Stabilising a Craton:

The Origin and Emplacement of the 3.1 Ga Mpuluzi Batholith

Rosanna C. L. Murphy

Australian Research Council Centre of Excellence for
Core to Crust Fluid Systems (CCFS) and GEMOC
Department of Earth and Planetary Sciences
Macquarie University
Sydney, Australia

This thesis has been submitted for fulfilment of the degree of Doctor of Philosophy,

June 2015

Table of Contents

Abstract 21

Chapter One – Introduction 27

1.1 Preamble 27

1.2 Aims and approach 28

1.3 Significance 29

1.4 Thesis structure 29

Chapter Two – Regional Geology 31

2.1 Overview 31

2.2 Ancient Gneiss Complex 31

2.3 Barberton Greenstone Belt 33

2.4 Granitoid rocks 33

2.4.1 TTG suite 33

2.4.2 GMS suite 35

2.4.3 Mswati Granites 35

2.5 Tectonic models 36

Chapter Three – Granite Petrogenesis 37

3.1 Granite classification schemes 37

3.1.1 IUGS modal classification 39

3.1.2 Source characteristics – I-S-A-M-type granites 40

3.1.3 Tectonic setting 44

3.2 Causes of compositional variation within granite suites 45

3.2.1 Source heterogeneity 45

3.2.2 Partial melting 46

3.2.3 Assimilation 47

3.2.4 Magma mixing/mingling 47

3.2.5 Fractional crystallisation 48

3.2.6 Alteration 50

Chapter Four - Analytical Methods 51

4.1 Whole-rock analyses 51

4.1.1 XRF major-element analyses 51

4.1.2 Trace-element analyses 53

4.1.3 Sr and Nd isotopic analyses 61

4.2 *In situ* analyses 63

4.2.1 Thin section analyses 63

4.2.2 Zircon separates 64

Chapter Five – Petrography and Mineral Chemistry 69

5.1 Petrography 69

5.2 Mineral Chemistry 74

5.2.1 Biotite 74

5.2.2 Allanite 82

5.3 Discussion 83

5.3.1 Post-crystallisation alteration 83

5.3.2 Host-rock effects on mineral chemistry 87

5.4 Conclusions 88

Chapter Six – Zircon Chemistry and Isotopic Composition 89

6.1 Introduction 89

6.2 Results 94

6.2.1 Zircon characteristics 94

6.2.2 Trace-element compositions 95

6.2.3 U-Pb data treatment 109

6.2.4 Calculated ages and Hf-isotope compositions 115

6.3 Discussion 154

6.3.1 Metamict zircon 154

6.3.2 Trace-element compositions 155

6.3.3 Timing and age constraints 160

6.3.4 Ti-in-zircon thermometry 169

6.4 Conclusions 169

Chapter Seven – Whole-Rock Chemistry and Isotopic Composition 171

7.1 Introduction 171

7.2 Results 171

7.2.1 Major-element compositions 171

7.2.2 Trace-element compositions 175

7.2.3 Sr and Nd isotopic compositions 181

7.3 Discussion 184

7.3.1 Granite classification 184

7.3.2 Comparison with other 3.1 Ga granitoids in the Barberton region 187

7.3.3 Constraints on source rocks 196

7.3.4 Factors influencing variation 197

7.4 Conclusions 205

Chapter Eight – Conclusions 207

8.1 Characteristics of Mpuluzi samples 207

8.2 Constraints on the source region 208

8.3 Processes involved in magma generation and emplacement 208

8.4 Tectonic implications 209

References 211

List of Figures

Figure 2.1. Simplified geological map of the eastern part of the Kaapvaal Craton, showing the Barberton Greenstone Belt, Ancient Gneiss Complex, and intrusions of the tonalite-trondhjemite-granodiorite (TTG) and granodiorite-monzogranite-syenite (GMS) suites. Modified from Wilson (1982); Belcher and Kisters (2006); Cutts *et al.* (2014). Sample localities for this study are marked with red crosses. 32

Figure 2.2. Simplified stratigraphy of the Barberton Greenstone Belt, showing the major divisions into the Onverwacht, Fig Tree, and Moodies Groups, the major discontinuities, and the relative ages of various intrusive units, divided into those north of the main greenstone belt and those to the south. Modified from Furnes *et al.* (2013). 34

Figure 2.3. Tectonic models for the formation of the eastern Kaapvaal Craton: (a) subduction-accretion; (b) vertical tectonics. Figure 2 from Van Kranendonk *et al.* (2014). 36

Figure 3.1. Descriptive classifications based on geochemical criteria: (a) the AFM diagram ($A = Na_2O+K_2O$, F = total Fe as FeO, M = MgO), separating the tholeiitic and calc-alkaline magma series (Kuno, 1968); (b) the low-K tholeiitic, medium- and high-K calc-alkaline, and shoshonitic series based on relative proportions of SiO_2 and K_2O (Le Maitre *et al.*, 1989). 38

Figure 3.2. Geochemical indices used in the geochemical classification scheme of Frost *et al.* (2001): (a) Fe number ($FeO^T/(FeO^T+MgO)$); (b) Modified alkali lime index ($Na_2O+K_2O–CaO$); (c) Aluminium saturation index ($Al_2O_3/(CaO+Na_2O+K_2O)$). 38

Figure 3.3. The IUGS modal classification diagram for igneous rocks with less than 90% mafic minerals, based on the modal proportions of quartz, alkali feldspar, plagioclase and feldspathoids (Streckeisen, 1967; 1974; 1976). 39

Figure 3.4. Zr *vs* Ga/Al discrimination diagram for separating A-type granites (blue) from S-type (red), I-type (yellow), and M-type granites (green), from Whalen *et al.* (1987). 43

Figure 3.5. Discrimination diagrams for the tectonic setting of granites from Pearce *et al.* (1984): (a) Nb *vs* Y; (b) Rb *vs* Y+Nb. COLG = collisional granites, WPG = within plate granites, ORG = ocean ridge granites, VAG = volcanic arc granites. The dashed line in (a) represents the upper compositional boundary for ORG from anomalous ridge segments. 45

Figure 3.6. Plot of Ba *vs* SiO_2 for the Boggy Plain pluton in the Lachlan Fold Belt, showing an inflection point at ~66% SiO_2 reflecting the onset of crystallisation of biotite (Wyborn *et al.*, 1987; 2001). 49

Figure 4.1. Accuracy of results obtained by: (a) solution ICPMS, and (b) laser ablation ICPMS, as percentage deviation from reference value. Strong negative peaks in the solution analysis of sample GSP (zircon-bearing granodiorite) indicate incomplete dissolution of zircon, which results in incomplete yields for zircon-hosted elements (Zr, Hf, Pb, Th, HREE). Strong positive peaks for Ni and Cr in the laser ablation ICPMS analyses indicate contamination from impurities in the flux. 59

Figure 4.2. Plot of $^{176}Yb/^{177}Hf$ *vs* $^{176}Hf/^{177}Hf$ (corrected) for: (a) Mud Tank and (b) Temora-2 reference zircons. 68

Figure 5.1. Photomicrographs (FOV = field of view; PPL = plane polarised light; XPL = cross polarised light; RL = reflected light): (a) plagioclase grains with strongly altered, euhedral cores (RSA02; FOV = 5 mm, PPL); (b) perthitic microcline (RSA02; FOV = 1.5 mm, XPL); (c) microcline with elongate blebs of perthite (RSA07; FOV = 5 mm, XPL); (d) partial replacement of microcline by myrmekite (RSA07; FOV = 2 mm, XPL); (e) deformed biotite grains (SWA07; FOV = 900 μm, PPL); (f) biotite partially altered to chlorite along cleavage planes (SWA18a; FOV = 900 μm, PPL); (g) unaltered biotite enclosed in quartz, other biotite altered to chlorite (RSA02; FOV = 1.5 mm, PPL); (h) small, euhedral hornblende (RSA03; FOV = 1.5 mm, PPL); (i) large, euhedral, orange-brown titanite with inclusions of quartz and feldspar (RSA03; FOV = 3 mm, PPL); (j) small, euhedral, dark-brown titanite (RSA01; FOV = 1.5 mm, PPL); (k) large, isolated allanite grain (RSA08; FOV = 4 mm, PPL); (l) allanite in cluster with biotite (SWA07; FOV = 3 mm, PPL); (m) zircon inclusion in muscovite (SWA05; FOV = 400 μm, PPL); (n) intergrown biotite and primary muscovite (SWA03; FOV = 1.5 mm, XPL); (o) secondary muscovite replacing plagioclase (SWA02a; FOV = 900 μm, XPL); (p) pyrite and chalcopyrite (RSA03; FOV = 900 μm, RL). 72

Figure 5.2. (a) Plot of octahedral Al *vs* Mg# in biotite, showing endmember compositions; (b) ternary plot of MgO, Al_2O_3, and FeO^T in biotite showing fields for coexisting phases (Nockolds, 1947). The colour of the points reflects the host-rock composition (warm colours = more mafic, cool colours = more felsic). 75

Figure 5.3. Plots of biotite compositions: (a) octahedral and (b) tetrahedral Al *vs* total Al content; (c) octahedral *vs* tetrahedral Al; (d) Fe^T *vs* Mg; (e) Ti, (f) Mn, and (g) F *vs* Mg# (atomic $Mg/(Mg+Fe^T)$); (h) and (i) same as (g) and (c) but with tie-lines connecting analyses of the same grain. The colour of the points reflects the host-rock composition (warm colours = more mafic, cool colours = more felsic). 76

Figure 5.4. Back-scatter electron (BSE) images of allanite showing (a) oscillatory zoning and (b) irregular patches. Scale bars are 50 μm. 82

Figure 5.5. Plots of allanite back-scatter electron signal intensity (approximate) *vs* (a) total REE content; (b) Ti content. 83

Figure 5.6. Plot of Ti in biotite *vs* ilmenite/magnetite in host rock. Red points represent samples with primary titanite. 87

Figure 6.1. Disturbances to the U-Th-Pb system: (a) addition of common Pb increases apparent ages; (b) recent loss of radiogenic Pb decreases the $^{207}Pb/^{235}U$ and $^{206}Pb/^{238}U$ ages but intersects the concordia at the true age; (c) ancient loss of radiogenic Pb decreases the apparent age; (d) the effect of common-Pb addition and ancient Pb loss on $^{207}Pb/^{206}Pb$ ages. 90

Figure 6.2. Plot of εHf *vs* age, showing a mixing trend between an evolved component and juvenile material. The main population lies at the crystallisation age of the rock (~2.5 Ga), and grains with inherited ages lie along an evolution line with Lu/Hf = 0.015 (average crust), which intersects the depleted mantle (DM) curve at the age of extraction of the source. Crustal model ages (T_{DM}^{C}) represent the intersection of an evolution line with the DM line; the mixing components in this example give model ages of ~3.2 Ga (evolved) and ~2.7 Ga (juvenile). 91

Figure 6.3. CL images of representative zircon grains from the Mpuluzi batholith: (a), (b) euhedral, oscillatory zoned (RSA01-101, RSA04-12); (c), (d) remnant oscillatory zoning (SWA03-45, SWA10a-75); (e) laminated (SWA18a-74); (f) distinct rim with dark CL response (SWA02a-42); (g), (h) distinct core with truncated zoning (RSA02-4, SWA05-2); (i), (j) multiple inclusions concentrated in dark (metamict) zones (RSA06-79, RSA01-110); (k), (l) inclusions cross cutting zoning (SWA03-32, SWA03-33); (m), (n) inclusions aligned with zoning (SWA10a-109, RSA06-115); (o), (p) fracturing concentrated in bright zones (RSA04-28, SWA07-13). Scale bars are 50 μm. For the full set of images see Appendix D. 92

Figure 6.4. Time-resolved analysis plots of trace-element analyses of Mpuluzi zircons: (a) pristine zircon with large apatite inclusion; (b) variable signal with small metamict zones included. 96

Figure 6.5. Plot of trace-element characteristics of the pristine (red), variable (yellow), and metamict (green) groups: (a) P; (b) Ca; (c) Ti; (d) Nb; (e) Ta; (f) Th; (g) U; (h) Th/U; (i) Y; (j) LREE; (k) MREE; (l) HREE; (m) $(Yb/Sm)_N$; (n) Ce/Ce*; (o) Eu/Eu*. Upper and lower bars represent maximum and minimum values; box represents upper quartile (75th percentile), median (black line), and lower quartile (25th percentile). 107

Figure 6.6. Chondrite-normalised REE plots for zircons from the Mpuluzi batholith (samples ordered from most mafic to most felsic): (a) RSA03; (b) RSA01; (c) SWA18a; (d) RSA05; (e) RSA02; (f) SWA07; (g) RSA04; (h) RSA08; (i) SWA10a; (j) RSA09; (k) SWA03; (l) RSA06; (m) SWA13a; (n) SWA11; (o) SWA09; (p) SWA02a; (q) RSA07; (r) SWA05. Red lines = pristine group; yellow field = variable group; green field = metamict group. 108

Figure 6.7. Collated age data for Mpuluzi samples: (a) U-Pb concordia plot showing the characteristic Pb-loss trend from ~3.1 Ga towards ~0 Ga; (b) plot of uncorrected $^{207}Pb/^{206}Pb$ ages showing the spread in ages down from ~3.1 Ga (Pb loss), a small plateau at ~3.5 Ga (inherited grains), and a spread towards higher ages (addition of common Pb). 109

Figure 6.8. Uncorrected $^{207}Pb/^{206}Pb$ ages *vs* U concentration, showing a decrease in the age obtained from grains with high U contents, indicating that these grains experienced ancient Pb loss. 110

Figure 6.9. Plot of uncorrected $^{207}Pb/^{206}Pb$ ages sorted by U content, showing calculated weighted averages for analyses with U <500, <1000, <1500, <2000 and <10000 ppm (all analyses), and the number of analyses included in these averages. Green line indicates 3100 Ma. Inherited grains and those with significant common Pb have been removed. 111

Figure 6.10. Plot of weighted averages of uncorrected $^{207}Pb/^{206}Pb$ ages calculated from analyses with different U contents. Maximum included U concentration starts at 100 ppm and increments by 100 ppm steps until 1500 ppm, then by 500 ppm steps until 5000 ppm; the final step includes analyses with <10000 ppm U (all analyses). 111

Figure 6.11. Uncorrected (blue) and corrected (pink) $^{207}Pb/^{206}Pb$ ages *vs* calculated proportion of common Pb, showing a strong positive correlation of uncorrected ages with common Pb above 10% calculated common Pb, and a negative correlation of corrected ages with calculated common Pb content. Common Pb calculated using the correction routine of Andersen (2002). 112

Figure 6.12. Effect of common-Pb correction on calculated ages for a representative sample (SWA18a). The uncorrected spectrum is on top and the corrected spectrum below; colours in the corrected spectrum correspond to the same-coloured bin in the uncorrected spectrum: (a) $^{206}Pb/^{238}U$ ages; (b) $^{207}Pb/^{235}U$ ages; (c) $^{207}Pb/^{206}Pb$ ages; (d) $^{208}Pb/^{232}Th$ ages. 114

Figure 6.13. Calculated ages and Hf isotopes from sample RSA03: (a) weighted average of $^{207}Pb/^{206}Pb$ ages and (b) intercept age on the U-Pb concordia diagram (uncorrected data); (c) weighted average of $^{207}Pb/^{206}Pb$ ages and (d) intercept age on the U-Pb concordia diagram (corrected data); histograms of (e) $^{176}Yb/^{177}Hf$ and (f) $^{176}Hf/^{177}Hf_i$, with kernel density estimate as a blue line; (g) εHf plot showing the range in crustal model ages (field) and the median (dashed line). 118

Figure 6.14. Calculated ages and Hf isotopes from sample RSA01: (a) weighted average of $^{207}Pb/^{206}Pb$ ages and (b) intercept age on the U-Pb concordia diagram (uncorrected data); (c) weighted average of $^{207}Pb/^{206}Pb$ ages and (d) intercept age on the U-Pb concordia diagram (corrected data); histograms of (e) $^{176}Yb/^{177}Hf$ and (f) $^{176}Hf/^{177}Hf_i$, with kernel density estimate as a blue line; (g) εHf plot showing the range in crustal model ages (field) and the median (dashed line). 120

Figure 6.15. Calculated ages and Hf isotopes from sample SWA18a: (a) weighted average of $^{207}Pb/^{206}Pb$ ages and (b) intercept age on the U-Pb concordia diagram (uncorrected data); (c) weighted average of $^{207}Pb/^{206}Pb$ ages and (d) intercept age on the U-Pb concordia diagram (corrected data); histograms of (e) $^{176}Yb/^{177}Hf$ and (f) $^{176}Hf/^{177}Hf_i$, with kernel density estimate as a blue line (main population shown in blue, inherited in pink); (g) εHf plot showing the range in crustal model ages (field), the median of the main population (dashed black line), and the inherited grain (dashed grey line). 122

Figure 6.16. Calculated ages and Hf isotopes from sample RSA05: (a) weighted average of $^{207}Pb/^{206}Pb$ ages and (b) intercept age on the U-Pb concordia diagram (uncorrected data); (c) weighted average of $^{207}Pb/^{206}Pb$ ages and (d) intercept age on the U-Pb concordia diagram (corrected data); histograms of (e) $^{176}Yb/^{177}Hf$ and (f) $^{176}Hf/^{177}Hf_i$, with kernel density estimate as a blue line; (g) εHf plot showing the range in crustal model ages (field) and the median (dashed line). 124

Figure 6.17. Calculated ages and Hf isotopes from sample RSA02: (a) weighted average of $^{207}Pb/^{206}Pb$ ages and (b) intercept age on the U-Pb concordia diagram (uncorrected data); (c) weighted average of $^{207}Pb/^{206}Pb$ ages and (d) intercept age on the U-Pb concordia diagram (corrected data); histograms of (e) $^{176}Yb/^{177}Hf$ and (f) $^{176}Hf/^{177}Hf_i$, with kernel density estimate as a blue line; (g) εHf plot showing the range in crustal model ages (field) and the median (dashed line). 126

Figure 6.18. Calculated ages and Hf isotopes from sample SWA07: (a) weighted average of $^{207}Pb/^{206}Pb$ ages and (b) intercept age on the U-Pb concordia diagram (uncorrected data); (c) weighted average of $^{207}Pb/^{206}Pb$ ages and (d) intercept age on the U-Pb concordia diagram (corrected data); (e) weighted average of $^{207}Pb/^{206}Pb$ ages and (f) intercept age on the U-Pb concordia diagram (inherited population); histograms of (g) $^{176}Yb/^{177}Hf$ and (h) $^{176}Hf/^{177}Hf_i$, with kernel density estimate as a blue line (main population shown in blue, inherited in pink); (i) εHf plot showing the range in crustal model ages (field), the median of the main population (dashed black line), and the maximum of the inherited grains (dashed grey line). 128

Figure 6.19. Calculated ages and Hf isotopes from sample RSA04: (a) weighted average of $^{207}Pb/^{206}Pb$ ages and (b) intercept age on the U-Pb concordia diagram (uncorrected data); (c) weighted average of $^{207}Pb/^{206}Pb$ ages and (d) intercept age on the U-Pb concordia diagram (corrected data); histograms of (e) $^{176}Yb/^{177}Hf$ and (f) $^{176}Hf/^{177}Hf_i$, with kernel density estimate as a blue line; (g) εHf plot showing the range in crustal model ages (field) and the median (dashed line). 130

Figure 6.20. Calculated ages and Hf isotopes from sample RSA08: (a) weighted average of $^{207}Pb/^{206}Pb$ ages and (b) intercept age on the U-Pb concordia diagram (uncorrected data); (c) weighted average of $^{207}Pb/^{206}Pb$ ages and (d) intercept age on the U-Pb concordia diagram (corrected data); histograms of (e) $^{176}Yb/^{177}Hf$ and (f) $^{176}Hf/^{177}Hf_i$, with kernel density estimate as a blue line; (g) εHf plot showing the range in crustal model ages (field) and the median (dashed line). 132

Figure 6.21. Calculated ages and Hf isotopes from sample SWA10a: (a) weighted average of $^{207}Pb/^{206}Pb$ ages and (b) intercept age on the U-Pb concordia diagram (uncorrected data); (c) weighted average of $^{207}Pb/^{206}Pb$ ages and (d) intercept age on the U-Pb concordia diagram (corrected data); histograms of (e) $^{176}Yb/^{177}Hf$ and (f) $^{176}Hf/^{177}Hf_i$, with kernel density estimate as a blue line (main population shown in blue, inherited in pink); (g) εHf plot showing the range in crustal model ages (field), the median of the main population (dashed black line), and the median of the inherited grains (dashed grey line). 134

Figure 6.22. Calculated ages and Hf isotopes from sample RSA09: (a) weighted average of $^{207}Pb/^{206}Pb$ ages and (b) intercept age on the U-Pb concordia diagram (uncorrected data); (c) intercept age on the U-Pb concordia diagram (corrected data; no weighted average could be calculated for this sample); histograms of (d) $^{176}Yb/^{177}Hf$ and (e) $^{176}Hf/^{177}Hf_i$, with kernel density estimate as a blue line; (f) εHf plot showing the range in crustal model ages (field) and the median (dashed line). 136

Figure 6.23. Calculated ages and Hf isotopes from sample SWA03: (a) weighted average of $^{207}Pb/^{206}Pb$ ages and (b) intercept age on the U-Pb concordia diagram (uncorrected data); (c) weighted average of $^{207}Pb/^{206}Pb$ ages and (d) intercept age on the U-Pb concordia diagram (corrected data); histograms of (e) $^{176}Yb/^{177}Hf$ and (f) $^{176}Hf/^{177}Hf_i$, with kernel density estimate as a blue line; (g) εHf plot showing the range in crustal model ages (field) and the median (dashed line). 138

Figure 6.24. Calculated ages and Hf isotopes from sample RSA06: (a) weighted average of $^{207}Pb/^{206}Pb$ ages and (b) intercept age on the U-Pb concordia diagram (uncorrected data); (c) weighted average of $^{207}Pb/^{206}Pb$ ages and (d) intercept age on the U-Pb concordia diagram (corrected data); histograms of (e) $^{176}Yb/^{177}Hf$ and (f) $^{176}Hf/^{177}Hf_i$, with kernel density estimate as a blue line; (g) εHf plot showing the range in crustal model ages (field) and the median (dashed line). 140

Figure 6.25. Calculated ages and Hf isotopes from sample SWA13a: (a) weighted average of $^{207}Pb/^{206}Pb$ ages and (b) intercept age on the U-Pb concordia diagram (uncorrected data); (c) weighted average of $^{207}Pb/^{206}Pb$ ages and (d) intercept age on the U-Pb concordia diagram (corrected data); histograms of (e) $^{176}Yb/^{177}Hf$ and (f) $^{176}Hf/^{177}Hf_i$, with kernel density estimate as a blue line; (g) εHf plot showing the range in crustal model ages (field) and the median (dashed line). 142

Figure 6.26. Calculated ages and Hf isotopes from sample SWA11: (a) weighted average of $^{207}Pb/^{206}Pb$ ages and (b) intercept age on the U-Pb concordia diagram (uncorrected data); (c) weighted average of $^{207}Pb/^{206}Pb$ ages and (d) intercept age on the U-Pb concordia diagram (corrected data); histograms of (e) $^{176}Yb/^{177}Hf$ and (f) $^{176}Hf/^{177}Hf_i$, with kernel density estimate as a blue line; (g) εHf plot showing the range in crustal model ages (field) and the median (dashed line). 144

Figure 6.27. Calculated ages and Hf isotopes from sample SWA09: (a) weighted average of $^{207}Pb/^{206}Pb$ ages and (b) intercept age on the U-Pb concordia diagram (uncorrected data); (c) weighted average of $^{207}Pb/^{206}Pb$ ages and (d) intercept age on the U-Pb concordia diagram (corrected data); histograms of (e) $^{176}Yb/^{177}Hf$ and (f) $^{176}Hf/^{177}Hf_i$, with kernel density estimate as a blue line (main population shown in blue, inherited in pink); (g) εHf plot showing the range in crustal model ages (field), the median of the main population (dashed black line), and the inherited grain (dashed grey line). 146

Figure 6.28. Calculated ages and Hf isotopes from sample SWA02a: (a) weighted average of $^{207}Pb/^{206}Pb$ ages and (b) intercept age on the U-Pb concordia diagram (uncorrected data); (c) weighted average of $^{207}Pb/^{206}Pb$ ages and (d) intercept age on the U-Pb concordia diagram (corrected data); histograms of (e) $^{176}Yb/^{177}Hf$ and (f) $^{176}Hf/^{177}Hf_i$, with kernel density estimate as a blue line (main population shown in blue, inherited in pink); (g) εHf plot showing the range in crustal model ages (field), the median of the main population (dashed black line), and the inherited grain (dashed grey line). 148

Figure 6.29. Calculated ages and Hf isotopes from sample RSA07: (a) weighted average of $^{207}Pb/^{206}Pb$ ages and (b) intercept age on the U-Pb concordia diagram (uncorrected data); (c) intercept age on the U-Pb concordia diagram (corrected data; no weighted average could be calculated for this sample); histograms of (d) $^{176}Yb/^{177}Hf$ and (e) $^{176}Hf/^{177}Hf_i$, with kernel density estimate as a blue line; (f) εHf plot showing the range in crustal model ages (field) and the median (dashed line). 150

Figure 6.30. Calculated ages and Hf isotopes from sample SWA05: (a) weighted average of $^{207}Pb/^{206}Pb$ ages and (b) intercept age on the U-Pb concordia diagram (uncorrected data); (c) weighted average of $^{207}Pb/^{206}Pb$ ages and (d) intercept age on the U-Pb concordia diagram (corrected data); histograms of (e) $^{176}Yb/^{177}Hf$ and (f) $^{176}Hf/^{177}Hf_i$, with kernel density estimate as a blue line; (g) εHf plot showing the range in crustal model ages (field) and the median (dashed line). 152

Figure 6.31. Plot of Y *vs* U in zircons from the Mpuluzi batholith (samples ordered from most mafic to most felsic; named sample in red, whole dataset in grey): (a) RSA03; (b) RSA01; (c) SWA18a; (d) RSA05; (e) RSA02; (f) SWA07; (g) RSA04; (h) RSA08; (i) SWA10a; (j) RSA09; (k) SWA03; (l) RSA06; (m) SWA13a; (n) SWA11; (o) SWA09; (p) SWA02a; (q) RSA07; (r) SWA05; (s) metamict grains; (t) fields for different host rock types (from Belousova *et al.,* 2002). 157

Figure 6.32. Plot of Hf *vs* Y in zircons from the Mpuluzi batholith (samples ordered from most mafic to most felsic; named sample in red, whole dataset in grey): (a) RSA03; (b) RSA01; (c) SWA18a; (d) RSA05; (e) RSA02; (f) SWA07; (g) RSA04; (h) RSA08; (i) SWA10a; (j) RSA09; (k) SWA03; (l) RSA06; (m) SWA13a; (n) SWA11; (o) SWA09; (p) SWA02a; (q) RSA07; (r) SWA05; (s) metamict grains; (t) fields for different host rock compositions (from Belousova *et al.,* 2002). The dashed line with Hf/Y=8.0 separates the fields for quartz-free rocks (-Q) from the fields for quartz-bearing rocks (+Q). 159

Figure 6.33. Plot of U concentration (blue) and accumulated radiation damage (pink) *vs* uncorrected $^{207}Pb/^{206}Pb$ ages. 162

Figure 6.34. Plot of total Th and U concentration *vs* accumulated radiation damage (in displacements per atom), showing the effect of errors in age caused by loss of radiogenic Pb and addition of common Pb on the calculated radiation dose. The black line is the calculated radiation dose for grains with an age of 3.1 Ga and a Th/U ratio of 0.65 (average for Mpuluzi zircons). 163

Figure 6.35. Plot of accumulated radiation damage (in displacements per atom) *vs* uncorrected $^{206}Pb/^{238}U$ ages. 164

Figure 6.36. Histogram of calculated ages with kernel density estimate prepared using DensityPlotter (Vermeesch, 2012): (a) corrected intercept ages; (b) uncorrected intercept ages; (c) uncorrected weighted mean of $^{207}Pb/^{206}Pb$ ages. 164

Figure 6.37. Plot of total Th + U content *vs* corrected (green) and uncorrected (red) intercept ages and uncorrected weighted averages of $^{207}Pb/^{206}Pb$ ages (blue) for the Mpuluzi samples. 165

Figure 6.38. Histogram of all inherited ages obtained from Mpuluzi samples (n=18). 166

Figure 6.39. Plot of $^{176}Yb/^{177}Hf$ *vs* εHf for the Mpuluzi samples. Red diamonds indicate inherited grains from sample SWA10a. 167

Figure 6.40. Ti-in-zircon crystallisation temperature estimates calculated from pristine analyses (red), variable analyses (orange), and metamict analyses (green). 168

List of Figures

Figure 7.1. Total-alkali *vs* silica (TAS) classification diagram of Le Bas *et al.* (1986), showing the samples from the Mpuluzi batholith. 173

Figure 7.2. Plot of Al/(Na+K) *vs* Al/(Ca+Na+K) for the Mpuluzi samples, showing the division into peraluminous, metaluminous, and peralkaline. 173

Figure 7.3. Harker variation diagrams for major elements *vs* SiO_2: (a) K_2O, showing the low- K tholeiitic, medium- and high-K calc-alkaline fields of Le Maitre *et al.* (1989); (b) MgO; (c) $Fe_2O_3^T$; (d) TiO_2; (e) P_2O_5; (f) CaO; (g) MnO; (h) Al_2O_3; (i) Na_2O; (j) Mg# (= $Mg/(Mg+Fe^T)$). 174

Figure 7.4. Trace elements *vs* SiO_2: (a) Rb; (b) Cs; (c) Sr; (d) Ba; (e) Rb/Sr; (f) K/Rb; (g) V; (h) Zr; (i) Hf; (j) Sc; (k) Nb; (l) Th; (m) U; (n) Th/U. 177

Figure 7.5. Chondrite-normalised rare earth element (REE) compositions of samples from the Mpuluzi batholith. 177

Figure 7.6. Rare earth element (REE) compositions and key parameters *vs* SiO_2: (a) $(La/Yb)_N$; (b) Eu/Eu* (chondrite-normalised $Eu/\sqrt{(Sm*Gd)}$); (c) Total REE; (d) La; (e) Ce; (f) Pr; (g) Nd; (h) Sm; (i) Eu; (j) Gd; (k) Tb; (l) Dy; (m) Ho; (n) Y; (o) Er; (p) Tm; (q) Yb; (r) Lu. 179

Figure 7.7. Plot of measured $^{87}Sr/^{86}Sr$ *vs* $^{87}Rb/^{86}Sr$ (isochron diagram). The samples define a single isochron with an initial ratio of 0.7012 ± 0.0016, and an age of 3113 ± 84 Ma. 183

Figure 7.8. Plot of measured $^{143}Nd/^{144}Nd$ *vs* $^{147}Sm/^{144}Nd$ (isochron diagram): (a) for all Mpuluzi samples; (b) excluding sample RSA09. The samples define a single isochron with an initial ratio of 0.50849 ± 0.00038, and an age of 3027 ± 530 Ma (excluding sample RSA09). 183

Figure 7.9. Plot of epsilon Nd *vs* initial Sr composition (excluding sample RSA09). 183

Figure 7.10. Compositions of Mpuluzi samples plotted on the AFM diagram of Kuno (1968). A = Na_2O+K_2O, F = FeO^T, and M = MgO. 184

Figure 7.11. Mpuluzi samples classified according to the key indices of Frost *et al.* (2001): (a) Division into magnesian and ferroan granites; and (b) Modified alkali-lime index. See also aluminium saturation index (Figure 7.2 above). 185

Figure 7.12. Plot of (a) aluminium saturation and (b) normative corundum/diopside *vs* SiO_2 for Mpuluzi samples. 185

Figure 7.13. Compositions of Mpuluzi samples plotted on the discrimination diagrams for the tectonic setting of granites from Pearce *et al.* (1984): (a) Nb *vs* Y; (b) Rb *vs* Y+Nb. COLG = collisional granites, WPG = within plate granites, ORG = ocean ridge granites, VAG = volcanic arc granites. The dashed line in (a) represents the upper compositional boundary for ORG from anomalous ridge segments. 186

Figure 7.14. Major-element analyses *vs* SiO_2 for the Mpuluzi batholith (blue) compared with published data for the Mpuluzi batholith (red), the Heerenveen batholith (orange) and the average composition of the Nelspruit batholith (green): (a) K_2O; (b) Na_2O; (c) CaO; (d) MgO; (e) MnO; (f) Al_2O_3; (g) TiO_2; (h) P_2O_5; (i) $Fe_2O_3^T$; (j) Mg#. Data from Anhaeusser and Robb (1983; circles) and Yearron (2003; crosses). 192

Figure 7.15. Trace-element analyses *vs* K_2O for the Mpuluzi batholith (blue) compared with published data for the Mpuluzi batholith (red) and Heerenveen batholith (orange): (a) Rb; (b) Sr. Data from Anhaeuser and Robb (1983; circles) and Yearron (2003; crosses). 193

Figure 7.16. Trace-element analyses *vs* SiO_2 for the Mpuluzi batholith (blue) compared with published data for the Mpuluzi batholith (red) and Heerenveen batholith (orange): (a) Rb; (b) Sr; (c) Rb/Sr; (d) Ba; (e) V; (f) Zn; (g) Zr; (h) Nb; (i) Y; (j) La; (k) Ce; (l) Nd; (m) Sm; (n) Eu; (o) Gd; (p) Tb; (q) Yb; (r) Lu; (s) $(La/Yb)_N$; (t) Eu/Eu*. Data from Anhaeusser and Robb (1983; circles) and Yearron (2003; crosses). 194

Figure 7.17. Plot of εHf *vs* age for samples from the TTG suite (green) and the Ancient Gneiss Complex (AGC; red), with all analyses from the Mpuluzi samples in this study plotted in grey for reference (filled diamonds are analyses from the main age population; open diamonds are inherited grains). Average (3.5 Ga) and oldest (4.13 Ga) crustal evolution lines shown for reference. Data from Zeh *et al.* (2009; 2011) and Kröner *et al.* (2014). 197

Figure 7.18. Plot of zircon Hf isotope T_{DM}^C (crustal) model ages *vs* T_{CHUR} model ages calculated from whole-rock Sr isotope compositions. 198

Figure 7.19. Estimates of magma temperature calculated from zircon saturation, plotted *vs* whole-rock SiO_2 content. Data points in red are samples with at least one inherited core detected. 199

Figure 7.20. Plot of calculated zircon U-Pb ages *vs* whole-rock SiO_2 for Mpuluzi samples: (a) intercept ages (corrected); (b) intercept ages (uncorrected); (c) weighted mean of $^{207}Pb/^{206}Pb$ ages (uncorrected). 201

Figure 7.21. Plot of (a) CaO and (b) Mg# (= $Mg/(Mg+Fe^T)$) *vs* MgO for Mpuluzi samples. 202

Figure 7.22. Plot of measured $^{87}Sr/^{86}Sr$ *vs* 1/Sr for Mpuluzi samples. 202

Figure 7.23. Average εHf *vs* whole-rock SiO_2 contents. Data points in red are samples with at least one inherited core detected. 202

Figure 7.24. Ti-in-zircon crystallisation temperatures *vs* whole-rock SiO_2 content (note that the anomalous low-temperature sample is a single data point). 204

List of Tables

Table 3.1: Distinguishing characteristics of I-, S-, M-, and A-type granites (adapted from Winter, 2010). 41

Table 4.1: Operating conditions and lower limits of detection for determination of major-element concentrations by XRF. 51

Table 4.2: Results of repeated major-element analysis of standards AGV-2, BCR-2, BHVO-2 and GSP-2 by XRF during this study, and comparison to preferred values from the GeoReM database (Jochum et al., 2005). All values in wt%. 52

Table 4.3: Results of repeated trace-element analysis of standards BHVO-2, BIR-1 and GSP-SS by solution ICPMS during this study, and comparison to values from the GeoReM database (Jochum et al., 2005). For USGS standards BHVO-2 and BIR-1, the preferred values are used. GSP-SS was collected from the same locality as USGS standard GSP-1, and the reported values for both GSP-1 and GSP-2 are provided for comparison (GSP-1 has no reported uncertainties). All values in ppm. 54

Table 4.4: Results of repeated trace-element analysis of standards AGV-2, BHVO-2, BCR-2 and GSP-SS by LA-ICPMS during this study, and comparison to values from the GeoReM database (Jochum et al., 2005). For USGS standards AGV-2, BHVO-2 and BCR-2, the preferred values are used. GSP-SS was collected from the same locality as USGS standard GSP-1, and the reported values for both GSP-1 and GSP-2 are provided for comparison (GSP-1 has no reported uncertainties). All values in ppm. 56

Table 4.5: List of trace elements analysed in this study, showing the uncertainties and detection limits (in ppm) for each technique, which technique was chosen for the final compilation, and the reason for this choice. 60

Table 4.6: LA-ICPMS results for Cr and Ni in standards AGV-2, BHVO-2, BCR-2 and GSP-SS prepared at flux:sample ratios of 2.5:0.3 and 1.5:0.5. References values as in Table 4.4. All values in ppm. 62

Table 4.7: Results of Sr and Nd isotopic analysis of standards BHVO-2, JMC 321 and NIST SRM 987 by TIMS during this study, and comparison to GAU long-term averages and preferred values from: NIST (NIST SRM 987; http://www.nist.gov/srm/index.cfm) and GeoReM (BHVO-2 and JMC 321; Jochum et al., 2005). 62

Table 4.8: Results of repeated major-element analyses of reference materials Lehmi Biotite, Muscovite and GJ zircon by EMP during this study, and comparison to reference values. Reference values for biotite and muscovite standards from USGS. All values in wt%. 63

Table 4.9: U-Pb isotopic analyses obtained in this study for zircons 91500 and OG1, and ID-TIMS values. Reference values for 91500 from Wiedenbeck et al. (1995); values for OG1 from Stern et al. (2009). GJ-1 ratios used for calibration from Jackson et al. (2004). Full dataset in Appendix A1. 65

Table 4.10: Results of repeated trace-element analysis of zircon 91500 by LA-ICPMS during this study, and comparison with published values. Reference values from Wiedenbeck et al. (2004) except P, Ti, Ta (values from the GeoReM database; Jochum et al., 2005). All values in ppm. 66

Table 4.11: Results of repeated Hf-isotope analysis of zircons Mud Tank and Temora-2 by LA-MC-ICPMS during this study, and comparison with long term averages from the GAU and published values. Reference values for Mud Tank from Griffin et al. (2007); values for Temora-2 from Woodhead and Hergt (2005). Full dataset in Appendix A2. 67

Table 5.1: Summary of the petrography of the Mpuluzi samples (full descriptions in Appendix B). Mineral abbreviations from Kretz (1983). Alt. = alteration; Frac. = fractures; Und. = undulose extinction; Sut. = sutured boundaries; Def. twins = deformation twins; Myrm. = myrmekite; y = yes (observed); yy = very abundant; min = minor; v min = very minor; v fine = very fine. 70

Table 5.2: Representative analyses of biotite for the Mpuluzi samples. LLD = lower limit of detection. 77

Table 5.3: Representative analyses of allanite for the Mpuluzi samples. LLD = lower limit of detection. 84

Table 6.1: Trace-element compositions of zircons from the Mpuluzi batholith; averages calculated from 'pristine', 'variable' and 'metamict' groups for each sample. All values in ppm. For the full dataset see Appendix F. 97

Table 6.2: Summary of U and Th contents and U-Pb ages of zircons from the Mpuluzi batholith. Where a population is represented by only one analysis, the $^{207}Pb/^{206}Pb$ age and associated error is presented in lieu of a weighted average. Where the corrected U-Pb data shows two values for number of analyses, the number in parentheses represents the weighted average. The full dataset is provided in Appendix G. 116

Table 6.3: Summary of Hf isotopic compositions of zircons from the Mpuluzi batholith. Where a population is represented by only one analysis, the measured ratios and calculated εHf and T(DM)c are presented in lieu of an average, along with their associated errors. For the full dataset see Appendix H. 117

Table 6.4: Previously-determined ages for the Mpuluzi and Piggs Peak batholiths. 160

Table 6.5: Average crystallisation temperature estimates for the 'pristine', 'variable', and 'metamict' groups, calculated using the Ti-in-zircon thermometer (note that the anomalously low temperature estimate for sample RSA03 represents a single data point). All values in °C. Full dataset in Appendix F. 168

Table 7.1: Major-element compositions for samples from the Mpuluzi batholith. All values in wt%. Al sat = Classification based on the aluminium saturation index; Metal. = metaluminous; Peral. = peraluminous; A/CNK = $Al_2O_3/(CaO+Na_2O+K_2O)$; A/NK = $Al_2O_3/(Na_2O+K_2O)$; TAS = Classification based on the total alkali silica diagram; Q Monz = quartz monzonite. 172

Table 7.2: Trace-element compositions for samples from the Mpuluzi batholith. All values in ppm. 180

Table 7.3: Sr and Nd isotopic compositions for samples from the Mpuluzi batholith. 182

Table 7.4: Major- and trace-element analyses for the Mpuluzi (Mpz), Heerenveen (Hvn), and Nelspruit (Nsp) batholiths compiled from the literature. References: (1) Anhaeusser and Robb (1983); (2) Yearron (2003). 188

Table 7.5: Sr isotopic analyses for the Mpuluzi and other ~3.1 Ga granitoids in the region compiled from the literature (data from Allsopp et al., 1962; de Gasparis, 1967; Davies, 1971; Barton et al., 1983; Maphalala et al., 1989). 193

Table 7.6: Nd isotopic analyses for the ~3.1 Ga granitoids in the region compiled from the literature (data from Yearron, 2003; Schoene et al., 2009). 196

*Table 7.7: Zircon saturation temperatures calculated for samples from the Mpuluzi batholith (calculated using the method of Watson & Harrison, 1983). M = (Na+K+2Ca)/(Al*Si), in cation proportions.* 198

Abstract

The Barberton Greenstone Belt (BGB) and Ancient Gneiss Complex (AGC), located in the eastern part of the Kaapvaal Craton (Swaziland and adjacent South Africa), represent some of the best-preserved and most-studied Early- to Mid-Archaean (3.6–3.2 Ga) crustal remnants. The extensively-studied granite-greenstone belt is surrounded and overlain by several large granitoid bodies (Mpuluzi, Piggs Peak, Nelspruit, and Heerenveen batholiths), all emplaced at ~3.1 Ga, which coincides with the end of TTG magmatism and regional metamorphism in the area. This study focuses on the Mpuluzi batholith as a case study to constrain the prevailing conditions at 3.1 Ga that led to the generation and emplacement of these granitoids, and subsequent cratonisation.

The granitoids were emplaced as extensive, km-thick sheets and extend over more than 20,000 km^2. Zircon U-Pb ages vary from ~3.16 to ~3.09 Ga; the presence of inherited cores in some grains suggests the involvement of an older crustal component (~3.5 Ga) in the magma generation. This is confirmed by the Hf isotopic data, which show clear indications of mixing between an older crustal component and juvenile material. The Hf isotopic data also provide a good estimate of the age of extraction of the inherited component, with one sample showing a well-defined evolution trend back to ~4.1 Ga. The Hf data also suggest that the juvenile material may have been extracted from the mantle very close to the time of emplacement of the batholith, with the mixing trend intersecting the depleted mantle line in some samples.

Whole-rock Sr and Nd isotopic data yield tight isochrons for both systems (MSWD <1), and calculated isochron ages are within error of each other, and of the U-Pb ages (Sr: 3113 ± 84 Ma; Nd: 3027 ± 520 Ma). The close agreement between ages from the three isotopic systems strongly suggests that the whole mass formed and cooled together.

The isotopic evidence for mixing between an older crustal component and juvenile material suggests that the mantle may have both provided the heat for melting and contributed material to the magma itself. The variation within the batholith thus represents variable proportions of mixing between these components, and perhaps also a build-up of heat over time. These 3.1 Ga granitoids therefore represent the final stage in the cratonisation of the region; this could represent the “draining” of fusible material from the lower crust, increasing its rigidity and limiting further tectonism.

Declaration

I certify that the work in this thesis entitled "**Stabilising a Craton: The Origin and Emplacement of the 3.1 Ga Mpuluzi Batholith**" has not previously been submitted for a degree, nor has it been submitted as a partial requirement for a degree to any other university or institution other than Macquarie University.

I also certify that this thesis is an original piece of research and has been written by me. Any help and assistance that I have received in my research work and the preparation of the thesis itself have been properly acknowledged.

In addition, I certify that all data, information sources and literature used are indicated in the thesis.

Rosanna C. L. Murphy

Student ID: 40962679

Date: 17 June 2015

Acknowledgements

First and foremost, my thanks go to my supervisors, for all their support, advice, encouragement, and the occasional well-deserved berating. To Norm Pearson, without whom I would have thrown in the towel long ago; to Bill Griffin, who turns around draft chapters unbelievably fast; to Sue O'Reilly, who has managed (to my surprise) to turn me into a halfway decent public speaker: thank you all. I couldn't have done it without you.

Thanks also go to Dick Flood, for his expertise in all things granitic, and many other things besides. Elena Belousova is also gratefully acknowledged for her assistance with zircons, particularly advice concerning badly behaving ones.

This project involved a large amount of analytical work in which I was assisted by many people, including Peter Wieland (wet chemistry and entertainment), Will Powell (laser ablation and computer magic), Yoann Gréau (hafnium and sympathy), Steve Craven (sample prep and bad puns), Kevin Grant, and David Adams.

Many thanks to all the people who assisted with fieldwork: in January 2011 I was accompanied by Jacques Batumike, whose field experience and assistance with sampling was greatly appreciated; Kenneth Ndlovu, Futti and Tsami from the Swaziland Geological Survey are gratefully acknowledged for providing transport, maps and invaluable local knowledge; Alfred Kroner, Axel Hofmann, and the Geology department at the University of Johannesburg are thanked for the provision of their field experience in the region, as well as a car, maps, references, and sundry organisational and logistical assistance. In March 2012 I joined the field expedition of Jean-François Moyen, Simon Carrouée, and Michel Cuney from Université Jean-Monnet in Saint-Etienne, France, and they are thanked for allowing me to accompany them and sharing their knowledge and insights.

Analytical work, conference travel, and living expenses were generously funded by Macquarie University and the Australian government. The Department of Earth & Planetary Sciences is also acknowledged for the use of the state-of-the-art laboratory facilities in the Geochemical Analysis Unit.

To Felix Genske, Nicole McGowan, Irina Tretiakova, Sophia Bratenkov, and Bruno Colas, my thanks and my apologies for sharing an office with me throughout this ordeal.

Final thanks go to my friends and family, for understanding that I'm not an archaeologist or a palaeontologist, and that rocks actually can be very interesting!

And to Ed, for putting up with me.

Chapter One – Introduction

1.1 Preamble

The rocks exposed at the surface of the Earth encompass an enormous range in ages, from active volcanoes forming new crust today, to remnants of crust formed shortly after the formation of the Earth itself. Fragments of such ancient crust occur within blocks of stable crust known as cratons, which form the cores of modern continents.

The formation of the first stable, continental crust in the early part of Earth's history is poorly understood and the subject of much debate (e.g. Van Kranendonk *et al.*, 2007; Anhaeusser, 2014). The remnants of Archaean crust are generally small and highly deformed, and thus unravelling their early history is often made difficult by overprinting in multiple later events. Such ancient crustal remnants are known as granite-greenstone terranes, and consist of a complex succession of metamorphosed volcano-sedimentary rocks (greenstones) surrounded by granitic rocks (Anhaeusser, 2014).

Granite-greenstone terranes have been reported from all continents; particularly famous and well-studied examples of occur in Greenland (North Atlantic Craton; e.g. Fedo *et al.*, 2001; Myers, 2001), Australia (Pilbara and Yilgarn Cratons; e.g. Binns *et al.*, 1976; Gee *et al.*, 1981; Swager *et al.*, 1992; Hickman & Van Kranendonk, 2012), Canada (Superior and Slave Cratons; e.g. Henderson, 1981; Shirey & Hanson, 1986; Isachsen & Bowring, 1994; Polat & Kerrich, 2000), and southern Africa (Zimbabwe and Kaapvaal Cratons; e.g. Viljoen & Viljoen, 1969; Anhaeusser & Robb, 1981; Kröner *et al.*, 1991; Kusky & Kidd, 1992; Wilson *et al.*, 1995).

The greenstone components of such terranes often occur as elongate slivers, and show a progression from dominantly volcanic to dominantly sedimentary rocks (Anhaeusser, 2014). They consist of a diverse range of lithologies, including ultramafic volcanics (e.g. komatiites), intermediate to felsic volcanics and volcaniclastics, cherts, pelites, psammites, and conglomerates (Anhaeusser, 2014).

The granitic component of granite-greenstone terranes generally includes migmatites and granitic gneisses in addition to undeformed granitoid plutons and batholiths (Anhaeusser, 2014). The granitic rocks commonly show a progression from Na-rich tonalite-trondhjemite-granodiorite (TTG) gneisses to K-rich granites, monzogranites, and granodiorites; the potassic magmas often have emplacement ages which match the timing of the main stabilisation event in the region (e.g. Brazil; Romano *et al.*, 2013; Canada; Whalen *et al.*, 2004; South Africa; Anhaeusser & Robb, 1983). This has led some authors to suggest that their emplacement

causes cratonisation, as the emplacement of potassic magma both increases the buoyancy of the upper crust, and removes heat producing elements from the lower crust (e.g. Kusky, 1993; Moser *et al.*, 1996; Sandiford *et al.*, 2002; Sandiford *et al.*, 2004; Romano *et al.*, 2013).

1.2 Aims and approach

The overall aim of this thesis is to contribute to the understanding of the processes of fluid/melt extraction that stabilise, and thus preserve, Archaean cratonic lithosphere.

To achieve this aim, this study examines a section of ancient crust in southern Africa. The eastern part of the Kaapvaal Craton includes a granite-greenstone terrane which dates back as far as ~3.6 Ga, and records multiple deformational events, culminating in the emplacement of several large batholiths at ~3.1 Ga. The emplacement of the Mpuluzi batholith (one such 3.1 Ga granite) is used as a case study to constrain the conditions prevailing at the time of emplacement that led to the generation and emplacement of large volumes of granitic magma, and subsequent cratonisation. An overview of the regional geology is presented in Chapter Two.

There are several fundamental questions relating to the generation and emplacement of such large volumes of granitic magma:

- What was the heat source? Can the depth of melting be constrained? Did the mantle contribute heat and/or material to the melt?
- What was melted? What was the composition of the source region? What was the age of the source region? Did the source region include multiple components?
- How many pulses of magma were involved? Can multiple batches of magma be distinguished, and if so, are the emplacement ages resolvable?
- What was the time span for emplacement?

In order to address these questions, this study involves the following objectives:

- Characterise the Mpuluzi batholith in terms of its geochemical and isotopic composition (whole-rock Sr and Nd isotopes, Hf isotopes in zircon), the range of emplacement ages, and the composition of key phases. While the literature includes both compositional and age data for the Mpuluzi batholith, there has been no detailed characterisation linking the two. This study will enable an assessment of any changes in composition as a function of time.

- Assess the constraints on the age and composition of the source region. The granite-greenstone terrane includes several components which are possible candidates or analogues for the source region; the degree to which these match the isotopic constraints will be assessed.

- Assess the factors influencing the composition of the Mpuluzi batholith, including an estimate of the melting and crystallisation temperatures (from zircon saturation and the Ti content of zircon respectively). The combination of chemical and isotopic data obtained in this study will allow an assessment of the relative importance of source controls (e.g. multiple components), magma chamber processes (e.g. crystal fractionation), and post-crystallisation alteration.

1.3 Significance

The data obtained in this study constitute a significant addition to the pool of analyses of the Mpuluzi batholith. This is especially true for the zircon Hf isotopic data and the whole-rock Sr and Nd isotopic systems, for which few analyses are available in the literature.

The broader significance of this work is its contribution to understanding the processes involved in the stabilisation of continental crust in the Archaean, and thus the formation of the first continents. The extent to which the emplacement of large potassic batholiths during cratonisation influenced the ongoing stability of the region is an important part of this problem. The timing of the diversification of crustal magmas is another key point of dispute in relation to conditions on the early Earth, and this work provides evidence that this may have happened earlier than postulated by some authors (e.g. Laurent *et al.*, 2014).

In addition to crust formation, cratonic regions hold the key to the makeup of the Earth's early atmosphere, and the beginnings of life. They also host a variety of economically important mineral deposits, including gold, base metals, iron, nickel, and chrome (Anhaeusser, 2014), and a better understanding the processes that produced ancient crust can help target regions of potential economic interest. This is particularly important where the ancient crust is overlain by younger cover sequences, as better exploration targeting leads to significant increases in accuracy and therefore decreases in exploration costs.

1.4 Thesis structure

This thesis is divided into eight chapters. The first three chapters consist of introductory and background material, including an overview of the regional geology (Chapter Two) and a review of granite petrogenesis (Chapter Three).

Chapter Four outlines the analytical methodology used in this study, including both whole rock and *in situ* techniques.

Chapters Five, Six, and Seven present the results obtained in this study, and relevant discussion.

- Chapter Five outlines the petrography and mineral chemistry of the samples analysed, and discusses the effects of post-crystallisation alteration on the mineral assemblage, as well as the role of the mineral assemblage of the host rock in determining the composition of individual phases.
- Chapter Six presents the results of an extensive study of the geochemical and isotopic characteristics of over 600 individual zircon grains, and discusses the implications for emplacement timing and magma generation, as well as a general discussion of metamictisation.
- Chapter Seven presents the whole-rock geochemistry and isotopic compositions, and discusses the results in the context of published compositional data, constraints on the composition of the source region, and the factors involved in generating the geochemical variation within the Mpuluzi batholith.

Chapter Eight is a brief summary of the conclusions of this study.

Chapter Two – Regional Geology

2.1 Overview

This study focuses on the Mpuluzi batholith, a ~3.1 Ga intrusion that forms part of the Kaapvaal Craton in southern Africa (Figure 2.1; modified from Wilson, 1982). The Mpuluzi batholith straddles the border between South Africa and Swaziland, and outcrops over an area of ~5,000 km^2. It is bordered to the north by the 3.5–3.2 Ga Barberton Greenstone Belt (BGB), and to the south by the 3.7–3.3 Ga Ancient Gneiss Complex (AGC). The BGB and AGC represent some of the best-exposed and best- preserved remnants of early Archaean crust, and have been extensively studied for over five decades (e.g. Anhaeusser, 1971; Hunter *et al.*, 1978; Barton *et al.*, 1983; de Wit *et al.*, 1987; Tegtmeyer & Kröner, 1987; Compston & Kröner, 1988; Kröner & Todt, 1988; Kröner *et al.*, 1989; Armstrong *et al.*, 1990; de Ronde *et al.*, 1991; Kröner *et al.*, 1991; Kamo & Davis, 1994; Lowe, 1994; Kisters & Anhaeusser, 1995; Dziggel *et al.*, 2002; Diener *et al.*, 2005; Clemens *et al.*, 2006; Moyen *et al.*, 2006; Kisters *et al.*, 2010; Lana *et al.*, 2010b; Schoene & Bowring, 2010; Van Kranendonk, 2011; Hofmann *et al.*, 2013; Kröner *et al.*, 2013; Zeh *et al.*, 2013; Cutts *et al.*, 2014; Kröner *et al.*, 2014; Van Kranendonk *et al.*, 2014). The emplacement of the Mpluzi batholith at ~3.1 Ga coincides with the end of major tectonic activity, and represents the main stage of cratonisation in the region (e.g. Belcher & Kisters, 2006b; Schoene *et al.*, 2008; Anhaeusser, 2014).

2.2 Ancient Gneiss Complex

The oldest rocks of the region (as old as 3.66 Ga) lie in a package of tonalite-trondhjemite-granodiorite (TTG) gneisses in Swaziland, known as the Ancient Gneiss Complex (AGC; Compston & Kröner, 1988; Schoene *et al.*, 2009; Zeh *et al.*, 2011). The 3.66 Ga component reflects reworking of early-formed crust (zircon Hf model ages of 3.77–4.08 Ga; Zeh *et al.*, 2011), and subsequent magmatic events at 3.54, 3.45, and 3.32 Ga involved the addition of juvenile material. The AGC also records reworking at 3.23, 3.1, and 2.7 Ga without addition of significant amounts of juvenile material (Zeh *et al.*, 2011).

In northern Swaziland a remnant of the AGC (the Piggs Peak inlier) is preserved in tectonic contact with the Barberton Greenstone Belt along the Phophonyane shear zone; this section of tonalitic gneiss records the 3.66, 3.54, and 3.45 events, as well as younger zircon growth associated with the emplacement of the Piggs Peak batholith at 3.1 Ga (Compston & Kröner, 1988). This is the only section where the contact is exposed; elsewhere the two are separated by the 3.1 Ga Piggs Peak and Mpuluzi batholiths (see Figure 2.1).

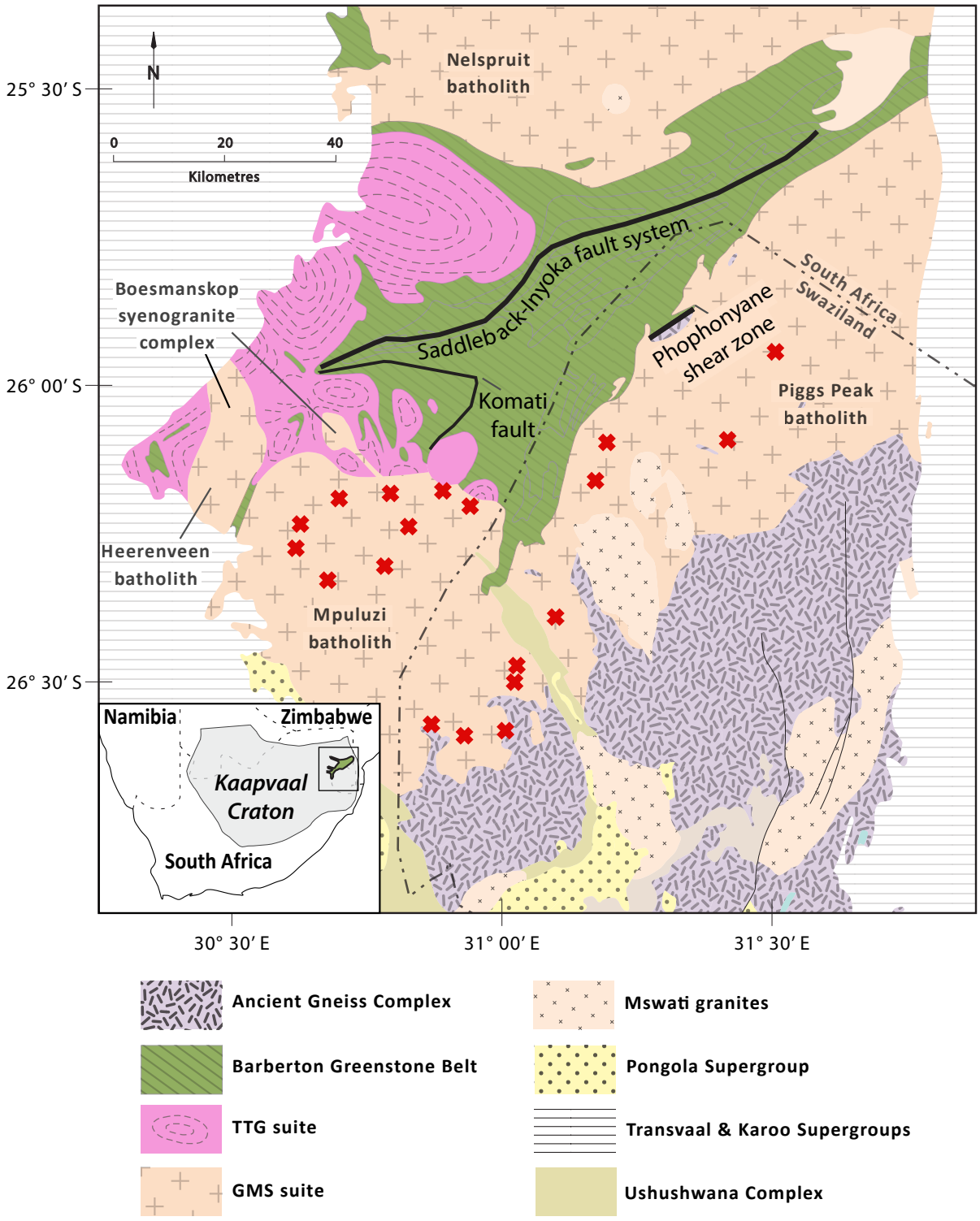


Figure 2.1. Simplified geological map of the eastern part of the Kaapvaal Craton, showing the Barberton Greenstone Belt, Ancient Gneiss Complex, and intrusions of the tonalite-trondhjemite-granodiorite (TTG) and granodiorite-monzogranite-syenite (GMS) suites. Modified from Wilson (1982); Belcher and Kisters (2006); Cutts *et al.* (2014). Sample localities for this study are marked with red crosses.

2.3 Barberton Greenstone Belt

The Barberton Greenstone Belt consists of a package of volcanic and sedimentary rocks ranging in age from ~3500 to ~3220 Ma. The greenstones have been subdivided into three terranes; the oldest component is the amphibolite-facies Stolzberg terrane (Kisters *et al.*, 2003), which is separated by the Komati fault from the younger greenstone-facies rocks of the southern Barberton terrane (Kröner *et al.*, 1996; Kisters *et al.*, 2010; Lana *et al.*, 2010a). The southern and northern Barberton terranes are in turn are separated by the Saddleback-Inyoka fault system (de Ronde & de Wit, 1994; Dziggel *et al.*, 2002; Zeh *et al.*, 2009).

The stratigraphy of the BGB is divided into three groups (Viljoen & Viljoen, 1969; SACS, 1980; see Figure 2.2), and progresses from dominantly volcanic rocks in the Onverwacht Group (3500–3300 Ma), through volcanic and sedimentary rocks of the Fig Tree Group (3260–3225 Ma), to the Moodies Group of dominantly sedimentary rocks (<3225 Ma; Viljoen & Viljoen, 1969; Kröner *et al.*, 1996).

The BGB records at least four phases of deformation; the two main phases occurred at ~3.45 and ~3.23 Ga, which correspond to the emplacement of the TTG suite (see Section 2.1.3 below; de Ronde & de Wit, 1994; de Ronde & Kamo, 2000; Dziggel *et al.*, 2002; Kisters *et al.*, 2003). The ~3.23 Ga event is responsible for the NE-SW trending structure of the main part of the greenstone belt, as well as the amphibolite-facies metamorphism in the lower part of the belt (see Figure 2.1; Belcher & Kisters, 2006).

2.4 Granitoid rocks

The BGB is surrounded by granitoid rocks ranging in age from ~3.5 to ~2.7 Ga. These can be divided into two main groups: the ~3.5–3.2 tonalite-trondhjemite-granodiorite (TTG) suite, and the ~3.1 Ga granodiorite-monzogranite-syenite (GMS) suite. A third, minor component is the ~2.8–2.7 Ga Mswati Granites.

2.4.1 TTG suite

The western edge of the BGB is intruded by 13 plutons, which make up the TTG suite (Robb & Anhaeusser, 1983; see Figure 2.1). The TTG suite can be subdivided according to emplacement age: most of the plutons were emplaced between ~3.5 and ~3.4 Ga, while the two largest, northernmost plutons were emplaced at ~3.2 Ga (Tegtmeyer & Kröner, 1987; Armstrong *et al.*, 1990; Kamo & Davis, 1994; Dziggel *et al.*, 2002). The older generation (e.g. the Stolzburg, Doornhoek, Steynsdorp, and Theespruit Plutons) generally displays more complex relationships with the greenstones than the younger plutons, and many contain large, deformed xenoliths of greenstone material (Robb & Anhaeusser, 1983; Yearron, 2003). The younger generation is made of the Kaap Valley tonalite (the largest pluton and the only

tonalite in the TTG suite), and the Nelshoogte trondhjemite (Kamo & Davis, 1994; de Ronde & Kamo, 2000). The margins of the TTG plutons are generally more strongly foliated than the cores; in some places the foliation appears to be concentric and this has been used to argue for diapiric emplacement (e.g. Hunter, 1974; Robb & Anhaeusser, 1983). However, in many of the plutons the foliation is heterogeneously distributed (e.g. Kisters & Anhaeusser, 1995).

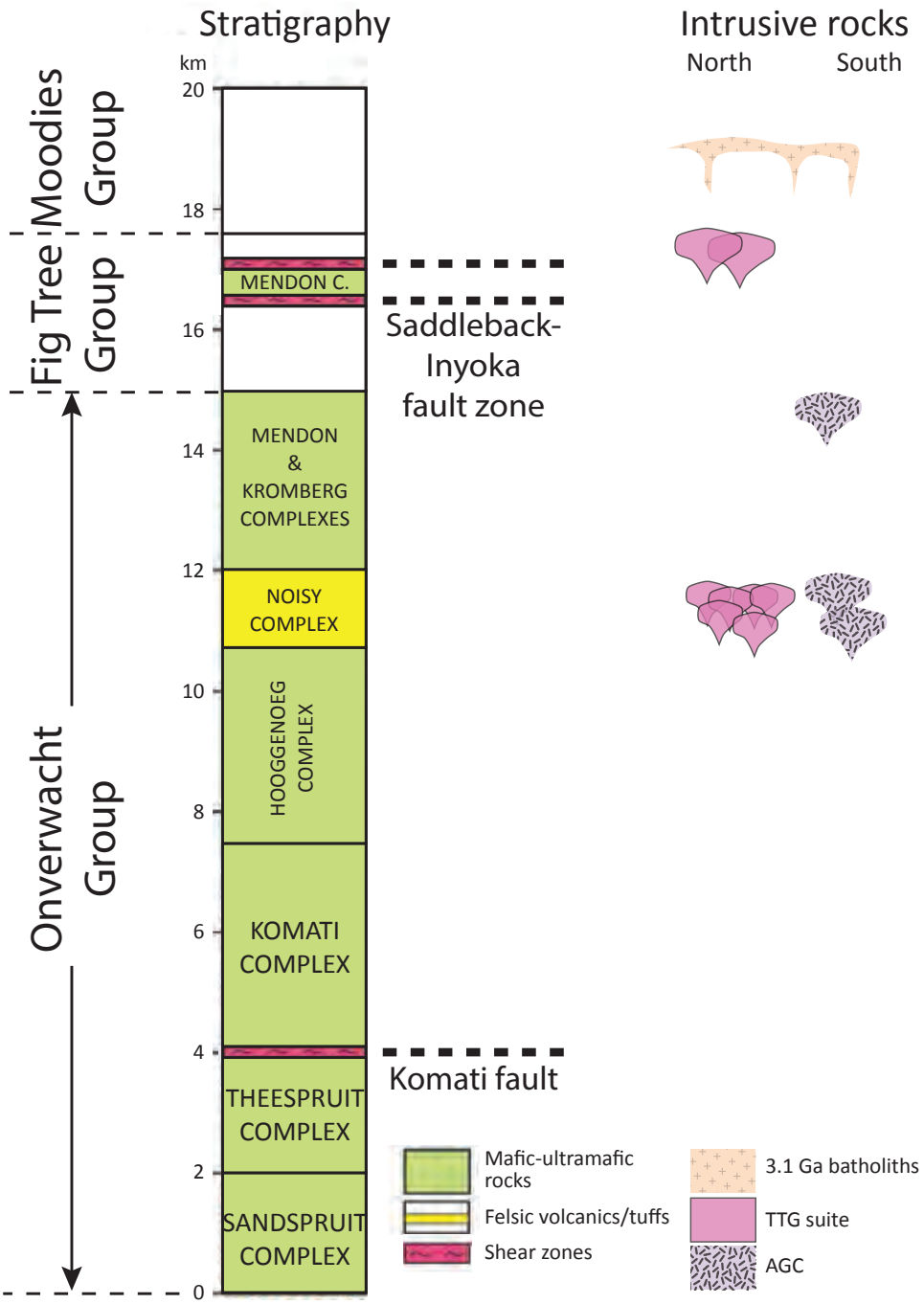


Figure 2.2. Simplified stratigraphy of the Barberton Greenstone Belt, showing the major divisions into the Onverwacht, Fig Tree, and Moodies Groups, the major discontinuities, and the relative ages of various intrusive units, divided into those north of the main greenstone belt and those to the south. Modified from Furnes *et al.* (2013).

2.4.2 GMS suite

The emplacement of the GMS suite marks a transition from sodic to potassic magmatism in the region. The GMS suite includes the large Mpuluzi, Piggs Peak, and Nelspruit batholiths, the smaller Heerenveen batholith, and the Boesmanskop syenogranite complex (Figure 2.1), all of which have been previously dated at ~3.11 Ga (Maphalala & Kröner, 1993; Kamo & Davis, 1994; Westraat *et al.*, 2005; Schoene & Bowring, 2007; Zeh *et al.*, 2009; this work). The batholiths occur as subhorizontal, tabular bodies, with estimated thicknesses of 700–1000 m (Hunter, 1973; Anhaeusser & Robb, 1983; Robb *et al.*, 1983; Westraat *et al.*, 2005; Belcher & Kisters, 2006). Textural characteristics and the low metamorphic grade of the greenstones suggest that the GMS suite was emplaced at shallow crustal levels (<5 km; Hunter, 1973; Anhaeusser & Robb, 1983; Robb *et al.*, 1983; Westraat *et al.*, 2005).

Early mapping in the Barberton region recognised what is now called the Nelspruit batholith to the north of the BGB, and to the south, the Lochiel granite (Hunter, 1974), which was later subdivided into the Mpuluzi, Heerenveen and Piggs Peak batholiths (Anhaeusser & Robb, 1983). The Heerenveen and Mpuluzi batholiths form a high plateau above the TTG suite, and are separated by the Schapenburg Greenstone Remnant. To the southwest they are overlain by Permian sedimentary rocks of the Karoo Supergroup; the Piggs Peak batholith intrudes the BGB to the north, and its eastern extent is also obscured by Karoo sediments (Figure 2.1). In Swaziland, the southeastern margins of the Mpuluzi and Piggs Peak batholith are eroded to expose the underlying Ancient Gneiss Complex; this is extensively cut by pegmatites and dykes related to the emplacement of the GMS suite batholiths (Hunter, 1974; Anhaeusser & Robb, 1983; Westraat *et al.*, 2005). This association of granite intruding basement gneisses is also seen in the Nelspruit batholith (Hunter, 1974), where a fragment of TTG gneiss in the granite has been dated at 3.3 Ga (Kamo & Davis, 1994). There is no exposure of the roof rocks of the batholiths (Westraat *et al.*, 2005; Clemens *et al.*, 2010). The Boesmanskop syenogranite complex is emplaced into the BGB and the surrounding TTGs to the north of the Mpuluzi batholith. The Mpuluzi batohlith largely outcrops as boulders, and attempting to define detailed field relationships was not pursued as part of this study (field photos are included in Appendix B).

2.4.3 Mswati Granites

After the formation of the GMS suite, the Mswati Granites were emplaced at ~2850–2700 Ma; these mainly occur in Swaziland, intruding rocks of the AGC, but also include the Mbabane, Nkalangeni, and Malandela plutons which intrude the Piggs Peak batholith, and the Mpageni pluton which intrudes the Nelspruit batholith (Wilson, 1982; Maphalala & Kröner, 1993; Kamo & Davis, 1994; Mukasa *et al.*, 2013). Meyer *et al.* (1994) divided the granites

into low- and high-Ca groups, and suggested that this distinction reflected a difference in source composition (low-Ca = sedimentary source, high-Ca = igneous source).

2.5 Tectonic models

Tectonic models for the formation of the eastern part of the Kaapvaal Craton can be broadly divided into two groups (Figure 2.3). (1) "Subduction-accretion" models, which involve the subduction of oceanic crust along the Saddleback-Inyoka fault system and the Phophonyane shear zone, thereby accreting first the northern and southern terranes of the Barberton Greenstone Belt together, and then the Ancient Gneiss Complex on the eastern margin (e.g. de Wit *et al.*, 1987; de Wit *et al.*, 1992; de Ronde & de Wit, 1994; Kamo & Davis, 1994; de Ronde & Kamo, 2000; Dziggel *et al.*, 2002; Kisters *et al.*, 2003; Diener *et al.*, 2005; Moyen *et al.*, 2006; Kisters *et al.*, 2010; Lana *et al.*, 2010a; Schoene & Bowring, 2010; Taylor *et al.*, 2012; Furnes *et al.*, 2013; Cutts *et al.*, 2014). (2) Models of "vertical tectonics", which posit a continental setting where sinking of dense greenstone material into the underlying felsic crust and corresponding diapiric ascent of the granitoids equalised a density imbalance in the crust (e.g. Hunter, 1974; Robb & Anhaeusser, 1983; Van Kranendonk *et al.*, 2009; Van Kranendonk, 2011; Van Kranendonk *et al.*, 2014). This is analogous to the dome-and-keel model for the formation of the granite-greenstone terrane in the Pilbara Craton in Western Australia (e.g. Collins *et al.*, 1998; Sandiford *et al.*, 2004).

Regardless of the tectonic processes operating before the emplacement of the 3.1 Ga granitoids, their formation marked the transition from active tectonics to a stable cratonic regime.

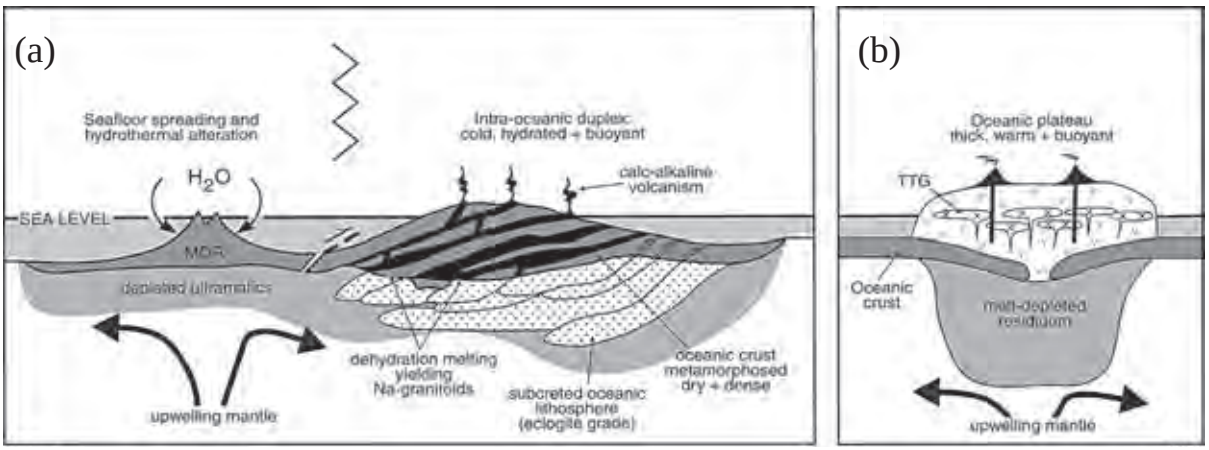


Figure 2.3. Tectonic models for the formation of the eastern Kaapvaal Craton: (a) subduction-accretion; (b) vertical tectonics. Figure 2 from Van Kranendonk *et al.* (2014).

Chapter Three – Granite Petrogenesis

3.1 Granite classification schemes

Since the earliest scientific studies of granites became a debate between the Neptunists (who believed granites were chemical precipitates from a primordial ocean) and the Plutonists (who saw granites as having solidified deep underground), these rocks have rarely ever been a matter of good agreement. In first half of the 20th century, the study of granites was dominated by the "granite controversy", where geologists were again divided into two camps: the Granitizers, who viewed granites as *in situ* products of a metasomatic process known as "granitization"; and the Magmatists, who saw them as products of igneous crystallisation. Their igneous origin was demonstrated by the seminal work of Tuttle and Bowen (1958), whose experiments showed that granitic magmas form by partial melting in equilibrium with quartz and feldspar.

Early classification schemes for granitic rocks focused on their emplacement level within the crust as the crucial factor (e.g. catazone, mesozone, epizone; Buddington, 1959; Cooma-, Murrumbidgee-, and Bathurst-types in eastern Australia; Vallance, 1969). While this type of classification is no longer widely used, emplacement depth is relevant when considering the likelihood of the association of granitic rocks with coeval volcanic rocks, as granites emplaced at high levels within the crust more commonly have erupted equivalents than those emplaced at depth (e.g. Kemp *et al.*, 2008).

More than 20 different classification schemes for granitoid rocks have been constructed (Barbarin, 1990; Frost *et al.*, 2001). These classification schemes can be divided into those that are purely descriptive, and those in which the categories defined carry some genetic implications.

Descriptive classifications may be based on mineralogy (e.g. the IUGS modal classification scheme; Streckeisen, 1967; 1974; 1976), or are more geochemical, relying on the molar proportions of major constituents (e.g. proportions of Na_2O+K_2O, FeO^t, and MgO in the AFM diagram of Kuno (1968); K_2O and SiO_2 in the division into low-K tholeiitic, medium- and high-K calc-alkaline, and shoshonitic series by Le Maitre *et al.* (1989); see Figure 3.1). More complex classification schemes combine multiple geochemical indices, for example Frost *et al.* (2001) developed a geochemical classification scheme for granitoid rocks using the aluminium saturation index (ASI = $Al_2O_3/CaO+Na_2O+K_2O$; Shand, 1950), a modified version of the alkali lime index (Peacock, 1931; MALI = $Na_2O+K_2O–CaO$), and the Fe number ($FeO^T/(FeO^T+MgO)$; Figure 3.2).

In genetic classification schemes, the implications may be related to the characteristics of the source region (e.g. the I- and S-type classification; Chappell & White, 1974; Chappell & White, 2001), the tectonic setting of magma generation (e.g. the system of Pearce *et al.*, 1984), or the processes involved (e.g. the division of A-type or 'ferroan' granites into different classes with compositions controlled by fractional crystallisation, partial melting, assimilation, or a combination of these factors; Frost & Frost, 2011).

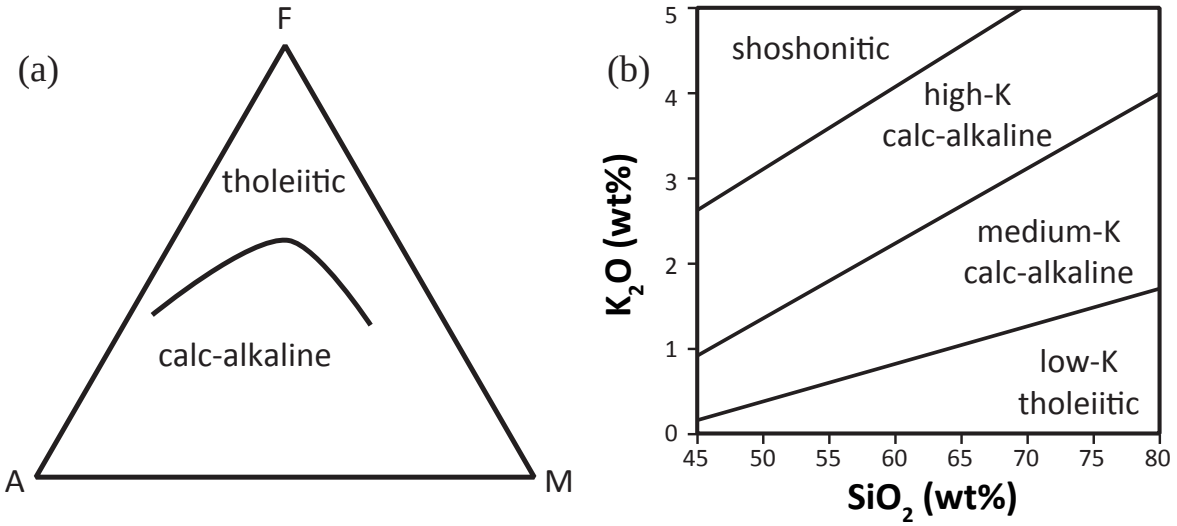


Figure 3.1. Descriptive classifications based on geochemical criteria: (a) the AFM diagram ($A = Na_2O+K_2O$, F = total Fe as FeO, M = MgO), separating the tholeiitic and calc-alkaline magma series (Kuno, 1968); (b) the low-K tholeiitic, medium- and high-K calc-alkaline, and shoshonitic series based on relative proportions of SiO_2 and K_2O (Le Maitre *et al.*, 1989).

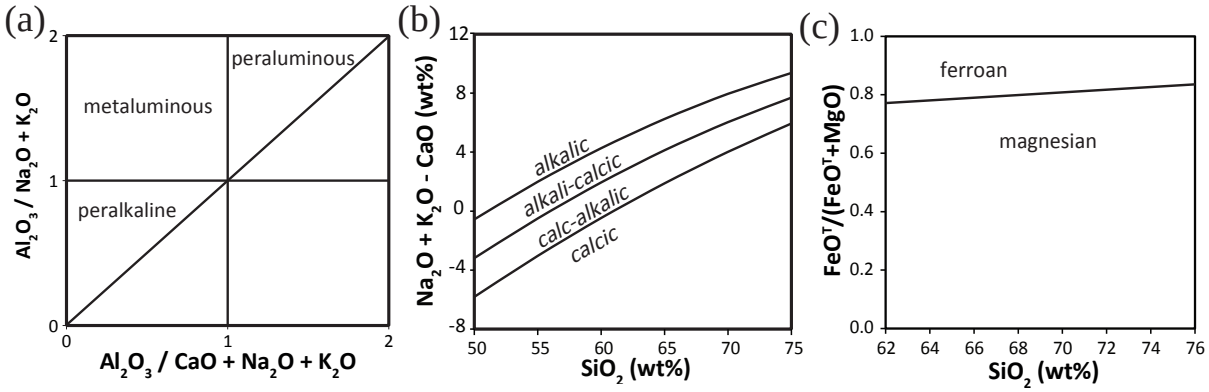


Figure 3.2. Geochemical indices used in the geochemical classification scheme of Frost *et al.* (2001): (a) Fe number ($FeO^T/(FeO^T+MgO)$); (b) Modified alkali lime index ($Na_2O+K_2O–CaO$); (c) Aluminium saturation index ($Al_2O_3/(CaO+Na_2O+K_2O)$).

3.1.1 IUGS modal classification

The IUGS classification system for igneous rocks (Streckeisen, 1967; 1974; 1976) is based on the modal abundances of quartz, alkali feldspar, plagioclase, and feldspathoid minerals in rocks with less than 90% mafic minerals (QAPF; see Figure 3.3). The reliance on the proportions of major phases makes the classification straightforward to apply, and has led to its widespread acceptance, ensuring consistency of nomenclature across the field. A geochemical equivalent of the QAPF classification was developed by Streckeisen and Le Maitre (1979) in order to extend the classification to volcanic rocks, where modal information is incomplete or cannot be obtained (as in the case of glassy rocks).

The purely descriptive nature of the scheme means that rocks with similar mineralogy are grouped together, even when formed through widely different processes. This is also a consequence of the simplicity of the scheme, as it takes into account neither the minor- and accessory-phase assemblage of the rocks, nor their trace-element and isotopic compositions.

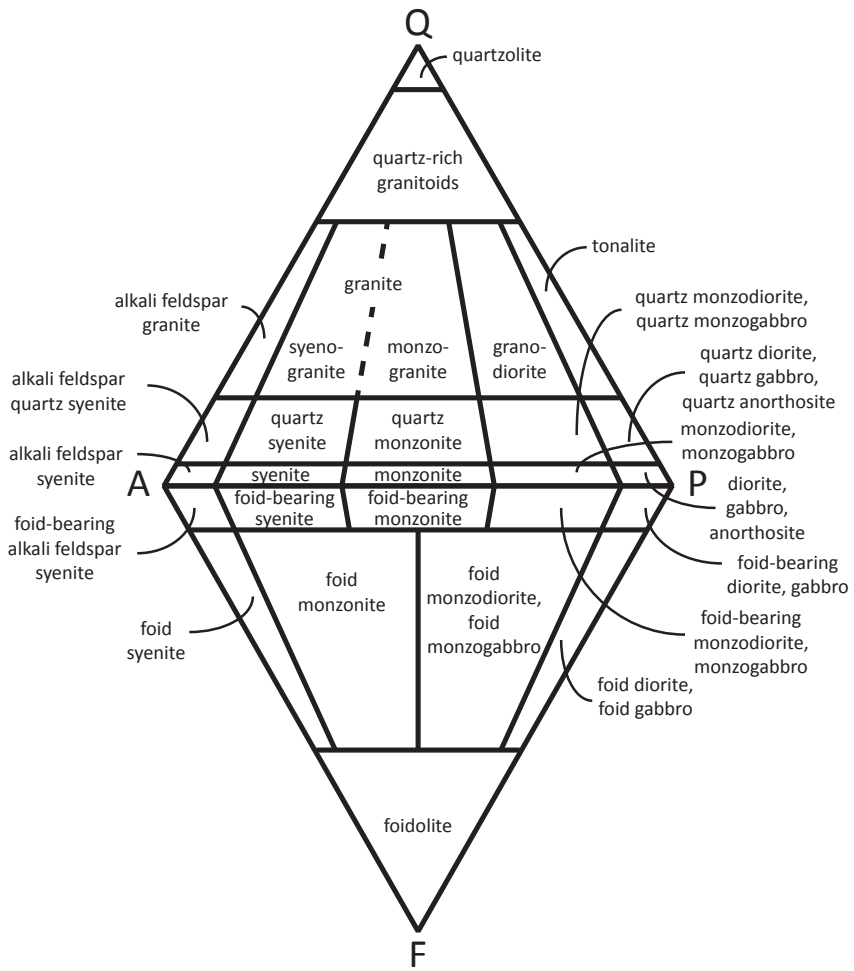


Figure 3.3. The IUGS modal classification diagram for igneous rocks with less than 90% mafic minerals, based on the modal proportions of quartz, alkali feldspar, plagioclase and feldspathoids (Streckeisen, 1967; 1974; 1976).

3.1.2 Source characteristics – I-S-A-M-type granites

The I- and S-type granite classification scheme pioneered by Chappell and White (1974), which divides granitoid suites into different types based on the characteristics of their source regions, is perhaps the most widely used of the classification systems with direct genetic implications. The original definition of the I- and S-types was based on a study of granitoids in the Lachlan Fold Belt (LFB) of eastern Australia, where Chappell and White (1974) identified two distinct groups, based mainly on mineralogical and major-element characteristics. They divided the granites into *I-type* – those derived from melting of older igneous material in the lower crust (*infra*crustal source), and *S-type* – those derived from melting of material that has experienced a weathering cycle (i.e. (meta-)sedimentary rocks; *supra*crustal source; Chappell & White, 1974; Chappell, 1984; Chappell & White, 2001).

This broad divide into two main groups in the LFB has been refined; in particular their isotopic characteristics have been defined in later studies (e.g. Sr and Nd isotopic characteristics: McCulloch & Chappell, 1982; whole-rock $\delta^{18}O$ characteristics: O'Neil & Chappell, 1977; zircon Hf and $\delta^{18}O$: Hawkesworth & Kemp, 2006; Kemp *et al.*, 2007). The I-type grouping has also been subdivided into high- and low-temperature members (Chappell *et al.*, 1998; Chappell *et al.*, 2004).

Additional types have also been added to the classification scheme in order to accommodate rocks with characteristics distinct from both the I- and S-type groups. The *M-type* designation (mantle source) was added by Pitcher (1979), denoting a minor but important group of granites formed from mantle-derived melts in island arc settings. A fourth group was added by Loiselle and Wones (1979), who suggested the use of the term *A-type* granites to denote the volumetrically minor yet distinct group of granitoids with **a**lkaline, **a**nhydrous, **a**luminous characteristics, commonly associated with rifting events (and therefore **a**norogenic). These two additional categories have been widely adopted, although they remain controversial, with some authors going so far as to suggest that they are both sub-groups of I-type granites (e.g. Whalen *et al.*, 1987). Other designations which have been proposed but not gained widespread acceptance include: *C-type*, for rocks with charnockitic affinities (Kilpatrick & Ellis, 1992); and *H-type*, for magmas inferred to be hybrids between mantle and crustal melts (Castro *et al.*, 1991). The main differences between the I-, S-, M-, and A-types are summarised in Table 3.1.

I- and S-type granites

Individual granite bodies had been recognised as the products of melting sedimentary or igneous rocks on a case by case basis before the definition of the I- and S-types (see summary in Carmichael *et al.*, 1974), however Chappell and White (1974) were the first to investigate

Table 3.1: Distinguishing characteristics of I-, S-, M-, and A-type granites (adapted from Winter, 2010).

	Source	SiO_2 (wt%)	K_2O/ Na_2O	Ca, Sr	ASI	$\delta^{18}O$	$^{87}Sr/^{86}Sr_i$	Mineralogy
I-type	Igneous	56–77	Low	High in mafic rocks	<1.1; metaluminous	Low; <10‰	Low; <0.706	Pyroxene, hornblende, magnetite; muscovite in felsic rocks
S-type	(Meta-) Sedimentary	64–77	High	Low	>1.1; peraluminous	High; >10‰	High; >0.708	Biotite, cordierite, garnet, aluminosilicates, ilmenite
M-type	Mantle	40–70	Low	High	<1.1; metaluminous	Low; <10‰	Low; <0.705	Pyroxene, hornblende, magnetite
A-type	Not source controlled	High; up to 77	Na_2O high	Low	Variable; often peralkaline	Variable	Variable	Aegirine, riebeckite, arfvedsonite

the two types together, and define the characteristics by which they could be clearly distinguished. In the Berridale Batholith of the LFB, they distinguished between the I- and S-type granites using primarily major-element characteristics. They found that the I-types are relatively high in Na_2O (>2.2 wt% in samples with ~2% K_2O; >3.2 wt% in samples with ~5% K_2O), whereas in S-types the Na content has been reduced through weathering of the source rocks (<2.2 wt% in samples with ~2% K_2O; <3.2 wt% in samples with ~5% K_2O); I-types are metaluminous to weakly peraluminous (ASI <1.1; ASI = $Al_2O_3/(Na_2O + K_2O + CaO)$) and usually have CIPW normative diopside (or <1% corundum) while S-types, being derived from peraluminous sedimentary material, are always peraluminous and can be strongly so, with >1% normative corundum and ASI >1.1; I-types display a large range in SiO_2 content (~56–77 wt%) whereas in S-types SiO_2 is high and relatively restricted (~64–77 wt%). Isotopically, the LFB I-type granites are characterised by low $^{87}Sr/^{86}Sr_i$ (0.704–0.706), while the enrichment of Rb relative to Sr in sedimentary rocks means the S-types generally have high $^{87}Sr/^{86}Sr_i$ (>0.708).

Extending the study of I- and S-type granites outside the LFB led to the revision of some of the compositional parameters, and the recognition of the S-type source in the LFB as chemically mature. The New England Orogen of eastern Australia was one of the first regions in which the classification scheme was applied, and its I- and S-type granites were found to be

less simple to distinguish, as the S-type source is relatively juvenile, and thus the weathering signature is much less distinct. The S-type suites in the New England Orogen have been found to have initial $^{87}Sr/^{86}Sr$ of 0.706, within the range of LFB I-type granites (Flood & Shaw, 1977), however they are still clearly distinguished based on oxygen isotope values ($\delta^{18}O$: I-types <10‰, S-types >10‰; O'Neil *et al.*, 1977).

Although the strict boundaries between I- and S-type granites delineated in the LFB are less distinct when applied to I- and S-type granites on a larger scale, the classification scheme is still able to broadly separate the two types of granites based on major-element and isotopic criteria. As with all classification schemes, the system becomes more difficult to apply in transitional cases, and there are examples where the source region has both sedimentary and older igneous material (e.g. the Uralla Plutonic Suite in the New England Batholith; Shaw & Flood, 1981).

M-type granites

The M-type designation of Pitcher (1979) comprises a minor but distinct group of granites generated in an island arc environment, through melting of subducted oceanic crust or the overlying mantle wedge. M-types typically have juvenile isotopic signatures, reflecting their derivation from mantle material (e.g. $^{87}Sr/^{86}Sr = 0.704$; Whalen, 1985).

A-type granites

Unlike the I-, S-, and M-type designations, A-type granites are not defined based on the characteristics of their source region. The original definition of A-type granites by Loiselle and Wones (1979) related to their tectonic setting – A-type granites are associated with periods of uplift and rifting, and are thus *anorogenic*, as opposed to the more common I- and S-type granites which are typically associated with orogenesis. A-type granites are commonly found in association with alkali basalts, and the original members of the A-type designation were thought to be extreme fractionates from such magmas (Loiselle & Wones, 1979).

A-type granites are distinguished based on their generally alkaline, anhydrous, aluminous nature. Other diagnostic characteristics include high Fe relative to Mg, and high Ga relative to Al. Whalen *et al.* (1987) developed discrimination diagrams for the separation of A-type granites from the I-, S-, and M-types, and found that identification was best achieved using combinations of diagnostic ratios (e.g. Fe/Mg, Ga/Al) and abundances of key trace elements (e.g. Zr, Ce, Y, Nb; the Zr *vs* Ga/Al discrimination diagram from Whalen *et al.* (1987) is included as Figure 3.4).

Several authors have posited possible source controls for A-type granites, in order to bring the designation into line with the other categories in the classification scheme. A-type granites have been suggested to be generated from: a residual source from which a granitic melt has already been extracted (Collins *et al.*, 1982; Whalen *et al.*, 1987); a diorite/tonalite/granodiorite source (Anderson, 1983; Creaser *et al.*, 1991); and undepleted granulites (e.g. Sheraton & Black, 1988). Bowden *et al.* (1984) took a different approach and suggested that if A-type granites were considered to be *anorogenic*, they should properly contrast with O-type (orogenic) granites, and form a higher-level division in the scheme; O-type granites could then be subdivided into I- and S-types.

The ambiguity associated with the A-type designation has led some authors to suggest it be abandoned altogether, and be replaced with the term "ferroan", as a geochemical classification with no implications as to the source of the magma (Creaser *et al.*, 1991; Frost & Frost, 2011). Frost and Frost (2011) studied these ferroan granites in detail, and divided them into groups based on their major-element characteristics. They classified the granites based on two key indices (the aluminium saturation index of Shand (1950), and a modified version of the alkali lime index of Peacock (1931)), and identified eight distinct naturally occurring types of ferroan granitoids, formed through combinations of fractional crystallisation, partial melting, and crustal assimilation. They concluded that both extreme fractional crystallisation from basaltic melts and partial melting of tonalitic to granodioritic crust are important end-member processes for the production of A-type granites, thus validating in part both the original concept and the source-control models, but ultimately highlighting the ambiguity inherent in the A-type designation, as it encompasses rocks formed through a variety of processes.

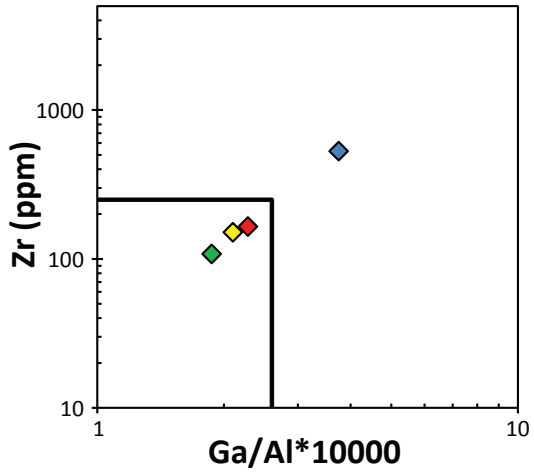


Figure 3.4. Zr *vs* Ga/Al discrimination diagram for separating A-type granites (blue) from S-type (red), I-type (yellow), and M-type granites (green), from Whalen *et al.* (1987).

3.1.3 Tectonic setting

Pearce *et al.* (1984) divided granites into groups based on their tectonic setting at the time of emplacement, and used their geochemical characteristics to produce discrimination diagrams for granites formed in the different tectonic environments. Granites were excluded from the dataset where their tectonic setting could not be verified by independent means, or where the tectonic mechanism was substantially disputed. The analyses were divided into four main groups: granites formed at mid-ocean ridges (ORG = ocean ridge granites); granites formed beneath volcanic arcs, either oceanic or continental (VAG = volcanic arc granites); granites formed in intracontinental or volcanic island settings (WPG = within plate granites); and granites formed during orogenesis, through continent-continent, continent-arc, or arc-arc collision (COLG = collision granites). The granites within each group were also divided into sub-groups based on minor differences in tectonic setting and/or petrology (Pearce *et al.*, 1984).

Pearce *et al.* (1984) found that diagrams involving the elements Rb, Y, Nb, Ta and Yb were most effective at discriminating between granites formed in different tectonic settings (e.g. Figure 3.5 shows the Nb *vs* Y and Rb *vs* Y+Nb discrimination diagrams from Pearce *et al.*, 1984). They note that although the boundaries were drawn arbitrarily to achieve the best separation of the different groups, there is a theoretical basis for the differences in composition according to the different petrogenetic histories of the groups (e.g. the derivation of ocean ridge and within plate granites from depleted and enriched mantle sources respectively).

The classification is simple to apply; however, discrimination is not complete for all groups on all diagrams, and a combination of several diagrams, as well as information from other sources, is necessary to confidently establish the tectonic setting in many cases. The classification scheme also cannot be applied if the geochemical characteristics of the samples have been substantially obscured by alteration, contamination, or loss of volatiles; cumulate rocks are also excluded. Pearce *et al.* (1984) also note that as the boundaries on the discrimination diagrams were drawn based on Phanerozoic rocks, the classification scheme cannot be extended to determine the tectonic setting of older rocks with any confidence. This caution is particularly applicable when considering Archaean granites, as the tectonic processes operating in the Archaean may have been substantially different to those in operation today; Archaean granites may also be affected by higher degrees of partial melting, a less fractionated mantle, and a greater relative importance of crustal melting (Pearce *et al.*, 1984).

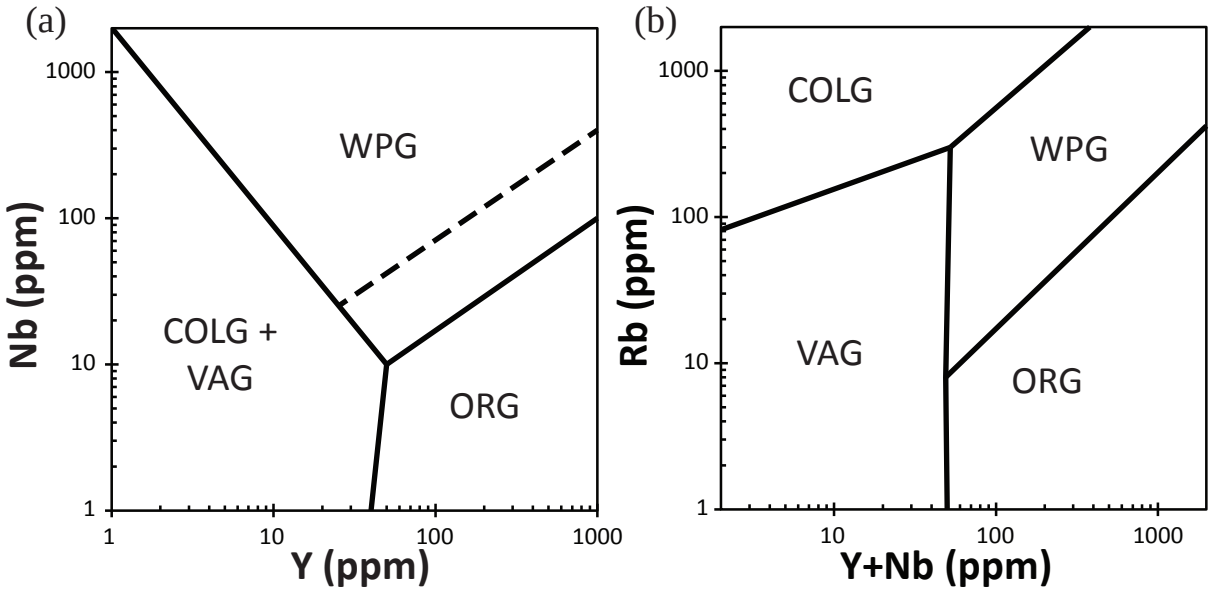


Figure 3.5. Discrimination diagrams for the tectonic setting of granites from Pearce *et al.* (1984): (a) Nb *vs* Y; (b) Rb *vs* Y+Nb. COLG = collisional granites, WPG = within plate granites, ORG = ocean ridge granites, VAG = volcanic arc granites. The dashed line in (a) represents the upper compositional boundary for ORG from anomalous ridge segments.

3.2 Causes of compositional variation within granite suites

An important component of the study of granites is the grouping of individual plutons into *suites*: groups of igneous rocks with common textural, mineralogical, and compositional characteristics (White *et al.*, 2001). A number of factors may influence the composition of a suite, including the characteristics of the source region and the processes operating during melt generation, transport, and emplacement. The exploration of the nature and extent of the variation may thus shed light on the formation of the suite itself.

Variation may be: inherited from the source region; related to the melt generation and transport processes (e.g. variation in the degree of partial melting and/or separation of solid material); caused by interaction of the magma with other material (e.g. mixing/mingling between different magmas; assimilation of country rock); a reflection of an evolving magma composition (fractional crystallisation in the magma chamber); or result from overprinting in a later event (e.g. hydrothermal alteration).

3.2.1 Source heterogeneity

The degree to which an igneous rock inherits the heterogeneity of its source region depends on the efficiency with which batches of melt from different parts of the source are homogenised once they have been extracted. This will be influenced by the degree and scale of heterogeneity of the source region (the greater the heterogeneity of the melt, the more difficult to homogenise), as well as physical factors which limit the physical and chemical

equilibration of the magma (e.g. high viscosity melts have limited ability to physically mix on large scales). Granitoid rocks are much more likely than mafic igneous rocks to inherit heterogeneity from their source regions, as their high SiO_2 contents and relatively low melting temperatures lead to high viscosities and thus inhibit mixing. Magma viscosity is also affected by volatile content, with volatile-poor magmas having higher viscosities than volatile-rich magmas, and thus less capacity for efficient mixing and a higher likelihood of retaining heterogeneity inherited from the source region.

In their original division of the granites of the LFB into I- and S-types, Chappell and White (1974) noted that the S-type granites generally showed more scatter in their compositions than their I-type counterparts, and suggested that this reflected a greater degree of heterogeneity in the source region of the S-type granites. This observation was based on the degree of dispersion seen on Harker diagrams for the two types of granites, as well as the variation in initial $^{87}Sr/^{86}Sr$ within a single pluton. A heterogeneous source for S-type suites has also been proposed to explain variation in zircon Hf-isotope data (Villaros *et al.*, 2012).

3.2.2 Partial melting

Magma produced by melting of continental crust is predominantly granitic in composition, as this corresponds to the 'minimum temperature melt' in a system containing quartz, plagioclase, and alkali feldspar. Tuttle and Bowen (1958) determined a thermal minimum in the eutectic, which favours the production of this melt; the temperature at which melting begins is influenced by both the pressure of the system and the availability of water. In most cases, the three phases are not present in the proportions required to produce a complete melt, and thus a partial melt is obtained, with melt production continuing until one phase is exhausted. After this point, melting will only continue at higher temperature, and the composition of this melt will shift away from the minimum-temperature melt. This exhaustion of a major phase strongly influences the major-element composition of the magma, but more subtle variations in composition may also be related to the degree of partial melting (percentage of melt produced), particularly in relation to elements that have a strong preference for either the melt phase (incompatible elements) or the residual phase (compatible elements). A small-percentage melt will be enriched in incompatible elements (e.g. Rb, REE) and depleted in those that are compatible (e.g. Sr, Ni), while this effect will be diluted as the proportion of melt increases.

Another model for a partial-melting control on variation within granitoid suites is that advocated by White and Chappell (1977). They proposed the *restite model* for granitoid genesis, where variation within a suite of granites with a common source is controlled by the proportion of solid material transported along with the melt as enclaves and, more importantly, as individual crystals. This solid material (restite) can represent either refractory

fragments of the source region, or solid products of the peritectic melt generation reactions (White & Chappell, 1977; Chappell *et al.*, 1987). White and Chappell (1977) argued that the linear inter-element variation trends observed in many suites could be explained by 'unmixing' entrained solid material from the melt to varying degrees. The trend line passes through the composition of the melt and restite end members, and mixtures of the two and the composition of the source region itself fall along the line; this model implies that the mafic members of a suite will have a large proportion of entrained material. The clearest evidence in favour of this model is the existence of strongly peraluminous S-type suites, which become more peraluminous as they become more mafic, a correlation that is not well explained by fractional crystallisation or mixing between mafic and felsic magmas. The variation in such suites has formed the basis for the peritectic assemblage entrainment (PAE) model of Clemens *et al.* (2011) and Clemens and Stevens (2012), where the variation is accounted for by differences in the degree of entrainment of peritectic material. The variation within S-type suites in particular has been ascribed to entrainment of peritectic garnet (e.g. Stevens *et al.*, 2007; Dorais & Spencer, 2014).

3.2.3 Assimilation

The emplacement of magma into relatively cool surrounding rock must necessarily be followed by a loss of heat from the magma to its surroundings, in order to reach thermal equilibrium. This heat transfer is achieved through conduction into the surrounding rock (commonly producing contact metamorphism), and incorporation of cool solid material into the magma. This means the assimilated material is likely to be concentrated in the margins of the intrusion, and to have little impact on the interior, thus producing minor local variations but not significantly influencing the composition of the magma on a larger scale. Assimilation is also a self-limiting process, as the magma close to the contact cools and crystallises, making it difficult to incorporate more material. For assimilation to be considered a major factor influencing the composition of a suite, the variation in both the chemical and isotopic compositions must be accounted for (e.g. the proportion of assimilated material needed to produce the variation in major-element composition must match that calculated from the isotopic variation).

3.2.4 Magma mixing/mingling

Mixing or mingling between two compositionally different magmas is frequently cited as the cause of variation in granitic suites, particularly in studies including isotopic data (e.g. whole-rock Sr and Nd isotopes: Gray, 1984; Kistler *et al.*, 1986; Keay *et al.*, 1997; Maas *et al.*, 1997; zircon Hf isotopes: Griffin *et al.*, 2002; Yang *et al.*, 2007). Mixing refers to complete homogenisation between two components, such that a hybrid magma is produced,

while in mingling some of the characteristics of both original components are retained. Field evidence for magma mingling includes the mafic enclaves common to many granitic rocks, argued to represent quenched globules of mafic magma (e.g. Vernon, 1984; Vernon *et al.*, 1988), however these are generally a volumetrically minor component of the pluton, and may be ascribed to localised dyking, rather than indicating magma mixing on a large scale (e.g. Wiebe, 1994).

Strong linear inter-element variations are frequently cited as evidence for magma mixing, but this type of variation between two end-member compositions can also be explained by assimilation, restite unmixing, or the formation of cumulates. As with models of assimilation-controlled variation, magma-mixing models must be able not only to account for variations in major-element compositions, but also to produce consistent end-member proportions when calculated from isotopic compositions. Based mainly on field evidence for magma mixing and mingling, Castro *et al.* (1991) suggested that many I-type granites are the product of mixing between mantle-derived magma and crustal melts (H-type: hybrid crust-mantle source), but stressed the necessity of field evidence supporting mixing to remove the ambiguity of the linear inter-element variation trends.

3.2.5 Fractional crystallisation

Crystals form in chemical equilibrium with the melt from which they precipitate. The composition of the mineral forming is not the same as that of the melt, so the melt composition evolves in response to the removal of the constituents of the mineral precipitating (note that the bulk composition of the magma (melt plus crystals) remains unchanged). This can lead to chemical zonation within crystals, reflecting continuous growth in equilibrium with an evolving melt composition. If the crystals are physically separated from the melt (e.g. by sinking to the bottom of the magma chamber), their removal alters the bulk composition of the magma, which in turn influences the composition of the next generation of crystals. The bulk composition of these crystal cumulates is not equal to the melt composition at any stage, but rather represents the solid component of the magma at a particular point in its evolution. Thus cumulate rocks are strong evidence that fractional crystallisation played a major role in producing the range of compositions observed, but cannot be considered to define the primitive melt composition.

Field evidence for compositional variation controlled by fractional crystallisation includes concentrically zoned plutons, where crystals accumulate on the edges of the magma chamber, and the melt migrates inwards as crystallisation progresses. This inward migration of the solidification front produces relatively mafic marginal rocks and progressively more felsic rocks towards the centre of the pluton (e.g. the Boggy Plain pluton in the LFB, which varies from marginal diorite to a monzogranitic core; Wyborn *et al.*, 1987; 2001). In some cases,

concentric zoning has been interpreted to reflect incremental assembly of the pluton, with injection (and in some cases subsequent fractional crystallisation) of different batches of magma, rather than a single fractionating magma chamber. This interpretation may be indicated by geochronological data (e.g. the Tuolumne Intrusive Suite of the Sierra Nevada was emplaced over a period of ~10 m.y.; Coleman *et al.*, 2004), or isotopic evidence for two or more distinct batches of magma (e.g. the Walcha Road pluton in the New England Orogen; Shaw & Flood, 2009).

The changes in bulk composition associated with fractional crystallisation are reflected as inflection points on inter-element variation diagrams, showing the onset of crystallisation of a particular phase. This is particularly striking for elements that are predominantly hosted in a single phase, where the concentration increases until the melt becomes saturated in the phase, at which point crystallisation commences and the concentration rapidly drops. The Boggy Plain pluton displays the characteristic inflection points on Harker diagrams reflecting a change in the mineral assembly (e.g. Figure 3.6 displays an inflection point in a plot of Ba *vs* SiO_2 from the Boggy Plain pluton in the LFB, reflecting the onset of crystallisation of biotite when the magma reached ~66% SiO_2; Wyborn *et al.*, 1987; 2001).

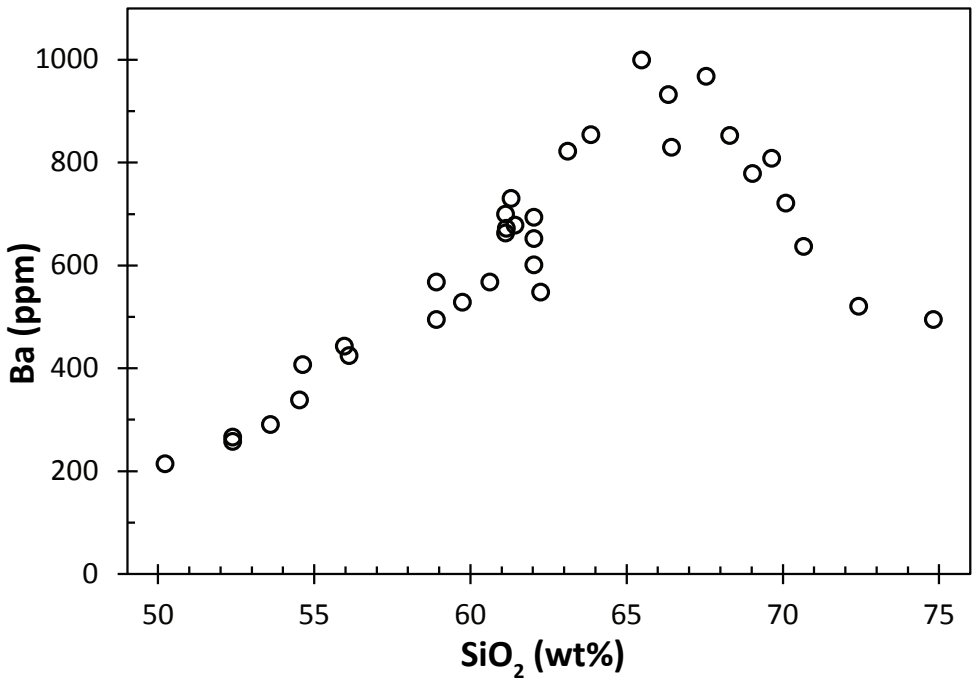


Figure 3.6. Plot of Ba *vs* SiO_2 for the Boggy Plain pluton in the Lachlan Fold Belt, showing an inflection point at ~66% SiO_2 reflecting the onset of crystallisation of biotite (Wyborn *et al.*, 1987; 2001).

3.2.6 Alteration

Many plutonic rocks experience deuteric alteration during the final stages of crystallisation, where late fluids react with earlier-formed minerals and produce low-temperature hydrothermal products (e.g. chloritization of biotite, seritization of feldspars). Such low-temperature re-equilibration may produce spurious estimates of temperature and pressure if the minerals involved in the calculations no longer reflect the conditions at the time of crystallisation. While this process alters the mineralogy and mineral chemistry of the rock, it generally has little to no impact on the bulk composition, as it occurs at scales much smaller than that at which the rock is sampled (Chappell, 1996).

Chapter Four - Analytical Methods

All analyses were carried out at the Geochemical Analysis Unit (GAU), ARC Centre of Excellence for Core to Crust Fluid Systems (CCFS) and GEMOC, Macquarie University, Sydney.

4.1 Whole-rock analyses

Samples were trimmed of weathered edges and crushed using a hydraulic press to a particle size of <1 cm. Samples were then powdered using a TEMA tungsten carbide ring mill to obtain a grainsize of <50 μm. Care was taken to thoroughly clean the mill with Milli-Q water and ethanol between samples to avoid cross-contamination.

4.1.1 XRF major-element analyses

Glass discs for major-element analysis were prepared by heating a platinum crucible with a mixture of 1 g sample and 10 g pre-ignited 12:22 lithium metaborate/tetraborate flux in a rocking furnace at 1050 °C for 20 minutes. An NH_4I release tablet was then added to increase surface tension and aid pouring, and discs were cast in a platinum mold. Discs were analysed using a PANalytical Axios 1 kW wavelength dispersive XRF spectrometer; operating conditions and average lower limits of detection are given in Table 4.1. Loss on ignition was also determined for each sample at 1050 °C for 1.5 hours. Results of repeat analyses of reference materials and preferred values are presented in Table 4.2.

Table 4.1: Operating conditions and lower limits of detection for determination of major-element concentrations by XRF.

Element	Counting time (s)	Accelerating voltage (KV)	Current (mA)	LLD (ppm)
Si	30	25	40	-
Ti	10	40	25	33
Al	30	25	40	34
Fe	8	55	18	18
Mn	10	55	18	12
Mg	40	25	40	37
Ca	10	30	33	30
Na	40	20	50	61
K	10	25	40	23
P	20	25	40	17

Table 4.2: Results of repeated major-element analysis of standards AGV-2, BCR-2, BHVO-2 and GSP-2 by XRF during this study, and comparison to preferred values from the GeoReM database (Jochum et al., 2005). All values in wt%.

	AGV-2				BCR-2				BHVO-2				GSP-2			
	This study		Reference values		This study		Reference values		This study		Reference values		This study		Reference values	
	Average	1σ	Average	1σ	Average	1σ	Average	1σ	Average	1σ	Average	1σ	Average	1σ	Average	1σ
	n=7				n=7				n=10				n=7			
SiO_2	59.31	0.09	59.30	0.70	54.07	0.12	54.10	0.80	50.17	0.07	49.90	0.60	66.46	0.19	66.60	0.80
TiO_2	1.06	0.01	1.05	0.22	2.27	0.01	2.26	0.05	2.79	0.01	2.73	0.04	0.68	0.01	0.66	0.02
Al_2O_3	17.04	0.03	16.91	0.21	13.58	0.03	13.50	0.20	13.93	0.03	13.50	0.20	14.99	0.04	14.90	0.20
$Fe_2O_3^t$	6.52	0.01	6.69	0.13	13.63	0.03	13.80	0.20	12.38	0.02	12.30	0.20	4.76	0.01	4.90	0.16
MnO	0.10	0.00	0.10	0.00	0.20	0.00	0.20	0.01	0.17	0.00	0.17	0.01	0.04	0.00	0.04	
MgO	1.80	0.00	1.79	0.03	3.61	0.01	3.59	0.05	7.41	0.02	7.23	0.12	0.98	0.00	0.96	0.03
CaO	5.17	0.01	5.20	0.13	7.11	0.01	7.12	0.11	11.58	0.02	11.40	0.20	2.07	0.01	2.10	0.06
Na_2O	4.32	0.01	4.19	0.13	3.27	0.02	3.16	0.11	2.31	0.01	2.22	0.08	2.83	0.01	2.78	0.09
K_2O	2.92	0.01	2.88	0.11	1.81	0.01	1.79	0.05	0.53	0.00	0.52	0.01	5.48	0.02	5.38	0.14
P_2O_5	0.48	0.01	0.48	0.02	0.36	0.00	0.35	0.02	0.27	0.00	0.27	0.02	0.29	0.00	0.29	0.02
Total	98.72		98.59		99.93		99.87		101.55		100.24		98.58		98.61	

4.1.2 Trace-element analyses

Whole-rock trace-element analyses were obtained at the GAU by two different techniques: solution analysis with an inductively coupled plasma mass spectrometer (ICPMS), and laser ablation ICPMS (LA-ICPMS) analysis of fused glass discs. The ablation analyses were performed in an attempt to circumvent the potential issue of incomplete dissolution of refractory phases (e.g. zircon) during preparation of samples for solution analysis. Complete dissolution of zircon is commonly achieved through high pressure digestion in teflon bombs, however this approach has been shown to result in considerable loss of volatile elements in granitic rocks (e.g. up to 20% loss of Sr, Th, light REE; up to 40% loss of Rb, Pb; Fitzpatrick & Bullen, 1999). Results for reference materials obtained using the two techniques are presented below, followed by a discussion of the relative merits of each technique and a justification of the selection criteria used to compile the final results.

Solution ICPMS trace-element analyses

Whole-rock digestions for solution ICPMS analysis were prepared using the following method: 0.1 g of sample powder was weighed into clean 15 mL Savillex Teflon beakers and the mass recorded to four decimal places. Samples were digested using a 1:1 mixture of concentrated HF (Merck, suprapur grade) and concentrated HNO_3 (Merck, AnalaR grade) at 120 °C for 24 hours, then dried down and repeated. Samples were then digested in 6 N HNO_3 for 24 hours, dried down, and diluted to 10 mL in 2% HNO_3 with trace HF. 1:1000 dilutions of each sample were then individually spiked with a 15 µL aliquot of a solution of ^{6}Li, As, Rh, In, Tm and Bi in 2% HNO_3, to correct for instrumental drift. Solutions were analysed using an Agilent 7500cs quadrupole ICPMS. BCR-2 was used as a calibration standard to correct for instrument sensitivity and drift, and background was measured on a 2% HNO_3 solution. Measured and reference values for standards BHVO-2, BIR-1 and GSP-SS are presented in Table 4.3 (sample GSP-SS was collected from the same locality as GSP-1, and reference values for both GSP-1 and GSP-2 are provided for comparison).

LA-ICPMS trace-element analyses

Trace-element compositions were also obtained by LA-ICPMS analysis of fused glass discs, as this allows accurate determination of low-concentration elements which typically reside in minerals resistant to classical acid-digestion methods (e.g. Zr, Hf from zircon). Glass discs were prepared by fusing a 0.5:1.5 g mixture of sample powder and 100% lithium metaborate flux in a platinum crucible at 1000 °C for 20 minutes, adding an NH_4I tablet as a releasing agent and quench pressing using a carbon die. Discs were glued together and set in resin, and the block of samples was then cut in half and polished to expose a cross section of each disc. Samples were analysed using an Agilent 7700cx quadrupole ICPMS attached to a Photon Machines Excite 193 nm excimer laser ablation system fitted with a HeLeX two-volume

Table 4.3: Results of repeated trace-element analysis of standards BHVO-2, BIR-1 and GSP-SS by solution ICPMS during this study, and comparison to values from the GeoReM database (Jochum et al., 2005). For USGS standards BHVO-2 and BIR-1, the preferred values are used. GSP-SS was collected from the same locality as USGS standard GSP-1, and the reported values for both GSP-1 and GSP-2 are provided for comparison (GSP-1 has no reported uncertainties). All values in ppm.

	BHVO-2					BIR-1					GSP-SS						
	This study		Preferred values		Deviation	This study		Preferred values		Deviation	This study		GSP-1	Deviation	GSP-2		Deviation
	Average	1σ	Value	1σ	%	Average	1σ	Value	1σ	%	Average	1σ	Value	%	Value	1σ	%
	n=6					n=6					n=3						
^{7}Li	4.60	0.20	4.8	0.2	-4.1	3.28	0.13	3.2	0.2	2.6	24.02	0.13	31	-23	36	1	-33
^{9}Be	1.38	0.15	1	0.1	38	0.116	0.010	0.12	0.01	0	1.302	0.017	1.4	-7.0	1.5	0.2	-13
^{45}Sc	33.61	0.56	32	1	5.0	44.9	1.2	43	2	4.4	5.99	0.10	6.2	-3.4	6.3	0.7	-4.9
^{47}Ti	17180	260	16300	2000	5.4	5990	43	5600	500	7.0	4085	77	3896	4.8	3956	120	3.3
^{51}V	312.2	3.1	317	11	-1.5	314.4	8.4	319	18	-1.4	50.27	0.91	53	-5.2	52	4	-3.3
^{53}Cr	246	18	280	19	-12	294	34	391	15	-25	10.29	0.17	13	-21	20	6	-49
^{55}Mn	1344	31	1317	39	2.1	1376	16	1363	62	0.94	291.8	4.0	310	-5.8	320	20	-8.8
^{60}Ni	129.2	4.1	119	7	8.6	184.5	4.0	166	7	11	8.06	0.19	8.8	-8.4	17	2	-53
^{65}Cu	138.8	2.4	127	7	9.3	125.6	1.7	119	8	5.5	39.97	0.81	33	21	43	4	-7.0
^{66}Zn	105.5	1.3	103	6	2.4	68.7	2.1	72	18	-4.6	102.25	0.42	104	-1.7	120	10	-15
^{71}Ga	20.98	0.26	22	2	-4.6	15.27	0.12	15.3	0.8	-0.20	24.14	0.64	23	4.9	22	2	9.7
^{85}Rb	9.56	0.14	9.11	0.04	5.0	0.224	0.023	0.2	0.01	12	202.5	1.7	254	-20	245	7	-17
^{88}Sr	389.8	6.8	396	1	-1.6	107.1	1.1	109	2	-1.7	216.7	4.7	234	-7.4	240	10	-9.7
^{89}Y	28.26	0.29	26	2	8.7	17.12	0.19	15.6	0.9	9.8	25.89	0.19	26	-0.44	28	2	-7.5
^{91}Zr	180.7	3.7	172	11	5.1	15.48	0.19	14	0.1	11	115.6	4.2	530	-78	550	30	-79
^{93}Nb	18.98	0.26	18.1	1	4.8	0.5528	0.0084	0.55	0.05	0.51	27.42	0.42	27.9	-1.7	27	2	1.6
^{95}Mo	3.71	0.32	4	0.2	-7.3	0.1143	0.0067	0.07		63	0.690	0.014	0.8	-14	2.1	0.6	-67
^{114}Cd	0.092	0.014	0.06	0.006	53	0.094	0.043	0.097		3.1	0.089	0.035	0.058	53			
^{133}Cs	0.105	0.003	0.1	0.01	5.0	0.00608	0.00057	0.007	0.003	-13	1.180	0.018	1.02	16	1.2	0.1	-1.6
^{137}Ba	130.3	3.0	131	1	-0.54	6.65	0.24	7.14		-6.8	1235	22	1310	-5.7	1340	44	-7.8

Table 4.3: Continued.

	BHVO-2					BIR-1					GSP-SS						
	This study		Preferred values		Deviation	This study		Preferred values		Deviation	This study		GSP-1	Deviation	GSP-2		Deviation
	Average	1σ	Value	1σ	%	Average	1σ	Value	1σ	%	Average	1σ	Value	%	Value	1σ	%
	n=6					n=6					n=3						
^{139}La	15.32	0.36	15.2	0.1	0.79	0.696	0.071	0.615	0.021	13	165.0	5.3	184	-10	180	12	-8.4
^{140}Ce	36.75	0.56	37.5	0.2	-2.0	2.04	0.11	1.92	0.08	6.4	405.9	6.6	399	1.7	410	30	-1.0
^{141}Pr	5.32	0.12	5.35	0.17	-0.51	0.404	0.014	0.37	0.02	9.3	51.3	1.2	52	-1.4	51	5	0.57
^{146}Nd	24.11	0.61	24.5	0.1	-1.6	2.404	0.067	2.38	0.01	1.0	188.6	4.1	196	-3.8	200	12	-5.7
^{147}Sm	6.09	0.16	6.07	0.01	0.34	1.116	0.030	1.12	0.02	-0.32	24.97	0.73	26.3	-5.1	27	1	-7.5
^{153}Eu	1.987	0.070	2.07	0.02	-4.0	0.502	0.019	0.53		-5.2	2.335	0.070	2.33	0.22	2.3	0.1	1.5
^{160}Gd	6.22	0.19	6.24	0.03	-0.30	1.910	0.055	1.87	0.04	2.1	13.13	0.38	12.1	8.5	12	2	9.4
^{159}Tb	0.946	0.024	0.92	0.03	2.8	0.358	0.012	0.36	0.03	-0.59	1.567	0.052	1.34	17			
^{163}Dy	5.17	0.15	5.31	0.02	-2.6	2.532	0.067	2.51		0.87	5.36	0.15	5.5	-2.5	6.1		-12
^{165}Ho	0.982	0.031	0.98	0.04	0.19	0.580	0.019	0.56	0.05	3.5	0.886	0.027	1.01	-12	1	0.1	-11
^{167}Er	2.500	0.085	2.54	0.01	-1.6	1.704	0.049	1.66		2.6	2.043	0.055	2.7	-24	2.2		-7.2
^{173}Yb	1.933	0.077	2	0.01	-3.3	1.609	0.056	1.65		-2.5	1.297	0.042	1.7	-24	1.6	0.2	-19
^{175}Lu	0.2669	0.0072	0.274	0.005	-2.6	0.243	0.010	0.25	0.02	-2.6	0.166	0.005	0.214	-23	0.23	0.03	-28
^{178}Hf	4.25	0.15	4.36	0.14	-2.6	0.571	0.019	0.582	0.004	-1.9	2.809	0.087	15.5	-82	14	1	-80
^{208}Pb	1.83	0.31	1.6	0.3	14	2.94	0.13	3.1	0.3	-5.2	43.2	2.3	55	-21	42	3	2.8
^{232}Th	1.221	0.094	1.22	0.06	0.10	0.0395	0.0034	0.032	0.004	23	104.3	5.8	106	-1.6	105	8	-0.66
^{238}U	0.403	0.033	0.403	0.001	-0.086	0.0107	0.0015	0.01	0.001	6.7	2.02	0.12	2.54	-20	2.4	0.19	-16

Table 4.4: Results of repeated trace-element analysis of standards AGV-2, BHVO-2, BCR-2 and GSP-SS by LA-ICPMS during this study, and comparison to values from the GeoReM database (Jochum et al., 2005). For USGS standards AGV-2, BHVO-2 and BCR-2, the preferred values are used. GSP-SS was collected from the same locality as USGS standard GSP-1, and the reported values for both GSP-1 and GSP-2 are provided for comparison (GSP-1 has no reported uncertainties). All values in ppm.

	AGV-2					BHVO-2				
	This study		Preferred values		Deviation	This study		Preferred values		Deviation
	Average	1σ	Value	1σ	%	Average	1σ	Value	1σ	%
	n=13					n=13				
^{9}Be	3.06	0.18	2.3	0.4	33	1.74	0.32	1.0	0.1	74
^{29}Si	Internal standard		277189	3272		Internal standard		233250	2805	
^{45}Sc	16.7	2.6	13	1	28	35.5	3.0	32	1	11
^{51}V	118.5	1.9	122	4	-2.9	320.8	8.1	317	11	1.2
^{53}Cr	75.9	2.4	16	1	370	301	13	280	19	7.5
^{60}Ni	51	12	20	1	160	137.9	3.7	119	7	16
^{65}Cu	50.2	1.6	53	4	-5.3	120.2	8.7	127	7	-5.4
^{66}Zn	94.1	4.9	86	8	9.4	106.6	5.9	103	6	3.5
^{71}Ga	21.13	0.85	20	1	5.7	21.75	0.22	22	2	-1.1
^{85}Rb	65.8	1.6	66.3	0.5	-0.75	9.04	0.30	9.11	0.04	-0.77
^{88}Sr	662	24	661	6	0.15	405	13	396	1	2.3
^{89}Y	18.8	1.3	19	2	-1.1	25.0	1.8	26	2	-3.8
^{90}Zr	238	14	230	4	3.5	174	11	172	11	1.2
^{93}Nb	13.56	0.62	14.5	0.8	-6.5	17.50	0.81	18.1	1	-3.3
^{133}Cs	0.984	0.062	1.2	0.1	-18	0.091	0.013	0.10	0.01	-9.0
^{138}Ba	1111	15	1130	11	-1.7	129.8	2.5	131	1	-0.92
^{139}La	42.0	2.2	37.90	0.04	11	17.11	0.87	15.2	0.1	13
^{140}Ce	69.4	1.5	68.6	0.5	1.2	37.9	1.0	37.5	0.2	1.1
^{141}Pr	7.95	0.34	7.84	0.31	1.4	5.28	0.25	5.35	0.17	-1.3
^{146}Nd	32.3	1.9	30.5	0.1	5.9	26.0	1.7	24.5	0.1	6.1
^{147}Sm	6.06	0.38	5.49	0.03	10	6.51	0.61	6.07	0.01	7.2
^{153}Eu	1.67	0.13	1.53	0.02	9.2	2.22	0.13	2.07	0.02	7.2
^{157}Gd	4.49	0.36	4.52	0.05	-0.66	6.11	0.57	6.24	0.03	-2.1
^{159}Tb	0.649	0.061	0.64	0.01	1.4	0.956	0.076	0.92	0.03	3.9
^{161}Dy	3.51	0.35	3.47	0.03	1.2	5.26	0.50	5.31	0.02	-0.94
^{165}Ho	0.681	0.081	0.65	0.03	4.8	1.008	0.067	0.98	0.04	2.9
^{167}Er	1.76	0.25	1.81	0.02	-2.8	2.54	0.17	2.54	0.01	0
^{169}Tm	0.265	0.028	0.26	0.01	1.9	0.328	0.029	0.33	0.01	-0.61
^{173}Yb	1.72	0.26	1.62	0.02	6.2	2.11	0.20	2.00	0.01	5.5
^{175}Lu	0.248	0.031	0.247	0.004	0.40	0.276	0.039	0.274	0.005	0.73
^{178}Hf	5.25	0.40	5.0	0.1	5.0	4.51	0.32	4.36	0.14	3.4
^{208}Pb	12.5	1.0	13.2	0.5	-5.3	1.84	0.22	1.6	0.3	15
^{232}Th	6.47	0.53	6.1	0.2	6.1	1.326	0.079	1.22	0.06	8.7
^{238}U	1.827	0.056	1.86	0.09	-1.8	0.413	0.020	0.403	0.001	2.5

Table 4.4: Continued.

	BCR-2					GSP-SS						
	This study		Preferred values		Deviation	This study		GSP-1	Deviation	GSP-2		Deviation
	Average	1σ	Value	1σ	%	Average	1σ	Value	%	Value	1σ	%
	n=17					n=13						
^{9}Be	3.22	0.39				1.94	0.30	1.40	39	1.5	0.2	29
^{29}Si	Internal standard		252882	3739		Internal standard		314210		311000	4000	
^{45}Sc	36.1	3.4	33	2	9.4	10.5	2.6	6.2	69	6.3	0.7	67
^{51}V	424	10	416	14	1.9	56.4	2.2	53	6.4	52	4	8.5
^{53}Cr	38.1	2.1	18	2	110	44.3	2.2	13.0	240	20	6	120
^{60}Ni	33.6	2.6	18	1	87	57.4	1.3	9	550	17	2	240
^{65}Cu	17.5	1.2	21	1	-17	34.9	1.0	33	5.8	43	4	-19
^{66}Zn	137	13	127	9	7.9	116.7	8.8	104	12	120	10	-2.8
^{71}Ga	22.69	0.70	23	2	-1.3	28.9	1.8	23	26	22	2	31
^{85}Rb	45.5	1.1	46.9	0.1	-3.0	232.9	8.2	254	-8.3	245	7	-4.9
^{88}Sr	339	11	340	3	-0.29	229	11	234	-2.1	240	10	-4.6
^{89}Y	33.1	2.9	37	2	-11	25.5	2.2	26	-1.9	28	2	-8.9
^{90}Zr	183	16	184	1	-0.54	622	48	530	17	550	30	13
^{93}Nb	11.63	0.56	12.6	0.4	-7.7	26.7	1.5	27.9	-4.3	27	2	-1.1
^{133}Cs	1.000	0.084	1.1	0.1	-9.1	1.002	0.070	1.02	-1.8	1.2	0.1	-16
^{138}Ba	659.3	4.8	677	2	-2.6	1255	36	1310	-4.2	1340	44	-6.3
^{139}La	26.9	1.8	24.9	0.2	8.0	204	13	184	11	180	12	13
^{140}Ce	52.8	1.5	52.9	0.2	-0.19	447	13	399	12	410	30	9.0
^{141}Pr	6.56	0.38	6.7	0.1	-2.1	54.4	2.5	52	4.6	51	5	6.7
^{146}Nd	29.5	2.2	28.7	0.1	2.8	216	14	196	10	200	12	8.0
^{147}Sm	6.73	0.67	6.58	0.02	2.3	27.5	2.3	26.3	4.6	27	1	1.9
^{153}Eu	2.12	0.15	1.96	0.01	8.2	2.39	0.21	2.33	2.6	2.3	0.1	3.9
^{157}Gd	6.34	0.70	6.75	0.03	-6.1	12.5	1.3	12.1	3.3	12	2	4.2
^{159}Tb	1.024	0.099	1.07	0.03	-4.3	1.31	0.11	1.34	-2.2			
^{161}Dy	6.22	0.66	6.41	0.05	-3.0	5.92	0.50	5.5	7.6	6.1		-3.0
^{165}Ho	1.27	0.12	1.28	0.03	-0.78	0.978	0.085	1.01	-3.2	1	0.1	-2.2
^{167}Er	3.35	0.51	3.66	0.01	-8.5	2.26	0.30	2.7	-16	2.2		2.7
^{169}Tm	0.488	0.054	0.54	0.04	-9.6	0.290	0.034	0.38	-24	0.29	0.02	0
^{173}Yb	3.45	0.33	3.38	0.02	2.1	1.68	0.30	1.7	-1.2	1.6	0.2	5.0
^{175}Lu	0.491	0.047	0.503	0.009	-2.4	0.233	0.026	0.214	8.9	0.23	0.03	1.3
^{178}Hf	4.81	0.53	4.9	0.1	-1.8	15.9	1.4	15.5	2.6	14	1	14
^{208}Pb	9.12	0.75	11	1	-17	41.9	2.8	55	-24	42	3	-0.24
^{232}Th	5.99	0.58	5.7	0.5	5.1	115.7	9.2	106	9.2	105	8	10
^{238}U	1.630	0.056	1.69	0.19	-3.6	2.525	0.097	2.54	-0.59	2.4	0.19	5.2

sample cell. Analyses were obtained using a laser spot of 55 μm rastered at 2 μm per second, at a pulse rate of 5 Hz and a laser energy of ~15 J cm^{-2}. The carrier gas was He in the sample cell, with Ar added downstream. The NIST 610 glass (Pearce *et al.*, 1997) was used as the calibration standard, and Si (obtained by XRF) was used as an internal standard to quantify trace-element compositions. The GLITTER™ software package (Version 4.4) was used to reduce the data (Griffin *et al.*, 2008; see http://www.glitter-gemoc.com/). Measured and reference values for reference materials AGV-2, BCR-2, BHVO-2 and GSP-SS are presented in Table 4.4 (sample GSP-SS was collected from the same locality as GSP-1, and reference values for both GSP-1 and GSP-2 are provided for comparison).

Comparison of techniques

Conventional acid digestion methods used to prepare samples for solution ICPMS analysis are often not completely effective when the sample contains significant amounts of refractory minerals (e.g. zircon, rutile). This can frequently be seen in the literature where analysed reference materials have lower-than-expected values for elements commonly residing in these phases (e.g. large spread in Zr (192-642 ppm, n=22) and Hf (4.5-16.7 ppm, n=20) concentrations for standard GSP-2 (zircon-bearing granodiorite) reported in the GeoReM database; Jochum *et al.*, 2005). More aggressive acid digestion methods may succeed in completely dissolving the refractory phases, but solution analyses in general are subject to complications related to adsorption and precipitation of samples stored and analysed as dilute acid solutions, leading to incomplete analyte recovery (Eggins, 2003). The direct ablation of glass discs negates these potential issues, although the possibility remains of contaminating the sample with impurities in the flux; this is addressed below.

Comparison of results obtained from the solution and laser ablation analyses shows that the solution-ICPMS analyses generally have better precision and lower limits of detection, and are therefore preferred for most elements (see Tables 4.3 and 4.4). Both techniques produce results with only small deviations from reference values for most elements (Figure 4.1), however there are some significant deviations in the case of the zircon-bearing standard GSP-SS. The values obtained by laser ablation are closer to the reference values for elements typically residing in zircon (Zr, Hf, U and the heavy rare earth elements (HREE); see the strong negative deviations for these elements in the solution-ICPMS data, Figure 4.1a). Table 4.5 presents a list of elements analysed in this study, showing which technique was selected for the final compilation and the rationale for this selection.

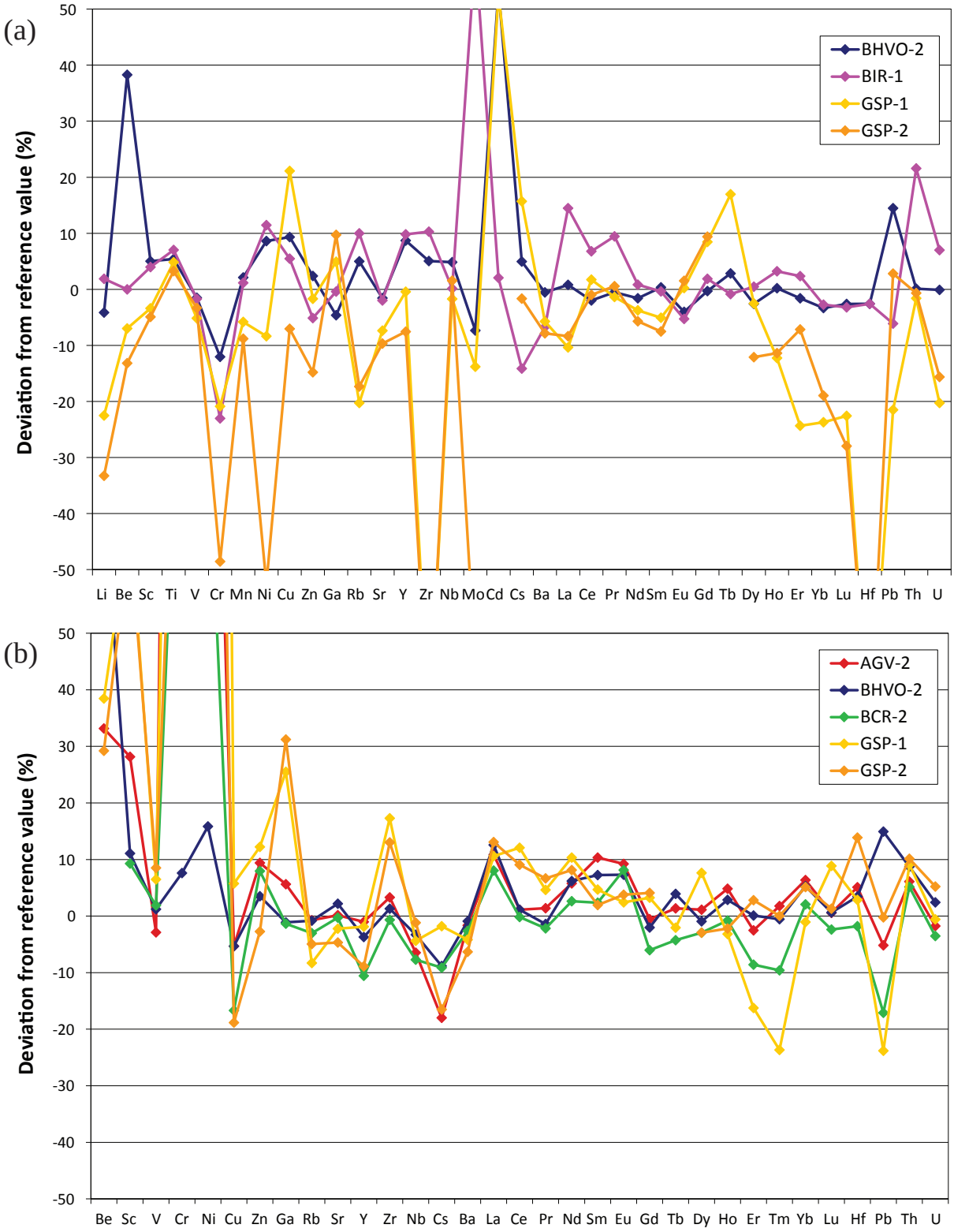


Figure 4.1. Accuracy of results obtained by: (a) solution ICPMS, and (b) laser ablation ICPMS, as percentage deviation from reference value. Strong negative peaks in the solution analysis of sample GSP (zircon-bearing granodiorite) indicate incomplete dissolution of zircon, which results in incomplete yields for zircon-hosted elements (Zr, Hf, Pb, Th, HREE). Strong positive peaks for Ni and Cr in the laser ablation ICPMS analyses indicate contamination from impurities in the flux.

Table 4.5: List of trace elements analysed in this study, showing the uncertainties and detection limits (in ppm) for each technique, which technique was chosen for the final compilation, and the reason for this choice.

Element	Solution ICPMS			LA-ICPMS			Justification
	%rsd	LLD		%rsd	LLD		
Li	3.0	0.024	**Preferred**			n.d.	
Be	6.7	0.048	**Preferred**	13	0.21	Analysed	Better precision and agreement with standard values
Sc	2.1	0.81	**Preferred**	15	0.34	Analysed	
V	1.9	0.13	**Preferred**	2.6	0.11	Analysed	"
Cr	6.8	0.51	**Preferred**	4.5	2.6	Analysed	Flux contamination
Ni	2.6	0.20	**Preferred**	9.1	0.42	Analysed	"
Cu	1.8	0.43	Analysed	5.0	1.3	**Preferred**	Better agreement with standard values
Zn	1.6	3.2	**Preferred**	6.9	0.98	Analysed	Better precision and agreement with standard values
Ga	1.5	0.038	**Preferred**	3.6	0.18	Analysed	
Rb	4.1	0.098	**Preferred**	2.9	0.15	Analysed	"
Sr	1.6	0.39	**Preferred**	3.7	0.034	Analysed	"
Y	1.0	0.12	Analysed	7.9	0.031	**Preferred**	Zircon hosted, low in solution analysis
Zr	2.3	0.042	Analysed	7.2	0.062	**Preferred**	"
Nb	1.4	0.026	**Preferred**	4.9	0.034	Analysed	Better precision and agreement with standard values
Mo	5.0	0.13	**Preferred**			n.d.	
Cd	33.8	0.096	**Preferred**			n.d.	
Cs	4.9	0.0036	**Preferred**	9.0	0.075	Analysed	Better precision and agreement with standard values
Ba	2.7	1.2	**Preferred**	1.7	0.034	Analysed	Better agreement with standard values
La	5.4	0.16	**Preferred**	5.8	0.033	Analysed	"
Ce	3.0	0.27	**Preferred**	2.6	0.023	Analysed	"
Pr	2.9	0.055	**Preferred**	4.8	0.019	Analysed	Better precision and agreement with standard values
Nd	2.6	0.15	**Preferred**	6.6	0.12	Analysed	
Sm	2.9	0.059	**Preferred**	8.5	0.14	Analysed	"
Eu	3.6	0.040	**Preferred**	7.4	0.036	Analysed	"
Gd	3.0	0.053	Analysed	9.7	0.12	**Preferred**	Better agreement with standard values
Tb	3.2	0.039	Analysed	8.9	0.021	**Preferred**	"
Dy	2.8	0.050	Analysed	9.6	0.10	**Preferred**	"
Ho	3.2	0.040	Analysed	9.2	0.021	**Preferred**	Zircon hosted, low in solution analysis
Er	3.1	0.048	Analysed	12	0.084	**Preferred**	"
Tm			n.d.	11	0.017	**Preferred**	
Yb	3.7	0.059	Analysed	13	0.12	**Preferred**	Zircon hosted, low in solution analysis
Lu	3.5	0.054	Analysed	12	0.019	**Preferred**	"
Hf	3.3	0.008	Analysed	8.6	0.064	**Preferred**	"
Pb	8.9	0.074	**Preferred**	8.7	0.077	Analysed	Better agreement with standard values
Th	7.4	0.006	**Preferred**	7.9	0.027	Analysed	Better precision and agreement with standard values
U	9.7	0.012	Analysed	3.8	0.019	**Preferred**	Zircon hosted, low in solution analysis

Two elements (Cr and Ni) give anomalously high concentrations when analysed by LA-ICPMS, suggestive of flux contamination (Figure 4.1b). To resolve this issue, standards were prepared at two different flux:sample ratios, and comparison of the two sets of results shows that Cr and Ni are both generally higher in the preparations with higher flux:sample ratios. All analyses are higher than reference values, indicating that contamination from impurities in the flux is the most likely reason for the anomalously high concentrations obtained for these elements (Table 4.6).

4.1.3 Sr and Nd isotopic analyses

Samples were digested in 15 mL Savillex Teflon beakers using concentrated HF and HNO_3. Samples were then dried down and 10 drops of concentrated $HClO_4$ was added, followed by 4 mL 6 N HCl and H_2O_2. Samples were dried down again, dissolved in 6 N HCl, dried, dissolved in HCl and HF, and centrifuged to remove any undissolved residue. Samples were then loaded on to Teflon columns containing Biorad® AG50W-X8 (200-400 mesh) cation exchange resin, and eluted using a 2.5 N HCl/0.1 N HF solution. Strontium was collected after 34.9 mL, followed by Nd. Neodymium was separated from Sm, Ba, La and Ce using a second column (Eichrom® Ln spec resin (50-100 μm); e.g. Aulbach *et al.*, 2004).

Isotopic analyses of Sr and Nd were obtained using a Thermo Finnigan Triton thermal ionisation mass spectrometer (TIMS).

Samples for Sr isotopic analysis were loaded on to single rhenium filaments with a Ta activator. Analyses were made between 1380 and 1430 °C, with total Sr signals of 1-11 V; they were collected in static mode with amplifier rotation, and were collected in 10 blocks of 20 cycles each, with an integration time of 4.2 seconds per cycle. Ratios were normalised to $^{86}Sr/^{88}Sr = 0.1194$ to correct for mass fractionation. Measured $^{87}Sr/^{86}Sr$ ratios for BHVO-2 (average = 0.703457 ± 3, n=2) and NIST SRM 987 (average = 0.710208 ± 3, n=2) are in good agreement with reference values (Table 4.7).

Samples for Nd isotopic analysis were loaded on to double rhenium filaments and analysed with an evaporation filament current of 1200-1600 mA and a total Nd signal of 0.5-10 V. Analyses were collected in static mode with amplifier rotation, collected in 4 blocks of 50 cycles each, with an integration time of 8.4 seconds per cycle. Ratios were normalised to $^{146}Nd/^{144}Nd = 0.7219$ to correct for mass fractionation. Measured values for standards BHVO-2 (average = 0.512987 ± 21, n=4) and NIST JMC 321 (0.511118 ± 5, n=1) are in good agreement with reference values, and are presented in Table 4.7.

Table 4.6: LA-ICPMS results for Cr and Ni in standards AGV-2, BHVO-2, BCR-2 and GSP-SS prepared at flux:sample ratios of 2.5:0.3 and 1.5:0.5. References values as in Table 4.4. All values in ppm.

	Cr					
	2.5:0.3		1.5:0.5		Reference value	
	Average	1σ	Average	1σ	Average	1σ
AGV-2	46.7	6.5	75.9	2.4	16	1
BCR-2	42.9	4.6	38.1	2.1	18	2
BHVO-2	318	15	301	13	280	19
GSP-SS	45.6	5.4	44.3	2.2	13	

	Ni					
	2.5:0.3		1.5:0.5		Reference value	
	Average	1σ	Average	1σ	Average	1σ
AGV-2	62.2	4.3	51	12	20	1
BCR-2	54.6	3.8	33.6	2.6	18	1
BHVO-2	183	22	137.9	3.7	119	7
GSP-SS	58	14	57.4	1.3	8.8	

Table 4.7: Results of Sr and Nd isotopic analysis of standards BHVO-2, JMC 321 and NIST SRM 987 by TIMS during this study, and comparison to GAU long-term averages and preferred values from: NIST (NIST SRM 987; http://www.nist.gov/srm/index.cfm) and GeoReM (BHVO-2 and JMC 321; Jochum et al., 2005).

		BHVO-2		NIST SRM 987
		$^{87}Sr/^{86}Sr$		$^{87}Sr/^{86}Sr$
This study	n=2	0.703457 ± 3	n=2	0.710208 ± 3
Long term average	n=90	0.703477 ± 25	n=78	0.710242 ± 21
Published value		0.703469 ± 17		0.710223 ± 260

		BHVO-2		JMC 321
		$^{143}Nd/^{144}Nd$		$^{143}Nd/^{144}Nd$
This study	n=4	0.512987 ± 21	n=1	0.511118 ± 5
Long term average	n=71	0.512973 ± 12	n=58	0.511114 ± 17
Published value		0.512980 ± 12		0.511008 - 0.511125

4.2 *In situ* analyses

4.2.1 Thin section analyses

Major-element compositions of major (biotite) and accessory (allanite, zircon) phases were obtained from polished thin sections (30 µm) using a CAMECA SX100 electron microprobe (EMP) with five wavelength dispersive spectrometers. Analyses were carried out using a focused beam (1-2 µm), an accelerating voltage of 15 kV and a beam current of 20-50 nA. Mean lower limits of detection (LLD) are ≤0.03 wt% oxide for all elements except Cr (LLD = 0.04 wt% oxide) and Zr (LLD = 0.09 wt% oxide). Calibration standards used were: jadeite (Na), Fe_2O_3 (Fe), kyanite (Al), olivine (Mg), chromium metal (Cr), spessartine (Mn), orthoclase (K, Si), wollastonite (Ca), rutile (Ti), sodalite (Cl), apatite (F), yttrium aluminium garnet (Y), Hf metal (Hf), and zircon (Zr, zircon Si). Analyses of reference materials and published values are presented in Table 4.8. Back-scattered-electron images were obtained on a Zeiss EVO MA15 scanning electron microscope, using an accelerating voltage of 20 kV and a working distance of 9 mm.

Table 4.8: Results of repeated major-element analyses of reference materials Lehmi Biotite, Muscovite and GJ zircon by EMP during this study, and comparison to reference values. Reference values for biotite and muscovite standards from USGS. All values in wt%.

	Lemhi Biotite				Muscovite					GJ1 Zircon	
	This study		Reference value		This study		Reference value				
	Average	1σ	Average	1σ	Average	1σ	Average	1σ		Average	1σ
	n=5				n=5					n=18	
Na_2O	0.10	0.03	0.13	0.02	0.57	0.04	0.76	0.06	SiO_2	33.01	0.77
K_2O	9.03	0.10	9.04	0.25	10.75	0.07	10.87	0.18	ZrO_2	66.87	0.90
MgO	2.94	0.02	2.83	0.08	0.61	0.01	0.57	0.03	HfO_2	0.94	0.04
Al_2O_3	17.28	0.11	17.65	0.27	34.90	0.28	35.71	1.14	Y_2O_3	0.03	0.02
CaO	<LLD		0.10	0.03	<LLD		0.08	0.03	Total	100.85	
FeO	31.95	0.61	31.40	0.02	2.30	0.03	2.17	0.11			
Cl	1.18	0.05	1.11		0.02	0.01	0.04	0.01			
F	0.19	0.01	0.23		0.22	0.04	0.30	0.13			
TiO_2	1.39	0.02	1.30	0.04	0.15	0.01	0.16				
MnO	0.06	0.01	0.04		0.09	0.02	0.06				
SiO_2	32.93	0.27	33.09	0.44	44.89	0.06	44.95	1.46			
O=F,Cl	0.02	0.00	0.35		0.01	0.00	0.14				
Total	97.06	0.92	96.76		94.48	0.37	95.60				

4.2.2 Zircon separates

Zircon grains were separated using the selFrag electrostatic rock disaggregation facility. Rocks were trimmed of weathered edges, coarsely crushed to obtain pieces <3 cm at greatest dimension, and 500 to 1000 g rock was disaggregated for each sample. The disaggregated sample was sieved using 200 μm mesh, then panned to separate the dense fraction. Some separates were processed by heavy liquid separation using sodium polytungstate to further purify the zircon concentrate. Concentrates were hand-picked in optical light, mounted in epoxy and polished to expose internal structures.

Zircon CL images

Cathodoluminescence (CL) images were obtained using a Zeiss EVO MA15 scanning electron microscope. Images were obtained using an accelerating voltage of 20 kV and a working distance of 7-12 mm.

Zircon EMP major-element analyses

Zircon grains were analysed for major-element compositions (Zr, Si, Hf, Y) as outlined in Section 4.3.1 above. Where CL images revealed two or more distinct domains, EMP analyses were obtained of all domains large enough to analyse (≥5 μm). Results of repeat analyses of the GJ zircon standard and reference values are presented in Table 4.8.

Zircon trace-element analyses and U-Pb ages

In situ trace-element and U-Pb isotopic analyses of zircon were obtained simultaneously using an Agilent 7700cx quadrupole ICPMS. Two laser ablation microprobe systems were used during the study: ablation was initially performed using a New Wave UP 213 nm Nd:YAG laser microprobe (fitted with a large format two-volume cell) but this was later replaced with a Photon Machines Excite 193 nm excimer laser ablation system (fitted with a two-stage HeLeX cell). Counting times were 60 s on a gas background followed by up to 120 s of ablation/analysis, depending on the size of the zircon grain. Analyses were carried out using a spot size of 40 μm, pulse rate of 5 Hz, and laser energy of ~5 J cm^{-2} (UP 213 nm system) or ~15 J cm^{-2} (Excite 193 nm system). The carrier gas was He in the sample cell, with Ar added downstream. Zircon grains were analysed in runs of ~10 analyses bracketed by 4 analyses each of GJ-1 Red zircon standard (ID-TIMS $^{207}Pb/^{206}Pb$ age = 608.5 ± 0.4 Ma; Jackson *et al.*, 2004) and NIST 610 glass (Pearce *et al.*, 1997). The GJ-1 zircon and NIST 610 glass were used as calibration standards for U-Pb isotopic and trace-element analyses respectively to correct for instrument sensitivity and drift.

Zircon reference materials 91500 (ID-TIMS $^{207}Pb/^{206}Pb$ age = 1065.4 ± 0.3 Ma; Wiedenbeck *et al.*, 1995) and OG1 (ID-TIMS $^{207}Pb/^{206}Pb$ age = 3465.4 ± 0.6 Ma; Stern *et al.*, 2009) were used

Table 4.9: U-Pb isotopic analyses obtained in this study for zircons 91500 and OG1, and ID-TIMS values. Reference values for 91500 from Wiedenbeck et al. (1995); values for OG1 from Stern et al. (2009). GJ-1 ratios used for calibration from Jackson et al. (2004). Full dataset in Appendix A1.

	91500							
	This study (n=79)				Reference values			
	Ratio	1σ	Age	1σ	Ratio	1σ	Age	1σ
$^{207}Pb/^{206}Pb$	0.07500	0.00086	1068	23	0.07488	0.00001	1065.4	0.3
$^{207}Pb/^{235}U$	1.834	0.028	1058	10	1.8502	0.0008		
$^{206}Pb/^{238}U$	0.1774	0.0022	1053	12	0.17917	0.00008	1062.4	0.4
$^{208}Pb/^{232}Th$	0.0538	0.0021	1059	40	0.05374	0.00015	1058.1	2.8

	OG1							
	This study (n=49)				Reference values			
	Ratio	1σ	Age	1σ	Ratio	1σ	Age	1σ
$^{207}Pb/^{206}Pb$	0.2982	0.0024	3461	12	0.29907	0.00011	3465.4	0.6
$^{207}Pb/^{235}U$	29.22	0.91	3460	31				
$^{206}Pb/^{238}U$	0.710	0.020	3461	76	0.7053	0.0008	3440.7	3.2
$^{208}Pb/^{232}Th$	0.189	0.010	3506	170				

	GJ-1	
	Calibration values	
	Ratio	1σ
$^{207}Pb/^{206}Pb$	0.06014	0.000005
$^{207}Pb/^{235}U$	0.8093	0.00045
$^{206}Pb/^{238}U$	0.09761	0.000065
$^{208}Pb/^{232}Th$	0.03011	

as secondary standards to assess the accuracy and precision of U-Pb results (Table 4.9; for the full set of analyses see Appendix A1). Trace-element concentrations were quantified using the Hf concentration (obtained by EMP analysis) as an internal standard. The GLITTER™ software package (Version 4.4) was used to reduce both the U-Pb and trace-element data (Griffin *et al.*, 2008; see http://www.glitter-gemoc.com/). Age data were then processed using Isoplot (version 3; Ludwig, 2003). Time-resolved analysis of the signal for each analysis allowed selection of the most stable part of the signal for U-Pb isotopic age determination, as well as elimination of metamict zones and any included phases in the part of the signal used for trace-element compositions. Compiled trace-element compositions for zircon 91500 are presented in Table 4.10, together with reference values.

Table 4.10: Results of repeated trace-element analysis of zircon 91500 by LA-ICPMS during this study, and comparison with published values. Reference values from Wiedenbeck et al. (2004) except P, Ti, Ta (values from the GeoReM database; Jochum et al., 2005). All values in ppm.

	91500			
	This study		Reference values	
	Average	1σ	Average	1σ
	n=78			
^{31}P	37	22	24	1
^{43}Ca	17	22		
^{49}Ti	4.15	0.80	6.00	1.00
^{89}Y	125	12	140	14
^{93}Nb	1.14	0.45	0.79	0.06
^{139}La	0.00013	0.00044	0.006	0.003
^{140}Ce	2.29	0.23	2.56	0.26
^{141}Pr	0.0027	0.0049	0.024	0.015
^{146}Nd	0.098	0.037	0.24	0.04
^{147}Sm	0.272	0.063	0.50	0.08
^{151}Eu	0.190	0.026	0.24	0.03
^{157}Gd	1.92	0.21	2.21	0.24
^{159}Tb	0.767	0.080	0.86	0.07
^{163}Dy	10.2	1.0	11.8	0.8
^{165}Ho	4.24	0.43	4.84	0.34
^{166}Er	22.0	2.2	24.6	2.5
^{169}Tm	5.69	0.62	6.89	0.34
^{173}Yb	63.4	7.5	73.9	3.7
^{175}Lu	11.5	1.0	13.10	1.05
^{181}Ta	0.365	0.037	0.50	0.10
^{232}Th	26.2	3.4	29.9	2.1
^{238}U	73.5	9.1	80.0	8.0

Zircon Hf-isotope analyses

In situ Hf-isotope analyses of zircon were carried out using a Nu Plasma multi-collector ICPMS (MC-ICPMS) system, in conjunction with two different New Wave laser ablation microprobes: a New Wave UP 213 nm system and a New Wave UP 266 nm system. Zircon grains mounted in epoxy, and previously analysed for U-Pb isotopic compositions, were analysed using a spot size of 40-60 μm, pulse frequency of 5 Hz and laser energy of ~5 J cm^{-2}, and counting times of 30 s background and 60-150 s sample. These conditions gave Hf signal intensities in the range 1.5 to 11 volts for reference materials. Zircons Mud Tank

($^{176}Hf/^{177}Hf = 0.282522 \pm 42$; Griffin *et al.*, 2007) and Temora-2 ($^{176}Hf/^{177}Hf = 0.282680 \pm 11$; Woodhead & Hergt, 2005) were used as reference materials to assess accuracy and to monitor instrument stability; results of repeat analyses obtained in this study and long term averages for the GAU are presented in Table 4.11 (for the full set of analyses obtained in this study see Appendix A2). Interferences of ^{176}Yb and ^{176}Lu on the ^{176}Hf signal were corrected using the single-isotope method outlined in Griffin *et al.* (2002) and Pearson *et al.* (2008), with a $^{176}Yb/^{172}Yb$ ratio of 0.587 and a $^{176}Lu/^{175}Lu$ ratio of 0.02669 (the Yb ratio has been empirically determined at the GAU; the Lu ratio is from De Bievre & Taylor, 1993). The efficacy of the correction is attested by the accuracy and reproducibility of the results for the two reference zircons with widely different REE contents (average $^{176}Yb/^{176}Hf = 0.0044 \pm 12$ for Mud Tank, 0.032 ± 12 for Temora-2; average $^{176}Lu/^{176}Hf = 0.000107 \pm 25$ for Mud Tank, 0.00102 ± 29 for Temora-2), together with the absence of any correlation between $^{176}Yb/^{177}Hf$ and the corrected $^{176}Hf/^{177}Hf$ (r^2 of 0.04 and 0.005 for Mud Tank and Temora-2 respectively; Figure 4.2). During analysis, care was taken to ablate the same domain previously analysed for U-Pb and trace elements, using the internal structure revealed in the CL images to guide the choice of analytical spots, and monitoring elemental and isotopic ratios throughout the analysis in order to detect the presence of multiple domains. Initial $^{176}Hf/^{177}Hf$, εHf, and model ages were calculated using the ^{176}Lu decay constant of Scherer *et al.* (2001).

Table 4.11: Results of repeated Hf-isotope analysis of zircons Mud Tank and Temora-2 by LA-MC-ICPMS during this study, and comparison with long term averages from the GAU and published values. Reference values for Mud Tank from Griffin et al. (2007); values for Temora-2 from Woodhead and Hergt (2005). Full dataset in Appendix A2.

		This study		Long term		Reference value	
		Average	1σ	Average	1σ	Average	1σ
		n=63		n=6093			
Mud Tank	$^{176}Hf/^{177}Hf$	0.282516	0.000014	0.282528	0.000026	0.282522	0.000042
	$^{178}Hf/^{177}Hf$	1.46720	0.00010	1.46717	0.00024		
	$^{180}Hf/^{177}Hf$	1.88674	0.00015	1.88667	0.00026		
	$^{176}Yb/^{177}Hf$	0.0044	0.0012	0.0034	0.0025		
	$^{176}Lu/^{177}Hf$	0.000107	0.000025	0.00008	0.00005		
		n=33		n=399			
Temora-2	$^{176}Hf/^{177}Hf$	0.282701	0.000029	0.282686	0.000034	0.282680	0.000011
	$^{178}Hf/^{177}Hf$	1.46714	0.00017	1.46714	0.00037		
	$^{180}Hf/^{177}Hf$	1.88676	0.00019	1.88673	0.00035		
	$^{176}Yb/^{177}Hf$	0.032	0.012	0.035	0.014		
	$^{176}Lu/^{177}Hf$	0.00102	0.00029	0.00109	0.00038		

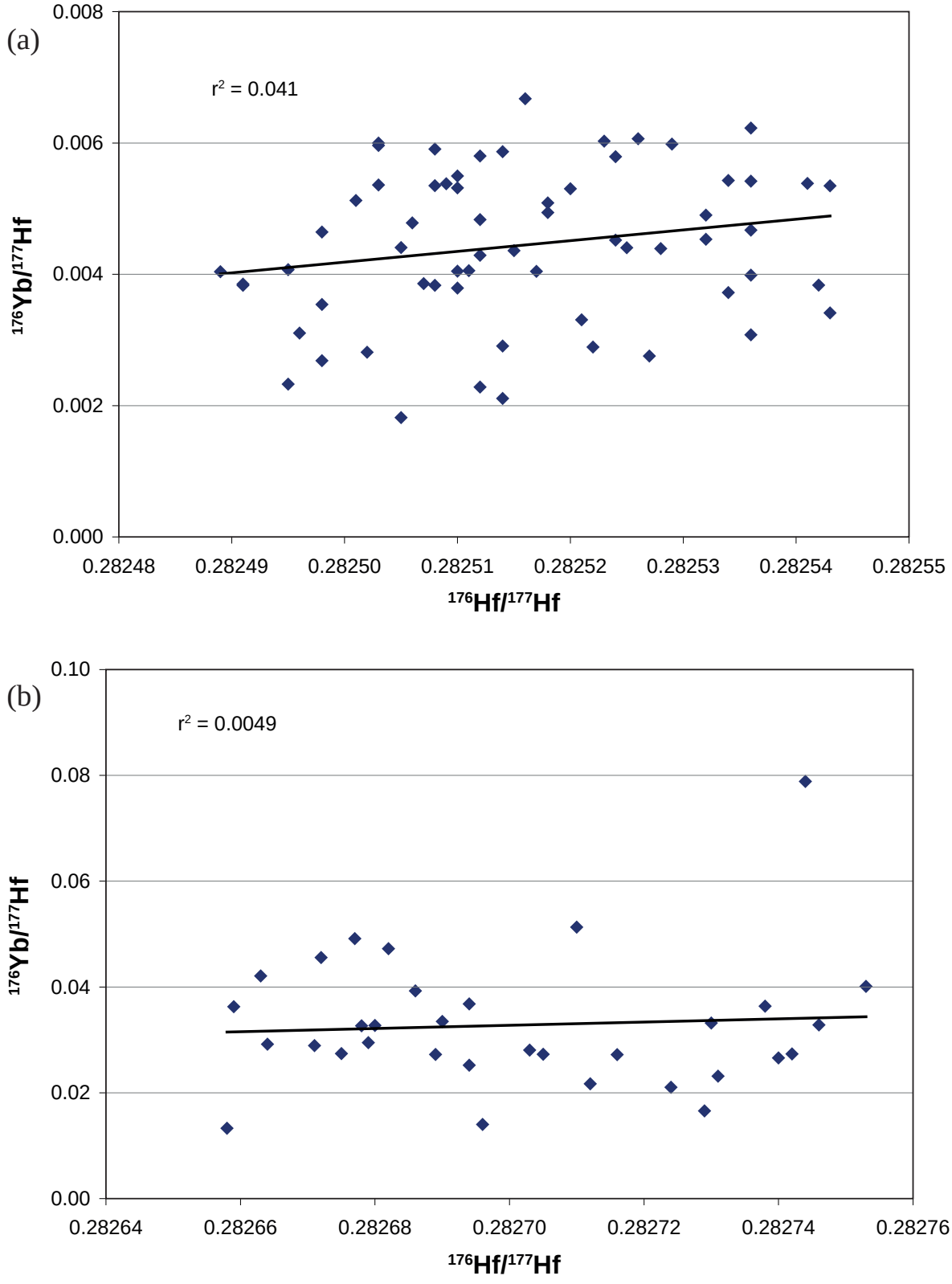


Figure 4.2. Plot of $^{176}Yb/^{177}Hf$ vs $^{176}Hf/^{177}Hf$ (corrected) for: (a) Mud Tank and (b) Temora-2 reference zircons.

Chapter Five – Petrography and Mineral Chemistry

5.1 Petrography

A summary of the petrography of the samples from the Mpuluzi batholith is presented in Table 5.1. For full descriptions and locations of individual samples, see Appendix B (note that four of the 19 samples in this study are from the Piggs Peak batholith; the Mpuluzi and Piggs Peak samples are not distinguishable in terms of mineralogical, chemical, or isotopic composition and are not noted separately in the presentation of results below).

All samples consist of quartz (~25–40%) + plagioclase (~20–35%) + microcline (~15–35%). Biotite (~5-15%) is the main ferromagnesian phase, and allanite, apatite, zircon, and ilmenite/magnetite are accessory phases in all samples. Hornblende, titanite, and fluorite occur in the more mafic samples (hornblende and titanite in sample RSA03; titanite in sample RSA01; fluorite inclusions in biotite in samples RSA03 and RSA02; see Table 5.1); primary muscovite occurs in the majority of the felsic samples (abundant in sample SWA05; occurs occasionally in samples SWA10a, SWA13a, SWA11, SWA09 and RSA07; see Table 5.1).

In hand specimen the Mpuluzi samples range from grey-green (e.g. SWA13a) to slightly pink (e.g. RSA09) to strongly pink (e.g. RSA07). No systematic variation was found between the colour in hand specimen and the degree of feldspar alteration or host rock composition. The grain size within the Mpuluzi samples ranges from medium (~2 mm, e.g. RSA03, SWA13a) to coarse (~15 mm, e.g. RSA07), with an average grain size of ~5 mm (e.g. RSA05). Most samples are equigranular (e.g. RSA03, SWA18a, SWA20, RSA07), some samples have large K-feldspar phenocrysts (e.g. ~25 mm in sample RSA08, largest ~50 mm in SWA07).

The majority of samples have no obvious foliation (e.g. RSA02, SWA05, RSA07) or display a weak foliation (e.g. SWA18a, SWA03), with a few samples showing a strongly developed foliation (e.g. RSA03, SWA11). The foliation is defined by aligned grains of biotite (e.g. RSA03, SWA07), elongated quartz (e.g. SWA10a, SWA02a), or bands of quartz and feldspar (e.g. SWA03, SWA13a). In some samples, there is a primary magmatic foliation defined mainly by the alignment of biotite and/or elongate feldspars (e.g. RSA03), while in other samples the foliation is a product of deformation, and they show evidence of recrystallisation (e.g. SWA10a). A few samples show evidence of brittle deformation (e.g. RSA07).

Most quartz occurs as large, anhedral grains; in some samples the quartz is large and contains many inclusions of other major phases (e.g. RSA02). In most samples the quartz displays slight to moderate undulose extinction; in some samples it is recrystallised and drawn out (e.g. SWA10a). Plagioclase is generally rectangular and commonly has strongly altered,

Table 5.1: Summary of the petrography of the Mpuluzi samples (full descriptions in Appendix B). Mineral abbreviations from Kretz (1983). Alt. = alteration; Frac. = fractures; Und. = undulose extinction; Sut. = sutured boundaries; Def. twins = deformation twins; Myrm. = myrmekite; y = yes (observed); yy = very abundant; min = minor; v min = very minor; v fine = very fine.

Sample	Grainsize		Colour	Foliation		Alt.	Frac.	Mineral assemblage													Quartz		Plagioclase	K-feldspar	
	mm	Kfs		Strength	Timing			Qtz	Pl	Kfs	Bt	Hbl	Aln	Ttn	Ap	Zrn	Ms	Mag	Ilm		Und.	Sut.	Def. twins	Perthite	Myrm.
RSA03	2		grey	strong	primary	min		y	y	y	y	min	y	y	y	y		y	min		v min		min	v fine	
RSA01	5		grey			y	y	y	y	y	y		y	y	y	y			min		min		y	min	y
SWA18a	5		pink	weak	primary	y		y	y	y	y		y		y	y		min	y		min		y	v fine	min
RSA05	5		grey			y		y	y	y	y		min		y	y		v min	y		min		min	min	y
RSA02	3		grey			y		y	y	y	y		y		y	y			min		min		min	fine	y
SWA07	7	50	pink	weak	sec.	y		y	y	y	y		y		y	y			min		y	y	min	min	y
RSA04	4		pink			y		y	y	y	y		y		y	y		y			min			y	y
RSA08	10	25	pink			y	y	y	y	y	y		y		y	y		y	min		v min		min	y	min
SWA10a	4		pink	weak	sec.	min		y	y	y	y		y		y	y		v min			y	y	min	fine	min
RSA09	10	25	slightly pink			y		y	y	y	y		min		y	y	min	min	y		min		min	y	y
SWA20	7		grey			y		y	y	y	y		y		y	y		min	min		y	min	min	y	y
SWA03	5		grey	weak	sec.	min		y	y	y	y		min		y	y			y		y	min	min	y	yy
RSA06	10	20	pink			y		y	y	y	y		y		y	y		min	min		y	min	min	fine	y
SWA13a	2		grey-green	strong	sec.	y	y	y	y	y	y		min		min	y	min		v min		min		min	y	min
SWA11	7		pink	strong	sec.	y	y	y	y	y	y		min		min	y	min	min			y	y	min	y	min
SWA09	3		pink	strong	primary	min		y	y	y	y		v min		min	y	v min	v min			min		min	min	min
SWA02a	5		grey	strong	sec.	y		y	y	y	y		y		v min	y			v min		y	y	y	y	min
RSA07	15		pink			y	y	y	y	y	y		y		v min	y	min	min	min		min		min	coarse	min
SWA05	7		grey			y		y	y	y	y		min		min	y	y		v min		min		min	min	min

euhedral cores (e.g. RSA02, Figure 5.1a). Deformation twinning is well developed in some samples, and others exhibit some brittle deformation (e.g. SWA11). K-feldspar is present as microcline in all samples, and generally occurs as roughly rectangular grains that commonly display simple twins; in some samples microcline occurs as phenocrysts up to ~50 mm across (e.g. SWA07). Most grains show the development of fine perthite, the alignment of which is strongly controlled by the crystal structure (e.g. RSA02, Figure 5.1b); in one sample the perthite has coalesced into elongate blebs (RSA07, Figure 5.1c). Partial replacement of microcline by myrmekite (symplectitically intergrown quartz and plagioclase) is common (e.g. RSA07, Figure 5.1d).

Biotite occurs as elongate plates; some grains show signs of deformation (e.g. SWA07, Figure 5.1e). Unaltered biotite is pleochroic, from straw to chocolate-brown; alteration to chlorite + epidote is common (e.g. SWA18a, Figure 5.1f) and in some samples no unaltered biotite is preserved (e.g. RSA04). In some samples unaltered biotite flakes are preserved enclosed in quartz grains, while the remaining biotite grains are altered (e.g. RSA02, Figure 5.1g). Inclusions are common and comprise zircon, apatite, titanite, and occasional fluorite, with titanite inclusions particularly prevalent in the more altered biotites (perhaps as a secondary product of the breakdown of biotite; Tulloch, 1979).

The most mafic sample (RSA03) is the only one to contain hornblende, which occurs as rare, small (100–200 μm), euhedral grains (Figure 5.1h). Euhedral grains of primary titanite occur in the two most mafic samples (RSA03 and RSA01); in sample RSA03 they occur as large grains (up to ~600 μm) which are pale orange-brown in thin section, commonly with inclusions of quartz and feldspar (Figure 5.1i), while in sample RSA01 they are generally smaller (200–400 μm) and more strongly coloured in thin section (RSA01, Figure 5.1j).

Allanite is present throughout the range in composition but is more abundant in the more mafic samples. It is generally euhedral to subhedral, ranges in size from ~100 μm to ~3 mm, and occurs as scattered grains (e.g. RSA08, Figure 5.1k) or in clusters with biotite, zircon, and oxides (e.g. SWA07, Figure 5.1l). Apatite is also more abundant in the more mafic samples, and commonly occurs as small needles, associated with biotite. Most zircon grains occur in clusters with biotite, allanite, and the oxide phases, or as inclusions in biotite or muscovite (e.g. SWA05, Figure 5.1m). Primary muscovite occurs in the felsic samples, commonly intergrown with biotite (e.g. SWA03, Figure 5.1n); most samples also contain some secondary muscovite replacing plagioclase (e.g. SWA02a, Figure 5.1o).

The abundance of oxide phases is higher in the more mafic samples, but the presence of ilmenite versus magnetite does not vary systematically with the composition of the host rock. The samples vary from ilmenite-only (e.g. SWA03), through dominant ilmenite (e.g. SWA18a), subequal ilmenite and magnetite (e.g. RSA07), dominant magnetite (e.g. RSA08),

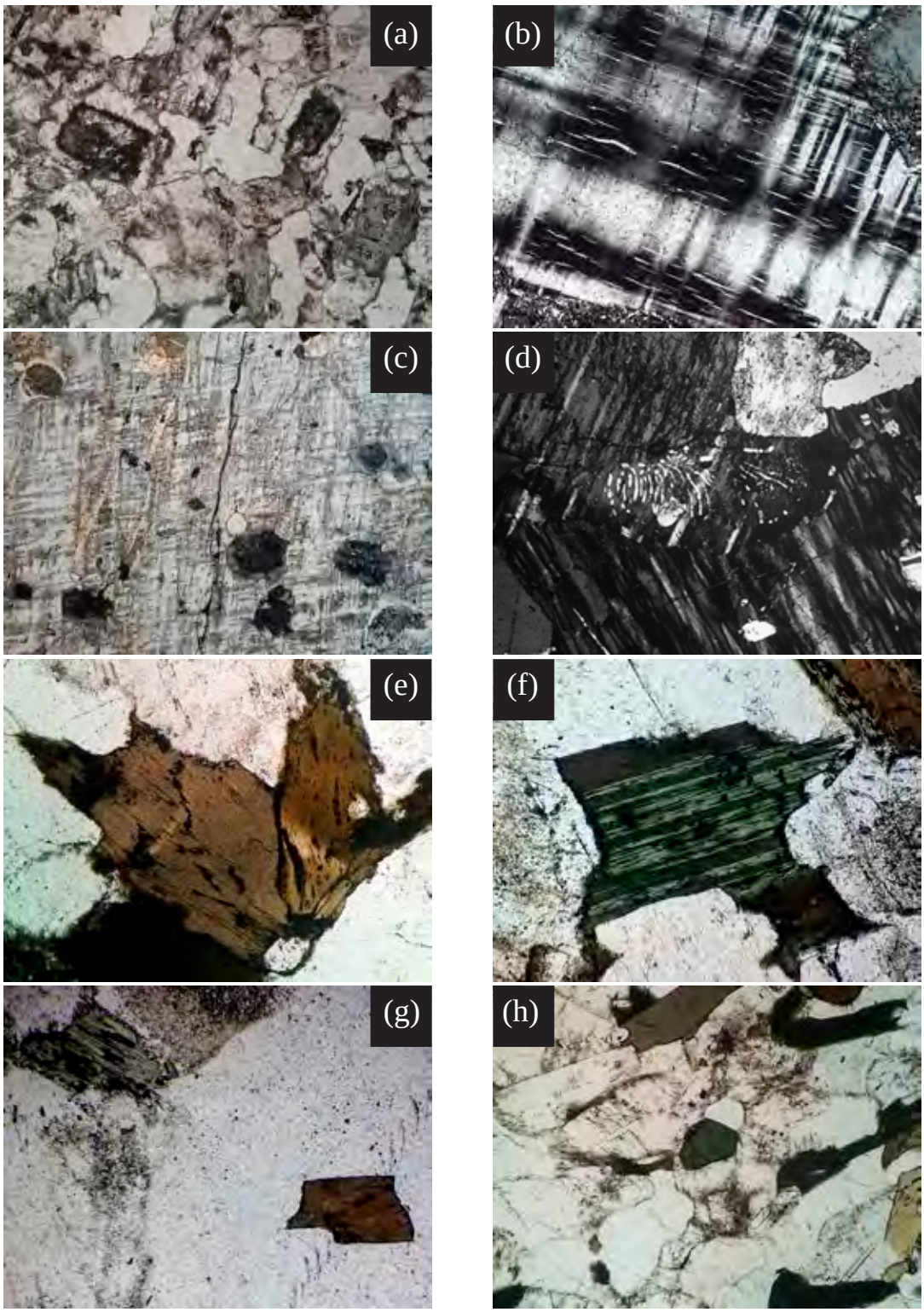
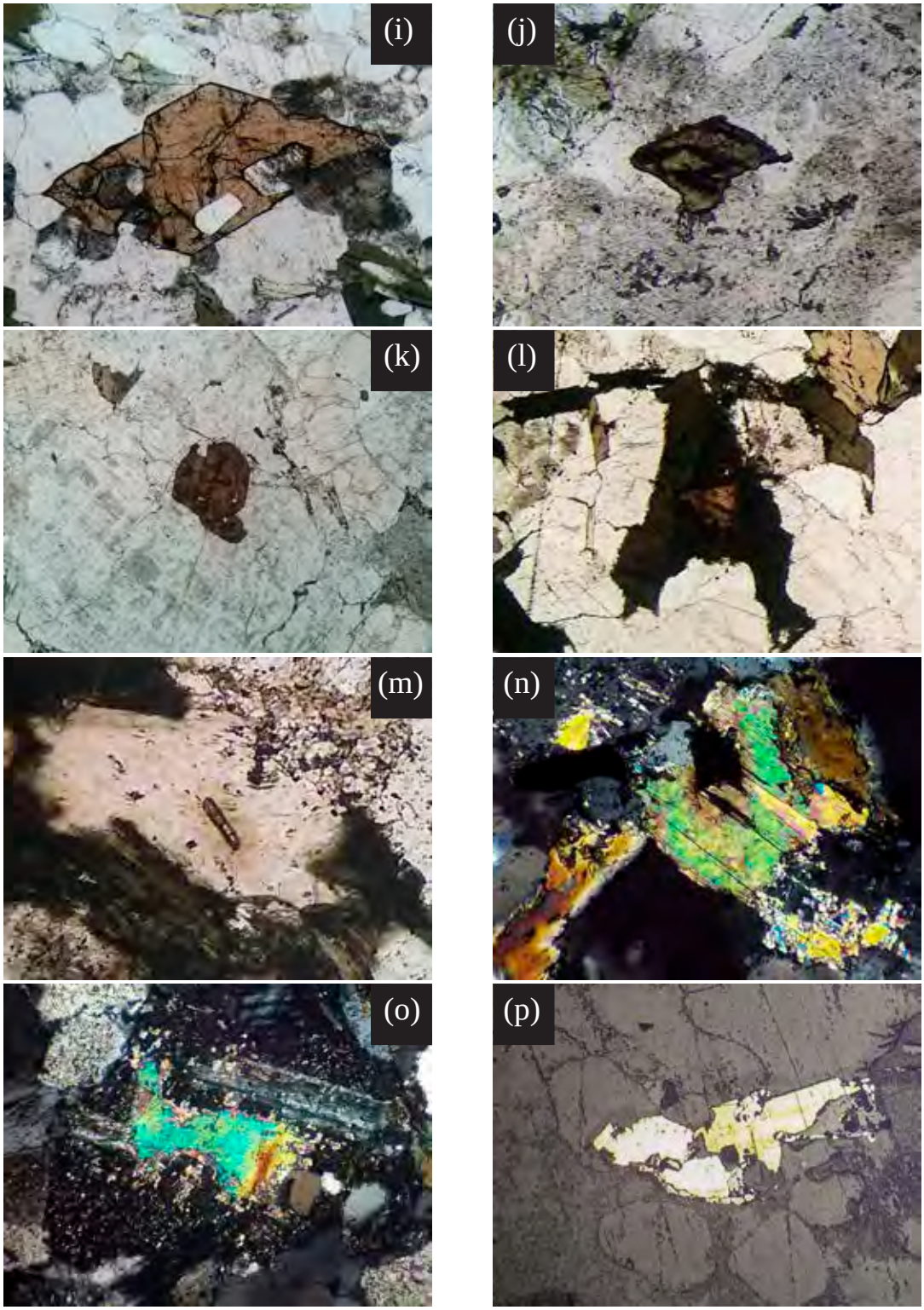


Figure 5.1. Photomicrographs (FOV = field of view; PPL = plane polarised light; XPL = cross polarised light; RL = reflected light): (a) plagioclase grains with strongly altered, euhedral cores (RSA02; FOV = 5 mm, PPL); (b) perthitic microcline (RSA02; FOV = 1.5 mm, XPL); (c) microcline with elongate blebs of perthite (RSA07; FOV = 5 mm, XPL); (d) partial replacement of microcline by myrmekite (RSA07; FOV = 2 mm, XPL); (e) deformed biotite grains (SWA07; FOV = 900 μm, PPL); (f) biotite partially altered to chlorite along cleavage planes (SWA18a; FOV = 900 μm, PPL); (g) unaltered biotite enclosed in quartz, other biotite altered to chlorite (RSA02; FOV = 1.5 mm, PPL); (h) small, euhedral



hornblende (RSA03; FOV = 1.5 mm, PPL); (i) large, euhedral, orange-brown titanite with inclusions of quartz and feldspar (RSA03; FOV = 3 mm, PPL); (j) small, euhedral, dark-brown titanite (RSA01; FOV = 1.5 mm, PPL); (k) large, isolated allanite grain (RSA08; FOV = 4 mm, PPL); (l) allanite in cluster with biotite (SWA07; FOV = 3 mm, PPL); (m) zircon inclusion in muscovite (SWA05; FOV = 400 μm, PPL); (n) intergrown biotite and primary muscovite (SWA03; FOV = 1.5 mm, XPL); (o) secondary muscovite replacing plagioclase (SWA02a; FOV = 900 μm, XPL); (p) pyrite and chalcopyrite (RSA03; FOV = 900 μm, RL).

to magnetite-only (e.g. RSA04). Sulphides are a minor component of the mafic samples and decrease in abundance as the samples become more felsic. They typically occur as small grains of pyrite, occasionally accompanied by chalcopyrite (e.g. RSA03, Figure 5.1p).

5.2 Mineral Chemistry

Determinations of mineral chemistry in this study focused on biotite as the main ferromagnesian phase (hornblende is only present in small amounts in one sample). The feldspars in most samples are highly altered and were not analysed.

5.2.1 Biotite

Representative analyses of biotite from each sample are presented in Table 5.2; for the complete dataset see Appendix C1. The extensive alteration of biotite to chlorite + epidote in many of the Mpuluzi samples prevented the analysis of biotite in some samples. No analyses of unaltered biotite were obtained from samples RSA04, RSA09, SWA02a, or RSA07, and sample SWA11 yielded only one analysis with minimal alteration to chlorite (biotite analyses containing >8.5 wt% K_2O were designated 'unaltered').

Analysed biotites from all samples have Mg# (= atomic Mg/(Mg+Fe^T); all iron is assumed to be Fe^{2+}) between 0.1 and 0.5, and octahedral Al (Al^{VI}) from 0.1 to 1.0 atoms per formula unit (pfu), and are accordingly classified as annite (Figure 5.2a). Biotites from the more felsic samples have higher Fe relative to Mg, reflecting the more iron-rich compositions of their host rocks (biotites from felsic samples have Mg# as low as ~0.1; mafic samples extend up to ~0.5). Biotites from the more felsic rocks are generally more Al-rich than those from more mafic samples (total Al content: ~18 wt% Al_2O_3 or ~3.4 atoms pfu in felsic samples; ~14.5 wt% Al_2O_3 or ~2.7 atoms pfu in mafic samples). More Al is present in both octahedral and tetrahedral sites in the more felsic samples, with a large increase in octahedral Al (mafic: ~0.2 atoms pfu; felsic: up to ~1 atom pfu), and a slight increase in tetrahedral Al (mafic: ~2.3 atoms pfu; felsic: ~2.5 atoms pfu). Low concentrations are observed for Ti (<4.5 wt% TiO_2; <0.5 atoms pfu) and Mn (<0.6 wt% MnO; <0.08 atoms pfu); Ti shows no systematic variation with host-rock composition, while Mn shows some scatter but is generally higher in the more felsic samples. Biotites from the more mafic samples generally have higher F contents (~1 wt%; ~0.03 atoms pfu) than those from more felsic samples (~0.3 wt%; ~0.01 atoms pfu). Concentrations of Ca and Na are low (generally <0.3 wt% oxide or <0.05 atoms pfu), and they show no correlation with whole-rock composition.

Consistent with the fact that biotite is the sole ferromagnesian mineral in most of the Mpuluzi samples, the majority of the biotites plot in the "biotite only" field of Nockolds (1947; Figure 5.2b). The more mafic samples extend into the "biotite + hornblende/pyroxene/olivine" field

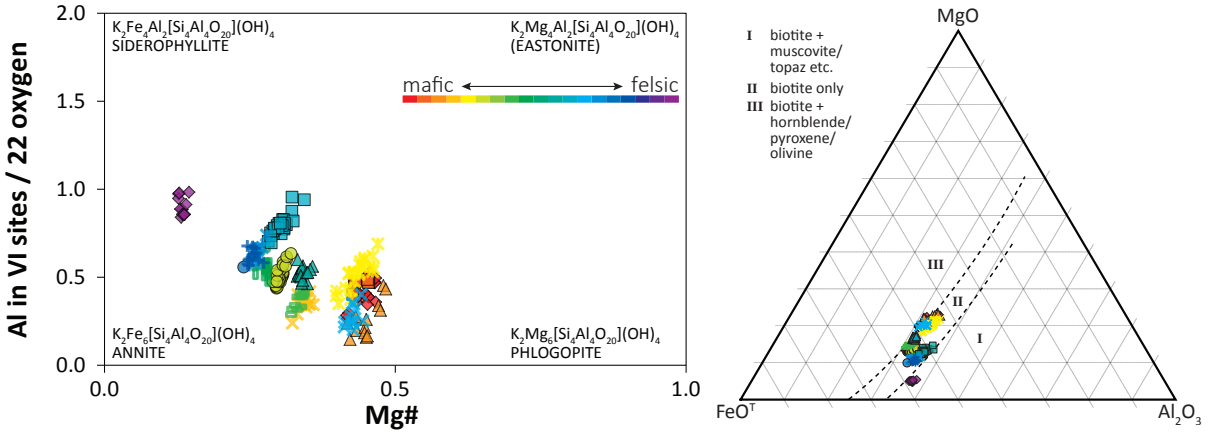


Figure 5.2. (a) Plot of octahedral Al *vs* Mg# in biotite, showing endmember compositions; (b) ternary plot of MgO, Al_2O_3, and FeO^T in biotite showing fields for coexisting phases (Nockolds, 1947). The colour of the points reflects the host-rock composition (warm colours = more mafic, cool colours = more felsic).

(consistent with the presence of minor hornblende in sample RSA03), while the felsic samples plot close to the boundary between the "biotite only" and "biotite + muscovite/topaz" fields, which is consistent with the presence of minor primary muscovite (particularly in sample SWA05, which plots entirely in the "biotite + muscovite/topaz" field).

Within each sample, octahedral Al (Al^{VI}) is positively correlated with the total Al content, while tetrahedral Al (Al^{IV}) is uncorrelated (Figure 5.3a, b). No correlation is observed between octahedral and tetrahedral Al (Figure 5.3c); this suggests that the Tschermak exchange ($Si^{IV} + (Mg,Fe^{2+}) \leftrightharpoons Al^{IV} + Al^{VI}$) does not completely balance the Al^{IV} component, and additional substitutions are involved (e.g. Fe^{3+} for Fe^{2+}). The other main substitution within the octahedral sites is the exchange of Mg for Fe^{2+} (Figure 5.3d); all Fe was assumed to be Fe^{2+}, and the strong negative correlation between Mg and Fe suggests that there is minimal substitution of Fe^{3+}. The simple case of direct substitution between Mg and Fe^{2+} would produce a 1:1 correlation; Figure 5.3d shows the slope is closer to 1:2 (Fe:Mg), which suggests a more complex coupled substitution. Ti and Mn generally show weak negative correlations with Mg# (Figure 5.3e, f). Substitution of Ca and Na for K in interlayer sites is very minor and shows no systematic variation. Substitution of F for OH is more pronounced in the grains with more magnesian compositions (Figure 5.3g; this is consistent with the stronger partitioning of F into phlogopite rather than annite; e.g. Munoz & Ludington, 1974). Substitution of Cl for OH is very minor (<0.003 atoms pfu), and shows no systematic variation.

The range of composition observed within a single grain is commonly very similar to the range shown by all analyses for that sample, suggesting that all biotites within a sample are from a single population (e.g. F *vs* Mg# and Al^{VI} *vs* Al^{IV}; Figure 5.3h, i).

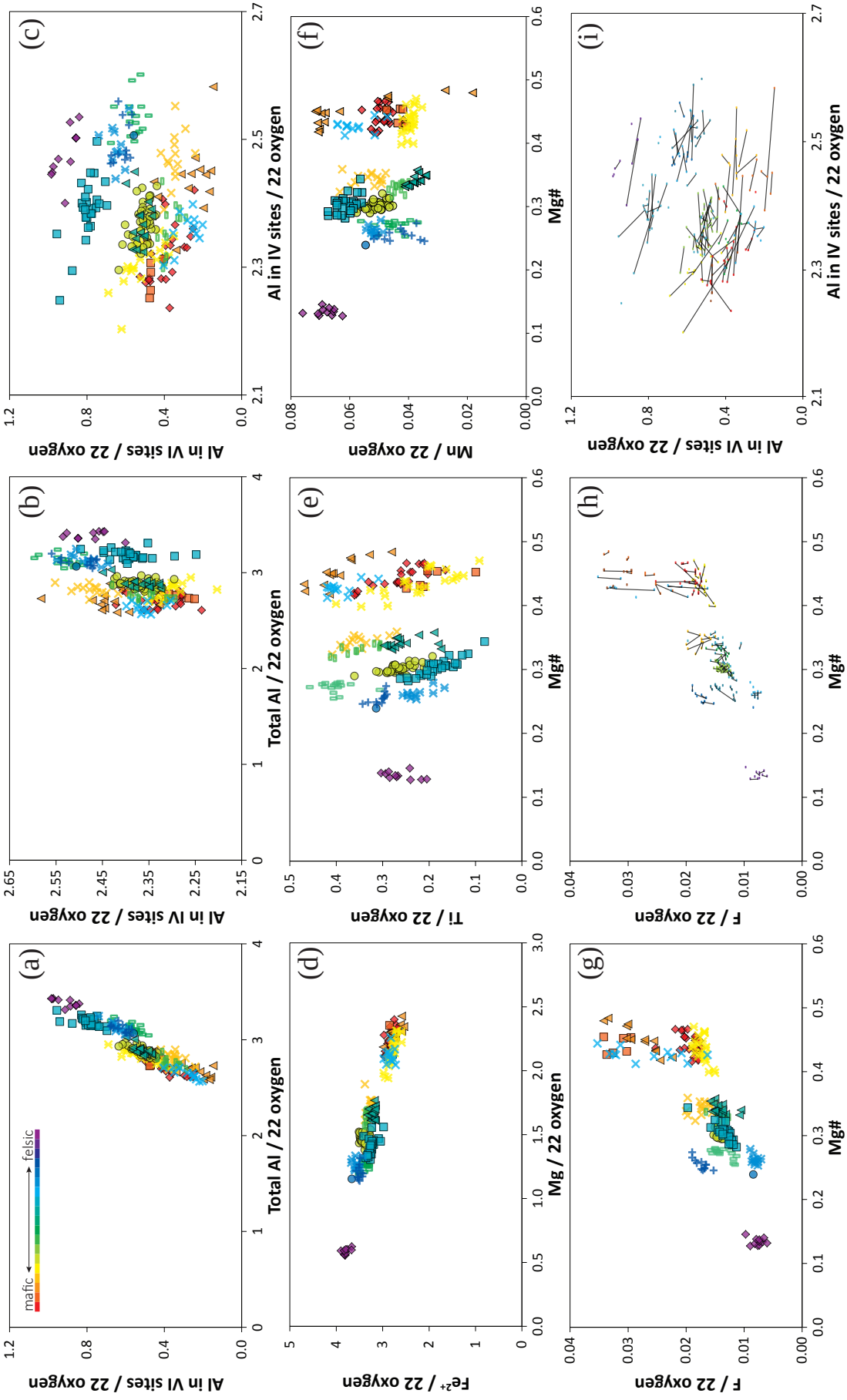


Figure 5.3. Plots of biotite compositions: (a) octahedral and (b) tetrahedral Al *vs* total Al content; (c) octahedral *vs* tetrahedral Al; (d) Fe^{T} *vs* Mg; (e) Ti, (f) Mn, and (g) F *vs* Mg# (atomic Mg/(Mg+Fe^{T})); (h) and (i) same as (g) and (c) but with tie-lines connecting analyses of the same grain. The colour of the points reflects the host-rock composition (warm colours = more mafic, cool colours = more felsic).

Table 5.2: Representative analyses of biotite for the Mpuluzi samples. LLD = lower limit of detection.

Analysis	Concentration (wt%)									- O equivalent			Structural formula (cations / 22 oxygen)												Cation	Mg#
	SiO	Al	TiO	FeO	MnO	MgO	CaO	Na	K	F	Cl	Total	Si	Al^{IV}	Al^{VI}	Ti	Fe^{2+}	Mn	Mg	Ca	Na	K	F	Cl	OH	total	
RSA03-01	37.29	15.21	1.92	20.86	0.36	10.18	<LLD	0.06	9.35	0.021	0.0008	96.05	5.722	2.278	0.473	0.222	2.677	0.047	2.329	0.000	0.018	1.830	0.021	0.001	3.880	15.596	0.47
RSA03-04	36.93	15.08	2.08	21.86	0.43	10.14	0.06	0.05	9.19	0.018	0.0008	96.56	5.666	2.334	0.393	0.240	2.805	0.056	2.319	0.010	0.015	1.799	0.018	0.001	3.420	15.637	0.45
RSA03-06	37.35	14.72	2.16	21.50	0.37	10.54	0.07	0.09	9.13	0.022	0.0013	96.83	5.708	2.292	0.359	0.248	2.748	0.048	2.401	0.011	0.027	1.780	0.022	0.001	3.150	15.622	0.47
RSA03-07	36.10	14.74	2.01	21.74	0.35	10.08	0.19	0.15	8.92	0.020	0.0014	95.12	5.634	2.366	0.345	0.236	2.837	0.046	2.345	0.032	0.045	1.776	0.020	0.001	3.979	15.662	0.45
RSA03-09	37.04	15.46	1.42	21.25	0.38	9.97	<LLD	<LLD	9.54	0.018	0.0008	95.80	5.715	2.285	0.526	0.165	2.742	0.050	2.293	0.000	0.000	1.878	0.018	0.001	3.981	15.654	0.46
RSA03-10	37.89	14.55	2.80	22.16	0.36	9.42	<LLD	0.05	9.38	0.018	0.0010	97.33	5.764	2.236	0.372	0.320	2.819	0.046	2.136	0.000	0.015	1.820	0.018	0.001	2.650	15.529	0.43
RSA03-13	37.03	14.99	2.87	21.79	0.39	9.49	<LLD	0.08	9.61	0.017	0.0013	96.98	5.666	2.334	0.369	0.330	2.788	0.051	2.165	0.000	0.024	1.876	0.017	0.001	3.000	15.602	0.44
RSA03-18	36.46	14.34	3.09	22.44	0.38	9.11	<LLD	0.05	9.20	0.018	0.0013	95.82	5.668	2.332	0.296	0.361	2.918	0.050	2.111	0.000	0.015	1.825	0.018	0.001	3.981	15.576	0.42
RSA03-20	36.26	14.25	3.02	22.64	0.40	9.29	0.08	0.07	9.28	0.019	0.0011	96.06	5.640	2.360	0.252	0.353	2.945	0.053	2.154	0.013	0.021	1.841	0.019	0.001	3.920	15.632	0.42
RSA03-21	36.91	14.44	3.12	23.02	0.39	9.21	0.05	<LLD	9.13	0.019	0.0010	97.04	5.669	2.331	0.283	0.361	2.957	0.051	2.109	0.008	0.000	1.789	0.019	0.001	2.940	15.558	0.42
RSA03-22	36.12	15.42	2.09	22.19	0.36	9.70	0.12	0.03	9.27	0.018	0.0014	96.08	5.594	2.406	0.408	0.243	2.874	0.047	2.239	0.020	0.009	1.831	0.018	0.001	3.850	15.672	0.44
RSA03-23	36.39	15.40	2.29	22.30	0.32	9.71	0.09	0.09	9.22	0.025	0.0010	96.81	5.601	2.399	0.395	0.265	2.871	0.042	2.228	0.015	0.027	1.811	0.025	0.001	3.070	15.653	0.44
RSA03-24	36.19	14.67	2.55	23.06	0.37	9.92	0.29	0.12	8.98	0.021	0.0017	97.05	5.579	2.421	0.245	0.296	2.973	0.048	2.280	0.048	0.036	1.766	0.021	0.002	2.920	15.692	0.43
RSA01-02	36.73	14.88	2.14	22.24	0.31	9.29	<LLD	<LLD	9.86	0.034	<LLD	96.70	5.687	2.313	0.403	0.249	2.880	0.041	2.144	0.000	0.000	1.948	0.034		3.150	15.664	0.43
RSA01-03	37.40	15.13	1.76	21.19	0.33	9.90	0.03	<LLD	9.88	0.034	0.0003	96.91	5.736	2.264	0.471	0.203	2.718	0.043	2.264	0.005	0.000	1.933	0.034	0.000	2.970	15.636	0.45
RSA01-04	36.82	15.24	1.57	21.34	0.32	9.94	0.02	<LLD	9.78	0.029	0.0003	96.14	5.693	2.307	0.470	0.183	2.760	0.042	2.291	0.003	0.000	1.929	0.029	0.000	3.730	15.678	0.45
RSA01-05	37.87	15.25	1.92	22.12	0.34	9.43	<LLD	<LLD	10.02	0.030	0.0003	98.09	5.748	2.252	0.476	0.219	2.808	0.044	2.134	0.000	0.000	1.940	0.030	0.000	1.830	15.621	0.43
RSA01-06	36.38	15.41	0.85	21.91	0.36	10.15	0.06	0.05	9.53	0.031	0.0003	95.86	5.662	2.338	0.488	0.100	2.852	0.047	2.355	0.010	0.015	1.892	0.031	0.000	3.969	15.759	0.45
SWA18a-01	34.62	14.80	3.97	22.84	0.53	9.37	0.04	0.07	8.57	0.022	0.0014	95.74	5.418	2.582	0.147	0.467	2.989	0.070	2.186	0.007	0.021	1.711	0.022	0.001	3.976	15.599	0.42
SWA18a-02	36.69	14.38	4.08	21.79	0.53	9.36	0.05	0.05	9.64	0.025	0.0014	97.60	5.607	2.393	0.198	0.469	2.785	0.069	2.133	0.008	0.015	1.880	0.025	0.001	2.320	15.555	0.43
SWA18a-03	35.97	14.77	3.66	21.54	0.54	9.20	0.02	0.03	9.47	0.025	0.0017	96.25	5.576	2.424	0.275	0.427	2.793	0.071	2.126	0.003	0.009	1.873	0.025	0.002	3.680	15.577	0.43
SWA18a-04	35.12	14.61	3.50	22.34	0.53	9.00	0.09	0.06	8.81	0.024	0.0014	95.06	5.529	2.471	0.239	0.415	2.941	0.071	2.112	0.015	0.018	1.769	0.024	0.001	3.974	15.581	0.42
SWA18a-07	35.59	14.72	3.46	21.06	0.48	9.68	0.13	0.17	8.95	0.027	0.0016	95.35	5.554	2.446	0.261	0.406	2.748	0.063	2.252	0.022	0.051	1.782	0.027	0.002	3.971	15.586	0.45
SWA18a-08	35.41	14.13	3.48	21.47	0.54	9.87	0.05	0.14	9.37	0.029	0.0013	95.64	5.549	2.451	0.159	0.410	2.814	0.072	2.306	0.008	0.043	1.873	0.029	0.001	3.969	15.685	0.45
SWA18a-09	35.88	14.10	3.60	21.34	0.54	9.88	0.16	0.09	9.32	0.030	0.0017	96.15	5.582	2.418	0.167	0.421	2.776	0.071	2.291	0.027	0.027	1.850	0.030	0.002	3.780	15.630	0.45
SWA18a-10	36.72	14.64	3.16	20.03	0.36	10.02	0.07	0.12	9.48	0.030	0.0016	95.83	5.673	2.327	0.339	0.367	2.588	0.047	2.308	0.012	0.036	1.868	0.030	0.002	3.968	15.565	0.47
SWA18a-11	35.96	15.15	3.18	20.24	0.36	10.26	0.02	0.05	9.78	0.030	0.0016	96.22	5.554	2.446	0.312	0.370	2.614	0.047	2.362	0.003	0.015	1.927	0.030	0.002	3.680	15.651	0.47
SWA18a-12	36.23	15.94	2.84	19.80	0.14	10.24	<LLD	0.09	9.68	0.034	0.0018	96.35	5.566	2.434	0.453	0.328	2.544	0.018	2.345	0.000	0.027	1.897	0.034	0.002	3.570	15.613	0.48
SWA18a-13	36.12	15.59	2.41	20.01	0.21	10.52	<LLD	0.11	9.34	0.033	0.0016	95.66	5.590	2.410	0.433	0.281	2.590	0.028	2.427	0.000	0.033	1.844	0.033	0.002	3.965	15.635	0.48
RSA05-01	34.68	15.64	2.28	25.75	0.47	8.09	0.02	0.05	8.69	0.020	0.0013	96.49	5.448	2.552	0.344	0.269	3.383	0.063	1.895	0.003	0.015	1.742	0.020	0.001	3.490	15.713	0.36
RSA05-03	35.59	15.13	3.33	24.76	0.44	7.10	<LLD	0.05	9.60	0.020	0.0014	96.84	5.558	2.442	0.343	0.391	3.234	0.058	1.653	0.000	0.015	1.913	0.020	0.001	3.080	15.607	0.34
RSA05-05	35.25	15.69	2.42	24.74	0.36	7.57	0.11	0.09	9.27	0.017	0.0020	96.26	5.521	2.479	0.418	0.285	3.241	0.048	1.768	0.018	0.027	1.852	0.017	0.002	3.620	15.658	0.35

Table 5.2 continued.

Analysis	Concentration (wt%)										- O equivalent		Structural formula (cations / 22 oxygen)												Cation	Mg#
	SiO	Al	TiO	FeO	MnO	MgO	CaO	Na	K	F	Cl	Total	Si	Al^{IV}	Al^{VI}	Ti	Fe^{2+}	Mn	Mg	Ca	Na	K	F	Cl	OH	total	
RSA05-06	35.41	15.41	2.85	24.98	0.37	7.27	0.21	0.17	9.07	0.017	0.0014	96.47	5.537	2.463	0.378	0.335	3.267	0.049	1.695	0.035	0.052	1.809	0.017	0.001	3.450	15.620	0.34
RSA05-09	34.47	15.17	2.93	24.54	0.39	7.44	0.11	0.08	8.63	0.015	0.0016	94.42	5.497	2.503	0.348	0.352	3.273	0.053	1.769	0.019	0.025	1.756	0.015	0.002	3.983	15.592	0.35
RSA05-10	36.02	15.22	3.13	24.65	0.41	7.34	0.05	0.08	9.52	0.017	0.0013	97.15	5.584	2.416	0.365	0.365	3.196	0.054	1.696	0.008	0.024	1.883	0.017	0.001	2.720	15.591	0.35
RSA05-11	35.01	14.96	3.11	24.54	0.37	7.17	0.20	0.14	8.86	0.017	0.0017	95.12	5.550	2.450	0.345	0.371	3.253	0.050	1.694	0.034	0.043	1.792	0.017	0.002	3.981	15.582	0.34
RSA05-12	33.95	14.18	3.34	24.86	0.46	6.66	0.19	0.14	8.83	0.018	0.0016	93.40	5.522	2.478	0.240	0.409	3.382	0.063	1.615	0.033	0.044	1.832	0.018	0.002	3.980	15.618	0.32
RSA05-13	35.23	15.07	2.94	24.72	0.38	7.36	0.08	0.16	9.40	0.016	0.0020	96.06	5.538	2.462	0.331	0.348	3.250	0.051	1.725	0.013	0.049	1.885	0.016	0.002	3.820	15.651	0.35
RSA05-14	34.34	14.92	3.17	25.20	0.44	7.01	0.03	0.03	9.28	0.020	0.0017	95.27	5.483	2.517	0.291	0.381	3.365	0.060	1.669	0.005	0.009	1.890	0.020	0.002	3.979	15.670	0.33
RSA02-01	36.45	15.64	1.73	20.80	0.31	9.97	<LLD	<LLD	9.16	0.017	0.0008	94.74	5.667	2.333	0.532	0.202	2.704	0.041	2.311	0.000	0.000	1.817	0.017	0.001	3.982	15.607	0.46
RSA02-02	36.50	15.80	1.69	20.68	0.29	10.00	<LLD	0.02	9.18	0.017	0.0007	94.83	5.663	2.337	0.552	0.197	2.683	0.038	2.313	0.000	0.006	1.817	0.017	0.001	3.982	15.607	0.46
RSA02-03	36.82	15.66	1.40	20.91	0.27	9.86	0.07	<LLD	9.65	0.018	0.0004	95.33	5.700	2.300	0.558	0.163	2.707	0.035	2.276	0.012	0.000	1.906	0.018	0.000	3.982	15.657	0.46
RSA02-04	37.64	16.41	0.80	20.37	0.29	10.14	<LLD	0.05	9.85	0.019	0.0006	96.28	5.740	2.260	0.690	0.092	2.598	0.037	2.305	0.000	0.015	1.916	0.019	0.001	3.670	15.653	0.47
RSA02-14	36.30	14.92	2.46	22.79	0.29	8.50	0.02	0.03	9.43	0.016	0.0007	95.38	5.674	2.326	0.422	0.289	2.979	0.038	1.981	0.003	0.009	1.880	0.016	0.001	3.983	15.602	0.40
RSA02-15	36.17	14.81	2.94	22.51	0.32	8.36	<LLD	0.06	9.32	0.015	0.0007	95.09	5.662	2.338	0.394	0.346	2.947	0.042	1.951	0.000	0.018	1.861	0.015	0.001	3.984	15.560	0.40
RSA02-16	38.83	16.05	1.74	20.77	0.30	9.98	0.12	0.07	9.31	0.017	0.0007	97.84	5.797	2.203	0.621	0.195	2.593	0.038	2.221	0.019	0.020	1.773	0.017	0.001	2.100	15.481	0.46
RSA02-17	36.50	14.69	2.79	21.88	0.31	9.03	0.26	0.13	8.91	0.018	0.0008	95.22	5.681	2.319	0.375	0.327	2.848	0.041	2.095	0.043	0.039	1.769	0.018	0.001	3.981	15.538	0.42
RSA02-19	36.72	14.88	3.46	22.39	0.31	8.47	0.25	0.04	9.36	0.015	0.0006	96.48	5.651	2.349	0.350	0.401	2.882	0.040	1.943	0.041	0.012	1.838	0.015	0.001	3.430	15.507	0.40
RSA02-23	36.76	15.66	1.42	21.37	0.32	9.38	0.06	0.05	9.52	0.019	0.0006	95.28	5.706	2.294	0.571	0.166	2.774	0.042	2.171	0.010	0.015	1.885	0.019	0.001	3.980	15.634	0.44
SWA07-03	35.82	15.78	2.17	25.96	0.35	6.38	<LLD	0.05	9.29	0.013	0.0014	96.37	5.617	2.383	0.533	0.256	3.405	0.046	1.491	0.000	0.015	1.858	0.013	0.001	3.620	15.606	0.30
SWA07-08	36.25	15.29	2.49	26.64	0.40	6.27	<LLD	0.06	9.53	0.013	0.0018	97.55	5.641	2.359	0.445	0.291	3.467	0.053	1.454	0.000	0.018	1.892	0.013	0.002	2.440	15.621	0.30
SWA07-09	35.83	15.24	2.18	26.43	0.43	6.25	0.05	0.06	9.36	0.013	0.0020	96.45	5.641	2.359	0.468	0.258	3.480	0.057	1.467	0.008	0.018	1.880	0.013	0.002	3.540	15.637	0.30
SWA07-13	35.11	14.98	2.30	26.07	0.39	6.19	0.21	0.11	8.69	0.014	0.0021	94.72	5.618	2.382	0.443	0.277	3.489	0.053	1.477	0.036	0.034	1.774	0.014	0.002	3.984	15.582	0.30
SWA07-14	35.34	15.12	2.18	26.20	0.41	6.28	0.16	0.10	8.53	0.014	0.0020	94.97	5.633	2.367	0.474	0.261	3.493	0.055	1.492	0.027	0.031	1.735	0.014	0.002	3.984	15.568	0.30
SWA07-16	34.79	15.29	1.74	26.01	0.37	6.33	0.07	<LLD	8.74	0.015	0.0013	93.97	5.612	2.388	0.519	0.211	3.509	0.051	1.522	0.012	0.000	1.799	0.015	0.001	3.984	15.623	0.30
SWA07-22	35.77	15.42	2.25	25.93	0.34	6.27	<LLD	0.07	9.70	0.015	0.0016	96.42	5.631	2.369	0.491	0.266	3.414	0.045	1.471	0.000	0.021	1.948	0.015	0.002	3.560	15.657	0.30
SWA07-23	35.90	15.35	2.45	26.30	0.39	6.17	<LLD	0.07	9.71	0.014	0.0014	96.95	5.620	2.380	0.452	0.289	3.443	0.052	1.440	0.000	0.021	1.939	0.014	0.001	2.960	15.635	0.29
SWA07-26	36.13	16.16	2.07	25.19	0.36	6.45	0.08	0.10	9.23	0.015	0.0010	96.38	5.634	2.366	0.603	0.243	3.285	0.048	1.499	0.013	0.030	1.836	0.015	0.001	3.550	15.557	0.31
SWA07-27	35.27	15.88	2.22	25.49	0.37	6.21	<LLD	0.08	9.58	0.013	0.0008	95.63	5.581	2.419	0.543	0.264	3.373	0.050	1.465	0.000	0.025	1.934	0.013	0.001	3.987	15.653	0.30
SWA07-29	35.67	15.59	3.06	25.82	0.40	5.91	<LLD	0.08	9.35	0.012	0.0017	96.45	5.594	2.406	0.475	0.361	3.386	0.053	1.382	0.000	0.024	1.871	0.012	0.002	3.540	15.552	0.29
SWA07-36	36.10	15.96	1.95	24.95	0.35	6.38	<LLD	<LLD	9.69	0.015	0.0011	96.01	5.665	2.335	0.616	0.230	3.274	0.047	1.492	0.000	0.000	1.940	0.015	0.001	3.970	15.599	0.31
SWA07-37	36.56	15.94	1.64	25.01	0.37	6.62	<LLD	<LLD	9.44	0.014	0.0010	96.17	5.704	2.296	0.636	0.193	3.264	0.049	1.540	0.000	0.000	1.879	0.014	0.001	3.760	15.559	0.32
RSA08-01	36.03	14.48	2.43	25.34	0.31	7.07	<LLD	0.09	9.00	0.014	0.0017	95.39	5.697	2.303	0.395	0.289	3.351	0.042	1.667	0.000	0.028	1.815	0.014	0.002	3.984	15.586	0.33
RSA08-02	35.63	14.45	2.99	25.60	0.35	6.88	<LLD	0.05	9.25	0.013	0.0017	95.81	5.628	2.372	0.318	0.355	3.382	0.047	1.620	0.000	0.015	1.864	0.013	0.002	3.985	15.602	0.32

Table 5.2 continued.

Analysis	Concentration (wt%)									- O equivalent			Structural formula (cations / 22 oxygen)												Cation	Mg#
	SiO	Al	TiO	FeO	MnO	MgO	CaO	Na	K	F	Cl	Total	Si	Al^{IV}	Al^{VI}	Ti	Fe^{2+}	Mn	Mg	Ca	Na	K	F	Cl	OH	total	
RSA08-03	35.51	14.25	3.38	25.65	0.34	6.55	<LLD	0.05	9.38	0.014	0.0017	95.76	5.627	2.373	0.288	0.403	3.399	0.046	1.547	0.000	0.015	1.896	0.014	0.002	3.984	15.595	0.31
RSA08-04	36.10	14.93	3.21	25.85	0.34	6.81	<LLD	0.05	9.43	0.013	0.0017	97.32	5.608	2.392	0.341	0.375	3.358	0.045	1.577	0.000	0.015	1.869	0.013	0.002	2.630	15.580	0.32
RSA08-05	35.77	14.64	3.50	25.60	0.31	6.60	0.04	<LLD	9.22	0.013	0.0020	96.30	5.613	2.387	0.321	0.413	3.360	0.041	1.544	0.007	0.000	1.846	0.013	0.002	3.640	15.531	0.31
RSA08-06	35.17	15.22	2.58	25.44	0.33	7.02	0.04	0.05	8.88	0.013	0.0021	95.37	5.570	2.430	0.411	0.307	3.370	0.044	1.657	0.007	0.015	1.794	0.013	0.002	3.984	15.607	0.33
RSA08-07	35.79	14.94	3.03	25.15	0.32	6.76	<LLD	0.05	9.32	0.013	0.0021	95.98	5.623	2.377	0.390	0.358	3.305	0.043	1.583	0.000	0.015	1.868	0.013	0.002	3.960	15.562	0.32
RSA08-08	35.98	14.98	2.69	24.68	0.30	6.99	<LLD	0.07	9.42	0.014	0.0023	95.78	5.659	2.341	0.436	0.318	3.246	0.040	1.639	0.000	0.021	1.890	0.014	0.002	3.984	15.590	0.34
RSA08-09	35.75	14.74	2.41	25.19	0.32	7.04	0.07	0.06	9.26	0.014	0.0021	95.52	5.652	2.348	0.399	0.287	3.331	0.043	1.659	0.012	0.018	1.868	0.014	0.002	3.983	15.616	0.33
RSA08-10	35.86	14.69	2.58	25.19	0.34	7.03	<LLD	0.05	9.31	0.017	0.0020	95.80	5.657	2.343	0.389	0.306	3.324	0.045	1.653	0.000	0.015	1.874	0.017	0.002	3.981	15.606	0.33
RSA08-13	35.59	14.29	2.53	24.68	0.31	6.97	0.05	0.05	8.58	0.014	0.0017	93.70	5.706	2.294	0.407	0.305	3.309	0.042	1.666	0.009	0.016	1.755	0.014	0.002	3.984	15.509	0.33
SWA10a-01	34.12	16.47	3.37	25.33	0.32	4.96	<LLD	0.10	9.40	0.012	0.0014	94.61	5.464	2.536	0.573	0.406	3.393	0.043	1.184	0.000	0.031	1.921	0.012	0.001	3.987	15.551	0.26
SWA10a-02	33.41	16.52	3.33	25.92	0.30	4.84	<LLD	0.05	8.73	0.012	0.0017	93.65	5.413	2.587	0.567	0.406	3.512	0.041	1.169	0.000	0.016	1.804	0.012	0.002	3.987	15.514	0.25
SWA10a-03	33.85	16.89	2.53	25.66	0.34	5.14	0.04	<LLD	8.99	0.011	0.0017	93.98	5.454	2.546	0.661	0.307	3.457	0.046	1.235	0.007	0.000	1.848	0.011	0.002	3.987	15.560	0.26
SWA10a-04	33.39	16.36	3.48	25.19	0.41	5.33	<LLD	0.05	8.78	0.014	0.0013	93.59	5.403	2.597	0.524	0.424	3.409	0.056	1.286	0.000	0.016	1.813	0.014	0.001	3.985	15.527	0.27
SWA10a-05	34.12	16.19	3.55	24.44	0.27	5.12	<LLD	<LLD	9.37	0.015	0.0016	93.71	5.500	2.500	0.576	0.431	3.295	0.037	1.230	0.000	0.000	1.927	0.015	0.002	3.984	15.495	0.27
SWA10a-09	34.38	16.14	3.30	24.90	0.33	5.28	0.05	<LLD	9.47	0.015	0.0014	94.50	5.508	2.492	0.555	0.398	3.336	0.045	1.261	0.009	0.000	1.935	0.015	0.001	3.984	15.539	0.27
SWA10a-10	34.04	15.97	3.21	25.49	0.31	5.29	<LLD	<LLD	8.98	0.015	0.0010	93.90	5.493	2.507	0.530	0.390	3.440	0.042	1.273	0.000	0.000	1.849	0.015	0.001	3.984	15.523	0.27
SWA10a-11	33.82	15.81	3.36	25.19	0.33	5.13	<LLD	<LLD	9.30	0.014	0.0016	93.57	5.488	2.512	0.512	0.410	3.419	0.045	1.241	0.000	0.000	1.925	0.014	0.002	3.984	15.552	0.27
SWA10a-12	33.71	16.08	3.23	25.93	0.37	4.89	<LLD	0.05	9.32	0.012	0.0016	94.13	5.454	2.546	0.519	0.393	3.508	0.051	1.179	0.000	0.016	1.924	0.012	0.002	3.987	15.590	0.25
SWA10a-13	33.83	15.82	3.30	25.33	0.35	5.32	<LLD	<LLD	9.59	0.016	0.0014	94.22	5.468	2.532	0.481	0.401	3.424	0.048	1.282	0.000	0.000	1.977	0.016	0.001	3.983	15.613	0.27
SWA10a-15	33.67	16.08	3.74	24.26	0.34	4.97	<LLD	0.07	9.43	0.012	0.0017	93.13	5.468	2.532	0.546	0.457	3.295	0.047	1.203	0.000	0.022	1.954	0.012	0.002	3.986	15.524	0.27
SWA10a-16	34.05	16.60	3.03	24.34	0.34	5.10	<LLD	<LLD	8.92	0.012	0.0020	92.98	5.510	2.490	0.677	0.369	3.294	0.047	1.230	0.000	0.000	1.842	0.012	0.002	3.986	15.458	0.27
SWA20-02	34.82	14.92	2.29	23.95	0.30	6.66	0.09	<LLD	9.04	0.014	0.0006	92.63	5.652	2.348	0.506	0.280	3.251	0.041	1.612	0.016	0.000	1.872	0.014	0.001	3.985	15.577	0.33
SWA20-05	35.86	15.51	2.09	24.05	0.27	6.99	<LLD	<LLD	9.46	0.015	0.0006	94.82	5.672	2.328	0.564	0.249	3.182	0.036	1.648	0.000	0.000	1.909	0.015	0.001	3.984	15.588	0.34
SWA20-06	34.11	15.66	1.47	24.26	0.27	7.01	<LLD	<LLD	9.58	0.011	<LLD	92.75	5.551	2.449	0.554	0.180	3.302	0.037	1.701	0.000	0.000	1.989	0.011		3.989	15.762	0.34
SWA20-07	34.13	15.76	1.42	24.36	0.29	6.80	0.21	<LLD	8.77	0.011	<LLD	92.14	5.569	2.431	0.600	0.174	3.324	0.040	1.654	0.037	0.000	1.826	0.011		3.989	15.654	0.33
SWA20-08	34.61	14.86	2.22	23.63	0.25	7.11	0.06	0.06	9.35	0.014	0.0004	92.69	5.620	2.380	0.463	0.271	3.209	0.034	1.721	0.010	0.019	1.937	0.014	0.000	3.986	15.665	0.35
SWA20-09	35.03	15.00	2.40	23.65	0.28	6.77	<LLD	0.10	9.41	0.016	0.0007	93.26	5.650	2.350	0.502	0.291	3.190	0.038	1.628	0.000	0.031	1.936	0.016	0.001	3.984	15.617	0.34
SWA20-10	35.34	14.97	2.46	23.57	0.28	6.74	<LLD	0.08	9.49	0.014	0.0004	93.47	5.676	2.324	0.510	0.297	3.166	0.038	1.614	0.000	0.025	1.945	0.014	0.000	3.986	15.594	0.34
SWA20-11	34.83	15.27	1.55	23.42	0.27	7.32	0.04	0.09	9.16	0.015	<LLD	92.50	5.645	2.355	0.562	0.189	3.175	0.037	1.769	0.007	0.028	1.894	0.015		3.985	15.661	0.36
SWA20-12	35.57	15.28	1.85	23.64	0.27	7.27	0.05	0.09	9.47	0.016	0.0006	94.11	5.672	2.328	0.544	0.222	3.153	0.036	1.728	0.009	0.028	1.927	0.016	0.001	3.984	15.647	0.35
SWA20-14	34.35	15.02	2.14	23.66	0.26	6.86	<LLD	0.06	9.78	0.014	0.0006	92.68	5.598	2.402	0.482	0.262	3.224	0.036	1.667	0.000	0.019	2.033	0.014	0.001	3.986	15.724	0.34
SWA20-15	34.99	15.37	2.18	23.65	0.28	7.06	<LLD	0.05	9.43	0.014	0.0004	93.58	5.617	2.383	0.525	0.263	3.175	0.038	1.690	0.000	0.016	1.931	0.014	0.000	3.985	15.639	0.35

Table 5.2 continued.

Analysis	Concentration (wt%)										- O equivalent		Structural formula (cations / 22 oxygen)												Cation	Mg#
	SiO	Al	TiO	FeO	MnO	MgO	CaO	Na	K	F	Cl	Total	Si	Al^{IV}	Al^{VI}	Ti	Fe^{2+}	Mn	Mg	Ca	Na	K	F	Cl	OH	total	
SWA03-01	37.24	17.56	1.36	24.12	0.43	6.43	<LLD	0.05	9.19	0.014	<LLD	96.90	5.705	2.295	0.876	0.157	3.090	0.056	1.469	0.000	0.015	1.796	0.014		3.090	15.458	0.32
SWA03-03	35.39	17.58	1.38	24.64	0.42	6.10	0.05	0.14	8.77	0.013	<LLD	94.94	5.568	2.432	0.828	0.163	3.242	0.056	1.431	0.008	0.043	1.760	0.013		3.987	15.532	0.31
SWA03-04	36.02	17.49	1.67	24.75	0.45	6.13	0.16	0.16	8.66	0.013	<LLD	95.96	5.599	2.401	0.803	0.195	3.217	0.059	1.420	0.027	0.048	1.717	0.013		3.987	15.487	0.31
SWA03-08	36.63	18.20	1.11	23.61	0.44	6.30	<LLD	<LLD	9.51	0.013	<LLD	96.29	5.648	2.352	0.955	0.129	3.045	0.057	1.448	0.000	0.000	1.871	0.013		3.700	15.505	0.32
SWA03-09	34.70	17.36	1.24	25.70	0.43	6.29	0.04	0.05	8.53	0.012	<LLD	94.80	5.503	2.497	0.748	0.148	3.409	0.058	1.487	0.007	0.015	1.726	0.012		3.988	15.597	0.30
SWA03-10	35.99	17.13	2.24	25.06	0.51	5.62	0.19	0.13	8.58	0.012	0.0004	95.93	5.607	2.393	0.753	0.263	3.265	0.067	1.305	0.032	0.039	1.705	0.012	0.000	3.987	15.430	0.29
SWA03-11	35.24	16.86	2.06	25.44	0.46	5.60	0.18	0.12	8.74	0.011	<LLD	95.12	5.566	2.434	0.705	0.245	3.361	0.062	1.319	0.030	0.037	1.761	0.011		3.989	15.519	0.28
SWA03-15	36.04	17.07	1.62	24.58	0.47	6.16	0.20	0.06	8.75	0.014	<LLD	95.49	5.636	2.364	0.782	0.191	3.215	0.062	1.436	0.034	0.018	1.746	0.014		3.986	15.482	0.31
SWA03-23	37.16	17.48	0.69	23.01	0.43	6.76	0.06	0.05	9.52	0.020	<LLD	95.89	5.752	2.248	0.941	0.080	2.979	0.056	1.560	0.010	0.015	1.880	0.020		3.980	15.521	0.34
SWA03-26	35.42	16.59	2.08	25.15	0.48	5.67	0.10	0.07	8.94	0.013	<LLD	94.97	5.603	2.397	0.696	0.248	3.327	0.064	1.337	0.017	0.021	1.804	0.013		3.987	15.515	0.29
RSA06-01	36.81	14.60	3.61	21.06	0.49	8.88	<LLD	0.08	9.54	0.021	0.0011	95.92	5.689	2.311	0.348	0.420	2.722	0.064	2.046	0.000	0.024	1.881	0.021	0.001	3.978	15.505	0.43
RSA06-02	35.59	14.57	3.42	21.00	0.48	8.90	<LLD	0.11	9.36	0.023	0.0014	94.39	5.613	2.387	0.321	0.406	2.770	0.064	2.093	0.000	0.034	1.883	0.023	0.001	3.975	15.571	0.43
RSA06-03	36.15	14.71	3.38	21.35	0.43	8.90	<LLD	0.06	9.27	0.016	0.0016	94.96	5.646	2.354	0.354	0.397	2.789	0.057	2.072	0.000	0.018	1.847	0.016	0.002	3.982	15.535	0.43
RSA06-04	36.52	14.05	3.60	22.57	0.47	8.88	0.03	0.08	9.52	0.029	0.0016	96.89	5.655	2.345	0.218	0.419	2.923	0.062	2.050	0.005	0.024	1.880	0.029	0.002	3.020	15.581	0.41
RSA06-05	36.09	14.26	3.20	22.83	0.39	9.01	0.16	0.03	9.08	0.020	0.0008	95.84	5.625	2.375	0.245	0.375	2.976	0.051	2.094	0.027	0.009	1.806	0.020	0.001	3.979	15.582	0.41
RSA06-06	36.44	14.31	3.19	22.54	0.45	9.27	0.08	0.02	9.38	0.023	0.0010	96.59	5.641	2.359	0.252	0.372	2.918	0.059	2.139	0.013	0.006	1.852	0.023	0.001	3.370	15.611	0.42
RSA06-07	35.91	14.42	2.95	21.66	0.39	9.71	0.17	0.07	9.44	0.035	0.0018	96.15	5.602	2.398	0.253	0.346	2.826	0.052	2.258	0.028	0.021	1.879	0.035	0.002	3.730	15.662	0.44
RSA06-08	36.76	14.82	2.65	21.16	0.36	9.39	0.23	0.06	9.18	0.031	0.0018	95.90	5.697	2.303	0.404	0.309	2.742	0.047	2.169	0.038	0.018	1.815	0.031	0.002	3.967	15.543	0.44
RSA06-10	35.97	14.14	3.43	21.71	0.46	9.05	<LLD	0.06	9.58	0.032	0.0007	95.64	5.636	2.364	0.247	0.404	2.845	0.061	2.114	0.000	0.018	1.915	0.032	0.001	3.967	15.603	0.43
RSA06-11	36.01	13.93	3.49	21.96	0.46	9.21	<LLD	0.10	9.37	0.033	0.0007	95.81	5.634	2.366	0.202	0.411	2.873	0.061	2.148	0.000	0.030	1.870	0.033	0.001	3.966	15.595	0.43
SWA13a-02	34.40	16.86	2.14	26.56	0.36	5.23	0.16	0.05	8.67	0.008	0.0004	94.74	5.488	2.512	0.659	0.257	3.544	0.049	1.244	0.027	0.015	1.765	0.008	0.000	3.992	15.560	0.26
SWA13a-04	35.27	16.63	2.08	26.50	0.39	5.31	0.08	0.03	9.14	0.007	0.0006	95.73	5.562	2.438	0.652	0.247	3.495	0.052	1.248	0.014	0.009	1.839	0.007	0.001	3.992	15.555	0.26
SWA13a-05	34.30	16.47	1.88	26.73	0.38	5.09	0.16	0.05	8.79	0.008	0.0006	94.17	5.519	2.481	0.642	0.228	3.597	0.052	1.221	0.028	0.016	1.804	0.008	0.001	3.992	15.587	0.25
SWA13a-07	34.83	17.46	1.61	26.01	0.37	5.64	0.17	0.09	8.99	0.009	0.0006	95.54	5.494	2.506	0.739	0.191	3.431	0.049	1.326	0.029	0.028	1.809	0.009	0.001	3.990	15.602	0.28
SWA13a-08	34.92	16.80	1.40	27.07	0.40	5.65	0.08	0.07	8.77	0.008	<LLD	95.47	5.532	2.468	0.669	0.167	3.587	0.054	1.334	0.014	0.022	1.772	0.008		3.992	15.618	0.27
SWA13a-09	34.19	16.66	1.92	27.56	0.39	5.39	0.19	0.07	8.60	0.008	0.0007	95.32	5.452	2.548	0.583	0.230	3.675	0.053	1.281	0.032	0.022	1.749	0.008	0.001	3.991	15.626	0.26
SWA13a-10	34.27	16.45	1.58	27.22	0.40	5.45	0.03	<LLD	8.73	0.008	0.0006	94.47	5.508	2.492	0.624	0.191	3.659	0.054	1.306	0.005	0.000	1.790	0.008	0.001	3.991	15.629	0.26
SWA13a-11	34.52	16.13	1.98	26.85	0.38	5.16	0.06	0.05	9.06	0.008	0.0006	94.53	5.548	2.452	0.603	0.239	3.609	0.052	1.236	0.010	0.016	1.857	0.008	0.001	3.991	15.622	0.26
SWA11-01	34.08	16.13	2.59	27.20	0.40	4.80	0.20	0.05	8.31	0.008	0.0020	94.21	5.494	2.506	0.558	0.314	3.667	0.055	1.153	0.035	0.016	1.709	0.008	0.002	3.990	15.506	0.24
SWA09-01	35.25	16.96	2.64	26.62	0.26	4.86	0.08	0.14	8.75	0.015	0.0016	96.23	5.538	2.462	0.678	0.312	3.497	0.035	1.138	0.013	0.043	1.754	0.015	0.002	3.730	15.470	0.25
SWA09-03	35.39	16.55	2.92	26.94	0.35	4.93	0.06	0.14	9.29	0.017	0.0017	97.32	5.529	2.471	0.576	0.343	3.520	0.046	1.148	0.010	0.042	1.851	0.017	0.002	2.620	15.537	0.25
SWA09-05	34.15	17.03	2.43	26.38	0.31	5.23	<LLD	0.06	9.03	0.018	0.0014	95.40	5.440	2.560	0.638	0.291	3.515	0.042	1.242	0.000	0.019	1.835	0.018	0.001	3.980	15.582	0.26

Table 5.2 continued.

Analysis	Concentration (wt%)									- O equivalent			Structural formula (cations / 22 oxygen)												Cation	
	SiO	Al	TiO	FeO	MnO	MgO	CaO	Na	K	F	Cl	Total	Si	Al^{IV}	Al^{VI}	Ti	Fe^{2+}	Mn	Mg	Ca	Na	K	F	Cl	OH	total	Mg#
SWA09-06	35.04	16.77	2.50	26.32	0.31	5.11	0.09	0.07	9.26	0.018	0.0017	96.26	5.523	2.477	0.639	0.296	3.470	0.041	1.201	0.015	0.021	1.862	0.018	0.002	3.640	15.546	0.26
SWA09-07	35.29	16.63	2.66	26.83	0.39	4.99	0.08	0.08	9.28	0.017	0.0014	96.95	5.532	2.468	0.604	0.314	3.517	0.052	1.166	0.013	0.024	1.856	0.017	0.001	2.960	15.546	0.25
SWA09-08	35.07	16.61	2.55	26.87	0.27	4.96	0.02	<LLD	9.83	0.017	0.0014	96.92	5.517	2.483	0.597	0.302	3.535	0.036	1.163	0.003	0.000	1.973	0.017	0.001	2.960	15.610	0.25
SWA09-09	34.80	16.74	2.47	26.50	0.28	5.61	0.02	<LLD	9.35	0.019	0.0020	96.61	5.478	2.522	0.583	0.292	3.488	0.037	1.316	0.003	0.000	1.878	0.019	0.002	3.260	15.599	0.27
SWA09-10	35.11	16.57	2.50	26.60	0.32	5.40	0.04	0.07	9.00	0.019	0.0024	96.48	5.524	2.476	0.597	0.296	3.500	0.043	1.267	0.007	0.021	1.806	0.019	0.002	3.420	15.536	0.27
SWA09-11	35.46	17.15	2.54	26.36	0.38	5.05	0.05	0.11	9.42	0.017	0.0018	97.26	5.525	2.475	0.674	0.298	3.435	0.050	1.173	0.008	0.033	1.872	0.017	0.002	2.680	15.544	0.25
SWA09-12	35.27	16.91	2.50	26.08	0.35	5.11	0.04	0.08	9.45	0.017	0.0016	96.54	5.536	2.464	0.664	0.295	3.423	0.047	1.196	0.007	0.024	1.892	0.017	0.002	3.400	15.548	0.26
SWA05-02	34.51	18.09	1.99	28.44	0.46	2.33	0.06	0.06	8.64	0.009	0.0007	94.96	5.531	2.469	0.947	0.240	3.812	0.062	0.557	0.010	0.019	1.766	0.009	0.001	3.990	15.414	0.13
SWA05-03	34.90	18.28	1.71	28.77	0.49	2.38	0.06	0.05	8.58	0.007	0.0007	95.54	5.552	2.448	0.979	0.205	3.827	0.066	0.564	0.010	0.015	1.741	0.007	0.001	3.992	15.408	0.13
SWA05-04	34.61	18.13	2.00	27.31	0.51	2.61	0.09	0.07	8.58	0.010	0.0006	94.31	5.555	2.445	0.984	0.241	3.666	0.069	0.624	0.015	0.022	1.757	0.010	0.001	3.990	15.379	0.15
SWA05-06	34.12	17.88	2.24	29.11	0.56	2.48	0.04	<LLD	8.74	0.006	0.0006	95.43	5.465	2.535	0.840	0.270	3.899	0.076	0.592	0.007	0.000	1.786	0.006	0.001	3.993	15.470	0.13
SWA05-07	34.71	18.37	2.40	28.77	0.53	2.43	0.07	<LLD	9.10	0.008	0.0007	96.73	5.473	2.527	0.887	0.285	3.794	0.071	0.571	0.012	0.000	1.831	0.008	0.001	3.260	15.450	0.13
SWA05-08	34.13	17.70	2.25	28.43	0.48	2.47	0.08	0.06	8.83	0.007	0.0006	94.74	5.498	2.502	0.858	0.273	3.830	0.065	0.593	0.014	0.019	1.815	0.007	0.001	3.992	15.466	0.13
SWA05-09	34.23	17.75	2.51	28.04	0.48	2.52	0.17	<LLD	8.73	0.008	0.0004	94.75	5.498	2.502	0.857	0.303	3.766	0.065	0.603	0.029	0.000	1.789	0.008	0.000	3.992	15.414	0.14
SWA05-11	35.41	17.78	2.41	27.75	0.50	2.54	0.21	0.07	8.67	0.007	0.0008	95.64	5.600	2.400	0.913	0.287	3.670	0.067	0.599	0.036	0.021	1.749	0.007	0.001	3.993	15.342	0.14

5.2.2 Allanite

Analyses of allanite were obtained from four samples (RSA03, RSA02, SWA07, RSA08). Representative analyses for each sample are presented in Table 5.3; for the complete dataset see Appendix C2.

Allanite occurs as euhedral to subhedral grains, occasionally in clusters with biotite, zircon, apatite, and the oxide phases. Grains vary in size from ~100 μm up to ~3 mm. A few grains display remnant oscillatory zoning (e.g. Figure 5.4a), while the majority are unzoned or display irregular patches (e.g. Figure 5.4b).

The composition of allanite is less obviously related to the whole-rock composition than that of biotite. There is a slight decrease in the concentration of Ca (~15 to ~10 wt% CaO; ~1.5 to ~1.1 atoms pfu) and La (~6.5 to ~4 wt% La_2O_3; ~0.2 to ~0.15 atoms pfu) in allanite from the more mafic to the more felsic samples, and a corresponding increase in the substitution of Th (~0.5 to ~1.25 wt% ThO_2; ~0.013 to ~0.026 atoms pfu) and the REE (~18 to ~23 wt% total REE; ~0.69 to ~0.80 atoms pfu total REE; see Table 5.3).

The back-scatter electron (BSE) images show the internal variation, as the intensity of the signal relates to the composition (higher average atomic number = brighter signal). The bright regions have higher concentrations of Fe, Y, and the REEs, and lower Al and Ti (e.g. Figure 5.5). The patchy zoning seen within many of the allanite grains is reminiscent of that seen in highly metamict zircons; this is consistent with the high concentrations of Th seen in the allanites (commonly ~1 wt% ThO_2), which suggests they have experienced high levels of radiation damage. This may account for the variable compositions seen in the allanites, as metamictisation disrupts the crystal lattice and promotes alteration.

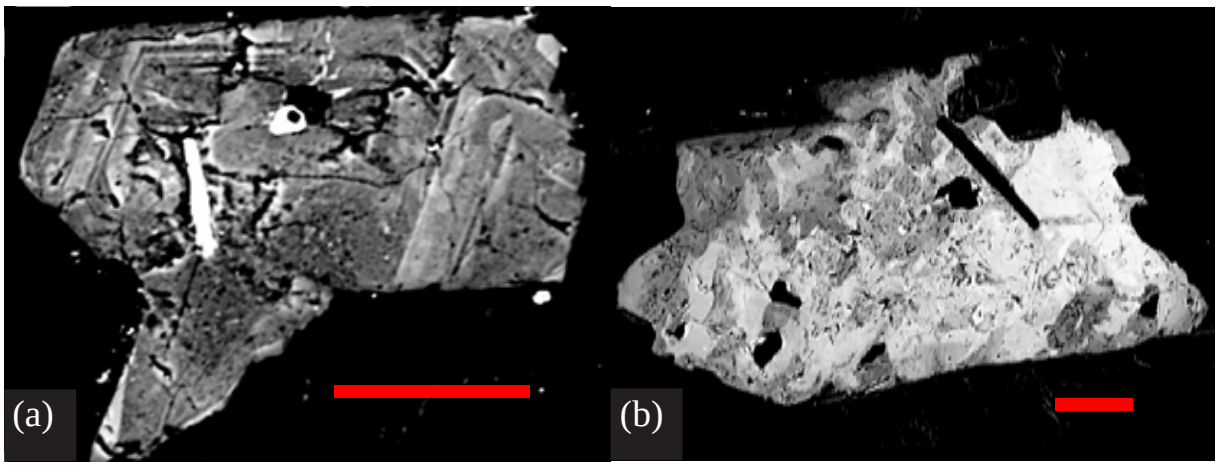


Figure 5.4. Back-scatter electron (BSE) images of allanite showing (a) oscillatory zoning and (b) irregular patches. Scale bars are 50 μm.

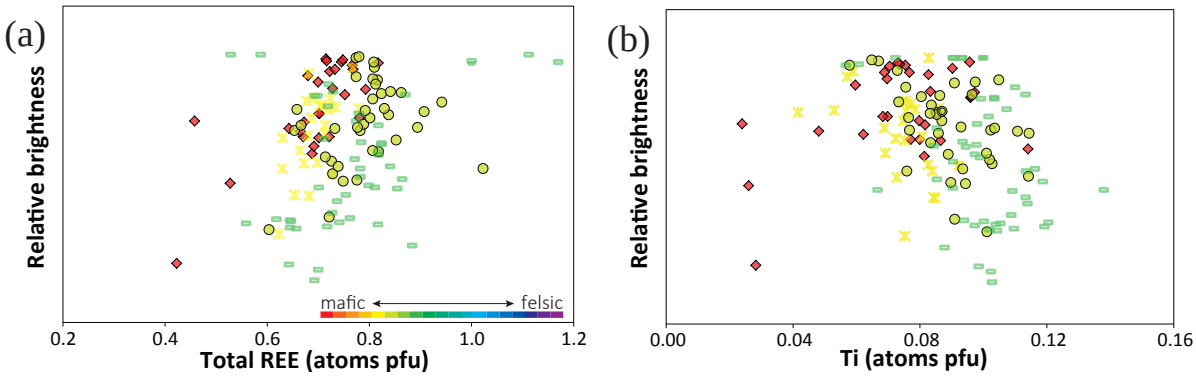


Figure 5.5. Plots of allanite back-scatter electron signal intensity (approximate) *vs* (a) total REE content; (b) Ti content.

5.3 Discussion

5.3.1 Post-crystallisation alteration

Deuteric alteration: chloritization and sericitization

Deuteric alteration (the reaction of late-stage, water-rich fluids with earlier-formed crystals) is common in granitic rocks (e.g. Putnis, 2002). The two main reactions involved are chloritization (biotite replaced by chlorite) and sericitization (plagioclase replaced by a fine-grained intergrowth of muscovite and clay minerals, known as sericite). Chlorite replaces biotite coherently, along cleavage planes, and incomplete replacement is observed as alternating biotite and chlorite layers within a grain (e.g. Figure 5.1g above). As described in detail by Tulloch (1979), the breakdown of biotite produces epidote and titanite in addition to chlorite. The two breakdown reactions are interrelated, as the K released from biotite breakdown contributes to the formation of sericite, and the breakdown of plagioclase in turn releases Ca, which contributes to the formation of epidote and titanite (Tulloch, 1979; Eggleton & Banfield, 1985; Shelley, 1993). Biotite and plagioclase are both extensively altered in many of the Mpuluzi samples, and all samples are altered to some degree, suggesting that deuteric fluids played an important role in the development of their present mineralogy.

K-feldspar: development of perthite, microcline, and myrmekite

Perthite develops as a result of low-temperature unmixing of Na-feldspar from K-feldspar. It reflects a reduced solubility of Na in K-feldspar as temperatures drop, and is thus common in slowly-cooled felsic igneous rocks (Shelley, 1993). In all the Mpuluzi samples microcline is at least slightly perthitic, and in some samples the perthite has coalesced into elongate blebs (e.g. sample RSA07; see Figure 5.1d above). The Mpuluzi samples commonly show the development of more abundant and coarser perthite in the samples which are more strongly altered, which suggests that the deuteric fluids were also responsible for the coarsening.

Table 5.3: Representative analyses of allanite for the Mpuluzi samples. LLD = lower limit of detection.

Analysis	Concentration (wt%)																				Structural formula (cations / 13 oxygen)												Cation
	Na_2O	MgO	Al	SiO_2	CaO	TiO_2	MnO	Fe_2O_3	SrO	Y_2O_3	La_2O_3	Ce_2O_3	Pr_2O_3	Nd_2O_3	SmO	Gd_2O_3	PbO	ThO_2	UO_2	Total	Si	Al^{IV}	Al^{VI}	Fe	Ti	Mg	Ca	Mn	REE	Y	Th	OH	Total
RSA03-04	0.16	0.22	12.08	32.29	13.38	0.95	0.44	14.61	0.23	<LLD	7.02	11.81	0.29	2.59	0.11	0.93	<LLD	0.61	<LLD	97.72	3.183	0.000	1.403	1.084	0.070	0.032	1.413	0.037	0.817	0.000	0.014	1	8.05
RSA03-05	0.06	0.26	13.01	33.16	14.75	1.12	0.73	13.63	0.54	<LLD	5.74	10.04	0.12	2.28	0.11	0.75	<LLD	0.49	<LLD	96.79	3.213	0.000	1.485	0.994	0.082	0.038	1.531	0.060	0.672	0.000	0.011	1	8.09
RSA03-07	0.07	0.31	15.13	34.03	14.78	0.68	0.69	13.08	0.39	<LLD	5.38	10.07	0.29	2.23	<LLD	0.78	<LLD	0.25	0.14	98.30	3.201	0.000	1.677	0.926	0.048	0.043	1.490	0.055	0.643	0.000	0.008	1	8.09
RSA03-09	0.05	0.22	11.63	31.92	13.43	1.22	0.58	16.39	0.38	<LLD	6.21	11.28	0.32	2.57	0.12	0.89	<LLD	0.72	<LLD	97.93	3.139	0.000	1.348	1.213	0.090	0.032	1.415	0.048	0.766	0.000	0.016	1	8.07
RSA03-12	0.04	0.27	12.36	31.96	13.50	1.04	0.59	15.55	0.45	<LLD	5.11	11.12	0.69	3.48	0.25	0.89	<LLD	0.77	<LLD	98.07	3.133	0.000	1.428	1.147	0.077	0.039	1.418	0.049	0.768	0.000	0.017	1	8.08
RSA03-14	0.17	<LLD	17.70	34.64	16.56	0.35	0.32	13.86	0.52	<LLD	4.05	7.28	0.20	1.70	0.07	0.51	<LLD	0.30	<LLD	98.23	3.151	0.000	1.898	0.949	0.024	0.000	1.614	0.025	0.458	0.000	0.006	1	8.12
RSA03-15	0.07	0.33	14.13	34.08	13.92	1.14	0.64	13.00	0.60	<LLD	6.00	10.44	0.22	2.36	0.08	0.80	<LLD	0.64	<LLD	98.45	3.233	0.000	1.580	0.928	0.081	0.047	1.415	0.051	0.688	0.000	0.014	1	8.04
RSA03-16	0.14	0.14	17.81	34.30	16.52	0.41	0.39	13.75	0.22	<LLD	3.58	6.80	0.20	1.55	<LLD	0.53	<LLD	0.34	<LLD	96.71	3.144	0.000	1.924	0.948	0.028	0.019	1.622	0.030	0.423	0.000	0.007	1	8.15
RSA03-17	0.06	0.16	12.46	33.15	14.28	0.96	0.69	15.57	0.61	<LLD	5.50	10.43	0.29	2.25	0.07	0.80	<LLD	0.68	0.13	98.09	3.197	0.000	1.416	1.130	0.070	0.023	1.475	0.056	0.680	0.000	0.018	1	8.06
RSA03-18	0.04	0.20	12.71	33.28	14.15	0.95	0.62	14.67	0.46	<LLD	6.12	11.24	0.24	2.36	<LLD	0.92	<LLD	0.48	0.12	98.56	3.205	0.000	1.443	1.063	0.069	0.029	1.460	0.051	0.733	0.000	0.013	1	8.06
RSA03-26	0.10	0.40	13.76	31.87	13.01	1.55	0.49	14.53	0.35	<LLD	5.51	10.30	0.23	2.44	0.11	0.81	<LLD	0.45	<LLD	95.95	3.119	0.000	1.587	1.070	0.114	0.058	1.364	0.041	0.691	0.000	0.010	1	8.05
RSA03-28	<LLD	0.35	12.21	32.64	13.77	1.31	0.52	14.97	0.36	<LLD	6.99	11.20	0.05	2.01	0.08	0.85	<LLD	0.67	<LLD	97.98	3.178	0.000	1.401	1.097	0.096	0.051	1.436	0.043	0.752	0.000	0.015	1	8.07
RSA02-03	0.11	0.35	15.17	33.65	12.96	1.00	0.68	11.30	0.59	0.34	4.63	9.88	0.50	3.08	0.37	0.98	<LLD	1.26	<LLD	96.94	3.235	0.000	1.719	0.817	0.072	0.050	1.335	0.055	0.679	0.017	0.028	1	8.01
RSA02-04	0.10	0.33	14.97	34.56	13.06	0.97	0.66	11.89	0.64	0.38	4.43	9.75	0.55	3.26	0.37	0.96	<LLD	1.20	<LLD	98.11	3.272	0.000	1.670	0.847	0.069	0.047	1.325	0.053	0.665	0.019	0.026	1	7.99
RSA02-07	0.10	0.39	14.61	32.51	12.17	1.09	0.77	9.44	0.58	0.27	4.76	9.93	0.36	2.83	0.35	0.82	<LLD	1.54	<LLD	92.54	3.273	0.000	1.734	0.715	0.083	0.059	1.313	0.066	0.698	0.014	0.035	1	7.99
RSA02-09	0.07	0.26	11.02	23.34	13.01	0.91	0.56	6.20	0.53	0.35	7.83	15.19	0.61	4.75	0.54	1.35	<LLD	2.31	<LLD	88.91	2.824	0.176	1.395	0.564	0.083	0.047	1.686	0.057	1.332	0.023	0.064	1	8.25
RSA02-10	0.04	0.32	16.29	33.58	14.48	0.58	0.71	9.57	0.55	0.32	5.15	10.24	0.51	3.52	0.36	1.02	<LLD	0.56	<LLD	97.80	3.201	0.000	1.830	0.686	0.042	0.045	1.479	0.057	0.721	0.016	0.012	1	8.09
RSA02-11	0.07	0.43	15.21	32.90	13.18	0.99	0.76	10.01	0.53	0.40	4.99	10.41	0.51	3.30	0.35	0.93	<LLD	0.83	<LLD	95.80	3.214	0.000	1.751	0.736	0.073	0.063	1.379	0.063	0.728	0.021	0.018	1	8.05
RSA02-14	0.08	0.39	14.90	34.39	12.82	1.08	0.71	11.75	0.53	0.31	5.11	9.95	0.40	2.92	0.32	0.88	0.27	1.23	<LLD	98.04	3.268	0.000	1.669	0.840	0.077	0.055	1.305	0.057	0.677	0.016	0.027	1	7.99
RSA02-15	0.06	0.45	14.07	32.35	13.57	0.80	0.70	12.09	0.39	0.18	5.82	10.85	0.43	3.24	0.25	0.92	<LLD	0.51	<LLD	96.68	3.172	0.000	1.626	0.892	0.059	0.066	1.426	0.058	0.768	0.009	0.011	1	8.09
RSA02-17	0.09	1.52	15.66	34.89	12.82	1.08	0.69	11.85	0.61	0.19	5.11	9.32	0.28	2.89	0.28	0.82	<LLD	1.18	<LLD	99.32	3.232	0.000	1.709	0.826	0.075	0.210	1.272	0.054	0.630	0.009	0.025	0.68	8.04
RSA02-21	0.12	0.28	14.80	33.86	12.46	1.11	0.86	10.61	0.55	0.36	5.56	10.23	0.38	2.84	0.28	0.97	0.25	1.17	<LLD	96.79	3.276	0.000	1.687	0.772	0.081	0.040	1.291	0.070	0.713	0.019	0.026	1	7.98
RSA02-22	0.09	0.38	15.89	35.30	13.37	1.21	0.95	10.85	0.62	0.38	4.96	9.66	0.55	3.06	0.30	0.87	<LLD	1.12	0.15	99.76	3.270	0.000	1.735	0.756	0.084	0.052	1.327	0.075	0.654	0.019	0.027	0.24	8.00
RSA02-23	0.07	0.31	14.08	31.83	13.41	1.21	0.79	10.12	0.56	0.20	4.98	9.29	0.28	2.61	0.27	0.81	<LLD	1.23	0.18	92.34	3.222	0.000	1.680	0.771	0.092	0.047	1.454	0.068	0.672	0.011	0.032	1	8.05
RSA02-24	0.05	0.35	14.71	32.71	12.55	1.00	0.73	10.56	0.63	0.21	4.41	8.77	0.43	2.47	0.23	0.80	<LLD	1.35	<LLD	92.00	3.272	0.000	1.734	0.795	0.075	0.052	1.345	0.062	0.623	0.011	0.031	1	8.00
SWA07-06	0.06	0.10	9.98	31.75	11.73	1.20	0.97	17.39	0.35	0.32	5.01	11.19	0.62	3.90	0.46	1.14	<LLD	0.89	0.13	97.21	3.195	0.000	1.184	1.317	0.091	0.015	1.265	0.083	0.816	0.017	0.023	1	8.00
SWA07-08	0.12	0.21	12.17	32.45	11.13	1.53	0.95	15.00	0.29	0.27	4.59	10.08	0.64	3.43	0.44	1.02	<LLD	1.94	<LLD	96.29	3.220	0.000	1.423	1.120	0.114	0.031	1.183	0.080	0.728	0.014	0.044	1	7.96
SWA07-11	0.14	0.12	13.65	33.51	11.70	1.17	0.68	14.02	0.35	0.28	4.02	9.22	0.58	3.22	0.45	0.97	<LLD	1.68	<LLD	95.80	3.267	0.000	1.568	1.028	0.086	0.017	1.222	0.056	0.653	0.015	0.037	1	7.95
SWA07-14	0.12	0.34	13.79	31.48	11.56	0.88	0.77	15.80	0.19	0.53	4.29	10.33	0.77	4.51	0.75	1.32	<LLD	0.50	0.16	98.09	3.082	0.000	1.591	1.164	0.065	0.050	1.212	0.064	0.780	0.028	0.015	1	8.05
SWA07-17	0.15	0.13	12.33	31.90	10.81	1.34	0.77	13.56	0.32	0.30	4.87	10.21	0.59	3.68	0.58	1.15	<LLD	1.77	<LLD	94.46	3.237	0.000	1.475	1.036	0.102	0.020	1.175	0.066	0.777	0.016	0.041	1	7.94
SWA07-19	0.13	0.23	13.44	31.50	11.81	0.78	0.86	15.29	0.17	0.79	4.08	10.08	0.86	5.10	1.04	1.51	<LLD	0.14	<LLD	97.81	3.103	0.000	1.560	1.133	0.058	0.034	1.247	0.072	0.808	0.041	0.003	1	8.06
SWA07-20	0.15	0.19	14.05	33.81	11.93	1.39	0.57	13.67	0.43	0.22	3.55	8.32	0.58	3.30	0.51	0.94	0.09	2.28	<LLD	96.03	3.269	0.000	1.601	0.995	0.101	0.027	1.236	0.047	0.603	0.011	0.050	1	7.94
SWA07-21	0.10	<LLD	11.58	31.30	12.43	1.16	0.81	16.61	0.35	0.36	4.85	11.02	0.63	3.97	0.55	1.13	<LLD	0.88	<LLD	97.73	3.118	0.000	1.359	1.245	0.087	0.000	1.326	0.068	0.801	0.019	0.020	1	8.04
SWA07-22	0.06	0.09	11.61	30.75	12.00	1.14	0.94	16.02	0.30	0.30	5.71	11.57	0.61	4.02	0.50	1.19	<LLD	0.92	<LLD	97.73	3.092	0.000	1.376	1.212	0.086	0.013	1.293	0.080	0.862	0.016	0.021	1	8.05
SWA07-23	0.18	0.27	13.26	32.80	11.40	1.39	0.68	14.99	0.35	0.26	4.68	10.04	0.57	3.42	0.45	0.99	<LLD	1.35	<LLD	97.12	3.197	0.000	1.523	1.099	0.102	0.039	1.190	0.056	0.714	0.013	0.030	1	7.96
SWA07-25	0.10	0.12	9.45	31.45	11.08	1.11	1.14	16.54	0.30	0.40	5.20	12.46	0.79	4.25	0.50	1.25	<LLD	1.02	<LLD	97.16	3.213	0.000	1.138	1.272	0.085	0.018	1.213	0.099	0.907	0.022	0.024	1	7.99
SWA07-28	0.08	0.13	10.40	29.75	10.78	0.96	0.84	14.53	0.28	0.39	5.45	13.72	0.85	4.82	0.64	1.33	<LLD	1.17	<LLD	96.14	3.125	0.000	1.287	1.148	0.076	0.020	1.213	0.075	1.023	0.022	0.028	1	8.02

Table 5.3 continued.

Analysis	Concentration (wt%)																				Structural formula (cations / 13 oxygen)												Cation
	Na_2O	MgO	Al	SiO_2	CaO	TiO_2	MnO	Fe_2O_3	SrO	Y_2O_3	La_2O_3	Ce_2O_3	Pr_2O_3	Nd_2O_3	SmO	Gd_2O_3	PbO	ThO_2	UO_2	Total	Si	Al^{IV}	Al^{VI}	Fe	Ti	Mg	Ca	Mn	REE	Y	Th	OH	Total
SWA07-30	0.12	0.66	12.97	32.12	10.88	1.22	0.84	14.72	0.31	0.29	4.79	9.81	0.56	3.44	0.46	0.97	<LLD	1.78	<LLD	96.04	3.183	0.000	1.515	1.098	0.091	0.098	1.155	0.071	0.721	0.015	0.040	1	7.99
SWA07-33	0.14	0.51	11.21	32.22	10.44	1.18	0.92	15.79	0.26	0.29	5.02	11.46	0.69	3.75	0.45	1.11	<LLD	1.06	<LLD	96.55	3.227	0.000	1.323	1.190	0.089	0.076	1.120	0.078	0.818	0.015	0.024	1	7.96
SWA07-38	0.12	0.19	11.75	32.17	10.87	1.23	0.94	14.77	0.34	0.31	4.86	9.78	0.48	3.46	0.53	1.02	0.37	1.60	<LLD	94.85	3.251	0.000	1.399	1.123	0.093	0.029	1.177	0.080	0.739	0.017	0.037	1	7.94
RSA08-03	0.14	<LLD	14.17	33.34	11.64	1.21	0.39	13.07	0.71	0.18	3.54	7.08	0.36	2.62	0.30	0.71	5.67	1.46	<LLD	96.59	3.286	0.000	1.646	0.969	0.090	0.000	1.229	0.033	0.523	0.009	0.033	1	7.82
RSA08-05	0.10	0.19	12.28	32.05	11.80	1.59	0.76	14.36	0.42	0.46	4.58	11.56	0.71	3.97	0.57	1.18	<LLD	0.94	<LLD	97.52	3.173	0.000	1.433	1.070	0.118	0.028	1.252	0.064	0.811	0.024	0.021	1	7.99
RSA08-07	0.08	<LLD	8.51	20.02	8.20	0.70	0.27	7.31	0.54	0.36	8.88	16.95	0.96	6.71	0.82	1.77	4.11	2.35	<LLD	88.54	2.718	0.282	1.079	0.747	0.071	0.000	1.192	0.031	1.779	0.026	0.073	1	8.00
RSA08-08	0.17	0.14	14.42	33.96	10.51	1.27	0.53	13.70	0.57	0.18	3.61	8.19	0.51	3.11	0.37	0.78	5.71	1.27	<LLD	99.02	3.284	0.000	1.643	0.997	0.092	0.020	1.089	0.043	0.582	0.009	0.028	0.98	7.79
RSA08-09	0.18	0.11	13.81	33.72	10.40	1.41	0.55	13.26	0.50	0.25	4.09	9.12	0.57	3.32	0.43	0.86	5.31	1.16	<LLD	99.07	3.289	0.000	1.587	0.973	0.103	0.016	1.087	0.045	0.652	0.013	0.026	0.93	7.79
RSA08-16	0.12	0.18	12.52	32.18	9.98	1.36	0.70	14.09	0.39	0.35	4.15	10.21	0.63	3.61	0.49	1.04	4.13	1.14	<LLD	97.32	3.240	0.000	1.486	1.067	0.103	0.027	1.076	0.060	0.736	0.019	0.026	1	7.84
RSA08-20	0.11	0.48	11.95	31.14	10.98	1.43	0.88	15.01	0.37	0.30	5.58	11.83	0.53	3.70	0.43	1.14	<LLD	0.56	<LLD	96.42	3.135	0.000	1.418	1.137	0.108	0.072	1.184	0.075	0.849	0.016	0.013	1	8.01
RSA08-21	0.13	0.36	10.72	31.04	11.18	1.55	0.92	16.31	0.27	0.37	5.53	11.68	0.65	3.89	0.49	1.14	<LLD	0.55	0.14	96.92	3.138	0.000	1.277	1.241	0.118	0.054	1.211	0.079	0.859	0.020	0.016	1	8.01
RSA08-22	0.11	0.16	12.55	31.92	9.87	1.56	0.55	14.03	0.56	0.24	4.40	8.40	0.33	2.96	0.37	0.80	5.51	1.24	<LLD	95.59	3.254	0.000	1.508	1.076	0.120	0.024	1.078	0.047	0.640	0.013	0.029	1	7.79
RSA08-23	0.09	0.32	11.65	31.19	11.57	1.82	0.79	15.62	0.45	0.31	5.09	11.01	0.66	3.77	0.51	1.10	<LLD	0.82	<LLD	96.77	3.123	0.000	1.375	1.177	0.137	0.048	1.241	0.067	0.805	0.017	0.019	1	8.01
RSA08-28	0.12	0.13	12.27	31.76	9.76	1.42	0.59	14.19	0.39	0.27	4.18	9.56	0.68	3.37	0.48	1.01	4.31	1.18	<LLD	95.72	3.246	0.000	1.478	1.091	0.109	0.020	1.069	0.051	0.715	0.015	0.027	1	7.82
RSA08-30	0.07	0.19	11.91	28.20	10.32	0.69	0.57	12.09	0.38	0.34	7.21	14.12	0.74	5.56	0.69	1.52	<LLD	0.73	<LLD	95.33	3.030	0.000	1.508	0.978	0.056	0.030	1.188	0.052	1.164	0.019	0.018	1	8.04
RSA08-32	0.13	0.18	12.10	31.21	11.51	1.54	0.67	15.77	0.47	0.32	5.28	11.73	0.59	3.83	0.50	1.15	<LLD	0.54	<LLD	97.52	3.109	0.000	1.421	1.182	0.115	0.027	1.229	0.057	0.835	0.017	0.012	1	8.00
RSA08-33	0.11	0.18	11.58	31.81	9.97	1.47	0.59	15.14	0.47	0.26	4.31	9.81	0.63	3.44	0.44	0.97	4.73	1.21	<LLD	97.19	3.235	0.000	1.388	1.158	0.112	0.027	1.086	0.051	0.724	0.014	0.028	1	7.82
RSA08-41	0.14	0.24	12.41	31.50	11.97	1.20	0.53	15.91	0.43	0.35	4.78	10.55	0.60	3.79	0.45	1.08	0.14	1.00	<LLD	97.07	3.126	0.000	1.452	1.188	0.090	0.036	1.273	0.045	0.766	0.018	0.023	1	8.02
RSA08-42	0.11	<LLD	12.53	32.13	13.20	0.90	0.47	17.46	0.57	0.36	4.10	9.86	0.62	3.59	0.51	1.03	<LLD	0.79	<LLD	98.23	3.123	0.000	1.435	1.277	0.066	0.000	1.375	0.039	0.696	0.019	0.017	1	8.05
RSA08-44	0.11	0.09	13.84	33.35	10.59	1.30	0.38	13.74	0.66	0.24	3.23	7.68	0.51	2.85	0.39	0.80	6.46	1.36	<LLD	97.61	3.289	0.000	1.608	1.019	0.096	0.013	1.119	0.032	0.553	0.013	0.031	1	7.77
RSA08-46	0.11	0.29	12.57	31.50	11.52	1.12	0.47	15.55	0.40	0.32	4.97	11.15	0.72	4.12	0.56	1.22	0.27	0.91	0.16	97.93	3.124	0.000	1.469	1.161	0.084	0.043	1.224	0.039	0.819	0.017	0.024	1	8.00

This is in accordance with previous studies linking perthite coarsening with low-temperature deuteric fluids (e.g. Parsons & Brown, 1984). The abundance of perthite has also been linked to deformation (e.g. Chayes, 1952), and the presence of abundant perthite in the Mpuluzi samples with strongly-developed secondary foliations (SWA11 and SWA02a) suggests that perthite may be linked to both deuteric alteration and subsequent deformation.

The transformation of K-feldspar from orthoclase (monoclinic) to microcline (triclinic) involves the development of a complex intergrowth of albite and pericline twins, and results in the distinctive tartan twinning typical of microcline (Shelley, 1993). The transition from submicroscopic or "tweed" textured feldspar to the cross-hatched variety requires additional energy which may be provided by contact metamorphism (e.g. Steiger & Hart, 1967), interaction with deuteric fluids, or tectonic strain (e.g. Brown & Parsons, 1989). The presence of tartan-twinned microcline in all the Mpuluzi samples, regardless of their degree of alteration or proximity to any subsequent intrusions, suggests that deuteric alteration may have promoted the development of microcline but that subsequent tectonic strain probably completed the process, particularly in the less-altered samples.

The replacement of K-feldspar by myrmekite (intergrown plagioclase and quartz) involves interaction with fluids rich in Na and/or Ca. The relative abundance of Na and Ca in the fluid influences both the composition of the plagioclase and the ratio of plagioclase to quartz in the myrmekite (Shelley, 1993). The proportion of quartz increases with the proportion of Ca in plagioclase, as albite ($NaAlSi_3O_8$) and anorthite ($CaAl_2Si_2O_8$) are related by the coupled substitution $Si^{4+} + Na^{+} \leftrightharpoons Al^{3+} + Ca^{2+}$, which means that anorthite has a lower silica content than both albite and orthoclase (therefore pure albite replacing K-feldspar will not form myrmekite as it requires no quartz to balance the reaction; Shelley, 1993). Myrmekite in the Mpuluzi samples consists of ~20–30% quartz, which suggests that the composition of the accompanying plagioclase is ~$An_{30–50}$ (Shelley, 1993); the breakdown of calcic plagioclase to form sericite is likely to be the source of the Ca.

Foliation: magma flow vs deformation

The Mpuluzi samples vary from massive to foliated, and display primary foliations as well as evidence for both ductile and minor brittle deformation. Primary foliations are generally defined by aligned grains (e.g. biotite, zircon, apatite; see Figure 5.1i above), while secondary foliations are commonly defined by deformed quartz grains and less frequently biotite (the strong alteration of biotite present in most samples somewhat obscures this). Evidence for brittle deformation includes both large, sample-scale fractures, and microfractures within grains (e.g. Figure 5.1b above).

The presence of a strong secondary foliation within only a few of the Mpuluzi samples suggests that the deformation was not related to major regional tectonic events. This is consistent with the overall geological history of the region, in which no major deformation events are recorded after the intrusion of the Mpuluzi batholith at ~3.1 Ga (see overview in Chapter Two).

5.3.2 Host-rock effects on mineral chemistry

Biotite and magnetite/ilmenite

The Ti content of biotite broadly correlates with the abundance of ilmenite and/or titanite in the host rock (Figure 5.6). The biotites in samples containing ilmenite as the only oxide phase generally contain less Ti than those in which magnetite is present (ilmenite-only samples average <0.3 atoms pfu; magnetite-only samples average >0.3 atoms pfu). The samples containing titanite show similarly low Ti contents in the biotites (despite containing only minor ilmenite).

Effects of changing Mg, Fe, and Mn

Biotites from more mafic rocks generally display higher Mg relative to Fe, reflecting the more magnesian composition of the host rock (see e.g. Figure 5.2a above). The Mn content of the biotites also changes with the host-rock composition, with biotite from mafic rocks having lower Mn than those from more felsic rocks. This is related to the fact that, along with Mg/Fe, the Fe/Mn ratio in the host rocks decreases with increasing silica content (Flood & Shaw, 2014).

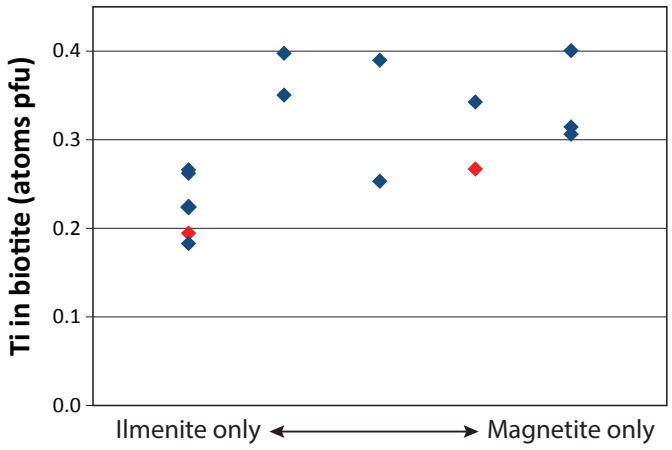


Figure 5.6. Plot of Ti in biotite *vs* ilmenite/magnetite in host rock. Red points represent samples with primary titanite.

5.4 Conclusions

The mineral assemblage of the Mpuluzi samples varies slightly over the range in composition, with the more mafic samples containing hornblende and titanite, and the more felsic samples containing primary muscovite. The abundances of accessory minerals also change, with allanite, apatite, and the oxide phases present in higher proportions in the more mafic samples.

Alteration within the Mpuluzi samples consists of chloritization of biotite and sericitization of plagioclase. This type of alteration is typical of granitic rocks, and is caused by the interaction of earlier-formed minerals with late-stage, water-rich fluids. The alteration varies from very minor to near-complete replacement of the original biotite and plagioclase, and shows no systematic variation with deformation or whole-rock composition.

The Mpuluzi samples display evidence of both primary and secondary foliations, as well as samples in which no foliation is observed. Primary foliations are generally defined by aligned grains of biotite and/or feldspar, while secondary foliations are defined by elongated quartz grains. Some samples show evidence of minor brittle deformation.

The chemistry of biotites within the Mpuluzi samples largely reflects the overall composition of the host rock, with biotites from more mafic samples having more magnesian compositions, while those from felsic samples are generally more iron-rich. The F content of the biotites is also higher in the more mafic samples, while the more felsic samples contain higher Mn. The Ti content of biotite is dependent on the accessory phase assemblage of the host rock – samples containing ilmenite and/or titanite have lower Ti contents in biotite than those which lack primary titanite and have magnetite as the dominant oxide.

Chapter Six – Zircon Chemistry and Isotopic Composition

6.1 Introduction

The chemical composition and isotope ratios of individual zircon grains formed during crystallisation of igneous rocks provide a wealth of information about the rocks themselves. The chemical fingerprint of a zircon provides information about the composition of the magma from which it crystallised (e.g. Belousova *et al.*, 2002; Hoskin & Schaltegger, 2003), and the isotopic composition provides the age of the crystal (using the U-Pb system; see overview in Davis *et al.*, 2003) as well as an estimate of the age of the source (using the Lu-Hf system; e.g. Patchett *et al.*, 1982; Griffin *et al.*, 2004; Hawkesworth & Kemp, 2006).

Imaging the zircons in cathodoluminescence (CL) prior to analysis allows for targeting of specific domains and provides confidence that the analysed trace-element compositions, U-Pb ages, and Hf-isotope compositions have all been obtained from the same part of the crystal and represent the composition of material formed in the same crystallisation event. Multiple analyses from different domains within a single zircon can provide information about the evolution of the magma composition through time.

U-Pb dating of zircons is one of the most commonly used tools in geochronology, and has a wide range of applications including dating of igneous rocks (e.g. Schärer & Allègre, 1983; Schaltegger *et al.*, 1996), dating of metamorphic events (e.g. Rowley *et al.*, 1997; Santosh *et al.*, 2007), provenance studies of sediment using detrital zircons (e.g. Cawood & Nemchin, 2000; Stewart *et al.*, 2001), and calibration of time scales based on stratigraphic sequences (e.g. Tucker *et al.*, 1990; Kaufmann, 2006). Zircon is common in many types of igneous rocks, and is extremely stable under surface conditions, being physically resistant to abrasion. It is also both chemically resistant and refractory, which means it commonly survives metamorphic and melting events. In addition to its durability, zircon is an ideal mineral for U-Pb dating because it does not incorporate any Pb at the time of formation, but readily holds U and Th in the crystal lattice in place of Zr. This means that ideally, all Pb in a given grain has been formed by the radioactive decay of U and Th. The three independent decay chains $^{238}U \rightarrow {}^{206}Pb$, $^{235}U \rightarrow {}^{207}Pb$, and $^{232}Th \rightarrow {}^{208}Pb$, together with ages calculated from the ratio of ^{207}Pb to ^{206}Pb, allow an accurate determination of the age of a grain, and in the case of disturbance, an assessment of the cause and severity of the error in age.

There are several common difficulties encountered when performing U-Pb analyses of zircon grains: (1) the presence of additional (common) Pb not produced by radioactive decay of U and Th; (2) the loss of radiogenic Pb at some point in the history of the crystal; (3) the

presence of other phases within the grain and along fractures, either as primary inclusions or alteration features. These problems are exacerbated as the zircons age, as radiation damage accumulates, disrupting the crystal lattice and facilitating alteration. In zircons with both high concentrations of radioactive U and Th, and long histories of radiation damage, these problems can be severe. Difficulty in obtaining an accurate age is compounded when more than one of these problems is encountered within an individual grain. A combination of common Pb and loss of radiogenic Pb is particularly difficult to resolve, as common Pb will tend to increase the apparent age of grains (Figure 6.1a), while loss of radiogenic lead results in a systematic decrease in calculated ages (Figure 6.1b). The calculated ages decrease as the proportion of lead lost to the total amount of the isotope increases; thus the systems are disturbed in proportion to their half-lives, and ages calculated from $^{208}Pb/^{232}Th$ will be the most strongly affected, followed by those calculated from the $^{206}Pb/^{238}U$ system, and then the $^{207}Pb/^{235}U$ system. The age calculated from the ratio of ^{207}Pb to ^{206}Pb is equal to the age of crystallisation if the lead loss is recent, and grains affected by ancient lead loss events provide a minimum estimate of the true age (Andersen, 2002; see Figure 6.1c, d).

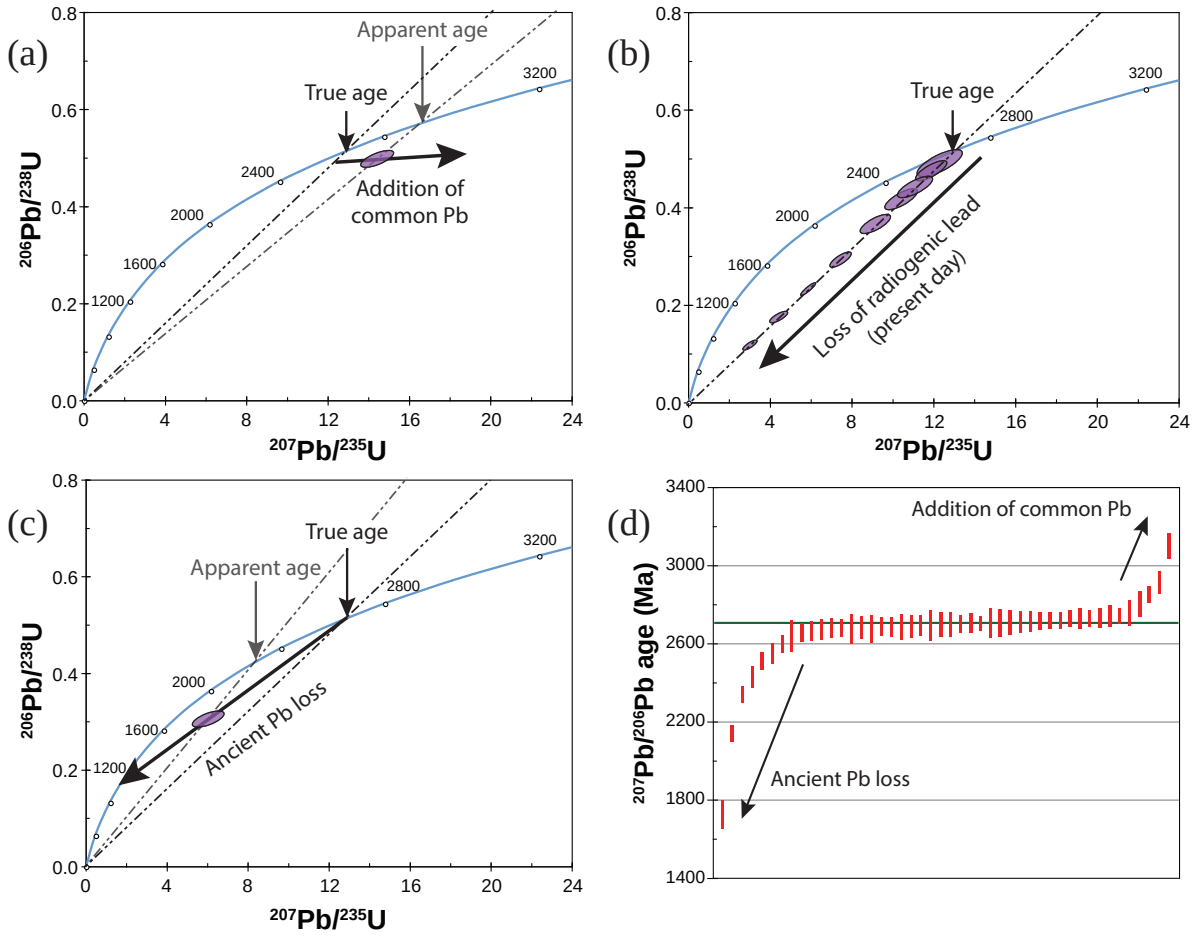


Figure 6.1. Disturbances to the U-Th-Pb system: (a) addition of common Pb increases apparent ages; (b) recent loss of radiogenic Pb decreases the $^{207}Pb/^{235}U$ and $^{206}Pb/^{238}U$ ages but intersects the concordia at the true age; (c) ancient loss of radiogenic Pb decreases the apparent age; (d) the effect of common-Pb addition and ancient Pb loss on $^{207}Pb/^{206}Pb$ ages.

The trace-element composition of a given zircon grain has been shown to correlate with the rock type in which the zircon crystallised (e.g. Belousova *et al.*, 2002). The combined analysis of trace elements and U-Pb isotopes can be used to identify different populations where they are indistinguishable within one dataset but clearly resolved in the other (e.g. two populations with similar ages but distinct chemical compositions). This approach has been used in studies of detrital zircons to provide a constraint on the source of different age populations (e.g. Wilde *et al.*, 2001; Veevers *et al.*, 2005); in studies of igneous zircons it has been used to provide evidence for mixing between different magma sources (e.g. Belousova *et al.*, 2006). Combined trace-element and U-Pb analysis has also been used in studies of metamorphic rocks to constrain the timing of metamorphic events or particular reactions (e.g. Whitehouse & Platt, 2003; Xia *et al.*, 2010).

The *in situ* analysis of the Lu-Hf isotopic system in igneous zircons is used to provide constraints on the source of the host rock (e.g. Griffin *et al.*, 2002; Belousova *et al.*, 2006; Kemp *et al.*, 2007). More evolved isotopic signatures indicate the melting of older crustal material (i.e. a recycled component), whereas more juvenile (radiogenic) isotopic signatures suggest that there has been a limited amount of time since extraction from the mantle. Igneous rocks frequently display a mixing trend between two isotopic end members, and this can be used to constrain the ages of these components (Figure 6.2). The evolved end of the mixing trend provides a minimum estimate of the age of extraction of the recycled component, while the radiogenic end provides a maximum estimate of the age of extraction of the juvenile component. The presence of inherited cores can better constrain the recycled component; if their Hf-isotopic compositions lie along an evolution line, this intersects the depleted mantle line at the age of extraction of the material from the mantle (Figure 6.2).

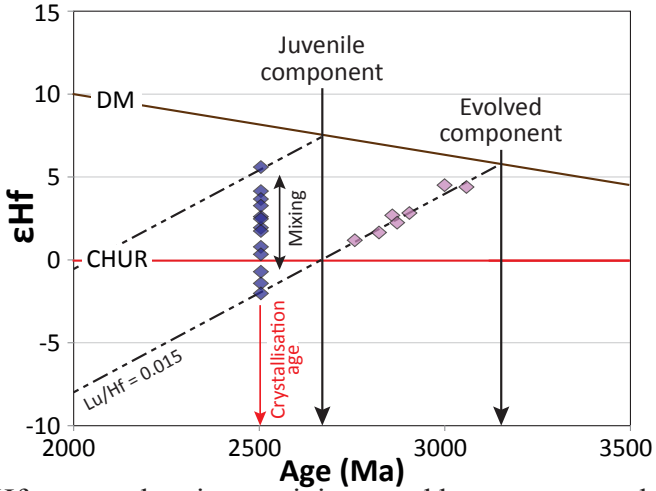


Figure 6.2. Plot of εHf *vs* age, showing a mixing trend between an evolved component and juvenile material. The main population lies at the crystallisation age of the rock (~2.5 Ga), and grains with inherited ages lie along an evolution line with Lu/Hf = 0.015 (average crust), which intersects the depleted mantle (DM) curve at the age of extraction of the source. Crustal model ages (T_{DM}^{C}) represent the intersection of an evolution line with the DM line; the mixing components in this example give model ages of ~3.2 Ga (evolved) and ~2.7 Ga (juvenile).

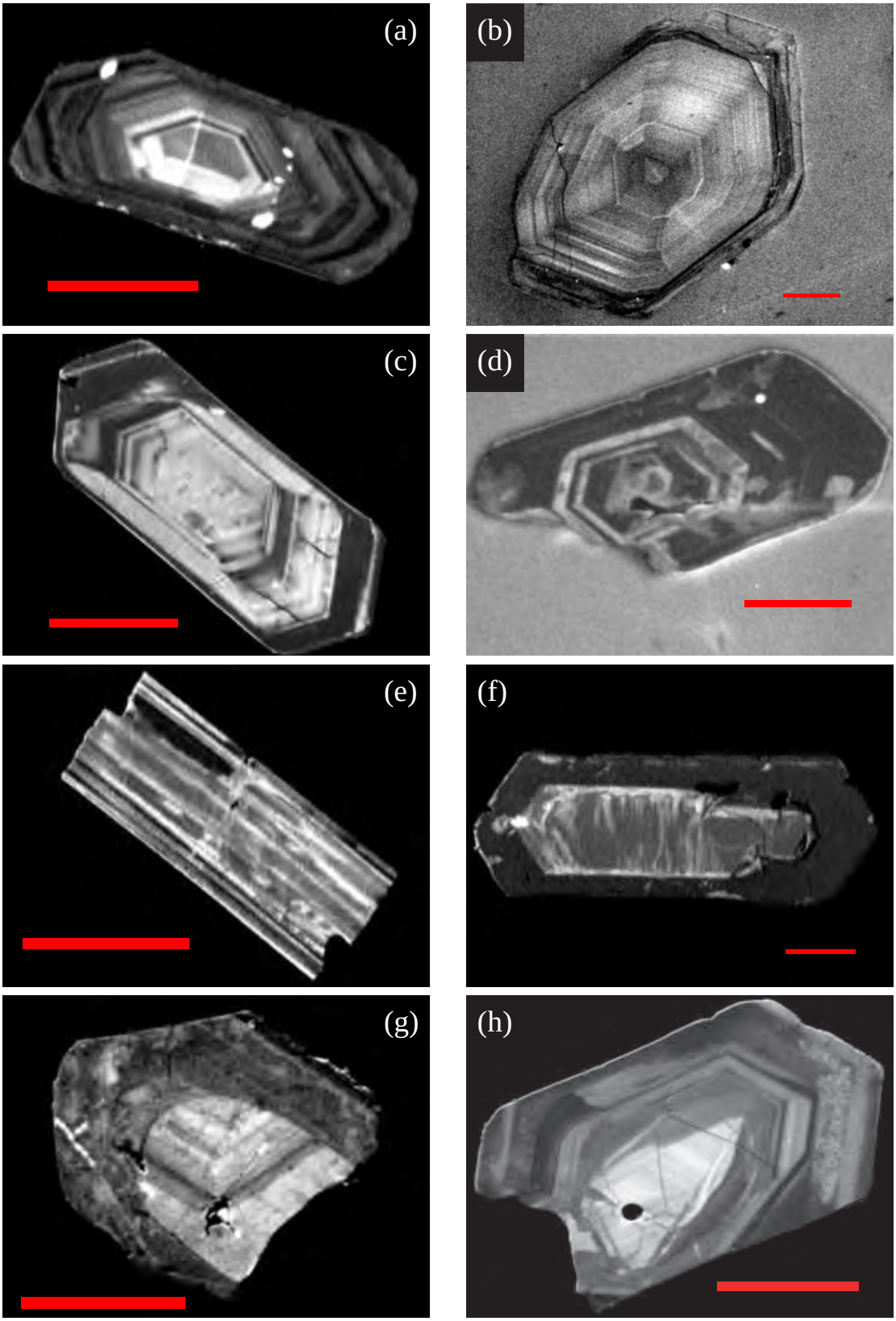
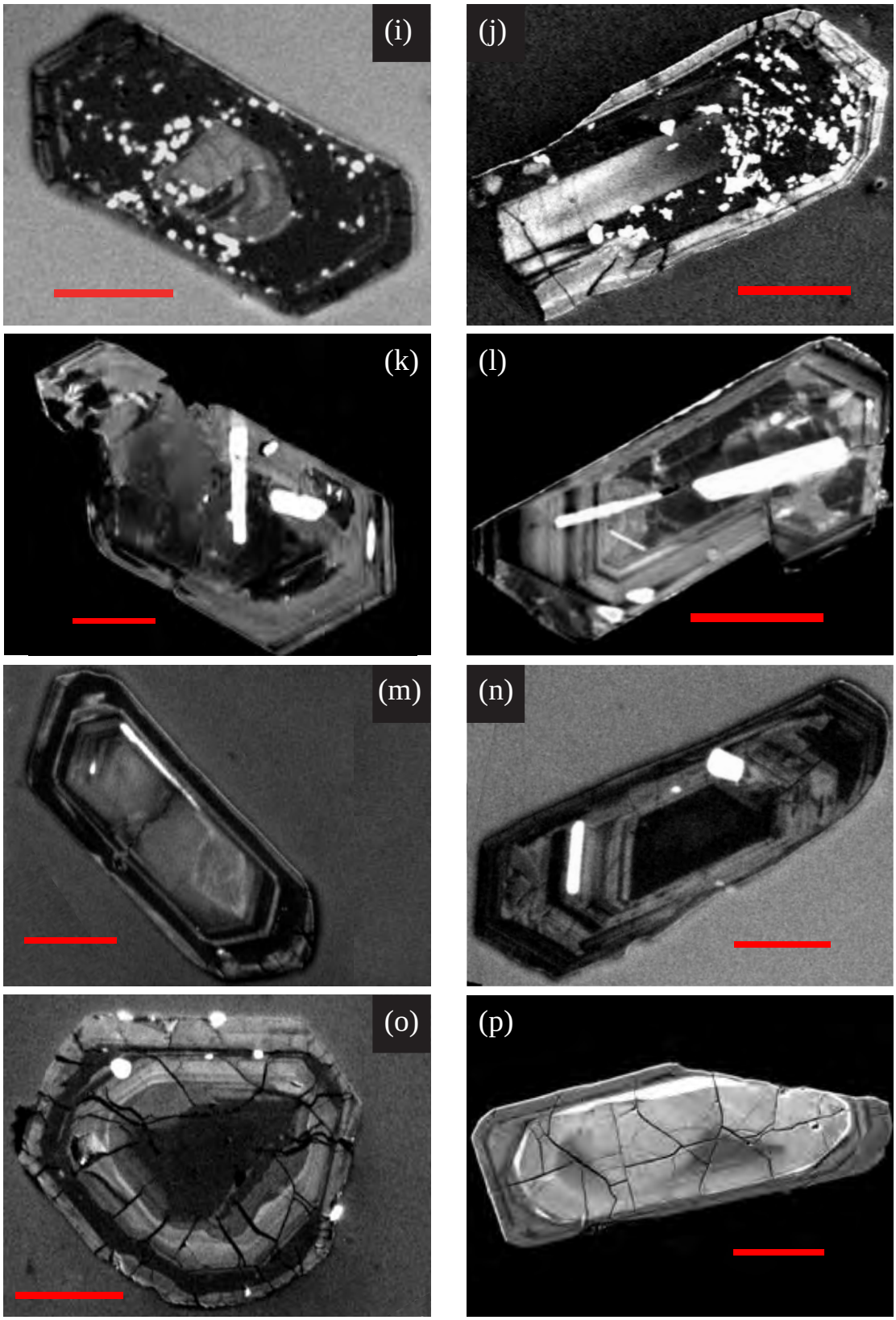


Figure 6.3. CL images of representative zircon grains from the Mpuluzi batholith: (a), (b) euhedral, oscillatory zoned (RSA01-101, RSA04-12); (c), (d) remnant oscillatory zoning (SWA03-45, SWA10a-75); (e) laminated (SWA18a-74); (f) distinct rim with dark CL response (SWA02a-42); (g), (h) distinct core with truncated zoning (RSA02-4, SWA05-2);



(i), (j) multiple inclusions concentrated in dark (metamict) zones (RSA06-79, RSA01-110); (k), (l) inclusions cross cutting zoning (SWA03-32, SWA03-33); (m), (n) inclusions aligned with zoning (SWA10a-109, RSA06-115); (o), (p) fracturing concentrated in bright zones (RSA04-28, SWA07-13). Scale bars are 50 μm. For the full set of images see Appendix D.

6.2 Results

6.2.1 Zircon characteristics

Zircons were extracted from 18 samples and imaged in CL to obtain information about their internal structure. The CL images were used to ensure analyses of major elements, U-Pb ages, trace-element compositions, and Hf isotopes were in the same domain. In the presentation of trace-element compositions, U-Pb ages, and Hf-isotopic compositions below, the samples are ordered from most mafic to most felsic.

Zircons from the Mpuluzi samples are small (~50–200 μm); they generally range in colour from pink to purple to brown with occasional colourless to pale yellow grains. They are usually euhedral to subhedral in shape and range from roughly equant to elongated (generally up to ~5:1, some up to ~10:1). The zircons commonly have a low CL response (grains appear dark in CL images), which is a common effect of metamictisation (e.g. Nasdala *et al.*, 2002). Many are euhedral and show clear oscillatory zoning patterns indicating a magmatic origin (e.g. Figure 6.3a, b), but in some grains the original oscillatory zoning has been partly erased, and only a remnant is present (Figure 6.3c, d). A minor proportion of the grains analysed show laminated zoning (parallel to the c axis; Figure 6.3e). Some grains have distinct cores and rims, and the rims commonly have a very dark CL response (Figure 6.3f); occasional grains show evidence of inheritance with rounded cores and truncated zoning (Figure 6.3g, h). Inclusions are abundant (e.g. apatite, titanite); in some grains they are mostly confined to the zones with dark CL response (Figure 6.3i, j), while in others they can be clearly seen to cross cut (Figure 6.3k, l) or parallel the zoning (Figure 6.3m, n). Many grains have abundant fractures, often largely confined to the sections with bright CL response (Figure 6.3o, p). The full set of CL images and ablation spot information is provided in Appendix D.

After obtaining CL images, grains were analysed for major-element compositions by EMP (see Appendix E). The EMP results provide a further means to identify grains which are substantially metamict, where this is not immediately apparent in the CL images. The main effect of metamictisation on the EMP data is a decrease in the total obtained (as low as ~75%), as strongly metamict grains typically have high concentrations of elements which are not typically present in zircon and thus not usually analysed by EMP (e.g. Al, P, Ca, Fe, Y, Ba, Pb, and the rare earth elements (REE), as well as water; Nasdala *et al.*, 2009). Grains with EMP totals <95% were not used for further analysis.

6.2.2 Trace-element compositions

The location of analysis points for trace-element compositions was determined based on the CL images, with the intention to avoid any inclusions, fractures, and metamict zones. Information about the structure in three dimensions cannot be obtained by CL imaging, so scrutinising the laser signal as a time-resolved spectrum is crucial to detecting the presence of different domains below the surface as the laser beam drills into the grain. The advantage of this is that it allows the selection of the 'cleanest' part of an individual analysis (i.e. the most stable part of the signal), and thus enables a reduction in the heterogeneity within individual analyses as far as possible. Where the change in composition is large and abrupt, this process is straightforward, for example in the case of large apatite inclusions which produce a sharp increase in the P and light rare earth element (LREE) signals (Figure 6.4a). When there is a gradational change in composition (as when there is an oblique boundary between two different zones), or multiple small-scale heterogeneities (small inclusions or metamict zones), this process is more difficult as it is often unclear where the boundary lies (e.g. Figure 6.4b). The analyses have accordingly been categorised into 'pristine' and 'variable', based on the quality and homogeneity of the signal, with the pristine group representing the most reliable analyses where any included phases and/or metamict zones could be excluded, while the variable group includes analyses where small but significant variations within the signal have been retained, reflecting either the presence of small inclusions or chemical zonation within the crystal. A third group has been labelled 'metamict', and comprises analyses where the only stable part of the signal had a distinctly metamict character; these are included in the following plots for comparison.

Average trace-element compositions for the three groups are presented in Table 6.1; for the full dataset see Appendix F. The pristine group of analyses generally shows lower and more homogenous concentrations of trace elements than the variable group, and the metamict group displays higher and more heterogeneous concentrations than either of the other two groups.

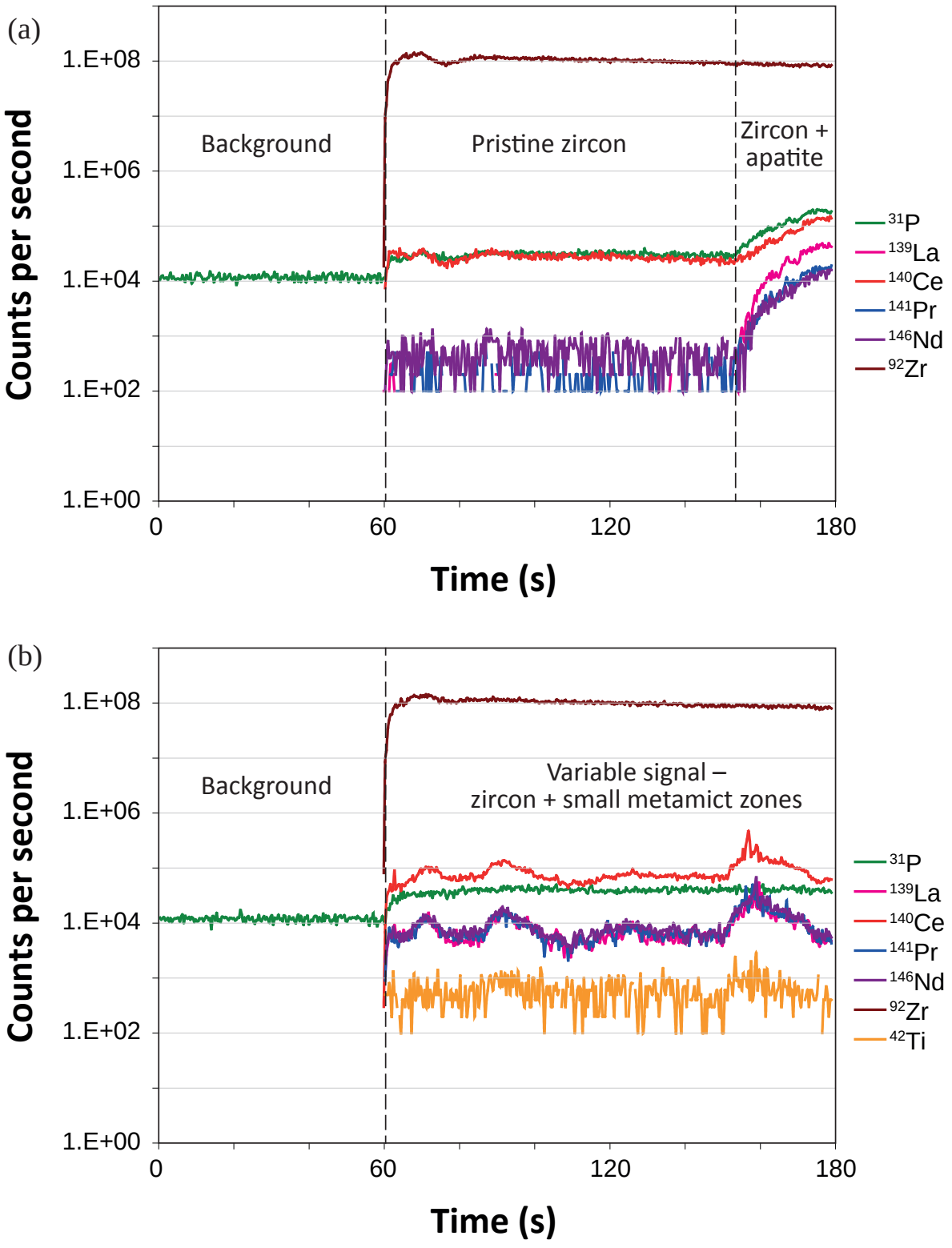


Figure 6.4. Time-resolved analysis plots of trace-element analyses of Mpuluzi zircons: (a) pristine zircon with large apatite inclusion; (b) variable signal with small metamict zones included.

Table 6.1: Trace-element compositions of zircons from the Mpuluzi batholith; averages calculated from 'pristine', 'variable' and 'metamict' groups for each sample. All values in ppm. For the full dataset see Appendix F.

	RSA03							
	Pristine (n=1)		Variable (n=51)					Metamict
	Value	1σ	Average	1σ	Min	Max	Median	-
P	34.9	9.6	60	48	0	230	44	
Ca	<LLD		300	460	0	2870	170	
Ti	0.64	0.35	19	69	0	406	3	
Y	120.3	4.5	400	460	90	2250	190	
Nb	1.154	0.078	2.4	1.8	0.6	10.2	1.5	
La	0.0206	0.0095	11	17	0	114	5	
Ce	2.92	0.14	74	81	4	429	51	
Pr	0.040	0.011	10	11	0	59	7	
Nd	0.234	0.067	68	69	1	352	51	
Sm	0.158	0.062	19	20	1	110	13	
Eu	0.041	0.017	4.9	4.6	0.2	19.5	3.5	
Gd	1.20	0.15	17	20	1	101	11	
Tb	0.649	0.048	3.8	5.0	0.4	23.4	1.8	
Dy	7.76	0.39	38	48	6	214	17	
Ho	3.21	0.14	13	15	2	72	6	
Er	18.04	0.71	54	59	14	282	27	
Tm	4.54	0.19	11	11	3	49	7	
Yb	57.2	2.1	114	91	40	440	72	
Lu	14.44	0.51	21	13	11	71	16	
Hf	11780	390	11800	1100	8300	15300	11600	
Ta	0.044	0.011	0.50	0.57	0.02	2.31	0.22	
Th	11.62	0.45	80	100	10	530	30	
U	127.2	4.0	171	69	88	447	149	

	RSA01														
	Pristine (n=2)					Variable (n=13)					Metamict (n=10)				
	Average	1σ	Min	Max	Median	Average	1σ	Min	Max	Median	Average	1σ	Min	Max	Median
P	210	160	100	320	210	250	160	100	600	190	320	200	140	750	250
Ti	10.00	0.21	9.85	10.15	10.00	26	17	8	70	23	73	28	43	121	68
Y	1080	820	500	1660	1080	1540	990	620	3700	1260	2100	610	1120	3130	2220
Nb	2.1	1.1	1.3	2.8	2.1	4.4	1.8	2.3	8.0	3.7	6.4	2.1	3.6	9.6	5.6
La	1.44	0.44	1.13	1.75	1.44	6.0	3.4	1.5	14.2	4.5	24	12	7	45	25
Ce	45	37	19	71	45	76	43	31	192	71	230	100	110	360	210
Pr	1.86	0.30	1.64	2.07	1.86	7.2	4.0	1.8	17.8	6.1	27	13	11	46	24
Nd	18.1	5.8	14.0	22.3	18.1	56	31	12	136	47	199	97	91	353	165
Sm	17	10	10	25	17	33	19	4	76	31	89	33	54	143	75
Eu	4.4	3.3	2.0	6.7	4.4	9.4	5.1	2.2	20.9	8.4	29	19	11	72	20
Gd	46	37	20	73	46	68	50	12	170	56	116	39	74	194	106
Tb	12	10	5	20	12	17	13	4	45	15	24.1	8.8	14.9	40.0	22.2
Dy	120	97	51	189	120	170	130	50	430	130	206	80	116	351	186
Ho	37	30	16	58	37	51	37	18	130	42	60	22	33	99	54
Er	140	110	70	220	140	190	130	80	490	160	226	77	120	353	218
Tm	29	22	13	44	29	38	24	16	92	32	43	14	22	64	42
Yb	260	180	130	390	260	350	210	150	810	280	390	130	200	570	390
Lu	42	25	25	60	42	55	30	26	123	41	63	20	32	85	66
Hf	9710	930	9050	10360	9710	11900	3200	8800	20800	10900	12300	2000	9500	15600	11900
Ta	0.37	0.24	0.20	0.54	0.37	0.91	0.50	0.28	2.16	0.83	0.89	0.28	0.47	1.28	0.81
Th	126	65	80	172	126	170	120	30	460	160	223	83	115	335	213
U	177	38	151	204	177	270	140	100	580	230	400	120	210	570	390

Table 6.1 continued.

	SWA18a														
	Pristine (n=7)					Variable (n=20)					Metamict (n=8)				
	Average	1σ	Min	Max	Median	Average	1σ	Min	Max	Median	Average	1σ	Min	Max	Median
P	550	300	260	1160	550	440	180	200	870	380	850	440	410	1730	740
Ca															
Ti	7.5	2.7	3.5	10.7	7.9	30	68	6	315	13	103	94	14	259	70
Y	1690	600	790	2580	1600	1680	860	980	4650	1430	6000	3500	2400	13200	4600
Nb	7.9	5.1	2.2	17.9	6.9	10.6	8.2	1.7	34.7	7.8	38	23	10	80	37
La	1.6	1.1	0.3	3.5	1.3	8	12	1	49	4	270	200	100	710	210
Ce	35	37	13	116	20	96	84	30	360	69	980	600	490	2110	710
Pr	1.7	1.4	0.4	4.2	1.4	5.7	7.3	1.3	33.2	3.5	143	95	48	323	100
Nd	12	12	4	38	10	33	37	10	176	24	700	480	210	1620	500
Sm	16	14	6	47	12	31	25	10	127	27	400	270	100	870	330
Eu	2.9	4.9	0.3	14.0	0.9	6.8	5.1	1.5	23.1	4.5	62	73	19	236	34
Gd	55	39	32	138	39	82	50	25	246	65	560	320	220	1120	470
Tb	19	10	10	37	15	25	15	9	76	23	160	93	58	302	140
Dy	210	100	90	350	180	240	130	100	670	220	1280	740	510	2380	1110
Ho	69	35	28	134	59	71	33	34	176	66	300	170	140	550	250
Er	290	150	110	570	250	270	110	140	600	260	940	510	480	1750	810
Tm	62	32	21	125	54	55	21	27	118	55	175	87	94	308	155
Yb	610	320	200	1240	540	550	210	240	1120	510	1590	780	850	2840	1420
Lu	89	46	31	182	77	79	29	41	151	79	191	86	116	343	156
Hf	11800	1700	8700	14100	12000	10000	2800	7400	17100	9000	11000	3700	7900	18400	9200
Ta	2.8	2.6	0.6	8.3	2.2	3.2	4.1	0.4	17.3	1.1	4.8	5.3	1.5	17.6	3.2
Th	210	150	70	440	120	270	200	80	820	190	800	460	400	1790	630
U	700	590	190	1820	380	470	340	100	1500	370	1370	980	510	3100	1030

	RSA05														
	Pristine (n=4)					Variable (n=19)					Metamict (n=7)				
	Average	1σ	Min	Max	Median	Average	1σ	Min	Max	Median	Average	1σ	Min	Max	Median
P	820	640	320	1690	630	1300	1100	300	4400	900	980	420	540	1820	950
Ca															
Ti	23	15	5	42	23	90	98	12	458	52	710	670	220	2060	370
Y	2600	1200	1000	3900	2700	4200	1600	2500	7700	3900	11000	3800	4600	16100	10900
Nb	30	16	11	50	29	80	54	11	187	60	300	140	40	510	350
La	37	32	5	77	33	50	25	9	89	48	420	480	130	1490	250
Ce	210	150	40	400	190	350	170	100	740	300	1730	640	1050	2970	1600
Pr	20	12	5	35	21	44	24	7	103	38	207	50	144	282	202
Nd	114	68	26	188	121	250	140	50	570	220	1090	230	820	1410	1010
Sm	52	26	14	72	62	157	94	36	386	117	600	200	270	890	530
Eu	9.6	5.3	2.0	14	11.1	21	11	5	47	20	82	29	35	119	74
Gd	101	50	28	139	118	260	130	90	560	200	850	320	310	1320	760
Tb	28	14	8	40	32	71	38	25	162	54	232	98	68	367	213
Dy	280	140	90	410	310	600	290	250	1280	470	1870	800	550	2920	1700
Ho	86	41	32	128	92	149	61	80	286	131	400	160	140	610	390
Er	330	150	150	490	350	510	180	300	880	460	1180	420	500	1740	1200
Tm	67	28	33	95	69	90	28	53	152	84	185	54	91	242	195
Yb	620	230	340	870	640	770	210	460	1210	720	1440	380	780	1850	1510
Lu	101	30	60	130	107	114	25	70	162	109	194	45	117	241	208
Hf	10600	370	10190	11050	10580	10050	860	8840	12250	9970	10300	640	9310	11100	10400
Ta	4.9	3.5	1.5	9.8	4.2	3.4	2.0	1.3	9.0	2.8	4.7	2.2	1.9	9.0	4.1
Th	310	220	60	550	320	360	180	160	880	300	640	470	300	1600	480
U	610	290	200	910	660	510	140	280	720	500	890	500	440	1850	700

Table 6.1 continued.

	RSA02										
	Pristine (n=8)					Variable (n=5)					Metamict
	Average	1σ	Min	Max	Median	Average	1σ	Min	Max	Median	-
P	350	140	190	560	340	640	470	210	1430	450	
Ca	490	550	60	1720	270	1800	1600	200	4400	1500	
Ti	150	400	10	1140	10	260	540	10	1230	10	
Y	2300	1000	1200	4100	2000	1900	1100	800	3500	1600	
Nb	30	26	6	67	15	21	29	3	73	12	
La	4.7	4.5	0.3	14.7	3.1	11.5	4.2	6.0	16.7	10.4	
Ce	49	29	14	84	47	75	30	31	107	70	
Pr	3.8	3.2	0.3	10.5	3.5	7.7	3.7	2.6	12.5	8.0	
Nd	28	25	3	83	27	56	33	18	98	51	
Sm	15	10	5	38	14	27	16	11	46	18	
Eu	2.9	1.4	1.1	5.7	2.8	4.4	2.4	1.8	7.8	4.6	
Gd	48	20	29	81	44	57	31	29	108	51	
Tb	16.7	6.4	10.5	24.5	14.9	15.7	8.2	8.1	29.7	13.4	
Dy	208	83	128	333	184	180	100	90	350	160	
Ho	80	34	47	135	72	66	40	31	126	56	
Er	350	160	190	620	320	280	180	120	500	230	
Tm	73	33	39	135	67	63	41	25	110	50	
Yb	680	310	360	1250	640	630	430	220	1200	510	
Lu	111	49	56	199	104	98	69	35	192	80	
Hf	11000	2100	9000	15300	10200	12200	2300	9200	14300	13500	
Ta	8.1	7.8	1.7	21.9	3.8	5.1	6.4	0.7	16.4	2.7	
Th	74	63	23	200	53	123	71	33	226	109	
U	146	98	54	335	128	320	180	70	520	360	

	SWA07														
	Pristine (n=13)					Variable (n=13)					Metamict (n=5)				
	Average	1σ	Min	Max	Median	Average	1σ	Min	Max	Median	Average	1σ	Min	Max	Median
P	490	220	160	950	460	750	680	170	2230	510	850	550	380	1770	710
Ca															
Ti	10.3	5.4	4.9	23.3	8.9	15.0	7.7	3.7	31.9	16.0	29	13	12	49	27
Y	1750	660	930	3460	1640	1900	1500	600	5800	1700	2860	780	2150	4170	2800
Nb	5.0	2.7	1.3	10.7	4.0	8.8	4.2	3.7	19.2	8.0	14.3	6.6	8.2	25.3	13.1
La	3.7	4.8	0.0	15.2	1.2	6.3	5.5	0.1	14.0	4.2	31	18	12	52	26
Ce	47	44	10	164	27	70	42	23	141	58	220	110	110	370	180
Pr	3.0	4.1	0.1	13.0	0.8	5.8	5.4	0.2	13.1	3.2	25	14	10	44	22
Nd	24	30	2	95	7	47	43	2	106	23	190	110	80	350	150
Sm	17	14	5	52	8	24	17	5	52	18	97	73	44	223	71
Eu	2.6	2.1	1.1	8.1	1.7	2.3	1.2	0.5	4.8	2.7	8.8	4.9	4.1	14.3	6.9
Gd	48	28	25	133	42	55	28	14	120	49	160	110	90	350	120
Tb	14.3	7.2	8.6	36.2	12.5	15	10	3	40	13	32	15	22	59	26
Dy	158	72	91	368	141	170	130	40	510	150	280	100	210	460	260
Ho	57	23	29	118	55	62	49	17	193	58	91	25	68	132	87
Er	246	87	125	459	242	270	210	90	840	260	377	96	275	530	364
Tm	53	17	27	92	53	59	45	19	180	55	80	18	63	109	77
Yb	520	160	270	850	530	570	420	180	1740	530	780	160	630	1030	770
Lu	92	28	48	138	88	98	65	33	270	90	132	23	108	162	140
Hf	11300	2300	7800	15500	10700	13800	2500	10300	19600	14000	13800	1900	10700	15400	14700
Ta	1.36	0.75	0.46	3.30	1.25	2.3	1.3	0.9	5.5	1.9	2.4	1.3	1.3	4.0	2.0
Th	148	88	63	377	112	180	180	30	670	110	270	110	120	380	300
U	290	190	90	700	200	410	350	90	1380	370	550	200	270	830	570

Table 6.1 continued.

	RSA04									
	Pristine (n=17)					Variable	Metamict (n=8)				
	Average	1σ	Min	Max	Median	-	Average	1σ	Min	Max	Median
P	290	170	80	830	270		260	120	100	430	220
Ca	600	1900	0	7800	100		2600	1500	700	4700	2600
Ti	14.7	7.0	8.1	27.7	11.7		330	320	40	880	250
Y	2200	2700	700	12300	1500		8700	8300	1900	24900	6500
Nb	7.2	6.1	1.8	26.6	6.6		110	110	20	280	70
La	7.7	9.5	0.0	27.4	3.1		160	120	30	300	170
Ce	150	190	20	750	80		890	780	150	2310	750
Pr	4.3	4.6	0.1	16	2.4		120	110	10	300	110
Nd	31	31	3	98	16		690	660	70	1850	570
Sm	31	41	5	180	18		420	420	50	1160	300
Eu	12	17	2	76	7		130	130	20	360	90
Gd	100	150	20	660	50		660	670	110	1840	450
Tb	27	40	7	178	16		170	170	30	480	120
Dy	250	350	70	1570	160		1300	1200	300	3600	1000
Ho	73	93	22	422	49		280	260	60	790	220
Er	270	300	90	1410	190		860	760	190	2330	690
Tm	53	53	17	249	39		150	130	40	390	130
Yb	490	430	160	2070	370		1270	980	320	3090	1100
Lu	73	55	27	271	59		180	130	50	420	160
Hf	9600	2300	6900	14200	8400		12300	3400	8600	19100	11600
Ta	0.91	0.56	0.32	2.23	0.71		4.5	3.3	1.5	11.4	3.2
Th	250	500	50	2170	130		550	420	120	1280	410
U	240	200	60	850	150		870	550	240	1680	840

	RSA08														
	Pristine (n=8)					Variable (n=9)					Metamict (n=3)				
	Average	1σ	Min	Max	Median	Average	1σ	Min	Max	Median	Average	1σ	Min	Max	Median
P	1030	980	360	3000	600	560	500	160	1560	300	224	44	189	274	210
Ca	2800	3100	0	7300	1900	1200	1500	200	4700	400	4500	2700	1400	6500	5500
Ti	10.2	5.9	4.2	23.1	9.7	52	51	8	137	30	1800	2900	100	5100	100
Y	3100	2400	1100	8400	2000	2800	1400	900	5200	2600	2190	990	1140	3130	2290
Nb	16	20	4	63	10	14.6	8.8	4.6	31.4	11.5	26	14	10	36	31
La	17	20	0	60	16	94	93	5	271	59	210	200	60	440	140
Ce	118	99	12	275	103	380	280	80	750	210	1150	930	450	2210	800
Pr	11	13	0	37	10	49	42	4	142	32	104	71	37	178	96
Nd	75	85	3	258	59	310	250	30	850	220	540	330	240	900	500
Sm	47	50	6	159	31	190	160	20	550	130	230	100	130	330	240
Eu	4.2	4.9	0.7	15.8	3.1	14	15	2	48	10	30	21	17	53	18
Gd	104	75	12	258	93	280	210	80	710	240	320	150	160	460	330
Tb	28	19	5	57	22	54	36	16	130	53	51	20	28	66	59
Dy	300	220	80	740	210	370	200	110	730	430	320	130	170	430	370
Ho	103	81	38	280	68	95	48	31	171	101	72	30	39	97	81
Er	440	350	200	1230	270	330	190	120	690	310	240	100	130	330	250
Tm	94	72	49	260	61	65	41	27	142	56	46	18	28	64	45
Yb	900	640	450	2380	660	600	370	250	1310	490	440	190	280	640	390
Lu	150	110	70	400	110	98	64	44	219	69	71	26	48	99	67
Hf	12100	1800	9700	14600	12200	12200	2100	8500	14300	13200	12100	1500	10500	13500	12300
Ta	8	14	0	40	2	4.2	2.9	0.8	9.3	2.8	6.2	2.9	2.9	8.4	7.5
Th	230	200	40	600	150	230	160	30	450	190	74	21	52	95	76
U	670	440	200	1290	600	480	300	190	1120	380	680	310	460	1030	540

Table 6.1 continued.

	SWA10a														
	Pristine (n=11)					Variable (n=13)					Metamict (n=8)				
	Average	1σ	Min	Max	Median	Average	1σ	Min	Max	Median	Average	1σ	Min	Max	Median
P	400	190	170	760	390	710	950	100	3740	360	1100	1000	300	3400	800
Ca	2300	2500	0	6900	2600	3200	4800	0	16700	1200	11900	6800	900	20600	12500
Ti	14	10	1	35	12	31	61	1	233	16	250	200	50	640	190
Y	2700	1500	900	5800	2400	2180	920	950	3670	2110	7300	6700	3400	23000	4600
Nb	21	22	3	77	9	14.7	8.2	2.6	35.4	13.4	93	67	22	241	73
La	21	27	2	96	15	30	18	2	68	30	320	210	160	730	230
Ce	57	42	18	150	47	97	74	14	287	71	1500	1500	300	4600	700
Pr	7.5	8.3	0.6	28.6	3.6	14	12	1	46	10	160	140	70	490	100
Nd	39	39	5	136	21	73	63	4	251	55	860	780	330	2650	480
Sm	22	12	5	46	20	34	24	5	98	30	390	450	110	1400	200
Eu	3.2	2.2	0.5	8.3	2.8	5.5	4.6	1.3	18.6	4.5	90	68	24	225	70
Gd	67	26	24	108	61	74	38	26	158	64	620	770	200	2380	270
Tb	22	10	8	41	20	20.6	9.0	8.8	36.2	18.3	140	180	50	570	60
Dy	250	130	90	510	230	210	88	108	360	196	1100	1300	400	4100	500
Ho	90	52	28	193	81	71	32	31	128	68	240	230	110	780	150
Er	390	220	110	820	330	300	130	110	510	290	710	490	400	1880	560
Tm	79	43	21	159	68	61	27	22	101	60	118	56	75	247	106
Yb	740	370	190	1370	640	570	250	210	960	570	990	330	650	1720	920
Lu	129	62	34	231	117	102	44	39	173	98	153	40	106	229	152
Hf	11400	2700	8100	18000	11400	10500	1700	7800	12600	10800	11400	2400	8700	15800	10500
Ta	7.6	7.8	0.4	24.6	4.6	4.3	3.1	0.8	10.4	3.8	17	17	2	47	7
Th	310	280	40	1000	300	240	160	70	520	170	830	910	190	2990	540
U	750	590	80	1720	620	700	420	160	1670	540	1640	970	450	3500	1310

	RSA09														
	Pristine (n=5)					Variable (n=12)					Metamict (n=14)				
	Average	1σ	Min	Max	Median	Average	1σ	Min	Max	Median	Average	1σ	Min	Max	Median
P	660	490	80	1210	600	640	300	140	1270	640	680	310	290	1400	620
Ca	800	1700	0	3800	100	3800	4700	300	15500	1300	8100	4800	800	15900	8200
Ti	12	12	5	33	7	31	25	5	95	23	129	87	33	274	101
Y	2900	2800	200	6200	1800	3900	1300	1800	6800	3500	10800	6000	2900	26600	10500
Nb	13	13	1	32	8	25	12	12	52	21	95	73	32	263	71
La	3.9	3.8	0	8.3	4.5	21	14	3	53	16	120	140	30	450	90
Ce	31	28	6	61	13	92	56	42	236	72	530	760	140	2990	310
Pr	1.8	2.0	0	4.6	1.2	8.5	5.9	1.7	24.0	7.0	55	75	16	309	40
Nd	12	13	1	29	6	44	28	12	117	38	280	370	80	1550	190
Sm	13	14	1	33	6	28	13	13	59	24	160	200	40	830	100
Eu	3.5	3.7	0.8	8.7	0.9	4.4	2.8	2.3	10.9	3.3	20	24	3	99	12
Gd	70	74	8	178	31	94	36	51	165	84	390	320	80	1360	290
Tb	25	25	2	59	13	33	12	16	53	31	124	92	26	368	100
Dy	270	260	20	610	160	370	130	170	620	340	1190	740	300	2780	1020
Ho	96	91	6	195	62	126	44	58	227	115	340	190	100	820	320
Er	400	370	20	810	280	520	180	230	960	470	1260	710	390	3250	1210
Tm	78	70	4	158	57	103	35	43	193	99	230	120	80	550	220
Yb	710	640	40	1450	530	940	330	370	1790	910	2000	1000	800	4800	1800
Lu	120	100	10	260	100	149	54	61	296	145	280	140	110	680	270
Hf	10100	1200	8500	11700	10000	10300	1900	7600	13800	10300	13200	2800	9000	19800	13800
Ta	1.7	1.5	0.4	4.1	1.0	5.0	4.4	1.3	12.7	2.9	12.4	6.9	1.0	27.5	13.5
Th	79	85	7	218	39	230	220	50	870	160	450	560	50	2040	210
U	200	290	10	710	90	720	440	230	1520	600	1720	870	650	3540	1600

Table 6.1 continued.

	SWA03														
	Pristine (n=9)					Variable (n=23)					Metamict (n=14)				
	Average	1σ	Min	Max	Median	Average	1σ	Min	Max	Median	Average	1σ	Min	Max	Median
P	1200	1700	200	5600	700	1500	1100	500	4800	1100	1800	1700	600	7000	1100
Ca															
Ti	18	13	5	46	17	120	470	10	2270	20	110	110	10	460	80
Y	2370	740	1510	3600	2240	2510	540	1410	3590	2490	4600	2400	2300	10800	3900
Nb	14.8	5.8	8.2	27.4	14.0	18	14	7	62	13	55	36	17	140	43
La	10	11	1	37	5	13	12	1	50	11	79	73	15	244	55
Ce	57	29	13	112	52	72	35	30	192	67	320	240	100	860	210
Pr	5.1	3.9	1.0	13.0	3.8	6.4	4.4	0.8	18.2	5.5	40	33	8	114	26
Nd	29	21	6	71	22	36	22	8	93	31	220	220	50	810	120
Sm	23	12	8	48	21	26	12	11	56	23	120	100	30	420	80
Eu	3.4	1.5	1.7	5.9	2.9	3.6	1.8	1.2	7.9	3.5	22	21	4	78	13
Gd	74	20	36	102	70	81	21	36	123	75	220	150	90	620	180
Tb	26.7	7.1	14.1	37.7	25.7	28.9	7.2	12.7	45.1	28.3	68	33	29	132	63
Dy	298	78	176	427	291	323	76	145	480	319	680	300	310	1310	650
Ho	102	32	67	157	93	109	24	52	150	109	201	83	105	420	185
Er	420	150	280	660	390	453	96	234	603	456	760	310	430	1660	710
Tm	87	30	55	135	81	93	20	49	122	91	146	55	87	306	138
Yb	800	280	510	1240	740	860	170	480	1100	860	1270	430	790	2480	1180
Lu	128	51	64	209	119	134	26	82	180	132	189	63	127	379	174
Hf	11100	1800	8900	14600	10300	10840	900	9150	12960	10850	12000	1900	10000	16400	11500
Ta	2.8	1.2	1.4	5.4	2.5	2.9	1.5	1.1	7.5	2.5	4.5	2.8	2.2	11.0	3.4
Th	310	160	50	560	320	390	200	90	980	350	680	240	350	1100	610
U	710	380	100	1260	600	690	330	330	1750	610	1150	720	540	2770	830

	RSA06														
	Pristine (n=5)					Variable (n=11)					Metamict (n=14)				
	Average	1σ	Min	Max	Median	Average	1σ	Min	Max	Median	Average	±1σ	Min	Max	Median
P	770	480	190	1430	730	910	460	410	1910	860	1000	1100	200	4700	700
Ca	900	830	30	1700	1070	2400	1700	400	5600	1900	8300	5900	2000	22400	6300
Ti	8.5	2.9	5.5	13.1	8.4	22	13	4	42	22	250	260	20	770	150
Y	2300	1200	500	3400	2900	2790	850	1510	4370	2810	3870	990	2410	5990	3710
Nb	6.4	3.3	2.2	10.1	7.1	13.9	5.4	8.0	24.2	12.5	35	22	13	95	32
La	9	16	0	38	2	32	20	3	65	23	200	160	60	610	150
Ce	90	88	20	243	65	250	140	70	460	250	1280	730	460	2540	1120
Pr	7	13	0	30	2	32	21	4	68	33	172	81	59	281	162
Nd	60	99	3	236	22	210	140	40	460	200	1090	460	460	1680	1120
Sm	35	42	3	109	22	109	67	26	219	108	630	280	230	1230	620
Eu	5.0	6.0	0.7	15.5	2.6	11.1	5.8	4.6	19.8	10.2	66	36	19	151	62
Gd	73	46	12	140	75	148	73	49	288	130	690	320	270	1420	650
Tb	21	11	4	31	25	31	13	15	55	29	104	50	44	224	97
Dy	220	110	50	320	280	284	97	153	450	260	610	240	340	1190	540
Ho	77	40	19	114	96	94	28	51	145	93	139	41	92	232	128
Er	320	170	80	480	400	390	110	230	590	430	470	110	300	680	450
Tm	66	35	18	101	79	83	23	49	117	89	92	19	59	122	90
Yb	620	320	170	950	710	810	240	470	1200	800	850	150	570	1090	830
Lu	101	50	30	152	123	136	44	86	230	132	135	24	85	166	136
Hf	9320	450	8690	9930	9360	12100	3000	9000	16300	11600	10300	1600	8800	13200	9600
Ta	1.34	0.72	0.46	2.14	1.64	4.2	3.5	1.6	12.1	2.9	5.0	4.6	1.7	19.7	3.5
Th	250	170	30	390	340	300	150	70	630	280	730	690	230	2890	540
U	350	240	40	540	500	620	220	230	1040	540	1050	470	530	2000	880

Table 6.1 continued.

	SWA13a														
	Pristine (n=19)					Variable (n=7)					Metamict (n=8)				
	Average	1σ	Min	Max	Median	Average	1σ	Min	Max	Median	Average	1σ	Min	Max	Median
P	520	210	260	1260	460	720	340	200	1240	580	440	150	250	670	410
Ca	53	60	0	214	27	170	150	30	460	100	720	610	300	1990	460
Ti	12.7	10.0	4.6	49	10.8	23	19	8	63	14	83	51	17	152	63
Y	1610	730	770	3750	1430	2230	740	1270	3060	1980	2460	940	1360	4170	2410
Nb	3.4	2.2	1.6	10.7	2.6	5.0	1.8	2.2	7.6	4.9	7.5	3.2	3.4	13.2	7.8
La	4.7	5.4	0.1	22.1	2.6	12	12	2	34	6	58	41	16	150	47
Ce	30	17	10	76	25	55	34	22	119	55	190	110	70	430	140
Pr	2.5	2.7	0.1	11.1	1.5	6.7	6.0	1.1	18.2	6.5	31	20	9	75	24
Nd	15	14	2	59	11	37	29	7	90	42	160	100	50	390	130
Sm	12.4	6.9	3.7	31.9	10.9	24	16	8	53	23	83	48	27	182	67
Eu	2.4	1.2	1.1	5.2	1.9	4.3	2.7	1.5	10	3.9	16.6	8.6	7.0	34.2	15.8
Gd	43	15	18	80	43	67	25	39	110	65	140	69	57	278	123
Tb	13.9	5.2	6.0	28.8	13.6	20.4	7.0	11.4	31.2	18.3	34	16	15	65	31
Dy	152	63	68	345	139	212	66	121	296	192	280	120	140	500	270
Ho	54	24	26	124	48	73	23	41	99	66	80	29	45	132	79
Er	230	100	110	520	200	300	94	175	410	280	291	97	182	458	294
Tm	46	20	24	103	40	60	19	35	83	57	55	17	34	81	57
Yb	430	180	230	960	380	550	170	330	750	540	490	140	320	670	510
Lu	76	31	44	163	66	98	30	60	136	92	82	21	54	110	84
Hf	9700	1300	8000	12500	9300	10100	1500	8300	12500	10400	10200	1900	8200	14000	10000
Ta	0.66	0.34	0.35	1.56	0.51	10.00	0.46	0.56	1.82	0.91	2.3	3.0	0.7	9.6	1.3
Th	109	49	38	240	97	169	51	100	264	162	230	130	90	440	210
U	180	100	70	520	150	290	110	130	440	300	450	280	190	1010	320

	SWA11														
	Pristine (n=19)					Variable (n=9)					Metamict (n=15)				
	Average	1σ	Min	Max	Median	Average	1σ	Min	Max	Median	Average	1σ	Min	Max	Median
P	430	150	260	860	400	570	310	220	1290	500	710	240	510	1430	590
Ca															
Ti	4.7	2.6	1.2	10.4	4.2	8.6	4.2	3.6	15.5	8.7	14.2	8.1	5.6	39.9	12.8
Y	1140	350	650	2110	1110	1700	650	830	2940	1770	2670	810	1520	4820	2570
Nb	3.6	1.9	1.7	8.9	2.9	8.5	5.0	2.6	16.9	8.3	18	19	4	66	10
La	0.5	1.1	0.0	4.9	0.0	1.7	1.6	0.1	5.4	1.4	11	10	1	32	6
Ce	14.6	6.0	7.4	27.4	14.1	24.6	8.6	10.9	37.1	22.8	53	25	19	107	49
Pr	0.26	0.48	0.02	2.07	0.07	0.81	0.50	0.17	1.91	0.80	4.5	3.6	0.6	11.5	3.2
Nd	2.4	2.4	0.5	10.9	1.7	5.9	3.0	2.3	12.2	5.9	28	20	6	70	20
Sm	4.4	2.1	1.8	10.5	4.1	7.5	2.2	3.5	10.4	7.5	22.0	9.5	9.0	40.5	21.9
Eu	0.72	0.55	0.15	2.25	0.57	1.44	0.72	0.57	2.89	1.28	5.4	3.6	2.0	14.6	4.7
Gd	23.7	7.2	12.5	38.1	23.5	36	11	13	51	39	76	24	35	113	79
Tb	8.6	2.3	4.7	13.1	8.0	12.9	4.0	6.1	19.9	13.7	23.2	7.1	12.3	39.1	23.3
Dy	102	29	58	171	99	151	51	75	245	158	240	77	136	441	227
Ho	37	11	22	66	37	54	19	28	92	56	81	27	49	153	76
Er	163	48	98	295	163	233	87	127	410	239	320	110	200	620	310
Tm	35	10	21	64	34	49	18	29	86	49	64	22	38	122	59
Yb	335	98	205	612	329	470	170	280	830	460	580	190	320	1060	540
Lu	58	17	37	103	57	78	30	46	140	82	99	33	58	187	92
Hf	11900	1500	9600	14800	11700	12100	1400	9800	15100	11900	11900	2600	9200	19900	11500
Ta	0.81	0.48	0.43	2.15	0.61	1.15	0.69	0.52	2.58	0.74	1.25	0.53	0.48	2.36	1.15
Th	72	25	30	139	74	138	84	60	318	124	201	92	81	418	184
U	174	79	74	328	148	280	170	130	650	200	330	100	170	610	290

Table 6.1 continued.

	SWA09														
	Pristine (n=11)					Variable (n=6)					Metamict (n=5)				
	Average	1σ	Min	Max	Median	Average	1σ	Min	Max	Median	Average	1σ	Min	Max	Median
P	480	140	240	750	480	470	310	130	960	400	760	370	310	1160	600
Ca	40	28	0	95	34	380	540	60	1430	120	2400	4700	100	10800	400
Ti	11.5	7.3	5.4	28.4	7.9	29	22	11	61	18	210	320	20	770	110
Y	1430	640	710	2960	1300	1800	1200	500	3800	1400	8100	7700	3000	20800	3500
Nb	7.7	4.3	1.6	13.7	7.0	27	27	3	79	22	150	220	10	530	40
La	4.5	3.8	0.1	10.0	4.5	17	17	1	44	9	200	300	30	740	60
Ce	28	16	8	53	30	87	87	8	249	52	1000	1800	100	4100	300
Pr	2.5	2.0	0.1	5.9	2.5	9.9	9.3	0.2	25.5	6.0	100	150	10	370	40
Nd	15	11	2	38	15	53	49	4	135	31	500	690	80	1710	210
Sm	11.3	7.3	3.5	29.7	9.4	32	29	6	82	22	260	310	50	800	110
Eu	1.40	0.78	0.34	3.23	1.39	4.3	3.4	0.8	9.4	3.0	35	52	5	128	11
Gd	39	21	18	96	37	70	52	24	156	54	440	460	140	1230	200
Tb	12.7	6.1	5.8	29.0	10.8	20	15	6	44	16	110	110	40	300	50
Dy	138	62	64	295	120	200	140	50	420	160	960	900	380	2430	400
Ho	48	21	23	97	44	58	38	15	116	47	240	220	90	590	110
Er	200	84	95	380	188	220	140	60	430	180	770	680	270	1890	410
Tm	41	16	17	71	39	44	27	12	82	36	120	100	40	290	80
Yb	380	150	150	630	380	400	230	110	740	350	980	790	320	2240	680
Lu	69	27	24	111	68	70	36	23	114	62	140	100	50	300	110
Hf	10500	1400	9300	14100	10300	12700	3000	9500	17300	12100	10100	2200	7400	13500	10200
Ta	0.87	0.47	0.32	1.66	0.77	10.00	0.66	0.45	2.15	0.74	4.0	3.5	0.8	9.5	3.6
Th	101	52	53	235	78	131	87	47	245	94	590	740	110	1900	280
U	200	150	90	610	120	250	220	90	670	170	700	900	240	2310	290

	SWA02a														
	Pristine (n=4)					Variable (n=4)					Metamict (n=13)				
	Average	1σ	Min	Max	Median	Average	1σ	Min	Max	Median	Average	1σ	Min	Max	Median
P	928	87	832	1043	917	380	200	160	660	350	1000	1400	100	4100	400
Ca															
Ti	9.5	4.5	4.9	15.2	9.0	12.9	7.8	3.9	23.1	12.2	63	73	16	257	30
Y	2600	270	2280	2900	2610	1140	550	540	1730	1150	4000	1900	2000	8200	3500
Nb	15.2	8.4	8.4	27.1	12.6	10.9	5.7	3.1	15.9	12.3	80	50	24	163	84
La	5.5	4.9	1.0	12.4	4.4	9.7	3.1	6.1	13.7	9.6	140	210	30	820	80
Ce	46	24	29	81	36	63	30	37	105	54	630	800	190	3270	430
Pr	2.9	3.0	0.4	7.2	2.0	6.2	3.8	2.9	11.4	5.2	75	96	19	391	54
Nd	18	14	5	37	14	43	31	15	86	35	450	500	130	2080	310
Sm	14.8	3.1	11.0	17.7	15.3	22	16	7	45	18	170	150	50	630	120
Eu	1.11	0.28	0.77	1.39	1.14	2.6	1.8	0.8	5.1	2.1	25	23	9	98	19
Gd	64.5	7.4	57.5	71.5	64.5	47	25	22	80	42	280	190	100	710	190
Tb	21.9	2.4	19.0	24.8	21.9	11.8	5.5	6.5	17.5	11.6	55	34	21	120	40
Dy	249	23	225	280	245	115	53	63	162	117	440	230	180	870	360
Ho	86.2	8.4	77.4	96.4	85.5	37	17	20	55	37	123	54	61	240	113
Er	366	31	334	399	366	153	70	73	229	156	460	190	260	940	400
Tm	79.9	5.7	73.0	84.6	81.0	35	16	15	53	36	98	39	59	200	88
Yb	789	47	728	840	794	360	160	150	550	380	970	380	610	1980	900
Lu	116	15	100	133	115	56	25	21	78	62	144	53	97	293	133
Hf	11800	1400	10100	13100	12000	11300	1300	10000	13000	11100	12700	2100	9800	17900	12300
Ta	3.11	0.58	2.25	3.50	3.34	1.83	0.98	1.07	3.24	1.51	9.7	8.6	2.4	25.0	6.0
Th	460	78	357	539	472	154	34	131	204	142	500	250	210	1070	430
U	1170	130	1010	1290	1200	490	270	210	840	460	1680	770	890	3790	1570

Table 6.1 continued.

	RSA07														
	Pristine (n=2)					Variable (n=5)					Metamict (n=5)				
	Average	1σ	Min	Max	Median	Average	1σ	Min	Max	Median	Average	1σ	Min	Max	Median
P	704	29	684	725	704	580	200	350	880	540	1070	650	460	1820	810
Ca															
Ti	11.1	4.3	8.1	14.1	11.1	60	68	7	172	27	600	490	200	1460	440
Y	2470	300	2250	2680	2470	3100	1400	1700	4900	2600	23000	14000	7000	41000	18000
Nb	13.6	2.2	12.0	15.2	13.6	14.5	8.6	6.3	26.7	13.4	170	150	30	410	110
La	14.6	7.2	9.5	19.7	14.6	34	31	5	86	28	320	120	140	470	340
Ce	74	21	59	90	74	170	140	60	390	100	2900	2400	700	5800	1800
Pr	9.2	5.2	5.5	12.8	9.2	27	24	5	68	19	350	240	100	630	280
Nd	54	30	33	75	54	150	140	30	370	110	2200	1700	500	4200	1600
Sm	32	17	20	44	32	91	86	22	231	63	1400	1100	300	2700	1000
Eu	2.95	0.15	2.84	3.05	2.95	7.5	6.3	2.2	17.5	7.1	75	51	23	140	62
Gd	83	24	66	100	83	180	150	60	410	120	2600	2100	500	5200	1700
Tb	23.4	5.2	19.8	27.1	23.4	45	33	19	97	30	600	460	130	1190	400
Dy	237	34	213	261	237	380	230	200	730	240	4200	3100	900	8300	3100
Ho	76.9	5.7	72.9	80.9	76.9	101	46	57	164	82	830	600	190	1630	600
Er	310	18	297	322	310	360	130	190	500	340	2000	1300	500	3700	1500
Tm	62.91	0.47	62.58	63.24	62.91	66	21	34	85	71	240	130	80	400	200
Yb	594.4	1.6	593.3	595.6	594.4	590	180	300	740	670	1600	670	640	2460	1480
Lu	96.6	2.8	94.6	98.6	96.6	94	29	47	120	106	211	74	96	297	222
Hf	10500	2700	8600	12400	10500	11320	490	10720	11930	11300	11600	2600	9100	15600	11700
Ta	4.1	3.2	1.8	6.4	4.1	2.3	1.4	0.7	4.4	2.0	11.1	7.4	5.2	23.8	9.7
Th	166	76	112	220	166	650	840	150	2150	340	3800	3800	700	10100	3300
U	490	210	340	630	490	300	150	90	440	380	1490	630	500	2010	1780

	SWA05														
	Pristine (n=5)					Variable (n=5)					Metamict (n=9)				
	Average	1σ	Min	Max	Median	Average	1σ	Min	Max	Median	Average	1σ	Min	Max	Median
P	292	63	196	358	305	360	110	240	520	370	1030	490	440	1810	890
Ca															
Ti	15.2	8.1	5.1	27.0	15.4	10.3	4.2	4.1	15.6	11.3	130	180	10	550	30
Y	890	270	450	1070	1060	1480	590	940	2340	1360	8000	10000	2000	32000	3000
Nb	2.8	1.1	1.1	4.1	3.0	8.4	7.7	1.6	20.8	6.4	66	76	17	228	29
La	4.3	2.7	1.8	8.2	3.6	8.4	7.0	2.0	18.5	5.0	340	270	50	760	230
Ce	37	23	8	64	39	81	66	26	169	49	1600	1600	200	5100	900
Pr	2.3	1.8	0.1	4.8	2.5	6.7	6.2	1.6	16.4	4.1	190	160	30	540	140
Nd	16	11	1	28	18	37	30	11	83	29	1200	1100	100	3200	500
Sm	14.3	8.4	3.0	21.7	17.5	19.0	9.0	9.3	29.6	17.1	610	770	90	2370	190
Eu	2.3	1.4	0.7	4.1	2.7	3.3	2.3	1.6	7.3	2.6	70	82	11	235	43
Gd	37	17	13	50	49	50	17	32	74	50	800	1100	200	2700	200
Tb	10.5	4.3	4.1	14.2	12.7	15.5	5.1	9.7	22.2	16.9	170	230	40	690	50
Dy	103	36	47	135	123	168	59	102	235	172	1300	1800	400	5900	500
Ho	32	10	16	40	38	58	23	34	82	62	360	490	120	1600	140
Er	125	36	65	149	145	240	100	140	370	260	1200	1500	400	5100	600
Tm	26.1	7.0	14.4	30.7	30.0	52	24	28	83	55	210	220	80	790	130
Yb	253	62	149	298	279	540	270	280	910	580	1900	1600	800	5900	1400
Lu	36.7	8.8	21.5	43.5	39.5	74	35	40	123	77	230	170	90	650	190
Hf	10450	310	9990	10800	10500	11300	1700	9200	13400	10800	17100	3000	12300	21800	16800
Ta	0.43	0.13	0.24	0.55	0.48	6	10	00.0	24	1	10.7	5.5	2.8	23.3	10.2
Th	113	43	42	153	118	240	230	80	640	140	800	1100	100	3600	300
U	228	80	96	300	234	420	340	130	950	250	3100	1700	700	6500	3300

The pristine group of analyses shows a range of average P contents from 35 to 1200 ppm with a median of 500 ppm; in the variable group this is slightly higher (60–1500 ppm, median = 580 ppm), while the metamict group ranges from 224 to 1800 ppm with a median value of 850 ppm (Figure 6.5a). Zircons from nine samples were analysed for Ca; the pristine group shows a range in average Ca from 40 to 2800 ppm and a median of 720 ppm; in the variable group this range is considerably extended (170–3800 ppm, median = 1500 ppm), and averages of the metamict group range from 720 to 12000 ppm with a median value of 4500 ppm (Figure 6.5b). Average Ti contents range from 0.64 to 150 ppm with a median of 11 ppm in the pristine group; the variable group ranges from 8.6 to 260 ppm with a median value of 29 ppm, and the metamict group shows much higher concentrations (14–1800 ppm, median = 130 ppm; Figure 6.5c).

Contents of Nb and Ta also show an increase from the pristine group (average Nb is 1.2–30 ppm, median = 5 ppm; Ta averages 0.044–8.1 ppm, median = 1.5 ppm) to the variable group (Nb averages 2.4–80 ppm, median = 14 ppm; Ta averages 0.50–5.6 ppm, median = 2.9 ppm), and the metamict group is higher still (range in average Nb: 6.4–300 ppm, median = 61 ppm; Ta range is 0.9–17, median = 4.8 ppm; Figure 6.5d, e).

The average values for Th and U also increase from the pristine group to the metamict group, with the pristine group showing a range in average Th of 12 to 460 ppm and U of 130 to 1200 ppm (median Th: 160 ppm; U: 260 ppm); in the variable group the range in average Th is 75 to 6500 ppm (median = 230 ppm), and U ranges from 170 to 720 ppm with a median value of 420 ppm. In the metamict group the range of both Th and U is considerably larger (Th: 74–3800 ppm, median = 570 ppm; U: 330–3100 ppm, median = 980 ppm; Figure 6.5f, g). The change in abundances of Th and U with increasing metamictisation does not appear to have any systematic effect on Th/U ratios – the range of Th/U in the pristine group is narrower than in the other two groups (pristine: 0.09–0.91; variable: 0.34–2.31; metamict: 0.12–2.28), but the median values are similar (pristine: 0.49; variable: 0.51; metamict: 0.59; Figure 6.5h).

Concentrations of Y and the rare earth elements (REE) also show an increase from the pristine group to the metamict group. Average Y contents range from 120 to 3100 ppm in the pristine group, with a median value of 2200 ppm; in the variable group the range is 400 to 4200 ppm with a median value of 1900 ppm, and the metamict group ranges from 2100 to 23000 ppm with a median value of 5300 ppm (Figure 6.5i). Among the REE, the increase is most pronounced in the light elements (La, Ce, Pr, Nd = LREE); average LREE contents range from 3.2 to 380 ppm with a median of 75 ppm in the pristine group; in the variable group the range is 33 to 830 ppm with a median of 150 ppm; the metamict group shows a range of 97 to 5700 ppm, with a median value of 1800 ppm (Figure 6.5j). The middle REE (Sm, Eu, Gd, Tb, Dy, Ho = MREE) show a less pronounced shift in average values (pristine group:

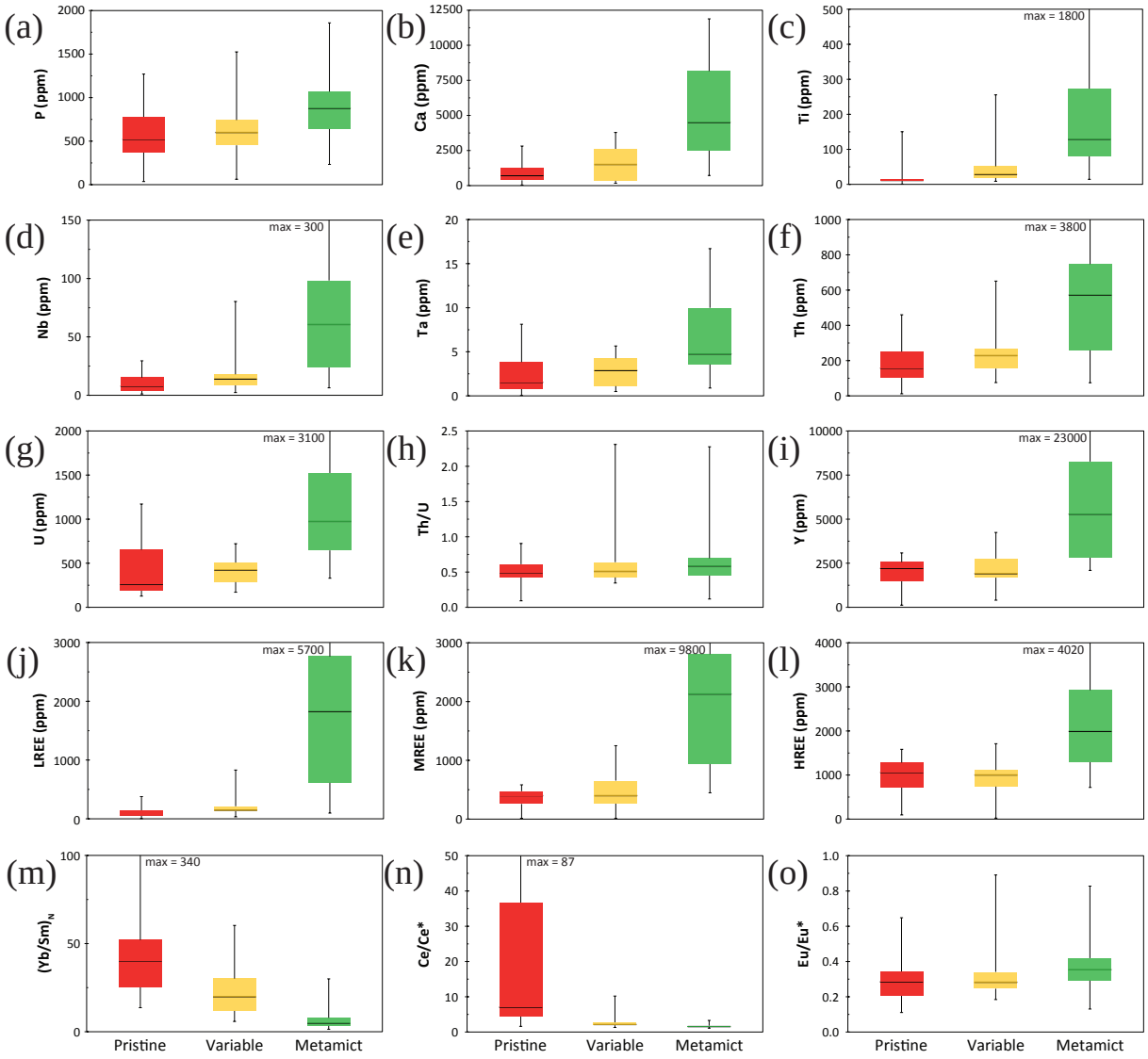


Figure 6.5. Plot of trace-element characteristics of the pristine (red), variable (yellow), and metamict (green) groups: (a) P; (b) Ca; (c) Ti; (d) Nb; (e) Ta; (f) Th; (g) U; (h) Th/U; (i) Y; (j) LREE; (k) MREE; (l) HREE; (m) $(Yb/Sm)_N$; (n) Ce/Ce*; (o) Eu/Eu*. Upper and lower bars represent maximum and minimum values; box represents upper quartile (75th percentile), median (black line), and lower quartile (25th percentile).

13–580 ppm, median = 400 ppm; variable group: 13–1200 ppm, median = 400 ppm; metamict group: 450–9800 ppm, median = 2100 ppm; Figure 6.5k), and the heavy REE (Er, Tm, Yb, Lu = HREE) show only a slight increase overall (pristine group: 94–1600 ppm, median = 1100 ppm; variable group: 21–1700 ppm, median = 1000 ppm; metamict group: 720–4000 ppm, median = 2000 ppm; Figure 6.5l). This more pronounced change in the lighter elements is reflected in the decrease in the slope of the REE patterns (see Figure 6.6); $(Yb/Sm)_N$ (as a proxy for the slope) shows an overall decrease from the pristine group (average $(Yb/Sm)_N$ = 14–340, median = 40), to the variable group (average $(Yb/Sm)_N$ = 5.8–60, median = 20), and the metamict group is lower still (average $(Yb/Sm)_N$ = 1.4–30, median = 4.9; Figure 6.5m).

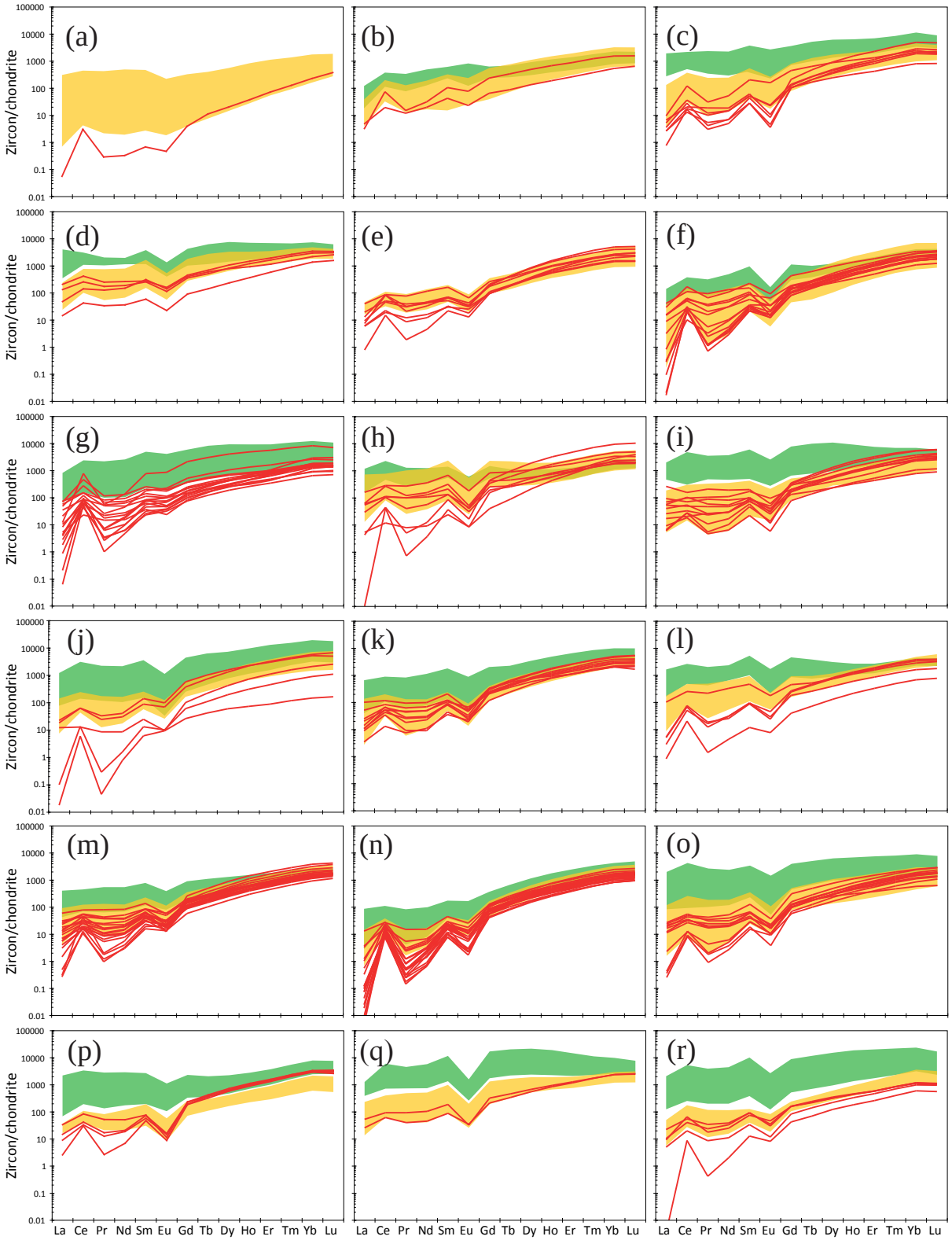


Figure 6.6. Chondrite-normalised REE plots for zircons from the Mpuluzi batholith (samples ordered from most mafic to most felsic): (a) RSA03; (b) RSA01; (c) SWA18a; (d) RSA05; (e) RSA02; (f) SWA07; (g) RSA04; (h) RSA08; (i) SWA10a; (j) RSA09; (k) SWA03; (l) RSA06; (m) SWA13a; (n) SWA11; (o) SWA09; (p) SWA02a; (q) RSA07; (r) SWA05. Red lines = pristine group; yellow field = variable group; green field = metamict group.

The other notable difference between the REE contents of the three groups is the magnitude of the Ce anomaly (Ce/Ce*: chondrite-normalised Ce content divided by the geometric mean of chondrite-normalised La and Pr). Ce anomalies are generally positive, and the average Ce/Ce* decreases in magnitude from the pristine group (average Ce/Ce* = 1.6–87, median = 7.0) to the variable group (average Ce/Ce* = 1.3–10, median = 2.1); the Ce anomaly in the metamict group is still less pronounced, ranging from 1.1 to 3.3, with a median value of 1.5 (Figure 6.5n). The Eu anomalies (Eu/Eu*: chondrite-normalised Eu content divided by the geometric mean of chondrite-normalised Sm and Gd) of the three groups also show a slight decrease in magnitude from the pristine to metamict groups. Eu anomalies are generally negative, and average Eu/Eu* in the pristine group ranges from 0.11 to 0.65 (median = 0.28), while the variable group shows a range of average Eu/Eu* from 0.18 to 0.89 (median = 0.28), and the metamict group ranges from 0.13 to 0.83 with a median value of 0.35 (Figure 6.5o).

6.2.3 U-Pb data treatment

Precise U-Pb ages were difficult to obtain as most samples show evidence of significant loss of radiogenic lead, coupled with variable addition of common Pb. All samples analysed in this study define a Pb-loss trend on the U-Pb concordia diagram extending from ~3.1 Ga towards ~0 Ga (Figure 6.7a), indicating that most of the loss of radiogenic lead has been recent. However, the $^{207}Pb/^{206}Pb$ ages also show a spread from ~3.1 Ga towards younger ages, suggesting there has been some Pb loss over the life of the zircons (Figure 6.7b). The $^{207}Pb/^{206}Pb$ ages also show a negative correlation with U content, which indicates that radiation damage is the primary facilitator of loss of radiogenic lead (Figure 6.8). The increase in the prevalence of 'ancient' Pb loss with increasing U content also suggests that there is a threshold of accumulated radiation damage which, when reached, allows loss of radiogenic lead; this threshold is necessarily reached earlier in grains with higher concentrations of U.

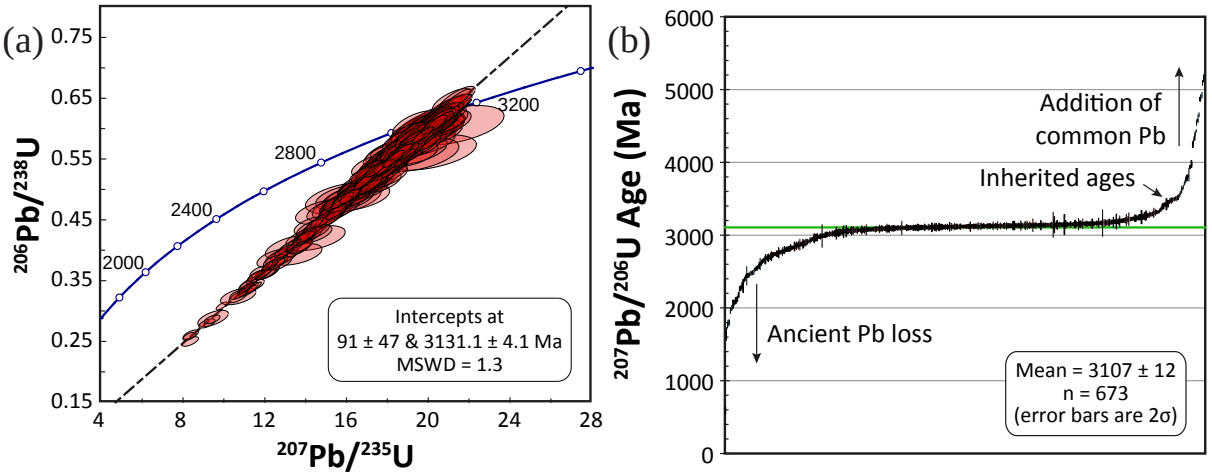


Figure 6.7. Collated age data for Mpuluzi samples: (a) U-Pb concordia plot showing the characteristic Pb-loss trend from ~3.1 Ga towards ~0 Ga; (b) plot of uncorrected $^{207}Pb/^{206}Pb$ ages showing the spread in ages down from ~3.1 Ga (Pb loss), a small plateau at ~3.5 Ga (inherited grains), and a spread towards higher ages (addition of common Pb).

Given the evident influence of loss of radiogenic Pb (recent and ancient) and common Pb addition on the $^{207}Pb/^{206}Pb$ ages, it was decided to attempt to define criteria to filter the analyses before attempting to calculate ages. The negative correlation of $^{207}Pb/^{206}Pb$ ages with U content observed in the dataset (Figure 6.8) suggested that filtering based on U concentration would reduce the effect of ancient Pb loss; recent Pb loss does not affect the $^{207}Pb/^{206}Pb$ ages, and concordia intercept ages have been calculated assuming all Pb loss is recent.

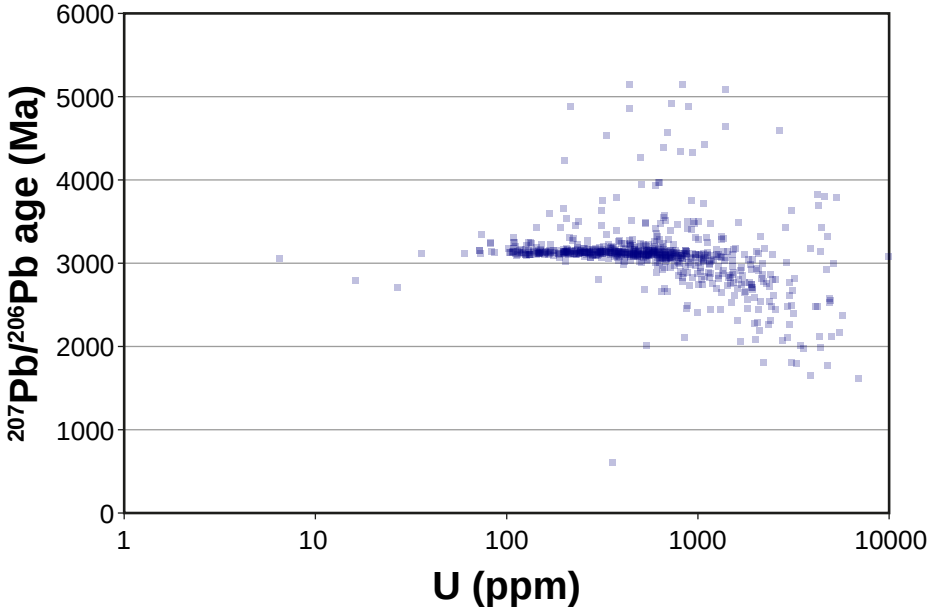


Figure 6.8. Uncorrected $^{207}Pb/^{206}Pb$ ages *vs* U concentration, showing a decrease in the age obtained from grains with high U contents, indicating that these grains experienced ancient Pb loss.

Firstly, grains with ages significantly older than the main population (~3.1 Ga) were removed from the dataset, as the intent was to observe the effect of U content on the U-Pb ages, and the presence of inherited grains and those with significant common Pb obscure this trend. The effect of addition of common Pb was removed by excluding analyses with $^{208}Pb/^{232}Th$ ages >3200 Ma, as this system is particularly sensitive to addition of common Pb; analyses with $^{207}Pb/^{206}Pb$ ages >3300 Ma were excluded as this system is the least susceptible to loss of radiogenic Pb and thus most likely to preserve inherited ages. A weighted average of $^{207}Pb/^{206}Pb$ ages was then calculated for grains with U concentration below a given threshold, starting at <100 ppm U and incremented in 100 ppm steps until 1500 ppm, then up by 500 ppm steps to 5000 ppm, with the final step including all grains (<10000 ppm U; see Figure 6.9). The ages calculated from each step clearly show that increasing the U content of analyses included in the calculation decreases the calculated ages, while simultaneously increasing the error on those ages (Figure 6.10; the <100 ppm U step consists of only four grains and therefore has a large standard deviation). The fact that the error on the average age increases with U content, despite the addition of more analyses in the average for each step,

suggests that there is real variation in the $^{207}Pb/^{206}Pb$ ages obtained from grains with different U contents. A filtering cut-off of 1000 ppm U was chosen as a compromise between the accuracy of the ages obtained and the need to have a sufficient dataset to analyse. Analyses with <1000 ppm U have an error on the weighted average age of <5 Ma and a MSWD of <10, and though the average age is lower than those calculated with a stricter cut-off, all the ages with a cut-off of <1000 ppm overlap within 2 standard deviations. Of the 414 analyses

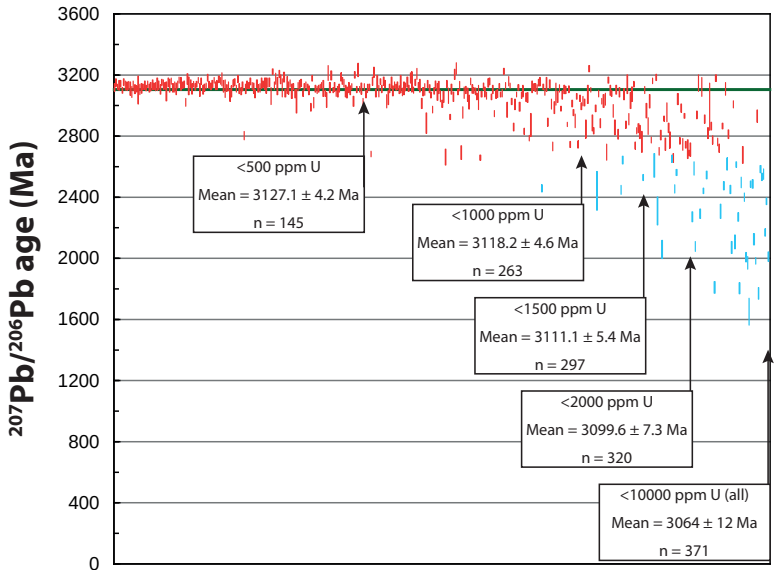


Figure 6.9. Plot of uncorrected $^{207}Pb/^{206}Pb$ ages sorted by U content, showing calculated weighted averages for analyses with U<500, <1000, <1500, <2000 and <10000 ppm (all analyses), and the number of analyses included in these averages. Green line indicates 3100 Ma. Inherited grains and those with significant common Pb have been removed.

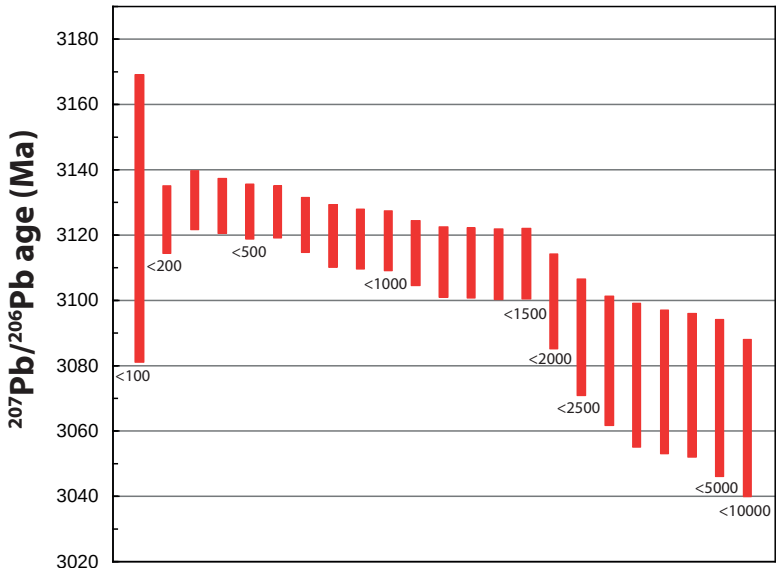


Figure 6.10. Plot of weighted averages of uncorrected $^{207}Pb/^{206}Pb$ ages calculated from analyses with different U contents. Maximum included U concentration starts at 100 ppm and increments by 100 ppm steps until 1500 ppm, then by 500 ppm steps until 5000 ppm; the final step includes analyses with <10000 ppm U (all analyses).

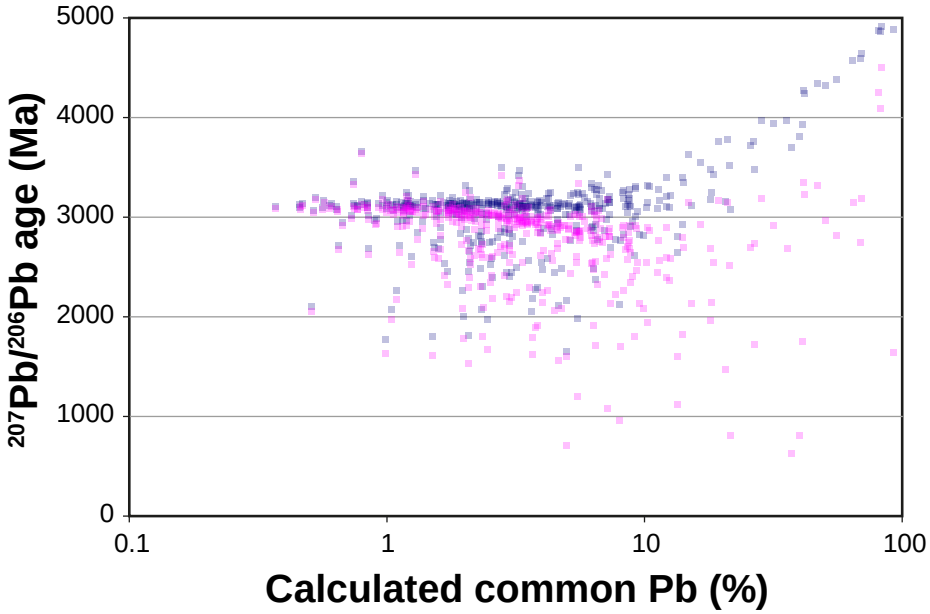


Figure 6.11. Uncorrected (blue) and corrected (pink) $^{207}Pb/^{206}Pb$ ages *vs* calculated proportion of common Pb, showing a strong positive correlation of uncorrected ages with common Pb above 10% calculated common Pb, and a negative correlation of corrected ages with calculated common Pb content. Common Pb calculated using the correction routine of Andersen (2002).

included in the trial, 127 were excluded on the basis of having U concentration greater than the 1000 ppm cut-off.

Filtering the dataset based on common Pb content was more problematic, as it is difficult to exclude those analyses affected by Pb loss from the calculations. On a plot of uncorrected $^{207}Pb/^{206}Pb$ ages *vs* the concentration of common Pb (calculated by the correction routine of Andersen, 2002), the main feature observed is a smear to lower ages caused by loss of radiogenic Pb (Figure 6.11). There is little correlation observed between the uncorrected $^{207}Pb/^{206}Pb$ age and the common Pb content for analyses with less than 10% calculated common Pb, however the corrected ages show a significant negative correlation between $^{207}Pb/^{206}Pb$ age and calculated common Pb (Figure 6.11). The correction routine appears to overcorrect the ages, and the overcorrection is more severe the higher the calculated common-Pb content. Filtering the dataset to exclude analyses with calculated common Pb >2% would minimise the overcorrection, but this would also leave less than half the number of analyses in the dataset, even before filtering for U content. A filtering cut-off of 10% calculated common Pb was therefore chosen, as this removes the analyses with a strong positive correlation between uncorrected $^{207}Pb/^{206}Pb$ ages and common Pb, without severely restricting the number of analyses available; the apparent overcorrection of the remaining ages is addressed below.

Because of this apparent overcorrection of $^{207}Pb/^{206}Pb$ ages by the common-Pb correction routine of Andersen (2002), both corrected and uncorrected ages for each sample have been processed and are presented below. Ideally, correcting for common Pb would affect only the grains with the oldest ages, as these would be the ones affected by common Pb, and the older the age the more significant the correction, with most of the grains in the middle and lower part of the population remaining uncorrected; as a result the peak of the main population is shifted slightly to younger ages and the scatter in the data is reduced (as shown by the uncorrected and corrected spectra for the $^{206}Pb/^{238}U$ and $^{207}Pb/^{235}U$ ages; see Figure 6.12a, b). Figure 6.12c shows the actual effect of the common Pb correction routine on the $^{207}Pb/^{206}Pb$ ages – analyses from all parts of the population are affected to varying degrees, and the resulting peak is both shifted and broadened.

The $^{208}Pb/^{232}Th$ ages are strongly affected by common Pb and show a large scatter in the uncorrected data; the corrected spectrum is scattered to lower ages, similar to the pattern seen in the $^{207}Pb/^{206}Pb$ ages, but this may be explained by the large uncertainties involved and in some cases the very large correction needed to remove the effect of common Pb (Figure 6.12d). The fact that the overcorrection apparent in the $^{207}Pb/^{206}Pb$ ages is not apparent to any significant extent in the U/Pb ages may indicate that only the $^{207}Pb/^{206}Pb$ ages are overcorrected, or any overcorrection may be obscured by the strong Pb-loss trends. The overcorrection does not appear to be caused by an incorrect assumption in the age of Pb loss (ages corrected to Pb loss = 0 Ga; increasing the assumed age of Pb loss slightly decreases the calculated proportion of common Pb without changing the ages significantly) or the age of common Pb addition (assumed present-day addition of common Pb; increasing this age simultaneously decreases the proportion of calculated common Pb and increases the difference between corrected and uncorrected ages, exacerbating the problem).

The following routine was used in processing analyses from each sample: (1) corrected for common Pb using the common-Pb correction routine of Andersen (2002); (2) analyses with >1000 ppm U were filtered out, as were those with >10% calculated common Pb; (3) the remaining analyses (both corrected and uncorrected) were scrutinised for any remaining problems – grains with anomalously low ages were excluded, as were those with large errors on the ages (>100 million years), and any with anomalously high ages which could be attributed to either common Pb or inheritance ($^{208}Pb/^{232}Th$ >3200 Ma, $^{207}Pb/^{206}Pb$ >3300 Ma); (4) the $^{207}Pb/^{206}Pb$ ages were plotted as a weighted mean using Isoplot (Ludwig, 2003), allowing Isoplot to reject any statistical outliers (these were excluded from further calculations); (5) the same analyses were plotted on the U-Pb concordia diagram to calculate an intercept age; (6) if the probability of fit of either of these was low (<0.05), the analyses were further culled based on the weighted residuals until the probability of fit exceeded 0.05.

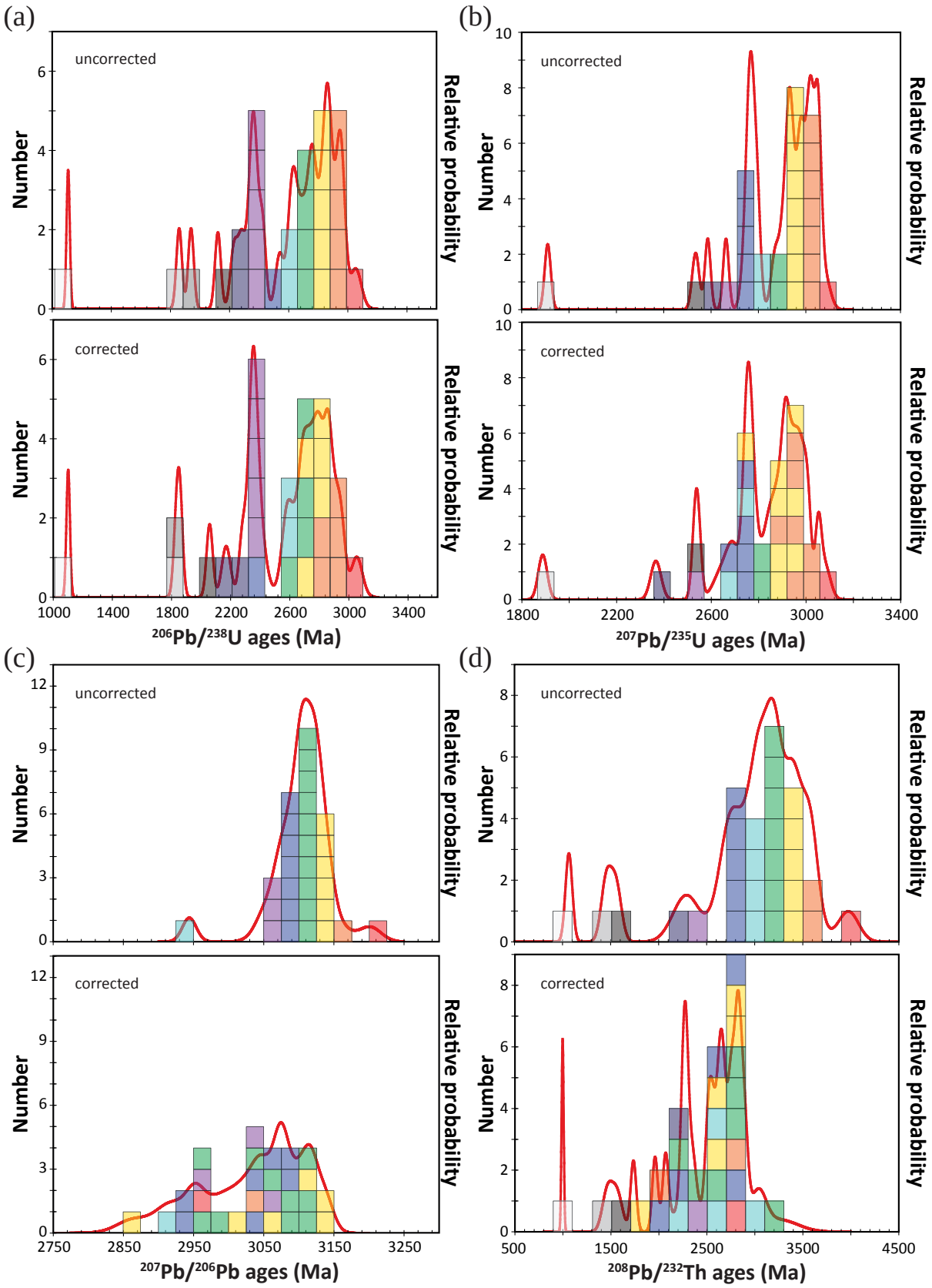


Figure 6.12. Effect of common-Pb correction on calculated ages for a representative sample (SWA18a). The uncorrected spectrum is on top and the corrected spectrum below; colours in the corrected spectrum correspond to the same-coloured bin in the uncorrected spectrum: (a) $^{206}Pb/^{238}U$ ages; (b) $^{207}Pb/^{235}U$ ages; (c) $^{207}Pb/^{206}Pb$ ages; (d) $^{208}Pb/^{232}Th$ ages.

For the corrected data, the overcorrection of the $^{207}Pb/^{206}Pb$ ages results in a bias towards younger ages calculated from a weighted average of these ages, partly because many grains are shifted to younger ages, shifting the mean, and partly because a large correction results in a large error, and culling based on weighted residuals will preferentially remove analyses with smaller errors as they have a lower probability of fit. This means that for the corrected data, some samples yield an anomalously low weighted average age or fail to achieve a statistically significant fit, while still yielding a reasonable intercept age. In these cases, the intercept age presented is that produced by culling to a probability of fit >0.05 for the intercept age, and the number of further analyses culled to produce the weighted average of $^{207}Pb/^{206}Pb$ ages is noted. Some samples with few analyses (e.g. RSA07) and/or significant ancient Pb loss (e.g. SWA02a) and/or significant calculated common Pb (e.g. RSA08) finished the filtering stage with very few analyses remaining and consequently have large errors on the calculated ages; the ages calculated from these samples are presented below along with the more reliable samples but are given less weight in the overall interpretation. A summary of the ages calculated from both uncorrected and corrected data is presented in Table 6.2.

6.2.4 Calculated ages and Hf-isotope compositions

The ages calculated from each sample (both uncorrected and corrected for common Pb) are presented below, together with the Th and U contents and Hf-isotope compositions. Initial $^{176}Hf/^{177}Hf$ and crustal model ages have been calculated using the intercept age obtained from the corrected dataset for all samples except RSA01 and RSA02, for which the weighted means of uncorrected $^{207}Pb/^{206}Pb$ ages have been used (see discussion of these samples). Crustal model ages have been calculated as the intersection between an evolution line with Lu/Hf = 0.015 (average crust) and the depleted mantle (DM) curve. The selection of an average crustal value for Lu/Hf was based on the sample with the largest number of inherited grains (SWA10a); in this sample the seven inherited grains clearly lie along an evolution line which intersects the spread of the main population at the lower end. A summary of the data from each sample is shown in Tables 6.2 and 6.3; for the full set of analyses see Appendices G and H. Concordia diagrams and weighted averages were calculated using Isoplot (Ludwig, 2003), and Hf kernel density estimates and histograms were prepared using DensityPlotter (Vermeesch, 2012).

Table 6.2: Summary of U and Th contents and U-Pb ages of zircons from the Mpuluzi batholith. Where a population is represented by only one analysis, the $^{207}Pb/^{206}Pb$ age and associated error is presented in lieu of a weighted average. Where the corrected U-Pb data shows two values for number of analyses, the number in parentheses represents the weighted average. The full dataset is provided in Appendix G.

	Th (ppm)		U (ppm)		Th/U		Calculated ages (uncorrected; Ma)					Calculated ages (corrected for common Pb; Ma)				
								Weighted average		Intercept			Weighted average		Intercept	
	Average	1σ	Average	1σ	Average	1σ	n	Age	1σ	Age	1σ	n	Age	1σ	Age	1σ
RSA03	120	100	190	82	0.56	0.30	34	3141.5	7.8	3144	20	31(28)	3077	11	3109	24
RSA01	240	120	430	170	0.6	0.29	22	3104.3	7.3	3107	15	26(11)	2971	17	3078	22
SWA18a	400	320	520	220	0.75	0.44	21	3113.0	6.5	3113	10	14(11)	3079	11	3117	21
(inherited)							1	3501	16			-				
RSA05	400	200	620	200	0.65	0.20	20	3087.4	6.5	3093	12	17(9)	3067	11	3100	17
RSA02	107	87	250	200	0.49	0.34	10	3111	13	3104	41	9(5)	2995	60	3063	49
SWA07	250	160	460	260	0.62	0.26	15	3131.5	7.5	3133.6	9.2	15(8)	3123	13	3123	13
(inherited)							3	3499	14	3502	26	-				
RSA04	340	200	460	210	0.82	0.41	12	3127	14	3128	24	8	3109	16	3119	27
RSA08	240	140	490	310	0.61	0.30	2	3131	21	3140	150	5(2)	3099	29	3105	48
SWA10a	290	170	560	260	0.53	0.18	5	3116.0	9.1	3122	15	7(3)	3121	12	3123	15
(inherited)							7[a]									
RSA09	290	310	510	310	0.59	0.32	4	3018	16	2996	57	5			3109	46
SWA03	440	180	630	160	0.69	0.21	25	3119.7	5.9	3120	12	22(11)	3040	19	3152	20
RSA06	900	1400	550	240	1.6	2.3	7	3028	15	3003	54	11(6)	2953	38	3105	29
SWA13a	210	110	320	190	0.71	0.25	24	3118.5	4.9	3117.6	8.0	19	3116.5	6.9	3117.7	8.8
SWA11	230	120	410	170	0.58	0.18	39	3135.9	4.3	3133.7	7.5	35(27)	3119.2	6.8	3130	10
SWA09	200	150	290	190	0.83	0.48	16	3141.9	7.0	3144	13	15	3139.6	7.3	3142	13
(inherited)							2[a]					-				
SWA02a	330	190	630	170	0.56	0.36	3	3116	30	3114	30	3(2)	3120	180	3119	30
(inherited)							1	3471	9			1	3373	13		
RSA07	1000	1000	440	170	2.2	1.7	3	3132	11	3141	24	3			3167	34
(inherited)							1	3575	13			-				
SWA05	310	240	460	280	0.67	0.27	7	3159.2	7.5	3165	18	5	3160	14	3165	18
(inherited)							1	3425	9			-				

[a] Inherited grains do not form a coherent population.

Table 6.3: Summary of Hf isotopic compositions of zircons from the Mpuluzi batholith. Where a population is represented by only one analysis, the measured ratios and calculated εHf and T(DM)c are presented in lieu of an average, along with their associated errors. For the full dataset see Appendix H.

	Age (Ma)		$^{176}Hf/^{177}Hf$		$^{176}Lu/^{177}Hf$		$^{176}Yb/^{177}Hf$		εHf				T(DM)c (Ga)		
		n	Average	1σ	Average	1σ	Average	1σ	Min	Max	Average	1σ	Median	Min	Max
RSA03	3109	15	0.280847	0.000040	0.00051	0.00017	0.0195	0.0072	-0.60	3.11	0.9	1.2	3.45	3.29	3.53
RSA01	3104.3	12	0.280871	0.000051	0.00063	0.00022	0.0201	0.0082	-1.67	4.55	1.4	1.6	3.41	3.20	3.60
SWA18a	3117	13	0.280887	0.000063	0.00113	0.00042	0.036	0.014	-2.48	3.33	1.2	1.7	3.42	3.29	3.66
(inherited)		1	0.280711	0.000014	0.00240	0.00007	0.0796	0.0022			0.61	0.49	3.75		
RSA05	3100	24	0.280852	0.000036	0.00216	0.00059	0.081	0.028	-6.32	0.26	-2.6	1.8	3.66	3.47	3.89
RSA02	3111	18	0.280862	0.000097	0.00098	0.00064	0.030	0.021	-3.64	6.32	0.5	2.4	3.50	3.09	3.73
SWA07	3123	17	0.280814	0.000073	0.00121	0.00041	0.036	0.012	-6.58	2.47	-1.4	2.2	3.63	3.35	3.92
(inherited)		5	0.280696	0.000084	0.00120	0.00039	0.036	0.015	-1.23	6.81	2.7	2.9	3.59	3.37	3.81
RSA04	3119	9	0.280926	0.000040	0.00138	0.00029	0.045	0.011	-0.70	4.11	2.1	1.5	3.34	3.24	3.55
RSA08	3105	3	0.280992	0.000064	0.00147	0.00056	0.044	0.015	2.89	5.87	4.0	1.6	3.29	3.11	3.31
SWA10a	3123	8	0.280755	0.000084	0.00175	0.00071	0.066	0.019	-10.39	0.56	-4.7	4.2	3.74	3.47	4.16
(inherited)		7	0.280512	0.000034	0.00173	0.00064	0.076	0.031	-7.00	-3.68	-5.1	1.2	4.13	4.03	4.15
RSA09	3109	8	0.280928	0.000040	0.00295	0.00060	0.142	0.041	-2.71	0.63	-1.4	1.0	3.58	3.45	3.67
SWA03	3152	36	0.280884	0.000045	0.00211	0.00049	0.068	0.013	-4.89	2.16	-0.2	1.5	3.53	3.39	3.84
RSA06	3105	12	0.280885	0.000054	0.00179	0.00064	0.072	0.021	-3.99	1.02	-0.5	1.4	3.51	3.43	3.75
SWA13a	3117.7	25	0.280911	0.000072	0.00162	0.00053	0.061	0.019	-2.96	5.65	1.1	2.3	3.45	3.14	3.69
SWA11	3130	37	0.280869	0.000038	0.00106	0.00028	0.035	0.010	-1.58	3.10	1.0	1.1	3.43	3.31	3.61
SWA09	3142	17	0.280893	0.000069	0.00129	0.00075	0.052	0.033	-4.16	5.04	1.5	2.4	3.44	3.20	3.78
(inherited)		1	0.280737	0.000029	0.00260	0.00005	0.1002	0.0023			-1.3	1.0	3.79		
SWA02a	3119	5	0.280863	0.000058	0.00137	0.00067	0.047	0.016	-1.82	2.13	-0.1	1.6	3.49	3.37	3.62
(inherited)		1	0.280689	0.000019	0.00150	0.00004	0.0435	0.0013			1.32	0.67	3.69		
RSA07	3167	6	0.280835	0.000033	0.00213	0.00042	0.078	0.024	-3.10	-0.34	-1.65	0.96	3.63	3.56	3.74
SWA05	3165	10	0.280861	0.000036	0.00108	0.00038	0.034	0.012	0.24	2.53	1.50	0.66	3.43	3.37	3.52

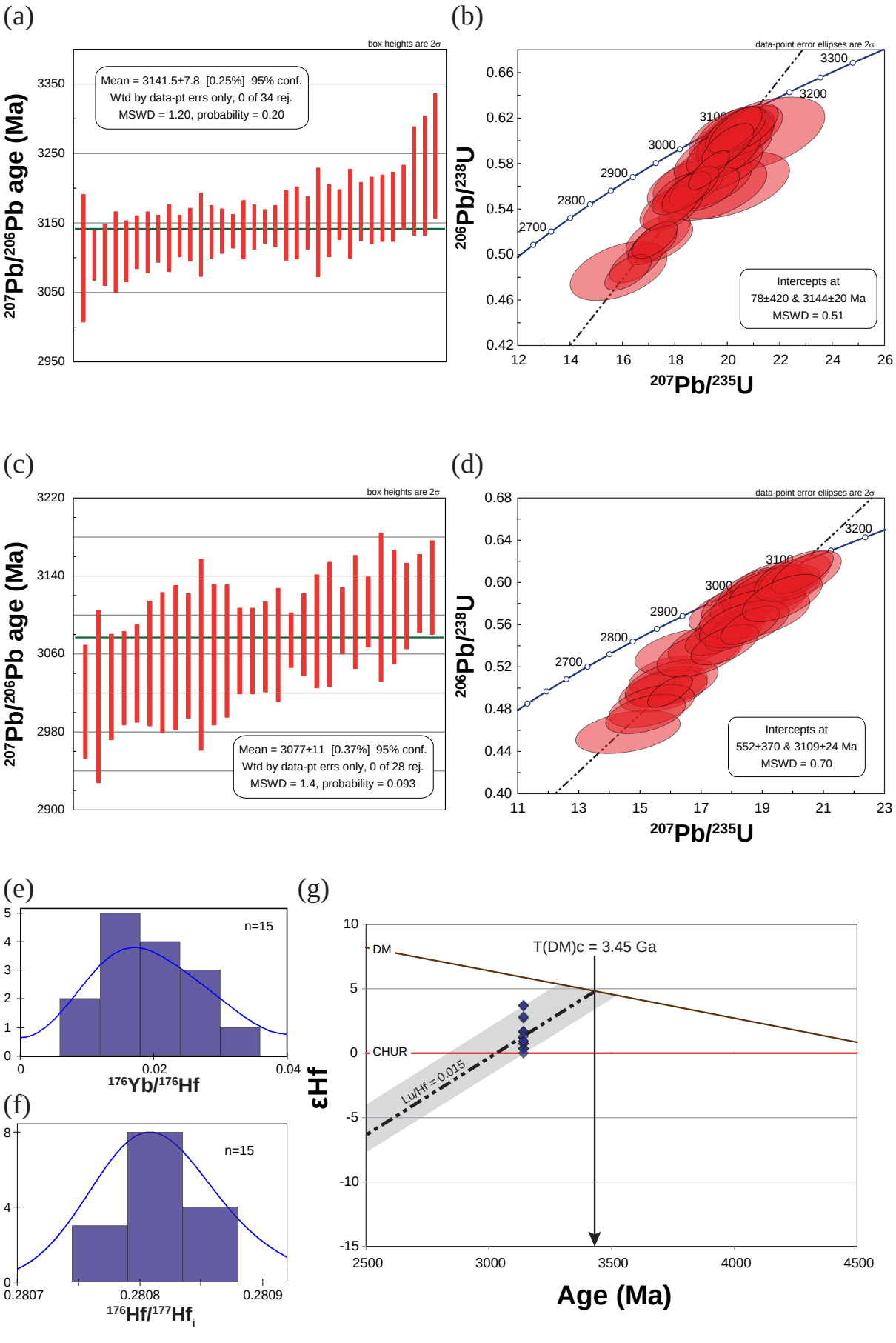
Sample RSA03

U-Pb ages were obtained from 52 grains from sample RSA03, 10 of which were filtered out due to high common Pb contents. The Th and U contents are relatively low (7–437 ppm Th, average = 120 ± 100 ppm; 73–388 ppm U, average = 190 ± 82 ppm), and Th/U ratios are low (0.10–1.15, average = 0.56 ± 0.30).

No inheritance was detected in this sample. Of the 42 analyses remaining after filtering, eight were determined to be statistical outliers from the main population and were rejected to give a probability of fit >0.05; the remaining 34 analyses give a weighted average of $^{207}Pb/^{206}Pb$ ages of 3141.5 ± 7.8 Ma and an intercept age of 3144 ± 20 Ma (Figure 6.13a, b). Eleven analyses were rejected from the corrected dataset to give an intercept age of 3109 ± 24 Ma (n=31; Figure 6.13c); excluding a further three analyses gave a weighted mean of $^{207}Pb/^{206}Pb$ ages of 3077 ± 11 Ma (n=28; Figure 6.13d). Although the two calculated ages overlap within error, the weighted average is substantially lower, suggesting that the overcorrection of $^{207}Pb/^{206}Pb$ ages by the common-Pb correction routine has artificially lowered this age.

Hf isotopic compositions were obtained on 15 grains; REE contents are low (average $^{176}Yb/^{177}Hf = 0.0195 \pm 0.0072$; Figure 6.13e) and the analyses form a cluster slightly above the CHUR line on the epsilon Hf plot with a tail up towards the DM line (εHf = -0.60–3.11, average = 0.9 ± 1.2). Crustal model ages range from 3.53 to 3.29 Ga, with a median of 3.45 Ga (Figure 6.13f, g).

Figure 6.13. (facing page) Calculated ages and Hf isotopes from sample RSA03: (a) weighted average of $^{207}Pb/^{206}Pb$ ages and (b) intercept age on the U-Pb concordia diagram (uncorrected data); (c) weighted average of $^{207}Pb/^{206}Pb$ ages and (d) intercept age on the U-Pb concordia diagram (corrected data); histograms of (e) $^{176}Yb/^{177}Hf$ and (f) $^{176}Hf/^{177}Hf_i$, with kernel density estimate as a blue line; (g) εHf plot showing the range in crustal model ages (field) and the median (dashed line).


(a)
box heights are 2σ
Mean = 3141.5±7.8 [0.25%] 95% conf.
Wtd by data-pt errs only, 0 of 34 rej.
MSWD = 1.20, probability = 0.20
207Pb/206Pb age (Ma)
(b)
data-point error ellipses are 2σ
Intercepts at
78±420 & 3144±20 Ma
MSWD = 0.51
206Pb/238U
207Pb/235U
(c)
box heights are 2σ
Mean = 3077±11 [0.37%] 95% conf.
Wtd by data-pt errs only, 0 of 28 rej.
MSWD = 1.4, probability = 0.093
207Pb/206Pb age (Ma)
(d)
data-point error ellipses are 2σ
Intercepts at
552±370 & 3109±24 Ma
MSWD = 0.70
206Pb/238U
207Pb/235U
(e)
n=15
176Yb/176Hf
(f)
n=15
176Hf/177Hfi
(g)
T(DM)c = 3.45 Ga
DM
CHUR
Lu/Hf = 0.015
εHf
Age (Ma)

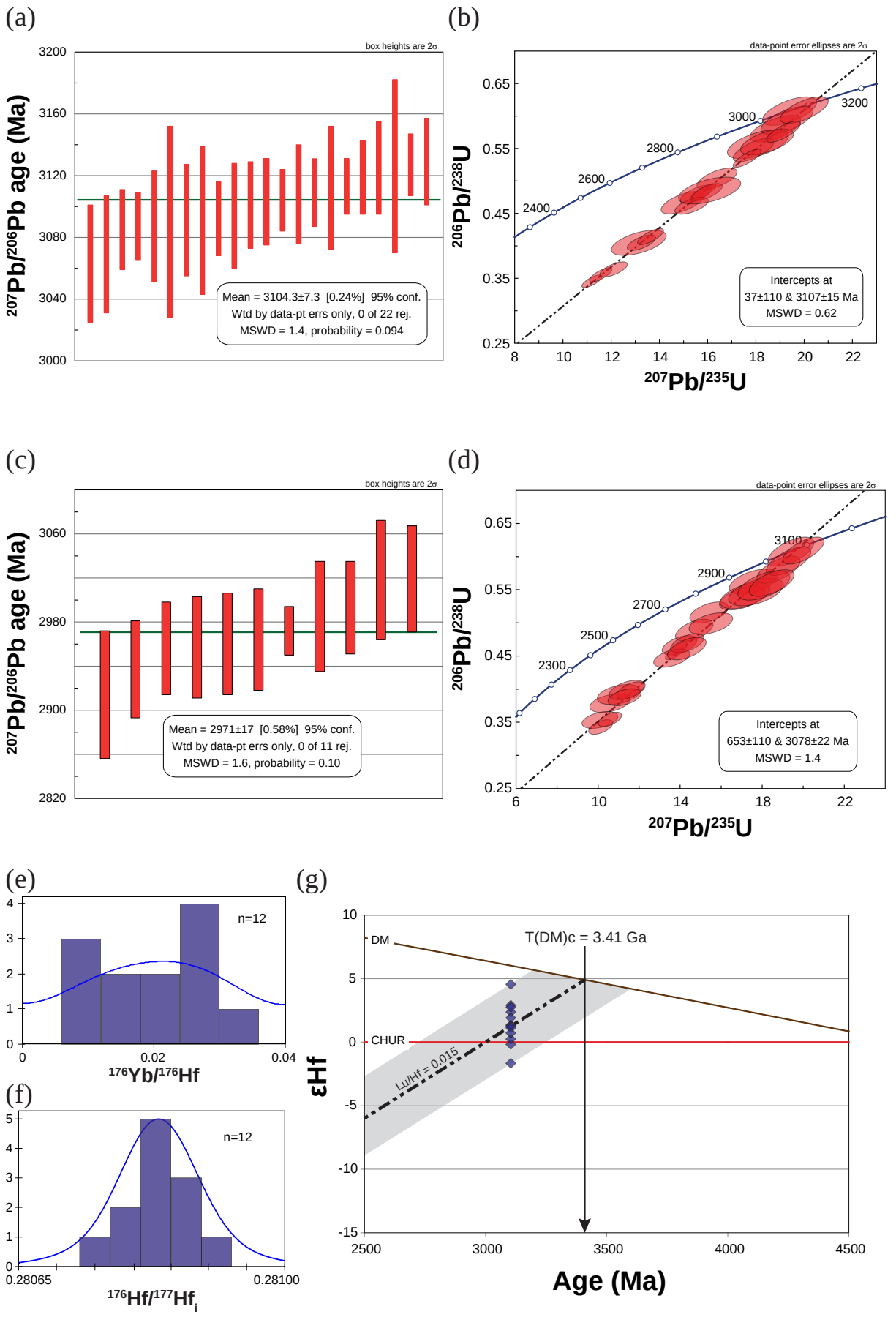
Sample RSA01

Ages were obtained from 55 spots on 54 grains from sample RSA01, 18 of which were excluded in the filtering stage, mainly due to high common Pb contents. Concentrations of Th and U are variable (58–503 ppm Th, average = 240 ± 120 ppm; 127–858 ppm U, average = 430 ± 170 ppm; 3 grains with U >1000 ppm excluded), and Th/U ratios range from 0.12 to 1.28 (average = 0.60 ± 0.29).

No inheritance was detected in this sample. Of the 37 grains remaining after filtering, 15 were determined to be statistical outliers from the main population and were excluded. The remaining 22 grains give a weighted mean of $^{207}Pb/^{206}Pb$ ages of 3104.3 ± 7.3 Ma, and an intercept age of 3107 ± 15 Ma (Figure 6.14a, b). This sample is strongly affected by common Pb and the corrected data show a large spread in $^{207}Pb/^{206}Pb$ ages. Eleven grains were rejected on a statistical basis to give an intercept age of 3078 ± 22 Ma (n=26), but to achieve a statistically significant fit for the weighted average of $^{207}Pb/^{206}Pb$ ages a further 15 analyses had to rejected, and the calculated age (2971 ± 17 Ma, n=11) is substantially lower than the intercept age, suggesting the overcorrection of $^{207}Pb/^{206}Pb$ ages is a major factor influencing the calculated age (Figure 6.14c, d).

Hf isotopic compositions were obtained from 12 grains; REE contents are low (average $^{176}Yb/^{177}Hf = 0.0201 \pm 0.0082$; Figure 6.14e) and on the epsilon Hf plot the analyses spread from slightly below the CHUR line up towards the DM line, with a range in εHf from -1.67 to 4.55, and an average of 1.4 ± 1.6. Crustal model ages range from 3.60 to 3.20 Ga with a median of 3.41 Ga (Figure 6.14f, g).

Figure 6.14. (facing page) Calculated ages and Hf isotopes from sample RSA01: (a) weighted average of $^{207}Pb/^{206}Pb$ ages and (b) intercept age on the U-Pb concordia diagram (uncorrected data); (c) weighted average of $^{207}Pb/^{206}Pb$ ages and (d) intercept age on the U-Pb concordia diagram (corrected data); histograms of (e) $^{176}Yb/^{177}Hf$ and (f) $^{176}Hf/^{177}Hf_i$, with kernel density estimate as a blue line; (g) εHf plot showing the range in crustal model ages (field) and the median (dashed line).


(a)
box heights are 2σ
$^{207}Pb/^{206}Pb$ age (Ma)
Mean = 3104.3±7.3 [0.24%] 95% conf.
Wtd by data-pt errs only, 0 of 22 rej.
MSWD = 1.4, probability = 0.094
(b)
data-point error ellipses are 2σ
$^{206}Pb/^{238}U$
$^{207}Pb/^{235}U$
Intercepts at
37±110 & 3107±15 Ma
MSWD = 0.62
(c)
box heights are 2σ
$^{207}Pb/^{206}Pb$ age (Ma)
Mean = 2971±17 [0.58%] 95% conf.
Wtd by data-pt errs only, 0 of 11 rej.
MSWD = 1.6, probability = 0.10
(d)
data-point error ellipses are 2σ
$^{206}Pb/^{238}U$
$^{207}Pb/^{235}U$
Intercepts at
653±110 & 3078±22 Ma
MSWD = 1.4
(e)
n=12
$^{176}Yb/^{176}Hf$
(f)
n=12
$^{176}Hf/^{177}Hf_i$
(g)
DM
T(DM)c = 3.41 Ga
CHUR
Lu/Hf = 0.015
εHf
Age (Ma)

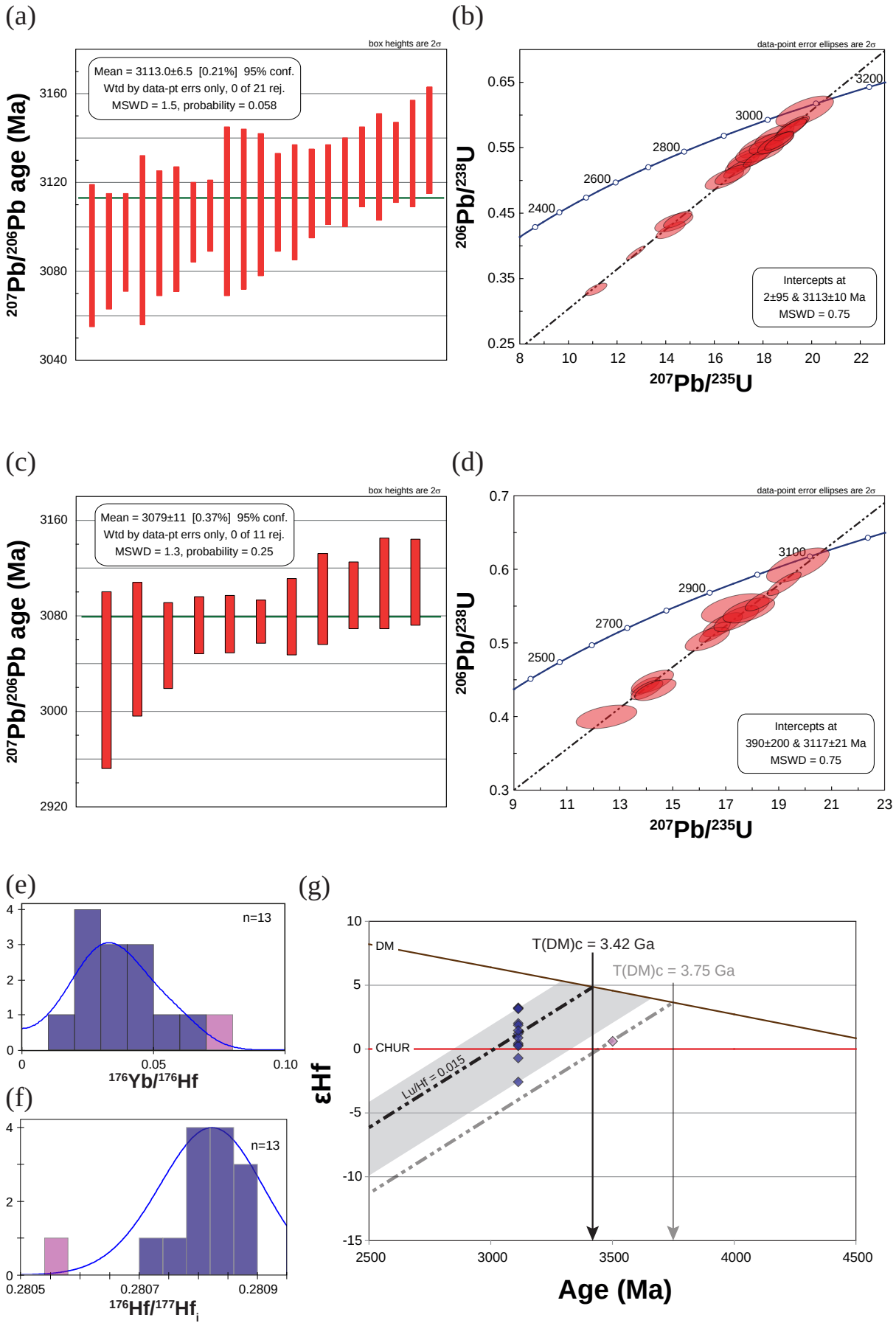
Sample SWA18a

Sample SWA18a yielded U-Pb analyses from 46 spots on 45 grains, 16 of which were rejected in the filtering stage due to high U contents. After filtering, Th and U contents are variable (Th = 55–1320 ppm, average = 400 ± 320 ppm; U = 159–935 ppm, average = 520 ± 220 ppm; those with U >1000 ppm excluded), as are Th/U ratios (0.17–2.11, average = 0.75 ± 0.44).

One grain with a $^{207}Pb/^{206}Pb$ age of 3501 ± 16 Ma is interpreted to be inherited. Of the 29 remaining grains, eight were rejected statistically to give a probability of fit of >0.05. The remaining 21 analyses give a weighted average of $^{207}Pb/^{206}Pb$ ages of 3113.0 ± 6.5 Ma, and an intercept age of 3113 ± 10 Ma (Figure 6.15a, b). The inherited grain and 16 outliers were excluded from the corrected data to give an intercept age of 3117 ± 21 Ma (n=14). Three further analyses had to be rejected to achieve a statistically significant fit for the weighted average of $^{207}Pb/^{206}Pb$ ages of 3079 ± 11 Ma (n=11); this age is significantly lower than the intercept age due to the overcorrection of $^{207}Pb/^{206}Pb$ ages in the common-Pb correction routine (Figure 6.15c, d).

Hf isotopic compositions were obtained from 14 grains, including the grain with the inherited age. REE contents are low (average $^{176}Yb/^{177}Hf = 0.036 \pm 0.014$; Figure 6.15e) and the main population lies above the CHUR line on the epsilon Hf plot (εHf = -2.48–3.33, average = 1.2 ± 1.7). Crustal model ages range from 3.66 to 3.29 Ga with a median of 3.42 Ga. The inherited grain also plots slightly above the CHUR line (εHf = 0.61 ± 0.49) and gives a crustal model age of 3.75 Ga (Figure 6.15f, g).

Figure 6.15. (facing page) Calculated ages and Hf isotopes from sample SWA18a: (a) weighted average of $^{207}Pb/^{206}Pb$ ages and (b) intercept age on the U-Pb concordia diagram (uncorrected data); (c) weighted average of $^{207}Pb/^{206}Pb$ ages and (d) intercept age on the U-Pb concordia diagram (corrected data); histograms of (e) $^{176}Yb/^{177}Hf$ and (f) $^{176}Hf/^{177}Hf_i$, with kernel density estimate as a blue line (main population shown in blue, inherited in pink); (g) εHf plot showing the range in crustal model ages (field), the median of the main population (dashed black line), and the inherited grain (dashed grey line).


(a)
box heights are 2σ
Mean = 3113.0±6.5 [0.21%] 95% conf.
Wtd by data-pt errs only, 0 of 21 rej.
MSWD = 1.5, probability = 0.058
207Pb/206Pb age (Ma)
(b)
data-point error ellipses are 2σ
Intercepts at
2±95 & 3113±10 Ma
MSWD = 0.75
206Pb/238U
207Pb/235U
(c)
box heights are 2σ
Mean = 3079±11 [0.37%] 95% conf.
Wtd by data-pt errs only, 0 of 11 rej.
MSWD = 1.3, probability = 0.25
207Pb/206Pb age (Ma)
(d)
data-point error ellipses are 2σ
Intercepts at
390±200 & 3117±21 Ma
MSWD = 0.75
206Pb/238U
207Pb/235U
(e)
n=13
176Yb/176Hf
(f)
n=13
176Hf/177Hfi
(g)
T(DM)c = 3.42 Ga
T(DM)c = 3.75 Ga
DM
CHUR
Lu/Hf = 0.015
εHf
Age (Ma)

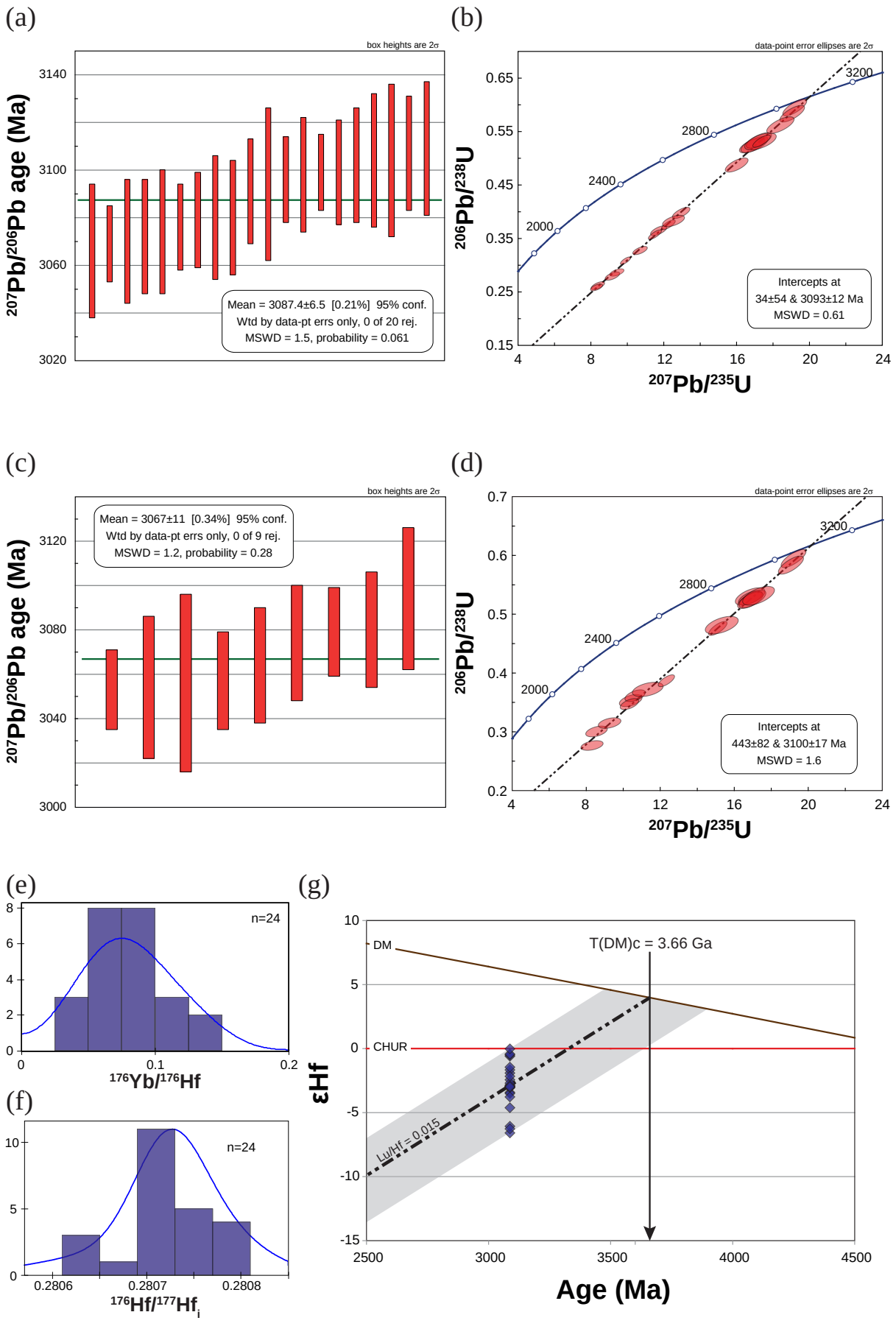
Sample RSA05

Ages were obtained from 41 grains from sample RSA05, 10 of which were filtered out with a combination of high U contents and high calculated common Pb. Thorium contents range from 138–1127 ppm (average = 400 ± 200 ppm) and U ranges from 291–998 ppm (average = 620 ± 200 ppm; 7 grains with U >1000 ppm excluded). Th/U ratios are variable, ranging from 0.16 to 1.16 (average = 0.65 ± 0.20).

No inheritance was detected in this sample. Of the 31 analyses remaining after filtering, 11 were determined to be statistical outliers, and the remaining 20 grains give a weighted average of $^{207}Pb/^{206}Pb$ ages of 3087.4 ± 6.5 Ma, and an intercept age of 3093 ± 12 Ma (Figure 6.16a, b). Fourteen analyses were rejected from the corrected dataset to give an intercept age of 3100 ± 17 Ma (n=17). A further eight analyses were rejected to achieve a statistically significant fit for the weighted mean of $^{207}Pb/^{206}Pb$ ages, and the resulting age (3067 ± 11 Ma, n=9) is significantly lower than the intercept age, suggesting that the average is skewed lower by the overcorrection of $^{207}Pb/^{206}Pb$ ages (Figure 6.16c, d).

Hf isotopic ratios were obtained on 24 grains; REE contents are generally low (average $^{176}Yb/^{177}Hf = 0.081 \pm 0.028$; Figure 6.16e) and the analyses lie below the CHUR line on the epsilon Hf plot ($\varepsilon Hf = -6.32–0.26$, average = -2.6 ± 1.8), and give crustal model ages ranging from 3.89 to 3.47 Ga (median = 3.66 Ga; Figure 6.16f, g).

Figure 6.16. (facing page) Calculated ages and Hf isotopes from sample RSA05: (a) weighted average of $^{207}Pb/^{206}Pb$ ages and (b) intercept age on the U-Pb concordia diagram (uncorrected data); (c) weighted average of $^{207}Pb/^{206}Pb$ ages and (d) intercept age on the U-Pb concordia diagram (corrected data); histograms of (e) $^{176}Yb/^{177}Hf$ and (f) $^{176}Hf/^{177}Hf_i$, with kernel density estimate as a blue line; (g) εHf plot showing the range in crustal model ages (field) and the median (dashed line).


(a)
box heights are 2σ
$^{207}Pb/^{206}Pb$ age (Ma)
Mean = 3087.4±6.5 [0.21%] 95% conf.
Wtd by data-pt errs only, 0 of 20 rej.
MSWD = 1.5, probability = 0.061
(b)
data-point error ellipses are 2σ
$^{206}Pb/^{238}U$
$^{207}Pb/^{235}U$
Intercepts at
34±54 & 3093±12 Ma
MSWD = 0.61
(c)
box heights are 2σ
$^{207}Pb/^{206}Pb$ age (Ma)
Mean = 3067±11 [0.34%] 95% conf.
Wtd by data-pt errs only, 0 of 9 rej.
MSWD = 1.2, probability = 0.28
(d)
data-point error ellipses are 2σ
$^{206}Pb/^{238}U$
$^{207}Pb/^{235}U$
Intercepts at
443±82 & 3100±17 Ma
MSWD = 1.6
(e)
n=24
$^{176}Yb/^{176}Hf$
(f)
n=24
$^{176}Hf/^{177}Hf_i$
(g)
DM
CHUR
T(DM)c = 3.66 Ga
Lu/Hf = 0.015
εHf
Age (Ma)

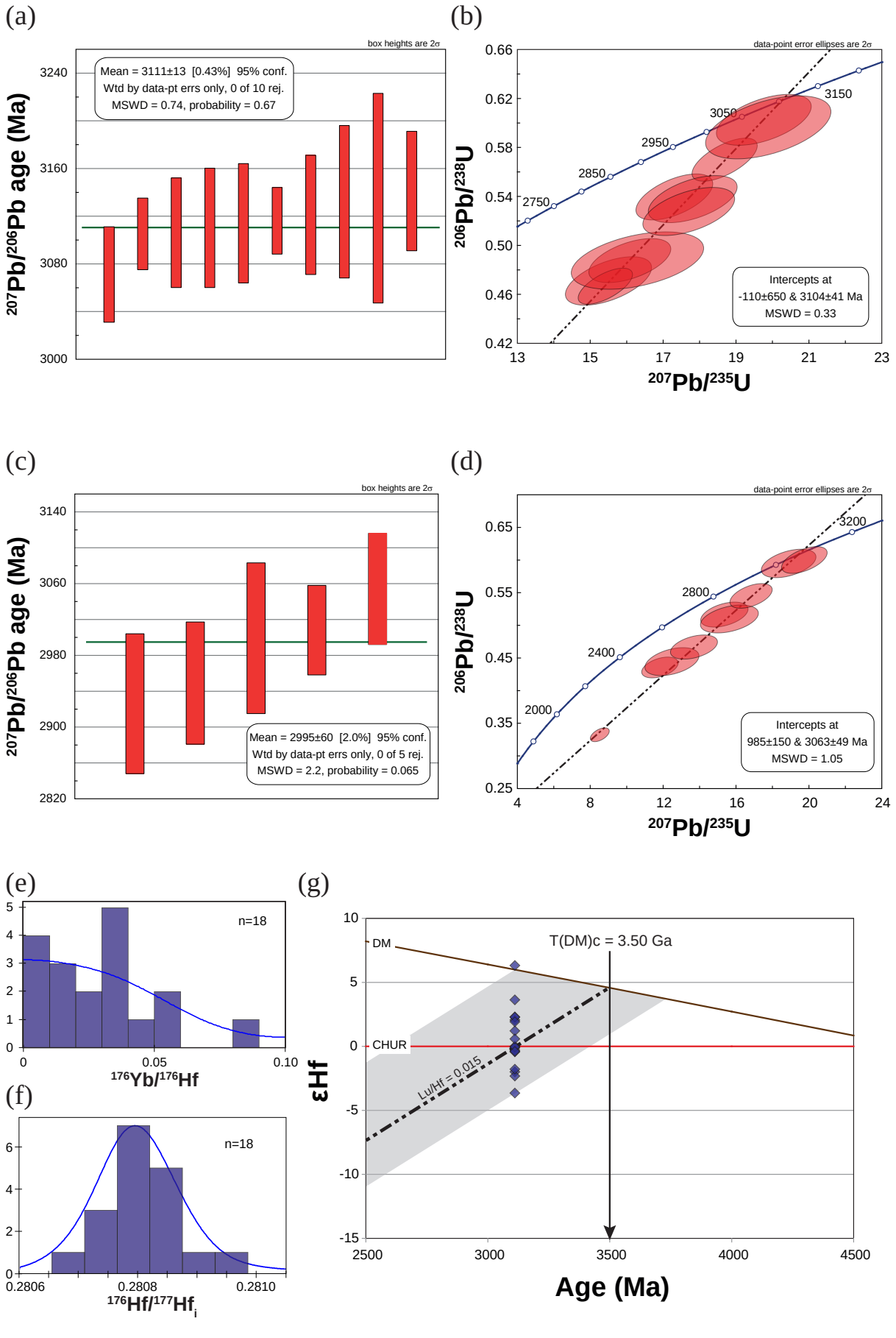
Sample RSA02

U-Pb ages were obtained on 22 spots from 20 grains, four of which were filtered out due to high U or common Pb contents. Thorium and U contents are variable (Th = 31–322 ppm, average = 107 ± 87 ppm; U = 74–790 ppm, average = 250 ± 200 ppm; 2 analyses with U >1000 ppm excluded), as are Th/U ratios (0.13–1.73, average = 0.49 ± 0.34).

No inheritance was detected in this sample. Of the 18 analyses remaining after filtering, eight were statistically rejected to achieve a probability of fit >0.05, and the remaining 10 analyses give a weighted average of $^{207}Pb/^{206}Pb$ ages of 3111 ± 13 Ma and an intercept age of 3104 ± 41 Ma (Figure 6.17a, b). Nine analyses were rejected from the corrected data to produce an intercept age of 3063 ± 49 Ma (n=9); excluding a further four analyses yields a statistically significant fit for the $^{207}Pb/^{206}Pb$ ages significantly and lowers the average (weighted average of $^{207}Pb/^{206}Pb$ ages = 2995 ± 60 Ma, n=5), suggesting that these ages were significantly overcorrected by the common-Pb correction routine (Figure 6.17c, d).

Hf isotopic compositions were obtained from 18 spots on 16 grains; REE contents are low (average $^{176}Yb/^{177}Hf$ = 0.030 ± 0.021; Figure 6.17e) and the analyses show a spread on the epsilon Hf diagram from -3.64 to 6.32, with an average of 0.5 ± 2.4. Crustal model ages range from 3.73 to 3.09 Ga, with a median of 3.50 Ga (Figure 6.17f, g).

Figure 6.17. (facing page) Calculated ages and Hf isotopes from sample RSA02: (a) weighted average of $^{207}Pb/^{206}Pb$ ages and (b) intercept age on the U-Pb concordia diagram (uncorrected data); (c) weighted average of $^{207}Pb/^{206}Pb$ ages and (d) intercept age on the U-Pb concordia diagram (corrected data); histograms of (e) $^{176}Yb/^{177}Hf$ and (f) $^{176}Hf/^{177}Hf_i$, with kernel density estimate as a blue line; (g) εHf plot showing the range in crustal model ages (field) and the median (dashed line).


(a)
box heights are 2σ
Mean = 3111±13 [0.43%] 95% conf.
Wtd by data-pt errs only, 0 of 10 rej.
MSWD = 0.74, probability = 0.67
207Pb/206Pb age (Ma)
(b)
data-point error ellipses are 2σ
Intercepts at
-110±650 & 3104±41 Ma
MSWD = 0.33
206Pb/238U
207Pb/235U
(c)
box heights are 2σ
Mean = 2995±60 [2.0%] 95% conf.
Wtd by data-pt errs only, 0 of 5 rej.
MSWD = 2.2, probability = 0.065
207Pb/206Pb age (Ma)
(d)
data-point error ellipses are 2σ
Intercepts at
985±150 & 3063±49 Ma
MSWD = 1.05
206Pb/238U
207Pb/235U
(e)
n=18
176Yb/176Hf
(f)
n=18
176Hf/177Hfi
(g)
DM
CHUR
T(DM)c = 3.50 Ga
Lu/Hf = 0.015
εHf
Age (Ma)

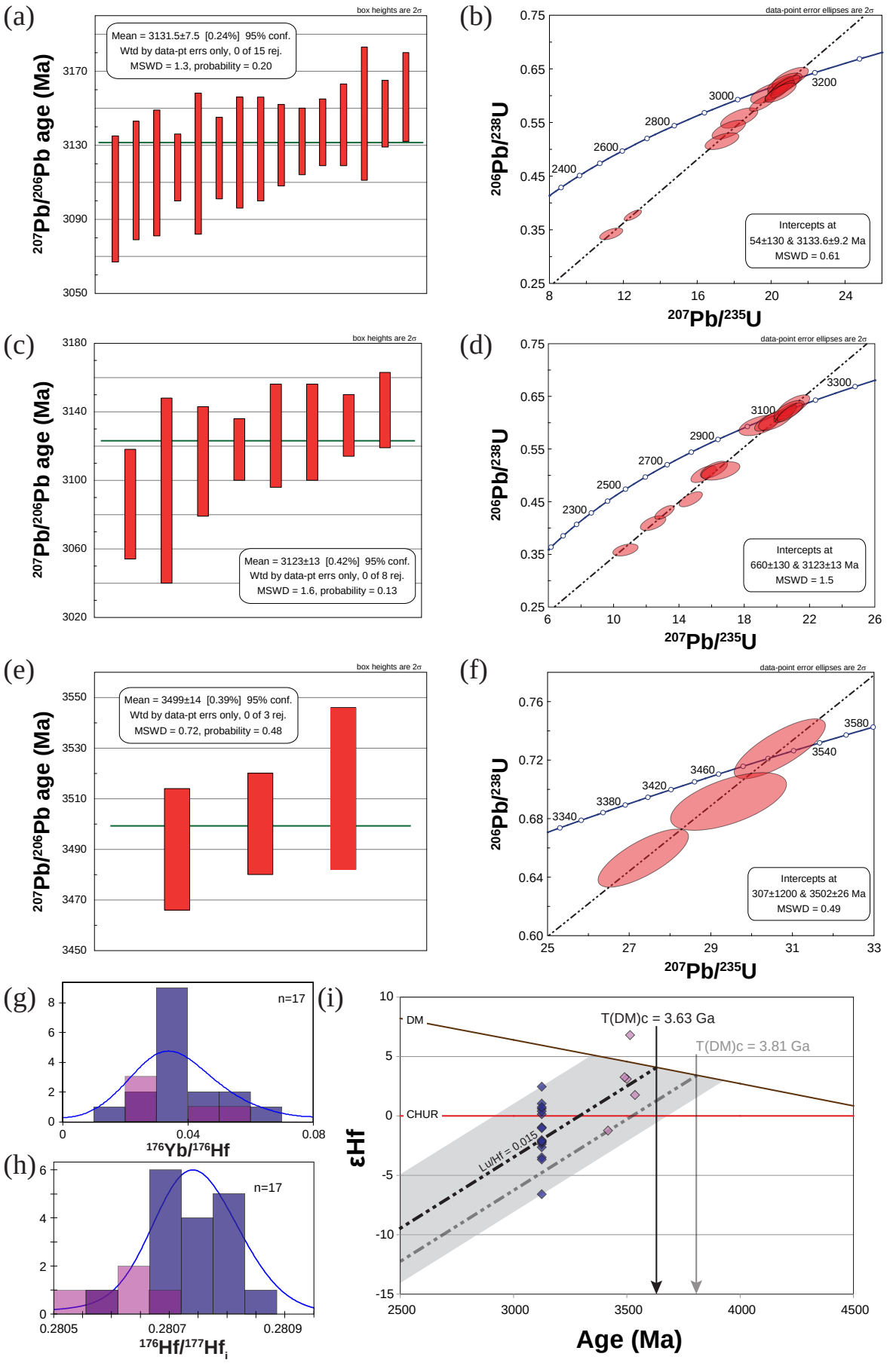
Sample SWA07

Ages were obtained from 40 grains, eight of which were removed in the filtering stage due to high common Pb or U contents. Thorium contents are variable (81–716 ppm, average = 250 ± 160 ppm), as are U contents (109–904 ppm, average = 460 ± 260 ppm; 4 grains with U >1000 ppm excluded). Th/U ratios are also variable (0.16–1.22, average = 0.62 ± 0.26).

Of the 32 analyses remaining after filtering, five were determined to be inherited, with a range in $^{207}Pb/^{206}Pb$ ages from 3536 to 3417 Ma. A further 17 analyses were culled from the main population on a statistical basis to give a probability of fit >0.05, and the remaining 15 analyses yield a weighted average of $^{207}Pb/^{206}Pb$ ages of 3131.5 ± 7.5 Ma and an intercept age of 3133.6 ± 9.2 Ma (Figure 6.18a, b). The corrected data give an intercept age of 3123 ± 13 Ma from 15 grains, and excluding a further seven analyses to achieve a probability of fit >0.05 for the weighted average of $^{207}Pb/^{206}Pb$ ages yields an identical age (3123 ± 13 Ma, n=8; Figure 6.18c, d). Of the five analyses with inherited ages, three form a coherent population with a weighted average of $^{207}Pb/^{206}Pb$ ages of 3499 ± 14 Ma and an intercept age of 3502 ± 26 Ma (Figure 6.18e, f; these grains have no calculated common Pb and are not affected by the correction routine).

Hf isotopic compositions were obtained from 17 grains from the main population and the five with inherited ages. REE contents are low (average $^{176}Yb/^{177}Hf = 0.036 \pm 0.012$; Figure 6.18g) and the analyses from the main population have a spread in εHf from -6.58 to 2.47, with an average of -1.4 ± 2.2. Crustal model ages range from 3.92 to 3.35 Ga, with a median of 3.63 Ga; the inherited grains show a spread from -1.23 to 6.81 epsilon units, with an average of 2.7 ± 2.9, and give crustal model ages ranging from 3.81 to 3.37 Ga (median = 3.59 Ga; Figure 6.18h, i). The large spread in both populations suggests that there may be mixing between the main population and the inherited component in both the analyses with inherited ages and those in the main population, shifting the εHf values of the main population down, and those of the inherited grains up towards the DM line. The median crustal model age for the main population is plotted on the εHf diagram, but for the inherited grains the crustal model age for the grain with the most evolved $^{177}Hf/^{176}Hf$ ratio has been plotted as this grain is the least affected by mixing (3.81 Ga; Figure 6.18i).

Figure 6.18. (facing page) Calculated ages and Hf isotopes from sample SWA07: (a) weighted average of $^{207}Pb/^{206}Pb$ ages and (b) intercept age on the U-Pb concordia diagram (uncorrected data); (c) weighted average of $^{207}Pb/^{206}Pb$ ages and (d) intercept age on the U-Pb concordia diagram (corrected data); (e) weighted average of $^{207}Pb/^{206}Pb$ ages and (f) intercept age on the U-Pb concordia diagram (inherited population); histograms of (g) $^{176}Yb/^{177}Hf$ and (h) $^{176}Hf/^{177}Hf_i$, with kernel density estimate as a blue line (main population shown in blue, inherited in pink); (i) εHf plot showing the range in crustal model ages (field), the median of the main population (dashed black line), and the maximum of the inherited grains (dashed grey line).


(a)
box heights are 2σ
Mean = 3131.5±7.5 [0.24%] 95% conf.
Wtd by data-pt errs only, 0 of 15 rej.
MSWD = 1.3, probability = 0.20
207Pb/206Pb age (Ma)
(b)
data-point error ellipses are 2σ
Intercepts at
54±130 & 3133.6±9.2 Ma
MSWD = 0.61
206Pb/238U
207Pb/235U
(c)
box heights are 2σ
Mean = 3123±13 [0.42%] 95% conf.
Wtd by data-pt errs only, 0 of 8 rej.
MSWD = 1.6, probability = 0.13
207Pb/206Pb age (Ma)
(d)
data-point error ellipses are 2σ
Intercepts at
660±130 & 3123±13 Ma
MSWD = 1.5
206Pb/238U
207Pb/235U
(e)
box heights are 2σ
Mean = 3499±14 [0.39%] 95% conf.
Wtd by data-pt errs only, 0 of 3 rej.
MSWD = 0.72, probability = 0.48
207Pb/206Pb age (Ma)
(f)
data-point error ellipses are 2σ
Intercepts at
307±1200 & 3502±26 Ma
MSWD = 0.49
206Pb/238U
207Pb/235U
(g)
n=17
176Yb/176Hf
(h)
n=17
176Hf/177Hfi
(i)
DM
CHUR
T(DM)c = 3.63 Ga
T(DM)c = 3.81 Ga
Lu/Hf = 0.015
εHf
Age (Ma)

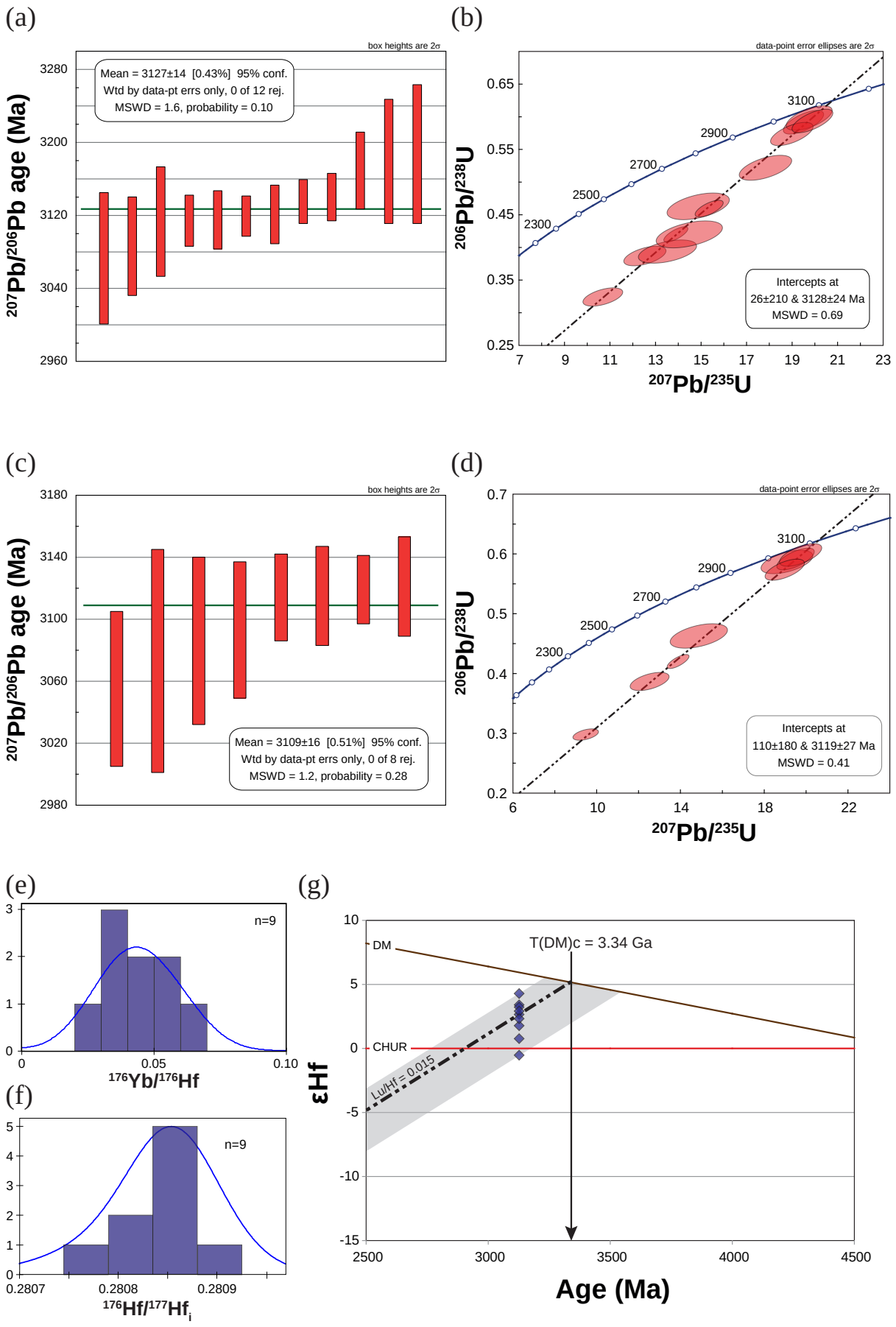
Sample RSA04

U-Pb ages were obtained from 32 spots on 25 grains, 15 of which were rejected in the filtering stage due to a combination of high U concentration and high common Pb. Thorium contents are variable (128–990 ppm, average = 340 ± 200 ppm), as are U contents (187–918 ppm, average = 460 ± 210 ppm; 5 analyses with U >1000 ppm excluded) and Th/U ratios (0.26–1.53, average = 0.82 ± 0.41).

No inheritance was detected in this sample. Of the 17 analyses remaining after filtering, five were determined to be statistical outliers and were rejected; the remaining 12 analyses give a weighted mean of $^{207}Pb/^{206}Pb$ ages of 3127 ± 14 Ma and an intercept age of 3128 ± 24 Ma (Figure 6.19a, b). Nine analyses were rejected from the corrected data; the remaining eight analyses give an intercept age of 3119 ± 27 Ma and a weighted average of $^{207}Pb/^{206}Pb$ ages of 3109 ± 16 Ma (Figure 6.19c, d).

Hf isotope analyses were obtained from nine grains; REE contents are low (average $^{176}Yb/^{177}Hf$ = 0.045 ± 0.011; Figure 6.19e) and the analyses generally lie above the CHUR line on the epsilon Hf plot (εHf = -0.70–4.11, average = 2.1 ± 1.5) and give crustal model ages ranging from 3.55 to 3.24 Ga (median = 3.34 Ga; Figure 6.19f, g).

Figure 6.19. (facing page) Calculated ages and Hf isotopes from sample RSA04: (a) weighted average of $^{207}Pb/^{206}Pb$ ages and (b) intercept age on the U-Pb concordia diagram (uncorrected data); (c) weighted average of $^{207}Pb/^{206}Pb$ ages and (d) intercept age on the U-Pb concordia diagram (corrected data); histograms of (e) $^{176}Yb/^{177}Hf$ and (f) $^{176}Hf/^{177}Hf_i$, with kernel density estimate as a blue line; (g) εHf plot showing the range in crustal model ages (field) and the median (dashed line).


(a)
box heights are 2σ
Mean = 3127±14 [0.43%] 95% conf.
Wtd by data-pt errs only, 0 of 12 rej.
MSWD = 1.6, probability = 0.10
207Pb/206Pb age (Ma)
(b)
data-point error ellipses are 2σ
Intercepts at
26±210 & 3128±24 Ma
MSWD = 0.69
206Pb/238U
207Pb/235U
(c)
box heights are 2σ
Mean = 3109±16 [0.51%] 95% conf.
Wtd by data-pt errs only, 0 of 8 rej.
MSWD = 1.2, probability = 0.28
207Pb/206Pb age (Ma)
(d)
data-point error ellipses are 2σ
Intercepts at
110±180 & 3119±27 Ma
MSWD = 0.41
206Pb/238U
207Pb/235U
(e)
n=9
176Yb/176Hf
(f)
n=9
176Hf/177Hfi
(g)
T(DM)c = 3.34 Ga
DM
CHUR
Lu/Hf = 0.015
εHf
Age (Ma)

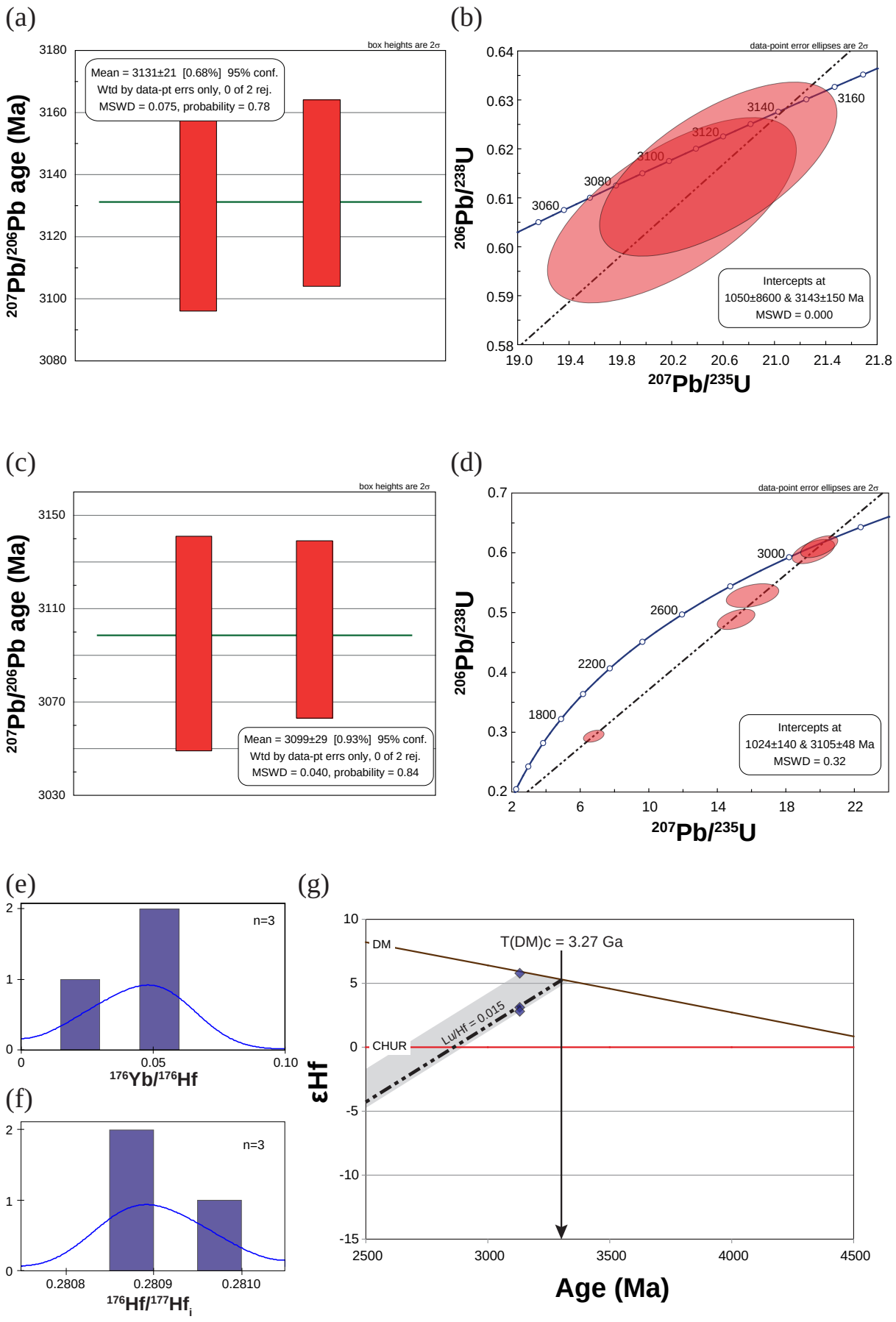
Sample RSA08

28 grains were analysed for U-Pb ages, 17 of which with calculated common Pb >10% and five with high U concentrations were filtered out, leaving six analyses. Thorium contents are variable (92–441 ppm, average = 240 ± 140 ppm), as are U contents (144–872 ppm, average = 490 ± 310 ppm; excluding those with U >1000 ppm); Th/U ratios range from 0.11 to 1.01 and average 0.61 ± 0.30.

No inheritance was detected in this sample. Of the six analyses remaining after filtering, one was anomalously low and was rejected, and a further three were determined to be significantly influenced by common Pb and were excluded, leaving only two analyses and thus yielding calculated ages of questionable significance. The weighted average of $^{207}Pb/^{206}Pb$ ages from these two grains is 3131 ± 21 Ma, and they yield an intercept age on the U-Pb concordia of 3140 ± 150 Ma (Figure 6.20a, b). When corrected for common Pb, five of the six analyses yield an intercept age of 3105 ± 48 Ma, but a further three analyses have to be excluded to achieve a probability of fit >0.05 for the weighted average of $^{207}Pb/^{206}Pb$ ages; this age has a large error but is consistent with the intercept age (weighted average = 3099 ± 29 Ma, n=2; Figure 6.20c, d).

Hf isotopic compositions were obtained from three grains; REE contents are low (average $^{176}Yb/^{177}Hf$ = 0.044 ± 0.015; Figure 6.20e) and the analyses sit above the CHUR line on the epsilon Hf plot (εHf = 2.89–5.87, average = 4.0 ± 1.6), and give crustal model ages ranging from 3.31 to 3.11 Ga (median = 3.29 Ga; Figure 6.20f, g).

Figure 6.20. (facing page) Calculated ages and Hf isotopes from sample RSA08: (a) weighted average of $^{207}Pb/^{206}Pb$ ages and (b) intercept age on the U-Pb concordia diagram (uncorrected data); (c) weighted average of $^{207}Pb/^{206}Pb$ ages and (d) intercept age on the U-Pb concordia diagram (corrected data); histograms of (e) $^{176}Yb/^{177}Hf$ and (f) $^{176}Hf/^{177}Hf_i$, with kernel density estimate as a blue line; (g) εHf plot showing the range in crustal model ages (field) and the median (dashed line).


(a)
box heights are 2σ
Mean = 3131±21 [0.68%] 95% conf.
Wtd by data-pt errs only, 0 of 2 rej.
MSWD = 0.075, probability = 0.78
207Pb/206Pb age (Ma)
(b)
data-point error ellipses are 2σ
Intercepts at
1050±8600 & 3143±150 Ma
MSWD = 0.000
206Pb/238U
207Pb/235U
(c)
box heights are 2σ
Mean = 3099±29 [0.93%] 95% conf.
Wtd by data-pt errs only, 0 of 2 rej.
MSWD = 0.040, probability = 0.84
207Pb/206Pb age (Ma)
(d)
data-point error ellipses are 2σ
Intercepts at
1024±140 & 3105±48 Ma
MSWD = 0.32
206Pb/238U
207Pb/235U
(e)
n=3
176Yb/176Hf
(f)
n=3
176Hf/177Hfi
(g)
DM
T(DM)c = 3.27 Ga
CHUR
Lu/Hf = 0.015
εHf
Age (Ma)

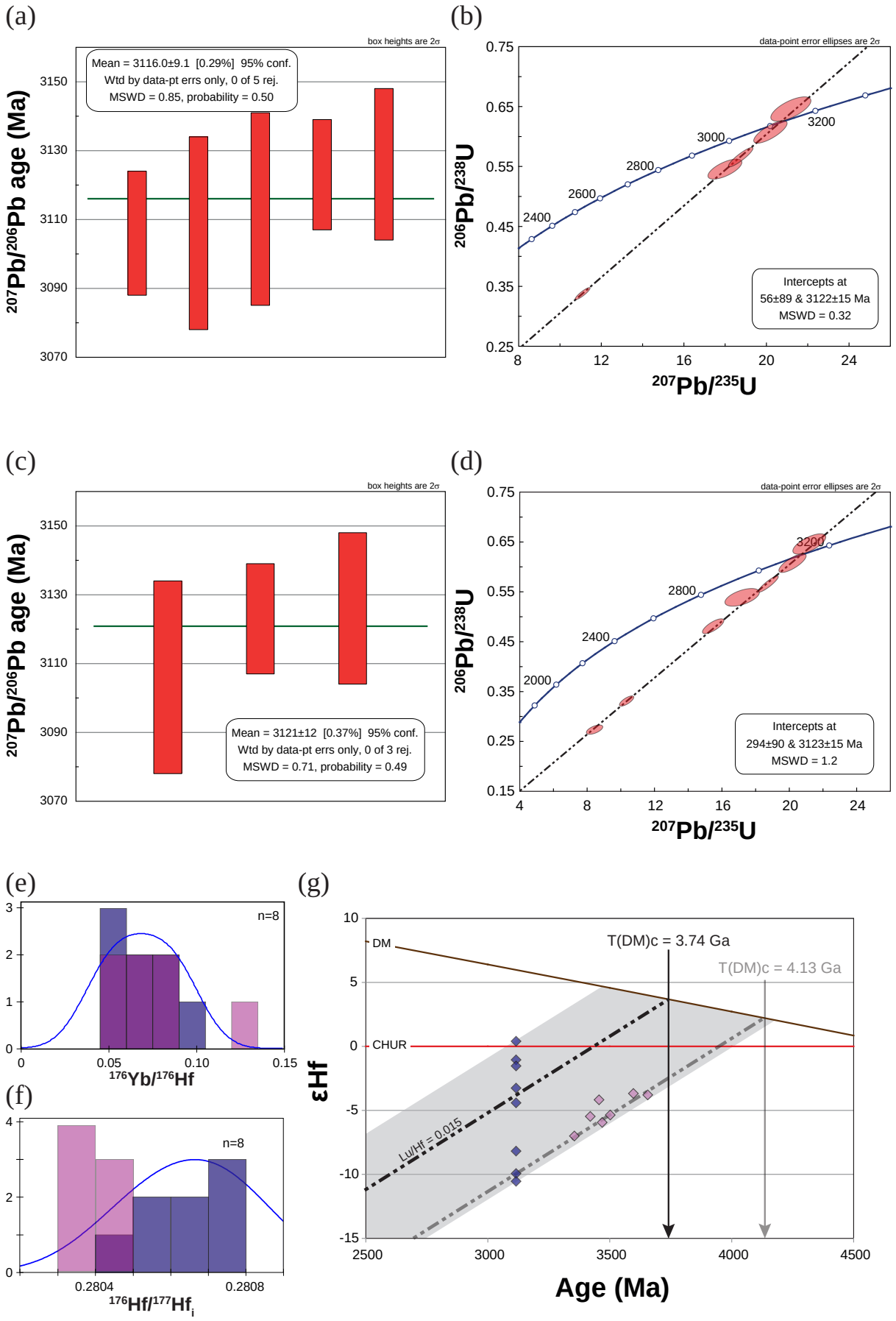
Sample SWA10a

Forty-four U-Pb analyses were obtained from 42 grains, 27 of which were filtered out due to high U contents. Concentrations of Th are variable (75–599 ppm, average = 290 ± 170 ppm), as are U contents (167–954 ppm, average = 560 ± 260 ppm; those with U >1000 ppm excluded); Th/U ratios range from 0.12 to 0.80 with an average of 0.53 ± 0.18.

Of the 17 analyses remaining after filtering, seven give $^{207}Pb/^{206}Pb$ ages ranging from 3656 to 3355 Ma and are interpreted to be inherited (range in corrected ages = 3318 to 3639 Ma). A further five analyses were statistically rejected to give a probability of fit of >0.05, and the remaining five analyses give a weighted mean of $^{207}Pb/^{206}Pb$ ages of 3116.0 ± 9.1 Ma and an intercept age of 3122 ± 15 Ma (Figure 6.21a, b). The seven analyses of inherited grains and a further three analyses were excluded from the corrected data to give an intercept age of 3123 ± 15 Ma (n=7); excluding a further four analyses produced a statistically significant fit and weighted average of $^{207}Pb/^{206}Pb$ ages of 3121 ± 12 Ma (n=3; Figure 6.21c, d).

Hf isotopic analyses were obtained from 15 spots on 14 grains, including the seven with inherited ages. REE contents are low (average $^{176}Yb/^{177}Hf = 0.066 \pm 0.019$; Figure 6.21e) and the analyses spread from close to the CHUR line on the epsilon Hf diagram down to strongly negative values (εHf = -10.39–0.56, average = -4.7 ± 4.2), and give crustal model ages ranging from 4.16 to 3.47 Ga, with a median of 3.74 Ga (Figure 6.21f, g). The inherited grains also lie below the CHUR line, with a range in εHf from -7.00 to -3.68 and an average of -5.1 ± 1.2; they yield crustal model ages ranging from 4.15 to 4.03 Ga with a median of 4.13 Ga. The inherited grains lie along an evolution line with the Lu/Hf ratio of the average continental crust (Lu/Hf = 0.015), which intersects the spread of the main population at the lower end, suggesting that the median crustal model age of the inherited population (4.13 Ga) is indeed the age of extraction from the source, and the main population has been generated by mixing between this recycled material and a more juvenile component (Figure 6.21g).

Figure 6.21. (facing page) Calculated ages and Hf isotopes from sample SWA10a: (a) weighted average of $^{207}Pb/^{206}Pb$ ages and (b) intercept age on the U-Pb concordia diagram (uncorrected data); (c) weighted average of $^{207}Pb/^{206}Pb$ ages and (d) intercept age on the U-Pb concordia diagram (corrected data); histograms of (e) $^{176}Yb/^{177}Hf$ and (f) $^{176}Hf/^{177}Hf_i$, with kernel density estimate as a blue line (main population shown in blue, inherited in pink); (g) εHf plot showing the range in crustal model ages (field), the median of the main population (dashed black line), and the median of the inherited grains (dashed grey line).


(a)
box heights are 2σ
Mean = 3116.0±9.1 [0.29%] 95% conf.
Wtd by data-pt errs only, 0 of 5 rej.
MSWD = 0.85, probability = 0.50
207Pb/206Pb age (Ma)
(b)
data-point error ellipses are 2σ
Intercepts at
56±89 & 3122±15 Ma
MSWD = 0.32
206Pb/238U
207Pb/235U
(c)
box heights are 2σ
Mean = 3121±12 [0.37%] 95% conf.
Wtd by data-pt errs only, 0 of 3 rej.
MSWD = 0.71, probability = 0.49
207Pb/206Pb age (Ma)
(d)
data-point error ellipses are 2σ
Intercepts at
294±90 & 3123±15 Ma
MSWD = 1.2
206Pb/238U
207Pb/235U
(e)
n=8
176Yb/176Hf
(f)
n=8
176Hf/177Hfi
(g)
DM
CHUR
T(DM)c = 3.74 Ga
T(DM)c = 4.13 Ga
Lu/Hf = 0.015
εHf
Age (Ma)

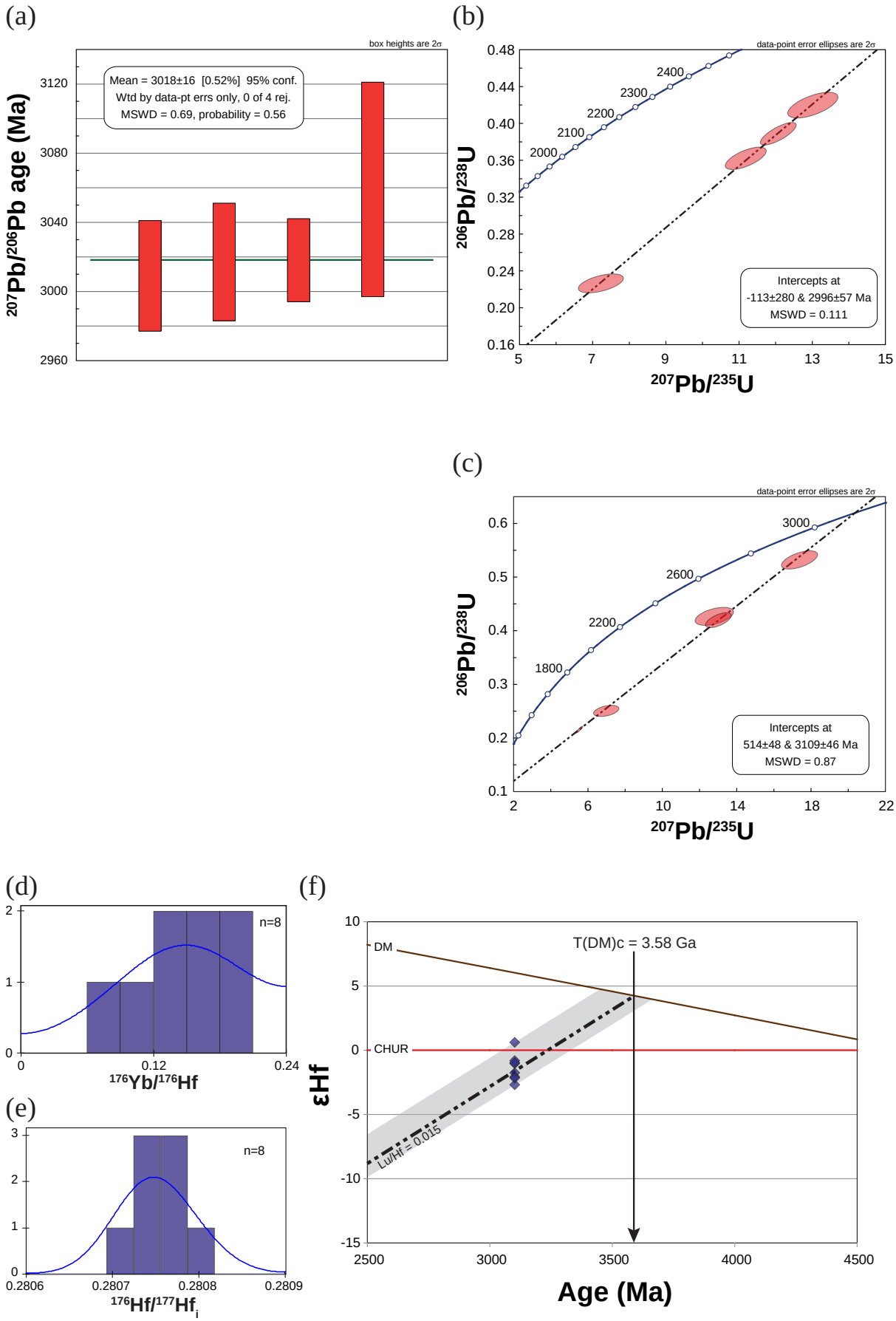
Sample RSA09

U-Pb ages were obtained on 40 spots from 35 grains, 27 of which were discarded at the filtering stage, mainly due to high U contents. Concentrations of Th and U are variable (Th = 16–1240 ppm, average = 290 ± 310 ppm; U = 27–997 ppm, average = 510 ± 310 ppm; 24 analyses with U >1000 ppm excluded), as are Th/U ratios (0.10–1.14, average = 0.59 ± 0.32).

No inheritance was detected in this sample. The 13 analyses remaining after filtering do not yield a consistent age unless a further nine analyses are rejected, the four remaining analyses give a weighted mean of $^{207}Pb/^{206}Pb$ ages of 3018 ± 16 Ma and an intercept age on the U-Pb concordia diagram of 2996 ± 57 Ma (Figure 6.22a, b). The corrected data yield an intercept age of 3109 ± 46 Ma from five analyses (Figure 6.22c), but fail to achieve a statistically significant fit for the weighted average of $^{207}Pb/^{206}Pb$ ages upon further culling, due to the large spread in $^{207}Pb/^{206}Pb$ ages attributed to a combination of ancient Pb loss and overcorrection of the $^{207}Pb/^{206}Pb$ ages by the common Pb correction routine.

Hf isotopic compositions were obtained from eight grains; the grains from this sample have high REE contents (average $^{176}Yb/^{177}Hf$ = 0.142 ± 0.041; Figure 6.22d) and the analyses cluster below the CHUR line on the epsilon Hf plot (εHf = -2.71–0.63, average = -1.4 ± 1.0), and give crustal model ages ranging from 3.67 to 3.45 Ga, and a median of 3.58 Ga (Figure 6.22e, f).

Figure 6.22. (facing page) Calculated ages and Hf isotopes from sample RSA09: (a) weighted average of $^{207}Pb/^{206}Pb$ ages and (b) intercept age on the U-Pb concordia diagram (uncorrected data); (c) intercept age on the U-Pb concordia diagram (corrected data; no weighted average could be calculated for this sample); histograms of (d) $^{176}Yb/^{177}Hf$ and (e) $^{176}Hf/^{177}Hf_i$, with kernel density estimate as a blue line; (f) εHf plot showing the range in crustal model ages (field) and the median (dashed line).


(a)
box heights are 2σ
Mean = 3018±16 [0.52%] 95% conf.
Wtd by data-pt errs only, 0 of 4 rej.
MSWD = 0.69, probability = 0.56
207Pb/206Pb age (Ma)
(b)
data-point error ellipses are 2σ
Intercepts at
-113±280 & 2996±57 Ma
MSWD = 0.111
206Pb/238U
207Pb/235U
(c)
data-point error ellipses are 2σ
Intercepts at
514±48 & 3109±46 Ma
MSWD = 0.87
206Pb/238U
207Pb/235U
(d)
n=8
176Yb/176Hf
(e)
n=8
176Hf/177Hfi
(f)
DM
CHUR
T(DM)c = 3.58 Ga
Lu/Hf = 0.015
εHf
Age (Ma)

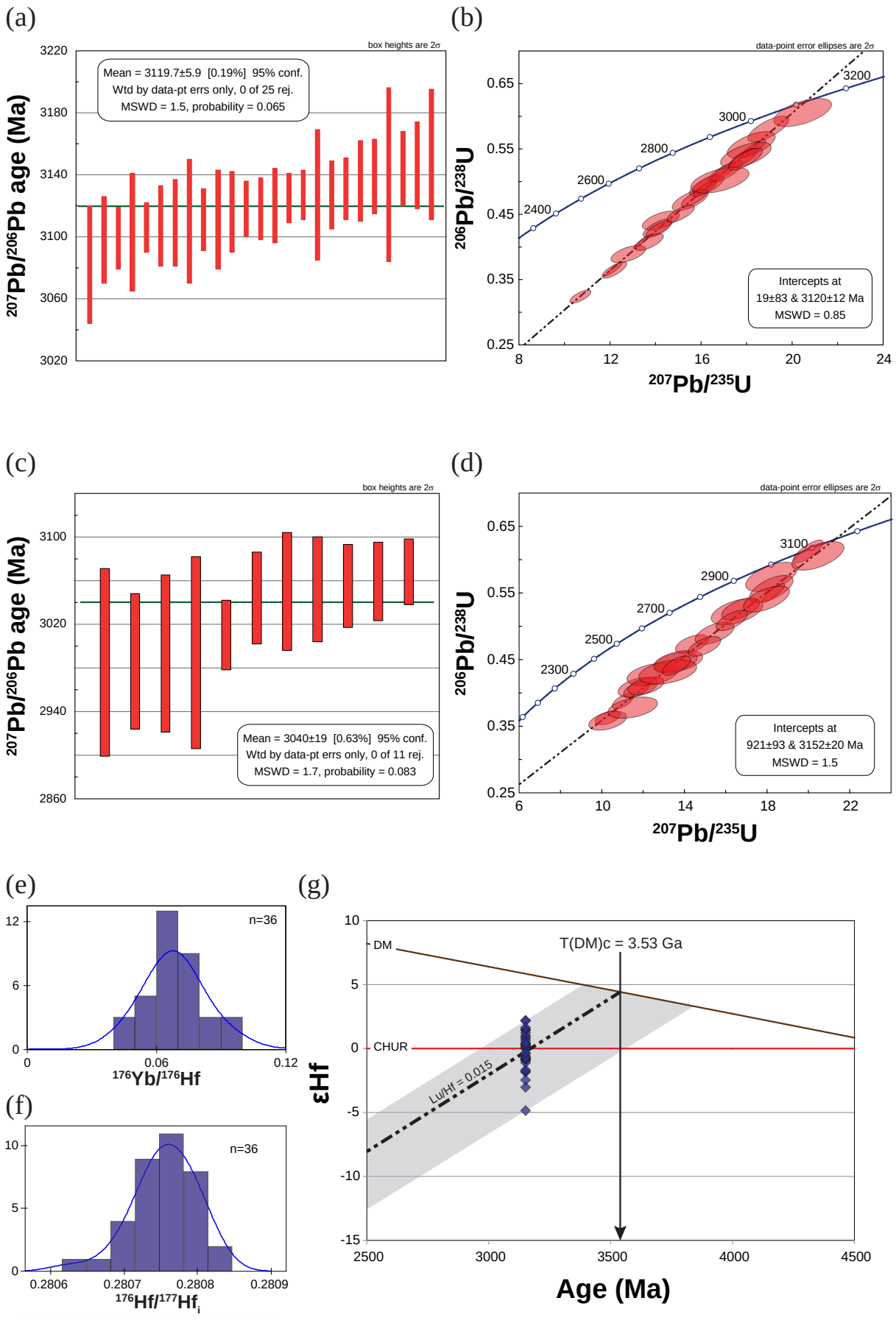
Sample SWA03

U-Pb ages were obtained from 56 spots on 48 grains, 23 of which were rejected at the filtering stage due mainly to high U contents. Thorium and U concentrations are variable (Th = 54–827 ppm, average = 440 ± 180 ppm; U = 109–966 ppm, average = 630 ± 160 ppm; 11 analyses with U >1000 ppm excluded), as are Th/U ratios (0.23–1.24, average = 0.69 ± 0.21).

No inheritance was detected in this sample. After filtering, 18 further analyses were excluded statistically, and the remaining 25 grains give a weighted average of $^{207}Pb/^{206}Pb$ ages of 3119.7 ± 5.9 Ma and an intercept age on the U-Pb concordia diagram of 3120 ± 12 Ma (Figure 6.23a, b). The corrected data give a statistically significant fit for the intercept age after rejection of 19 grains (3152 ± 20 Ma, n=24); however, there is a large spread in $^{207}Pb/^{206}Pb$ ages and a further 13 analyses had to be rejected to achieve a probability of fit >0.05 for the weighted mean of $^{207}Pb/^{206}Pb$ ages. The calculated age (3040 ± 19 Ma, n=11) is significantly lower than the intercept age and is most likely skewed younger than the 'true' age due to the overcorrection of the $^{207}Pb/^{206}Pb$ ages (Figure 6.23c, d).

Hf isotopic compositions were obtained from 36 spots on 34 grains; REE contents are low (average $^{176}Yb/^{177}Hf$ = 0.068 ± 0.013; Figure 6.23e) and the analyses form a cluster centred slightly below the CHUR line on the epsilon Hf diagram (εHf = -4.89–2.16, average = -0.2 ± 1.5), and give crustal model ages ranging from 3.84 to 3.39 Ga (median = 3.53 Ga; Figure 6.23f, g).

Figure 6.23. (facing page) Calculated ages and Hf isotopes from sample SWA03: (a) weighted average of $^{207}Pb/^{206}Pb$ ages and (b) intercept age on the U-Pb concordia diagram (uncorrected data); (c) weighted average of $^{207}Pb/^{206}Pb$ ages and (d) intercept age on the U-Pb concordia diagram (corrected data); histograms of (e) $^{176}Yb/^{177}Hf$ and (f) $^{176}Hf/^{177}Hf_i$, with kernel density estimate as a blue line; (g) εHf plot showing the range in crustal model ages (field) and the median (dashed line).


(a)
box heights are 2σ
Mean = 3119.7±5.9 [0.19%] 95% conf.
Wtd by data-pt errs only, 0 of 25 rej.
MSWD = 1.5, probability = 0.065
207Pb/206Pb age (Ma)
(b)
data-point error ellipses are 2σ
Intercepts at
19±83 & 3120±12 Ma
MSWD = 0.85
206Pb/238U
207Pb/235U
(c)
box heights are 2σ
Mean = 3040±19 [0.63%] 95% conf.
Wtd by data-pt errs only, 0 of 11 rej.
MSWD = 1.7, probability = 0.083
207Pb/206Pb age (Ma)
(d)
data-point error ellipses are 2σ
Intercepts at
921±93 & 3152±20 Ma
MSWD = 1.5
206Pb/238U
207Pb/235U
(e)
n=36
176Yb/176Hf
(f)
n=36
176Hf/177Hfi
(g)
DM
CHUR
T(DM)c = 3.53 Ga
Lu/Hf = 0.015
εHf
Age (Ma)

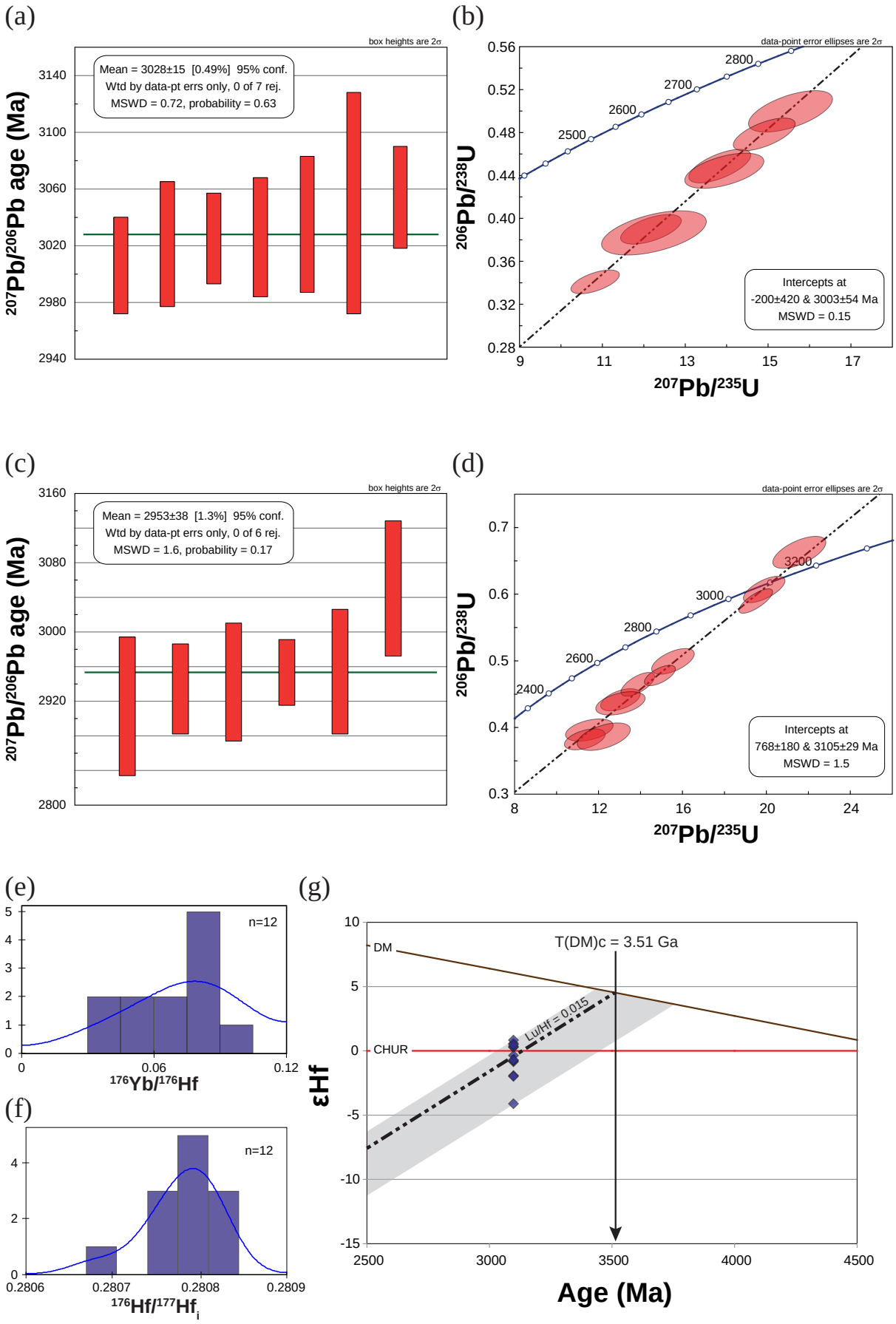
Sample RSA06

U-Pb analyses were obtained from 43 grains, 27 of which were filtered out due to high U contents. Thorium contents are variable to very high (Th = 35–4817 ppm, average = 900 ± 1400 ppm), U contents show considerable variation (U = 60–841 ppm, average = 550 ± 240 ppm; those with U >1000 ppm excluded), and Th/U ratios are variable to very high (0.28–8.24, average = 1.61 ± 2.29).

No inheritance was detected in this sample. After filtering, a further nine analyses were determined to be statistical outliers and were rejected; the remaining seven analyses give a weighted average of $^{207}Pb/^{206}Pb$ ages of 3028 ± 15 Ma and an intercept age of 3003 ± 54 Ma (Figure 6.24a, b). The corrected data give an intercept age of 3105 ± 29 Ma from 11 grains, but a further five analyses have to be rejected to achieve a statistically significant fit for the weighted average of $^{207}Pb/^{206}Pb$ ages (2953 ± 38 Ma, n=6; Figure 6.24c, d). The anomalously young ages obtained from this sample, particularly the weighted averages of $^{207}Pb/^{206}Pb$ ages, are probably a result of ancient Pb loss rather than an overcorrection of the $^{207}Pb/^{206}Pb$ ages, as the high Th content reduces the effectiveness of filtering by U content to remove the effect of Pb loss.

Hf isotopic compositions were obtained from 12 grains; REE contents are low (average $^{176}Yb/^{177}Hf = 0.072 \pm 0.021$; Figure 6.24e) and the analyses generally lie below the CHUR line on the epsilon Hf diagram (εHf = -3.99–1.02, average = -0.5 ± 1.4), and give crustal model ages ranging from 3.75 to 3.43 Ga, with a median of 3.51 Ga (Figure 6.24f, g).

Figure 6.24. (facing page) Calculated ages and Hf isotopes from sample RSA06: (a) weighted average of $^{207}Pb/^{206}Pb$ ages and (b) intercept age on the U-Pb concordia diagram (uncorrected data); (c) weighted average of $^{207}Pb/^{206}Pb$ ages and (d) intercept age on the U-Pb concordia diagram (corrected data); histograms of (e) $^{176}Yb/^{177}Hf$ and (f) $^{176}Hf/^{177}Hf_i$, with kernel density estimate as a blue line; (g) εHf plot showing the range in crustal model ages (field) and the median (dashed line).


(a)
box heights are 2σ
Mean = 3028±15 [0.49%] 95% conf.
Wtd by data-pt errs only, 0 of 7 rej.
MSWD = 0.72, probability = 0.63
207Pb/206Pb age (Ma)
(b)
data-point error ellipses are 2σ
Intercepts at
-200±420 & 3003±54 Ma
MSWD = 0.15
206Pb/238U
207Pb/235U
(c)
box heights are 2σ
Mean = 2953±38 [1.3%] 95% conf.
Wtd by data-pt errs only, 0 of 6 rej.
MSWD = 1.6, probability = 0.17
207Pb/206Pb age (Ma)
(d)
data-point error ellipses are 2σ
Intercepts at
768±180 & 3105±29 Ma
MSWD = 1.5
206Pb/238U
207Pb/235U
(e)
n=12
176Yb/176Hf
(f)
n=12
176Hf/177Hfi
(g)
T(DM)c = 3.51 Ga
DM
CHUR
Lu/Hf = 0.015
εHf
Age (Ma)

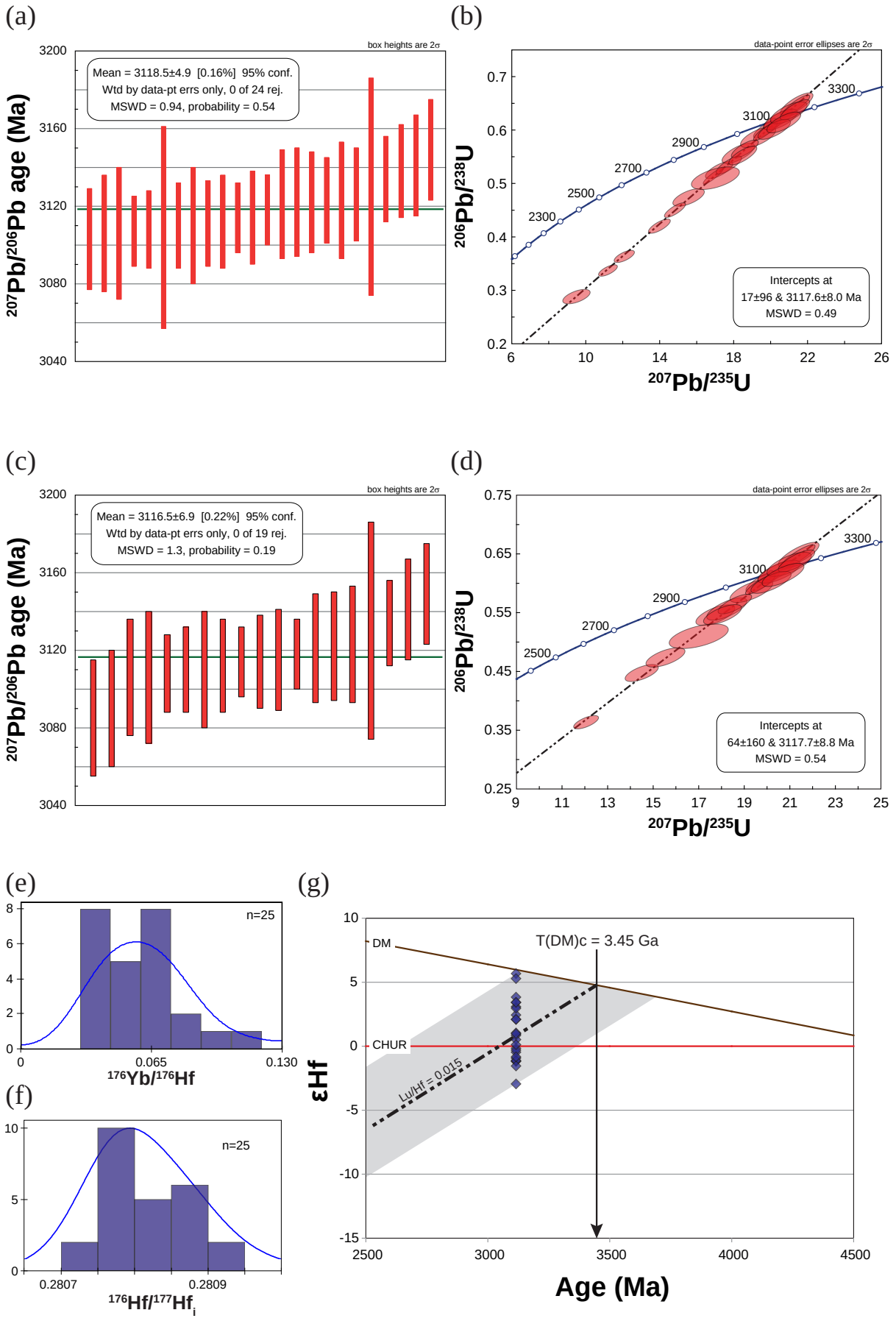
Sample SWA13a

Ages were obtained from 37 grains, three of which were filtered out due to high U contents and a further one with high common Pb. Concentrations of Th and U are variable (Th = 44–498 ppm, average = 210 ± 110 ppm; U = 73–918 ppm, average = 320 ± 190 ppm; those with U >1000 ppm excluded), as are Th/U ratios (0.33–1.57, average = 0.71 ± 0.25).

No inheritance was detected in this sample. Nine further analyses were rejected after filtering as statistical outliers, and the remaining 24 grains give a weighted average of $^{207}Pb/^{206}Pb$ ages of 3118.5 ± 4.9 Ma and an intercept age of 3117.6 ± 8.0 Ma (Figure 6.25a, b). Fourteen analyses were rejected from the corrected data on a statistical basis; the remaining 19 analyses yield an intercept age of 3117.7 ± 8.8 Ma and a weighted mean of $^{207}Pb/^{206}Pb$ ages of 3116.5 ± 6.9 Ma (Figure 6.25c, d).

Hf isotopic compositions were obtained from 25 grains; REE contents are low (average $^{176}Yb/^{177}Hf = 0.061 \pm 0.019$; Figure 6.25e) and the analyses have a spread in εHf from -2.96 to 5.65 with an average of 1.1 ± 2.3, and give crustal model ages ranging from 3.69 to 3.14 Ga, with a median of 3.45 Ga (Figure 6.25f, g).

Figure 6.25. (facing page) Calculated ages and Hf isotopes from sample SWA13a: (a) weighted average of $^{207}Pb/^{206}Pb$ ages and (b) intercept age on the U-Pb concordia diagram (uncorrected data); (c) weighted average of $^{207}Pb/^{206}Pb$ ages and (d) intercept age on the U-Pb concordia diagram (corrected data); histograms of (e) $^{176}Yb/^{177}Hf$ and (f) $^{176}Hf/^{177}Hf_i$, with kernel density estimate as a blue line; (g) εHf plot showing the range in crustal model ages (field) and the median (dashed line).


(a)
box heights are 2σ
Mean = 3118.5±4.9 [0.16%] 95% conf.
Wtd by data-pt errs only, 0 of 24 rej.
MSWD = 0.94, probability = 0.54
207Pb/206Pb age (Ma)
(b)
data-point error ellipses are 2σ
Intercepts at
17±96 & 3117.6±8.0 Ma
MSWD = 0.49
206Pb/238U
207Pb/235U
(c)
box heights are 2σ
Mean = 3116.5±6.9 [0.22%] 95% conf.
Wtd by data-pt errs only, 0 of 19 rej.
MSWD = 1.3, probability = 0.19
207Pb/206Pb age (Ma)
(d)
data-point error ellipses are 2σ
Intercepts at
64±160 & 3117.7±8.8 Ma
MSWD = 0.54
206Pb/238U
207Pb/235U
(e)
n=25
176Yb/176Hf
(f)
n=25
176Hf/177Hfi
(g)
T(DM)c = 3.45 Ga
DM
CHUR
Lu/Hf = 0.015
εHf
Age (Ma)

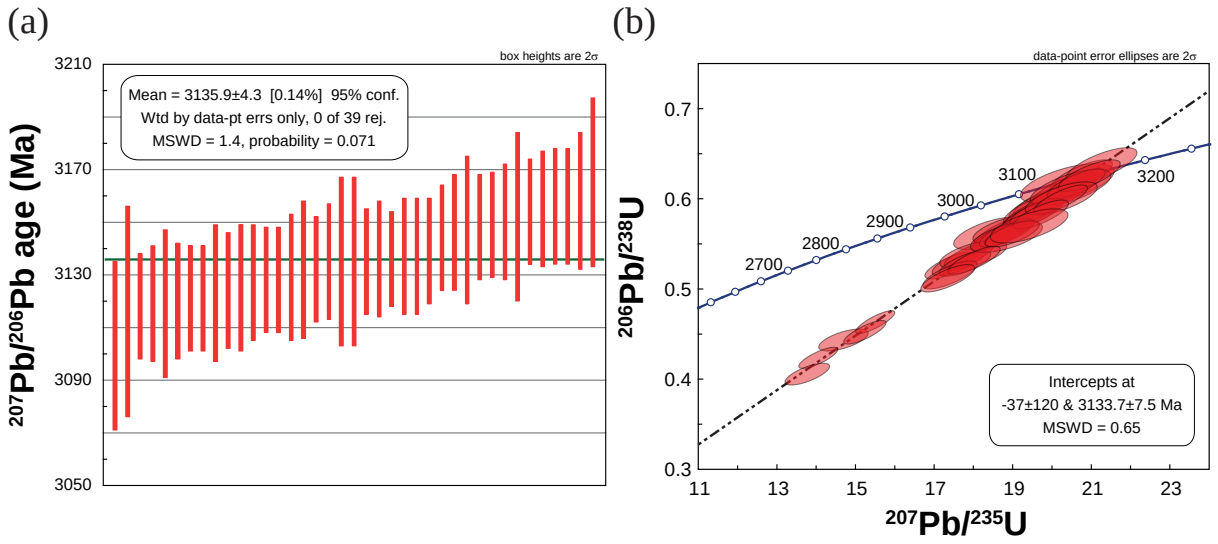
Sample SWA11

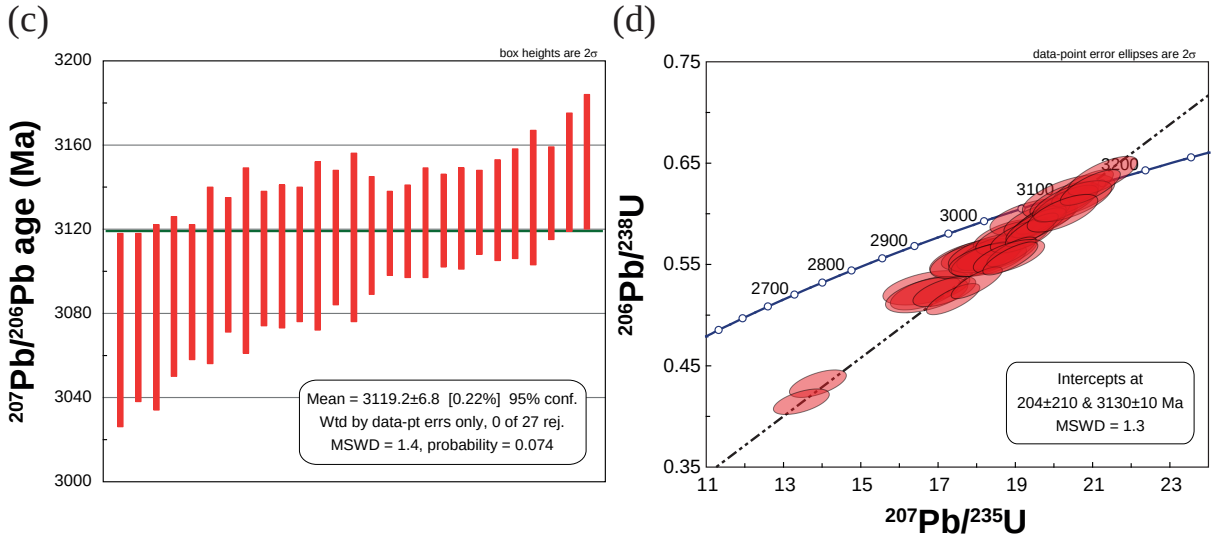
Ages were obtained from 50 grains, five of which were filtered out due to high common Pb contents. Concentrations of Th and U are variable (Th = 60–614 ppm, average = 230 ± 120 ppm; U = 0.23–0.94, average = 410 ± 170 ppm); Th/U ratios range from 0.23 to 0.94, with an average of 0.58 ± 0.18.

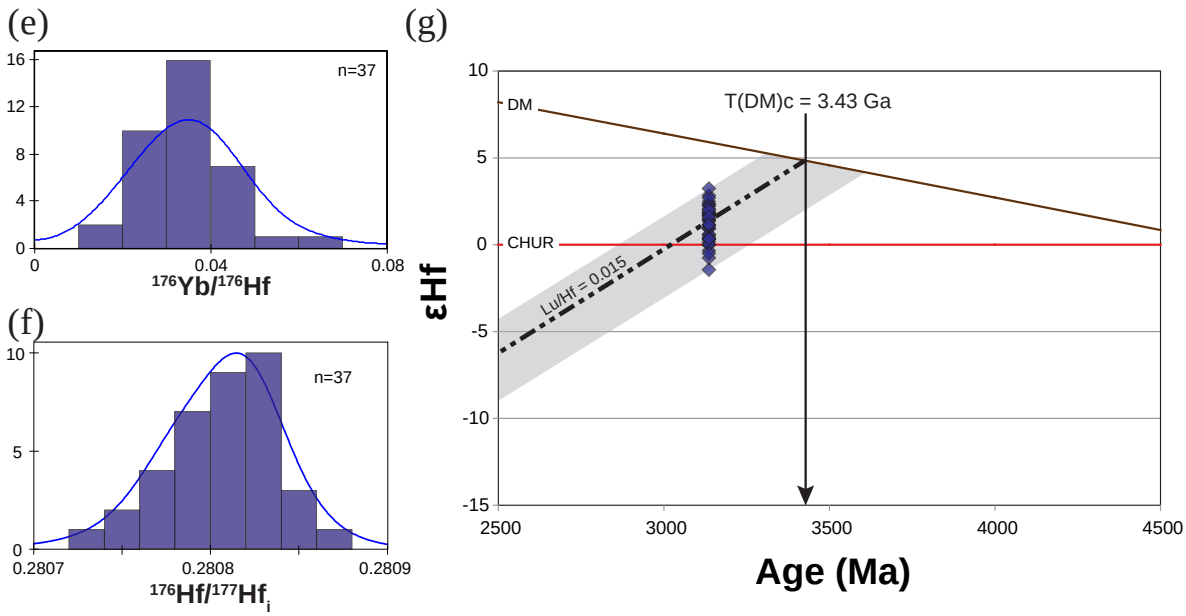
No inheritance was detected in this sample. Of the 45 analyses remaining after the filtering stage, six further analyses were statistically rejected to achieve a probability of fit >0.05; the remaining 39 analyses give a weighted mean of $^{207}Pb/^{206}Pb$ ages of 3135.9 ± 4.3 Ma and an intercept age of 3133.7 ± 7.5 Ma (Figure 6.26a, b). For the corrected data, 10 analyses were excluded on a statistical basis to give an intercept age of 3130 ± 10 Ma (n=35), and after rejecting a further eight analyses the remaining 27 grains yield a weighted mean of $^{207}Pb/^{206}Pb$ ages of 3119.2 ± 6.8 Ma (Figure 6.26c, d). This is significantly younger than the intercept age and those calculated from the uncorrected data, suggesting the overcorrection of $^{207}Pb/^{206}Pb$ ages by the common-Pb correction routine has artificially lowered the calculated average age.

Hf isotopic compositions were obtained from 37 grains; REE contents are low (average $^{176}Yb/^{177}Hf = 0.035 \pm 0.010$; Figure 6.26e) and the analyses mainly plot above the CHUR line on the εHf diagram (εHf = -1.58–3.10, average = 1.0 ± 1.1), and give crustal model ages ranging from 3.61 to 3.31 Ga, and a median of 3.43 Ga (Figure 6.26f, g).

Figure 6.26. (facing page) Calculated ages and Hf isotopes from sample SWA11: (a) weighted average of $^{207}Pb/^{206}Pb$ ages and (b) intercept age on the U-Pb concordia diagram (uncorrected data); (c) weighted average of $^{207}Pb/^{206}Pb$ ages and (d) intercept age on the U-Pb concordia diagram (corrected data); histograms of (e) $^{176}Yb/^{177}Hf$ and (f) $^{176}Hf/^{177}Hf_i$, with kernel density estimate as a blue line; (g) εHf plot showing the range in crustal model ages (field) and the median (dashed line).


(a)
box heights are 2σ
Mean = 3135.9±4.3 [0.14%] 95% conf.
Wtd by data-pt errs only, 0 of 39 rej.
MSWD = 1.4, probability = 0.071
207Pb/206Pb age (Ma)
(b)
data-point error ellipses are 2σ
Intercepts at
-37±120 & 3133.7±7.5 Ma
MSWD = 0.65
206Pb/238U
207Pb/235U


(c)
box heights are 2σ
Mean = 3119.2±6.8 [0.22%] 95% conf.
Wtd by data-pt errs only, 0 of 27 rej.
MSWD = 1.4, probability = 0.074
207Pb/206Pb age (Ma)
(d)
data-point error ellipses are 2σ
Intercepts at
204±210 & 3130±10 Ma
MSWD = 1.3
206Pb/238U
207Pb/235U


(e)
n=37
176Yb/176Hf
(f)
n=37
176Hf/177Hfi
(g)
T(DM)c = 3.43 Ga
DM
CHUR
Lu/Hf = 0.015
εHf
Age (Ma)

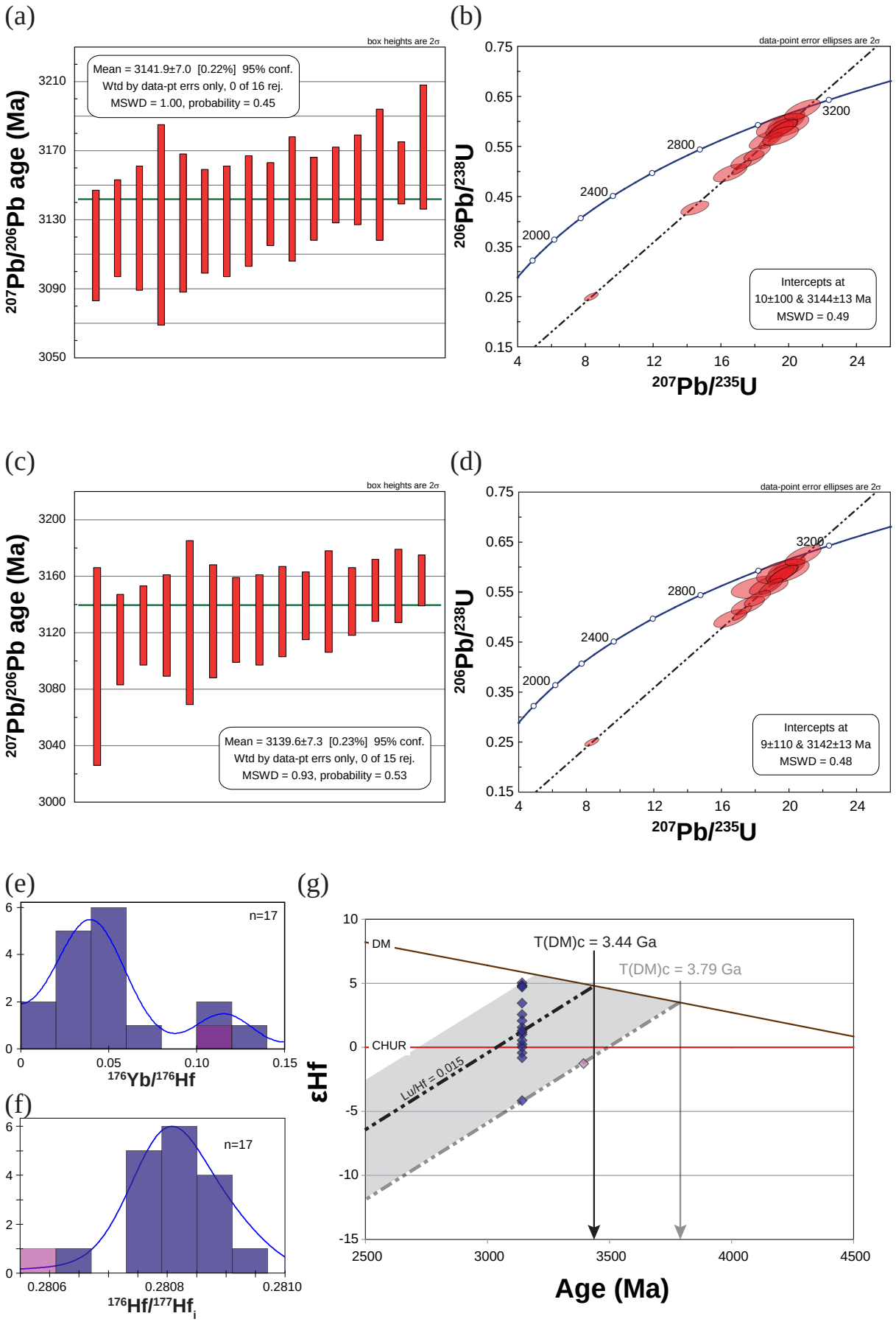
Sample SWA09

Ages were obtained from 24 grains from sample SWA09, four of which were filtered out due to high U contents. Concentrations of Th and U are variable (Th = 61–631 ppm, average = 210 ± 150 ppm; U = 86–867 ppm, average = 290 ± 190 ppm; those with U >1000 ppm excluded), as are Th/U ratios (0.20–2.25, average = 0.83 ± 0.48).

Two grains with $^{207}Pb/^{206}Pb$ ages of 3394 ± 23 and 3478 ± 13 Ma are interpreted to be inherited, and two were statistically rejected to achieve a probability of fit of >0.05. The remaining 16 analyses give a weighted mean of $^{207}Pb/^{206}Pb$ ages of 3141.9 ± 7.0 Ma and an intercept age of 3144 ± 13 Ma (Figure 6.27a, b). The two inherited grains and three further analyses were excluded from the corrected data, and the remaining 15 analyses yield an intercept age of 3142 ± 13 Ma and a weighted average of $^{207}Pb/^{206}Pb$ ages of 3139.6 ± 7.3 Ma (Figure 6.27c, d).

Hf isotopic compositions were obtained from 18 grains, including the two with inherited ages. REE contents are low (average $^{176}Yb/^{177}Hf$ = 0.052 ± 0.033; Figure 6.27e); one of the grains with an inherited age has an isotopic composition consistent with the main population and is treated as such, while the other has an εHf value of -1.3 ± 1.0 and a crustal model age of 3.79 Ga. The main population mainly lies above the CHUR line on the epsilon Hf diagram, with a range in εHf from -4.16 to 5.04 and an average of 1.5 ± 2.4. Crustal model ages range from 3.78 to 3.20 Ga, with a median of 3.44 Ga (Figure 6.27f, g).

Figure 6.27. (facing page) Calculated ages and Hf isotopes from sample SWA09: (a) weighted average of $^{207}Pb/^{206}Pb$ ages and (b) intercept age on the U-Pb concordia diagram (uncorrected data); (c) weighted average of $^{207}Pb/^{206}Pb$ ages and (d) intercept age on the U-Pb concordia diagram (corrected data); histograms of (e) $^{176}Yb/^{177}Hf$ and (f) $^{176}Hf/^{177}Hf_i$, with kernel density estimate as a blue line (main population shown in blue, inherited in pink); (g) εHf plot showing the range in crustal model ages (field), the median of the main population (dashed black line), and the inherited grain (dashed grey line).


(a)
box heights are 2σ
Mean = 3141.9±7.0 [0.22%] 95% conf.
Wtd by data-pt errs only, 0 of 16 rej.
MSWD = 1.00, probability = 0.45
207Pb/206Pb age (Ma)
(b)
data-point error ellipses are 2σ
Intercepts at
10±100 & 3144±13 Ma
MSWD = 0.49
206Pb/238U
207Pb/235U
(c)
box heights are 2σ
Mean = 3139.6±7.3 [0.23%] 95% conf.
Wtd by data-pt errs only, 0 of 15 rej.
MSWD = 0.93, probability = 0.53
207Pb/206Pb age (Ma)
(d)
data-point error ellipses are 2σ
Intercepts at
9±110 & 3142±13 Ma
MSWD = 0.48
206Pb/238U
207Pb/235U
(e)
n=17
176Yb/176Hf
(f)
n=17
176Hf/177Hfi
(g)
DM
T(DM)c = 3.44 Ga
T(DM)c = 3.79 Ga
CHUR
Lu/Hf = 0.015
εHf
Age (Ma)

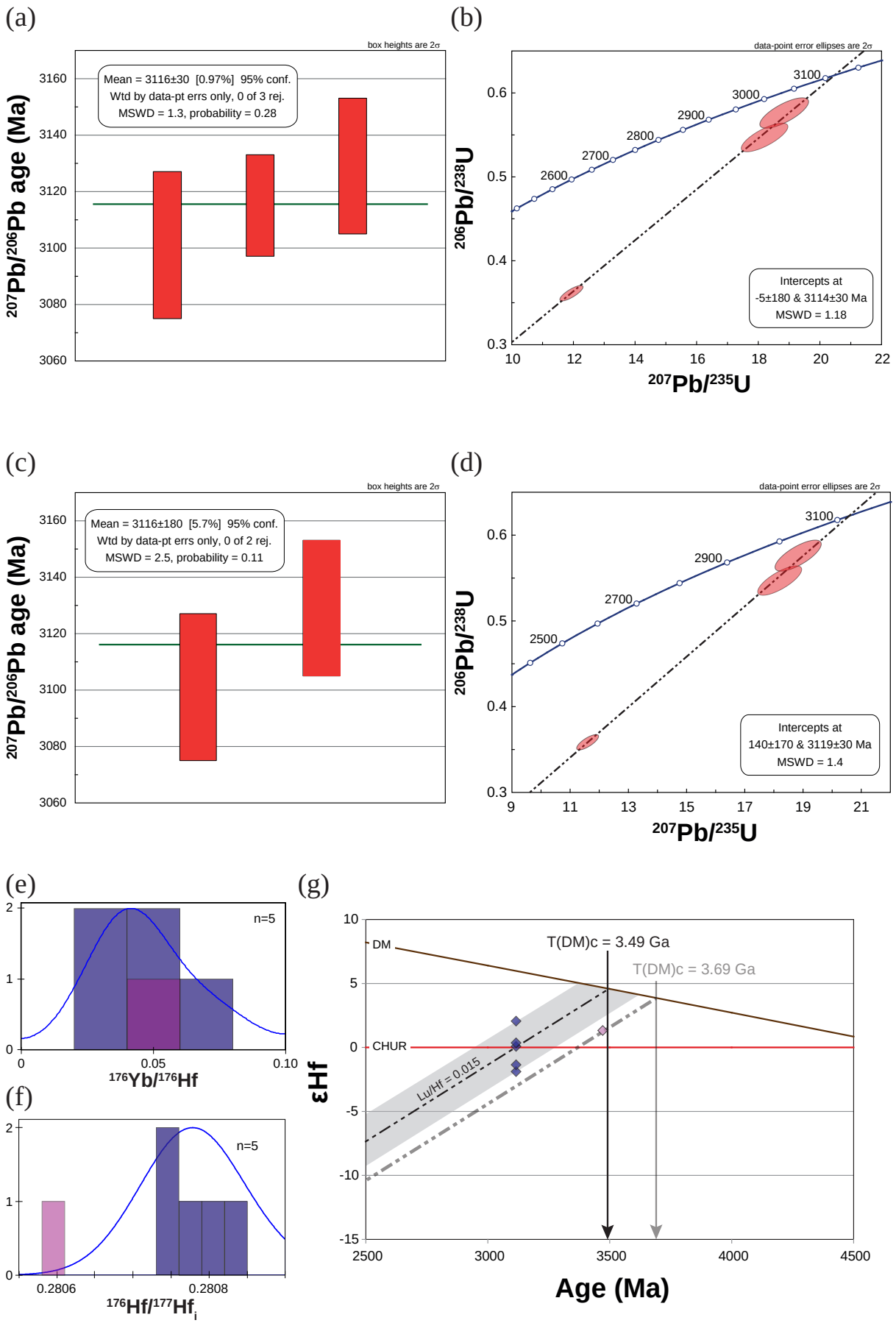
Sample SWA02a

U-Pb analyses were obtained from 24 spots on 23 grains, 18 of which were rejected in the filtering stage due mainly to high concentrations of U. Concentrations of Th and U are variable (Th = 133–681 ppm, average = 330 ± 190 ppm; U = 441–868 ppm, average = 630 ± 170 ppm; 17 analyses with U >1000 ppm excluded), as are Th/U ratios (0.17–1.22, average = 0.56 ± 0.36).

One grain gives a $^{207}Pb/^{206}Pb$ age of 3471 ± 9 Ma and is interpreted to be inherited. Two further analyses were rejected on a statistical basis, leaving only three analyses which yield a weighted mean of $^{207}Pb/^{206}Pb$ ages of 3116 ± 30 Ma and an intercept age of 3114 ± 30 Ma (Figure 6.28a, b). For the corrected data, the inherited grain (corrected $^{207}Pb/^{206}Pb$ age = 3373 ± 13 Ma) and two other analyses were excluded to give an intercept age of 3119 ± 30 Ma (n=3); one further analysis was rejected to achieve a probability of fit >0.05 for the weighted average of $^{207}Pb/^{206}Pb$ ages, leaving only two grains which nevertheless give an imprecise but consistent calculated age of 3120 ± 180 Ma (Figure 6.28c, d).

Hf isotopic compositions were obtained from the six grains not excluded at the filtering stage, including the inherited grain. REE contents are low (average $^{176}Yb/^{177}Hf$ = 0.047 ± 0.016; Figure 6.28e) and the five grains from the main population cluster about the CHUR line on the epsilon Hf diagram (εHf = -1.82–2.13, average = -0.1 ± 1.6). Crustal model ages range from 3.62 to 3.37 Ga, with a median of 3.49 Ga. The inherited grain gives an εHf value of 1.32 ± 0.67 and a crustal model age of 3.69 Ga (Figure 6.28f, g).

Figure 6.28. (facing page) Calculated ages and Hf isotopes from sample SWA02a: (a) weighted average of $^{207}Pb/^{206}Pb$ ages and (b) intercept age on the U-Pb concordia diagram (uncorrected data); (c) weighted average of $^{207}Pb/^{206}Pb$ ages and (d) intercept age on the U-Pb concordia diagram (corrected data); histograms of (e) $^{176}Yb/^{177}Hf$ and (f) $^{176}Hf/^{177}Hf_i$, with kernel density estimate as a blue line (main population shown in blue, inherited in pink); (g) εHf plot showing the range in crustal model ages (field), the median of the main population (dashed black line), and the inherited grain (dashed grey line).


(a)
box heights are 2σ
Mean = 3116±30 [0.97%] 95% conf.
Wtd by data-pt errs only, 0 of 3 rej.
MSWD = 1.3, probability = 0.28
207Pb/206Pb age (Ma)
(b)
data-point error ellipses are 2σ
Intercepts at
-5±180 & 3114±30 Ma
MSWD = 1.18
206Pb/238U
207Pb/235U
(c)
box heights are 2σ
Mean = 3116±180 [5.7%] 95% conf.
Wtd by data-pt errs only, 0 of 2 rej.
MSWD = 2.5, probability = 0.11
207Pb/206Pb age (Ma)
(d)
data-point error ellipses are 2σ
Intercepts at
140±170 & 3119±30 Ma
MSWD = 1.4
206Pb/238U
207Pb/235U
(e)
n=5
176Yb/176Hf
(f)
n=5
176Hf/177Hfi
(g)
T(DM)c = 3.49 Ga
T(DM)c = 3.69 Ga
DM
CHUR
Lu/Hf = 0.015
εHf
Age (Ma)

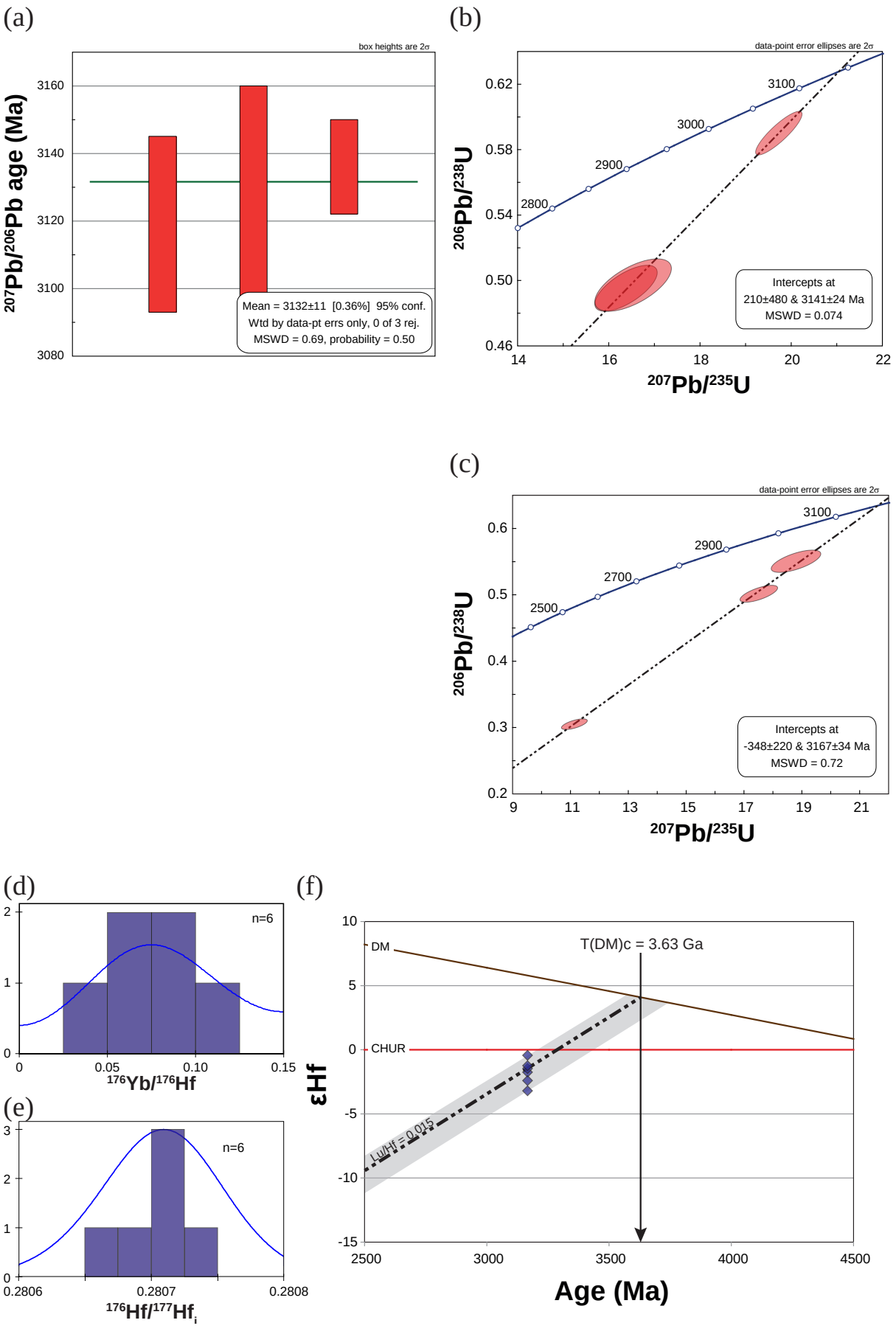
Sample RSA07

Ages were obtained from 15 spots on 13 grains from sample RSA07, seven of which had high U contents or calculated common Pb and were filtered out. Concentrations of Th are high and extremely variable (133–2835 ppm, average = 1000 ± 1000 ppm), while U contents are relatively low (131–667 ppm, average = 440 ± 170 ppm; 6 analyses with U >1000 ppm excluded); Th/U ratios are correspondingly high (0.31–4.67, average = 2.2 ± 1.7).

Of the eight analyses remaining after filtering, one has a $^{207}Pb/^{206}Pb$ age of 3575 ± 13 Ma and is interpreted as inherited, and a further four were rejected to achieve a probability of fit >0.05, leaving three analyses which give a weighted mean of $^{207}Pb/^{206}Pb$ ages of 3132 ± 11 Ma and an intercept age of 3141 ± 24 Ma (Figure 6.29a, b). After excluding the inherited grain and four others, the corrected ages give a statistically significant intercept age of 3167 ± 34 Ma from three analyses, but there is a large spread in the $^{207}Pb/^{206}Pb$ ages and they fail to achieve a probability of fit >0.05 even when a further analysis is excluded (Figure 6.29c).

Hf compositions were obtained from six grains; REE contents are low (average $^{176}Yb/^{177}Hf$ = 0.078 ± 0.024; Figure 6.29d) and the analyses lie below the CHUR line on the epsilon Hf diagram, with a range in εHf from -3.10 to -0.34 (average = -1.65 ± 0.96). Crustal model ages range from 3.74 to 3.56 Ga, with a median of 3.63 Ga (Figure 6.29e, f).

Figure 6.29. (facing page) Calculated ages and Hf isotopes from sample RSA07: (a) weighted average of $^{207}Pb/^{206}Pb$ ages and (b) intercept age on the U-Pb concordia diagram (uncorrected data); (c) intercept age on the U-Pb concordia diagram (corrected data; no weighted average could be calculated for this sample); histograms of (d) $^{176}Yb/^{177}Hf$ and (e) $^{176}Hf/^{177}Hf_i$, with kernel density estimate as a blue line; (f) εHf plot showing the range in crustal model ages (field) and the median (dashed line).


(a)
box heights are 2σ
$^{207}Pb/^{206}Pb$ age (Ma)
3160
3140
3120
3100
3080
Mean = 3132±11 [0.36%] 95% conf.
Wtd by data-pt errs only, 0 of 3 rej.
MSWD = 0.69, probability = 0.50
(b)
data-point error ellipses are 2σ
$^{206}Pb/^{238}U$
0.62
0.58
0.54
0.50
0.46
3100
3000
2900
2800
Intercepts at
210±480 & 3141±24 Ma
MSWD = 0.074
14
16
18
20
22
$^{207}Pb/^{235}U$
(c)
data-point error ellipses are 2σ
$^{206}Pb/^{238}U$
0.6
0.5
0.4
0.3
0.2
3100
2900
2700
2500
Intercepts at
-348±220 & 3167±34 Ma
MSWD = 0.72
9
11
13
15
17
19
21
$^{207}Pb/^{235}U$
(d)
n=6
2
1
0
0
0.05
0.10
0.15
$^{176}Yb/^{176}Hf$
(e)
n=6
3
2
1
0
0.2806
0.2807
0.2808
$^{176}Hf/^{177}Hf_i$
(f)
εHf
10
5
0
-5
-10
-15
DM
CHUR
T(DM)c = 3.63 Ga
Lu/Hf = 0.015
2500
3000
3500
4000
4500
Age (Ma)

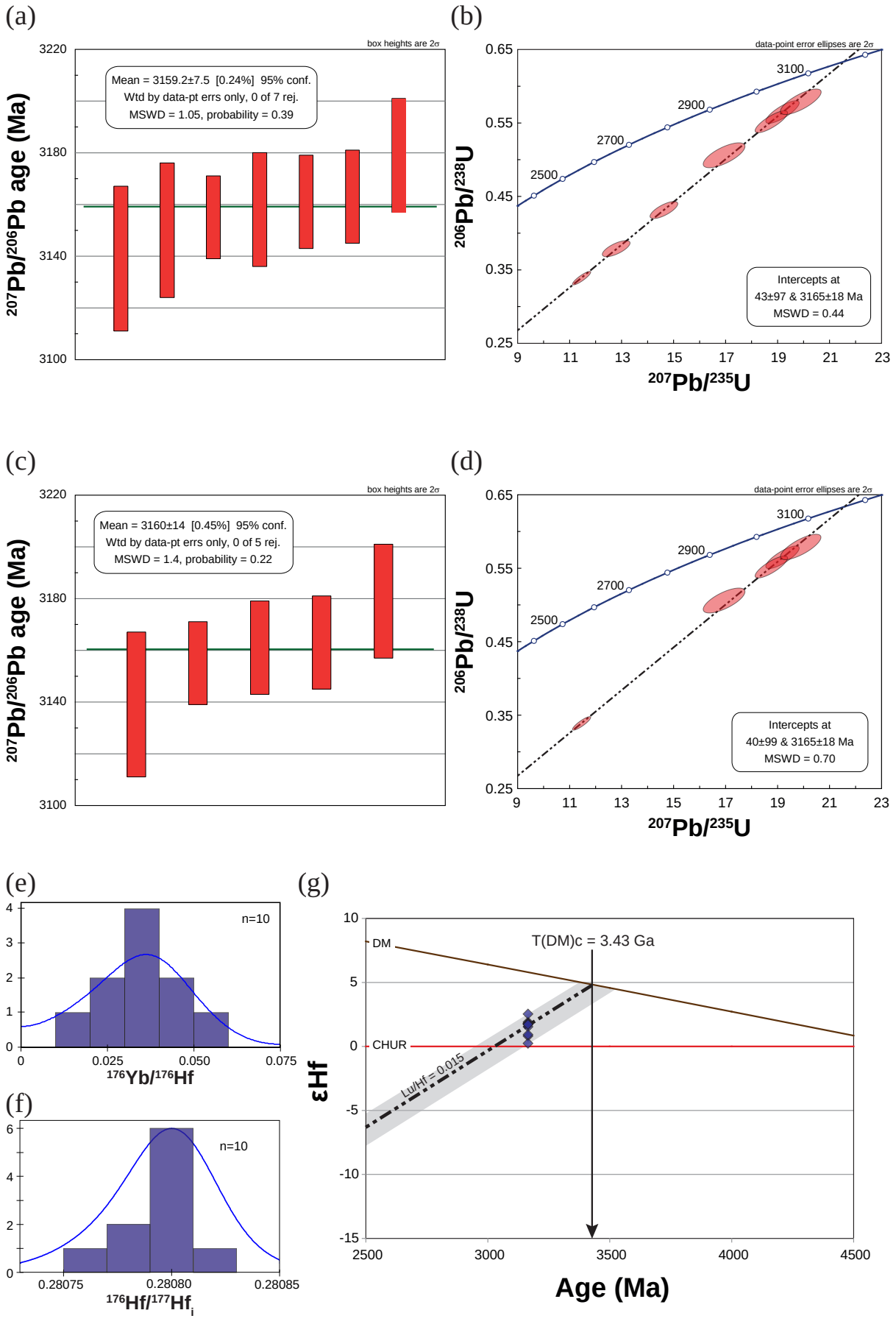
Sample SWA05

U-Pb ages were obtained from 25 spots on 18 grains, 14 of which were excluded in the filtering stage, mainly due to high U contents. Thorium and U contents are variable (Th = 117–853 ppm, average = 310 ± 240 ppm; U = 119–889, average = 460 ± 280 ppm; 11 analyses with U >1000 ppm excluded), Th/U ranges from 0.41 to 1.17 with an average of 0.67 ± 0.27.

Of the 11 analyses remaining after the filtering stage, one has a $^{207}Pb/^{206}Pb$ age of 3425 ± 9 Ma and is interpreted to be inherited. Three further analyses were rejected on a statistical basis in order to get a probability of fit >0.05, the remaining seven analyses give a weighted mean of $^{207}Pb/^{206}Pb$ ages of 3159.2 ± 7.5 Ma and an intercept age on the U-Pb concordia diagram of 3165 ± 18 Ma (Figure 6.30a, b). This sample, with only a minor common Pb component, gives ages calculated from the corrected data that are consistent with the uncorrected data: five analyses give a weighted mean of $^{207}Pb/^{206}Pb$ ages of 3160 ± 14 Ma and an intercept age of 3165 ± 18 Ma (Figure 6.30c, d).

Hf isotopic compositions were obtained from 10 spots on nine grains, including analyses of both the core and rim of the grain with the inherited core; however, both spots gave identical results and have been included in the calculations with the rest of the main population, the old material having apparently all been ablated during U-Pb analysis. REE contents are low (average $^{176}Yb/^{177}Hf = 0.034 \pm 0.012$; Figure 6.30e) and the analyses form a cluster above the CHUR line on the epsilon Hf diagram ($\varepsilon Hf = 0.24–2.53$, average = 1.50 ± 0.66), and give crustal model ages ranging from 3.52 to 3.37 Ga, with a median of 3.43 Ga (Figure 6.30f, g).

Figure 6.30. (facing page) Calculated ages and Hf isotopes from sample SWA05: (a) weighted average of $^{207}Pb/^{206}Pb$ ages and (b) intercept age on the U-Pb concordia diagram (uncorrected data); (c) weighted average of $^{207}Pb/^{206}Pb$ ages and (d) intercept age on the U-Pb concordia diagram (corrected data); histograms of (e) $^{176}Yb/^{177}Hf$ and (f) $^{176}Hf/^{177}Hf_i$, with kernel density estimate as a blue line; (g) εHf plot showing the range in crustal model ages (field) and the median (dashed line).


(a)
box heights are 2σ
Mean = 3159.2±7.5 [0.24%] 95% conf.
Wtd by data-pt errs only, 0 of 7 rej.
MSWD = 1.05, probability = 0.39
207Pb/206Pb age (Ma)
(b)
data-point error ellipses are 2σ
Intercepts at
43±97 & 3165±18 Ma
MSWD = 0.44
206Pb/238U
207Pb/235U
(c)
box heights are 2σ
Mean = 3160±14 [0.45%] 95% conf.
Wtd by data-pt errs only, 0 of 5 rej.
MSWD = 1.4, probability = 0.22
207Pb/206Pb age (Ma)
(d)
data-point error ellipses are 2σ
Intercepts at
40±99 & 3165±18 Ma
MSWD = 0.70
206Pb/238U
207Pb/235U
(e)
n=10
176Yb/176Hf
(f)
n=10
176Hf/177Hfi
(g)
T(DM)c = 3.43 Ga
DM
CHUR
Lu/Hf = 0.015
εHf
Age (Ma)

6.3 Discussion

6.3.1 Metamict zircon

Interpretation of zircon trace-element and isotopic compositions becomes more difficult as the grains age. This difficulty in interpretation is caused by the metamictisation process – the accumulation of damage to the crystal lattice caused by α-decay of U and Th. The disrupted crystal lattice is more susceptible to alteration, including both the introduction of trace elements and the loss of radiogenic Pb. Identification of metamict grains and parts of grains is therefore an important part of the interpretation of trace-element and U-Pb isotopic data, as these compositions may reflect substantial alteration rather than the original composition.

CL images

One of the most characteristic consequences of metamictisation is a strong dampening of the CL response (e.g. Nasdala *et al.*, 2002). CL imaging also shows the presence of inclusions, and these are generally more abundant in metamict grains (or zones within grains) than in the corresponding non-metamict grains (or zones; see Figure 6.3i, j). Another characteristic of metamictisation is a volume increase; this is most obvious when only part of a grain is metamict, as this increase in volume is accommodated by brittle deformation in the surrounding material (Murakami *et al.*, 1991; see Figure 6.3o, p).

Zircon chemistry

The difference in the chemical composition of zircon between metamict and non-metamict grains can be summarised as greater degree of substitution of trace elements (e.g. P, Ca, Ti, Nb, Y, Ta, Th, U, and the REE) for Zr and Si in metamict grains (Nasdala *et al.*, 2009).

The tetravalent cations (Hf, Th, U) substitute directly for Zr^{4+} in zircon, however the trivalent REE are accommodated by a coupled substitution involving a replacement of Si^{4+} by P^{5+}, except in the case of Ce and Eu. The variability in the valence states of these two elements (Ce^{3+} or Ce^{4+}, Eu^{2+} or Eu^{3+}) accounts for the positive Ce anomaly and negative Eu anomaly commonly seen in zircon REE patterns, as Ce^{4+} is more readily accommodated than the trivalent REE, and if Eu is in the divalent state it readily substitutes for Ca^{2+} in plagioclase and thus is relatively less available for incorporation into the zircon lattice.

The higher concentrations of Th and U in metamict grains is at least in part a cause of metamictisation rather than an effect (higher Th and U leads to more radiation damage), but to what extent the higher concentrations of the other trace elements existed before the radiation damage is unclear. Grains with high Th and U crystallising from a late-stage, fractionated melt are also likely to incorporate higher concentrations of other incompatible elements, and the increase in LREE relative to HREE in metamict zircons could be explained by the fact that the

LREE are more incompatible and are thus more strongly enriched in late-stage melts. Another possible explanation for the increased trace-element concentrations seen within particular zones is that these represent 'hydrothermal' zircon, either produced by hydrothermal alteration or precipitated directly from hydrothermal fluids (e.g. Hoskin, 2005). Such zircon has been shown to be enriched in trace elements including Th, U, and the REE, and has been documented to occur as oscillatory variation alternating with normal zircon growth (Hoskin, 2005).

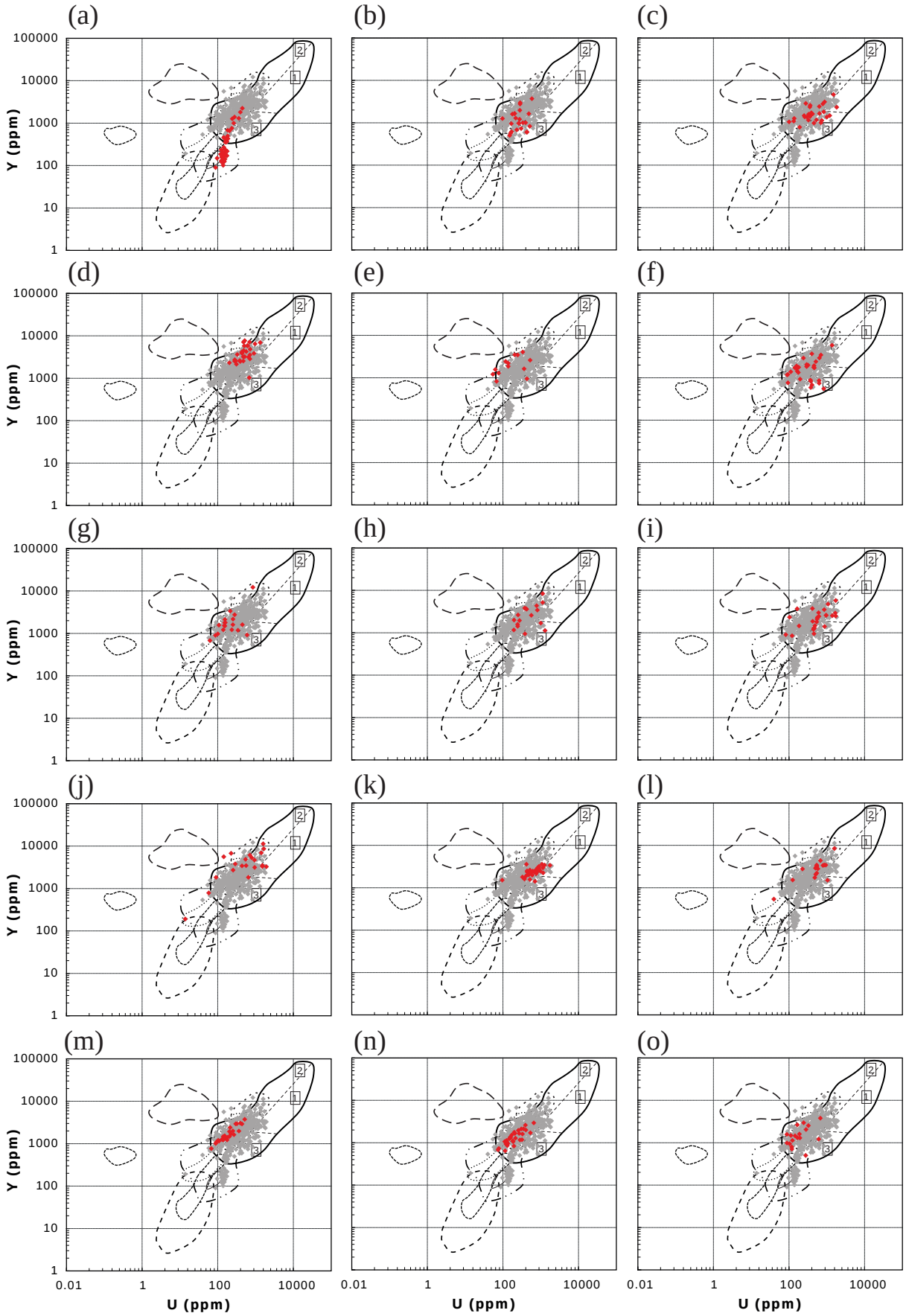
U-Pb ages

The effect of metamictisation on the U-Pb system is to promote the loss of radiogenic Pb and thus to produce artificially young ages. The problem is necessarily more severe in grains with higher concentrations of U and Th, as they have more accumulated radiation damage and are thus more susceptible to mobilisation of Pb. Although the loss of radiogenic Pb prevents the calculation of concordia ages, precise ages can still be obtained by finding the intersection of the Pb-loss chord with the concordia (i.e. the intercept age). This process becomes more difficult where there is a component of ancient Pb loss, as the lower intercept of the Pb-loss chord is the age of Pb loss, and if there are multiple Pb-loss events a single chord through the data will not yield an accurate age. Relative to grains with low Th and U contents, grains with higher concentrations of these elements are more susceptible to Pb loss, as the radiation damage accumulates faster and the loss of radiogenic Pb is promoted earlier in the history of the crystal. They are thus more likely to have experienced ancient Pb loss, and so excluding grains with high Th and U contents (and high accumulated radiation damage) is necessary to remove the effect of ancient Pb loss and obtain accurate intercept ages.

6.3.2 Trace-element compositions

The range of original trace-element (TE) compositions of Mpuluzi zircons is somewhat obscured by the effects of metamictisation. Metamictisation is more pronounced in the more felsic samples, which is to be expected as these are generally more enriched in Th and U, but zircons crystallising from late-stage melts would also be expected to incorporate higher concentrations of other incompatible elements (e.g. REE). Thus, distinguishing between higher TE contents caused by metamictisation-facilitated alteration and higher concentrations as a primary feature of the zircons is problematic.

When compared to the zircon trace-element classification fields of Belousova *et al.* (2002), the 'pristine' group of Mpuluzi zircons plot within or close to the granitoid field (e.g. Y *vs* U, Figure 6.31a-r), while the metamict group overlap the high Y and U end of the pristine analyses and extend outside the field to still higher values (Figure 6.31s). One notable exception to this is the most mafic sample (RSA03), which tends to extend to lower


(a)
(b)
(c)
(d)
(e)
(f)
(g)
(h)
(i)
(j)
(k)
(l)
(m)
(n)
(o)
Y (ppm)
U (ppm)
100000
10000
1000
100
10
1
0.01
1
100
10000
1
2
3

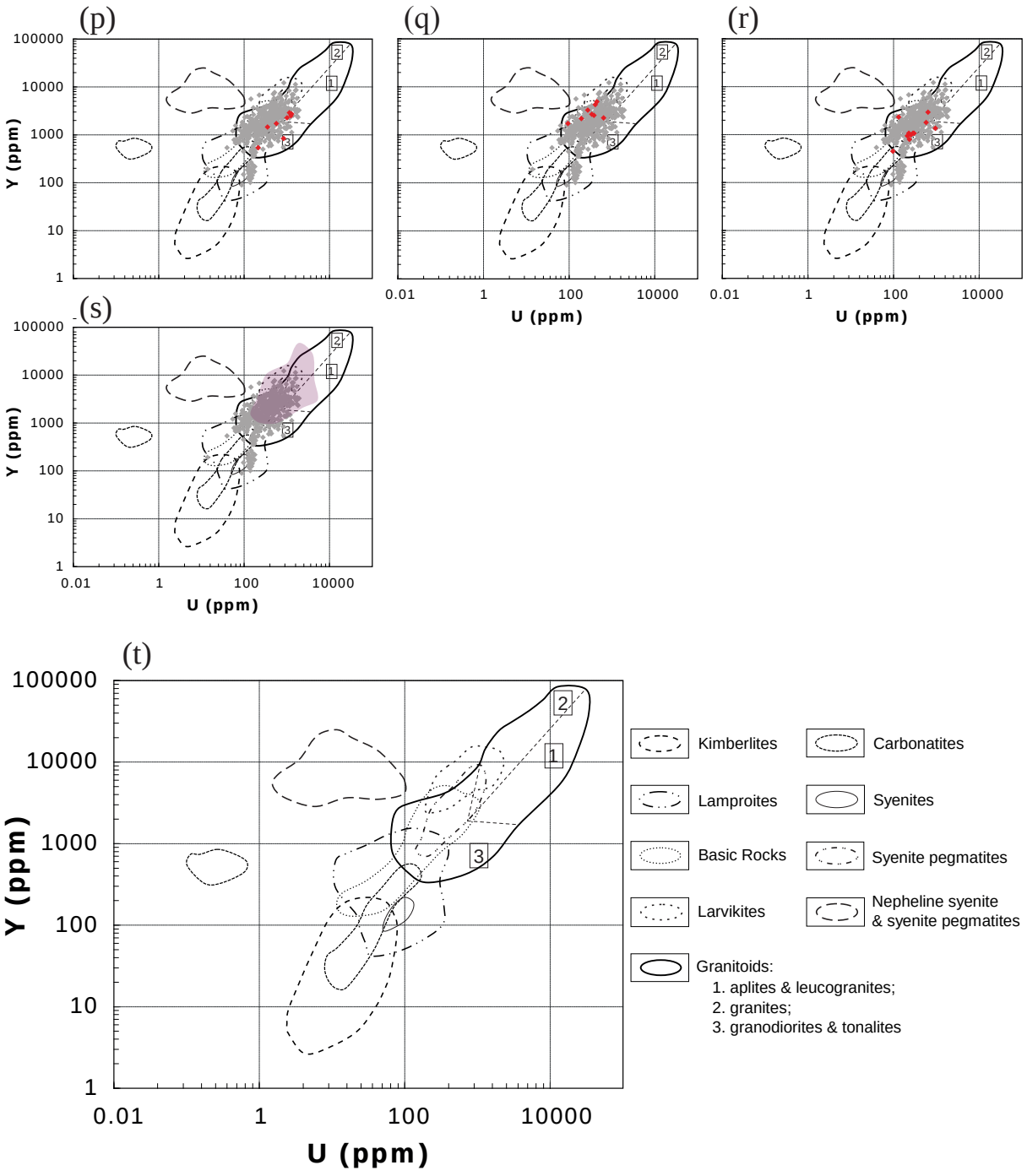
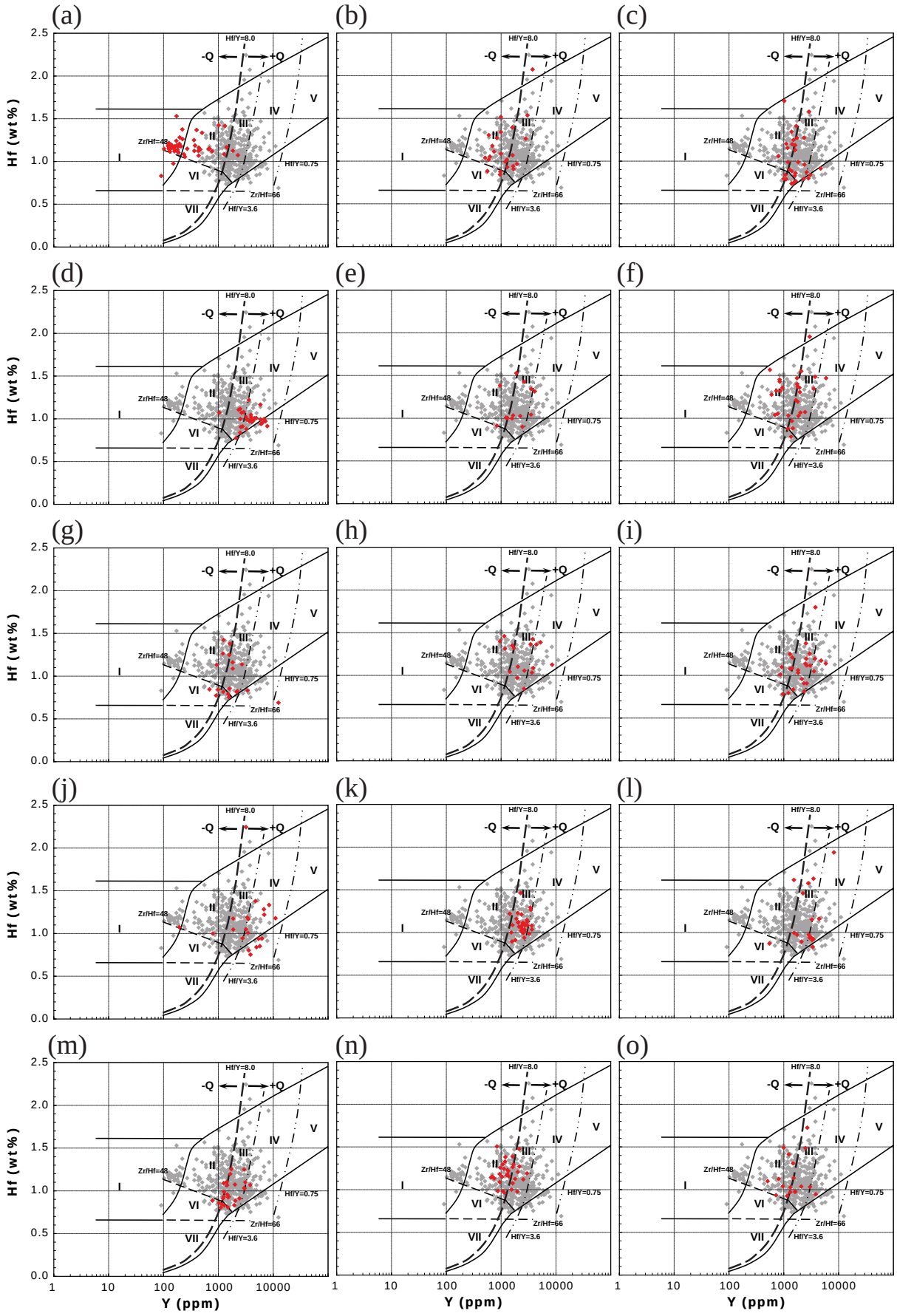


Figure 6.31. Plot of Y *vs* U in zircons from the Mpuluzi batholith (samples ordered from most mafic to most felsic; named sample in red, whole dataset in grey): (a) RSA03; (b) RSA01; (c) SWA18a; (d) RSA05; (e) RSA02; (f) SWA07; (g) RSA04; (h) RSA08; (i) SWA10a; (j) RSA09; (k) SWA03; (l) RSA06; (m) SWA13a; (n) SWA11; (o) SWA09; (p) SWA02a; (q) RSA07; (r) SWA05; (s) metamict grains; (t) fields for different host rock types (from Belousova *et al.*, 2002).


(a)
(b)
(c)
(d)
(e)
(f)
(g)
(h)
(i)
(j)
(k)
(l)
(m)
(n)
(o)
Hf (wt %)
Y (ppm)
Hf/Y=8.0
-Q
+Q
Zr/Hf=48
Hf/Y=0.75
Zr/Hf=66
Hf/Y=3.6
I
II
III
IV
V
VI
VII

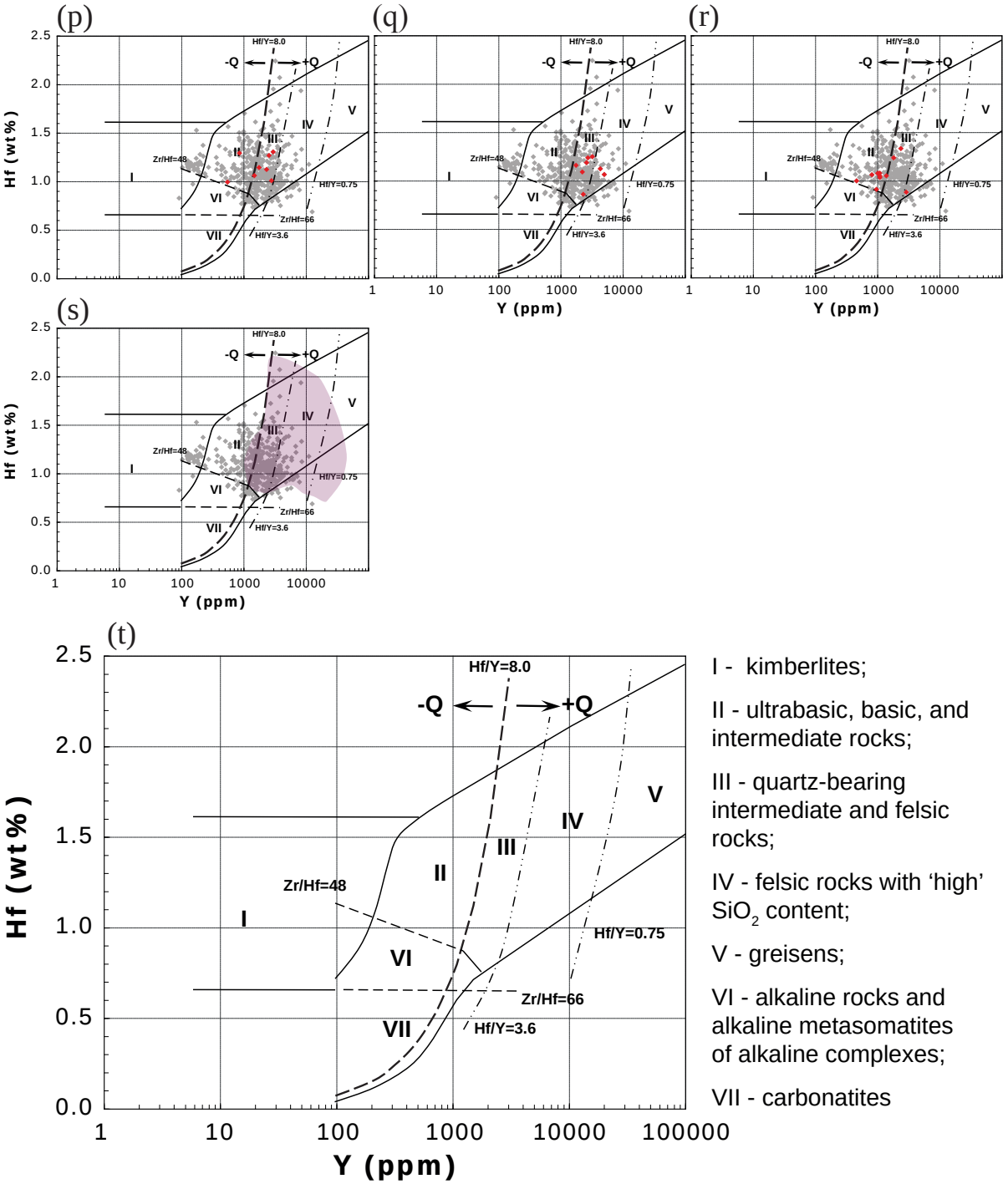


Figure 6.32. Plot of Hf *vs* Y in zircons from the Mpuluzi batholith (samples ordered from most mafic to most felsic; named sample in red, whole dataset in grey): (a) RSA03; (b) RSA01; (c) SWA18a; (d) RSA05; (e) RSA02; (f) SWA07; (g) RSA04; (h) RSA08; (i) SWA10a; (j) RSA09; (k) SWA03; (l) RSA06; (m) SWA13a; (n) SWA11; (o) SWA09; (p) SWA02a; (q) RSA07; (r) SWA05; (s) metamict grains; (t) fields for different host rock compositions (from Belousova *et al.*, 2002). The dashed line with Hf/Y=8.0 separates the fields for quartz-free rocks (-Q) from the fields for quartz-bearing rocks (+Q).

concentrations and outside the granitoid field (Figure 6.31a). When the pristine group of analyses are plotted on the Hf *vs* Y plot (Figure 6.32a-r; Belousova *et al.*, 2002), zircons from the most mafic sample plot almost entirely in the quartz-free region (Figure 6.32a), and most samples spread from the quartz-free region to the quartz-present region, suggesting that zircon started crystallising early in the sequence (i.e. before quartz), and most likely continued throughout the crystallisation history of the samples. The metamict group of analyses plot almost exclusively in the quartz-present region, which is consistent with their crystallisation from late-stage melts (Figure 6.32s).

The suggestion that zircon may have had a long crystallisation history in the Mpuluzi samples also has implications for the resolvability of differences in the U-Pb ages of different samples if the intrusions are closely spaced in time. The crystallisation ages for individual grains within a sample may have a large range, potentially large enough that the late-stage zircons in an earlier intrusion crystallised after the onset of zircon crystallisation in a later intrusion. When the errors on the individual ages are large, as when the grains are old and have a significant degree of accumulated radiation damage, the difference in ages between closely spaced intrusions is likely to be unresolvable with the technique used in this study.

6.3.3 Timing and age constraints

Although the U-Pb dating was somewhat problematic and some samples give anomalous results, the overall picture presented by the age data is consistent with the age of ~3.1 Ga determined for the Mpuluzi and Piggs Peak batholiths in previous studies (Allsopp *et al.*, 1962; Oosthuyzen, 1970; Davies, 1971; Maphalala *et al.*, 1989; Maphalala & Kröner, 1993;

Table 6.4: Previously-determined ages for the Mpuluzi and Piggs Peak batholiths.

Unit sampled	Age (Ma)	Method	Reference
Mpuluzi batholith	3070 ± 60	Whole-rock Rb-Sr	Allsopp *et al.* (1962)
Mpuluzi batholith	3075 ± 100	Whole-rock Rb-Sr	Oosthuyzen (1970)
Piggs Peak batholith	3050 ± 35	Whole-rock Rb-Sr	Davies (1971)
Mpuluzi batholith *(granodiorite)*	2979 ± 33	Whole-rock Rb-Sr	Maphalala *et al.* (1989)
Mpuluzi batholith *(alkali feldspar granite)*	3000 ± 125	Whole-rock Rb-Sr	Maphalala *et al.* (1989)
Mpuluzi batholith	3074 ± 6	Zircon Pb-Pb evaporation	Maphalala and Kroner (1993)
Mpuluzi batholith	3107 +4/-2	Zircon ID-TIMS	Kamo and Davis (1994)
Mpuluzi batholith	3113.2 ± 2.4	Zircon ID-TIMS	Westraat *et al.* (2005)
Piggs Peak batholith	3140.3 ± 0.3	Zircon ID-TIMS, chemically abraded	Schoene and Bowring (2007)
Mpuluzi batholith	3082 ± 6	Zircon LA-SF-ICP-MS	Zeh *et al.* (2009)
Piggs Peak batholith	3099 ± 8	Zircon LA-SF-ICP-MS	Zeh *et al.* (2009)

Kamo & Davis, 1994; Westraat *et al.*, 2005; Schoene & Bowring, 2007; Zeh *et al.*, 2009; see Table 6.4).

Anomalous ages

Sample RSA06 gives an anomalously young weighted average of $^{207}Pb/^{206}Pb$ ages for both corrected and uncorrected data (3028 ± 15 and 2953 ± 38 Ma respectively; see Figure 6.24a, c). This sample had 27 analyses removed at the filtering stage due to U contents >1000 ppm, but the remaining analyses still show considerable evidence of loss of radiogenic lead. This is most likely due to the very high Th contents in this sample (average = 900 ± 1400 ppm). Although most samples have Th/U between 0.5 and 0.8, the analyses from this sample have an average Th/U of 1.6 ± 2.3, and this likely accounts for the extreme Pb loss, as analyses with U below the 1000 ppm cut-off still have very high levels of accumulated radiation damage due to the larger influence of Th decay. The intercept age calculated from the uncorrected data is also anomalously young (3003 ± 54 Ma; see Figure 6.24b), but this is expected as the culling criteria for the uncorrected data focused on the $^{207}Pb/^{206}Pb$ ages. The intercept age calculated from the corrected data is consistent with the majority of the ages obtained from the Mpuluzi samples, and suggests that the other ages obtained from this sample are anomalously young, rather than that there is a real difference in age.

Anomalously young ages were also obtained from the uncorrected data for sample RSA09 (weighted average of $^{207}Pb/^{206}Pb$ ages = 3018 ± 16 Ma, intercept age = 2996 ± 57 Ma; see Figure 6.22a, b), and no statistically significant weighted average was obtained for the corrected $^{207}Pb/^{206}Pb$ ages. As with sample RSA06, the intercept age obtained from the corrected ages is consistent with the other Mpuluzi samples (3109 ± 46 Ma; see Figure 6.22c), suggesting that this sample also does not represent a real difference in age, but that the effect of Pb loss has not been sufficiently removed by filtering for U content.

Samples RSA01 and RSA02 also produced anomalously young ages, but in these samples it is the corrected ages which are young (weighted averages of $^{207}Pb/^{206}Pb$ ages = 2971 ± 17 and 2995 ± 60 Ma respectively; intercept ages = 3078 ± 22 and 3063 ± 49 Ma respectively; see Figures 6.14c, d and 6.17c, d), while the uncorrected ages are consistent with the majority of the samples. This suggests that the issue in these samples is the amount of common Pb in the grains. Sample RSA01 had 12 analyses rejected with calculated common Pb >10%, and nine of the remaining 37 analyses have >5% calculated common Pb; sample RSA02 had only two analyses rejected due to common Pb >10%, but six of the remaining 18 analyses have common Pb >5%. This large amount of common Pb necessitates a large correction, with a large associated uncertainty, and also amplifies the problem of overcorrection of the $^{207}Pb/^{206}Pb$ ages by the common-Pb correction routine. Although the $^{207}Pb/^{235}U$ and $^{206}Pb/^{238}U$ ages do not appear to be overcorrected, the large proportion of calculated common Pb

increases the error on the corrected age, and the intercept ages calculated from the corrected data, though low, are within error of the majority of the rest of the samples (see Figures 6.14d and 6.17d).

The weighted averages of $^{207}Pb/^{206}Pb$ ages obtained from the corrected dataset are substantially lower than the corresponding intercept ages in most samples; this is most likely due to the overcorrection of the $^{207}Pb/^{206}Pb$ ages by the common Pb correction routine. These ages are therefore considered to be unreliable and not discussed further below.

Degree of radiation damage

Filtering based on the degree of radiation damage (the radiation dose in displacements per atom (D_{dpa}), calculated using the Th and U contents and the age of the zircon; see Palenik *et al.*, 2003; Gao *et al.*, 2014) rather than the U content may slightly improve the ages obtained for the samples with high Th contents (RSA06 and RSA09; see discussion above). Any improvement is likely to be minor as the D_{dpa} strongly parallels the U concentration (Figure 6.33), and the calculated D_{dpa} is also affected by errors in the ages used in the calculation. This is likely to reduce the efficacy of filtering based on D_{dpa}, as loss of radiogenic Pb, producing artificially low ages, reduces the calculated D_{dpa} (Figure 6.34); this may result in grains with high U and Th (and therefore highly damaged) not being filtered out as they have artificially low D_{dpa}. Addition of common Pb, with the opposite effect on the age, increases the calculated D_{dpa}, which may result in the removal of grains which have not experienced substantial Pb loss (Figure 6.34).

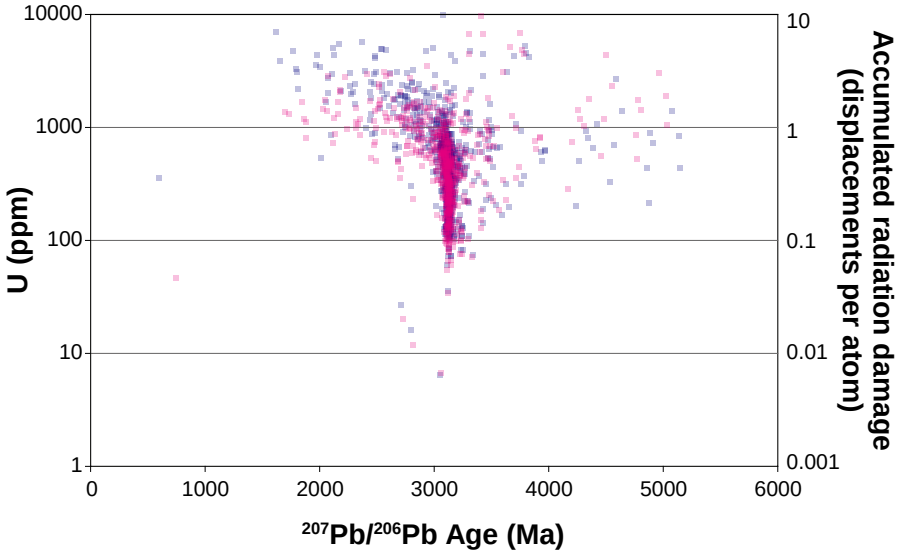


Figure 6.33. Plot of U concentration (blue) and accumulated radiation damage (pink) *vs* uncorrected $^{207}Pb/^{206}Pb$ ages.

Differences in the degree of radiation damage between the calibration standard and the sample have been shown to cause systematic errors in U-Pb ages, as the radiation damage causes subtle changes in the ablation behaviour of the zircon (Allen & Campbell, 2012). Marillo-Sialer *et al.* (2014) showed that this matrix effect is due to an increase in drill rate with increasing radiation dose, which changes the degree of U-Pb downhole fractionation. The calculated U-Pb ages vary systematically, with older ages obtained for samples with a higher D_{dpa} than the calibration standard, and younger ages where the calibration standard has accumulated more radiation damage than the sample (Allen & Campbell, 2012; Marillo-Sialer *et al.*, 2014). Thermally annealing the grains prior to analysis reduces the offset in age (Allen & Campbell, 2012), but does not eliminate it entirely (Marillo-Sialer *et al.*, 2014). Allen and Campbell (2012) measured an offset in $^{206}Pb/^{238}U$ age of +1.17% in one Archaean zircon (OG1, TIMS age = 3465.4 Ma); the Mpuluzi zircons have substantially higher D_{dpa} than OG1 (average D_{dpa} for Mpuluzi zircons = 0.67, OG1 = 0.15) and thus the effect may be expected to be larger in these grains. Any correlation between calculated D_{dpa} and $^{206}Pb/^{238}U$ age is obscured by the strong Pb-loss trend, as the more severely damaged grains are also subject to a larger degree of Pb loss (Figure 6.35).

Emplacement timing

Once the anomalous data discussed above are discarded, the ages obtained for both the uncorrected and corrected datasets are indistinguishable. The uncorrected weighted averages

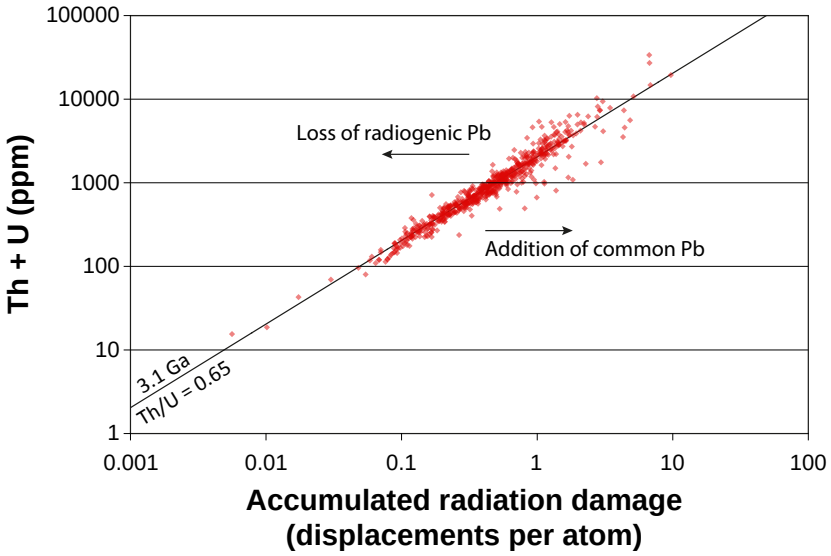


Figure 6.34. Plot of total Th and U concentration *vs* accumulated radiation damage (in displacements per atom), showing the effect of errors in age caused by loss of radiogenic Pb and addition of common Pb on the calculated radiation dose. The black line is the calculated radiation dose for grains with an age of 3.1 Ga and a Th/U ratio of 0.65 (average for Mpuluzi zircons).

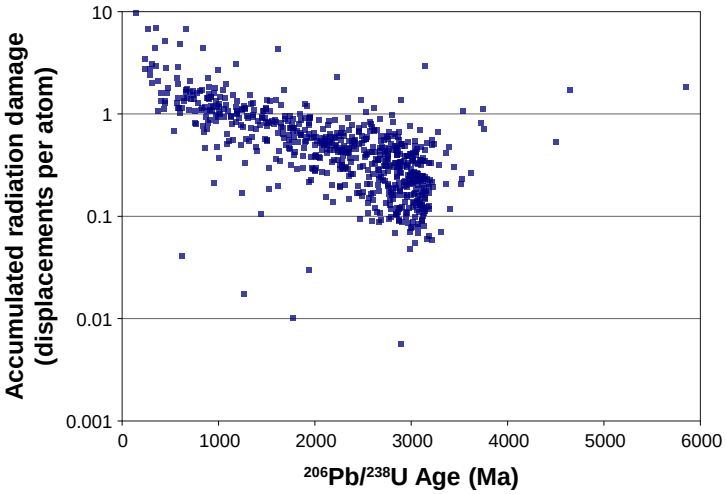


Figure 6.35. Plot of accumulated radiation damage (in displacements per atom) *vs* uncorrected $^{206}Pb/^{238}U$ ages.

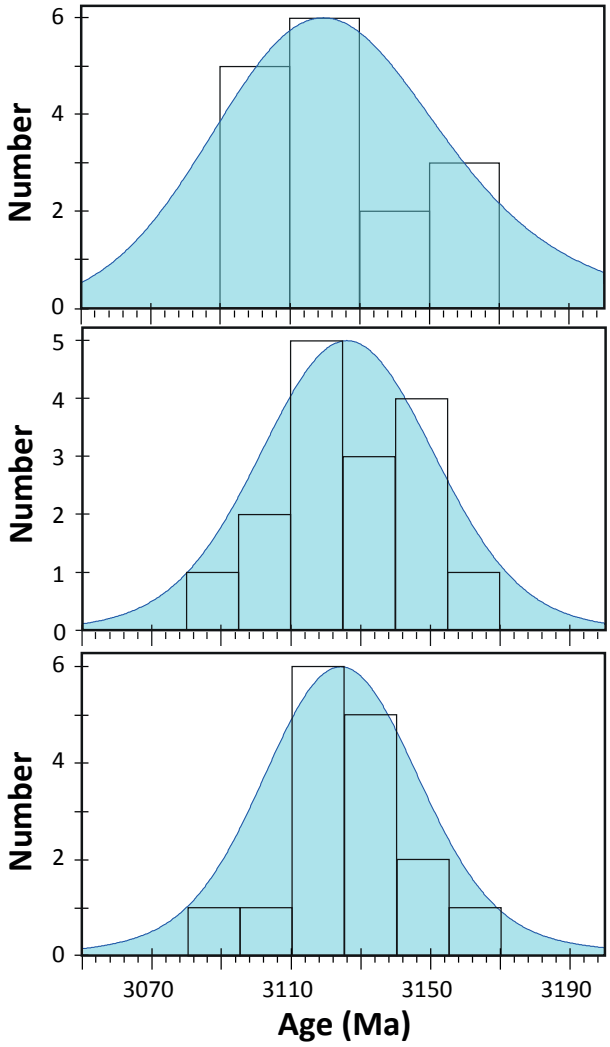


Figure 6.36. Histogram of calculated ages with kernel density estimate prepared using DensityPlotter (Vermeesch, 2012): (a) corrected intercept ages; (b) uncorrected intercept ages; (c) uncorrected weighted mean of $^{207}Pb/^{206}Pb$ ages.

of $^{207}Pb/^{206}Pb$ ages range from 3165 ± 18 to 3087.4 ± 6.5 Ma, with a total spread of 77 Ma, and the intercept ages range from 3159.2 ± 7.5 to 3093 ± 12 Ma (spread of 66 Ma); the corrected data yield intercept ages ranging from 3167 ± 34 to 3100 ± 17 Ma (spread of 67 Ma). All three sets of ages show a single peak centred at ~3.12 Ga (Figure 6.36).

Fifty analyses of reference zircon OG1 (ID-TIMS $^{207}Pb/^{206}Pb$ age = 3465.4 ± 0.6 Ma; Stern *et al.*, 2009) were obtained during this study (Appendix A1); excluding one discordant analysis yields a weighted mean of $^{207}Pb/^{206}Pb$ ages of 3461.7 ± 5.5 Ma. This is comparable to the errors obtained for individual Mpuluzi samples (see Table 6.2), however the overall range in ages far exceeds this and cannot be attributed to analytical uncertainty. There are two possible explanations for the large spread in ages between the Mpuluzi samples: (1) the large range is an artefact, most likely due to the high degree of radiation damage in the zircons (e.g. old ages produced by matrix effects during ablation and/or young ages resulting from ancient Pb loss or overcorrection of common Pb); (2) the range in ages is real, and reflects a long-lived magmatic system.

The fact that both the spread in ages and the absolute maximum and minimum ages are identical within error in all three datasets (corrected and uncorrected intercept ages, uncorrected $^{207}Pb/^{206}Pb$ ages) suggests that the large spread is unlikely to be an artefact caused by matrix effects or the common-Pb correction, as these factors do not affect the U-Pb and Pb-Pb ages in the same way. The matrix effects produce artificially old U-Pb ages but do not affect the $^{207}Pb/^{206}Pb$ ratios, while the common-Pb correction routine only shows a systematic overcorrection in the $^{207}Pb/^{206}Pb$ ratios, producing young ages. Failure to remove the effect of ancient Pb loss would artificially lower both the intercept ages and the weighted means

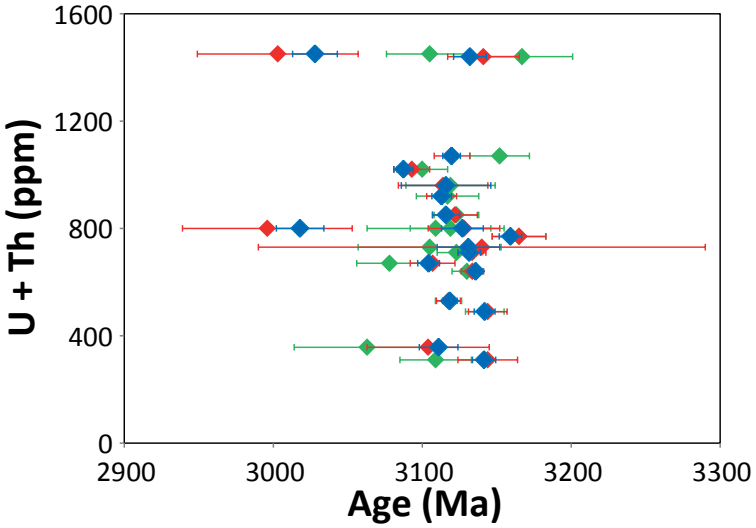


Figure 6.37. Plot of total Th + U content *vs* corrected (green) and uncorrected (red) intercept ages and uncorrected weighted averages of $^{207}Pb/^{206}Pb$ ages (blue) for the Mpuluzi samples.

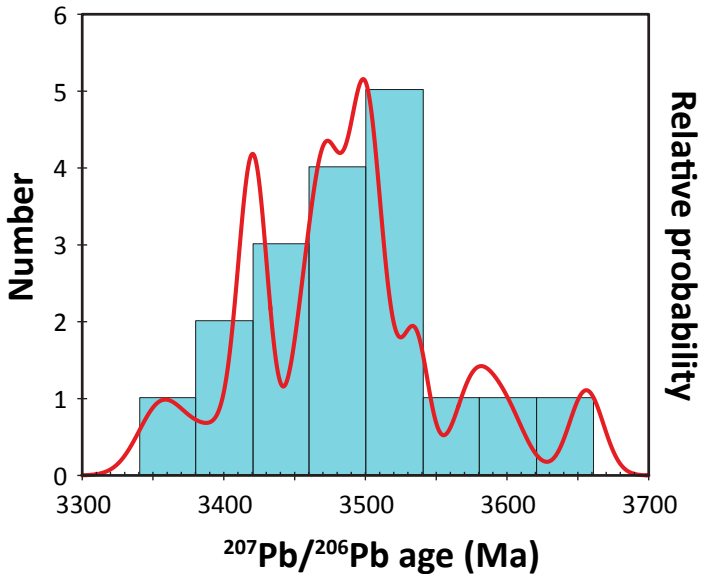


Figure 6.38. Histogram of all inherited ages obtained from Mpuluzi samples (n=18).

calculated from the $^{207}Pb/^{206}Pb$ ages, however there is no correlation between contents of U and Th and the calculated ages (Figure 6.37). This suggests that the range in ages is not an artefact but rather indicates that the Mpuluzi batholith was emplaced over a timespan of ~70 million years; this will be discussed further in Chapter Seven, in the context of the whole rock compositions.

Source characteristics

The U-Pb ages identified as inherited (18 analyses from 7 samples) do not form a single population, but range from 3656 ± 12 Ma to 3355 ± 16 Ma. The small number of inherited ages obtained, and the large spread in their ages, makes it difficult to pinpoint the age of the source, but the population centres around ~3.5 Ga (Figure 6.38), suggesting that the source region is at least this old, and may include even older material.

The Hf isotopic data are consistent with the limited number of analyses available in the literature (average $^{176}Hf/^{177}Hf_i$ of 0.28078 ± 4 and 0.28075 ± 5 for the Mpuluzi and Piggs Peak batholiths respectively; Zeh *et al.*, 2009). These data confirm that there is an older component involved in the magma generation, as suggested by the presence of inherited cores in some grains. The large spread in εHf seen in these data is generally considered to reflect incomplete mixing between an evolved crustal component and juvenile material; however it is also possible to create such variation by low degree partial melting in the presence of zircon (e.g. Zeh *et al.*, 2009; 2011; Tang *et al.*, 2014). Sample SWA10a, with 7 inherited grains, provides the best evidence for mixing as the explanation for the Hf variability, as the grains with older ages lie along an evolution line which intersects the main population at the more evolved

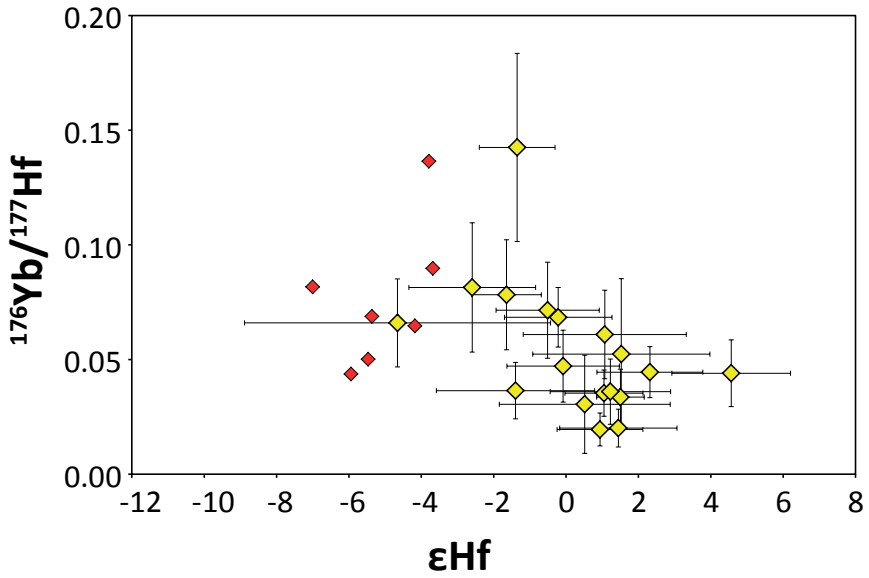


Figure 6.39. Plot of $^{176}Yb/^{177}Hf$ *vs* εHf for the Mpuluzi samples. Red diamonds indicate inherited grains from sample SWA10a.

end of the spread (see Figure 6.21e). This sample therefore provides the best estimate for the age of extraction of the inherited component, with a crustal model age of 4.13 Ga for the inherited grains, and provides further evidence that the Mpuluzi batholith was generated from melting of previously existing crust, with additional input from a more juvenile source. Of the six other samples with inherited grains, four had enough material available to ablate for Hf isotopic compositions, and the crustal model ages for these grains range from 3.79 to 3.59 Ga, again suggesting that the evolved component was extracted from the mantle at least 500 million years before the emplacement of the Mpuluzi batholith.

The uppermost εHf values provide an estimate of the age of the juvenile component. Crustal model ages calculated from the analyses with the highest εHf values in each sample range from 3.58 to 3.09 Ga, suggesting that the juvenile component may have been extracted from the mantle very close to the time of emplacement of the batholith, and that there was a variable amount of mixing between the juvenile material and the crustal component.

The Mpuluzi samples show a range in average $^{176}Yb/^{177}Hf$ from 0.02 to 0.14; a plot of average $^{176}Yb/^{177}Hf$ for each sample *vs* εHf shows a broad negative correlation (Figure 6.39). The inherited grains from sample SWA10a have also been plotted on Figure 6.39, as they lie on an evolution line (see Figure 6.21g) and can therefore be confidently assumed to represent inherited material (as opposed to the inherited grains in SWA07 which exhibit clear signs of mixing between inherited material and the 3.1 Ga population; see Figure 6.18g). They have scattered compositions but generally fall at the low εHf, high $^{176}Yb/^{177}Hf$ end of the spread, which suggests that the Hf in the evolved component was most likely controlled by zircon, while the juvenile component probably contained little zircon.

Table 6.5: Average crystallisation temperature estimates for the 'pristine', 'variable', and 'metamict' groups, calculated using the Ti-in-zircon thermometer (note that the anomalously low temperature estimate for sample RSA03 represents a single data point). All values in °C. Full dataset in Appendix F.

	Pristine		Variable		Metamict	
	Average	1σ	Average	1σ	Average	1σ
RSA03	546		670	140		
RSA01	741	2	816	63	945	47
SWA18a	711	34	790	100	960	130
RSA05	803	84	650	100	1280	180
RSA02	820	260	900	320		
SWA07	736	41	767	54	837	52
RSA04	769	41			1120	190
RSA08	734	46	860	120	1290	560
SWA10a	750	82	780	130	1090	140
RSA09	736	75	826	82	1000	100
SWA03	778	70	820	190	950	130
RSA06	724	29	802	67	1070	180
SWA13a	748	54	798	72	948	91
SWA11	667	46	720	43	764	44
SWA09	742	51	823	78	1020	210
SWA02a	730	42	751	64	890	110
RSA07	748	35	870	140	1260	150
SWA05	769	56	737	43	940	190

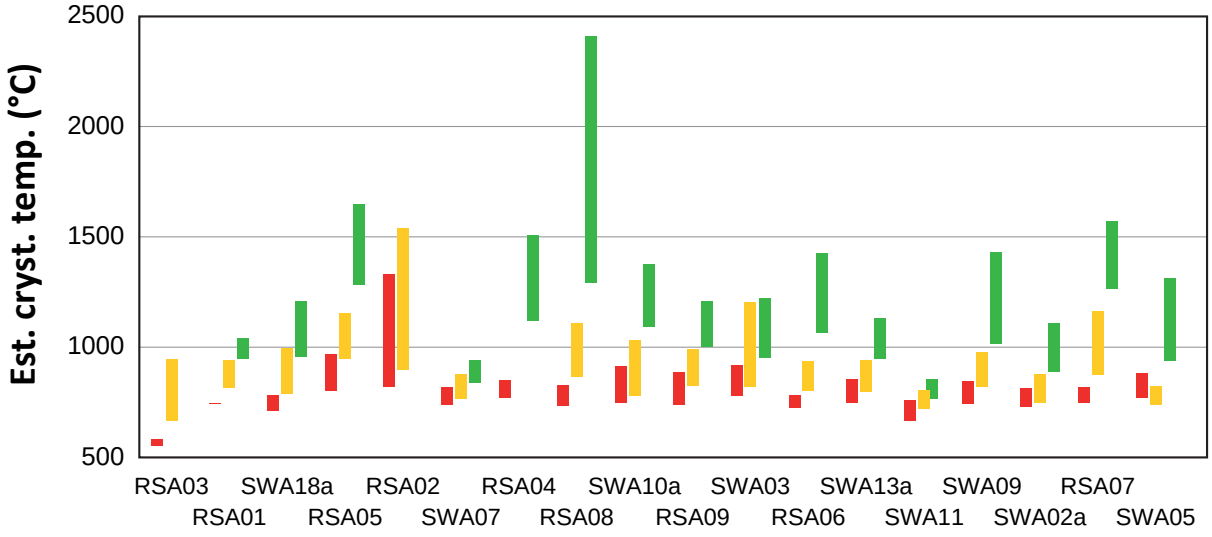


Figure 6.40. Ti-in-zircon crystallisation temperature estimates calculated from pristine analyses (red), variable analyses (orange), and metamict analyses (green).

6.3.4 Ti-in-zircon thermometry

Estimates of zircon crystallisation temperature have been calculated using the Ti-in-zircon thermometer (Watson & Harrison, 2005; Watson *et al.*, 2006). Titanium generally exists as a tetravalent cation and thus in zircon substitutes directly for Si^{4+}, and the presence of Ti phases (generally titanite and/or ilmenite in igneous rocks) and Ti-bearing silicates constrains the activity of Ti close to 1, two facts which make it ideal for use as a thermometer. Even when there is no Ti phase present in the rock, the activity of Ti is generally ≥0.5, and a discrepancy of this magnitude will only result in an underestimate of the crystallisation temperature by ~50–60 °C (Watson & Harrison, 2005).

The crystallisation temperature estimates calculated from the Ti contents of zircons from the Mpuluzi batholith range from 386 to 1935 °C, with an average of 840 ± 180 °C (summary in Table 6.5; for the full dataset see Appendix F). However, the calculated temperatures are strongly influenced by the increased Ti contents of metamict zircons (see Figure 6.5c). Taking only the pristine group of analyses yields a much more reasonable estimate of crystallisation temperatures, with average temperatures for the 18 samples ranging from 667 to 820 °C with a median temperature estimate of 742 °C (excluding one anomalous analysis from sample RSA03 which gives T = 546 °C), which is consistent with fluid-present, minimum-melting conditions. The variable group of analyses yields higher average temperature estimates (650–900 °C, median = 798 °C), and the metamict group yields estimates ranging from 764 to 1290 °C, with a median of 980 °C. This is clearly an unreasonable crystallisation temperature for granitic rocks, and demonstrates that failing to identify metamict zircon may result in significant overestimates of crystallisation temperatures when calculated using the Ti-in-zircon thermometer (Figure 6.40).

6.4 Conclusions

Although the absolute U-Pb ages are difficult to constrain precisely due to the high degree of accumulated radiation damage in most grains, the aggregate of the U-Pb and Hf datasets provide some robust constraints on the timing and duration of the melting and emplacement events. The emplacement itself appears to have occurred in a single episode, spanning a range of up to 70 million years, centred at approximately 3.12 Ga.

The presence of inherited cores in some grains suggests the involvement of an older crustal component (~3.5 Ga) in the magma generation, and this is confirmed by the Hf isotopic data, which show clear indications of mixing between an older crustal component and juvenile material. The Hf isotopic data also provide a good estimate of the age of extraction of the inherited component, with one sample showing a well-defined evolution trend back to ~4.1 Ga. The Hf data also suggest that the juvenile material may have been extracted from

the mantle very close to the time of emplacement of the batholith, with the mixing trend intersecting the depleted mantle line in some samples. This suggests that magma generation, transport and emplacement happened over a period of ~100 million years.

Chapter Seven – Whole-Rock Chemistry and Isotopic Composition

7.1 Introduction

Nineteen samples from the Mpuluzi batholith were analysed for their major- and trace-element concentrations, as well as their Sr and Nd isotopic compositions. This chapter includes a presentation of these results, and classifies the Mpuluzi samples according to the schemes described in Chapter Three. The Mpuluzi samples analysed in this study are discussed in the context of published compositions of the Mpuluzi batholith and the other 3.1 Ga batholiths in the region. Constraints on the composition of the source region are also discussed, along with how the geochemical data can be used to unravel the processes involved in magma generation.

7.2 Results

7.2.1 Major-element compositions

Whole-rock major-element compositions of samples from the Mpuluzi batholith are presented in Table 7.1, along with calculated CIPW normative mineral abundances. Samples show a range in SiO_2 content from 63.3 to 74.6 wt% and alkali contents (Na_2O+K_2O) vary from 7.33 to 9.26 wt%, and plot in the granite and quartz monzonite fields on the TAS (total alkali silica; Le Bas *et al.*, 1986) diagram (Figure 7.1). The samples cluster at the high-silica end of the compositional range, with a gap of >5 wt% SiO_2 between the two most mafic samples (63.3 and 68.6 wt% SiO_2 in samples RSA03 and RSA01 respectively). The aluminium saturation index (ASI = $Al_2O_3/(CaO+Na_2O+K_2O)$) ranges from 0.89 to 1.08, and the Mpuluzi samples are accordingly classified as metaluminous to weakly peraluminous (Figure 7.2).

K_2O concentrations range from 2.32 to 5.48 wt%, and there is a positive correlation of K_2O with SiO_2; the samples plot in the high-K calc-alkaline field of Le Maitre *et al.* (1989; Figure 7.3a). Harker variation diagrams show strong negative correlations of MgO (0.11–1.76 wt%), $Fe_2O_3^T$ (0.91–5.49 wt%), TiO_2 (0.07–1.20 wt%), P_2O_5 (0.01–0.67 wt%), and CaO (0.52–3.66 wt%) with SiO_2 (r^2 >0.8; Figure 7.3b-f); MnO (0.07–0.74 wt%) and Al_2O_3 (13.59–15.29 wt%) show more scattered negative correlations with SiO_2 (r^2 = 0.69 and 0.61 respectively; Figure 7.3g, h). Na_2O contents vary from 3.48 to 5.24 wt%, and Na_2O is weakly negatively correlated with SiO_2 (r^2 = 0.24; Figure 7.3i). Magnesium number (Mg#; wt% $Mg/(Mg+Fe^T)$) ranges from 0.21 to 0.47, and is moderately negatively correlated with SiO_2 (r^2 = 0.51; Figure 7.3j).

Table 7.1: Major-element compositions for samples from the Mpuluzi batholith. All values in wt%. Al sat = Classification based on the aluminium saturation index; Metal. = metaluminous; Peral. = peraluminous; A/CNK = $Al_2O_3/(CaO+Na_2O+K_2O)$; A/NK = $Al_2O_3/(Na_2O+K_2O)$; TAS = Classification based on the total alkali silica diagram; Q Monz = quartz monzonite.

	RSA03 n=2	RSA01 n=2	SWA18a	RSA05 n=2	RSA02 n=2	SWA07	RSA04 n=2	RSA08 n=2	SWA10a	RSA09 n=2	SWA20	SWA03	RSA06 n=2	SWA13a	SWA11	SWA09	SWA02a	RSA07 n=2	SWA05
SiO_2	63.29	68.60	68.86	69.90	70.34	70.53	71.19	71.48	72.18	72.35	72.78	72.78	72.87	73.01	73.70	73.76	74.09	74.25	74.58
TiO_2	1.20	0.67	0.34	0.44	0.32	0.45	0.26	0.35	0.20	0.20	0.20	0.26	0.23	0.23	0.15	0.18	0.11	0.15	0.07
Al_2O_3	15.07	14.48	14.85	14.57	15.29	14.36	14.84	14.16	14.36	14.26	13.81	14.14	13.59	14.02	13.75	13.98	13.69	13.59	13.85
$Fe_2O_3^T$	5.49	3.00	2.55	2.79	1.92	2.92	1.96	2.35	1.55	1.93	1.63	1.60	1.53	1.60	1.20	1.43	1.00	1.27	0.91
MnO	0.07	0.04	0.06	0.06	0.03	0.06	0.05	0.05	0.03	0.04	0.02	0.04	0.03	0.03	0.03	0.04	0.03	0.02	0.02
MgO	1.76	0.98	0.72	0.57	0.76	0.65	0.36	0.42	0.27	0.33	0.39	0.40	0.29	0.32	0.19	0.24	0.20	0.17	0.11
CaO	3.66	2.19	1.70	1.40	2.29	1.50	0.92	1.04	0.93	0.99	1.11	1.31	0.89	0.91	0.62	0.77	0.71	0.52	0.85
Na_2O	4.25	4.28	4.94	4.20	5.24	4.41	4.64	4.15	4.08	4.07	3.48	4.15	3.66	3.91	3.89	4.04	3.97	3.49	4.05
K_2O	3.09	3.80	3.43	4.58	2.32	3.87	4.62	4.53	4.96	4.70	5.48	4.00	5.33	4.69	5.02	4.84	5.05	5.45	4.77
P_2O_5	0.67	0.25	0.19	0.14	0.11	0.16	0.07	0.11	0.05	0.04	0.07	0.05	0.05	0.05	0.03	0.05	0.03	0.03	0.01
LOI	1.22	1.70	1.65	1.50	1.18	0.92	1.19	1.13	0.98	1.11	1.13	1.03	1.29	1.01	0.76	0.88	0.86	1.64	0.73
Total	99.77	99.97	99.29	100.15	99.80	99.83	100.09	99.75	99.59	100.02	100.09	99.76	99.77	99.78	99.34	100.21	99.73	100.58	99.95
Mg#	0.42	0.42	0.39	0.31	0.47	0.33	0.29	0.29	0.28	0.28	0.35	0.35	0.30	0.31	0.26	0.27	0.30	0.22	0.21
Al sat	Metal.	Metal.	Metal.	Peral.	Metal.	Peral.	Peral.	Peral.	Peral.	Peral.	Peral.	Peral.	Peral.	Peral.	Peral.	Peral.	Peral.	Peral.	Peral.
ASI	0.89	0.96	1.00	1.01	1.00	1.01	1.04	1.04	1.04	1.05	1.01	1.04	1.01	1.07	1.06	1.05	1.03	1.08	1.04
A/NK	1.46	1.30	1.25	1.23	1.37	1.26	1.17	1.21	1.19	1.21	1.18	1.27	1.15	1.22	1.16	1.18	1.14	1.17	1.17
TAS	Q Monz	Q Monz	Q Monz	Granite	Granite	Granite	Granite	Granite	Granite	Granite	Granite	Granite	Granite	Granite	Granite	Granite	Granite	Granite	Granite
CIPW normative mineralogy (%)																			
Quartz	15.88	22.62	21.87	23.16	24.44	25.05	23.05	26.55	26.71	27.36	28.14	29.52	28.5	29.42	30.04	29.22	29.71	31.4	30.46
Plagioclase	49.84	46.2	50.49	42.6	56.17	44.4	44.64	40.29	39.5	39.71	35.06	42.06	35.88	38.01	36.49	38.1	37.41	32.39	38.86
Orthoclase	18.62	22.93	20.8	27.48	13.95	23.17	27.66	27.18	29.78	28.13	32.74	23.99	32.03	28.13	30.14	28.84	30.2	32.62	28.43
Corundum			0.31	0.38	0.15	0.55	0.45	0.77	0.67	0.73	0.25	0.66	0.21	0.92	0.82	0.77	0.46	1.04	0.48
Diopside	1.16	0.4																	
Hypersthene	9.86	5.56	5.05	4.81	4.16	5.13	3.38	3.93	2.58	3.3	3.03	2.93	2.59	2.75	1.98	2.41	1.8	2.02	1.5
Ilmenite	2.34	1.29	0.66	0.85	0.63	0.87	0.49	0.66	0.4	0.38	0.38	0.49	0.46	0.44	0.3	0.34	0.21	0.28	0.13
Magnetite	0.81	0.45	0.38	0.41	0.29	0.43	0.29	0.35	0.23	0.29	0.23	0.23	0.23	0.23	0.17	0.2	0.14	0.19	0.13
Apatite	1.58	0.58	0.44	0.32	0.25	0.39	0.16	0.25	0.12	0.09	0.16	0.12	0.12	0.12	0.07	0.12	0.07	0.07	0.02
Zircon	0.04	0.06	0.04	0.09	0.04	0.06	0.06	0.06	0.04	0.04	0.04	0.04	0.04	0.04	0.03	0.04	0.03	0.03	0.01

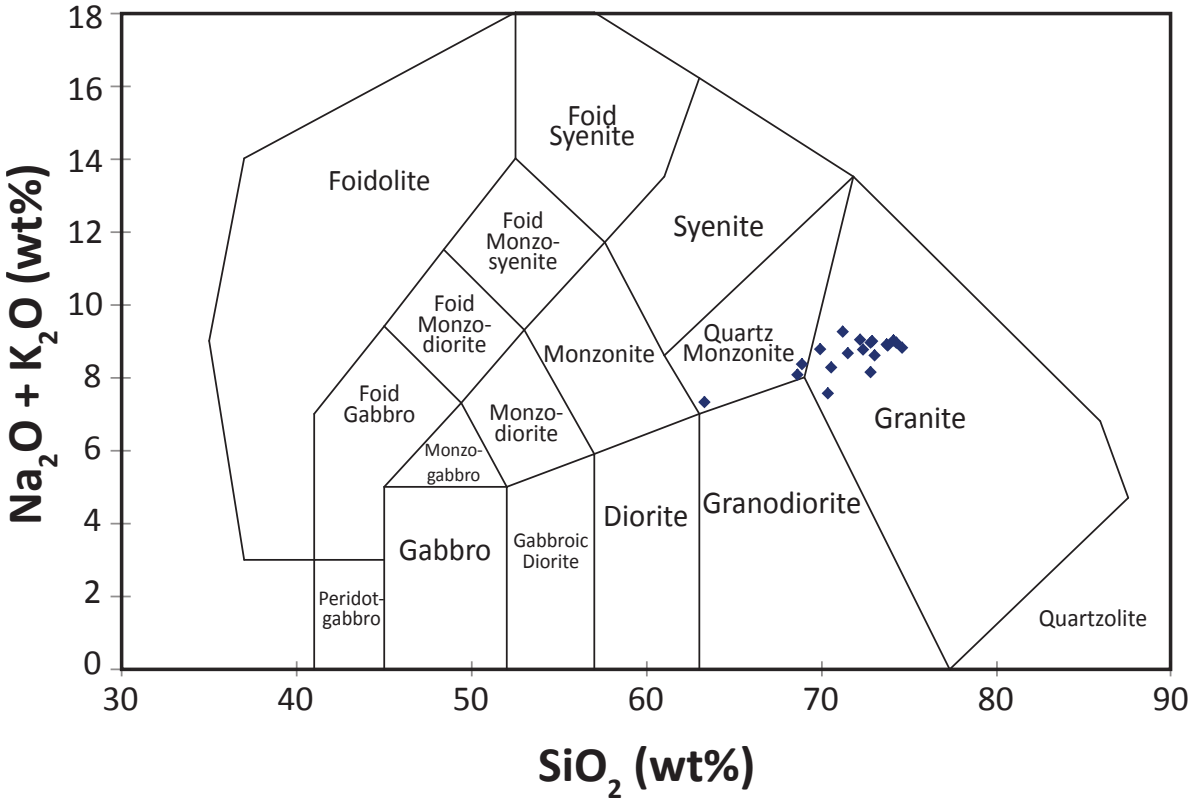


Figure 7.1. Total-alkali *vs* silica (TAS) classification diagram of Le Bas *et al.* (1986), showing the samples from the Mpuluzi batholith.

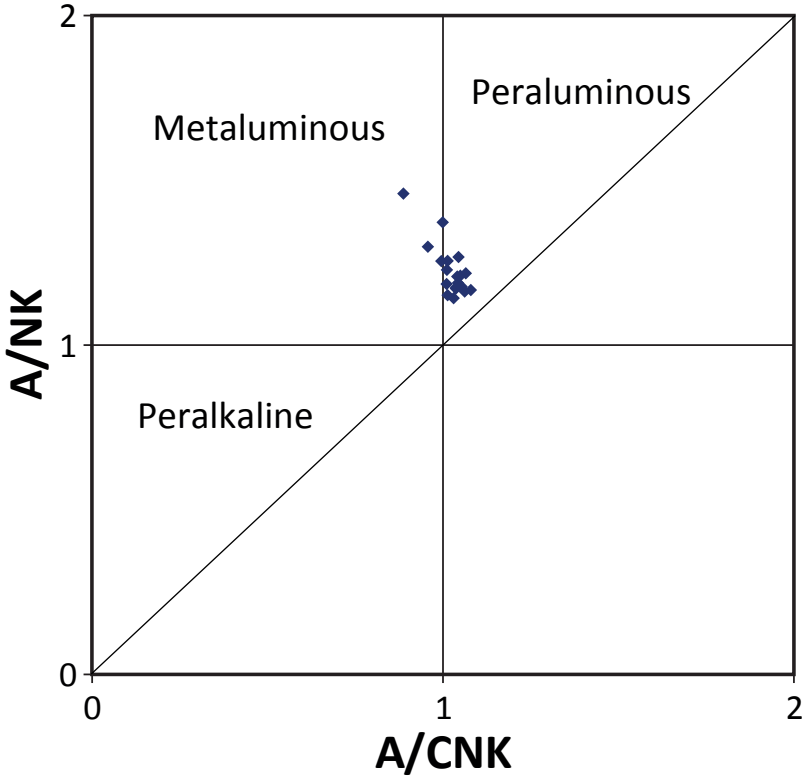


Figure 7.2. Plot of Al/(Na+K) *vs* Al/(Ca+Na+K) for the Mpuluzi samples, showing the division into peraluminous, metaluminous, and peralkaline.

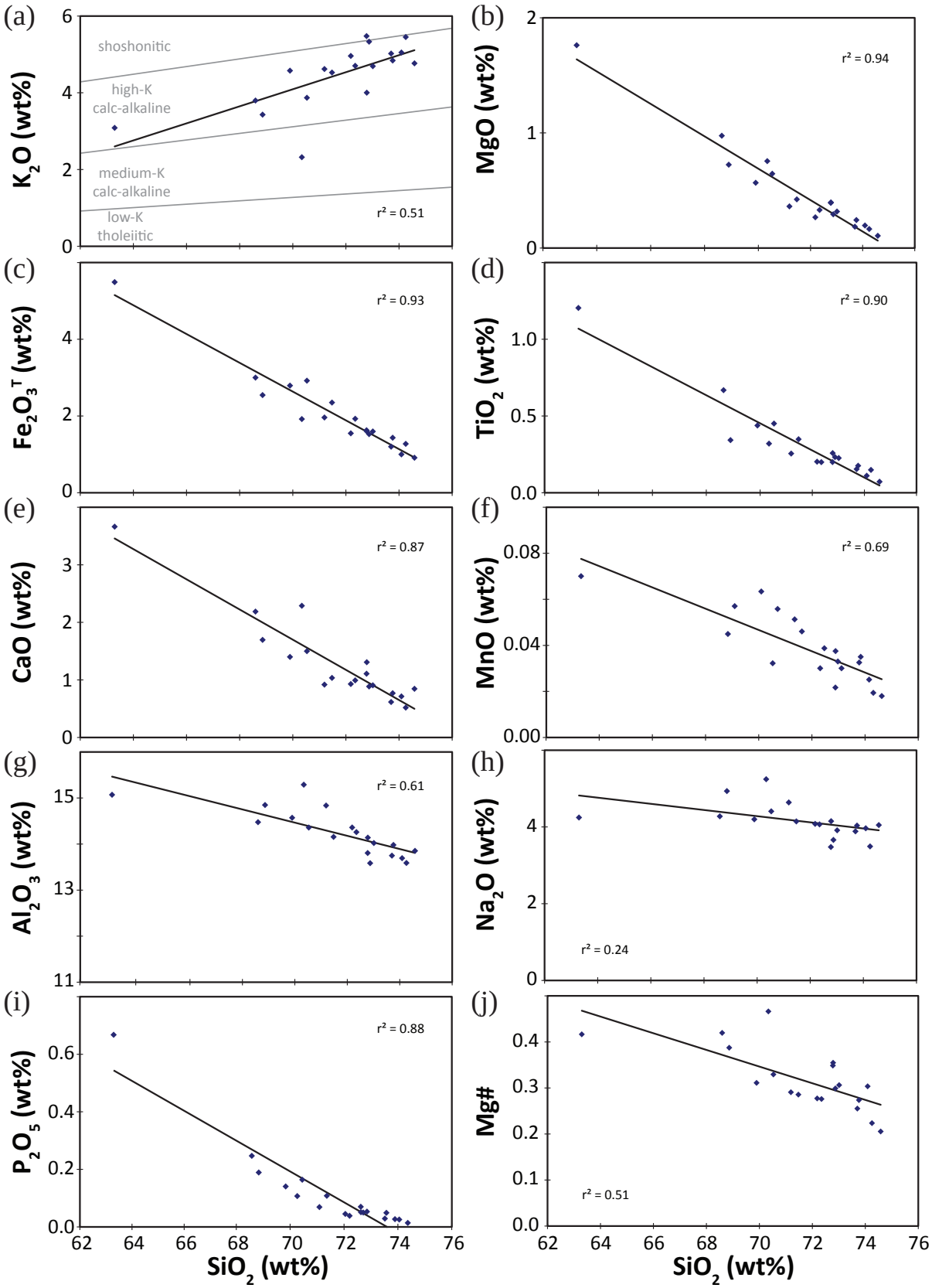


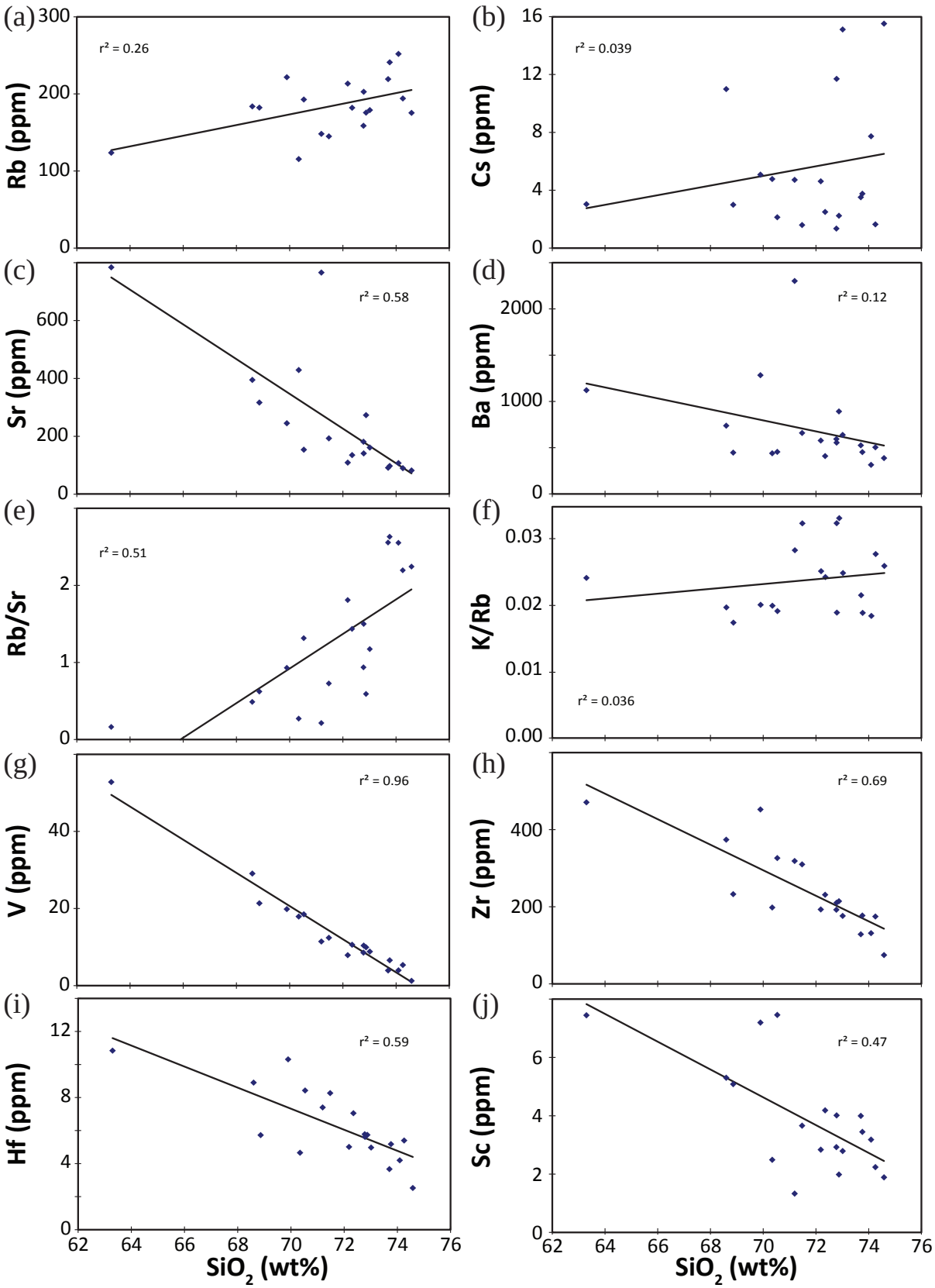
Figure 7.3. Harker variation diagrams for major elements *vs* SiO_2: (a) K_2O, showing the low-K tholeiitic, medium- and high-K calc-alkaline fields of Le Maitre *et al.* (1989); (b) MgO; (c) $Fe_2O_3^T$; (d) TiO_2; (e) P_2O_5; (f) CaO; (g) MnO; (h) Al_2O_3; (i) Na_2O; (j) Mg# (= $Mg/(Mg+Fe^T)$).

7.2.2 Trace-element compositions

Trace-element compositions for the Mpuluzi samples are presented in Table 7.2.

Among the large ion lithophile elements (LILE), Rb (120–270 ppm) and Cs (1.3–15.5 ppm) follow K, and are weakly positively correlated with SiO_2, whereas Sr (82–784 ppm) and Ba (310–2300 ppm) display moderate negative correlations with SiO_2; Rb/Sr (0.16–2.63) is positively correlated with SiO_2, while K/Rb (0.02–0.03) is uncorrelated (Figure 7.4a-f). The high field strength elements (HFSE) generally display negative correlations with SiO_2; V (1.2–52.8 ppm) displays the strongest correlation with SiO_2 ($r^2 = 0.96$) and is also strongly correlated with TiO_2 ($r^2 = 0.97$); Zr (75–471 ppm) and Hf (2.5–10.8 ppm) are strongly correlated with each other and display moderate correlations with SiO_2, while Sc (1.3–7.5 ppm) and Nb (5.6–41.2 ppm) display more scattered correlations (Figure 7.4g-k). Positive correlations with SiO_2 are shown by Th (9.2–31.5 ppm) and U (0.77–6.77 ppm), although Th/U (3.5–23.3) decreases with increasing SiO_2 (Figure 7.4l-n).

With the exception of one sample (RSA09), the rare earth elements (REE) for each sample display similar chondrite-normalised patterns (Figure 7.5), which are light REE (LREE) enriched (LREE: 100–1000 times chondrite, heavy REE (HREE): ~10 times chondrite) with moderate negative Eu anomalies (average Eu/Eu* ~ 0.5; Eu/Eu* = chondrite normalised Eu/√(Sm*Gd)). The chondrite-normalised La/Yb ratio ($(La/Yb)_N$) is a proxy for the slope of the REE pattern and decreases with increasing SiO_2 ($(La/Yb)_N$ = 1.1–55; Figure 7.6a). Eu anomalies are generally negative (Eu/Eu* <1) and become more pronounced with increasing SiO_2 (Eu/Eu* = 0.25–1.11; a value of 1 indicates no Eu anomaly; Figure 7.6b). Total REE content ranges from 121 to 819 ppm, and shows an overall decrease with increasing SiO_2 (Figure 7.6a-c). Individual elements are weakly negatively correlated to uncorrelated with SiO_2 (Figure 7.6c), with the strongest correlations displayed by the LREE ($r^2 = 0.35–0.13$; Figure 7.6d-g), whereas Y and the HREE are uncorrelated ($r^2 \leq 0.01$; Figure 7.6m-r). Sample RSA09 has an anomalous HREE-enriched pattern, and an elevated Y content (~10 times higher Y and HREE contents than those with similar SiO_2; see Table 7.2).


(a)
Rb (ppm)
r² = 0.26
(b)
Cs (ppm)
r² = 0.039
(c)
Sr (ppm)
r² = 0.58
(d)
Ba (ppm)
r² = 0.12
(e)
Rb/Sr
r² = 0.51
(f)
K/Rb
r² = 0.036
(g)
V (ppm)
r² = 0.96
(h)
Zr (ppm)
r² = 0.69
(i)
Hf (ppm)
r² = 0.59
(j)
Sc (ppm)
r² = 0.47
SiO2 (wt%)
SiO2 (wt%)

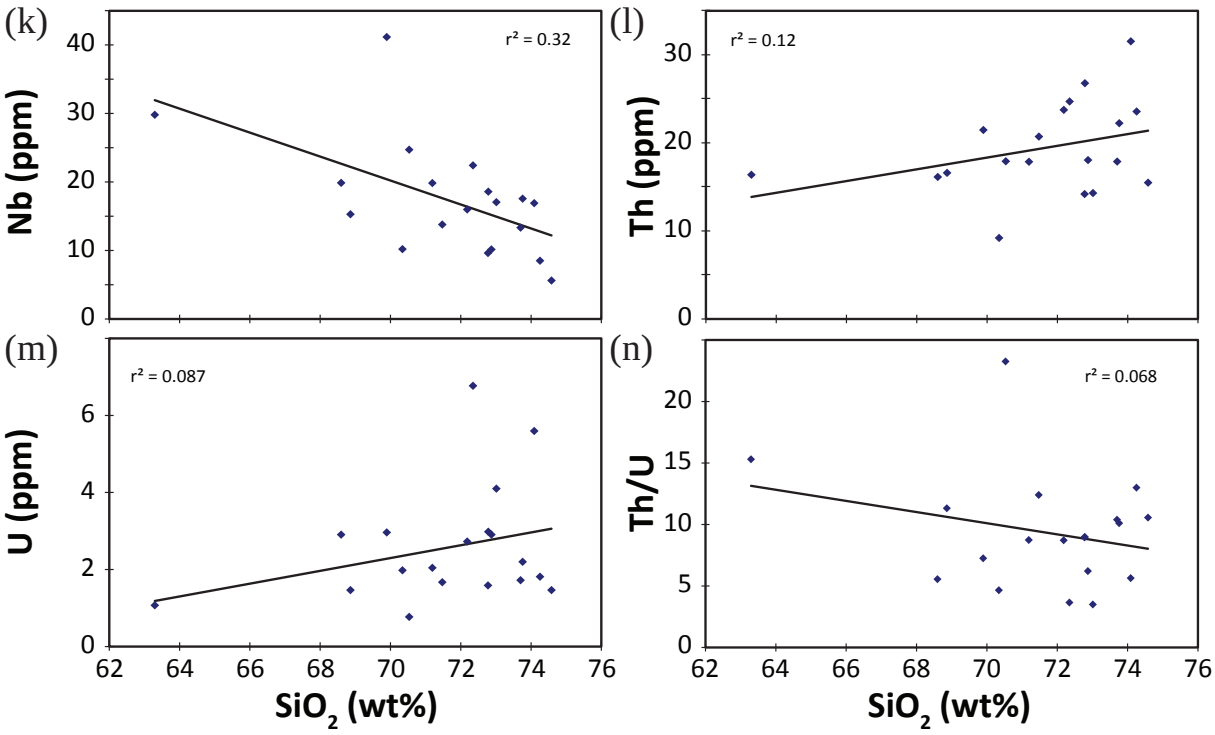


Figure 7.4. Trace elements *vs* SiO_2: (a) Rb; (b) Cs; (c) Sr; (d) Ba; (e) Rb/Sr; (f) K/Rb; (g) V; (h) Zr; (i) Hf; (j) Sc; (k) Nb; (l) Th; (m) U; (n) Th/U.

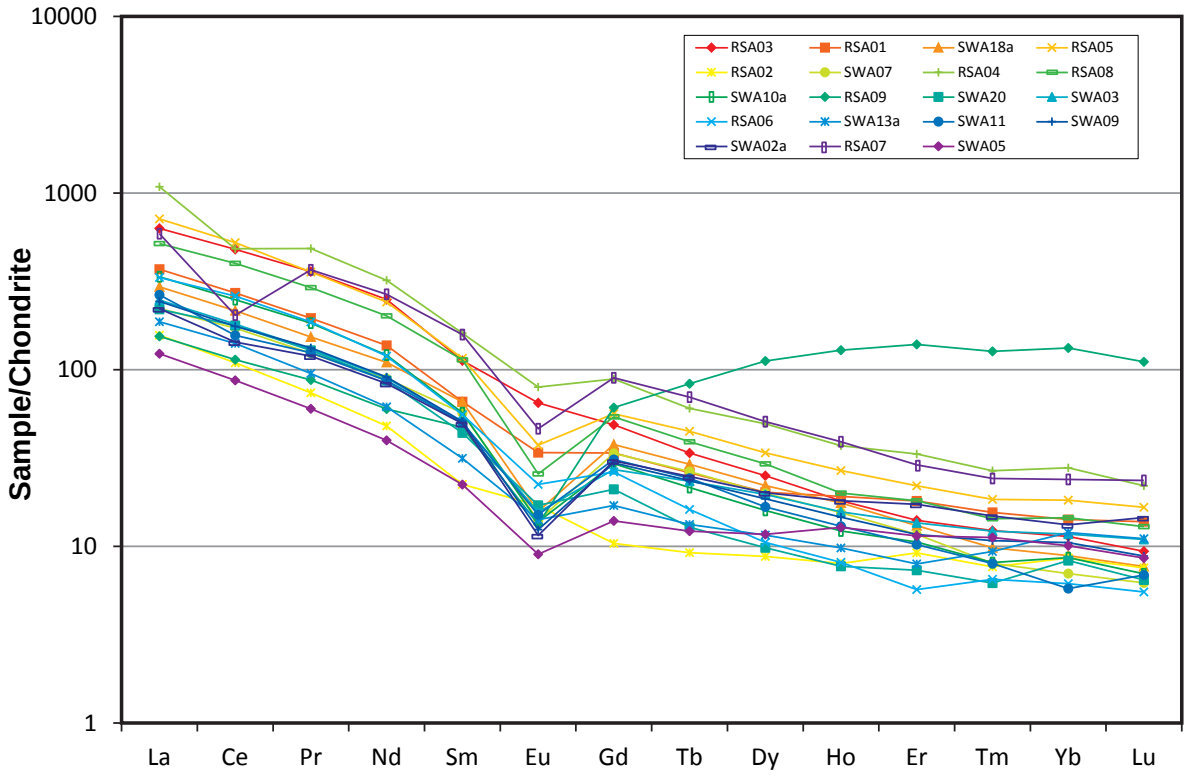
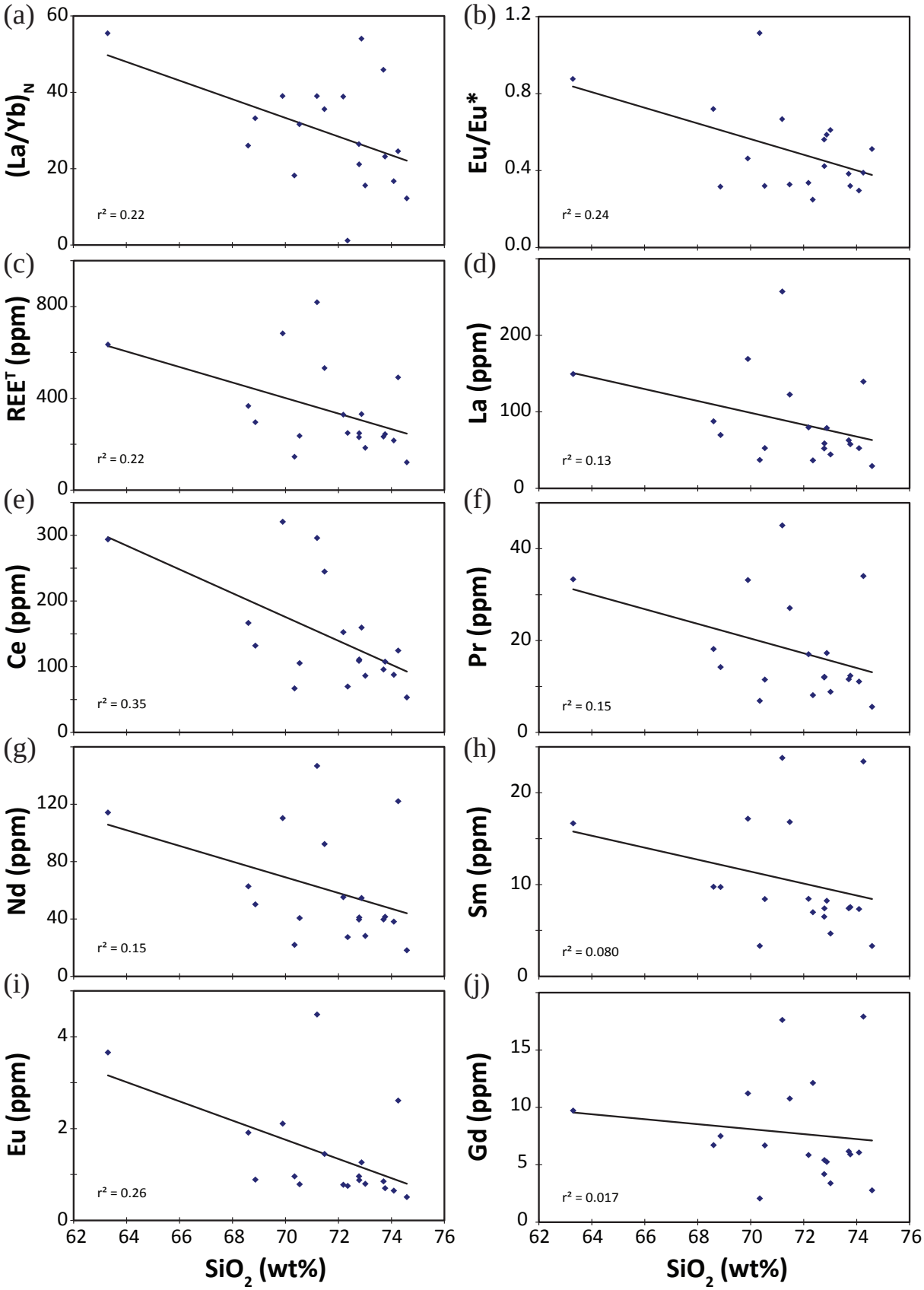


Figure 7.5. Chondrite-normalised rare earth element (REE) compositions of samples from the Mpuluzi batholith.


(a)
(La/Yb)N
r² = 0.22
(b)
Eu/Eu*
r² = 0.24
(c)
REET (ppm)
r² = 0.22
(d)
La (ppm)
r² = 0.13
(e)
Ce (ppm)
r² = 0.35
(f)
Pr (ppm)
r² = 0.15
(g)
Nd (ppm)
r² = 0.15
(h)
Sm (ppm)
r² = 0.080
(i)
Eu (ppm)
r² = 0.26
(j)
Gd (ppm)
r² = 0.017
SiO2 (wt%)
SiO2 (wt%)

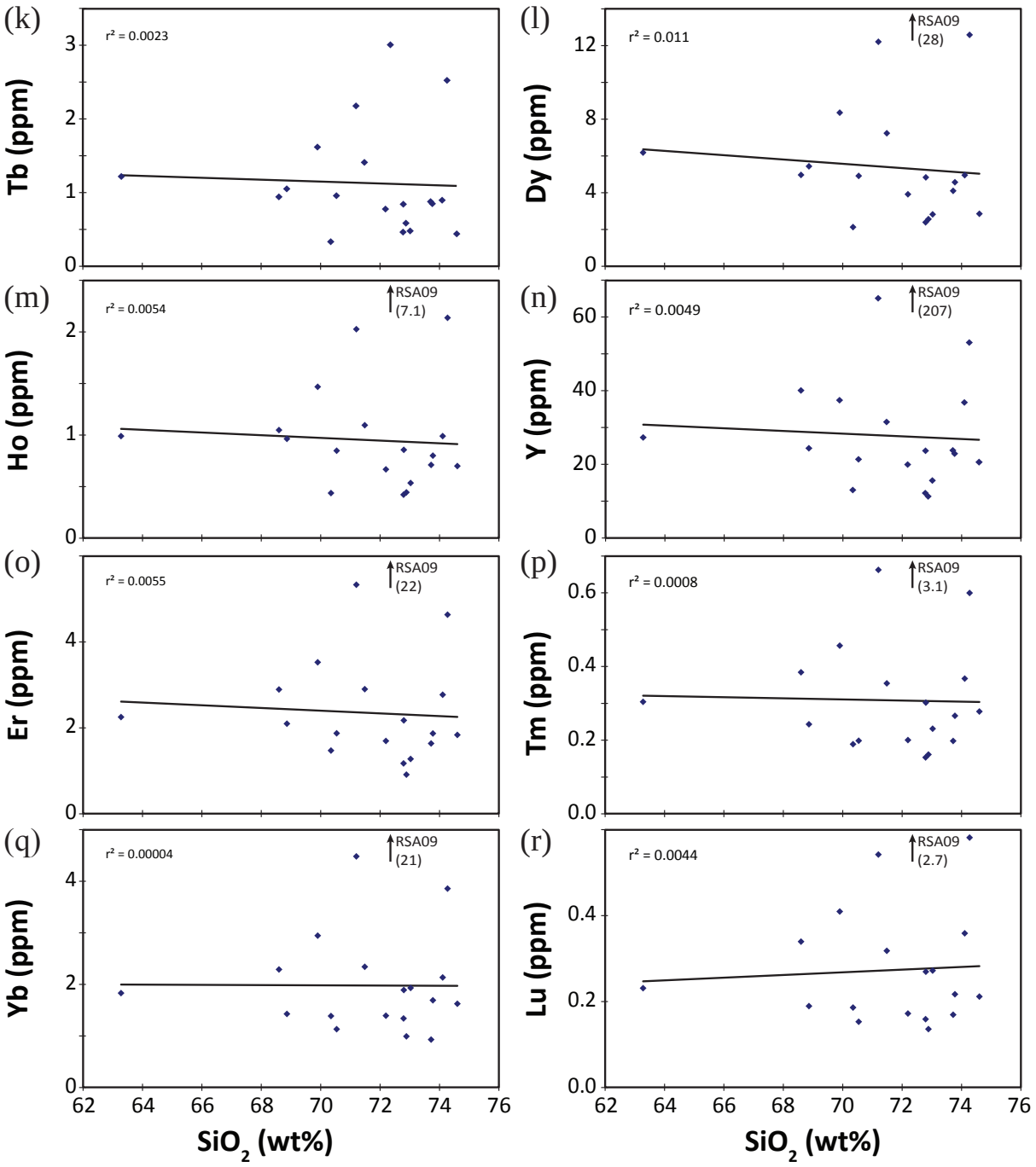


Figure 7.6. Rare earth element (REE) compositions and key parameters *vs* SiO_2: (a) $(La/Yb)_N$; (b) Eu/Eu* (chondrite-normalised Eu/√(Sm*Gd)); (c) Total REE; (d) La; (e) Ce; (f) Pr; (g) Nd; (h) Sm; (i) Eu; (j) Gd; (k) Tb; (l) Dy; (m) Ho; (n) Y; (o) Er; (p) Tm; (q) Yb; (r) Lu.

Table 7.2: Trace-element compositions for samples from the Mpuluzi batholith. All values in ppm.

	RSA03	RSA01	SWA18a	RSA05	RSA02	SWA07	RSA04	RSA08	SWA10a	RSA09	SWA20	SWA03	RSA06	SWA13a	SWA11	SWA09	SWA02a	RSA07	SWA05
Li	51.50	60.66	35.50	40.94	52.53	32.01	19.99	19.23	26.79	32.61	18.26	98.71	22.24	38.50	29.56	27.47	18.55	16.00	79.07
Be	1.973	4.242	3.744	3.688	2.535	1.888	3.311	1.913	2.866	2.969	1.445	3.249	2.407	3.608	1.967	2.258	4.721	1.502	6.126
Sc	7.45	5.30	5.09	7.20	2.49	7.46	1.33	3.66	2.84	4.18	2.92	4.01	1.98	2.79	4.00	3.45	3.18	2.24	1.89
V	52.82	29.06	21.37	19.85	17.92	18.51	11.43	12.40	7.89	10.60	8.56	10.39	9.94	8.83	3.92	6.57	3.97	5.35	1.24
Cr	29.71	24.72	5.06	5.86	11.92	8.77	4.01	4.68	4.38	5.39	6.21	8.11	3.96	3.47	2.32	5.17	3.87	2.54	2.04
Ni	15.52	11.90	3.55	3.93	7.03	5.20	1.01	2.58	2.41	2.58	3.69	4.11	1.75	1.71	0.81	2.21	1.32	0.79	0.54
Cu	42.9	25.4	15.6	20.9	24.3	20.5	17.9	9.2	14.3	12.1	13.8	3.7	13.8	12.6	5.8	14.4	4.7	2.4	3.6
Zn	102.56	78.90	76.61	83.49	53.71	79.49	53.27	204.39	40.96	62.43	35.38	49.42	40.64	41.47	39.20	45.13	21.24	31.84	36.14
Ga	20.11	20.44	21.60	22.50	17.46	20.58	17.59	19.45	18.36	18.91	15.98	19.64	16.39	17.49	16.73	18.13	18.48	18.28	18.20
Rb	128.0	192.8	196.9	227.8	116.3	202.1	163.6	140.2	197.4	194.1	169.6	211.5	161.3	188.9	233.3	256.5	274.1	197.0	184.0
Sr	784.1	395.0	316.6	245.0	429.0	153.7	765.9	192.8	109.1	135.2	181.1	141.0	273.2	161.0	91.3	97.5	107.4	89.7	82.0
Y	27.1	39.8	24.2	37.2	12.9	21.2	64.8	31.3	19.8	206.5	12.0	23.5	11.2	15.5	23.6	22.7	36.6	52.8	20.4
Zr	471	374	233	453	198	326	319	310	193	231	192	210	214	176	128	177	131	175	75
Nb	29.81	19.88	15.29	41.18	10.19	24.73	19.84	13.78	15.99	22.44	9.63	18.59	10.15	17.05	13.33	17.57	16.91	8.51	5.62
Mo	1.736	0.804	0.316	0.945	0.403	0.235	0.357	1.922	0.187	0.225	1.467	0.411	3.403	0.263	0.153	0.360	0.183	0.232	0.304
Cd	0.076	0.138	0.125	0.178	0.060	0.072	0.171	0.227	0.045	0.095	0.067	0.167	0.099	0.048	0.056	0.010	0.171	0.035	0.166
Cs	3.032	10.992	2.995	5.077	4.773	2.130	4.714	1.594	4.617	2.496	1.345	11.701	2.237	15.116	3.515	3.758	7.731	1.640	15.516
Ba	1121	738	447	1283	439	455	2302	659	577	409	593	554	892	638	526	452	315	504	387
La	149.4	87.7	69.7	169.1	37.1	52.6	257.3	122.6	79.7	36.6	52.1	58.8	78.8	44.3	62.8	57.6	52.5	139.5	29.2
Ce	294.3	166.8	132.3	321.1	67.0	105.5	296.4	245.2	152.8	69.9	109.1	111.2	159.8	86.4	95.9	107.9	87.9	124.7	53.3
Pr	33.3	18.2	14.2	33.2	6.9	11.5	45.1	27.1	17.0	8.1	12.0	12.1	17.3	8.8	11.6	12.3	11.1	34.1	5.6
Nd	114.2	62.8	50.2	110.3	22.0	40.7	146.7	92.2	55.3	27.4	39.6	41.1	54.6	28.2	39.7	41.6	38.2	122.1	18.2
Sm	16.67	9.76	9.74	17.17	3.32	8.42	23.80	16.82	8.45	6.99	6.50	7.41	8.23	4.67	7.42	7.55	7.34	23.41	3.31
Eu	3.659	1.912	0.888	2.107	0.959	0.788	4.485	1.447	0.776	0.752	0.961	0.879	1.265	0.797	0.850	0.701	0.648	2.611	0.509
Gd	9.7	6.7	7.5	11.2	2.1	6.7	17.6	10.8	5.9	12.1	4.2	5.4	5.3	3.4	6.2	5.9	6.1	17.9	2.8
Tb	1.22	0.94	1.05	1.62	0.33	0.96	2.18	1.41	0.78	3.01	0.46	0.84	0.59	0.48	0.88	0.85	0.90	2.53	0.44
Dy	6.18	4.98	5.44	8.33	2.16	4.92	12.15	7.22	3.93	27.54	2.42	4.84	2.59	2.85	4.12	4.58	4.96	12.52	2.88
Ho	0.989	1.048	0.962	1.467	0.437	0.847	2.026	1.095	0.667	7.050	0.421	0.856	0.444	0.535	0.710	0.800	0.989	2.136	0.699
Er	2.25	2.89	2.10	3.52	1.47	1.87	5.33	2.90	1.69	22.23	1.17	2.17	0.91	1.28	1.64	1.87	2.77	4.63	1.84
Tm	0.304	0.384	0.243	0.456	0.189	0.198	0.662	0.354	0.200	3.140	0.153	0.302	0.161	0.231	0.198	0.266	0.367	0.599	0.278
Yb	1.83	2.29	1.43	2.94	1.39	1.13	4.48	2.34	1.39	21.38	1.34	1.89	0.99	1.93	0.93	1.69	2.13	3.86	1.62
Lu	0.231	0.339	0.189	0.409	0.186	0.153	0.542	0.318	0.172	2.730	0.159	0.269	0.136	0.272	0.169	0.217	0.359	0.581	0.212
Hf	10.8	8.9	5.7	10.3	4.7	8.4	7.4	8.3	5.0	7.1	5.8	5.6	5.7	5.0	3.7	5.2	4.2	5.4	2.5
Pb	15.8	21.0	27.9	26.4	18.1	22.4	26.9	182.7	30.5	27.1	20.2	30.1	23.7	25.5	35.6	31.5	30.5	28.9	40.2
Th	16.4	16.1	16.6	21.5	9.2	17.9	17.9	20.7	23.7	24.7	14.2	26.8	18.0	14.3	17.9	22.2	31.5	23.6	15.5
U	1.071	2.906	1.466	2.961	1.978	0.770	2.044	1.671	2.726	6.770	1.587	2.980	2.906	4.100	1.722	2.200	5.597	1.814	1.466

7.2.3 Sr and Nd isotopic compositions

Sr and Nd isotopic compositions were obtained from the same 19 samples, and are presented in Table 7.3. $^{87}Rb/^{86}Sr$ and $^{147}Sm/^{144}Nd$ ratios were calculated from concentrations obtained by solution ICPMS (Table 7.2), and the errors on the ratios were propagated from the uncertainties on the concentrations. Initial ratios and isochron ages were calculated using Isoplot (Ludwig, 2003). The $^{87}Sr/^{86}Sr$ initial ratios and isochron ages were calculated using the updated value of 1.398×10^{-11} for the ^{87}Rb decay constant (Boehnke & Harrison, 2014), as the value of 1.42×10^{-11} (Steiger & Jäger, 1977) typically used in these calculations has been shown to consistently give younger Rb-Sr ages than those obtained using other isotopic systems (Nebel *et al.*, 2011; Rotenberg *et al.*, 2012; Boehnke & Harrison, 2014).

The samples produce a range in $^{87}Rb/^{86}Sr$ from ~0.5 to ~7.5, and yield $^{87}Sr/^{86}Sr$ ratios ranging from 0.721573 to 1.022424. They define a single isochron with a mean square of weighted derivatives (MSWD) of 0.74, indicating that the scatter in the data is accommodated by the analytical error; the isochron yields an initial $^{87}Sr/^{86}Sr$ ratio of 0.7012 ± 0.0016, and an age of 3113 ± 84 Ma (Figure 7.7). This initial ratio yields a model age of extraction from the chondritic uniform reservoir (T_{CHUR}) of 2.8 ± 1.3 Ga. Individual samples yield model ages ranging from 2.97 to 3.45 Ga, and initial $^{87}Sr/^{86}Sr$ ratios range from 0.682881 to 0.708823.

The range in $^{147}Sm/^{144}Nd$ is relatively restricted (0.09–0.16), and $^{143}Nd/^{144}Nd$ ratios range from 0.510372 to 0.511480. The 19 samples yield an isochron with a MSWD of 0.36 (indicating that the variation is within the analytical uncertainty). However, the age obtained from this isochron is considerably younger than that for the Rb-Sr system (2823 ± 400 Ma; Figure 7.8a). Excluding the sample with anomalously high REE concentrations (RSA09, see Section 7.2.2 above) significantly improves the agreement between the two systems, and produces an isochron with initial $^{143}Nd/^{144}Nd = 0.50849 \pm 0.00038$ and a corresponding age of 3027 ± 520 Ma (Figure 7.8b). The large uncertainty on this age is a consequence of the narrow range in Sm/Nd in the Mpuluzi samples, which means that the slope of the isochron is poorly constrained. The initial ratio of the isochron yields a T_{CHUR} model age of 3.19 ± 0.29 Ga; individual samples yield older model ages ranging from 3.23 to 3.64 Ga; initial $^{143}Nd/^{144}Nd$ ratios range from 0.508335 to 508513, and εNd ranges from -4.47 to -1.70. These calculations exclude sample RSA09, which yields $^{143}Nd/^{144}Nd_i = 0.508180$, an unrealistic $T_{CHUR} = 4.85$ Ga, and a strongly negative εNd = -8.25.

Plotting epsilon Nd vs initial Sr composition shows no correlation between the two isotopic systems (Figure 7.9).

Table 7.3: Sr and Nd isotopic compositions for samples from the Mpuluzi batholith.

	$^{87}Rb/^{86}Sr$	$^{87}Sr/^{86}Sr$	st err	$T_{(CHUR)}$	$^{87}Sr/^{86}Sr_i$	$^{147}Sm/^{144}Nd$	$^{143}Nd/^{144}Nd$	st err	$T_{(CHUR)}$	$^{143}Nd/^{144}Nd_i$	εNd
RSA03	0.46 ± 0.02	0.721573	± 3	3.15	0.701111	0.0919 ± 0.0036	0.510401	± 4	3.23	0.508513	-1.70
RSA01	1.38 ± 0.06	0.760985	± 3	3.05	0.699832	0.0980 ± 0.0038	0.510487	± 11	3.30	0.508476	-2.48
SWA18a	1.76 ± 0.08	0.778180	± 3	3.08	0.699999	0.1221 ± 0.0048	0.510902	± 4	3.52	0.508388	-3.96
RSA05	2.62 ± 0.12	0.815610	± 3	3.06	0.699406	0.0980 ± 0.0038	0.510432	± 5	3.38	0.508424	-3.68
RSA02	0.77 ± 0.03	0.736544	± 4	3.28	0.702607	0.0952 ± 0.0037	0.510403	± 9	3.33	0.508450	-3.06
SWA07	3.71 ± 0.16	0.861538	± 3	3.03	0.695925	0.1304 ± 0.0051	0.511045	± 4	3.64	0.508354	-4.47
RSA04	0.60 ± 0.03	0.726693	± 5	2.99	0.699829	0.1022 ± 0.0040	0.510581	± 6	3.29	0.508476	-2.18
RSA08	2.05 ± 0.09	0.797355	± 4	3.29	0.706266	0.1148 ± 0.0045	0.510771	± 2	3.45	0.508415	-3.73
SWA10a	5.11 ± 0.22	0.928168	± 6	3.12	0.700261	0.0963 ± 0.0037	0.510383	± 2	3.40	0.508396	-3.64
RSA09	4.05 ± 0.18	0.882987	± 8	3.15	0.703028	0.1606 ± 0.0063	0.511480	± 4	4.85	0.508180	-8.25
SWA20	2.64 ± 0.12	0.820062	± 4	3.16	0.702237	0.1034 ± 0.0040	0.510534	± 2	3.41	0.508403	-3.58
SWA03	4.23 ± 0.19	0.891498	± 4	3.15	0.700749	0.1135 ± 0.0044	0.510772	± 5	3.40	0.508408	-2.66
RSA06	1.67 ± 0.07	0.782771	± 4	3.45	0.708823	0.0949 ± 0.0037	0.510372	± 4	3.37	0.508424	-3.55
SWA13a	3.31 ± 0.15	0.850497	± 7	3.16	0.702975	0.1042 ± 0.0041	0.510533	± 3	3.44	0.508386	-3.97
SWA11	7.21 ± 0.32	1.022424	± 4	3.12	0.699782	0.1176 ± 0.0046	0.510914	± 3	3.30	0.508481	-1.79
SWA09	7.43 ± 0.33	1.018711	± 5	3.00	0.685210	0.1144 ± 0.0045	0.510802	± 4	3.38	0.508427	-2.53
SWA02a	7.20 ± 0.32	1.010230	± 5	3.01	0.689219	0.1211 ± 0.0047	0.510930	± 3	3.42	0.508434	-3.01
RSA07	6.20 ± 0.27	0.963341	± 4	2.97	0.682881	0.1207 ± 0.0047	0.510938	± 4	3.39	0.508411	-2.22
SWA05	6.33 ± 0.28	0.983628	± 4	3.13	0.697241	0.1144 ± 0.0045	0.510728	± 5	3.51	0.508335	-3.76

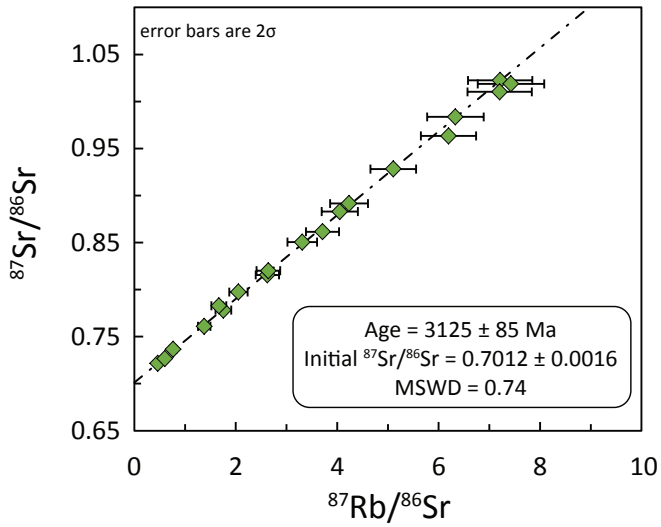


Figure 7.7. Plot of measured $^{87}Sr/^{86}Sr$ *vs* $^{87}Rb/^{86}Sr$ (isochron diagram). The samples define a single isochron with an initial ratio of 0.7012 ± 0.0016, and an age of 3113 ± 84 Ma.

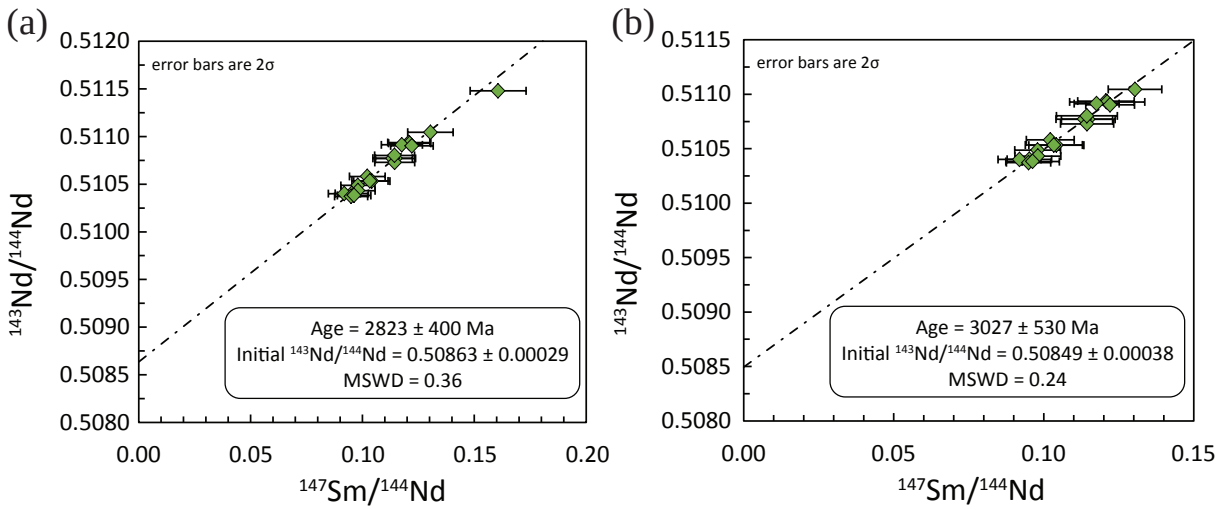


Figure 7.8. Plot of measured $^{143}Nd/^{144}Nd$ *vs* $^{147}Sm/^{144}Nd$ (isochron diagram): (a) for all Mpuluzi samples; (b) excluding sample RSA09. The samples define a single isochron with an initial ratio of 0.50849 ± 0.00038, and an age of 3027 ± 530 Ma (excluding sample RSA09).

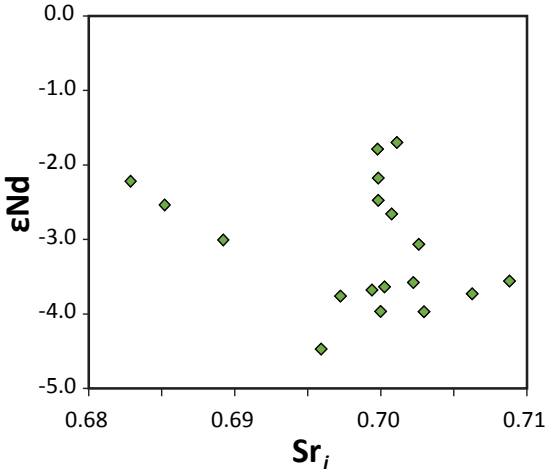


Figure 7.9. Plot of epsilon Nd *vs* initial Sr composition (excluding sample RSA09).

7.3 Discussion

7.3.1 Granite classification

A review of granite classification schemes is presented in Chapter Three. Classification schemes range from purely descriptive (e.g. the geochemical classification scheme of Frost *et al.*, 2001) to those with implications for the source of the magma (e.g. the I- and S-type classification; Chappell & White, 1974; Chappell & White, 2001) or the tectonic setting at the time of emplacement (Pearce *et al.*, 1984).

Geochemical classification

The Mpuluzi samples plot in the calc-alkaline field on the AFM diagram (Figure 7.10; A = Na_2O+K_2O, F = FeO^T, and M = MgO; Kuno, 1968); a plot of K_2O *vs* SiO_2 further classifies them as high-K calc-alkaline (see Figure 7.3a above; fields from Le Maitre *et al.*, 1989). In the geochemical classification scheme of Frost *et al.* (2001) the Mpuluzi samples classify as magnesian, alkali-calcic, and generally metaluminous; the most felsic samples have slightly peraluminous compositions (Figure 7.11; see also Figure 7.2 above). Of the suites analysed by Frost *et al.* (2001), the Mpuluzi compositions are most similar to the high-K alkali-calcic granitoids generally considered to be post-orogenic (e.g. the Caledonian granitoids of Britain and Ireland; note that TTGs were the only Archaean suites included by Frost *et al.* (2001)).

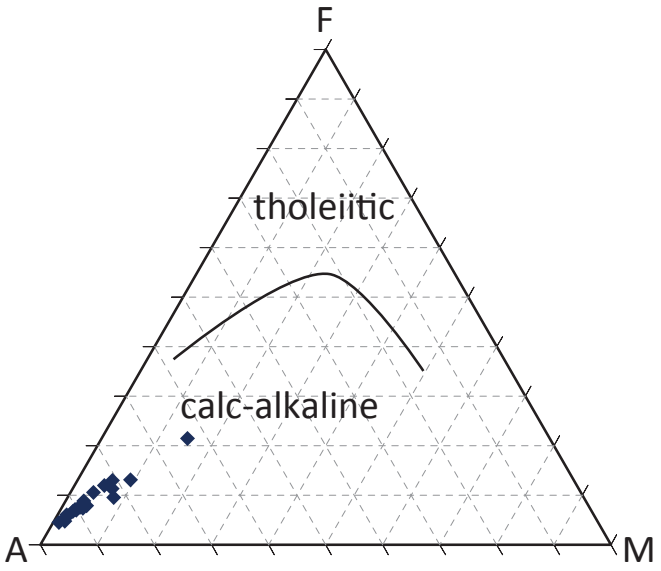


Figure 7.10. Compositions of Mpuluzi samples plotted on the AFM diagram of Kuno (1968). A = Na_2O+K_2O, F = FeO^T, and M = MgO.

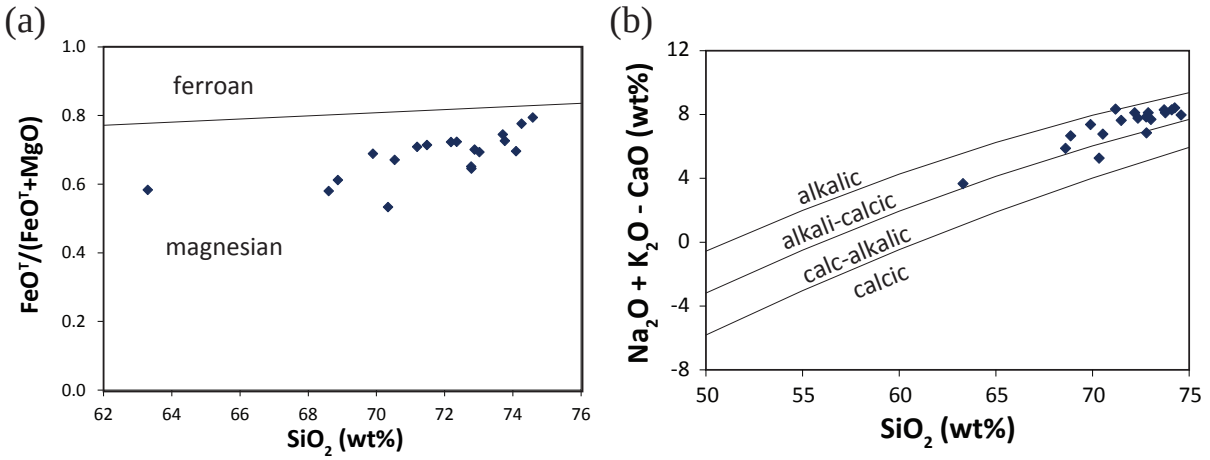


Figure 7.11. Mpuluzi samples classified according to the key indices of Frost *et al.* (2001): (a) Division into magnesian and ferroan granites; and (b) Modified alkali-lime index. See also aluminium saturation index (Figure 7.2 above).

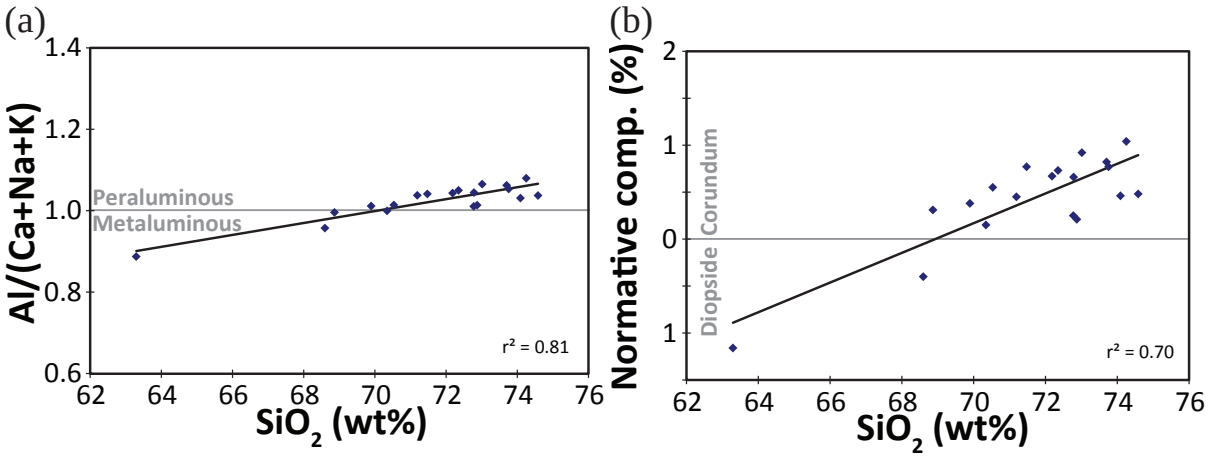


Figure 7.12. Plot of (a) aluminium saturation and (b) normative corundum/diopside *vs* SiO_2 for Mpuluzi samples.

Source classification – I-S-A-M-type granites

The Mpuluzi samples classify as I-type (igneous source) granites using the classification scheme of Chappell and White (1974); this is consistent with the findings of previous studies which classified the ~3.1 Ga granitoids as I-type (e.g. Yearron, 2003). As is typical of I-type granites, the Mpuluzi samples are metaluminous to weakly peraluminous (ASI = 0.89–1.1), and have relatively high Na_2O contents (>3.2 wt% in all samples). Normative compositions range from 1.16% diopside to 1.04% corundum (Figure 7.12), and the samples also display the mineralogical characteristics of I-type granites, with hornblende present in the most mafic sample, and primary muscovite in the felsic samples (see Chapter Five). The low initial $^{87}Sr/^{86}Sr$ calculated from the Rb-Sr isochron is also consistent with the characteristics of I-type granites.

Tectonic setting

The tectonic classification of Pearce *et al.* (1984) was constructed based on granites where the tectonic setting is known, and thus can be used to infer the tectonic setting of granites where that information is not available through other means. However, the application of the classification scheme to Archaean granites presents a problem, as the tectonic processes in the Archaean may have been substantially different to those in modern settings. Magmas formed in the Archaean may also differ compositionally from modern magmas, even if the tectonic environments were similar; these differences may be caused by higher degrees of partial melting, less fractionated mantle compositions, and differences in the relative importance of crustal and mantle melting (Pearce *et al.*, 1984; Keller & Schoene, 2012).

When the Mpuluzi samples are plotted on the tectonic setting discrimination diagrams of Pearce *et al.* (1984; Figure 7.13), they plot across all fields on the Nb *vs* Y diagram, and in both the within plate granite (WPG) and volcanic arc granite (VAG) fields on the Rb *vs* Y+Nb diagram, suggesting that this classification scheme is not useful in discriminating the tectonic environment of these granites.

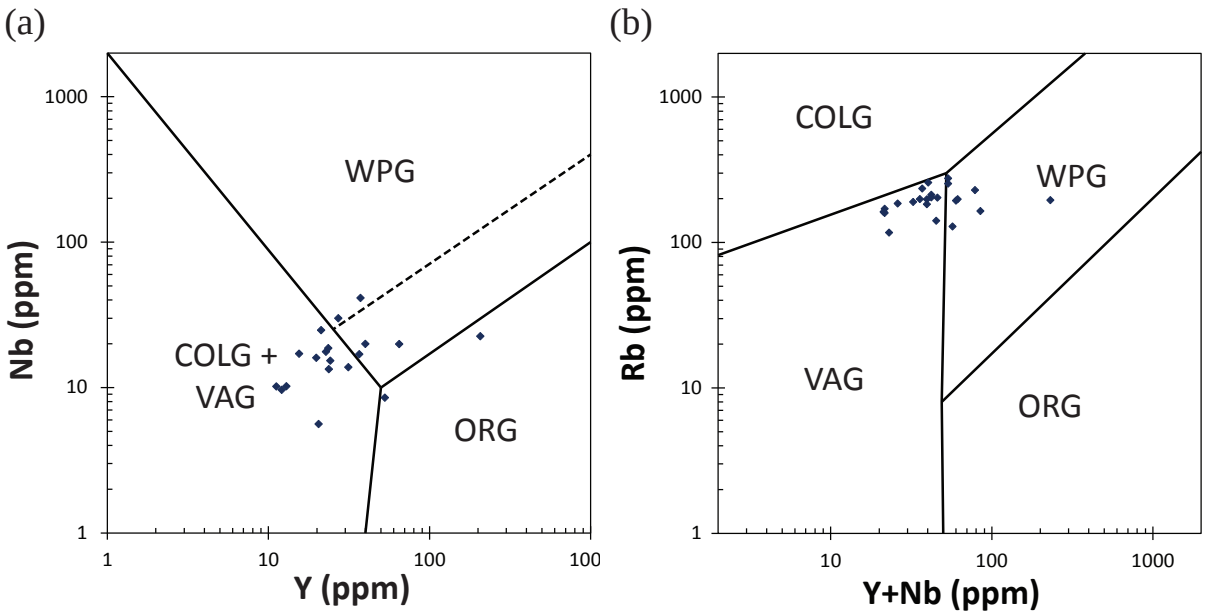


Figure 7.13. Compositions of Mpuluzi samples plotted on the discrimination diagrams for the tectonic setting of granites from Pearce *et al.* (1984): (a) Nb *vs* Y; (b) Rb *vs* Y+Nb. COLG = collisional granites, WPG = within plate granites, ORG = ocean ridge granites, VAG = volcanic arc granites. The dashed line in (a) represents the upper compositional boundary for ORG from anomalous ridge segments.

7.3.2 Comparison with other 3.1 Ga granitoids in the Barberton region

Major- and trace-element analyses of the Mpuluzi batholith compiled from the literature are presented in Table 7.4, together with available analyses of the ~3.1 Ga Heerenveen and Nelspruit batholiths (Mpuluzi: n=21; Heerenveen: n=23; Nelspruit: average of 3 analyses; data from Anhaeusser & Robb, 1983; Yearron, 2003).

The major-element compositions of the Mpuluzi samples analysed in this study generally fall within the range of reported values for the Mpuluzi, Heerenveen, and Nelspruit batholiths (Figure 7.14). The reported values for the Mpuluzi batholith cover the entire range of SiO_2 analysed in this study (63.2–75.9 wt% SiO_2), and show the same compositional gap between ~63 and ~68 wt% SiO_2. The literature data generally scatter around the trend line defined by the analyses obtained in this study; the similarity in the datasets suggests that all major components of the Mpuluzi batholith are represented. The samples from the Heerenveen batholith are generally more felsic than the Mpuluzi batholith (71.7–75.4 wt% SiO_2), and show a greater degree of compositional variability, with some analyses having distinctly lower K_2O and higher Na_2O, CaO, and Al_2O_3 than the Mpuluzi samples. The average composition of the Nelspruit batholith (72.2% SiO_2) falls close to the main trend of the Mpuluzi samples for most major elements, with higher Fe_2O_3 and lower K_2O.

Comparison of the limited number of published trace-element analyses for the Mpuluzi and Heerenveen batholiths with the analyses obtained in this study shows that the compositions of the two batholiths define similar trends for most elements (Figures 7.15 and 7.16). Compared to the trend defined by analyses of the Mpuluzi batholith, the Heerenveen batholith has a component with distinctly low Rb, high Sr, and low Rb/Sr (this corresponds to the low-K_2O component seen in Figure 7.14a); Ba is also generally somewhat lower (Figures 7.15 and 7.16a-d). The high field strength elements display similar trends within both batholiths (Figure 7.16e-g); only a subset of the REE were available in the literature and these show scattered but similar trends to those obtained in this study, as does Y (Figure 7.16h-r). The two batholiths also display similar values for $(La/Yb)_N$ and Eu/Eu* (Figure 7.16s, t).

Table 7.4: Major- and trace-element analyses for the Mpuluzi (Mpz), Heerenveen (Hvn), and Nelspruit (Nsp) batholiths compiled from the literature. References: (1) Anhaeusser and Robb (1983); (2) Yearron (2003).

Batholith	Mpz	Mpz	Mpz	Mpz	Mpz	Mpz	Mpz	Mpz	Mpz	Mpz	Mpz	Mpz
Sample	JV36	GM7	LR4A	JG7A	JG5	JG7B	LR2	LR4B	MF13	LO3	LO5	MF8
Reference	1	1	1	1	1	1	1	1	1	1	1	1
Major elements (wt%)												
SiO_2	74.15	73.78	73.00	72.95	63.15	69.64	74.00	70.68	75.47	71.11	70.54	73.75
TiO_2	0.24	0.14	0.23	0.17	1.43	0.45	0.25	0.50	0.14	0.25	0.65	0.20
Al_2O_3	13.55	14.27	13.78	13.03	15.30	13.90	14.14	14.67	13.53	14.78	14.41	13.75
$Fe_2O_3^T$	1.32	1.29	1.67	1.65	5.75	2.92	2.10	3.05	1.36	1.60	2.89	1.56
MnO	0.01	0.01	0.03	0.02	0.12	0.03	0.02	0.05	0.03	0.05	0.08	0.02
MgO	0.27	0.26	0.43	0.75	2.17	0.62	0.21	0.55	0.17	0.43	1.08	0.07
CaO	1.11	0.46	1.03	0.92	3.78	1.23	1.03	1.54	0.82	1.30	2.06	1.78
Na_2O	3.69	3.00	3.28	3.60	4.20	4.64	3.41	4.68	4.11	3.50	3.68	4.50
K_2O	5.01	5.36	5.49	5.02	2.86	3.98	5.81	4.17	4.26	4.85	3.96	4.17
P_2O_5	0.05	0.06	0.07	0.07	0.57	0.19	0.06	0.20	0.05	0.07	0.11	0.06
LOI	0.69	0.60	0.53	0.63	0.62	1.31	0.92	0.60	0.62	1.08	0.65	0.50
Total	100.09	99.23	99.54	98.81	99.95	98.91	101.95	100.69	100.56	99.02	100.11	100.36
Mg#	0.31	0.31	0.36	0.50	0.46	0.32	0.18	0.29	0.22	0.37	0.45	0.09
Trace elements (ppm)												
V												
Zn												
Rb	230	184	205	272	240	225	142	184	214	189	137	227
Sr	195	66	244	224	737	743	166	342	146	791	325	177
Y												
Zr												
Nb												
Ba	995	349	185	656	1008	967	1103	432	373	2024	880	482
La												
Ce												
Nd												
Sm												
Eu												
Gd												
Tb												
Yb												
Lu												
Rb/Sr	1.18	2.79	0.84	1.21	0.33	0.30	0.86	0.54	1.47	0.24	0.42	1.28
Eu/Eu*												
$(La/Yb)_N$												

Table 7.4 continued.

Batholith	Mpz	Mpz	Mpz	Mpz	Mpz	Mpz	Mpz	Mpz	Mpz	Hvn	Hvn	Hvn
Sample	OK7	BB10	H506	MPZ1	MPZ2B	MPZ3	TMP1	TMP2	TMP3	BC11	BP13	BC29
Reference	1	1	1	2	2	2	2	2	2	1	1	1
Major elements (wt%)												
SiO_2	75.92	73.99	74.95	75.03	71.31	70.21	72.49	71.81	70.69	75.03	73.42	73.39
TiO_2	0.07	0.23	0.09	0.12	0.33	0.65	0.00	0.13	0.36	0.17	0.11	0.13
Al_2O_3	13.82	14.01	13.87	13.46	16.11	14.84	15.61	16.28	16.08	13.62	14.99	14.97
$Fe_2O_3^T$	1.00	1.96	1.07	2.78	4.38	6.85	1.33	3.07	6.65	1.20	1.01	1.20
MnO	0.02	0.03	0.04	0.01	0.03	0.05	0.23	0.02	0.06	0.03	0.04	0.02
MgO	0.09	0.16	0.25	0.20	0.60	0.92	0.06	0.51	0.70	0.37	0.00	0.00
CaO	0.55	0.93	1.05	0.39	2.24	2.31	0.34	1.92	2.60	1.34	1.03	1.49
Na_2O	3.51	3.58	4.04	3.37	5.60	4.13	4.77	6.04	5.28	5.72	5.97	6.33
K_2O	5.81	5.52	4.79	6.13	1.69	3.54	5.89	1.87	1.14	2.75	3.12	2.32
P_2O_5	0.04	0.06	0.02	0.04	0.12	0.26	0.02	0.05	0.10	0.12	0.05	0.05
LOI	0.57	1.56	0.53							0.47	0.50	0.69
Total	101.40	102.03	100.70	100.05	99.55	99.55	101.25	100.45	100.35	100.82	100.24	100.59
Mg#	0.17	0.15	0.34	0.22	0.35	0.35	0.15	0.40	0.29	0.41		
Trace elements (ppm)												
V				3.25	15.83	28.43		9.93	22.22			
Zn				25.04	47.06	85.57	10.43	34.83	83.1			
Rb	292	188		246.57	137.29	123.83	498.22	90.95	124.96	53	118	44
Sr	61	319		107.55	713.48	432.41	50.56	437.32	481.73	655	487	623
Y				5.59	3.12	36.14	69.83	1.52	31.62			
Zr				150.77	165.01	303.98	56.6	94.48	197.05			
Nb				7.5	6.22	16.33	88.61	1.77	7.58			
Ba	233	886		248.74	376.34	722.16	148.1	2	121.82	426	252	322
La				37.36	21.99	73.79	10.05	12.12	46.7			
Ce				103.41	38.05	136.59	26.48	20.11	60.47			
Nd				26.57	13	49.24	15.26	8.87	40.51			
Sm				4.8	1.95	7.74		1.95	8.51			
Eu				0.33	0.72	1.24		0.65	1.19			
Gd				3.31	1.62	6.39		0.76	6.78			
Tb				0.46	0.2	0.77						
Yb				0.86	0.35	1.62		0.46	2.35			
Lu				0.17	0.05	0.26						
Rb/Sr	4.79	0.59		2.29	0.19	0.29	9.85	0.21	0.26	0.08	0.24	0.07
Eu/Eu*				0.24	1.2	0.52		1.37	0.46			
$(La/Yb)_N$				29.36	42.46	30.78		17.65	13.43			

Table 7.4 continued.

Batholith	Hvn	Hvn	Hvn	Hvn	Hvn	Hvn	Hvn	Hvn	Hvn	Hvn	Hvn	Hvn
Sample	BC1	BC4	BC7	BC2	BC8	BP10	BP4	ET1	JV27	BC19	BC20	HVN1A
Reference	1	1	1	1	1	1	1	1	1	1	1	2
Major elements (wt%)												
SiO_2	74.90	72.66	72.24	73.00	75.39	71.70	72.84	72.37	72.82	72.10	74.90	74.67
TiO_2	0.15	0.16	0.15	0.25	0.10	0.21	0.23	0.12	0.27	0.15	0.16	0.15
Al_2O_3	14.30	14.93	14.53	13.80	14.41	14.71	13.84	13.11	13.51	13.43	13.90	13.85
$Fe_2O_3^T$	0.92	1.31	1.12	1.85	0.98	1.82	2.02	1.02	1.76	1.33	1.14	3.40
MnO	0.03	0.02	0.02	0.01	0.01	0.02	0.05	0.02	0.07	0.04	0.05	0.04
MgO	0.30	0.53	0.00	0.40	0.00	1.65	0.39	0.18	0.63	0.11	0.30	0.17
CaO	1.46	1.56	1.30	1.15	0.83	2.02	0.92	0.58	0.98	0.68	0.95	0.79
Na_2O	4.20	6.40	6.67	3.40	5.06	5.38	4.82	5.34	3.34	4.43	3.50	3.57
K_2O	2.37	2.01	1.72	4.81	4.13	2.15	5.38	4.48	4.93	4.70	4.18	5.17
P_2O_5	0.06	0.07	0.05	0.08	0.05	0.11	0.10	0.08	0.03	0.05	0.04	0.05
LOI	0.39	0.54	0.83	0.67	0.62	0.38	0.59	0.49	1.14	0.30	0.22	
Total	99.08	100.19	98.63	99.42	101.58	100.15	101.18	97.79	99.48	97.32	99.34	99.50
Mg#	0.42	0.47		0.32		0.67	0.30	0.28	0.44	0.16	0.37	0.17
Trace elements (ppm)												
V												9.53
Zn												50.84
Rb	60	69	76	190	207	69	105	317	218	231	170	221.3
Sr	640	827	312	190	126	696	633	137	217	117	195	184.66
Y												38.24
Zr												178.77
Nb												21.48
Ba	260	264	150	520	236	285	514	225	940	545	460	720.53
La												66.56
Ce												139.9
Nd												51.69
Sm												8.52
Eu												1.17
Gd												6.76
Tb												1.15
Yb												2.66
Lu												0.39
Rb/Sr	0.09	0.08	0.24	1.00	1.64	0.10	0.17	2.31	1.00	1.97	0.87	1.2
Eu/Eu*												0.46
$(La/Yb)_N$												16.91

Table 7.4 continued.

Batholith	Hvn	Hvn	Hvn	Hvn	Hvn	Hvn	Hvn	Hvn	Nsp
Sample	HVN2	HVN3	HVN4	HVN5	HVN6	HVN7A	HVN7B	HVN8B	n=3
Reference	2	2	2	2	2	2	2	2	1
Major elements (wt%)									
SiO_2	73.72	74.65	74.45	73.02	75.51	74.57	73.88	72.70	72.21
TiO_2	0.21	0.09	0.02	0.29	0.04	0.13	0.11	0.12	0.25
Al_2O_3	14.38	15.09	15.17	15.44	14.62	14.37	15.49	16.18	14.39
$Fe_2O_3^T$	3.82	1.80	1.02	3.31	1.42	2.78	1.98	2.04	3.62
MnO	0.03	0.01	0.01	0.01	0.01	0.03	0.02	0.02	0.03
MgO	0.40	0.21	0.04	0.54	0.11	0.25	0.24	0.24	0.60
CaO	1.58	1.35	0.71	2.22	0.74	1.29	1.60	1.66	1.58
Na_2O	3.72	5.25	4.35	5.74	4.61	3.77	5.38	5.69	4.37
K_2O	4.16	2.52	4.75	1.13	3.70	4.29	2.34	2.43	3.57
P_2O_5	0.08	0.03	0.03	0.12	0.03	0.06	0.04	0.04	0.10
LOI									1.17
Total	99.90	99.90	99.60	100.40	99.90	99.60	99.80	100.00	101.89
Mg#	0.29	0.31	0.14	0.39	0.24	0.26	0.33	0.32	0.27
Trace elements (ppm)									
V	13.66	7.21	5.54	13.81	3.15	8.78	7.36	8.16	
Zn	45.48	31.63	11.78	46.78	19.63	36.17	33.3	33.73	
Rb	164.19	77.24	170.2	45.95	93.55	184.28	72.27	59.86	
Sr	196.77	524	301.7	756.28	229.87	180.11	613.71	664.88	
Y	21.36			3.86	4.9	23.73	1.94	3.23	
Zr	198.76	92.24	25.89	228.87	51.62	145.55	102.7	96.69	
Nb	14.89	3.33	4.5	2.42	3.94	16.37	2.92	2.66	
Ba	608.73	296.58	401.16	174.09	297.12	481.2	315.75	284.34	
La	69.33	13.39		27.42	8.34	48.07	14.07	21.41	
Ce	120.01	24.53	22.56	56.17	273.34	89.62	23.36	35.96	
Nd	41.82	10.94		19.07		28.56	10.78	14.39	
Sm		1.6				4.57	1.53	2.17	
Eu		0.41				0.63	0.46	0.64	
Gd		1.09				4.19	1.03	1.76	
Tb		0.15				0.66	0.14	0.22	
Yb		0.3				2.14	0.25	0.19	
Lu		0.04				0.4	0.04	0.07	
Rb/Sr	0.83	0.15	0.56	0.06	0.41	1.02	0.12	0.09	
Eu/Eu*		0.9				0.43	1.06	0.97	
$(La/Yb)_N$		30.16				15.18	38.03	76.15	

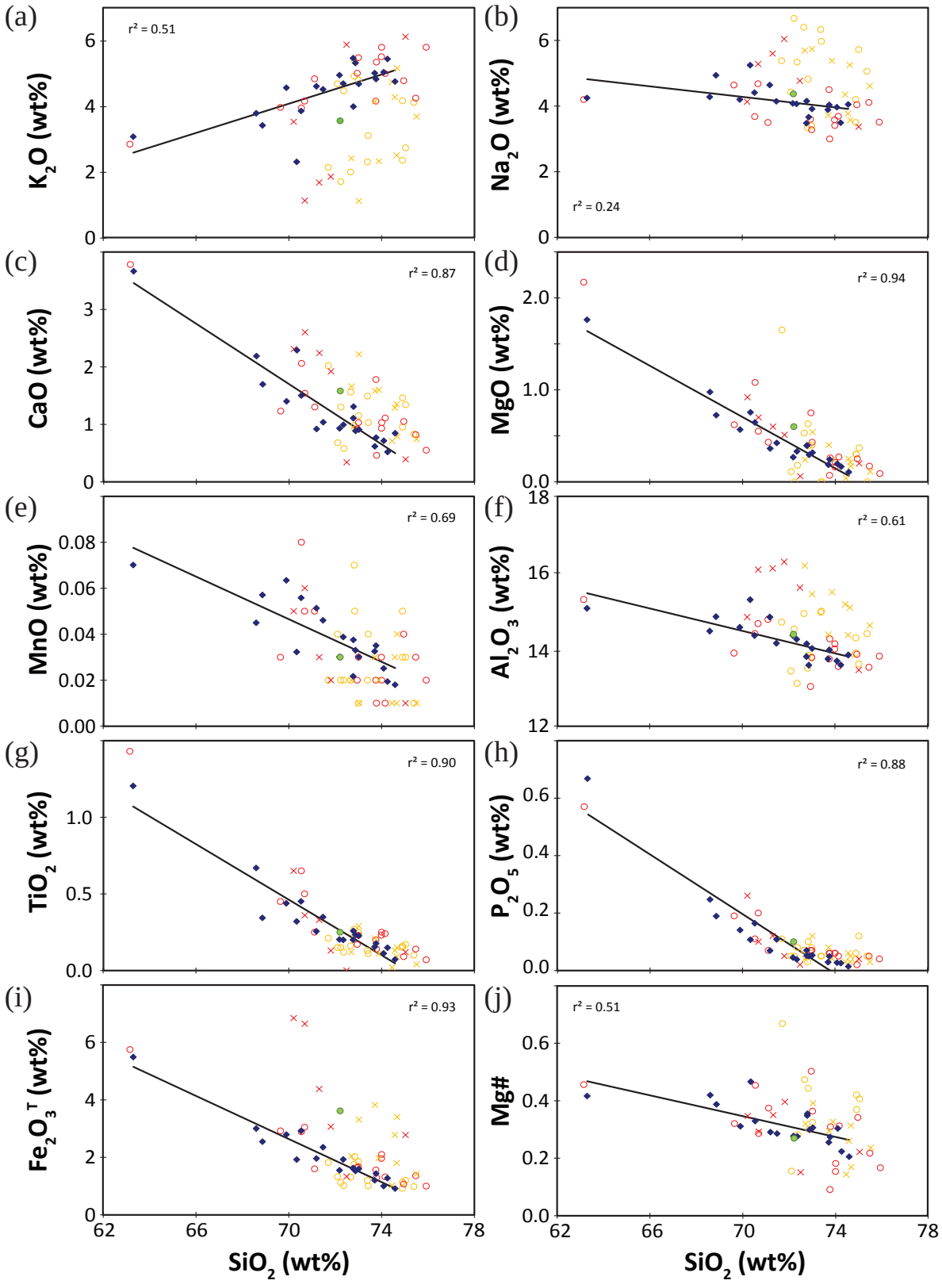


Figure 7.14. Major-element analyses *vs* SiO_2 for the Mpuluzi batholith (blue) compared with published data for the Mpuluzi batholith (red), the Heerenveen batholith (orange) and the average composition of the Nelspruit batholith (green): (a) K_2O; (b) Na_2O; (c) CaO; (d) MgO; (e) MnO; (f) Al_2O_3; (g) TiO_2; (h) P_2O_5; (i) $Fe_2O_3^T$; (j) Mg#. Data from Anhaeusser and Robb (1983; circles) and Yearron (2003; crosses).

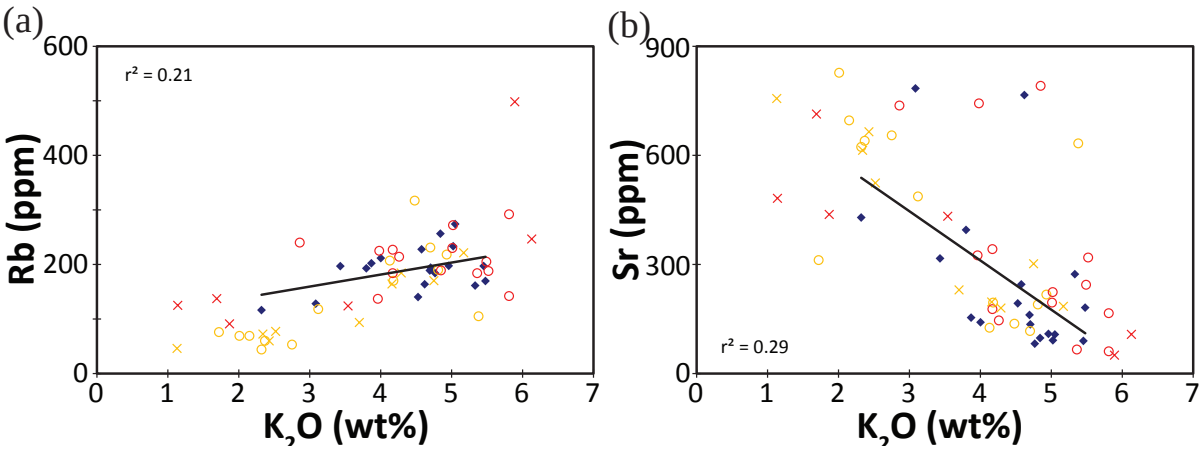


Figure 7.15. Trace-element analyses *vs* K_2O for the Mpuluzi batholith (blue) compared with published data for the Mpuluzi batholith (red) and Heerenveen batholith (orange): (a) Rb; (b) Sr. Data from Anhaeuser and Robb (1983; circles) and Yearron (2003; crosses).

The isotopic compositions obtained in this study are also consistent with the limited isotopic data available in the literature (Allsopp *et al.*, 1962; de Gasparis, 1967; Davies, 1971; Barton *et al.*, 1983; Maphalala *et al.*, 1989; Yearron, 2003; Schoene *et al.*, 2009; see Tables 7.5 and 7.6). The reported $^{87}Sr/^{86}Sr$ initial ratios are similarly low (0.7013–0.7052), and while the reported ages are lower than that determined in this study, this may reflect the use of a higher value for the ^{87}Rb decay constant with which the ages were calculated. Schoene *et al.* (2009) obtained Nd isotopic analyses of 11 samples from the Mpuluzi and other ~3.1 Ga batholiths; these show predominantly negative εNd values similar to those obtained in this study, and are considered to reflect crustal recycling after craton stabilisation. Four analyses of the contemporaneous Boesmanskop syenite complex were obtained by Yearron (2003); these show a similar range in εNd (-4.62 to 4.85) and were interpreted as indicating mixing between mantle and crustal material in the generation of the ~3.1 Ga granitoids; the older TTG suites exposed in the region were suggested as a candidate for the crustal component.

Table 7.5: Sr isotopic analyses for the Mpuluzi and other ~3.1 Ga granitoids in the region compiled from the literature (data from Allsopp et al., 1962; de Gasparis, 1967; Davies, 1971; Barton et al., 1983; Maphalala et al., 1989).

Unit sampled	Age (Ma)	$^{87}Sr/^{86}Sr_i$	err	Reference
Mpuluzi batholith *(alkali feldspar granite)*	3000 ± 125	0.7047	0.0103	Maphalala *et al.* (1989)
Mpuluzi batholith *(granodiorite)*	2979 ± 33	0.7017	0.0005	Maphalala *et al.* (1989)
Piggs Peak batholith	2986 ± 69			Davies (1971)
Heerenveen batholith	3028 ±14	0.7013	0.0002	Barton *et al.* (1983)
Mpuluzi batholith	3070 ± 60	fixed at 0.71		Allsopp *et al.* (1962)
Nelspruit batholith	2990 ± 70	0.7052	0.001	de Gasparis (1967)
Piggs Peak batholith	3050 ± 35	0.7054	0.0018	Davies (1971)

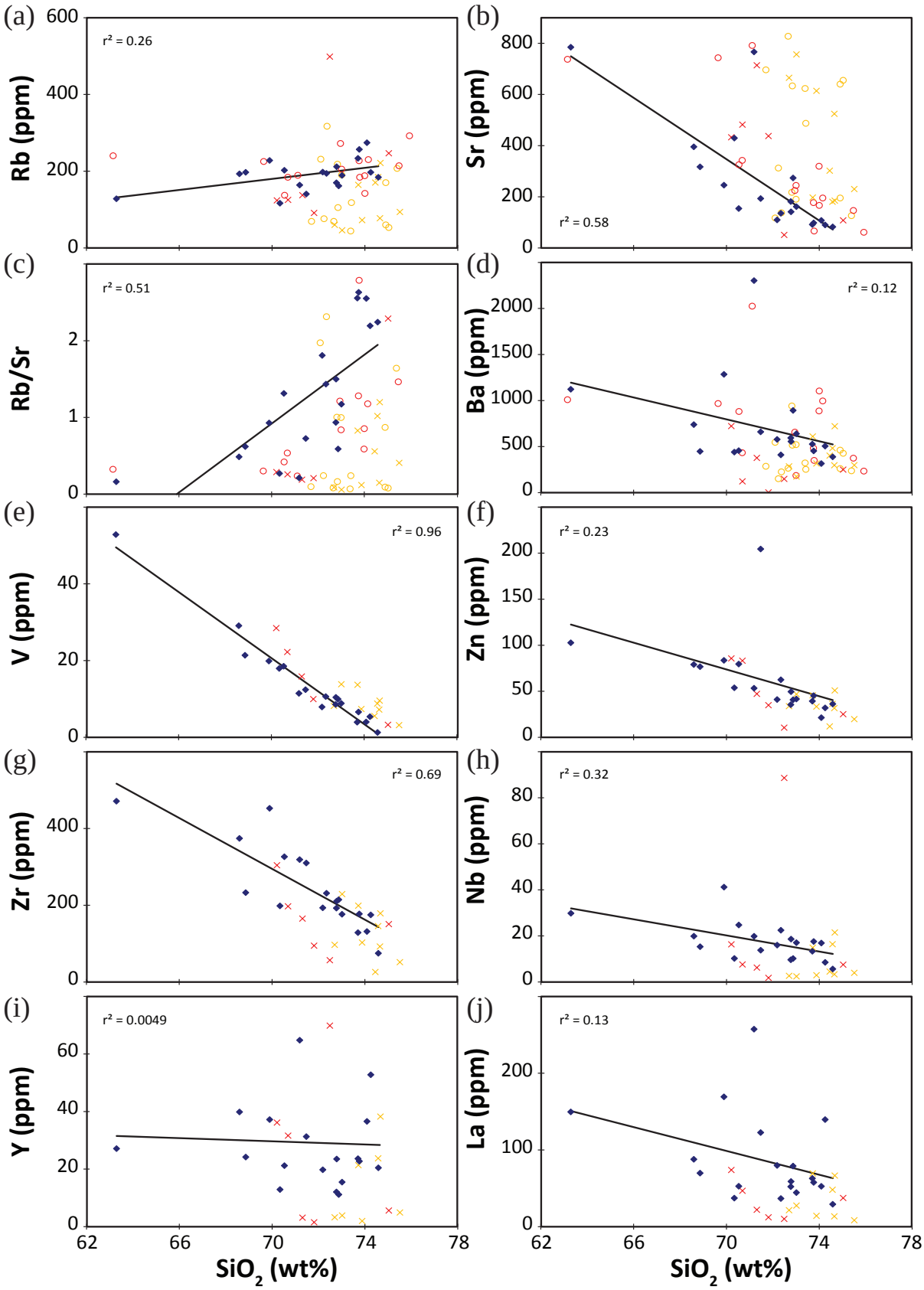
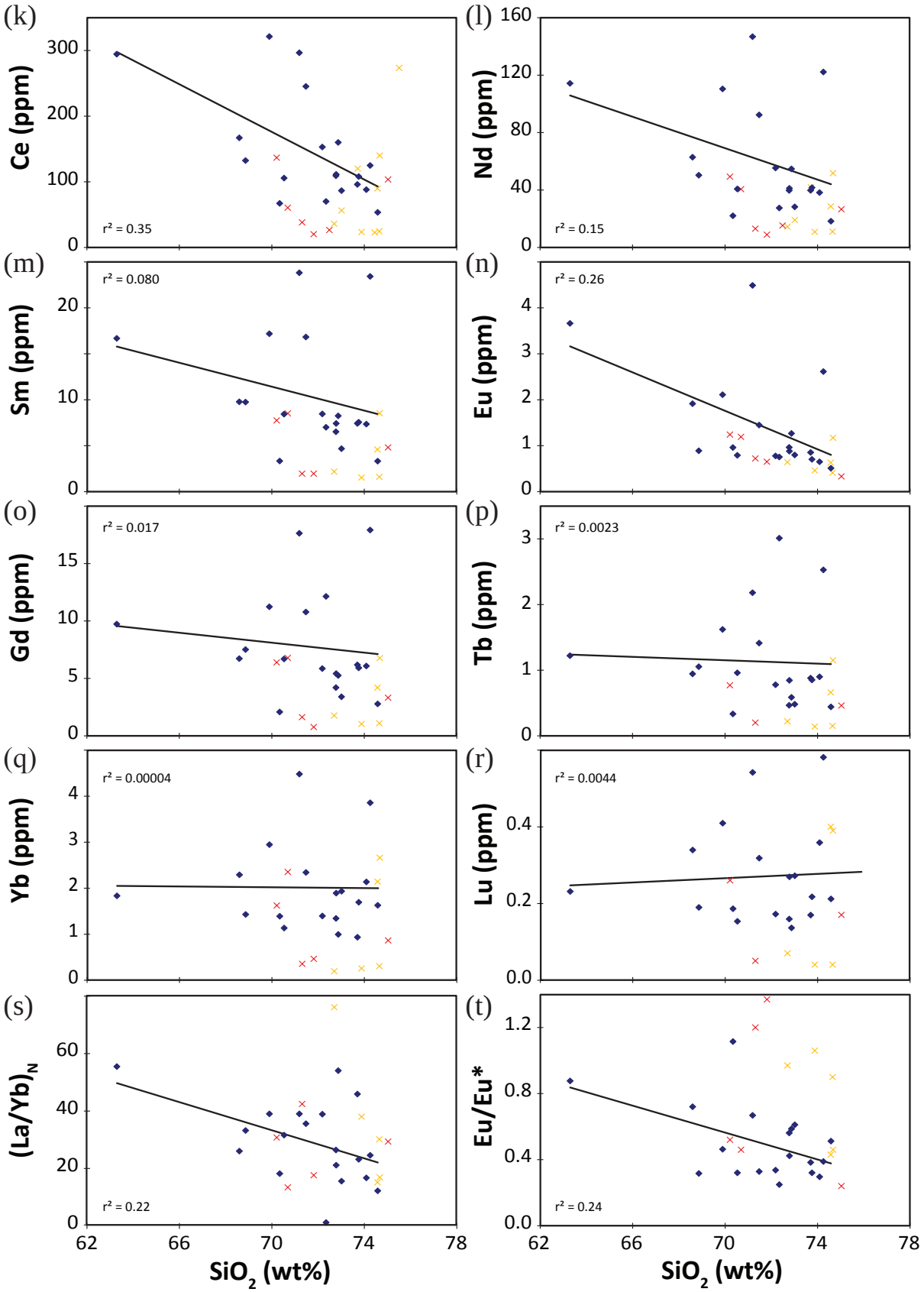


Figure 7.16. Trace-element analyses *vs* SiO_2 for the Mpuluzi batholith (blue) compared with published data for the Mpuluzi batholith (red) and Heerenveen batholith (orange): (a) Rb; (b) Sr; (c) Rb/Sr; (d) Ba; (e) V; (f) Zn; (g) Zr; (h) Nb; (i) Y; (j) La;



(k) Ce; (l) Nd; (m) Sm; (n) Eu; (o) Gd; (p) Tb; (q) Yb; (r) Lu; (s) $(La/Yb)_N$; (t) Eu/Eu*. Data from Anhaeusser and Robb (1983; circles) and Yearron (2003; crosses).

Table 7.6: Nd isotopic analyses for the ~3.1 Ga granitoids in the region compiled from the literature (data from Yearron, 2003; Schoene et al., 2009).

Unit sampled	$^{174}Sm/^{144}Nd$	$^{143}Nd/^{144}Nd$	err	eNd	Reference
Mpuluzi batholith	0.08895	0.510190	0.000008	-4.64	Schoene *et al.* (2009)
Mpuluzi batholith	0.11254	0.510754	0.000006	-3.08	Schoene *et al.* (2009)
Mpuluzi batholith	0.10510	0.510625	0.000006	-2.61	Schoene *et al.* (2009)
Mpuluzi batholith	0.10970	0.510699	0.000006	-3.01	Schoene *et al.* (2009)
Piggs Peak bathoilth	0.09667	0.510474	0.000006	-2.09	Schoene *et al.* (2009)
Piggs Peak batholith	0.11003	0.510780	0.000006	-1.54	Schoene *et al.* (2009)
Nelspruit batholith	0.10568	0.510758	0.000012	-0.23	Schoene *et al.* (2009)
Nelspruit batholith	0.15456	0.512098	0.000008	6.39	Schoene *et al.* (2009)
Nelspruit batholith	0.09584	0.510581	0.000008	0.24	Schoene *et al.* (2009)
Nelspruit batholith	0.10049	0.510523	0.000006	-2.76	Schoene *et al.* (2009)
Nelspruit batholith	0.09292	0.510478	0.000008	-0.59	Schoene *et al.* (2009)
Boesmanskop syenite (head)	0.10689	0.510573	0.000027	-4.35	Yearron (2003)
Boesmanskop syenite (head)	0.1025	0.510952	0.000017	4.85	Yearron (2003)
Boesmanskop syenite (head)	0.0946	0.510621	0.000009	1.54	Yearron (2003)
Boesmanskop syenite (tail)	0.1116	0.510655	0.000022	-4.62	Yearron (2003)

7.3.3 Constraints on source rocks

The presence of an older crustal component in the source region is indicated by the negative εNd values obtained for the Mpuluzi samples (see Section 7.2.3 above), as well as the inherited cores identified within Mpuluzi zircons (ranging in age from ~3.66 to ~3.36 Ga) and their Hf-isotopic compositions (which yield crustal model ages extending back to ~4.1 Ga; see discussion of source characteristics in Chapter Six).

The most likely candidate for the crustal component is the TTG suite intruding the Barberton Greenstone Belt (BGB) to the north of the Mpuluzi batholith, and the Ancient Gneiss Complex (AGC) to the southeast, which range in age from ~3.66 to ~3.2 Ga. In addition to covering the age range of the inherited cores found in the Mpuluzi zircons, the TTG suites also have Hf-isotopic compositions which are consistent with the values obtained for the majority of the Mpuluzi samples (Figure 7.17; $\varepsilon Hf = 1.2 \pm 1.0$ and -0.4 ± 1.9 for the TTG suite and the AGC respectively; Zeh *et al.*, 2009; 2011; Kröner *et al.*, 2014). The spread in εHf within the oldest AGC samples overlaps the ~4.1 Ga evolution line obtained for sample SWA10a (Figure 7.17), suggesting that the crustal component involved in the generation of the Mpuluzi magmas probably includes the ~3.66 Ga gneisses, and possibly even older material of which there is presently no exposure. The negative Eu anomalies observed in the Mpuluzi samples suggest melting of a plagioclase-bearing source, which is also consistent with their derivation from older tonalitic crust.

The low Zr content of the TTG suites (average of ~130 and ~215 ppm for the TTG suite and the AGC respectively; Hunter *et al.*, 1984; Yearron, 2003) suggests that the TTGs contain relatively few zircons. This is consistent with the inheritance-poor nature of the Mpuluzi samples (only 18 inherited cores identified in >600 grains analysed), which suggests that

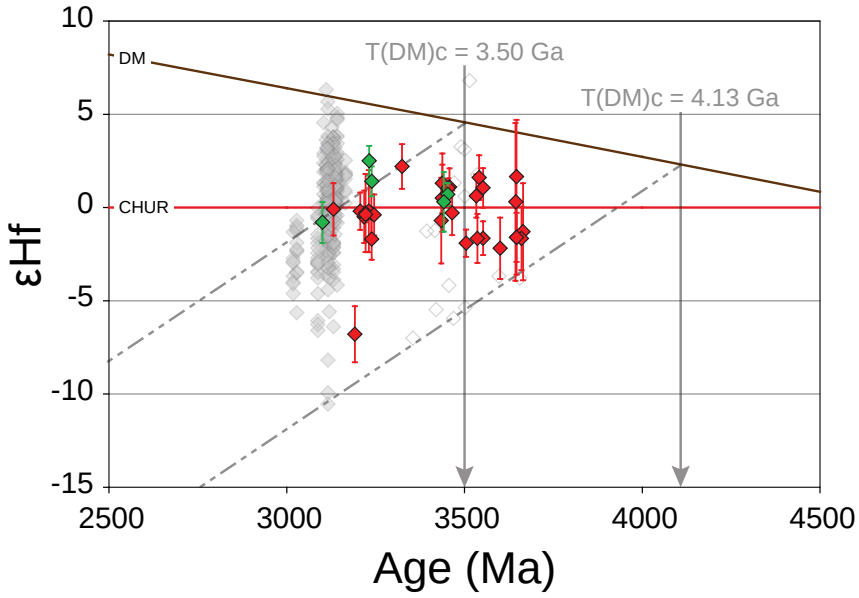


Figure 7.17. Plot of εHf *vs* age for samples from the TTG suite (green) and the Ancient Gneiss Complex (AGC; red), with all analyses from the Mpuluzi samples in this study plotted in grey for reference (filled diamonds are analyses from the main age population; open diamonds are inherited grains). Average (3.5 Ga) and oldest (4.13 Ga) crustal evolution lines shown for reference. Data from Zeh *et al.* (2009; 2011) and Kröner *et al.* (2014).

the source region was undersaturated in Zr; this makes the preservation of inherited grains unlikely (Miller *et al.*, 2003).

7.3.4 Factors influencing variation

The compositional variation within the Mpuluzi batholith is unlikely to be the result of a single factor. The factors controlling variation within a suite of related granites include characteristics of the source region and the processes operating during melt generation, transport, and emplacement (partial melting, assimilation, magma mixing, fractional crystallisation, and alteration; these are discussed in detail in Chapter Three); the evidence for and against each of these factors influencing the variation within the Mpuluzi batholith is discussed below.

Source heterogeneity

An isotopically heterogeneous source region is one possible explanation for the scatter in the initial $^{87}Sr/^{86}Sr$ ratios; the large range in model ages calculated from zircon Lu-Hf isotopes could also indicate that there were multiple components of different ages within the source region. The presence of components with different ages should produce a correlation between model ages calculated from different isotopic systems, but a plot of zircon Hf crustal model ages *vs* Sr T_{CHUR} model ages shows no correlation (Figure 7.18). This suggests that the scatter in initial $^{87}Sr/^{86}Sr$ may reflect the uncertainty on the $^{87}Rb/^{86}Sr$ ratio, rather than scatter in

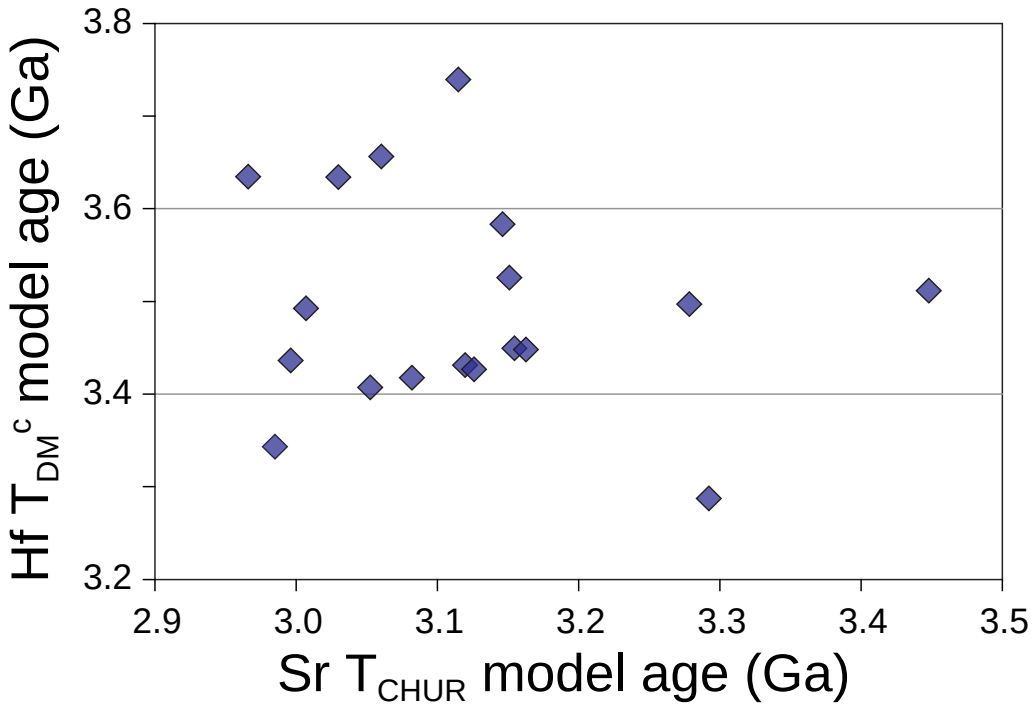


Figure 7.18. Plot of zircon Hf isotope T_{DM}^{c} (crustal) model ages *vs* T_{CHUR} model ages calculated from whole-rock Sr isotope compositions.

*Table 7.7: Zircon saturation temperatures calculated for samples from the Mpuluzi batholith (calculated using the method of Watson & Harrison, 1983). M = (Na+K+2Ca)/(Al*Si), in cation proportions.*

	Zr (ppm)	M	T (°C)
RSA03	471	1.9	848
RSA01	374	1.6	848
SWA18a	233	1.5	809
RSA05	453	1.5	876
RSA02	198	1.5	796
SWA07	326	1.5	845
RSA04	319	1.4	846
RSA08	310	1.4	845
SWA10a	193	1.4	802
RSA09	231	1.4	819
SWA20	192	1.4	799
SWA03	210	1.4	811
RSA06	214	1.4	810
SWA13a	176	1.4	797
SWA11	128	1.4	771
SWA09	177	1.4	797
SWA02a	131	1.4	770
RSA07	175	1.3	800
SWA05	75	1.4	725

the source region, whereas the range in zircon Lu-Hf isotopes results from mixing between different components or low-degree partial melting in the presence of zircon (e.g. Zeh *et al.*, 2009; 2011; Tang *et al.*, 2014). This is discussed further in the section on magma mixing below.

Partial melting

If variation in the degree of partial melting has controlled the geochemical variation within the Mpuluzi batholith, this should be reflected in higher estimated melting temperatures for the more mafic samples relative to the felsic samples. Melting temperatures were estimated from the zircon saturation of the Mpuluzi samples and are presented in Table 7.7. Calculated temperatures rely on the whole-rock Zr content, the peraluminosity of the melt (M), and the partitioning of Zr between zircon and the melt (Watson & Harrison, 1983). This simple relationship makes for straightforward temperature calculations, but interpretation of the data is made more complicated by the need to determine whether the source was saturated in zircon at the time of melting. This determination is based on the presence of inherited cores in zircon grains: abundant inheritance indicates that the source was saturated in zircon, whereas minimal or no inheritance indicates undersaturation (Miller *et al.*, 2003). For saturated sources, temperature estimates calculated using this method are maximum estimates of magma temperatures, while samples from undersaturated sources provide minimum temperature estimates.

Samples from the Mpuluzi batholith, with a total of 18 inherited cores detected in all samples, are clearly inheritance-poor, and therefore likely to represent a zircon-undersaturated source, and give minimum estimates of melting temperatures. Calculated saturation temperatures

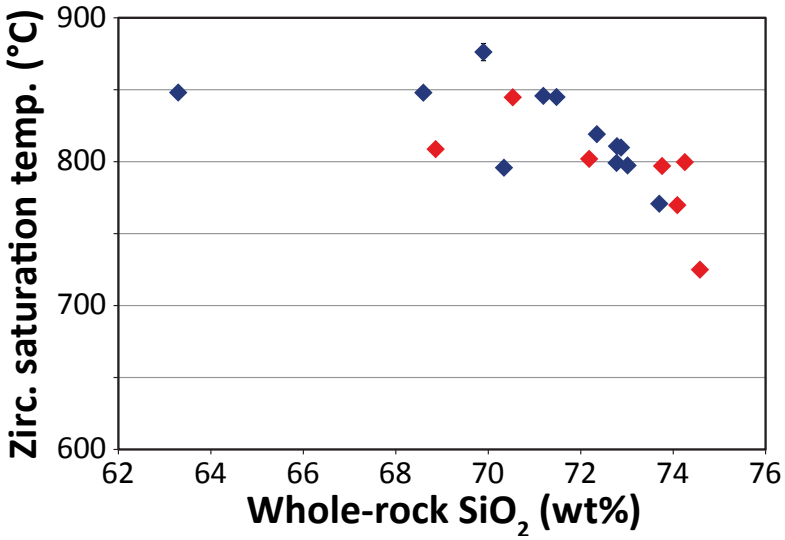


Figure 7.19. Estimates of magma temperature calculated from zircon saturation, plotted *vs* whole-rock SiO_2 content. Data points in red are samples with at least one inherited core detected.

range from 725 to 876 °C, with an average of 811 ± 35 °C (Table 7.7). A plot of magma temperatures calculated from zircon saturation *vs* the whole-rock SiO_2 content shows a weak inverse correlation (Figure 7.19; samples with inherited grains detected are shown in red). The strength of the correlation is likely to be underestimated as the mafic samples generally have less inheritance and may therefore be more strongly undersaturated than the felsic samples.

Plots of calculated ages for the Mpuluzi samples versus the whole rock SiO_2 content show a weak positive correlation (Figure 7.20). Although the samples generally overlap within error, the presence of the correlation in all three age datasets (weighted average of uncorrected $^{207}Pb/^{206}Pb$ ages, intercept ages from corrected and uncorrected data) suggests that the trend indicates a real age progression, with the more felsic samples being generally older than the more mafic samples. This age progression is consistent with the decrease in calculated melting temperature with increasing SiO_2, and supports the suggestion that partial melting has controlled at least some of the geochemical variation within the Mpuluzi batholith. The combination of the age and temperature data suggests that felsic, low-temperature magmas were produced at the onset of melting, and a build-up in heat over time produced higher degrees of partial melting and shifted the magmas towards increasingly more mafic compositions. However, these two trends could also be explained by changes in the proportion of juvenile material mixed into the generated melt, as a juvenile component would most likely be more mafic (and higher temperature) and would thus shift the magma towards more mafic compositions. This is discussed further below.

Assimilation

The strong correlations seen within the geochemical and isotopic datasets (particularly the tight isochrons obtained from the Sr and Nd isotopic data) suggest that any assimilant must be a relatively homogeneous single component. Based on the assumption that the most felsic samples represent the uncontaminated magma composition, the assimilant must also be more mafic. The large geographic extent of the Mpuluzi batholith makes it unlikely that contamination of the magma could be coeval with emplacement, particularly as SiO_2 content does not vary systematically with the spatial distribution of the samples.

Magma mixing

The well-defined linear trends between the major elements and SiO_2 are consistent with mixing between two chemically distinct components (see Figure 7.3 above); linear correlations observed between other major elements (e.g. CaO, Mg# *vs* MgO; Figure 7.21) are also consistent with mixing (Clemens *et al.*, 2010).

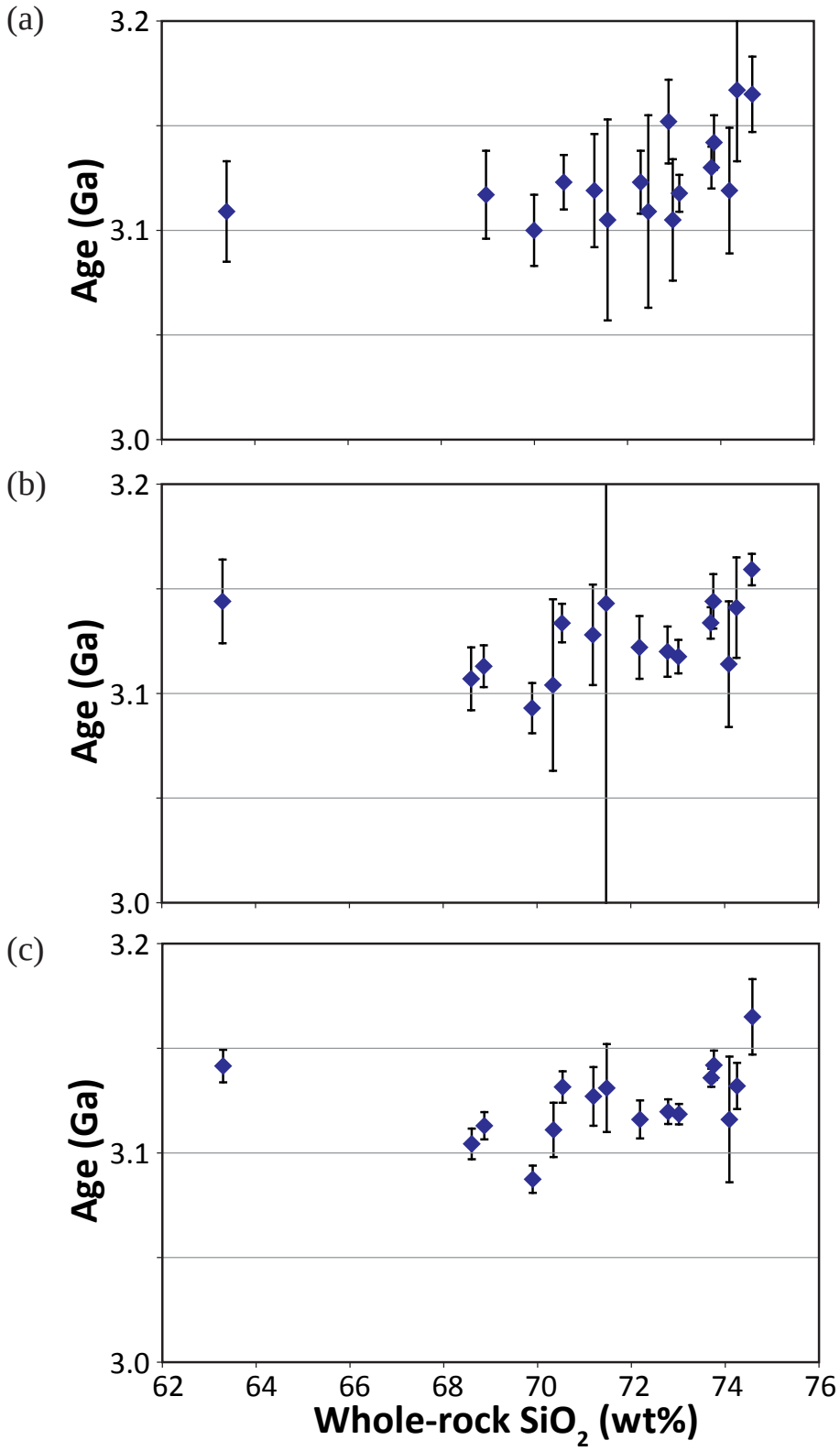


Figure 7.20. Plot of calculated zircon U-Pb ages *vs* whole-rock SiO_2 for Mpuluzi samples: (a) intercept ages (corrected); (b) intercept ages (uncorrected); (c) weighted mean of $^{207}Pb/^{206}Pb$ ages (uncorrected).

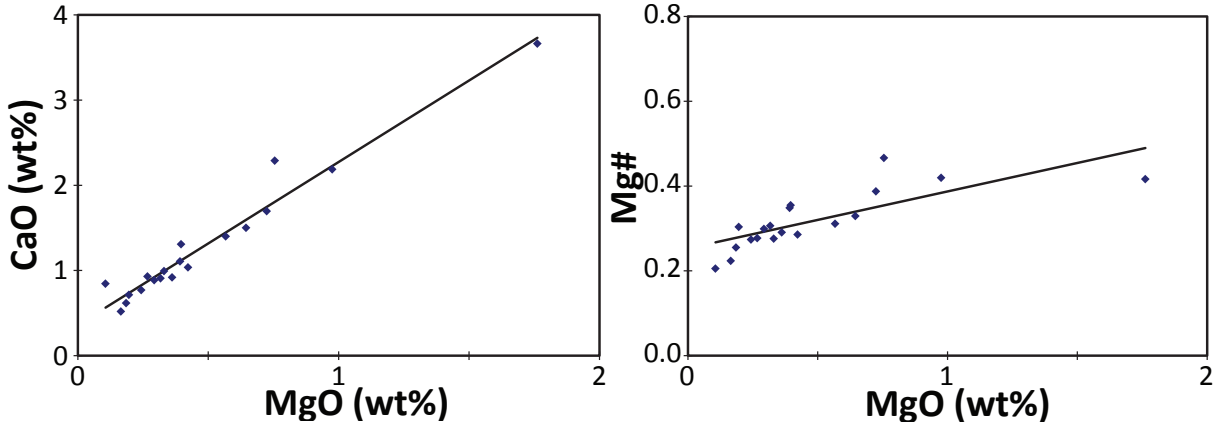


Figure 7.21. Plot of (a) CaO and (b) Mg# (= Mg/(Mg+Fe^T)) *vs* MgO for Mpuluzi samples.

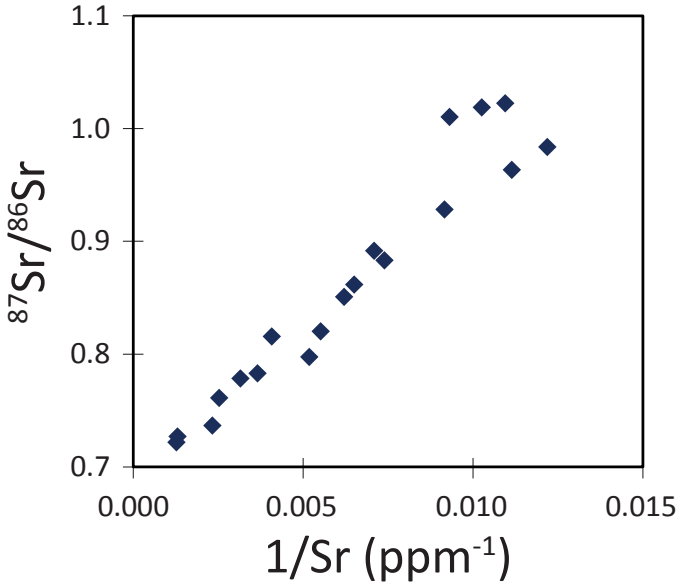


Figure 7.22. Plot of measured $^{87}Sr/^{86}Sr$ *vs* 1/Sr for Mpuluzi samples.

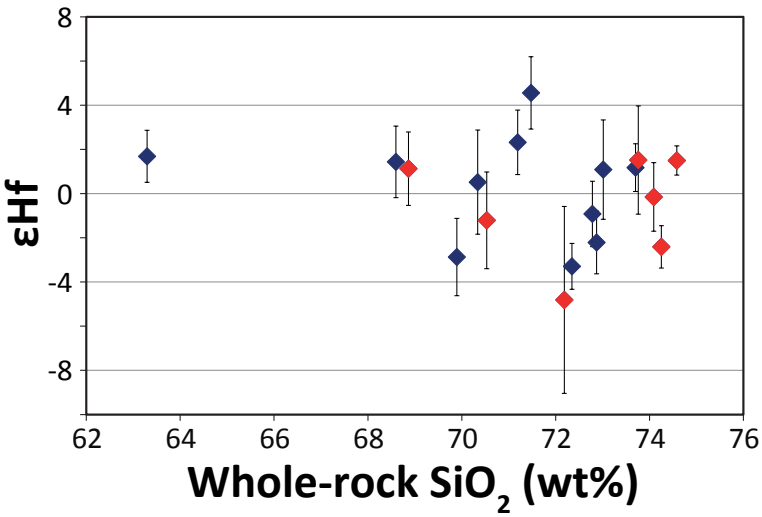


Figure 7.23. Average εHf *vs* whole-rock SiO_2 contents. Data points in red are samples with at least one inherited core detected.

The whole-rock isotopic data are also consistent with mixing between two isotopically distinct components. Figure 7.22 shows a linear trend between $^{87}Sr/^{86}Sr$ and the inverse of the Sr content; this correlation does not necessarily require mixing, as samples which form a true isochron may coincidentally produce such a trend; rather, the absence of a correlation would indicate that mixing was not involved (Faure, 1986).

A mixed source makes interpretation of the Sr and Nd isotopic compositions more complex, as true isochrons cannot be obtained if the source region contains multiple components. The good agreement of the ages obtained from the 'isochrons' with the zircon U-Pb ages suggests that any such effect of mixing on the Sr and Nd isotopic compositions is negligible.

The case for magma mixing is supported by the zircon Hf-isotopic data, which show a spread within each sample, suggesting mixing between an evolved (crustal) component (with ages extending back to ~4 Ga), and a juvenile (mantle) component (~3.2 Ga). If the proportion of juvenile material is controlling the variation in whole-rock composition this should be reflected in the Hf-isotopic data as a more juvenile isotopic composition for the more mafic samples, and a more evolved composition for the more felsic samples. A plot of εHf versus whole-rock SiO_2 shows considerable scatter and only a weak negative correlation, suggesting that other factors contribute to the variation within the Mpuluzi samples (Figure 7.23). One possible alternate explanation for the spread in Hf isotopic compositions is that the variation is a result of low-degree partial melting in the presence of zircon (e.g. Zeh *et al.*, 2009; 2011; Tang *et al.*, 2014). In this model, the vairation in Hf is a consequence of the fact that ^{177}Hf is controlled by zircon, while ^{176}Hf resides in the phase controlling the Lu budget (e.g. garnet), and incongruent melting may release the two at different rates and result in large variations in $^{176}Hf/^{177}Hf$ ratios. While this process may have played a role in producing the Hf variation in the Mpuluzi samples, the presence of a strong evolution line in the most evolved sample (SWA10a) suggests that at least some of this variation results from mixing between an evolved source and juvenile material.

Fractional crystallisation

Previous studies have invoked fractional crystallisation to explain the compositional variation within the Mpuluzi batholith (e.g. fractionation of plagioclase; Anhaeusser & Robb, 1983; K-feldspar fractionation; Yearron, 2003). Progressive fractional crystallisation would be expected to produce a sequence of rocks with increasingly felsic compositions crystallised at decreasing temperatures. The combination of zircon data (ages and compositions; presented in Chapter Six) and whole-rock compositions obtained in this study allows an examination of the relationship between the ages, crystallisation temperatures, and compositions of the Mpuluzi samples.

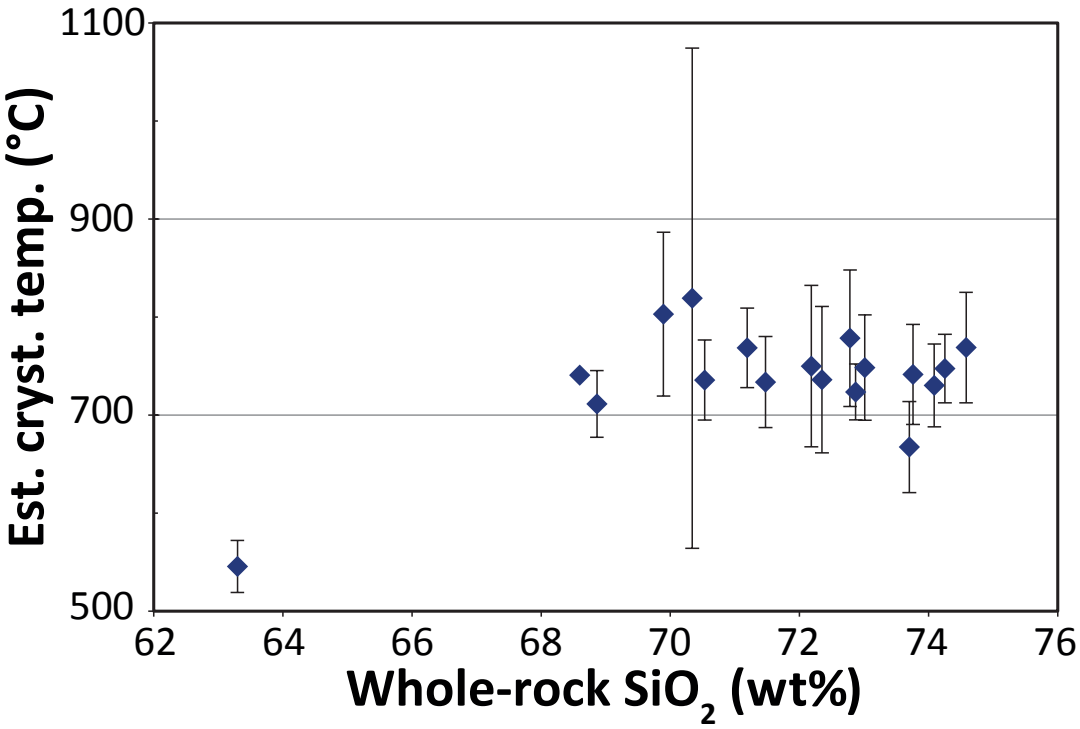


Figure 7.24. Ti-in-zircon crystallisation temperatures *vs* whole-rock SiO_2 content (note that the anomalous low-temperature sample is a single data point).

One of the most common lines of evidence for fractional crystallisation is the presence of inflection points on inter-element variation diagrams, reflecting the onset of crystallisation of a particular phase. This is commonly shown by elements that are essential stoichiometric components in accessory phases (e.g. Zr in zircon, Ti in ilmenite or titanite, P in apatite). Such inflection points are absent from the Mpuluzi samples; this may be a result of their similar mineralogy, relatively high SiO_2, and their narrow range in SiO_2 (~63–75%), and thus does not necessarily indicate the absence of fractional crystallisation.

The weak positive correlation seen between the calculated ages and whole rock SiO_2 (see Figure 7.20 above) contradicts the relationship expected from fractional crystallisation, which operates to produce a series of progressively more felsic rocks through time. While the correlation is suggestive, the uncertainties on the ages are large enough that they all overlap within two standard deviations, and thus the possibility that the correlation is entirely coincidental cannot be ruled out. Nevertheless, the mafic rocks are clearly not *older* than the felsic samples and at best this does not constitute evidence for fractionation.

A plot of crystallisation temperature (calculated using Ti-in-zircon thermometry; see Section 6.3.4) *vs* whole rock SiO_2 content does not show the inverse correlation expected from progressive fractional crystallisation (Figure 7.24; note that the anomalously low temperature estimate from the most mafic sample represents only a single grain). This lack of correlation

on its own does not rule out fractional crystallisation, but when taken together with the inverse age progression and lack of inflection points, it becomes very difficult to argue that fractional crystallisation has played a significant role in producing the geochemical variation within the Mpuluzi batholith.

Alteration

Although many of the Mpuluzi samples have experienced extensive alteration (mainly of biotite to chlorite + epidote, and of plagioclase to sericite; see Chapter Five), this is interpreted to be late-stage re-equilibration of crystals with residual fluids (deuteric alteration), rather than interaction with an external agent. This means that the alteration affects the mineral composition but not the bulk composition of the samples, and thus does not contribute to the compositional variation within the Mpuluzi batholith.

7.4 Conclusions

The Mpuluzi samples display geochemical and isotopic characteristics consistent with their derivation from melting of older igneous material (i.e. they classify as I-type granites). The most likely candidate for the source material is the TTG gneisses of the Ancient Gneiss Complex and the TTG suite intruding the Barberton Greenstone Belt; melting of these is consistent with the characteristics of the Mpuluzi batholith in terms of their crystallisation ages (inherited grains in the Mpuluzi samples match with the ages of the TTG gneisses) and model ages (calculated from both Hf isotopes in zircon and whole-rock Nd isotopes). The TTGs also have low Zr contents, and this is consistent with the limited inheritance observed in the Mpuluzi samples.

The geochemical, isotopic, and geochronological data obtained in this study allow an assessment of the processes operating to produce the range of compositions in the Mpuluzi batholith. The zircon Hf isotopic data clearly indicate mixing between a crustal component (likely derived from the older TTG gneisses) and a juvenile component. The lack of correlation between εHf and SiO_2 indicates that while mixing controls the isotopic variation, it is not the dominant control on the variations in whole-rock chemistry; a negative correlation between estimated melting temperatures (calculated from zircon saturation) and whole-rock SiO_2 contents suggests that this variation may rather be produced by changes in the temperature at which the magmas formed. This is supported by the calculated ages which, while generally overlapping within error, show a weak positive correlation between age and SiO_2. This suggests that the most felsic magmas were formed first and as more heat was introduced into the system the degree of partial melting increased, shifting the magmas towards more mafic compositions. The presence of a juvenile component also indicates that

the intrusion of mantle-derived material into the lower crust may be the heat source for crustal melting. The low Zr content of the source region means that a small addition of juvenile material would be visible in the Hf-isotopic composition without substantially altering the whole-rock chemistry.

Chapter Eight – Conclusions

This study has carried out a detailed characterisation of the Mpuluzi batholith in terms of its geochemical and isotopic composition, range of emplacement ages, and the composition of key phases. These compositional data were then used to examine the processes which were involved in magma generation and emplacement, as well as the age and composition of the source region.

8.1 Characteristics of Mpuluzi samples

The samples of the Mpuluzi batholith analysed in this study classify as granite and quartz monzonite. They display high-K, calc-alkaline, metaluminous to slightly peraluminous compositions. The samples range from ~63 to 75 wt% SiO_2, and define broad linear trends for most elements, with no obvious divisions into multiple groups, and no inflection points.

The Mpuluzi samples have a major phase assemblage of quartz + microcline + plagioclase + biotite; all samples have accessory allanite, apatite, zircon, and oxides (ilmenite and/or magnetite); hornblende and titanite are present in the more mafic samples, while primary muscovite is present in felsic samples. Many samples show evidence of deuteric alteration (biotite → chloritization + epidote; plagioclase → sericite); some display primary or secondary foliations (defined by aligned biotite and elongated quartz respectively).

Zircon U-Pb ages obtained from Mpuluzi samples range from 3165 to 3090 Ma, and form a single broad peak centred at ~3120 Ma. Inherited cores are scarce, and yield ages ranging from 3660 to 3360 Ma (average = ~3.5 Ga). Zircon Hf isotopic compositions yield crustal model ages ranging from 4.1 to 3.1 Ga. Whole-rock Sr-isotope analyses yield an isochron age of 3113 ± 84 Ma, and model ages ranging from 3.5 to 3.0 Ga; Nd isotopic compositions yield an isochron age of 3027 ± 520 Ma and model ages ranging from 3.6 to 3.2 Ga.

The composition of biotite in the Mpuluzi samples is controlled by the whole-rock composition (except Ti which is influenced by the presence of ilmenite and/or titanite). Zircon compositions are strongly affected by metamictisation, but indicate that zircon had a long crystallisation history (which may affect the resolvability of U-Pb ages). Metamict zircons may be a product of late-stage crystallisation, with higher concentrations of U, Th, and other incompatible elements.

The samples from the Mpuluzi batholith examined in this study cannot be subdivided on mineralogical, geochemical, or isotopic grounds. Although the samples show a range in

composition and age, they form a continuum of compositions, and no distinct batches of magma were distinguished.

8.2 Constraints on the source region

The mineralogical, geochemical, and isotopic characteristics of the Mpuluzi batholith are consistent with their derivation from melting of igneous rocks. The U-Pb ages of inherited zircons indicate that the source region included material ranging in age from ~3.6 to 3.3 Ga. Zircon Hf-isotope composition and whole-rock Sr and Nd isotopic composition also indicate an older component in the source region, with model ages extending back to ~4.1 Ga.

The most likely candidates for the source region are the Ancient Gneiss Complex (AGC) and the TTG suite that intrudes the Barberton Greenstone Belt. These have crystallisation ages and model ages consistent with the characteristics of the Mpuluzi batholith. The AGC and TTG suite also have low Zr contents, which is consistent with the limited number of inherited zircons obtained from the Mpuluzi samples.

8.3 Processes involved in magma generation and emplacement

The zircon Hf isotopic data clearly indicate mixing between an evolved, crustal component (likely derived from the older AGC and/or TTG suite), and juvenile material. However, the zircon Hf isotope composition does not show a systematic variation with whole-rock chemistry, which indicates that while mixing controls the isotopic variation, it is not the dominant control on the variations in whole-rock chemistry.

A systematic relationship is observed between estimates of melting temperatures (calculated from zircon saturation) and whole-rock composition, which suggests that changes in melting temperature produced the variation seen within the Mpuluzi samples. The oldest U-Pb ages are obtained from the most felsic samples, while the mafic samples yield younger ages. This suggests that a build-up of heat over time progressively increased the degree of partial melting, shifting the magmas towards more mafic compositions. In this model, the heat source is probably also the source of the juvenile component observed in the isotopic data; this provided enough material to affect the isotopic composition without substantially altering the whole-rock chemistry. The addition of juvenile material, although minor, suggests that magma underplating probably provided the heat for melting.

8.4 Tectonic implications

As outlined in Chapter Two, there are two competing models for the evolution of the eastern Kaapvaal Craton (1) subduction-accretion models, in which distinct terranes are juxtaposed along major suture zones and the dome-and-keel structure resulted from orogenic collapse; (2) vertical tectonic models, in which dense greenstone material sinks into partially molten granitoid crust (see Section 2.5 for further details). In both sets of models, most of the activity was over by 3.2 Ga.

Dating of the Mpuluzi batholith in this study confirms that its emplacement was significantly later than the 3.2 Ga event (emplacement of the Mpuluzi batholith occurred at ~3.12 Ga, nearly 100 million years later), which suggests that the question of which tectonic regime was operating at 3.2 Ga is irrelevant to the formation of these granites. The new Hf isotopic data, combined with the whole-rock Sr and Nd isotopic compositions, suggest that the Mpuluzi batholith was generated melting of the older TTGs, while the Hf isotopic compositions also require a juvenile input.

These isotopic constraints, combined with the time gap between the 3.2 Ga tectono-metamorphic event and the emplacement of the Mpuluzi batholith, and the large volume of crust that must have melted to give the 3.1 Ga batholiths, indicate that this melting requires a new heat source. The most obvious possibility is that the trigger was asthenospheric uprise associated with extension, but if so this was clearly unsuccessful in breaking up the eastern part of the Kaapvaal Craton. The subsequent stability of the craton was a result of this melting, as this exhausted the fusible material from a large volume of the crust, rendering it refractory and welding it to the lithospheric mantle.

References

Allen, C. M. & Campbell, I. H. (2012). Identification and elimination of a matrix-induced systematic error in LA–ICP–MS $^{206}Pb/^{238}U$ dating of zircon. *Chemical Geology* **332–333**, 157-165.

Allsopp, H. L., Roberts, H. R., Schreiner, G. D. L. & Hunter, D. R. (1962). Rb-Sr Age Measurements on Various Swaziland Granites. *Journal of Geophysical Research* **67**, 5307-5313.

Andersen, T. (2002). Correction of common lead in U-Pb analyses that do not report ^{204}Pb. *Chemical Geology* **192**, 59-79.

Anderson, J. L. (1983). Proterozoic anorogenic granite plutonism of North America. *Geological Society of America Memoirs* **161**, 133-154.

Anhaeusser, C. R. (1971). The Barberton Mountain land, South Africa: a guide to the understanding of the archaean geology of Western Australia. *Special Publications of the Geological Society of Australia* **3**, 103-119.

Anhaeusser, C. R. (2014). Archaean greenstone belts and associated granitic rocks – A review. *Journal of African Earth Sciences* **100**, 684-732.

Anhaeusser, C. R. & Robb, L. J. (1981). Magmatic cycles and the evolution of the Archaean granitic crust in the Eastern Transvaal and Swaziland. *Special Publications of the Geological Society of South Africa* **7**, 457-467.

Anhaeusser, C. R. & Robb, L. J. (1983a). Chemical analyses of granitoid rocks from the Barberton Mountain Land. *Geological Society of South Africa Special Publication* **9**, 189-219.

Anhaeusser, C. R. & Robb, L. J. (1983b). Geological and Geochemical Characteristics of the Heerenveen and Mpuluzi Batholiths South of the Barberton Greenstone Belt and Preliminary Thoughts on Their Petrogenesis. *Special Publications of the Geological Society of South Africa* **9**, 131-151.

Armstrong, R. A., Compston, W., de Wit, M. J. & Williams, I. S. (1990). The stratigraphy of the 3.5-3.2 Ga Barberton Greenstone Belt revisited: A single zircon ion microprobe study. *Earth and Planetary Science Letters* **101**, 90-106.

Aulbach, S., Griffin, W. L., O'Reilly, S. Y. & McCandless, T. E. (2004). Genesis and evolution of the lithospheric mantle beneath the Buffalo Head Terrane, Alberta (Canada). *Lithos* **77**, 413-451.

Baasner, A., Schmidt, B. C. & Webb, S. L. (2013). The effect of chlorine, fluorine and water on the viscosity of aluminosilicate melts. *Chemical Geology* **357**, 134-149.

Barbarin, B. (1990). Granitoids: Main petrogenetic classifications in relation to origin and tectonic setting. *Geological Journal* **25**, 227-238.

Barton, J. M. J., Robb, L. J., Anhaeusser, C. R. & Van Nierop, D. A. (1983). Geochronologic and Sr-isotopic studies of certain units in the Barberton granite-greenstone terrane, South Africa. *Special Publications of the Geological Society of South Africa* **9**, 63-72.

Belcher, R. W. & Kisters, A. F. M. (2006a). Progressive adjustments of ascent and emplacement controls during incremental construction of the 3.1 Ga Heerenveen batholith, South Africa. *Journal of Structural Geology* **28**, 1406-1421.

Belcher, R. W. & Kisters, A. F. M. (2006b). Syntectonic emplacement and deformation of the Heerenveen batholith: Conjectures on the structural setting of the 3.1 Ga granite magmatism in the Barberton granite-greenstone terrain, South Africa. *Geological Society of America Special Papers* **405**, 211-231.

Belousova, E. A., Griffin, W. L. & O'Reilly, S. Y. (2006). Zircon Crystal Morphology, Trace Element Signatures and Hf Isotope Composition as a Tool for Petrogenetic Modelling: Examples From Eastern Australian Granitoids. *Journal of Petrology* **47**, 329-353.

Belousova, E. A., Griffin, W. L., O'Reilly, S. Y. & Fisher, N. I. (2002). Igneous Zircon: Trace Element Composition as an Indicator of Source Rock Type. *Contributions to Mineralogy and Petrology* **143**, 602-622.

Binns, R. A., Gunthorpe, R. J. & Groves, D. I. (1976). Metamorphic patterns and development of greenstone belts in the eastern Yilgarn Block, Western Australia. *The early history of the Earth*, 303-313.

Boehnke, P. & Harrison, T. M. (2014). A meta-analysis of geochronologically relevant half-lives: what's the best decay constant? *International Geology Review* **56**, 905-914.

Bowden, P., Batchelor, R. A., Chappell, B. W., Didier, J. & Lameyre, J. (1984). Petrological, geochemical and source criteria for the classification of granitic rocks: a discussion. *Physics of the earth and planetary interiors* **35**, 1-11.

Brown, W. L. & Parsons, I. (1989). Alkali feldspars: ordering rates, phase transformations and behaviour diagrams for igneous rocks. *Mineral Mag* **53**, 25-42.

Buddington, A. F. (1959). Granite emplacement with special reference to North America. *Geological Society of America Bulletin* **70**, 671.

Carmichael, I. S. E., Turner, F. J. & Verhoogen, J. (1974). *Igneous petrology*: McGraw-Hill.

Castro, A., Moreno-Ventas, I. & de la Rosa, J. D. (1991). H-type (hybrid) granitoids: a proposed revision of the granite-type classification and nomenclature. *Earth-Science Reviews* **31**, 237-253.

Cawood, P. A. & Nemchin, A. A. (2000). Provenance record of a rift basin: U/Pb ages of detrital zircons from the Perth Basin, Western Australia. *Sedimentary Geology* **134**, 209-234.

Chappell, B. W. (1984). Source Rocks of I- and S-Type Granites in the Lachlan Fold Belt, Southeastern Australia. *Philosophical Transactions of the Royal Society of London. Series A, Mathematical and Physical Sciences* **310**, 693-706.

Chappell, B. W. (1996). Compositional variation within granite suites of the Lachlan Fold Belt: its causes and implications for the physical state of granite magma. *Transactions of the Royal Society of Edinburgh-Earth Sciences* **87**, 159-170.

Chappell, B. W. (2004). Towards a unified model for granite genesis. *Transactions of the Royal Society of Edinburgh: Earth Sciences* **95**, 1-10.

Chappell, B. W., Bryant, C. J., Wyborn, D., White, A. J. R. & Williams, I. S. (1998). High- and Low-Temperature I-type Granites. *Resource Geology* **48**, 225-235.

Chappell, B. W. & White, A. J. R. (1974). Two contrasting granite types. *Pacific Geology* **8**, 173-174.

Chappell, B. W. & White, A. J. R. (2001). Two contrasting granite types: 25 years later. *Australian Journal of Earth Sciences* **48**, 489-499.

Chappell, B. W., White, A. J. R., Williams, I. S. & Wyborn, D. (2004). Low-and high-temperature granites. *Transactions of the Royal Society of Edinburgh: Earth Sciences* **95**, 125-140.

Chappell, B. W., White, A. J. R. & Wyborn, D. (1987). The Importance of Residual Source Material (Restite) in Granite Petrogenesis. *Journal of Petrology* **28**, 1111-1138.

Chayes, F. (1952). On the association of perthitic microcline with highly undulant or granular quartz in some calcalkaline granites. *American Journal of Science* **250**, 281-296.

Clemens, J. D., Belcher, R. W. & Kisters, A. F. M. (2010). The Heerenveen Batholith, Barberton Mountain Land, South Africa: Mesoarchaean, Potassic, Felsic Magmas Formed by Melting of an Ancient Subduction Complex. *Journal of Petrology* **51**, 1099-1120.

Clemens, J. D. & Stevens, G. (2012). What controls chemical variation in granitic magmas? *Lithos* **134-135**, 317-329.

Clemens, J. D., Stevens, G. & Farina, F. (2011). The enigmatic sources of I-type granites: The peritectic connexion. *Lithos* **126**, 174-181.

Clemens, J. D., Yearron, L. M. & Stevens, G. (2006). Barberton (South Africa) TTG magmas: Geochemical and experimental constraints on source-rock petrology, pressure of formation and tectonic setting. *Precambrian Research* **151**, 53-78.

Coleman, D. S., Gray, W. & Glazner, A. F. (2004). Rethinking the emplacement and evolution of zoned plutons: Geochronologic evidence for incremental assembly of the Tuolumne Intrusive Suite, California. *Geology* **32**, 433-436.

Collins, W. J., Beams, S. D., White, A. J. R. & Chappell, B. W. (1982). Nature and origin of A-type granites with particular reference to southeastern Australia. *Contributions to Mineralogy and Petrology* **80**, 189-200.

Collins, W. J., Van Kranendonk, M. J. & Teyssier, C. (1998). Partial convective overturn of Archaean crust in the east Pilbara Craton, Western Australia: driving mechanisms and tectonic implications. *Journal of Structural Geology* **20**, 1405-1424.

Compston, W. & Kröner, A. (1988). Multiple zircon growth within early Archaean tonalitic gneiss from the Ancient Gneiss Complex, Swaziland. *Earth and Planetary Science Letters* **87**, 13-28.

Creaser, R. A., Price, R. C. & Wormald, R. J. (1991). A-type granites revisited: Assessment of a residual-source model. *Geology* **19**, 163-166.

Cutts, K. A., Stevens, G., Hoffmann, J. E., Buick, I. S., Frei, D. & Münker, C. (2014). Paleo- to Mesoarchean polymetamorphism in the Barberton Granite-Greenstone Belt, South Africa: Constraints from U-Pb monazite and Lu-Hf garnet geochronology on the tectonic processes that shaped the belt. *Geological Society of America Bulletin* **126**, 251-270.

Davies, R. D., (1971). *Geochronology and isotopic evolution of the early Precambrian crustal rocks in Swaziland.* PhD Thesis, University of the Witwatersrand.

Davis, D. W., Krogh, T. E. & Williams, I. S. (2003). Historical development of zircon geochronology. *Reviews in Mineralogy and Geochemistry* **53**, 145-181.

De Bievre, P. & Taylor, P. D. P. (1993). Table of the isotopic compositions of the elements. *International Journal of Mass Spectrometry and Ion Processes* **123**, 149-166.

de Gasparis, A. A. A., (1967). *Rb-Sr isotopic studies relating to problems of geochronology on the Nelspruit and Mpageni granites.* MSc Thesis, University of the Witwatersrand.

de Ronde, C. E. J. & de Wit, M. J. (1994). Tectonic history of the Barberton greenstone belt, South Africa: 490 million years of Archean crustal evolution. *Tectonics* **13**, 983-1005.

de Ronde, C. E. J., Kamo, S., Davis, D. W., de Wit, M. J. & Spooner, E. T. C. (1991). Field, geochemical and U-Pb isotopic constraints from hypabyssal felsic intrusions within the Barberton greenstone belt, South Africa: Implications for tectonics and the timing of gold mineralization. *Precambrian Research* **49**, 261-280.

de Ronde, C. E. J. & Kamo, S. L. (2000). An Archæan arc-arc collisional event: a short-lived (ca 3 Myr) episode, Weltevreden area, Barberton greenstone belt, South Africa. *Journal of African Earth Sciences* **30**, 219-248.

de Wit, M. J., Armstrong, R., Hart, R. J. & Wilson, A. H. (1987). Felsic igneous rocks within the 3.3- to 3.5-Ga Barbeton Greenstone Belt: High crustal level equivalents of the surrounding tonalite-trondhjemite terrain, emplaced during thrusting. *Tectonics* **6**, 529-549.

de Wit, M. J., de Ronde, C. E. J., Tredoux, M., Roering, C., Hart, R. J., Armstrong, R. A., Green, R. W. E., Peberdy, E. & Hart, R. A. (1992). Formation of an Archaean continent. *Nature* **357**, 553-562.

Diener, J. F. A., Stevens, G., Kisters, A. F. M. & Poujol, M. (2005). Metamorphism and exhumation of the basal parts of the Barberton greenstone belt, South Africa: Constraining the rates of Mesoarchaean tectonism. *Precambrian Research* **143**, 87-112.

Dorais, M. J. & Spencer, C. J. (2014). Revisiting the importance of residual source material (restite) in granite petrogenesis: The Cardigan Pluton, New Hampshire. *Lithos* **202-203**, 237-249.

Dziggel, A., Stevens, G., Poujol, M., Anhaeusser, C. R. & Armstrong, R. A. (2002). Metamorphism of the granite–greenstone terrane south of the Barberton greenstone belt, South Africa: an insight into the tectono-thermal evolution of the 'lower' portions of the Onverwacht Group. *Precambrian Research* **114**, 221-247.

Eggins, S. M. (2003). Laser Ablation ICP-MS Analysis of Geological Materials Prepared as Lithium Borate Glasses. *Geostandards Newsletter* **27**, 147-162.

Eggleton, R. A. & Banfield, J. F. (1985). The alteration of granitic biotite to chlorite. *American Mineralogist* **70**, 902-910.

Faure, G. (1986). *Principles of isotope geology*: Wiley New York.

Fedo, C. M., Myers, J. S. & Appel, P. W. (2001). Depositional setting and paleogeographic implications of earth's oldest supracrustal rocks, the> 3.7 Ga Isua Greenstone belt, West Greenland. *Sedimentary Geology* **141**, 61-77.

Fitzpatrick, J. A. & Bullen, T. D. (1999). Elemental Losses From Teflon Digestion Bombs as Determined by ICP-MS: A Cautionary Tale. *AGU Fall Meeting.*

Flood, R. H. & Shaw, S. E. (1977). Two 'S-type' granite suites with low initial $^{87}Sr/^{86}Sr$ ratios from the New England Batholith, Australia. *Contributions to Mineralogy and Petrology* **61**, 163-173.

Flood, R. H. & Shaw, S. E. (2014). Microgranitoid enclaves in the felsic Looanga monzogranite, New England Batholith, Australia: Pressure quench cumulates. *Lithos* **198-199**, 92-102.

Frost, B. R., Barnes, C. G., Collins, W. J., Arculus, R. J., Ellis, D. J. & Frost, C. D. (2001). A Geochemical Classification for Granitic Rocks. *Journal of Petrology* **42**, 2033-2048.

Frost, C. D. & Frost, B. R. (2011). On Ferroan (A-type) Granitoids: their Compositional Variability and Modes of Origin. *Journal of Petrology* **52**, 39-53.

Furnes, H., de Wit, M. & Robins, B. (2013). A review of new interpretations of the tectonostratigraphy, geochemistry and evolution of the Onverwacht Suite, Barberton Greenstone Belt, South Africa. *Gondwana Research* **23**, 403-428.

Gao, Y.-Y., Li, X.-H., Griffin, W. L., O'Reilly, S. Y. & Wang, Y.-F. (2014). Screening criteria for reliable U-Pb geochronology and oxygen isotope analysis in uranium-rich zircons: A case study from the Suzhou A-type granites, SE China. *Lithos* **192-195**, 180-191.

Gee, R. D., Baxter, J. L., Wilde, S. A. & Williams, I. R. (1981). Crustal development in the Archaean Yilgarn Block, Western Australia. *Spec. Publ. Geol. Soc. Aust* **7**, 43-56.

Gray, C. M. (1984). An isotopic mixing model for the origin of granitic rocks in southeastern Australia. *Earth and Planetary Science Letters* **70**, 47-60.

Griffin, W. L., Belousova, E. A., Shee, S. R., Pearson, N. J. & O'Reilly, S. Y. (2004). Archean crustal evolution in the northern Yilgarn Craton: U–Pb and Hf-isotope evidence from detrital zircons. *Precambrian Research* **131**, 231-282.

Griffin, W. L., Pearson, N. J., Belousova, E. A. & Saeed, A. (2007). Reply to "Comment to short-communication 'Comment: Hf-isotope heterogeneity in zircon 91500' by W.L. Griffin, N.J. Pearson, E.A. Belousova and A. Saeed (Chemical Geology 233 (2006) 358-363)" by F. Corfu. *Chemical Geology* **244**, 354-356.

Griffin, W. L., Powell, W. J., Pearson, N. J. & O'Reilly, S. Y. (2008). GLITTER: data reduction software for laser ablation ICP-MS. In: Sylvester, P. (ed.) *Laser Ablation-ICP-MS in the Earth Sciences, Mineralogical Association of Canada Short Course Series*, 204-207.

Griffin, W. L., Wang, X., Jackson, S. E., Pearson, N. J., O'Reilly, S. Y., Xu, X. & Zhou, X. (2002). Zircon chemistry and magma mixing, SE China: In-situ analysis of Hf isotopes, Tonglu and Pingtan igneous complexes. *Lithos* **61**, 237-269.

Hawkesworth, C. J. & Kemp, A. I. S. (2006). Using hafnium and oxygen isotopes in zircons to unravel the record of crustal evolution. *Chemical Geology* **226**, 144-162.

Henderson, J. B. (1981). Archaean basin evolution in the Slave Province, Canada. *Developments in Precambrian geology* **4**, 213-235.

Hickman, A. H. & Van Kranendonk, M. J. (2012). Early Earth evolution: Evidence from the 3.5-1.8 Ga geological history of the Pilbara region of Western Australia. *Episodes-Newsmagazine of the International Union of Geological Sciences* **35**, 283.

Hofmann, A., Bolhar, R., Orberger, B. & Foucher, F. (2013). Cherts of the Barberton Greenstone Belt, South Africa: Petrology and trace-element geochemistry of 3.5 to 3.3 Ga old silicified volcaniclastic sediments. *South African Journal of Geology* **116**, 297-322.

Hoskin, P. W. O. (2005). Trace-element composition of hydrothermal zircon and the alteration of Hadean zircon from the Jack Hills, Australia. *Geochimica et Cosmochimica Acta* **69**, 637-648.

Hoskin, P. W. O. & Schaltegger, U. (2003). The Composition of Zircon and Igneous and Metamorphic Petrogenesis. *Reviews in Mineralogy and Geochemistry* **53**, 27-62.

Hunter, D. R. (1973). The granitic rocks of the Precambrian in Swaziland. *Special Publications of the Geological Society of Australia* **3**, 131-145.

Hunter, D. R. (1974). Crustal development in the Kaapvaal craton, I. The Archaean. *Precambrian Research* **1**, 259-294.

Hunter, D. R., Barker, F. & Millard, J., H.T. (1978). The geochemical nature of the Archean Ancient Gneiss Complex and granodiorite suite, Swaziland: A preliminary study. *Precambrian Research* **7**, 105-127.

Hunter, D. R., Barker, F. & Millard Jr, H. T. (1984). Geochemical investigation of Archaean Bimodal and Dwalile metamorphic suites, Ancient Gneiss Complex, Swaziland. *Precambrian Research* **24**, 131-155.

Isachsen, C. & Bowring, S. (1994). Evolution of the Slave craton. *Geology* **22**, 917-920.

Jackson, S. E., Pearson, N. J., Griffin, W. L. & Belousova, E. A. (2004). The Application of Laser Ablation-Inductively Coupled Plasma-Mass Spectrometry to *in situ* U-Pb Zircon Geochronology. *Chemical Geology* **211**, 47-69.

Jochum, K. P., Nohl, U., Herwig, K., Lammel, E., Stoll, B. & Hofmann, A. W. (2005). GeoReM: A New Geochemical Database for Reference Materials and Isotopic Standards. *Geostandards and Geoanalytical Research* **29**, 333-338.

Kamo, S. L. & Davis, D. W. (1994). Reassessment of Archean crustal development in the Barbeton Mountain Land, South Africa, based on U-Pb dating. *Tectonics* **13**, 167-192.

Kaufmann, B. (2006). Calibrating the Devonian Time Scale: A synthesis of U–Pb ID–TIMS ages and conodont stratigraphy. *Earth-Science Reviews* **76**, 175-190.

Keay, S., Collins, W. J. & McCulloch, M. T. (1997). A three-component Sr-Nd isotopic mixing model for granitoid genesis, Lachlan fold belt, eastern Australia. *Geology* **25**, 307-310.

Keller, C. B. & Schoene, B. (2012). Statistical geochemistry reveals disruption in secular lithospheric evolution about 2.5 Gyr ago. *Nature* **485**, 490-493.

Kemp, A. I. S., Hawkesworth, C. J., Foster, G. L., Paterson, B. A., Woodhead, J. D., Hergt, J. M., Gray, C. M. & Whitehouse, M. J. (2007). Magmatic and Crustal Differentiation History of Granitic Rocks from Hf-O Isotopes in Zircon. *Science* **315**, 980-983.

Kemp, A. I. S., Hawkesworth, C. J., Paterson, B. A., Foster, G. L., Kinny, P. D., Whitehouse, M. J., Maas, R., EIMF. (2008). Exploring the Plutonic-Volcanic Link: a Zircon U-Pb, Lu-Hf and O Isotope Study of Paired Volcanic and Granitic Units from Southeastern Australia. *Transactions of the Royal Society of Edinburgh: Earth Sciences* **97**, 337-355.

Kilpatrick, J. A. & Ellis, D. J. (1992). C-type magmas: igneous charnockites and their extrusive equivalents. *Geological Society of America Special Papers* **272**, 155-164.

Kisters, A. F. M. & Anhaeusser, C. R. (1995). Emplacement features of Archaean TTG plutons along the southern margin of the Barberton greenstone belt, South Africa. *Precambrian Research* **75**, 1-15.

Kisters, A. F. M., Belcher, R. W., Poujol, M. & Dziggel, A. (2010). Continental growth and convergence-related arc plutonism in the Mesoarchaean: Evidence from the Barberton granitoid-greenstone terrain, South Africa. *Precambrian Research* **178**, 15-26.

Kisters, A. F. M., Stevens, G., Dziggel, A. & Armstrong, R. A. (2003). Extensional detachment faulting and core-complex formation in the southern Barberton granite–greenstone terrain, South Africa: evidence for a 3.2 Ga orogenic collapse. *Precambrian Research* **127**, 355-378.

Kistler, R. W., Chappell, B. W., Peck, D. L. & Bateman, P. C. (1986). Isotopic variation in the Tuolumne Intrusive Suite, central Sierra Nevada, California. *Contributions to Mineralogy and Petrology* **94**, 205-220.

Kretz, R. (1983). Symbols for rock-forming minerals. *American Mineralogist* **68**, 277-279.

Kröner, A., Byerly, G. R. & Lowe, D. R. (1991). Chronology of early Archaean granite-greenstone evolution in the Barberton Mountain Land, South Africa, based on precise dating by single zircon evaporation. *Earth and Planetary Science Letters* **103**, 41-54.

Kröner, A., Compston, W. & Williams, I. S. (1989). Growth of early Archaean crust in the Ancient Gneiss Complex of Swaziland as revealed by single zircon dating. *Tectonophysics* **161**, 271-298.

Kröner, A., Elis Hoffmann, J., Xie, H., Wu, F., Münker, C., Hegner, E., Wong, J., Wan, Y. & Liu, D. (2013). Generation of early Archaean felsic greenstone volcanic rocks through crustal melting in the Kaapvaal, craton, southern Africa. *Earth and Planetary Science Letters* **381**, 188-197.

Kröner, A., Hegner, E., Wendt, J. I. & Byerly, G. R. (1996). The oldest part of the Barberton granitoid-greenstone terrain, South Africa: evidence for crust formation between 3.5 and 3.7 Ga. *Precambrian Research* **78**, 105-124.

Kröner, A., Hoffmann, J. E., Xie, H., Münker, C., Hegner, E., Wan, Y., Hofmann, A., Liu, D. & Yang, J. (2014). Generation of early Archaean grey gneisses through melting of older crust in the eastern Kaapvaal craton, southern Africa. *Precambrian Research* **255, Part 3**, 823-846.

Kröner, A. & Todt, W. (1988). Single zircon dating constraining the maximum age of the Barberton Greenstone Belt, southern Africa. *Journal of Geophysical Research: Solid Earth* **93**, 15329-15337.

Kuno, H. (1968). Differentiation of basalt magmas. *Basalts* **2**, 623-688.

Kusky, T. M. (1993). Collapse of Archean orogens and the generation of late- to postkinematic granitoids. *Geology* **21**, 925-928.

Kusky, T. M. & Kidd, W. S. (1992). Remnants of an Archean oceanic plateau, Belingwe greenstone belt, Zimbabwe. *Geology* **20**, 43-46.

Lana, C., Kisters, A. & Stevens, G. (2010a). Exhumation of Mesoarchean TTG gneisses from the middle crust: Insights from the Steynsdorp core complex, Barberton granitoid-greenstone terrain, South Africa. *Geological Society of America Bulletin* **122**, 183-197.

Lana, C., Tohver, E. & Cawood, P. (2010b). Quantifying rates of dome-and-keel formation in the Barberton granitoid-greenstone belt, South Africa. *Precambrian Research* **177**, 199-211.

Laurent, O., Rapopo, M., Stevens, G., Moyen, J. F., Martin, H., Doucelance, R., Bosq, C. (2014). Contrasting petrogenesis of Mg–K and Fe–K granitoids and implications for post-collisional magmatism: Case study from the Late-Archean Matok pluton (Pietersburg block, South Africa). *Lithos* **196-197**, 131-149.

Le Bas, M. J., Le Maitre, R. W., Streckeisen, A. & Zanettin, B. (1986). A chemical classification of volcanic rocks based on the total alkali-silica diagram. *Journal of Petrology* **27**, 745-750.

Le Maitre, R., Bateman, P., Dudek, A., Keller, J., Lameyre, L., Sabine, P., Schmid, R., Sorensen, H., Streckeisen, A. & Wooley, A. (1989). A classification of igneous rocks and glossary of terms. Recommendations of the IUGS Commission on the Systematics of Igneous Rocks. Oxford: Blackwell.

Loiselle, M. C. & Wones, D. R. (1979). Characteristics and origin of anorogenic granites. *Geological Society of America Abstracts with Programs*, 468.

Lowe, D. R. (1994). Accretionary history of the Archean Barberton Greenstone Belt (3.55-3.22 Ga), southern Africa. *Geology* **22**, 1099-1102.

Ludwig, K. R. (2003). *User's manual for Isoplot 3.00: A geochronological toolkit for Microsoft Excel*: Kenneth R. Ludwig.

Maas, R., Nicholls, I. A. & Legg, C. (1997). Igneous and Metamorphic Enclaves in the S-type Deddick Granodiorite, Lachlan Fold Belt, SE Australia: Petrographic, Geochemical and Nd-Sr Isotopic Evidence for Crustal Melting and Magma Mixing. *Journal of Petrology* **38**, 815-841.

Maphalala, R., Kröner, A. & Kramers, J. D. (1989). Rb-Sr ages for Archaean granitoids and tin-bearing pegmatites in Swaziland, southern Africa. *Journal of African Earth Sciences (and the Middle East)* **9**, 749-757.

Maphalala, R. M. & Kröner, A. (1993). Pb-Pb single zircon ages for the younger Archaean granitoids of Swaziland, southern Africa. *Ext. Abstr. 16th International Colloquium on African Geology, Mbabane, Swaziland*, 201-206.

Marillo-Sialer, E., Woodhead, J., Hergt, J., Greig, A., Guillong, M., Gleadow, A., Evans, N. & Paton, C. (2014). The zircon 'matrix effect': evidence for an ablation rate control on the accuracy of U-Pb age determinations by LA-ICP-MS. *Journal of Analytical Atomic Spectrometry* **29**, 981-989.

McCulloch, M. T. & Chappell, B. W. (1982). Nd isotopic characteristics of S- and I-type granites. *Earth and Planetary Science Letters* **58**, 51-64.

Meyer, F. M., Robb, L. J., Reimold, W. U. & de Bruiyn, H. (1994). Contrasting low- and high-Ca granites in the Archean Barberton Mountain Land, Southern Africa. *Lithos* **32**, 63-76.

Miller, C. F., McDowell, S. M. & Mapes, R. W. (2003). Hot and cold granites? Implications of zircon saturation temperatures and preservation of inheritance. *Geology* **31**, 529-532.

Moser, D. E., Heaman, L. M., Krogh, T. E. & Hanes, J. A. (1996). Intracrustal extension of an Archean orogen revealed using single-grain U-Pb zircon geochronology. *Tectonics* **15**, 1093-1109.

Moyen, J.-F., Stevens, G. & Kisters, A. (2006). Record of mid-Archaean subduction from metamorphism in the Barberton terrain, South Africa. *Nature* **442**, 559-562.

Mukasa, S. B., Wilson, A. H. & Young, K. R. (2013). Geochronological constraints on the magmatic and tectonic development of the Pongola Supergroup (Central Region), South Africa. *Precambrian Research* **224**, 268-286.

Munoz, J. L. & Ludington, S. D. (1974). Fluoride-hydroxyl exchange in biotite. *American Journal of Science* **274**, 396-413.

Murakami, T., Chakoumakos, B. C., Ewing, R. C., Lumpkin, G. R. & Weber, W. J. (1991). Alpha-decay event damage in zircon. *American Mineralogist* **76**, 1510-1532.

Myers, J. S. (2001). Protoliths of the 3.8–3.7 Ga Isua greenstone belt, west Greenland. *Precambrian Research* **105**, 129-141.

Nasdala, L., Kronz, A., Wirth, R., Váczi, T., Pérez-Soba, C., Willner, A. & Kennedy, A. K. (2009). The phenomenon of deficient electron microprobe totals in radiation-damaged and altered zircon. *Geochimica et Cosmochimica Acta* **73**, 1637-1650.

Nasdala, L., Lengauer, C. L., Hanchar, J. M., Kronz, A., Wirth, R., Blanc, P., Kennedy, A. K. & Seydoux-Guillaume, A.-M. (2002). Annealing radiation damage and the recovery of cathodoluminescence. *Chemical Geology* **191**, 121-140.

Nebel, O., Scherer, E. E. & Mezger, K. (2011). Evaluation of the ^{87}Rb decay constant by age comparison against the U-Pb system. *Earth and Planetary Science Letters* **301**, 1-8.

Nockolds, S. R. (1947). The relation between chemical composition and paragenesis in the biotite micas of igneous rocks. *American Journal of Science* **245**, 401-420.

O'Neil, J. R. & Chappell, B. W. (1977). Oxygen and hydrogen isotope relations in the Berridale batholith. *Journal of the Geological Society* **133**, 559-571.

O'Neil, J. R., Shaw, S. E. & Flood, R. H. (1977). Oxygen and hydrogen isotope compositions as indicators of granite genesis in the New England Batholith, Australia. *Contributions to Mineralogy and Petrology* **62**, 313-328.

Oosthuyzen, E. J., (1970). *The Geochronology of a Suite of Rocks from the Granitic Terrain Surrounding the Barberton Mountain Land.* PhD Thesis, University of the Witwatersrand, Johannesburg.

Palenik, C. S., Nasdala, L. & Ewing, R. C. (2003). Radiation damage in zircon. *American Mineralogist* **88**, 770-781.

Parsons, I. & Brown, W. L. (1984). Feldspars and the thermal history of igneous rocks. *Feldspars and feldspathoids*: Springer, 317-371.

Patchett, P. J., Kouvo, O., Hedge, C. E. & Tatsumoto, M. (1982). Evolution of continental crust and mantle heterogeneity: Evidence from Hf isotopes. *Contributions to Mineralogy and Petrology* **78**, 279-297.

Peacock, M. A. (1931). Classification of igneous rock series. *The Journal of Geology*, 54-67.

Pearce, J. A., Harris, N. B. W. & Tindle, A. G. (1984). Trace Element Discrimination Diagrams for the Tectonic Interpretation of Granitic Rocks. *Journal of Petrology* **25**, 956-983.

Pearce, N. J. G., Perkins, W. T., Westgate, J. A., Gorton, M. P., Jackson, S. E., Neal, C. R. & Chenery, S. P. (1997). A Compilation of New and Published Major and Trace Element Data for NIST SRM 610 and NIST SRM 612 Glass Reference Materials. *Geostandards Newsletter* **21**, 115-144.

Pearson, N. J., Griffin, W. L. & O'Reilly, S. Y. (2008). Mass fractionation correction in laser ablation multiple-collector ICP-MS: implications for overlap corrections and precise and accurate in situ isotope ratio measurement. In: Sylvester, P. (ed.) *Laser ablation ICP-MS in the earth sciences: current practices and outstanding issues*. Quebec: Mineralogical Association of Canada, 93-116.

Pitcher, W. S. (1979). The nature, ascent and emplacement of granitic magmas. *Journal of the Geological Society* **136**, 627-662.

Polat, A. & Kerrich, R. (2000). Archean greenstone belt magmatism and the continental growth–mantle evolution connection: constraints from Th–U–Nb–LREE systematics of the 2.7 Ga Wawa subprovince, Superior Province, Canada. *Earth and Planetary Science Letters* **175**, 41-54.

Putnis, A. (2002). Mineral replacement reactions: from macroscopic observations to microscopic mechanisms. *Mineralogical Magazine* **66**, 689-708.

Robb, L. J. & Anhaeusser, C. R. (1983). Chemical and petrogenetic characteristics of Archaean tonalite-trondhjemite gneiss plutons in the Barberton Mountain Land. *Special Publication of the Geological Society of South Africa* **9**, 103-117.

Robb, L. J., Anhaeusser, C. R. & Van Nierop, D. A. (1983). The recognition of the Nelspruit batholith north of the Barberton greenstone belt and its significance in terms of Archaean crustal evolution. *Special Publication of the Geological Society of South Africa* **9**, 117-130.

Romano, R., Lana, C., Alkmim, F. F., Stevens, G. & Armstrong, R. (2013). Stabilization of the southern portion of the São Francisco craton, SE Brazil, through a long-lived period of potassic magmatism. *Precambrian Research* **224**, 143-159.

Rotenberg, E., Davis, D. W., Amelin, Y., Ghosh, S. & Bergquist, B. A. (2012). Determination of the decay-constant of ^{87}Rb by laboratory accumulation of ^{87}Sr. *Geochimica et Cosmochimica Acta* **85**, 41-57.

Rowley, D. B., Xue, F., Tucker, R. D., Peng, Z. X., Baker, J. & Davis, A. (1997). Ages of ultrahigh pressure metamorphism and protolith orthogneisses from the eastern Dabie Shan: U/Pb zircon geochronology. *Earth and Planetary Science Letters* **151**, 191-203.

Sandiford, M., McLaren, S. & Neumann, N. (2002). Long-term thermal consequences of the redistribution of heat-producing elements associated with large-scale granitic complexes. *Journal of Metamorphic Geology* **20**, 87-98.

Sandiford, M., Van Kranendonk, M. J. & Bodorkos, S. (2004). Conductive incubation and the origin of dome-and-keel structure in Archean granite-greenstone terrains: A model based on the eastern Pilbara Craton, Western Australia. *Tectonics* **23**, 1-19.

Santosh, M., Wilde, S. A. & Li, J. H. (2007). Timing of Paleoproterozoic ultrahigh-temperature metamorphism in the North China Craton: Evidence from SHRIMP U–Pb zircon geochronology. *Precambrian Research* **159**, 178-196.

Schaltegger, U., Schneider, J.-L., Maurin, J.-C. & Corfu, F. (1996). Precise UPb chronometry of 345-340 Ma old magmatism related to syn-convergence extension in the Southern Vosges (Central Variscan Belt). *Earth and Planetary Science Letters* **144**, 403-419.

Schärer, U. & Allègre, C. J. (1983). The Palung granite (Himalaya); high-resolution UPb systematics in zircon and monazite. *Earth and Planetary Science Letters* **63**, 423-432.

Scherer, E., Münker, C., Mezger, K. (2001). Calibration of the Lutetium-Hafnium Clock. *Science* **293**, 683-687.

Schoene, B. & Bowring, S. A. (2007). Determining accurate temperature–time paths from U-Pb thermochronology: An example from the Kaapvaal craton, southern Africa. *Geochimica et Cosmochimica Acta* **71**, 165-185.

Schoene, B. & Bowring, S. A. (2010). Rates and mechanisms of Mesoarchean magmatic arc construction, eastern Kaapvaal craton, Swaziland. *Geological Society of America Bulletin* **122**, 408-429.

Schoene, B., Dudas, F. O. L., Bowring, S. A. & De Wit, M. (2009). Sm-Nd isotopic mapping of lithospheric growth and stabilization in the eastern Kaapvaal craton. *Terra Nova* **21**, 219-228.

Shand, S. J. (1950). *Eruptive Rocks*. New York: Wiley, 4th edition.

Shaw, S. E. & Flood, R. H. (1981). The New England Batholith, Eastern Australia: Geochemical Variations in Time and Space. *Journal of Geophysical Research* **86**, 10530-10544.

Shaw, S. E. & Flood, R. H. (2009). Zircon Hf Isotopic Evidence for Mixing of Crustal and Silicic Mantle-derived Magmas in a Zoned Granite Pluton, Eastern Australia. *Journal of Petrology* **50**, 147-168.

Shaw, S. E., Flood, R. H. & Pearson, N. J. (2011). The New England Batholith of eastern Australia: Evidence of silicic magma mixing from zircon 176Hf/177Hf ratios. *Lithos* **126**, 115-126.

Shelley, D. (1993). *Igneous and metamorphic rocks under the microscope: classification, textures, microstructures and mineral preferred-orientations*: Chapman & Hall London.

Sheraton, J. W. & Black, L. P. (1988). Chemical evolution of granitic rocks in the East Antarctic Shield, with particular reference to post-orogenic granites. *Lithos* **21**, 37-52.

Shirey, S. B. & Hanson, G. N. (1986). Mantle heterogeneity and crustal recycling in Archean granite-greenstone belts: evidence from Nd isotopes and trace elements in the Rainy Lake area, Superior Province, Ontario, Canada. *Geochimica et Cosmochimica Acta* **50**, 2631-2651.

SACS (South African Committee for Stratigraphy), (1980). Stratigraphy of South Africa. *Handbook of the South African Geological Survey* **8**, 690.

Steiger, R. H. & Hart, S. R. (1967). Microcline-orthoclase transition within a contact aureole. *American Mineralogist* **52**, 87-116.

Steiger, R. H. & Jäger, E. (1977). Subcommission on geochronology: Convention on the use of decay constants in geo- and cosmochronology. *Earth and Planetary Science Letters* **36**, 359-362.

Stern, R. A., Bodorkos, S., Kamo, S. L., Hickman, A. H. & Corfu, F. (2009). Measurement of SIMS Instrumental Mass Fractionation of Pb Isotopes During Zircon Dating. *Geostandards and Geoanalytical Research* **33**, 145-168.

Stevens, G., Villaros, A. & Moyen, J.-F. (2007). Selective Peritectic Garnet Entrainment as the Origin of Geochemical Diversity in S-type Granites. *Geology* **39**, 9-12.

Stewart, J. H., Gehrels, G. E., Barth, A. P., Link, P. K., Christie-Blick, N. & Wrucke, C. T. (2001). Detrital zircon provenance of Mesoproterozoic to Cambrian arenites in the western United States and northwestern Mexico. *Geological Society of America Bulletin* **113**, 1343-1356.

Streckeisen, A. (1967). Classification and nomenclature of igneous rocks. *Neues Jahrbuch für Mineralogie, Abhandlungen* **107**, 144-214.

Streckeisen, A. (1974). Classification and nomenclature of plutonic rocks recommendations of the IUGS subcommission on the systematics of Igneous Rocks. *Geologische Rundschau* **63**, 773-786.

Streckeisen, A. (1976). To each plutonic rock its proper name. *Earth-Science Reviews* **12**, 1-33.

Streckeisen, A. & Le Maitre, R. W. (1979). A chemical approximation to the modal QAPF classification of the igneous rocks. *Neues Jahrbuch für Mineralogie, Abhandlungen* **136**, 169-206.

Swager, C. P., Witt, W. K., Griffin, T. J., Ahmat, A. L., Hunter, W. M., McGoldrick, P. J. & Wyche, S. (1992). Late Archaean granite-greenstones of the Kalgoorlie Terrane, Yilgarn Craton, Western Australia. *The Archaean: terrains, processes and metallogeny* **22**, 107-122.

Tang, M., Wang, X.-L., Shu, X.-J., Wang, D., Yang, T., Gopon, P. (2014). Hafnium isotopic heterogeneity in zircons from granitic rocks: Geochemical evaluation and modeling of "zircon effect" in crustal anatexis. *Earth and Planetary Science Letters* **389**, 188-199.

Taylor, J., Stevens, G., Buick, I. S. & Lana, C. (2012). Successive midcrustal, high-grade metamorphic events provide insight into Mid-Archean mountain-building along the SE margin of the proto-Kaapvaal craton. *Geological Society of America Bulletin* **124**, 1191-1211.

Tegtmeyer, A. R. & Kröner, A. (1987). U-Pb zircon ages bearing on the nature of early Archaean greenstone belt evolution, Barberton Mountain Land, southern Africa. *Precambrian Research* **36**, 1-20.

Tucker, R. D., Krogh, T. E., Ross Jr, R. J. & Williams, S. H. (1990). Time-scale calibration by high-precision UPb zircon dating of interstratified volcanic ashes in the Ordovician and Lower Silurian stratotypes of Britain. *Earth and Planetary Science Letters* **100**, 51-58.

Tulloch, A. J. (1979). Secondary Ca-Al silicates as low-grade alteration products of granitoid biotite. *Contributions to Mineralogy and Petrology* **69**, 105-117.

Tuttle, O. F. & Bowen, N. L. (1958). Origin of granite in the light of experimental studies in the system $NaAlSi_3O_8$–$KAlSi_3O_8$–SiO_2–H_2O. *Geological Society of America Memoirs* **74**, 1-146.

Vallance, T. G. (1969). III Southern and Central Highlands Fold Belt: Plutonic and metamorphic rocks. *Journal of the Geological Society of Australia* **16**, 180-200.

Van Kranendonk, M. J. (2011). Cool greenstone drips and the role of partial convective overturn in Barberton greenstone belt evolution. *Journal of African Earth Sciences* **60**, 346-352.

Van Kranendonk, M. J., Kröner, A., Hegner, E. & Connelly, J. (2009). Age, lithology and structural evolution of the c. 3.53 Ga Theespruit Formation in the Tjakastad area, southwestern Barberton Greenstone Belt, South Africa, with implications for Archaean tectonics. *Chemical Geology* **261**, 115-139.

Van Kranendonk, M. J., Kröner, A., Hoffmann, J. E., Nagel, T. & Anhaeusser, C. R. (2014). Just another drip: Re-analysis of a proposed Mesoarchean suture from the Barberton Mountain Land, South Africa. *Precambrian Research* **254**, 19-35.

Van Kranendonk, M. J., Smithies, H. R. H. & Bennett, V. (2007). *Earth's oldest rocks*: Elsevier.

Veevers, J. J., Saeed, A., Belousova, E. A. & Griffin, W. L. (2005). U-Pb ages and source composition by Hf-isotope and trace-element analysis of detrital zircons in Permian sandstone and modern sand from southwestern Australia and a review of the paleogeographical and denudational history of the Yilgarn Craton. *Earth-Science Reviews* **68**, 245-279.

Vermeesch, P. (2012). On the visualisation of detrital age distributions. *Chemical Geology* **312-313**, 190-194.

Vernon, R. H. (1984). Microgranitoid enclaves in granites—globules of hybrid magma quenched in a plutonic environment. *Nature* **309**, 438-439.

Vernon, R. H., Etheridge, M. A. & Wall, V. J. (1988). Shape and Microstructure of Microgranitoid Enclaves: Indicators of Magma Mingling and Flow. *Lithos* **22**, 1-11.

Viljoen, M. J. & Viljoen, R. P. (1969). An introduction to the geology of the Barberton granite-greenstone terrain. *Geological Society of South Africa Special Publication* **2**, 9-28.

Villaros, A., Buick, I. S. & Stevens, G. (2012). Isotopic variations in S-type granites: an inheritance from a heterogeneous source? *Contributions to Mineralogy and Petrology* **163**, 243-257.

Watson, E. B. & Harrison, T. M. (1983). Zircon saturation revisited: temperature and composition effects in a variety of crustal magma types. *Earth and Planetary Science Letters* **64**, 295-304.

Watson, E. B. & Harrison, T. M. (2005). Zircon thermometer reveals minimum melting conditions on earliest Earth. *Science* **308**, 841-844.

Watson, E. B., Wark, D. A. & Thomas, J. B. (2006). Crystallization thermometers for zircon and rutile. *Contributions to Mineralogy and Petrology* **151**, 413-433.

Westraat, J. D., Kisters, A. F. M., Poujol, M. & Stevens, G. (2005). Transcurrent shearing, granite sheeting and the incremental construction of the tabular 3.1 Ga Mpuluzi batholith, Barberton granite-greenstone terrane, South Africa. *Journal of the Geological Society* **162**, 373-388.

Whalen, J. B. (1985). Geochemistry of an Island-Arc Plutonic Suite: the Uasilau-Yau Yau Intrusive Complex, New Britain, P.N.G. *Journal of Petrology* **26**, 603-632.

Whalen, J. B., Currie, K. L. & Chappell, B. W. (1987). A-type granites: geochemical characteristics, discrimination and petrogenesis. *Contributions to Mineralogy and Petrology* **95**, 407-419.

Whalen, J. B., Percival, J. A., McNicoll, V. J. & Longstaffe, F. J. (2004). Geochemical and isotopic (Nd–O) evidence bearing on the origin of late- to post-orogenic high-K granitoid rocks in the Western Superior Province: implications for late Archean tectonomagmatic processes. *Precambrian Research* **132**, 303-326.

White, A. J. R., Allen, C. M., Beams, S. D., Carr, P. F., Champion, D. C., Chappell, B. W., Wyborn, D. & Wyborn, L. A. I. (2001). Granite suites and supersuites of eastern Australia. *Australian Journal of Earth Sciences* **48**, 515-530.

White, A. J. R. & Chappell, B. W. (1977). Ultrametamorphism and granitoid genesis. *Tectonophysics* **43**, 7-22.

Whitehouse, M. J. & Platt, J. P. (2003). Dating high-grade metamorphism—constraints from rare-earth elements in zircon and garnet. *Contributions to Mineralogy and Petrology* **145**, 61-74.

Wiebe, R. A. (1994). Silicic magma chambers as traps for basaltic magmas: the Cadillac Mountain intrusive complex, Mount Desert Island, Maine. *The Journal of Geology*, 423-437.

Wiedenbeck, M., Allé, P., Corfu, F., Griffin, W. L., Meier, M., Oberli, F., Von Quadt, A., Roddick, J. C. & Spiegel, W. (1995). Three natural zircon standards for U-Th-Pb, Lu-Hf, trace element and REE analyses. *Geostandards Newsletter* **19**, 1-23.

Wiedenbeck, M., Hanchar, J. M., Peck, W. H., Sylvester, P., Valley, J., Whitehouse, M., Kronz, A., Morishita, Y., Nasdala, L., Fiebig, J., Franchi, I., Girard, J. P., Greenwood, R. C., Hinton, R., Kita, N., Mason, P. R. D., Norman, M., Ogasawara, M., Piccoli, P. M., Rhede, D., Satoh, H., Schulz-Dobrick, B., Skår, O., Spicuzza, M. J., Terada, K., Tindle, A., Togashi, S., Vennemann, T., Xie, Q. & Zheng, Y. F. (2004). Further Characterisation of the 91500 Zircon Crystal. *Geostandards and Geoanalytical Research* **28**, 9-39.

Wilde, S. A., Valley, J. W., Peck, W. H. & Graham, C. M. (2001). Evidence from detrital zircons for the existence of continental crust and oceans on the Earth 4.4 Gyr ago. *Nature* **409**, 175-178.

Wilson, A. C. (1982). 1: 250,000 Geological map of Swaziland. Swaziland Geological Survey Mines Department.

Wilson, J. F., Nesbitt, R. W. & Fanning, C. M. (1995). Zircon geochronology of Archaean felsic sequences in the Zimbabwe craton: a revision of greenstone stratigraphy and a model for crustal growth. *Geological Society, London, Special Publications* **95**, 109-126.

Winter, J. D. (2010). *Principles of igneous and metamorphic petrology*: Prentice Hall New York.

Woodhead, J. D. & Hergt, J. M. (2005). A Preliminary Appraisal of Seven Natural Zircon Reference Materials for In Situ Hf Isotope Determination. *Geostandards and Geoanalytical Research* **29**, 183-195.

Wyborn, D., Chappell, B. W. & James, M. (2001). Examples of convective fractionation in high-temperature granites from the Lachlan Fold Belt. *Australian Journal of Earth Sciences* **48**, 531-541.

Wyborn, D., Turner, B. S. & Chappell, B. W. (1987). The Boggy Plain Supersuite: A distinctive belt of I-type igneous rocks of potential economic significance in the Lachlan Fold Belt. *Australian Journal of Earth Sciences* **34**, 21-43.

Xia, Q.-X., Zheng, Y.-F. & Hu, Z. (2010). Trace elements in zircon and coexisting minerals from low-T/UHP metagranite in the Dabie orogen: Implications for action of supercritical fluid during continental subduction-zone metamorphism. *Lithos* **114**, 385-412.

Yang, J.-H., Wu, F.-Y., Wilde, S. A., Xie, L.-W., Yang, Y.-H. & Liu, X.-M. (2007). Tracing magma mixing in granite genesis: in situ U-Pb dating and Hf-isotope analysis of zircons. *Contributions to Mineralogy and Petrology* **153**, 177-190.

Yearron, L. M., (2003). *Archaean granite petrogenesis and implications for the evolution of the Barberton mountain land, South Africa.* PhD Thesis, Kingston University.

Zeh, A., Gerdes, A. & Barton, J. M. (2009). Archean Accretion and Crustal Evolution of the Kalahari Craton—the Zircon Age and Hf Isotope Record of Granitic Rocks from Barberton/Swaziland to the Francistown Arc. *Journal of Petrology* **50**, 933-966.

Zeh, A., Gerdes, A. & Heubeck, C. (2013). U-Pb and Hf isotope data of detrital zircons from the Barberton Greenstone Belt: constraints on provenance and Archaean crustal evolution. *Journal of the Geological Society* **170**, 215-223.

Zeh, A., Gerdes, A. & Millonig, L. (2011). Hafnium isotope record of the Ancient Gneiss Complex, Swaziland, southern Africa: evidence for Archaean crust–mantle formation and crust reworking between 3.66 and 2.73 Ga. *Journal of the Geological Society* **168**, 953-964.

Contents of Appendices

Appendix A – Standard Compilation A-3

Appendix A1 – Zircon standards for U-Pb analysis A-4

Appendix A2 – Zircon standards for Hf-isotope analysis A-10

Appendix B – Sample Descriptions A-17

Appendix C – Mineral Chemistry A-39

Appendix C1 – Biotite compositions A-40

Appendix C2 – Allanite compositions A-48

Appendix D – Zircon CL Images A-53

Appendix E – Zircon Major-Element Analyses A-83

Appendix F – Zircon Trace-Element Analyses A-101

Appendix G – Zircon U-Pb Analyses A-199

Appendix H – Zircon Hf-Isotope Analyses A-255

Appendix A – Standard Compilation

Appendix A1 – Zircon standards for U-Pb analysis (uncorrected):

OG1: ID-TIMS $^{207}Pb/^{206}Pb$ age = 3465.4 ± 0.6 Ma.

Reference:

Stern, R. A., Bodorkos, S., Kamo, S. L., Hickman, A. H. & Corfu, F. (2009). Measurement of SIMS Instrumental Mass Fractionation of Pb Isotopes During Zircon Dating. *Geostandards and Geoanalytical Research* **33**, 145-168.

91500: ID-TIMS $^{207}Pb/^{206}Pb$ age = 1065.4 ± 0.3 Ma.

Reference:

Wiedenbeck, M., Allé, P., Corfu, F., Griffin, W. L., Meier, M., Oberli, F., Von Quadt, A., Roddick, J. C. & Spiegel, W. (1995). Three natural zircon standards for U-Th-Pb, Lu-Hf, trace element and REE analyses. *Geostandards Newsletter* **19**, 1-23.

Appendix A2 – Zircon standards for Hf-isotope analysis:

Mud Tank: $^{176}Hf/^{177}Hf$ = 0.282522 ± 42.

Reference:

Griffin, W. L., Pearson, N. J., Belousova, E. A. & Saeed, A. (2007). Reply to "Comment to short-communication 'Comment: Hf-isotope heterogeneity in zircon 91500' by W.L. Griffin, N.J. Pearson, E.A. Belousova and A. Saeed (Chemical Geology 233 (2006) 358-363)" by F. Corfu. *Chemical Geology* **244**, 354-356.

Temora-2: $^{176}Hf/^{177}Hf$ = 0.282680 ± 11.

Reference:

Woodhead, J. D. & Hergt, J. M. (2005). A Preliminary Appraisal of Seven Natural Zircon Reference Materials for In Situ Hf Isotope Determination. *Geostandards and Geoanalytical Research* **29**, 183-195.

	Ratio								Age (Ma)							
	$^{207}Pb/^{206}Pb$	± 1σ	$^{207}Pb/^{235}U$	± 1σ	$^{206}Pb/^{238}U$	± 1σ	$^{208}Pb/^{232}Th$	± 1σ	$^{207}Pb/^{206}Pb$	± 1σ	$^{207}Pb/^{235}U$	± 1σ	$^{206}Pb/^{238}U$	± 1σ	$^{208}Pb/^{232}Th$	± 1σ
OG1-01	0.295	0.012	27.3	1.1	0.671	0.012	0.174	0.021	3446	36	3395	39	3311	46	3250	360
OG1-02	0.3011	0.0042	29.85	0.42	0.7189	0.0082	0.1858	0.0056	3476	10	3482	14	3492	31	3444	96
OG1-03	0.2977	0.0039	29.12	0.39	0.7095	0.0081	0.1860	0.0050	3458	9	3458	13	3456	31	3448	85
OG1-04	0.2999	0.0036	29.95	0.35	0.7242	0.0074	0.2017	0.0048	3470	7	3485	11	3512	28	3715	81
OG1-05	0.2975	0.0036	29.21	0.34	0.7124	0.0073	0.2003	0.0048	3457	8	3461	11	3468	28	3690	81
OG1-06	0.2968	0.0035	28.83	0.34	0.7046	0.0073	0.1912	0.0045	3454	8	3448	11	3438	28	3537	76
OG1-07	0.2993	0.0039	30.15	0.39	0.7311	0.0081	0.2016	0.0055	3466	8	3492	13	3537	30	3713	93
OG1-08	0.2983	0.0038	29.29	0.37	0.7122	0.0077	0.1925	0.0051	3461	8	3463	12	3467	29	3558	86
OG1-09	0.2990	0.0037	29.34	0.36	0.7118	0.0076	0.1830	0.0045	3465	8	3465	12	3465	29	3396	77
OG1-10	0.2988	0.0038	29.33	0.37	0.7121	0.0077	0.1881	0.0047	3464	8	3465	12	3466	29	3484	80
OG1-11	0.2994	0.0039	28.72	0.37	0.6958	0.0076	0.1991	0.0054	3423	17	3401	22	3364	35	3353	39
OG1-12	0.3027	0.0046	29.92	0.45	0.7169	0.0083	0.1894	0.0064	3484	10	3484	15	3484	31	3510	110
OG1-13	0.2995	0.0038	29.47	0.37	0.7137	0.0076	0.1900	0.0049	3467	8	3469	12	3472	29	3517	83
OG1-14	0.2979	0.0036	29.18	0.35	0.7105	0.0076	0.1964	0.0045	3459	8	3460	12	3460	29	3625	77
OG1-15	0.2999	0.0037	29.20	0.36	0.7062	0.0076	0.1882	0.0045	3470	8	3460	12	3444	29	3486	77
OG1-16	0.2994	0.0041	29.54	0.40	0.7156	0.0079	0.1936	0.0055	3467	9	3472	13	3480	30	3577	93
OG1-17	0.2992	0.0038	29.30	0.37	0.7104	0.0078	0.1895	0.0048	3466	8	3464	13	3460	29	3508	82
OG1-18	0.2992	0.0052	29.87	0.52	0.7242	0.0092	0.1941	0.0080	3466	12	3483	17	3512	35	3590	136
OG1-19	0.2988	0.0040	29.52	0.42	0.7165	0.0085	0.1881	0.0039	3464	9	3471	14	3483	32	3484	67
OG1-20	0.2909	0.0050	25.43	0.46	0.6341	0.0085	0.1823	0.0054	3396	16	3300	22	3143	35	3101	39
OG1-21	0.2925	0.0043	29.66	0.45	0.7356	0.0091	0.1959	0.0046	3431	10	3476	15	3554	34	3617	78
OG1-22	0.2941	0.0045	29.50	0.47	0.7274	0.0096	0.1689	0.0040	3440	11	3470	16	3524	36	3154	70
OG1-23	0.2956	0.0040	27.91	0.41	0.6850	0.0087	0.1818	0.0039	3447	10	3416	15	3364	33	3377	66
OG1-24	0.2740	0.0037	25.85	0.37	0.6848	0.0085	0.1411	0.0028	3329	9	3341	14	3363	33	2667	49
OG1-25	0.2986	0.0043	29.67	0.44	0.7205	0.0086	0.1889	0.0044	3463	10	3476	15	3498	32	3498	75

	Ratio								Age (Ma)							
	$^{207}Pb/^{206}Pb$	± 1σ	$^{207}Pb/^{235}U$	± 1σ	$^{206}Pb/^{238}U$	± 1σ	$^{208}Pb/^{232}Th$	± 1σ	$^{207}Pb/^{206}Pb$	± 1σ	$^{207}Pb/^{235}U$	± 1σ	$^{206}Pb/^{238}U$	± 1σ	$^{208}Pb/^{232}Th$	± 1σ
OG1-26	0.2988	0.0043	28.39	0.42	0.6892	0.0082	0.1803	0.0041	3464	10	3433	15	3379	31	3351	70
OG1-27	0.2933	0.0036	29.60	0.39	0.7320	0.0086	0.1826	0.0031	3435	8	3474	13	3541	32	3389	52
OG1-28	0.2985	0.0040	29.33	0.41	0.7125	0.0083	0.1669	0.0032	3463	10	3465	14	3468	31	3120	56
OG1-29	0.2994	0.0042	28.99	0.42	0.7024	0.0082	0.1826	0.0040	3467	10	3453	14	3430	31	3391	69
OG1-30	0.2960	0.0036	28.77	0.37	0.7050	0.0081	0.1846	0.0031	3449	8	3446	13	3439	30	3424	53
OG1-31	0.2984	0.0036	30.51	0.40	0.7417	0.0088	0.1967	0.0033	3462	8	3503	13	3577	33	3629	56
OG1-32	0.2985	0.0046	29.19	0.46	0.7093	0.0086	0.2174	0.0058	3462	11	3460	16	3456	32	3976	97
OG1-33	0.2995	0.0035	28.18	0.36	0.6826	0.0079	0.1715	0.0026	3468	8	3426	13	3354	30	3199	45
OG1-34	0.2984	0.0044	27.62	0.42	0.6712	0.0081	0.1851	0.0044	3462	10	3406	15	3311	31	3433	75
OG1-35	0.2948	0.0036	28.94	0.38	0.7122	0.0084	0.1789	0.0030	3443	8	3451	13	3467	32	3327	51
OG1-36	0.2944	0.0036	28.80	0.38	0.7098	0.0083	0.1767	0.0029	3441	9	3447	13	3458	31	3289	50
OG1-37	0.2968	0.0036	28.14	0.36	0.6876	0.0080	0.1760	0.0029	3454	9	3424	13	3374	30	3276	49
OG1-38	0.2982	0.0038	27.66	0.38	0.6728	0.0080	0.1781	0.0034	3461	9	3407	13	3316	31	3313	58
OG1-39	0.2991	0.0039	29.81	0.39	0.7229	0.0079	0.1948	0.0037	3466	9	3481	13	3507	30	3597	63
OG1-40	0.2999	0.0047	30.32	0.47	0.7333	0.0086	0.1978	0.0051	3470	11	3497	15	3546	32	3649	87
OG1-41	0.2994	0.0050	29.85	0.49	0.7232	0.0085	0.1974	0.0056	3467	11	3482	16	3508	32	3641	95
OG1-42	0.3000	0.0018	29.46	0.39	0.7124	0.0078	0.1953	0.0039	3470	9	3469	13	3467	29	3606	66
OG1-43	0.2989	0.0056	29.74	0.56	0.7215	0.0091	0.1867	0.0061	3464	14	3478	18	3502	34	3460	100
OG1-44	0.2992	0.0027	30.10	0.56	0.7297	0.0091	0.1992	0.0067	3466	13	3490	18	3532	34	3670	110
OG1-45	0.2987	0.0040	29.25	0.40	0.7103	0.0078	0.1983	0.0041	3463	9	3462	13	3460	30	3656	69
OG1-47	0.2999	0.0055	29.99	0.55	0.7253	0.0090	0.2063	0.0070	3470	13	3487	18	3516	34	3790	120
OG1-48	0.3025	0.0050	29.61	0.50	0.7099	0.0086	0.1898	0.0054	3483	12	3474	17	3458	32	3512	92
OG1-49	0.3010	0.0043	30.18	0.44	0.7273	0.0086	0.2015	0.0046	3476	10	3493	14	3523	32	3711	77
OG1-50	0.2958	0.0042	30.16	0.44	0.7394	0.0088	0.1926	0.0045	3449	10	3492	14	3568	33	3560	76
OG1-51	0.3003	0.0042	29.74	0.43	0.7185	0.0083	0.1959	0.0043	3472	9	3478	14	3490	31	3616	73

	Ratio								Age (Ma)							
	$^{207}Pb/^{206}Pb$	± 1σ	$^{207}Pb/^{235}U$	± 1σ	$^{206}Pb/^{238}U$	± 1σ	$^{208}Pb/^{232}Th$	± 1σ	$^{207}Pb/^{206}Pb$	± 1σ	$^{207}Pb/^{235}U$	± 1σ	$^{206}Pb/^{238}U$	± 1σ	$^{208}Pb/^{232}Th$	± 1σ
91500-01	0.0749	0.0013	1.806	0.030	0.1749	0.0020	0.0560	0.0017	1065	16	1047	11	1039	11	1101	32
91500-02	0.0748	0.0012	1.790	0.028	0.1736	0.0020	0.0535	0.0014	1063	14	1042	10	1032	11	1054	26
91500-03	0.0750	0.0013	1.820	0.032	0.1761	0.0022	0.0566	0.0017	1067	16	1053	12	1046	12	1113	32
91500-04	0.0749	0.0013	1.803	0.031	0.1747	0.0020	0.0532	0.0016	1065	16	1046	11	1038	11	1048	31
91500-05	0.0749	0.0011	1.810	0.027	0.1754	0.0020	0.0532	0.0013	1064	13	1049	10	1042	11	1047	25
91500-06	0.0749	0.0012	1.804	0.028	0.1748	0.0020	0.0550	0.0014	1065	13	1047	10	1038	11	1081	26
91500-07	0.0748	0.0012	1.858	0.030	0.1801	0.0021	0.0536	0.0014	1064	15	1066	11	1068	11	1056	27
91500-08	0.0748	0.0012	1.846	0.028	0.1789	0.0020	0.0532	0.0014	1064	14	1062	10	1061	11	1047	26
91500-09	0.0749	0.0012	1.844	0.028	0.1787	0.0021	0.0542	0.0014	1065	14	1061	10	1060	11	1068	27
91500-10	0.0748	0.0012	1.829	0.029	0.1773	0.0021	0.0540	0.0015	1064	14	1056	11	1052	11	1064	29
91500-11	0.0726	0.0012	1.781	0.027	0.1779	0.0019	0.0558	0.0014	1003	14	1038	10	1056	10	1097	27
91500-12	0.0752	0.0011	1.781	0.024	0.1718	0.0018	0.0521	0.0012	1074	12	1039	9	1022	10	1026	22
91500-13	0.0750	0.0013	1.802	0.028	0.1744	0.0019	0.0526	0.0015	1067	15	1046	10	1036	10	1036	29
91500-14	0.0749	0.0011	1.794	0.025	0.1737	0.0019	0.0523	0.0013	1067	13	1043	9	1032	10	1030	24
91500-15	0.0748	0.0012	1.808	0.028	0.1754	0.0020	0.0555	0.0014	1062	14	1048	10	1042	11	1091	27
91500-16	0.0748	0.0011	1.854	0.027	0.1798	0.0020	0.0572	0.0014	1063	13	1065	9	1066	11	1125	26
91500-17	0.0774	0.0011	1.878	0.026	0.1760	0.0020	0.0559	0.0012	1070	29	1051	15	1042	11	1041	11
91500-18	0.0749	0.0012	1.875	0.030	0.1816	0.0021	0.0582	0.0015	1065	14	1072	11	1076	12	1144	29
91500-19	0.0765	0.0017	1.887	0.040	0.1790	0.0023	0.0562	0.0028	1107	22	1076	14	1061	12	1105	54
91500-20	0.0749	0.0011	1.834	0.026	0.1776	0.0020	0.0560	0.0012	1065	12	1058	9	1054	11	1102	24
91500-21	0.0753	0.0011	1.827	0.023	0.1760	0.0015	0.0533	0.0011	1077	13	1055	8	1045	8	1049	20
91500-22	0.0750	0.0011	1.833	0.025	0.1773	0.0016	0.0521	0.0011	1068	12	1057	9	1052	9	1026	21
91500-23	0.0748	0.0011	1.836	0.024	0.1780	0.0017	0.0531	0.0010	1063	12	1058	9	1056	9	1046	20
91500-24	0.0749	0.0011	1.873	0.025	0.1814	0.0017	0.0547	0.0012	1065	12	1071	9	1075	9	1077	22
91500-25	0.0749	0.0011	1.861	0.025	0.1802	0.0017	0.0538	0.0011	1065	12	1067	9	1068	10	1059	21

	Ratio								Age (Ma)							
	$^{207}Pb/^{206}Pb$	± 1σ	$^{207}Pb/^{235}U$	± 1σ	$^{206}Pb/^{238}U$	± 1σ	$^{208}Pb/^{232}Th$	± 1σ	$^{207}Pb/^{206}Pb$	± 1σ	$^{207}Pb/^{235}U$	± 1σ	$^{206}Pb/^{238}U$	± 1σ	$^{208}Pb/^{232}Th$	± 1σ
91500-26	0.0748	0.0011	1.849	0.025	0.1793	0.0017	0.0568	0.0012	1063	12	1063	9	1063	9	1117	23
91500-29	0.0747	0.0014	1.810	0.032	0.1756	0.0021	0.0503	0.0021	1062	17	1049	12	1043	11	991	41
91500-30	0.0750	0.0018	1.803	0.041	0.1744	0.0022	0.0510	0.0029	1068	24	1047	15	1037	12	1005	56
91500-31	0.0753	0.0024	1.842	0.056	0.1774	0.0027	0.0506	0.0043	1077	35	1061	20	1053	15	998	83
91500-32	0.0748	0.0012	1.832	0.028	0.1776	0.0020	0.0511	0.0014	1064	14	1057	10	1054	11	1008	27
91500-33	0.0747	0.0011	1.845	0.027	0.1792	0.0020	0.0535	0.0013	1060	13	1062	10	1063	11	1054	25
91500-34	0.0753	0.0011	1.869	0.027	0.1802	0.0019	0.0542	0.0014	1075	13	1070	10	1068	11	1066	27
91500-35	0.0748	0.0012	1.823	0.028	0.1768	0.0019	0.0548	0.0016	1063	15	1054	10	1049	10	1078	31
91500-36	0.0749	0.0011	1.821	0.026	0.1763	0.0019	0.0555	0.0015	1067	13	1053	9	1047	11	1091	28
91500-37	0.0753	0.0013	1.888	0.031	0.1820	0.0021	0.0538	0.0016	1077	15	1077	11	1078	12	1059	30
91500-38	0.0747	0.0014	1.843	0.033	0.1788	0.0021	0.0562	0.0019	1062	17	1061	12	1061	12	1106	36
91500-39	0.0750	0.0016	1.847	0.038	0.1788	0.0023	0.0511	0.0019	1067	20	1062	13	1060	13	1007	37
91500-40	0.0748	0.0012	1.841	0.029	0.1785	0.0020	0.0541	0.0014	1063	14	1060	10	1059	11	1064	28
91500-41	0.0748	0.0011	1.818	0.026	0.1763	0.0019	0.0526	0.0014	1063	13	1052	10	1047	11	1035	26
91500-42	0.0750	0.0013	1.861	0.032	0.1801	0.0021	0.0544	0.0017	1067	16	1067	11	1067	11	1071	32
91500-43	0.0755	0.0012	1.839	0.030	0.1767	0.0020	0.0529	0.0015	1081	15	1060	11	1049	11	1043	28
91500-44	0.0746	0.0012	1.840	0.029	0.1790	0.0020	0.0554	0.0015	1057	14	1060	10	1062	11	1089	29
91500-45	0.0750	0.0019	1.846	0.044	0.1784	0.0024	0.0538	0.0025	1069	26	1062	16	1058	13	1059	47
91500-46	0.0750	0.0014	1.854	0.033	0.1794	0.0022	0.0547	0.0017	1067	17	1065	12	1064	12	1076	33
91500-47	0.0749	0.0015	1.848	0.036	0.1791	0.0022	0.0553	0.0019	1065	19	1063	13	1062	12	1088	37
91500-48	0.0749	0.0015	1.855	0.035	0.1798	0.0023	0.0539	0.0019	1065	18	1065	13	1066	12	1061	37
91500-49	0.0750	0.0011	1.835	0.028	0.1776	0.0022	0.0541	0.0010	1068	13	1058	10	1054	12	1064	19
91500-50	0.0748	0.0012	1.830	0.029	0.1775	0.0022	0.0523	0.0011	1062	14	1056	10	1053	12	1031	21
91500-51	0.0742	0.0011	1.813	0.028	0.1772	0.0022	0.0543	0.0010	1047	13	1050	10	1052	12	1068	19
91500-52	0.0751	0.0013	1.849	0.032	0.1785	0.0023	0.0546	0.0011	1072	16	1063	11	1059	12	1074	22

	Ratio								Age (Ma)							
	$^{207}Pb/^{206}Pb$	± 1σ	$^{207}Pb/^{235}U$	± 1σ	$^{206}Pb/^{238}U$	± 1σ	$^{208}Pb/^{232}Th$	± 1σ	$^{207}Pb/^{206}Pb$	± 1σ	$^{207}Pb/^{235}U$	± 1σ	$^{206}Pb/^{238}U$	± 1σ	$^{208}Pb/^{232}Th$	± 1σ
91500-53	0.0764	0.0011	1.871	0.029	0.1777	0.0022	0.0525	0.0010	1105	13	1071	10	1054	12	1035	18
91500-54	0.0736	0.0011	1.827	0.027	0.1801	0.0022	0.0478	0.0008	1030	13	1055	10	1068	12	945	16
91500-55	0.0767	0.0012	1.820	0.030	0.1721	0.0021	0.0518	0.0010	1114	14	1053	11	1024	12	1022	20
91500-56	0.0729	0.0012	1.754	0.029	0.1746	0.0021	0.0514	0.0010	1011	15	1029	11	1037	12	1013	20
91500-57	0.0733	0.0011	1.779	0.028	0.1760	0.0021	0.0524	0.0010	1022	14	1038	10	1045	12	1032	20
91500-58	0.0760	0.0012	1.886	0.030	0.1799	0.0022	0.0511	0.0010	1096	14	1076	10	1066	12	1008	18
91500-59	0.0744	0.0012	1.815	0.030	0.1770	0.0022	0.0496	0.0010	1051	16	1051	11	1051	12	979	20
91500-60	0.0749	0.0013	1.848	0.032	0.1789	0.0022	0.0527	0.0012	1067	16	1063	11	1061	12	1037	24
91500-61	0.0754	0.0012	1.861	0.029	0.1790	0.0021	0.0538	0.0010	1079	14	1067	10	1062	12	1059	20
91500-62	0.0750	0.0011	1.833	0.028	0.1772	0.0022	0.0554	0.0010	1069	13	1057	10	1052	12	1089	19
91500-63	0.0767	0.0012	1.838	0.029	0.1737	0.0022	0.0525	0.0010	1115	14	1059	10	1032	12	1035	19
91500-64	0.0754	0.0013	1.834	0.032	0.1765	0.0022	0.0530	0.0012	1079	16	1058	12	1048	12	1043	22
91500-65	0.0750	0.0012	1.785	0.028	0.1727	0.0021	0.0509	0.0010	1068	14	1040	10	1027	11	1003	19
91500-66	0.0744	0.0011	1.804	0.028	0.1759	0.0021	0.0514	0.0009	1052	14	1047	10	1045	12	1013	18
91500-67	0.0762	0.0012	1.854	0.029	0.1764	0.0022	0.0509	0.0009	1101	14	1065	10	1047	12	1004	18
91500-68	0.0753	0.0012	1.823	0.029	0.1756	0.0021	0.0512	0.0010	1076	15	1054	10	1043	12	1010	19
91500-69	0.0772	0.0012	1.864	0.029	0.1751	0.0021	0.0531	0.0010	1127	14	1069	10	1040	12	1046	19
91500-70	0.0743	0.0012	1.827	0.029	0.1783	0.0020	0.0553	0.0011	1050	15	1055	11	1058	11	1087	22
91500-71	0.0749	0.0014	1.847	0.033	0.1789	0.0021	0.0547	0.0013	1065	18	1062	12	1061	12	1075	25
91500-72	0.0746	0.0013	1.817	0.032	0.1767	0.0021	0.0551	0.0013	1057	16	1051	11	1049	11	1084	24
91500-73	0.0747	0.0006	1.843	0.032	0.1790	0.0021	0.0553	0.0012	1060	16	1061	11	1061	11	1088	24
91500-74	0.0750	0.0008	1.838	0.036	0.1777	0.0022	0.0537	0.0014	1069	20	1059	13	1054	12	1056	28
91500-75	0.0748	0.0008	1.813	0.037	0.1758	0.0022	0.0562	0.0016	1063	20	1050	13	1044	12	1105	30
91500-76	0.0750	0.0014	1.820	0.033	0.1760	0.0021	0.0541	0.0013	1068	17	1053	12	1045	12	1065	25
91500-78	0.0751	0.0019	1.845	0.045	0.1783	0.0025	0.0608	0.0024	1071	26	1062	16	1057	14	1193	46

	Ratio								Age (Ma)							
	$^{207}Pb/^{206}Pb$	± 1σ	$^{207}Pb/^{235}U$	± 1σ	$^{206}Pb/^{238}U$	± 1σ	$^{208}Pb/^{232}Th$	± 1σ	$^{207}Pb/^{206}Pb$	± 1σ	$^{207}Pb/^{235}U$	± 1σ	$^{206}Pb/^{238}U$	± 1σ	$^{208}Pb/^{232}Th$	± 1σ
91500-79	0.0751	0.0016	1.846	0.038	0.1784	0.0023	0.0542	0.0017	1071	21	1062	14	1058	13	1067	32
91500-80	0.0782	0.0021	1.913	0.050	0.1775	0.0026	0.0562	0.0021	1152	27	1086	17	1053	14	1105	41
91500-81	0.0736	0.0014	1.832	0.034	0.1805	0.0023	0.0547	0.0014	1031	18	1057	12	1070	12	1077	26
91500-82	0.0736	0.0014	1.814	0.034	0.1788	0.0022	0.0554	0.0014	1031	18	1051	12	1060	12	1091	27

	$^{176}Hf/^{177}Hf$	± 1σ	$^{178}Hf/^{177}Hf$	± 1σ	$^{180}Hf/^{177}Hf$	± 1σ	$^{176}Lu/^{177}Hf$	± 1σ	$^{176}Yb/^{177}Hf$	± 1σ	Total Hf	1σ
MT-11-460	0.282536	0.000011	1.467190	0.000026	1.886780	0.000054	0.000109	0.000000	0.005417	0.000025	2.864	0.087
MT-11-461	0.282524	0.000010	1.467240	0.000019	1.886700	0.000061	0.000093	0.000000	0.004520	0.000017	3.048	0.081
MT-11-462	0.282536	0.000012	1.467270	0.000026	1.886770	0.000054	0.000084	0.000000	0.003987	0.000029	2.991	0.095
MT-11-463	0.282512	0.000013	1.467260	0.000020	1.886820	0.000098	0.000098	0.000000	0.004833	0.000028	2.880	0.071
MT-11-507	0.282513	0.000010	1.466900	0.000027	1.887120	0.000078	0.000089	0.000000	0.004118	0.000042	1.789	0.066
MT-11-508	0.282503	0.000011	1.467140	0.000025	1.886940	0.000068	0.000127	0.000001	0.005962	0.000070	2.404	0.072
MT-11-518	0.282529	0.000009	1.467260	0.000025	1.886640	0.000054	0.000138	0.000000	0.005983	0.000027	4.088	0.079
MT-11-519	0.282516	0.000011	1.467230	0.000016	1.886630	0.000063	0.000145	0.000000	0.006674	0.000020	3.599	0.110
MT-11-520	0.282527	0.000009	1.467150	0.000025	1.886830	0.000100	0.000063	0.000001	0.002756	0.000039	3.632	0.120
MT-11-521	0.282551	0.000010	1.467210	0.000027	1.886930	0.000062	0.000035	0.000000	0.001449	0.000010	3.498	0.092
MT-11-522	0.282505	0.000011	1.467180	0.000022	1.887020	0.000098	0.000047	0.000000	0.001819	0.000012	3.295	0.083
MT-11-523	0.282521	0.000011	1.467180	0.000020	1.886930	0.000053	0.000078	0.000000	0.003308	0.000005	3.517	0.095
MT-11-562	0.282522	0.000008	1.467110	0.000022	1.886800	0.000052	0.000077	0.000000	0.002892	0.000013	3.984	0.082
MT-11-563	0.282507	0.000010	1.467150	0.000025	1.886730	0.000060	0.000101	0.000000	0.003859	0.000029	3.268	0.100
MT-11-564	0.282505	0.000011	1.467140	0.000022	1.886870	0.000052	0.000108	0.000000	0.004408	0.000014	3.398	0.099
MT-11-565	0.282543	0.000010	1.467390	0.000017	1.886860	0.000060	0.000127	0.000000	0.005348	0.000027	3.528	0.110
MT-11-566	0.282546	0.000010	1.467310	0.000022	1.886830	0.000062	0.000119	0.000000	0.004905	0.000033	3.235	0.130
MT-11-567	0.282536	0.000009	1.467280	0.000022	1.886780	0.000060	0.000081	0.000000	0.003079	0.000016	3.381	0.083
MT-11-626	0.282547	0.000007	1.467250	0.000024	1.886600	0.000053	0.000124	0.000000	0.005040	0.000024	4.730	0.110
MT-11-627	0.282512	0.000008	1.467290	0.000017	1.886610	0.000048	0.000136	0.000000	0.005803	0.000033	4.660	0.140
MT-11-628	0.282510	0.000010	1.467220	0.000021	1.886460	0.000062	0.000133	0.000000	0.005496	0.000033	4.184	0.100
MT-11-629	0.282523	0.000010	1.467270	0.000013	1.886550	0.000051	0.000135	0.000000	0.006029	0.000037	4.317	0.140
MT-11-630	0.282520	0.000008	1.467310	0.000020	1.886760	0.000053	0.000114	0.000000	0.005302	0.000043	4.073	0.110
MT-11-901	0.282532	0.000013	1.467260	0.000058	1.886850	0.000050	0.000126	0.000000	0.004532	0.000028	2.565	0.078
MT-11-902	0.282540	0.000012	1.467390	0.000033	1.887120	0.000059	0.000122	0.000000	0.004326	0.000029	2.074	0.054
MT-11-903	0.282508	0.000011	1.467250	0.000037	1.887250	0.000054	0.000107	0.000001	0.003758	0.000065	1.776	0.051
MT-11-904	0.282510	0.000017	1.467160	0.000050	1.886980	0.000071	0.000110	0.000000	0.004047	0.000044	1.683	0.029
MT-11-905	0.282509	0.000011	1.467340	0.000036	1.887200	0.000061	0.000103	0.000000	0.003677	0.000022	1.848	0.040

	$^{176}Hf/^{177}Hf$	± 1σ	$^{178}Hf/^{177}Hf$	± 1σ	$^{180}Hf/^{177}Hf$	± 1σ	$^{176}Lu/^{177}Hf$	± 1σ	$^{176}Yb/^{177}Hf$	± 1σ	Total Hf	1σ
MT-11-906	0.282528	0.000018	1.467400	0.000048	1.887190	0.000081	0.000122	0.000000	0.004835	0.000032	1.596	0.054
MT-11-907	0.282532	0.000010	1.467240	0.000040	1.886710	0.000089	0.000124	0.000000	0.004902	0.000044	1.580	0.042
MT-11-908	0.282518	0.000015	1.467260	0.000037	1.887180	0.000088	0.000113	0.000001	0.004408	0.000019	1.522	0.049
MT-11-909	0.282556	0.000014	1.467330	0.000056	1.887230	0.000075	0.000121	0.000000	0.004899	0.000028	1.450	0.052
MT-11-910	0.282514	0.000019	1.467260	0.000050	1.886800	0.000081	0.000080	0.000000	0.002907	0.000006	1.500	0.036
MT-11-911	0.282503	0.000018	1.467250	0.000050	1.887250	0.000062	0.000086	0.000000	0.003139	0.000021	1.460	0.041
MT-11-912	0.282515	0.000017	1.467280	0.000039	1.887150	0.000085	0.000102	0.000000	0.003887	0.000047	1.474	0.033
MT-13-069	0.282508	0.000007	1.467280	0.000019	1.886840	0.000024	0.000145	0.000000	0.005906	0.000036	9.349	0.140
MT-13-070	0.282514	0.000006	1.467290	0.000021	1.886870	0.000028	0.000140	0.000000	0.005868	0.000065	9.521	0.180
MT-13-071	0.282554	0.000008	1.467800	0.000065	1.888670	0.000044	0.000124	0.000000	0.004944	0.000026	9.869	0.100
MT-13-072	0.282502	0.000006	1.467520	0.000026	1.887080	0.000031	0.000124	0.000000	0.005383	0.000031	10.393	0.200
MT-13-073	0.282493	0.000005	1.467880	0.000059	1.887300	0.000020	0.000119	0.000000	0.005098	0.000019	11.372	0.220
MT-13-074	0.282509	0.000004	1.467320	0.000016	1.886910	0.000026	0.000113	0.000001	0.005380	0.000012	11.159	0.180
MT-13-075	0.282524	0.000004	1.467350	0.000024	1.886880	0.000026	0.000120	0.000000	0.005792	0.000033	9.137	0.160
MT-13-076	0.282526	0.000005	1.467350	0.000016	1.886930	0.000024	0.000125	0.000000	0.006066	0.000037	8.831	0.170
MT-13-077	0.282495	0.000005	1.467260	0.000016	1.887010	0.000022	0.000087	0.000001	0.004070	0.000092	8.932	0.140
MT-13-078	0.282512	0.000005	1.467340	0.000017	1.886890	0.000035	0.000051	0.000001	0.002283	0.000037	10.219	0.200
MT-13-079	0.282525	0.000005	1.467300	0.000017	1.886880	0.000028	0.000093	0.000000	0.004404	0.000018	9.856	0.140
MT-13-080	0.282528	0.000007	1.467220	0.000016	1.886890	0.000029	0.000093	0.000000	0.004391	0.000008	9.971	0.190
MT-13-223	0.282521	0.000007	1.468250	0.000044	1.887340	0.000041	0.000166	0.000003	0.007688	0.000200	8.489	0.300
MT-13-224	0.282514	0.000005	1.467290	0.000023	1.886790	0.000032	0.000045	0.000000	0.002108	0.000020	8.913	0.200
MT-13-225	0.282523	0.000006	1.466570	0.000030	1.887220	0.000034	0.000039	0.000001	0.001809	0.000022	9.653	0.250
MT-13-226	0.282517	0.000005	1.467280	0.000031	1.886880	0.000030	0.000081	0.000000	0.004044	0.000036	7.450	0.190
MT-13-227	0.282557	0.000004	1.467310	0.000014	1.886640	0.000021	0.000073	0.000000	0.003594	0.000017	7.117	0.200
MT-13-228	0.282510	0.000006	1.467210	0.000029	1.886640	0.000028	0.000073	0.000000	0.003790	0.000016	6.907	0.200
MT-13-229	0.282544	0.000006	1.467260	0.000014	1.886650	0.000023	0.000080	0.000000	0.004025	0.000011	7.543	0.240
MT-13-230	0.282510	0.000005	1.467300	0.000018	1.886810	0.000020	0.000103	0.000001	0.005316	0.000009	7.417	0.150
MT-13-231	0.282480	0.000005	1.467350	0.000020	1.886920	0.000030	0.000111	0.000000	0.005610	0.000019	7.253	0.150

	$^{176}Hf/^{177}Hf$	± 1σ	$^{178}Hf/^{177}Hf$	± 1σ	$^{180}Hf/^{177}Hf$	± 1σ	$^{176}Lu/^{177}Hf$	± 1σ	$^{176}Yb/^{177}Hf$	± 1σ	Total Hf	1σ
MT-13-266	0.282503	0.000006	1.467380	0.000017	1.887030	0.000033	0.000144	0.000000	0.006000	0.000040	8.530	0.140
MT-13-267	0.282534	0.000007	1.467260	0.000018	1.886820	0.000029	0.000128	0.000000	0.005429	0.000037	9.007	0.170
MT-13-268	0.282518	0.000005	1.467300	0.000018	1.887010	0.000024	0.000122	0.000000	0.005088	0.000017	9.460	0.180
MT-13-269	0.282492	0.000004	1.466700	0.000019	1.887450	0.000025	0.000115	0.000000	0.004741	0.000028	9.535	0.210
MT-13-270	0.282518	0.000007	1.467240	0.000014	1.886740	0.000033	0.000112	0.000000	0.004940	0.000024	9.117	0.200
MT-13-271	0.282508	0.000005	1.467420	0.000016	1.887140	0.000033	0.000120	0.000000	0.005379	0.000039	10.012	0.210
MT-13-272	0.282519	0.000005	1.467850	0.000019	1.887250	0.000032	0.000130	0.000000	0.005920	0.000023	10.032	0.200
MT-13-273	0.282536	0.000005	1.467320	0.000014	1.886770	0.000030	0.000128	0.000000	0.006227	0.000039	9.089	0.170
MT-13-274	0.282578	0.000006	1.467150	0.000021	1.886640	0.000030	0.000111	0.000000	0.005212	0.000025	8.962	0.160
MT-13-275	0.282541	0.000008	1.467120	0.000017	1.886690	0.000026	0.000112	0.000000	0.005384	0.000029	8.956	0.150
MT-13-276	0.282503	0.000007	1.467220	0.000013	1.886860	0.000033	0.000114	0.000000	0.005361	0.000053	8.871	0.160
MT-14-312	0.282614	0.000010	1.467070	0.000020	1.886150	0.000046	0.000143	0.000000	0.004897	0.000028	3.161	0.065
MT-14-313	0.282513	0.000011	1.466880	0.000019	1.886630	0.000061	0.000136	0.000000	0.005094	0.000038	3.253	0.077
MT-14-314	0.282512	0.000010	1.467040	0.000017	1.886510	0.000057	0.000119	0.000000	0.004289	0.000034	3.322	0.085
MT-14-315	0.282508	0.000010	1.467090	0.000025	1.886510	0.000068	0.000143	0.000000	0.005350	0.000040	3.386	0.068
MT-14-316	0.282505	0.000012	1.467070	0.000023	1.886570	0.000059	0.000144	0.000000	0.005365	0.000035	3.333	0.073
MT-14-317	0.282472	0.000011	1.466990	0.000020	1.886780	0.000045	0.000090	0.000002	0.003158	0.000066	3.506	0.073
MT-14-318	0.282553	0.000008	1.467150	0.000021	1.886450	0.000045	0.000088	0.000001	0.003307	0.000013	3.204	0.059
MT-14-319	0.282494	0.000008	1.466940	0.000026	1.886600	0.000039	0.000118	0.000000	0.004594	0.000039	3.321	0.059
MT-14-320	0.282476	0.000009	1.466990	0.000022	1.886770	0.000070	0.000129	0.000000	0.005092	0.000046	3.248	0.062
MT-14-321	0.282501	0.000010	1.467080	0.000018	1.886650	0.000044	0.000131	0.000000	0.005125	0.000031	3.320	0.078
MT-14-322	0.282462	0.000007	1.467000	0.000021	1.886880	0.000047	0.000131	0.000000	0.005162	0.000036	3.202	0.072
MT-14-323	0.282506	0.000009	1.467140	0.000021	1.886660	0.000056	0.000121	0.000001	0.004784	0.000098	3.358	0.082
MT-14-324	0.282491	0.000011	1.466930	0.000032	1.886570	0.000048	0.000133	0.000000	0.004875	0.000041	3.223	0.069
MT-14-325	0.282479	0.000013	1.466970	0.000023	1.886650	0.000067	0.000127	0.000000	0.004713	0.000045	3.409	0.061
MT-14-326	0.282499	0.000009	1.466950	0.000023	1.886650	0.000054	0.000129	0.000000	0.004760	0.000040	3.078	0.055
MT-14-327	0.282536	0.000009	1.467230	0.000024	1.886510	0.000045	0.000124	0.000000	0.004674	0.000046	3.154	0.067
MT-14-382	0.282516	0.000015	1.466890	0.000026	1.886500	0.000061	0.000029	0.000000	0.001002	0.000020	2.855	0.068

	$^{176}Hf/^{177}Hf$	± 1σ	$^{178}Hf/^{177}Hf$	± 1σ	$^{180}Hf/^{177}Hf$	± 1σ	$^{176}Lu/^{177}Hf$	± 1σ	$^{176}Yb/^{177}Hf$	± 1σ	Total Hf	1σ
MT-14-383	0.282468	0.000013	1.466990	0.000020	1.886790	0.000092	0.000100	0.000000	0.003462	0.000038	2.945	0.058
MT-14-384	0.282534	0.000013	1.467100	0.000019	1.886650	0.000062	0.000105	0.000000	0.003723	0.000035	2.585	0.063
MT-14-385	0.282491	0.000011	1.467120	0.000033	1.886610	0.000072	0.000105	0.000002	0.003850	0.000049	2.387	0.056
MT-14-386	0.282513	0.000011	1.467060	0.000027	1.886630	0.000075	0.000102	0.000000	0.003540	0.000030	2.913	0.060
MT-14-387	0.282495	0.000011	1.467020	0.000027	1.886630	0.000055	0.000069	0.000000	0.002326	0.000036	2.479	0.056
MT-14-388	0.282475	0.000010	1.467080	0.000025	1.886770	0.000061	0.000093	0.000001	0.003422	0.000026	2.766	0.044
MT-14-389	0.282542	0.000009	1.467190	0.000022	1.886600	0.000053	0.000110	0.000000	0.003836	0.000050	2.666	0.057
MT-14-390	0.282543	0.000012	1.467180	0.000024	1.886530	0.000067	0.000095	0.000001	0.003412	0.000066	2.445	0.041
MT-14-391	0.282491	0.000011	1.467110	0.000024	1.886560	0.000068	0.000103	0.000000	0.003831	0.000038	2.280	0.050
MT-14-392	0.282498	0.000014	1.467080	0.000017	1.886610	0.000077	0.000097	0.000000	0.003541	0.000028	2.382	0.051
MT-14-393	0.282453	0.000017	1.467050	0.000028	1.886750	0.000078	0.000097	0.000000	0.003554	0.000031	2.443	0.041
MT-14-394	0.282498	0.000015	1.467010	0.000023	1.886590	0.000053	0.000081	0.000000	0.002684	0.000019	2.990	0.043
MT-14-395	0.282524	0.000010	1.467050	0.000021	1.886580	0.000073	0.000100	0.000000	0.003471	0.000022	2.948	0.042
MT-14-396	0.282447	0.000011	1.466980	0.000025	1.886840	0.000061	0.000059	0.000000	0.001918	0.000017	2.812	0.050
MT-14-397	0.282515	0.000014	1.467130	0.000017	1.886550	0.000066	0.000123	0.000000	0.004361	0.000019	2.736	0.053
MT-14-398	0.282496	0.000011	1.467040	0.000017	1.886630	0.000054	0.000090	0.000000	0.003105	0.000033	2.992	0.044
MT-14-399	0.282502	0.000011	1.467090	0.000036	1.886560	0.000075	0.000080	0.000001	0.002814	0.000008	2.729	0.033
MT-14-400	0.282512	0.000010	1.467090	0.000024	1.886420	0.000068	0.000106	0.000000	0.003850	0.000017	2.725	0.033
MT-14-401	0.282508	0.000011	1.467030	0.000022	1.886620	0.000072	0.000106	0.000000	0.003832	0.000039	2.566	0.043
MT-14-402	0.282489	0.000011	1.467100	0.000022	1.886730	0.000061	0.000112	0.000000	0.004039	0.000024	2.614	0.032
MT-14-403	0.282511	0.000009	1.467130	0.000022	1.886690	0.000055	0.000113	0.000001	0.004054	0.000028	2.711	0.034
MT-14-404	0.282498	0.000011	1.467090	0.000024	1.886560	0.000066	0.000126	0.000000	0.004643	0.000036	2.634	0.045
MT-14-405	0.282473	0.000011	1.467080	0.000030	1.886540	0.000068	0.000121	0.000002	0.004486	0.000031	2.694	0.038

	$^{176}Hf/^{177}Hf$	± 1σ	$^{178}Hf/^{177}Hf$	± 1σ	$^{180}Hf/^{177}Hf$	± 1σ	$^{176}Lu/^{177}Hf$	± 1σ	$^{176}Yb/^{177}Hf$	± 1σ	Total Hf	1σ
TEM-11-107	0.282659	0.000009	1.467230	0.000025	1.886720	0.000048	0.001049	0.000009	0.036276	0.000220	2.625	0.064
TEM-11-114	0.282694	0.000008	1.466940	0.000032	1.887060	0.000059	0.001159	0.000005	0.036816	0.000096	1.856	0.050
TEM-11-116	0.282678	0.000013	1.467160	0.000037	1.886590	0.000083	0.001075	0.000043	0.032680	0.001300	3.789	0.170
TEM-11-123	0.282682	0.000008	1.467230	0.000016	1.886550	0.000061	0.001595	0.000085	0.047228	0.002600	3.858	0.140
TEM-11-124	0.282712	0.000012	1.467340	0.000024	1.886880	0.000073	0.000752	0.000007	0.021716	0.000072	2.886	0.061
TEM-11-135	0.282675	0.000009	1.467300	0.000019	1.886630	0.000069	0.000948	0.000036	0.027424	0.001300	5.005	0.100
TEM-11-136	0.282677	0.000010	1.467340	0.000024	1.886880	0.000074	0.001618	0.000040	0.049139	0.000580	3.762	0.210
TEM-11-178	0.282690	0.000013	1.467170	0.000040	1.886770	0.000055	0.001163	0.000039	0.033488	0.001400	2.246	0.035
TEM-11-179	0.282679	0.000015	1.467320	0.000049	1.887100	0.000110	0.001069	0.000005	0.029471	0.000420	1.611	0.057
TEM-13-024	0.282689	0.000008	1.467290	0.000042	1.886850	0.000042	0.000862	0.000024	0.027234	0.000580	8.141	0.120
TEM-13-025	0.282663	0.000007	1.468640	0.000045	1.887470	0.000021	0.001109	0.000013	0.041008	0.000960	8.657	0.110
TEM-13-026	0.282663	0.000013	1.467300	0.000050	1.887070	0.000043	0.001127	0.000033	0.042096	0.000900	8.813	0.180
TEM-13-027	0.282744	0.000010	1.467150	0.000013	1.886980	0.000031	0.001891	0.000022	0.078859	0.000350	6.484	0.110
TEM-13-132	0.282671	0.000008	1.467290	0.000032	1.886840	0.000042	0.000803	0.000027	0.028930	0.001700	7.856	0.260
TEM-13-133	0.282710	0.000006	1.467230	0.000020	1.886590	0.000038	0.001177	0.000012	0.051307	0.000750	7.389	0.054
TEM-13-134	0.282672	0.000010	1.467440	0.000036	1.887020	0.000030	0.001004	0.000010	0.045557	0.000830	7.558	0.130
TEM-13-198	0.282664	0.000006	1.467350	0.000016	1.886990	0.000039	0.000846	0.000012	0.029193	0.000760	7.913	0.140
TEM-13-199	0.282721	0.000006	1.467760	0.000030	1.887200	0.000023	0.001434	0.000029	0.053656	0.000820	8.490	0.110
TEM-13-200	0.282686	0.000006	1.467230	0.000016	1.886880	0.000036	0.001040	0.000010	0.039263	0.000630	8.587	0.140
TEM-14-162	0.282746	0.000012	1.467170	0.000038	1.886550	0.000097	0.001200	0.000034	0.032842	0.000540	2.838	0.130
TEM-14-163	0.282859	0.000013	1.467090	0.000022	1.886340	0.000056	0.001736	0.000018	0.055211	0.000820	2.446	0.034
TEM-14-164	0.282680	0.000014	1.466890	0.000028	1.886810	0.000062	0.001064	0.000038	0.032743	0.001900	2.515	0.038
TEM-14-165	0.282738	0.000013	1.466830	0.000020	1.886990	0.000058	0.001105	0.000028	0.036388	0.001400	2.845	0.028
TEM-14-166	0.282724	0.000014	1.466950	0.000021	1.886870	0.000050	0.000659	0.000007	0.021037	0.000380	2.713	0.055
TEM-14-167	0.282806	0.000014	1.467040	0.000030	1.886850	0.000058	0.001554	0.000043	0.052473	0.001100	2.125	0.044
TEM-14-168	0.282694	0.000013	1.466840	0.000030	1.886730	0.000069	0.000925	0.000041	0.025205	0.001400	2.707	0.039
TEM-14-169	0.282705	0.000011	1.466950	0.000024	1.886640	0.000054	0.000971	0.000009	0.027282	0.000520	2.962	0.061
TEM-14-387	0.282696	0.000012	1.466920	0.000023	1.886610	0.000080	0.000511	0.000017	0.014033	0.000300	3.362	0.038

	$^{176}Hf/^{177}Hf$	± 1σ	$^{178}Hf/^{177}Hf$	± 1σ	$^{180}Hf/^{177}Hf$	± 1σ	$^{176}Lu/^{177}Hf$	± 1σ	$^{176}Yb/^{177}Hf$	± 1σ	Total Hf	1σ
TEM-14-388	0.282729	0.000011	1.466970	0.000036	1.886560	0.000099	0.000629	0.000014	0.016563	0.000380	2.778	0.070
TEM-14-389	0.282740	0.000013	1.466970	0.000025	1.886570	0.000091	0.000904	0.000004	0.026594	0.000270	2.524	0.047
TEM-14-390	0.282753	0.000012	1.467170	0.000034	1.886540	0.000096	0.001272	0.000022	0.040110	0.000390	2.064	0.020
TEM-14-391	0.282776	0.000012	1.467110	0.000033	1.886470	0.000120	0.001191	0.000006	0.038782	0.000200	2.206	0.024
TEM-14-392	0.282730	0.000017	1.467140	0.000024	1.886560	0.000092	0.001062	0.000009	0.033189	0.000270	2.084	0.019
TEM-14-393	0.282731	0.000013	1.467060	0.000029	1.886500	0.000071	0.000790	0.000022	0.023134	0.000790	2.460	0.025
TEM-14-394	0.282703	0.000014	1.467000	0.000030	1.886740	0.000078	0.000885	0.000019	0.028066	0.000540	1.776	0.031
TEM-14-395	0.282658	0.000014	1.467070	0.000034	1.886540	0.000086	0.000481	0.000005	0.013291	0.000230	2.027	0.031
TEM-14-396	0.282716	0.000014	1.467100	0.000028	1.886680	0.000059	0.000980	0.000018	0.027201	0.000180	2.294	0.028
TEM-14-397	0.282742	0.000015	1.467220	0.000033	1.886870	0.000082	0.001047	0.000022	0.027348	0.000810	2.085	0.040

Appendix B – Sample Descriptions

The following information is provided for each sample:

Photograph of hand specimen.

Scan of thin section.

Appearance in hand specimen (grain size, colour, texture).

List of the primary phases and their characteristics.

Any other comments (e.g. extent of alteration, description of foliation).

Page A-37 displays a selection of field photographs showing the typical outcrop style of the Mpuluzi batholith.

RSA03



Left: photograph of hand specimen (scale bar = 2 cm). Right: scan of thin section (base = 2cm).

Sample location: 30°45.554 E
26°09.300 S

Medium-grained, grey, strongly foliated.

Phase assemblage:

- Quartz: minor undulose extinction
- Microcline: very fine perthite
- Plagioclase: minor alteration, no deformation twinning
- Biotite: aligned, undeformed, minor alteration to chlorite + epidote
- Titanite: up to ~600 μm, yellow-brown
- Hornblende: small, euhedral
- Allanite: small, subhedral, some minor remnant oscillatory zoning
- Apatite: aligned with foliation
- Zircon: abundant, tabular, aligned with foliation
- Oxides: abundant magnetite; minor ilmenite
- Fluorite: inclusions in biotite

Foliation is a magmatic alignment defined by alignment of biotite, also zircon, apatite. Biotite is undeformed, quartz only slightly strained, no deformation twinning in plagioclase.

Only slightly altered: feldspars are white, minor alteration of biotite to chlorite + epidote, plagioclase to sericite.

This is the only sample with hornblende.

RSA01



Left: photograph of hand specimen (scale bar = 2 cm). Right: scan of thin section (base = 2cm).

Sample location: 30°54.980 E
26°10.724 S

Medium-grained, grey, massive.

Phase assemblage:

- Quartz: undulose extinction
- Microcline: myrmekite; minor perthite
- Plagioclase: strongly altered to sericite, deformation twinning
- Biotite: partly altered to chlorite + epidote; aggregates of biotite, biotite + titanite
- Titanite: up to ~400 μm, euhedral, dark brown
- Allanite: ~100-200 μm, subhedral-anhedral, red-brown
- Apatite: abundant needles
- Zircon: commonly associated with biotite
- Oxides: minor ilmenite; magnetite absent

Unfoliated; fractures indicate brittle deformation.

Alteration is moderate: feldspars are white; plagioclase is strongly altered to sericite; biotite is partially altered to chlorite.

Biotites are deformed and commonly recrystallised to form aggregates of small grains.

SWA18a





Left: photograph of hand specimen (scale bar = 2 cm). Right: scan of thin section (base = 2cm).

Sample location: 31°25.040 E
26°03.540 S

Note: This sample is from the Piggs Peak batholith.

Medium-grained, pink, foliated.

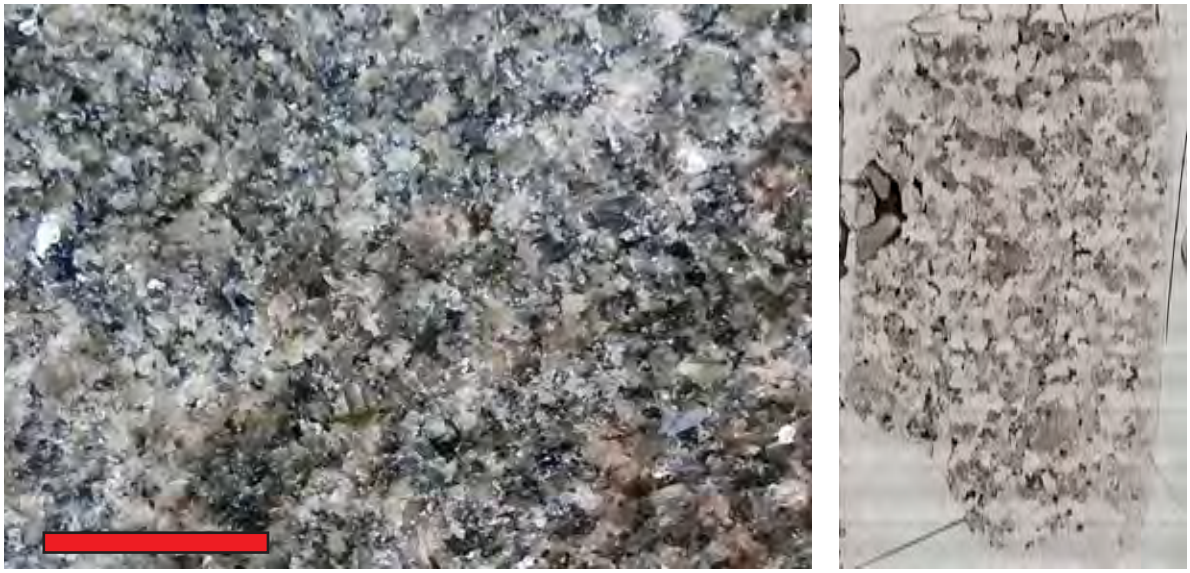
Phase assemblage:

- Quartz: minor undulose extinction
- Microcline: minor myrmekite; very fine perthite
- Plagioclase: deformation twinning; cores altered to sericite
- Biotite: euhedral, aligned; partly altered to chlorite + epidote along cleavage planes
- Allanite: rare, euhedral grains
- Apatite: abundant
- Zircon: euhedral, associated with biotite
- Oxides: ilmenite; minor magnetite

Weak foliation defined by aligned biotite.

Alteration is moderate: feldspars are pink; plagioclase cores are altered to sericite; biotite is partially altered to chlorite.

RSA05



Left: photograph of hand specimen (scale bar = 2 cm). Right: scan of thin section (base = 2cm).

Sample location: 30°35.094 E
26°12.596 S

Coarse-grained, grey, massive.

Phase assemblage:

- Quartz: minor undulose extinction
- Microcline: minor perthite; extensive replacement by myrmekite
- Plagioclase: altered to sericite; minor deformation twinning
- Biotite: altered to chlorite + epidote except where enclosed in quartz or feldspar
- Allanite: minor
- Apatite: occasional fine needles
- Zircon: commonly included in biotite
- Oxides: abundant ilmenite; very minor magnetite

Alteration is moderate: feldspars are white; plagioclase is extensively altered to sericite; biotite is partially altered to chlorite, with some unaltered grains enclosed in large quartz or feldspar.

RSA02





Left: photograph of hand specimen (scale bar = 2 cm). Right: scan of thin section (base = 2cm).

Sample location: 30°51.678 E
26°09.080 S

Medium-grained, grey, massive.

Phase assemblage:

- Quartz: minor undulose extinction
- Microcline: fine perthite; myrmekite
- Plagioclase: euhedral cores strongly altered to sericite; minor deformation twinning
- Biotite: partly altered to chlorite + epidote
- Allanite: small, euhedral grains
- Apatite: abundant needles
- Zircon: rare, euhedral grains, often included in biotite
- Oxides: minor ilmenite; magnetite absent
- Fluorite: inclusions in biotite

Alteration is moderate: feldspars are white; plagioclase cores are extensively altered to sericite; biotite is partially replaced by chlorite.

SWA07



Left: photograph of hand specimen (scale bar = 2 cm). Right: scan of thin section (base = 2cm).

Sample location: 31°00.374 E
26°27.716 S

Coarse-grained, pink, slightly foliated.

Phase assemblage:

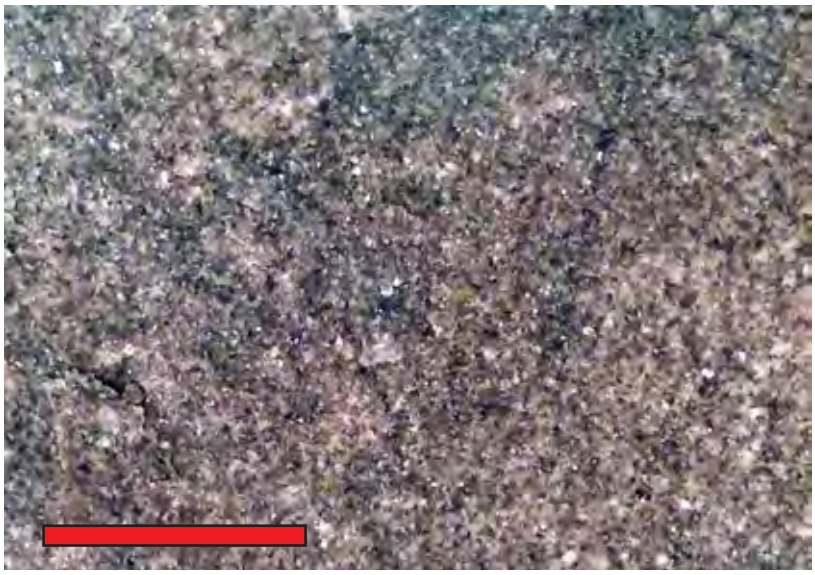
- Quartz: undulose extinction, sutured boundaries
- Microcline: myrmekite; minor perthite
- Plagioclase: minor deformation twinning; slightly altered
- Biotite: minor alteration to chlorite + epidote along boundaries, some deformation
- Allanite: rare, large, subhedral-euhedral
- Apatite: abundant, up to ~200 μm
- Zircon: commonly included in biotite, pleochroic haloes
- Oxides: minor ilmenite; magnetite absent
- Titanite: inclusions in biotite

Strongly porphyritic, with K-feldspar phenocrysts up to ~50 mm.

Weak foliation defined by aggregates of biotite and elongate quartz. Biotites show signs of deformation (bent cleavage).

Alteration is minor: feldspars are pink; biotite is mostly fresh with some alteration along grain boundaries; plagioclase is partially altered, especially the cores.

RSA04





Left: photograph of hand specimen (scale bar = 2 cm). Right: scan of thin section (base = 2cm).

Sample location: 30°39.595 E
26°09.898 S

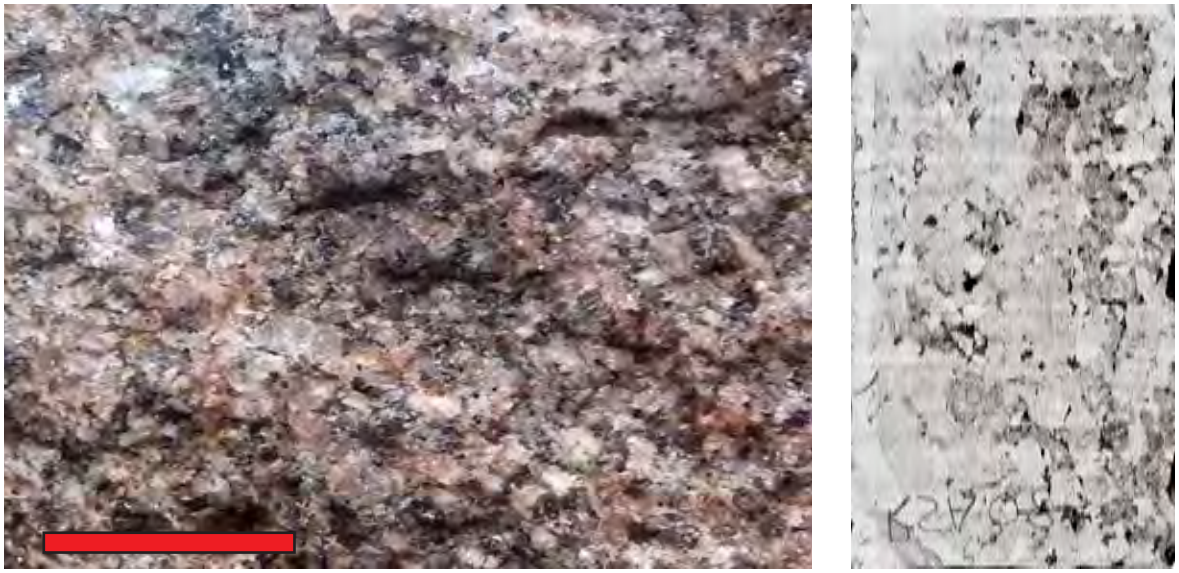
Medium-grained, pink, massive.

Phase assemblage:

- Quartz: minor undulose extinction
- Microcline: perthitic; myrmekiteu
- Plagioclase: cores altered to sericite; deformation twinning not observed (maybe obscured by extensive alteration)
- Biotite: extensively altered to chlorite + epidote
- Allanite: rare small, euhedral grains
- Zircon: associated with biotite
- Apatite: rare, small needles
- Oxides: very abundant magnetite; ilmenite absent

Alteration is extensive: feldspars are pink; plagioclase is extensively altered to sericite (and some recrystallised to muscovite); biotite is almost completely replaced by chlorite + epidote.

RSA08



Left: photograph of hand specimen (scale bar = 2 cm). Right: scan of thin section (base = 2cm).

Sample location: 30°44.963 E
26°17.164 S

Coarse-grained, pink, massive.

Phase assemblage:

- Quartz: very minor undulose extinction
- Microcline: perthitic; minor myrmekite
- Plagioclase: minor deformation twinning; altered cores
- Biotite: partly altered to chlorite + epidote
- Allanite: rare, large, euhedral to subhedral
- Zircon: commonly included in biotite
- Apatite: rare, small grains
- Oxides: abundant magnetite; minor ilmenite

Alteration is moderate: feldspars are pink; plagioclase cores are strongly altered to sericite; biotite partially altered to chlorite + epidote.

Microcline phenocrysts are ~rectangular, up to ~25 mm. Often display simple twins and enclose small grains of quartz, plagioclase, and occasional biotite.

SWA10a





Left: photograph of hand specimen (scale bar = 2 cm). Right: scan of thin section (base = 2cm).

Sanple location: 30°59.026 E
26°34.695 S

Medium-grained, pink, slightly foliated.

Phase assemblage:

- Quartz: undulose extinction, sutured boundaries
- Microcline: fine perthite; minor myrmekite
- Plagioclase: cores altered; minor deformation twinning
- Biotite: small, generally unaltered, randomly oriented
- Allanite: minor, euhedral
- Apatite: abundant small grains
- Zircon: associated with biotite
- Oxides: very minor magnetite; ilmenite absent

Weak foliation defined by drawn-out quartz.

Alteration is minor: feldspars are pink; plagioclase cores are partially altered to sericite; biotite shows incipient alteration to chlorite along cleavage planes.

RSA09



Left: photograph of hand specimen (scale bar = 2 cm). Right: scan of thin section (base = 2cm).

Sample location: 30°47.732 E
26°12.846 S

Coarse-grained, slightly pink, massive.

Phase assemblage:

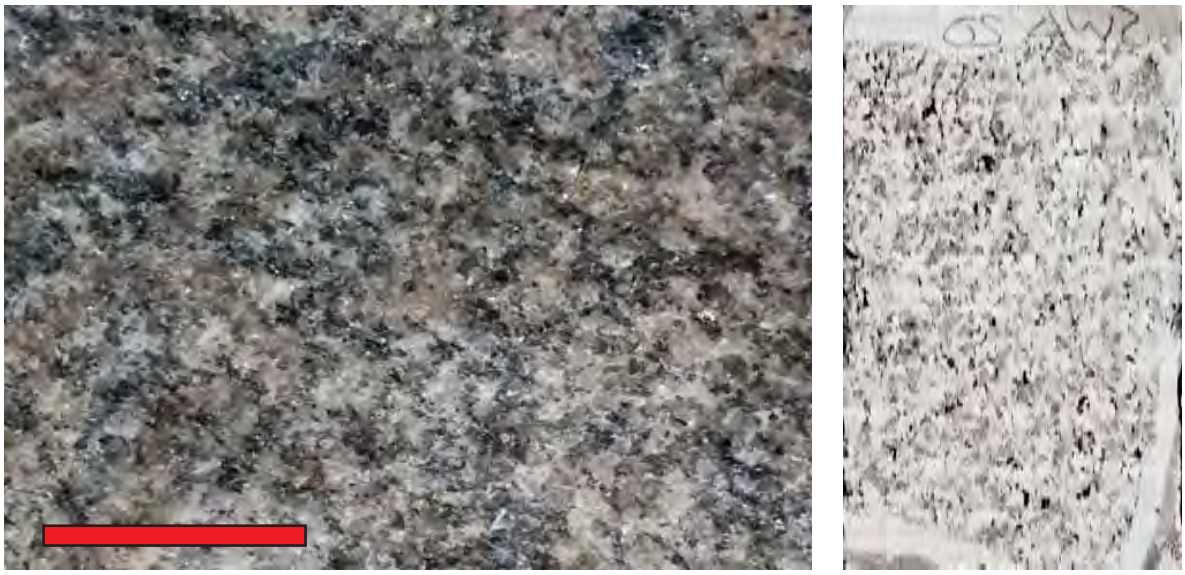
- Quartz: minor undulose extinction
- Microcline: perthitic; myrmekite; simple twins
- Plagioclase: minor deformation twinning; cores strongly altered
- Biotite: extensively altered to chlorite + epidote
- Allanite: rare, small grains
- Oxides: abundant ilmenite; minor magnetite
- Zircon: commonly with biotite
- Apatite: small needles
- Titanite: inclusions in biotite

Microcline phenocrysts are ~rectangular, up to ~25 mm. Often display simple twins and enclose small grains of quartz, plagioclase, and occasional biotite.

Alteration is extensive: feldspars are pink; plagioclase cores are strongly altered to sericite and in some cases recrystallised to muscovite; biotite is extensively altered to chlorite + epidote.

Clusters of biotite, allanite, zircon, apatite, and oxides.

SWA20



Left: photograph of hand specimen (scale bar = 2 cm). Right: scan of thin section (base = 2cm).

Sample location: 31°30.669 E
25°54.147 S

Note: This sample is from the Piggs Peak batholith.

Medium-grained, grey, massive.

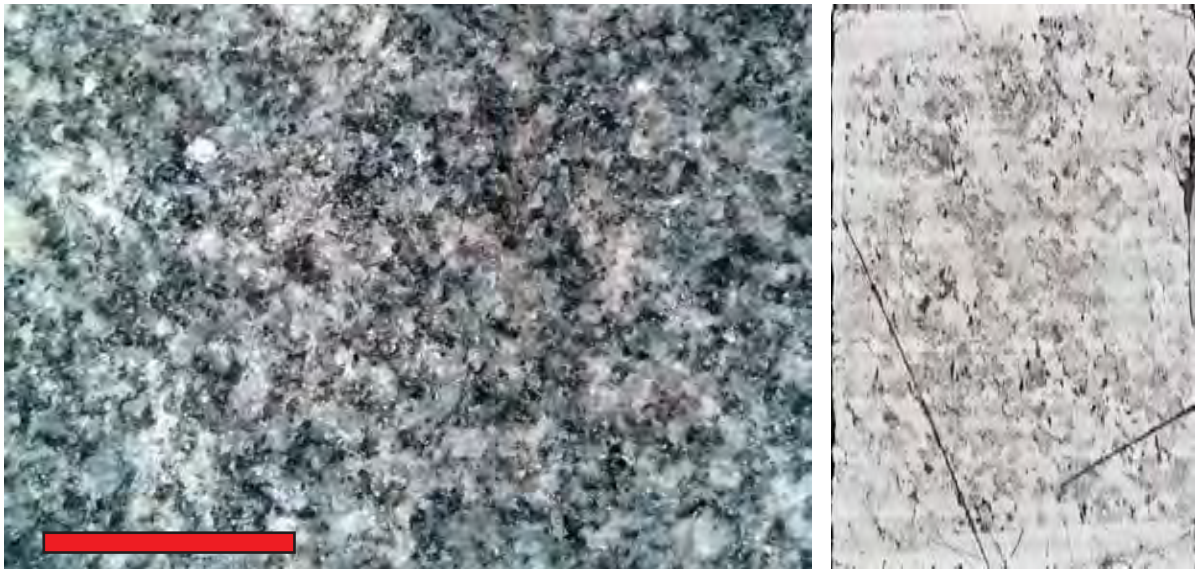
Phase assemblage:

- Quartz: undulose extinction, boundaries slightly sutured
- Microcline: perthitic; abundant myrmekite; simple twins
- Plagioclase: strongly altered cores; minor deformation twinning
- Biotite: partially altered to chlorite + epidote; large grains recrystallised
- Allanite: scattered euhedral grains
- Apatite: abundant small needles
- Zircon: abundant, commonly associated with biotite
- Oxides: minor magnetite and ilmenite

Alteration is extensive: feldspars are white; extensive replacement of microcline by myrmekite; plagioclase is strongly altered to sericite and sometimes replaced by muscovite; biotite is partially altered to chlorite + epidote and large grains are commonly recrystallised into aggregates of small grains.

Biotite commonly occurs as clusters with zircon, apatite, allanite, and opaques.

SWA03



Left: photograph of hand specimen (scale bar = 2 cm). Right: scan of thin section (base = 2cm).

Sample location: 31°10.872 E
26°03.921 S

Note: This sample is from the Piggs Peak batholith.

Coarse-grained, grey, slightly foliated.

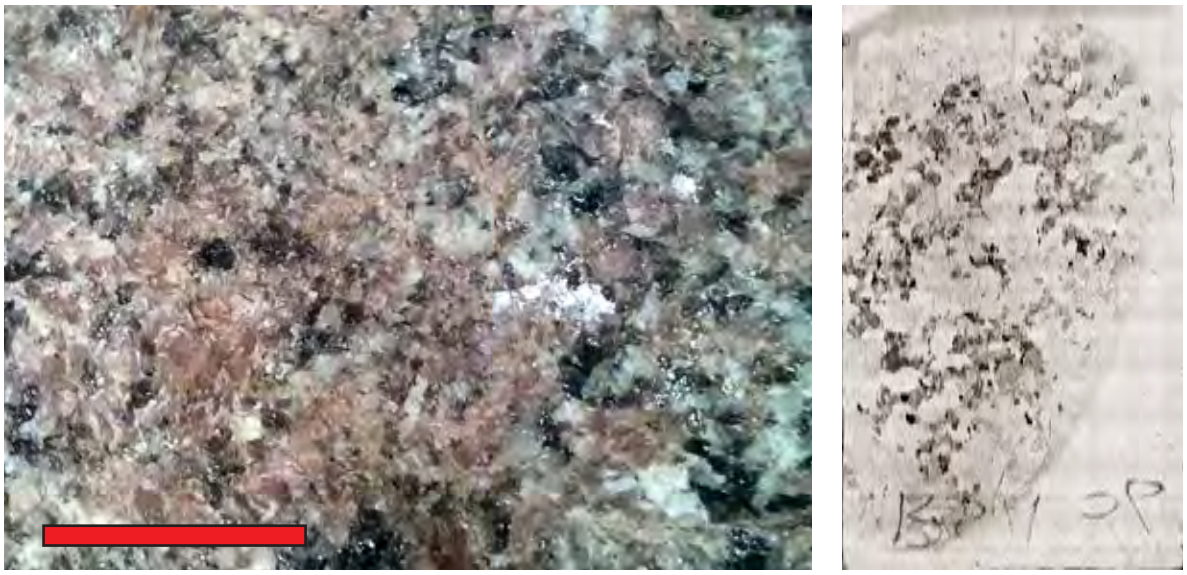
Phase assemblage:

- Quartz: undulose extinction, minor sutured boundaries
- Microcline: perthitic; extensively replaced by myrmekite
- Plagioclase: cores altered; minor deformation twins
- Biotite: minor alteration to chlorite + epidote, randomly oriented
- Zircon: associated with biotite
- Oxides: ilmenite; magnetite absent
- Apatite: rare, small needles
- Allanite: minor

Weak foliation defined by bands of quartz and feldspar

Alteration is moderate: feldspars are white; plagioclase is extensively altered to sericite and in some cases the cores are replaced by muscovite; biotite commonly shows incipient alteration to chlorite along cleavage planes.

RSA06



Left: photograph of hand specimen (scale bar = 2 cm). Right: scan of thin section (base = 2cm).

Sample location: 30°34.596 E
26°15.272 S

Coarse-grained, pink, massive.

Phase assemblage:

- Quartz: undulose extinction, boundaries slightly sutured
- Microcline: fine perthite; myrmekite; simple twins
- Plagioclase: minor deformation twinning
- Biotite: partly altered to chlorite + epidote
- Allanite: small, euhedral grains
- Zircon: abundant, associated with biotite/allanite/magnetite
- Apatite: rare, small grains
- Oxides: minor ilemnite (rare, large) and magnetite (small, euhedral)

Weakly portphyritic (microcline up to ~20 mm).

Alteration is moderate: feldspars are pink; plagioclase is partially altered to sericite; biotite is extensively altered to chlorite + epidote.

Zircon commonly appears in clusters with biotite, allanite, apatite, and magnetite.

SWA13a



Left: photograph of hand specimen (scale bar = 2 cm). Right: scan of thin section (base = 2cm).

Sanple location: 30°50.448 E
26°34.036 S

Medium-grained, grey-green, foliated.

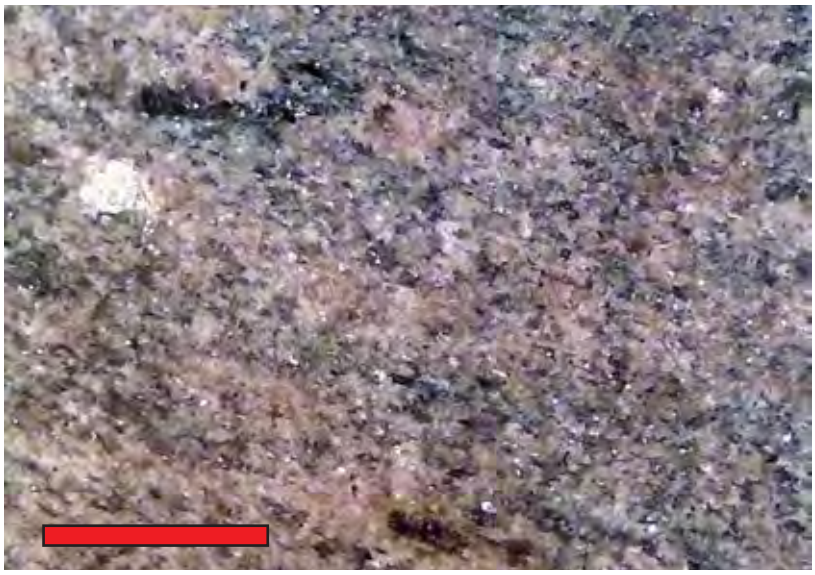
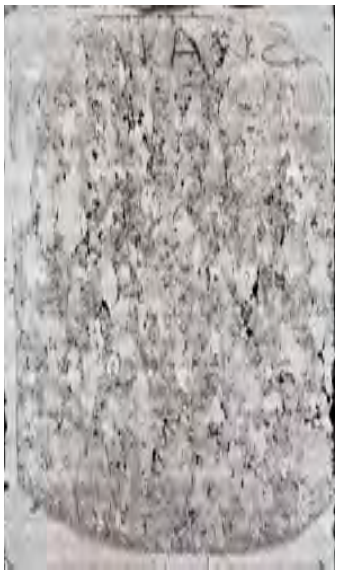
Phase assemblage:

- Quartz: minor undulose extinction
- Microcline: perthitic; minor myrmekite
- Plagioclase: altered to sericite; minor deformation twinning
- Biotite: partly altered to chlorite + epidote; euhedral, undeformed
- Zircon: commonly associated with biotite
- Allanite: rare, small grains
- Muscovite: minor
- Apatite: rare, small needles
- Oxides: very minor ilmenite; magnetite absent

Foliation is defined by bands of quartz and feldspar.

Alteration is moderate: feldspars are white; plagioclase is partially altered to sericite; biotite is partially altered to chlorite + epidote.

SWA11

Left: photograph of hand specimen (scale bar = 2 cm). Right: scan of thin section (base = 2cm).

Sample location: 30°54.231 E
26°35.265 S

Medium-grained, pink, foliated.

Phase assemblage:

- Quartz: undulose extinction, sutured boundaries, development of sub-grains, fractured
- Microcline: perthitic; minor myrmekite
- Plagioclase: fractures; minor deformation twinning; altered, especially cores
- Biotite: extensively altered to chlorite + epidote; some deformed
- Allanite: minor, subhedral
- Mucovite: minor
- Zircon: rare
- Oxides: minor magnetite; ilmenite absent
- Apatite: rare, small

Foliation is a result of deformation. Quartz is strongly undulose and grains appear drawn out.

Alteration is strong: feldspars are pink; plagioclase cores are altered to sericite; biotite is extensively replaced by chlorite + epidote.

SWA09



Left: photograph of hand specimen (scale bar = 2 cm). Right: scan of thin section (base = 2cm).

Sample location: 31°00.087 E
26°29.619 S

Medium-grained, pink, foliated.

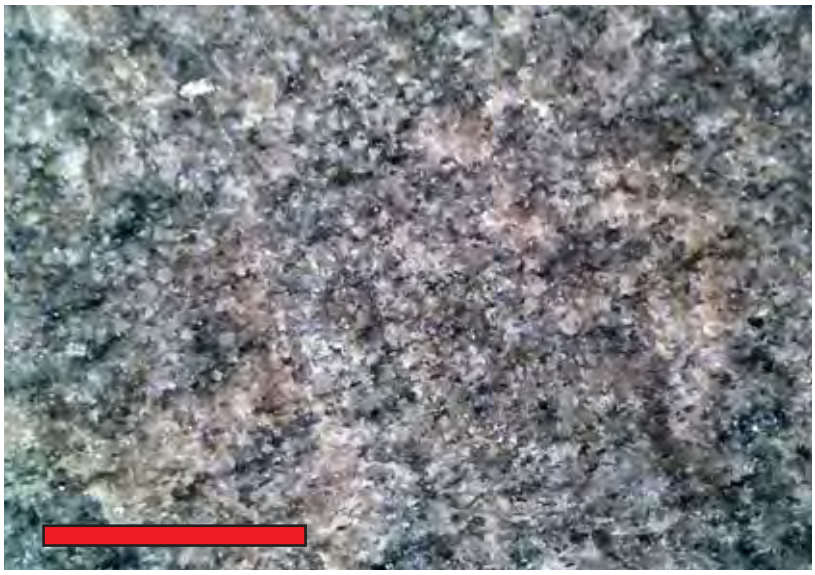
Phase assemblage:

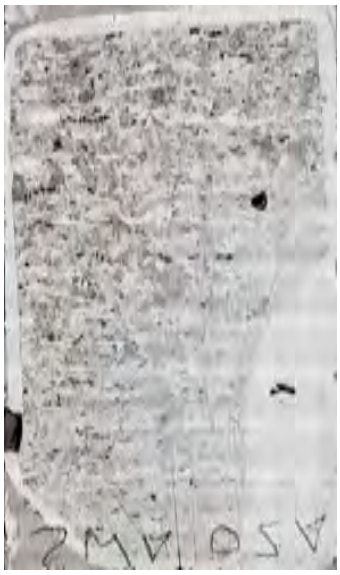
- Quartz: slight undulose extinction; boundaries are smooth and curved
- Microcline: minor perthite; minor myrmekite
- Plagioclase: minor deformation twinning, partially altered to sericite
- Biotite: some grains partially altered to chlorite; generally ehuedral, undeformed
- Zircon: rare, often associated with biotite
- Muscovite: minor
- Apatite: rare, acicular
- Oxides: very minor magnetite; ilmenite absent
- Allanite: very rare

Foliation appears to be primary, and is defined by aligned grains of undeformed biotite.

Alteration is minor. Feldpsars are pink; plagioclase is partially altered to sericite, and some biotite grains show incipient chloritisation.

SWA02a





Left: photograph of hand specimen (scale bar = 2 cm). Right: scan of thin section (base = 2cm).

Sample location: 31°09.640 E
26°08.017 S

Note: This sample is from the Piggs Peak batholith.

Medium-grained, grey, foliated.

Phase assemblage:

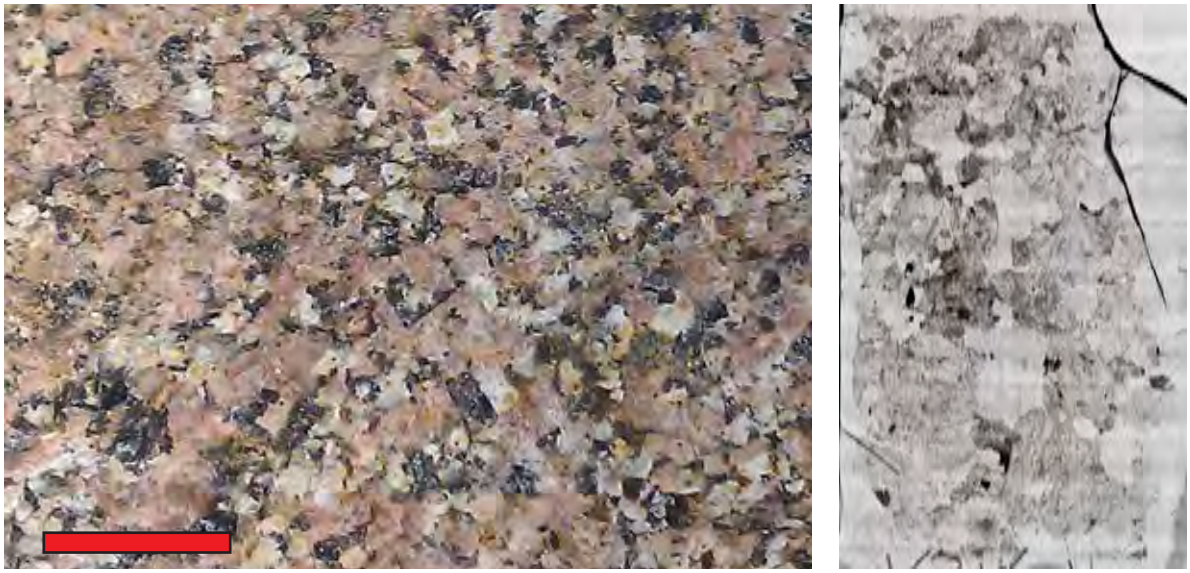
- Quartz: undulose extinction, sutured boundaries
- Microcline: minor perthite; minor myrmekite
- Plagioclase: deformation twinning; altered to sericite
- Biotite: ~completely replaced by chlorite + epidote
- Allanite: rare, small, euhedral grains
- Zircon: rare, small, euhdral
- Apatite: very rare, small needles
- Oxides: very minor ilmenite; magnetite absent

Foliation is a result of deformation, and is defined by elongated grains of quartz. The remnants of deformed biotites (replaced by chlorite + epidote) form elongate strings with allanite, zircon, and oxide grains.

Alteration is extensive: feldspars are white; plagioclase is strongly altered to sericite; biotite is extensively altered to chlorite + epidote.

Sericite replacing plagioclase is occasionally recrystallised to form single grains of muscovite.

RSA07



Left: photograph of hand specimen (scale bar = 2 cm). Right: scan of thin section (base = 2cm).

Sample location: 30°38.253 E
26°18.635 S

Coarse-grained, pink, massive.

Phase assemblage:

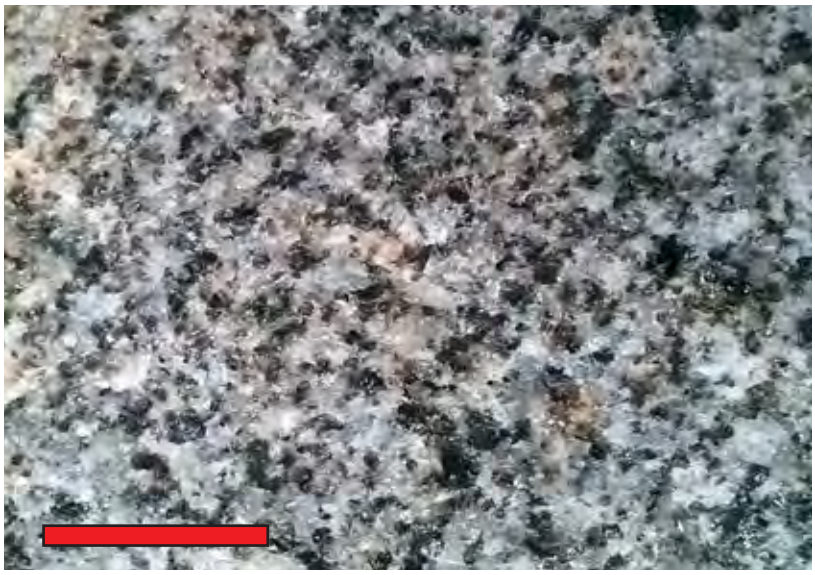
- Quartz: minor undulose extinction
- Microcline: coarse veins of perthite; minor myrmekite
- Plagioclase: minor deformation twinning
- Biotite: extensively altered to chlorite + epidote; undeformed
- Zircon: rare, euhedral grains, often associated with biotite
- Muscovite: minor
- Oxides: rare large (~2 mm) ilmenite; small (~0.5 mm) magnetite
- Apatite: very minor

Heavily fractured, however the fractures are not spatially associated with alteration.

Strongly altered: feldspars are pink; biotite is extensively altered to chlorite + epidote; plagioclase is also strongly altered to sericite, particularly the cores.

Very large microcline grains display simple twins and include small, euhedral grains of quartz and plagioclase.

SWA05





Left: photograph of hand specimen (scale bar = 2 cm). Right: scan of thin section (base = 2cm).

Sample location: 31°04.993 E
26°22.642 S

Coarse-grained, grey, massive.

Phase assemblage:

- Quartz: minor undulose extinction, boudaries generally smooth
- Microcline: minor perthite; minor mymekite
- Plagioclase: minor deformation twinning; cores altered to sericite
- Biotite: extensively altered to chlorite (+ epidote)
- Muscovite: large anastomosing grains, intergrown with quartz and feldspars
- Allanite: rare small, euhedral grains
- Zircon: rare, pleochroic halos when included in biotite or muscovite
- Apatite: very rare, small needles (<100 μm)
- Oxides: very rare ilmenite; magnetite absent

Muscovite occurs as large anastomosing grains, intergrown with microcline, plagioclase, and quartz.

Alteration is extensive: feldpsars are white; plagioclase is strongly altered to sericite (particularly the calcic cores); biotite is strongly altered to to chlorite + epidote.

Typical outcrop style of the Mpuluzi batholith



RSA01



RSA05



SWA07



SWA03



RSA06



SWA072a

Appendix C – Mineral Chemistry

Appendix C1 – Biotite compositions

The following information is presented for each biotite analysis:

Sample, Grain, Spot: Analyses are numbered sequentially per sample.

Composition, – O equiv.: Measured compositions are given in wt% oxide for cations; the oxide total is adjusted for F and Cl oxygen equivalents.

Structural formula: Calculated on the basis of 22 oxygens.

At%: Mg and Fe are given calculated in atomic percent, and the calculated magnesium number (Mg# = Mg/(Mg+Fe)).

Samples are ordered from mafic to felsic.

Appendix C2 – Allanite compositions

The following information is presented for each allanite analysis:

Sample, Grain, Spot: Analyses are numbered sequentially per sample.

Composition: Measured compositions are given in wt%.

Structural formula: Calculated on the basis of 13 oxygens.

Samples are ordered from mafic to felsic.

			Composition (wt%)									– O equiv.			Structural formula (cations / 22 oxygen)												Cation	at%		
Sample	Grain	Spot	SiO_2	Al_2O_3	TiO_2	FeO	MnO	MgO	CaO	Na_2O	K_2O	F	Cl	Total	Si	Al^{IV}	Al^{VI}	Ti	Fe^{2+}	Mn	Mg	Ca	Na	K	F	Cl	OH	total	Mg	Fe	Mg#
RSA03	1	1	37.29	15.21	1.92	20.86	0.36	10.18	<LLD	0.06	9.35	0.0205	0.0008	95.21	5.722	2.278	0.473	0.222	2.677	0.047	2.329	0.000	0.018	1.830	0.021	0.001	3.880	15.60	6.13	7.05	0.47
RSA03	1	2	36.79	15.33	1.84	21.07	0.38	10.27	<LLD	<LLD	9.12	0.0208	0.0011	94.78	5.679	2.321	0.468	0.214	2.720	0.050	2.363	0.000	0.000	1.796	0.021	0.001	3.978	15.61	6.22	7.15	0.46
RSA03	1	3	37.50	15.41	1.83	20.94	0.39	10.27	<LLD	<LLD	9.38	0.0197	0.0010	95.70	5.724	2.276	0.496	0.210	2.673	0.050	2.337	0.000	0.000	1.827	0.020	0.001	3.460	15.59	6.15	7.04	0.47
RSA03	2	4	36.93	15.08	2.08	21.86	0.43	10.14	0.06	0.05	9.19	0.0184	0.0008	95.80	5.666	2.334	0.393	0.240	2.805	0.056	2.319	0.010	0.015	1.799	0.018	0.001	3.420	15.64	6.10	7.38	0.45
RSA03	2	5	37.05	14.95	2.26	21.60	0.37	10.10	0.06	0.06	9.15	0.0203	0.0013	95.58	5.684	2.316	0.388	0.261	2.771	0.048	2.310	0.010	0.018	1.791	0.020	0.001	3.480	15.60	6.08	7.29	0.45
RSA03	3	6	37.35	14.72	2.16	21.50	0.37	10.54	0.07	0.09	9.13	0.0218	0.0013	95.91	5.708	2.292	0.359	0.248	2.748	0.048	2.401	0.011	0.027	1.780	0.022	0.001	3.150	15.62	6.31	7.22	0.47
RSA03	3	7	36.10	14.74	2.01	21.74	0.35	10.08	0.19	0.15	8.92	0.0200	0.0014	94.26	5.634	2.366	0.345	0.236	2.837	0.046	2.345	0.032	0.045	1.776	0.020	0.001	3.979	15.66	6.16	7.45	0.45
RSA03	4	8	37.17	15.23	1.75	21.67	0.36	9.90	<LLD	0.06	9.24	0.0184	0.0010	95.36	5.717	2.283	0.478	0.202	2.787	0.047	2.270	0.000	0.018	1.813	0.018	0.001	3.850	15.62	5.98	7.34	0.45
RSA03	4	9	37.04	15.46	1.42	21.25	0.38	9.97	<LLD	<LLD	9.54	0.0184	0.0008	95.04	5.715	2.285	0.526	0.165	2.742	0.050	2.293	0.000	0.000	1.878	0.018	0.001	3.981	15.65	6.03	7.21	0.46
RSA03	5	10	37.89	14.55	2.80	22.16	0.36	9.42	<LLD	0.05	9.38	0.0176	0.0010	96.59	5.764	2.236	0.372	0.320	2.819	0.046	2.136	0.000	0.015	1.820	0.018	0.001	2.650	15.53	5.64	7.44	0.43
RSA03	5	11	37.26	15.25	1.76	21.50	0.39	10.05	<LLD	<LLD	9.24	0.0203	0.0010	95.43	5.720	2.280	0.479	0.203	2.760	0.051	2.300	0.000	0.000	1.810	0.020	0.001	3.710	15.60	6.05	7.26	0.45
RSA03	6	12	37.18	15.11	2.26	21.71	0.35	9.91	<LLD	0.07	9.38	0.0176	0.0011	95.95	5.686	2.314	0.409	0.260	2.777	0.045	2.259	0.000	0.021	1.830	0.018	0.001	3.220	15.60	5.95	7.32	0.45
RSA03	6	13	37.03	14.99	2.87	21.79	0.39	9.49	<LLD	0.08	9.61	0.0174	0.0013	96.23	5.666	2.334	0.369	0.330	2.788	0.051	2.165	0.000	0.024	1.876	0.017	0.001	3.000	15.60	5.70	7.35	0.44
RSA03	7	14	37.10	15.02	2.33	22.13	0.36	9.57	0.05	0.09	9.36	0.0195	0.0011	95.99	5.690	2.310	0.405	0.269	2.838	0.047	2.188	0.008	0.027	1.831	0.019	0.001	3.170	15.61	5.76	7.47	0.44
RSA03	7	15	37.17	14.88	2.22	22.08	0.37	9.52	0.07	<LLD	9.38	0.0182	0.0010	95.67	5.718	2.282	0.416	0.257	2.841	0.048	2.183	0.012	0.000	1.841	0.018	0.001	3.550	15.60	5.75	7.48	0.43
RSA03	8	16	36.51	14.80	2.24	22.32	0.39	9.58	<LLD	0.05	9.60	0.0184	0.0016	95.47	5.656	2.344	0.359	0.261	2.892	0.051	2.213	0.000	0.015	1.897	0.018	0.002	3.700	15.69	5.81	7.60	0.43
RSA03	8	17	37.29	14.79	2.33	22.10	0.37	9.62	<LLD	0.06	9.45	0.0203	0.0011	95.99	5.719	2.281	0.392	0.269	2.834	0.048	2.199	0.000	0.018	1.849	0.020	0.001	3.140	15.61	5.79	7.46	0.44
RSA03	9	18	36.46	14.34	3.09	22.44	0.38	9.11	<LLD	0.05	9.20	0.0179	0.0013	95.05	5.668	2.332	0.296	0.361	2.918	0.050	2.111	0.000	0.015	1.825	0.018	0.001	3.981	15.58	5.57	7.69	0.42
RSA03	9	19	36.92	14.48	3.10	23.06	0.40	9.29	<LLD	0.07	9.44	0.0179	0.0011	96.74	5.652	2.348	0.264	0.357	2.952	0.052	2.120	0.000	0.021	1.844	0.018	0.001	2.440	15.61	5.58	7.78	0.42
RSA03	11	20	36.26	14.25	3.02	22.64	0.40	9.29	0.08	0.07	9.28	0.0187	0.0011	95.27	5.640	2.360	0.252	0.353	2.945	0.053	2.154	0.013	0.021	1.841	0.019	0.001	3.920	15.63	5.67	7.75	0.42
RSA03	11	21	36.91	14.44	3.12	23.02	0.39	9.21	0.05	<LLD	9.13	0.0189	0.0010	96.25	5.669	2.331	0.283	0.361	2.957	0.051	2.109	0.008	0.000	1.789	0.019	0.001	2.940	15.56	5.56	7.80	0.42
RSA03	12	22	36.12	15.42	2.09	22.19	0.36	9.70	0.12	0.03	9.27	0.0184	0.0014	95.28	5.594	2.406	0.408	0.243	2.874	0.047	2.239	0.020	0.009	1.831	0.018	0.001	3.850	15.67	5.89	7.55	0.44
RSA03	13	23	36.39	15.40	2.29	22.30	0.32	9.71	0.09	0.09	9.22	0.0253	0.0010	95.78	5.601	2.399	0.395	0.265	2.871	0.042	2.228	0.015	0.027	1.811	0.025	0.001	3.070	15.65	5.84	7.53	0.44
RSA03	14	24	36.19	14.67	2.55	23.06	0.37	9.92	0.29	0.12	8.98	0.0211	0.0017	96.13	5.579	2.421	0.245	0.296	2.973	0.048	2.280	0.048	0.036	1.766	0.021	0.002	2.920	15.69	5.98	7.80	0.43
RSA01	1	1	36.97	15.18	1.83	21.99	0.32	9.29	0.04	<LLD	9.87	0.0326		95.46	5.708	2.292	0.470	0.213	2.839	0.042	2.138	0.007	0.000	1.944	0.033		3.170	15.65	5.59	7.42	0.43
RSA01	1	2	36.73	14.88	2.14	22.24	0.31	9.29	<LLD	<LLD	9.86	0.0337		95.42	5.687	2.313	0.403	0.249	2.880	0.041	2.144	0.000	0.000	1.948	0.034		3.150	15.66	5.60	7.52	0.43
RSA01	2	3	37.40	15.13	1.76	21.19	0.33	9.90	0.03	<LLD	9.88	0.0342	0.0003	95.59	5.736	2.264	0.471	0.203	2.718	0.043	2.264	0.005	0.000	1.933	0.034	0.000	2.970	15.64	5.91	7.10	0.45
RSA01	2	4	36.82	15.24	1.57	21.34	0.32	9.94	0.02	<LLD	9.78	0.0295	0.0003	95.00	5.693	2.307	0.470	0.183	2.760	0.042	2.291	0.003	0.000	1.929	0.029	0.000	3.730	15.68	5.99	7.22	0.45
RSA01	3	5	37.87	15.25	1.92	22.12	0.34	9.43	<LLD	<LLD	10.02	0.0303	0.0003	96.92	5.748	2.252	0.476	0.219	2.808	0.044	2.134	0.000	0.000	1.940	0.030	0.000	1.830	15.62	5.59	7.35	0.43
RSA01	4	6	36.38	15.41	0.85	21.91	0.36	10.15	0.06	0.05	9.53	0.0308	0.0003	94.67	5.662	2.338	0.488	0.100	2.852	0.047	2.355	0.010	0.015	1.892	0.031	0.000	3.969	15.76	6.14	7.44	0.45
SWA18a	1	1	34.62	14.80	3.97	22.84	0.53	9.37	0.04	0.07	8.57	0.0224	0.0014	94.79	5.418	2.582	0.147	0.467	2.989	0.070	2.186	0.007	0.021	1.711	0.022	0.001	3.976	15.60	5.74	7.85	0.42
SWA18a	1	2	36.69	14.38	4.08	21.79	0.53	9.36	0.05	0.05	9.64	0.0253	0.0014	96.54	5.607	2.393	0.198	0.469	2.785	0.069	2.133	0.008	0.015	1.880	0.025	0.001	2.320	15.56	5.60	7.32	0.43
SWA18a	2	3	35.97	14.77	3.66	21.54	0.54	9.20	0.02	0.03	9.47	0.0253	0.0017	95.17	5.576	2.424	0.275	0.427	2.793	0.071	2.126	0.003	0.009	1.873	0.025	0.002	3.680	15.58	5.58	7.33	0.43
SWA18a	2	4	35.12	14.61	3.50	22.34	0.53	9.00	0.09	0.06	8.81	0.0245	0.0014	94.03	5.529	2.471	0.239	0.415	2.941	0.071	2.112	0.015	0.018	1.769	0.024	0.001	3.974	15.58	5.55	7.72	0.42
SWA18a	3	5	35.78	14.60	3.55	21.62	0.52	9.85	0.06	0.08	9.08	0.0255	0.0016	95.11	5.547	2.453	0.215	0.414	2.803	0.068	2.276	0.010	0.024	1.796	0.026	0.002	3.770	15.61	5.97	7.35	0.45
SWA18a	3	6	35.80	14.38	3.36	21.93	0.53	9.95	0.07	0.06	9.20	0.0271	0.0016	95.25	5.555	2.445	0.185	0.392	2.846	0.070	2.302	0.012	0.018	1.821	0.027	0.002	3.540	15.65	6.03	7.45	0.45

			Composition (wt%)									– O equiv.			Structural formula (cations / 22 oxygen)													Cation	at%		
Sample	Grain	Spot	SiO_2	Al_2O_3	TiO_2	FeO	MnO	MgO	CaO	Na_2O	K_2O	F	Cl	Total	Si	Al^{IV}	Al^{VI}	Ti	Fe^{2+}	Mn	Mg	Ca	Na	K	F	Cl	OH	total	Mg	Fe	Mg#
SWA18a	4	7	35.59	14.72	3.46	21.06	0.48	9.68	0.13	0.17	8.95	0.0271	0.0016	94.21	5.554	2.446	0.261	0.406	2.748	0.063	2.252	0.022	0.051	1.782	0.027	0.002	3.971	15.59	5.91	7.21	0.45
SWA18a	5	8	35.41	14.13	3.48	21.47	0.54	9.87	0.05	0.14	9.37	0.0295	0.0013	94.43	5.549	2.451	0.159	0.410	2.814	0.072	2.306	0.008	0.043	1.873	0.029	0.001	3.969	15.68	6.03	7.35	0.45
SWA18a	5	9	35.88	14.10	3.60	21.34	0.54	9.88	0.16	0.09	9.32	0.0303	0.0017	94.88	5.582	2.418	0.167	0.421	2.776	0.071	2.291	0.027	0.027	1.850	0.030	0.002	3.780	15.63	5.99	7.26	0.45
SWA18a	6	10	36.72	14.64	3.16	20.03	0.36	10.02	0.07	0.12	9.48	0.0303	0.0016	94.57	5.673	2.327	0.339	0.367	2.588	0.047	2.308	0.012	0.036	1.868	0.030	0.002	3.968	15.56	6.05	6.78	0.47
SWA18a	6	11	35.96	15.15	3.18	20.24	0.36	10.26	0.02	0.05	9.78	0.0300	0.0016	94.97	5.554	2.446	0.312	0.370	2.614	0.047	2.362	0.003	0.015	1.927	0.030	0.002	3.680	15.65	6.18	6.84	0.47
SWA18a	7	12	36.23	15.94	2.84	19.80	0.14	10.24	<LLD	0.09	9.68	0.0342	0.0018	94.92	5.566	2.434	0.453	0.328	2.544	0.018	2.345	0.000	0.027	1.897	0.034	0.002	3.570	15.61	6.13	6.65	0.48
SWA18a	7	13	36.12	15.59	2.41	20.01	0.21	10.52	<LLD	0.11	9.34	0.0334	0.0016	94.28	5.590	2.410	0.433	0.281	2.590	0.028	2.427	0.000	0.033	1.844	0.033	0.002	3.965	15.63	6.34	6.76	0.48
RSA05	1	1	34.68	15.64	2.28	25.75	0.47	8.09	0.02	0.05	8.69	0.0197	0.0013	95.65	5.448	2.552	0.344	0.269	3.383	0.063	1.895	0.003	0.015	1.742	0.020	0.001	3.490	15.71	4.97	8.88	0.36
RSA05	1	2	35.50	15.53	3.10	24.98	0.40	7.65	<LLD	0.09	9.21	0.0176	0.0018	96.44	5.508	2.492	0.348	0.362	3.241	0.053	1.769	0.000	0.027	1.823	0.018	0.002	2.720	15.62	4.66	8.53	0.35
RSA05	1	3	35.59	15.13	3.33	24.76	0.44	7.10	<LLD	0.05	9.60	0.0200	0.0014	95.98	5.558	2.442	0.343	0.391	3.234	0.058	1.653	0.000	0.015	1.913	0.020	0.001	3.080	15.61	4.35	8.51	0.34
RSA05	2	4	35.26	15.40	2.64	24.80	0.43	7.44	0.04	0.06	9.44	0.0161	0.0016	95.49	5.534	2.466	0.383	0.312	3.255	0.057	1.741	0.007	0.018	1.890	0.016	0.002	3.700	15.66	4.58	8.57	0.35
RSA05	2	5	35.25	15.69	2.42	24.74	0.36	7.57	0.11	0.09	9.27	0.0168	0.0020	95.48	5.521	2.479	0.418	0.285	3.241	0.048	1.768	0.018	0.027	1.852	0.017	0.002	3.620	15.66	4.65	8.52	0.35
RSA05	3	6	35.41	15.41	2.85	24.98	0.37	7.27	0.21	0.17	9.07	0.0171	0.0014	95.72	5.537	2.463	0.378	0.335	3.267	0.049	1.695	0.035	0.052	1.809	0.017	0.001	3.450	15.62	4.46	8.60	0.34
RSA05	3	7	35.93	15.17	2.93	24.88	0.39	6.95	0.10	0.16	9.34	0.0174	0.0014	95.83	5.610	2.390	0.402	0.344	3.249	0.052	1.618	0.017	0.048	1.860	0.017	0.001	3.350	15.59	4.26	8.56	0.33
RSA05	4	8	35.16	15.24	3.20	24.93	0.37	7.07	0.18	0.14	9.14	0.0155	0.0018	95.41	5.522	2.478	0.344	0.378	3.275	0.049	1.655	0.030	0.043	1.831	0.016	0.002	3.770	15.61	4.36	8.63	0.34
RSA05	5	9	34.47	15.17	2.93	24.54	0.39	7.44	0.11	0.08	8.63	0.0150	0.0016	93.74	5.497	2.503	0.348	0.352	3.273	0.053	1.769	0.019	0.025	1.756	0.015	0.002	3.983	15.59	4.66	8.63	0.35
RSA05	5	10	36.02	15.22	3.13	24.65	0.41	7.34	0.05	0.08	9.52	0.0174	0.0013	96.40	5.584	2.416	0.365	0.365	3.196	0.054	1.696	0.008	0.024	1.883	0.017	0.001	2.720	15.59	4.47	8.42	0.35
RSA05	6	11	35.01	14.96	3.11	24.54	0.37	7.17	0.20	0.14	8.86	0.0174	0.0017	94.34	5.550	2.450	0.345	0.371	3.253	0.050	1.694	0.034	0.043	1.792	0.017	0.002	3.981	15.58	4.46	8.57	0.34
RSA05	6	12	33.95	14.18	3.34	24.86	0.46	6.66	0.19	0.14	8.83	0.0184	0.0016	92.59	5.522	2.478	0.240	0.409	3.382	0.063	1.615	0.033	0.044	1.832	0.018	0.002	3.980	15.62	4.25	8.89	0.32
RSA05	7	13	35.23	15.07	2.94	24.72	0.38	7.36	0.08	0.16	9.40	0.0158	0.0020	95.32	5.538	2.462	0.331	0.348	3.250	0.051	1.725	0.013	0.049	1.885	0.016	0.002	3.820	15.65	4.54	8.55	0.35
RSA05	7	14	34.34	14.92	3.17	25.20	0.44	7.01	0.03	0.03	9.28	0.0197	0.0017	94.40	5.483	2.517	0.291	0.381	3.365	0.060	1.669	0.005	0.009	1.890	0.020	0.002	3.979	15.67	4.38	8.84	0.33
RSA02	1	1	36.45	15.64	1.73	20.80	0.31	9.97	<LLD	<LLD	9.16	0.0168	0.0008	94.04	5.667	2.333	0.532	0.202	2.704	0.041	2.311	0.000	0.000	1.817	0.017	0.001	3.982	15.61	6.09	7.13	0.46
RSA02	1	2	36.50	15.80	1.69	20.68	0.29	10.00	<LLD	0.02	9.18	0.0168	0.0007	94.14	5.663	2.337	0.552	0.197	2.683	0.038	2.313	0.000	0.006	1.817	0.017	0.001	3.982	15.61	6.10	7.07	0.46
RSA02	2	3	36.82	15.66	1.40	20.91	0.27	9.86	0.07	<LLD	9.65	0.0179	0.0004	94.62	5.700	2.300	0.558	0.163	2.707	0.035	2.276	0.012	0.000	1.906	0.018	0.000	3.982	15.66	5.99	7.12	0.46
RSA02	2	4	37.64	16.41	0.80	20.37	0.29	10.14	<LLD	0.05	9.85	0.0187	0.0006	95.53	5.740	2.260	0.690	0.092	2.598	0.037	2.305	0.000	0.015	1.916	0.019	0.001	3.670	15.65	6.07	6.84	0.47
RSA02	3	5	36.92	15.89	1.28	21.48	0.30	9.47	0.05	0.05	9.71	0.0187	0.0007	95.13	5.699	2.301	0.590	0.149	2.773	0.039	2.179	0.008	0.015	1.912	0.019	0.001	3.981	15.67	5.73	7.29	0.44
RSA02	4	6	36.29	15.65	1.77	21.74	0.29	9.18	<LLD	<LLD	9.59	0.0184	0.0006	94.49	5.655	2.345	0.530	0.208	2.833	0.038	2.133	0.000	0.000	1.907	0.018	0.001	3.981	15.65	5.61	7.45	0.43
RSA02	4	7	36.43	14.95	2.51	22.00	0.32	8.75	0.12	<LLD	9.34	0.0166	0.0007	94.40	5.688	2.312	0.439	0.295	2.873	0.042	2.037	0.020	0.000	1.860	0.017	0.001	3.983	15.57	5.37	7.58	0.41
RSA02	5	8	36.51	15.57	1.89	21.56	0.29	9.09	0.10	<LLD	9.62	0.0168	0.0004	94.61	5.677	2.323	0.530	0.221	2.803	0.038	2.107	0.017	0.000	1.908	0.017	0.000	3.983	15.62	5.55	7.39	0.43
RSA02	7	9	36.62	15.68	2.14	21.18	0.29	9.27	<LLD	0.04	9.59	0.0166	0.0006	94.79	5.668	2.332	0.528	0.249	2.741	0.038	2.139	0.000	0.012	1.893	0.017	0.001	3.983	15.60	5.64	7.23	0.44
RSA02	7	10	36.39	15.75	2.18	21.28	0.30	9.28	<LLD	0.04	9.48	0.0166	0.0004	94.68	5.639	2.361	0.516	0.254	2.758	0.039	2.144	0.000	0.012	1.874	0.017	0.000	3.983	15.60	5.65	7.27	0.44
RSA02	8	11	36.51	15.55	1.21	21.40	0.30	9.55	0.13	0.05	9.20	0.0179	0.0006	93.88	5.702	2.298	0.563	0.142	2.795	0.040	2.223	0.022	0.015	1.833	0.018	0.001	3.982	15.63	5.85	7.36	0.44
RSA02	8	12	36.44	15.68	1.07	21.10	0.29	9.55	0.08	0.04	9.52	0.0184	0.0007	93.75	5.704	2.296	0.597	0.126	2.762	0.038	2.229	0.013	0.012	1.901	0.018	0.001	3.981	15.68	5.86	7.26	0.45
RSA02	9	13	36.80	15.76	1.19	21.00	0.29	9.54	0.12	0.05	9.26	0.0171	0.0007	93.99	5.722	2.278	0.610	0.139	2.731	0.038	2.211	0.020	0.015	1.837	0.017	0.001	3.982	15.60	5.83	7.20	0.45
RSA02	10	14	36.30	14.92	2.46	22.79	0.29	8.50	0.02	0.03	9.43	0.0161	0.0007	94.72	5.674	2.326	0.422	0.289	2.979	0.038	1.981	0.003	0.009	1.880	0.016	0.001	3.983	15.60	5.22	7.86	0.40
RSA02	10	15	36.17	14.81	2.94	22.51	0.32	8.36	<LLD	0.06	9.32	0.0150	0.0007	94.47	5.662	2.338	0.394	0.346	2.947	0.042	1.951	0.000	0.018	1.861	0.015	0.001	3.984	15.56	5.15	7.78	0.40

			Composition (wt%)									– O equiv.			Structural formula (cations / 22 oxygen)														Cation	at%		
Sample	Grain	Spot	SiO_2	Al_2O_3	TiO_2	FeO	MnO	MgO	CaO	Na_2O	K_2O	F	Cl	Total	Si	Al^{IV}	Al^{VI}	Ti	Fe^{2+}	Mn	Mg	Ca	Na	K	F	Cl	OH	total	Mg	Fe	Mg#
RSA02	11	16	38.83	16.05	1.74	20.77	0.30	9.98	0.12	0.07	9.31	0.0168	0.0007	97.15	5.797	2.203	0.621	0.195	2.593	0.038	2.221	0.019	0.020	1.773	0.017	0.001	2.100	15.48	5.88	6.86	0.46
RSA02	11	17	36.50	14.69	2.79	21.88	0.31	9.03	0.26	0.13	8.91	0.0179	0.0008	94.48	5.681	2.319	0.375	0.327	2.848	0.041	2.095	0.043	0.039	1.769	0.018	0.001	3.981	15.54	5.53	7.52	0.42
RSA02	12	18	36.92	15.43	2.11	22.06	0.30	9.33	<LLD	0.04	9.47	0.0174	0.0006	95.64	5.679	2.321	0.477	0.244	2.838	0.039	2.140	0.000	0.012	1.858	0.017	0.001	3.610	15.61	5.64	7.48	0.43
RSA02	12	19	36.72	14.88	3.46	22.39	0.31	8.47	0.25	0.04	9.36	0.0153	0.0006	95.86	5.651	2.349	0.350	0.401	2.882	0.040	1.943	0.041	0.012	1.838	0.015	0.001	3.430	15.51	5.14	7.62	0.40
RSA02	13	20	37.02	15.39	1.94	22.08	0.30	8.97	0.06	0.06	9.43	0.0168	0.0007	95.23	5.718	2.282	0.520	0.225	2.852	0.039	2.065	0.010	0.018	1.858	0.017	0.001	3.982	15.59	5.45	7.52	0.42
RSA02	13	21	36.79	15.57	1.88	22.13	0.32	9.02	0.04	0.03	9.42	0.0168	0.0006	95.18	5.688	2.312	0.525	0.219	2.861	0.042	2.079	0.007	0.009	1.858	0.017	0.001	3.983	15.60	5.48	7.54	0.42
RSA02	14	22	36.21	15.14	2.54	21.67	0.30	8.94	0.08	0.06	9.73	0.0168	0.0006	94.65	5.643	2.357	0.424	0.298	2.824	0.040	2.077	0.013	0.018	1.934	0.017	0.001	3.983	15.63	5.47	7.44	0.42
RSA02	14	23	36.76	15.66	1.42	21.37	0.32	9.38	0.06	0.05	9.52	0.0189	0.0006	94.52	5.706	2.294	0.571	0.166	2.774	0.042	2.171	0.010	0.015	1.885	0.019	0.001	3.980	15.63	5.71	7.30	0.44
SWA07	1	1	35.67	15.75	2.35	25.79	0.36	6.40	<LLD	<LLD	9.49	0.0129	0.0014	95.80	5.598	2.402	0.511	0.277	3.385	0.048	1.497	0.000	0.000	1.900	0.013	0.001	3.600	15.62	3.95	8.93	0.31
SWA07	1	2	35.89	15.78	2.13	26.24	0.39	6.40	<LLD	<LLD	9.63	0.0132	0.0018	96.45	5.606	2.394	0.511	0.250	3.428	0.052	1.490	0.000	0.000	1.919	0.013	0.002	2.910	15.65	3.93	9.04	0.30
SWA07	2	3	35.82	15.78	2.17	25.96	0.35	6.38	<LLD	0.05	9.29	0.0126	0.0014	95.79	5.617	2.383	0.533	0.256	3.405	0.046	1.491	0.000	0.015	1.858	0.013	0.001	3.620	15.61	3.94	8.99	0.30
SWA07	2	4	35.82	15.52	2.29	25.96	0.37	6.37	<LLD	<LLD	9.53	0.0134	0.0016	95.85	5.624	2.376	0.496	0.270	3.409	0.049	1.491	0.000	0.000	1.909	0.013	0.002	3.520	15.62	3.93	8.99	0.30
SWA07	3	5	36.37	15.49	2.31	26.28	0.37	6.35	0.13	<LLD	9.32	0.0137	0.0013	96.61	5.653	2.347	0.491	0.270	3.416	0.049	1.471	0.022	0.000	1.848	0.014	0.001	2.720	15.57	3.89	9.02	0.30
SWA07	3	6	35.78	15.63	2.36	26.06	0.37	6.40	0.12	0.06	8.95	0.0132	0.0010	95.72	5.611	2.389	0.500	0.278	3.418	0.049	1.496	0.020	0.018	1.791	0.013	0.001	3.700	15.57	3.95	9.03	0.30
SWA07	4	7	35.64	15.55	2.62	26.48	0.39	6.24	<LLD	0.10	9.43	0.0132	0.0017	96.44	5.573	2.427	0.439	0.308	3.463	0.052	1.455	0.000	0.030	1.881	0.013	0.002	2.880	15.63	3.84	9.13	0.30
SWA07	4	8	36.25	15.29	2.49	26.64	0.40	6.27	<LLD	0.06	9.53	0.0132	0.0018	96.92	5.641	2.359	0.445	0.291	3.467	0.053	1.454	0.000	0.018	1.892	0.013	0.002	2.440	15.62	3.84	9.15	0.30
SWA07	6	9	35.83	15.24	2.18	26.43	0.43	6.25	0.05	0.06	9.36	0.0129	0.0020	95.82	5.641	2.359	0.468	0.258	3.480	0.057	1.467	0.008	0.018	1.880	0.013	0.002	3.540	15.64	3.87	9.18	0.30
SWA07	6	10	35.22	15.75	2.09	26.48	0.43	6.08	0.15	0.08	8.97	0.0126	0.0017	95.24	5.576	2.424	0.515	0.249	3.506	0.058	1.435	0.025	0.025	1.812	0.013	0.002	3.986	15.62	3.79	9.25	0.29
SWA07	7	11	35.88	15.54	2.31	25.39	0.38	6.32	<LLD	0.11	9.55	0.0142	0.0017	95.46	5.643	2.357	0.523	0.273	3.340	0.051	1.482	0.000	0.034	1.916	0.014	0.002	3.860	15.62	3.91	8.81	0.31
SWA07	7	12	36.09	15.20	2.32	26.47	0.37	6.22	<LLD	0.08	9.17	0.0134	0.0017	95.90	5.664	2.336	0.475	0.274	3.474	0.049	1.455	0.000	0.024	1.836	0.013	0.002	3.450	15.59	3.84	9.17	0.30
SWA07	8	13	35.11	14.98	2.30	26.07	0.39	6.19	0.21	0.11	8.69	0.0142	0.0021	94.03	5.618	2.382	0.443	0.277	3.489	0.053	1.477	0.036	0.034	1.774	0.014	0.002	3.984	15.58	3.90	9.20	0.30
SWA07	8	14	35.34	15.12	2.18	26.20	0.41	6.28	0.16	0.10	8.53	0.0139	0.0020	94.30	5.633	2.367	0.474	0.261	3.493	0.055	1.492	0.027	0.031	1.735	0.014	0.002	3.984	15.57	3.94	9.22	0.30
SWA07	9	15	35.87	15.18	2.20	26.03	0.38	6.25	0.07	0.08	9.20	0.0145	0.0016	95.24	5.664	2.336	0.490	0.261	3.438	0.051	1.471	0.012	0.024	1.853	0.014	0.002	3.984	15.60	3.88	9.07	0.30
SWA07	9	16	34.79	15.29	1.74	26.01	0.37	6.33	0.07	<LLD	8.74	0.0147	0.0013	93.32	5.612	2.388	0.519	0.211	3.509	0.051	1.522	0.012	0.000	1.799	0.015	0.001	3.984	15.62	4.01	9.25	0.30
SWA07	10	17	35.47	15.23	2.20	26.10	0.38	6.27	<LLD	0.07	9.28	0.0147	0.0020	94.98	5.628	2.372	0.476	0.263	3.463	0.051	1.483	0.000	0.022	1.878	0.015	0.002	3.983	15.64	3.91	9.12	0.30
SWA07	10	18	35.59	15.33	2.15	25.91	0.41	6.26	<LLD	0.08	9.40	0.0145	0.0016	95.11	5.635	2.365	0.496	0.256	3.431	0.055	1.478	0.000	0.025	1.899	0.014	0.002	3.984	15.64	3.89	9.04	0.30
SWA07	11	19	35.24	15.44	1.97	26.36	0.35	6.41	<LLD	<LLD	9.58	0.0142	0.0014	95.33	5.588	2.412	0.473	0.235	3.496	0.047	1.515	0.000	0.000	1.938	0.014	0.001	3.984	15.70	3.99	9.20	0.30
SWA07	11	20	35.37	15.44	1.93	25.85	0.37	6.40	0.07	0.05	8.95	0.0137	0.0013	94.42	5.629	2.371	0.525	0.231	3.440	0.050	1.518	0.012	0.015	1.817	0.014	0.001	3.985	15.61	4.01	9.08	0.31
SWA07	12	21	35.63	15.35	2.33	26.06	0.41	6.27	<LLD	<LLD	9.50	0.0139	0.0017	95.53	5.621	2.379	0.475	0.277	3.438	0.055	1.475	0.000	0.000	1.912	0.014	0.002	3.800	15.63	3.89	9.07	0.30
SWA07	12	22	35.77	15.42	2.25	25.93	0.34	6.27	<LLD	0.07	9.70	0.0153	0.0016	95.73	5.631	2.369	0.491	0.266	3.414	0.045	1.471	0.000	0.021	1.948	0.015	0.002	3.560	15.66	3.87	8.99	0.30
SWA07	13	23	35.90	15.35	2.45	26.30	0.39	6.17	<LLD	0.07	9.71	0.0139	0.0014	96.32	5.620	2.380	0.452	0.289	3.443	0.052	1.440	0.000	0.021	1.939	0.014	0.001	2.960	15.64	3.80	9.08	0.29
SWA07	13	24	35.73	15.49	2.37	26.22	0.35	6.27	<LLD	<LLD	9.67	0.0139	0.0013	96.08	5.609	2.391	0.474	0.280	3.442	0.047	1.467	0.000	0.000	1.936	0.014	0.001	3.280	15.65	3.87	9.07	0.30
SWA07	14	25	36.41	15.48	2.40	26.20	0.41	6.30	0.19	0.07	8.74	0.0132	0.0016	96.19	5.669	2.331	0.510	0.281	3.412	0.054	1.462	0.032	0.021	1.736	0.013	0.002	3.190	15.51	3.87	9.03	0.30
SWA07	14	26	36.13	16.16	2.07	25.19	0.36	6.45	0.08	0.10	9.23	0.0147	0.0010	95.75	5.634	2.366	0.603	0.243	3.285	0.048	1.499	0.013	0.030	1.836	0.015	0.001	3.550	15.56	3.96	8.68	0.31
SWA07	15	27	35.27	15.88	2.22	25.49	0.37	6.21	<LLD	0.08	9.58	0.0126	0.0008	95.09	5.581	2.419	0.543	0.264	3.373	0.050	1.465	0.000	0.025	1.934	0.013	0.001	3.987	15.65	3.86	8.90	0.30
SWA07	15	28	36.03	15.30	2.46	25.64	0.37	6.02	<LLD	<LLD	9.48	0.0137	0.0014	95.28	5.679	2.321	0.521	0.292	3.380	0.049	1.414	0.000	0.000	1.906	0.014	0.001	3.985	15.56	3.74	8.93	0.30

			Composition (wt%)									– O equiv.			Structural formula (cations / 22 oxygen)													Cation	at%		
Sample	Grain	Spot	SiO_2	Al_2O_3	TiO_2	FeO	MnO	MgO	CaO	Na_2O	K_2O	F	Cl	Total	Si	Al^{IV}	Al^{VI}	Ti	Fe^{2+}	Mn	Mg	Ca	Na	K	F	Cl	OH	total	Mg	Fe	Mg#
SWA07	16	29	35.67	15.59	3.06	25.82	0.40	5.91	<LLD	0.08	9.35	0.0121	0.0017	95.87	5.594	2.406	0.475	0.361	3.386	0.053	1.382	0.000	0.024	1.871	0.012	0.002	3.540	15.55	3.65	8.96	0.29
SWA07	16	30	36.16	15.73	2.68	25.86	0.41	6.13	<LLD	0.07	9.50	0.0124	0.0014	96.53	5.626	2.374	0.510	0.314	3.365	0.054	1.422	0.000	0.021	1.886	0.012	0.001	2.890	15.57	3.76	8.89	0.30
SWA07	17	31	36.45	16.09	2.34	25.38	0.40	6.31	<LLD	0.11	9.28	0.0142	0.0011	96.34	5.649	2.351	0.588	0.273	3.289	0.053	1.458	0.000	0.033	1.835	0.014	0.001	2.970	15.53	3.85	8.70	0.31
SWA07	18	32	35.53	15.58	2.39	26.21	0.41	6.19	<LLD	<LLD	9.67	0.0145	0.0016	95.96	5.589	2.411	0.477	0.283	3.448	0.055	1.452	0.000	0.000	1.940	0.014	0.002	3.360	15.65	3.82	9.08	0.30
SWA07	18	33	36.21	15.61	2.46	25.86	0.38	6.14	<LLD	<LLD	9.16	0.0147	0.0018	95.80	5.663	2.337	0.541	0.289	3.383	0.050	1.432	0.000	0.000	1.828	0.015	0.002	3.490	15.52	3.78	8.94	0.30
SWA07	19	34	36.02	15.65	2.04	25.51	0.39	6.34	<LLD	0.11	9.13	0.0142	0.0016	95.17	5.667	2.333	0.570	0.241	3.357	0.052	1.487	0.000	0.034	1.833	0.014	0.002	3.984	15.57	3.93	8.86	0.31
SWA07	19	35	35.92	15.70	1.81	25.62	0.39	6.50	<LLD	0.06	9.40	0.0147	0.0016	95.38	5.652	2.348	0.563	0.214	3.371	0.052	1.525	0.000	0.018	1.887	0.015	0.002	3.930	15.63	4.02	8.89	0.31
SWA07	20	36	36.10	15.96	1.95	24.95	0.35	6.38	<LLD	<LLD	9.69	0.0150	0.0011	95.36	5.665	2.335	0.616	0.230	3.274	0.047	1.492	0.000	0.000	1.940	0.015	0.001	3.970	15.60	3.94	8.64	0.31
SWA07	20	37	36.56	15.94	1.64	25.01	0.37	6.62	<LLD	<LLD	9.44	0.0139	0.0010	95.57	5.704	2.296	0.636	0.193	3.264	0.049	1.540	0.000	0.000	1.879	0.014	0.001	3.760	15.56	4.07	8.62	0.32
RSA08	1	1	36.03	14.48	2.43	25.34	0.31	7.07	<LLD	0.09	9.00	0.0142	0.0017	94.73	5.697	2.303	0.395	0.289	3.351	0.042	1.667	0.000	0.028	1.815	0.014	0.002	3.984	15.59	4.40	8.84	0.33
RSA08	2	2	35.63	14.45	2.99	25.60	0.35	6.88	<LLD	0.05	9.25	0.0132	0.0017	95.19	5.628	2.372	0.318	0.355	3.382	0.047	1.620	0.000	0.015	1.864	0.013	0.002	3.985	15.60	4.28	8.93	0.32
RSA08	2	3	35.51	14.25	3.38	25.65	0.34	6.55	<LLD	0.05	9.38	0.0145	0.0017	95.09	5.627	2.373	0.288	0.403	3.399	0.046	1.547	0.000	0.015	1.896	0.014	0.002	3.984	15.60	4.08	8.97	0.31
RSA08	4	4	36.10	14.93	3.21	25.85	0.34	6.81	<LLD	0.05	9.43	0.0129	0.0017	96.71	5.608	2.392	0.341	0.375	3.358	0.045	1.577	0.000	0.015	1.869	0.013	0.002	2.630	15.58	4.17	8.87	0.32
RSA08	5	5	35.77	14.64	3.50	25.60	0.31	6.60	0.04	<LLD	9.22	0.0132	0.0020	95.66	5.613	2.387	0.321	0.413	3.360	0.041	1.544	0.007	0.000	1.846	0.013	0.002	3.640	15.53	4.08	8.88	0.31
RSA08	5	6	35.17	15.22	2.58	25.44	0.33	7.02	0.04	0.05	8.88	0.0134	0.0021	94.71	5.570	2.430	0.411	0.307	3.370	0.044	1.657	0.007	0.015	1.794	0.013	0.002	3.984	15.61	4.37	8.89	0.33
RSA08	6	7	35.79	14.94	3.03	25.15	0.32	6.76	<LLD	0.05	9.32	0.0126	0.0021	95.35	5.623	2.377	0.390	0.358	3.305	0.043	1.583	0.000	0.015	1.868	0.013	0.002	3.960	15.56	4.18	8.73	0.32
RSA08	6	8	35.98	14.98	2.69	24.68	0.30	6.99	<LLD	0.07	9.42	0.0139	0.0023	95.09	5.659	2.341	0.436	0.318	3.246	0.040	1.639	0.000	0.021	1.890	0.014	0.002	3.984	15.59	4.32	8.57	0.34
RSA08	7	9	35.75	14.74	2.41	25.19	0.32	7.04	0.07	0.06	9.26	0.0145	0.0021	94.82	5.652	2.348	0.399	0.287	3.331	0.043	1.659	0.012	0.018	1.868	0.014	0.002	3.983	15.62	4.37	8.78	0.33
RSA08	8	10	35.86	14.69	2.58	25.19	0.34	7.03	<LLD	0.05	9.31	0.0166	0.0020	95.03	5.657	2.343	0.389	0.306	3.324	0.045	1.653	0.000	0.015	1.874	0.017	0.002	3.981	15.61	4.36	8.75	0.33
RSA08	8	11	35.98	14.67	3.30	25.27	0.32	6.98	<LLD	<LLD	9.24	0.0147	0.0021	95.74	5.628	2.372	0.332	0.388	3.305	0.042	1.628	0.000	0.000	1.844	0.015	0.002	3.480	15.54	4.30	8.73	0.33
RSA08	9	12	36.02	14.52	2.90	24.96	0.33	6.86	0.05	0.07	9.01	0.0139	0.0020	94.70	5.688	2.312	0.390	0.345	3.296	0.044	1.615	0.008	0.021	1.815	0.014	0.002	3.984	15.53	4.27	8.71	0.33
RSA08	9	13	35.59	14.29	2.53	24.68	0.31	6.97	0.05	0.05	8.58	0.0145	0.0017	93.03	5.706	2.294	0.407	0.305	3.309	0.042	1.666	0.009	0.016	1.755	0.014	0.002	3.984	15.51	4.40	8.75	0.33
SWA10a	1	1	34.12	16.47	3.37	25.33	0.32	4.96	<LLD	0.10	9.40	0.0118	0.0014	94.06	5.464	2.536	0.573	0.406	3.393	0.043	1.184	0.000	0.031	1.921	0.012	0.001	3.987	15.55	3.13	8.97	0.26
SWA10a	1	2	33.41	16.52	3.33	25.92	0.30	4.84	<LLD	0.05	8.73	0.0116	0.0017	93.09	5.413	2.587	0.567	0.406	3.512	0.041	1.169	0.000	0.016	1.804	0.012	0.002	3.987	15.51	3.09	9.30	0.25
SWA10a	2	3	33.85	16.89	2.53	25.66	0.34	5.14	0.04	<LLD	8.99	0.0113	0.0017	93.43	5.454	2.546	0.661	0.307	3.457	0.046	1.235	0.007	0.000	1.848	0.011	0.002	3.987	15.56	3.26	9.14	0.26
SWA10a	3	4	33.39	16.36	3.48	25.19	0.41	5.33	<LLD	0.05	8.78	0.0137	0.0013	92.98	5.403	2.597	0.524	0.424	3.409	0.056	1.286	0.000	0.016	1.813	0.014	0.001	3.985	15.53	3.40	9.01	0.27
SWA10a	4	5	34.12	16.19	3.55	24.44	0.27	5.12	<LLD	<LLD	9.37	0.0147	0.0016	93.04	5.500	2.500	0.576	0.431	3.295	0.037	1.230	0.000	0.000	1.927	0.015	0.002	3.984	15.50	3.25	8.71	0.27
SWA10a	4	6	33.94	16.51	3.24	24.90	0.29	5.31	<LLD	0.07	9.29	0.0150	0.0013	93.53	5.453	2.547	0.580	0.392	3.346	0.039	1.272	0.000	0.022	1.904	0.015	0.001	3.984	15.55	3.36	8.84	0.28
SWA10a	5	7	33.88	16.28	3.33	24.71	0.30	5.13	<LLD	0.08	9.24	0.0142	0.0014	92.93	5.477	2.523	0.579	0.405	3.341	0.041	1.236	0.000	0.025	1.906	0.014	0.001	3.984	15.53	3.27	8.83	0.27
SWA10a	5	8	33.89	16.11	3.49	24.79	0.33	5.09	<LLD	<LLD	9.36	0.0145	0.0014	93.04	5.479	2.521	0.548	0.424	3.352	0.045	1.227	0.000	0.000	1.930	0.014	0.001	3.984	15.53	3.24	8.86	0.27
SWA10a	6	9	34.38	16.14	3.30	24.90	0.33	5.28	0.05	<LLD	9.47	0.0150	0.0014	93.83	5.508	2.492	0.555	0.398	3.336	0.045	1.261	0.009	0.000	1.935	0.015	0.001	3.984	15.54	3.33	8.81	0.27
SWA10a	6	10	34.04	15.97	3.21	25.49	0.31	5.29	<LLD	<LLD	8.98	0.0147	0.0010	93.27	5.493	2.507	0.530	0.390	3.440	0.042	1.273	0.000	0.000	1.849	0.015	0.001	3.984	15.52	3.36	9.09	0.27
SWA10a	8	11	33.82	15.81	3.36	25.19	0.33	5.13	<LLD	<LLD	9.30	0.0142	0.0016	92.92	5.488	2.512	0.512	0.410	3.419	0.045	1.241	0.000	0.000	1.925	0.014	0.002	3.984	15.55	3.28	9.03	0.27
SWA10a	8	12	33.71	16.08	3.23	25.93	0.37	4.89	<LLD	0.05	9.32	0.0118	0.0016	93.57	5.454	2.546	0.519	0.393	3.508	0.051	1.179	0.000	0.016	1.924	0.012	0.002	3.987	15.59	3.12	9.27	0.25
SWA10a	9	13	33.83	15.82	3.30	25.33	0.35	5.32	<LLD	<LLD	9.59	0.0158	0.0014	93.52	5.468	2.532	0.481	0.401	3.424	0.048	1.282	0.000	0.000	1.977	0.016	0.001	3.983	15.61	3.38	9.02	0.27
SWA10a	9	14	34.23	16.13	3.28	25.14	0.38	5.15	<LLD	0.07	9.46	0.0155	0.0014	93.82	5.495	2.505	0.547	0.396	3.375	0.052	1.233	0.000	0.022	1.937	0.016	0.001	3.983	15.56	3.25	8.91	0.27

			Composition (wt%)									– O equiv.			Structural formula (cations / 22 oxygen)													Cation	at%		
Sample	Grain	Spot	SiO_2	Al_2O_3	TiO_2	FeO	MnO	MgO	CaO	Na_2O	K_2O	F	Cl	Total	Si	Al^{IV}	Al^{VI}	Ti	Fe^{2+}	Mn	Mg	Ca	Na	K	F	Cl	OH	total	Mg	Fe	Mg#
SWA10a	10	15	33.67	16.08	3.74	24.26	0.34	4.97	<LLD	0.07	9.43	0.0121	0.0017	92.55	5.468	2.532	0.546	0.457	3.295	0.047	1.203	0.000	0.022	1.954	0.012	0.002	3.986	15.52	3.18	8.72	0.27
SWA10a	10	16	34.05	16.60	3.03	24.34	0.34	5.10	<LLD	<LLD	8.92	0.0124	0.0020	92.37	5.510	2.490	0.677	0.369	3.294	0.047	1.230	0.000	0.000	1.842	0.012	0.002	3.986	15.46	3.26	8.73	0.27
SWA20	1	1	34.99	15.13	2.32	23.94	0.29	6.72	0.07	<LLD	9.05	0.0132	0.0004	92.50	5.646	2.354	0.523	0.282	3.230	0.040	1.616	0.012	0.000	1.863	0.013	0.000	3.986	15.57	4.27	8.54	0.33
SWA20	1	2	34.82	14.92	2.29	23.95	0.30	6.66	0.09	<LLD	9.04	0.0139	0.0006	92.06	5.652	2.348	0.506	0.280	3.251	0.041	1.612	0.016	0.000	1.872	0.014	0.001	3.985	15.58	4.26	8.59	0.33
SWA20	2	3	35.27	15.31	2.34	23.49	0.28	6.74	<LLD	0.10	9.50	0.0147	0.0006	93.01	5.655	2.345	0.548	0.282	3.150	0.038	1.611	0.000	0.031	1.943	0.015	0.001	3.985	15.60	4.25	8.31	0.34
SWA20	2	4	34.86	15.11	2.25	23.96	0.30	6.77	<LLD	<LLD	9.32	0.0145	0.0007	92.55	5.633	2.367	0.511	0.274	3.238	0.041	1.631	0.000	0.000	1.921	0.014	0.001	3.985	15.62	4.30	8.54	0.33
SWA20	3	5	35.86	15.51	2.09	24.05	0.27	6.99	<LLD	<LLD	9.46	0.0150	0.0006	94.21	5.672	2.328	0.564	0.249	3.182	0.036	1.648	0.000	0.000	1.909	0.015	0.001	3.984	15.59	4.35	8.40	0.34
SWA20	4	6	34.11	15.66	1.47	24.26	0.27	7.01	<LLD	<LLD	9.58	0.0105		92.35	5.551	2.449	0.554	0.180	3.302	0.037	1.701	0.000	0.000	1.989	0.011		3.989	15.76	4.48	8.70	0.34
SWA20	4	7	34.13	15.76	1.42	24.36	0.29	6.80	0.21	<LLD	8.77	0.0108		91.73	5.569	2.431	0.600	0.174	3.324	0.040	1.654	0.037	0.000	1.826	0.011		3.989	15.65	4.37	8.78	0.33
SWA20	5	8	34.61	14.86	2.22	23.63	0.25	7.11	0.06	0.06	9.35	0.0137	0.0004	92.14	5.620	2.380	0.463	0.271	3.209	0.034	1.721	0.010	0.019	1.937	0.014	0.000	3.986	15.67	4.54	8.46	0.35
SWA20	6	9	35.03	15.00	2.40	23.65	0.28	6.77	<LLD	0.10	9.41	0.0155	0.0007	92.62	5.650	2.350	0.502	0.291	3.190	0.038	1.628	0.000	0.031	1.936	0.016	0.001	3.984	15.62	4.29	8.41	0.34
SWA20	6	10	35.34	14.97	2.46	23.57	0.28	6.74	<LLD	0.08	9.49	0.0137	0.0004	92.92	5.676	2.324	0.510	0.297	3.166	0.038	1.614	0.000	0.025	1.945	0.014	0.000	3.986	15.59	4.26	8.36	0.34
SWA20	7	11	34.83	15.27	1.55	23.42	0.27	7.32	0.04	0.09	9.16	0.0150		91.93	5.645	2.355	0.562	0.189	3.175	0.037	1.769	0.007	0.028	1.894	0.015		3.985	15.66	4.66	8.36	0.36
SWA20	7	12	35.57	15.28	1.85	23.64	0.27	7.27	0.05	0.09	9.47	0.0158	0.0006	93.47	5.672	2.328	0.544	0.222	3.153	0.036	1.728	0.009	0.028	1.927	0.016	0.001	3.984	15.65	4.55	8.31	0.35
SWA20	8	13	34.48	14.90	2.17	23.83	0.28	6.86	0.04	0.06	9.69	0.0150	0.0006	92.29	5.609	2.391	0.466	0.266	3.242	0.039	1.664	0.007	0.019	2.011	0.015	0.001	3.984	15.71	4.38	8.53	0.34
SWA20	8	14	34.35	15.02	2.14	23.66	0.26	6.86	<LLD	0.06	9.78	0.0137	0.0006	92.12	5.598	2.402	0.482	0.262	3.224	0.036	1.667	0.000	0.019	2.033	0.014	0.001	3.986	15.72	4.39	8.48	0.34
SWA20	9	15	34.99	15.37	2.18	23.65	0.28	7.06	<LLD	0.05	9.43	0.0145	0.0004	93.00	5.617	2.383	0.525	0.263	3.175	0.038	1.690	0.000	0.016	1.931	0.014	0.000	3.985	15.64	4.46	8.37	0.35
SWA20	9	16	34.96	15.35	2.22	23.49	0.25	7.09	<LLD	0.06	9.39	0.0153		92.79	5.619	2.381	0.527	0.268	3.158	0.034	1.699	0.000	0.019	1.925	0.015		3.985	15.63	4.48	8.33	0.35
SWA03	1	1	37.24	17.56	1.36	24.12	0.43	6.43	<LLD	0.05	9.19	0.0139		96.37	5.705	2.295	0.876	0.157	3.090	0.056	1.469	0.000	0.015	1.796	0.014		3.090	15.46	3.89	8.19	0.32
SWA03	1	2	35.53	17.02	1.69	24.35	0.44	6.10	0.09	0.05	8.95	0.0134		94.21	5.608	2.392	0.775	0.201	3.214	0.059	1.435	0.015	0.015	1.802	0.013		3.987	15.52	3.80	8.51	0.31
SWA03	2	3	35.39	17.58	1.38	24.64	0.42	6.10	0.05	0.14	8.77	0.0126		94.46	5.568	2.432	0.828	0.163	3.242	0.056	1.431	0.008	0.043	1.760	0.013		3.987	15.53	3.79	8.58	0.31
SWA03	3	4	36.02	17.49	1.67	24.75	0.45	6.13	0.16	0.16	8.66	0.0126		95.48	5.599	2.401	0.803	0.195	3.217	0.059	1.420	0.027	0.048	1.717	0.013		3.987	15.49	3.77	8.53	0.31
SWA03	3	5	35.55	17.38	1.52	24.24	0.46	6.06	0.20	0.10	8.69	0.0129		94.19	5.600	2.400	0.827	0.180	3.193	0.061	1.423	0.034	0.031	1.746	0.013		3.987	15.50	3.77	8.46	0.31
SWA03	3	6	35.95	17.24	1.43	24.43	0.47	6.24	0.07	0.07	9.21	0.0158		95.09	5.622	2.378	0.800	0.168	3.195	0.062	1.455	0.012	0.021	1.837	0.016		3.984	15.55	3.84	8.44	0.31
SWA03	4	7	36.01	17.51	0.99	24.86	0.46	6.70	<LLD	<LLD	8.89	0.0150		95.40	5.607	2.393	0.820	0.116	3.237	0.061	1.555	0.000	0.000	1.766	0.015		3.985	15.55	4.11	8.56	0.32
SWA03	4	8	36.63	18.20	1.11	23.61	0.44	6.30	<LLD	<LLD	9.51	0.0132		95.79	5.648	2.352	0.955	0.129	3.045	0.057	1.448	0.000	0.000	1.871	0.013		3.700	15.50	3.84	8.07	0.32
SWA03	5	9	34.70	17.36	1.24	25.70	0.43	6.29	0.04	0.05	8.53	0.0124		94.33	5.503	2.497	0.748	0.148	3.409	0.058	1.487	0.007	0.015	1.726	0.012		3.988	15.60	3.93	9.01	0.30
SWA03	6	10	35.99	17.13	2.24	25.06	0.51	5.62	0.19	0.13	8.58	0.0121	0.0004	95.44	5.607	2.393	0.753	0.263	3.265	0.067	1.305	0.032	0.039	1.705	0.012	0.000	3.987	15.43	3.47	8.67	0.29
SWA03	6	11	35.24	16.86	2.06	25.44	0.46	5.60	0.18	0.12	8.74	0.0113		94.69	5.566	2.434	0.705	0.245	3.361	0.062	1.319	0.030	0.037	1.761	0.011		3.989	15.52	3.49	8.91	0.28
SWA03	7	12	35.73	17.17	1.54	24.57	0.45	5.91	<LLD	<LLD	9.33	0.0137		94.69	5.622	2.378	0.806	0.182	3.233	0.060	1.386	0.000	0.000	1.873	0.014		3.986	15.54	3.67	8.55	0.30
SWA03	7	13	35.38	17.31	1.62	24.80	0.44	5.88	<LLD	<LLD	9.20	0.0126		94.62	5.578	2.422	0.794	0.192	3.270	0.059	1.382	0.000	0.000	1.850	0.013		3.987	15.55	3.66	8.65	0.30
SWA03	8	14	36.08	17.26	1.86	25.49	0.49	5.85	<LLD	0.06	9.25	0.0124		96.33	5.594	2.406	0.749	0.217	3.305	0.064	1.352	0.000	0.018	1.830	0.012		3.190	15.54	3.58	8.75	0.29
SWA03	9	15	36.04	17.07	1.62	24.58	0.47	6.16	0.20	0.06	8.75	0.0145		94.94	5.636	2.364	0.782	0.191	3.215	0.062	1.436	0.034	0.018	1.746	0.014		3.986	15.48	3.80	8.51	0.31
SWA03	10	16	35.57	17.37	1.18	25.08	0.48	6.26	0.10	0.05	8.61	0.0134		94.69	5.590	2.410	0.808	0.140	3.296	0.064	1.467	0.017	0.015	1.726	0.013		3.987	15.53	3.88	8.72	0.31
SWA03	11	17	36.11	17.05	1.22	24.65	0.49	6.20	<LLD	<LLD	9.32	0.0137		95.03	5.658	2.342	0.806	0.144	3.230	0.065	1.448	0.000	0.000	1.863	0.014		3.986	15.56	3.83	8.54	0.31
SWA03	11	18	35.35	17.34	1.66	25.21	0.45	5.76	<LLD	0.11	9.47	0.0124		95.34	5.553	2.447	0.763	0.196	3.312	0.060	1.349	0.000	0.034	1.898	0.012		3.988	15.61	3.56	8.75	0.29

			Composition (wt%)										– O equiv.		Structural formula (cations / 22 oxygen)												Cation	at%		
Sample	Grain	Spot	SiO_2	Al_2O_3	TiO_2	FeO	MnO	MgO	CaO	Na_2O	K_2O	F	Cl	Total	Si	Al^{IV}	Al^{VI}	Ti	Fe^{2+}	Mn	Mg	Ca	Na	K	F	Cl	OH	total	Mg	Fe	Mg#
SWA03	12	19	35.60	16.91	1.39	24.47	0.48	6.04	<LLD	<LLD	9.18	0.0142		94.06	5.638	2.362	0.794	0.166	3.241	0.064	1.426	0.000	0.000	1.855	0.014		3.986	15.55	3.77	8.57	0.31
SWA03	12	20	35.87	17.12	1.87	24.76	0.45	5.77	<LLD	0.06	9.31	0.0118		95.20	5.616	2.384	0.776	0.220	3.242	0.060	1.347	0.000	0.018	1.860	0.012		3.988	15.52	3.57	8.59	0.29
SWA03	13	21	35.99	17.20	1.75	25.04	0.51	5.80	<LLD	0.09	9.19	0.0121		95.56	5.616	2.384	0.779	0.205	3.268	0.067	1.349	0.000	0.027	1.829	0.012		3.970	15.53	3.57	8.66	0.29
SWA03	13	22	35.35	17.45	1.73	24.94	0.47	5.95	0.15	0.15	8.61	0.0126		94.79	5.552	2.448	0.782	0.204	3.276	0.063	1.393	0.025	0.046	1.725	0.013		3.987	15.51	3.69	8.68	0.30
SWA03	14	23	37.16	17.48	0.69	23.01	0.43	6.76	0.06	0.05	9.52	0.0197		95.14	5.752	2.248	0.941	0.080	2.979	0.056	1.560	0.010	0.015	1.880	0.020		3.980	15.52	4.12	7.86	0.34
SWA03	15	24	35.49	16.86	1.92	25.07	0.47	5.63	0.18	0.16	8.83	0.0118		94.60	5.600	2.400	0.736	0.228	3.309	0.063	1.324	0.030	0.049	1.778	0.012		3.988	15.52	3.51	8.77	0.29
SWA03	15	25	35.43	17.14	1.45	24.63	0.48	5.99	0.07	<LLD	8.77	0.0137		93.95	5.610	2.390	0.808	0.173	3.261	0.064	1.414	0.012	0.000	1.771	0.014		3.986	15.50	3.74	8.64	0.30
SWA03	16	26	35.42	16.59	2.08	25.15	0.48	5.67	0.10	0.07	8.94	0.0126		94.49	5.603	2.397	0.696	0.248	3.327	0.064	1.337	0.017	0.021	1.804	0.013		3.987	15.52	3.54	8.81	0.29
RSA06	1	1	36.81	14.60	3.61	21.06	0.49	8.88	<LLD	0.08	9.54	0.0208	0.0011	95.05	5.689	2.311	0.348	0.420	2.722	0.064	2.046	0.000	0.024	1.881	0.021	0.001	3.978	15.51	5.40	7.18	0.43
RSA06	1	2	35.59	14.57	3.42	21.00	0.48	8.90	<LLD	0.11	9.36	0.0232	0.0014	93.41	5.613	2.387	0.321	0.406	2.770	0.064	2.093	0.000	0.034	1.883	0.023	0.001	3.975	15.57	5.50	7.28	0.43
RSA06	1	3	36.15	14.71	3.38	21.35	0.43	8.90	<LLD	0.06	9.27	0.0163	0.0016	94.23	5.646	2.354	0.354	0.397	2.789	0.057	2.072	0.000	0.018	1.847	0.016	0.002	3.982	15.54	5.47	7.36	0.43
RSA06	2	4	36.52	14.05	3.60	22.57	0.47	8.88	0.03	0.08	9.52	0.0287	0.0016	95.69	5.655	2.345	0.218	0.419	2.923	0.062	2.050	0.005	0.024	1.880	0.029	0.002	3.020	15.58	5.37	7.66	0.41
RSA06	3	5	36.09	14.26	3.20	22.83	0.39	9.01	0.16	0.03	9.08	0.0197	0.0008	95.03	5.625	2.375	0.245	0.375	2.976	0.051	2.094	0.027	0.009	1.806	0.020	0.001	3.979	15.58	5.51	7.84	0.41
RSA06	3	6	36.44	14.31	3.19	22.54	0.45	9.27	0.08	0.02	9.38	0.0226	0.0010	95.66	5.641	2.359	0.252	0.372	2.918	0.059	2.139	0.013	0.006	1.852	0.023	0.001	3.370	15.61	5.62	7.67	0.42
RSA06	4	7	35.91	14.42	2.95	21.66	0.39	9.71	0.17	0.07	9.44	0.0353	0.0018	94.68	5.602	2.398	0.253	0.346	2.826	0.052	2.258	0.028	0.021	1.879	0.035	0.002	3.730	15.66	5.89	7.37	0.44
RSA06	4	8	36.76	14.82	2.65	21.16	0.36	9.39	0.23	0.06	9.18	0.0313	0.0018	94.58	5.697	2.303	0.404	0.309	2.742	0.047	2.169	0.038	0.018	1.815	0.031	0.002	3.967	15.54	5.68	7.19	0.44
RSA06	5	9	35.86	14.35	3.40	21.60	0.43	8.92	<LLD	0.02	9.56	0.0255	0.0008	94.11	5.627	2.373	0.281	0.401	2.834	0.057	2.087	0.000	0.006	1.914	0.026	0.001	3.974	15.58	5.48	7.44	0.42
RSA06	5	10	35.97	14.14	3.43	21.71	0.46	9.05	<LLD	0.06	9.58	0.0321	0.0007	94.37	5.636	2.364	0.247	0.404	2.845	0.061	2.114	0.000	0.018	1.915	0.032	0.001	3.967	15.60	5.53	7.44	0.43
RSA06	5	11	36.01	13.93	3.49	21.96	0.46	9.21	<LLD	0.10	9.37	0.0332	0.0007	94.50	5.634	2.366	0.202	0.411	2.873	0.061	2.148	0.000	0.030	1.870	0.033	0.001	3.966	15.60	5.62	7.51	0.43
RSA06	5	12	36.16	14.06	3.54	21.79	0.46	9.14	<LLD	0.06	9.39	0.0324	0.0007	94.57	5.647	2.353	0.235	0.416	2.846	0.061	2.128	0.000	0.018	1.871	0.032	0.001	3.967	15.58	5.57	7.45	0.43
SWA13a	1	1	34.64	16.66	2.05	26.50	0.38	5.20	0.07	0.07	9.06	0.0087	0.0006	94.62	5.520	2.480	0.649	0.246	3.532	0.051	1.235	0.012	0.022	1.842	0.009	0.001	3.991	15.59	3.27	9.35	0.26
SWA13a	1	2	34.40	16.86	2.14	26.56	0.36	5.23	0.16	0.05	8.67	0.0076	0.0004	94.42	5.488	2.512	0.659	0.257	3.544	0.049	1.244	0.027	0.015	1.765	0.008	0.000	3.992	15.56	3.30	9.40	0.26
SWA13a	2	3	34.65	16.49	1.96	26.77	0.39	5.35	0.13	0.05	8.98	0.0084	0.0006	94.76	5.520	2.480	0.617	0.235	3.567	0.053	1.271	0.022	0.015	1.825	0.008	0.001	3.991	15.60	3.36	9.44	0.26
SWA13a	2	4	35.27	16.63	2.08	26.50	0.39	5.31	0.08	0.03	9.14	0.0071	0.0006	95.42	5.562	2.438	0.652	0.247	3.495	0.052	1.248	0.014	0.009	1.839	0.007	0.001	3.992	15.56	3.31	9.27	0.26
SWA13a	3	5	34.30	16.47	1.88	26.73	0.38	5.09	0.16	0.05	8.79	0.0076	0.0006	93.84	5.519	2.481	0.642	0.228	3.597	0.052	1.221	0.028	0.016	1.804	0.008	0.001	3.992	15.59	3.23	9.53	0.25
SWA13a	3	6	34.51	17.02	1.84	26.68	0.38	5.38	0.13	0.06	8.91	0.0076	0.0007	94.90	5.482	2.518	0.669	0.220	3.545	0.051	1.274	0.022	0.018	1.806	0.008	0.001	3.992	15.60	3.37	9.38	0.26
SWA13a	4	7	34.83	17.46	1.61	26.01	0.37	5.64	0.17	0.09	8.99	0.0089	0.0006	95.16	5.494	2.506	0.739	0.191	3.431	0.049	1.326	0.029	0.028	1.809	0.009	0.001	3.990	15.60	3.51	9.08	0.28
SWA13a	5	8	34.92	16.80	1.40	27.07	0.40	5.65	0.08	0.07	8.77	0.0084		95.15	5.532	2.468	0.669	0.167	3.587	0.054	1.334	0.014	0.022	1.772	0.008		3.992	15.62	3.53	9.49	0.27
SWA13a	6	9	34.19	16.66	1.92	27.56	0.39	5.39	0.19	0.07	8.60	0.0082	0.0007	94.96	5.452	2.548	0.583	0.230	3.675	0.053	1.281	0.032	0.022	1.749	0.008	0.001	3.991	15.63	3.39	9.72	0.26
SWA13a	7	10	34.27	16.45	1.58	27.22	0.40	5.45	0.03	<LLD	8.73	0.0082	0.0006	94.12	5.508	2.492	0.624	0.191	3.659	0.054	1.306	0.005	0.000	1.790	0.008	0.001	3.991	15.63	3.45	9.68	0.26
SWA13a	7	11	34.52	16.13	1.98	26.85	0.38	5.16	0.06	0.05	9.06	0.0082	0.0006	94.18	5.548	2.452	0.603	0.239	3.609	0.052	1.236	0.010	0.016	1.857	0.008	0.001	3.991	15.62	3.27	9.55	0.26
SWA11	8	1	34.08	16.13	2.59	27.20	0.40	4.80	0.20	0.05	8.31	0.0084	0.0020	93.75	5.494	2.506	0.558	0.314	3.667	0.055	1.153	0.035	0.016	1.709	0.008	0.002	3.990	15.51	3.06	9.72	0.24
SWA09	1	1	35.25	16.96	2.64	26.62	0.26	4.86	0.08	0.14	8.75	0.0153	0.0016	95.54	5.538	2.462	0.678	0.312	3.497	0.035	1.138	0.013	0.043	1.754	0.015	0.002	3.730	15.47	3.01	9.25	0.25
SWA09	1	2	34.58	16.69	2.79	26.84	0.36	4.98	0.06	0.14	9.34	0.0168	0.0017	95.76	5.461	2.539	0.567	0.331	3.545	0.048	1.172	0.010	0.043	1.882	0.017	0.002	3.390	15.60	3.09	9.34	0.25
SWA09	1	3	35.39	16.55	2.92	26.94	0.35	4.93	0.06	0.14	9.29	0.0171	0.0017	96.55	5.529	2.471	0.576	0.343	3.520	0.046	1.148	0.010	0.042	1.851	0.017	0.002	2.620	15.54	3.03	9.29	0.25
SWA09	2	4	34.45	16.88	2.52	26.92	0.29	5.15	0.06	<LLD	8.99	0.0166	0.0020	95.24	5.462	2.538	0.616	0.301	3.569	0.039	1.217	0.010	0.000	1.818	0.017	0.002	3.910	15.57	3.21	9.41	0.25

			Composition (wt%)										– O equiv.		Structural formula (cations / 22 oxygen)												Cation	at%		
Sample	Grain	Spot	SiO_2	Al_2O_3	TiO_2	FeO	MnO	MgO	CaO	Na_2O	K_2O	F	Cl	Total	Si	Al^{IV}	Al^{VI}	Ti	Fe^{2+}	Mn	Mg	Ca	Na	K	F	Cl	OH	total	Mg	Fe	Mg#
SWA09	2	5	34.15	17.03	2.43	26.38	0.31	5.23	<LLD	0.06	9.03	0.0184	0.0014	94.60	5.440	2.560	0.638	0.291	3.515	0.042	1.242	0.000	0.019	1.835	0.018	0.001	3.980	15.58	3.27	9.26	0.26
SWA09	3	6	35.04	16.77	2.50	26.32	0.31	5.11	0.09	0.07	9.26	0.0182	0.0017	95.45	5.523	2.477	0.639	0.296	3.470	0.041	1.201	0.015	0.021	1.862	0.018	0.002	3.640	15.55	3.17	9.15	0.26
SWA09	4	7	35.29	16.63	2.66	26.83	0.39	4.99	0.08	0.08	9.28	0.0168	0.0014	96.21	5.532	2.468	0.604	0.314	3.517	0.052	1.166	0.013	0.024	1.856	0.017	0.001	2.960	15.55	3.08	9.28	0.25
SWA09	4	8	35.07	16.61	2.55	26.87	0.27	4.96	0.02	<LLD	9.83	0.0174	0.0014	96.16	5.517	2.483	0.597	0.302	3.535	0.036	1.163	0.003	0.000	1.973	0.017	0.001	2.960	15.61	3.06	9.31	0.25
SWA09	5	9	34.80	16.74	2.47	26.50	0.28	5.61	0.02	<LLD	9.35	0.0189	0.0020	95.75	5.478	2.522	0.583	0.292	3.488	0.037	1.316	0.003	0.000	1.878	0.019	0.002	3.260	15.60	3.46	9.18	0.27
SWA09	5	10	35.11	16.57	2.50	26.60	0.32	5.40	0.04	0.07	9.00	0.0189	0.0024	95.59	5.524	2.476	0.597	0.296	3.500	0.043	1.267	0.007	0.021	1.806	0.019	0.002	3.420	15.54	3.34	9.22	0.27
SWA09	6	11	35.46	17.15	2.54	26.36	0.38	5.05	0.05	0.11	9.42	0.0166	0.0018	96.50	5.525	2.475	0.674	0.298	3.435	0.050	1.173	0.008	0.033	1.872	0.017	0.002	2.680	15.54	3.10	9.06	0.25
SWA09	6	12	35.27	16.91	2.50	26.08	0.35	5.11	0.04	0.08	9.45	0.0174	0.0016	95.77	5.536	2.464	0.664	0.295	3.423	0.047	1.196	0.007	0.024	1.892	0.017	0.002	3.400	15.55	3.15	9.03	0.26
SWA05	2	1	34.67	18.21	1.80	28.45	0.52	2.34	<LLD	0.06	8.77	0.0076	0.0007	94.81	5.543	2.457	0.974	0.216	3.804	0.070	0.558	0.000	0.019	1.789	0.008	0.001	3.992	15.43	1.48	10.12	0.13
SWA05	2	2	34.51	18.09	1.99	28.44	0.46	2.33	0.06	0.06	8.64	0.0089	0.0007	94.57	5.531	2.469	0.947	0.240	3.812	0.062	0.557	0.010	0.019	1.766	0.009	0.001	3.990	15.41	1.48	10.14	0.13
SWA05	5	3	34.90	18.28	1.71	28.77	0.49	2.38	0.06	0.05	8.58	0.0074	0.0007	95.21	5.552	2.448	0.979	0.205	3.827	0.066	0.564	0.010	0.015	1.741	0.007	0.001	3.992	15.41	1.50	10.19	0.13
SWA05	8	4	34.61	18.13	2.00	27.31	0.51	2.61	0.09	0.07	8.58	0.0097	0.0006	93.90	5.555	2.445	0.984	0.241	3.666	0.069	0.624	0.015	0.022	1.757	0.010	0.001	3.990	15.38	1.66	9.75	0.15
SWA05	9	5	34.62	17.78	2.22	28.43	0.50	2.46	0.05	<LLD	8.90	0.0068	0.0006	94.95	5.535	2.465	0.885	0.267	3.801	0.068	0.586	0.009	0.000	1.815	0.007	0.001	3.993	15.43	1.56	10.12	0.13
SWA05	9	6	34.12	17.88	2.24	29.11	0.56	2.48	0.04	<LLD	8.74	0.0061	0.0006	95.16	5.465	2.535	0.840	0.270	3.899	0.076	0.592	0.007	0.000	1.786	0.006	0.001	3.993	15.47	1.57	10.37	0.13
SWA05	12	7	34.71	18.37	2.40	28.77	0.53	2.43	0.07	<LLD	9.10	0.0082	0.0007	96.37	5.473	2.527	0.887	0.285	3.794	0.071	0.571	0.012	0.000	1.831	0.008	0.001	3.260	15.45	1.52	10.09	0.13
SWA05	13	8	34.13	17.70	2.25	28.43	0.48	2.47	0.08	0.06	8.83	0.0074	0.0006	94.42	5.498	2.502	0.858	0.273	3.830	0.065	0.593	0.014	0.019	1.815	0.007	0.001	3.992	15.47	1.58	10.18	0.13
SWA05	13	9	34.23	17.75	2.51	28.04	0.48	2.52	0.17	<LLD	8.73	0.0079	0.0004	94.42	5.498	2.502	0.857	0.303	3.766	0.065	0.603	0.029	0.000	1.789	0.008	0.000	3.992	15.41	1.61	10.02	0.14
SWA05	14	10	34.37	17.81	2.44	28.36	0.51	2.53	0.16	<LLD	8.70	0.0074	0.0008	94.87	5.498	2.502	0.855	0.294	3.794	0.069	0.603	0.027	0.000	1.775	0.007	0.001	3.992	15.42	1.61	10.10	0.14
SWA05	14	11	35.41	17.78	2.41	27.75	0.50	2.54	0.21	0.07	8.67	0.0066	0.0008	95.33	5.600	2.400	0.913	0.287	3.670	0.067	0.599	0.036	0.021	1.749	0.007	0.001	3.993	15.34	1.60	9.79	0.14

Sample	Grain	Spot	Concentration (wt%)																					Structural formula (cations / 13 oxygen)												Cation Total
			Na_2O	MgO	Al_2O_3	SiO_2	P_2O_5	K_2O	CaO	TiO_2	MnO	Fe_2O_3	SrO	Y_2O_3	La_2O_3	Ce_2O_3	Pr_2O_3	Nd_2O_3	SmO	Gd_2O_3	PbO	ThO_2	UO_2	Total	Si	Al	Al	Fe	Ti	Mg	Ca	Mn	REE	Y	Th	OH	
RSA03	1	1	0.06	0.20	12.63	33.43	<LLD	<LLD	14.47	0.96	0.66	14.22	0.50	<LLD	5.95	10.45	0.18	2.38	0.12	0.84	<LLD	0.61	<LLD	97.66	3.230	0.000	1.438	1.034	0.070	0.029	1.498	0.054	0.701	0.000	0.013	1	8.07
RSA03	1	2	0.05	0.24	12.51	33.68	<LLD	<LLD	14.43	1.20	0.63	14.56	0.46	<LLD	5.85	10.49	0.31	2.41	0.11	0.92	<LLD	0.65	<LLD	98.50	3.228	0.000	1.413	1.050	0.087	0.034	1.482	0.051	0.701	0.000	0.014	1	8.06
RSA03	1	3	0.11	0.17	12.71	32.98	<LLD	<LLD	14.06	0.82	0.49	15.55	0.47	<LLD	6.30	10.31	0.15	2.22	0.10	0.76	<LLD	0.59	<LLD	97.79	3.189	0.000	1.449	1.132	0.060	0.025	1.457	0.040	0.700	0.000	0.013	1	8.06
RSA03	2	4	0.16	0.22	12.08	32.29	<LLD	<LLD	13.38	0.95	0.44	14.61	0.23	<LLD	7.02	11.81	0.29	2.59	0.11	0.93	<LLD	0.61	<LLD	97.72	3.183	0.000	1.403	1.084	0.070	0.032	1.413	0.037	0.817	0.000	0.014	1	8.05
RSA03	2	5	0.06	0.26	13.01	33.16	<LLD	<LLD	14.75	1.12	0.73	13.63	0.54	<LLD	5.74	10.04	0.12	2.28	0.11	0.75	<LLD	0.49	<LLD	96.79	3.213	0.000	1.485	0.994	0.082	0.038	1.531	0.060	0.672	0.000	0.011	1	8.09
RSA03	2	6	0.15	0.18	16.92	33.27	<LLD	<LLD	15.53	0.37	0.35	14.08	0.28	<LLD	4.64	8.03	0.24	1.83	0.09	0.65	<LLD	0.36	<LLD	96.97	3.111	0.000	1.865	0.991	0.026	0.025	1.556	0.028	0.527	0.000	0.008	1	8.14
RSA03	2	7	0.07	0.31	15.13	34.03	<LLD	<LLD	14.78	0.68	0.69	13.08	0.39	<LLD	5.38	10.07	0.29	2.23	<LLD	0.78	<LLD	0.25	0.14	98.30	3.201	0.000	1.677	0.926	0.048	0.043	1.490	0.055	0.643	0.000	0.008	1	8.09
RSA03	3	8	0.05	0.23	12.85	32.25	<LLD	<LLD	14.37	0.93	0.58	14.93	0.50	<LLD	5.84	10.33	0.27	2.40	0.08	0.81	<LLD	0.53	<LLD	96.95	3.151	0.000	1.480	1.098	0.068	0.034	1.504	0.048	0.702	0.000	0.012	1	8.10
RSA03	3	9	0.05	0.22	11.63	31.92	<LLD	<LLD	13.43	1.22	0.58	16.39	0.38	<LLD	6.21	11.28	0.32	2.57	0.12	0.89	<LLD	0.72	<LLD	97.93	3.139	0.000	1.348	1.213	0.090	0.032	1.415	0.048	0.766	0.000	0.016	1	8.07
RSA03	3	10	0.05	0.19	12.48	33.45	<LLD	<LLD	14.34	1.32	0.58	14.30	0.46	<LLD	5.90	10.77	0.27	2.53	0.09	0.81	<LLD	0.55	<LLD	98.09	3.223	0.000	1.417	1.037	0.096	0.027	1.480	0.047	0.715	0.000	0.012	1	8.06
RSA03	3	11	0.04	0.26	13.05	33.26	<LLD	<LLD	13.83	1.06	0.47	14.14	0.33	<LLD	6.30	10.67	0.19	2.39	0.08	0.85	<LLD	0.69	<LLD	97.61	3.215	0.000	1.487	1.029	0.077	0.037	1.432	0.038	0.721	0.000	0.015	1	8.05
RSA03	4	12	0.04	0.27	12.36	31.96	<LLD	<LLD	13.50	1.04	0.59	15.55	0.45	<LLD	5.11	11.12	0.69	3.48	0.25	0.89	<LLD	0.77	<LLD	98.07	3.133	0.000	1.428	1.147	0.077	0.039	1.418	0.049	0.768	0.000	0.017	1	8.08
RSA03	4	13	0.07	0.29	13.93	33.45	<LLD	<LLD	14.20	1.11	0.63	13.55	0.56	<LLD	5.71	10.06	0.24	2.33	0.09	0.79	<LLD	0.53	<LLD	97.54	3.202	0.000	1.572	0.976	0.080	0.041	1.456	0.051	0.670	0.000	0.012	1	8.06
RSA03	4	14	0.17	<LLD	17.70	34.64	<LLD	<LLD	16.56	0.35	0.32	13.86	0.52	<LLD	4.05	7.28	0.20	1.70	0.07	0.51	<LLD	0.30	<LLD	98.23	3.151	0.000	1.898	0.949	0.024	0.000	1.614	0.025	0.458	0.000	0.006	1	8.12
RSA03	4	15	0.07	0.33	14.13	34.08	<LLD	<LLD	13.92	1.14	0.64	13.00	0.60	<LLD	6.00	10.44	0.22	2.36	0.08	0.80	<LLD	0.64	<LLD	98.45	3.233	0.000	1.580	0.928	0.081	0.047	1.415	0.051	0.688	0.000	0.014	1	8.04
RSA03	4	16	0.14	0.14	17.81	34.30	<LLD	0.03	16.52	0.41	0.39	13.75	0.22	<LLD	3.58	6.80	0.20	1.55	<LLD	0.53	<LLD	0.34	<LLD	96.71	3.144	0.000	1.924	0.948	0.028	0.019	1.622	0.030	0.423	0.000	0.007	1	8.15
RSA03	5	17	0.06	0.16	12.46	33.15	<LLD	<LLD	14.28	0.96	0.69	15.57	0.61	<LLD	5.50	10.43	0.29	2.25	0.07	0.80	<LLD	0.68	0.13	98.09	3.197	0.000	1.416	1.130	0.070	0.023	1.475	0.056	0.680	0.000	0.018	1	8.06
RSA03	5	18	0.04	0.20	12.71	33.28	<LLD	<LLD	14.15	0.95	0.62	14.67	0.46	<LLD	6.12	11.24	0.24	2.36	<LLD	0.92	<LLD	0.48	0.12	98.56	3.205	0.000	1.443	1.063	0.069	0.029	1.460	0.051	0.733	0.000	0.013	1	8.06
RSA03	5	19	0.08	0.18	12.46	33.16	<LLD	<LLD	14.27	1.01	0.58	14.68	0.45	<LLD	6.30	10.59	0.13	2.36	0.08	0.82	<LLD	0.55	<LLD	97.70	3.214	0.000	1.423	1.070	0.074	0.026	1.482	0.048	0.716	0.000	0.012	1	8.06
RSA03	5	20	0.04	0.32	12.25	32.92	<LLD	<LLD	14.15	1.13	0.54	14.73	0.37	<LLD	5.94	10.86	0.23	2.44	0.09	0.82	<LLD	0.74	<LLD	97.57	3.203	0.000	1.404	1.078	0.083	0.046	1.475	0.044	0.722	0.000	0.016	1	8.07
RSA03	5	21	0.07	0.24	12.24	33.04	<LLD	<LLD	14.12	1.03	0.62	14.39	0.44	<LLD	6.19	10.85	0.26	2.72	0.14	0.88	<LLD	0.66	<LLD	97.89	3.215	0.000	1.403	1.054	0.075	0.035	1.472	0.051	0.746	0.000	0.015	1	8.07
RSA03	6	22	0.08	0.15	12.06	33.14	<LLD	<LLD	14.02	1.00	0.66	14.91	0.45	<LLD	6.50	11.18	0.20	2.38	<LLD	0.89	<LLD	0.63	<LLD	98.25	3.217	0.000	1.380	1.089	0.073	0.022	1.458	0.054	0.748	0.000	0.014	1	8.05
RSA03	6	23	0.06	0.20	12.17	32.68	<LLD	<LLD	14.07	1.13	0.62	14.60	0.47	<LLD	6.13	10.64	0.30	2.40	0.08	0.84	<LLD	0.59	<LLD	96.98	3.202	0.000	1.405	1.076	0.083	0.029	1.477	0.051	0.728	0.000	0.013	1	8.07
RSA03	7	24	0.06	0.29	11.70	32.59	<LLD	<LLD	13.75	1.32	0.57	14.63	0.41	<LLD	5.85	11.65	0.44	3.23	0.18	0.88	<LLD	0.69	<LLD	98.24	3.192	0.000	1.351	1.078	0.097	0.042	1.443	0.047	0.793	0.000	0.015	1	8.06
RSA03	7	25	0.13	0.19	12.38	32.86	<LLD	<LLD	13.56	1.09	0.44	14.75	0.24	<LLD	6.54	11.62	0.22	2.60	0.12	0.93	<LLD	0.66	<LLD	98.33	3.196	0.000	1.419	1.079	0.080	0.028	1.413	0.036	0.781	0.000	0.015	1	8.05
RSA03	7	26	0.10	0.40	13.76	31.87	<LLD	0.04	13.01	1.55	0.49	14.53	0.35	<LLD	5.51	10.30	0.23	2.44	0.11	0.81	<LLD	0.45	<LLD	95.95	3.119	0.000	1.587	1.070	0.114	0.058	1.364	0.041	0.691	0.000	0.010	1	8.05
RSA03	8	27	0.07	0.32	13.51	32.94	<LLD	<LLD	14.45	0.86	0.42	15.00	0.46	<LLD	5.65	10.07	0.13	2.25	0.07	0.82	<LLD	0.63	<LLD	97.65	3.165	0.000	1.530	1.085	0.062	0.046	1.488	0.034	0.665	0.000	0.014	1	8.09
RSA03	8	28	<LLD	0.35	12.21	32.64	<LLD	<LLD	13.77	1.31	0.52	14.97	0.36	<LLD	6.99	11.20	0.05	2.01	0.08	0.85	<LLD	0.67	<LLD	97.98	3.178	0.000	1.401	1.097	0.096	0.051	1.436	0.043	0.752	0.000	0.015	1	8.07
RSA02	1	1	0.12	0.37	14.69	33.92	<LLD	0.03	12.42	1.08	0.68	11.15	0.54	0.40	4.59	10.27	0.59	3.24	0.38	0.98	<LLD	1.15	<LLD	96.60	3.276	0.000	1.672	0.810	0.078	0.053	1.285	0.056	0.704	0.021	0.025	1	7.98
RSA02	1	2	0.05	0.32	14.88	33.81	<LLD	<LLD	12.45	1.04	0.78	11.15	0.51	0.36	4.47	10.03	0.57	3.29	0.35	0.96	<LLD	1.10	<LLD	96.12	3.272	0.000	1.697	0.812	0.076	0.046	1.291	0.064	0.692	0.019	0.024	1	7.99
RSA02	1	3	0.11	0.35	15.17	33.65	0.04	0.05	12.96	1.00	0.68	11.30	0.59	0.34	4.63	9.88	0.50	3.08	0.37	0.98	<LLD	1.26	<LLD	96.94	3.235	0.000	1.719	0.817	0.072	0.050	1.335	0.055	0.679	0.017	0.028	1	8.01
RSA02	1	4	0.10	0.33	14.97	34.56	<LLD	0.03	13.06	0.97	0.66	11.89	0.64	0.38	4.43	9.75	0.55	3.26	0.37	0.96	<LLD	1.20	<LLD	98.11	3.272	0.000	1.670	0.847	0.069	0.047	1.325	0.053	0.665	0.019	0.026	1	7.99
RSA02	1	5	0.08	0.33	14.33	33.31	<LLD	0.02	12.58	1.17	0.73	11.45	0.61	0.36	4.96	10.23	0.42	3.02	0.32	0.93	<LLD	0.96	<LLD	95.81	3.252	0.000	1.648	0.841	0.086	0.048	1.316	0.060	0.706	0.019	0.021	1	8.00
RSA02	2	6	0.05	0.41	14.76	32.64	<LLD	0.02	12.42	1.12	0.76	8.91	0.60	0.33	4.58	9.67	0.45	2.76	0.27	0.90	<LLD	1.61	<LLD	92.26	3.284	0.000	1.750	0.675	0.085	0.062	1.339	0.065	0.682	0.018	0.037	1	8.00
RSA02	2	7	0.10	0.39	14.61	32.51	<LLD	0.02	12.17	1.09	0.77	9.44	0.58	0.27	4.76	9.93	0.36	2.83	0.35	0.82	<LLD	1.54	<LLD	92.54	3.273	0.000	1.734	0.715	0.083	0.059	1.313	0.066	0.698	0.014	0.035	1	7.99
RSA02	2	8	<LLD	0.30	14.39	33.22	<LLD	<LLD	13.96	0.78	0.70	11.83	0.47	0.35	5.08	9.61	0.44	2.98	0.29	0.89	<LLD	0.84	<LLD	96.13	3.228	0.000	1.648	0.865	0.057	0.043	1.453	0.058	0.682	0.018	0.019	1	8.07
RSA02	2	9	0.07	0.26	11.02	23.34	0.08	<LLD	13.01	0.91	0.56	6.20	0.53	0.35	7.83	15.19	0.61	4.75	0.54	1.35	<LLD	2.31	<LLD	88.91	2.824	0.176	1.395	0.564	0.083	0.047	1.686	0.057	1.332	0.023	0.064	1	8.25
RSA02	3	10	0.04	0.32	16.29	33.58	<LLD	<LLD	14.48	0.58	0.71	9.57	0.55	0.32	5.15	10.24	0.51	3.52	0.36	1.02	<LLD	0.56	<LLD	97.80	3.201	0.000	1.830	0.686	0.042	0.045	1.479	0.057	0.721	0.016	0.012	1	8.09
RSA02	3	11	0.07	0.43	15.21	32.90	<LLD	<LLD	13.18	0.99	0.76	10.01	0.53	0.40	4.99	10.41	0.51	3.30	0.35	0.93	<LLD	0.83	<LLD	95.80	3.214	0.000	1.751	0.736	0.073	0.063	1.379	0.063	0.728	0.021	0.018	1	8.05
RSA02	3	12	0.06	0.42	15.43	33.63	<LLD	<LLD	13.88	0.73	0.90	9.46	0.53	0.34	5.30	10.35	0.51	3.41	0.33	1.03	<LLD	0.55	<LLD	96.86	3.243	0.000	1.754	0.686	0.053	0.060	1.434	0.074	0.734	0.017	0.012	1	8.07
RSA02	4	13	0.12	0.29	15.59	34.29	0.06	<LLD	13.05	1.17	0.67	10.74	0.61	0.27	4.83	9.33	0.28	2.61	0.26	0.85	0.25	1.70	0.15	97.12	3.267	0.000	1.750	0.770	0.084	0.041	1.332	0.054	0.629	0.014	0.040	1	7.98
RSA02	4	14	0.08	0.39	14.90	34.39	<LLD	<LLD	12.82	1.08	0.71	11.75	0.53	0.31	5.11	9.95	0.40	2.92	0.32	0.88	0.27	1.23	<LLD	98.04	3.268	0.000	1.669	0.840	0.077	0.055	1.305	0.057	0.677	0.016	0.027	1	7.99
RSA02	4	15	0.06	0.45	14.07	32.35	<LLD	<LLD	13.57	0.80	0.70	12.09	0.39	0.18	5.82	10.85	0.43	3.24	0.25	0.92	<LLD	0.51	<LLD	96.68	3.172	0.000	1.626	0.892	0.059	0.066	1.426	0.058	0.768	0.009	0.011	1	8.09

Sample	Grain	Spot	Concentration (wt%)																					Structural formula (cations / 13 oxygen)												Cation
			Na_2O	MgO	Al_2O_3	SiO_2	P_2O_5	K_2O	CaO	TiO_2	MnO	Fe_2O_3	SrO	Y_2O_3	La_2O_3	Ce_2O_3	Pr_2O_3	Nd_2O_3	SmO	Gd_2O_3	PbO	ThO_2	UO_2	Total	Si	Al	Al	Fe	Ti	Mg	Ca	Mn	REE	Y	Th	OH	Total
RSA02	4	16	0.06	0.40	14.48	33.52	<LLD	<LLD	13.00	1.03	0.74	11.83	0.52	0.20	5.45	10.32	0.44	3.20	0.29	0.93	<LLD	1.04	<LLD	97.45	3.231	0.000	1.645	0.858	0.075	0.057	1.342	0.060	0.723	0.010	0.023	1	8.02
RSA02	4	17	0.09	1.52	15.66	34.89	<LLD	0.04	12.82	1.08	0.69	11.85	0.61	0.19	5.11	9.32	0.28	2.89	0.28	0.82	<LLD	1.18	<LLD	99.32	3.232	0.000	1.709	0.826	0.075	0.210	1.272	0.054	0.630	0.009	0.025	0.68	8.04
RSA02	4	18	0.09	0.34	15.22	34.79	<LLD	0.02	13.06	1.06	0.71	11.92	0.58	0.23	5.21	10.09	0.44	3.13	0.31	0.98	<LLD	1.17	<LLD	99.35	3.260	0.000	1.681	0.841	0.075	0.047	1.311	0.056	0.687	0.011	0.025	0.65	7.99
RSA02	5	19	0.08	0.39	13.75	32.89	<LLD	0.02	12.27	1.02	0.83	11.29	0.52	0.39	5.66	10.92	0.52	3.28	0.37	0.97	<LLD	0.97	<LLD	96.14	3.246	0.000	1.599	0.838	0.076	0.057	1.297	0.069	0.780	0.020	0.022	1	8.01
RSA02	5	20	0.06	0.39	14.63	33.58	0.06	0.02	12.81	0.94	0.91	10.69	0.52	0.34	5.41	10.12	0.36	3.04	0.31	0.92	<LLD	1.08	<LLD	96.19	3.266	0.000	1.677	0.782	0.069	0.057	1.335	0.075	0.713	0.018	0.024	1	8.02
RSA02	5	21	0.12	0.28	14.80	33.86	0.07	0.03	12.46	1.11	0.86	10.61	0.55	0.36	5.56	10.23	0.38	2.84	0.28	0.97	0.25	1.17	<LLD	96.79	3.276	0.000	1.687	0.772	0.081	0.040	1.291	0.070	0.713	0.019	0.026	1	7.98
RSA02	6	22	0.09	0.38	15.89	35.30	<LLD	0.05	13.37	1.21	0.95	10.85	0.62	0.38	4.96	9.66	0.55	3.06	0.30	0.87	<LLD	1.12	0.15	99.76	3.270	0.000	1.735	0.756	0.084	0.052	1.327	0.075	0.654	0.019	0.027	0.24	8.00
RSA02	6	23	0.07	0.31	14.08	31.83	0.08	0.03	13.41	1.21	0.79	10.12	0.56	0.20	4.98	9.29	0.28	2.61	0.27	0.81	<LLD	1.23	0.18	92.34	3.222	0.000	1.680	0.771	0.092	0.047	1.454	0.068	0.672	0.011	0.032	1	8.05
RSA02	6	24	0.05	0.35	14.71	32.71	<LLD	0.04	12.55	1.00	0.73	10.56	0.63	0.21	4.41	8.77	0.43	2.47	0.23	0.80	<LLD	1.35	<LLD	92.00	3.272	0.000	1.734	0.795	0.075	0.052	1.345	0.062	0.623	0.011	0.031	1	8.00
SWA07	1	1	0.12	0.17	11.34	32.29	<LLD	0.04	11.30	1.52	1.00	14.99	0.31	0.29	4.82	10.94	0.67	3.55	0.44	1.09	<LLD	1.58	<LLD	96.46	3.230	0.000	1.337	1.128	0.114	0.025	1.211	0.085	0.782	0.015	0.036	1	7.96
SWA07	1	2	0.06	0.11	10.09	31.29	<LLD	<LLD	12.18	1.28	1.04	17.02	0.37	0.27	4.82	10.94	0.72	3.87	0.50	1.11	<LLD	1.12	<LLD	96.79	3.165	0.000	1.203	1.295	0.097	0.017	1.320	0.089	0.807	0.015	0.026	1	8.03
SWA07	1	3	0.10	<LLD	9.89	31.56	<LLD	0.02	11.33	1.26	0.98	16.81	0.37	0.29	5.05	11.64	0.63	3.82	0.47	1.15	<LLD	1.02	<LLD	96.39	3.211	0.000	1.186	1.287	0.096	0.000	1.235	0.084	0.841	0.016	0.024	1	7.98
SWA07	1	4	0.11	0.16	11.36	31.78	<LLD	0.03	11.35	1.23	0.87	15.88	0.34	0.26	4.88	10.73	0.64	3.72	0.54	1.11	<LLD	1.44	<LLD	96.43	3.192	0.000	1.345	1.200	0.093	0.024	1.221	0.074	0.789	0.014	0.033	1	7.99
SWA07	1	5	0.13	0.34	11.53	32.33	<LLD	0.03	11.09	1.40	0.91	15.56	0.30	0.28	5.16	10.75	0.54	3.43	0.47	1.04	<LLD	1.30	<LLD	96.59	3.219	0.000	1.353	1.166	0.105	0.050	1.183	0.077	0.774	0.015	0.029	1	7.97
SWA07	1	6	0.06	0.10	9.98	31.75	<LLD	0.02	11.73	1.20	0.97	17.39	0.35	0.32	5.01	11.19	0.62	3.90	0.46	1.14	<LLD	0.89	0.13	97.21	3.195	0.000	1.184	1.317	0.091	0.015	1.265	0.083	0.816	0.017	0.023	1	8.00
SWA07	1	7	0.14	0.19	12.82	33.03	<LLD	0.04	11.32	1.39	0.83	14.27	0.33	0.28	5.11	9.81	0.50	3.39	0.50	1.02	<LLD	1.61	<LLD	96.58	3.245	0.000	1.484	1.055	0.103	0.028	1.191	0.069	0.726	0.015	0.036	1	7.95
SWA07	1	8	0.12	0.21	12.17	32.45	<LLD	0.03	11.13	1.53	0.95	15.00	0.29	0.27	4.59	10.08	0.64	3.43	0.44	1.02	<LLD	1.94	<LLD	96.29	3.220	0.000	1.423	1.120	0.114	0.031	1.183	0.080	0.728	0.014	0.044	1	7.96
SWA07	1	9	0.09	0.26	13.29	31.16	<LLD	<LLD	11.85	0.99	0.83	16.04	0.18	0.50	4.76	10.90	0.66	4.35	0.68	1.24	<LLD	0.36	<LLD	98.14	3.066	0.000	1.541	1.188	0.073	0.038	1.249	0.069	0.806	0.026	0.008	1	8.07
SWA07	1	10	0.09	0.24	11.89	30.92	0.05	<LLD	11.90	1.06	0.81	15.50	0.30	0.44	4.90	10.97	0.63	4.21	0.57	1.21	<LLD	0.79	<LLD	96.48	3.120	0.000	1.414	1.177	0.080	0.036	1.286	0.069	0.824	0.024	0.018	1	8.05
SWA07	2	11	0.14	0.12	13.65	33.51	<LLD	0.04	11.70	1.17	0.68	14.02	0.35	0.28	4.02	9.22	0.58	3.22	0.45	0.97	<LLD	1.68	<LLD	95.80	3.267	0.000	1.568	1.028	0.086	0.017	1.222	0.056	0.653	0.015	0.037	1	7.95
SWA07	2	12	0.06	0.17	11.94	32.55	<LLD	<LLD	11.80	0.90	0.97	15.50	0.34	0.40	4.67	10.49	0.69	3.98	0.59	1.14	<LLD	1.10	<LLD	97.29	3.218	0.000	1.391	1.153	0.067	0.025	1.250	0.081	0.774	0.021	0.025	1	8.01
SWA07	2	13	0.16	0.17	13.73	33.38	<LLD	0.04	11.63	1.16	0.65	14.14	0.37	0.31	4.11	9.25	0.50	3.24	0.52	0.99	<LLD	1.74	<LLD	96.09	3.251	0.000	1.576	1.036	0.085	0.025	1.214	0.054	0.658	0.016	0.039	1	7.95
SWA07	2	14	0.12	0.34	13.79	31.48	<LLD	<LLD	11.56	0.88	0.77	15.80	0.19	0.53	4.29	10.33	0.77	4.51	0.75	1.32	<LLD	0.50	0.16	98.09	3.082	0.000	1.591	1.164	0.065	0.050	1.212	0.064	0.780	0.028	0.015	1	8.05
SWA07	2	15	0.15	0.22	13.01	33.09	<LLD	<LLD	11.22	1.40	0.68	14.65	0.38	0.35	4.12	9.29	0.51	3.28	0.49	0.97	<LLD	1.70	<LLD	95.51	3.253	0.000	1.507	1.084	0.104	0.032	1.182	0.057	0.666	0.018	0.038	1	7.94
SWA07	2	16	0.08	<LLD	11.27	32.10	<LLD	<LLD	11.85	0.97	0.97	15.91	0.38	0.45	4.68	10.78	0.73	4.25	0.68	1.23	<LLD	0.96	<LLD	97.29	3.205	0.000	1.326	1.195	0.073	0.000	1.268	0.082	0.810	0.024	0.022	1	8.00
SWA07	2	17	0.15	0.13	12.33	31.90	<LLD	<LLD	10.81	1.34	0.77	13.56	0.32	0.30	4.87	10.21	0.59	3.68	0.58	1.15	<LLD	1.77	<LLD	94.46	3.237	0.000	1.475	1.036	0.102	0.020	1.175	0.066	0.777	0.016	0.041	1	7.94
SWA07	2	18	0.13	0.18	12.42	32.59	<LLD	0.04	10.89	1.48	0.79	14.44	0.31	0.35	4.48	10.02	0.64	3.54	0.53	1.07	<LLD	1.91	<LLD	95.81	3.242	0.000	1.456	1.081	0.111	0.027	1.160	0.067	0.732	0.019	0.043	1	7.94
SWA07	2	19	0.13	0.23	13.44	31.50	<LLD	<LLD	11.81	0.78	0.86	15.29	0.17	0.79	4.08	10.08	0.86	5.10	1.04	1.51	<LLD	0.14	<LLD	97.81	3.103	0.000	1.560	1.133	0.058	0.034	1.247	0.072	0.808	0.041	0.003	1	8.06
SWA07	2	20	0.15	0.19	14.05	33.81	<LLD	0.05	11.93	1.39	0.57	13.67	0.43	0.22	3.55	8.32	0.58	3.30	0.51	0.94	0.09	2.28	<LLD	96.03	3.269	0.000	1.601	0.995	0.101	0.027	1.236	0.047	0.603	0.011	0.050	1	7.94
SWA07	3	21	0.10	<LLD	11.58	31.30	<LLD	<LLD	12.43	1.16	0.81	16.61	0.35	0.36	4.85	11.02	0.63	3.97	0.55	1.13	<LLD	0.88	<LLD	97.73	3.118	0.000	1.359	1.245	0.087	0.000	1.326	0.068	0.801	0.019	0.020	1	8.04
SWA07	3	22	0.06	0.09	11.61	30.75	<LLD	<LLD	12.00	1.14	0.94	16.02	0.30	0.30	5.71	11.57	0.61	4.02	0.50	1.19	<LLD	0.92	<LLD	97.73	3.092	0.000	1.376	1.212	0.086	0.013	1.293	0.080	0.862	0.016	0.021	1	8.05
SWA07	3	23	0.18	0.27	13.26	32.80	<LLD	0.04	11.40	1.39	0.68	14.99	0.35	0.26	4.68	10.04	0.57	3.42	0.45	0.99	<LLD	1.35	<LLD	97.12	3.197	0.000	1.523	1.099	0.102	0.039	1.190	0.056	0.714	0.013	0.030	1	7.96
SWA07	3	24	0.09	0.11	11.15	31.21	<LLD	<LLD	11.86	1.00	0.75	17.11	0.37	0.27	5.43	11.06	0.56	3.67	0.46	1.09	<LLD	1.08	<LLD	97.27	3.133	0.000	1.319	1.292	0.076	0.016	1.275	0.064	0.812	0.014	0.025	1	8.03
SWA07	4	25	0.10	0.12	9.45	31.45	<LLD	<LLD	11.08	1.11	1.14	16.54	0.30	0.40	5.20	12.46	0.79	4.25	0.50	1.25	<LLD	1.02	<LLD	97.16	3.213	0.000	1.138	1.272	0.085	0.018	1.213	0.099	0.907	0.022	0.024	1	7.99
SWA07	4	26	0.09	0.17	10.48	30.11	<LLD	<LLD	11.56	1.08	1.09	15.85	0.19	0.45	5.55	13.06	0.69	4.09	0.50	1.31	<LLD	0.76	<LLD	97.03	3.098	0.000	1.271	1.227	0.084	0.026	1.274	0.095	0.942	0.025	0.018	1	8.06
SWA07	4	27	0.10	0.25	11.41	31.70	<LLD	0.02	11.08	1.01	0.89	14.61	0.27	0.33	5.45	12.30	0.69	4.29	0.48	1.17	<LLD	0.91	0.13	97.09	3.200	0.000	1.357	1.110	0.077	0.038	1.198	0.076	0.894	0.018	0.024	1	7.99
SWA07	4	28	0.08	0.13	10.40	29.75	<LLD	0.02	10.78	0.96	0.84	14.53	0.28	0.39	5.45	13.72	0.85	4.82	0.64	1.33	<LLD	1.17	<LLD	96.14	3.125	0.000	1.287	1.148	0.076	0.020	1.213	0.075	1.023	0.022	0.028	1	8.02
SWA07	4	29	0.15	0.11	12.28	32.43	<LLD	0.04	11.23	1.20	0.90	14.84	0.31	0.28	5.04	10.73	0.60	3.55	0.48	1.08	<LLD	1.21	<LLD	96.46	3.223	0.000	1.438	1.110	0.090	0.016	1.196	0.076	0.776	0.015	0.027	1	7.97
SWA07	4	30	0.12	0.66	12.97	32.12	0.05	0.05	10.88	1.22	0.84	14.72	0.31	0.29	4.79	9.81	0.56	3.44	0.46	0.97	<LLD	1.78	<LLD	96.04	3.183	0.000	1.515	1.098	0.091	0.098	1.155	0.071	0.721	0.015	0.040	1	7.99
SWA07	4	31	0.16	0.15	11.48	32.48	<LLD	0.05	10.85	1.26	0.82	16.25	0.32	0.34	4.85	10.42	0.57	3.41	0.45	1.00	<LLD	1.62	<LLD	96.48	3.233	0.000	1.347	1.217	0.094	0.022	1.157	0.069	0.749	0.018	0.037	1	7.94
SWA07	4	32	0.08	<LLD	10.35	31.36	<LLD	0.03	11.08	1.09	1.14	16.73	0.30	0.42	5.40	11.57	0.55	3.91	0.51	1.14	<LLD	0.97	<LLD	96.63	3.187	0.000	1.240	1.279	0.083	0.000	1.206	0.098	0.852	0.023	0.022	1	7.99
SWA07	4	33	0.14	0.51	11.21	32.22	<LLD	0.05	10.44	1.18	0.92	15.79	0.26	0.29	5.02	11.46	0.69	3.75	0.45	1.11	<LLD	1.06	<LLD	96.55	3.227	0.000	1.323	1.190	0.089	0.076	1.120	0.078	0.818	0.015	0.024	1	7.96
SWA07	5	34	0.13	0.34	12.75	31.06	<LLD	<LLD	11.58	1.02	0.78	15.38	0.25	0.45	5.00	11.07	0.77	4.34	0.72	1.27	<LLD	0.59	<LLD	97.50	3.094	0.000	1.497	1.153	0.076	0.050	1.236	0.066	0.838	0.024	0.013	1	8.05

			Concentration (wt%)																					Structural formula (cations / 13 oxygen)												Cation
Sample	Grain	Spot	Na_2O	MgO	Al_2O_3	SiO_2	P_2O_5	K_2O	CaO	TiO_2	MnO	Fe_2O_3	SrO	Y_2O_3	La_2O_3	Ce_2O_3	Pr_2O_3	Nd_2O_3	SmO	Gd_2O_3	PbO	ThO_2	UO_2	Total	Si	Al	Al	Fe	Ti	Mg	Ca	Mn	REE	Y	Th	OH	Total
SWA07	5	35	0.15	0.29	11.52	31.76	<LLD	0.04	10.58	1.31	0.82	13.83	0.25	0.39	5.40	10.50	0.51	3.64	0.50	1.11	0.30	1.19	<LLD	94.09	3.254	0.000	1.391	1.066	0.101	0.044	1.161	0.071	0.806	0.021	0.028	1	7.94
SWA07	5	36	0.11	0.16	11.36	30.73	<LLD	0.02	11.38	1.13	0.89	15.50	0.26	0.43	5.16	10.76	0.66	3.94	0.62	1.19	0.10	0.92	0.13	95.45	3.143	0.000	1.369	1.193	0.087	0.024	1.247	0.077	0.829	0.023	0.024	1	8.02
SWA07	5	37	0.15	0.17	11.74	32.19	<LLD	0.03	11.14	1.11	0.99	15.58	0.31	0.38	5.28	10.55	0.54	3.79	0.56	1.16	0.24	1.15	<LLD	97.06	3.207	0.000	1.379	1.168	0.083	0.025	1.189	0.084	0.792	0.020	0.026	1	7.97
SWA07	5	38	0.12	0.19	11.75	32.17	<LLD	0.06	10.87	1.23	0.94	14.77	0.34	0.31	4.86	9.78	0.48	3.46	0.53	1.02	0.37	1.60	<LLD	94.85	3.251	0.000	1.399	1.123	0.093	0.029	1.177	0.080	0.739	0.017	0.037	1	7.94
RSA08	0	1	0.13	0.11	13.56	32.59	<LLD	<LLD	10.06	1.24	0.47	13.11	0.52	0.20	3.98	8.45	0.47	3.19	0.32	0.83	5.04	1.07	<LLD	95.34	3.286	0.000	1.611	0.995	0.094	0.017	1.087	0.040	0.631	0.011	0.025	1	7.80
RSA08	1	2	0.07	0.15	13.59	33.09	<LLD	<LLD	10.11	1.35	0.54	13.08	0.53	0.23	3.85	8.82	0.49	3.20	0.38	0.95	5.21	1.09	<LLD	96.73	3.296	0.000	1.595	0.980	0.101	0.022	1.079	0.046	0.640	0.012	0.025	1	7.79
RSA08	1	3	0.14	<LLD	14.17	33.34	<LLD	<LLD	11.64	1.21	0.39	13.07	0.71	0.18	3.54	7.08	0.36	2.62	0.30	0.71	5.67	1.46	<LLD	96.59	3.286	0.000	1.646	0.969	0.090	0.000	1.229	0.033	0.523	0.009	0.033	1	7.82
RSA08	1	4	0.14	0.17	14.04	33.64	<LLD	0.02	10.13	1.33	0.55	13.46	0.48	0.23	4.04	8.88	0.51	3.25	0.38	0.91	5.39	1.13	<LLD	98.68	3.284	0.000	1.615	0.989	0.098	0.025	1.059	0.045	0.637	0.012	0.025	1	7.79
RSA08	1	5	0.10	0.19	12.28	32.05	<LLD	<LLD	11.80	1.59	0.76	14.36	0.42	0.46	4.58	11.56	0.71	3.97	0.57	1.18	<LLD	0.94	<LLD	97.52	3.173	0.000	1.433	1.070	0.118	0.028	1.252	0.064	0.811	0.024	0.021	1	7.99
RSA08	1	6	0.14	0.18	12.67	32.53	<LLD	0.04	9.63	1.50	0.59	14.03	0.44	0.31	4.37	10.03	0.49	3.64	0.53	1.05	4.00	1.12	<LLD	97.29	3.259	0.000	1.496	1.058	0.113	0.027	1.034	0.050	0.732	0.017	0.026	1	7.81
RSA08	1	7	0.08	<LLD	8.51	20.02	<LLD	<LLD	8.20	0.70	0.27	7.31	0.54	0.36	8.88	16.95	0.96	6.71	0.82	1.77	4.11	2.35	<LLD	88.54	2.718	0.282	1.079	0.747	0.071	0.000	1.192	0.031	1.779	0.026	0.073	1	8.00
RSA08	1	8	0.17	0.14	14.42	33.96	<LLD	0.02	10.51	1.27	0.53	13.70	0.57	0.18	3.61	8.19	0.51	3.11	0.37	0.78	5.71	1.27	<LLD	99.02	3.284	0.000	1.643	0.997	0.092	0.020	1.089	0.043	0.582	0.009	0.028	0.98	7.79
RSA08	1	9	0.18	0.11	13.81	33.72	<LLD	0.02	10.40	1.41	0.55	13.26	0.50	0.25	4.09	9.12	0.57	3.32	0.43	0.86	5.31	1.16	<LLD	99.07	3.289	0.000	1.587	0.973	0.103	0.016	1.087	0.045	0.652	0.013	0.026	0.93	7.79
RSA08	1	10	0.09	0.16	13.05	32.30	<LLD	<LLD	12.12	1.53	0.67	14.57	0.47	0.39	4.34	10.58	0.70	3.80	0.54	1.15	1.13	1.01	<LLD	98.60	3.156	0.000	1.503	1.071	0.112	0.023	1.269	0.055	0.749	0.020	0.022	1	7.98
RSA08	1	11	0.17	0.15	14.05	33.59	<LLD	0.02	10.28	1.42	0.58	12.88	0.50	0.24	4.17	8.95	0.39	3.20	0.43	0.89	5.46	1.27	<LLD	98.64	3.286	0.000	1.620	0.948	0.105	0.022	1.078	0.048	0.641	0.012	0.028	1	7.79
RSA08	2	12	0.07	0.10	10.24	26.08	0.07	0.02	8.57	1.05	0.44	11.15	0.43	0.30	6.09	12.39	0.78	4.84	0.62	1.31	5.17	1.93	<LLD	91.65	3.053	0.000	1.413	0.982	0.092	0.017	1.075	0.044	1.107	0.019	0.051	1	7.85
RSA08	2	13	0.10	<LLD	9.81	24.51	0.06	<LLD	8.69	0.98	0.37	8.68	0.45	0.37	7.75	15.22	0.75	5.42	0.70	1.54	4.63	2.02	<LLD	92.05	2.976	0.024	1.380	0.793	0.090	0.000	1.131	0.038	1.385	0.024	0.056	1	7.90
RSA08	2	14	0.12	0.22	13.44	32.67	<LLD	<LLD	9.66	1.35	0.57	13.38	0.48	0.26	4.28	9.33	0.54	3.53	0.46	1.00	4.64	1.07	<LLD	97.00	3.265	0.000	1.583	1.006	0.101	0.033	1.034	0.048	0.695	0.014	0.024	1	7.80
RSA08	2	15	0.15	0.22	12.66	32.55	<LLD	<LLD	9.69	1.44	0.59	13.81	0.40	0.33	4.33	9.81	0.58	3.42	0.40	0.98	4.65	1.21	<LLD	97.22	3.269	0.000	1.498	1.044	0.109	0.033	1.043	0.050	0.712	0.018	0.028	1	7.80
RSA08	2	16	0.12	0.18	12.52	32.18	0.05	<LLD	9.98	1.36	0.70	14.09	0.39	0.35	4.15	10.21	0.63	3.61	0.49	1.04	4.13	1.14	<LLD	97.32	3.240	0.000	1.486	1.067	0.103	0.027	1.076	0.060	0.736	0.019	0.026	1	7.84
RSA08	2	17	0.15	0.19	13.29	32.50	<LLD	0.02	9.74	1.34	0.55	12.68	0.44	0.29	4.32	9.28	0.42	3.23	0.44	1.03	4.98	1.19	<LLD	96.08	3.284	0.000	1.583	0.964	0.102	0.029	1.054	0.047	0.687	0.016	0.027	1	7.79
RSA08	2	18	0.10	0.19	12.65	32.01	<LLD	<LLD	9.88	1.42	0.61	13.98	0.39	0.33	4.30	9.85	0.54	3.53	0.47	0.98	4.41	1.23	<LLD	96.87	3.235	0.000	1.506	1.063	0.108	0.029	1.070	0.052	0.722	0.018	0.028	1	7.83
RSA08	2	19	0.11	0.20	11.75	31.37	<LLD	<LLD	11.44	1.15	0.88	14.94	0.40	0.46	5.03	11.71	0.74	4.56	0.72	1.33	<LLD	0.63	<LLD	97.42	3.152	0.000	1.391	1.130	0.087	0.030	1.232	0.075	0.878	0.025	0.014	1	8.01
RSA08	3	20	0.11	0.48	11.95	31.14	<LLD	<LLD	10.98	1.43	0.88	15.01	0.37	0.30	5.58	11.83	0.53	3.70	0.43	1.14	<LLD	0.56	<LLD	96.42	3.135	0.000	1.418	1.137	0.108	0.072	1.184	0.075	0.849	0.016	0.013	1	8.01
RSA08	3	21	0.13	0.36	10.72	31.04	<LLD	<LLD	11.18	1.55	0.92	16.31	0.27	0.37	5.53	11.68	0.65	3.89	0.49	1.14	<LLD	0.55	0.14	96.92	3.138	0.000	1.277	1.241	0.118	0.054	1.211	0.079	0.859	0.020	0.016	1	8.01
RSA08	3	22	0.11	0.16	12.55	31.92	<LLD	0.03	9.87	1.56	0.55	14.03	0.56	0.24	4.40	8.40	0.33	2.96	0.37	0.80	5.51	1.24	<LLD	95.59	3.254	0.000	1.508	1.076	0.120	0.024	1.078	0.047	0.640	0.013	0.029	1	7.79
RSA08	3	23	0.09	0.32	11.65	31.19	<LLD	<LLD	11.57	1.82	0.79	15.62	0.45	0.31	5.09	11.01	0.66	3.77	0.51	1.10	<LLD	0.82	<LLD	96.77	3.123	0.000	1.375	1.177	0.137	0.048	1.241	0.067	0.805	0.017	0.019	1	8.01
RSA08	4	24	0.14	0.22	12.58	32.22	<LLD	<LLD	9.94	1.29	0.62	13.64	0.43	0.35	4.05	9.33	0.59	3.29	0.50	0.91	4.91	1.35	<LLD	96.36	3.267	0.000	1.503	1.041	0.098	0.033	1.080	0.053	0.688	0.019	0.031	1	7.81
RSA08	4	25	0.16	0.31	12.81	31.78	<LLD	<LLD	10.67	1.28	0.71	13.38	0.41	0.42	4.20	10.38	0.67	3.97	0.65	1.13	2.48	0.84	<LLD	96.25	3.207	0.000	1.524	1.016	0.097	0.047	1.154	0.061	0.769	0.023	0.019	1	7.92
RSA08	4	26	0.11	0.23	12.62	31.64	<LLD	<LLD	9.79	1.33	0.53	13.70	0.41	0.31	3.92	9.35	0.63	3.38	0.43	0.90	4.60	1.17	<LLD	95.05	3.245	0.000	1.525	1.057	0.103	0.035	1.076	0.046	0.693	0.017	0.027	1	7.82
RSA08	4	27	0.16	0.30	12.96	32.30	0.05	<LLD	10.84	1.35	0.77	13.74	0.44	0.33	4.77	10.88	0.58	3.62	0.54	1.09	2.00	0.88	<LLD	97.60	3.206	0.000	1.516	1.026	0.101	0.044	1.153	0.065	0.774	0.017	0.020	1	7.92
RSA08	4	28	0.12	0.13	12.27	31.76	<LLD	0.05	9.76	1.42	0.59	14.19	0.39	0.27	4.18	9.56	0.68	3.37	0.48	1.01	4.31	1.18	<LLD	95.72	3.246	0.000	1.478	1.091	0.109	0.020	1.069	0.051	0.715	0.015	0.027	1	7.82
RSA08	4	29	0.12	0.24	12.28	31.75	<LLD	<LLD	11.50	1.24	0.78	13.89	0.39	0.46	4.72	11.20	0.67	4.01	0.64	1.20	0.65	0.88	<LLD	96.62	3.188	0.000	1.453	1.049	0.094	0.036	1.237	0.066	0.818	0.025	0.020	1	7.99
RSA08	4	30	0.07	0.19	11.91	28.20	<LLD	<LLD	10.32	0.69	0.57	12.09	0.38	0.34	7.21	14.12	0.74	5.56	0.69	1.52	<LLD	0.73	<LLD	95.33	3.030	0.000	1.508	0.978	0.056	0.030	1.188	0.052	1.164	0.019	0.018	1	8.04
RSA08	5	31	0.11	0.15	12.09	31.43	<LLD	<LLD	12.14	1.51	0.67	16.16	0.49	0.28	4.83	10.79	0.64	3.77	0.49	1.05	<LLD	0.82	<LLD	97.42	3.114	0.000	1.412	1.205	0.113	0.022	1.289	0.056	0.776	0.015	0.018	1	8.02
RSA08	5	32	0.13	0.18	12.10	31.21	<LLD	<LLD	11.51	1.54	0.67	15.77	0.47	0.32	5.28	11.73	0.59	3.83	0.50	1.15	<LLD	0.54	<LLD	97.52	3.109	0.000	1.421	1.182	0.115	0.027	1.229	0.057	0.835	0.017	0.012	1	8.00
RSA08	5	33	0.11	0.18	11.58	31.81	0.07	<LLD	9.97	1.47	0.59	15.14	0.47	0.26	4.31	9.81	0.63	3.44	0.44	0.97	4.73	1.21	<LLD	97.19	3.235	0.000	1.388	1.158	0.112	0.027	1.086	0.051	0.724	0.014	0.028	1	7.82
RSA08	5	34	0.11	0.22	11.88	31.19	<LLD	<LLD	11.89	1.29	0.66	16.61	0.45	0.26	5.38	11.29	0.58	3.71	0.44	1.07	<LLD	0.64	<LLD	97.67	3.102	0.000	1.392	1.243	0.096	0.033	1.267	0.056	0.812	0.014	0.014	1	8.03
RSA08	5	35	0.14	0.10	12.90	32.03	<LLD	0.03	10.49	1.30	0.50	13.84	0.56	0.18	4.21	7.98	0.42	2.80	0.36	0.83	5.81	1.34	<LLD	95.82	3.252	0.000	1.544	1.057	0.099	0.015	1.141	0.043	0.612	0.010	0.031	1	7.80
RSA08	5	36	0.12	0.18	12.19	31.82	<LLD	<LLD	10.04	1.40	0.55	14.98	0.47	0.28	4.42	9.64	0.55	3.42	0.43	0.97	4.63	1.13	<LLD	97.22	3.217	0.000	1.453	1.140	0.106	0.027	1.088	0.047	0.714	0.015	0.026	1	7.83
RSA08	5	37	0.09	0.24	12.04	31.34	0.05	<LLD	11.98	1.31	0.71	15.81	0.54	0.24	5.08	11.51	0.52	3.82	0.43	1.13	<LLD	0.63	<LLD	97.47	3.119	0.000	1.412	1.184	0.098	0.036	1.277	0.060	0.813	0.013	0.014	1	8.03
RSA08	6	38	0.11	0.18	12.72	31.78	<LLD	<LLD	11.99	1.14	0.46	15.69	0.37	0.40	4.50	10.75	0.69	4.05	0.59	1.16	0.55	1.06	<LLD	98.19	3.130	0.000	1.477	1.163	0.084	0.026	1.265	0.038	0.777	0.021	0.024	1	8.01
RSA08	6	39	0.08	<LLD	9.34	24.95	<LLD	<LLD	8.23	1.09	0.31	10.69	0.44	0.36	6.70	14.34	0.69	4.97	0.60	1.45	5.42	1.64	<LLD	91.30	3.015	0.000	1.330	0.972	0.099	0.000	1.065	0.032	1.262	0.023	0.045	1	7.84

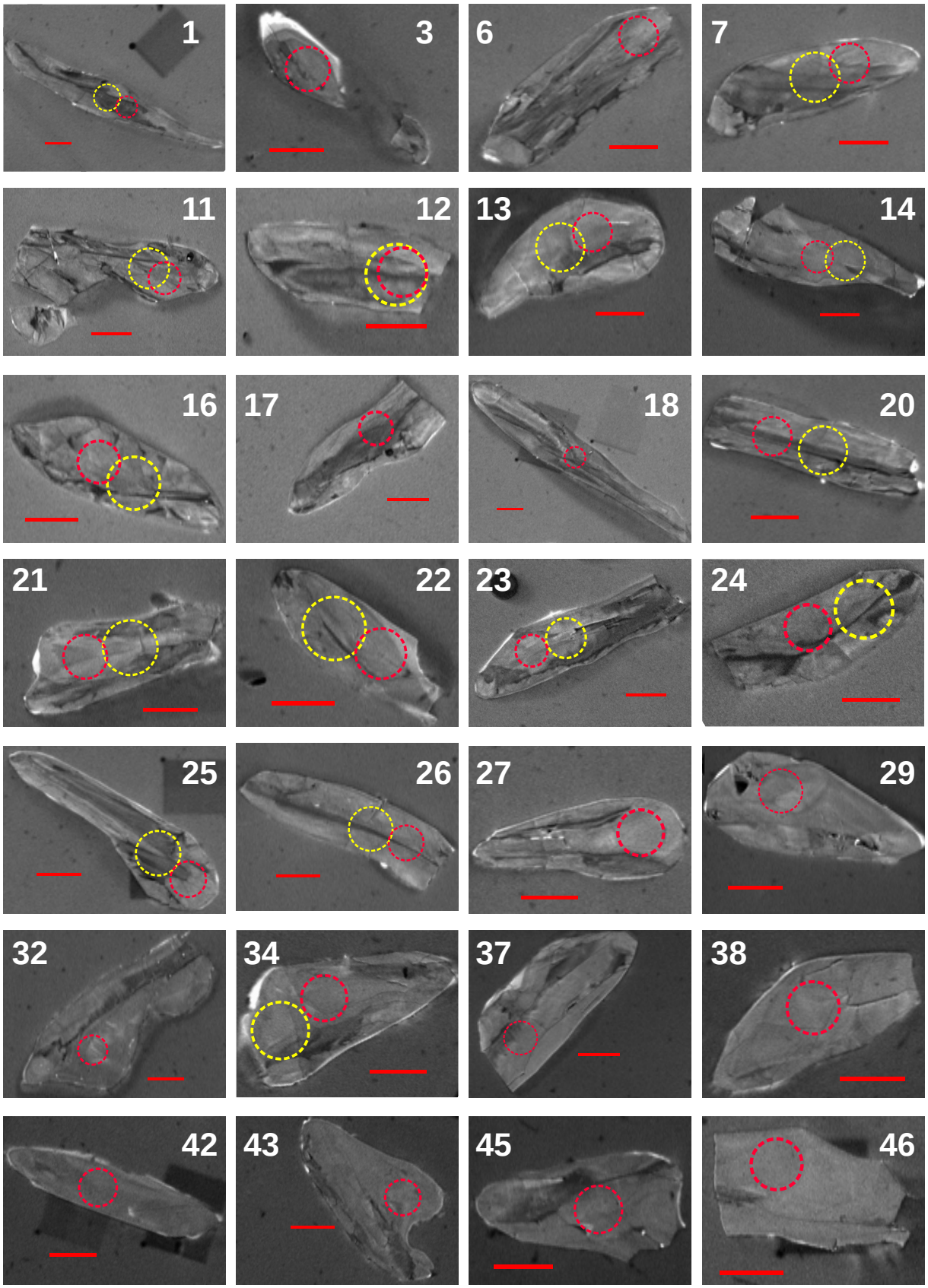
			Concentration (wt%)																					Structural formula (cations / 13 oxygen)												Cation
Sample	Grain	Spot	Na_2O	MgO	Al_2O_3	SiO_2	P_2O_5	K_2O	CaO	TiO_2	MnO	Fe_2O_3	SrO	Y_2O_3	La_2O_3	Ce_2O_3	Pr_2O_3	Nd_2O_3	SmO	Gd_2O_3	PbO	ThO_2	UO_2	Total	Si	Al	Al	Fe	Ti	Mg	Ca	Mn	REE	Y	Th	OH	Total
RSA08	6	40	0.13	0.11	11.92	31.83	<LLD	<LLD	10.33	1.22	0.49	15.96	0.42	0.29	4.34	9.58	0.46	3.45	0.45	0.99	4.03	1.15	<LLD	97.15	3.211	0.000	1.417	1.212	0.093	0.017	1.117	0.042	0.706	0.016	0.026	1	7.86
RSA08	6	41	0.14	0.24	12.41	31.50	<LLD	<LLD	11.97	1.20	0.53	15.91	0.43	0.35	4.78	10.55	0.60	3.79	0.45	1.08	0.14	1.00	<LLD	97.07	3.126	0.000	1.452	1.188	0.090	0.036	1.273	0.045	0.766	0.018	0.023	1	8.02
RSA08	6	42	0.11	<LLD	12.53	32.13	<LLD	<LLD	13.20	0.90	0.47	17.46	0.57	0.36	4.10	9.86	0.62	3.59	0.51	1.03	<LLD	0.79	<LLD	98.23	3.123	0.000	1.435	1.277	0.066	0.000	1.375	0.039	0.696	0.019	0.017	1	8.05
RSA08	6	43	0.14	0.20	12.17	31.25	0.06	<LLD	11.76	1.19	0.61	15.75	0.45	0.37	4.72	10.86	0.64	3.95	0.50	1.17	<LLD	0.97	<LLD	96.76	3.127	0.000	1.435	1.186	0.090	0.030	1.261	0.052	0.793	0.020	0.022	1	8.01
RSA08	6	44	0.11	0.09	13.84	33.35	<LLD	0.03	10.59	1.30	0.38	13.74	0.66	0.24	3.23	7.68	0.51	2.85	0.39	0.80	6.46	1.36	<LLD	97.61	3.289	0.000	1.608	1.019	0.096	0.013	1.119	0.032	0.553	0.013	0.031	1	7.77
RSA08	6	45	0.13	0.11	13.04	31.48	<LLD	<LLD	12.57	1.31	0.45	15.27	0.39	0.45	4.48	10.73	0.73	4.18	0.55	1.14	<LLD	0.94	<LLD	97.95	3.097	0.000	1.512	1.130	0.097	0.016	1.325	0.037	0.779	0.024	0.021	1	8.04
RSA08	6	46	0.11	0.29	12.57	31.50	<LLD	<LLD	11.52	1.12	0.47	15.55	0.40	0.32	4.97	11.15	0.72	4.12	0.56	1.22	0.27	0.91	0.16	97.93	3.124	0.000	1.469	1.161	0.084	0.043	1.224	0.039	0.819	0.017	0.024	1	8.00
RSA08	6	47	0.14	0.21	12.43	31.07	<LLD	<LLD	9.83	1.20	0.43	14.04	0.40	0.33	4.44	10.06	0.63	3.58	0.49	1.03	4.32	1.14	<LLD	95.77	3.200	0.000	1.509	1.088	0.093	0.032	1.085	0.038	0.757	0.018	0.027	1	7.85
RSA08	6	48	0.10	<LLD	11.70	28.44	<LLD	<LLD	9.68	0.74	0.48	14.03	0.32	0.21	5.81	12.53	0.73	4.50	0.60	1.29	3.04	1.13	<LLD	95.33	3.060	0.000	1.483	1.136	0.060	0.000	1.116	0.044	0.995	0.012	0.028	1	7.93
RSA08	6	49	0.10	0.14	12.50	31.62	<LLD	<LLD	11.85	1.13	0.51	15.28	0.40	0.39	5.00	11.10	0.66	4.04	0.54	1.18	<LLD	0.94	<LLD	97.38	3.141	0.000	1.464	1.142	0.084	0.021	1.261	0.043	0.812	0.021	0.021	1	8.01
RSA08	6	50	0.13	0.21	11.98	31.57	<LLD	<LLD	11.34	1.37	0.62	15.47	0.34	0.33	5.56	11.90	0.62	4.15	0.51	1.21	<LLD	0.71	<LLD	98.02	3.140	0.000	1.404	1.158	0.103	0.031	1.208	0.052	0.865	0.017	0.016	1	8.00

Appendix D – Zircon CL Images

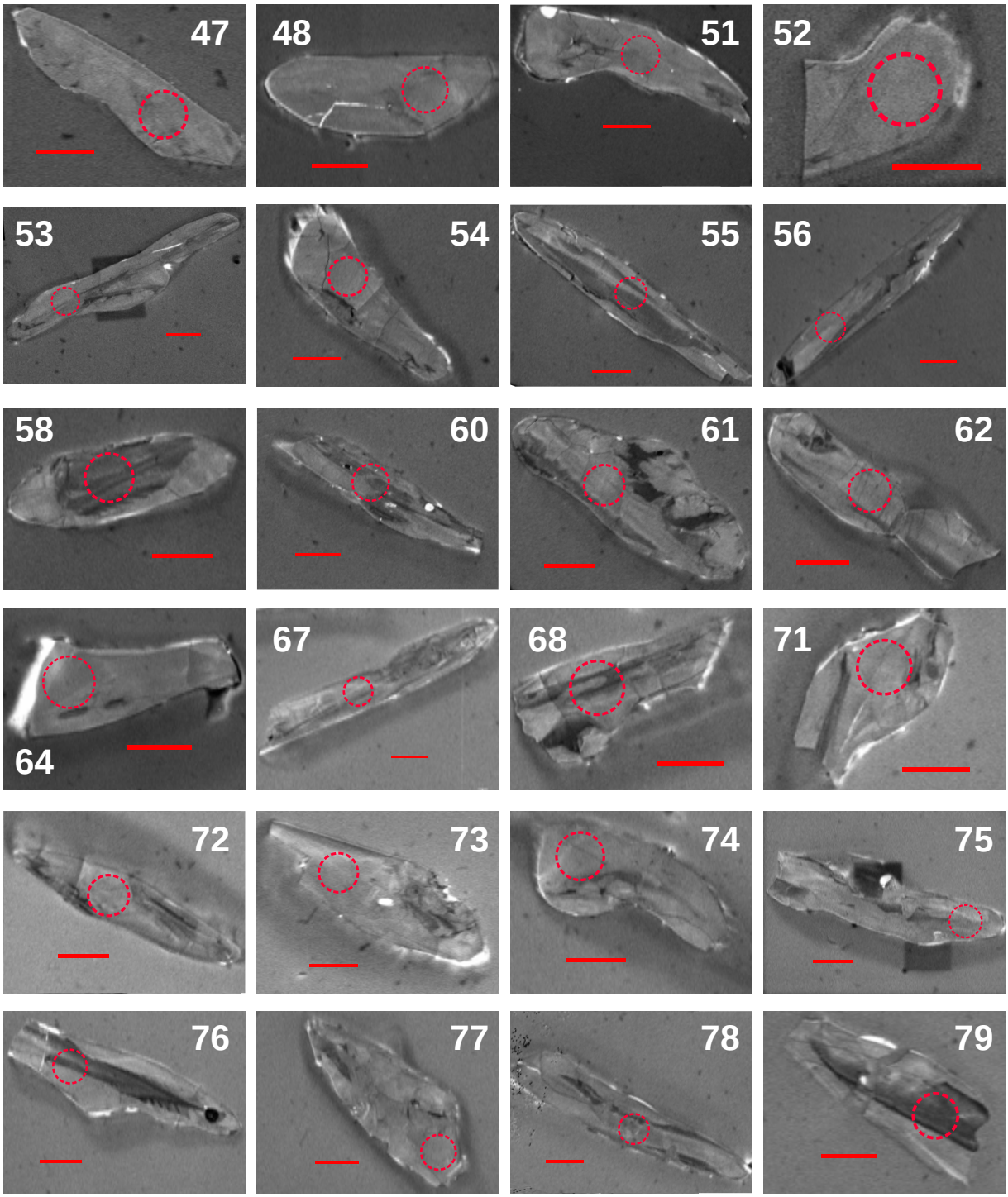
Cathodoluminescence (CL) images for each analysed grain are shown, with the following annotations:

- White numbers correspond to analysis number in datasets of major-element analyses (Appendix E), trace-element analyses (Appendix F), U-Pb analyses (Appendix G), and Hf-isotope analyses (Appendix H).
- Scale bars on all images are 50 μm.
- Circles represent locations of laser ablation spots for U-Pb and trace-element analysis (red) and Hf-isotope analysis (yellow).

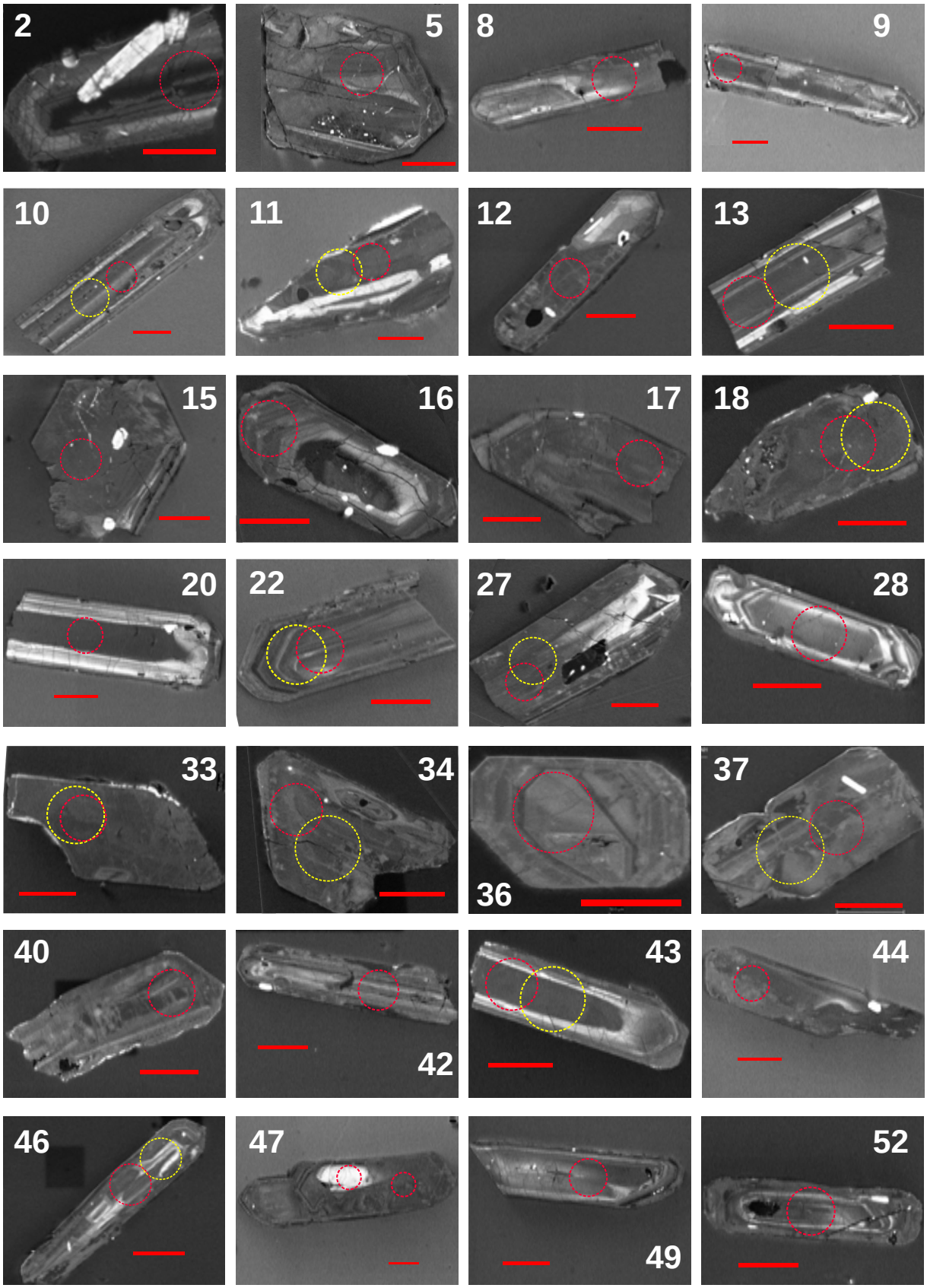
Samples are ordered from mafic to felsic.



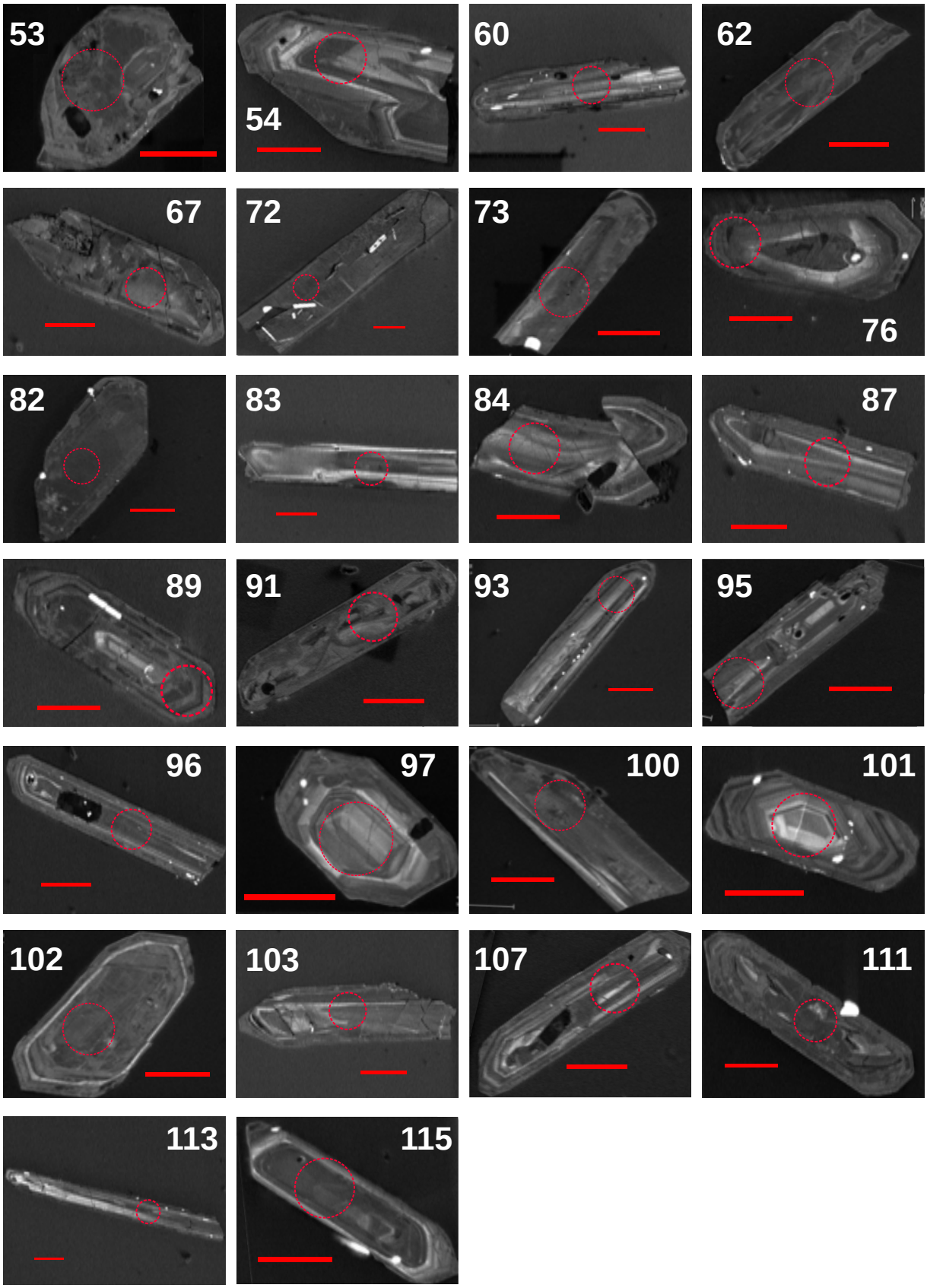
CL images from sample RSA03, showing location of spots used for U-Pb + TE analysis (red circles) and Hf isotope analysis (yellow circles). Scale bars are 50 µm. White number corresponds to the analysis number in the zircon EMP, U-Pb, TE and Hf datasets.



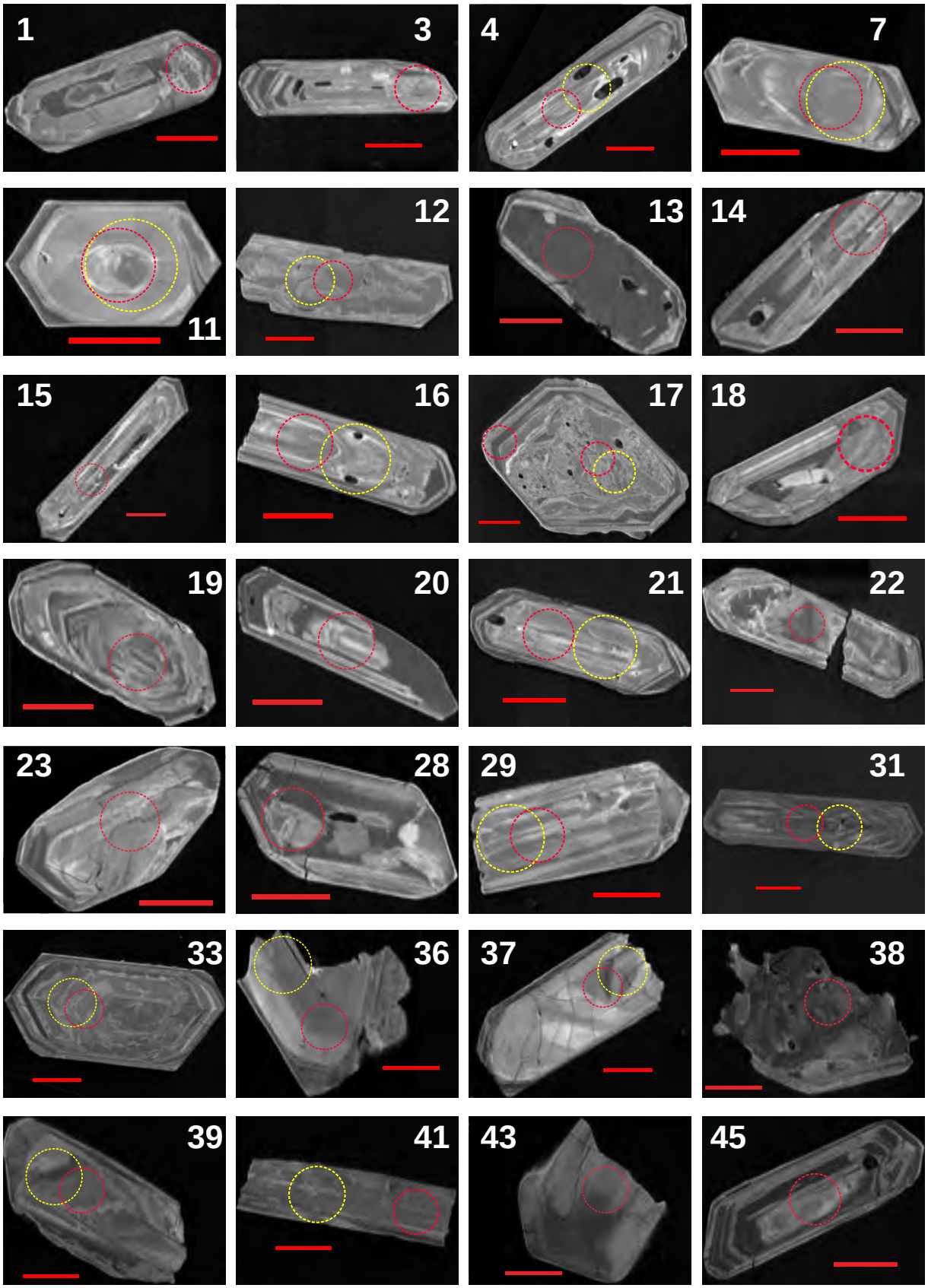
CL images from sample RSA03 (continued), showing location of spots used for U-Pb + TE analysis (red circles) and Hf isotope analysis (yellow circles). Scale bars are 50 µm. White number corresponds to the analysis number in the zircon EMP, U-Pb, TE and Hf datasets.



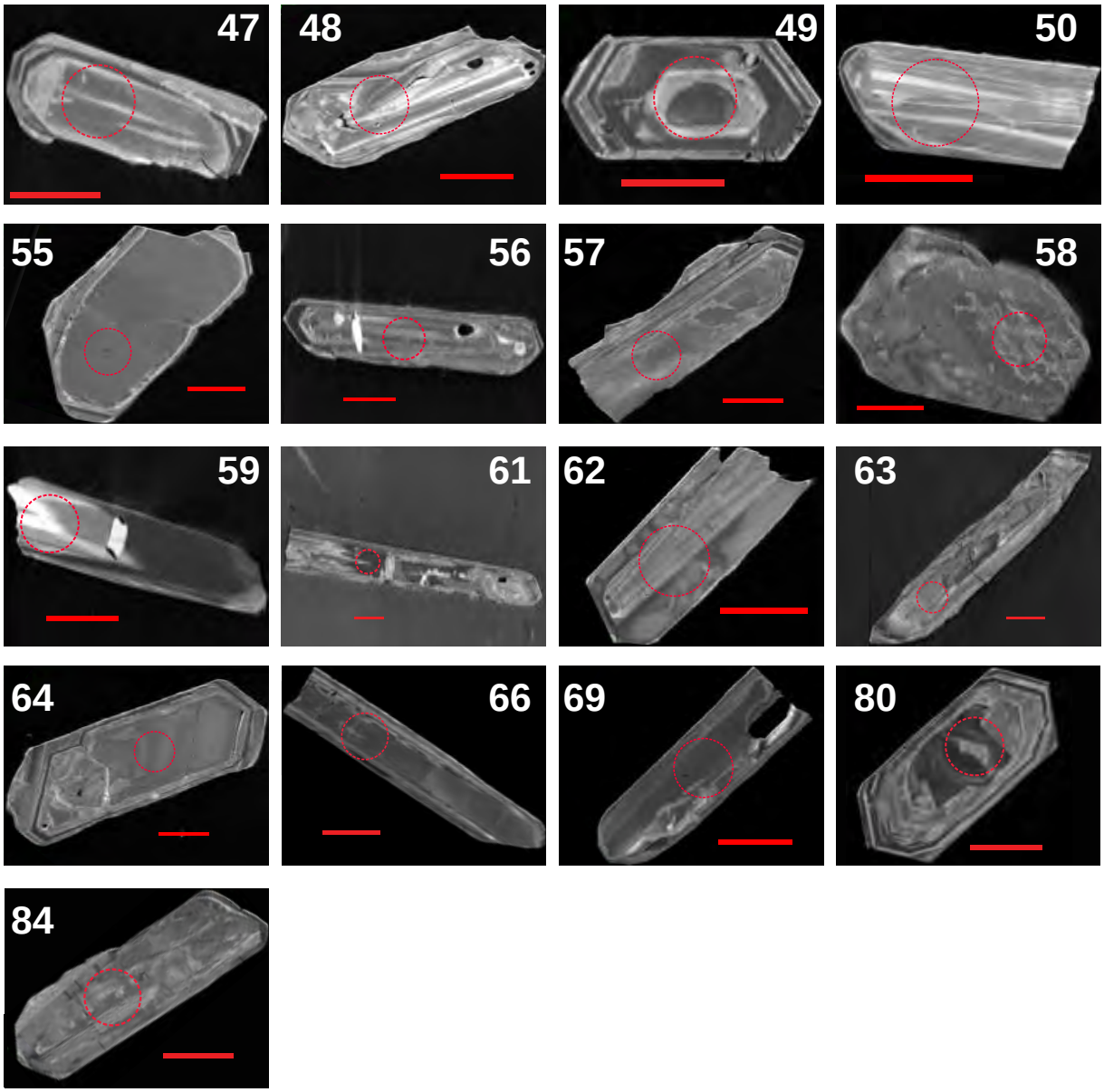
CL images from sample RSA01, showing location of spots used for U-Pb + TE analysis (red circles) and Hf isotope analysis (yellow circles). Scale bars are 50 µm. White number corresponds to the analysis number in the zircon EMP, U-Pb, TE and Hf datasets.



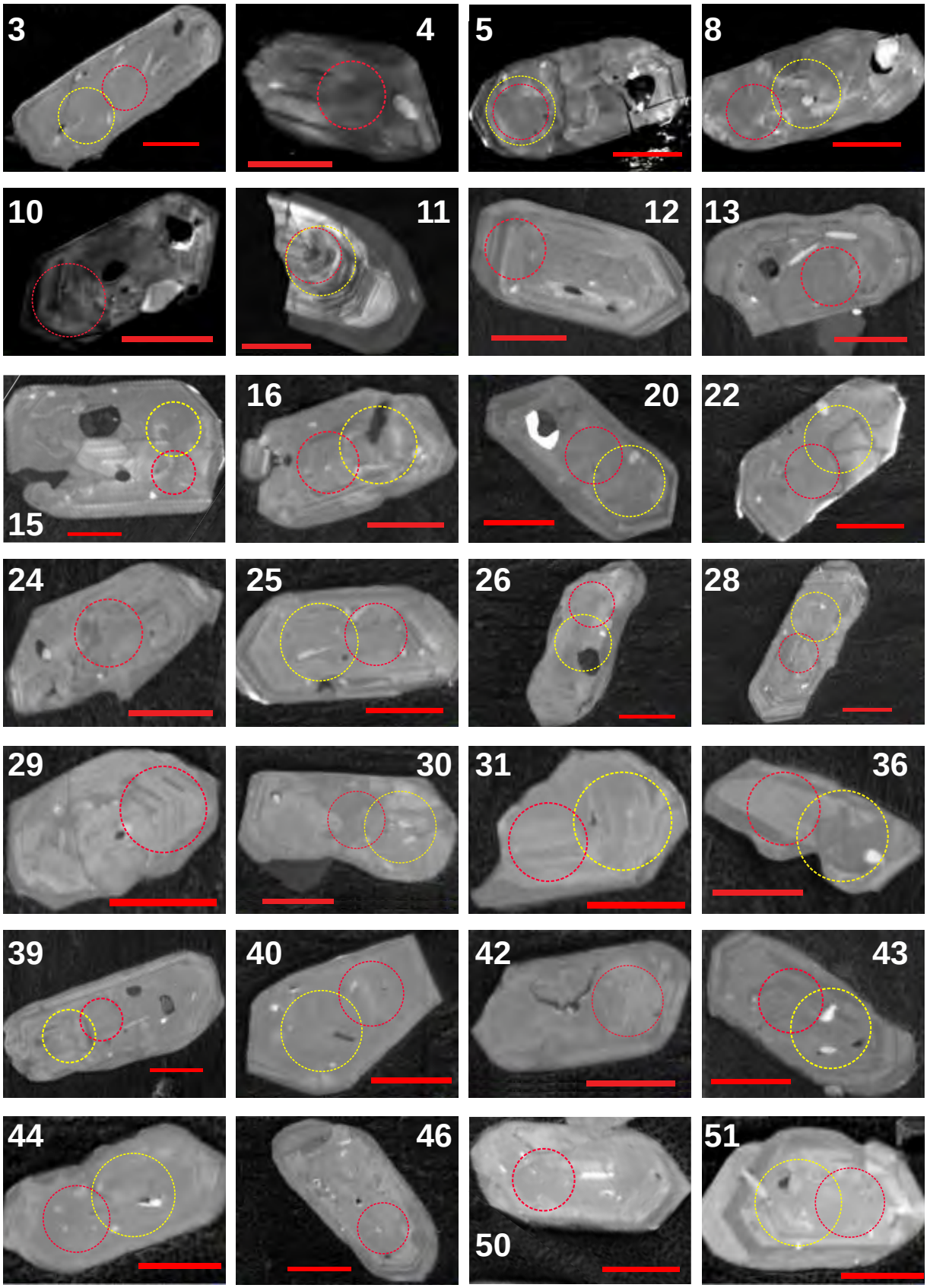
CL images from sample RSA01 (continued), showing location of spots used for U-Pb + TE analysis (red circles) and Hf isotope analysis (yellow circles). Scale bars are 50 µm. White number corresponds to the analysis number in the zircon EMP, U-Pb, TE and Hf datasets.



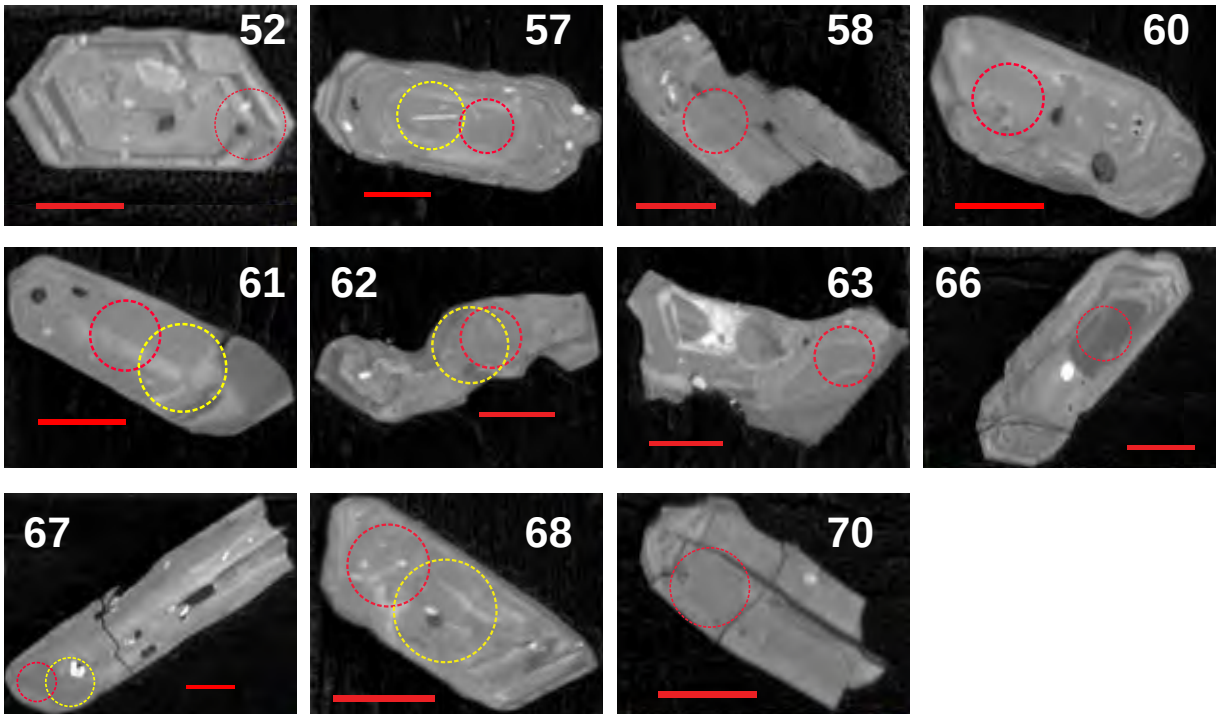
CL images from sample SWA18a, showing location of spots used for U-Pb + TE analysis (red circles) and Hf isotope analysis (yellow circles). Scale bars are 50 µm. White number corresponds to the analysis number in the zircon EMP, U-Pb, TE and Hf datasets.



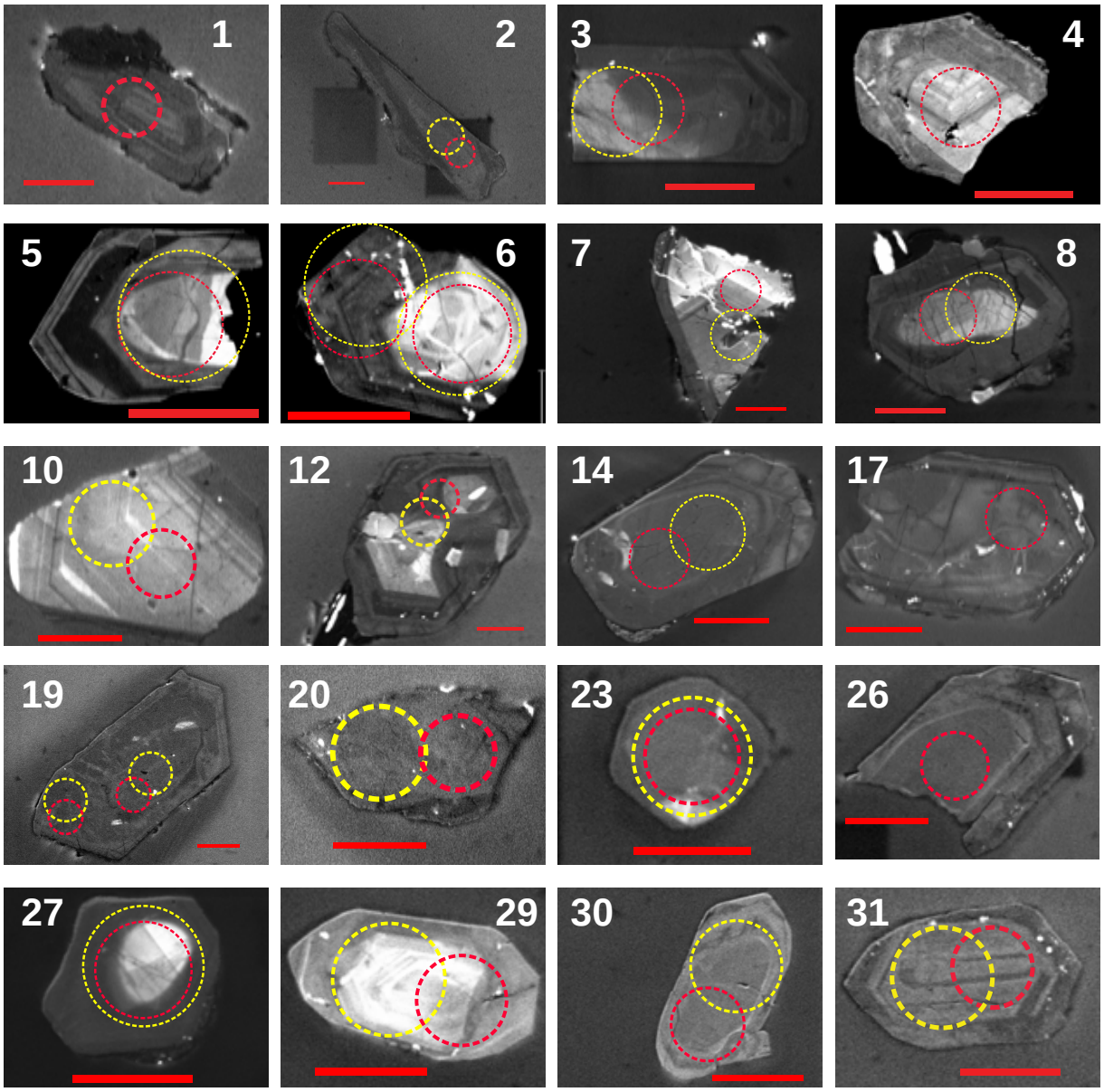
CL images from sample SWA18a (continued), showing location of spots used for U-Pb + TE analysis (red circles) and Hf isotope analysis (yellow circles). Scale bars are 50 µm. White number corresponds to the analysis number in the zircon EMP, U-Pb, TE and Hf datasets.



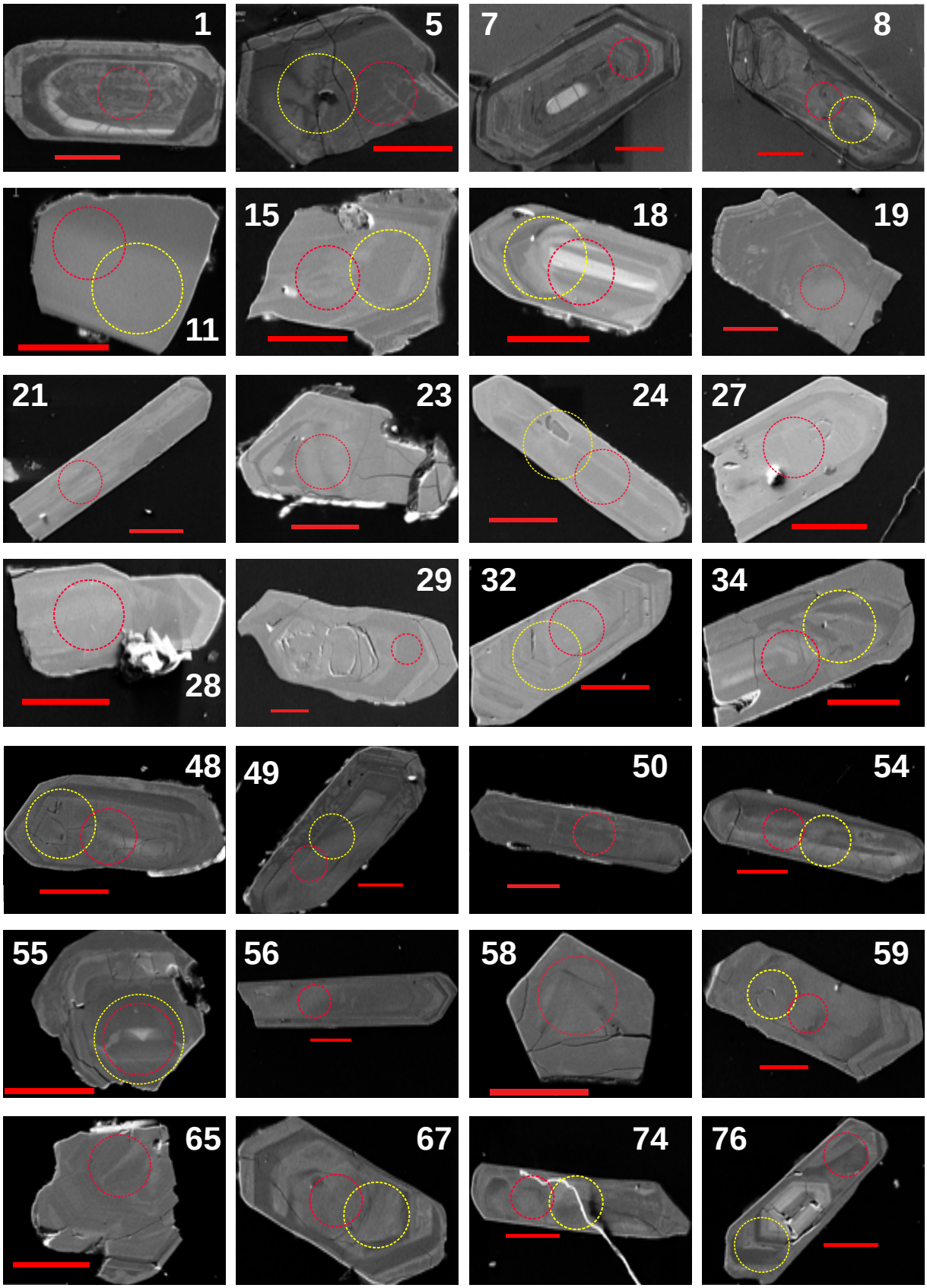
CL images from sample RSA05, showing location of spots used for U-Pb + TE analysis (red circles) and Hf isotope analysis (yellow circles). Scale bars are 50 µm. White number corresponds to the analysis number in the zircon EMP, U-Pb, TE and Hf datasets.



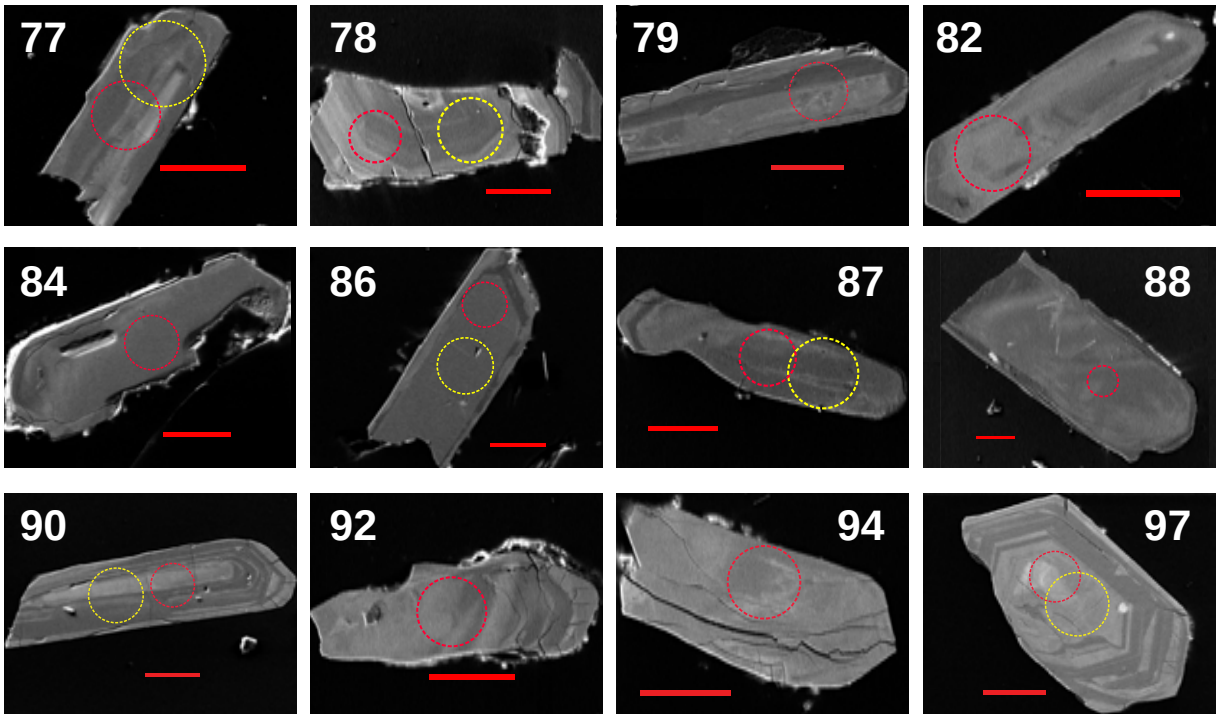
CL images from sample RSA05 (continued), showing location of spots used for U-Pb + TE analysis (red circles) and Hf isotope analysis (yellow circles). Scale bars are 50 µm. White number corresponds to the analysis number in the zircon EMP, U-Pb, TE and Hf datasets.



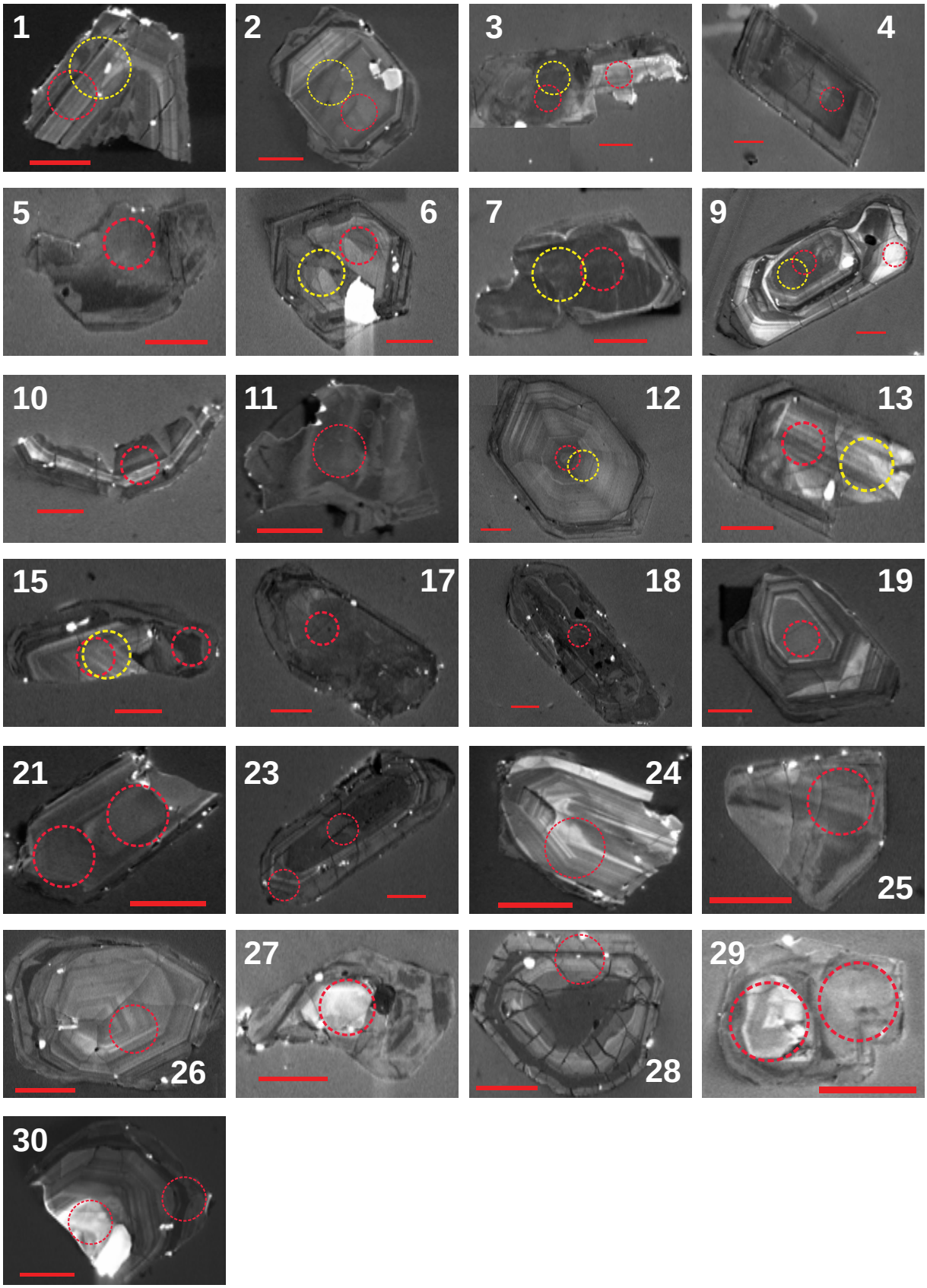
CL images from sample RSA02, showing location of spots used for U-Pb + TE analysis (red circles) and Hf isotope analysis (yellow circles). Scale bars are 50 µm. White number corresponds to the analysis number in the zircon EMP, U-Pb, TE and Hf datasets.



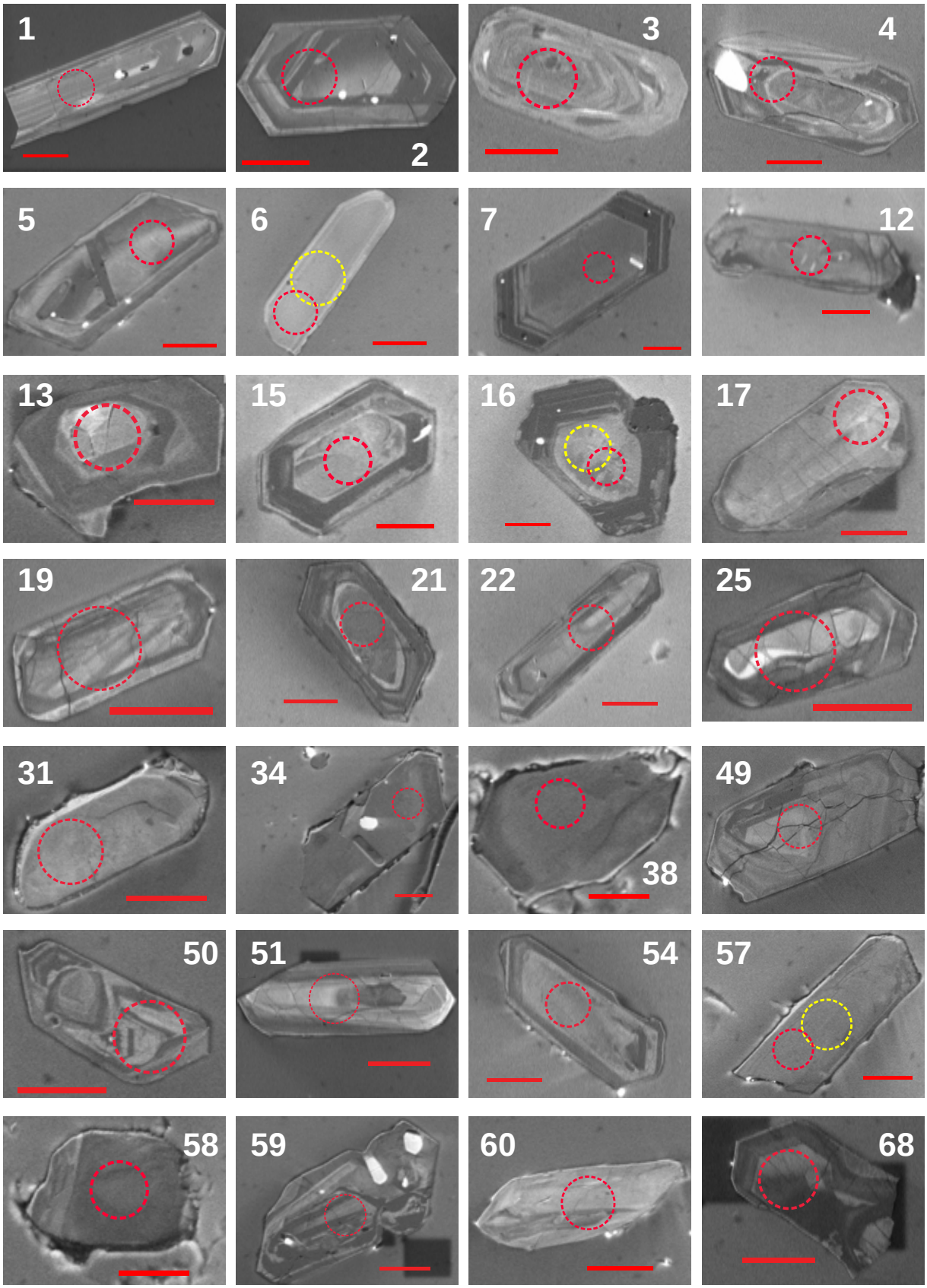
CL images from sample SWA07, showing location of spots used for U-Pb + TE analysis (red circles) and Hf isotope analysis (yellow circles). Scale bars are 50 µm. White number corresponds to the analysis number in the zircon EMP, U-Pb, TE and Hf datasets.



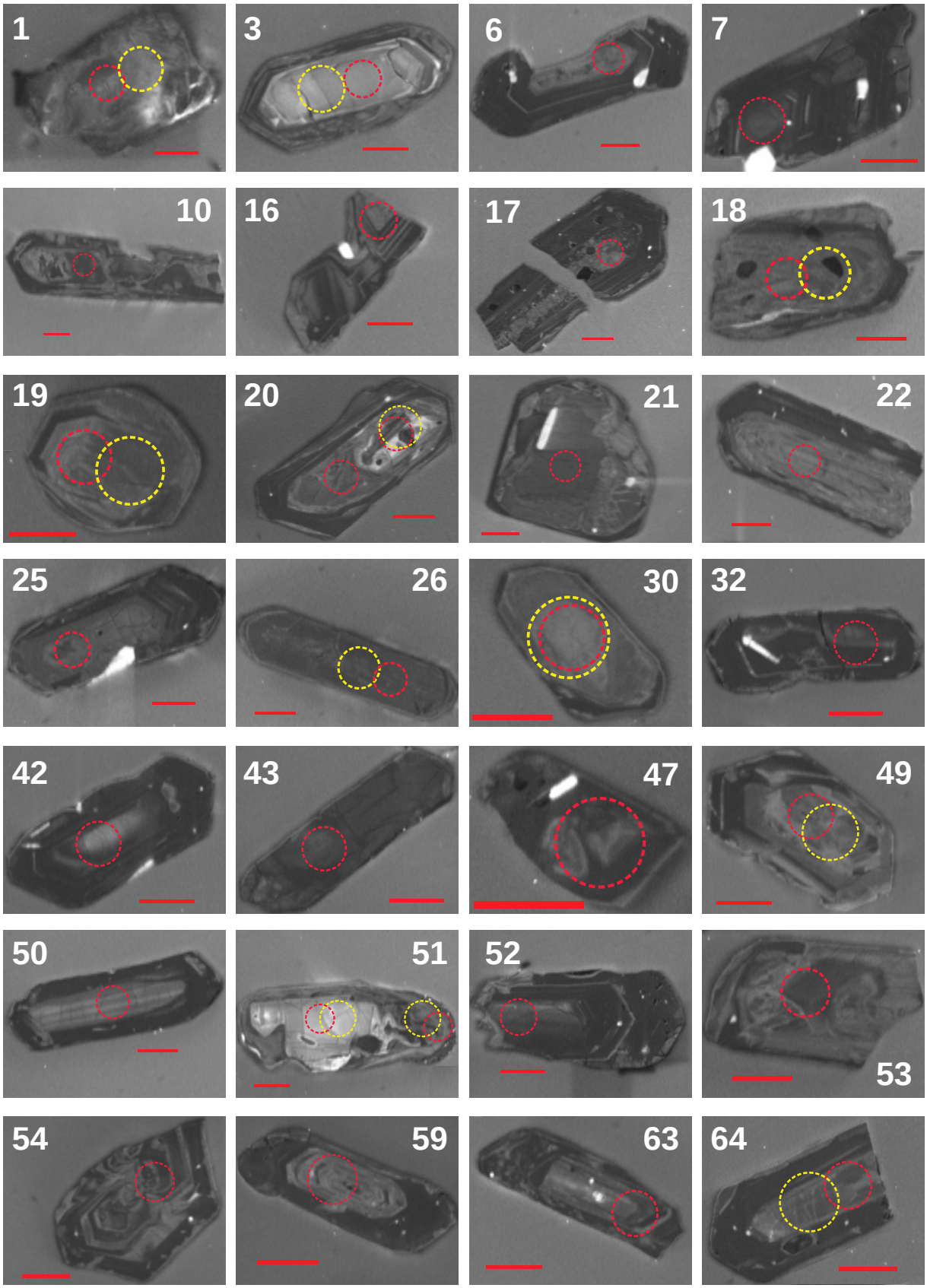
CL images from sample SWA07, (continued) showing location of spots used for U-Pb + TE analysis (red circles) and Hf isotope analysis (yellow circles). Scale bars are 50 µm. White number corresponds to the analysis number in the zircon EMP, U-Pb, TE and Hf datasets.



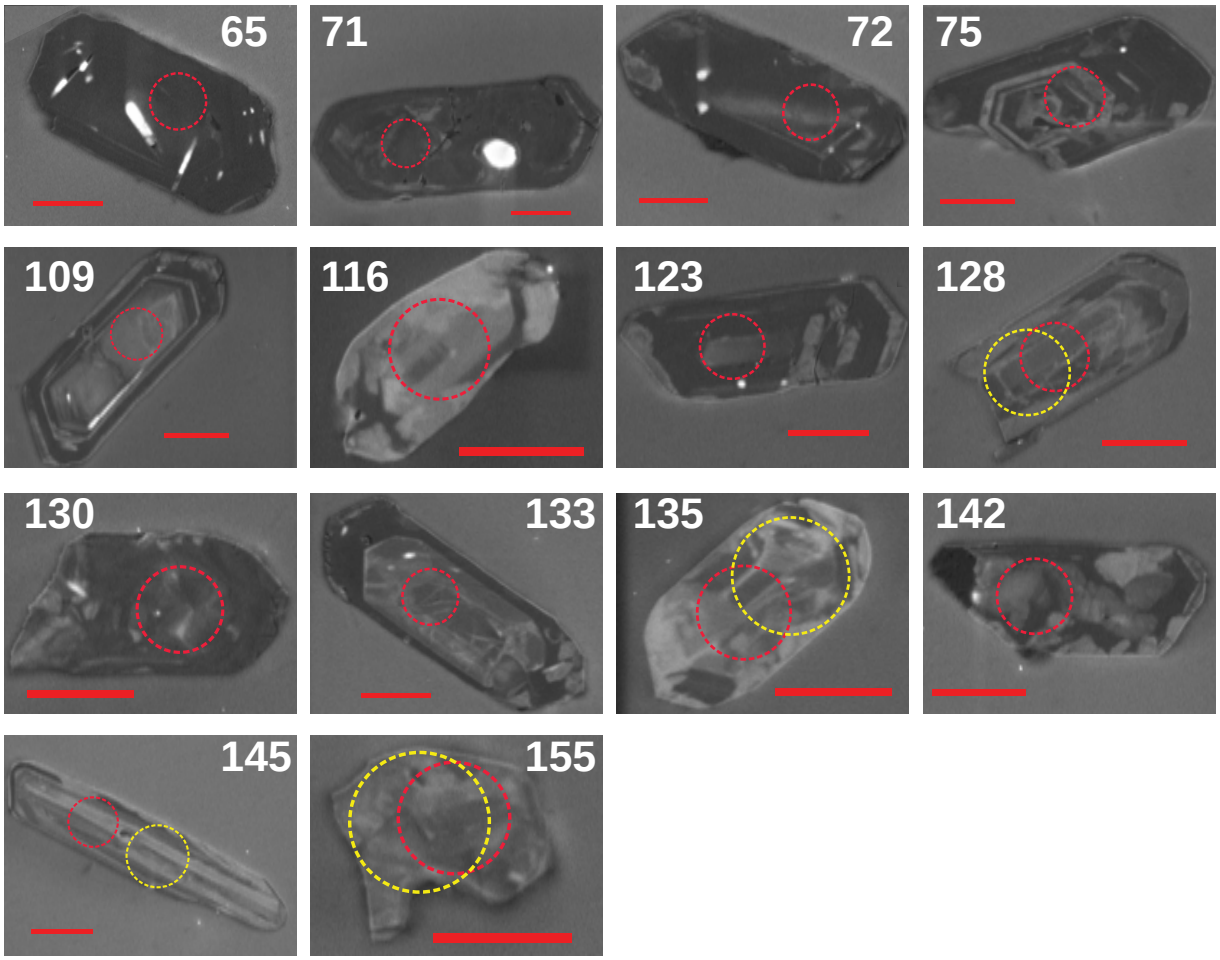
CL images from sample RSA04, showing location of spots used for U-Pb + TE analysis (red circles) and Hf isotope analysis (yellow circles). Scale bars are 50 µm. White number corresponds to the analysis number in the zircon EMP, U-Pb, TE and Hf datasets.



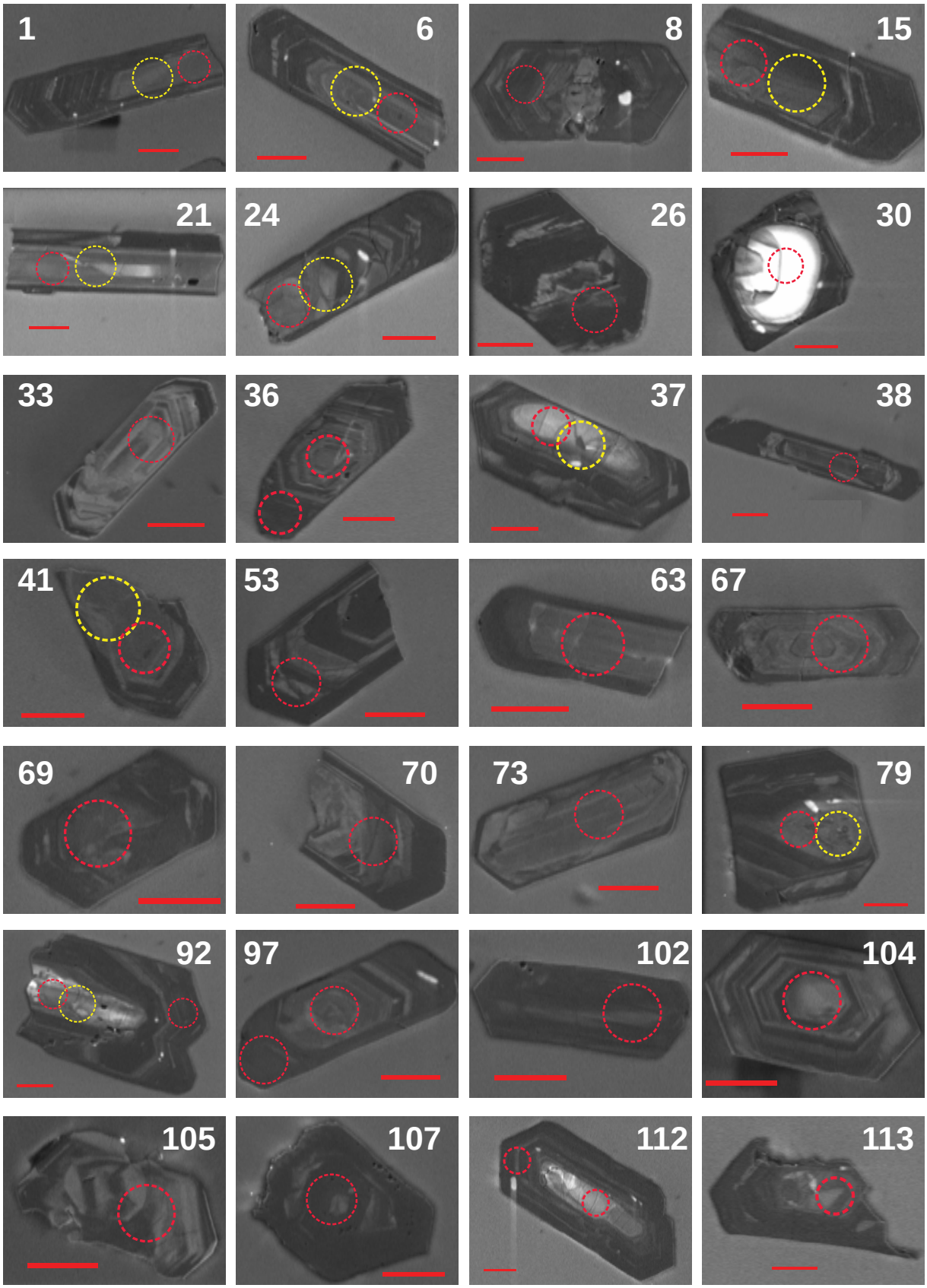
CL images from sample RSA08, showing location of spots used for U-Pb + TE analysis (red circles) and Hf isotope analysis (yellow circles). Scale bars are 50 µm. White number corresponds to the analysis number in the zircon EMP, U-Pb, TE and Hf datasets.



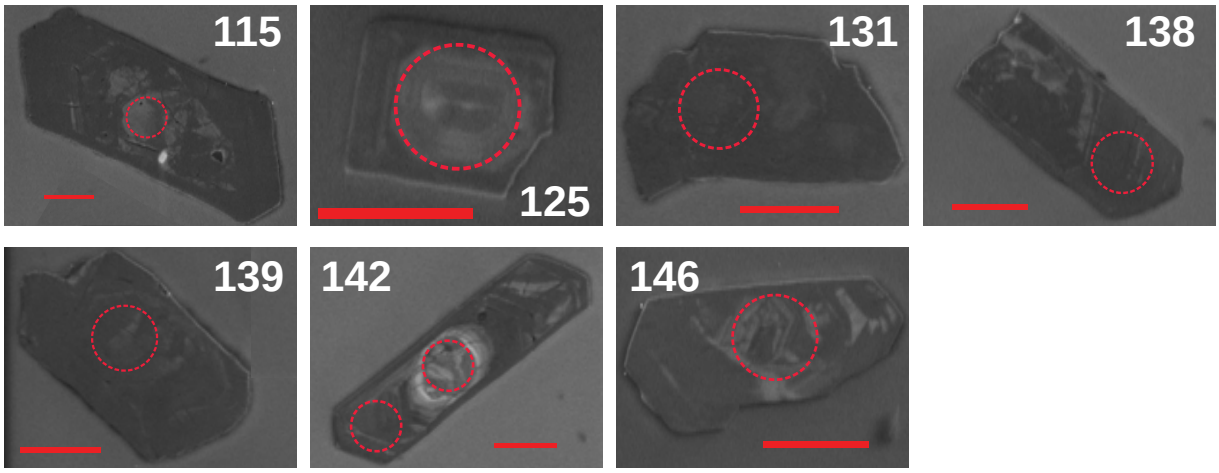
CL images from sample SWA10a, showing location of spots used for U-Pb + TE analysis (red circles) and Hf isotope analysis (yellow circles). Scale bars are 50 µm. White number corresponds to the analysis number in the zircon EMP, U-Pb, TE and Hf datasets.



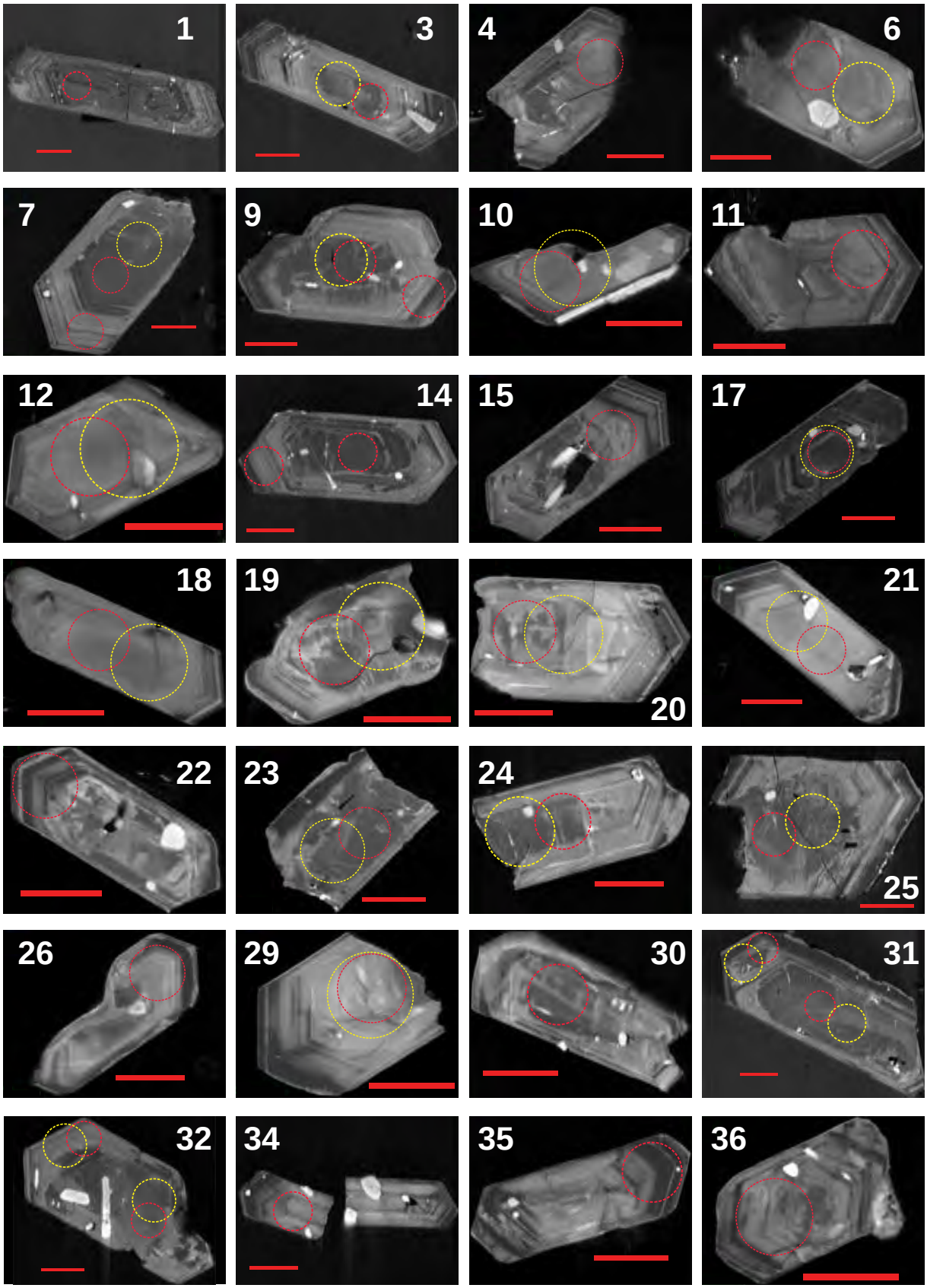
CL images from sample SWA10a (continued), showing location of spots used for U-Pb + TE analysis (red circles) and Hf isotope analysis (yellow circles). Scale bars are 50 µm. White number corresponds to the analysis number in the zircon EMP, U-Pb, TE and Hf datasets.



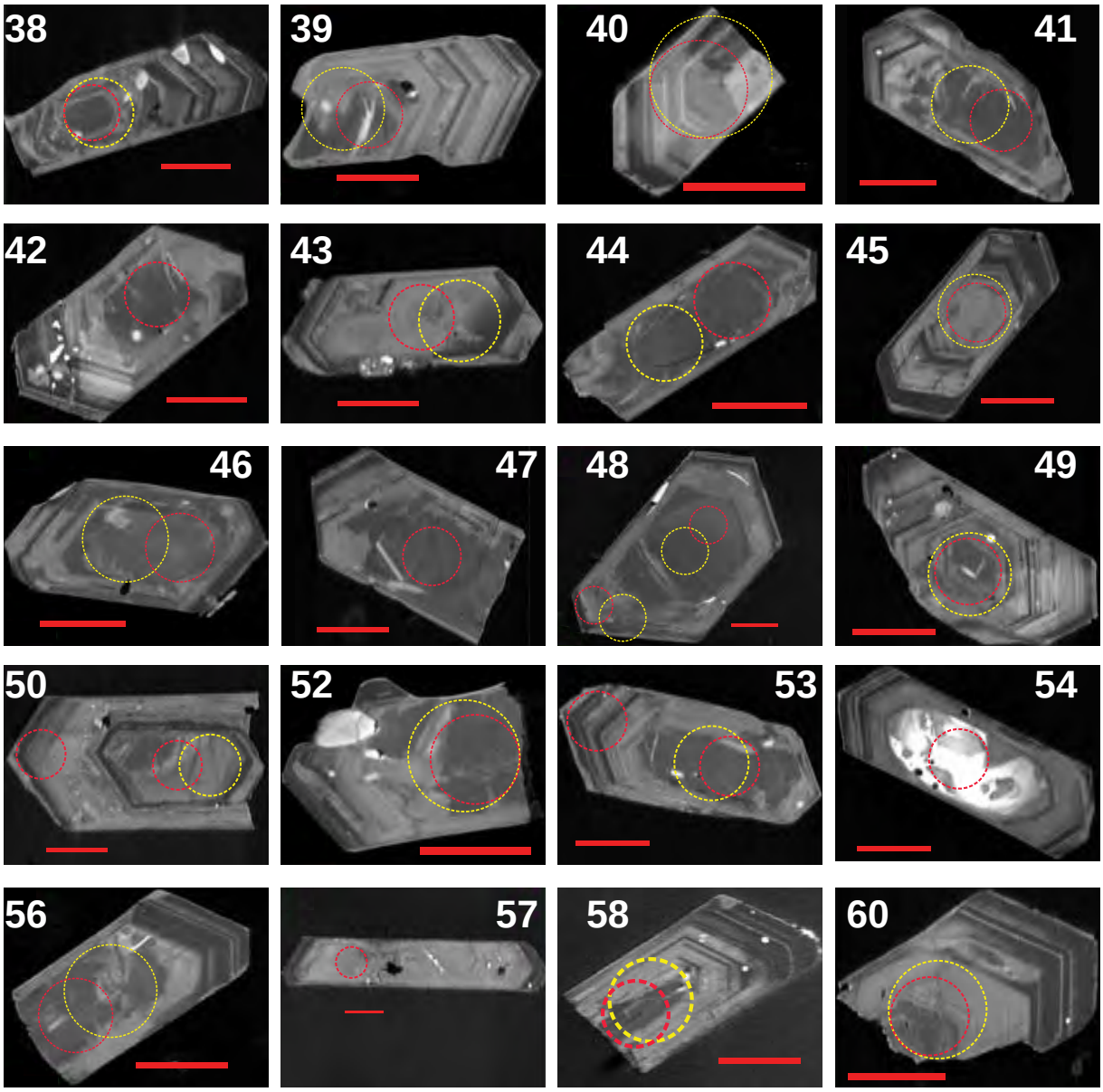
CL images from sample RSA09, showing location of spots used for U-Pb + TE analysis (red circles) and Hf isotope analysis (yellow circles). Scale bars are 50 µm. White number corresponds to the analysis number in the zircon EMP, U-Pb, TE and Hf datasets.



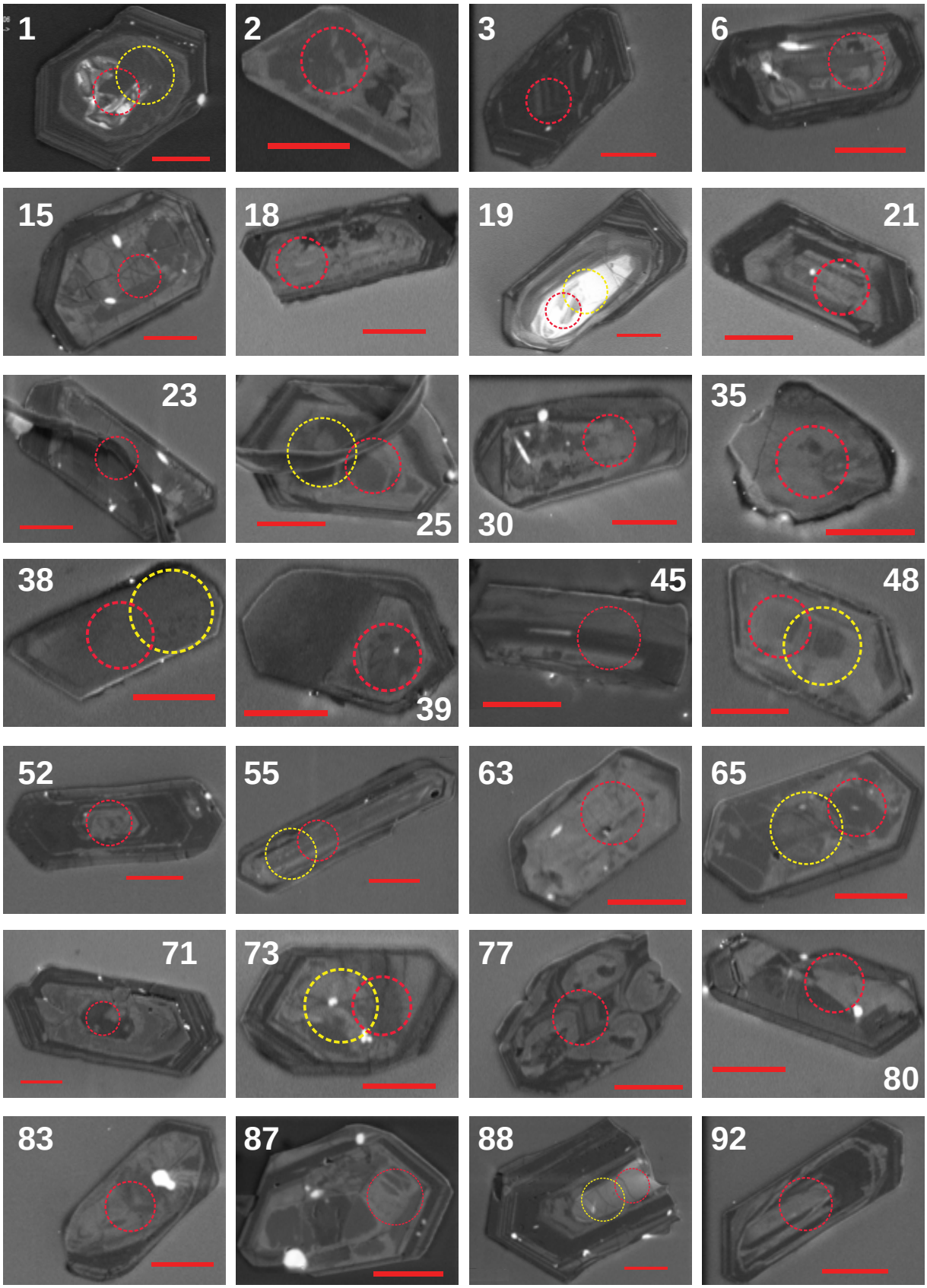
CL images from sample RSA09 (continued), showing location of spots used for U-Pb + TE analysis (red circles) and Hf isotope analysis (yellow circles). Scale bars are 50 µm. White number corresponds to the analysis number in the zircon EMP, U-Pb, TE and Hf datasets.



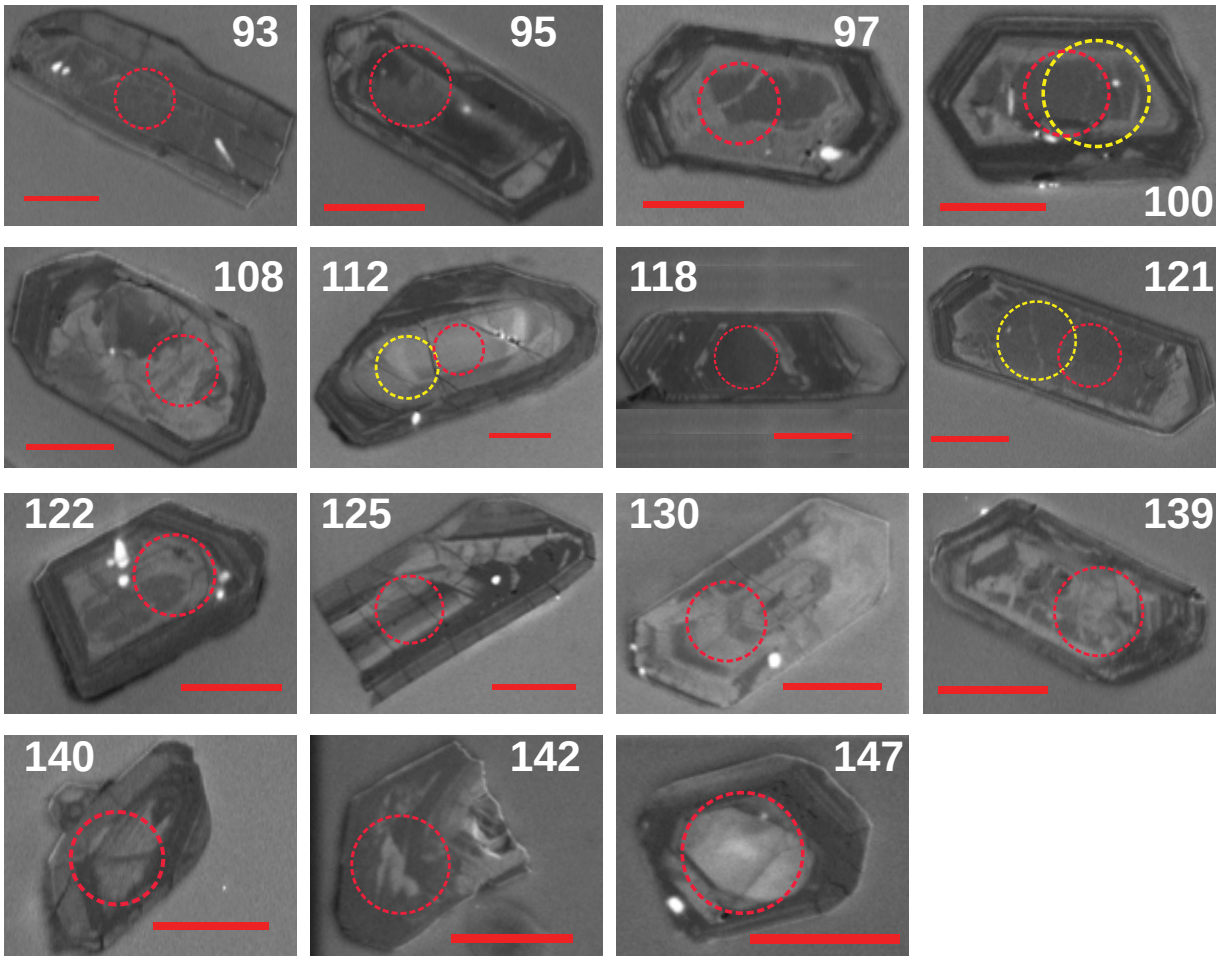
CL images from sample SWA03, showing location of spots used for U-Pb + TE analysis (red circles) and Hf isotope analysis (yellow circles). Scale bars are 50 µm. White number corresponds to the analysis number in the zircon EMP, U-Pb, TE and Hf datasets.



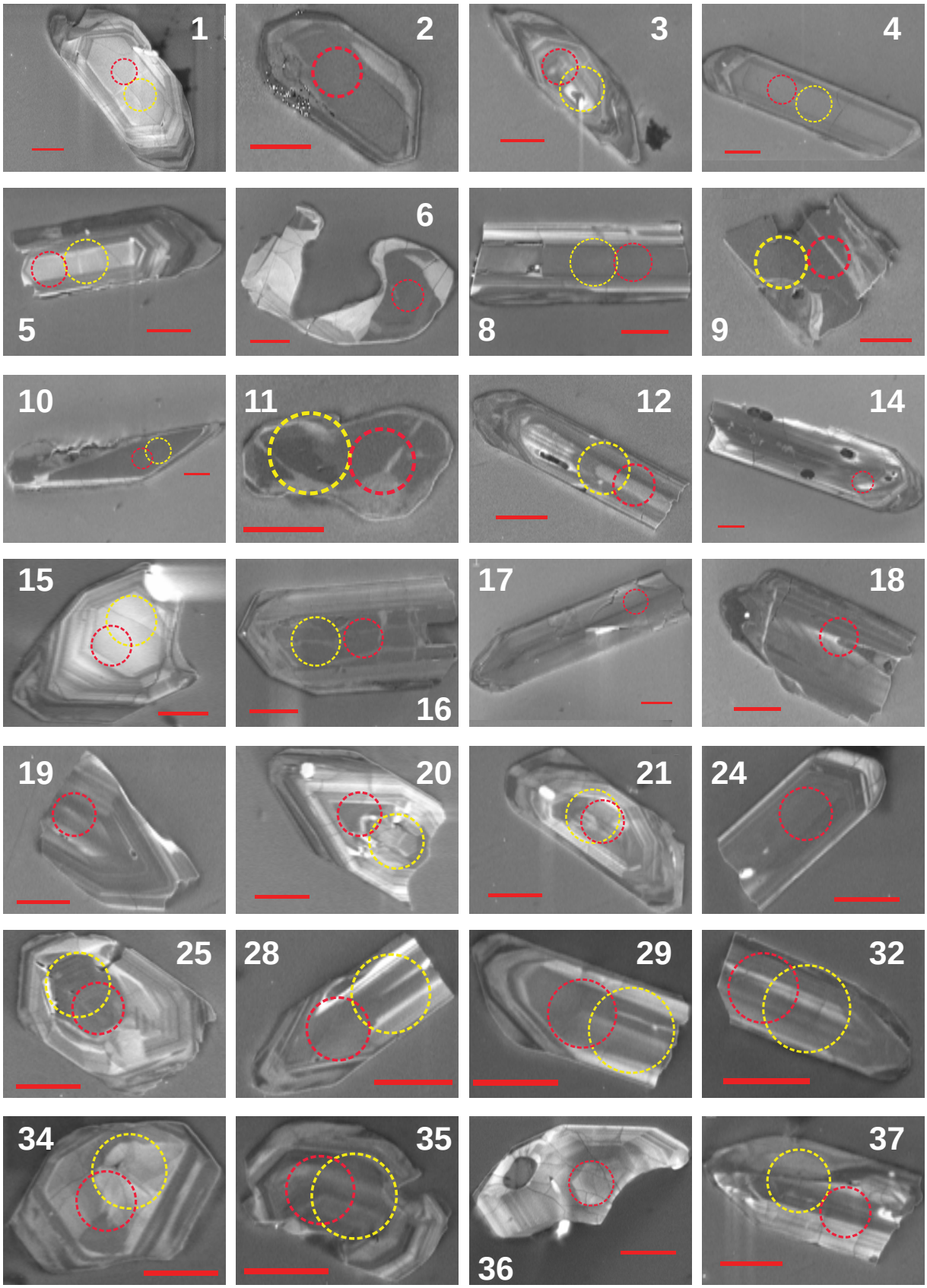
CL images from sample SWA03 (continued), showing location of spots used for U-Pb + TE analysis (red circles) and Hf isotope analysis (yellow circles). Scale bars are 50 µm. White number corresponds to the analysis number in the zircon EMP, U-Pb, TE and Hf datasets.



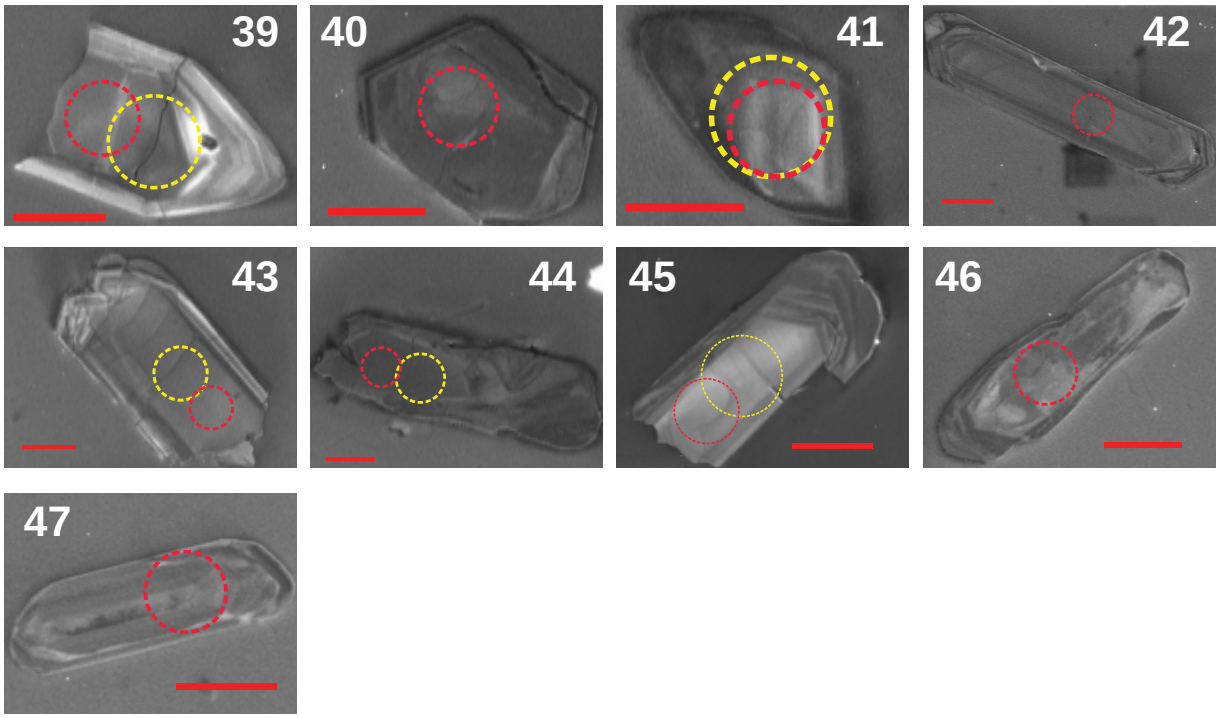
CL images from sample RSA06, showing location of spots used for U-Pb + TE analysis (red circles) and Hf isotope analysis (yellow circles). Scale bars are 50 µm. White number corresponds to the analysis number in the zircon EMP, U-Pb, TE and Hf datasets.



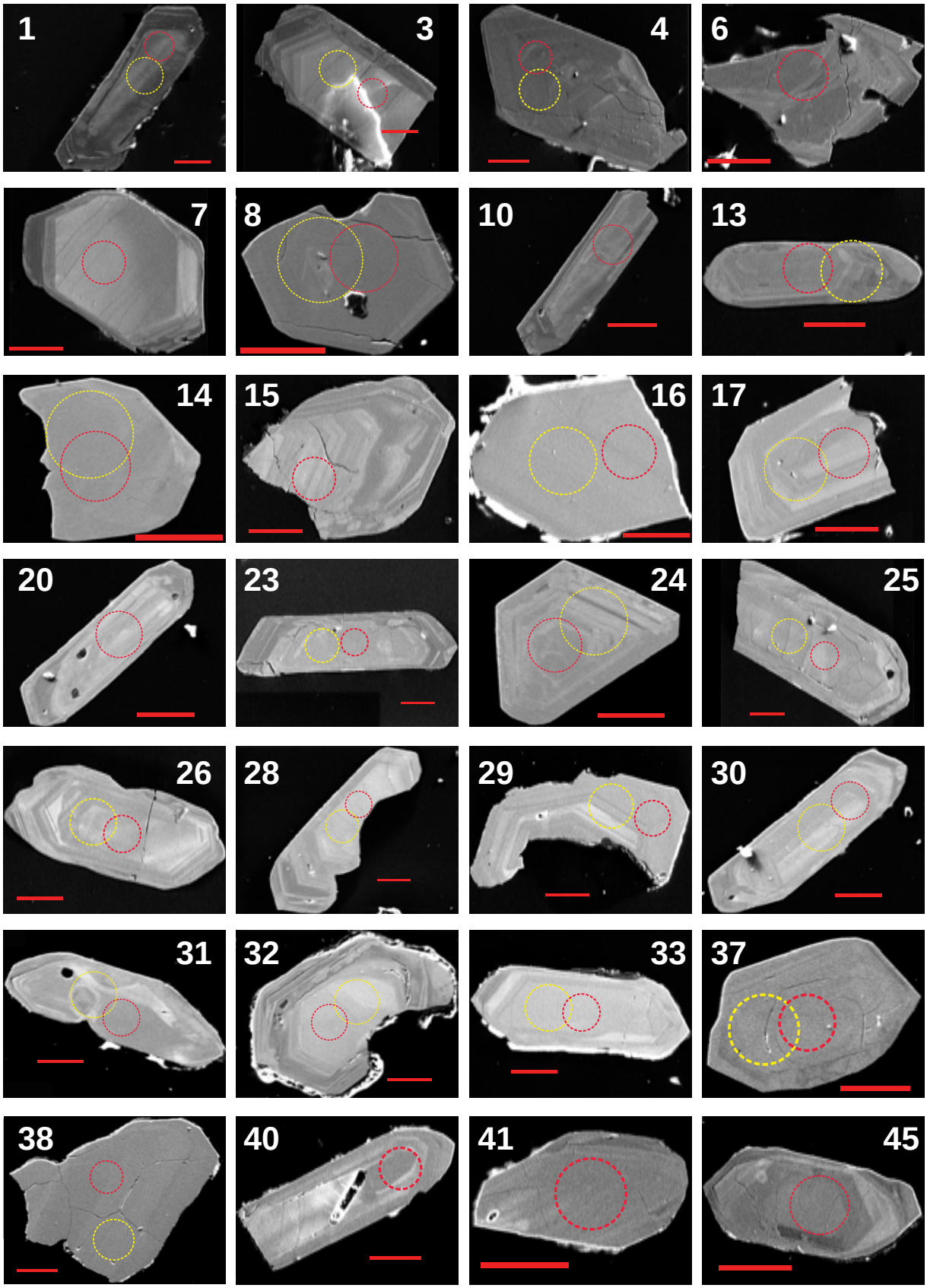
CL images from sample RSA06 (continued), showing location of spots used for U-Pb + TE analysis (red circles) and Hf isotope analysis (yellow circles). Scale bars are 50 µm. White number corresponds to the analysis number in the zircon EMP, U-Pb, TE and Hf datasets.



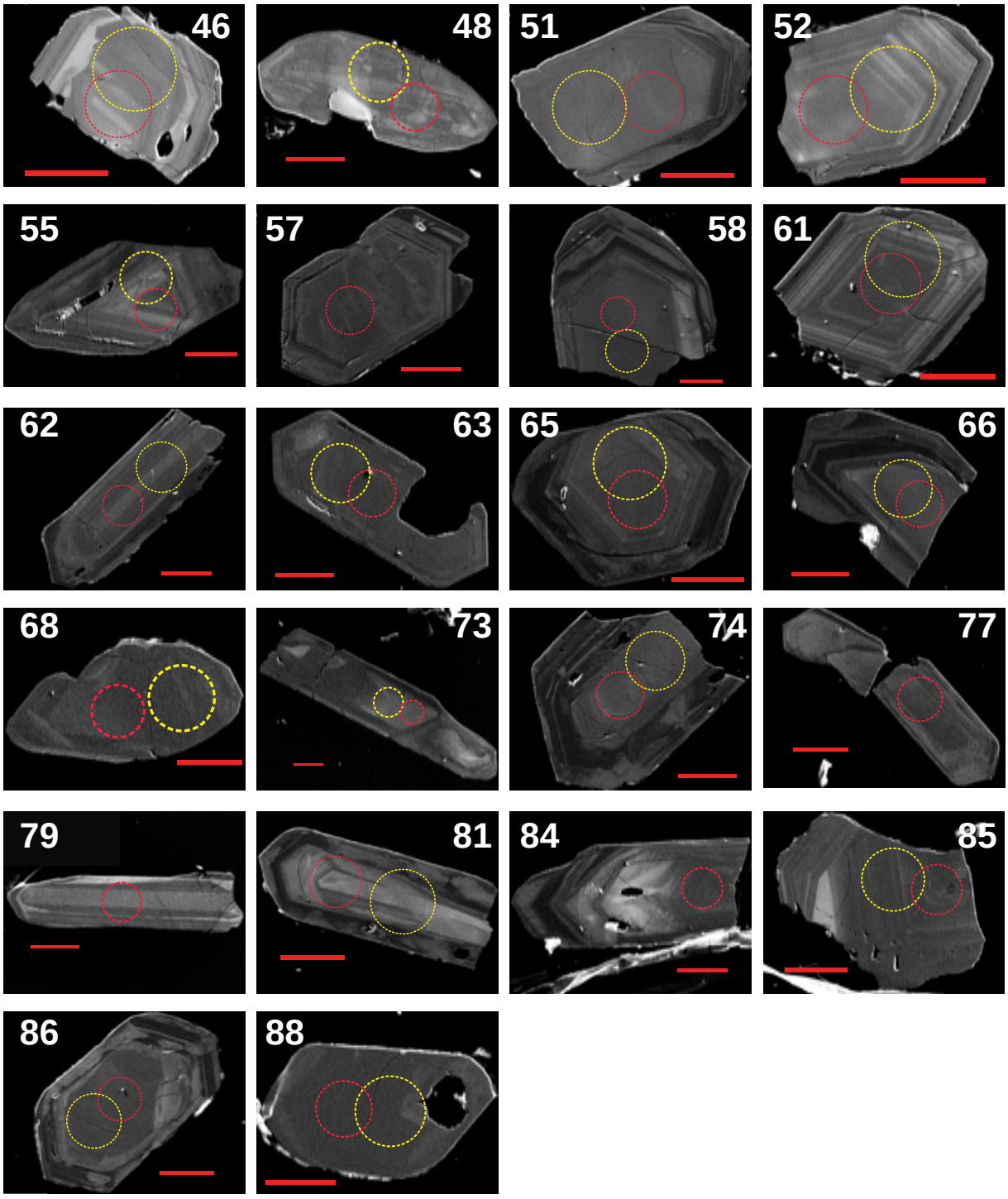
CL images from sample SWA13a, showing location of spots used for U-Pb + TE analysis (red circles) and Hf isotope analysis (yellow circles). Scale bars are 50 µm. White number corresponds to the analysis number in the zircon EMP, U-Pb, TE and Hf datasets.



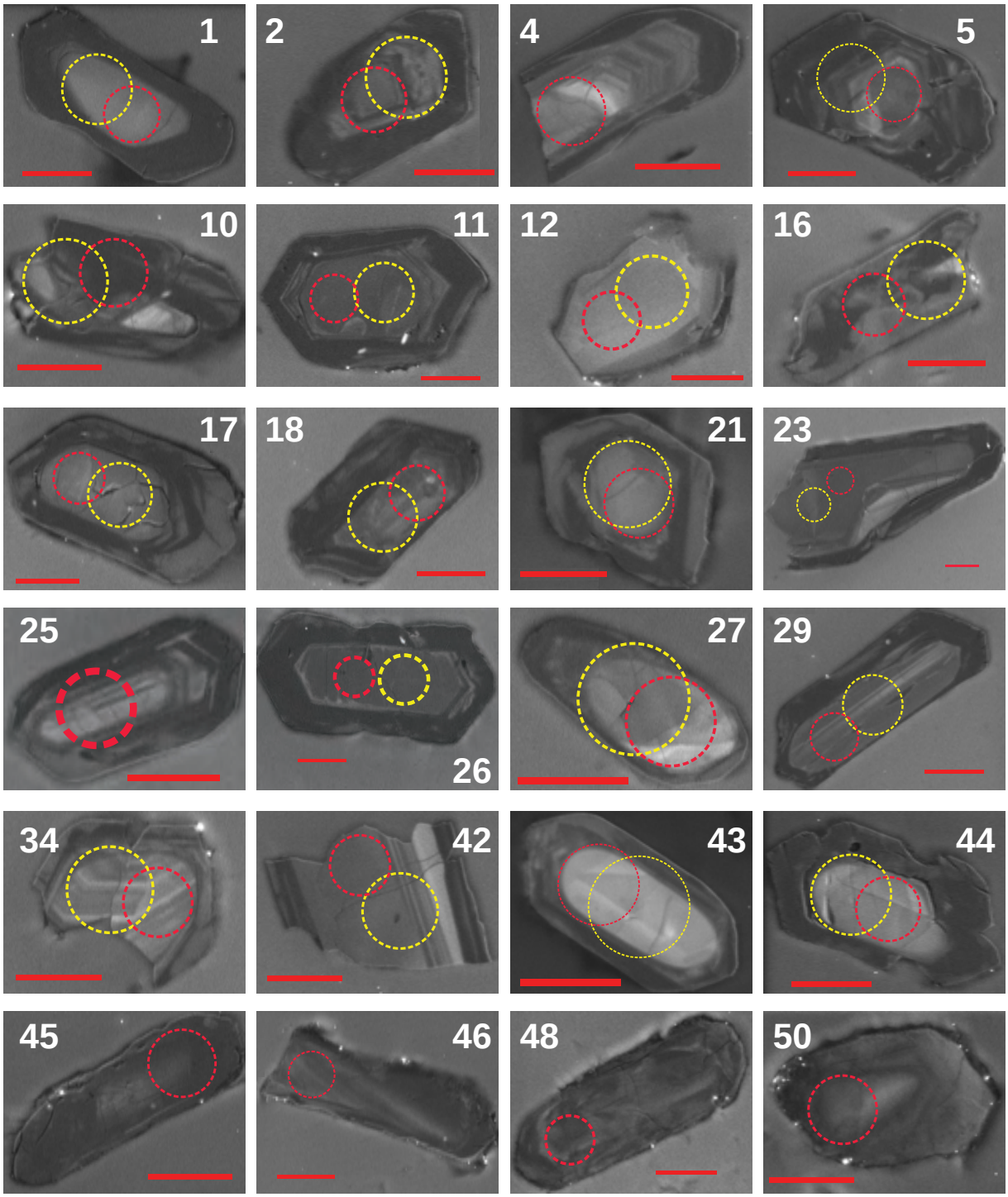
CL images from sample SWA13a (continued), showing location of spots used for U-Pb + TE analysis (red circles) and Hf isotope analysis (yellow circles). Scale bars are 50 µm. White number corresponds to the analysis number in the zircon EMP, U-Pb, TE and Hf datasets.



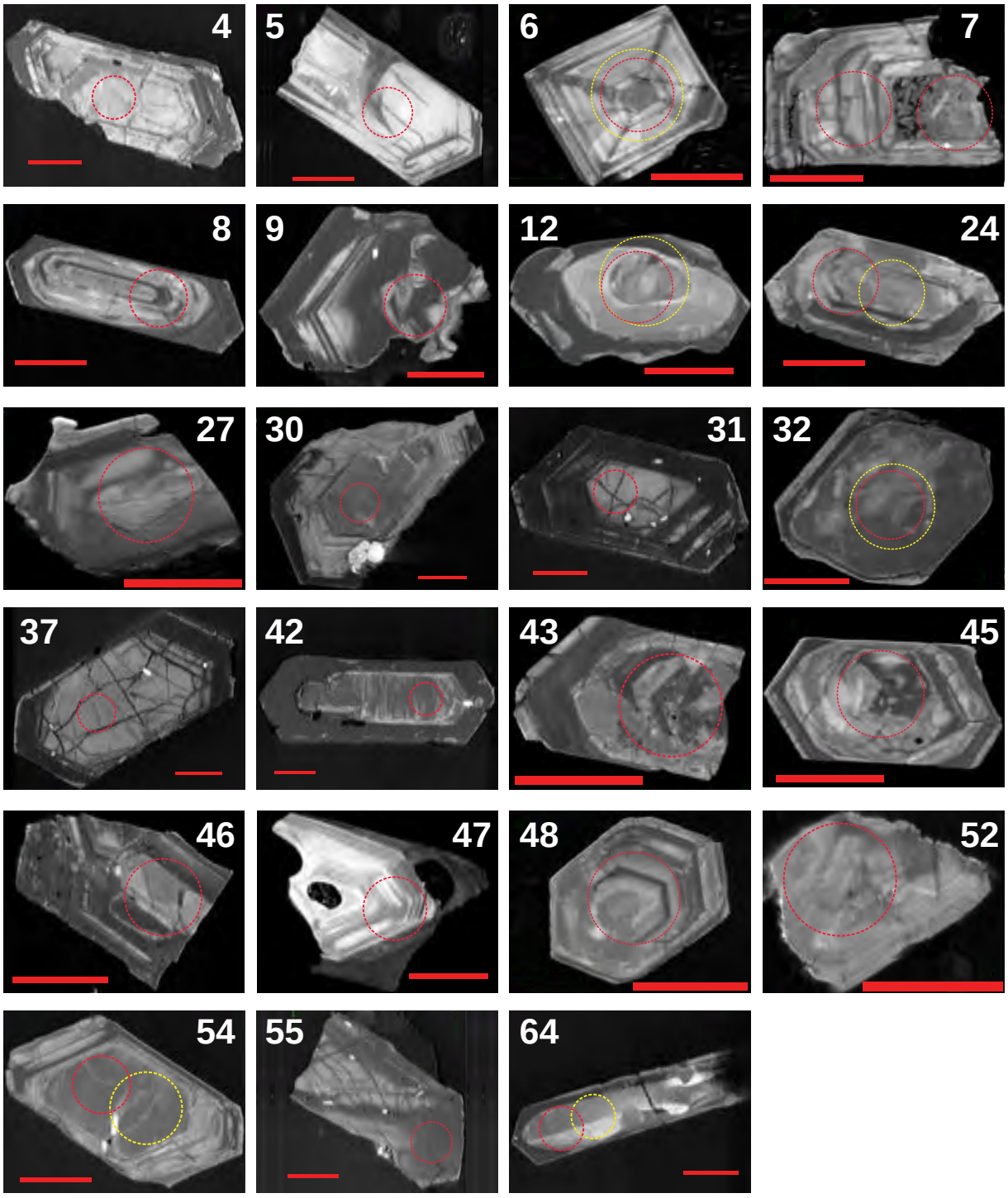
CL images from sample SWA11, showing location of spots used for U-Pb + TE analysis (red circles) and Hf isotope analysis (yellow circles). Scale bars are 50 µm. White number corresponds to the analysis number in the zircon EMP, U-Pb, TE and Hf datasets.



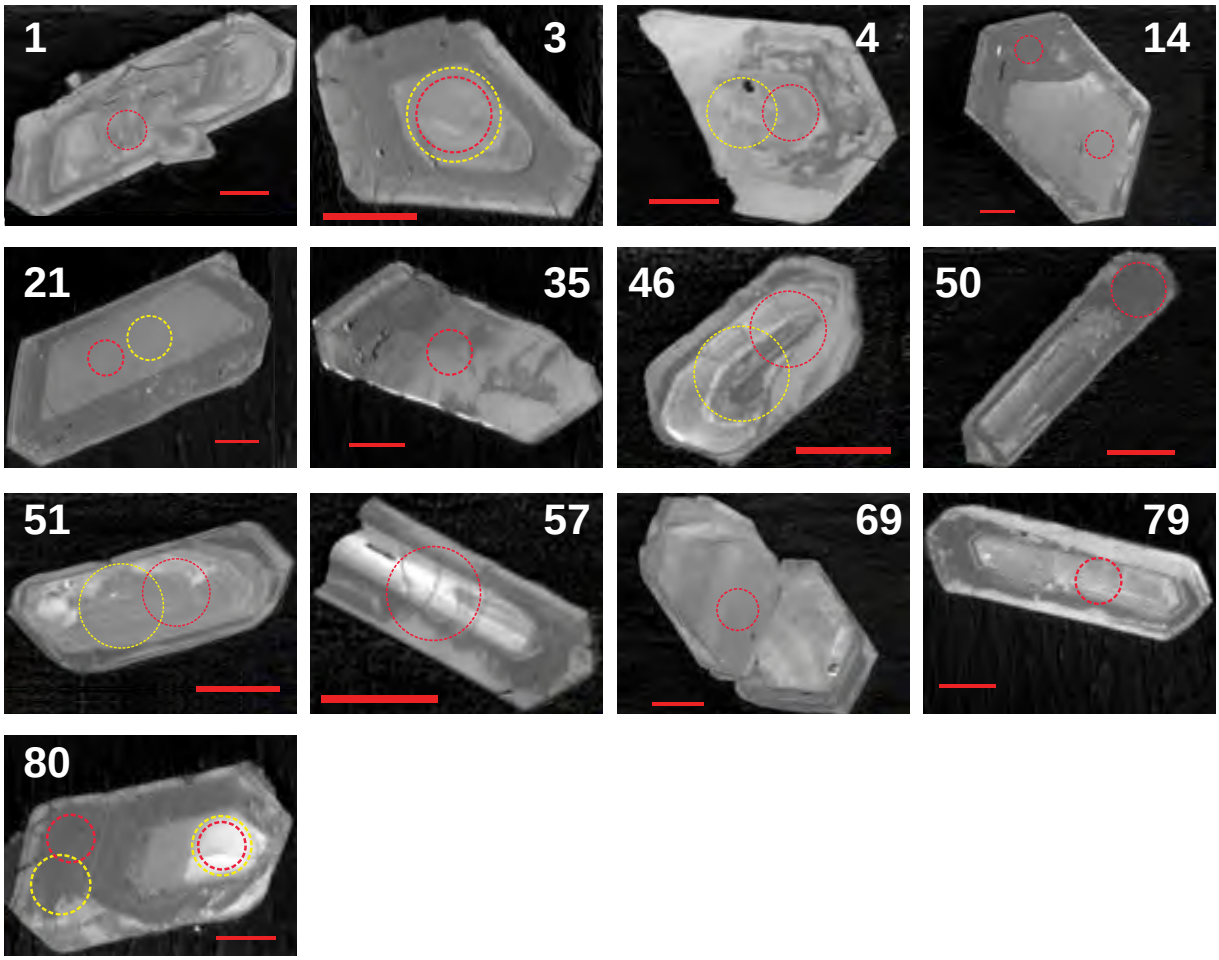
CL images from sample SWA11 (continued), showing location of spots used for U-Pb + TE analysis (red circles) and Hf isotope analysis (yellow circles). Scale bars are 50 µm. White number corresponds to the analysis number in the zircon EMP, U-Pb, TE and Hf datasets.



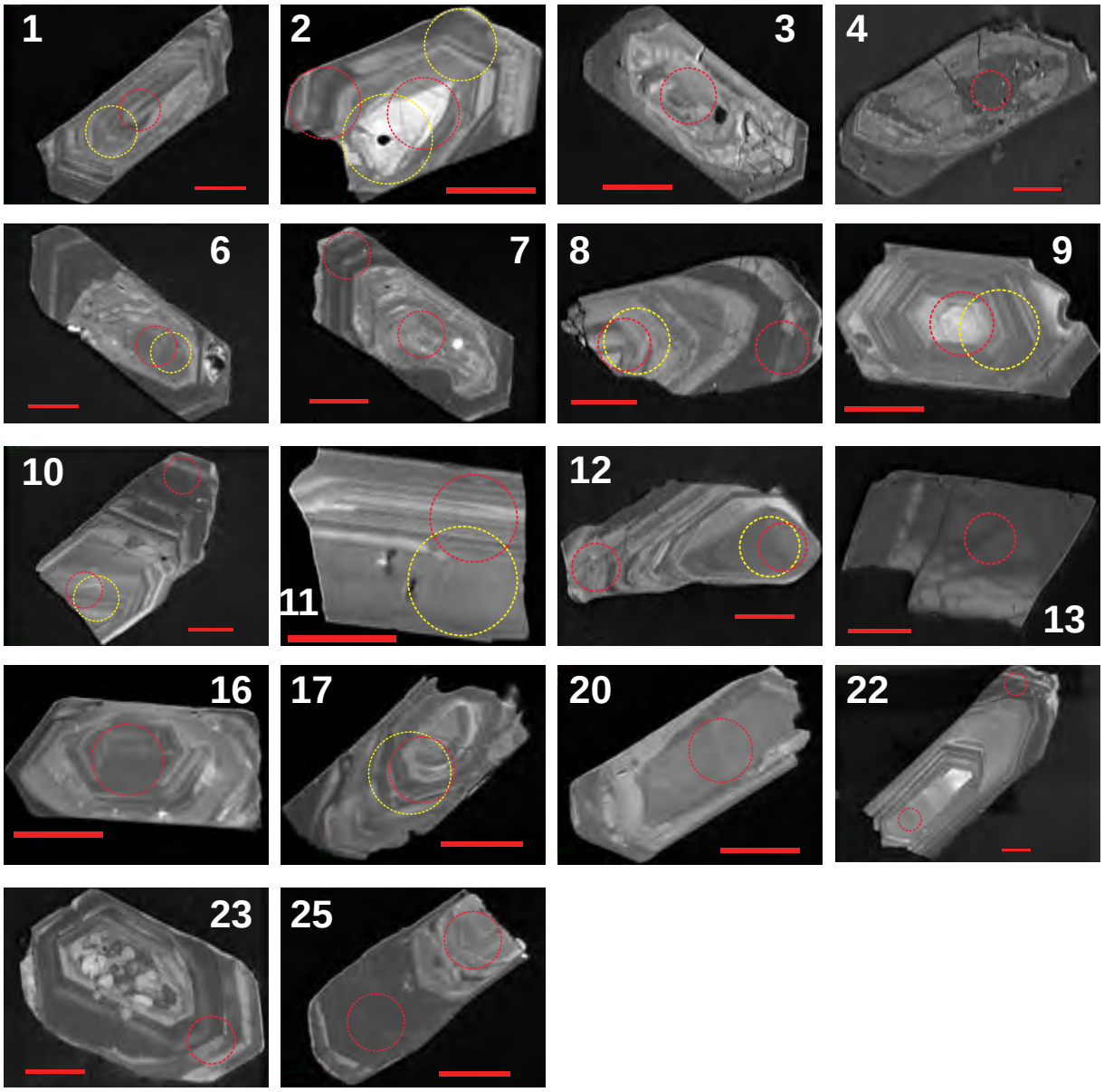
CL images from sample SWA09, showing location of spots used for U-Pb + TE analysis (red circles) and Hf isotope analysis (yellow circles). Scale bars are 50 µm. White number corresponds to the analysis number in the zircon EMP, U-Pb, TE and Hf datasets.



CL images from sample SWA02a, showing location of spots used for U-Pb + TE analysis (red circles) and Hf isotope analysis (yellow circles). Scale bars are 50 µm. White number corresponds to the analysis number in the zircon EMP, U-Pb, TE and Hf datasets.



CL images from sample RSA07, showing location of spots used for U-Pb + TE analysis (red circles) and Hf isotope analysis (yellow circles). Scale bars are 50 µm. White number corresponds to the analysis number in the zircon EMP, U-Pb, TE and Hf datasets.



CL images from sample SWA05, showing location of spots used for U-Pb + TE analysis (red circles) and Hf isotope analysis (yellow circles). Scale bars are 50 µm. White number corresponds to the analysis number in the zircon EMP, U-Pb, TE and Hf datasets.

Appendix E – Zircon Major-Element Analyses

Major-element compositions analysed by electron microprobe are shown for each analysed grain.

Samples are ordered from mafic to felsic.

	HfO_2	SiO_2	ZrO_2	Y_2O_3	Total
RSA03-001	1.27	33.74	65.77	0.09	100.86
RSA03-003	1.32	33.96	66.21	<LLD	101.50
RSA03-006	1.35	33.88	66.15	<LLD	101.38
RSA03-007	1.35	33.98	66.30	0.03	101.66
RSA03-011	1.44	33.91	65.61	<LLD	100.97
RSA03-012	1.32	33.20	64.09	0.30	98.91
RSA03-013	1.33	33.91	65.83	<LLD	101.06
RSA03-014	1.32	33.93	66.20	0.04	101.49
RSA03-016	1.33	33.95	66.13	<LLD	101.42
RSA03-017	1.14	33.93	66.12	0.09	101.28
RSA03-018	1.79	33.97	65.80	0.04	101.61
RSA03-020	1.66	33.95	65.50	<LLD	101.12
RSA03-021	1.36	33.96	66.19	<LLD	101.52
RSA03-022	1.32	33.92	66.23	<LLD	101.48
RSA03-023	1.62	33.90	66.05	<LLD	101.59
RSA03-024	1.35	33.86	66.00	<LLD	101.21
RSA03-025	1.38	33.97	65.61	<LLD	100.99
RSA03-026	1.47	33.94	65.82	<LLD	101.25
RSA03-027	1.29	33.99	65.86	<LLD	101.12
RSA03-029	1.30	33.88	66.15	<LLD	101.35
RSA03-032	1.39	34.05	66.15	<LLD	101.58
RSA03-034	1.33	33.56	64.72	0.03	99.64
RSA03-037	1.36	33.92	66.14	<LLD	101.44
RSA03-038	1.38	33.95	66.01	<LLD	101.36
RSA03-042	1.36	33.93	66.60	<LLD	101.90
RSA03-043	1.38	33.89	66.35	<LLD	101.62
RSA03-045	1.30	33.77	66.45	<LLD	101.53
RSA03-046	1.38	33.92	66.29	<LLD	101.61
RSA03-047	1.27	33.74	66.08	<LLD	101.11
RSA03-048	1.27	33.88	65.99	<LLD	101.16
RSA03-051	1.64	33.85	65.81	<LLD	101.29
RSA03-052	1.29	33.82	66.35	<LLD	101.47
RSA03-053	1.34	33.90	66.51	<LLD	101.76
RSA03-054	1.34	33.76	66.27	0.03	101.40
RSA03-055	1.69	33.85	65.89	0.04	101.47
RSA03-056	1.53	33.96	66.28	<LLD	101.78
RSA03-058	0.99	33.39	65.44	0.33	100.14
RSA03-060	1.28	33.88	66.30	<LLD	101.47
RSA03-061	1.35	33.81	66.50	<LLD	101.67
RSA03-062	1.58	33.98	65.83	<LLD	101.42
RSA03-064	1.49	33.99	65.92	0.04	101.44
RSA03-067	1.42	33.99	66.01	0.03	101.47

	HfO_2	SiO_2	ZrO_2	Y_2O_3	Total
RSA03-068	1.38	33.99	66.17	0.06	101.60
RSA03-071	1.31	33.85	66.32	<LLD	101.49
RSA03-072	1.36	33.91	66.07	<LLD	101.33
RSA03-073	1.30	33.75	66.26	0.04	101.35
RSA03-074	1.35	33.95	66.29	<LLD	101.60
RSA03-075	1.25	33.96	66.17	0.03	101.41
RSA03-076	1.37	33.96	66.53	<LLD	101.84
RSA03-077	1.34	33.83	66.18	<LLD	101.36
RSA03-078	1.35	33.98	66.55	<LLD	101.88
RSA03-079	1.36	34.02	66.13	<LLD	101.53
RSA03-079	1.36	34.02	66.13	<LLD	101.53
RSA01-002	1.64	31.87	64.45	0.15	98.11
RSA01-005	2.87	31.94	63.37	<LLD	98.20
RSA01-008	1.53	32.57	65.34	0.11	99.54
RSA01-009	1.08	32.49	65.72	0.21	99.50
RSA01-010c	1.12	32.47	65.15	0.33	99.08
RSA01-011	1.49	32.23	65.23	0.10	99.05
RSA01-012	1.62	32.65	65.69	0.09	100.04
RSA01-013	1.12	32.59	65.07	0.22	99.00
RSA01-015	1.64	32.17	65.12	0.18	99.12
RSA01-016r	1.58	32.23	65.35	0.21	99.37
RSA01-017	1.61	32.07	64.43	0.11	98.23
RSA01-018	1.75	32.52	65.95	<LLD	100.21
RSA01-020	1.07	32.57	65.50	0.20	99.35
RSA01-022	1.49	32.01	64.56	0.18	98.25
RSA01-027	1.39	32.61	65.92	0.03	99.95
RSA01-028	1.26	32.72	66.05	0.06	100.09
RSA01-033	1.76	32.62	64.94	<LLD	99.33
RSA01-034	2.17	31.84	64.23	<LLD	98.24
RSA01-036c	1.61	32.51	65.58	0.05	99.75
RSA01-037	2.45	32.46	64.81	<LLD	99.72
RSA01-040	1.32	32.49	66.04	<LLD	99.86
RSA01-042	1.84	32.37	65.40	0.03	99.64
RSA01-043	1.15	32.39	65.31	0.34	99.18
RSA01-044	1.82	32.15	64.93	0.06	98.95
RSA01-046	1.10	32.63	65.74	0.28	99.74
RSA01-047c	1.25	32.31	65.16	0.07	98.79
RSA01-047r	1.54	32.26	65.61	0.13	99.54
RSA01-049	1.21	32.53	65.74	0.09	99.57
RSA01-052	1.14	32.29	65.38	0.30	99.12
RSA01-053	1.79	32.32	65.57	0.05	99.73
RSA01-054	1.29	32.63	66.28	0.08	100.29

	HfO_2	SiO_2	ZrO_2	Y_2O_3	Total
RSA01-060	1.04	32.68	65.32	0.12	99.15
RSA01-062	1.65	32.39	65.43	0.09	99.56
RSA01-067	1.45	32.63	65.70	0.08	99.86
RSA01-072	1.36	32.37	65.61	0.12	99.46
RSA01-073	1.32	32.47	65.22	0.12	99.13
RSA01-076r	1.39	32.07	65.07	0.17	98.71
RSA01-082	1.79	32.61	65.79	0.04	100.23
RSA01-083	1.05	32.69	66.15	0.23	100.11
RSA01-084	1.11	32.61	65.99	0.08	99.79
RSA01-087	2.49	31.97	63.62	0.30	98.38
RSA01-089	1.58	32.25	65.15	0.11	99.09
RSA01-091	1.40	31.92	64.70	0.28	98.29
RSA01-093	1.44	32.48	65.88	0.05	99.85
RSA01-095	1.70	32.52	65.85	0.03	100.10
RSA01-096	1.18	32.60	65.95	0.21	99.94
RSA01-097	1.03	32.26	66.25	0.11	99.65
RSA01-100	1.51	32.37	65.70	0.03	99.62
RSA01-101c	1.20	32.51	66.43	0.10	100.23
RSA01-102	1.50	32.35	65.57	0.12	99.54
RSA01-103	1.00	32.30	65.54	0.32	99.16
RSA01-107	1.33	32.61	66.03	0.08	100.05
RSA01-111	1.12	32.44	65.70	0.03	99.29
RSA01-113	1.46	32.35	65.25	0.15	99.21
RSA01-115	1.22	32.33	65.98	0.12	99.65
SWA18a-001r	1.32	32.04	66.71	0.29	100.36
SWA18a-003	0.94	32.08	67.66	0.34	101.02
SWA18a-004	1.07	32.05	67.40	0.27	100.79
SWA18a-007	0.87	31.67	67.72	0.14	100.40
SWA18a-011c	1.25	32.17	68.29	0.03	101.73
SWA18a-012	1.34	31.89	67.78	0.05	101.04
SWA18a-013c	0.98	29.65	61.38	0.72	92.73
SWA18a-014	1.42	32.23	68.52	0.03	102.21
SWA18a-015	1.13	30.30	65.41	0.60	97.44
SWA18a-016	1.02	32.22	67.63	0.14	101.01
SWA18a-017	1.17	31.14	66.59	0.23	99.13
SWA18a-018	1.08	31.94	68.22	0.24	101.48
SWA18a-019	1.42	32.07	68.04	0.12	101.66
SWA18a-020	1.03	31.82	67.25	0.33	100.42
SWA18a-021	0.98	31.76	67.27	0.25	100.26
SWA18a-022	1.50	31.54	66.51	0.24	99.80
SWA18a-023	1.59	31.07	66.55	0.05	99.26
SWA18a-028	0.95	31.00	65.48	0.18	97.61

	HfO_2	SiO_2	ZrO_2	Y_2O_3	Total
SWA18a-029	0.91	31.91	67.42	0.37	100.60
SWA18a-031	1.50	32.10	67.92	0.10	101.62
SWA18a-033	1.47	32.14	67.90	0.04	101.55
SWA18a-036	1.21	32.24	67.95	0.12	101.51
SWA18a-037	1.87	32.06	67.31	0.15	101.39
SWA18a-038	2.17	31.63	66.51	0.05	100.36
SWA18a-039	2.02	30.94	64.88	0.13	97.97
SWA18a-041	0.94	31.99	67.66	0.24	100.83
SWA18a-043	1.47	30.60	65.36	0.36	97.79
SWA18a-045c	0.99	31.44	66.30	0.26	98.99
SWA18a-047	1.66	32.05	67.48	0.11	101.31
SWA18a-048	1.37	32.24	68.15	0.05	101.80
SWA18a-049c	1.28	31.01	66.04	0.07	98.41
SWA18a-050	1.05	32.16	67.72	0.26	101.18
SWA18a-055	1.64	32.22	67.86	<LLD	101.72
SWA18a-056	0.94	31.80	67.76	0.27	100.76
SWA18a-057	0.88	31.43	66.88	0.30	99.49
SWA18a-058	1.40	31.80	66.99	0.20	100.39
SWA18a-059	0.99	32.02	68.02	0.16	101.20
SWA18a-061	0.93	30.65	65.66	0.42	97.66
SWA18a-062	1.14	32.16	68.23	0.10	101.63
SWA18a-063	1.71	31.94	67.43	0.06	101.13
SWA18a-064	1.41	32.24	68.03	0.12	101.80
SWA18a-066	1.04	31.88	68.13	0.17	101.22
SWA18a-069	1.02	32.03	67.53	0.33	100.91
SWA18a-080	1.75	31.57	65.96	0.26	99.54
SWA18a-084	1.95	32.23	67.88	<LLD	102.06
RSA05-003	1.15	32.17	66.89	0.24	100.45
RSA05-004	1.19	31.94	66.72	0.26	100.11
RSA05-005	1.38	32.16	66.50	0.26	100.30
RSA05-008	1.21	31.91	65.69	0.66	99.47
RSA05-010	1.20	32.02	67.01	0.28	100.51
RSA05-011	1.30	32.03	65.73	0.40	99.46
RSA05-012	1.23	32.08	66.21	0.33	99.85
RSA05-013	1.15	31.49	64.90	0.98	98.52
RSA05-015	1.27	32.03	66.19	0.18	99.67
RSA05-016	1.31	32.35	66.93	0.03	100.62
RSA05-020	1.14	32.09	66.17	0.20	99.60
RSA05-022	1.10	31.72	65.09	0.75	98.66
RSA05-024	1.20	32.05	65.98	0.49	99.72
RSA05-025	1.17	31.93	66.49	0.49	100.07
RSA05-026	1.16	31.91	66.25	0.33	99.64

	HfO_2	SiO_2	ZrO_2	Y_2O_3	Total
RSA05-028	1.08	31.81	66.28	0.32	99.49
RSA05-029	1.23	32.05	65.96	0.33	99.58
RSA05-030	1.28	31.90	66.26	0.28	99.72
RSA05-031	1.16	32.01	66.27	0.20	99.64
RSA05-036	1.19	31.99	65.88	0.42	99.48
RSA05-039	1.18	31.77	65.78	0.31	99.03
RSA05-040	1.08	31.89	65.66	0.36	98.99
RSA05-042	1.04	31.78	65.57	0.30	98.68
RSA05-043	1.27	32.07	66.29	0.24	99.87
RSA05-044	1.18	32.07	65.28	0.44	98.97
RSA05-046	1.11	32.04	65.60	0.49	99.25
RSA05-049	1.18	32.26	65.77	0.29	99.50
RSA05-050	1.14	31.93	65.77	0.38	99.22
RSA05-051	1.19	32.07	65.98	0.36	99.60
RSA05-052r	1.18	31.24	64.74	0.36	97.51
RSA05-057	1.07	31.92	66.00	0.41	99.40
RSA05-058	1.13	31.92	66.28	0.27	99.60
RSA05-060	1.26	31.97	66.10	0.13	99.46
RSA05-061	0.99	31.90	66.04	0.19	99.13
RSA05-062	1.32	31.81	65.90	0.38	99.40
RSA05-063	1.94	31.89	65.22	0.03	99.08
RSA05-066	1.14	31.77	65.58	0.54	99.03
RSA05-067	1.45	32.11	66.62	0.10	100.28
RSA05-068	0.92	31.43	64.52	0.95	97.82
RSA05-070	1.27	32.06	65.74	0.30	99.37
RSA02-001	1.14	33.63	65.57	0.09	100.44
RSA02-002	1.59	33.45	64.48	0.48	100.00
RSA02-003	1.14	33.84	65.92	0.25	101.15
RSA02-004c	1.21	33.67	65.89	0.17	100.94
RSA02-005c	1.80	33.73	65.01	0.16	100.71
RSA02-006c	1.45	33.62	65.41	0.18	100.66
RSA02-006r	1.60	32.93	63.77	0.08	98.38
RSA02-007c	1.19	33.88	65.73	0.19	101.00
RSA02-008c	1.02	33.51	63.50	0.22	98.24
RSA02-010	1.18	33.91	65.18	0.16	100.43
RSA02-012c	1.04	33.90	66.29	<LLD	101.25
RSA02-014	1.22	33.65	65.36	0.46	100.69
RSA02-017	2.36	33.19	63.90	0.30	99.76
RSA02-019c	1.67	33.81	65.75	0.09	101.32
RSA02-019r	2.10	33.84	65.29	0.11	101.33
RSA02-020	1.69	33.21	64.08	0.15	99.13
RSA02-023	1.26	34.01	65.92	0.04	101.24

	HfO_2	SiO_2	ZrO_2	Y_2O_3	Total
RSA02-023	1.26	34.01	65.92	0.04	101.24
RSA02-026	1.53	33.71	65.23	0.42	100.90
RSA02-027c	1.43	33.84	66.27	<LLD	101.53
RSA02-029c	1.06	33.80	66.36	0.22	101.44
RSA02-030	1.19	33.76	65.99	0.14	101.07
RSA02-031	1.41	33.89	66.05	0.05	101.39
SWA07-001c	1.60	32.51	65.80	0.03	99.94
SWA07-005	1.41	32.31	65.87	0.15	99.74
SWA07-007c	1.25	32.23	66.22	0.08	99.77
SWA07-008	1.60	31.83	64.64	0.07	98.13
SWA07-011	1.22	32.13	66.09	0.11	99.55
SWA07-015	1.25	31.76	64.95	0.31	98.28
SWA07-018	1.14	32.30	65.75	0.14	99.33
SWA07-019c	1.44	31.98	65.29	0.06	98.77
SWA07-021	1.59	32.50	65.92	0.04	100.05
SWA07-023	1.74	32.05	64.04	0.18	98.01
SWA07-024	1.85	32.36	65.63	<LLD	99.86
SWA07-027	1.76	32.44	65.80	0.05	100.05
SWA07-028	1.23	31.57	64.55	0.33	97.68
SWA07-029	1.43	31.69	64.90	0.07	98.09
SWA07-032	1.54	31.81	64.51	0.17	98.02
SWA07-034	2.31	32.22	65.08	0.08	99.69
SWA07-048	1.72	32.03	63.71	0.08	97.54
SWA07-049	1.51	31.86	64.92	0.11	98.40
SWA07-050	1.73	32.13	65.32	0.10	99.27
SWA07-054	1.56	31.93	64.79	0.08	98.36
SWA07-055	0.92	32.38	65.93	0.26	99.50
SWA07-056	1.04	32.27	66.14	0.20	99.64
SWA07-058	1.55	31.59	64.64	0.08	97.85
SWA07-059	1.76	31.76	64.67	0.13	98.31
SWA07-065	1.22	32.03	65.81	0.16	99.22
SWA07-067	1.66	31.84	64.65	0.15	98.30
SWA07-074	1.59	31.89	64.94	0.18	98.60
SWA07-076	1.61	31.69	64.46	0.27	98.03
SWA07-077	1.83	32.15	65.18	0.07	99.23
SWA07-078	1.03	32.30	65.80	0.22	99.35
SWA07-079	1.49	31.73	64.88	0.06	98.17
SWA07-082	1.74	31.57	64.03	0.27	97.61
SWA07-084	1.69	32.20	65.80	0.07	99.76
SWA07-086	1.26	31.94	65.20	0.26	98.66
SWA07-087	1.82	32.31	65.59	0.09	99.81
SWA07-088	1.62	32.66	66.06	0.05	100.39

	HfO_2	SiO_2	ZrO_2	Y_2O_3	Total
SWA07-090	1.26	32.42	66.00	0.11	99.79
SWA07-092c	1.82	31.82	64.73	0.16	98.52
SWA07-094	1.56	31.68	64.55	0.08	97.87
SWA07-097	1.31	32.18	65.37	0.16	99.03
RSA04-001r	1.07	33.66	66.45	0.15	101.33
RSA04-002c	0.98	33.69	66.14	0.37	101.17
RSA04-003c	1.24	33.61	66.25	0.12	101.22
RSA04-003r	1.48	33.77	66.18	0.04	101.46
RSA04-004c	0.81	32.50	63.37	1.11	97.79
RSA04-005	1.40	33.25	65.31	0.05	100.00
RSA04-006c	0.96	33.57	66.73	0.14	101.39
RSA04-007c	1.50	33.44	66.10	0.11	101.14
RSA04-009c	1.37	33.54	65.71	0.33	100.96
RSA04-009r	0.99	33.88	66.85	0.09	101.81
RSA04-010	1.70	33.61	65.96	0.08	101.34
RSA04-011	1.34	33.29	65.12	0.11	99.86
RSA04-012	0.92	33.77	66.13	0.22	101.04
RSA04-013c	0.98	33.92	66.34	0.09	101.33
RSA04-015c	0.89	33.81	66.75	0.10	101.55
RSA04-015r	1.31	33.46	65.75	0.18	100.71
RSA04-017	1.31	33.72	66.25	0.19	101.47
RSA04-018	2.25	33.73	65.69	0.07	101.73
RSA04-019c	0.96	33.80	66.58	0.13	101.47
RSA04-021c	0.91	33.67	66.54	0.15	101.28
RSA04-021r	1.62	33.71	66.01	0.04	101.37
RSA04-023c	1.74	33.14	64.93	0.09	99.90
RSA04-023r	1.49	33.43	65.43	0.03	100.37
RSA04-024	1.00	33.90	66.72	0.05	101.66
RSA04-025	1.24	33.79	66.26	0.08	101.38
RSA04-026	0.96	33.76	66.30	0.15	101.17
RSA04-027c	1.00	34.00	66.95	0.10	102.05
RSA04-028r	1.37	33.61	65.52	0.17	100.66
RSA04-029c	1.08	33.70	65.85	0.12	100.75
RSA04-029r	1.37	33.36	65.16	0.08	99.97
RSA04-030c	1.29	33.97	66.39	<LLD	101.65
RSA04-030r	1.41	33.43	65.34	0.04	100.22
RSA08-001c	1.23	33.47	65.30	0.50	100.50
RSA08-002c	1.09	33.19	65.41	0.40	100.10
RSA08-003	1.29	33.87	66.27	0.05	101.47
RSA08-004c	1.00	33.51	65.58	0.14	100.23
RSA08-005	1.55	33.18	64.88	0.16	99.77
RSA08-006	1.32	33.79	65.82	0.24	101.17

	HfO_2	SiO_2	ZrO_2	Y_2O_3	Total
RSA08-007c	1.15	33.62	65.55	0.27	100.58
RSA08-012	1.44	33.49	65.14	0.18	100.25
RSA08-013c	1.56	33.78	65.82	0.22	101.38
RSA08-015c	1.50	32.89	64.41	0.19	99.00
RSA08-016c	1.29	33.22	64.83	0.52	99.86
RSA08-017	1.28	33.78	66.14	0.11	101.31
RSA08-019c	1.59	32.65	64.40	0.11	98.74
RSA08-021c	1.48	33.79	65.96	<LLD	101.24
RSA08-022	1.24	33.77	66.45	0.14	101.59
RSA08-025c	1.59	33.78	65.85	0.09	101.31
RSA08-031	1.67	33.58	64.62	0.08	99.94
RSA08-034	1.66	33.66	65.94	0.12	101.38
RSA08-038	1.73	33.18	64.60	0.13	99.64
RSA08-049c	1.25	33.92	66.47	0.07	101.71
RSA08-050r	1.77	32.79	64.09	0.17	98.83
RSA08-051	1.38	33.55	66.06	0.14	101.14
RSA08-054c	1.53	33.50	65.63	0.07	100.73
RSA08-057	1.54	33.64	65.97	0.09	101.24
RSA08-058	1.54	33.46	65.37	0.12	100.49
RSA08-059	1.12	33.73	66.15	0.19	101.19
RSA08-060	1.30	33.85	66.27	<LLD	101.44
RSA08-068	2.11	32.63	63.49	0.08	98.31
SWA10a-001	2.14	30.98	61.81	0.17	95.10
SWA10a-003c	1.30	32.17	64.20	0.20	97.87
SWA10a-006	1.36	30.29	60.66	1.17	93.49
SWA10a-007	1.14	29.85	59.06	0.73	90.78
SWA10a-010	1.43	30.29	60.93	0.38	93.04
SWA10a-016	1.87	31.35	62.49	0.24	95.95
SWA10a-017	1.16	31.12	63.20	0.16	95.64
SWA10a-018	1.25	31.96	64.52	0.40	98.12
SWA10a-019	1.23	32.13	64.50	0.17	98.03
SWA10a-020c	0.93	30.51	61.23	1.28	93.96
SWA10a-021	1.38	30.04	57.62	1.63	90.67
SWA10a-022c	1.39	31.29	63.16	0.38	96.21
SWA10a-025	1.28	31.97	64.35	0.35	97.94
SWA10a-026	1.49	32.09	64.41	0.05	98.04
SWA10a-030	1.26	32.07	64.01	0.34	97.67
SWA10a-032	1.15	30.20	58.67	0.83	90.85
SWA10a-042c	1.26	32.41	64.71	0.07	98.45
SWA10a-043	1.54	31.18	62.36	0.17	95.25
SWA10a-047	1.03	30.65	60.55	0.57	92.80
SWA10a-049c	1.35	32.00	63.88	0.26	97.48

	HfO_2	SiO_2	ZrO_2	Y_2O_3	Total
SWA10a-050c	1.20	31.57	63.23	0.21	96.22
SWA10a-051c	0.96	31.67	64.26	0.42	97.31
SWA10a-051r	1.44	30.73	61.13	0.82	94.12
SWA10a-052c	1.33	30.30	60.86	0.35	92.83
SWA10a-053	1.64	31.62	63.32	0.07	96.64
SWA10a-054	2.92	31.08	61.57	0.16	95.73
SWA10a-059c	1.17	28.90	52.52	1.93	84.52
SWA10a-063c	1.18	31.98	63.73	0.81	97.71
SWA10a-064c	1.43	31.96	64.97	0.12	98.48
SWA10a-065	1.44	30.20	59.93	0.44	92.02
SWA10a-071	1.54	30.42	61.00	0.23	93.18
SWA10a-072c	1.27	30.50	61.20	0.56	93.52
SWA10a-075	1.49	30.21	60.50	0.41	92.61
SWA10a-109c	1.31	31.08	63.94	0.46	96.78
SWA10a-116	1.09	31.71	63.93	0.39	97.11
SWA10a-123	1.05	30.33	59.35	0.71	91.43
SWA10a-128	1.17	32.26	65.53	0.16	99.11
SWA10a-130	1.56	30.82	63.08	0.13	95.59
SWA10a-133c	1.06	30.73	60.15	1.35	93.29
SWA10a-135	1.08	31.61	64.07	0.89	97.65
SWA10a-142	1.34	29.52	57.95	0.41	89.23
SWA10a-145	1.15	31.17	62.18	0.76	95.26
SWA10a-155	0.98	32.04	64.15	0.39	97.57
RSA09-001c	1.41	31.60	64.29	0.35	97.64
RSA09-006	1.13	31.92	64.15	0.99	98.19
RSA09-008	1.54	30.95	62.28	0.46	95.24
RSA09-015c	1.42	31.07	60.34	2.35	95.18
RSA09-021	1.14	31.95	63.97	0.50	97.56
RSA09-024	1.01	31.65	61.89	1.13	95.68
RSA09-026	1.75	30.10	58.47	0.37	90.70
RSA09-030c	1.29	31.76	63.66	0.04	96.75
RSA09-033	1.27	31.83	64.31	0.36	97.77
RSA09-036c	1.09	31.97	64.64	0.25	97.95
RSA09-036r	2.37	29.79	57.82	1.10	91.08
RSA09-037	1.47	30.64	60.36	2.25	94.72
RSA09-038c	0.97	30.58	58.72	0.88	91.15
RSA09-041	1.21	31.66	63.70	0.41	96.97
RSA09-053r	1.64	30.18	58.23	0.68	90.74
RSA09-063c	1.11	31.42	62.39	1.41	96.33
RSA09-067	1.33	31.87	63.98	0.33	97.51
RSA09-069	1.69	30.52	60.19	0.35	92.75
RSA09-070	1.36	31.28	62.31	1.17	96.11

	HfO_2	SiO_2	ZrO_2	Y_2O_3	Total
RSA09-073	1.39	31.88	63.80	0.79	97.86
RSA09-079	1.83	30.82	61.44	0.45	94.54
RSA09-092c	1.00	31.58	62.68	1.87	97.12
RSA09-092r	1.54	30.29	57.29	2.15	91.27
RSA09-097c	1.25	30.69	61.81	0.43	94.17
RSA09-097r	1.59	30.22	57.74	0.76	90.30
RSA09-102	1.46	30.27	58.32	2.08	92.13
RSA09-104c	1.18	31.89	64.29	0.24	97.60
RSA09-105	2.66	31.24	61.94	0.15	95.98
RSA09-107c	1.85	30.82	61.28	0.14	94.08
RSA09-112c	1.39	32.28	64.93	0.15	98.74
RSA09-112r	1.64	30.18	56.69	2.09	90.60
RSA09-113c	0.90	31.93	64.97	0.62	98.40
RSA09-115c	1.75	30.62	59.70	0.38	92.45
RSA09-125c	1.12	31.77	63.96	0.61	97.46
RSA09-131	1.65	30.06	57.69	1.23	90.63
RSA09-138	1.26	29.67	56.67	3.02	90.62
RSA09-139	1.43	30.40	58.65	0.28	90.77
RSA09-142c	1.67	31.58	62.43	1.02	96.70
RSA09-142r	1.72	30.42	60.69	0.20	93.03
RSA09-146	1.82	29.36	55.28	3.63	90.09
SWA03-001c	1.94	32.16	67.43	0.06	101.60
SWA03-003c	1.22	31.86	68.17	0.10	101.35
SWA03-004c	1.73	31.67	67.35	0.06	100.80
SWA03-006c	1.29	30.74	65.99	0.34	98.36
SWA03-007c	1.28	31.84	68.10	0.18	101.40
SWA03-007r	1.33	31.08	65.93	0.26	98.60
SWA03-009c	1.32	31.76	66.97	0.27	100.32
SWA03-009r	1.38	31.07	65.99	0.34	98.77
SWA03-010	1.28	31.29	66.86	0.50	99.93
SWA03-011	1.31	30.80	65.32	0.50	97.93
SWA03-012	1.22	31.26	66.63	0.38	99.50
SWA03-014c	1.21	31.70	67.36	0.35	100.61
SWA03-014r	1.43	31.13	65.87	0.36	98.78
SWA03-015	1.26	31.29	66.77	0.30	99.63
SWA03-017c	1.18	31.76	68.07	0.25	101.26
SWA03-018	1.36	31.47	67.00	0.28	100.10
SWA03-019	1.25	31.06	65.98	0.33	98.62
SWA03-020	1.32	31.45	66.53	0.37	99.66
SWA03-021c	1.31	31.08	66.59	0.36	99.34
SWA03-022r	1.40	30.87	64.93	0.35	97.55
SWA03-023	1.32	31.91	68.01	0.21	101.46

	HfO_2	SiO_2	ZrO_2	Y_2O_3	Total
SWA03-024	1.48	31.83	67.54	0.09	100.95
SWA03-025c	1.44	31.88	67.64	0.14	101.11
SWA03-026	1.30	31.40	66.83	0.31	99.84
SWA03-029	1.32	31.66	67.45	0.25	100.67
SWA03-030	1.42	31.79	68.18	0.14	101.54
SWA03-031c	1.50	31.44	66.61	0.42	99.96
SWA03-031r	1.89	31.87	67.88	0.12	101.76
SWA03-032c	1.37	31.51	67.18	0.23	100.30
SWA03-032r	1.32	31.37	66.34	0.36	99.39
SWA03-034c	1.17	31.25	66.86	0.36	99.64
SWA03-035r	1.78	31.02	64.86	0.06	97.72
SWA03-036	1.21	30.89	65.89	0.46	98.45
SWA03-038c	1.20	31.25	66.48	0.58	99.51
SWA03-039c	1.20	31.46	67.01	0.36	100.03
SWA03-040	1.22	31.43	66.38	0.38	99.41
SWA03-041	1.17	31.80	67.90	0.18	101.05
SWA03-042	1.23	31.91	68.20	0.21	101.55
SWA03-043c	1.28	31.52	67.32	0.07	100.18
SWA03-044	1.31	32.12	67.86	0.23	101.51
SWA03-045c	1.32	31.15	66.31	0.32	99.11
SWA03-046c	1.20	31.68	67.94	0.22	101.03
SWA03-047c	1.08	31.71	68.01	0.20	101.00
SWA03-048c	1.45	32.10	68.07	0.06	101.68
SWA03-048r	1.05	31.47	66.95	0.28	99.76
SWA03-049c	1.11	31.68	67.39	0.24	100.41
SWA03-050c	1.58	31.43	66.79	0.07	99.87
SWA03-050r	1.53	31.12	66.46	0.28	99.39
SWA03-052	1.19	31.62	67.79	0.30	100.91
SWA03-053c	1.28	31.89	67.95	0.23	101.35
SWA03-053r	1.20	31.78	66.94	0.22	100.14
SWA03-054c	1.18	32.11	68.23	0.15	101.67
SWA03-056c	1.49	31.56	67.35	0.24	100.64
SWA03-057c	1.19	31.43	67.34	0.27	100.22
SWA03-058c	1.24	31.94	67.57	0.32	101.08
SWA03-060c	1.43	31.86	67.47	0.22	100.98
RSA06-001c	1.90	32.46	65.07	0.21	99.63
RSA06-002	1.17	32.49	65.40	0.39	99.45
RSA06-003	1.58	30.40	58.17	0.70	90.85
RSA06-006c	1.10	30.64	62.28	1.01	95.03
RSA06-015c	1.13	30.03	59.90	1.36	92.42
RSA06-018	1.29	30.53	61.84	1.06	94.73
RSA06-019c	1.04	32.29	65.44	0.22	98.99

	HfO_2	SiO_2	ZrO_2	Y_2O_3	Total
RSA06-021c	1.17	31.87	65.12	0.46	98.62
RSA06-023	1.17	32.06	65.40	0.47	99.11
RSA06-025c	1.38	32.17	65.83	0.33	99.71
RSA06-030	1.94	31.90	64.54	0.18	98.57
RSA06-035	1.51	31.46	64.37	0.15	97.48
RSA06-038	1.40	30.91	61.99	0.04	94.35
RSA06-039c	1.23	32.02	65.69	0.48	99.42
RSA06-045c	1.38	30.57	61.11	0.11	93.17
RSA06-048	1.13	31.82	63.29	0.87	97.10
RSA06-052c	1.35	30.77	59.87	0.62	92.60
RSA06-055c	0.90	32.22	65.24	0.49	98.85
RSA06-063	1.08	31.50	63.68	0.87	97.14
RSA06-065	1.10	31.92	64.79	0.48	98.30
RSA06-071	1.76	31.37	63.63	0.29	97.05
RSA06-073	1.13	31.78	64.73	0.49	98.13
RSA06-077c	1.65	30.45	60.35	0.37	92.80
RSA06-080c	1.10	31.11	62.80	0.57	95.58
RSA06-083c	2.00	32.57	65.27	0.09	99.93
RSA06-087	1.12	30.99	62.75	0.98	95.84
RSA06-088c	1.31	32.38	64.74	0.09	98.52
RSA06-092c	1.39	31.35	63.17	0.43	96.34
RSA06-093	1.25	32.25	65.24	0.33	99.06
RSA06-095	1.61	30.46	61.19	0.16	93.43
RSA06-097c	1.11	32.26	64.98	0.47	98.82
RSA06-100	1.10	32.23	64.75	0.49	98.56
RSA06-108	1.12	30.98	62.37	0.72	95.19
RSA06-112c	1.19	32.26	65.23	0.16	98.84
RSA06-118c	1.66	31.40	62.55	0.26	95.86
RSA06-121	1.13	31.24	63.47	0.54	96.39
RSA06-122c	1.09	31.82	64.06	0.63	97.60
RSA06-125c	1.59	31.47	63.18	0.14	96.37
RSA06-130	1.02	30.48	61.19	0.55	93.24
RSA06-139	1.08	31.51	63.72	0.55	96.86
RSA06-140	1.40	31.17	62.06	0.37	95.00
RSA06-142	2.31	29.99	54.85	3.22	90.37
RSA06-147c	1.01	32.26	65.14	0.14	98.55
SWA13a-001	1.02	32.17	64.79	0.18	98.16
SWA13a-002	1.39	32.26	64.52	0.29	98.45
SWA13a-003	1.05	32.23	64.58	0.26	98.12
SWA13a-004	1.31	32.14	64.90	0.24	98.59
SWA13a-005c	0.96	32.00	65.41	0.12	98.48
SWA13a-006	1.29	32.17	65.02	0.23	98.71

	HfO_2	SiO_2	ZrO_2	Y_2O_3	Total
SWA13a-008c	1.14	32.01	65.51	0.36	99.01
SWA13a-009	1.32	31.93	64.61	0.74	98.60
SWA13a-010	1.23	31.90	64.93	0.53	98.60
SWA13a-011	1.27	32.11	64.69	0.66	98.73
SWA13a-012c	0.96	30.24	62.21	1.65	95.05
SWA13a-014	1.12	32.08	65.03	0.34	98.57
SWA13a-015c	1.05	32.16	65.56	0.07	98.84
SWA13a-016	1.50	32.10	64.74	0.44	98.78
SWA13a-017	1.10	32.25	65.45	0.37	99.16
SWA13a-018	1.23	32.23	65.48	0.14	99.08
SWA13a-019	1.10	32.50	64.76	0.42	98.78
SWA13a-020	1.00	32.22	65.38	0.22	98.82
SWA13a-021c	1.03	32.33	64.89	0.17	98.42
SWA13a-024c	1.19	32.13	65.23	0.40	98.94
SWA13a-025	1.29	31.66	64.09	0.53	97.58
SWA13a-028	1.08	32.32	65.49	0.49	99.37
SWA13a-029	0.99	32.39	65.14	0.35	98.87
SWA13a-032	0.98	32.22	64.64	0.39	98.22
SWA13a-034	1.49	32.37	65.11	0.09	99.07
SWA13a-035c	1.25	32.05	65.54	0.11	98.95
SWA13a-036	1.16	32.35	65.76	0.10	99.36
SWA13a-037	1.07	32.31	65.31	0.28	98.97
SWA13a-039	1.00	32.06	65.79	0.21	99.06
SWA13a-040	1.67	31.50	63.70	0.46	97.32
SWA13a-041	0.99	32.21	66.11	0.11	99.42
SWA13a-042	1.27	32.39	65.52	0.21	99.39
SWA13a-043	1.17	32.44	66.07	0.21	99.90
SWA13a-044	1.42	31.79	64.16	0.69	98.06
SWA13a-045	1.08	32.19	65.36	0.19	98.81
SWA13a-046c	1.23	32.06	64.38	0.40	98.06
SWA13a-047	1.60	31.77	64.32	0.08	97.77
SWA11-001c	1.64	32.30	65.44	0.14	99.51
SWA11-003	1.38	32.65	66.13	0.08	100.23
SWA11-004	1.43	32.45	65.88	0.16	99.92
SWA11-006	1.53	32.25	65.39	0.24	99.42
SWA11-007	1.48	32.37	65.87	0.08	99.81
SWA11-008	1.41	32.01	64.72	0.60	98.73
SWA11-010	1.09	32.05	65.56	0.37	99.08
SWA11-013	2.35	31.97	63.54	0.10	97.96
SWA11-014	1.59	32.06	64.68	0.50	98.83
SWA11-015	1.38	32.38	65.94	0.07	99.77
SWA11-016	1.53	32.32	65.46	0.19	99.50

	HfO_2	SiO_2	ZrO_2	Y_2O_3	Total
SWA11-017	1.35	32.37	65.55	0.31	99.58
SWA11-020	1.22	32.17	65.39	0.26	99.04
SWA11-023c	1.17	32.38	66.09	0.15	99.79
SWA11-024	1.53	31.72	64.44	0.27	97.96
SWA11-025	1.30	32.31	65.72	0.16	99.49
SWA11-026	1.40	32.44	65.92	0.13	99.89
SWA11-028c	1.62	32.52	65.79	<LLD	99.93
SWA11-029	1.56	32.46	65.79	0.11	99.91
SWA11-030	1.27	32.40	64.87	0.30	98.84
SWA11-031	1.21	32.55	65.91	0.24	99.91
SWA11-032c	1.47	32.49	66.08	0.03	100.06
SWA11-033	1.36	32.41	66.05	0.11	99.92
SWA11-037	1.45	32.37	65.58	0.20	99.60
SWA11-038	1.57	32.53	65.99	0.08	100.17
SWA11-040	1.35	32.31	65.05	0.35	99.06
SWA11-041	1.16	32.27	65.68	0.18	99.28
SWA11-045	1.33	32.34	65.51	0.22	99.40
SWA11-046	1.16	32.36	66.11	0.15	99.78
SWA11-048	1.28	32.32	65.75	0.18	99.53
SWA11-051	1.13	32.41	66.11	0.13	99.78
SWA11-052	1.16	32.34	66.07	0.10	99.66
SWA11-055	1.33	32.42	66.07	0.08	99.91
SWA11-057	1.54	32.22	65.38	0.23	99.36
SWA11-058c	1.36	32.49	66.01	0.08	99.94
SWA11-061	1.16	32.44	65.75	0.31	99.66
SWA11-062	1.46	32.19	65.10	0.37	99.12
SWA11-063	1.49	32.35	65.71	0.17	99.72
SWA11-065	1.28	32.48	66.14	0.08	99.97
SWA11-066	1.39	32.47	65.87	0.06	99.79
SWA11-068	1.74	32.46	65.62	0.19	100.01
SWA11-073	1.44	32.43	65.86	0.12	99.85
SWA11-074	1.78	32.54	65.75	0.03	100.10
SWA11-077	1.33	32.42	65.46	0.41	99.61
SWA11-079	1.36	32.66	65.53	0.19	99.73
SWA11-081	1.36	32.53	64.93	0.25	99.07
SWA11-084	1.18	32.46	65.76	0.22	99.61
SWA11-085	1.15	32.43	65.35	0.17	99.10
SWA11-086	1.50	32.64	65.79	0.17	100.10
SWA11-088	1.63	32.45	65.25	0.16	99.49
SWA09-001c	1.10	31.98	64.07	0.08	97.22
SWA09-002	1.23	29.89	59.54	1.36	92.03
SWA09-004	1.22	31.90	63.99	0.13	97.24

	HfO_2	SiO_2	ZrO_2	Y_2O_3	Total
SWA09-005c	1.60	32.04	63.55	0.34	97.53
SWA09-010	2.06	29.57	58.57	0.62	90.82
SWA09-011c	1.31	32.39	65.52	0.03	99.25
SWA09-012	1.23	32.01	65.13	0.17	98.54
SWA09-016	1.77	29.97	60.05	0.36	92.15
SWA09-017c	1.35	31.90	64.04	0.19	97.48
SWA09-018	1.23	29.19	58.56	2.16	91.14
SWA09-021c	1.16	32.16	64.00	0.28	97.60
SWA09-023c	1.15	31.78	64.33	0.31	97.57
SWA09-025	1.22	31.10	60.88	1.30	94.50
SWA09-026c	1.68	31.96	63.99	0.11	97.74
SWA09-027c	1.58	32.02	64.46	0.20	98.27
SWA09-029c	1.08	32.06	64.79	0.34	98.27
SWA09-034c	1.11	31.78	64.76	0.07	97.71
SWA09-042c	1.23	31.38	59.99	0.41	93.01
SWA09-043c	1.34	32.20	64.94	0.06	98.54
SWA09-044c	1.16	32.15	64.56	0.22	98.08
SWA09-045	0.88	29.91	56.41	2.99	90.19
SWA09-046	1.14	30.28	61.04	0.67	93.14
SWA09-048	1.55	30.27	60.17	0.34	92.34
SWA09-050	1.76	30.72	60.83	0.27	93.58
SWA02a-004c	1.33	31.27	66.30	0.29	99.19
SWA02a-005c	2.23	31.23	64.28	0.14	97.87
SWA02a-006	1.19	30.75	65.54	0.29	97.77
SWA02a-007c	1.39	31.96	67.01	0.26	100.62
SWA02a-007r	1.54	31.16	64.75	0.12	97.57
SWA02a-008	1.34	31.31	66.11	0.21	98.97
SWA02a-009	1.59	31.70	67.39	0.13	100.81
SWA02a-012c	1.34	31.82	66.50	0.11	99.77
SWA02a-024c	1.60	32.15	67.71	0.08	101.54
SWA02a-027c	1.77	32.17	67.69	<LLD	101.64
SWA02a-030c	1.54	32.05	67.74	0.10	101.43
SWA02a-031c	1.28	31.37	66.89	0.24	99.79
SWA02a-032	1.53	32.31	67.65	<LLD	101.51
SWA02a-037c	1.24	31.47	66.88	0.23	99.82
SWA02a-042c	1.36	31.99	67.63	0.18	101.16
SWA02a-043	1.45	31.30	65.40	0.22	98.37
SWA02a-045c	1.16	31.30	65.23	0.30	97.98
SWA02a-046c	1.44	31.50	65.26	0.20	98.40
SWA02a-047c	1.18	32.25	68.37	0.03	101.82
SWA02a-048	1.56	31.59	66.81	0.12	100.08
SWA02a-052	1.50	32.09	67.78	0.09	101.45

	HfO_2	SiO_2	ZrO_2	Y_2O_3	Total
SWA02a-052	1.50	32.09	67.78	0.09	101.45
SWA02a-054c	1.26	32.08	67.67	0.19	101.21
SWA02a-055	2.11	31.54	65.76	0.12	99.54
SWA02a-064c	1.48	31.80	66.93	0.19	100.39
RSA07-001	1.84	31.97	65.33	0.19	99.34
RSA07-003	1.48	31.97	66.07	0.18	99.70
RSA07-004	1.41	31.93	65.75	0.26	99.34
RSA07-014	1.42	31.94	65.82	0.23	99.41
RSA07-021	1.46	31.63	65.55	0.31	98.96
RSA07-035	1.69	31.44	64.35	0.24	97.72
RSA07-046	1.26	32.10	65.11	0.20	98.67
RSA07-050	1.08	32.28	65.72	0.23	99.31
RSA07-051	1.33	32.37	65.73	0.06	99.49
RSA07-057	1.12	32.26	66.13	0.10	99.61
RSA07-069	1.29	31.98	65.58	0.24	99.10
RSA07-079	1.02	31.91	65.09	0.54	98.56
RSA07-080	1.38	31.85	65.70	0.08	99.00
SWA05-001	1.58	32.30	68.06	<LLD	101.94
SWA05-002c	1.58	31.00	64.99	0.25	97.82
SWA05-002r	1.99	30.83	64.60	0.29	97.72
SWA05-003	1.31	32.10	67.84	0.13	101.38
SWA05-004	1.68	32.12	68.29	0.04	102.13
SWA05-006c	1.47	31.67	67.20	0.33	100.66
SWA05-007c	1.25	31.79	67.33	0.17	100.53
SWA05-007r	2.36	29.44	58.06	0.43	90.28
SWA05-008c	1.45	32.04	67.63	0.05	101.17
SWA05-008r	3.11	30.38	61.46	0.34	95.29
SWA05-009	1.24	32.01	68.42	0.05	101.72
SWA05-010c	1.28	31.95	68.19	0.05	101.46
SWA05-010r	2.00	29.74	61.72	0.36	93.82
SWA05-011	1.22	31.95	68.25	0.06	101.49
SWA05-012c	1.25	32.05	68.17	0.09	101.56
SWA05-012r	1.46	31.55	67.28	0.24	100.52
SWA05-013	1.92	30.45	62.51	0.37	95.25
SWA05-016	1.08	30.90	66.23	0.46	98.68
SWA05-017	1.27	32.13	67.85	0.05	101.30
SWA05-020	1.44	32.06	67.89	0.04	101.42
SWA05-022c	1.18	31.83	68.18	0.08	101.27
SWA05-022r	2.34	29.30	58.65	0.77	91.06
SWA05-023r	2.57	30.28	61.32	0.15	94.32
SWA05-025c	1.05	31.56	66.87	0.36	99.84
SWA05-025r	1.79	27.56	52.72	3.26	85.33

Appendix F – Zircon Trace-Element Analyses

Trace-element compositions analysed by laser ablation ICPMS are shown for each analysed grain. For each analysis, the following two values are given for each element measured:

Conc: Concentration of element in ppm. Detection limit filtered.

1σ: Internal precision.

Each analysis also has a crystallisation temperature estimate calculated from the Ti content (Ti-in-zirc; following the method of Watson & Harrison, 2005).

Analyses are divided into three groups based on the quality and homogeneity of the signal:

Pristine: stable signal with no included phases or metamict zones.

Variable: small inclusions and/or chemical zonation within the crystal.

Metamict: metamict zircon; included for comparison.

Samples are ordered from mafic to felsic.

Analysis Group		RSA03-001 variable	RSA03-003 variable	RSA03-006 variable	RSA03-007 variable	RSA03-011 variable	RSA03-012 variable	RSA03-013 variable	RSA03-014 variable	RSA03-016 variable	RSA03-017 variable	RSA03-018 variable	RSA03-020 variable
^{31}P	Conc	34	123	29.5	27.9	37	45	60	30.5	29.2	26.9	35	181
	1σ	11	30	8.5	7.9	10	13	15	7.7	8.2	7.0	11	43
^{43}Ca	Conc	<76	512	<61	80	220	252	815	143	201	62	<96	440
	1σ	53	57	30	34	54	55	58	25	47	22	45	56
^{49}Ti	Conc	5.5	10.3	0.85	2.37	2.27	1.56	4.45	2.57	3.88	1.05	2.65	3.65
	1σ	1.0	1.0	0.36	0.56	0.79	0.54	0.57	0.40	0.82	0.32	0.62	0.70
^{89}Y	Conc	234.2	760	130.1	159.4	169.2	429	360	179.8	182.6	149.3	170.3	1302
	1σ	8.2	26	4.5	5.6	6.0	15	12	6.3	6.5	5.3	6.0	46
^{93}Nb	Conc	1.72	4.39	1.267	1.526	1.29	2.44	2.42	1.886	1.53	1.547	1.83	6.44
	1σ	0.13	0.20	0.079	0.099	0.11	0.14	0.11	0.095	0.12	0.088	0.11	0.29
^{139}La	Conc	5.84	32.0	3.03	1.91	4.59	26.15	8.44	5.14	7.90	1.770	0.959	34.9
	1σ	0.29	1.1	0.15	0.12	0.28	0.97	0.32	0.21	0.36	0.097	0.070	1.3
^{140}Ce	Conc	58.8	287.3	15.27	17.55	55.7	119.7	72.2	51.5	84.2	20.15	18.39	182.2
	1σ	2.0	9.6	0.55	0.64	2.0	4.1	2.4	1.8	2.9	0.72	0.67	6.3
^{141}Pr	Conc	8.03	33.5	1.641	2.26	7.62	13.02	12.16	8.93	12.51	3.01	2.50	16.55
	1σ	0.33	1.1	0.083	0.11	0.35	0.48	0.42	0.32	0.48	0.13	0.12	0.60
^{146}Nd	Conc	58.2	213.5	10.18	15.45	60.1	61.9	87.5	75.6	103.7	20.40	21.58	86.3
	1σ	2.3	7.1	0.51	0.76	2.6	2.4	3.0	2.6	3.8	0.85	0.93	3.2
^{147}Sm	Conc	16.20	41.0	2.53	4.68	12.61	12.54	19.77	19.49	33.1	5.66	8.59	26.0
	1σ	0.96	1.6	0.23	0.37	0.93	0.74	0.83	0.82	1.5	0.36	0.51	1.2
^{151}Eu	Conc	3.54	15.28	0.674	1.57	5.69	3.29	4.43	5.82	10.78	1.344	2.19	5.24
	1σ	0.23	0.58	0.064	0.12	0.34	0.20	0.20	0.24	0.49	0.093	0.14	0.28
^{157}Gd	Conc	9.20	37.2	2.94	3.60	8.81	13.45	16.00	11.58	16.90	4.61	6.41	40.5
	1σ	0.64	1.5	0.24	0.30	0.71	0.74	0.68	0.53	0.92	0.30	0.40	1.7
^{159}Tb	Conc	1.88	8.14	0.740	0.995	1.45	3.94	3.38	1.655	1.91	1.104	1.084	12.73
	1σ	0.12	0.30	0.050	0.067	0.11	0.18	0.14	0.078	0.12	0.062	0.067	0.47

Analysis		RSA03-001	RSA03-003	RSA03-006	RSA03-007	RSA03-011	RSA03-012	RSA03-013	RSA03-014	RSA03-016	RSA03-017	RSA03-018	RSA03-020
^{163}Dy	Conc	17.16	78.1	8.10	12.20	13.57	40.0	34.1	15.46	18.81	11.30	11.66	134.7
	1σ	0.84	2.7	0.39	0.58	0.76	1.6	1.2	0.62	0.89	0.50	0.54	4.8
^{165}Ho	Conc	6.49	25.68	3.66	4.34	5.03	13.52	11.52	5.26	6.20	4.57	4.74	44.0
	1σ	0.28	0.87	0.15	0.19	0.24	0.50	0.40	0.20	0.27	0.18	0.19	1.5
^{166}Er	Conc	32.5	100.7	19.26	23.07	23.04	58.0	48.6	24.52	26.6	21.65	23.96	175.6
	1σ	1.3	3.4	0.73	0.89	0.97	2.1	1.7	0.88	1.1	0.80	0.90	5.9
^{169}Tm	Conc	7.09	19.86	4.83	5.48	5.72	11.78	10.04	6.13	6.08	4.76	6.35	37.8
	1σ	0.30	0.67	0.19	0.22	0.25	0.43	0.35	0.22	0.26	0.18	0.24	1.3
^{173}Yb	Conc	71.8	177.0	56.5	62.8	62.7	110.7	102.7	72.1	69.7	56.5	77.7	354
	1σ	2.8	6.1	2.1	2.4	2.5	4.1	3.6	2.6	2.8	2.1	2.9	12
^{175}Lu	Conc	15.82	29.9	13.90	15.17	15.42	20.60	19.44	14.33	13.18	10.94	19.17	48.7
	1σ	0.58	1.0	0.48	0.54	0.56	0.72	0.65	0.49	0.50	0.38	0.66	1.6
^{181}Ta	Conc	0.246	1.165	0.0287	0.139	0.067	0.583	0.586	0.385	0.217	0.331	0.089	2.17
	1σ	0.036	0.067	0.0085	0.022	0.025	0.051	0.037	0.029	0.033	0.029	0.016	0.11
^{232}Th	Conc	33.1	205.9	14.62	18.95	27.7	84.5	80.4	25.47	39.7	17.27	18.81	261.1
	1σ	1.2	6.9	0.54	0.70	1.1	2.9	2.7	0.89	1.4	0.62	0.68	8.8
^{238}U	Conc	122.7	234.6	124.6	128.4	133.9	174.4	170.6	134.4	159.3	96.2	174.6	360
	1σ	4.0	7.5	4.0	4.2	4.4	5.7	5.5	4.4	5.2	3.2	5.7	12
Ti-in-zirc	T (°C)	691	743.3	562	628	625	600	674.3	634	664	575	636	659
	1σ	14	8.3	22	15	22	20	9.6	11	15	17	16	14

Analysis Group		RSA03-021 variable	RSA03-022 variable	RSA03-023 variable	RSA03-024 variable	RSA03-025 variable	RSA03-026 variable	RSA03-027 variable	RSA03-029 variable	RSA03-032 variable	RSA03-034 variable	RSA03-037 variable	RSA03-038 variable
^{31}P	Conc	37	27.0	73	61	64	45	38.3	34.1	41	33.7	62	21.9
	1σ	11	6.9	18	16	19	11	9.9	9.1	11	9.3	15	7.1
^{43}Ca	Conc	<110	33	49	862	215	98	401	<36	69	158	181	113
	1σ	60	21	35	76	92	32	53	29	38	39	43	45
^{49}Ti	Conc	3.26	0.58	3.38	406	10.4	2.38	8.14	0.95	2.02	7.01	2.96	1.04
	1σ	0.76	0.25	0.77	16	1.9	0.42	0.99	0.43	0.56	0.84	0.69	0.48
^{89}Y	Conc	124.0	124.7	396	267.1	206.8	356	176.9	101.2	135.5	155.9	370	124.2
	1σ	4.5	4.5	14	9.7	7.7	13	6.6	3.8	5.1	5.9	14	4.8
^{93}Nb	Conc	1.057	1.355	3.29	2.17	1.10	2.49	1.311	1.23	1.269	1.308	2.85	1.10
	1σ	0.089	0.076	0.19	0.12	0.13	0.12	0.093	0.10	0.098	0.083	0.17	0.11
^{139}La	Conc	0.880	2.63	4.40	21.72	9.31	3.66	15.95	0.255	0.438	4.50	30.9	1.74
	1σ	0.080	0.12	0.23	0.80	0.48	0.16	0.61	0.042	0.054	0.20	1.2	0.14
^{140}Ce	Conc	6.52	29.04	35.6	74.0	77.6	42.8	57.8	4.09	7.12	45.2	64.1	23.06
	1σ	0.29	0.99	1.3	2.5	2.8	1.4	2.0	0.21	0.31	1.6	2.2	0.88
^{141}Pr	Conc	0.690	4.20	4.35	9.50	13.95	5.85	7.38	0.298	0.835	7.61	6.78	3.04
	1σ	0.060	0.16	0.21	0.35	0.59	0.21	0.29	0.040	0.066	0.28	0.29	0.17
^{146}Nd	Conc	4.48	33.5	33.4	70.4	101.0	50.7	47.0	1.37	5.65	60.8	34.0	23.4
	1σ	0.38	1.3	1.5	2.6	4.1	1.8	1.8	0.21	0.43	2.2	1.5	1.2
^{147}Sm	Conc	0.87	8.17	11.26	27.0	26.9	13.71	14.27	0.63	1.89	16.28	8.47	6.02
	1σ	0.17	0.43	0.75	1.2	1.7	0.61	0.77	0.15	0.25	0.77	0.62	0.56
^{151}Eu	Conc	0.160	2.74	4.04	9.29	7.23	4.17	4.12	0.208	0.492	4.08	1.87	2.24
	1σ	0.041	0.14	0.25	0.39	0.46	0.19	0.23	0.047	0.070	0.20	0.15	0.19
^{157}Gd	Conc	2.25	5.33	13.03	18.33	16.0	12.24	10.24	1.21	2.31	9.54	11.41	4.42
	1σ	0.27	0.31	0.78	0.84	1.1	0.54	0.59	0.20	0.26	0.50	0.70	0.45
^{159}Tb	Conc	0.624	0.940	3.20	2.74	2.02	3.06	1.488	0.504	0.765	1.453	3.28	0.937
	1σ	0.058	0.053	0.17	0.13	0.16	0.12	0.089	0.053	0.064	0.078	0.17	0.083

Analysis		RSA03-021	RSA03-022	RSA03-023	RSA03-024	RSA03-025	RSA03-026	RSA03-027	RSA03-029	RSA03-032	RSA03-034	RSA03-037	RSA03-038
^{163}Dy	Conc	7.67	10.08	37.6	23.88	16.9	30.1	14.16	6.76	9.53	12.03	34.2	9.31
	1σ	0.46	0.44	1.6	0.98	1.0	1.1	0.67	0.44	0.53	0.55	1.5	0.59
^{165}Ho	Conc	3.47	3.81	13.31	7.93	5.74	11.07	5.22	2.91	4.34	4.75	12.12	3.89
	1σ	0.17	0.15	0.52	0.31	0.31	0.39	0.22	0.16	0.20	0.20	0.48	0.21
^{166}Er	Conc	15.87	17.85	57.1	34.9	30.3	47.3	24.42	15.14	20.50	22.58	50.9	18.91
	1σ	0.69	0.66	2.1	1.3	1.4	1.6	0.94	0.68	0.84	0.84	1.9	0.86
^{169}Tm	Conc	4.73	4.55	12.75	7.36	6.41	10.40	5.62	4.38	5.16	5.13	11.06	5.38
	1σ	0.21	0.17	0.49	0.28	0.33	0.37	0.23	0.20	0.23	0.21	0.44	0.25
^{173}Yb	Conc	54.8	55.7	132.1	78.7	73.7	103.9	64.6	54.2	61.8	57.5	110.6	60.2
	1σ	2.2	2.0	4.8	2.9	3.2	3.6	2.5	2.2	2.4	2.2	4.1	2.5
^{175}Lu	Conc	14.31	12.35	20.00	17.33	16.69	20.31	13.92	11.49	15.59	13.62	17.89	12.61
	1σ	0.53	0.43	0.73	0.61	0.69	0.70	0.51	0.45	0.58	0.49	0.67	0.51
^{181}Ta	Conc	0.077	0.146	1.226	0.219	0.026	0.540	0.104	0.062	0.091	0.132	0.902	0.017
	1σ	0.018	0.017	0.087	0.026	0.016	0.035	0.019	0.017	0.020	0.019	0.071	0.010
^{232}Th	Conc	11.55	19.17	58.7	52.4	29.0	54.6	24.87	12.90	13.43	19.04	56.9	19.68
	1σ	0.47	0.69	2.1	1.9	1.2	1.9	0.92	0.53	0.54	0.71	2.1	0.80
^{238}U	Conc	137.5	142.4	164.9	144.9	133.8	158.7	131.5	139.0	138.2	128.2	174.2	149.3
	1σ	4.4	4.5	5.3	4.6	4.4	5.0	4.2	4.5	4.4	4.1	5.6	4.8
Ti-in-zirc	T (°C)	651	540	654	1220.1	745	629	723.1	569	617	710.5	644	575
	1σ	16	22	16	3.0	15	12	9.8	24	17	9.5	16	25

Analysis Group		RSA03-042 variable	RSA03-043 variable	RSA03-045 variable	RSA03-046 pristine	RSA03-047 variable	RSA03-048 variable	RSA03-051 variable	RSA03-052 variable	RSA03-053 variable	RSA03-054 variable	RSA03-055 variable	RSA03-056 variable
^{31}P	Conc	28.3	44	<140	34.9	167	66	45	24.4	230	38.6	125	54
	1σ	7.6	11	74	9.6	47	16	12	6.2	56	9.8	30	14
^{43}Ca	Conc	94	<35	<1000	<76	2870	368	<36	47	1670	175	409	161
	1σ	31	35	540	39	360	49	34	19	190	36	55	46
^{49}Ti	Conc	0.91	1.15	10.8	0.64	24.5	5.57	2.91	1.93	13.7	82.2	5.30	2.29
	1σ	0.39	0.50	5.3	0.35	4.6	0.75	0.75	0.30	2.2	4.0	0.80	0.62
^{89}Y	Conc	142.7	172.8	185.0	120.3	2247	431	217.8	128.6	1819	138.2	1001	194.6
	1σ	5.3	6.4	7.6	4.5	84	16	8.3	4.9	69	5.4	39	7.7
^{93}Nb	Conc	1.357	1.36	0.55	1.154	10.20	2.66	1.95	1.200	6.79	1.270	4.69	1.44
	1σ	0.097	0.11	0.19	0.078	0.71	0.14	0.14	0.062	0.38	0.087	0.23	0.10
^{139}La	Conc	1.79	2.01	4.08	0.0206	114.0	14.76	7.43	2.66	27.0	1.64	8.94	4.81
	1σ	0.12	0.14	0.51	0.0095	4.4	0.57	0.36	0.11	1.1	0.10	0.37	0.23
^{140}Ce	Conc	19.77	28.4	41.7	2.92	429	120.6	57.1	29.3	227.9	15.80	103.4	45.2
	1σ	0.72	1.0	2.0	0.14	15	4.1	2.0	1.0	7.8	0.59	3.6	1.6
^{141}Pr	Conc	2.86	4.18	8.60	0.040	59.1	17.59	10.00	5.02	29.4	2.10	11.55	7.01
	1σ	0.14	0.20	0.67	0.011	2.3	0.61	0.41	0.18	1.1	0.11	0.42	0.28
^{146}Nd	Conc	25.8	33.6	71.0	0.234	352	112.9	68.5	38.1	209.8	15.79	89.9	50.8
	1σ	1.1	1.5	4.9	0.067	14	3.9	2.7	1.3	7.6	0.75	3.2	2.0
^{147}Sm	Conc	7.51	9.31	18.1	0.158	109.8	31.5	20.9	8.35	63.1	3.35	28.1	10.01
	1σ	0.52	0.69	2.5	0.062	5.9	1.4	1.2	0.39	2.9	0.30	1.3	0.64
^{151}Eu	Conc	2.38	2.78	3.69	0.041	19.5	5.44	4.34	2.040	16.80	1.45	7.42	2.99
	1σ	0.16	0.20	0.60	0.017	1.2	0.26	0.28	0.098	0.79	0.11	0.34	0.19
^{157}Gd	Conc	5.27	7.53	12.4	1.20	100.8	25.6	13.16	4.91	69.2	2.87	35.2	7.47
	1σ	0.40	0.57	1.9	0.15	5.2	1.1	0.83	0.25	3.0	0.26	1.4	0.50
^{159}Tb	Conc	1.080	1.61	0.58	0.649	23.4	4.90	1.97	0.857	18.70	1.069	9.12	1.544
	1σ	0.074	0.11	0.17	0.048	1.1	0.20	0.13	0.043	0.74	0.068	0.35	0.094

Analysis		RSA03-042	RSA03-043	RSA03-045	RSA03-046	RSA03-047	RSA03-048	RSA03-051	RSA03-052	RSA03-053	RSA03-054	RSA03-055	RSA03-056
^{163}Dy	Conc	11.04	16.18	9.8	7.76	213.5	45.2	19.58	9.68	182.4	10.64	95.9	16.08
	1σ	0.55	0.81	1.4	0.39	8.5	1.7	0.95	0.39	6.6	0.51	3.4	0.75
^{165}Ho	Conc	4.10	5.49	4.44	3.21	71.5	14.28	6.63	3.83	59.9	4.03	32.7	5.60
	1σ	0.19	0.26	0.47	0.14	2.8	0.52	0.30	0.15	2.2	0.18	1.2	0.25
^{166}Er	Conc	20.87	26.7	16.9	18.04	282	57.8	31.8	18.47	231.8	19.85	135.4	26.4
	1σ	0.84	1.1	1.6	0.71	10	2.1	1.3	0.66	8.1	0.79	4.7	1.1
^{169}Tm	Conc	5.35	6.45	4.92	4.54	49.1	12.26	7.63	5.03	42.9	5.18	27.22	6.64
	1σ	0.22	0.28	0.48	0.19	2.0	0.45	0.33	0.19	1.6	0.22	0.98	0.28
^{173}Yb	Conc	70.9	75.4	69.4	57.2	440	112.1	87.9	60.4	380	61.7	248.5	65.5
	1σ	2.7	3.0	4.9	2.1	17	4.0	3.5	2.1	14	2.4	8.7	2.6
^{175}Lu	Conc	14.94	14.46	16.5	14.44	71.1	20.84	16.48	13.44	60.9	13.41	41.3	16.42
	1σ	0.54	0.55	1.0	0.51	2.7	0.73	0.63	0.46	2.2	0.49	1.4	0.61
^{181}Ta	Conc	0.098	0.318	<0.068	0.044	2.31	0.562	0.411	0.0464	1.35	0.136	1.404	0.150
	1σ	0.019	0.042	0.045	0.011	0.25	0.045	0.050	0.0074	0.12	0.021	0.083	0.024
^{232}Th	Conc	19.30	23.50	18.0	11.62	534	157.9	28.7	12.93	421	18.81	181.2	23.90
	1σ	0.73	0.91	1.2	0.45	19	5.5	1.1	0.47	15	0.72	6.4	0.91
^{238}U	Conc	154.6	149.7	118.6	127.2	447	184.8	178.1	136.6	396	147.3	263.4	137.6
	1σ	4.9	4.8	4.3	4.0	14	5.9	5.7	4.3	13	4.7	8.4	4.4
Ti-in-zirc	T (°C)	566	581	748	546	826	692	643	614	769	967.4	688	626
	1σ	23	24	37	27	17	10	17	10	14	4.5	11	17

Analysis Group		RSA03-058 variable	RSA03-060 variable	RSA03-061 variable	RSA03-062 variable	RSA03-064 variable	RSA03-067 variable	RSA03-068 variable	RSA03-071 variable	RSA03-072 variable	RSA03-073 variable	RSA03-074 variable	RSA03-075 variable
^{31}P	Conc	29.8	155	62	65	48	39	187	27.8	83	29.3	35.9	46
	1σ	7.8	37	15	16	12	11	44	7.1	20	7.5	9.7	13
^{43}Ca	Conc	<54	541	191	38	278	<65	535	333	401	198	320	288
	1σ	27	39	43	30	40	40	44	32	43	29	42	56
^{49}Ti	Conc	<0.54	4.14	1.07	2.93	1.13	<0.57	10.95	0.89	7.75	1.01	1.79	2.57
	1σ	0.27	0.43	0.40	0.69	0.34	0.39	0.78	0.28	0.78	0.29	0.41	0.70
^{89}Y	Conc	89.7	1265	446	499	220.1	192.1	1394	124.7	659	150.7	161.0	242.9
	1σ	3.6	44	16	17	7.7	6.8	49	4.4	23	5.4	5.7	8.7
^{93}Nb	Conc	0.841	4.70	2.83	3.13	1.720	1.294	5.11	1.272	3.13	1.272	1.323	1.260
	1σ	0.052	0.18	0.16	0.17	0.097	0.090	0.20	0.067	0.14	0.073	0.080	0.099
^{139}La	Conc	0.632	13.39	27.8	5.23	9.72	7.53	20.58	3.97	19.40	2.44	5.09	20.34
	1σ	0.043	0.48	1.0	0.25	0.38	0.32	0.73	0.16	0.71	0.12	0.22	0.79
^{140}Ce	Conc	5.54	147.1	90.9	53.3	69.7	41.8	223.2	30.8	202.4	21.14	34.7	120.6
	1σ	0.21	4.8	3.1	1.8	2.3	1.4	7.3	1.0	6.7	0.73	1.2	4.1
^{141}Pr	Conc	0.675	15.21	11.09	6.77	8.12	6.51	32.5	4.39	28.94	3.02	3.82	18.43
	1σ	0.039	0.50	0.42	0.28	0.30	0.26	1.1	0.16	0.97	0.12	0.16	0.66
^{146}Nd	Conc	5.65	100.0	66.9	42.7	45.8	44.6	254.2	30.0	199.8	20.65	26.6	119.4
	1σ	0.29	3.3	2.5	1.7	1.7	1.7	8.3	1.1	6.6	0.83	1.1	4.3
^{147}Sm	Conc	1.86	33.0	16.96	13.45	10.85	13.77	72.7	8.34	43.9	6.40	7.11	32.7
	1σ	0.16	1.2	0.94	0.79	0.58	0.76	2.6	0.41	1.7	0.38	0.43	1.6
^{151}Eu	Conc	0.391	8.19	4.82	3.03	2.26	2.54	17.93	2.28	14.09	1.169	2.40	7.15
	1σ	0.038	0.30	0.27	0.19	0.13	0.16	0.63	0.11	0.52	0.080	0.14	0.35
^{157}Gd	Conc	2.11	58.5	17.59	15.77	10.51	9.57	76.5	5.97	33.6	5.16	5.75	19.07
	1σ	0.16	2.0	0.91	0.83	0.53	0.56	2.6	0.30	1.3	0.30	0.35	0.97
^{159}Tb	Conc	0.440	15.01	3.89	4.53	1.819	1.535	16.90	1.042	7.37	1.136	1.192	2.70
	1σ	0.030	0.50	0.18	0.20	0.090	0.089	0.57	0.052	0.27	0.060	0.066	0.14

Analysis		RSA03-058	RSA03-060	RSA03-061	RSA03-062	RSA03-064	RSA03-067	RSA03-068	RSA03-071	RSA03-072	RSA03-073	RSA03-074	RSA03-075
^{163}Dy	Conc	5.57	142.6	46.2	49.3	18.34	14.89	156.4	10.72	65.5	12.94	13.67	21.56
	1σ	0.26	4.7	1.8	1.9	0.75	0.68	5.3	0.44	2.3	0.54	0.59	0.97
^{165}Ho	Conc	2.38	44.7	14.67	16.01	6.84	5.88	48.9	3.92	21.82	4.85	4.55	7.57
	1σ	0.10	1.5	0.55	0.59	0.26	0.24	1.6	0.15	0.75	0.19	0.18	0.32
^{166}Er	Conc	13.58	167.4	59.8	68.3	29.5	26.6	185.7	18.02	87.1	21.50	21.83	30.9
	1σ	0.52	5.5	2.2	2.4	1.1	1.0	6.2	0.66	3.0	0.80	0.83	1.2
^{169}Tm	Conc	3.28	31.9	13.03	14.92	7.21	6.60	36.5	4.41	18.41	5.59	5.03	7.08
	1σ	0.13	1.0	0.48	0.54	0.27	0.26	1.2	0.16	0.63	0.21	0.19	0.29
^{173}Yb	Conc	40.4	275.8	126.4	147.3	74.5	65.3	318	56.3	168.8	67.7	59.7	70.5
	1σ	1.5	9.1	4.5	5.2	2.7	2.5	11	2.0	5.8	2.4	2.2	2.7
^{175}Lu	Conc	10.54	44.5	19.00	21.26	16.87	15.96	51.9	11.41	29.9	14.23	12.81	17.58
	1σ	0.38	1.5	0.68	0.75	0.58	0.57	1.7	0.39	1.0	0.49	0.45	0.64
^{181}Ta	Conc	0.0327	1.082	0.805	1.175	0.080	0.125	1.452	0.0572	0.868	0.088	0.125	0.096
	1σ	0.0071	0.047	0.063	0.078	0.014	0.021	0.064	0.0091	0.050	0.013	0.017	0.021
^{232}Th	Conc	8.81	223.8	76.4	76.8	37.1	25.05	245.6	16.26	140.9	17.68	25.82	38.6
	1σ	0.34	7.6	2.7	2.7	1.3	0.91	8.3	0.58	4.8	0.64	0.92	1.4
^{238}U	Conc	87.9	241.5	174.7	183.4	164.2	136.6	277.4	134.6	203.0	145.9	135.1	154.2
	1σ	2.8	7.6	5.5	5.8	5.2	4.3	8.7	4.2	6.4	4.6	4.3	4.9
Ti-in-zirc	T (°C)	495	668.8	576	643	580	526	748.9	565	718.9	573	609	634
	1σ	40	7.8	21	16	17	36	6.0	17	8.1	16	14	18

Analysis Group		RSA03-076 variable	RSA03-077 variable	RSA03-078 variable	RSA03-079 variable	RSA01-012 metamict	RSA01-013 metamict	RSA01-020 pristine	RSA01-022 variable	RSA01-027 variable	RSA01-028 variable	RSA01-037 variable	RSA01-040 variable
^{31}P	Conc	67	27.1	45	77	620	236	324	600	125	193	560	156
	1σ	16	7.0	12	19	180	68	94	170	37	57	160	49
^{43}Ca	Conc	117	78	100	434								
	1σ	32	21	50	65								
^{49}Ti	Conc	4.15	<0.37	7.7	284	47.2	77.0	10.15	11.56	70.4	23.7	17.9	7.73
	1σ	0.59	0.21	1.1	12	2.9	3.8	0.74	0.74	3.5	1.7	1.4	0.71
^{89}Y	Conc	434	121.2	463	679	1660	2482	1660	2780	684	1603	3700	734
	1σ	15	4.4	17	25	62	92	64	110	24	56	130	25
^{93}Nb	Conc	2.67	0.988	3.03	4.44	3.64	4.51	2.84	3.66	3.20	3.01	7.95	5.58
	1σ	0.13	0.060	0.17	0.25	0.19	0.21	0.13	0.16	0.15	0.15	0.35	0.21
^{139}La	Conc	1.198	1.557	6.16	10.94	10.99	6.69	1.129	5.92	3.86	10.41	14.24	4.48
	1σ	0.074	0.082	0.29	0.49	0.45	0.28	0.059	0.23	0.17	0.41	0.55	0.17
^{140}Ce	Conc	21.12	19.13	54.8	83.4	206.7	108.8	71.2	71.0	99.5	80.2	191.7	42.4
	1σ	0.74	0.66	1.9	2.9	6.9	3.6	2.4	2.4	3.3	2.7	6.4	1.4
^{141}Pr	Conc	1.402	3.23	8.67	10.34	14.44	10.57	2.071	4.71	4.47	9.60	17.76	3.99
	1σ	0.072	0.13	0.34	0.42	0.52	0.38	0.085	0.17	0.17	0.35	0.63	0.15
^{146}Nd	Conc	9.22	26.1	57.6	82.6	122.2	90.7	22.25	41.3	34.0	77.3	135.7	28.4
	1σ	0.47	1.0	2.3	3.2	4.3	3.2	0.85	1.5	1.3	2.7	4.6	1.0
^{147}Sm	Conc	4.30	6.82	19.0	25.0	64.6	64.3	24.57	40.5	17.44	44.1	75.8	11.72
	1σ	0.31	0.39	1.0	1.4	2.5	2.4	0.94	1.5	0.73	1.7	2.7	0.51
^{151}Eu	Conc	0.966	1.576	4.26	6.72	17.82	15.64	6.72	11.37	5.14	11.41	20.85	4.93
	1σ	0.075	0.094	0.25	0.37	0.67	0.58	0.25	0.40	0.22	0.44	0.75	0.20
^{157}Gd	Conc	10.04	4.76	16.79	28.2	91.1	146.5	72.5	135.4	22.97	84.7	170.1	19.18
	1σ	0.50	0.28	0.88	1.4	3.3	5.0	2.5	4.6	0.92	3.0	5.9	0.74
^{159}Tb	Conc	3.05	0.885	3.88	6.08	18.74	35.3	19.84	36.4	4.99	20.43	44.8	5.49
	1σ	0.13	0.050	0.18	0.28	0.66	1.2	0.67	1.2	0.18	0.69	1.5	0.20

Analysis		RSA03-076	RSA03-077	RSA03-078	RSA03-079	RSA01-012	RSA01-013	RSA01-020	RSA01-022	RSA01-027	RSA01-028	RSA01-037	RSA01-040
^{163}Dy	Conc	38.8	8.22	43.4	67.3	167.1	314	189.0	342	49.8	188.7	426	58.0
	1σ	1.4	0.37	1.7	2.6	5.7	10	6.3	11	1.7	6.3	14	2.0
^{165}Ho	Conc	13.38	3.36	15.03	21.69	48.1	90.2	58.3	103.9	17.94	56.0	129.7	19.83
	1σ	0.48	0.14	0.57	0.81	1.6	3.0	1.9	3.4	0.61	1.9	4.2	0.67
^{166}Er	Conc	56.5	17.30	62.2	85.7	182.9	320	221.1	374	78.0	201.2	486	89.4
	1σ	2.0	0.66	2.3	3.2	6.0	10	7.2	12	2.6	6.6	16	3.0
^{169}Tm	Conc	12.69	4.71	13.21	17.93	34.4	59.8	44.1	71.2	17.02	37.8	92.1	20.32
	1σ	0.44	0.18	0.49	0.67	1.1	1.9	1.4	2.3	0.57	1.2	3.0	0.68
^{173}Yb	Conc	117.4	60.4	124.6	165.3	300.7	508	385	622	165.2	334	811	200.3
	1σ	4.1	2.2	4.6	6.1	9.9	16	12	20	5.4	11	26	6.5
^{175}Lu	Conc	20.88	12.81	21.35	27.39	47.2	75.1	60.2	92.4	26.98	49.9	123.2	37.6
	1σ	0.72	0.45	0.77	0.99	1.6	2.4	1.9	3.0	0.89	1.6	4.0	1.2
^{181}Ta	Conc	0.685	0.0360	0.941	1.281	0.582	0.852	0.538	0.914	1.011	0.674	2.159	1.099
	1σ	0.044	0.0080	0.070	0.095	0.044	0.049	0.029	0.039	0.051	0.043	0.096	0.051
^{232}Th	Conc	72.7	12.65	73.6	114.5	142.6	335	172.2	332	50.7	160.3	460	93.4
	1σ	2.5	0.47	2.6	4.0	4.7	11	5.6	11	1.7	5.3	15	3.1
^{238}U	Conc	151.0	140.8	144.0	182.6	287.2	333	204.2	283.6	231.5	178.0	584	302.5
	1σ	4.8	4.5	4.6	5.8	9.3	11	6.7	9.4	7.2	5.5	18	9.9
Ti-in-zirc	T (°C)	669	390	718	1155.1	898.4	958.8	742.1	753.7	947.3	822.8	794.9	718.7
	1σ	10	110	11	3.7	5.7	4.6	6.1	5.4	4.5	6.3	7.0	7.4

Analysis Group		RSA01-042 metamict	RSA01-043 metamict	RSA01-044 variable	RSA01-046 variable	RSA01-047c variable	RSA01-054 variable	RSA01-060 variable	RSA01-072 metamict	RSA01-073 metamict	RSA01-084 variable	RSA01-089 metamict	RSA01-093 metamict
^{31}P	Conc	240	154	301	124	241	102	119	260	279	260	750	139
	1σ	76	49	96	40	77	32	37	82	88	83	230	43
^{43}Ca	Conc												
	1σ												
^{49}Ti	Conc	84.4	59.0	23.2	19.7	23.7	34.4	23.5	71.2	42.6	48.6	44.9	65.0
	1σ	4.0	2.4	1.8	1.5	1.3	2.1	1.4	2.8	2.3	2.1	2.0	3.5
^{89}Y	Conc	2617	1471	2980	1289	617	982	957	2108	1125	1640	1648	2377
	1σ	88	50	100	44	21	33	33	73	39	58	55	79
^{93}Nb	Conc	9.16	5.29	7.27	3.68	3.46	4.43	2.60	5.98	4.80	3.99	7.74	4.90
	1σ	0.35	0.19	0.30	0.17	0.14	0.20	0.12	0.22	0.21	0.16	0.29	0.23
^{139}La	Conc	44.6	15.04	5.33	3.48	4.27	7.68	4.23	13.02	27.27	8.56	22.10	27.99
	1σ	1.5	0.52	0.23	0.16	0.16	0.30	0.17	0.44	0.96	0.30	0.75	0.99
^{140}Ce	Conc	312	138.1	115.8	51.5	41.0	93.8	58.7	122.7	134.7	73.8	205.3	354
	1σ	10	4.6	3.9	1.8	1.4	3.2	2.0	4.1	4.6	2.6	6.6	11
^{141}Pr	Conc	45.1	20.10	9.07	5.45	6.10	8.57	6.37	15.19	19.08	10.46	26.96	33.5
	1σ	1.5	0.66	0.34	0.21	0.21	0.32	0.23	0.50	0.66	0.35	0.88	1.1
^{146}Nd	Conc	341	133.6	74.0	46.7	45.7	64.9	49.4	119.0	127.8	72.3	221.4	196.0
	1σ	11	4.4	2.7	1.8	1.6	2.3	1.8	3.9	4.4	2.4	7.2	6.6
^{147}Sm	Conc	119.0	54.0	52.0	30.4	19.10	34.6	30.7	65.0	61.5	39.2	85.4	95.4
	1σ	4.1	1.9	2.0	1.3	0.75	1.4	1.2	2.2	2.3	1.4	2.9	3.4
^{151}Eu	Conc	71.9	15.24	17.31	7.67	7.13	8.35	6.73	18.47	10.75	10.16	31.1	20.69
	1σ	2.4	0.53	0.66	0.33	0.27	0.35	0.27	0.62	0.42	0.36	1.1	0.78
^{157}Gd	Conc	147.0	73.6	135.0	55.9	26.57	41.2	46.3	112.6	79.6	73.1	82.6	99.0
	1σ	4.9	2.4	4.6	2.0	0.96	1.6	1.6	3.6	2.8	2.4	2.8	3.5
^{159}Tb	Conc	30.2	16.14	35.0	14.67	6.35	9.10	10.97	25.76	14.85	18.28	15.83	18.10
	1σ	1.0	0.53	1.2	0.51	0.22	0.33	0.38	0.83	0.51	0.60	0.52	0.63

Analysis		RSA01-042	RSA01-043	RSA01-044	RSA01-046	RSA01-047c	RSA01-054	RSA01-060	RSA01-072	RSA01-073	RSA01-084	RSA01-089	RSA01-093
^{163}Dy	Conc	258.5	141.1	342	144.5	56.2	84.8	98.0	226.9	115.9	161.0	144.1	137.4
	1σ	8.7	4.7	12	5.0	2.0	3.0	3.4	7.7	4.1	5.7	4.8	4.7
^{165}Ho	Conc	76.8	43.0	102.5	43.7	18.86	26.30	29.80	66.3	33.2	49.2	46.9	41.2
	1σ	2.6	1.4	3.4	1.5	0.64	0.89	0.99	2.2	1.1	1.6	1.5	1.4
^{166}Er	Conc	292.1	157.4	369	160.3	77.3	108.4	111.8	239.1	119.7	184.9	198.8	157.8
	1σ	9.6	5.1	12	5.3	2.6	3.6	3.7	7.8	4.0	6.1	6.4	5.2
^{169}Tm	Conc	56.3	29.40	70.1	31.7	15.88	22.14	21.36	43.8	21.67	34.9	41.0	29.08
	1σ	1.9	0.98	2.4	1.1	0.54	0.76	0.72	1.5	0.75	1.2	1.3	0.98
^{173}Yb	Conc	519	258.6	595	279.3	153.7	216.5	193.8	378	196.3	306.6	403	265.8
	1σ	17	8.3	19	9.2	5.0	7.2	6.4	12	6.5	9.9	13	9.1
^{175}Lu	Conc	84.6	44.6	89.6	41.1	25.60	34.7	30.4	59.9	32.0	53.1	72.4	44.5
	1σ	2.8	1.5	2.9	1.4	0.85	1.2	1.0	1.9	1.1	1.7	2.4	1.5
^{181}Ta	Conc	1.191	0.768	1.239	0.826	0.276	0.734	0.356	0.771	0.472	0.552	1.279	0.750
	1σ	0.067	0.035	0.072	0.053	0.020	0.049	0.026	0.031	0.036	0.025	0.057	0.056
^{232}Th	Conc	313	150.7	264.0	176.2	28.47	97.1	93.0	220.4	115.5	185.3	206.6	150.9
	1σ	11	5.1	8.9	6.0	0.98	3.3	3.1	7.4	3.9	6.3	6.9	5.1
^{238}U	Conc	510	371	285.2	217.1	169.1	259.3	166.4	404	210.4	201.6	533	284.6
	1σ	17	12	9.4	7.2	5.6	8.4	5.4	13	6.9	6.7	17	9.3
Ti-in-zirc	T (°C)	970.8	925.1	820.5	804.0	823.0	862.6	822.1	948.7	886.5	901.7	892.5	937.2
	1σ	4.3	3.5	6.9	6.7	4.8	5.5	5.2	3.2	5.0	3.7	4.0	5.0

Analysis Group		RSA01-095 metamict	RSA01-101c variable	RSA01-102 variable	RSA01-107 metamict	RSA01-115 pristine	SWA18a-003 variable	SWA18a-004 variable	SWA18a-007 variable	SWA18a-011c pristine	SWA18a-012 variable	SWA18a-013c metamict
^{31}P	Conc	232	248	164	291	96	309	360	590	260	222	1730
	1σ	72	76	51	88	30	90	100	170	75	65	500
^{43}Ca	Conc											
	1σ											
^{49}Ti	Conc	121.3	17.6	10.1	116.0	9.85	9.04	9.93	315	10.73	18.7	241
	1σ	5.4	1.0	1.3	5.4	0.62	0.82	0.72	13	0.59	1.5	10
^{89}Y	Conc	2335	1257	830	3130	503	985	1268	1369	786	1597	8890
	1σ	78	42	28	100	17	35	46	49	28	58	320
^{93}Nb	Conc	8.43	2.34	5.73	9.60	1.313	14.47	1.685	7.96	2.155	7.84	26.63
	1σ	0.35	0.10	0.28	0.38	0.059	0.55	0.081	0.32	0.087	0.33	0.99
^{139}La	Conc	32.1	3.77	1.48	36.2	1.753	8.88	1.350	3.09	0.972	7.46	369
	1σ	1.1	0.15	0.11	1.3	0.074	0.33	0.064	0.14	0.041	0.30	12
^{140}Ce	Conc	363	39.6	31.3	323	18.64	87.3	44.5	87.4	17.12	59.0	1752
	1σ	12	1.3	1.1	11	0.63	2.9	1.5	2.9	0.56	2.0	57
^{141}Pr	Conc	40.4	5.58	1.79	46.5	1.642	6.80	1.342	2.65	1.387	6.42	214.4
	1σ	1.4	0.20	0.11	1.5	0.066	0.24	0.058	0.11	0.051	0.24	6.8
^{146}Nd	Conc	286.5	47.2	11.86	353	14.04	38.3	12.06	18.10	10.42	36.4	1049
	1σ	9.5	1.6	0.71	12	0.53	1.4	0.50	0.76	0.39	1.4	36
^{147}Sm	Conc	133.7	26.44	3.51	143.3	9.86	35.2	15.41	23.00	11.94	32.2	600
	1σ	4.6	0.97	0.37	5.0	0.41	1.4	0.62	0.94	0.45	1.3	20
^{151}Eu	Conc	39.0	9.37	2.24	48.0	2.014	6.75	4.38	6.31	1.979	4.30	236.2
	1σ	1.4	0.35	0.17	1.7	0.093	0.27	0.18	0.26	0.079	0.21	7.7
^{157}Gd	Conc	137.2	58.9	12.02	194.1	20.01	73.5	49.2	79.1	32.9	59.5	870
	1σ	4.7	2.0	0.73	6.5	0.73	2.6	1.7	2.8	1.1	2.2	29
^{159}Tb	Conc	25.66	14.93	4.28	40.0	5.14	22.10	15.03	24.63	9.85	22.76	263.3
	1σ	0.87	0.50	0.20	1.3	0.18	0.74	0.50	0.82	0.32	0.77	8.5

Analysis		RSA01-095	RSA01-101c	RSA01-102	RSA01-107	RSA01-115	SWA18a-003	SWA18a-004	SWA18a-007	SWA18a-011c	SWA18a-012	SWA18a-013c
^{163}Dy	Conc	205.8	134.9	60.3	351	51.5	215.1	147.0	250.7	93.6	217.8	2226
	1σ	7.0	4.6	2.3	12	1.7	7.1	4.8	8.3	3.1	7.2	72
^{165}Ho	Conc	59.5	41.7	24.34	99.5	16.21	62.0	44.5	79.4	28.19	64.2	550
	1σ	2.0	1.4	0.87	3.3	0.54	2.0	1.4	2.6	0.91	2.1	18
^{166}Er	Conc	236.9	157.0	129.4	353	66.3	233.3	177.0	305.0	105.5	250.0	1748
	1σ	7.7	5.1	4.4	11	2.2	7.5	5.7	9.8	3.4	8.1	56
^{169}Tm	Conc	48.0	28.75	33.4	64.3	13.49	47.7	36.7	63.2	21.34	53.6	308
	1σ	1.6	0.93	1.1	2.1	0.44	1.6	1.2	2.1	0.70	1.8	10
^{173}Yb	Conc	489	247.7	409	566	134.2	482	356	673	199.2	515	2674
	1σ	16	8.4	14	19	4.5	16	12	22	6.5	17	86
^{175}Lu	Conc	84.2	41.2	74.3	82.8	24.77	63.5	52.3	84.5	31.3	76.8	309.1
	1σ	2.8	1.4	2.5	2.7	0.82	2.1	1.7	2.7	1.0	2.5	9.9
^{181}Ta	Conc	0.967	0.573	1.373	1.260	0.199	4.23	0.420	0.690	1.049	1.264	4.61
	1σ	0.062	0.032	0.091	0.078	0.015	0.16	0.025	0.042	0.040	0.069	0.17
^{232}Th	Conc	269.5	105.5	184.1	328	80.5	222.3	128.5	303.5	73.7	165.0	1793
	1σ	9.0	3.5	6.3	11	2.7	7.3	4.2	10.0	2.4	5.5	59
^{238}U	Conc	567	97.0	513	457	150.7	456	136.6	299	190.6	329	3100
	1σ	18	3.2	17	15	5.1	15	4.6	10	6.5	11	110
Ti-in-zirc	T (°C)	1020.8	792.8	742	1014.3	739.5	732.0	740.2	1173.5	747.1	799.1	1126.9
	1σ	4.0	5.1	10	4.2	5.3	7.5	6.1	3.5	4.6	6.9	3.6

Analysis		SWA18a-015	SWA18a-016	SWA18a-017c	SWA18a-017r	SWA18a-018	SWA18a-019	SWA18a-020	SWA18a-021	SWA18a-022	SWA18a-023
Group		metamict	variable	variable	variable	variable	metamict	metamict	variable	pristine	variable
^{31}P	Conc	580	470	690	570	610	690	410	480	1160	318
	1σ	170	140	200	170	220	200	120	140	330	91
^{43}Ca	Conc										
	1σ										
^{49}Ti	Conc	36.5	16.4	18.2	10.58	69.3	86.0	88.3	11.52	3.51	15.8
	1σ	1.8	1.3	1.6	0.67	3.5	3.7	3.7	0.89	0.24	1.1
^{89}Y	Conc	3310	1617	1813	1172	4650	4730	2411	1573	2325	1367
	1σ	120	60	68	41	170	160	84	55	81	48
^{93}Nb	Conc	33.3	7.28	22.28	12.16	34.7	58.8	15.76	4.63	17.87	18.20
	1σ	1.2	0.31	0.89	0.45	1.3	2.1	0.58	0.20	0.66	0.70
^{139}La	Conc	101.4	1.756	16.19	5.88	48.6	261.3	134.3	6.65	1.315	7.27
	1σ	3.4	0.095	0.60	0.21	1.7	8.7	4.5	0.25	0.051	0.28
^{140}Ce	Conc	487	170.7	64.6	32.2	360	913	681	109.2	26.84	62.9
	1σ	16	5.6	2.2	1.0	12	29	22	3.5	0.86	2.0
^{141}Pr	Conc	74.1	1.808	7.60	3.85	33.2	201.3	83.1	5.49	0.573	4.73
	1σ	2.4	0.086	0.29	0.14	1.1	6.5	2.7	0.20	0.023	0.18
^{146}Nd	Conc	392	17.70	37.4	21.19	176.3	970	384	37.3	5.07	24.47
	1σ	14	0.79	1.6	0.78	5.9	32	13	1.4	0.20	0.97
^{147}Sm	Conc	250.8	27.1	30.4	21.43	126.8	616	165.3	38.1	10.14	19.94
	1σ	8.5	1.1	1.3	0.79	4.6	20	5.5	1.4	0.37	0.83
^{151}Eu	Conc	26.26	10.19	4.19	2.63	23.13	43.6	19.07	10.78	0.726	3.84
	1σ	0.88	0.40	0.22	0.11	0.85	1.4	0.64	0.40	0.033	0.17
^{157}Gd	Conc	395	102.1	65.0	64.4	246.5	725	256.6	109.5	65.5	46.9
	1σ	13	3.6	2.5	2.2	8.2	24	8.4	3.7	2.2	1.7
^{159}Tb	Conc	114.8	29.56	23.63	23.24	76.1	221.1	65.7	32.1	27.88	15.63
	1σ	3.7	0.99	0.81	0.75	2.7	7.1	2.1	1.1	0.89	0.53

Analysis		SWA18a-015	SWA18a-016	SWA18a-017c	SWA18a-017r	SWA18a-018	SWA18a-019	SWA18a-020	SWA18a-021	SWA18a-022	SWA18a-023
^{163}Dy	Conc	950	297.9	223.4	230.0	669	1671	546	309	355	154.5
	1σ	31	9.9	7.5	7.5	23	54	18	10	12	5.1
^{165}Ho	Conc	223.2	94.2	67.6	68.8	175.8	342	140.6	90.9	133.8	49.3
	1σ	7.2	3.1	2.2	2.2	5.9	11	4.5	3.0	4.3	1.6
^{166}Er	Conc	725	350	298.7	265.5	601	994	483	333	575	205.2
	1σ	23	11	9.7	8.5	19	32	15	11	18	6.7
^{169}Tm	Conc	138.5	72.7	75.7	57.4	118.0	181.2	93.8	68.1	124.6	47.3
	1σ	4.6	2.4	2.6	1.9	3.8	5.8	3.0	2.2	4.0	1.6
^{173}Yb	Conc	1261	759	873	597	1119	1617	851	651	1237	510
	1σ	41	25	29	19	36	52	27	21	40	16
^{175}Lu	Conc	148.8	94.6	151.0	91.8	139.1	164.1	115.8	93.1	182.1	80.5
	1σ	4.8	3.1	4.9	3.0	4.5	5.3	3.7	3.0	5.9	2.6
^{181}Ta	Conc	1.513	0.882	9.18	5.31	5.12	3.10	4.89	0.639	8.32	17.27
	1σ	0.059	0.052	0.34	0.18	0.19	0.11	0.17	0.037	0.27	0.57
^{232}Th	Conc	568	485	157.2	94.5	685	528	571	343	359	176.0
	1σ	19	16	5.2	3.1	23	17	19	11	12	5.8
^{238}U	Conc	506	419	832	530	1498	1121	1030	358	1823	1000
	1σ	18	15	30	18	49	39	36	13	64	36
Ti-in-zirc	T (°C)	868.9	786.3	796.1	745.8	945.3	973.3	976.8	753.4	656.5	782.9
	1σ	4.4	7.0	7.7	5.3	4.6	3.7	3.6	6.5	5.3	6.1

Analysis		SWA18a-028	SWA18a-029	SWA18a-031	SWA18a-033	SWA18a-037	SWA18a-038	SWA18a-039	SWA18a-047	SWA18a-048	SWA18a-050
Group		variable	variable	variable	pristine	variable	metamict	variable	pristine	variable	variable
^{31}P	Conc	380	530	630	286	870	530	196	570	270	300
	1σ	140	150	180	82	420	250	92	210	130	140
^{43}Ca	Conc										
	1σ										
^{49}Ti	Conc	19.01	11.71	12.9	9.96	13.3	259	5.97	6.60	7.80	6.89
	1σ	0.95	0.81	1.4	0.71	1.5	11	0.59	0.54	0.83	0.55
^{89}Y	Conc	2786	1632	1726	1482	2860	4540	1006	1664	1158	1381
	1σ	100	57	61	52	110	170	37	60	43	52
^{93}Nb	Conc	20.40	6.24	5.92	10.75	7.67	40.3	14.41	6.03	11.97	4.26
	1σ	0.76	0.25	0.29	0.43	0.33	1.5	0.54	0.24	0.47	0.17
^{139}La	Conc	34.8	2.36	4.48	1.935	2.63	165.1	2.029	2.47	2.13	4.26
	1σ	1.2	0.10	0.22	0.084	0.14	5.7	0.085	0.10	0.10	0.16
^{140}Ce	Conc	260.5	140.0	96.5	35.2	31.0	588	29.7	19.62	55.3	73.1
	1σ	9.0	4.5	3.2	1.1	1.1	20	1.0	0.70	1.9	2.5
^{141}Pr	Conc	16.46	3.16	4.71	1.660	2.43	80.9	1.872	2.571	1.724	4.04
	1σ	0.53	0.12	0.20	0.068	0.11	2.6	0.071	0.096	0.078	0.14
^{146}Nd	Conc	80.7	27.8	27.4	10.54	22.89	382	9.84	13.22	11.48	25.73
	1σ	2.7	1.0	1.2	0.45	0.96	12	0.39	0.51	0.51	0.90
^{147}Sm	Conc	61.4	35.5	29.2	12.02	37.1	197.6	9.52	14.16	12.40	26.58
	1σ	2.2	1.3	1.3	0.50	1.5	6.7	0.40	0.59	0.58	0.99
^{151}Eu	Conc	15.38	10.27	7.16	2.089	4.50	27.37	1.527	0.937	3.17	5.45
	1σ	0.54	0.37	0.33	0.096	0.21	0.91	0.070	0.054	0.15	0.20
^{157}Gd	Conc	140.8	110.7	93.5	43.0	136.1	313	24.50	39.0	39.6	62.9
	1σ	4.6	3.7	3.4	1.5	4.8	11	0.89	1.4	1.5	2.2
^{159}Tb	Conc	38.6	32.7	29.4	15.84	39.6	89.3	9.05	15.49	12.38	18.04
	1σ	1.4	1.1	1.0	0.52	1.3	2.9	0.30	0.56	0.42	0.59

Analysis		SWA18a-028	SWA18a-029	SWA18a-031	SWA18a-033	SWA18a-037	SWA18a-038	SWA18a-039	SWA18a-047	SWA18a-048	SWA18a-050
^{163}Dy	Conc	331	314	292.9	188.0	348	694	101.4	175.1	129.6	174.8
	1σ	11	10	9.8	6.2	11	22	3.3	6.0	4.3	5.7
^{165}Ho	Conc	90.9	96.9	87.4	67.5	92.3	160.8	34.1	58.7	41.4	50.9
	1σ	3.0	3.2	2.9	2.2	3.0	5.2	1.1	2.0	1.4	1.7
^{166}Er	Conc	326	362	327	290.2	305.5	533	147.8	245.0	167.6	191.4
	1σ	10	12	11	9.4	9.8	17	4.7	7.9	5.4	6.1
^{169}Tm	Conc	62.2	73.6	67.4	66.7	56.7	105.3	34.9	53.5	35.1	39.1
	1σ	2.0	2.4	2.2	2.2	1.8	3.4	1.1	1.7	1.1	1.3
^{173}Yb	Conc	543	710	683	711	477	966	385	535	338	382
	1σ	17	23	22	23	15	31	12	17	11	12
^{175}Lu	Conc	84.1	97.7	95.8	101.4	71.9	142.2	57.4	77.4	48.0	54.9
	1σ	2.7	3.2	3.2	3.3	2.3	4.6	1.8	2.5	1.6	1.8
^{181}Ta	Conc	6.41	0.795	0.879	2.69	1.616	17.58	4.24	1.992	3.55	0.679
	1σ	0.21	0.039	0.063	0.10	0.081	0.57	0.14	0.077	0.13	0.030
^{232}Th	Conc	821	463	289.4	248.8	133.3	397	109.2	111.4	140.5	220.4
	1σ	27	15	9.5	8.1	4.4	13	3.6	3.7	4.6	7.2
^{238}U	Conc	781	392	389	1187	277.9	2708	700	635	326	261.1
	1σ	26	14	14	44	8.9	87	22	21	11	8.6
Ti-in-zirc	T (°C)	800.6	754.9	763.6	740.5	766.3	1139.1	697.4	705.6	719.4	709.1
	1σ	4.3	5.9	9.0	6.0	9.6	3.8	7.8	6.6	8.6	6.4

Analysis		SWA18a-056	SWA18a-057	SWA18a-058	SWA18a-059	SWA18a-061	SWA18a-063	SWA18a-064	SWA18a-066	SWA18a-069	RSA05-003
Group		variable	variable	pristine	variable	metamict	metamict	pristine	metamict	pristine	variable
^{31}P	Conc	290	380	550	250	1260	780	560	800	420	1860
	1σ	120	160	230	110	530	330	240	290	180	440
^{43}Ca	Conc										
	1σ										
^{49}Ti	Conc	12.0	13.26	4.58	12.2	55.0	43.4	7.88	14.27	9.16	42.9
	1σ	1.1	0.97	0.40	1.0	2.5	2.4	0.62	0.70	0.67	2.2
^{89}Y	Conc	1093	1474	1597	1052	13190	6690	1401	4140	2582	3620
	1σ	40	54	58	39	480	250	52	150	96	120
^{93}Nb	Conc	3.80	4.29	6.85	2.81	80.4	41.3	7.25	9.97	4.40	44.9
	1σ	0.18	0.18	0.26	0.13	3.0	1.6	0.29	0.38	0.18	1.5
^{139}La	Conc	2.19	4.18	0.974	1.493	712	146.6	0.282	248.9	3.53	41.1
	1σ	0.11	0.17	0.043	0.077	25	5.2	0.021	8.5	0.14	1.4
^{140}Ce	Conc	48.5	75.0	12.50	31.5	2105	748	15.85	604	116.2	253.6
	1σ	1.7	2.6	0.44	1.1	74	27	0.58	21	4.2	8.3
^{141}Pr	Conc	1.458	2.323	0.747	1.291	323	117.1	0.419	47.5	4.24	30.59
	1σ	0.073	0.092	0.031	0.061	10	3.8	0.023	1.5	0.15	0.98
^{146}Nd	Conc	12.03	16.65	4.94	10.30	1618	614	3.56	209.8	37.6	182.0
	1σ	0.56	0.65	0.20	0.46	53	20	0.18	6.9	1.3	6.1
^{147}Sm	Conc	14.08	19.49	6.54	12.55	873	403	6.48	97.7	47.3	114.4
	1σ	0.67	0.79	0.28	0.58	31	14	0.30	3.5	1.8	3.8
^{151}Eu	Conc	3.48	4.50	0.398	4.03	81.2	40.9	0.311	20.06	14.00	15.81
	1σ	0.17	0.18	0.025	0.17	2.6	1.4	0.026	0.71	0.48	0.55
^{157}Gd	Conc	42.3	54.7	31.5	41.9	1117	551	32.2	218.6	137.8	204.3
	1σ	1.6	1.9	1.1	1.5	37	19	1.2	7.2	4.8	6.6
^{159}Tb	Conc	13.14	17.80	12.12	12.81	301.9	164.8	12.08	57.8	37.5	54.1
	1σ	0.45	0.59	0.39	0.43	9.6	5.3	0.40	2.1	1.2	1.8

Analysis		SWA18a-056	SWA18a-057	SWA18a-058	SWA18a-059	SWA18a-061	SWA18a-063	SWA18a-064	SWA18a-066	SWA18a-069	RSA05-003
^{163}Dy	Conc	128.2	177.3	149.8	119.5	2377	1279	135.8	515	340	471
	1σ	4.4	6.0	5.0	4.1	80	43	4.7	18	12	15
^{165}Ho	Conc	40.0	52.5	55.3	35.9	532	285.7	48.3	146.3	93.8	126.4
	1σ	1.3	1.7	1.8	1.2	17	9.3	1.6	4.9	3.1	4.2
^{166}Er	Conc	157.0	200.5	242.7	139.9	1667	891	205.5	517	335	444
	1σ	5.1	6.4	7.7	4.5	53	28	6.6	17	11	14
^{169}Tm	Conc	31.8	41.3	54.4	27.19	304.5	170.6	45.9	101.3	65.4	80.5
	1σ	1.1	1.3	1.7	0.89	9.7	5.5	1.5	3.3	2.1	2.7
^{173}Yb	Conc	304.8	410	535	243.6	2838	1571	472	936	612	711
	1σ	9.9	13	17	7.9	90	50	15	30	20	23
^{175}Lu	Conc	45.9	54.3	86.8	41.5	343	179.8	69.0	126.8	76.4	104.8
	1σ	1.5	1.8	2.8	1.4	11	5.8	2.2	4.1	2.5	3.4
^{181}Ta	Conc	0.389	0.572	2.223	0.450	1.872	1.551	2.506	3.38	0.561	1.539
	1σ	0.030	0.032	0.078	0.029	0.065	0.066	0.091	0.11	0.027	0.069
^{232}Th	Conc	118.0	209.1	90.8	82.5	1134	709	117.6	680	440	297
	1σ	3.9	6.8	3.0	2.7	37	23	3.8	23	14	10
^{238}U	Conc	133.4	250.5	375	100.5	1022	927	359	514	362	327
	1σ	4.3	8.1	12	3.3	33	31	12	17	12	10
Ti-in-zirc	T (°C)	757.2	766.2	676.5	758.9	916.6	888.7	720.3	773.1	733.2	887.4
	1σ	8.1	6.3	6.7	7.0	4.0	5.0	6.4	4.2	6.1	4.5

Analysis Group		RSA05-005 variable	RSA05-008 variable	RSA05-010 pristine	RSA05-011 pristine	RSA05-012 pristine	RSA05-013 variable	RSA05-015 variable	RSA05-016 metamict	RSA05-022 metamict	RSA05-024 variable	RSA05-026 variable	RSA05-028 variable
^{31}P	Conc	1460	1570	890	378	1690	900	254	1820	950	2210	450	890
	1σ	350	370	210	91	410	220	62	440	230	540	110	220
^{43}Ca	Conc												
	1σ												
^{49}Ti	Conc	102.0	40.6	18.29	42.1	28.0	87.2	34.6	235	1105	458	51.7	197.8
	1σ	4.7	1.8	0.98	1.9	1.3	3.9	1.8	10	41	17	2.2	8.5
^{89}Y	Conc	5760	3890	3150	2312	3870	7120	2612	8480	4560	4860	4270	7700
	1σ	190	130	110	78	130	240	89	290	150	160	150	260
^{93}Nb	Conc	142.2	59.3	24.53	49.9	33.1	135.4	52.9	259.3	43.6	128.2	63.4	187.2
	1σ	4.8	2.0	0.85	1.7	1.1	4.7	1.9	9.0	1.5	4.4	2.2	6.5
^{139}La	Conc	89.3	48.8	49.0	17.71	76.8	72.1	27.41	159.4	1493	76.3	47.6	86.0
	1σ	3.0	1.6	1.6	0.60	2.6	2.4	0.94	5.4	49	2.5	1.6	2.9
^{140}Ce	Conc	581	304.1	245.7	136.1	400	623	223.1	1198	2974	420	337	742
	1σ	19	10.0	8.1	4.5	13	21	7.5	40	100	14	11	25
^{141}Pr	Conc	73.9	33.3	24.03	17.53	34.5	74.2	27.33	151.8	282	55.9	39.7	103.4
	1σ	2.4	1.1	0.77	0.56	1.1	2.4	0.88	4.8	11	2.2	1.6	4.2
^{146}Nd	Conc	428	190.2	134.8	107.3	188.3	472	164.7	894	1013	320	225.7	571
	1σ	14	6.4	4.6	3.6	6.4	16	5.7	31	32	10	7.3	19
^{147}Sm	Conc	248.7	99.9	59.4	72.0	64.0	322	113.3	532	270.7	211.2	139.0	386
	1σ	8.2	3.3	2.0	2.4	2.1	10	3.7	17	8.9	6.9	4.6	13
^{151}Eu	Conc	29.7	19.29	9.94	12.31	14.01	42.9	13.17	72.6	34.9	22.80	20.14	47.1
	1σ	1.0	0.63	0.34	0.41	0.46	1.4	0.45	2.3	1.2	0.77	0.68	1.6
^{157}Gd	Conc	387	183.4	110.1	125.3	139.3	522	175.9	723	315	338	229.6	559
	1σ	12	5.9	3.6	4.0	4.5	17	5.7	23	10	11	7.5	18
^{159}Tb	Conc	109.7	49.0	30.0	34.9	40.5	136.8	46.1	177.0	67.8	93.1	63.4	162.0
	1σ	3.7	1.6	1.0	1.2	1.4	4.6	1.6	6.1	2.3	3.2	2.2	5.8

Analysis		RSA05-005	RSA05-008	RSA05-010	RSA05-011	RSA05-012	RSA05-013	RSA05-015	RSA05-016	RSA05-022	RSA05-024	RSA05-026	RSA05-028
^{163}Dy	Conc	918	459	316	305.2	412	1112	371	1331	552	753	545	1278
	1σ	29	15	10	9.8	13	36	12	43	18	24	18	41
^{165}Ho	Conc	210.6	131.5	103.7	79.6	127.5	262.9	89.8	288.8	144.7	178.3	146.3	285.6
	1σ	7.1	4.4	3.5	2.7	4.3	9.0	3.1	10.0	4.9	6.1	5.0	9.9
^{166}Er	Conc	693	485	412	290.4	489	838	295.5	885	500	573	514	884
	1σ	22	15	13	9.3	16	27	9.4	28	16	18	16	28
^{169}Tm	Conc	117.3	91.3	81.8	56.7	95.0	140.1	53.0	147.5	91.2	96.7	93.5	151.9
	1σ	3.9	3.0	2.7	1.9	3.2	4.7	1.8	5.0	3.1	3.3	3.3	5.4
^{173}Yb	Conc	963	819	740	545	869	1156	462	1213	782	798	805	1209
	1σ	31	26	24	17	28	37	15	39	25	26	26	39
^{175}Lu	Conc	134.1	124.6	116.5	98.4	130.5	159.8	70.0	167.4	117.5	120.3	120.4	161.9
	1σ	4.3	4.0	3.8	3.2	4.2	5.2	2.3	5.4	3.8	3.9	3.9	5.3
^{181}Ta	Conc	2.97	2.023	3.61	1.457	4.75	3.15	3.09	4.10	1.913	3.97	2.753	2.74
	1σ	0.12	0.074	0.13	0.055	0.16	0.11	0.11	0.14	0.072	0.14	0.097	0.13
^{232}Th	Conc	572	293	435	213.3	552	875	191.0	297	297	523	352	368
	1σ	20	10	15	7.4	19	30	6.6	10	10	18	12	13
^{238}U	Conc	620	439	648	203.9	905	693	382	549	436	716	566	516
	1σ	20	14	21	6.5	29	22	12	17	14	23	18	16
Ti-in-zirc	T (°C)	996.4	881.0	796.8	885.1	840.3	975.1	863.2	1122.8	1439.2	1243.6	909.2	1094.7
	1σ	4.2	4.0	4.7	3.9	4.0	4.0	4.7	3.8	1.9	2.6	3.6	3.7

Analysis Group		RSA05-029 metamict	RSA05-030 variable	RSA05-031 variable	RSA05-036 metamict	RSA05-039 variable	RSA05-040 variable	RSA05-042 variable	RSA05-043 metamict	RSA05-044 variable	RSA05-046 variable	RSA05-049 variable	RSA05-051 variable
^{31}P	Conc	950	840	760	540	860	690	382	1140	2480	4400	920	3410
	1σ	230	210	190	130	210	170	93	280	600	1100	220	830
^{43}Ca	Conc												
	1σ												
^{49}Ti	Conc	355	51.4	60.2	219.0	133.4	92.0	51.4	613	45.7	94.8	51.3	63.2
	1σ	14	2.3	2.8	9.0	5.6	4.4	2.3	23	2.5	4.1	3.0	2.5
^{89}Y	Conc	9870	2864	3980	10880	5790	2744	3210	13310	2483	5900	3230	4510
	1σ	340	98	140	380	200	94	110	460	85	200	110	160
^{93}Nb	Conc	269.5	68.2	35.8	351	187.4	17.24	59.9	350	11.39	111.8	49.6	91.2
	1σ	9.3	2.4	1.3	12	6.4	0.65	2.1	12	0.44	3.9	1.8	3.2
^{139}La	Conc	128.4	57.4	40.8	327	83.6	23.12	24.19	184.0	26.91	79.0	30.2	58.9
	1σ	4.3	1.9	1.4	11	2.8	0.83	0.83	6.2	0.95	2.7	1.1	2.0
^{140}Ce	Conc	1053	288.9	307	1604	516	183.1	191.9	1462	151.8	487	234.6	368
	1σ	36	10.0	11	56	17	6.2	6.5	49	5.2	17	8.1	13
^{141}Pr	Conc	143.5	38.0	40.7	192.2	70.3	24.28	24.58	202.1	14.93	68.3	27.0	48.4
	1σ	5.8	1.6	1.7	8.3	2.7	0.97	0.97	7.9	0.62	2.8	1.1	2.0
^{146}Nd	Conc	818	216.6	234.0	975	397	148.2	128.4	1159	83.3	394	172.0	274.8
	1σ	26	7.1	7.7	32	13	5.0	4.2	37	2.9	13	5.8	8.8
^{147}Sm	Conc	531	114.4	152.0	533	251.8	78.9	79.7	751	40.1	224.0	109.3	153.3
	1σ	17	3.9	5.1	18	8.5	2.9	2.8	25	1.6	7.6	4.0	5.1
^{151}Eu	Conc	65.6	16.86	20.88	73.9	33.1	10.14	10.12	100.4	4.92	26.79	14.53	21.55
	1σ	2.2	0.58	0.73	2.5	1.2	0.43	0.37	3.4	0.23	0.95	0.58	0.74
^{157}Gd	Conc	756	188.7	238.3	761	379	135.7	137.6	1095	86.3	367	191.2	250.2
	1σ	25	6.2	7.9	25	12	4.7	4.6	35	3.0	12	6.5	8.2
^{159}Tb	Conc	213.4	50.0	66.7	211.0	111.0	33.9	42.1	308	24.92	100.2	50.1	67.4
	1σ	7.6	1.8	2.4	7.8	4.0	1.2	1.5	11	0.94	3.7	1.9	2.5

Analysis		RSA05-029	RSA05-030	RSA05-031	RSA05-036	RSA05-039	RSA05-040	RSA05-042	RSA05-043	RSA05-044	RSA05-046	RSA05-049	RSA05-051
^{163}Dy	Conc	1676	416	546	1698	903	302.8	401	2403	250.5	848	450	576
	1σ	54	13	18	55	29	9.9	13	77	8.2	27	15	19
^{165}Ho	Conc	345	102.8	136.1	387	212.5	87.8	111.0	471	81.0	208.6	113.0	149.0
	1σ	12	3.6	4.8	14	7.0	2.9	3.7	16	2.7	6.9	3.8	5.0
^{166}Er	Conc	1019	350	462	1196	671	335	400	1373	326	706	394	528
	1σ	33	11	15	38	21	11	13	44	10	23	13	17
^{169}Tm	Conc	163.6	65.0	84.3	195.2	115.1	64.2	76.2	227.3	67.0	123.4	72.5	95.7
	1σ	5.8	2.3	3.1	7.2	4.2	2.4	2.8	8.4	2.5	4.7	2.8	3.8
^{173}Yb	Conc	1265	577	715	1510	944	578	652	1748	592	1007	645	798
	1σ	41	19	23	49	31	19	21	57	19	33	21	26
^{175}Lu	Conc	166.6	91.1	109.1	207.7	133.3	89.6	100.7	232.7	96.0	149.7	94.9	125.1
	1σ	5.5	3.0	3.6	6.9	4.3	2.9	3.2	7.5	3.1	4.8	3.1	4.0
^{181}Ta	Conc	3.81	7.77	1.508	4.90	3.71	1.341	3.93	5.05	1.849	2.76	4.68	2.671
	1σ	0.13	0.26	0.066	0.18	0.15	0.080	0.15	0.20	0.093	0.12	0.20	0.095
^{232}Th	Conc	314	226.0	238.7	852	427	176.6	349	477	234.1	592	450	299
	1σ	11	7.7	8.2	29	15	6.1	12	16	8.0	20	15	10
^{238}U	Conc	540	710	428	1108	502	281.4	472	700	393	609	515	484
	1σ	17	22	14	35	16	8.9	15	22	12	19	16	15
Ti-in-zirc	T (°C)	1195.1	908.5	927.7	1111.2	1034.5	982.3	908.5	1303.2	894.5	986.3	908.4	933.6
	1σ	2.9	3.9	4.1	3.4	3.7	4.4	4.0	2.3	5.0	3.8	5.4	3.3

Analysis Group		RSA05-057 variable	RSA05-060 pristine	RSA05-066 metamict	RSA05-067 variable	RSA05-070 metamict	RSA02-002 variable	RSA02-003 pristine	RSA02-004c pristine	RSA02-005c pristine	RSA02-006r variable	RSA02-007c pristine	RSA02-008c pristine
^{31}P	Conc	530	316	850	440	630	436	234	560	445	209	204	294
	1σ	130	76	210	110	150	90	48	120	92	43	42	61
^{43}Ca	Conc						162	<61	323	211	1511	221	1718
	1σ						48	24	31	27	77	23	77
^{49}Ti	Conc	11.86	5.44	371	45.7	2061	19.9	5.79	6.17	9.25	12.70	6.95	1138
	1σ	0.63	0.32	13	1.9	71	1.7	0.32	0.49	0.52	0.80	0.41	39
^{89}Y	Conc	2538	1029	16080	3570	13530	3500	1563	2198	1863	946	1209	2417
	1σ	84	34	530	120	450	120	52	73	62	31	40	80
^{93}Nb	Conc	25.32	10.60	347	55.4	511	15.61	6.28	18.36	62.3	12.13	8.50	11.03
	1σ	0.84	0.36	11	1.8	17	0.60	0.22	0.63	2.1	0.43	0.29	0.38
^{139}La	Conc	8.87	5.39	253.0	36.8	400	9.64	2.173	3.45	7.20	14.66	0.290	14.73
	1σ	0.30	0.18	8.3	1.2	13	0.40	0.080	0.14	0.25	0.51	0.018	0.50
^{140}Ce	Conc	97.2	40.9	1842	261.8	1966	97.6	18.46	44.5	48.9	107.2	14.46	83.8
	1σ	3.3	1.4	65	9.4	72	3.2	0.60	1.5	1.6	3.5	0.48	2.7
^{141}Pr	Conc	7.45	4.64	239.2	32.0	241	9.31	1.668	4.17	5.36	12.53	0.257	10.54
	1σ	0.29	0.19	10.0	1.4	11	0.36	0.059	0.15	0.18	0.42	0.015	0.35
^{146}Nd	Conc	48.1	25.88	1408	194.1	1350	81.4	11.49	33.2	31.9	97.9	3.26	83.0
	1σ	1.6	0.86	45	6.2	43	3.0	0.40	1.2	1.1	3.3	0.15	2.7
^{147}Sm	Conc	35.6	13.70	888	116.7	713	45.6	7.00	16.46	12.11	43.2	5.07	37.7
	1σ	1.2	0.48	28	3.8	23	1.9	0.27	0.65	0.46	1.5	0.22	1.3
^{151}Eu	Conc	7.70	1.966	118.7	19.86	110.3	7.77	2.209	3.74	2.68	5.23	1.133	5.74
	1σ	0.27	0.076	3.9	0.67	3.6	0.36	0.083	0.15	0.11	0.20	0.052	0.20
^{157}Gd	Conc	92.1	28.02	1316	197.2	1017	108.4	29.3	53.8	29.8	58.6	29.3	81.2
	1σ	3.0	0.93	42	6.4	33	4.1	1.0	2.0	1.1	2.2	1.1	3.0
^{159}Tb	Conc	26.1	8.33	367	53.6	280	29.7	10.94	18.29	10.84	12.50	10.52	22.32
	1σ	1.1	0.35	16	2.4	13	1.0	0.36	0.60	0.36	0.42	0.35	0.73

Analysis		RSA05-057	RSA05-060	RSA05-066	RSA05-067	RSA05-070	RSA02-002	RSA02-003	RSA02-004c	RSA02-005c	RSA02-006r	RSA02-007c	RSA02-008c
^{163}Dy	Conc	259.0	89.8	2924	459	2486	347	139.9	221.2	146.9	109.8	127.6	242.9
	1σ	8.3	2.9	93	15	79	11	4.5	7.2	4.8	3.6	4.2	8.0
^{165}Ho	Conc	79.7	31.7	610	115.5	526	125.6	55.9	81.8	61.9	32.0	47.0	87.9
	1σ	3.0	1.2	24	4.7	22	4.1	1.8	2.6	2.0	1.1	1.5	2.8
^{166}Er	Conc	315	146.7	1740	391	1545	502	250.0	336	297.4	120.7	192.7	365
	1σ	10	4.7	55	13	49	16	8.0	11	9.5	3.9	6.2	12
^{169}Tm	Conc	60.7	32.6	242	70.4	229	103.2	52.8	67.3	67.6	24.62	38.9	72.9
	1σ	2.6	1.4	12	3.4	12	3.4	1.7	2.2	2.2	0.84	1.3	2.5
^{173}Yb	Conc	556	343	1850	631	1738	933	500	605	669	223.5	360	665
	1σ	18	11	61	21	58	30	16	19	21	7.2	11	21
^{175}Lu	Conc	87.8	60.4	240.6	100.5	224.3	144.6	86.0	93.6	114.0	35.5	56.2	117.3
	1σ	2.9	2.0	8.3	3.5	7.9	4.7	2.8	3.0	3.7	1.2	1.8	3.8
^{181}Ta	Conc	2.222	9.77	4.10	9.01	9.03	3.95	1.688	4.95	21.87	2.72	2.479	2.476
	1σ	0.081	0.32	0.15	0.30	0.31	0.18	0.059	0.17	0.70	0.10	0.087	0.089
^{232}Th	Conc	164.6	57.1	608	196.8	1602	97.2	31.3	65.4	44.9	148.8	23.11	60.8
	1σ	5.6	1.9	21	6.7	54	3.4	1.1	2.2	1.5	5.1	0.80	2.1
^{238}U	Conc	280.0	679	1085	708	1845	204.8	63.0	137.5	138.5	430	54.1	118.1
	1σ	8.8	21	34	22	58	6.6	2.0	4.4	4.4	14	1.8	3.8
Ti-in-zirc	T (°C)	756.0	690.0	1203.2	894.6	1611.25	805.0	695.0	700.1	734.0	762.3	709.8	1446.6
	1σ	4.5	4.7	2.3	3.6	0.44	7.6	4.5	6.3	4.7	5.4	4.8	1.2

Analysis Group		RSA02-010 pristine	RSA02-014 pristine	RSA02-019c variable	RSA02-026 pristine	RSA02-029c variable	RSA02-030 variable	SWA07-005 pristine	SWA07-007c variable	SWA07-008 pristine	SWA07-011 pristine	SWA07-015 pristine
^{31}P	Conc	195	384	680	490	1430	450	600	238	221	400	780
	1σ	40	89	160	110	340	110	180	71	66	120	230
^{43}Ca	Conc	364	838	1880	179	4440	1175					
	1σ	30	63	100	23	230	85					
^{49}Ti	Conc	12.71	15.0	1228	8.69	9.8	6.81	9.47	19.0	23.3	8.25	6.14
	1σ	0.69	1.2	44	0.50	1.3	0.92	0.62	1.0	1.1	0.38	0.35
^{89}Y	Conc	1293	3460	2606	4050	826	1628	1766	765	930	1196	1984
	1σ	43	120	90	140	29	57	59	26	31	40	65
^{93}Nb	Conc	9.32	53.6	72.7	66.9	3.03	3.83	8.87	7.45	8.21	3.71	3.96
	1σ	0.33	1.9	2.5	2.3	0.18	0.19	0.31	0.26	0.29	0.13	0.14
^{139}La	Conc	2.251	2.74	10.42	4.80	6.02	16.73	15.18	10.43	5.51	0.0062	0.306
	1σ	0.091	0.13	0.40	0.17	0.29	0.64	0.52	0.37	0.20	0.0017	0.016
^{140}Ce	Conc	21.58	79.4	70.3	80.4	31.1	67.6	107.5	127.8	55.3	22.77	30.26
	1σ	0.72	2.7	2.4	2.7	1.1	2.4	3.5	4.1	1.8	0.73	0.99
^{141}Pr	Conc	1.186	2.89	7.97	4.40	2.58	6.23	13.03	12.84	5.18	0.0972	0.341
	1σ	0.049	0.12	0.29	0.15	0.14	0.25	0.43	0.42	0.18	0.0061	0.016
^{146}Nd	Conc	8.75	23.67	50.9	29.8	17.76	33.3	94.9	100.9	39.3	2.056	3.94
	1σ	0.35	0.96	1.9	1.0	0.95	1.4	3.1	3.3	1.3	0.088	0.16
^{147}Sm	Conc	7.57	15.41	18.18	15.59	10.94	16.50	35.7	36.4	25.29	4.99	7.45
	1σ	0.33	0.72	0.82	0.56	0.74	0.85	1.3	1.3	0.94	0.19	0.28
^{151}Eu	Conc	1.577	3.07	2.56	2.86	1.76	4.55	2.98	3.35	1.254	1.091	1.269
	1σ	0.073	0.16	0.14	0.11	0.15	0.24	0.13	0.14	0.065	0.043	0.054
^{157}Gd	Conc	34.2	65.1	36.2	59.0	29.1	51.3	55.1	51.4	47.7	25.02	41.9
	1σ	1.3	2.3	1.4	1.9	1.4	2.0	1.9	1.8	1.6	0.84	1.4
^{159}Tb	Conc	11.51	24.45	13.42	24.42	8.11	15.02	14.69	9.88	9.56	8.96	14.52
	1σ	0.38	0.82	0.47	0.80	0.34	0.54	0.48	0.33	0.32	0.29	0.47

Analysis		RSA02-010	RSA02-014	RSA02-019c	RSA02-026	RSA02-029c	RSA02-030	SWA07-005	SWA07-007c	SWA07-008	SWA07-011	SWA07-015
^{163}Dy	Conc	137.7	314	189.5	333	88.9	163.6	155.4	85.1	90.7	106.0	173.9
	1σ	4.5	10	6.2	11	3.2	5.5	5.1	2.8	3.0	3.5	5.8
^{165}Ho	Conc	49.8	123.0	83.7	135.2	30.6	56.3	55.5	26.46	28.98	40.2	64.3
	1σ	1.6	4.0	2.7	4.4	1.1	1.9	1.8	0.86	0.94	1.3	2.1
^{166}Er	Conc	204.4	538	428	622	119.5	231.2	242.4	98.7	124.9	180.5	277.1
	1σ	6.6	17	14	20	4.1	7.6	7.8	3.2	4.0	5.8	8.9
^{169}Tm	Conc	42.3	109.5	109.8	134.6	26.07	49.9	53.2	19.49	27.37	39.0	58.8
	1σ	1.4	3.5	3.5	4.3	0.91	1.7	1.7	0.64	0.89	1.2	1.9
^{173}Yb	Conc	387	1002	1196	1251	263.2	513	526	183.2	271.7	385	568
	1σ	12	33	39	42	9.3	18	17	6.0	8.8	12	18
^{175}Lu	Conc	58.8	159.4	192.3	199.3	39.0	79.6	88.2	32.6	47.5	68.9	96.6
	1σ	1.9	5.1	6.2	6.4	1.3	2.6	2.8	1.1	1.5	2.2	3.1
^{181}Ta	Conc	2.725	11.76	16.38	17.05	0.663	1.667	2.146	1.125	1.853	1.154	1.297
	1σ	0.099	0.41	0.55	0.55	0.061	0.092	0.082	0.050	0.072	0.041	0.047
^{232}Th	Conc	26.67	141.0	108.7	200.3	33.2	225.7	79.7	51.6	108.9	66.7	169.4
	1σ	0.93	4.7	3.7	6.7	1.2	7.6	2.6	1.7	3.6	2.2	5.6
^{238}U	Conc	77.1	245.7	524	335	67.7	363	449	93.5	196.8	92.7	318
	1σ	2.5	7.8	17	11	2.3	12	15	3.2	6.7	3.2	10
Ti-in-zirc	T (°C)	762.3	777.6	1466.1	728.6	739	708	736.1	800.6	820.8	724.2	699.7
	1σ	4.6	7.0	1.5	4.8	11	11	5.5	4.6	4.2	3.8	4.6

Analysis		SWA07-018	SWA07-021	SWA07-023	SWA07-024	SWA07-027	SWA07-028	SWA07-029	SWA07-032	SWA07-034	SWA07-048	SWA07-049
Group		pristine	pristine	variable	variable	metamict	variable	pristine	pristine	variable	variable	variable
^{31}P	Conc	460	400	1780	182	900	266	530	660	690	174	178
	1σ	140	120	530	55	270	80	160	200	210	53	55
^{43}Ca	Conc											
	1σ											
^{49}Ti	Conc	6.11	7.86	11.28	7.97	49.3	15.0	18.71	10.36	31.9	18.8	19.3
	1σ	0.38	0.47	0.88	0.96	2.8	1.1	0.93	0.55	2.1	1.2	1.0
^{89}Y	Conc	1388	3460	5850	551	4170	681	1643	1933	2927	832	591
	1σ	46	110	190	18	140	23	55	65	96	27	19
^{93}Nb	Conc	2.94	10.74	19.15	7.99	25.28	7.83	5.67	5.91	11.09	11.61	9.05
	1σ	0.11	0.37	0.67	0.33	0.90	0.30	0.20	0.21	0.42	0.42	0.32
^{139}La	Conc	0.0350	10.89	8.61	4.19	46.6	11.20	5.83	5.65	1.514	13.79	13.95
	1σ	0.0054	0.37	0.32	0.20	1.6	0.41	0.21	0.20	0.093	0.49	0.48
^{140}Ce	Conc	18.95	163.6	89.4	25.10	366	92.6	49.5	61.5	58.1	109.7	95.8
	1σ	0.63	5.3	3.0	0.89	12	3.1	1.7	2.1	1.9	3.5	3.1
^{141}Pr	Conc	0.167	9.11	5.19	3.20	43.6	12.62	2.84	4.62	1.712	13.10	11.64
	1σ	0.011	0.30	0.19	0.15	1.4	0.44	0.10	0.16	0.090	0.44	0.38
^{146}Nd	Conc	3.30	77.0	42.9	23.4	353	103.6	21.94	33.5	16.46	105.8	96.0
	1σ	0.15	2.6	1.6	1.1	12	3.6	0.79	1.2	0.76	3.6	3.2
^{147}Sm	Conc	6.12	52.2	26.6	9.55	222.5	43.2	13.37	21.52	17.98	51.6	35.8
	1σ	0.26	1.8	1.1	0.59	7.7	1.6	0.52	0.77	0.86	1.9	1.3
^{151}Eu	Conc	1.405	8.11	2.91	0.503	14.34	2.32	2.95	1.942	2.88	2.74	2.86
	1σ	0.063	0.29	0.15	0.066	0.58	0.13	0.12	0.083	0.17	0.14	0.12
^{157}Gd	Conc	31.5	133.4	99.0	13.81	347	49.4	41.7	52.9	64.9	67.4	41.5
	1σ	1.1	4.4	3.4	0.73	12	1.8	1.4	1.8	2.4	2.4	1.4
^{159}Tb	Conc	10.81	36.2	40.0	3.38	58.6	8.05	12.49	15.90	21.86	10.06	6.91
	1σ	0.35	1.2	1.3	0.16	1.9	0.29	0.41	0.52	0.74	0.35	0.23

Analysis		SWA07-018	SWA07-021	SWA07-023	SWA07-024	SWA07-027	SWA07-028	SWA07-029	SWA07-032	SWA07-034	SWA07-048	SWA07-049
^{163}Dy	Conc	125.3	368	509	39.8	462	69.5	141.5	170.9	250.7	82.3	59.7
	1σ	4.2	12	17	1.6	16	2.5	4.8	5.9	8.3	2.8	2.0
^{165}Ho	Conc	45.8	118.1	192.6	17.31	132.3	23.39	54.6	61.5	92.4	25.80	19.40
	1σ	1.5	3.8	6.2	0.62	4.3	0.79	1.8	2.0	3.1	0.88	0.66
^{166}Er	Conc	196.1	459	840	91.1	530	94.8	248.1	270.8	413	115.8	85.1
	1σ	6.3	15	27	3.1	17	3.2	8.1	8.8	13	3.8	2.8
^{169}Tm	Conc	41.3	92.0	180.4	25.66	108.9	21.24	54.2	58.8	91.8	27.36	19.52
	1σ	1.3	3.0	5.9	0.89	3.6	0.72	1.8	1.9	3.0	0.91	0.65
^{173}Yb	Conc	389	850	1738	370	1026	215.5	542	586	868	283.8	207.9
	1σ	12	27	56	12	33	7.1	17	19	29	9.5	6.9
^{175}Lu	Conc	69.0	135.7	270.1	66.6	161.5	41.0	100.5	103.3	148.8	50.7	41.6
	1σ	2.2	4.3	8.7	2.2	5.2	1.4	3.2	3.3	4.9	1.7	1.4
^{181}Ta	Conc	0.926	3.30	5.49	3.15	3.51	2.33	1.251	1.542	1.912	2.93	2.560
	1σ	0.037	0.11	0.20	0.14	0.15	0.10	0.050	0.057	0.094	0.12	0.094
^{232}Th	Conc	80.3	377	667	29.6	301	44.9	97.8	194.2	198.6	69.3	77.8
	1σ	2.7	12	22	1.1	10	1.5	3.2	6.4	6.6	2.3	2.6
^{238}U	Conc	111.1	698	1377	827	570	403	160.3	459	241.1	376	375
	1σ	3.5	22	44	27	18	13	5.2	15	7.7	12	12
Ti-in-zirc	T (°C)	699.3	720.1	751.5	721.3	903.6	777.8	799.0	743.9	854.2	799.3	802.3
	1σ	5.0	4.9	6.6	9.7	5.2	6.4	4.3	4.5	5.9	5.8	4.6

Analysis		SWA07-050	SWA07-055	SWA07-056	SWA07-059	SWA07-065	SWA07-067	SWA07-074	SWA07-076	SWA07-077	SWA07-078	SWA07-082
Group		metamict	pristine	pristine	variable	variable	variable	metamict	variable	pristine	pristine	variable
^{31}P	Conc	1770	164	460	1540	690	2230	380	510	340	390	400
	1σ	540	51	140	480	220	700	120	160	110	120	130
^{43}Ca	Conc											
	1σ											
^{49}Ti	Conc	27.1	4.92	8.92	19.0	5.51	16.0	26.3	19.6	9.63	14.27	3.66
	1σ	1.8	0.48	0.70	1.4	0.71	1.1	1.1	1.1	0.90	0.64	0.56
^{89}Y	Conc	2147	1336	1443	3690	1836	1724	2802	1901	2047	1172	1717
	1σ	71	44	47	120	60	57	92	63	68	39	57
^{93}Nb	Conc	13.06	1.287	3.11	12.35	4.73	4.39	14.19	4.86	3.23	3.34	10.14
	1σ	0.48	0.062	0.13	0.46	0.21	0.18	0.47	0.18	0.14	0.12	0.38
^{139}La	Conc	52.0	0.116	1.172	12.18	0.609	3.80	12.35	1.666	3.29	0.0076	0.063
	1σ	1.8	0.015	0.062	0.45	0.052	0.16	0.41	0.078	0.15	0.0021	0.015
^{140}Ce	Conc	288.2	9.82	24.36	141.1	34.9	40.2	107.2	39.4	26.84	20.30	23.13
	1σ	9.3	0.34	0.81	4.6	1.2	1.3	3.5	1.3	0.91	0.66	0.79
^{141}Pr	Conc	34.3	0.449	0.769	10.71	0.778	2.049	10.42	1.570	2.155	0.1530	0.162
	1σ	1.1	0.028	0.041	0.37	0.053	0.090	0.33	0.068	0.099	0.0087	0.021
^{146}Nd	Conc	254.4	6.70	7.35	84.7	5.76	13.70	78.6	16.49	22.22	2.89	2.23
	1σ	8.4	0.31	0.35	2.9	0.37	0.59	2.5	0.65	0.91	0.12	0.20
^{147}Sm	Conc	97.4	8.38	8.01	49.1	6.89	10.40	44.4	16.69	19.64	5.26	4.95
	1σ	3.5	0.39	0.39	1.9	0.44	0.50	1.5	0.67	0.85	0.20	0.35
^{151}Eu	Conc	13.67	3.12	1.723	4.79	1.168	1.97	4.09	2.78	5.68	1.357	0.855
	1σ	0.52	0.14	0.093	0.22	0.094	0.11	0.14	0.13	0.25	0.054	0.077
^{157}Gd	Conc	132.4	30.1	34.4	119.8	38.6	42.4	94.7	53.6	58.0	25.00	31.5
	1σ	4.5	1.1	1.3	4.1	1.5	1.6	3.1	1.9	2.1	0.85	1.3
^{159}Tb	Conc	23.93	10.06	11.63	31.8	13.58	13.14	26.13	16.01	16.27	8.55	11.26
	1σ	0.80	0.34	0.39	1.0	0.47	0.45	0.83	0.53	0.55	0.28	0.40

Analysis		SWA07-050	SWA07-055	SWA07-056	SWA07-059	SWA07-065	SWA07-067	SWA07-074	SWA07-076	SWA07-077	SWA07-078	SWA07-082
^{163}Dy	Conc	214.0	110.5	130.5	343	161.2	152.2	267.4	175.0	173.9	101.5	149.9
	1σ	7.1	3.7	4.3	11	5.4	5.0	8.6	5.7	5.7	3.3	5.0
^{165}Ho	Conc	67.8	39.8	46.8	117.7	60.3	57.9	92.6	61.9	64.2	39.1	55.8
	1σ	2.3	1.4	1.6	4.0	2.1	1.9	3.0	2.0	2.1	1.3	1.8
^{166}Er	Conc	274.9	185.3	200.8	498	264.0	263.5	392	266.6	298.4	176.6	242.7
	1σ	8.9	6.0	6.5	16	8.6	8.5	12	8.6	9.6	5.7	7.9
^{169}Tm	Conc	62.8	42.9	43.3	100.9	55.5	58.1	82.1	55.9	67.6	38.9	51.2
	1σ	2.1	1.4	1.4	3.4	1.9	1.9	2.6	1.8	2.2	1.3	1.7
^{173}Yb	Conc	653	450	408	948	538	566	794	531	714	387	482
	1σ	22	15	14	32	18	18	25	17	23	12	16
^{175}Lu	Conc	109.5	80.7	68.7	161.2	89.7	102.0	140.5	93.9	138.3	69.4	76.9
	1σ	3.6	2.7	2.3	5.3	3.0	3.3	4.6	3.1	4.5	2.3	2.6
^{181}Ta	Conc	3.97	0.455	0.795	1.934	1.437	1.200	1.957	0.916	0.758	0.821	3.42
	1σ	0.16	0.027	0.041	0.089	0.077	0.059	0.067	0.045	0.047	0.031	0.14
^{232}Th	Conc	116.6	143.3	112.0	434	149.7	105.1	358	141.5	242.3	63.3	206.6
	1σ	3.9	4.8	3.8	15	5.1	3.6	12	4.9	8.3	2.2	7.2
^{238}U	Conc	830	176.0	164.3	402	292.1	143.1	591	158.6	292.7	88.7	466
	1σ	26	5.6	5.3	13	9.5	4.5	19	5.0	9.3	2.8	15
Ti-in-zirc	T (°C)	836.6	682.1	730.9	800.5	691.0	784.1	833.4	803.6	737.5	773.1	660
	1σ	5.9	7.5	6.5	6.3	9.9	6.0	3.5	5.1	7.8	3.8	11

Analysis		SWA07-086	SWA07-088	SWA07-090	SWA07-092c	RSA04-002c	RSA04-004c	RSA04-006c	RSA04-007c	RSA04-009c	RSA04-009r	RSA04-010
Group		pristine	variable	metamict	metamict	pristine	pristine	pristine	pristine	pristine	pristine	pristine
^{31}P	Conc	950	840	480	710	189	830	288	480	294	168	294
	1σ	300	260	150	220	39	170	61	100	63	37	61
^{43}Ca	Conc					111	7840	99	71	86	119	87
	1σ					25	360	21	24	32	22	28
^{49}Ti	Conc	6.04	8.01	30.9	12.31	14.80	23.8	27.7	8.90	11.35	10.63	9.51
	1σ	0.55	0.67	1.3	0.98	0.79	1.6	1.2	0.64	0.92	0.54	0.69
^{89}Y	Conc	2410	1770	2796	2392	3370	12270	2136	1191	1794	678	1220
	1σ	80	59	94	80	130	490	87	49	74	28	42
^{93}Nb	Conc	4.44	3.67	10.71	8.17	6.56	26.6	13.54	6.83	6.44	1.831	7.23
	1σ	0.17	0.15	0.37	0.31	0.31	1.3	0.66	0.35	0.35	0.099	0.27
^{139}La	Conc	0.105	0.199	25.95	16.12	7.74	4.44	25.5	1.96	21.1	1.041	3.84
	1σ	0.014	0.021	0.86	0.57	0.34	0.23	1.2	0.11	1.0	0.055	0.15
^{140}Ce	Conc	21.83	27.51	184.5	132.1	116.5	754	450	22.2	144.6	42.2	56.1
	1σ	0.73	0.90	5.9	4.3	5.8	39	24	1.2	8.1	2.4	1.9
^{141}Pr	Conc	0.174	0.264	22.21	12.67	3.58	7.68	15.99	2.03	6.91	0.476	3.03
	1σ	0.017	0.022	0.71	0.43	0.17	0.38	0.77	0.11	0.36	0.028	0.12
^{146}Nd	Conc	2.49	3.64	148.9	102.8	32.1	98.5	94.3	11.05	35.0	4.45	19.89
	1σ	0.17	0.22	4.8	3.5	1.8	5.9	5.8	0.75	2.3	0.31	0.76
^{147}Sm	Conc	7.12	6.29	70.6	49.5	41.5	180.1	59.5	8.56	19.24	5.38	14.46
	1σ	0.35	0.33	2.3	1.8	1.7	7.4	2.5	0.44	0.96	0.26	0.60
^{151}Eu	Conc	1.055	1.343	6.94	4.90	19.59	75.7	17.16	2.09	4.45	2.78	3.97
	1σ	0.066	0.080	0.24	0.22	0.84	3.3	0.78	0.12	0.25	0.14	0.17
^{157}Gd	Conc	42.8	35.8	121.6	92.1	161.7	663	114.3	25.8	44.4	23.4	36.2
	1σ	1.5	1.3	3.9	3.1	8.5	37	6.5	1.6	2.8	1.5	1.3
^{159}Tb	Conc	16.55	13.01	27.87	22.14	44.2	178.4	30.1	9.16	15.01	7.22	11.52
	1σ	0.55	0.44	0.89	0.74	1.9	7.7	1.3	0.42	0.70	0.34	0.39

Analysis		SWA07-086	SWA07-088	SWA07-090	SWA07-092c	RSA04-002c	RSA04-004c	RSA04-006c	RSA04-007c	RSA04-009c	RSA04-009r	RSA04-010
^{163}Dy	Conc	202.8	160.2	260.1	221.5	408	1568	258	111.1	169	72.4	114.5
	1σ	6.6	5.2	8.3	7.2	22	88	15	6.7	10	4.5	3.8
^{165}Ho	Conc	77.5	58.9	86.8	77.7	115.8	422	68.0	39.6	59.4	22.42	38.5
	1σ	2.5	1.9	2.8	2.5	4.6	17	2.8	1.7	2.5	0.96	1.3
^{166}Er	Conc	341	264.2	364	323	406	1411	239	183.3	270	86.9	163.3
	1σ	11	8.5	12	10	16	58	10	7.9	12	3.8	5.3
^{169}Tm	Conc	74.6	56.4	77.4	67.2	76.0	249	44.8	43.5	66.2	17.03	37.1
	1σ	2.4	1.8	2.5	2.2	3.2	11	2.0	1.9	3.0	0.78	1.2
^{173}Yb	Conc	721	535	769	635	659	2065	400	462	732	162.4	373
	1σ	23	17	25	21	24	75	15	17	28	6.2	12
^{175}Lu	Conc	123.9	98.5	139.9	108.4	95.7	270.6	58.6	72.8	116.2	27.2	61.9
	1σ	4.1	3.2	4.5	3.5	3.4	9.8	2.2	2.7	4.4	1.0	2.0
^{181}Ta	Conc	1.422	1.187	1.299	1.252	0.631	2.23	0.709	1.817	1.199	0.318	1.378
	1σ	0.062	0.055	0.047	0.063	0.035	0.12	0.038	0.098	0.076	0.019	0.061
^{232}Th	Conc	184.9	102.5	385	196.4	331	2170	183.8	53.6	84.4	53.5	77.8
	1σ	6.5	3.5	13	6.7	15	100	8.8	2.6	4.2	2.7	2.7
^{238}U	Conc	512	180.0	485	274.1	215	847	154.4	343	153.1	62.1	235.8
	1σ	16	5.7	15	8.6	11	47	9.0	21	9.4	3.9	7.4
Ti-in-zirc	T (°C)	698.4	721.7	850.7	759.4	776.5	823.2	839.1	730.7	752.1	746.2	736.4
	1σ	7.2	6.8	3.5	6.8	4.6	5.9	3.8	6.0	6.9	4.3	6.0

Analysis Group		RSA04-011 pristine	RSA04-012 pristine	RSA04-013c pristine	RSA04-015c pristine	RSA04-015r metamict	RSA04-018 metamict	RSA04-019c pristine	RSA04-021c pristine	RSA04-021r pristine	RSA04-023c metamict	RSA04-023r metamict
^{31}P	Conc	76	346	181	247	169	206	304	265	343	417	350
	1σ	16	73	38	52	36	44	65	56	73	89	74
^{43}Ca	Conc	1230	66	272	54	3470	2560	<68	46	66	4290	2550
	1σ	66	18	38	21	140	100	35	19	43	160	110
^{49}Ti	Conc	14.87	13.18	26.5	27.3	315	179.9	8.07	8.48	11.7	763	372
	1σ	0.95	0.55	1.6	1.2	12	6.5	0.63	0.50	1.0	27	13
^{89}Y	Conc	919	1493	2178	1536	5790	7260	974	899	1602	17650	7260
	1σ	31	51	75	53	200	250	34	31	56	590	240
^{93}Nb	Conc	10.79	8.70	10.00	6.85	40.7	85.3	2.125	1.805	4.79	267.5	87.0
	1σ	0.40	0.30	0.38	0.25	1.4	3.0	0.096	0.075	0.21	9.1	3.0
^{139}La	Conc	12.80	3.05	27.40	17.75	228.3	118.5	0.0232	0.323	0.076	303	242.4
	1σ	0.46	0.11	0.96	0.60	7.7	4.0	0.0069	0.021	0.017	10	8.1
^{140}Ce	Conc	83.1	82.7	145.7	265.9	712	780	52.6	44.9	94.3	1809	884
	1σ	2.8	2.7	4.9	8.8	24	26	1.8	1.5	3.2	58	29
^{141}Pr	Conc	7.33	2.428	11.32	9.34	111.7	106.5	0.138	0.447	0.361	262.9	124.8
	1σ	0.26	0.081	0.39	0.31	3.6	3.4	0.014	0.023	0.032	8.4	4.0
^{146}Nd	Conc	45.2	16.49	66.6	52.4	506	628	3.44	4.55	7.05	1503	651
	1σ	1.6	0.55	2.3	1.8	16	20	0.20	0.20	0.40	48	21
^{147}Sm	Conc	26.2	17.09	47.9	32.9	264.0	345	6.09	7.38	13.05	998	380
	1σ	1.0	0.58	1.8	1.1	8.7	11	0.31	0.31	0.65	32	12
^{151}Eu	Conc	8.75	6.66	15.24	9.84	66.9	109.2	3.17	3.35	5.97	285.4	111.5
	1σ	0.33	0.22	0.55	0.33	2.2	3.5	0.14	0.13	0.26	9.1	3.6
^{157}Gd	Conc	45.9	56.7	117.6	69.8	372	529	30.5	31.3	53.4	1558	570
	1σ	1.6	1.9	4.1	2.3	12	18	1.1	1.1	2.0	51	19
^{159}Tb	Conc	11.88	16.86	33.0	19.24	112.2	133.1	9.91	9.56	16.03	396	145.8
	1σ	0.40	0.54	1.1	0.62	3.6	4.3	0.34	0.32	0.55	13	4.7

Analysis		RSA04-011	RSA04-012	RSA04-013c	RSA04-015c	RSA04-015r	RSA04-018	RSA04-019c	RSA04-021c	RSA04-021r	RSA04-023c	RSA04-023r
^{163}Dy	Conc	101.1	161.9	278.6	171.9	915	999	99.5	95.5	162.7	2772	1055
	1σ	3.4	5.3	9.2	5.6	30	33	3.4	3.2	5.5	89	34
^{165}Ho	Conc	27.03	49.3	73.8	49.0	201.5	229.8	32.0	29.90	52.2	585	234.9
	1σ	0.89	1.6	2.4	1.6	6.5	7.4	1.1	0.98	1.7	19	7.5
^{166}Er	Conc	109.6	188.5	251.6	188.1	665	720	122.4	116.7	210.1	1697	726
	1σ	3.6	6.1	8.3	6.1	22	24	4.1	3.9	7.1	54	23
^{169}Tm	Conc	26.05	38.2	47.4	38.9	129.0	128.7	24.34	24.14	45.5	290.1	130.9
	1σ	0.86	1.2	1.6	1.3	4.2	4.2	0.82	0.80	1.5	9.4	4.3
^{173}Yb	Conc	300.0	353	432	367	1186	1095	222.2	232.8	450	2365	1101
	1σ	9.7	11	14	12	38	35	7.2	7.5	15	76	36
^{175}Lu	Conc	54.4	56.4	58.8	59.7	161.9	158.1	38.7	35.6	69.5	321	159.2
	1σ	1.8	1.8	1.9	1.9	5.2	5.0	1.3	1.2	2.3	10	5.1
^{181}Ta	Conc	1.587	0.735	0.881	0.620	2.73	3.72	0.404	0.383	1.078	11.37	4.62
	1σ	0.070	0.027	0.051	0.027	0.10	0.13	0.026	0.020	0.062	0.37	0.16
^{232}Th	Conc	116.0	132.5	183.3	162.3	456	302	87.3	68.5	153.3	1282	736
	1σ	4.0	4.5	6.3	5.5	15	10	3.0	2.3	5.3	43	25
^{238}U	Conc	597	153.6	252.6	148.9	864	888	100.8	86.9	250.7	1652	816
	1σ	19	4.8	8.0	4.7	27	28	3.2	2.8	8.0	52	26
Ti-in-zirc	T (°C)	776.9	765.7	834.5	837.5	1173.6	1079.7	722.3	726.5	754.5	1351.1	1203.7
	1σ	5.5	3.5	5.2	3.6	2.6	2.8	6.4	4.9	7.3	1.7	2.4

Analysis Group		RSA04-024 pristine	RSA04-025 metamict	RSA04-026 pristine	RSA04-027c metamict	RSA04-029c metamict	RSA04-030c pristine	RSA04-030r metamict	RSA08-001c pristine	RSA08-003 variable	RSA08-004c variable	RSA08-005 pristine
^{31}P	Conc	159	227	218	194	99	255	430	630	212	161	2130
	1σ	34	48	46	41	21	54	91	130	44	34	450
^{43}Ca	Conc	<47	673	94	1542	1035	<53	4690	775	778	1868	3120
	1σ	21	51	22	91	48	30	170	44	40	98	150
^{49}Ti	Conc	12.68	59.5	11.10	36.1	77.5	9.03	875	23.1	125.1	88.0	9.55
	1σ	0.67	2.7	0.64	2.1	3.0	0.69	31	1.1	4.6	3.9	0.91
^{89}Y	Conc	1569	3160	1217	1909	1897	1802	24910	3600	3810	2586	4340
	1σ	52	110	41	64	63	60	830	120	130	87	150
^{93}Nb	Conc	1.926	56.4	4.24	19.48	21.69	2.78	280.0	9.45	11.48	31.4	10.69
	1σ	0.078	2.0	0.16	0.72	0.76	0.12	9.7	0.33	0.39	1.1	0.40
^{139}La	Conc	0.665	50.0	1.592	25.08	47.5	1.432	291.4	59.7	227.8	95.1	10.88
	1σ	0.034	1.7	0.068	0.89	1.6	0.072	9.7	2.0	7.6	3.2	0.41
^{140}Ce	Conc	61.0	218.0	76.6	152.2	296.4	64.3	2307	275.3	726	422	100.0
	1σ	2.0	7.1	2.5	5.0	9.6	2.1	75	9.0	24	14	3.3
^{141}Pr	Conc	0.966	25.58	0.856	13.69	31.6	1.002	303.0	37.5	142.3	60.3	5.57
	1σ	0.040	0.84	0.038	0.48	1.0	0.050	9.6	1.2	4.5	2.0	0.21
^{146}Nd	Conc	12.69	136.5	7.41	75.0	161.4	14.16	1849	257.9	852	410	40.8
	1σ	0.47	4.5	0.31	2.7	5.2	0.58	59	8.4	27	13	1.5
^{147}Sm	Conc	17.77	88.5	10.57	53.0	91.5	19.70	1157	158.9	554	296.8	30.7
	1σ	0.65	3.0	0.42	2.0	3.0	0.78	37	5.2	18	9.9	1.3
^{151}Eu	Conc	8.79	24.79	4.16	16.48	27.74	8.54	362	15.83	28.22	48.2	3.85
	1σ	0.30	0.85	0.16	0.61	0.91	0.32	12	0.54	0.92	1.6	0.19
^{157}Gd	Conc	67.7	172.0	41.4	109.5	137.8	76.6	1841	258.3	714	499	107.1
	1σ	2.3	5.8	1.4	3.9	4.6	2.7	61	8.4	23	16	3.7
^{159}Tb	Conc	18.78	52.2	12.63	31.1	37.6	21.87	483	52.7	130.4	80.0	35.7
	1σ	0.61	1.7	0.42	1.0	1.2	0.72	15	1.7	4.2	2.6	1.2

Analysis		RSA04-024	RSA04-025	RSA04-026	RSA04-027c	RSA04-029c	RSA04-030c	RSA04-030r	RSA08-001c	RSA08-003	RSA08-004c	RSA08-005
^{163}Dy	Conc	180.1	433	124.1	259.7	275.8	204.6	3590	419	726	452	414
	1σ	5.8	14	4.0	8.5	8.9	6.7	120	14	24	15	14
^{165}Ho	Conc	54.7	105.4	40.4	67.2	60.9	61.3	792	122.8	134.4	89.9	148.6
	1σ	1.8	3.4	1.3	2.2	2.0	2.0	25	3.9	4.3	2.9	4.8
^{166}Er	Conc	197.3	347	159.6	229.7	194.2	228.0	2328	462	342	255.9	624
	1σ	6.3	11	5.1	7.5	6.2	7.4	75	15	11	8.3	20
^{169}Tm	Conc	38.4	63.0	33.1	43.3	36.3	43.5	392	91.7	55.9	45.0	127.1
	1σ	1.3	2.1	1.1	1.5	1.2	1.5	13	2.9	1.8	1.5	4.1
^{173}Yb	Conc	346	556	329	407	325	374	3090	856	488	419	1174
	1σ	11	18	11	13	11	12	100	28	16	14	38
^{175}Lu	Conc	52.5	75.8	51.9	58.3	52.8	60.3	416	128.1	75.4	65.5	189.2
	1σ	1.7	2.5	1.7	1.9	1.7	2.0	13	4.1	2.4	2.1	6.1
^{181}Ta	Conc	0.339	2.67	0.706	1.467	2.165	0.464	7.46	1.657	9.30	2.69	2.72
	1σ	0.019	0.11	0.033	0.077	0.078	0.030	0.25	0.065	0.30	0.12	0.12
^{232}Th	Conc	126.9	356	102.5	158.8	116.7	182.9	991	269.4	169.7	269.9	440
	1σ	4.3	12	3.5	5.4	4.0	6.3	34	9.2	5.8	9.2	15
^{238}U	Conc	107.4	396	140.0	238.8	410	158.8	1678	426	374	562	780
	1σ	3.4	12	4.4	7.5	13	5.0	53	13	12	18	24
Ti-in-zirc	T (°C)	762.1	926.2	750.1	867.7	959.6	731.9	1382.8	820.2	1025.1	976.4	736.8
	1σ	4.5	4.0	4.9	5.3	3.1	6.3	1.8	4.2	2.9	4.0	7.9

Analysis		RSA08-006	RSA08-007c	RSA08-013c	RSA08-015c	RSA08-016c	RSA08-017	RSA08-019c	RSA08-022	RSA08-025c	RSA08-031	RSA08-034
Group		pristine	pristine	pristine	pristine	pristine	variable	variable	variable	metamict	variable	variable
^{31}P	Conc	364	570	530	650	3000	362	1560	272	210	217	1140
	1σ	76	120	110	140	630	76	330	57	44	46	240
^{43}Ca	Conc	<38	92	86	4240	7270	384	4720	317	5530	191	279
	1σ	25	20	35	160	260	51	220	35	230	40	56
^{49}Ti	Conc	5.35	11.41	11.77	9.76	6.79	137.3	37.0	14.51	131.4	12.24	30.2
	1σ	0.53	0.56	0.72	0.62	0.48	6.0	2.2	0.96	5.5	0.95	1.9
^{89}Y	Conc	1997	1945	1572	1690	8400	2633	5170	1426	3130	944	3710
	1σ	67	65	53	57	280	89	170	48	110	32	130
^{93}Nb	Conc	4.02	6.37	11.14	4.53	20.76	9.39	22.21	6.54	36.3	13.57	10.01
	1σ	0.16	0.22	0.39	0.17	0.71	0.37	0.80	0.25	1.3	0.49	0.38
^{139}La	Conc	0.0038	23.26	22.10	20.15	1.592	82.8	270.5	44.2	438	23.87	33.9
	1σ	0.0032	0.78	0.76	0.69	0.069	2.8	9.1	1.5	15	0.84	1.2
^{140}Ce	Conc	40.0	260.1	105.5	108.8	43.2	749	718	211.4	2212	133.7	211.1
	1σ	1.3	8.6	3.5	3.6	1.5	24	23	6.9	73	4.4	7.0
^{141}Pr	Conc	0.100	16.76	13.88	13.77	0.696	59.6	77.2	31.6	178.5	16.39	26.82
	1σ	0.013	0.54	0.46	0.45	0.033	2.0	2.5	1.0	5.8	0.56	0.91
^{146}Nd	Conc	2.69	112.3	93.3	77.3	8.98	350	458	224.7	897	105.3	211.4
	1σ	0.18	3.7	3.1	2.6	0.36	12	15	7.4	29	3.6	7.1
^{147}Sm	Conc	8.56	73.8	49.5	31.3	20.10	233.3	172.5	131.7	330	57.5	134.0
	1σ	0.42	2.4	1.7	1.1	0.74	7.9	5.9	4.5	11	2.1	4.7
^{151}Eu	Conc	0.739	4.51	3.50	2.72	1.451	11.52	11.51	10.20	53.3	4.39	8.73
	1σ	0.055	0.16	0.14	0.11	0.069	0.47	0.46	0.38	1.8	0.20	0.36
^{157}Gd	Conc	48.2	130.5	78.7	60.4	137.6	318	261.5	193.8	461	83.3	242.6
	1σ	1.7	4.3	2.7	2.1	4.6	11	8.7	6.4	15	2.9	8.1
^{159}Tb	Conc	17.79	26.49	16.02	15.08	57.1	70.8	59.3	30.08	66.5	15.57	52.8
	1σ	0.59	0.85	0.53	0.50	1.8	2.3	2.0	0.99	2.2	0.53	1.7

Analysis		RSA08-006	RSA08-007c	RSA08-013c	RSA08-015c	RSA08-016c	RSA08-017	RSA08-019c	RSA08-022	RSA08-025c	RSA08-031	RSA08-034
^{163}Dy	Conc	202.2	217.8	143.6	150.3	741	465	525	190.4	429	111.6	431
	1σ	6.7	7.2	4.8	5.0	25	15	17	6.3	14	3.8	14
^{165}Ho	Conc	71.0	64.3	49.9	52.2	280.4	100.9	171.1	47.0	97.1	31.0	123.3
	1σ	2.3	2.1	1.6	1.7	9.0	3.3	5.5	1.5	3.2	1.0	4.0
^{166}Er	Conc	286.3	245.2	246.0	228.9	1234	307.6	687	158.8	329	122.3	471
	1σ	9.2	7.9	7.9	7.4	40	10.0	22	5.2	11	4.0	15
^{169}Tm	Conc	59.1	49.2	63.6	49.6	259.8	56.8	142.2	30.66	63.7	27.85	94.8
	1σ	1.9	1.6	2.0	1.6	8.3	1.9	4.6	0.99	2.1	0.91	3.0
^{173}Yb	Conc	542	451	729	468	2378	509	1308	286.5	643	291.0	873
	1σ	18	15	24	15	78	17	42	9.4	21	9.6	29
^{175}Lu	Conc	78.4	71.4	153.0	79.9	398	69.1	219.2	46.8	98.9	50.0	142.7
	1σ	2.6	2.3	5.0	2.6	13	2.3	7.1	1.5	3.2	1.6	4.7
^{181}Ta	Conc	0.890	0.835	7.51	0.456	5.75	2.76	5.10	2.49	8.38	7.79	1.888
	1σ	0.046	0.033	0.25	0.025	0.20	0.13	0.20	0.10	0.30	0.28	0.092
^{232}Th	Conc	129.2	167.2	39.9	113.7	596	397	447	55.7	94.5	74.0	192.4
	1σ	4.4	5.7	1.4	3.9	20	13	15	1.9	3.2	2.6	6.6
^{238}U	Conc	196.2	272.8	243.7	1000	1124	251.7	1121	245.7	1031	382	403
	1σ	6.2	8.5	7.6	31	35	8.0	35	7.8	33	12	13
Ti-in-zirc	T (°C)	688.7	752.6	755.4	738.7	707.9	1038.7	870.4	774.6	1032.3	758.9	848.1
	1σ	7.7	4.1	5.2	5.3	5.7	3.9	5.5	5.7	3.6	6.6	5.7

Analysis Group		RSA08-038 pristine	RSA08-049c metamict	RSA08-051 metamict	RSA08-054c variable	RSA08-058 variable	SWA10a-001 pristine	SWA10a-003c pristine	SWA10a-006 pristine	SWA10a-016 metamict	SWA10a-018 variable	SWA10a-019 variable
^{31}P	Conc	373	189	274	800	303	390	290	410	380	300	350
	1σ	79	40	58	170	63	320	230	330	330	260	310
^{43}Ca	Conc	6960	6550	1436	1900	202	124	<23	6900	7090	2280	228
	1σ	300	260	91	110	37	23	12	410	430	170	26
^{49}Ti	Conc	4.20	5130	52.7	7.93	12.66	12.0	1.16	9.54	46.2	26.1	15.5
	1σ	0.67	190	2.6	0.83	0.80	1.1	0.39	0.91	3.2	2.3	1.3
^{89}Y	Conc	1125	1145	2291	3420	1164	3720	903	5780	3610	3510	1808
	1σ	38	39	77	110	39	150	37	230	150	150	76
^{93}Nb	Conc	62.8	31.1	9.88	22.07	4.63	6.59	3.26	77.5	82.0	17.49	12.82
	1σ	2.2	1.1	0.37	0.79	0.18	0.30	0.18	3.3	3.5	0.78	0.56
^{139}La	Conc	2.00	58.1	139.7	4.82	58.6	9.45	3.37	20.66	197.7	40.9	26.5
	1σ	0.12	2.0	4.7	0.21	2.0	0.37	0.16	0.78	7.4	1.6	1.0
^{140}Ce	Conc	11.51	447	799	78.3	153.7	31.6	17.57	99.2	674	139.1	63.3
	1σ	0.44	15	26	2.6	5.0	1.1	0.65	3.4	24	5.0	2.3
^{141}Pr	Conc	1.094	36.5	95.8	3.54	24.61	3.18	0.640	8.02	91.2	16.86	9.63
	1σ	0.073	1.2	3.1	0.15	0.81	0.12	0.045	0.28	3.2	0.62	0.35
^{146}Nd	Conc	6.63	241.5	496	27.4	142.2	21.01	4.59	38.3	430	93.3	51.6
	1σ	0.44	8.0	16	1.1	4.7	0.80	0.30	1.4	15	3.4	1.9
^{147}Sm	Conc	5.59	128.3	235.1	19.28	79.9	20.98	5.10	23.59	170.2	49.2	29.4
	1σ	0.43	4.4	7.9	0.88	2.7	0.81	0.33	0.88	5.8	1.8	1.1
^{151}Eu	Conc	0.749	17.44	18.00	2.17	4.25	3.33	0.503	2.54	30.0	4.45	5.34
	1σ	0.080	0.62	0.65	0.13	0.17	0.14	0.052	0.11	1.0	0.20	0.20
^{157}Gd	Conc	12.40	163.4	332	77.2	117.1	87.7	23.93	107.8	225.7	120.3	64.0
	1σ	0.68	5.5	11	2.9	4.2	3.0	0.96	3.6	7.6	4.2	2.2
^{159}Tb	Conc	5.26	28.23	58.6	28.20	20.83	29.86	8.08	40.9	46.5	34.6	18.26
	1σ	0.22	0.93	1.9	0.95	0.69	0.99	0.29	1.4	1.5	1.2	0.61

Analysis		RSA08-038	RSA08-049c	RSA08-051	RSA08-054c	RSA08-058	SWA10a-001	SWA10a-003c	SWA10a-006	SWA10a-016	SWA10a-018	SWA10a-019
^{163}Dy	Conc	82.3	174.8	368	326	144.2	335	89.0	510	365	349	175.7
	1σ	2.9	5.8	12	11	4.8	11	3.0	17	12	12	5.8
^{165}Ho	Conc	37.7	38.8	80.7	117.1	38.9	122.3	31.1	192.8	105.0	120.2	57.7
	1σ	1.3	1.3	2.6	3.8	1.3	4.0	1.1	6.3	3.4	4.0	1.9
^{166}Er	Conc	199.1	127.3	251.3	518	138.6	518	131.8	823	418	496	234.7
	1σ	6.6	4.2	8.2	17	4.5	17	4.4	27	14	16	7.7
^{169}Tm	Conc	52.8	28.00	45.4	107.1	27.23	102.8	27.26	159.3	86.6	101.1	47.2
	1σ	1.7	0.91	1.5	3.5	0.92	3.3	0.91	5.2	2.8	3.3	1.5
^{173}Yb	Conc	594	280.0	393	1001	254.2	935	265.7	1373	847	956	446
	1σ	20	9.3	13	32	8.3	30	8.7	44	28	31	15
^{175}Lu	Conc	95.0	48.3	66.8	170.7	43.7	164.7	44.6	230.8	148.7	167.1	83.7
	1σ	3.1	1.6	2.2	5.6	1.4	5.3	1.5	7.4	4.8	5.4	2.7
^{181}Ta	Conc	40.4	7.45	2.87	5.47	0.764	1.525	0.669	14.53	47.2	3.97	1.092
	1σ	1.3	0.26	0.12	0.21	0.039	0.059	0.039	0.47	1.5	0.14	0.042
^{232}Th	Conc	46.6	52.2	76.3	423	27.68	314	40.9	995	370	518	174.7
	1σ	1.7	1.8	2.7	14	0.97	10	1.4	32	12	17	5.6
^{238}U	Conc	1293	544	458	810	193.4	414	81.9	1723	1143	852	537
	1σ	41	17	15	26	6.3	13	2.6	54	35	26	17
Ti-in-zirc	T (°C)	670	1935.40	911.5	720.8	762.0	757.3	581	736.7	895.8	832.8	781.0
	1σ	12	0.73	4.5	8.5	5.4	7.8	19	7.9	6.6	8.0	7.1

Analysis Group		SWA10a-020c variable	SWA10a-020b variable	SWA10a-022c pristine	SWA10a-025 variable	SWA10a-026 variable	SWA10a-032 metamict	SWA10a-047 metamict	SWA10a-049c pristine	SWA10a-050c pristine	SWA10a-051c pristine
^{31}P	Conc	96	113	410	360	540	820	3400	270	180	170
	1σ	99	84	360	320	480	740	3100	240	170	150
^{43}Ca	Conc	1043	798	3430	1162	<26	18600	16480	2680	115	130
	1σ	76	75	230	91	8.1	1100	990	180	22	18
^{49}Ti	Conc	16.1	16.2	9.9	12.3	0.94	305	218	23.6	9.1	17.1
	1σ	1.7	1.3	1.0	1.2	0.58	19	14	1.9	1.0	1.4
^{89}Y	Conc	951	1197	4750	1287	1281	4980	3420	2440	852	2333
	1σ	51	40	210	56	53	210	140	100	36	98
^{93}Nb	Conc	15.29	13.38	18.88	22.7	2.64	69.2	74.7	36.8	6.26	6.59
	1σ	0.61	0.67	0.84	1.0	0.20	2.9	3.2	1.6	0.29	0.30
^{139}La	Conc	29.8	37.6	14.67	13.01	1.91	533	161.2	96.5	34.1	6.26
	1σ	1.5	1.1	0.58	0.52	0.14	20	6.2	3.7	1.3	0.26
^{140}Ce	Conc	115.7	124.9	51.5	61.2	13.86	2324	632	149.7	67.7	19.50
	1σ	4.6	4.2	1.9	2.3	0.59	83	23	5.4	2.5	0.73
^{141}Pr	Conc	16.11	19.16	3.52	8.07	0.598	219.8	82.3	28.6	12.03	3.60
	1σ	0.71	0.58	0.14	0.31	0.063	7.7	2.9	1.0	0.45	0.14
^{146}Nd	Conc	85.5	99.1	20.91	39.0	4.26	900	404	135.8	57.9	20.67
	1σ	3.7	3.1	0.85	1.5	0.41	32	14	4.9	2.2	0.81
^{147}Sm	Conc	37.8	49.1	20.04	16.58	4.82	205.7	140.0	46.3	22.56	16.72
	1σ	1.8	1.4	0.79	0.67	0.47	7.2	5.0	1.7	0.91	0.66
^{151}Eu	Conc	7.30	7.84	4.28	3.07	1.29	126.1	72.2	5.22	3.46	2.80
	1σ	0.32	0.27	0.18	0.14	0.13	4.3	2.5	0.21	0.15	0.12
^{157}Gd	Conc	59.5	75.5	100.0	35.5	25.8	271.7	200.9	91.9	40.5	60.9
	1σ	2.7	2.1	3.5	1.3	1.3	9.0	6.7	3.1	1.4	2.1
^{159}Tb	Conc	13.71	17.88	35.6	10.57	8.79	57.0	45.5	23.02	9.98	20.36
	1σ	0.61	0.46	1.2	0.37	0.35	1.9	1.5	0.77	0.35	0.68

Analysis		SWA10a-020c	SWA10a-020b	SWA10a-022c	SWA10a-025	SWA10a-026	SWA10a-032	SWA10a-047	SWA10a-049c	SWA10a-050c	SWA10a-051c
^{163}Dy	Conc	108.9	142.6	436	114.8	108.3	497	382	225.8	89.2	226.8
	1σ	4.8	3.6	15	3.9	3.8	16	13	7.5	3.0	7.5
^{165}Ho	Conc	30.5	38.6	164.9	43.3	40.6	152.7	109.1	78.5	27.68	80.8
	1σ	1.3	1.0	5.4	1.4	1.4	5.0	3.6	2.6	0.93	2.7
^{166}Er	Conc	113.4	140.4	713	193.0	182.5	592	404	333	108.6	333
	1σ	4.7	3.7	23	6.4	6.1	19	13	11	3.6	11
^{169}Tm	Conc	22.29	25.67	145.0	40.3	40.6	116.1	75.4	67.7	20.96	63.8
	1σ	0.85	0.73	4.7	1.3	1.4	3.7	2.5	2.2	0.69	2.1
^{173}Yb	Conc	206.7	240.0	1324	389	410	1055	655	644	194.5	570
	1σ	8.0	6.8	43	13	14	34	21	21	6.4	18
^{175}Lu	Conc	38.8	41.8	222.3	73.2	77.4	166.8	106.2	116.7	34.4	96.3
	1σ	1.4	1.3	7.2	2.4	2.5	5.4	3.4	3.8	1.1	3.1
^{181}Ta	Conc	3.760	2.55	9.27	10.42	0.840	7.33	6.00	15.33	0.387	1.213
	1σ	0.099	0.13	0.31	0.34	0.063	0.24	0.21	0.49	0.022	0.046
^{232}Th	Conc	66.4	84.7	513	83.5	143.6	989	514	248.6	48.1	61.4
	1σ	2.7	2.1	16	2.7	4.7	32	16	8.0	1.6	2.0
^{238}U	Conc	458	444	1073	466	450	2337	1020	616	120.5	103.2
	1σ	14	14	33	14	14	73	32	19	3.8	3.2
Ti-in-zirc	T (°C)	784.5	785.1	739.9	759.6	568	1167.4	1110.5	822.1	732.3	790.5
	1σ	7.0	9.0	8.6	8.4	31	7.0	7.3	7.4	9.2	7.3

Analysis		SWA10a-051r	SWA10a-052c	SWA10a-053	SWA10a-059c	SWA10a-064c	SWA10a-065	SWA10a-071	SWA10a-072c	SWA10a-075	SWA10a-109c
Group		pristine	variable	pristine	metamict	variable	variable	metamict	metamict	variable	variable
^{31}P	Conc	370	1000	420	840	300	3700	660	1400	1020	630
	1σ	330	910	380	760	270	3400	600	1300	930	580
^{43}Ca	Conc	2580	3410	6210	6430	481	16700	14070	10920	9770	3790
	1σ	190	210	380	400	73	1000	880	680	600	280
^{49}Ti	Conc	35.2	28.9	23.9	122.2	8.3	233	438	153	5.35	8.4
	1σ	3.0	1.9	1.9	8.1	1.4	16	29	11	0.82	1.4
^{89}Y	Conc	1408	2980	2490	4270	3670	2540	9540	5920	2930	2590
	1σ	60	120	100	180	150	110	400	250	120	110
^{93}Nb	Conc	32.3	14.90	24.4	71.7	8.76	35.4	128.0	56.9	20.22	11.16
	1σ	1.4	0.65	1.1	3.2	0.46	1.7	5.9	2.7	0.97	0.56
^{139}La	Conc	25.4	68.1	19.49	171.5	37.4	50.9	256	207.0	8.97	14.38
	1σ	1.0	2.6	0.76	6.6	1.5	2.0	10	8.2	0.39	0.60
^{140}Ce	Conc	92.8	287	46.5	586	38.6	179.1	1852	778	24.66	75.2
	1σ	3.5	10	1.7	22	1.5	6.8	70	30	0.98	2.9
^{141}Pr	Conc	14.33	45.6	6.43	65.9	10.04	23.25	179.7	100.8	1.929	6.88
	1σ	0.55	1.6	0.24	2.4	0.41	0.87	6.5	3.7	0.092	0.29
^{146}Nd	Conc	78.5	251.2	33.4	329	54.7	115.3	1184	528	7.75	35.4
	1σ	3.0	8.5	1.2	11	2.2	4.2	41	18	0.39	1.5
^{147}Sm	Conc	39.4	98.4	18.14	114.8	35.2	43.8	689	225.9	6.50	19.20
	1σ	1.5	3.4	0.73	4.1	1.6	1.8	24	8.1	0.36	0.95
^{151}Eu	Conc	8.31	18.62	2.16	67.6	5.52	8.30	224.6	43.6	1.414	2.30
	1σ	0.33	0.64	0.10	2.3	0.28	0.36	7.8	1.6	0.086	0.15
^{157}Gd	Conc	61.4	157.9	50.3	200.5	116.7	90.0	1054	338	37.1	60.2
	1σ	2.2	5.3	1.8	6.9	4.3	3.3	36	12	1.4	2.3
^{159}Tb	Conc	16.45	36.2	17.56	50.9	33.5	24.41	213.1	78.2	15.78	20.02
	1σ	0.57	1.2	0.59	1.7	1.1	0.84	7.0	2.6	0.54	0.71

Analysis		SWA10a-051r	SWA10a-052c	SWA10a-053	SWA10a-059c	SWA10a-064c	SWA10a-065	SWA10a-071	SWA10a-072c	SWA10a-075	SWA10a-109c
^{163}Dy	Conc	152.1	312	213.1	462	360	252.7	1408	661	223.7	229.3
	1σ	5.1	10	7.1	15	12	8.5	47	22	7.6	7.9
^{165}Ho	Conc	48.0	93.0	82.5	138.5	127.7	84.0	291.9	186.6	91.4	84.7
	1σ	1.6	3.1	2.7	4.6	4.3	2.8	9.7	6.2	3.1	2.8
^{166}Er	Conc	212.0	349	383	519	514	348	810	658	434	367
	1σ	7.0	11	13	17	17	11	27	22	14	12
^{169}Tm	Conc	51.0	66.3	82.4	95.5	99.2	71.0	126.7	117.9	94.5	76.9
	1σ	1.7	2.1	2.7	3.1	3.2	2.3	4.1	3.8	3.1	2.5
^{173}Yb	Conc	599	597	807	840	939	654	1077	986	913	720
	1σ	19	19	26	27	31	22	35	32	30	23
^{175}Lu	Conc	117.4	97.5	150.4	128.8	172.6	106.2	177.8	155.8	164.5	122.2
	1σ	3.8	3.1	4.8	4.1	5.6	3.4	5.7	5.0	5.3	4.0
^{181}Ta	Conc	24.58	2.298	8.25	4.95	4.89	7.14	34.8	4.57	9.72	2.59
	1σ	0.79	0.078	0.27	0.17	0.19	0.25	1.1	0.17	0.33	0.12
^{232}Th	Conc	57.9	256.9	301.1	572	87.9	479	284.1	723	408	365
	1σ	1.9	8.2	9.6	18	2.9	15	9.1	23	13	12
^{238}U	Conc	872	606	1723	1089	164.5	1399	2111	1476	1674	967
	1σ	27	19	55	35	5.3	45	68	48	54	32
Ti-in-zirc	T (°C)	865.1	843.4	823.8	1021.8	724	1121.2	1235.0	1055.0	689	726
	1σ	8.1	6.2	7.4	6.9	14	7.6	7.8	7.7	12	13

Analysis Group		SWA10a-116 pristine	SWA10a-128 metamict	SWA10a-130 metamict	SWA10a-135 pristine	SWA10a-145 variable	SWA10a-155 variable	RSA09-001c metamict	RSA09-006 pristine	RSA09-021 variable	RSA09-024 variable
^{31}P	Conc	760	260	1400	730	400	350	1400	1110	1050	580
	1σ	700	240	1300	680	370	320	1100	850	810	450
^{43}Ca	Conc	2660	930	20600	293	1252	900	4470	3830	626	528
	1σ	190	100	1200	41	89	140	280	240	70	63
^{49}Ti	Conc	2.65	73.7	639	13.0	6.03	23.7	76.5	33.4	13.1	48.0
	1σ	0.58	5.6	36	1.4	0.64	3.4	4.9	2.2	1.5	3.7
^{89}Y	Conc	2590	3760	23020	2297	2110	1468	8870	6160	2730	4890
	1σ	110	160	980	99	92	65	380	270	120	220
^{93}Nb	Conc	8.92	21.9	241	7.04	7.78	9.17	36.5	31.7	12.98	21.1
	1σ	0.43	1.0	11	0.35	0.37	0.55	1.7	1.4	0.64	1.0
^{139}La	Conc	2.42	269	734	2.22	19.80	37.9	38.3	8.30	8.27	25.9
	1σ	0.12	10	27	0.11	0.76	1.6	1.5	0.34	0.38	1.1
^{140}Ce	Conc	26.7	291	4650	26.1	70.6	68.8	164.7	60.8	41.8	133.1
	1σ	1.0	11	180	1.1	2.9	2.9	6.4	2.4	1.7	5.5
^{141}Pr	Conc	1.473	90.7	487	0.752	8.80	13.02	17.57	4.56	2.55	11.80
	1σ	0.076	3.3	18	0.046	0.34	0.58	0.65	0.18	0.12	0.47
^{146}Nd	Conc	11.93	431	2646	7.28	45.0	70.0	90.4	29.0	16.47	64.4
	1σ	0.56	15	94	0.38	1.7	3.1	3.4	1.1	0.79	2.6
^{147}Sm	Conc	13.55	184.4	1396	10.78	25.68	30.5	67.9	32.8	13.35	40.0
	1σ	0.63	6.6	48	0.52	0.96	1.6	2.5	1.2	0.67	1.6
^{151}Eu	Conc	0.995	23.92	129.7	1.168	3.49	2.42	20.31	8.66	2.45	4.08
	1σ	0.072	0.92	4.5	0.077	0.15	0.20	0.74	0.32	0.14	0.20
^{157}Gd	Conc	61.3	276.4	2382	52.5	63.7	60.6	293	177.6	60.6	130.2
	1σ	2.2	9.5	80	1.9	2.2	2.6	10	6.3	2.4	4.9
^{159}Tb	Conc	21.18	68.8	574	17.67	19.21	15.34	101.2	59.3	21.41	44.6
	1σ	0.73	2.3	19	0.62	0.66	0.60	3.3	2.0	0.73	1.5

Analysis		SWA10a-116	SWA10a-128	SWA10a-130	SWA10a-135	SWA10a-145	SWA10a-155	RSA09-001c	RSA09-006	RSA09-021	RSA09-024
^{163}Dy	Conc	240.0	517	4150	206.0	196.1	153.5	993	606	253.3	476
	1σ	8.2	18	140	7.1	6.8	5.7	33	20	8.5	16
^{165}Ho	Conc	86.6	132.6	782	74.2	68.5	48.3	284.0	195.4	89.9	160.6
	1σ	2.9	4.4	26	2.5	2.3	1.7	9.3	6.4	3.0	5.3
^{166}Er	Conc	377	430	1885	320	288.2	202.8	1006	753	381	634
	1σ	12	14	60	10	9.3	6.8	33	24	12	21
^{169}Tm	Conc	79.2	77.9	247.4	65.9	59.7	42.5	186.5	146.0	78.9	120.7
	1σ	2.6	2.5	7.9	2.1	1.9	1.5	6.0	4.7	2.6	3.9
^{173}Yb	Conc	757	701	1721	617	570	408	1552	1308	734	1079
	1σ	25	23	55	20	18	14	50	42	24	35
^{175}Lu	Conc	130.4	110.0	228.6	107.6	102.5	78.4	227.6	192.2	120.1	161.7
	1σ	4.2	3.6	7.3	3.5	3.3	2.6	7.3	6.2	3.9	5.2
^{181}Ta	Conc	4.55	1.623	27.12	2.95	1.446	5.39	7.52	2.371	1.546	1.501
	1σ	0.17	0.080	0.88	0.11	0.055	0.24	0.25	0.084	0.071	0.070
^{232}Th	Conc	394	187.8	2991	418	350	125.3	277.5	217.8	122.5	147.4
	1σ	13	6.1	96	14	11	4.2	8.9	7.0	4.0	4.8
^{238}U	Conc	951	455	3500	563	552	484	1079	709	254.3	543
	1σ	31	15	120	19	19	17	36	24	8.8	19
Ti-in-zirc	T (°C)	636	953.2	1312.1	764.6	698.2	823	958.0	859.2	765.3	900.4
	1σ	15	7.8	6.2	9.1	8.3	13	6.4	6.2	9.8	7.6

Analysis Group		RSA09-030c pristine	RSA09-033 variable	RSA09-036c metamict	RSA09-036r metamict	RSA09-037 variable	RSA09-038c variable	RSA09-041 variable	RSA09-053r metamict	RSA09-063c metamict	RSA09-067 metamict	RSA09-073 variable
^{31}P	Conc	82	650	1170	880	1270	690	470	430	870	410	670
	1σ	63	500	900	680	980	530	360	330	670	310	530
^{43}Ca	Conc	14.2	5220	847	15860	715	15500	524	13120	3760	2240	930
	1σ	6.8	380	96	900	49	870	67	790	230	170	110
^{49}Ti	Conc	4.92	4.9	274	190	30.2	13.5	19.7	180	125.7	36.0	26.8
	1σ	0.45	1.3	16	11	1.8	1.1	2.1	11	7.2	3.0	2.9
^{89}Y	Conc	191.5	3150	9120	15410	6770	3530	3430	3320	10560	2930	3480
	1σ	7.9	130	380	640	280	150	150	140	450	130	140
^{93}Nb	Conc	1.353	11.68	46.3	51.3	17.72	25.0	19.79	35.2	91.1	32.4	14.59
	1σ	0.067	0.60	2.0	2.2	0.74	1.1	0.89	1.5	3.8	1.4	0.71
^{139}La	Conc	0.0066	2.77	91.3	449	25.64	53.0	15.81	424	52.5	34.7	16.09
	1σ	0.0025	0.18	3.5	17	0.98	2.0	0.66	16	2.0	1.4	0.68
^{140}Ce	Conc	5.80	53.9	239.3	2990	113.3	126.6	59.1	1171	272.1	146.7	103.6
	1σ	0.21	2.0	8.4	100	4.0	4.5	2.2	42	9.7	5.3	3.9
^{141}Pr	Conc	0.0061	1.74	40.0	309	10.74	7.14	5.84	77.4	27.35	16.37	11.43
	1σ	0.0020	0.12	1.4	10	0.37	0.25	0.24	2.7	0.94	0.60	0.46
^{146}Nd	Conc	0.550	12.48	184.1	1546	55.8	42.0	29.0	347	148.7	75.3	58.7
	1σ	0.045	0.77	6.5	52	1.9	1.5	1.2	12	5.1	2.8	2.5
^{147}Sm	Conc	1.428	16.43	111.2	833	42.0	22.31	21.88	87.3	93.6	35.3	34.4
	1σ	0.085	0.97	4.1	28	1.5	0.84	0.99	3.2	3.2	1.4	1.6
^{151}Eu	Conc	0.822	2.27	7.16	99.0	8.69	3.96	2.44	16.72	11.46	2.93	2.38
	1σ	0.040	0.18	0.33	3.3	0.30	0.16	0.15	0.65	0.42	0.16	0.17
^{157}Gd	Conc	8.09	78.6	272.4	1363	153.9	79.1	79.6	132.3	294	77.5	91.7
	1σ	0.31	3.1	9.5	46	5.2	2.8	3.0	4.8	10	2.9	3.4
^{159}Tb	Conc	2.435	27.97	98.9	368	53.5	26.75	30.3	32.5	96.1	26.48	31.4
	1σ	0.086	0.98	3.3	12	1.7	0.88	1.0	1.1	3.1	0.90	1.1

Analysis		RSA09-030c	RSA09-033	RSA09-036c	RSA09-036r	RSA09-037	RSA09-038c	RSA09-041	RSA09-053r	RSA09-063c	RSA09-067	RSA09-073
^{163}Dy	Conc	22.94	312	1030	2597	621	308	346	324	1023	297	334
	1σ	0.78	11	34	85	20	10	12	11	34	10	11
^{165}Ho	Conc	6.28	101.7	299.8	519	227.2	113.6	114.5	101.3	335	97.9	116.3
	1σ	0.21	3.4	9.8	17	7.4	3.7	3.8	3.3	11	3.2	3.9
^{166}Er	Conc	22.21	434	1125	1537	959	489	459	426	1288	391	454
	1σ	0.73	14	36	49	31	16	15	14	41	13	15
^{169}Tm	Conc	4.24	88.5	197.4	273.7	193.2	108.8	93.4	94.1	240.8	84.3	90.2
	1σ	0.14	2.9	6.4	8.8	6.2	3.5	3.0	3.1	7.7	2.7	3.0
^{173}Yb	Conc	36.8	901	1597	2358	1794	1065	851	966	2040	793	792
	1σ	1.2	30	52	77	59	35	28	32	67	26	26
^{175}Lu	Conc	6.30	129.2	220.0	318	296.5	165.9	126.8	157.3	303.6	113.8	128.5
	1σ	0.21	4.2	7.1	10	9.5	5.3	4.1	5.1	9.7	3.7	4.2
^{181}Ta	Conc	0.419	2.05	1.024	27.45	3.77	12.70	1.731	15.87	7.90	6.14	1.895
	1σ	0.018	0.11	0.061	0.90	0.13	0.42	0.083	0.55	0.27	0.23	0.098
^{232}Th	Conc	7.05	404	2043	351	129.8	874	181.8	105.3	332	256.2	189.8
	1σ	0.24	13	67	11	4.2	29	6.0	3.5	11	8.5	6.2
^{238}U	Conc	13.84	946	648	2645	225.0	1520	436	1912	1047	835	564
	1σ	0.43	29	20	82	7.0	47	14	60	33	26	18
Ti-in-zirc	T (°C)	682.1	682	1149.0	1087.9	848.4	768.0	804.3	1079.9	1025.8	867.6	836
	1σ	7.1	18	6.2	5.7	5.5	7.1	9.5	6.4	5.7	8.0	10

Analysis Group		RSA09-092c pristine	RSA09-097c variable	RSA09-102 metamict	RSA09-104c pristine	RSA09-107c metamict	RSA09-112c pristine	RSA09-112r variable	RSA09-113c variable	RSA09-115c metamict	RSA09-125c variable	RSA09-131 metamict
^{31}P	Conc	1210	140	690	330	290	600	720	370	450	630	660
	1σ	950	110	540	260	230	470	570	290	350	500	520
^{43}Ca	Conc	145	1630	10100	<24	8370	138	5740	265	6850	3830	13670
	1σ	24	120	590	13	520	37	360	43	430	230	880
^{49}Ti	Conc	11.3	11.8	48.3	6.87	32.8	4.74	31.0	52.9	63.6	95.5	163
	1σ	1.0	1.2	3.3	0.85	2.8	0.95	2.4	3.9	4.4	5.5	11
^{89}Y	Conc	5640	1843	13420	785	4410	1838	4700	3810	9270	5350	26600
	1σ	230	77	570	33	180	75	190	160	380	220	1100
^{93}Nb	Conc	20.97	32.1	150.8	2.24	34.8	8.00	42.6	51.9	35.5	20.64	109.5
	1σ	0.91	1.4	6.6	0.13	1.5	0.40	1.9	2.3	1.6	0.91	4.9
^{139}La	Conc	6.74	11.16	45.0	0.0372	94.7	4.51	22.93	16.09	138.2	43.3	95.1
	1σ	0.27	0.44	1.7	0.0094	3.6	0.22	0.89	0.65	5.2	1.6	3.7
^{140}Ce	Conc	60.9	49.3	198.1	13.11	393	12.44	85.8	55.6	387	235.6	384
	1σ	2.3	1.9	7.5	0.53	14	0.51	3.2	2.1	14	8.8	15
^{141}Pr	Conc	3.38	4.53	21.00	0.0399	39.9	1.182	10.41	6.88	47.0	23.99	42.0
	1σ	0.13	0.18	0.76	0.0082	1.4	0.075	0.38	0.27	1.7	0.83	1.5
^{146}Nd	Conc	21.67	25.7	109.0	1.13	199.1	6.15	48.7	33.1	251.0	117.0	238.6
	1σ	0.87	1.1	4.2	0.11	7.2	0.41	1.9	1.4	9.2	4.3	9.1
^{147}Sm	Conc	20.56	16.70	74.7	3.06	89.6	5.74	25.4	27.0	142.5	59.0	184.5
	1σ	0.81	0.72	2.7	0.21	3.3	0.41	1.0	1.2	5.1	2.1	6.9
^{151}Eu	Conc	6.07	2.60	11.35	0.887	19.36	0.836	5.20	2.31	7.07	10.89	34.9
	1σ	0.24	0.13	0.43	0.061	0.74	0.080	0.22	0.14	0.30	0.39	1.4
^{157}Gd	Conc	115.7	50.7	309	18.73	200.6	31.2	89.8	88.4	334	164.7	720
	1σ	4.0	1.8	11	0.76	6.9	1.3	3.2	3.2	11	5.6	25
^{159}Tb	Conc	42.4	15.54	120.2	6.33	46.6	12.65	36.7	31.6	103.7	52.3	266.8
	1σ	1.4	0.54	4.0	0.23	1.6	0.46	1.2	1.1	3.4	1.7	8.8

Analysis		RSA09-092c	RSA09-097c	RSA09-102	RSA09-104c	RSA09-107c	RSA09-112c	RSA09-112r	RSA09-113c	RSA09-115c	RSA09-125c	RSA09-131
^{163}Dy	Conc	506	167.6	1378	75.1	393	161.2	437	367	1016	526	2781
	1σ	17	5.7	47	2.6	13	5.5	15	12	34	18	93
^{165}Ho	Conc	190.9	57.7	430	26.82	118.8	62.5	142.5	134.1	300.6	162.6	824
	1σ	6.2	1.9	14	0.90	3.9	2.1	4.7	4.4	9.8	5.3	27
^{166}Er	Conc	811	228.7	1643	114.2	452	277.5	564	554	1088	613	3250
	1σ	27	7.5	54	3.8	15	9.0	18	18	35	20	100
^{169}Tm	Conc	158.1	42.9	309	23.80	88.6	56.9	106.9	104.6	203.5	114.7	551
	1σ	5.1	1.4	10	0.79	2.9	1.9	3.5	3.4	6.6	3.7	18
^{173}Yb	Conc	1452	371	2685	225.7	801	526	942	919	1662	1012	4840
	1σ	48	12	90	7.7	26	17	31	30	54	33	160
^{175}Lu	Conc	256.4	61.0	385	42.3	134.3	97.6	156.4	148.2	230.5	157.2	683
	1σ	8.2	2.0	12	1.4	4.3	3.2	5.0	4.8	7.4	5.0	22
^{181}Ta	Conc	4.07	1.273	11.20	0.626	15.65	0.986	10.55	4.36	13.19	7.19	17.71
	1σ	0.14	0.055	0.37	0.033	0.52	0.057	0.35	0.16	0.44	0.23	0.61
^{232}Th	Conc	97.8	45.0	163.1	32.5	52.8	38.7	82.9	244.0	142.0	242.9	161.9
	1σ	3.2	1.5	5.3	1.1	1.7	1.3	2.7	7.9	4.6	7.9	5.3
^{238}U	Conc	144.3	644	1988	57.7	1467	90.4	937	290.0	1399	792	3540
	1σ	4.6	21	64	1.9	45	2.8	29	9.0	43	25	110
Ti-in-zirc	T (°C)	751.6	755.4	901.2	708.9	857.1	679	851.0	912.0	934.6	987.4	1064.8
	1σ	7.5	8.6	6.5	9.8	8.1	15	7.1	7.3	6.8	5.6	7.4

Analysis		RSA09-138	RSA09-139	RSA09-142c	RSA09-142r	RSA09-146	SWA03-001c	SWA03-004c	SWA03-006c	SWA03-007c	SWA03-007r	SWA03-009c
Group		metamict	variable	metamict	metamict	metamict	metamict	pristine	variable	variable	variable	variable
^{31}P	Conc	570	400	630	440	610	1010	430	660	970	640	1060
	1σ	450	320	500	350	480	360	150	230	340	230	290
^{43}Ca	Conc	7960	9920	2260	10700	12790						
	1σ	510	630	150	640	740						
^{49}Ti	Conc	253	20.0	245	56.5	60.5	133.9	28.8	5.58	48.4	19.6	18.5
	1σ	15	2.1	13	3.9	3.7	5.4	1.7	0.73	2.5	1.7	1.5
^{89}Y	Conc	14480	3320	10370	10870	12020	8970	2242	1603	3590	2960	2015
	1σ	610	140	410	430	480	310	79	56	130	100	72
^{93}Nb	Conc	263	27.1	208.6	142.7	97.6	88.9	27.4	7.72	43.7	26.3	9.97
	1σ	12	1.3	8.7	6.0	4.1	3.2	1.0	0.33	1.7	1.0	0.41
^{139}La	Conc	62.3	14.40	87.9	83.5	28.8	155.3	37.3	34.7	15.68	6.04	11.44
	1σ	2.4	0.60	3.3	3.2	1.1	5.4	1.3	1.3	0.58	0.27	0.45
^{140}Ce	Conc	169.2	51.9	386	350	135.1	746	112.1	72.4	107.1	67.4	47.0
	1σ	6.5	2.0	14	13	4.9	28	4.3	2.9	4.3	2.8	1.6
^{141}Pr	Conc	26.05	5.43	47.7	40.1	17.87	114.3	12.96	6.69	13.83	4.41	3.69
	1σ	0.94	0.23	1.6	1.4	0.62	3.7	0.45	0.25	0.48	0.19	0.16
^{146}Nd	Conc	135.1	27.8	242.2	211.9	119.0	810	70.6	30.7	69.5	23.03	21.95
	1σ	5.2	1.2	8.4	7.5	4.2	26	2.4	1.2	2.4	0.99	0.96
^{147}Sm	Conc	124.1	18.33	124.9	98.2	127.8	418	48.1	11.40	55.6	18.20	14.79
	1σ	4.6	0.89	4.3	3.5	4.4	14	1.8	0.59	2.1	0.89	0.74
^{151}Eu	Conc	24.18	5.85	7.26	9.23	12.75	77.5	4.92	1.195	7.94	2.69	1.70
	1σ	0.92	0.28	0.29	0.37	0.47	2.6	0.20	0.088	0.31	0.16	0.12
^{157}Gd	Conc	482	64.1	288.7	264.0	377	625	102.1	35.8	121.9	67.1	57.1
	1σ	17	2.4	9.6	8.9	13	20	3.4	1.4	4.1	2.5	2.1
^{159}Tb	Conc	163.3	23.12	96.1	86.4	130.1	131.7	31.6	12.68	45.1	27.80	21.12
	1σ	5.4	0.80	3.1	2.8	4.2	4.2	1.0	0.44	1.5	0.94	0.72

Analysis		RSA09-138	RSA09-139	RSA09-142c	RSA09-142r	RSA09-146	SWA03-001c	SWA03-004c	SWA03-006c	SWA03-007c	SWA03-007r	SWA03-009c
^{163}Dy	Conc	1550	286.0	1009	935	1340	1120	300.4	145.5	480	309	247.8
	1σ	52	9.8	33	31	44	36	9.7	4.8	16	10	8.2
^{165}Ho	Conc	456	94.8	334	296.5	394	290.8	79.3	52.4	136.3	101.3	88.9
	1σ	15	3.1	11	9.6	13	9.6	2.6	1.8	4.6	3.4	2.9
^{166}Er	Conc	1647	416	1298	1085	1449	989	280.1	234.1	519	407	379
	1σ	53	14	42	35	47	32	9.0	7.6	17	13	12
^{169}Tm	Conc	288.9	88.4	233.4	191.8	263.0	187.5	55.1	49.4	108.1	89.7	79.9
	1σ	9.3	2.9	7.5	6.2	8.4	6.1	1.8	1.6	3.6	3.0	2.6
^{173}Yb	Conc	2296	849	1955	1612	2244	1696	507	477	1017	861	752
	1σ	76	28	63	52	73	57	17	16	35	30	24
^{175}Lu	Conc	348	142.3	306.4	245.5	303.7	238.2	64.4	82.2	133.1	111.4	124.9
	1σ	11	4.6	9.8	7.9	9.7	7.6	2.1	2.7	4.3	3.6	4.0
^{181}Ta	Conc	15.69	11.68	2.527	13.76	17.33	8.92	2.496	2.84	1.909	5.30	1.628
	1σ	0.52	0.40	0.095	0.46	0.56	0.29	0.099	0.12	0.080	0.21	0.084
^{232}Th	Conc	1181	85.9	923	162.9	104.0	809	152.3	136.9	237.4	590	215.0
	1σ	38	2.8	30	5.3	3.4	26	5.0	4.5	7.8	19	7.1
^{238}U	Conc	3095	1508	860	1736	1858	2771	1154	371	420	1142	481
	1σ	96	47	27	54	57	92	39	13	14	39	15
Ti-in-zirc	T (°C)	1135.0	805.8	1129.7	919.9	928.2	1035.1	843.1	692	901.3	803.8	798.1
	1σ	6.4	9.4	5.7	6.8	6.0	3.4	5.3	10	4.8	7.6	7.4

Analysis Group		SWA03-010 variable	SWA03-011 metamict	SWA03-012 variable	SWA03-014r metamict	SWA03-017c metamict	SWA03-018 variable	SWA03-020 variable	SWA03-022r metamict	SWA03-023 pristine	SWA03-024 metamict
^{31}P	Conc	1090	1170	1240	740	1230	1200	1060	690	810	7000
	1σ	300	320	340	200	340	330	300	190	230	2000
^{43}Ca	Conc										
	1σ										
^{49}Ti	Conc	9.18	17.71	7.56	11.94	75.5	7.1	9.8	98.5	45.9	96.4
	1σ	0.72	0.94	0.87	0.70	3.3	1.1	1.2	4.1	2.2	4.4
^{89}Y	Conc	2690	2860	2643	2561	3790	2930	2476	3970	2041	4590
	1σ	97	100	97	94	140	110	90	150	75	170
^{93}Nb	Conc	13.26	20.29	10.51	27.01	33.1	10.27	7.13	45.4	14.08	69.8
	1σ	0.49	0.73	0.43	0.98	1.2	0.46	0.32	1.6	0.52	2.5
^{139}La	Conc	1.747	76.2	7.15	14.79	62.7	1.007	3.47	35.8	4.09	50.9
	1σ	0.082	2.7	0.30	0.53	2.2	0.089	0.18	1.3	0.16	1.8
^{140}Ce	Conc	43.8	196.8	46.5	103.1	219.7	34.2	31.5	197.3	41.4	249.3
	1σ	1.4	6.4	1.6	3.4	7.1	1.2	1.1	6.4	1.4	8.2
^{141}Pr	Conc	1.158	19.27	2.28	7.84	27.08	0.814	1.197	20.07	3.52	34.6
	1σ	0.054	0.63	0.11	0.26	0.89	0.068	0.077	0.65	0.13	1.1
^{146}Nd	Conc	8.71	89.5	14.73	54.7	126.9	7.83	7.61	109.2	19.87	176.4
	1σ	0.39	3.0	0.69	1.8	4.2	0.54	0.49	3.7	0.75	6.1
^{147}Sm	Conc	12.79	39.7	17.86	32.0	76.4	12.76	11.88	61.6	18.64	108.9
	1σ	0.54	1.4	0.83	1.1	2.6	0.78	0.67	2.1	0.70	3.7
^{151}Eu	Conc	1.314	6.00	1.61	9.62	12.30	1.67	1.44	7.85	2.44	13.27
	1σ	0.074	0.22	0.11	0.33	0.41	0.14	0.12	0.27	0.10	0.46
^{157}Gd	Conc	72.9	104.4	75.4	91.9	171.1	75.0	66.5	149.1	65.5	227.9
	1σ	2.5	3.4	2.7	3.0	5.5	2.8	2.5	4.9	2.2	7.6
^{159}Tb	Conc	28.46	35.5	28.68	29.52	63.0	29.9	24.57	51.9	23.70	80.1
	1σ	0.93	1.1	0.96	0.96	2.0	1.0	0.84	1.7	0.77	2.6

Analysis		SWA03-010	SWA03-011	SWA03-012	SWA03-014r	SWA03-017c	SWA03-018	SWA03-020	SWA03-022r	SWA03-023	SWA03-024
^{163}Dy	Conc	344	389	335	336	641	365	299.2	566	271.7	800
	1σ	11	13	11	11	21	12	9.8	18	8.8	26
^{165}Ho	Conc	124.6	131.4	122.5	116.7	186.7	136.1	108.7	181.6	93.3	225.2
	1σ	4.1	4.3	4.0	3.8	6.1	4.5	3.6	5.9	3.0	7.3
^{166}Er	Conc	532	542	520	477	700	576	470	713	389	836
	1σ	17	18	17	16	23	19	15	23	13	27
^{169}Tm	Conc	111.4	112.1	108.5	96.6	135.4	121.7	98.9	138.5	80.6	161.8
	1σ	3.6	3.6	3.6	3.2	4.4	4.1	3.2	4.5	2.6	5.2
^{173}Yb	Conc	1003	1018	1022	868	1167	1094	938	1183	738	1406
	1σ	32	33	33	28	38	36	30	38	24	45
^{175}Lu	Conc	161.6	159.9	156.2	135.5	171.9	179.7	147.9	175.4	118.9	205.5
	1σ	5.2	5.1	5.0	4.3	5.5	5.8	4.8	5.6	3.8	6.6
^{181}Ta	Conc	3.10	4.19	2.58	5.95	2.669	2.43	1.623	6.57	1.664	2.247
	1σ	0.12	0.14	0.11	0.20	0.090	0.13	0.089	0.21	0.064	0.086
^{232}Th	Conc	509	438	462	848	556	471	359	897	316	592
	1σ	17	14	15	28	18	16	12	29	10	19
^{238}U	Conc	848	898	807	1478	621	872	613	1553	442	667
	1σ	26	28	25	46	19	27	19	48	14	21
Ti-in-zirc	T (°C)	733.4	793.7	716.8	756.7	956.3	712	739.2	991.6	895.1	988.6
	1σ	6.5	4.6	9.2	5.0	3.9	12	9.7	3.6	4.2	4.0

Analysis Group		SWA03-025c variable	SWA03-026 variable	SWA03-029 metamict	SWA03-030 metamict	SWA03-032c variable	SWA03-032r metamict	SWA03-034c variable	SWA03-035r metamict	SWA03-036 variable	SWA03-038c variable	SWA03-039c pristine
^{31}P	Conc	530	700	3350	3260	4800	1050	1460	1020	1670	1650	740
	1σ	150	200	940	920	1400	300	420	290	480	470	210
^{43}Ca	Conc											
	1σ											
^{49}Ti	Conc	9.78	5.96	19.6	75.1	7.65	191.2	6.30	458	29.8	15.4	11.45
	1σ	0.53	0.62	1.0	3.5	0.75	8.6	0.67	21	2.0	1.3	0.96
^{89}Y	Conc	1414	2690	2281	4750	1873	4940	3200	10840	2491	2308	2304
	1σ	53	100	86	180	68	180	120	400	93	87	88
^{93}Nb	Conc	11.51	16.14	16.76	40.0	6.75	85.8	11.40	139.6	22.41	14.33	17.61
	1σ	0.42	0.62	0.62	1.5	0.28	3.2	0.46	5.3	0.89	0.59	0.71
^{139}La	Conc	4.24	1.883	58.6	33.3	11.48	62.6	6.27	216.8	15.04	9.00	5.18
	1σ	0.16	0.094	2.1	1.2	0.45	2.3	0.26	8.0	0.59	0.38	0.22
^{140}Ce	Conc	30.17	48.0	164.6	181.7	62.8	292	56.8	861	101.7	72.9	65.1
	1σ	0.99	1.6	5.4	6.0	2.2	10	2.1	31	3.7	2.7	2.4
^{141}Pr	Conc	3.47	1.334	17.81	24.93	7.02	41.2	3.08	102.9	10.23	6.60	3.84
	1σ	0.12	0.065	0.59	0.82	0.27	1.5	0.13	3.7	0.40	0.27	0.16
^{146}Nd	Conc	19.35	10.61	85.9	123.0	41.0	193.3	21.53	564	56.5	42.3	21.67
	1σ	0.69	0.49	3.0	4.4	1.6	7.0	0.90	21	2.3	1.8	0.94
^{147}Sm	Conc	15.71	13.97	38.7	88.7	26.2	129.2	22.30	247.3	38.3	27.7	20.33
	1σ	0.55	0.61	1.3	3.0	1.0	4.3	0.90	8.4	1.5	1.1	0.84
^{151}Eu	Conc	2.74	2.25	3.83	13.88	3.54	17.21	5.40	40.5	4.83	5.67	2.11
	1σ	0.10	0.12	0.14	0.48	0.16	0.57	0.22	1.4	0.22	0.25	0.11
^{157}Gd	Conc	48.9	75.5	89.1	202.8	69.8	244.0	94.9	447	100.2	86.8	70.4
	1σ	1.7	2.7	3.0	6.9	2.5	8.3	3.4	15	3.7	3.2	2.6
^{159}Tb	Conc	17.64	27.97	29.24	76.6	22.58	94.8	35.0	128.0	35.1	28.34	25.70
	1σ	0.57	0.92	0.94	2.5	0.76	3.1	1.2	4.2	1.2	0.97	0.88

Analysis		SWA03-025c	SWA03-026	SWA03-029	SWA03-030	SWA03-032c	SWA03-032r	SWA03-034c	SWA03-035r	SWA03-036	SWA03-038c	SWA03-039c
^{163}Dy	Conc	192.1	340	312	777	245.4	931	408	1309	368	304	291.0
	1σ	6.2	11	10	25	8.0	30	13	42	12	10	9.5
^{165}Ho	Conc	63.3	123.2	104.6	225.9	84.3	247.1	143.8	420	114.1	101.9	103.3
	1σ	2.1	4.0	3.4	7.4	2.8	8.0	4.7	14	3.8	3.4	3.4
^{166}Er	Conc	267.9	525	427	839	353	889	603	1657	456	411	440
	1σ	8.7	17	14	27	11	29	19	53	15	13	14
^{169}Tm	Conc	56.1	108.5	86.7	161.0	74.7	170.1	121.7	306.0	91.0	82.4	91.1
	1σ	1.8	3.5	2.8	5.2	2.4	5.5	4.0	9.9	3.0	2.7	3.0
^{173}Yb	Conc	523	993	788	1388	711	1467	1099	2482	825	750	828
	1σ	17	32	25	45	23	47	36	80	27	25	27
^{175}Lu	Conc	85.0	157.7	127.3	213.3	112.0	199.8	175.3	379	127.1	118.9	133.7
	1σ	2.7	5.1	4.1	6.8	3.6	6.4	5.6	12	4.1	3.8	4.3
^{181}Ta	Conc	3.65	4.14	2.627	2.354	1.593	4.18	2.73	11.03	3.72	2.228	2.98
	1σ	0.12	0.15	0.090	0.087	0.071	0.14	0.11	0.36	0.14	0.098	0.12
^{232}Th	Conc	87.3	503	349	549	194.6	631	589	1097	604	351	338
	1σ	2.8	16	11	18	6.3	20	19	36	20	11	11
^{238}U	Conc	701	911	542	717	403	754	897	2557	964	468	542
	1σ	22	28	17	22	13	24	29	82	31	15	18
Ti-in-zirc	T (°C)	738.9	697.3	803.4	955.6	717.8	1089.3	701.8	1243.8	847.0	780.5	752.9
	1σ	4.5	8.2	4.5	4.3	7.9	4.0	8.4	4.3	6.1	7.3	7.1

Analysis Group		SWA03-040 pristine	SWA03-041 variable	SWA03-042 variable	SWA03-043c variable	SWA03-045c metamict	SWA03-046c metamict	SWA03-047c variable	SWA03-048c pristine	SWA03-048r pristine	SWA03-049c variable
^{31}P	Conc	1070	1000	1020	2250	1790	830	3170	670	410	2810
	1σ	310	280	290	650	510	240	910	190	120	810
^{43}Ca	Conc										
	1σ										
^{49}Ti	Conc	8.47	27.9	18.5	10.73	19.5	83.3	10.4	20.4	21.4	31.8
	1σ	0.83	2.1	1.8	0.97	1.1	5.0	1.0	1.3	1.4	2.6
^{89}Y	Conc	3600	2499	2380	2990	2830	3840	1795	1987	1563	2610
	1σ	140	92	88	110	110	150	69	77	61	100
^{93}Nb	Conc	13.31	12.77	14.83	11.47	16.50	36.8	8.09	12.79	17.69	16.27
	1σ	0.56	0.54	0.64	0.48	0.65	1.5	0.36	0.53	0.73	0.73
^{139}La	Conc	3.87	16.06	10.80	13.38	23.69	25.7	34.6	7.55	9.19	15.71
	1σ	0.18	0.65	0.47	0.54	0.91	1.0	1.4	0.31	0.38	0.68
^{140}Ce	Conc	51.7	79.6	56.0	70.5	156.1	158.8	102.5	50.1	62.1	97.1
	1σ	2.0	3.0	2.2	2.7	6.0	6.2	4.0	2.0	2.5	4.0
^{141}Pr	Conc	2.50	8.47	5.46	5.27	16.56	22.31	11.80	6.47	6.01	10.36
	1σ	0.12	0.34	0.25	0.22	0.63	0.87	0.48	0.26	0.24	0.45
^{146}Nd	Conc	16.19	41.6	27.0	30.6	97.1	106.3	65.1	34.7	35.7	61.6
	1σ	0.75	1.8	1.3	1.3	3.8	4.3	2.7	1.5	1.5	2.8
^{147}Sm	Conc	21.44	30.6	22.6	23.16	49.4	75.8	35.0	28.6	24.37	42.8
	1σ	0.90	1.3	1.1	0.95	1.7	2.8	1.4	1.1	0.90	1.8
^{151}Eu	Conc	2.88	4.97	2.59	2.58	9.98	11.39	4.33	4.45	5.87	4.87
	1σ	0.14	0.24	0.18	0.14	0.37	0.46	0.21	0.18	0.23	0.26
^{157}Gd	Conc	98.9	91.7	73.9	88.8	116.4	166.3	81.5	76.9	63.7	115.0
	1σ	3.7	3.4	2.9	3.3	4.1	6.1	3.1	2.9	2.4	4.5
^{159}Tb	Conc	37.7	33.1	27.41	31.3	36.1	62.7	24.22	27.36	20.98	36.6
	1σ	1.3	1.2	0.99	1.1	1.2	2.2	0.87	0.97	0.75	1.3

Analysis		SWA03-040	SWA03-041	SWA03-042	SWA03-043c	SWA03-045c	SWA03-046c	SWA03-047c	SWA03-048c	SWA03-048r	SWA03-049c
^{163}Dy	Conc	427	356	308	364	380	651	248.5	282.9	220.5	374
	1σ	14	12	10	12	12	21	8.2	9.3	7.3	12
^{165}Ho	Conc	156.8	114.3	106.2	129.3	128.0	184.3	80.9	87.9	69.9	117.2
	1σ	5.2	3.8	3.6	4.3	4.3	6.2	2.7	3.0	2.4	4.0
^{166}Er	Conc	658	464	439	552	519	696	327	349	275.9	471
	1σ	21	15	14	18	17	23	11	12	9.1	16
^{169}Tm	Conc	128.5	95.5	88.9	115.6	105.3	137.0	67.1	71.8	56.3	94.3
	1σ	4.2	3.1	3.0	3.8	3.4	4.5	2.2	2.4	1.9	3.2
^{173}Yb	Conc	1156	844	857	1075	951	1177	611	673	511	862
	1σ	38	28	28	35	31	38	20	22	17	28
^{175}Lu	Conc	199.5	132.5	129.2	170.1	149.9	168.1	97.4	105.6	80.0	131.6
	1σ	6.4	4.3	4.2	5.5	4.9	5.5	3.2	3.4	2.6	4.3
^{181}Ta	Conc	3.13	1.631	1.81	2.51	2.332	2.215	1.121	1.362	2.176	1.810
	1σ	0.12	0.082	0.10	0.10	0.080	0.094	0.059	0.053	0.077	0.091
^{232}Th	Conc	561	336	321	495	456	451	207.8	229.8	325	372
	1σ	18	11	10	16	15	15	6.8	7.4	11	12
^{238}U	Conc	1075	435	489	836	645	571	327	598	514	518
	1σ	35	14	16	27	21	19	11	20	17	17
Ti-in-zirc	T (°C)	726.4	839.8	798.0	747.1	803.1	969.1	744.0	807.7	812.2	853.7
	1σ	8.0	6.9	8.8	7.6	5.1	5.8	8.3	5.8	5.7	7.6

Analysis Group		SWA03-050c metamict	SWA03-050r variable	SWA03-052 variable	SWA03-053c variable	SWA03-053r metamict	SWA03-054c pristine	SWA03-056c pristine	SWA03-057c pristine	SWA03-060c variable	RSA06-001c variable
^{31}P	Conc	1400	650	730	2940	570	240	5600	1070	520	860
	1σ	400	190	210	850	170	69	1600	310	150	630
^{43}Ca	Conc										427
	1σ										66
^{49}Ti	Conc	146.5	21.6	2270	75.7	46.1	16.71	5.14	5.83	32.4	25.7
	1σ	6.1	1.6	98	4.2	2.1	0.91	0.50	0.98	1.8	2.7
^{89}Y	Conc	4430	3390	2480	2357	3560	1512	3440	2653	2322	2770
	1σ	160	120	90	86	130	55	130	98	87	110
^{93}Nb	Conc	95.4	33.8	61.7	10.09	60.7	8.19	13.96	8.41	33.0	21.13
	1σ	3.5	1.3	2.6	0.43	2.3	0.32	0.55	0.40	1.3	0.96
^{139}La	Conc	243.7	50.2	11.13	17.38	45.9	1.291	19.15	3.32	11.42	22.93
	1σ	8.7	1.9	0.63	0.69	1.7	0.058	0.73	0.19	0.45	0.90
^{140}Ce	Conc	640	192.3	64.4	82.7	344	12.65	80.5	33.1	81.5	250.7
	1σ	22	6.8	2.5	3.0	12	0.47	3.0	1.3	3.1	8.7
^{141}Pr	Conc	75.1	18.15	4.90	8.97	37.6	1.039	8.65	1.277	7.79	40.5
	1σ	2.5	0.65	0.32	0.35	1.3	0.044	0.32	0.089	0.29	1.4
^{146}Nd	Conc	335	93.0	30.1	50.5	263.8	7.81	49.2	6.44	42.0	281.6
	1σ	12	3.4	2.0	2.0	9.3	0.33	1.9	0.49	1.6	9.7
^{147}Sm	Conc	148.1	49.7	24.1	32.7	121.9	8.29	28.2	10.28	28.6	108.0
	1σ	4.9	1.9	1.8	1.4	4.1	0.33	1.1	0.67	1.1	4.0
^{151}Eu	Conc	30.8	5.01	3.81	6.22	52.1	1.898	4.04	1.67	3.67	10.15
	1σ	1.1	0.24	0.37	0.30	1.8	0.083	0.17	0.14	0.16	0.43
^{157}Gd	Conc	250.0	122.6	67.5	91.7	194.9	36.2	89.7	66.3	71.7	130.1
	1σ	8.2	4.3	3.4	3.3	6.5	1.3	3.1	2.6	2.5	4.6
^{159}Tb	Conc	84.3	42.2	27.5	30.1	53.7	14.09	33.9	25.39	26.80	26.21
	1σ	2.8	1.4	1.1	1.0	1.8	0.48	1.2	0.92	0.92	0.90

Analysis		SWA03-050c	SWA03-050r	SWA03-052	SWA03-053c	SWA03-053r	SWA03-054c	SWA03-056c	SWA03-057c	SWA03-060c	RSA06-001c
^{163}Dy	Conc	791	456	319	314	525	175.9	397	314	300.5	253.5
	1σ	26	15	11	10	17	5.7	13	10	9.8	8.4
^{165}Ho	Conc	208.1	149.8	102.8	106.6	157.5	67.0	146.0	117.1	99.5	92.5
	1σ	6.8	5.0	3.6	3.6	5.2	2.2	4.8	4.0	3.3	3.1
^{166}Er	Conc	740	583	452	433	581	287.4	640	492	436	432
	1σ	24	19	15	14	19	9.4	21	16	14	14
^{169}Tm	Conc	141.0	116.7	85.9	88.5	110.7	59.8	135.0	107.2	89.4	107.7
	1σ	4.5	3.8	3.0	2.9	3.6	1.9	4.4	3.5	2.9	3.5
^{173}Yb	Conc	1231	1032	805	830	958	553	1245	973	837	1203
	1σ	40	33	27	27	31	18	40	32	27	39
^{175}Lu	Conc	185.1	153.4	131.8	126.1	140.0	88.9	208.8	154.8	141.2	230.4
	1σ	6.0	5.0	4.5	4.1	4.5	2.9	6.8	5.1	4.6	7.4
^{181}Ta	Conc	2.696	7.47	4.27	1.959	5.12	5.44	3.86	2.15	4.19	12.07
	1σ	0.091	0.27	0.28	0.097	0.17	0.18	0.14	0.12	0.15	0.42
^{232}Th	Conc	1060	979	308	279.2	785	46.0	436	420	289.4	74.7
	1σ	35	32	10	9.2	26	1.5	14	14	9.5	2.4
^{238}U	Conc	1114	1754	492	436	1274	95.6	1257	747	759	226.6
	1σ	35	55	16	14	40	3.0	40	24	24	7.0
Ti-in-zirc	T (°C)	1048.3	813.2	1641.0	956.7	895.5	788.1	685.5	696	855.9	831.2
	1σ	3.6	6.7	3.0	5.3	4.1	4.7	7.5	13	4.9	9.6

Analysis Group		RSA06-002 variable	RSA06-003 metamict	RSA06-006c metamict	RSA06-015c metamict	RSA06-019c pristine	RSA06-021c variable	RSA06-023 metamict	RSA06-025c variable	RSA06-030 variable	RSA06-035 metamict	RSA06-038 variable
^{31}P	Conc	430	500	800	900	190	1240	890	1090	410	420	1900
	1σ	320	370	590	660	140	920	660	810	310	310	1400
^{43}Ca	Conc	779	4250	6420	3740	34.3	1920	4670	970	5270	3840	3740
	1σ	83	270	520	250	8.7	150	280	100	350	310	230
^{49}Ti	Conc	22.0	24.9	94.2	32.4	5.47	8.1	565	4.32	22.5	181	14.0
	1σ	2.2	2.1	9.1	2.8	0.50	1.2	32	0.92	2.5	13	1.3
^{89}Y	Conc	1731	3190	4860	3810	541	2810	5000	3220	1509	2410	4370
	1σ	70	130	200	150	22	110	200	130	62	100	180
^{93}Nb	Conc	9.73	19.55	32.6	13.56	2.19	7.95	47.6	8.30	24.2	20.84	12.93
	1σ	0.46	0.85	1.6	0.62	0.10	0.40	2.0	0.42	1.1	0.98	0.56
^{139}La	Conc	3.19	127.6	121.0	61.0	0.305	16.67	204.8	15.04	17.57	82.5	50.2
	1σ	0.16	4.7	4.6	2.3	0.019	0.66	7.5	0.61	0.71	3.1	1.9
^{140}Ce	Conc	69.1	796	987	462	19.62	131.4	1381	138.6	117.9	568	461
	1σ	2.4	28	34	16	0.69	4.6	48	4.9	4.1	20	16
^{141}Pr	Conc	3.57	90.0	156.7	58.7	0.195	11.89	244.7	17.23	16.56	109.0	55.9
	1σ	0.16	3.1	5.4	2.0	0.012	0.44	8.3	0.63	0.60	3.7	1.9
^{146}Nd	Conc	39.0	575	1065	461	3.12	78.1	1495	131.3	104.9	690	369
	1σ	1.5	19	37	16	0.14	2.9	50	4.7	3.8	24	13
^{147}Sm	Conc	25.6	260.7	632	270.8	2.75	39.6	977	69.0	69.8	479	192.4
	1σ	1.1	9.0	22	9.4	0.14	1.6	33	2.7	2.7	17	6.6
^{151}Eu	Conc	5.28	33.8	45.5	33.0	0.670	4.63	75.5	8.64	5.78	37.0	17.87
	1σ	0.24	1.2	1.8	1.2	0.035	0.22	2.5	0.37	0.28	1.4	0.63
^{157}Gd	Conc	48.8	265.6	668	307	12.27	83.0	1123	114.7	93.4	536	227.7
	1σ	1.8	8.8	23	10	0.45	3.0	37	4.0	3.4	18	7.6
^{159}Tb	Conc	14.51	44.1	108.4	54.2	4.24	24.08	185.3	28.89	18.41	84.6	49.8
	1σ	0.51	1.5	3.7	1.8	0.14	0.82	6.0	0.98	0.64	2.8	1.6

Analysis		RSA06-002	RSA06-003	RSA06-006c	RSA06-015c	RSA06-019c	RSA06-021c	RSA06-023	RSA06-025c	RSA06-030	RSA06-035	RSA06-038
^{163}Dy	Conc	158.6	343	725	427	50.3	260.3	998	307	152.8	459	450
	1σ	5.3	11	24	14	1.7	8.6	32	10	5.2	15	15
^{165}Ho	Conc	59.3	106.0	182.7	130.9	18.72	92.6	194.6	107.0	51.0	91.7	145.2
	1σ	2.0	3.5	6.1	4.3	0.62	3.1	6.4	3.5	1.7	3.1	4.7
^{166}Er	Conc	256.0	430	626	516	82.6	400	587	461	229.2	300.1	590
	1σ	8.3	14	21	17	2.7	13	19	15	7.5	9.9	19
^{169}Tm	Conc	55.6	88.0	121.5	106.9	17.63	81.5	103.4	97.1	49.1	59.3	117.1
	1σ	1.8	2.8	4.0	3.4	0.57	2.6	3.3	3.1	1.6	2.0	3.8
^{173}Yb	Conc	545	830	1085	993	170.8	753	889	922	472	570	1103
	1σ	18	27	36	32	5.5	24	28	30	15	19	35
^{175}Lu	Conc	86.1	143.0	166.0	157.3	29.75	129.8	144.9	151.1	85.6	84.9	178.2
	1σ	2.8	4.6	5.4	5.1	0.96	4.2	4.7	4.9	2.8	2.8	5.7
^{181}Ta	Conc	3.48	3.58	2.71	1.700	0.460	1.967	2.564	2.38	10.11	6.67	2.147
	1σ	0.14	0.13	0.17	0.077	0.020	0.089	0.095	0.11	0.36	0.27	0.084
^{232}Th	Conc	246.8	249.5	688	394	25.14	298.2	2893	274.1	202.6	231.7	374
	1σ	8.0	8.0	22	13	0.82	9.6	93	8.9	6.6	7.6	12
^{238}U	Conc	479	804	953	759	39.7	581	532	542	1044	763	677
	1σ	15	25	30	24	1.2	18	17	17	33	25	22
Ti-in-zirc	T (°C)	815.0	828.1	986	855.9	690.4	723	1286.1	672	818	1081.0	771.2
	1σ	9.0	7.7	11	8.1	7.2	12	6.2	15	10	7.6	8.3

Analysis Group		RSA06-039c metamict	RSA06-045c metamict	RSA06-048 pristine	RSA06-063 metamict	RSA06-065 variable	RSA06-071 variable	RSA06-073 pristine	RSA06-080c metamict	RSA06-083c variable	RSA06-087 variable	RSA06-093 metamict
^{31}P	Conc	640	170	730	1400	740	660	1400	870	440	870	480
	1σ	480	130	550	1000	550	500	1100	660	340	660	370
^{43}Ca	Conc	7320	11200	1073	22400	1910	1720	1670	6310	2210	5550	2010
	1σ	430	660	97	1300	160	140	110	390	240	340	170
^{49}Ti	Conc	166	506	8.4	658	16.3	14.2	13.1	773	42.4	40.7	61.2
	1σ	10	29	1.2	39	2.0	1.6	1.2	45	5.0	3.1	5.1
^{89}Y	Conc	4240	2760	3060	3590	2078	2209	2900	5990	3440	3360	2780
	1σ	180	110	130	150	88	92	120	250	140	140	120
^{93}Nb	Conc	22.43	31.9	10.11	94.6	12.54	10.70	8.76	34.0	15.24	18.96	12.97
	1σ	0.96	1.4	0.47	4.0	0.59	0.51	0.40	1.5	0.83	0.86	0.65
^{139}La	Conc	214.9	357	1.93	477	22.44	65.0	37.9	182.1	46.2	39.2	62.8
	1σ	7.9	13	0.11	17	0.89	2.5	1.5	7.0	1.9	1.5	2.5
^{140}Ce	Conc	1653	2529	73.3	2286	170.6	452	242.8	1352	405	295	505
	1σ	57	87	2.6	78	5.9	17	9.3	53	16	12	21
^{141}Pr	Conc	227.4	267.7	2.59	281.0	15.44	67.7	30.0	265.5	54.9	33.2	66.8
	1σ	7.6	8.9	0.12	9.4	0.56	2.4	1.1	9.6	2.1	1.2	2.5
^{146}Nd	Conc	1453	1644	18.19	1606	94.7	458	236.0	1682	387	208.4	464
	1σ	49	56	0.80	55	3.5	17	9.0	65	16	8.3	19
^{147}Sm	Conc	790	750	20.51	753	45.3	187.4	109.1	1234	218.9	127.4	234.3
	1σ	27	25	0.91	26	1.9	6.7	3.9	43	8.4	4.6	8.6
^{151}Eu	Conc	71.6	96.5	2.11	150.6	4.76	18.33	15.53	115.0	19.81	15.11	18.74
	1σ	2.4	3.3	0.12	5.1	0.24	0.69	0.56	3.9	0.88	0.56	0.74
^{157}Gd	Conc	901	630	75.4	938	86.2	189.9	139.8	1419	288	195.2	296
	1σ	30	21	2.7	31	3.1	6.7	4.9	49	11	6.9	11
^{159}Tb	Conc	136.2	74.3	25.27	106.2	20.96	29.8	30.6	224.0	54.9	41.7	55.0
	1σ	4.4	2.4	0.85	3.5	0.73	1.0	1.0	7.3	1.9	1.4	1.9

Analysis		RSA06-039c	RSA06-045c	RSA06-048	RSA06-063	RSA06-065	RSA06-071	RSA06-073	RSA06-080c	RSA06-083c	RSA06-087	RSA06-093
^{163}Dy	Conc	733	403	288.2	560	208.3	230.6	283.1	1188	404	361	377
	1σ	24	13	9.6	19	7.0	7.7	9.4	39	14	12	13
^{165}Ho	Conc	148.6	95.8	104.2	123.7	71.7	72.9	96.1	231.8	118.0	114.8	96.3
	1σ	4.9	3.2	3.4	4.1	2.4	2.4	3.1	7.6	3.9	3.8	3.2
^{166}Er	Conc	455	352	437	424	302.2	293.2	395	677	478	457	353
	1σ	15	11	14	14	9.9	9.6	13	22	16	15	12
^{169}Tm	Conc	80.2	74.1	91.3	82.3	67.2	60.2	79.3	117.7	101.7	89.7	72.0
	1σ	2.6	2.4	2.9	2.7	2.2	2.0	2.5	3.8	3.4	2.9	2.4
^{173}Yb	Conc	736	732	851	791	650	568	711	1024	1037	831	702
	1σ	24	24	27	26	21	18	23	33	34	27	23
^{175}Lu	Conc	120.9	119.3	131.9	127.7	102.3	98.6	123.3	159.7	166.3	132.3	108.6
	1σ	3.9	3.8	4.3	4.1	3.3	3.2	4.0	5.1	5.4	4.2	3.5
^{181}Ta	Conc	5.42	8.29	2.144	4.39	2.75	3.01	1.751	2.150	3.63	2.90	1.903
	1σ	0.19	0.29	0.091	0.17	0.12	0.12	0.067	0.090	0.19	0.11	0.093
^{232}Th	Conc	437	311	386	781	277.1	143.4	345	728	369	630	371
	1σ	14	10	13	25	9.1	4.6	11	23	12	20	12
^{238}U	Conc	1001	1700	532	2002	510	544	503	655	853	788	663
	1σ	32	55	17	66	17	18	17	23	30	28	24
Ti-in-zirc	T (°C)	1067.2	1263.6	726	1318.5	786	772.6	764.8	1354.2	886	881.3	929.7
	1σ	6.3	6.4	11	6.8	11	9.9	7.8	6.7	12	7.3	8.4

Analysis Group		RSA06-095 metamict	RSA06-097c pristine	RSA06-100 variable	RSA06-108 metamict	RSA06-112c pristine	RSA06-122c metamict	RSA06-139 metamict	SWA13a-001 pristine	SWA13a-002 metamict	SWA13a-003 pristine	SWA13a-004 pristine
^{31}P	Conc	630	1000	1400	770	480	4700	320	420	670	450	460
	1σ	490	770	1000	600	370	3600	250	400	630	420	430
^{43}Ca	Conc	14400	1700	2060	5440	29.0	17200	6250	<19	320	106	40
	1σ	890	130	150	370	9.1	1100	460	7.1	55	15	19
^{49}Ti	Conc	124.0	6.51	36.9	248	9.12	40.9	62.8	13.2	127.5	49.0	5.03
	1σ	9.2	0.97	2.8	16	0.74	3.2	5.6	1.2	8.9	3.1	0.83
^{89}Y	Conc	3610	3420	3240	4580	1521	3930	3410	1008	2600	2005	1402
	1σ	160	150	140	200	66	170	150	44	110	88	62
^{93}Nb	Conc	67.3	7.09	11.46	36.5	3.80	33.6	22.2	1.629	7.57	5.79	2.33
	1σ	3.1	0.36	0.55	1.7	0.19	1.6	1.2	0.092	0.41	0.28	0.14
^{139}La	Conc	608	1.85	58.2	73.6	1.043	130.3	166.5	1.132	43.4	8.54	2.53
	1σ	24	0.11	2.3	3.0	0.051	5.4	7.2	0.059	1.8	0.35	0.13
^{140}Ce	Conc	2540	64.7	297	630	49.0	958	1252	16.17	130.4	50.3	17.79
	1σ	110	2.7	12	26	2.1	42	58	0.65	5.2	2.0	0.74
^{141}Pr	Conc	248.2	1.689	34.0	104.6	2.260	120.9	166.7	0.893	21.39	5.23	1.241
	1σ	9.4	0.088	1.3	4.0	0.092	4.8	6.9	0.044	0.82	0.20	0.068
^{146}Nd	Conc	1438	21.9	199.2	682	22.30	833	1176	7.27	109.4	27.9	8.10
	1σ	60	1.0	8.0	27	0.94	35	53	0.33	4.2	1.1	0.43
^{147}Sm	Conc	710	21.65	114.3	478	22.35	588	609	6.88	65.0	19.30	9.07
	1σ	25	0.95	4.2	17	0.85	22	23	0.32	2.6	0.72	0.47
^{151}Eu	Conc	72.7	3.99	11.61	45.4	2.57	71.4	52.4	1.920	9.35	4.33	1.73
	1σ	2.6	0.19	0.45	1.7	0.10	2.6	2.1	0.092	0.42	0.17	0.10
^{157}Gd	Conc	730	82.6	173.7	568	56.1	631	690	27.1	120.7	53.1	37.5
	1σ	26	3.1	6.3	20	2.0	23	26	1.0	4.5	1.9	1.5
^{159}Tb	Conc	102.4	27.41	37.0	96.5	15.16	85.8	97.4	8.63	31.5	17.46	12.19
	1σ	3.4	0.93	1.2	3.2	0.50	2.9	3.3	0.30	1.1	0.60	0.44

Analysis		RSA06-095	RSA06-097c	RSA06-100	RSA06-108	RSA06-112c	RSA06-122c	RSA06-139	SWA13a-001	SWA13a-002	SWA13a-003	SWA13a-004
^{163}Dy	Conc	526	317	334	653	151.7	526	570	94.9	286.1	185.5	135.6
	1σ	18	10	11	21	5.0	17	19	3.2	9.7	6.2	4.6
^{165}Ho	Conc	124.7	114.4	107.1	168.4	52.0	131.8	123.7	34.1	85.6	66.1	48.3
	1σ	4.1	3.8	3.5	5.5	1.7	4.3	4.1	1.1	2.9	2.2	1.6
^{166}Er	Conc	452	478	439	599	216.1	468	407	143.6	325	276.3	202.0
	1σ	15	16	14	20	7.1	15	14	4.9	11	9.4	6.9
^{169}Tm	Conc	99.3	100.7	88.9	115.0	43.4	91.5	78.8	29.84	64.5	55.6	41.8
	1σ	3.2	3.3	2.9	3.7	1.4	3.0	2.6	0.98	2.1	1.8	1.4
^{173}Yb	Conc	987	950	800	1049	404	839	730	285.2	579	521	395
	1σ	32	31	26	34	13	27	24	9.3	19	17	13
^{175}Lu	Conc	156.7	151.6	138.6	160.4	68.2	128.9	112.6	52.4	97.1	89.9	69.9
	1σ	5.1	4.9	4.5	5.2	2.2	4.2	3.7	1.7	3.2	2.9	2.3
^{181}Ta	Conc	19.66	1.636	1.553	3.06	0.710	3.45	3.91	0.346	0.900	1.078	0.506
	1σ	0.67	0.072	0.064	0.13	0.028	0.13	0.17	0.019	0.054	0.040	0.031
^{232}Th	Conc	334	389	384	1317	107.9	637	860	57.4	442	162.9	80.3
	1σ	11	12	12	42	3.5	20	28	1.9	14	5.3	2.6
^{238}U	Conc	1869	537	539	792	125.1	1120	1150	88.5	655	250.4	154.0
	1σ	68	19	19	28	4.5	41	44	2.9	22	8.3	5.2
Ti-in-zirc	T (°C)	1023.9	704	870.3	1132.0	732.8	881.8	932.9	766.0	1028.0	902.9	684
	1σ	8.0	12	7.1	7.0	6.7	7.5	9.2	7.5	7.4	6.0	12

Analysis		SWA13a-005c	SWA13a-006	SWA13a-008c	SWA13a-009	SWA13a-010	SWA13a-011	SWA13a-012c	SWA13a-014	SWA13a-015c	SWA13a-016
Group		pristine	variable	pristine	variable	pristine	pristine	pristine	variable	pristine	variable
^{31}P	Conc	570	580	570	1200	790	1300	540	200	270	910
	1σ	540	550	540	1200	740	1200	510	180	250	850
^{43}Ca	Conc	27	100	24	42	<8.6	58	214	30	23.1	457
	1σ	12	38	13	23	2.7	20	30	31	5.8	64
^{49}Ti	Conc	9.12	13.3	10.8	8.1	11.9	4.57	21.8	33.4	11.30	15.5
	1σ	0.87	2.0	1.1	1.4	1.6	0.82	1.8	4.3	0.81	1.9
^{89}Y	Conc	1095	1980	1433	3060	2960	3750	1477	1492	769	2910
	1σ	49	89	65	140	140	180	64	65	34	130
^{93}Nb	Conc	1.700	3.82	2.74	4.87	10.67	6.14	2.56	4.86	1.898	7.64
	1σ	0.096	0.26	0.16	0.30	0.58	0.35	0.14	0.34	0.092	0.40
^{139}La	Conc	1.489	5.77	4.31	1.57	0.112	2.10	22.14	15.03	0.181	21.65
	1σ	0.074	0.30	0.20	0.11	0.023	0.12	0.89	0.72	0.012	0.91
^{140}Ce	Conc	14.48	54.8	28.5	22.21	41.4	25.5	75.7	64.5	10.40	66.5
	1σ	0.60	2.3	1.2	0.99	1.8	1.1	2.9	2.6	0.41	2.7
^{141}Pr	Conc	0.735	6.54	2.30	1.249	0.274	1.402	11.06	8.55	0.1660	8.74
	1σ	0.038	0.30	0.10	0.085	0.031	0.079	0.42	0.40	0.0096	0.36
^{146}Nd	Conc	5.51	41.9	14.22	9.53	4.01	10.23	59.3	47.8	2.109	44.8
	1σ	0.26	1.9	0.63	0.59	0.31	0.53	2.2	2.2	0.098	1.8
^{147}Sm	Conc	6.81	23.1	13.18	12.23	10.24	15.68	31.9	31.6	3.69	27.7
	1σ	0.31	1.2	0.58	0.71	0.59	0.74	1.3	1.7	0.16	1.2
^{151}Eu	Conc	2.076	3.93	2.35	1.45	1.51	1.089	5.00	4.59	1.178	4.45
	1σ	0.097	0.24	0.12	0.12	0.11	0.081	0.21	0.31	0.050	0.23
^{157}Gd	Conc	29.1	59.7	43.0	64.7	57.0	80.3	62.3	71.7	18.05	82.9
	1σ	1.1	2.5	1.6	2.6	2.3	3.1	2.2	3.0	0.65	3.1
^{159}Tb	Conc	9.36	17.96	13.55	24.26	21.57	28.8	16.83	18.30	5.99	25.81
	1σ	0.33	0.67	0.49	0.89	0.79	1.0	0.58	0.71	0.21	0.91

Analysis		SWA13a-005c	SWA13a-006	SWA13a-008c	SWA13a-009	SWA13a-010	SWA13a-011	SWA13a-012c	SWA13a-014	SWA13a-015c	SWA13a-016
^{163}Dy	Conc	103.7	192.3	139.0	269.8	248.5	345	161.1	168.3	68.4	267.0
	1σ	3.5	6.7	4.8	9.3	8.6	12	5.3	5.9	2.2	8.8
^{165}Ho	Conc	37.0	66.1	48.3	98.7	96.7	124.1	49.9	52.2	25.59	93.7
	1σ	1.2	2.3	1.6	3.3	3.3	4.2	1.7	1.8	0.85	3.1
^{166}Er	Conc	156.4	279.8	199.7	410	424	520	197.6	198.2	113.7	390
	1σ	5.4	9.8	6.9	14	15	18	6.7	7.0	3.9	13
^{169}Tm	Conc	31.8	57.2	40.2	82.7	84.3	103.2	39.3	39.3	23.64	78.3
	1σ	1.1	1.9	1.3	2.8	2.8	3.4	1.3	1.4	0.77	2.6
^{173}Yb	Conc	304.0	541	380	748	793	957	366	353	231.1	733
	1σ	9.9	18	12	25	26	31	12	12	7.5	24
^{175}Lu	Conc	55.8	92.3	66.5	136.0	144.4	162.7	62.5	61.3	43.9	126.2
	1σ	1.8	3.0	2.2	4.4	4.7	5.2	2.0	2.1	1.4	4.1
^{181}Ta	Conc	0.385	0.586	0.448	0.913	1.558	1.189	0.478	0.728	0.496	1.820
	1σ	0.020	0.046	0.025	0.057	0.075	0.057	0.025	0.065	0.019	0.083
^{232}Th	Conc	67.5	158.9	106.1	161.6	177.0	239.6	96.7	190.5	38.1	171.9
	1σ	2.2	5.2	3.5	5.3	5.8	7.8	3.1	6.2	1.2	5.6
^{238}U	Conc	91.9	363	157.0	395	321	515	140.2	205.3	67.6	438
	1σ	3.1	12	5.4	14	11	18	4.5	6.7	2.2	14
Ti-in-zirc	T (°C)	732.8	766	747.4	723	756	676	814.1	859	751.7	781
	1σ	7.9	13	8.8	14	11	13	7.5	12	6.1	10

Analysis		SWA13a-017	SWA13a-018	SWA13a-019	SWA13a-020	SWA13a-021c	SWA13a-025	SWA13a-028	SWA13a-029	SWA13a-032	SWA13a-034
Group		pristine	variable	pristine	metamict	metamict	pristine	pristine	variable	metamict	pristine
^{31}P	Conc	540	970	530	350	340	370	460	540	310	580
	1σ	510	910	490	330	310	350	430	510	290	540
^{43}Ca	Conc	<15	182	40	537	389	<26	19	257	563	125
	1σ	10	36	12	51	46	12	15	37	68	17
^{49}Ti	Conc	5.68	62.6	13.3	49.6	16.5	8.8	20.3	13.8	56.8	10.13
	1σ	0.79	4.8	1.1	3.6	1.6	1.1	2.1	1.3	4.4	0.85
^{89}Y	Conc	1235	2930	1532	1742	1358	1230	2400	1933	2219	1703
	1σ	55	130	69	79	62	51	100	81	93	72
^{93}Nb	Conc	2.17	6.95	3.22	5.58	3.41	2.58	5.34	4.84	3.93	4.00
	1σ	0.13	0.36	0.16	0.28	0.19	0.15	0.29	0.24	0.22	0.19
^{139}La	Conc	2.61	33.9	5.62	44.4	15.81	3.56	4.88	1.802	49.1	9.74
	1σ	0.13	1.4	0.24	1.8	0.68	0.17	0.23	0.091	1.9	0.38
^{140}Ce	Conc	17.25	119.3	31.8	121.8	66.9	23.58	42.9	30.3	151.3	53.9
	1σ	0.71	4.8	1.3	5.1	2.8	0.89	1.6	1.1	5.6	2.0
^{141}Pr	Conc	1.168	18.20	3.07	20.10	8.80	2.039	2.24	1.097	25.72	5.96
	1σ	0.061	0.70	0.12	0.77	0.35	0.096	0.11	0.056	0.95	0.22
^{146}Nd	Conc	7.34	89.9	16.00	102.9	49.5	13.55	13.56	7.19	139.3	36.5
	1σ	0.37	3.4	0.62	3.8	1.9	0.60	0.65	0.35	4.9	1.3
^{147}Sm	Conc	7.80	53.2	13.87	51.2	27.3	11.70	10.85	8.21	69.8	20.09
	1σ	0.40	2.1	0.56	2.0	1.1	0.58	0.59	0.41	2.8	0.79
^{151}Eu	Conc	1.136	10.01	2.73	10.98	7.02	1.638	2.78	2.66	15.81	5.23
	1σ	0.072	0.42	0.12	0.44	0.30	0.098	0.15	0.13	0.62	0.20
^{157}Gd	Conc	31.8	110.2	45.9	87.5	56.6	33.4	48.1	39.8	124.5	49.5
	1σ	1.2	4.0	1.7	3.2	2.1	1.3	1.8	1.5	4.4	1.7
^{159}Tb	Conc	10.26	31.2	14.38	22.52	15.22	11.36	16.85	14.02	30.6	15.01
	1σ	0.37	1.1	0.50	0.79	0.55	0.39	0.58	0.47	1.0	0.50

Analysis		SWA13a-017	SWA13a-018	SWA13a-019	SWA13a-020	SWA13a-021c	SWA13a-025	SWA13a-028	SWA13a-029	SWA13a-032	SWA13a-034
^{163}Dy	Conc	115.8	295.6	150.7	195.6	144.4	120.3	206.6	168.2	256.8	160.3
	1σ	3.9	9.7	4.9	6.4	4.8	4.0	6.8	5.5	8.5	5.2
^{165}Ho	Conc	40.5	94.7	51.6	57.2	45.4	40.3	78.8	62.4	73.0	56.0
	1σ	1.4	3.2	1.7	1.9	1.5	1.3	2.6	2.0	2.4	1.8
^{166}Er	Conc	177.8	377	215.2	218.7	182.3	172.7	335	270.2	263.4	238.4
	1σ	6.1	13	7.5	7.6	6.4	5.6	11	8.7	8.6	7.7
^{169}Tm	Conc	35.5	72.6	43.4	40.8	37.8	34.7	69.4	55.1	49.5	48.5
	1σ	1.2	2.4	1.4	1.4	1.3	1.1	2.3	1.8	1.6	1.6
^{173}Yb	Conc	346	669	404	359	373	323	629	502	437	459
	1σ	11	22	13	12	12	11	21	16	14	15
^{175}Lu	Conc	62.0	117.6	71.6	62.0	65.8	58.8	109.4	89.6	71.5	81.6
	1σ	2.0	3.8	2.3	2.0	2.1	1.9	3.5	2.9	2.3	2.6
^{181}Ta	Conc	0.401	1.367	0.516	0.873	1.654	0.624	0.961	0.991	0.745	1.006
	1σ	0.024	0.063	0.022	0.038	0.067	0.035	0.052	0.044	0.043	0.038
^{232}Th	Conc	68.8	264.1	117.2	101.5	86.4	90.1	161.4	133.0	147.5	98.8
	1σ	2.2	8.5	3.8	3.3	2.8	3.0	5.3	4.4	4.9	3.3
^{238}U	Conc	139.9	298.4	152.8	188.4	264.2	176.6	213.0	203.3	325	223.2
	1σ	4.6	9.9	5.1	6.3	8.9	5.4	6.6	6.3	10	6.9
Ti-in-zirc	T (°C)	693	932.6	766.7	904.2	787.0	730	807.2	769.9	920.5	742.0
	1σ	11	7.6	7.0	7.1	8.5	10	9.4	8.3	7.7	7.0

Analysis		SWA13a-035c	SWA13a-036	SWA13a-039	SWA13a-040	SWA13a-041	SWA13a-042	SWA13a-043	SWA13a-044	SWA13a-045	SWA13a-046c
Group		metamict	metamict	pristine	metamict	variable	pristine	pristine	pristine	pristine	metamict
^{31}P	Conc	570	250	400	570	580	450	490	260	400	470
	1σ	540	240	380	540	560	430	470	250	380	440
^{43}Ca	Conc	301	336	<24	1990	88	145	72	100	<18	1320
	1σ	35	59	16	180	22	26	23	24	12	120
^{49}Ti	Conc	144.7	68.3	5.5	152	12.1	11.0	5.90	10.4	13.9	47.4
	1σ	9.1	5.5	1.2	11	1.1	1.2	0.91	1.2	1.4	3.9
^{89}Y	Conc	2900	1541	1151	4170	1269	1425	1242	1627	1206	3140
	1σ	120	66	50	180	52	59	52	68	51	130
^{93}Nb	Conc	9.71	8.11	1.63	13.16	2.23	3.43	2.09	3.18	1.66	8.30
	1σ	0.47	0.44	0.14	0.69	0.12	0.18	0.13	0.17	0.10	0.42
^{139}La	Conc	59.7	26.7	0.099	149.8	5.90	6.73	0.540	11.47	2.05	74.2
	1σ	2.3	1.1	0.025	5.9	0.24	0.28	0.045	0.46	0.10	2.8
^{140}Ce	Conc	209.7	133.7	12.36	434	28.6	27.4	16.73	42.7	19.49	250.5
	1σ	7.8	5.1	0.54	17	1.1	1.0	0.64	1.6	0.75	9.3
^{141}Pr	Conc	34.7	20.60	0.133	75.4	2.56	3.41	0.244	5.15	1.543	39.5
	1σ	1.3	0.79	0.025	2.8	0.10	0.14	0.024	0.20	0.075	1.4
^{146}Nd	Conc	177.5	121.3	2.31	392	15.93	20.92	2.85	26.0	10.81	208.0
	1σ	6.1	4.4	0.26	14	0.64	0.83	0.21	1.0	0.49	7.4
^{147}Sm	Conc	103.3	59.2	4.44	182.2	10.73	15.18	5.50	19.56	10.68	103.1
	1σ	3.9	2.5	0.40	7.3	0.47	0.65	0.34	0.83	0.51	3.9
^{151}Eu	Conc	15.78	17.78	1.81	34.2	3.21	1.94	1.352	2.42	2.84	22.01
	1σ	0.59	0.72	0.14	1.3	0.14	0.10	0.088	0.12	0.14	0.83
^{157}Gd	Conc	167.8	100.5	28.7	278	39.3	45.0	31.8	50.7	36.1	182.4
	1σ	5.8	3.7	1.3	10	1.4	1.6	1.2	1.9	1.4	6.5
^{159}Tb	Conc	43.3	22.10	9.81	64.8	11.41	13.84	10.18	16.08	11.19	41.3
	1σ	1.4	0.77	0.37	2.2	0.38	0.47	0.36	0.54	0.38	1.4

Analysis		SWA13a-035c	SWA13a-036	SWA13a-039	SWA13a-040	SWA13a-041	SWA13a-042	SWA13a-043	SWA13a-044	SWA13a-045	SWA13a-046c
^{163}Dy	Conc	353	180.4	106.5	504	121.1	140.7	116.2	172.1	120.4	348
	1σ	11	6.0	3.7	17	4.0	4.7	3.9	5.7	4.0	11
^{165}Ho	Conc	96.6	50.5	39.1	132.5	41.4	48.7	41.8	55.3	41.4	97.7
	1σ	3.2	1.7	1.3	4.4	1.4	1.6	1.4	1.8	1.4	3.2
^{166}Er	Conc	343	182.0	171.1	458	174.8	199.6	179.6	227.2	170.2	357
	1σ	11	6.0	5.7	15	5.7	6.5	5.8	7.4	5.5	12
^{169}Tm	Conc	67.0	34.4	36.6	80.8	34.9	40.6	37.6	45.5	34.3	68.2
	1σ	2.2	1.1	1.2	2.6	1.1	1.3	1.2	1.5	1.1	2.2
^{173}Yb	Conc	607	316	357	669	327	381	362	414	327	617
	1σ	20	11	12	22	11	13	12	14	11	21
^{175}Lu	Conc	98.5	53.9	61.4	109.8	59.7	65.7	65.2	70.1	57.7	99.1
	1σ	3.2	1.8	2.0	3.5	1.9	2.1	2.1	2.3	1.9	3.2
^{181}Ta	Conc	1.524	9.56	0.424	2.032	0.560	0.645	0.396	0.719	0.395	0.980
	1σ	0.060	0.34	0.038	0.094	0.028	0.032	0.027	0.036	0.024	0.052
^{232}Th	Conc	308	122.6	72.7	335	100.2	127.7	90.3	128.6	81.0	276.6
	1σ	10	4.1	2.5	11	3.3	4.2	3.0	4.3	2.7	9.2
^{238}U	Conc	232.9	318.9	108.0	1015	129.5	183.6	135.2	267.8	102.7	566
	1σ	7.2	9.9	3.4	31	4.0	5.7	4.2	8.2	3.2	17
Ti-in-zirc	T (°C)	1046.5	943.4	690	1053.8	757.6	749.5	696	744.3	770.8	898.8
	1σ	6.6	8.2	16	7.7	8.0	8.8	12	9.4	8.7	8.0

Analysis		SWA11-001c	SWA11-003	SWA11-004	SWA11-007	SWA11-008	SWA11-010	SWA11-013	SWA11-014	SWA11-015	SWA11-016	SWA11-017
Group		pristine	pristine	variable	pristine	variable	metamict	metamict	metamict	metamict	pristine	pristine
^{31}P	Conc	610	480	520	330	1290	540	1000	880	580	330	275
	1σ	190	150	160	100	390	170	310	270	180	100	86
^{43}Ca	Conc											
	1σ											
^{49}Ti	Conc	4.88	5.31	4.40	4.24	3.56	11.01	13.08	15.1	39.9	1.53	2.72
	1σ	0.40	0.42	0.63	0.30	0.48	0.87	0.82	1.3	2.7	0.13	0.22
^{89}Y	Conc	1611	1248	1994	954	2937	2572	3260	2628	2641	1055	645
	1σ	54	42	68	32	98	86	110	88	89	36	22
^{93}Nb	Conc	8.89	2.362	8.30	2.367	14.67	11.14	9.91	65.8	57.1	4.47	2.393
	1σ	0.32	0.095	0.33	0.090	0.53	0.41	0.36	2.3	2.0	0.16	0.090
^{139}La	Conc	4.85	<0.0021	0.121	0.0034	1.830	20.89	5.40	25.40	32.1	0.0446	0.0031
	1σ	0.18	0.0018	0.022	0.0019	0.093	0.72	0.20	0.90	1.1	0.0041	0.0016
^{140}Ce	Conc	26.12	16.40	22.80	14.14	35.2	54.6	51.3	59.9	48.0	8.69	7.43
	1σ	0.85	0.54	0.78	0.46	1.2	1.8	1.7	2.0	1.6	0.28	0.24
^{141}Pr	Conc	2.069	0.0681	0.170	0.0445	0.862	3.23	3.15	9.74	11.54	0.0340	0.0243
	1σ	0.078	0.0080	0.023	0.0051	0.050	0.13	0.12	0.36	0.43	0.0030	0.0035
^{146}Nd	Conc	10.91	1.75	2.32	1.502	6.31	19.76	21.67	52.0	69.5	0.525	0.459
	1σ	0.43	0.11	0.22	0.085	0.35	0.79	0.80	2.0	2.6	0.032	0.039
^{147}Sm	Conc	10.47	4.80	5.88	3.83	8.77	18.73	22.81	32.6	40.5	2.273	1.779
	1σ	0.43	0.23	0.40	0.17	0.46	0.78	0.86	1.4	1.7	0.096	0.096
^{151}Eu	Conc	2.254	0.714	0.572	0.558	1.180	5.93	4.73	6.48	10.21	0.191	0.196
	1σ	0.099	0.044	0.063	0.031	0.083	0.25	0.19	0.30	0.45	0.012	0.016
^{157}Gd	Conc	38.1	26.08	39.5	22.79	51.2	68.3	90.1	79.2	106.5	16.50	12.47
	1σ	1.3	0.91	1.5	0.78	1.9	2.4	3.0	2.9	3.9	0.56	0.45
^{159}Tb	Conc	13.03	9.39	15.18	7.71	19.90	22.83	28.32	23.29	24.78	7.02	4.72
	1σ	0.43	0.31	0.53	0.25	0.67	0.76	0.92	0.79	0.86	0.23	0.16

Analysis		SWA11-001c	SWA11-003	SWA11-004	SWA11-007	SWA11-008	SWA11-010	SWA11-013	SWA11-014	SWA11-015	SWA11-016	SWA11-017
^{163}Dy	Conc	150.0	112.6	176.6	89.0	245.4	241.6	299.2	221.2	215.3	90.3	57.8
	1σ	4.9	3.7	5.8	2.9	8.0	7.8	9.6	7.3	7.2	2.9	1.9
^{165}Ho	Conc	52.4	40.4	63.0	32.0	92.0	83.0	101.4	70.3	61.8	36.1	21.58
	1σ	1.7	1.3	2.1	1.0	3.0	2.7	3.3	2.3	2.1	1.2	0.70
^{166}Er	Conc	225.5	174.9	267.6	138.6	410	327	415	277.3	218.1	165.8	97.5
	1σ	7.3	5.6	8.7	4.5	13	11	13	9.1	7.3	5.4	3.2
^{169}Tm	Conc	46.6	37.4	54.4	28.86	85.9	65.2	83.4	53.4	37.7	36.2	21.25
	1σ	1.5	1.2	1.8	0.94	2.8	2.1	2.7	1.8	1.3	1.2	0.69
^{173}Yb	Conc	432	362	496	272.7	825	584	760	468	318	355	207.8
	1σ	14	12	16	8.8	27	19	25	16	11	12	6.8
^{175}Lu	Conc	76.4	60.5	84.8	48.9	140.3	95.6	130.4	83.9	57.6	63.6	36.6
	1σ	2.5	2.0	2.8	1.6	4.5	3.1	4.2	2.7	1.9	2.0	1.2
^{181}Ta	Conc	1.149	0.546	1.635	0.643	2.58	1.075	1.229	2.36	2.24	1.367	0.614
	1σ	0.048	0.027	0.083	0.027	0.11	0.054	0.053	0.11	0.12	0.047	0.025
^{232}Th	Conc	139.4	82.3	205.7	66.0	318	256.0	259.0	144.2	159.2	69.1	40.2
	1σ	4.8	2.8	7.1	2.3	10	8.4	8.5	4.8	5.3	2.3	1.3
^{238}U	Conc	328	148.3	404	135.4	652	344	367	356	378	185.0	114.8
	1σ	10	4.7	13	4.3	20	11	12	11	12	5.8	3.6
Ti-in-zirc	T (°C)	681.5	688.1	673	670.6	657.5	749.4	765.0	778.4	879.0	598.9	638.0
	1σ	6.4	6.2	11	5.5	9.8	6.7	5.4	7.6	6.3	6.0	6.0

Analysis		SWA11-020	SWA11-023c	SWA11-025	SWA11-026	SWA11-028c	SWA11-029	SWA11-031	SWA11-032c	SWA11-033	SWA11-037	SWA11-038
Group		metamict	metamict	metamict	variable	metamict	metamict	metamict	pristine	metamict	pristine	pristine
^{31}P	Conc	520	700	590	500	570	660	510	520	580	470	282
	1σ	160	220	190	160	180	210	160	160	180	150	88
^{43}Ca	Conc											
	1σ											
^{49}Ti	Conc	9.71	17.54	9.47	8.7	5.56	16.0	14.07	2.28	6.71	3.27	1.76
	1σ	0.68	0.84	0.86	1.1	0.49	1.0	0.89	0.31	0.76	0.32	0.28
^{89}Y	Conc	2524	2666	1980	1281	1585	2449	2382	1106	1521	1283	1164
	1σ	85	90	66	43	53	81	79	37	51	43	39
^{93}Nb	Conc	8.52	15.15	7.48	2.76	11.56	9.05	7.67	3.86	3.64	2.87	5.97
	1σ	0.31	0.53	0.29	0.15	0.41	0.33	0.28	0.15	0.17	0.11	0.23
^{139}La	Conc	22.93	21.53	6.03	0.254	3.28	3.08	1.037	0.207	2.55	0.0271	0.0397
	1σ	0.78	0.72	0.25	0.038	0.13	0.13	0.056	0.019	0.13	0.0059	0.0087
^{140}Ce	Conc	107.3	103.6	27.08	20.49	18.82	42.6	41.7	10.58	24.45	11.35	10.59
	1σ	3.4	3.3	0.92	0.74	0.64	1.4	1.4	0.37	0.86	0.39	0.38
^{141}Pr	Conc	9.15	9.56	3.19	0.228	1.811	1.558	0.576	0.166	1.730	0.0677	0.0423
	1σ	0.31	0.32	0.13	0.031	0.075	0.070	0.033	0.015	0.088	0.0082	0.0078
^{146}Nd	Conc	55.7	52.8	18.24	2.44	11.41	10.83	5.64	2.06	13.09	1.67	0.632
	1σ	1.9	1.8	0.79	0.26	0.48	0.49	0.29	0.14	0.65	0.11	0.077
^{147}Sm	Conc	28.4	34.9	16.13	6.59	8.97	12.38	9.60	4.14	10.46	4.67	2.46
	1σ	1.0	1.2	0.73	0.49	0.41	0.55	0.43	0.23	0.56	0.23	0.18
^{151}Eu	Conc	14.64	9.78	3.46	0.842	2.62	2.27	2.00	0.579	2.19	0.558	0.260
	1σ	0.51	0.33	0.17	0.092	0.12	0.11	0.10	0.043	0.13	0.038	0.030
^{157}Gd	Conc	83.4	92.4	59.6	32.0	34.8	55.8	47.1	23.53	44.0	26.53	17.17
	1σ	2.8	3.1	2.2	1.4	1.3	2.0	1.7	0.88	1.7	0.96	0.69
^{159}Tb	Conc	22.66	26.83	17.71	10.37	12.32	18.53	16.48	8.67	13.43	9.79	8.02
	1σ	0.75	0.87	0.60	0.39	0.42	0.62	0.55	0.30	0.48	0.33	0.28

Analysis		SWA11-020	SWA11-023c	SWA11-025	SWA11-026	SWA11-028c	SWA11-029	SWA11-031	SWA11-032c	SWA11-033	SWA11-037	SWA11-038
^{163}Dy	Conc	226.9	254.3	183.0	126.0	136.4	208.0	194.2	98.9	146.7	115.1	100.3
	1σ	7.3	8.2	6.1	4.3	4.5	6.8	6.4	3.3	5.0	3.8	3.4
^{165}Ho	Conc	76.2	80.2	60.0	43.4	48.9	75.2	72.3	37.8	50.8	42.1	38.4
	1σ	2.5	2.6	2.0	1.5	1.6	2.4	2.4	1.2	1.7	1.4	1.3
^{166}Er	Conc	293.6	308	237.5	191.9	206.1	325	321	163.1	204.6	181.3	173.6
	1σ	9.6	10	7.8	6.4	6.7	11	10	5.4	6.8	6.0	5.8
^{169}Tm	Conc	58.4	58.1	47.0	40.4	43.8	68.6	68.8	34.1	41.4	39.2	39.2
	1σ	1.9	1.9	1.5	1.4	1.4	2.2	2.2	1.1	1.4	1.3	1.3
^{173}Yb	Conc	537	511	448	421	429	634	651	318	391	381	395
	1σ	18	17	15	14	14	21	21	11	13	13	13
^{175}Lu	Conc	87.4	86.7	70.8	62.4	71.0	116.1	112.8	57.3	68.7	63.5	65.2
	1σ	2.8	2.8	2.3	2.1	2.3	3.8	3.7	1.9	2.3	2.1	2.2
^{181}Ta	Conc	0.952	1.153	0.481	0.532	1.219	1.486	1.383	0.721	0.612	0.596	2.145
	1σ	0.044	0.044	0.035	0.048	0.053	0.066	0.060	0.036	0.043	0.029	0.086
^{232}Th	Conc	184.3	237.0	117.3	80.7	81.0	158.9	169.9	75.1	95.5	86.3	83.8
	1σ	6.1	7.8	3.9	2.7	2.7	5.2	5.6	2.5	3.2	2.9	2.8
^{238}U	Conc	257.7	380	254.4	156.0	253.5	282.3	293.4	182.3	168.3	214.1	280.8
	1σ	8.1	12	8.0	5.0	8.0	8.9	9.3	5.8	5.4	6.8	9.0
Ti-in-zirc	T (°C)	738.2	792.7	736.1	729	691.7	784.0	771.8	625.6	706.9	651.3	608
	1σ	5.9	4.1	7.5	10	6.9	5.5	5.4	9.4	9.0	7.2	10

Analysis Group		SWA11-040 metamict	SWA11-041 variable	SWA11-045 variable	SWA11-046 pristine	SWA11-051 pristine	SWA11-052 pristine	SWA11-055 pristine	SWA11-058c pristine	SWA11-061 metamict	SWA11-062 metamict	SWA11-065 pristine
^{31}P	Conc	580	410	660	316	400	440	276	680	790	1430	370
	1σ	180	130	200	99	120	140	87	210	250	450	110
^{43}Ca	Conc											
	1σ											
^{49}Ti	Conc	20.3	15.54	9.57	9.27	5.94	7.67	6.09	4.12	11.53	12.8	7.41
	1σ	1.3	0.89	0.91	0.56	0.36	0.51	0.40	0.59	0.79	1.4	0.49
^{89}Y	Conc	2868	1959	1775	857	1129	1065	735	1366	3660	4820	929
	1σ	95	65	59	28	37	35	24	46	120	160	31
^{93}Nb	Conc	18.25	16.90	5.32	3.18	2.384	1.742	1.983	2.48	8.14	34.4	4.69
	1σ	0.65	0.59	0.22	0.12	0.089	0.073	0.078	0.12	0.29	1.2	0.17
^{139}La	Conc	12.69	1.407	1.291	0.381	0.0159	0.0092	<0.0028	0.457	1.884	2.40	1.358
	1σ	0.47	0.066	0.080	0.024	0.0033	0.0034	0.00087	0.043	0.085	0.15	0.059
^{140}Ce	Conc	59.4	37.1	31.2	22.15	17.50	14.42	16.60	18.65	62.6	42.5	16.92
	1σ	2.0	1.2	1.1	0.74	0.59	0.49	0.56	0.67	2.0	1.4	0.55
^{141}Pr	Conc	5.57	0.847	0.799	0.329	0.1081	0.117	0.0343	0.361	1.803	1.72	0.753
	1σ	0.21	0.041	0.052	0.019	0.0078	0.011	0.0051	0.032	0.076	0.10	0.034
^{146}Nd	Conc	35.9	6.66	7.30	3.14	2.15	2.17	1.134	3.63	18.06	14.44	4.84
	1σ	1.4	0.31	0.42	0.16	0.11	0.13	0.077	0.27	0.70	0.79	0.22
^{147}Sm	Conc	25.4	9.91	8.64	4.81	5.02	5.22	2.78	6.84	24.75	21.8	5.49
	1σ	1.0	0.43	0.49	0.23	0.21	0.24	0.14	0.42	0.93	1.1	0.25
^{151}Eu	Conc	5.71	2.013	1.69	1.001	0.965	1.118	0.470	0.904	4.78	2.86	1.240
	1σ	0.24	0.095	0.11	0.052	0.044	0.058	0.030	0.077	0.19	0.19	0.061
^{157}Gd	Conc	88.4	42.6	41.7	23.73	26.13	25.11	17.27	34.3	103.6	113.0	22.65
	1σ	3.0	1.5	1.6	0.83	0.88	0.88	0.61	1.3	3.5	4.1	0.81
^{159}Tb	Conc	25.48	14.46	13.69	7.63	8.96	9.00	6.02	11.05	32.7	39.1	7.92
	1σ	0.85	0.48	0.48	0.26	0.30	0.30	0.20	0.40	1.1	1.3	0.27

Analysis		SWA11-040	SWA11-041	SWA11-045	SWA11-046	SWA11-051	SWA11-052	SWA11-055	SWA11-058c	SWA11-061	SWA11-062	SWA11-065
^{163}Dy	Conc	252.1	167.5	158.3	83.0	102.3	100.1	67.8	126.2	351	441	87.3
	1σ	8.3	5.5	5.3	2.7	3.4	3.3	2.3	4.3	12	15	2.9
^{165}Ho	Conc	83.0	60.1	55.5	28.44	36.9	35.6	24.53	46.2	116.5	152.8	30.22
	1σ	2.7	2.0	1.8	0.93	1.2	1.2	0.80	1.5	3.8	5.0	0.98
^{166}Er	Conc	320	257.2	238.7	119.7	158.2	151.6	105.2	192.9	468	624	129.1
	1σ	10	8.3	7.8	3.9	5.1	4.9	3.4	6.3	15	21	4.3
^{169}Tm	Conc	62.5	53.7	49.4	25.92	33.8	32.4	21.82	39.4	93.4	121.9	27.30
	1σ	2.0	1.7	1.6	0.84	1.1	1.0	0.70	1.3	3.0	4.0	0.88
^{173}Yb	Conc	545	509	458	240.8	329	316	208.0	378	868	1064	270.0
	1σ	18	16	15	7.8	11	10	6.7	12	28	35	8.9
^{175}Lu	Conc	94.3	85.3	82.1	41.0	56.2	52.9	37.3	68.1	136.8	187.3	44.5
	1σ	3.1	2.8	2.7	1.4	1.9	1.8	1.2	2.3	4.4	6.0	1.4
^{181}Ta	Conc	1.042	1.483	0.736	0.565	0.605	0.432	0.510	0.432	1.097	1.70	0.483
	1σ	0.055	0.061	0.048	0.027	0.025	0.023	0.024	0.035	0.051	0.10	0.024
^{232}Th	Conc	183.5	170.5	123.6	74.1	73.7	64.2	48.5	87.1	418	355	50.9
	1σ	6.1	5.6	4.1	2.4	2.4	2.1	1.6	2.9	14	12	1.7
^{238}U	Conc	294.3	255.5	199.0	130.7	123.9	111.5	77.4	156.9	435	609	127.1
	1σ	9.3	8.1	6.3	4.1	3.9	3.6	2.5	5.1	14	19	4.0
Ti-in-zirc	T (°C)	807.3	781.1	737.0	734.2	697.0	718.0	699.0	668	753.5	763.0	715.1
	1σ	5.6	4.9	7.9	5.0	4.9	5.5	5.3	11	5.8	9.3	5.4

Analysis Group		SWA11-066 pristine	SWA11-068 pristine	SWA11-073 variable	SWA11-074 variable	SWA11-079 pristine	SWA11-081 variable	SWA11-084 pristine	SWA11-085 metamict	SWA11-086 variable	SWA11-088 pristine	SWA09-001c pristine
^{31}P	Conc	400	860	460	330	262	224	410	710	760	460	390
	1σ	130	270	140	100	82	69	130	220	230	140	310
^{43}Ca	Conc											24
	1σ											15
^{49}Ti	Conc	5.31	2.18	13.77	10.5	3.27	5.11	10.37	10.89	6.49	1.16	15.5
	1σ	0.33	0.31	0.77	1.2	0.33	0.62	0.72	0.76	0.50	0.20	1.3
^{89}Y	Conc	930	2112	1344	832	678	1029	1528	2472	2128	1178	1132
	1σ	31	70	44	28	22	34	51	82	71	39	45
^{93}Nb	Conc	2.016	4.39	10.35	6.07	1.804	2.55	6.54	8.79	9.53	4.95	13.21
	1σ	0.075	0.17	0.36	0.27	0.076	0.12	0.24	0.31	0.33	0.18	0.58
^{139}La	Conc	0.0069	0.0448	5.38	1.68	0.0278	0.756	1.205	6.37	2.86	0.0345	4.18
	1σ	0.0023	0.0091	0.20	0.11	0.0062	0.054	0.061	0.24	0.12	0.0074	0.18
^{140}Ce	Conc	14.01	7.45	26.10	10.87	8.19	18.95	27.42	48.8	18.90	9.35	25.83
	1σ	0.46	0.26	0.85	0.42	0.28	0.65	0.90	1.6	0.63	0.32	0.95
^{141}Pr	Conc	0.0642	0.0649	1.908	0.910	0.0769	0.745	0.419	3.63	0.788	0.0200	2.353
	1σ	0.0059	0.0094	0.074	0.070	0.0090	0.047	0.027	0.14	0.039	0.0048	0.094
^{146}Nd	Conc	1.388	1.044	12.24	3.96	1.003	5.62	4.17	24.95	5.94	0.483	13.94
	1σ	0.078	0.097	0.47	0.35	0.084	0.33	0.23	0.92	0.27	0.059	0.57
^{147}Sm	Conc	3.52	3.91	10.43	3.54	2.41	6.59	6.79	21.93	7.52	1.88	9.25
	1σ	0.16	0.23	0.43	0.35	0.15	0.39	0.34	0.86	0.34	0.14	0.41
^{151}Eu	Conc	0.574	0.198	2.89	0.808	0.241	1.66	1.558	3.86	1.280	0.149	1.487
	1σ	0.031	0.025	0.12	0.093	0.024	0.10	0.084	0.16	0.068	0.020	0.077
^{157}Gd	Conc	20.47	30.7	35.2	13.42	13.60	30.1	35.0	75.9	41.4	17.68	32.2
	1σ	0.71	1.1	1.2	0.76	0.53	1.2	1.3	2.7	1.5	0.70	1.2
^{159}Tb	Conc	7.36	13.11	11.62	6.08	5.06	9.35	11.61	23.49	15.12	7.70	10.50
	1σ	0.24	0.44	0.39	0.26	0.18	0.33	0.39	0.77	0.50	0.26	0.36

Analysis		SWA11-066	SWA11-068	SWA11-073	SWA11-074	SWA11-079	SWA11-081	SWA11-084	SWA11-085	SWA11-086	SWA11-088	SWA09-001c
^{163}Dy	Conc	83.8	170.7	123.4	74.8	61.9	101.8	137.7	234.0	182.4	98.9	113.2
	1σ	2.8	5.7	4.1	2.7	2.1	3.5	4.6	7.7	6.1	3.3	3.7
^{165}Ho	Conc	30.9	65.7	42.3	28.43	23.49	35.5	49.0	75.6	66.2	39.3	38.6
	1σ	1.0	2.1	1.4	0.98	0.77	1.2	1.6	2.4	2.1	1.3	1.3
^{166}Er	Conc	134.5	294.6	172.5	126.8	103.2	144.0	213.5	305	287.3	182.3	156.8
	1σ	4.4	9.8	5.7	4.4	3.5	4.9	7.2	10	9.7	6.2	5.1
^{169}Tm	Conc	28.64	63.6	35.4	30.2	21.58	29.35	43.6	59.1	60.4	40.1	32.6
	1σ	0.92	2.0	1.1	1.0	0.70	0.97	1.4	1.9	1.9	1.3	1.1
^{173}Yb	Conc	280.6	612	331	294	205.2	280.8	409	551	591	388	305
	1σ	9.2	20	11	10	6.8	9.4	13	18	19	13	10
^{175}Lu	Conc	49.3	102.7	55.2	48.4	36.6	45.8	73.2	92.0	97.1	71.1	54.2
	1σ	1.6	3.3	1.8	1.6	1.2	1.5	2.4	3.0	3.1	2.3	1.7
^{181}Ta	Conc	0.485	0.957	0.708	1.434	0.467	0.522	0.836	0.790	0.744	1.769	0.411
	1σ	0.021	0.046	0.033	0.089	0.025	0.037	0.041	0.040	0.036	0.071	0.022
^{232}Th	Conc	56.7	57.4	69.4	60.5	30.4	70.9	108.1	197.5	145.0	84.1	77.8
	1σ	1.9	1.9	2.3	2.1	1.0	2.4	3.6	6.6	4.8	2.8	2.5
^{238}U	Conc	120.4	305.3	156.7	195.1	74.3	128.2	170.9	275.1	350	317	122.7
	1σ	3.8	9.5	4.9	6.1	2.3	4.0	5.4	8.6	11	10	3.8
Ti-in-zirc	T (°C)	688.1	622.5	769.7	745.0	651.3	685.1	744.0	748.4	704.2	581	780.7
	1σ	5.0	9.7	4.8	9.7	7.5	9.3	5.8	5.9	6.2	11	7.0

Analysis Group		SWA09-002 pristine	SWA09-004 variable	SWA09-005c metamict	SWA09-010 variable	SWA09-011c variable	SWA09-012 pristine	SWA09-016 variable	SWA09-017c pristine	SWA09-018 metamict	SWA09-021c pristine	SWA09-023c pristine
^{31}P	Conc	620	270	600	960	130	390	470	480	1160	530	520
	1σ	490	210	470	760	100	310	370	390	920	420	410
^{43}Ca	Conc	65	71	212	461	58	23	135	57	723	<22	<21
	1σ	21	23	24	78	17	14	47	18	63	8.7	11
^{49}Ti	Conc	19.8	19.2	108.9	51.6	10.61	5.43	12.6	28.4	107.2	7.54	6.47
	1σ	1.5	1.7	6.2	4.5	0.86	0.72	2.0	2.2	6.3	0.61	0.63
^{89}Y	Conc	2048	1305	3400	2660	502	946	987	1489	9920	1605	1300
	1σ	82	52	140	110	20	38	40	59	400	64	52
^{93}Nb	Conc	13.70	21.58	42.0	27.8	6.50	2.49	2.72	11.37	112.2	5.50	4.16
	1σ	0.60	0.95	1.8	1.3	0.30	0.14	0.20	0.50	4.6	0.24	0.19
^{139}La	Conc	4.54	9.47	41.0	30.0	7.06	0.133	0.588	9.95	116.9	0.157	0.852
	1σ	0.19	0.39	1.6	1.2	0.28	0.018	0.069	0.40	4.3	0.012	0.044
^{140}Ce	Conc	34.0	56.7	120.6	118.2	47.8	8.82	7.63	53.3	327	12.49	11.83
	1σ	1.3	2.1	4.4	4.4	1.8	0.35	0.36	1.9	12	0.45	0.44
^{141}Pr	Conc	2.459	5.59	22.69	16.48	5.14	0.247	0.246	4.26	67.7	0.280	0.594
	1σ	0.099	0.21	0.78	0.62	0.18	0.021	0.037	0.17	2.3	0.015	0.030
^{146}Nd	Conc	15.20	31.6	119.4	90.0	26.7	2.72	3.68	22.53	370	3.69	4.44
	1σ	0.62	1.3	4.2	3.5	1.0	0.18	0.36	0.91	13	0.17	0.21
^{147}Sm	Conc	13.97	23.16	79.0	49.3	13.42	4.32	5.65	14.38	238.8	6.84	6.57
	1σ	0.58	0.95	2.7	2.1	0.52	0.26	0.49	0.63	8.1	0.28	0.29
^{151}Eu	Conc	1.998	3.48	9.09	7.76	2.58	0.336	0.840	1.392	23.62	0.914	0.941
	1σ	0.098	0.17	0.34	0.38	0.11	0.034	0.098	0.084	0.83	0.044	0.050
^{157}Gd	Conc	49.1	55.7	159.5	107.9	26.42	21.56	24.4	39.9	472	36.9	30.0
	1σ	1.7	2.0	5.3	4.0	0.94	0.83	1.2	1.4	15	1.2	1.0
^{159}Tb	Conc	16.77	15.58	47.4	31.0	5.97	7.35	8.94	13.38	138.3	12.55	10.50
	1σ	0.56	0.53	1.6	1.1	0.20	0.26	0.35	0.46	4.5	0.41	0.35

Analysis		SWA09-002	SWA09-004	SWA09-005c	SWA09-010	SWA09-011c	SWA09-012	SWA09-016	SWA09-017c	SWA09-018	SWA09-021c	SWA09-023c
^{163}Dy	Conc	190.4	143.3	402	304	52.9	89.4	95.0	144.1	1189	142.5	119.8
	1σ	6.3	4.8	13	10	1.8	3.0	3.4	4.8	39	4.6	3.9
^{165}Ho	Conc	68.4	42.3	100.6	92.4	15.00	32.1	33.7	50.4	300.1	54.1	44.5
	1σ	2.2	1.4	3.3	3.1	0.50	1.1	1.2	1.7	9.8	1.8	1.5
^{166}Er	Conc	298.3	153.6	322	363	58.5	139.3	141.7	211.8	968	238.4	188.5
	1σ	9.6	5.0	10	12	1.9	4.5	4.8	6.9	31	7.7	6.1
^{169}Tm	Conc	62.4	28.51	52.6	68.0	11.66	29.59	29.5	43.2	158.0	49.7	39.3
	1σ	2.0	0.93	1.7	2.2	0.38	0.96	1.0	1.4	5.1	1.6	1.3
^{173}Yb	Conc	606	265.3	418	604	114.0	279.1	274.7	408	1235	473	375
	1σ	20	8.8	14	20	3.8	9.2	9.4	13	40	15	12
^{175}Lu	Conc	108.9	51.4	65.3	110.7	22.75	49.8	51.6	71.3	173.3	90.2	68.4
	1σ	3.5	1.7	2.1	3.6	0.74	1.6	1.7	2.3	5.6	2.9	2.2
^{181}Ta	Conc	1.660	0.526	3.58	1.369	0.525	0.417	0.452	1.255	4.99	1.291	0.590
	1σ	0.064	0.031	0.12	0.080	0.023	0.025	0.043	0.055	0.17	0.046	0.026
^{232}Th	Conc	124.6	78.2	110.3	233.4	68.7	65.8	47.5	141.4	431	93.8	76.6
	1σ	4.0	2.5	3.6	7.6	2.2	2.1	1.6	4.6	14	3.1	2.5
^{238}U	Conc	282.0	168.2	236.5	165.0	274.8	103.1	88.3	111.8	386	188.1	194.2
	1σ	8.7	5.2	7.3	5.1	8.5	3.2	2.8	3.5	12	5.8	6.0
Ti-in-zirc	T (°C)	804.8	801.7	1005.4	909.0	746.1	690	762	841.5	1003.3	716.6	703.9
	1σ	6.9	8.0	5.6	8.8	6.8	10	13	7.1	5.9	6.6	7.7

Analysis		SWA09-025	SWA09-026c	SWA09-027c	SWA09-029c	SWA09-034c	SWA09-042c	SWA09-043c	SWA09-044c	SWA09-045	SWA09-046
Group		metamict	pristine	variable	metamict	pristine	pristine	pristine	pristine	metamict	variable
^{31}P	Conc	310	430	330	600	310	750	240	560	1130	690
	1σ	250	350	260	480	250	600	190	450	910	550
^{43}Ca	Conc	431	51	111	106	<23	59	95	34.5	10760	1430
	1σ	40	16	38	30	10	22	19	8.6	590	130
^{49}Ti	Conc	54.9	5.73	17.1	19.0	7.92	13.8	10.00	5.68	772	61.4
	1σ	3.4	0.65	2.2	1.9	0.58	1.3	0.90	0.45	46	4.9
^{89}Y	Conc	2970	1223	1460	3450	712	2960	798	1571	20830	3800
	1σ	120	49	59	140	29	120	32	62	830	150
^{93}Nb	Conc	37.0	7.00	22.4	9.34	1.602	11.35	9.01	5.66	535	78.9
	1σ	1.6	0.32	1.0	0.45	0.076	0.52	0.39	0.24	22	3.3
^{139}La	Conc	59.8	6.15	8.99	30.9	0.0936	8.89	7.00	7.97	740	43.9
	1σ	2.2	0.25	0.41	1.2	0.0080	0.36	0.27	0.30	27	1.7
^{140}Ce	Conc	267.3	30.4	44.4	89.5	7.87	47.0	42.0	33.3	4110	249.5
	1σ	9.6	1.1	1.7	3.3	0.29	1.8	1.5	1.1	140	8.6
^{141}Pr	Conc	39.5	3.36	6.38	14.03	0.1245	5.85	4.82	2.751	368	25.51
	1σ	1.3	0.13	0.27	0.51	0.0081	0.22	0.17	0.097	12	0.90
^{146}Nd	Conc	214.9	17.55	31.1	84.8	1.977	37.6	28.3	15.02	1714	135.0
	1σ	7.5	0.70	1.4	3.2	0.097	1.5	1.0	0.53	58	4.8
^{147}Sm	Conc	114.5	10.79	20.6	53.6	3.53	29.7	15.61	9.37	796	82.4
	1σ	3.9	0.46	1.1	2.1	0.15	1.2	0.61	0.35	27	3.1
^{151}Eu	Conc	11.04	0.860	1.95	4.64	0.805	3.23	1.777	1.653	127.8	9.42
	1σ	0.40	0.053	0.15	0.23	0.037	0.15	0.082	0.064	4.2	0.40
^{157}Gd	Conc	198.1	30.0	52.0	139.4	17.92	96.4	39.4	38.6	1227	156.1
	1σ	6.5	1.1	2.1	4.8	0.61	3.3	1.4	1.3	40	5.4
^{159}Tb	Conc	48.9	10.28	17.04	39.1	5.82	28.97	10.82	12.55	296.8	44.2
	1σ	1.6	0.35	0.61	1.3	0.19	0.96	0.36	0.41	9.6	1.5

Analysis		SWA09-025	SWA09-026c	SWA09-027c	SWA09-029c	SWA09-034c	SWA09-042c	SWA09-043c	SWA09-044c	SWA09-045	SWA09-046
^{163}Dy	Conc	378	114.7	168.0	375	63.8	295.4	98.7	141.7	2432	418
	1σ	12	3.8	5.7	12	2.1	9.6	3.2	4.6	79	14
^{165}Ho	Conc	88.4	41.0	51.0	110.1	23.04	96.7	26.99	51.3	590	116.3
	1σ	2.9	1.4	1.7	3.6	0.75	3.2	0.89	1.7	19	3.8
^{166}Er	Conc	265.9	175.6	199.0	412	101.7	380	95.0	218.7	1885	434
	1σ	8.6	5.7	6.6	13	3.3	12	3.1	7.1	61	14
^{169}Tm	Conc	41.3	36.7	43.2	76.8	21.80	71.5	17.01	44.5	287.3	82.1
	1σ	1.3	1.2	1.4	2.5	0.70	2.3	0.56	1.4	9.2	2.7
^{173}Yb	Conc	321	366	424	676	215.0	627	146.2	428	2242	740
	1σ	10	12	14	22	7.0	20	4.8	14	72	24
^{175}Lu	Conc	49.4	66.9	72.3	109.7	41.7	111.5	24.07	77.5	298.4	113.9
	1σ	1.6	2.2	2.4	3.6	1.3	3.6	0.78	2.5	9.5	3.7
^{181}Ta	Conc	1.108	1.491	0.961	0.804	0.317	0.766	0.561	0.838	9.52	2.149
	1σ	0.045	0.058	0.063	0.047	0.014	0.038	0.026	0.030	0.30	0.098
^{232}Th	Conc	252.0	103.9	110.7	278.6	57.0	234.7	77.9	53.2	1901	245.0
	1σ	8.2	3.4	3.7	9.1	1.9	7.7	2.5	1.7	62	8.0
^{238}U	Conc	269.1	607	144.5	294.8	119.0	244.2	117.6	87.5	2306	674
	1σ	8.3	19	4.5	9.1	3.7	7.6	3.7	2.7	72	21
Ti-in-zirc	T (°C)	916.3	694.1	790	800.5	720.7	770.0	740.8	693.4	1353.8	930.1
	1σ	5.9	8.8	11	9.1	6.0	8.2	7.5	6.3	7.0	8.1

Analysis		SWA02a-004c	SWA02a-006	SWA02a-007c	SWA02a-007r	SWA02a-008	SWA02a-009	SWA02a-024c	SWA02a-027c	SWA02a-030c	SWA02a-031c
Group		pristine	pristine	metamict	metamict	metamict	metamict	metamict	metamict	pristine	metamict
^{31}P	Conc	920	1040	280	4100	380	390	174	213	920	1120
	1σ	340	390	100	1500	140	150	65	79	330	410
^{43}Ca	Conc										
	1σ										
^{49}Ti	Conc	4.85	10.71	26.7	24.5	25.8	30.1	16.39	257	7.32	17.2
	1σ	0.76	0.71	1.4	1.3	1.4	1.7	0.95	11	0.40	1.0
^{89}Y	Conc	2277	2732	3500	2304	2696	2556	2048	3750	2900	3160
	1σ	80	96	120	81	94	89	72	130	100	110
^{93}Nb	Conc	10.43	8.44	128.4	94.1	23.96	33.2	26.8	143.4	27.1	36.6
	1σ	0.44	0.33	4.8	3.5	0.91	1.3	1.0	5.6	1.0	1.4
^{139}La	Conc	3.34	0.956	87.2	78.2	75.7	169.1	25.32	102.1	12.40	72.5
	1σ	0.16	0.047	3.0	2.7	2.7	6.0	0.91	3.7	0.43	2.5
^{140}Ce	Conc	31.9	29.3	433	315	320	522	186.1	515	80.7	431
	1σ	1.2	1.0	15	11	11	19	6.8	19	2.9	15
^{141}Pr	Conc	1.737	0.364	54.6	41.1	38.9	61.6	18.61	77.6	7.21	54.3
	1σ	0.091	0.021	1.8	1.4	1.3	2.1	0.64	2.7	0.24	1.8
^{146}Nd	Conc	13.44	4.94	343	224.3	238.1	309	125.1	517	36.8	353
	1σ	0.65	0.22	11	7.3	7.8	10	4.1	17	1.2	11
^{147}Sm	Conc	13.55	10.99	197.6	115.1	84.1	87.1	55.3	214.1	17.66	114.4
	1σ	0.70	0.45	6.7	4.0	2.9	3.1	2.0	7.6	0.63	4.0
^{151}Eu	Conc	1.292	0.768	19.52	10.93	11.57	17.79	13.30	26.69	0.994	16.35
	1σ	0.099	0.044	0.66	0.38	0.40	0.61	0.46	0.94	0.042	0.58
^{157}Gd	Conc	57.5	58.9	351	192.0	136.7	138.1	103.6	278	71.5	161.6
	1σ	2.2	2.1	12	6.7	4.8	4.9	3.8	10	2.3	5.3
^{159}Tb	Conc	19.01	21.60	65.4	36.2	30.4	29.68	21.11	51.2	24.80	32.9
	1σ	0.66	0.71	2.1	1.2	1.0	0.99	0.70	1.7	0.84	1.1

Analysis		SWA02a-004c	SWA02a-006	SWA02a-007c	SWA02a-007r	SWA02a-008	SWA02a-009	SWA02a-024c	SWA02a-027c	SWA02a-030c	SWA02a-031c
^{163}Dy	Conc	225.4	251.0	451	268.9	264.0	260.2	183.5	414	280.2	301
	1σ	7.7	8.4	15	9.1	9.0	8.9	6.4	15	9.4	10
^{165}Ho	Conc	77.4	89.1	116.7	72.7	81.9	80.1	61.4	112.9	96.4	94.9
	1σ	2.6	3.0	3.9	2.4	2.8	2.7	2.1	3.9	3.2	3.2
^{166}Er	Conc	334	386	405	283.9	318	315	255.7	396	399	379
	1σ	11	13	13	9.3	10	10	8.5	13	13	12
^{169}Tm	Conc	73.0	84.6	79.8	62.3	68.8	66.1	58.8	87.7	84.5	82.8
	1σ	2.4	2.8	2.6	2.1	2.3	2.2	2.0	2.9	2.7	2.7
^{173}Yb	Conc	728	840	718	663	726	613	651	905	801	826
	1σ	24	28	24	22	24	21	22	31	26	27
^{175}Lu	Conc	100.4	132.6	111.7	102.2	104.3	97.1	100.2	132.8	123.0	121.7
	1σ	3.3	4.3	3.7	3.4	3.4	3.2	3.3	4.5	3.9	3.9
^{181}Ta	Conc	2.25	3.50	24.63	25.03	6.49	6.97	3.55	18.87	3.32	2.445
	1σ	0.11	0.13	0.82	0.84	0.23	0.25	0.13	0.67	0.11	0.091
^{232}Th	Conc	357	495	435	365	452	425	317	259.7	539	375
	1σ	12	16	14	12	15	14	10	8.5	18	12
^{238}U	Conc	1006	1288	915	1390	978	1282	894	1854	1150	1234
	1σ	32	42	30	45	32	42	30	62	38	41
Ti-in-zirc	T (°C)	681	746.9	835.2	826.4	831.6	847.8	786.2	1138.0	714.1	790.8
	1σ	12	5.6	4.7	4.7	4.7	5.0	5.0	3.6	4.5	5.1

Analysis		SWA02a-032	SWA02a-037c	SWA02a-042c	SWA02a-043	SWA02a-045c	SWA02a-046c	SWA02a-047c	SWA02a-048	SWA02a-052	SWA02a-054c
Group		variable	metamict	variable	metamict	metamict	metamict	variable	metamict	pristine	variable
^{31}P	Conc	163	1000	660	132	210	1080	340	4100	830	360
	1σ	60	360	240	49	78	400	130	1500	300	130
^{43}Ca	Conc										
	1σ										
^{49}Ti	Conc	3.94	42.6	12.36	88.2	53.0	21.4	23.1	32.8	15.2	12.05
	1σ	0.31	1.9	0.95	3.8	2.7	1.4	1.6	1.8	1.1	0.75
^{89}Y	Conc	840	3980	1729	6830	6600	3500	538	3250	2495	1456
	1σ	30	140	62	240	240	130	19	120	87	51
^{93}Nb	Conc	14.20	124.6	10.35	84.0	105.3	23.81	3.09	48.9	14.84	15.88
	1σ	0.53	4.6	0.42	3.2	4.0	0.94	0.15	1.9	0.56	0.59
^{139}La	Conc	6.06	91.9	9.68	122.8	31.4	77.5	9.48	83.2	5.47	13.70
	1σ	0.22	3.2	0.36	4.2	1.1	2.7	0.36	2.9	0.22	0.49
^{140}Ce	Conc	36.9	538	63.4	586	292	403	45.5	318	40.5	105.0
	1σ	1.3	20	2.4	22	11	15	1.8	13	1.5	3.8
^{141}Pr	Conc	3.66	70.1	6.74	67.5	29.38	41.7	2.90	32.9	2.341	11.37
	1σ	0.13	2.3	0.24	2.2	0.98	1.4	0.12	1.1	0.096	0.38
^{146}Nd	Conc	26.46	446	43.6	435	291.8	205.7	14.76	237.4	14.87	85.5
	1σ	0.89	14	1.5	14	9.6	6.8	0.62	7.8	0.61	2.8
^{147}Sm	Conc	14.16	167.0	22.78	225.4	219.7	45.1	7.14	123.3	17.03	44.6
	1σ	0.53	5.8	0.93	7.9	7.9	1.8	0.39	4.6	0.71	1.6
^{151}Eu	Conc	2.515	18.78	1.772	27.44	30.3	9.29	0.845	19.60	1.392	5.10
	1σ	0.097	0.65	0.096	0.96	1.1	0.37	0.064	0.72	0.081	0.19
^{157}Gd	Conc	32.5	262.0	52.0	510	527	103.0	22.14	186.1	70.2	79.6
	1σ	1.1	8.4	1.8	16	17	3.5	0.87	6.1	2.4	2.6
^{159}Tb	Conc	7.66	51.9	15.47	112.5	98.6	29.9	6.46	40.4	22.20	17.53
	1σ	0.27	1.8	0.55	3.9	3.5	1.1	0.25	1.5	0.73	0.57

Analysis		SWA02a-032	SWA02a-037c	SWA02a-042c	SWA02a-043	SWA02a-045c	SWA02a-046c	SWA02a-047c	SWA02a-048	SWA02a-052	SWA02a-054c
^{163}Dy	Conc	74.7	425	161.9	815	738	325	63.0	357	238.2	158.5
	1σ	2.5	14	5.6	28	25	11	2.3	12	7.7	5.1
^{165}Ho	Conc	26.03	122.8	54.9	199.1	191.9	114.7	19.50	105.9	81.9	48.0
	1σ	0.88	4.1	1.9	6.8	6.6	4.0	0.70	3.7	2.7	1.6
^{166}Er	Conc	121.2	470	229.1	665	644	497	73.5	413	347	190.2
	1σ	3.9	15	7.4	21	21	16	2.4	13	11	6.1
^{169}Tm	Conc	31.9	100.5	53.1	134.8	130.6	114.5	15.26	89.8	77.4	39.3
	1σ	1.0	3.3	1.7	4.4	4.3	3.7	0.52	2.9	2.5	1.3
^{173}Yb	Conc	378	965	547	1267	1279	1112	150.8	949	787	373
	1σ	12	32	18	42	43	37	5.2	32	26	12
^{175}Lu	Conc	65.0	145.0	78.3	171.9	180.9	168.6	20.68	141.6	107.3	59.1
	1σ	2.1	4.7	2.5	5.5	5.8	5.4	0.69	4.6	3.4	1.9
^{181}Ta	Conc	3.24	3.50	1.759	5.98	3.41	3.73	1.068	3.61	3.36	1.257
	1σ	0.11	0.12	0.075	0.20	0.13	0.14	0.054	0.13	0.13	0.050
^{232}Th	Conc	149.4	526	130.6	207.0	1070	545	133.8	609	448	204.1
	1σ	4.9	17	4.3	6.8	35	18	4.5	20	15	6.7
^{238}U	Conc	838	1575	567	2057	2328	1824	213.2	1708	1244	352
	1σ	28	52	19	69	79	62	7.4	59	40	12
Ti-in-zirc	T (°C)	665.1	886.4	759.8	976.6	912.2	812.3	820.0	857.1	779.2	757.5
	1σ	6.0	3.8	6.6	3.8	4.6	5.9	6.0	4.8	6.2	5.3

Analysis Group		SWA02a-055 metamict	RSA07-001 metamict	RSA07-004 variable	RSA07-014c metamict	RSA07-021 pristine	RSA07-046 variable	RSA07-050 metamict	RSA07-051 variable	RSA07-057 metamict	RSA07-069 variable	RSA07-079 pristine
^{31}P	Conc	228	1710	460	1820	680	880	550	540	460	660	720
	1σ	82	410	110	430	160	210	130	130	110	160	170
^{43}Ca	Conc											
	1σ											
^{49}Ti	Conc	178.2	444	6.55	444	14.14	171.6	453	78.3	196.6	19.0	8.12
	1σ	7.1	16	0.75	16	0.74	6.7	17	3.4	8.0	1.4	0.46
^{89}Y	Conc	8150	18400	2554	15660	2679	4920	33300	4260	6550	2185	2254
	1σ	290	620	86	530	91	170	1100	150	220	75	78
^{93}Nb	Conc	162.7	110.6	13.35	64.7	12.01	26.73	245.2	19.34	34.3	6.93	15.19
	1σ	5.9	3.7	0.49	2.2	0.41	0.91	8.3	0.68	1.2	0.28	0.52
^{139}La	Conc	816	342	21.59	262.2	19.69	86.4	393	29.6	143.6	5.03	9.53
	1σ	28	11	0.76	8.7	0.66	2.9	13	1.0	4.8	0.21	0.33
^{140}Ce	Conc	3270	1829	101.2	964	89.7	390	5020	236.2	694	61.6	59.3
	1σ	120	67	3.8	36	3.5	16	200	9.8	22	2.0	1.9
^{141}Pr	Conc	391	276	12.65	179.3	12.81	67.5	564	28.6	101.2	5.35	5.51
	1σ	13	11	0.54	7.4	0.55	3.0	26	1.4	3.3	0.21	0.19
^{146}Nd	Conc	2076	1628	62.8	937	74.8	370	3790	171.6	534	29.5	32.6
	1σ	67	53	2.3	30	2.5	12	130	5.8	18	1.2	1.1
^{147}Sm	Conc	626	1015	27.6	655	43.8	231.1	2480	111.0	315	21.70	20.45
	1σ	21	33	1.1	21	1.5	7.6	81	3.7	10	0.94	0.70
^{151}Eu	Conc	97.9	62.0	2.25	34.6	2.84	17.54	113.6	7.10	22.87	2.23	3.05
	1σ	3.2	2.0	0.13	1.1	0.11	0.60	3.8	0.27	0.77	0.13	0.11
^{157}Gd	Conc	712	1697	75.8	1189	99.7	409	4480	237.9	538	59.7	65.8
	1σ	23	54	2.7	38	3.3	13	140	7.8	17	2.2	2.1
^{159}Tb	Conc	120.5	403	21.35	290	27.1	97.2	961	55.5	129.2	18.73	19.77
	1σ	3.9	16	0.91	12	1.2	4.4	45	2.7	4.1	0.64	0.63

Analysis		SWA02a-055	RSA07-001	RSA07-004	RSA07-014c	RSA07-021	RSA07-046	RSA07-050	RSA07-051	RSA07-057	RSA07-069	RSA07-079
^{163}Dy	Conc	868	3120	239.6	2259	261.1	731	6560	485	911	200.3	213.2
	1σ	28	100	7.8	72	8.4	24	210	16	29	6.6	6.9
^{165}Ho	Conc	240.3	603	82.4	450	80.9	163.8	1289	133.5	194.1	66.3	72.9
	1σ	7.9	23	3.3	18	3.4	7.1	57	6.0	6.2	2.2	2.4
^{166}Er	Conc	944	1520	344	1244	322	501	2890	469	535	279.9	297.3
	1σ	30	49	11	40	11	16	95	15	17	9.2	9.6
^{169}Tm	Conc	200.0	196.0	70.6	181.6	63.2	84.4	321	84.8	82.0	57.9	62.6
	1σ	6.5	8.3	3.1	8.1	3.0	4.2	16	4.4	2.6	1.9	2.0
^{173}Yb	Conc	1977	1478	665	1458	593	715	1977	743	645	547	596
	1σ	65	48	22	48	20	24	66	25	21	18	19
^{175}Lu	Conc	293.1	196.7	106.3	221.7	98.6	108.7	245.2	119.9	96.1	90.5	94.6
	1σ	9.3	6.9	3.8	7.9	3.6	4.0	9.2	4.6	3.1	2.9	3.0
^{181}Ta	Conc	18.38	6.48	2.88	9.69	1.775	4.38	10.16	2.000	5.21	1.303	6.36
	1σ	0.59	0.23	0.13	0.32	0.067	0.15	0.35	0.082	0.19	0.073	0.21
^{232}Th	Conc	922	3320	189.3	1243	112.1	2146	3600	341	692	152.5	219.8
	1σ	30	110	6.4	42	3.8	72	120	12	23	5.2	7.4
^{238}U	Conc	3790	1779	379	1244	338	443	2007	408	498	192.9	635
	1σ	120	56	12	39	11	14	64	13	16	6.1	20
Ti-in-zirc	T (°C)	1078.2	1237.6	704.9	1237.7	772.2	1072.3	1241.5	960.9	1093.8	800.4	722.8
	1σ	3.3	2.5	9.0	2.4	4.5	3.2	2.8	3.8	3.4	6.6	4.7

Analysis		RSA07-080c	RSA07-080r	SWA05-002c	SWA05-002r	SWA05-004	SWA05-006c	SWA05-007c	SWA05-007r	SWA05-009	SWA05-010c	SWA05-010r
Group		variable	metamict	variable	metamict	metamict	variable	variable	metamict	pristine	variable	metamict
^{31}P	Conc	352	810	240	550	1810	370	520	1040	305	400	810
	1σ	83	190	86	200	650	130	150	300	89	120	240
^{43}Ca	Conc											
	1σ											
^{49}Ti	Conc	26.7	1457	11.6	31.2	279	11.3	8.96	11.88	11.11	15.63	138.9
	1σ	1.3	61	1.2	1.4	11	1.0	0.66	0.76	0.55	0.83	6.6
^{89}Y	Conc	1724	41100	2337	3400	16250	1789	1358	2950	1070	990	5390
	1σ	60	1400	83	120	580	64	47	100	37	34	190
^{93}Nb	Conc	6.30	407	20.82	28.0	161.6	6.37	10.01	32.3	3.27	3.06	55.6
	1σ	0.23	14	0.81	1.0	5.9	0.27	0.36	1.1	0.12	0.12	1.9
^{139}La	Conc	27.82	469	5.04	102.2	318	18.47	12.79	762	3.43	3.78	226.6
	1σ	0.96	16	0.22	3.5	11	0.66	0.45	26	0.12	0.14	7.7
^{140}Ce	Conc	68.9	5790	48.8	632	3020	168.9	134.2	5150	63.5	26.34	959
	1σ	2.2	190	1.7	21	100	5.8	4.3	170	2.1	0.87	31
^{141}Pr	Conc	18.55	631	4.12	78.5	328	16.35	9.26	543	2.454	2.075	135.3
	1σ	0.63	21	0.17	2.5	10	0.55	0.32	18	0.086	0.078	4.6
^{146}Nd	Conc	106.0	4150	28.9	467	3200	82.7	51.9	2849	17.79	11.83	753
	1σ	3.6	140	1.2	15	100	2.9	1.8	91	0.60	0.43	24
^{147}Sm	Conc	62.9	2705	17.08	157.9	2368	29.6	27.06	763	17.47	12.14	340
	1σ	2.1	87	0.84	5.4	81	1.2	0.99	25	0.61	0.46	11
^{151}Eu	Conc	8.36	139.9	2.61	18.33	188.6	7.27	2.95	43.1	4.07	1.965	49.4
	1σ	0.29	4.6	0.16	0.63	6.4	0.30	0.13	1.4	0.14	0.081	1.7
^{157}Gd	Conc	119.3	5240	49.8	181.8	2690	58.3	74.2	556	49.1	37.5	500
	1σ	3.9	170	1.9	5.9	87	2.1	2.5	18	1.6	1.3	17
^{159}Tb	Conc	30.00	1192	17.40	41.2	436	16.89	22.17	81.3	13.26	11.22	117.6
	1σ	0.96	38	0.63	1.4	15	0.61	0.73	2.6	0.43	0.37	3.8

Analysis		RSA07-080c	RSA07-080r	SWA05-002c	SWA05-002r	SWA05-004	SWA05-006c	SWA05-007c	SWA05-007r	SWA05-009	SWA05-010c	SWA05-010r
^{163}Dy	Conc	238.5	8290	216.2	370	2676	172.5	234.7	575	123.0	113.1	1002
	1σ	7.7	270	7.4	12	90	5.9	7.6	19	4.0	3.7	32
^{165}Ho	Conc	57.4	1635	81.9	116.5	569	61.7	77.6	161.7	38.1	35.9	270.0
	1σ	1.9	53	2.7	3.8	19	2.1	2.5	5.2	1.2	1.2	8.8
^{166}Er	Conc	191.3	3670	370	483	1697	260.1	315	633	148.9	141.2	921
	1σ	6.2	120	12	15	54	8.4	10	21	4.9	4.6	30
^{169}Tm	Conc	34.4	402	82.6	106.5	283.2	55.4	66.7	140.6	30.7	29.15	167.1
	1σ	1.1	13	2.7	3.4	9.1	1.8	2.2	4.6	1.0	0.97	5.6
^{173}Yb	Conc	299.7	2455	907	1057	2473	578	667	1462	293.4	285.6	1504
	1σ	9.7	79	29	34	79	19	22	48	9.8	9.6	51
^{175}Lu	Conc	47.0	297.1	123.1	158.4	313	77.2	89.1	194.4	43.5	40.4	186.5
	1σ	1.5	9.5	4.0	5.1	10	2.5	2.9	6.3	1.4	1.3	6.1
^{181}Ta	Conc	0.710	23.81	24.34	23.34	10.45	1.427	1.645	11.14	0.479	0.462	8.11
	1σ	0.033	0.82	0.82	0.76	0.36	0.070	0.068	0.38	0.020	0.022	0.31
^{232}Th	Conc	427	10130	84.9	260.4	1422	220.3	640	776	153.1	143.3	322
	1σ	14	340	2.9	8.6	47	7.3	21	26	5.2	4.9	11
^{238}U	Conc	93.3	1900	131.5	715	3250	575	948	4460	227.5	254.0	3320
	1σ	3.0	60	4.2	23	100	19	31	150	7.6	8.6	110
Ti-in-zirc	T (°C)	835.2	1511.4	754.3	851.8	1151.8	751.6	731.3	756.2	750.2	781.7	1040.4
	1σ	4.4	2.9	8.7	3.9	3.2	7.6	6.1	5.4	4.2	4.6	4.4

Analysis Group		SWA05-011 pristine	SWA05-012c pristine	SWA05-012r metamict	SWA05-013 metamict	SWA05-016 variable	SWA05-017 pristine	SWA05-022c pristine	SWA05-022r metamict	SWA05-023r metamict	SWA05-025r metamict
^{31}P	Conc	360	269	440	770	272	333	196	890	1190	1790
	1σ	110	79	130	230	80	98	58	260	350	530
^{43}Ca	Conc										
	1σ										
^{49}Ti	Conc	17.68	15.39	91.9	19.3	4.11	27.0	5.08	13.29	22.1	552
	1σ	0.88	0.73	4.3	1.5	0.27	1.4	0.40	0.61	1.1	23
^{89}Y	Conc	1069	797	2003	2405	944	1062	451	2641	2810	31700
	1σ	37	29	73	87	34	39	17	99	110	1200
^{93}Nb	Conc	3.04	2.69	18.84	29.3	1.635	4.11	1.058	16.81	22.17	227.9
	1σ	0.11	0.10	0.70	1.1	0.064	0.17	0.050	0.60	0.80	8.2
^{139}La	Conc	8.24	1.843	46.1	161.9	2.042	3.82	<0.0024	224.7	765	443
	1σ	0.29	0.069	1.6	5.4	0.075	0.15	0.0016	7.5	26	15
^{140}Ce	Conc	53.1	19.20	243.0	628	26.47	39.2	8.48	769	916	2400
	1σ	1.7	0.63	7.9	20	0.86	1.3	0.29	25	30	79
^{141}Pr	Conc	4.75	1.186	27.65	88.3	1.599	3.28	0.0576	107.7	147.6	289.7
	1σ	0.17	0.044	0.93	2.9	0.057	0.12	0.0068	3.5	4.9	9.6
^{146}Nd	Conc	27.73	7.95	143.6	442	11.18	23.84	1.441	531	509	1740
	1σ	0.93	0.29	4.8	14	0.39	0.86	0.093	17	16	56
^{147}Sm	Conc	21.28	7.85	88.9	177.6	9.25	21.69	2.97	188.3	126.1	1311
	1σ	0.75	0.30	3.1	6.1	0.34	0.82	0.16	6.2	4.2	43
^{151}Eu	Conc	3.09	1.031	10.71	15.38	1.609	2.65	0.714	53.0	20.03	234.6
	1σ	0.11	0.045	0.41	0.58	0.062	0.12	0.041	1.7	0.67	7.6
^{157}Gd	Conc	49.7	25.64	161.1	204.9	32.5	49.5	13.07	247.0	165.8	2735
	1σ	1.7	0.86	5.4	6.9	1.1	1.7	0.49	8.0	5.4	88
^{159}Tb	Conc	14.24	8.25	47.9	43.0	9.67	12.72	4.07	50.4	41.9	685
	1σ	0.47	0.27	1.6	1.4	0.32	0.43	0.14	1.6	1.4	22

Analysis		SWA05-011	SWA05-012c	SWA05-012r	SWA05-013	SWA05-016	SWA05-017	SWA05-022c	SWA05-022r	SWA05-023r	SWA05-025r
^{163}Dy	Conc	134.7	85.6	450	364	102.1	123.2	47.4	425	423	5860
	1σ	4.4	2.8	15	12	3.3	4.1	1.6	14	14	190
^{165}Ho	Conc	39.7	28.72	122.7	122.4	33.8	38.6	15.71	131.0	143.9	1601
	1σ	1.3	0.93	4.0	4.0	1.1	1.3	0.52	4.3	4.7	52
^{166}Er	Conc	147.8	118.0	439	533	136.2	144.8	65.3	513	613	5070
	1σ	4.9	3.8	14	17	4.4	4.7	2.1	16	20	160
^{169}Tm	Conc	30.0	25.14	82.7	117.2	28.17	30.4	14.35	112.5	134.2	787
	1σ	1.0	0.81	2.7	3.8	0.91	1.0	0.48	3.7	4.4	26
^{173}Yb	Conc	279.3	246.6	788	1167	275.9	298.5	149.4	1131	1369	5880
	1σ	9.5	8.1	26	39	9.1	9.9	5.0	38	46	200
^{175}Lu	Conc	39.5	37.1	89.7	154.1	41.2	41.6	21.53	171.6	191.0	653
	1σ	1.3	1.2	2.9	5.0	1.3	1.4	0.70	5.5	6.2	21
^{181}Ta	Conc	0.349	0.552	2.81	9.74	0.393	0.522	0.240	8.49	10.15	12.32
	1σ	0.017	0.023	0.12	0.35	0.017	0.029	0.015	0.27	0.33	0.40
^{232}Th	Conc	114.1	118.4	583	173.4	117.8	137.0	41.5	104.9	142.0	3630
	1σ	3.9	3.9	19	5.8	3.9	4.6	1.4	3.5	4.8	120
^{238}U	Conc	283.8	234.0	1036	2521	209.0	300.0	96.1	2386	3410	6450
	1σ	9.7	7.4	33	80	6.6	9.5	3.1	76	110	210
Ti-in-zirc	T (°C)	793.5	780.2	982.2	802.2	668.3	836.2	684.6	766.5	815.7	1281.1
	1σ	4.3	4.1	4.3	7.0	5.1	4.6	6.2	3.9	4.4	3.2

Appendix G – Zircon U-Pb Analyses

U-Pb isotopic compositions are shown for each analysis.

Analyses are presented as uncorrected data (left hand page) and corrected for common Pb (right hand page). Analyses were corrected for common Pb using the method of Andersen (2002).

The following information is presented for each analysis:

Th, U, Th/U: Measured concentrations of Th and U in ppm, and the ratio.

Common Pb: Calculated percentage of common Pb and associated uncertainty.

Discordance: Calculated discordance as a percentage.

Correction type: None or Disc (discordance).

^{204}Pb: Measured ^{204}Pb in counts per second, background subtracted.

Ratios: Uncorrected and corrected for common Pb and associated uncertainties.

Ages: Calculated from uncorrected and corrected ratios; ages and associated uncertainties in Ma.

Inc.?: Included in the intercept (Int.) and weighted average (W/A) ages calculated for each sample (for the uncorrected data these are the same and not shown separately).

Samples are ordered from mafic to felsic.

						Ratios (uncorrected)								Ages (uncorrected; Ma)								
	Th	U	Th/U	Common Pb		$^{207}Pb/^{206}Pb$		$^{207}Pb/^{235}U$		$^{206}Pb/^{238}U$		$^{208}Pb/^{232}Th$		$^{207}Pb/^{206}Pb$		$^{207}Pb/^{235}U$		$^{206}Pb/^{238}U$		$^{208}Pb/^{232}Th$		Inc.?
	ppm	ppm		%	1σ	Ratio	1σ	Ratio	1σ	Ratio	1σ	Ratio	1σ	Age	1σ	Age	1σ	Age	1σ	Age	1σ	
RSA03-001	56	109	0.51	2.96	0.52	0.2478	0.0071	17.51	0.48	0.5127	0.0076	0.198	0.011	3171	24	2963	26	2668	33	3658	182	y
RSA03-003	215	225	0.96	6.22	0.91	0.2687	0.0067	18.12	0.44	0.4892	0.0067	0.193	0.009	3298	20	2996	23	2567	29	3562	154	
RSA03-006	58	221	0.26			0.2433	0.0090	21.40	0.76	0.6381	0.0114	0.298	0.023	3142	32	3157	35	3182	45	5274	355	
RSA03-007	34	219	0.15	1.24	0.21	0.2450	0.0076	20.29	0.61	0.6009	0.0097	0.264	0.017	3153	26	3105	29	3034	39	4740	276	y
RSA03-011	7	73	0.10	1.66	0.19	0.2446	0.0075	20.33	0.61	0.6029	0.0098	0.375	0.024	3150	26	3107	29	3041	39	6443	357	y
RSA03-012	50	110	0.45	4.31	1.12	0.2600	0.0129	20.06	0.95	0.5612	0.0120	0.260	0.029	3246	45	3094	46	2871	49	4678	464	y
RSA03-013	41	125	0.33	1.39	0.41	0.2466	0.0089	19.68	0.68	0.5789	0.0097	0.206	0.015	3163	32	3076	34	2944	40	3793	252	y
RSA03-014	177	209	0.85	2.44	1.16	0.2447	0.0104	19.06	0.77	0.5649	0.0102	0.184	0.016	3151	39	3045	39	2887	42	3410	265	y
RSA03-016	245	213	1.15	9.26	1.89	0.2698	0.0099	14.91	0.53	0.4009	0.0068	0.169	0.013	3305	32	2810	34	2173	31	3158	222	
RSA03-017	435	588	0.74			0.2431	0.0144	20.17	1.14	0.6031	0.0143	0.199	0.027	3140	56	3100	55	3042	58	3673	452	
RSA03-018	21	108	0.20			0.2423	0.0064	20.89	0.53	0.6253	0.0088	0.239	0.013	3135	22	3133	25	3131	35	4335	214	
RSA03-020	112	132	0.84	3.22	1.51	0.2368	0.0117	15.86	0.76	0.4857	0.0106	0.168	0.018	3099	46	2868	46	2552	46	3132	303	y
RSA03-021	10	103	0.10	1.05	0.13	0.2404	0.0059	19.61	0.47	0.5916	0.0088	0.291	0.016	3122	19	3072	23	2996	35	5165	245	y
RSA03-022	175	249	0.71			0.2417	0.0049	20.32	0.41	0.6099	0.0082	0.094	0.004	3131	15	3107	20	3070	33	1807	65	y
RSA03-023	66	138	0.48	1.77	0.31	0.2428	0.0051	18.74	0.38	0.5599	0.0074	0.193	0.007	3138	16	3029	20	2866	30	3566	126	y
RSA03-024	80	137	0.58	3.99	0.5	0.2446	0.0056	17.15	0.38	0.5084	0.0070	0.208	0.009	3150	19	2943	22	2650	30	3816	148	y
RSA03-025	158	199	0.79	1.97	0.59	0.2430	0.0062	16.52	0.41	0.4930	0.0071	0.157	0.007	3140	21	2907	24	2584	31	2943	131	y
RSA03-026	56	134	0.42	2.2	0.3	0.2410	0.0051	18.45	0.39	0.5552	0.0074	0.210	0.008	3127	17	3013	20	2847	31	3845	139	y
RSA03-027	25	150	0.17	2.49	0.25	0.2474	0.0069	20.75	0.56	0.6084	0.0093	0.356	0.019	3168	24	3127	26	3064	37	6154	290	y
RSA03-029	18	126	0.15			0.2376	0.0060	20.36	0.50	0.6215	0.0090	0.207	0.011	3104	21	3109	24	3116	36	3799	181	
RSA03-032	28	218	0.13			0.2393	0.0066	20.42	0.54	0.6194	0.0094	0.439	0.023	3115	23	3111	26	3107	37	7353	329	
RSA03-034	28	114	0.25	1.86	0.25	0.2377	0.0062	19.16	0.49	0.5846	0.0085	0.251	0.013	3104	22	3050	24	2967	35	4520	206	y
RSA03-037	138	307	0.45			0.2501	0.0128	21.45	1.06	0.6238	0.0136	0.246	0.025	3185	50	3159	48	3125	54	4438	400	
RSA03-038	143	162	0.88	1.82	0.58	0.2427	0.0056	16.21	0.36	0.4846	0.0065	0.150	0.006	3137	19	2889	21	2547	28	2822	114	y
RSA03-042	73	267	0.27	0.57	0.19	0.2471	0.0062	20.05	0.50	0.5889	0.0090	0.184	0.009	3166	21	3094	24	2985	36	3406	148	y

				Ratios (corrected)								Ages (corrected; Ma)									
	Disc.	Correction type	^{204}Pb	^{207}Pb/^{206}Pb		^{207}Pb/^{235}U		^{206}Pb/^{238}U		^{208}Pb/^{232}Th		^{207}Pb/^{206}Pb		^{207}Pb/^{235}U		^{206}Pb/^{238}U		^{208}Pb/^{232}Th		Inc.?	
	%		cps	Ratio	1σ	Ratio	1σ	Ratio	1σ	Ratio	1σ	Age	1σ	Age	1σ	Age	1σ	Age	1σ	Int	W/A
RSA03-001	17.8	Disc	78	0.2298	0.0054	15.76	0.59	0.4975	0.0082	0.1339	0.0022	3051	36	2862	36	2603	35	2540	39	y	y
RSA03-003	24.46	Disc	257	0.2311	0.0073	14.62	0.70	0.4588	0.0083	0.1235	0.0021	3059	49	2791	45	2434	37	2353	38	y	y
RSA03-006	-1.6	None	63	0.2433	0.0052	21.40	0.76	0.6381	0.0114	0.2982	0.0228	3142	32	3157	35	3182	45	5274	355		
RSA03-007	4.01	Disc	28	0.2375	0.0044	19.43	0.62	0.5935	0.0095	0.1593	0.0027	3103	29	3063	31	3004	38	2987	47	y	y
RSA03-011	3.34	Disc	79	0.2345	0.0043	19.17	0.61	0.5928	0.0095	0.1593	0.0037	3083	29	3050	30	3001	38	2988	64	y	y
RSA03-012	12.15	Disc	112	0.2333	0.0110	17.27	1.20	0.5370	0.0135	0.1444	0.0034	3075	73	2950	66	2771	57	2725	60		
RSA03-013	7.86	Disc	113	0.2382	0.0059	18.75	0.74	0.5709	0.0099	0.1532	0.0025	3108	38	3029	38	2911	41	2880	43	y	y
RSA03-014	8.98	Disc	98	0.2300	0.0099	17.47	1.11	0.5511	0.0125	0.1484	0.0029	3052	67	2961	61	2830	52	2796	51		
RSA03-016	36.54	Disc	208	0.2120	0.0149	10.63	1.03	0.3638	0.0105	0.0987	0.0024	2921	112	2492	90	2000	49	1902	43		
RSA03-017	4.13	None	122	0.2431	0.0089	20.17	1.14	0.6031	0.0143	0.1993	0.0268	3140	56	3100	55	3042	58	3673	452		
RSA03-018	0.16	None	34	0.2423	0.0035	20.89	0.53	0.6253	0.0088	0.2392	0.0132	3135	22	3133	25	3131	35	4335	214		
RSA03-020	19.26	Disc	57	0.2169	0.0125	14.06	1.17	0.4701	0.0132	0.1272	0.0030	2958	91	2754	79	2484	58	2421	54		
RSA03-021	4.43	Disc	34	0.2341	0.0031	18.89	0.47	0.5854	0.0084	0.1573	0.0027	3080	21	3036	24	2971	34	2953	48	y	y
RSA03-022	2.5	None	90	0.2417	0.0024	20.32	0.41	0.6099	0.0082	0.0935	0.0035	3131	15	3107	20	3070	33	1807	65	y	
RSA03-023	9.72	Disc	56	0.2321	0.0033	17.60	0.45	0.5500	0.0076	0.1479	0.0020	3067	23	2968	25	2825	32	2788	35	y	y
RSA03-024	16.97	Disc	94	0.2200	0.0046	14.81	0.51	0.4882	0.0078	0.1320	0.0022	2981	34	2803	33	2563	34	2505	39		
RSA03-025	20.43	Disc	82	0.2311	0.0052	15.40	0.57	0.4833	0.0082	0.1300	0.0020	3059	36	2840	35	2541	36	2471	37	y	y
RSA03-026	9.72	Disc	72	0.2276	0.0034	17.04	0.46	0.5430	0.0078	0.1463	0.0021	3035	24	2937	26	2796	33	2760	38	y	y
RSA03-027	2.69	Disc	55	0.2324	0.0042	19.01	0.59	0.5932	0.0094	0.1595	0.0035	3069	29	3042	30	3003	38	2992	61	y	y
RSA03-029	-0.49	None	56	0.2376	0.0032	20.36	0.50	0.6215	0.0090	0.2068	0.0108	3104	21	3109	24	3116	36	3799	181		
RSA03-032	0.37	None	105	0.2393	0.0035	20.42	0.54	0.6194	0.0094	0.4387	0.0234	3115	23	3111	26	3107	37	7353	329		
RSA03-034	4.24	Disc	81	0.2264	0.0038	17.91	0.53	0.5737	0.0087	0.1547	0.0025	3026	27	2985	28	2923	36	2907	44	y	y
RSA03-037	2.65	None	117	0.2501	0.0079	21.45	1.06	0.6238	0.0136	0.2455	0.0247	3185	50	3159	48	3125	54	4438	400		
RSA03-038	21.78	Disc	101	0.2316	0.0049	15.19	0.53	0.4758	0.0076	0.1280	0.0019	3063	34	2827	33	2509	33	2434	34	y	y
RSA03-042	6.84	Disc	81	0.2436	0.0035	19.67	0.53	0.5855	0.0092	0.1568	0.0024	3144	23	3075	26	2971	37	2943	41	y	

						Ratios (uncorrected)								Ages (uncorrected; Ma)								
	Th	U	Th/U	Common Pb		$^{207}Pb/^{206}Pb$		$^{207}Pb/^{235}U$		$^{206}Pb/^{238}U$		$^{208}Pb/^{232}Th$		$^{207}Pb/^{206}Pb$		$^{207}Pb/^{235}U$		$^{206}Pb/^{238}U$		$^{208}Pb/^{232}Th$		Inc.?
	ppm	ppm		%	1σ	Ratio	1σ	Ratio	1σ	Ratio	1σ	Ratio	1σ	Age	1σ	Age	1σ	Age	1σ	Age	1σ	
RSA03-043	61	115	0.53	2.23	0.51	0.2440	0.0074	17.37	0.50	0.5164	0.0085	0.184	0.011	3146	25	2956	28	2684	36	3407	179	y
RSA03-045	77	148	0.52	1.56	0.44	0.2404	0.0065	17.94	0.47	0.5412	0.0083	0.179	0.010	3122	22	2986	25	2788	35	3326	165	y
RSA03-046	26	112	0.24			0.2387	0.0046	20.11	0.38	0.6115	0.0077	0.180	0.007	3111	15	3097	18	3076	31	3341	111	
RSA03-047	312	388	0.81	2.91	0.89	0.2631	0.0094	19.16	0.66	0.5282	0.0093	0.179	0.012	3266	32	3050	33	2734	39	3328	208	
RSA03-048	114	152	0.75	5.14	0.5	0.2557	0.0046	19.04	0.34	0.5402	0.0067	0.219	0.007	3220	13	3044	17	2784	28	4002	116	
RSA03-051	33	235	0.14	0.96	0.25	0.2553	0.0126	21.29	1.00	0.6062	0.0133	0.250	0.024	3218	43	3152	45	3055	53	4518	385	y
RSA03-052	22	207	0.11	1.01	0.11	0.2464	0.0057	20.78	0.48	0.6116	0.0087	0.290	0.013	3162	18	3128	22	3076	35	5146	209	y
RSA03-053	186	261	0.71			0.2382	0.0080	18.42	0.60	0.5608	0.0092	0.159	0.010	3108	29	3012	31	2870	38	2985	178	y
RSA03-054	27	204	0.13			0.2421	0.0081	21.00	0.68	0.6286	0.0107	0.386	0.026	3134	28	3138	31	3144	42	6605	374	
RSA03-055	294	312	0.94			0.2332	0.0044	15.99	0.30	0.4973	0.0062	0.142	0.005	3074	14	2876	18	2602	27	2681	86	
RSA03-056	72	133	0.55			0.2375	0.0055	18.12	0.40	0.5535	0.0074	0.144	0.007	3103	18	2996	21	2840	31	2728	115	y
RSA03-058	16	105	0.15	1.73	0.17	0.2420	0.0058	20.33	0.47	0.6093	0.0084	0.314	0.015	3133	19	3107	22	3067	33	5519	230	y
RSA03-060	246	255	0.96	2.01	0.43	0.2438	0.0039	19.31	0.32	0.5745	0.0070	0.178	0.005	3145	12	3058	16	2926	29	3305	82	y
RSA03-061	189	333	0.57			0.2412	0.0071	20.17	0.58	0.6065	0.0099	0.173	0.010	3128	24	3100	28	3056	40	3229	168	y
RSA03-062	131	282	0.46			0.2458	0.0092	20.94	0.76	0.6174	0.0116	0.199	0.014	3158	32	3136	35	3100	46	3660	243	
RSA03-064	60	169	0.36	3.32	0.23	0.2561	0.0042	20.40	0.33	0.5778	0.0070	0.268	0.007	3223	11	3111	16	2940	28	4795	118	
RSA03-067	36	111	0.32	1.8	0.2	0.2519	0.0046	19.80	0.36	0.5700	0.0072	0.219	0.007	3197	13	3082	17	2908	29	4010	119	
RSA03-068	190	204	0.93	3.31	0.49	0.2428	0.0042	18.14	0.31	0.5421	0.0065	0.184	0.005	3138	12	2997	16	2792	27	3406	93	y
RSA03-071	25	199	0.12			0.2417	0.0058	20.98	0.49	0.6297	0.0092	0.365	0.017	3131	19	3137	23	3148	37	6295	248	
RSA03-072	94	144	0.65	4.18	0.64	0.2504	0.0068	19.25	0.50	0.5578	0.0079	0.222	0.012	3187	23	3055	25	2858	33	4053	195	y
RSA03-073	134	264	0.51	2.55	0.32	0.2438	0.0049	20.03	0.40	0.5960	0.0079	0.222	0.008	3145	15	3093	19	3014	32	4053	133	y
RSA03-074	20	103	0.19	2.09	0.26	0.2482	0.0073	20.31	0.58	0.5936	0.0089	0.298	0.018	3173	25	3106	27	3004	36	5267	281	y
RSA03-075	47	127	0.37	1.39	0.48	0.2540	0.0110	19.53	0.81	0.5577	0.0112	0.193	0.016	3210	39	3068	40	2857	46	3571	274	y
RSA03-076	63	126	0.50			0.2383	0.0063	17.78	0.45	0.5413	0.0078	0.145	0.007	3109	22	2978	25	2789	33	2740	132	y
RSA03-077	245	304	0.80	2.73	0.81	0.2420	0.0083	20.19	0.67	0.6052	0.0100	0.204	0.013	3133	30	3101	32	3051	40	3745	219	y

				Ratios (corrected)								Ages (corrected; Ma)									
	Disc.	Correction	^{204}Pb	^{207}Pb/^{206}Pb		^{207}Pb/^{235}U		^{206}Pb/^{238}U		^{208}Pb/^{232}Th		^{207}Pb/^{206}Pb		^{207}Pb/^{235}U		^{206}Pb/^{238}U		^{208}Pb/^{232}Th		Inc.?	
	%	type	cps	Ratio	1σ	Ratio	1σ	Ratio	1σ	Ratio	1σ	Age	1σ	Age	1σ	Age	1σ	Age	1σ	Int	W/A
RSA03-043	16.75	Disc	80	0.2305	0.0053	16.04	0.62	0.5048	0.0092	0.1359	0.0024	3056	37	2879	37	2635	40	2575	42	y	y
RSA03-045	12.25	Disc	71	0.2309	0.0046	16.96	0.58	0.5327	0.0090	0.1434	0.0023	3058	32	2933	33	2753	38	2708	40	y	y
RSA03-046	1.47	None	24	0.2387	0.0022	20.11	0.38	0.6115	0.0077	0.1798	0.0065	3111	15	3097	18	3076	31	3341	111		
RSA03-047	18.88	Disc	283	0.2459	0.0082	17.39	0.91	0.5129	0.0111	0.1372	0.0027	3158	51	2956	50	2669	47	2599	48		
RSA03-048	13.93	Disc	119	0.2242	0.0042	15.84	0.49	0.5124	0.0075	0.1383	0.0021	3011	29	2867	30	2667	32	2617	37	y	y
RSA03-051	5.83	Disc	46	0.2491	0.0076	20.62	1.01	0.6003	0.0133	0.1604	0.0034	3179	46	3121	47	3031	54	3007	59		
RSA03-052	2.85	Disc	42	0.2404	0.0031	20.06	0.49	0.6054	0.0086	0.1623	0.0027	3122	20	3094	23	3052	35	3040	48	y	y
RSA03-053	9.48	None	68	0.2382	0.0046	18.42	0.60	0.5608	0.0092	0.1592	0.0102	3108	29	3012	31	2870	38	2985	178	y	y
RSA03-054	-0.49	None	63	0.2421	0.0045	21.00	0.68	0.6286	0.0107	0.3865	0.0257	3134	28	3138	31	3144	42	6605	374		
RSA03-055	18.62	None	62	0.2332	0.0022	15.99	0.30	0.4973	0.0062	0.1418	0.0049	3074	14	2876	18	2602	27	2681	86	y	y
RSA03-056	10.52	None	39	0.2375	0.0028	18.12	0.40	0.5535	0.0074	0.1445	0.0065	3103	18	2996	21	2840	31	2728	115	y	y
RSA03-058	1.55	Disc	38	0.2316	0.0033	19.12	0.49	0.5988	0.0084	0.1611	0.0029	3063	22	3048	25	3025	34	3019	50	y	y
RSA03-060	7.46	Disc	119	0.2316	0.0034	17.98	0.47	0.5630	0.0081	0.1514	0.0021	3063	22	2989	25	2879	33	2850	36	y	y
RSA03-061	2.88	None	77	0.2412	0.0038	20.17	0.58	0.6065	0.0099	0.1732	0.0098	3128	24	3100	28	3056	40	3229	168	y	y
RSA03-062	2.28	None	54	0.2458	0.0052	20.94	0.76	0.6174	0.0116	0.1985	0.0144	3158	32	3136	35	3100	46	3660	243		
RSA03-064	9.32	Disc	113	0.2362	0.0026	18.19	0.38	0.5586	0.0072	0.1500	0.0024	3094	17	3000	20	2861	30	2825	42	y	y
RSA03-067	10.38	Disc	60	0.2412	0.0027	18.62	0.40	0.5598	0.0074	0.1500	0.0021	3128	17	3022	20	2866	30	2825	36	y	
RSA03-068	11.5	Disc	76	0.2224	0.0039	16.07	0.47	0.5241	0.0076	0.1415	0.0019	2998	27	2881	28	2717	32	2675	34		
RSA03-071	-0.67	None	40	0.2417	0.0030	20.98	0.49	0.6297	0.0092	0.3654	0.0168	3131	19	3137	23	3148	37	6295	248		
RSA03-072	10.39	Disc	83	0.2248	0.0063	16.57	0.71	0.5345	0.0091	0.1442	0.0024	3016	44	2910	41	2760	38	2722	42	y	y
RSA03-073	3.59	Disc	119	0.2282	0.0036	18.28	0.51	0.5808	0.0086	0.1565	0.0023	3040	25	3004	27	2952	35	2938	40	y	y
RSA03-074	5.52	Disc	59	0.2356	0.0049	18.88	0.64	0.5811	0.0092	0.1561	0.0029	3090	32	3036	33	2953	37	2931	51	y	y
RSA03-075	12.99	Disc	38	0.2458	0.0079	18.64	0.94	0.5499	0.0118	0.1471	0.0029	3158	50	3023	49	2825	49	2774	51		
RSA03-076	12.67	None	47	0.2383	0.0034	17.78	0.45	0.5413	0.0078	0.1452	0.0075	3109	22	2978	25	2789	33	2740	132	y	y
RSA03-077	1.45	Disc	123	0.2253	0.0079	18.29	0.96	0.5887	0.0118	0.1588	0.0028	3019	55	3005	51	2984	48	2978	49		

						Ratios (uncorrected)								Ages (uncorrected; Ma)								
	Th	U	Th/U	Common Pb		$^{207}Pb/^{206}Pb$		$^{207}Pb/^{235}U$		$^{206}Pb/^{238}U$		$^{208}Pb/^{232}Th$		$^{207}Pb/^{206}Pb$		$^{207}Pb/^{235}U$		$^{206}Pb/^{238}U$		$^{208}Pb/^{232}Th$		Inc.?
	ppm	ppm		%	1σ	Ratio	1σ	Ratio	1σ	Ratio	1σ	Ratio	1σ	Age	1σ	Age	1σ	Age	1σ	Age	1σ	
RSA03-078	437	384	1.14	3.85	1.63	0.2265	0.0096	13.29	0.54	0.4255	0.0080	0.143	0.013	3027	39	2700	39	2285	36	2700	228	
RSA03-079	313	329	0.95	2.28	0.54	0.2436	0.0050	17.24	0.35	0.5132	0.0066	0.162	0.006	3144	16	2948	20	2670	28	3033	104	y
RSA01-002	986	2169	0.45			0.2213	0.0173	4.87	0.37	0.1597	0.0048	0.127	0.029	2990	78	1797	63	955	27	2424	513	
RSA01-005	168	590	0.28	7.31	2.15	0.2439	0.0172	10.44	0.71	0.3105	0.0086	0.248	0.050	3145	69	2475	63	1743	42	4481	811	
RSA01-008	124	373	0.33			0.2470	0.0224	14.92	1.32	0.4381	0.0147	0.222	0.059	3166	92	2810	84	2342	66	4053	972	
RSA01-009	183	371	0.49			0.2430	0.0209	14.44	1.20	0.4310	0.0137	0.193	0.048	3140	86	2779	79	2310	62	3561	816	
RSA01-010c	217	551	0.39	6	0.47	0.2455	0.0042	14.37	0.25	0.4248	0.0056	0.249	0.010	3156	13	2775	17	2282	25	4492	164	
RSA01-011	98	281	0.35			0.2357	0.0054	19.29	0.44	0.5937	0.0088	0.133	0.008	3091	18	3057	22	3004	36	2527	136	y
RSA01-012	213	421	0.51	8.66	0.44	0.2464	0.0032	13.63	0.18	0.4013	0.0045	0.249	0.006	3162	9	2724	12	2175	21	4495	105	
RSA01-013	401	419	0.96	5.47	0.71	0.2384	0.0038	13.64	0.22	0.4151	0.0051	0.158	0.006	3109	11	2725	15	2238	23	2971	105	y
RSA01-015	168	553	0.30	6.51	0.32	0.2569	0.0034	13.44	0.18	0.3794	0.0042	0.272	0.007	3228	9	2711	12	2074	20	4868	119	
RSA01-016r	276	1125	0.25	18.11	0.67	0.2604	0.0034	7.46	0.10	0.2078	0.0023	0.380	0.010	3249	9	2168	12	1217	12	6516	154	
RSA01-017	131	316	0.42	1.86	0.43	0.2459	0.0060	18.90	0.46	0.5576	0.0084	0.201	0.012	3158	19	3037	23	2857	35	3707	203	
RSA01-018	143	375	0.38			0.2357	0.0069	18.09	0.52	0.5569	0.0090	0.134	0.010	3091	24	2995	28	2854	37	2542	179	y
RSA01-020	248	275	0.90			0.2315	0.0055	19.40	0.46	0.6080	0.0090	0.150	0.009	3063	19	3062	23	3062	36	2816	162	y
RSA01-022	379	297	1.28			0.2381	0.0048	20.01	0.41	0.6095	0.0083	0.165	0.009	3108	16	3092	20	3068	33	3084	149	y
RSA01-027	119	298	0.40	3.51	0.35	0.2359	0.0038	11.58	0.19	0.3559	0.0045	0.161	0.006	3092	12	2571	15	1963	21	3014	109	y
RSA01-028	88	316	0.28	19.29	1.62	0.3614	0.0097	27.58	0.71	0.5538	0.0077	0.948	0.067	3756	21	3404	25	2841	32	13479	690	
RSA01-033	92	413	0.22	1.16	0.26	0.2325	0.0057	14.96	0.36	0.4669	0.0071	0.178	0.012	3069	19	2813	23	2470	31	3304	199	y
RSA01-034	126	643	0.20	3.35	0.27	0.2318	0.0041	13.18	0.24	0.4125	0.0055	0.261	0.012	3065	13	2693	17	2226	25	4690	191	
RSA01-036c	436	627	0.69	11.36	0.7	0.2657	0.0039	12.62	0.18	0.3444	0.0038	0.206	0.007	3281	10	2651	13	1908	18	3783	112	
RSA01-037	391	497	0.79	3.28	0.44	0.2376	0.0033	15.80	0.22	0.4826	0.0055	0.170	0.005	3104	10	2865	13	2538	24	3172	89	y
RSA01-040	354	618	0.57			0.2188	0.0034	13.82	0.21	0.4580	0.0054	0.123	0.005	2972	11	2737	15	2431	24	2339	83	
RSA01-042	377	676	0.56	21.32	1.56	0.3085	0.0060	18.20	0.35	0.4278	0.0055	0.406	0.021	3514	14	3001	18	2296	25	6885	304	
RSA01-043	292	450	0.65	3.6	0.44	0.2390	0.0033	17.64	0.24	0.5354	0.0058	0.196	0.006	3113	9	2971	13	2764	24	3625	104	y

				Ratios (corrected)								Ages (corrected; Ma)									
	Disc.	Correction type	^{204}Pb	^{207}Pb/^{206}Pb		^{207}Pb/^{235}U		^{206}Pb/^{238}U		^{208}Pb/^{232}Th		^{207}Pb/^{206}Pb		^{207}Pb/^{235}U		^{206}Pb/^{238}U		^{208}Pb/^{232}Th		Inc.?	
	%		cps	Ratio	1σ	Ratio	1σ	Ratio	1σ	Ratio	1σ	Age	1σ	Age	1σ	Age	1σ	Age	1σ	Int	W/A
RSA03-078	26.18	Disc	157	0.2020	0.0133	11.40	1.04	0.4091	0.0113	0.1115	0.0025	2843	106	2556	85	2211	52	2136	45		
RSA03-079	17.11	Disc	143	0.2297	0.0048	15.88	0.54	0.5015	0.0078	0.1350	0.0019	3050	32	2870	32	2620	33	2560	34	y	y
RSA01-002	72.94	None	3828	0.2213	0.0111	4.87	0.37	0.1597	0.0048	0.1274	0.0286	2990	78	1797	63	955	27	2424	513		
RSA01-005	47.16	Disc	2352	0.1972	0.0195	7.82	1.04	0.2878	0.0108	0.0786	0.0032	2803	159	2211	120	1630	54	1529	59		
RSA01-008	30.89	None	1760	0.2470	0.0148	14.92	1.32	0.4381	0.0147	0.2221	0.0588	3166	92	2810	84	2342	66	4053	972		
RSA01-009	31.33	None	1630	0.2430	0.0137	14.44	1.20	0.4310	0.0137	0.1926	0.0481	3140	86	2779	79	2310	62	3561	816		
RSA01-010c	29.35	Disc	2167	0.2077	0.0040	11.43	0.35	0.3993	0.0060	0.1085	0.0023	2888	30	2559	29	2166	28	2082	42	y	
RSA01-011	3.54	None	1542	0.2357	0.0027	19.29	0.44	0.5937	0.0088	0.1332	0.0077	3091	18	3057	22	3004	36	2527	136	y	
RSA01-012	30.99	Disc	1639	0.1904	0.0038	9.62	0.29	0.3665	0.0049	0.1004	0.0022	2746	31	2399	27	2013	23	1934	40		
RSA01-013	29.65	Disc	1433	0.2038	0.0053	11.03	0.43	0.3923	0.0062	0.1068	0.0016	2857	41	2525	36	2134	29	2051	29	y	
RSA01-015	39.01	Disc	1949	0.2166	0.0029	10.59	0.23	0.3548	0.0044	0.0960	0.0025	2956	21	2488	20	1957	21	1853	46	y	y
RSA01-016r	56.78	Disc	2761	0.1332	0.0068	3.12	0.19	0.1701	0.0025	0.0483	0.0038	2140	87	1439	48	1013	14	953	73		
RSA01-017	10.82	Disc	1454	0.2347	0.0043	17.70	0.54	0.5472	0.0085	0.1470	0.0022	3084	28	2974	29	2813	36	2772	39	y	
RSA01-018	9.51	None	1333	0.2357	0.0037	18.09	0.52	0.5569	0.0090	0.1340	0.0100	3091	24	2995	28	2854	37	2542	179	y	
RSA01-020	0.06	None	1095	0.2315	0.0028	19.40	0.46	0.6080	0.0090	0.1495	0.0092	3063	19	3062	23	3062	36	2816	162	y	
RSA01-022	1.62	None	1320	0.2381	0.0024	20.01	0.41	0.6095	0.0083	0.1648	0.0086	3108	16	3092	20	3068	33	3084	149	y	
RSA01-027	40.48	Disc	1299	0.2141	0.0030	10.14	0.24	0.3435	0.0045	0.0931	0.0014	2937	22	2447	22	1903	22	1799	26	y	y
RSA01-028	29.66	Disc	3188	0.2479	0.0141	15.28	1.23	0.4470	0.0113	0.1195	0.0115	3171	88	2833	77	2382	50	2281	207		
RSA01-033	22.73	Disc	1113	0.2253	0.0034	14.34	0.39	0.4615	0.0069	0.1245	0.0019	3019	24	2772	26	2446	30	2371	34	y	y
RSA01-034	30.19	Disc	1365	0.2108	0.0028	11.59	0.27	0.3986	0.0053	0.1082	0.0024	2912	21	2572	22	2163	25	2076	43	y	
RSA01-036c	43.01	Disc	2000	0.1927	0.0058	8.11	0.34	0.3053	0.0044	0.0836	0.0018	2765	48	2243	38	1717	22	1622	33		
RSA01-037	19.92	Disc	1342	0.2173	0.0033	13.98	0.35	0.4667	0.0060	0.1263	0.0016	2960	23	2748	24	2469	26	2404	29	y	y
RSA01-040	21.8	None	92	0.2188	0.0015	13.82	0.21	0.4580	0.0054	0.1227	0.0046	2972	11	2737	15	2431	24	2339	83	y	y
RSA01-042	29.49	Disc	1786	0.1658	0.0144	7.70	0.84	0.3366	0.0083	0.0935	0.0040	2516	143	2196	99	1870	40	1806	73		
RSA01-043	11.3	Disc	226	0.2167	0.0033	15.43	0.38	0.5162	0.0065	0.1397	0.0018	2957	23	2842	24	2683	28	2643	32	y	y

						Ratios (uncorrected)								Ages (uncorrected; Ma)								
	Th	U	Th/U	Common Pb		$^{207}Pb/^{206}Pb$		$^{207}Pb/^{235}U$		$^{206}Pb/^{238}U$		$^{208}Pb/^{232}Th$		$^{207}Pb/^{206}Pb$		$^{207}Pb/^{235}U$		$^{206}Pb/^{238}U$		$^{208}Pb/^{232}Th$		Inc.?
	ppm	ppm		%	1σ	Ratio	1σ	Ratio	1σ	Ratio	1σ	Ratio	1σ	Age	1σ	Age	1σ	Age	1σ	Age	1σ	
RSA01-044	294	293	1.00			0.2365	0.0051	19.25	0.40	0.5904	0.0080	0.179	0.010	3097	16	3054	20	2991	33	3322	174	
RSA01-046	408	370	1.10			0.2389	0.0060	18.46	0.45	0.5606	0.0082	0.159	0.011	3112	20	3014	23	2869	34	2980	187	y
RSA01-047c	34	192	0.18	18.46	1.72	0.2923	0.0089	8.55	0.25	0.2122	0.0037	0.472	0.038	3430	23	2292	26	1241	20	7820	524	
RSA01-047r	200	858	0.23	1.1	0.33	0.2165	0.0058	15.86	0.41	0.5314	0.0080	0.191	0.014	2955	22	2868	25	2747	34	3531	243	
RSA01-049	208	792	0.26	6.89	0.43	0.2350	0.0036	11.22	0.17	0.3463	0.0039	0.262	0.010	3087	11	2542	14	1917	19	4701	159	y
RSA01-052	354	601	0.59	41.05	2.03	0.4062	0.0064	21.44	0.33	0.3829	0.0043	0.576	0.023	3932	10	3159	15	2090	20	9189	296	
RSA01-053	503	634	0.79	2.71	0.67	0.2241	0.0039	11.24	0.19	0.3639	0.0043	0.120	0.005	3010	12	2544	16	2001	20	2291	97	
RSA01-054	84	258	0.33	3.26	0.41	0.2408	0.0048	15.33	0.28	0.4623	0.0052	0.211	0.011	3125	15	2836	18	2449	23	3871	179	y
RSA01-060	123	333	0.37	14.2	0.59	0.2773	0.0034	13.79	0.17	0.3608	0.0038	0.355	0.009	3348	8	2736	12	1986	18	6146	136	
RSA01-062	366	469	0.78	2.35	0.53	0.2410	0.0036	19.15	0.29	0.5763	0.0067	0.186	0.007	3127	10	3049	15	2934	27	3442	116	y
RSA01-067	167	923	0.18	26.61	1.28	0.3617	0.0058	14.97	0.24	0.3003	0.0036	0.924	0.037	3757	11	2813	15	1693	18	13231	387	
RSA01-072	273	455	0.60	12.12	0.81	0.2541	0.0038	12.42	0.18	0.3547	0.0041	0.226	0.008	3211	10	2637	14	1957	19	4121	133	
RSA01-073	244	347	0.70	8.57	1	0.2414	0.0047	12.12	0.23	0.3641	0.0048	0.178	0.009	3129	14	2614	18	2002	22	3311	155	y
RSA01-076r	332	659	0.50	16.43	1.15	0.3152	0.0055	15.28	0.26	0.3516	0.0043	0.304	0.014	3547	12	2833	16	1942	20	5361	215	
RSA01-082	191	383	0.50	2.14	0.45	0.2427	0.0043	18.39	0.33	0.5496	0.0068	0.191	0.009	3138	13	3010	17	2824	28	3530	150	
RSA01-083	200	353	0.57	2.55	0.93	0.2409	0.0081	16.09	0.52	0.4858	0.0084	0.170	0.014	3126	28	2882	31	2552	36	3179	248	y
RSA01-084	246	242	1.02	6.43	0.97	0.2398	0.0040	15.98	0.26	0.4834	0.0053	0.183	0.008	3119	12	2875	15	2542	23	3398	134	y
RSA01-087	97	1190	0.08	3.35	0.19	0.1917	0.0030	6.09	0.09	0.2306	0.0026	0.249	0.009	2756	11	1989	13	1337	14	4490	153	
RSA01-089	239	616	0.39	10.27	0.54	0.2730	0.0037	16.86	0.23	0.4482	0.0051	0.344	0.010	3323	9	2927	13	2387	23	5973	155	
RSA01-091	348	499	0.70	2.87	0.93	0.2574	0.0072	14.76	0.40	0.4164	0.0067	0.142	0.010	3231	22	2800	26	2244	30	2691	177	
RSA01-093	492	544	0.90			0.2296	0.0067	12.55	0.36	0.3967	0.0065	0.123	0.009	3049	23	2646	27	2154	30	2343	156	
RSA01-095	150	465	0.32	4.2	0.44	0.2374	0.0045	13.26	0.24	0.4054	0.0048	0.210	0.010	3103	14	2698	17	2194	22	3851	173	y
RSA01-096	196	222	0.88	8.29	1.61	0.2638	0.0074	20.90	0.56	0.5748	0.0087	0.250	0.019	3269	23	3134	26	2927	36	4503	303	
RSA01-097	114	176	0.65	2.34	0.99	0.2355	0.0088	13.16	0.47	0.4051	0.0079	0.136	0.011	3090	31	2691	33	2192	36	2574	203	y
RSA01-100	58	504	0.12	2.93	0.27	0.2361	0.0050	16.40	0.34	0.5041	0.0067	0.386	0.022	3094	17	2900	20	2631	29	6599	322	y

				Ratios (corrected)								Ages (corrected; Ma)									
	Disc.	Correction type	^{204}Pb	^{207}Pb/^{206}Pb		^{207}Pb/^{235}U		^{206}Pb/^{238}U		^{208}Pb/^{232}Th		^{207}Pb/^{206}Pb		^{207}Pb/^{235}U		^{206}Pb/^{238}U		^{208}Pb/^{232}Th		Inc.?	
	%		cps	Ratio	1σ	Ratio	1σ	Ratio	1σ	Ratio	1σ	Age	1σ	Age	1σ	Age	1σ	Age	1σ	Int	W/A
RSA01-044	4.29	None	15	0.2365	0.0025	19.25	0.40	0.5904	0.0080	0.1786	0.0101	3097	16	3054	20	2991	33	3322	174		
RSA01-046	9.67	None	111	0.2389	0.0031	18.46	0.45	0.5606	0.0082	0.1589	0.0107	3112	20	3014	23	2869	34	2980	187	y	
RSA01-047c	64.35	Disc	260	0.1693	0.0158	4.04	0.48	0.1730	0.0051	0.0480	0.0051	2550	152	1642	97	1029	28	947	99		
RSA01-047r	7.57	Disc	275	0.2095	0.0038	15.18	0.46	0.5255	0.0081	0.1427	0.0022	2902	28	2827	29	2722	34	2696	38		
RSA01-049	39.32	Disc	461	0.1906	0.0037	8.47	0.24	0.3224	0.0042	0.0883	0.0024	2747	30	2283	26	1801	20	1711	44		
RSA01-052	27.6	Disc	2987	0.1070	0.0276	3.33	0.98	0.2257	0.0087	0.0655	0.0054	1749	508	1488	230	1312	46	1282	103		
RSA01-053	37.21	Disc	313	0.2071	0.0048	10.11	0.36	0.3541	0.0052	0.0963	0.0013	2883	36	2445	33	1954	25	1857	24	y	
RSA01-054	24.06	Disc	84	0.2206	0.0036	13.60	0.36	0.4472	0.0056	0.1209	0.0018	2985	25	2722	25	2383	25	2306	33	y	y
RSA01-060	40.41	Disc	509	0.1848	0.0053	7.89	0.31	0.3096	0.0043	0.0851	0.0034	2697	46	2218	36	1739	21	1650	64		
RSA01-062	6.17	Disc	249	0.2267	0.0038	17.59	0.48	0.5627	0.0078	0.1517	0.0020	3029	25	2967	26	2878	32	2854	35	y	
RSA01-067	58.38	Disc	2713	0.1897	0.0131	5.76	0.52	0.2204	0.0051	0.0604	0.0106	2739	109	1941	78	1284	27	1186	203		
RSA01-072	37.1	Disc	331	0.1738	0.0067	7.47	0.39	0.3117	0.0051	0.0862	0.0020	2595	61	2169	47	1749	25	1670	37		
RSA01-073	36.13	Disc	187	0.1857	0.0077	8.52	0.49	0.3329	0.0062	0.0914	0.0017	2705	66	2289	52	1852	30	1768	32		
RSA01-076r	48.88	Disc	1300	0.2128	0.0096	8.62	0.54	0.2938	0.0059	0.0797	0.0031	2927	70	2299	57	1661	30	1549	58		
RSA01-082	11.08	Disc	263	0.2296	0.0036	17.03	0.45	0.5379	0.0074	0.1448	0.0019	3050	24	2937	25	2774	31	2733	34	y	
RSA01-083	20.6	Disc	208	0.2247	0.0076	14.66	0.76	0.4734	0.0098	0.1277	0.0024	3014	52	2794	49	2498	43	2429	43		
RSA01-084	17.44	Disc	128	0.1988	0.0071	12.40	0.62	0.4523	0.0075	0.1234	0.0018	2816	55	2635	47	2405	33	2352	33		
RSA01-087	54.09	Disc	285	0.1693	0.0020	5.20	0.10	0.2228	0.0026	0.0618	0.0024	2550	18	1853	17	1297	13	1211	45		
RSA01-089	29.01	Disc	1023	0.2085	0.0044	11.56	0.37	0.4022	0.0056	0.1093	0.0033	2894	33	2570	30	2179	26	2096	59		
RSA01-091	35.05	Disc	692	0.2400	0.0071	13.38	0.63	0.4044	0.0080	0.1084	0.0020	3120	45	2707	44	2189	37	2081	36		
RSA01-093	34.44	None	402	0.2296	0.0035	12.55	0.36	0.3967	0.0065	0.1229	0.0087	3049	23	2646	27	2154	30	2343	156		
RSA01-095	32.02	Disc	398	0.2110	0.0039	11.30	0.33	0.3884	0.0052	0.1054	0.0018	2914	29	2548	27	2115	24	2025	33	y	y
RSA01-096	8.03	Disc	219	0.2120	0.0123	15.41	1.24	0.5271	0.0132	0.1430	0.0032	2921	93	2841	77	2729	56	2701	56		
RSA01-097	32.95	Disc	1	0.2212	0.0083	12.07	0.69	0.3956	0.0092	0.1069	0.0022	2989	59	2610	54	2149	43	2052	41		
RSA01-100	16.18	Disc	217	0.2178	0.0032	14.69	0.38	0.4893	0.0068	0.1324	0.0036	2964	23	2796	24	2568	29	2513	65	y	y

						Ratios (uncorrected)								Ages (uncorrected; Ma)								
	Th	U	Th/U	Common Pb		$^{207}Pb/^{206}Pb$		$^{207}Pb/^{235}U$		$^{206}Pb/^{238}U$		$^{208}Pb/^{232}Th$		$^{207}Pb/^{206}Pb$		$^{207}Pb/^{235}U$		$^{206}Pb/^{238}U$		$^{208}Pb/^{232}Th$		Inc.?
	ppm	ppm		%	1σ	Ratio	1σ	Ratio	1σ	Ratio	1σ	Ratio	1σ	Age	1σ	Age	1σ	Age	1σ	Age	1σ	
RSA01-101c	134	127	1.05			0.2351	0.0055	18.81	0.43	0.5809	0.0084	0.172	0.010	3087	18	3032	22	2952	34	3214	177	y
RSA01-102	271	762	0.36	2.1	0.32	0.2347	0.0040	15.52	0.26	0.4800	0.0057	0.183	0.008	3085	13	2848	16	2527	25	3396	135	y
RSA01-103	499	717	0.70	12.2	1.07	0.2854	0.0052	18.23	0.33	0.4635	0.0060	0.273	0.013	3393	13	3002	18	2455	26	4873	199	
RSA01-107	311	523	0.59	8.64	0.64	0.2572	0.0038	14.72	0.22	0.4152	0.0049	0.224	0.008	3229	10	2797	14	2239	22	4082	128	
RSA01-111	249	492	0.51	3.14	0.47	0.2445	0.0043	17.37	0.30	0.5155	0.0060	0.199	0.009	3149	13	2956	16	2680	25	3660	150	
RSA01-113	320	406	0.79	2.19	0.56	0.2207	0.0036	14.38	0.23	0.4728	0.0057	0.152	0.006	2986	12	2775	15	2496	25	2859	106	
RSA01-115	142	233	0.61	1.16	0.48	0.2372	0.0046	17.91	0.34	0.5479	0.0072	0.167	0.008	3101	14	2985	18	2816	30	3115	138	y
SWa18a-001r	299	1205	0.25	2.43	0.39	0.2283	0.0055	11.76	0.29	0.3736	0.0056	0.166	0.010	3040	20	2585	23	2046	26	3096	182	
SWa18a-003	412	1032	0.40	1.37	0.15	0.2160	0.0030	9.31	0.13	0.3126	0.0038	0.116	0.003	2951	10	2369	13	1753	19	2210	57	
SWa18a-004	223	270	0.83	3.11	0.47	0.2401	0.0033	19.13	0.27	0.5779	0.0067	0.192	0.005	3120	10	3048	14	2940	27	3555	88	y
SWa18a-007	470	471	1.00			0.2362	0.0058	19.72	0.49	0.6059	0.0096	0.176	0.011	3094	19	3078	24	3053	38	3269	185	y
SWa18a-011c	79	202	0.39	1.91	0.21	0.2393	0.0034	19.24	0.27	0.5833	0.0066	0.218	0.006	3115	10	3054	14	2962	27	3985	105	y
SWa18a-012	392	542	0.72			0.2429	0.0041	14.21	0.24	0.4245	0.0053	0.081	0.003	3139	12	2764	16	2281	24	1565	56	y
SWa18a-013c	2176	4331	0.50	7.97	0.73	0.1320	0.0028	0.90	0.02	0.0496	0.0006	0.030	0.001	2124	18	653	10	312	4	603	29	
SWa18a-014	431	1007	0.43	2.18	0.28	0.1900	0.0026	4.80	0.07	0.1834	0.0021	0.065	0.002	2742	10	1786	12	1085	11	1274	33	
SWa18a-015	754	658	1.15	5.85	1.1	0.2525	0.0051	16.81	0.34	0.4828	0.0065	0.175	0.009	3201	16	2924	20	2539	28	3268	147	
SWa18a-016	495	463	1.07	3.37	0.9	0.2385	0.0048	18.34	0.37	0.5577	0.0073	0.182	0.009	3110	16	3008	19	2857	30	3387	146	y
SWa18a-017c	146	878	0.17			0.3060	0.0065	20.76	0.42	0.4923	0.0058	0.129	0.007	3501	16	3127	19	2581	25	2460	119	
SWa18a-017r	198	1004	0.20	0.37	0.11	0.2376	0.0037	9.58	0.15	0.2924	0.0035	0.089	0.003	3104	11	2395	14	1654	17	1730	58	
SWa18a-018	905	2017	0.45	4.6	0.38	0.2140	0.0034	5.30	0.09	0.1795	0.0022	0.092	0.003	2936	12	1869	14	1064	12	1776	64	
SWa18a-019	593	1335	0.44	6.61	0.58	0.2717	0.0049	9.74	0.18	0.2601	0.0034	0.144	0.006	3316	14	2411	17	1490	17	2712	109	
SWa18a-020	900	2145	0.42	9.93	0.71	0.1987	0.0051	3.01	0.07	0.1099	0.0018	0.074	0.003	2816	18	1410	18	672	10	1439	54	
SWa18a-021	513	530	0.97	3.5	0.88	0.2351	0.0048	17.94	0.37	0.5536	0.0076	0.187	0.009	3087	16	2987	20	2840	31	3465	160	y
SWa18a-022	468	2374	0.20	2.12	0.19	0.1872	0.0031	3.78	0.06	0.1465	0.0018	0.075	0.003	2718	13	1589	13	881	10	1462	56	
SWa18a-023	499	1345	0.37	2.04	0.23	0.2058	0.0032	7.19	0.11	0.2533	0.0030	0.105	0.004	2873	12	2135	14	1455	15	2014	69	

				Ratios (corrected)								Ages (corrected; Ma)									
	Disc.	Correction type	^{204}Pb	^{207}Pb/^{206}Pb		^{207}Pb/^{235}U		^{206}Pb/^{238}U		^{208}Pb/^{232}Th		^{207}Pb/^{206}Pb		^{207}Pb/^{235}U		^{206}Pb/^{238}U		^{208}Pb/^{232}Th		Inc.?	
	%		cps	Ratio	1σ	Ratio	1σ	Ratio	1σ	Ratio	1σ	Age	1σ	Age	1σ	Age	1σ	Age	1σ	Int	W/A
RSA01-101c	5.52	None	124	0.2351	0.0028	18.81	0.43	0.5809	0.0084	0.1724	0.0103	3087	18	3032	22	2952	34	3214	177	y	
RSA01-102	20.47	Disc	354	0.2217	0.0029	14.36	0.33	0.4699	0.0060	0.1269	0.0017	2993	21	2774	22	2483	26	2415	30	y	y
RSA01-103	28.24	Disc	1381	0.2087	0.0087	11.71	0.68	0.4070	0.0080	0.1105	0.0027	2896	66	2582	55	2201	37	2119	49		
RSA01-107	31.64	Disc	507	0.2024	0.0052	10.58	0.40	0.3793	0.0057	0.1033	0.0020	2845	41	2487	35	2073	27	1988	37	y	
RSA01-111	16.39	Disc	353	0.2252	0.0039	15.51	0.43	0.4993	0.0066	0.1347	0.0018	3018	27	2847	27	2611	29	2554	33	y	y
RSA01-113	17.93	Disc	93	0.2069	0.0041	13.19	0.41	0.4625	0.0067	0.1257	0.0017	2881	30	2693	30	2451	30	2394	31		
RSA01-115	10.59	Disc	65	0.2300	0.0039	17.17	0.49	0.5415	0.0081	0.1458	0.0021	3052	25	2945	28	2790	34	2750	36	y	
SWa18a-001r	36.64	Disc	209	0.2131	0.0040	10.71	0.34	0.3645	0.0058	0.0988	0.0017	2930	29	2498	29	2003	27	1905	31		
SWa18a-003	45.4	Disc	297	0.2074	0.0018	8.82	0.16	0.3083	0.0038	0.0838	0.0011	2886	13	2319	16	1732	19	1626	20		
SWa18a-004	5.01	Disc	137	0.2209	0.0035	17.05	0.47	0.5599	0.0078	0.1513	0.0021	2987	25	2938	26	2866	32	2848	36		
SWa18a-007	1.7	None	146	0.2362	0.0029	19.72	0.49	0.6059	0.0096	0.1755	0.0108	3094	19	3078	24	3053	38	3269	185	y	y
SWa18a-011c	4.86	Disc	207	0.2277	0.0022	17.96	0.33	0.5722	0.0068	0.1542	0.0020	3036	15	2988	18	2917	28	2898	34		
SWa18a-012	32.33	None	156	0.2429	0.0020	14.21	0.24	0.4245	0.0053	0.0805	0.0030	3139	12	2764	16	2281	24	1565	56		
SWa18a-013c	71.46	Disc	471	0.0710	0.0066	0.45	0.05	0.0457	0.0008	0.0138	0.0002	957	188	375	33	288	5	278	4		
SWa18a-014	64.09	Disc	207	0.1756	0.0023	4.34	0.10	0.1794	0.0023	0.0495	0.0006	2612	21	1702	19	1064	12	977	12		
SWa18a-015	21.78	Disc	430	0.2163	0.0081	13.55	0.74	0.4545	0.0090	0.1231	0.0022	2953	59	2719	52	2415	40	2346	40		
SWa18a-016	7.67	Disc	170	0.2177	0.0066	16.17	0.74	0.5389	0.0097	0.1458	0.0023	2964	48	2887	44	2779	40	2751	41		
SWa18a-017c	31.77	None	122	0.3060	0.0033	20.76	0.42	0.4923	0.0058	0.1294	0.0066	3501	16	3127	19	2581	25	2460	119		
SWa18a-017r	52.6	Disc	184	0.2353	0.0019	9.45	0.16	0.2913	0.0035	0.0783	0.0009	3089	12	2383	16	1648	18	1523	18		
SWa18a-018	66.92	Disc	415	0.1841	0.0032	4.35	0.12	0.1713	0.0024	0.0471	0.0008	2690	28	1702	23	1019	13	930	16		
SWa18a-019	60.09	Disc	948	0.2318	0.0049	7.76	0.27	0.2429	0.0039	0.0653	0.0014	3064	33	2204	31	1402	20	1279	26		
SWa18a-020	73.98	Disc	38	0.1285	0.0066	1.75	0.12	0.0990	0.0020	0.0282	0.0007	2078	89	1028	44	608	12	561	14		
SWa18a-021	7.2	Disc	134	0.2133	0.0065	15.71	0.72	0.5342	0.0097	0.1448	0.0024	2931	48	2859	44	2759	41	2734	42		
SWa18a-022	70.98	Disc	262	0.1731	0.0021	3.42	0.07	0.1434	0.0018	0.0396	0.0006	2588	20	1510	17	864	10	786	12		
SWa18a-023	53.68	Disc	206	0.1927	0.0023	6.59	0.14	0.2481	0.0031	0.0679	0.0009	2765	19	2058	19	1429	16	1328	18		

						Ratios (uncorrected)								Ages (uncorrected; Ma)								
	Th	U	Th/U	Common Pb		$^{207}Pb/^{206}Pb$		$^{207}Pb/^{235}U$		$^{206}Pb/^{238}U$		$^{208}Pb/^{232}Th$		$^{207}Pb/^{206}Pb$		$^{207}Pb/^{235}U$		$^{206}Pb/^{238}U$		$^{208}Pb/^{232}Th$		Inc.?
	ppm	ppm		%	1σ	Ratio	1σ	Ratio	1σ	Ratio	1σ	Ratio	1σ	Age	1σ	Age	1σ	Age	1σ	Age	1σ	
SWa18a-028	3143	1905	1.65			0.1900	0.0030	4.04	0.06	0.1544	0.0018	0.037	0.001	2742	11	1643	13	926	10	732	27	
SWa18a-029	642	601	1.07	1.41	0.7	0.2354	0.0041	18.48	0.33	0.5692	0.0071	0.168	0.007	3089	13	3015	17	2904	29	3133	124	y
SWa18a-031	460	510	0.90			0.2382	0.0053	14.34	0.32	0.4366	0.0060	0.123	0.007	3108	18	2772	21	2335	27	2347	123	y
SWa18a-033	180	935	0.19	0.96	0.12	0.2387	0.0039	14.51	0.24	0.4409	0.0053	0.170	0.006	3111	11	2783	16	2354	24	3168	111	y
SWa18a-036	55	159	0.35	1.73	0.3	0.2368	0.0047	16.43	0.33	0.5031	0.0067	0.188	0.009	3099	14	2902	19	2627	29	3478	159	y
SWa18a-037	119	348	0.34	3.49	0.18	0.2378	0.0028	12.78	0.16	0.3897	0.0043	0.195	0.004	3105	8	2663	12	2121	20	3607	70	y
SWa18a-038	680	3010	0.23	2.85	0.15	0.1756	0.0022	2.65	0.03	0.1097	0.0012	0.064	0.002	2611	9	1316	9	671	7	1255	30	
SWa18a-039	177	621	0.29	0.46	0.14	0.2359	0.0039	17.15	0.29	0.5275	0.0066	0.163	0.006	3093	11	2943	16	2731	28	3047	108	y
SWa18a-041	402	460	0.87	2.98	0.48	0.2336	0.0036	14.71	0.22	0.4568	0.0051	0.158	0.006	3077	10	2797	14	2425	22	2961	98	
SWa18a-043	503	1923	0.26	1.59	0.13	0.1836	0.0023	3.97	0.05	0.1570	0.0017	0.065	0.002	2686	9	1629	10	940	10	1270	31	
SWa18a-045c	535	722	0.74	0.67	0.33	0.2151	0.0033	5.56	0.08	0.1875	0.0020	0.055	0.002	2944	10	1910	13	1108	11	1075	36	
SWa18a-047	129	616	0.21	0.52	0.1	0.2324	0.0035	14.22	0.21	0.4439	0.0051	0.146	0.005	3069	10	2765	14	2368	23	2753	91	
SWa18a-048	188	463	0.40	0.77	0.24	0.2386	0.0042	16.76	0.30	0.5095	0.0063	0.159	0.007	3111	13	2921	17	2654	27	2986	124	y
SWa18a-049c	264	1147	0.23	1.94	0.15	0.2007	0.0030	5.97	0.09	0.2157	0.0026	0.107	0.004	2832	10	1971	13	1259	14	2056	67	
SWa18a-050	467	487	0.96			0.2366	0.0046	17.40	0.34	0.5338	0.0072	0.144	0.007	3097	14	2957	19	2757	30	2724	125	y
SWa18a-055	108	641	0.17	0.64	0.08	0.2373	0.0033	16.96	0.23	0.5185	0.0058	0.186	0.006	3102	9	2932	13	2693	25	3443	96	y
SWa18a-056	264	240	1.10	2.91	0.47	0.2410	0.0032	17.78	0.23	0.5351	0.0059	0.172	0.004	3127	9	2978	13	2763	25	3201	76	y
SWa18a-057	204	189	1.08			0.2381	0.0056	17.86	0.40	0.5446	0.0070	0.154	0.009	3107	19	2982	22	2803	29	2893	160	y
SWa18a-058	116	439	0.27	0.46	0.1	0.2414	0.0032	18.67	0.24	0.5610	0.0060	0.173	0.005	3129	9	3025	13	2871	25	3223	79	y
SWa18a-059	154	271	0.57	6.15	0.34	0.2433	0.0031	11.77	0.15	0.3509	0.0039	0.183	0.004	3142	9	2586	12	1939	19	3396	71	
SWa18a-061	1641	1327	1.24	9.27	0.71	0.2665	0.0035	12.61	0.17	0.3432	0.0040	0.147	0.004	3285	9	2651	13	1902	19	2775	67	
SWa18a-062	1320	626	2.11			0.2420	0.0039	11.15	0.18	0.3342	0.0039	0.075	0.003	3133	12	2535	15	1859	19	1463	53	y
SWa18a-063	680	767	0.89	3.18	0.71	0.2457	0.0050	14.00	0.28	0.4132	0.0055	0.143	0.007	3157	15	2750	19	2230	25	2709	127	
SWa18a-064	152	397	0.38			0.2399	0.0032	19.21	0.26	0.5807	0.0065	0.163	0.004	3119	9	3052	13	2952	27	3047	74	y
SWa18a-066	1023	830	1.23	2.21	1.04	0.2302	0.0042	15.87	0.29	0.5002	0.0063	0.149	0.007	3053	13	2869	17	2615	27	2808	120	

				Ratios (corrected)								Ages (corrected; Ma)									
	Disc.	Correction type	^{204}Pb	^{207}Pb/^{206}Pb		^{207}Pb/^{235}U		^{206}Pb/^{238}U		^{208}Pb/^{232}Th		^{207}Pb/^{206}Pb		^{207}Pb/^{235}U		^{206}Pb/^{238}U		^{208}Pb/^{232}Th		Inc.?	
	%		cps	Ratio	1σ	Ratio	1σ	Ratio	1σ	Ratio	1σ	Age	1σ	Age	1σ	Age	1σ	Age	1σ	Int	W/A
SWa18a-028	70.88	None	261	0.1900	0.0014	4.04	0.06	0.1544	0.0018	0.0369	0.0014	2742	11	1643	13	926	10	732	27		
SWa18a-029	6.47	Disc	188	0.2268	0.0050	17.55	0.62	0.5612	0.0089	0.1513	0.0022	3030	35	2965	34	2871	37	2847	39		
SWa18a-031	29.53	None	141	0.2382	0.0028	14.34	0.32	0.4366	0.0060	0.1231	0.0068	3108	18	2772	21	2335	27	2347	123	y	y
SWa18a-033	28.47	Disc	113	0.2328	0.0019	14.02	0.25	0.4366	0.0054	0.1174	0.0015	3072	12	2751	17	2335	24	2244	27	y	y
SWa18a-036	17.47	Disc	117	0.2263	0.0030	15.42	0.38	0.4944	0.0070	0.1333	0.0019	3026	20	2842	24	2589	30	2529	33		
SWa18a-037	35.26	Disc	150	0.2162	0.0017	11.21	0.18	0.3761	0.0045	0.1018	0.0016	2952	12	2541	15	2058	21	1960	29		
SWa18a-038	76.55	Disc	402	0.1562	0.0014	2.29	0.04	0.1065	0.0012	0.0298	0.0005	2415	14	1210	12	653	7	593	9		
SWa18a-039	14.05	Disc	61	0.2331	0.0020	16.87	0.31	0.5250	0.0067	0.1412	0.0017	3073	12	2928	17	2720	28	2669	31	y	y
SWa18a-041	23.45	Disc	370	0.2151	0.0036	13.14	0.36	0.4432	0.0059	0.1201	0.0015	2944	25	2690	26	2365	26	2292	27		
SWa18a-043	68.71	Disc	279	0.1731	0.0013	3.69	0.06	0.1545	0.0018	0.0427	0.0005	2587	12	1569	13	926	10	846	10		
SWa18a-045c	67.38	Disc	176	0.2109	0.0026	5.42	0.12	0.1863	0.0023	0.0506	0.0006	2912	18	1888	19	1101	12	997	11		
SWa18a-047	26.91	Disc	38	0.2292	0.0017	13.96	0.22	0.4416	0.0051	0.1189	0.0014	3047	11	2747	15	2358	23	2271	25	y	
SWa18a-048	17.42	Disc	102	0.2339	0.0025	16.30	0.34	0.5056	0.0066	0.1359	0.0017	3079	16	2895	20	2638	28	2575	30	y	y
SWa18a-049c	59.8	Disc	98	0.1881	0.0017	5.49	0.10	0.2116	0.0026	0.0580	0.0009	2725	14	1898	15	1237	14	1140	17		
SWa18a-050	13.54	None	65	0.2366	0.0023	17.40	0.34	0.5338	0.0072	0.1443	0.0071	3097	14	2957	19	2757	30	2724	125	y	y
SWa18a-055	15.73	Disc	190	0.2334	0.0015	16.58	0.24	0.5152	0.0058	0.1385	0.0016	3075	9	2911	14	2679	25	2622	28	y	y
SWa18a-056	12.45	Disc	189	0.2231	0.0033	15.98	0.41	0.5195	0.0070	0.1402	0.0018	3003	23	2876	25	2697	30	2653	31		
SWa18a-057	12.13	None	162	0.2381	0.0029	17.86	0.40	0.5446	0.0070	0.1539	0.0091	3107	19	2982	22	2803	29	2893	160	y	y
SWa18a-058	10	Disc	127	0.2386	0.0015	18.37	0.26	0.5585	0.0060	0.1498	0.0016	3111	10	3009	14	2860	25	2822	28	y	
SWa18a-059	41.08	Disc	281	0.2045	0.0029	9.28	0.22	0.3293	0.0042	0.0896	0.0016	2862	22	2366	22	1835	20	1735	30		
SWa18a-061	45	Disc	1234	0.2083	0.0054	8.94	0.35	0.3114	0.0050	0.0846	0.0014	2892	40	2332	36	1748	24	1642	27		
SWa18a-062	46.61	None	285	0.2420	0.0019	11.15	0.18	0.3342	0.0039	0.0750	0.0028	3133	12	2535	15	1859	19	1463	53		
SWa18a-063	33.22	Disc	294	0.2263	0.0054	12.49	0.47	0.4001	0.0065	0.1079	0.0016	3026	37	2642	35	2170	30	2070	30	y	y
SWa18a-064	6.7	None	97	0.2399	0.0015	19.21	0.26	0.5807	0.0065	0.1627	0.0043	3119	9	3052	13	2952	27	3047	74	y	
SWa18a-066	15.84	Disc	321	0.2164	0.0070	14.59	0.70	0.4892	0.0088	0.1324	0.0021	2954	51	2789	46	2567	38	2514	37		

						Ratios (uncorrected)								Ages (uncorrected; Ma)								
	Th	U	Th/U	Common Pb		$^{207}Pb/^{206}Pb$		$^{207}Pb/^{235}U$		$^{206}Pb/^{238}U$		$^{208}Pb/^{232}Th$		$^{207}Pb/^{206}Pb$		$^{207}Pb/^{235}U$		$^{206}Pb/^{238}U$		$^{208}Pb/^{232}Th$		Inc.?
	ppm	ppm		%	1σ	Ratio	1σ	Ratio	1σ	Ratio	1σ	Ratio	1σ	Age	1σ	Age	1σ	Age	1σ	Age	1σ	
SWa18a-069	379	350	1.08	1.83	0.58	0.2411	0.0039	18.53	0.31	0.5576	0.0068	0.170	0.006	3127	12	3018	16	2857	28	3175	108	y
SWa18a-080	95	1536	0.06	1.61	0.08	0.1935	0.0027	4.76	0.07	0.1784	0.0020	0.161	0.005	2772	10	1777	12	1058	11	3010	81	
SWa18a-084	1063	926	1.15			0.2304	0.0052	14.23	0.33	0.4479	0.0064	0.117	0.007	3055	18	2765	22	2386	29	2241	127	
RSA05-003	319	382	0.84			0.2333	0.0041	16.86	0.28	0.5244	0.0057	0.128	0.005	3074	13	2927	16	2718	24	2436	87	y
RSA05-004	928	1123	0.83	8.8	0.49	0.2373	0.0029	7.34	0.08	0.2244	0.0019	0.100	0.002	3102	7	2154	10	1305	10	1925	37	
RSA05-005	526	794	0.66			0.2324	0.0030	9.90	0.12	0.3092	0.0028	0.082	0.002	3069	8	2426	11	1737	14	1600	35	y
RSA05-008	279	459	0.61	0.84	0.24	0.2368	0.0030	17.39	0.20	0.5327	0.0047	0.156	0.003	3099	8	2957	11	2753	20	2922	60	y
RSA05-010	452	834	0.54	2.07	0.27	0.1950	0.0026	8.28	0.10	0.3078	0.0028	0.104	0.003	2785	9	2262	11	1730	14	2006	46	
RSA05-011	260	291	0.89			0.2478	0.0041	15.07	0.24	0.4412	0.0046	0.113	0.004	3171	12	2820	15	2356	21	2171	73	
RSA05-012	759	1290	0.59	2.26	0.55	0.1981	0.0040	9.09	0.18	0.3328	0.0038	0.113	0.005	2811	16	2347	18	1852	18	2160	96	
RSA05-013	1127	969	1.16			0.2376	0.0043	9.18	0.16	0.2805	0.0031	0.055	0.002	3104	14	2357	16	1594	16	1084	43	y
RSA05-015	240	518	0.46	3.18	0.36	0.2329	0.0037	11.73	0.18	0.3655	0.0037	0.142	0.005	3072	12	2583	14	2008	18	2678	85	y
RSA05-016	322	655	0.49	2.78	0.47	0.2375	0.0047	12.55	0.24	0.3833	0.0043	0.140	0.006	3104	16	2646	18	2091	20	2652	113	y
RSA05-020	374	531	0.70			0.2340	0.0042	16.98	0.30	0.5262	0.0061	0.135	0.005	3080	13	2934	17	2725	26	2561	92	y
RSA05-022	328	539	0.61	1.24	0.37	0.2380	0.0040	16.02	0.26	0.4879	0.0054	0.148	0.005	3107	12	2878	15	2562	23	2790	90	y
RSA05-024	621	742	0.84	12.59	0.79	0.2558	0.0038	11.73	0.17	0.3325	0.0035	0.173	0.005	3221	10	2583	14	1851	17	3224	87	
RSA05-025	431	740	0.58	8.73	0.58	0.2401	0.0037	12.88	0.20	0.3890	0.0042	0.206	0.006	3120	11	2671	14	2118	20	3779	107	
RSA05-026	422	719	0.59			0.2301	0.0033	15.11	0.21	0.4763	0.0049	0.125	0.003	3053	9	2822	13	2511	21	2388	62	
RSA05-028	460	723	0.64	5.4	0.59	0.2326	0.0041	8.31	0.13	0.2593	0.0026	0.108	0.004	3070	13	2266	15	1486	13	2066	76	y
RSA05-029	366	679	0.54	4.6	0.43	0.2357	0.0037	12.96	0.20	0.3986	0.0043	0.166	0.005	3091	11	2677	14	2162	20	3107	93	y
RSA05-030	329	549	0.60	3.43	0.51	0.2383	0.0044	9.44	0.16	0.2873	0.0028	0.106	0.004	3109	14	2382	15	1628	14	2028	78	y
RSA05-031	332	677	0.49	3.76	0.31	0.2365	0.0033	12.27	0.16	0.3764	0.0036	0.152	0.004	3096	9	2625	12	2059	17	2852	70	y
RSA05-036	628	967	0.65	2	0.5	0.2321	0.0043	8.40	0.15	0.2624	0.0030	0.084	0.003	3066	14	2275	17	1502	16	1639	64	y
RSA05-039	971	1041	0.93			0.2309	0.0032	7.79	0.10	0.2447	0.0023	0.063	0.002	3058	9	2207	11	1411	12	1238	31	
RSA05-040	262	423	0.62			0.2368	0.0036	19.06	0.28	0.5839	0.0063	0.152	0.005	3099	11	3045	14	2965	26	2860	81	y

				Ratios (corrected)								Ages (corrected; Ma)									
	Disc.	Correction type	^{204}Pb	^{207}Pb/^{206}Pb		^{207}Pb/^{235}U		^{206}Pb/^{238}U		^{208}Pb/^{232}Th		^{207}Pb/^{206}Pb		^{207}Pb/^{235}U		^{206}Pb/^{238}U		^{208}Pb/^{232}Th		Inc.?	
	%		cps	Ratio	1σ	Ratio	1σ	Ratio	1σ	Ratio	1σ	Age	1σ	Age	1σ	Age	1σ	Age	1σ	Int	W/A
SWa18a-069	9.58	Disc	168	0.2299	0.0042	17.36	0.53	0.5474	0.0081	0.1474	0.0020	3052	28	2955	29	2814	34	2778	36	y	y
SWa18a-080	65.94	Disc	246	0.1829	0.0014	4.43	0.07	0.1755	0.0020	0.0483	0.0015	2679	12	1717	13	1042	11	953	29		
SWa18a-084	26.15	None	175	0.2304	0.0027	14.23	0.33	0.4479	0.0064	0.1173	0.0070	3055	18	2765	22	2386	29	2241	127	y	y
RSA05-003	14.2	None	1875	0.2333	0.0020	16.86	0.28	0.5244	0.0057	0.1281	0.0048	3074	13	2927	16	2718	24	2436	87	y	y
RSA05-004	59.72	Disc	1924	0.1796	0.0040	5.07	0.16	0.2047	0.0023	0.0564	0.0007	2649	35	1831	26	1200	12	1109	14		
RSA05-005	49.29	None	1208	0.2324	0.0012	9.90	0.12	0.3092	0.0028	0.0824	0.0019	3069	8	2426	11	1737	14	1600	35		
RSA05-008	13.2	Disc	1183	0.2317	0.0020	16.87	0.26	0.5282	0.0049	0.1421	0.0013	3064	13	2928	15	2734	21	2685	22	y	y
RSA05-010	41.17	Disc	1104	0.1815	0.0022	7.54	0.15	0.3014	0.0029	0.0830	0.0008	2667	19	2178	18	1698	15	1611	15		
RSA05-011	30.58	None	1323	0.2478	0.0020	15.07	0.24	0.4412	0.0046	0.1134	0.0040	3171	12	2820	15	2356	21	2171	73		
RSA05-012	36.98	Disc	1277	0.1833	0.0044	8.22	0.28	0.3253	0.0042	0.0895	0.0010	2683	38	2255	31	1815	20	1732	19		
RSA05-013	54.66	None	1423	0.2376	0.0022	9.18	0.16	0.2805	0.0031	0.0551	0.0023	3104	14	2357	16	1594	16	1084	43		
RSA05-015	38.47	Disc	1218	0.2130	0.0031	10.39	0.25	0.3539	0.0042	0.0959	0.0012	2929	22	2471	22	1953	20	1852	22	y	
RSA05-016	36.68	Disc	1084	0.2203	0.0041	11.32	0.34	0.3726	0.0049	0.1007	0.0013	2983	28	2550	28	2042	23	1939	24	y	
RSA05-020	14.07	None	797	0.2340	0.0021	16.98	0.30	0.5262	0.0061	0.1351	0.0052	3080	13	2934	17	2725	26	2561	92	y	y
RSA05-022	20.56	Disc	1074	0.2306	0.0031	15.32	0.36	0.4819	0.0061	0.1297	0.0016	3056	20	2835	23	2535	27	2465	28	y	y
RSA05-024	40.96	Disc	1651	0.1724	0.0068	6.91	0.37	0.2907	0.0047	0.0804	0.0015	2581	62	2100	47	1645	23	1563	27		
RSA05-025	31.17	Disc	1297	0.1832	0.0048	8.97	0.34	0.3551	0.0051	0.0977	0.0017	2682	41	2335	35	1959	24	1883	32		
RSA05-026	21.36	None	985	0.2301	0.0014	15.11	0.21	0.4763	0.0049	0.1254	0.0034	3053	9	2822	13	2511	21	2388	62	y	y
RSA05-028	55.13	Disc	1040	0.1982	0.0047	6.70	0.23	0.2453	0.0032	0.0670	0.0009	2811	37	2073	31	1414	16	1310	17		
RSA05-029	32.52	Disc	1159	0.2069	0.0035	10.85	0.30	0.3803	0.0049	0.1034	0.0014	2881	26	2510	25	2077	23	1988	26		
RSA05-030	52.38	Disc	927	0.2171	0.0042	8.30	0.25	0.2774	0.0034	0.0751	0.0009	2959	29	2265	27	1578	17	1463	17	y	
RSA05-031	37.01	Disc	983	0.2130	0.0026	10.64	0.22	0.3622	0.0041	0.0982	0.0012	2929	19	2492	20	1993	19	1893	22	y	
RSA05-036	56.24	Disc	1155	0.2198	0.0040	7.79	0.23	0.2571	0.0036	0.0695	0.0009	2979	29	2207	27	1475	18	1358	17		
RSA05-039	59.71	None	1028	0.2309	0.0013	7.79	0.10	0.2447	0.0023	0.0632	0.0016	3058	9	2207	11	1411	12	1238	31		
RSA05-040	5.39	None	937	0.2368	0.0016	19.06	0.28	0.5839	0.0063	0.1520	0.0046	3099	11	3045	14	2965	26	2860	81	y	

						Ratios (uncorrected)								Ages (uncorrected; Ma)								
	Th	U	Th/U	Common Pb		$^{207}Pb/^{206}Pb$		$^{207}Pb/^{235}U$		$^{206}Pb/^{238}U$		$^{208}Pb/^{232}Th$		$^{207}Pb/^{206}Pb$		$^{207}Pb/^{235}U$		$^{206}Pb/^{238}U$		$^{208}Pb/^{232}Th$		Inc.?
	ppm	ppm		%	1σ	Ratio	1σ	Ratio	1σ	Ratio	1σ	Ratio	1σ	Age	1σ	Age	1σ	Age	1σ	Age	1σ	
RSA05-042	1193	1167	1.02	2.33	0.43	0.2262	0.0030	9.69	0.12	0.3109	0.0031	0.096	0.002	3025	9	2406	12	1745	15	1861	43	
RSA05-043	450	749	0.60	5.64	0.43	0.2411	0.0036	10.61	0.15	0.3193	0.0035	0.141	0.004	3127	11	2490	14	1786	17	2673	75	
RSA05-044	256	443	0.58			0.2339	0.0034	19.20	0.27	0.5954	0.0064	0.158	0.004	3079	10	3052	14	3011	26	2960	78	y
RSA05-046	1222	1288	0.95	4.31	0.79	0.2371	0.0046	8.34	0.16	0.2550	0.0031	0.089	0.004	3101	15	2268	17	1464	16	1727	74	
RSA05-049	687	686	1.00			0.2307	0.0035	12.32	0.18	0.3873	0.0041	0.077	0.002	3057	11	2629	14	2110	19	1503	45	
RSA05-050	674	652	1.03			0.2123	0.0026	5.36	0.06	0.1831	0.0017	0.030	0.001	2923	8	1878	10	1084	9	599	12	
RSA05-051	403	673	0.60	3.84	0.45	0.2367	0.0040	10.71	0.16	0.3281	0.0032	0.127	0.005	3098	12	2498	14	1829	16	2424	86	y
RSA05-052r	679	695	0.98			0.1804	0.0023	3.57	0.04	0.1437	0.0013	0.039	0.001	2656	8	1544	9	866	7	782	17	
RSA05-057	219	382	0.57	2.09	0.37	0.2374	0.0040	18.41	0.30	0.5625	0.0065	0.190	0.007	3102	12	3012	16	2877	27	3514	120	y
RSA05-058	611	998	0.61	3	0.24	0.2060	0.0024	4.17	0.04	0.1468	0.0014	0.054	0.001	2875	7	1668	9	883	8	1055	19	
RSA05-060	151	938	0.16	4.38	0.19	0.2003	0.0026	6.42	0.08	0.2325	0.0024	0.189	0.005	2828	9	2035	11	1348	12	3497	78	
RSA05-061	198	390	0.51	2.91	0.27	0.2334	0.0032	11.52	0.15	0.3581	0.0036	0.135	0.004	3076	9	2566	12	1973	17	2568	63	y
RSA05-062	254	302	0.84			0.1969	0.0036	4.32	0.07	0.1590	0.0016	0.033	0.001	2801	13	1696	14	951	9	655	25	
RSA05-063	222	1445	0.15	2.98	0.17	0.2007	0.0030	6.50	0.09	0.2351	0.0025	0.155	0.005	2832	10	2047	13	1361	13	2904	85	
RSA05-066	744	977	0.76	12.49	0.88	0.2369	0.0040	6.34	0.10	0.1941	0.0019	0.112	0.004	3099	12	2024	13	1144	10	2141	76	
RSA05-067	138	365	0.38	0.64	0.22	0.2341	0.0040	17.24	0.28	0.5340	0.0059	0.161	0.006	3080	12	2948	16	2758	25	3017	106	y
RSA05-068	356	552	0.65			0.2361	0.0050	17.31	0.35	0.5318	0.0065	0.126	0.006	3094	16	2952	20	2749	28	2403	112	y
RSA05-070	1714	2073	0.83	4.29	1.3	0.2399	0.0087	4.57	0.16	0.1382	0.0024	0.050	0.004	3119	31	1744	29	834	13	992	80	
RSA02-001	456	1751	0.26	6.57	0.65	0.1935	0.0062	5.83	0.18	0.2183	0.0036	0.176	0.011	2772	27	1950	27	1273	19	3273	192	
RSA02-002	61	130	0.47	8.24	0.55	0.2606	0.0053	22.51	0.44	0.6265	0.0077	0.393	0.014	3250	14	3206	19	3136	30	6705	203	
RSA02-003	36	74	0.48	6.22	0.39	0.2759	0.0046	24.35	0.40	0.6404	0.0078	0.338	0.009	3340	11	3283	16	3190	31	5891	141	
RSA02-004c	117	234	0.50			0.2500	0.0054	21.60	0.46	0.6271	0.0084	0.238	0.009	3185	16	3166	21	3138	33	4317	152	
RSA02-005c	44	135	0.33	5.74	0.37	0.2589	0.0050	20.66	0.40	0.5788	0.0074	0.365	0.013	3240	14	3123	19	2944	30	6296	187	
RSA02-006c	79	204	0.39	5.55	0.65	0.2384	0.0076	15.50	0.48	0.4712	0.0081	0.266	0.016	3110	25	2847	30	2489	35	4766	254	y
RSA02-006r	322	790	0.41	2.75	0.27	0.2037	0.0036	9.62	0.17	0.3425	0.0042	0.141	0.004	2856	13	2399	16	1899	20	2668	78	

				Ratios (corrected)								Ages (corrected; Ma)									
	Disc.	Correction type	^{204}Pb	^{207}Pb/^{206}Pb		^{207}Pb/^{235}U		^{206}Pb/^{238}U		^{208}Pb/^{232}Th		^{207}Pb/^{206}Pb		^{207}Pb/^{235}U		^{206}Pb/^{238}U		^{208}Pb/^{232}Th		Inc.?	
	%		cps	Ratio	1σ	Ratio	1σ	Ratio	1σ	Ratio	1σ	Age	1σ	Age	1σ	Age	1σ	Age	1σ	Int	W/A
RSA05-042	46.95	Disc	1308	0.2116	0.0032	8.86	0.22	0.3037	0.0036	0.0824	0.0009	2918	24	2324	23	1710	18	1600	17		
RSA05-043	46.31	Disc	1106	0.2056	0.0036	8.54	0.24	0.3013	0.0038	0.0820	0.0012	2871	28	2290	25	1698	19	1592	22	y	
RSA05-044	2.76	None	724	0.2339	0.0015	19.20	0.27	0.5954	0.0064	0.1577	0.0044	3079	10	3052	14	3011	26	2960	78	y	y
RSA05-046	57.18	Disc	1656	0.2102	0.0060	7.07	0.30	0.2440	0.0038	0.0662	0.0009	2907	46	2120	37	1407	20	1296	18		
RSA05-049	36.17	None	1253	0.2307	0.0016	12.32	0.18	0.3873	0.0041	0.0772	0.0024	3057	11	2629	14	2110	19	1503	45	y	y
RSA05-050	68.09	None	661	0.2123	0.0011	5.36	0.06	0.1831	0.0017	0.0301	0.0006	2923	8	1878	10	1084	9	599	12		
RSA05-051	45.09	Disc	1145	0.2127	0.0038	9.25	0.25	0.3155	0.0036	0.0856	0.0010	2926	28	2363	25	1768	18	1659	19	y	
RSA05-052r	71.82	None	708	0.1804	0.0009	3.57	0.04	0.1437	0.0013	0.0395	0.0009	2656	8	1544	9	866	7	782	17		
RSA05-057	7.61	Disc	1027	0.2246	0.0032	17.06	0.42	0.5507	0.0069	0.1486	0.0018	3014	22	2938	23	2828	29	2800	32		
RSA05-058	72.77	Disc	687	0.1866	0.0019	3.66	0.07	0.1424	0.0014	0.0391	0.0004	2712	16	1564	14	858	8	775	8		
RSA05-060	54.59	Disc	907	0.1712	0.0019	5.25	0.10	0.2223	0.0023	0.0615	0.0017	2569	18	1860	16	1294	12	1207	32		
RSA05-061	39.99	Disc	885	0.2153	0.0024	10.32	0.20	0.3477	0.0038	0.0942	0.0011	2946	17	2464	18	1924	18	1819	21	y	
RSA05-062	70.8	None	402	0.1969	0.0017	4.32	0.07	0.1590	0.0016	0.0330	0.0013	2801	13	1696	14	951	9	655	25		
RSA05-063	55.43	Disc	959	0.1812	0.0019	5.70	0.11	0.2281	0.0024	0.0628	0.0013	2664	17	1931	16	1324	13	1231	25		
RSA05-066	61.62	Disc	1687	0.1514	0.0077	3.55	0.23	0.1699	0.0026	0.0476	0.0009	2362	83	1538	51	1011	14	940	18		
RSA05-067	12.44	Disc	667	0.2303	0.0024	16.85	0.33	0.5306	0.0060	0.1428	0.0016	3054	16	2926	19	2744	25	2698	28	y	y
RSA05-068	13.67	None	713	0.2361	0.0026	17.31	0.35	0.5318	0.0065	0.1262	0.0063	3094	16	2952	20	2749	28	2403	112	y	y
RSA05-070	77.02	Disc	2127	0.2133	0.0104	3.89	0.27	0.1322	0.0031	0.0359	0.0007	2931	75	1611	56	801	17	712	14		
RSA02-001	53.07	Disc	532	0.1483	0.0063	4.17	0.24	0.2040	0.0038	0.0573	0.0016	2327	67	1669	48	1197	20	1125	31		
RSA02-002	-1.3	Disc	98	0.2089	0.0050	16.56	0.60	0.5749	0.0085	0.1562	0.0036	2897	35	2910	35	2928	35	2933	63		
RSA02-003	3.2	Disc	35	0.2387	0.0035	19.77	0.51	0.6005	0.0084	0.1611	0.0031	3111	21	3080	25	3032	34	3019	55	y	
RSA02-004c	1.91	None	68	0.2500	0.0027	21.60	0.46	0.6271	0.0084	0.2381	0.0093	3185	16	3166	21	3138	33	4317	152		
RSA02-005c	8.23	Disc	84	0.2238	0.0038	16.83	0.47	0.5456	0.0077	0.1473	0.0034	3008	25	2925	27	2807	32	2776	60	y	y
RSA02-006c	20.11	Disc	61	0.2035	0.0065	12.49	0.60	0.4451	0.0088	0.1212	0.0028	2855	47	2642	45	2373	39	2312	50	y	
RSA02-006r	36.13	Disc	155	0.1858	0.0027	8.54	0.21	0.3331	0.0044	0.0915	0.0013	2706	22	2290	23	1853	21	1769	23	y	

						Ratios (uncorrected)								Ages (uncorrected; Ma)								
	Th	U	Th/U	Common Pb		$^{207}Pb/^{206}Pb$		$^{207}Pb/^{235}U$		$^{206}Pb/^{238}U$		$^{208}Pb/^{232}Th$		$^{207}Pb/^{206}Pb$		$^{207}Pb/^{235}U$		$^{206}Pb/^{238}U$		$^{208}Pb/^{232}Th$		Inc.?
	ppm	ppm		%	1σ	Ratio	1σ	Ratio	1σ	Ratio	1σ	Ratio	1σ	Age	1σ	Age	1σ	Age	1σ	Age	1σ	
RSA02-007c	37	82	0.46	1.19	0.31	0.2605	0.0060	21.90	0.49	0.6099	0.0085	0.195	0.008	3250	17	3179	22	3070	34	3603	139	
RSA02-008c	82	189	0.43	6.25	0.58	0.2328	0.0060	17.31	0.43	0.5398	0.0077	0.306	0.014	3071	20	2952	24	2782	32	5393	221	y
RSA02-010	41	109	0.37	3.15	0.34	0.2597	0.0059	17.71	0.39	0.4947	0.0067	0.218	0.009	3245	17	2974	21	2591	29	3990	148	
RSA02-012c	52	120	0.43	6.66	0.48	0.2394	0.0048	15.41	0.31	0.4670	0.0060	0.278	0.010	3116	14	2841	19	2470	26	4955	162	y
RSA02-014	153	266	0.58	2.1	0.35	0.2637	0.0050	23.33	0.44	0.6417	0.0081	0.219	0.008	3269	14	3241	18	3196	32	4001	130	
RSA02-017	503	1083	0.46	3.95	0.68	0.2022	0.0067	8.89	0.29	0.3187	0.0052	0.144	0.010	2844	30	2326	29	1784	25	2718	176	
RSA02-019c	55	199	0.28	4.24	0.45	0.2392	0.0071	16.09	0.46	0.4879	0.0074	0.291	0.017	3114	25	2882	27	2562	32	5162	266	y
RSA02-019r	31	224	0.14	3.94	0.34	0.2402	0.0070	17.82	0.50	0.5381	0.0078	0.474	0.028	3121	25	2980	27	2775	33	7843	381	y
RSA02-020	88	672	0.13	1.53	0.16	0.1841	0.0047	8.09	0.20	0.3188	0.0044	0.168	0.008	2690	22	2241	22	1784	22	3141	145	
RSA02-023	227	132	1.73	3.46	1.06	0.2378	0.0047	18.70	0.37	0.5703	0.0072	0.174	0.006	3105	15	3026	19	2909	30	3244	109	y
RSA02-026	229	384	0.60			0.2624	0.0072	23.31	0.63	0.6443	0.0093	0.189	0.010	3261	23	3240	26	3206	36	3505	174	
RSA02-027c	130	283	0.46	1.26	0.4	0.2378	0.0066	19.77	0.53	0.6028	0.0085	0.196	0.011	3106	23	3080	26	3041	34	3622	187	y
RSA02-029c	82	108	0.76	2.49	0.9	0.2418	0.0088	19.89	0.70	0.5967	0.0105	0.200	0.015	3132	32	3086	34	3016	42	3679	244	y
RSA02-030	277	509	0.54	3.38	0.61	0.2433	0.0072	17.71	0.51	0.5280	0.0080	0.210	0.012	3141	25	2974	28	2733	34	3847	207	y
RSA02-031	133	310	0.43	4.61	0.96	0.2423	0.0114	16.30	0.74	0.4879	0.0095	0.241	0.023	3135	44	2895	44	2562	41	4370	381	y
SWA07-001c	302	510	0.59	1.22	0.5	0.2247	0.0045	11.26	0.21	0.3635	0.0041	0.112	0.006	3014	15	2545	18	1999	19	2149	106	
SWA07-005	170	818	0.21	1	0.18	0.2353	0.0043	16.75	0.31	0.5164	0.0064	0.187	0.009	3088	14	2920	18	2684	27	3463	150	
SWA07-007c	222	831	0.27	1.61	0.29	0.2298	0.0048	13.21	0.27	0.4168	0.0056	0.161	0.009	3051	16	2694	19	2246	25	3012	149	
SWA07-008	150	311	0.48			0.2386	0.0052	19.92	0.42	0.6058	0.0082	0.171	0.010	3111	16	3088	21	3053	33	3194	168	y
SWA07-011	93	123	0.76			0.2412	0.0046	20.75	0.38	0.6240	0.0075	0.168	0.008	3128	14	3127	18	3126	30	3144	144	y
SWA07-015	222	395	0.56			0.2419	0.0031	20.57	0.26	0.6167	0.0067	0.170	0.004	3132	9	3118	12	3097	27	3173	76	y
SWA07-018	105	145	0.72			0.2396	0.0032	20.49	0.27	0.6201	0.0067	0.166	0.005	3118	9	3115	13	3110	27	3109	80	y
SWA07-019c	1071	4104	0.26	4.77	0.29	0.1627	0.0023	3.33	0.05	0.1486	0.0017	0.094	0.003	2484	10	1489	11	893	9	1823	55	
SWA07-021	571	803	0.71			0.2215	0.0042	13.13	0.24	0.4301	0.0054	0.114	0.005	2991	14	2689	18	2306	24	2187	96	
SWA07-023	806	1494	0.54	2.52	0.33	0.1669	0.0024	3.49	0.05	0.1517	0.0017	0.056	0.002	2527	10	1525	11	910	9	1093	33	

				Ratios (corrected)								Ages (corrected; Ma)									
	Disc.	Correction type	^{204}Pb	^{207}Pb/^{206}Pb		^{207}Pb/^{235}U		^{206}Pb/^{238}U		^{208}Pb/^{232}Th		^{207}Pb/^{206}Pb		^{207}Pb/^{235}U		^{206}Pb/^{238}U		^{208}Pb/^{232}Th		Inc.?	
	%		cps	Ratio	1σ	Ratio	1σ	Ratio	1σ	Ratio	1σ	Age	1σ	Age	1σ	Age	1σ	Age	1σ	Int	W/A
RSA02-007c	6.49	Disc	47	0.2535	0.0036	21.06	0.56	0.6026	0.0089	0.1608	0.0023	3207	21	3141	26	3040	36	3013	40		
RSA02-008c	5.4	Disc	83	0.1923	0.0055	13.42	0.57	0.5060	0.0084	0.1385	0.0029	2762	43	2709	40	2640	36	2622	51		
RSA02-010	23.22	Disc	48	0.2409	0.0039	15.92	0.45	0.4792	0.0070	0.1284	0.0021	3126	23	2872	27	2524	30	2442	38		
RSA02-012c	19.88	Disc	131	0.1969	0.0044	11.83	0.41	0.4359	0.0065	0.1191	0.0025	2800	35	2591	32	2332	29	2274	46	y	
RSA02-014	2.03	Disc	100	0.2515	0.0035	21.78	0.54	0.6283	0.0085	0.1677	0.0023	3194	21	3174	24	3143	34	3134	39		
RSA02-017	38.86	Disc	124	0.1761	0.0065	7.43	0.39	0.3061	0.0056	0.0845	0.0015	2617	59	2165	47	1722	28	1640	28		
RSA02-019c	18.67	Disc	92	0.2127	0.0053	13.70	0.53	0.4672	0.0076	0.1267	0.0028	2926	39	2729	36	2471	33	2411	51	y	y
RSA02-019r	10.89	Disc	85	0.2157	0.0048	15.38	0.53	0.5169	0.0078	0.1400	0.0048	2949	34	2839	33	2686	33	2648	85	y	y
RSA02-020	36.71	Disc	138	0.1740	0.0029	7.53	0.21	0.3139	0.0043	0.0868	0.0015	2596	26	2177	25	1760	21	1682	28		
RSA02-023	5.28	Disc	43	0.2164	0.0076	16.42	0.85	0.5506	0.0103	0.1491	0.0024	2954	54	2902	49	2828	43	2808	42		
RSA02-026	2.16	None	86	0.2624	0.0040	23.31	0.63	0.6443	0.0093	0.1893	0.0102	3261	23	3240	26	3206	36	3505	174		
RSA02-027c	1.77	Disc	57	0.2302	0.0046	18.89	0.61	0.5952	0.0089	0.1602	0.0022	3054	31	3036	31	3010	36	3003	39	y	y
RSA02-029c	2.97	Disc	34	0.2266	0.0081	18.18	0.98	0.5818	0.0121	0.1568	0.0029	3028	55	2999	52	2956	49	2945	51		
RSA02-030	13.89	Disc	279	0.2225	0.0061	15.65	0.65	0.5101	0.0087	0.1377	0.0023	2999	42	2856	40	2657	37	2608	41	y	y
RSA02-031	19.23	Disc	136	0.2136	0.0101	13.71	0.92	0.4654	0.0106	0.1262	0.0028	2933	74	2730	64	2463	46	2401	51		
SWA07-001c	38.36	Disc	138	0.2170	0.0041	10.74	0.32	0.3591	0.0047	0.0972	0.0012	2959	29	2501	27	1978	22	1875	22	y	
SWA07-005	15.36	Disc	152	0.2292	0.0025	16.15	0.34	0.5113	0.0065	0.1377	0.0018	3046	17	2886	20	2662	28	2607	32	y	
SWA07-007c	30.2	Disc	57	0.2199	0.0032	12.43	0.32	0.4102	0.0057	0.1109	0.0016	2980	22	2638	24	2216	26	2125	29	y	
SWA07-008	2.33	None	122	0.2386	0.0026	19.92	0.42	0.6058	0.0082	0.1712	0.0097	3111	16	3088	21	3053	33	3194	168	y	y
SWA07-011	0.08	None	57	0.2412	0.0022	20.75	0.38	0.6240	0.0075	0.1683	0.0084	3128	14	3127	18	3126	30	3144	144	y	y
SWA07-015	1.44	None	23	0.2419	0.0014	20.57	0.26	0.6167	0.0067	0.1700	0.0044	3132	9	3118	12	3097	27	3173	76	y	y
SWA07-018	0.3	None	25	0.2396	0.0014	20.49	0.27	0.6201	0.0067	0.1663	0.0046	3118	9	3115	13	3110	27	3109	80	y	y
SWA07-019c	62.92	Disc	1544	0.1290	0.0026	2.52	0.07	0.1415	0.0018	0.0403	0.0008	2084	33	1277	21	853	10	798	15		
SWA07-021	27.18	None	41	0.2215	0.0020	13.13	0.24	0.4301	0.0054	0.1143	0.0053	2991	14	2689	18	2306	24	2187	96	y	
SWA07-023	66.24	Disc	163	0.1496	0.0027	3.05	0.08	0.1479	0.0018	0.0415	0.0005	2341	29	1420	21	889	10	821	10		

						Ratios (uncorrected)								Ages (uncorrected; Ma)								
	Th	U	Th/U	Common Pb		$^{207}Pb/^{206}Pb$		$^{207}Pb/^{235}U$		$^{206}Pb/^{238}U$		$^{208}Pb/^{232}Th$		$^{207}Pb/^{206}Pb$		$^{207}Pb/^{235}U$		$^{206}Pb/^{238}U$		$^{208}Pb/^{232}Th$		Inc.?
	ppm	ppm		%	1σ	Ratio	1σ	Ratio	1σ	Ratio	1σ	Ratio	1σ	Age	1σ	Age	1σ	Age	1σ	Age	1σ	
SWA07-024	181	562	0.32			0.2349	0.0043	19.51	0.35	0.6022	0.0074	0.171	0.008	3086	13	3067	17	3039	30	3193	132	
SWA07-027	209	275	0.76	5.65	1.05	0.2329	0.0056	16.95	0.39	0.5277	0.0074	0.214	0.013	3072	19	2932	22	2732	31	3925	222	
SWA07-028	288	546	0.53	3.4	0.64	0.2372	0.0054	18.28	0.41	0.5589	0.0078	0.218	0.013	3101	17	3005	21	2862	32	3983	212	y
SWA07-029	84	133	0.63	5.48	0.71	0.2598	0.0050	22.54	0.41	0.6294	0.0072	0.268	0.013	3245	14	3207	18	3147	28	4807	201	
SWA07-032	227	550	0.41	1.31	0.42	0.2440	0.0055	17.35	0.37	0.5158	0.0064	0.169	0.010	3147	18	2954	21	2681	27	3163	172	y
SWA07-034	148	160	0.93	2.03	0.5	0.2425	0.0032	20.30	0.26	0.6073	0.0064	0.185	0.005	3137	9	3106	12	3059	26	3436	89	y
SWA07-048	716	845	0.85	2.7	1.01	0.2400	0.0056	11.35	0.26	0.3431	0.0045	0.111	0.007	3120	19	2553	21	1902	21	2125	128	y
SWA07-049	304	706	0.43			0.2405	0.0038	12.52	0.19	0.3777	0.0041	0.106	0.004	3123	11	2644	14	2066	19	2027	74	y
SWA07-050	142	904	0.16	2.99	0.27	0.1887	0.0035	6.81	0.13	0.2619	0.0033	0.165	0.008	2731	15	2087	16	1500	17	3086	137	
SWA07-054	97	484	0.20	1.53	0.19	0.2334	0.0040	16.43	0.28	0.5107	0.0062	0.210	0.009	3075	12	2902	16	2659	27	3849	147	
SWA07-055	164	237	0.69			0.3059	0.0045	30.69	0.45	0.7279	0.0084	0.202	0.007	3500	10	3509	15	3526	31	3710	114	
SWA07-056	229	269	0.85			0.2389	0.0038	20.55	0.33	0.6238	0.0075	0.174	0.007	3113	11	3117	16	3125	30	3237	114	
SWA07-058	382	2491	0.15	9.13	0.73	0.1762	0.0042	2.57	0.06	0.1056	0.0014	0.147	0.009	2617	20	1291	17	647	8	2771	159	
SWA07-059	269	270	0.99	2.58	0.67	0.2415	0.0037	19.54	0.29	0.5870	0.0063	0.183	0.006	3130	11	3069	14	2977	26	3398	111	y
SWA07-065	225	414	0.54			0.2417	0.0040	21.26	0.36	0.6380	0.0077	0.183	0.008	3131	12	3150	16	3181	30	3403	129	
SWA07-067	120	130	0.92	2.7	0.47	0.2441	0.0032	20.62	0.26	0.6129	0.0065	0.195	0.005	3147	9	3121	12	3081	26	3609	85	y
SWA07-074	308	530	0.58			0.3038	0.0049	27.35	0.45	0.6532	0.0081	0.183	0.007	3490	12	3396	16	3241	32	3399	119	
SWA07-076	150	151	0.99	3.62	0.74	0.2455	0.0042	20.52	0.34	0.6064	0.0074	0.201	0.008	3156	12	3116	16	3055	30	3694	130	y
SWA07-077	163	206	0.79			0.3131	0.0042	31.34	0.41	0.7261	0.0079	0.204	0.006	3536	9	3530	13	3519	29	3755	93	
SWA07-078	81	109	0.75			0.2432	0.0037	20.80	0.32	0.6203	0.0073	0.167	0.006	3141	11	3129	15	3111	29	3113	97	y
SWA07-079	455	880	0.52	4.04	0.45	0.2080	0.0034	9.59	0.16	0.3344	0.0039	0.139	0.005	2890	12	2396	15	1860	19	2629	93	
SWA07-082	251	429	0.59			0.2416	0.0049	20.98	0.41	0.6299	0.0076	0.185	0.009	3130	16	3138	19	3149	30	3424	158	
SWA07-084	456	707	0.64			0.2349	0.0047	14.74	0.29	0.4552	0.0058	0.129	0.006	3086	16	2799	19	2418	26	2445	113	
SWA07-086	243	668	0.36			0.2410	0.0046	21.04	0.40	0.6332	0.0081	0.170	0.008	3126	15	3140	18	3162	32	3182	138	y
SWA07-087	547	448	1.22			0.3086	0.0064	29.44	0.58	0.6919	0.0081	0.188	0.010	3514	16	3468	19	3390	31	3481	171	

				Ratios (corrected)								Ages (corrected; Ma)									
	Disc.	Correction	^{204}Pb	^{207}Pb/^{206}Pb		^{207}Pb/^{235}U		^{206}Pb/^{238}U		^{208}Pb/^{232}Th		^{207}Pb/^{206}Pb		^{207}Pb/^{235}U		^{206}Pb/^{238}U		^{208}Pb/^{232}Th		Inc.?	
	%	type	cps	Ratio	1σ	Ratio	1σ	Ratio	1σ	Ratio	1σ	Age	1σ	Age	1σ	Age	1σ	Age	1σ	Int	W/A
SWA07-024	1.92	None	32	0.2349	0.0021	19.51	0.35	0.6022	0.0074	0.1711	0.0077	3086	13	3067	17	3039	30	3193	132	y	
SWA07-027	8.45	Disc	185	0.1968	0.0080	13.51	0.78	0.4979	0.0097	0.1360	0.0024	2799	63	2716	54	2605	42	2577	43		
SWA07-028	7.05	Disc	205	0.2162	0.0053	16.09	0.61	0.5399	0.0089	0.1462	0.0024	2952	38	2882	36	2783	37	2758	42		
SWA07-029	0.69	Disc	101	0.2263	0.0056	18.57	0.70	0.5949	0.0090	0.1604	0.0026	3026	38	3019	36	3009	37	3007	45		
SWA07-032	17.35	Disc	122	0.2361	0.0041	16.57	0.48	0.5090	0.0071	0.1367	0.0018	3094	27	2910	28	2652	31	2590	32	y	y
SWA07-034	1.79	Disc	59	0.2302	0.0035	18.88	0.49	0.5950	0.0079	0.1601	0.0020	3053	23	3036	25	3009	32	3002	35	y	
SWA07-048	43.8	Disc	495	0.2235	0.0074	10.29	0.51	0.3339	0.0061	0.0901	0.0015	3006	51	2461	46	1857	30	1744	27		
SWA07-049	39.43	None	95	0.2405	0.0017	12.52	0.19	0.3777	0.0041	0.1055	0.0041	3123	11	2644	14	2066	19	2027	74		
SWA07-050	47.5	Disc	85	0.1687	0.0027	5.91	0.16	0.2541	0.0035	0.0704	0.0015	2545	26	1963	23	1460	18	1376	28		
SWA07-054	15.49	Disc	61	0.2240	0.0024	15.53	0.32	0.5028	0.0065	0.1357	0.0020	3009	16	2848	20	2626	28	2572	35	y	
SWA07-055	-0.93	None	20	0.3059	0.0021	30.69	0.45	0.7279	0.0084	0.2015	0.0068	3500	10	3509	15	3526	31	3710	114		
SWA07-056	-0.5	None	54	0.2389	0.0018	20.55	0.33	0.6238	0.0075	0.1737	0.0066	3113	11	3117	16	3125	30	3237	114		
SWA07-058	70.17	Disc	433	0.1099	0.0068	1.45	0.11	0.0960	0.0016	0.0278	0.0014	1798	109	912	45	591	10	553	27		
SWA07-059	4.38	Disc	6	0.2258	0.0047	17.80	0.59	0.5719	0.0083	0.1542	0.0021	3022	32	2979	32	2916	34	2899	36		
SWA07-065	-2.0	None	89	0.2417	0.0019	21.26	0.36	0.6380	0.0077	0.1834	0.0076	3131	12	3150	16	3181	30	3403	129		
SWA07-067	0.85	Disc	19	0.2277	0.0033	18.72	0.48	0.5963	0.0079	0.1607	0.0021	3036	23	3027	25	3015	32	3012	36		
SWA07-074	9.09	None	89	0.3038	0.0023	27.35	0.45	0.6532	0.0081	0.1831	0.0070	3490	12	3396	16	3241	32	3399	119		
SWA07-076	1.57	Disc	153	0.2233	0.0053	17.99	0.66	0.5844	0.0092	0.1578	0.0023	3005	37	2989	35	2967	37	2961	40		
SWA07-077	0.64	None	13	0.3131	0.0018	31.34	0.41	0.7261	0.0079	0.2042	0.0056	3536	9	3530	13	3519	29	3755	93		
SWA07-078	1.22	None	80	0.2432	0.0017	20.80	0.32	0.6203	0.0073	0.1665	0.0056	3141	11	3129	15	3111	29	3113	97	y	y
SWA07-079	37.38	Disc	105	0.1815	0.0036	8.03	0.24	0.3209	0.0042	0.0883	0.0013	2667	33	2235	27	1794	21	1711	23		
SWA07-082	-0.76	None	150	0.2416	0.0024	20.98	0.41	0.6299	0.0076	0.1846	0.0093	3130	16	3138	19	3149	30	3424	158		
SWA07-084	25.88	None	77	0.2349	0.0023	14.74	0.29	0.4552	0.0058	0.1286	0.0063	3086	16	2799	19	2418	26	2445	113	y	y
SWA07-086	-1.4	None	48	0.2410	0.0023	21.04	0.40	0.6332	0.0081	0.1705	0.0080	3126	15	3140	18	3162	32	3182	138	y	y
SWA07-087	4.54	None	17	0.3086	0.0032	29.44	0.58	0.6919	0.0081	0.1880	0.0100	3514	16	3468	19	3390	31	3481	171		

						Ratios (uncorrected)								Ages (uncorrected; Ma)								
	Th	U	Th/U	Common Pb		$^{207}Pb/^{206}Pb$		$^{207}Pb/^{235}U$		$^{206}Pb/^{238}U$		$^{208}Pb/^{232}Th$		$^{207}Pb/^{206}Pb$		$^{207}Pb/^{235}U$		$^{206}Pb/^{238}U$		$^{208}Pb/^{232}Th$		Inc.?
	ppm	ppm		%	1σ	Ratio	1σ	Ratio	1σ	Ratio	1σ	Ratio	1σ	Age	1σ	Age	1σ	Age	1σ	Age	1σ	
SWA07-088	95	161	0.59			0.2417	0.0034	20.67	0.28	0.6201	0.0066	0.192	0.006	3131	9	3123	13	3110	26	3552	98	
SWA07-090	486	604	0.80			0.2899	0.0040	21.35	0.29	0.5340	0.0060	0.125	0.004	3417	9	3154	13	2758	25	2382	65	
SWA07-092c	191	226	0.84	3.82	0.9	0.2392	0.0051	17.71	0.37	0.5370	0.0072	0.188	0.010	3115	17	2974	20	2771	30	3475	176	y
SWA07-094	612	1158	0.53	7.11	0.56	0.2198	0.0034	8.26	0.13	0.2724	0.0031	0.142	0.005	2979	11	2259	14	1553	16	2683	92	
SWA07-097	141	447	0.32			0.2516	0.0048	21.38	0.41	0.6162	0.0081	0.172	0.009	3195	14	3156	19	3095	32	3215	147	
RSA04-001r	277	656	0.42	6.4	0.46	0.2306	0.0046	9.62	0.19	0.3026	0.0038	0.176	0.006	3056	16	2399	18	1704	19	3278	108	
RSA04-002c	482	318	1.51			0.2391	0.0045	19.51	0.36	0.5919	0.0074	0.170	0.006	3114	14	3067	18	2997	30	3179	99	y
RSA04-003c	239	356	0.67	4.53	0.89	0.2389	0.0082	10.70	0.35	0.3249	0.0057	0.131	0.009	3113	30	2498	31	1813	28	2495	152	y
RSA04-003r	280	918	0.31			0.2331	0.0089	14.89	0.56	0.4635	0.0083	0.101	0.008	3073	36	2808	36	2455	37	1938	143	y
RSA04-004c	990	647	1.53			0.1807	0.0051	6.01	0.16	0.2412	0.0033	0.070	0.004	2659	26	1977	23	1393	17	1365	71	
RSA04-005	143	1549	0.09	1.25	0.2	0.1750	0.0074	6.74	0.28	0.2798	0.0053	0.158	0.014	2606	39	2078	36	1590	27	2961	242	
RSA04-006c	285	217	1.31			0.2398	0.0037	13.90	0.21	0.4206	0.0048	0.103	0.003	3119	11	2743	15	2263	22	1980	47	y
RSA04-007c	128	486	0.26			0.2393	0.0050	19.75	0.41	0.5986	0.0077	0.154	0.006	3115	16	3079	20	3024	31	2898	108	y
RSA04-009c	203	198	1.02	4.91	0.53	0.2423	0.0041	15.37	0.25	0.4600	0.0052	0.166	0.005	3135	12	2838	16	2439	23	3105	82	y
RSA04-009r	74	84	0.88			0.2421	0.0051	22.41	0.47	0.6716	0.0088	0.191	0.007	3134	16	3202	20	3312	34	3527	127	
RSA04-010	121	312	0.39			0.2423	0.0045	20.96	0.39	0.6274	0.0079	0.199	0.007	3135	13	3137	18	3139	31	3670	113	
RSA04-011	137	1054	0.13	1.52	0.1	0.1900	0.0032	7.72	0.13	0.2949	0.0036	0.154	0.005	2742	12	2199	15	1666	18	2902	81	
RSA04-012	288	313	0.92	1.18	0.44	0.2430	0.0045	19.90	0.37	0.5940	0.0074	0.174	0.006	3140	13	3086	18	3005	30	3244	99	y
RSA04-013c	340	445	0.77	7.3	0.98	0.2541	0.0076	13.08	0.38	0.3738	0.0060	0.171	0.010	3210	24	2686	28	2047	28	3192	175	
RSA04-015c	268	256	1.05			0.2476	0.0067	17.83	0.47	0.5225	0.0079	0.106	0.006	3169	21	2981	25	2710	33	2041	102	y
RSA04-015r	864	1515	0.57			0.2047	0.0064	7.26	0.22	0.2574	0.0040	0.057	0.004	2864	27	2144	27	1477	21	1125	72	
RSA04-017	434	599	0.73	7.23	1.29	0.2491	0.0099	13.54	0.52	0.3942	0.0072	0.184	0.015	3179	34	2718	36	2142	33	3419	258	y
RSA04-018	235	583	0.40	3.03	0.33	0.2488	0.0055	10.56	0.23	0.3079	0.0038	0.130	0.005	3177	17	2485	20	1730	19	2474	97	
RSA04-019c	178	208	0.86			0.2406	0.0055	20.48	0.46	0.6176	0.0083	0.185	0.008	3124	19	3114	22	3100	33	3428	137	
RSA04-021c	121	149	0.82			0.2418	0.0057	21.15	0.49	0.6345	0.0088	0.186	0.008	3132	19	3146	23	3167	35	3441	144	

				Ratios (corrected)								Ages (corrected; Ma)									
	Disc.	Correction type	^{204}Pb	^{207}Pb/^{206}Pb		^{207}Pb/^{235}U		^{206}Pb/^{238}U		^{208}Pb/^{232}Th		^{207}Pb/^{206}Pb		^{207}Pb/^{235}U		^{206}Pb/^{238}U		^{208}Pb/^{232}Th		Inc.?	
	%		cps	Ratio	1σ	Ratio	1σ	Ratio	1σ	Ratio	1σ	Age	1σ	Age	1σ	Age	1σ	Age	1σ	Int	W/A
SWA07-088	0.87	None	0	0.2417	0.0015	20.67	0.28	0.6201	0.0066	0.1922	0.0058	3131	9	3123	13	3110	26	3552	98		
SWA07-090	23.62	None	10	0.2899	0.0018	21.35	0.29	0.5340	0.0060	0.1251	0.0036	3417	9	3154	13	2758	25	2382	65		
SWA07-092c	10.9	Disc	234	0.2155	0.0066	15.35	0.70	0.5165	0.0090	0.1399	0.0023	2947	48	2837	43	2684	38	2646	40		
SWA07-094	48.67	Disc	287	0.1727	0.0046	6.02	0.23	0.2531	0.0035	0.0700	0.0012	2584	44	1979	33	1454	18	1367	23		
SWA07-097	3.96	None	132	0.2516	0.0023	21.38	0.41	0.6162	0.0081	0.1724	0.0085	3195	14	3156	19	3095	32	3215	147		
RSA04-001r	46.41	Disc	412	0.1892	0.0043	7.39	0.26	0.2832	0.0042	0.0777	0.0016	2735	37	2160	31	1608	21	1512	31		
RSA04-002c	4.71	None	94	0.2391	0.0022	19.51	0.36	0.5919	0.0074	0.1703	0.0057	3114	14	3067	18	2997	30	3179	99	y	y
RSA04-003c	45.64	Disc	250	0.2106	0.0080	9.01	0.51	0.3102	0.0068	0.0842	0.0018	2910	61	2339	52	1741	34	1634	33		
RSA04-003r	24.14	None	128	0.2331	0.0053	14.89	0.56	0.4635	0.0083	0.1006	0.0078	3073	36	2808	36	2455	37	1938	143	y	y
RSA04-004c	52.77	None	80	0.1807	0.0029	6.01	0.16	0.2412	0.0033	0.0699	0.0038	2659	26	1977	23	1393	17	1365	71		
RSA04-005	42.31	Disc	203	0.1665	0.0046	6.34	0.27	0.2763	0.0051	0.0767	0.0016	2523	43	2024	38	1573	26	1493	30		
RSA04-006c	32.42	None	114	0.2398	0.0017	13.90	0.21	0.4206	0.0048	0.1029	0.0026	3119	11	2743	15	2263	22	1980	47	y	y
RSA04-007c	3.67	None	62	0.2393	0.0026	19.75	0.41	0.5986	0.0077	0.1542	0.0061	3115	16	3079	20	3024	31	2898	108	y	y
RSA04-009c	23.61	Disc	65	0.2117	0.0042	12.76	0.40	0.4374	0.0060	0.1187	0.0016	2918	30	2662	29	2339	27	2266	28		
RSA04-009r	-7.3	None	53	0.2421	0.0026	22.41	0.47	0.6716	0.0088	0.1907	0.0075	3134	16	3202	20	3312	34	3527	127		
RSA04-010	-0.15	None	90	0.2423	0.0022	20.96	0.39	0.6274	0.0079	0.1991	0.0067	3135	13	3137	18	3139	31	3670	113		
RSA04-011	42.95	Disc	126	0.1800	0.0017	7.21	0.13	0.2904	0.0035	0.0800	0.0013	2653	14	2137	17	1644	17	1556	24		
RSA04-012	4.66	Disc	32	0.2359	0.0035	19.09	0.51	0.5869	0.0081	0.1576	0.0020	3093	22	3046	26	2977	33	2958	36	y	y
RSA04-013c	38.75	Disc	206	0.2080	0.0083	9.94	0.57	0.3465	0.0070	0.0942	0.0019	2890	60	2429	53	1918	34	1819	35		
RSA04-015c	17.73	None	104	0.2476	0.0036	17.83	0.47	0.5225	0.0079	0.1063	0.0056	3169	21	2981	25	2710	33	2041	102		
RSA04-015r	54.01	None	495	0.2047	0.0037	7.26	0.22	0.2574	0.0040	0.0572	0.0037	2864	27	2144	27	1477	21	1125	72		
RSA04-017	34.31	Disc	387	0.2033	0.0110	10.25	0.77	0.3657	0.0087	0.0996	0.0022	2853	82	2458	70	2009	41	1919	40		
RSA04-018	50.77	Disc	330	0.2305	0.0037	9.49	0.25	0.2985	0.0039	0.0803	0.0012	3055	25	2386	24	1684	19	1562	22	y	y
RSA04-019c	0.96	None	20	0.2406	0.0029	20.48	0.46	0.6176	0.0083	0.1848	0.0080	3124	19	3114	22	3100	33	3428	137		
RSA04-021c	-1.4	None	25	0.2418	0.0030	21.15	0.49	0.6345	0.0088	0.1856	0.0085	3132	19	3146	23	3167	35	3441	144		

						Ratios (uncorrected)								Ages (uncorrected; Ma)								
	Th	U	Th/U	Common Pb		$^{207}Pb/^{206}Pb$		$^{207}Pb/^{235}U$		$^{206}Pb/^{238}U$		$^{208}Pb/^{232}Th$		$^{207}Pb/^{206}Pb$		$^{207}Pb/^{235}U$		$^{206}Pb/^{238}U$		$^{208}Pb/^{232}Th$		Inc.?
	ppm	ppm		%	1σ	Ratio	1σ	Ratio	1σ	Ratio	1σ	Ratio	1σ	Age	1σ	Age	1σ	Age	1σ	Age	1σ	
RSA04-021r	169	266	0.63			0.2415	0.0082	21.50	0.71	0.6458	0.0107	0.195	0.014	3130	30	3162	32	3212	42	3594	236	
RSA04-023c	940	956	0.98	18.1	1.2	0.3019	0.0061	9.30	0.18	0.2233	0.0027	0.138	0.005	3480	15	2368	18	1299	14	2619	90	
RSA04-023r	775	978	0.79	10.43	1.12	0.2710	0.0072	11.24	0.29	0.3007	0.0043	0.158	0.008	3312	22	2543	24	1695	21	2967	146	
RSA04-024	178	145	1.23			0.2417	0.0042	20.50	0.35	0.6153	0.0076	0.175	0.005	3131	13	3115	17	3091	30	3266	87	
RSA04-025	599	627	0.96			0.2350	0.0073	12.55	0.38	0.3874	0.0062	0.084	0.005	3086	27	2646	28	2111	29	1639	92	y
RSA04-026	224	238	0.94			0.2392	0.0048	20.45	0.40	0.6205	0.0077	0.184	0.007	3115	15	3113	19	3112	31	3408	115	
RSA04-027c	228	350	0.65	8.32	1.3	0.2503	0.0107	14.49	0.60	0.4206	0.0084	0.220	0.017	3187	38	2783	39	2263	38	4020	282	y
RSA04-028r	278	928	0.30	14.08	0.88	0.2866	0.0072	10.53	0.25	0.2665	0.0036	0.331	0.016	3399	20	2483	22	1523	18	5783	237	
RSA04-029c	224	650	0.35	1.95	0.36	0.2316	0.0067	13.03	0.37	0.4083	0.0061	0.158	0.009	3063	25	2682	27	2207	28	2959	153	
RSA04-029r	229	1491	0.15	2.32	0.32	0.1920	0.0069	6.87	0.24	0.2593	0.0042	0.154	0.012	2759	34	2094	30	1486	21	2896	205	
RSA04-030c	208	187	1.12			0.2401	0.0050	18.99	0.38	0.5739	0.0073	0.166	0.006	3121	16	3042	19	2924	30	3098	108	y
RSA04-030r	1221	2031	0.60	7.28	0.86	0.2438	0.0075	3.88	0.11	0.1153	0.0017	0.059	0.003	3145	27	1609	23	704	10	1161	64	
RSA08-001c	332	507	0.65	31.54	1.21	0.4082	0.0061	30.78	0.46	0.5470	0.0062	0.667	0.016	3940	10	3512	15	2813	26	10331	196	
RSA08-002c	505	621	0.81	35.72	2.63	0.4169	0.0121	20.23	0.56	0.3520	0.0048	0.393	0.022	3971	24	3103	27	1944	23	6707	323	
RSA08-003	226	441	0.51			0.9383	0.0130	382.75	5.34	2.9590	0.0326	13.929	0.305	5148	9	6042	14	8870	53	54639	413	
RSA08-004c	558	938	0.59	50.23	2.01	0.5288	0.0087	20.52	0.33	0.2815	0.0032	0.548	0.016	4324	11	3116	16	1599	16	8826	203	
RSA08-005	336	594	0.57	6.81	0.63	0.2626	0.0059	20.52	0.45	0.5674	0.0073	0.289	0.012	3262	18	3116	21	2897	30	5139	189	
RSA08-006	183	273	0.67	0.82	0.37	0.2412	0.0048	20.20	0.40	0.6075	0.0077	0.178	0.006	3128	16	3101	19	3060	31	3305	109	y
RSA08-007c	256	375	0.68	20.98	1.48	0.3680	0.0090	34.68	0.82	0.6839	0.0091	0.596	0.027	3783	20	3630	23	3359	35	9445	347	
RSA08-012	266	894	0.30	92.51	3.45	0.7808	0.0150	32.13	0.59	0.2985	0.0035	1.997	0.070	4887	14	3554	18	1684	17	22184	469	
RSA08-013c	36	202	0.18	41.78	2.27	0.4989	0.0121	51.88	1.22	0.7541	0.0097	3.926	0.181	4238	19	4029	23	3623	36	32230	743	
RSA08-015c	92	809	0.11	6.22	0.38	0.2092	0.0049	9.05	0.21	0.3138	0.0041	0.449	0.021	2900	20	2343	21	1759	20	7499	287	
RSA08-016c	441	872	0.51	0.84	0.27	0.2422	0.0045	20.56	0.38	0.6160	0.0073	0.186	0.006	3134	15	3118	18	3094	29	3447	107	y
RSA08-017	508	216	2.35	80.95	6.57	0.7743	0.0215	68.85	1.83	0.6462	0.0089	0.511	0.026	4875	22	4312	27	3213	35	8341	353	
RSA08-019c	322	662	0.49	55.43	2.76	0.5518	0.0119	41.35	0.85	0.5436	0.0066	1.402	0.056	4386	16	3804	20	2799	28	17713	475	

				Ratios (corrected)								Ages (corrected; Ma)									
	Disc.	Correction type	^{204}Pb	^{207}Pb/^{206}Pb		^{207}Pb/^{235}U		^{206}Pb/^{238}U		^{208}Pb/^{232}Th		^{207}Pb/^{206}Pb		^{207}Pb/^{235}U		^{206}Pb/^{238}U		^{208}Pb/^{232}Th		Inc.?	
	%		cps	Ratio	1σ	Ratio	1σ	Ratio	1σ	Ratio	1σ	Age	1σ	Age	1σ	Age	1σ	Age	1σ	Int	W/A
RSA04-021r	-3.3	None	0	0.2415	0.0047	21.50	0.71	0.6458	0.0107	0.1946	0.0139	3130	30	3162	32	3212	42	3594	236		
RSA04-023c	64.67	Disc	1441	0.1840	0.0113	4.64	0.38	0.1829	0.0039	0.0503	0.0013	2689	100	1757	68	1083	21	992	26		
RSA04-023r	51.94	Disc	976	0.2053	0.0098	7.62	0.51	0.2694	0.0057	0.0733	0.0017	2868	76	2188	60	1537	29	1429	31		
RSA04-024	1.62	None	23	0.2417	0.0020	20.50	0.35	0.6153	0.0076	0.1754	0.0050	3131	13	3115	17	3091	30	3266	87		
RSA04-025	36.94	None	169	0.2350	0.0041	12.55	0.38	0.3874	0.0062	0.0845	0.0050	3086	27	2646	28	2111	29	1639	92	y	y
RSA04-026	0.18	None	75	0.2392	0.0024	20.45	0.40	0.6205	0.0077	0.1837	0.0067	3115	15	3113	19	3112	31	3408	115		
RSA04-027c	29.1	Disc	273	0.1968	0.0123	10.46	0.90	0.3856	0.0103	0.1053	0.0027	2800	101	2477	80	2103	48	2024	50		
RSA04-028r	57.86	Disc	1157	0.1966	0.0089	6.21	0.38	0.2290	0.0043	0.0626	0.0035	2798	73	2006	54	1329	23	1227	66		
RSA04-029c	31.8	Disc	282	0.2195	0.0047	12.11	0.42	0.4003	0.0064	0.1082	0.0017	2977	34	2613	33	2170	29	2077	31		
RSA04-029r	49.53	Disc	161	0.1767	0.0050	6.17	0.26	0.2533	0.0042	0.0699	0.0015	2622	46	2000	37	1455	22	1366	28		
RSA04-030c	7.88	None	25	0.2401	0.0025	18.99	0.38	0.5739	0.0073	0.1657	0.0062	3121	16	3042	19	2924	30	3098	108	y	y
RSA04-030r	80.37	Disc	837	0.1973	0.0081	2.91	0.17	0.1069	0.0020	0.0292	0.0006	2804	66	1384	44	655	12	582	12		
RSA08-001c	34.47	Disc	3336	0.2111	0.0139	10.90	0.95	0.3745	0.0090	0.1016	0.0074	2914	105	2515	81	2050	42	1956	136		
RSA08-002c	56.31	Disc	3335	0.1842	0.0314	5.75	1.23	0.2263	0.0104	0.0622	0.0044	2691	296	1938	186	1315	55	1220	84		
RSA08-003	-142	None	59756	0.9383	0.0059	382.75	5.34	2.9590	0.0326	13.9287	0.3049	5148	9	6042	14	8870	53	54639	413		
RSA08-004c	76.08	Disc	5677	0.2188	0.0303	4.23	0.77	0.1401	0.0063	0.0379	0.0064	2972	232	1679	149	845	36	752	125		
RSA08-005	10.14	Disc	906	0.2203	0.0057	16.06	0.63	0.5288	0.0082	0.1429	0.0027	2983	41	2881	37	2736	34	2700	48	y	
RSA08-006	2.23	Disc	59	0.2363	0.0034	19.63	0.50	0.6026	0.0082	0.1618	0.0021	3095	23	3073	25	3040	33	3031	36	y	y
RSA08-007c	14	Disc	2403	0.2435	0.0138	18.14	1.45	0.5404	0.0136	0.1447	0.0066	3143	90	2997	77	2785	57	2731	117		
RSA08-012	92.32	Disc	10584	0.1013	0.3874	0.31	1.33	0.0224	0.0104	0.0065	0.0489	1647	17625	276	1031	143	65	131	981		
RSA08-013c	32.5	Disc	2807	0.2573	0.0282	15.57	2.35	0.4391	0.0192	0.1170	0.0511	3230	177	2851	144	2347	86	2236	924		
RSA08-015c	38.91	Disc	579	0.1677	0.0042	6.80	0.25	0.2942	0.0041	0.0816	0.0044	2534	42	2086	32	1663	20	1586	83	y	
RSA08-016c	1.11	Disc	272	0.2371	0.0029	19.97	0.44	0.6108	0.0075	0.1639	0.0019	3101	19	3090	21	3073	30	3068	33	y	y
RSA08-017	86.84	Disc	4978	0.5052	0.1477	8.57	5.36	0.1231	0.0429	0.0309	0.0159	4256	18296	2294	568	748	246	614	313		
RSA08-019c	55.7	Disc	8009	0.1984	0.0465	6.63	1.97	0.2423	0.0160	0.0661	0.0164	2813	435	2063	263	1399	83	1294	310		

						Ratios (uncorrected)								Ages (uncorrected; Ma)								
	Th	U	Th/U	Common Pb		$^{207}Pb/^{206}Pb$		$^{207}Pb/^{235}U$		$^{206}Pb/^{238}U$		$^{208}Pb/^{232}Th$		$^{207}Pb/^{206}Pb$		$^{207}Pb/^{235}U$		$^{206}Pb/^{238}U$		$^{208}Pb/^{232}Th$		Inc.?
	ppm	ppm		%	1σ	Ratio	1σ	Ratio	1σ	Ratio	1σ	Ratio	1σ	Age	1σ	Age	1σ	Age	1σ	Age	1σ	
RSA08-021c	278	503	0.55	41.51	2.31	0.5094	0.0116	55.42	1.23	0.7893	0.0104	1.398	0.059	4269	17	4095	22	3751	37	17682	498	
RSA08-022	248	835	0.30			0.9342	0.0298	190.65	5.94	1.4800	0.0232	11.312	0.734	5142	26	5337	31	5855	60	50744	1205	
RSA08-025c	359	1397	0.26			0.8953	0.0207	77.58	1.73	0.6288	0.0080	5.664	0.253	5081	17	4431	22	3145	32	38337	766	
RSA08-031	1092	1067	1.02	25.8	1.29	0.3526	0.0060	14.16	0.23	0.2914	0.0033	0.218	0.006	3718	12	2761	16	1648	16	3981	107	
RSA08-034	156	331	0.47			0.6119	0.0158	85.23	2.14	1.0113	0.0139	2.796	0.140	4537	20	4526	25	4505	45	26961	743	
RSA08-038	165	315	0.52	14.88	1.13	0.3328	0.0089	30.52	0.78	0.6654	0.0091	0.559	0.029	3630	22	3504	25	3288	35	8981	373	
RSA08-049c	78	729	0.11	83.19	5.64	0.7960	0.0189	62.23	1.44	0.5673	0.0074	9.540	0.432	4915	18	4211	23	2897	30	47603	829	
RSA08-050r	292	1391	0.21	69.77	2.78	0.6589	0.0121	37.63	0.68	0.4142	0.0049	2.998	0.099	4644	13	3710	18	2234	22	28010	499	
RSA08-051	165	812	0.20	46.81	3.14	0.5359	0.0166	37.03	1.13	0.5008	0.0080	2.559	0.158	4343	25	3694	30	2617	34	25658	897	
RSA08-054c	332	693	0.48	64.45	2.14	0.6257	0.0088	68.06	0.96	0.7889	0.0086	2.361	0.054	4569	9	4300	14	3749	31	24503	322	
RSA08-057	111	144	0.78	7.16	1.51	0.2915	0.0122	24.04	0.96	0.5983	0.0111	0.267	0.024	3425	37	3270	39	3023	45	4788	381	
RSA08-058	53	441	0.12	82.23	3.92	0.7673	0.0156	82.72	1.65	0.7820	0.0098	11.472	0.440	4862	14	4496	20	3724	35	51005	712	
RSA08-059	863	2666	0.32	68.84	4.62	0.6343	0.0224	24.91	0.86	0.2847	0.0049	1.327	0.097	4589	29	3305	34	1615	25	17073	839	
RSA08-060	267	263	1.01	4.24	0.52	0.2499	0.0040	17.61	0.28	0.5110	0.0058	0.178	0.005	3184	12	2968	15	2661	25	3314	84	
RSA08-068	354	4216	0.08			0.3782	0.0185	7.29	0.34	0.1399	0.0027	1.649	0.166	3825	45	2147	42	844	15	19687	1267	
SWA10a-001	250	314	0.80			0.2973	0.0045	28.93	0.45	0.7061	0.0087	0.182	0.005	3456	10	3451	15	3444	33	3380	84	
SWA10a-003c	117	186	0.63	1.24	0.34	0.2389	0.0045	17.99	0.33	0.5462	0.0068	0.168	0.006	3113	14	2989	18	2810	28	3137	97	y
SWA10a-006	233	1088	0.21	1.06	0.26	0.2327	0.0080	10.57	0.36	0.3293	0.0059	0.122	0.008	3071	30	2486	32	1835	28	2333	146	
SWA10a-007	931	2050	0.45	3.86	0.37	0.1452	0.0027	1.95	0.04	0.0974	0.0013	0.044	0.002	2290	15	1098	13	599	7	879	31	
SWA10a-010	144	1125	0.13	1.29	0.07	0.2406	0.0033	16.24	0.24	0.4894	0.0061	0.237	0.005	3124	10	2891	14	2568	26	4294	83	
SWA10a-016	469	1272	0.37	1.92	0.14	0.2336	0.0028	6.19	0.08	0.1921	0.0022	0.073	0.001	3077	9	2003	11	1133	12	1416	22	
SWA10a-017	585	1258	0.46	5.43	0.48	0.2367	0.0053	7.63	0.17	0.2338	0.0032	0.119	0.005	3098	17	2188	20	1354	17	2280	88	
SWA10a-018	535	779	0.69	1.29	0.32	0.2998	0.0053	20.45	0.37	0.4946	0.0064	0.149	0.004	3469	13	3113	18	2591	28	2801	78	
SWA10a-019	211	596	0.35			0.2409	0.0038	20.20	0.33	0.6081	0.0077	0.162	0.004	3126	11	3101	16	3062	31	3032	73	y
SWA10a-020c	375	954	0.39	5.55	0.28	0.3063	0.0043	13.40	0.20	0.3172	0.0040	0.176	0.004	3502	10	2708	14	1776	19	3280	66	

				Ratios (corrected)								Ages (corrected; Ma)									
	Disc.	Correction type	^{204}Pb	^{207}Pb/^{206}Pb		^{207}Pb/^{235}U		^{206}Pb/^{238}U		^{208}Pb/^{232}Th		^{207}Pb/^{206}Pb		^{207}Pb/^{235}U		^{206}Pb/^{238}U		^{208}Pb/^{232}Th		Inc.?	
	%		cps	Ratio	1σ	Ratio	1σ	Ratio	1σ	Ratio	1σ	Age	1σ	Age	1σ	Age	1σ	Age	1σ	Int	W/A
RSA08-021c	32.24	Disc	6967	0.2776	0.0272	17.67	2.48	0.4616	0.0205	0.1221	0.0182	3349	157	2972	135	2447	91	2329	327		
RSA08-022	-21.3	None	49221	0.9342	0.0171	190.65	5.94	1.4800	0.0232	11.3120	0.7341	5142	26	5337	31	5855	60	50744	1205		
RSA08-025c	47.61	None	38365	0.8953	0.0109	77.58	1.73	0.6288	0.0080	5.6640	0.2526	5081	17	4431	22	3145	32	38337	766		
RSA08-031	58.31	Disc	3815	0.1845	0.0131	5.50	0.51	0.2162	0.0051	0.0594	0.0021	2693	116	1900	79	1262	27	1167	40		
RSA08-034	1.08	None	8145	0.6119	0.0086	85.23	2.14	1.0113	0.0139	2.7959	0.1395	4537	20	4526	25	4505	45	26961	743		
RSA08-038	10.15	Disc	1358	0.2447	0.0104	19.11	1.18	0.5664	0.0120	0.1516	0.0060	3151	66	3047	59	2893	49	2853	105		
RSA08-049c	90.56	Disc	14365	0.5973	0.1266	7.85	4.20	0.0953	0.0324	0.0235	0.4363	4501	359	2214	482	587	191	470	8616		
RSA08-050r	80.43	Disc	16788	0.2505	0.0668	4.32	1.55	0.1252	0.0120	0.0334	0.0405	3188	498	1698	295	760	69	665	792		
RSA08-051	60.48	Disc	6846	0.2726	0.0409	10.01	2.12	0.2664	0.0173	0.0706	0.0348	3321	244	2436	196	1522	88	1379	657		
RSA08-054c	55.51	Disc	14132	0.2448	0.0450	9.46	2.32	0.2804	0.0182	0.0751	0.0305	3151	309	2384	225	1594	91	1463	573		
RSA08-057	12.94	Disc	251	0.2495	0.0127	19.11	1.44	0.5555	0.0148	0.1484	0.0037	3181	79	3047	73	2848	61	2797	65		
RSA08-058	84.3	Disc	11556	0.4504	0.1178	8.63	4.09	0.1390	0.0312	0.0352	0.2555	4086	501	2300	431	839	176	699	4988		
RSA08-059	83.31	Disc	18655	0.1907	0.1099	2.33	1.68	0.0887	0.0135	0.0243	0.0326	2748	1323	1222	513	548	80	485	644		
RSA08-060	17.76	Disc	283	0.2240	0.0040	15.11	0.45	0.4893	0.0069	0.1320	0.0018	3009	28	2822	28	2568	30	2507	32	y	
RSA08-068	82.74	None	7982	0.3782	0.0116	7.29	0.34	0.1399	0.0027	1.6486	0.1660	3825	45	2147	42	844	15	19687	1267		
SWA10a-001	0.49	None	33	0.2973	0.0021	28.93	0.45	0.7061	0.0087	0.1820	0.0049	3456	10	3451	15	3444	33	3380	84		
SWA10a-003c	11.27	Disc	44	0.2314	0.0031	17.21	0.42	0.5395	0.0072	0.1451	0.0018	3062	20	2947	23	2781	30	2739	32	y	
SWA10a-006	45.61	Disc	147	0.2263	0.0049	10.17	0.37	0.3259	0.0058	0.0879	0.0015	3026	32	2450	33	1818	28	1702	28		
SWA10a-007	72.93	Disc	213	0.1173	0.0032	1.51	0.06	0.0937	0.0013	0.0269	0.0004	1915	46	936	23	577	8	537	8		
SWA10a-010	20.87	Disc	234	0.2329	0.0016	15.51	0.25	0.4831	0.0061	0.1299	0.0021	3072	10	2847	15	2541	27	2468	38		
SWA10a-016	68.14	Disc	523	0.2219	0.0015	5.76	0.09	0.1884	0.0023	0.0509	0.0007	2994	11	1941	14	1113	13	1003	13		
SWA10a-017	60.13	Disc	805	0.2022	0.0047	6.16	0.23	0.2211	0.0036	0.0602	0.0011	2844	36	1999	32	1288	19	1182	22		
SWA10a-018	30.57	Disc	279	0.2928	0.0033	19.71	0.46	0.4883	0.0071	0.1285	0.0018	3433	16	3077	22	2563	31	2444	32		
SWA10a-019	2.53	None	76	0.2409	0.0018	20.20	0.33	0.6081	0.0077	0.1619	0.0042	3126	11	3101	16	3062	31	3032	73	y	y
SWA10a-020c	55.79	Disc	645	0.2752	0.0028	11.37	0.24	0.2996	0.0042	0.0793	0.0017	3336	15	2554	20	1690	21	1543	32		

						Ratios (uncorrected)								Ages (uncorrected; Ma)								
	Th	U	Th/U	Common Pb		$^{207}Pb/^{206}Pb$		$^{207}Pb/^{235}U$		$^{206}Pb/^{238}U$		$^{208}Pb/^{232}Th$		$^{207}Pb/^{206}Pb$		$^{207}Pb/^{235}U$		$^{206}Pb/^{238}U$		$^{208}Pb/^{232}Th$		Inc.?
	ppm	ppm		%	1σ	Ratio	1σ	Ratio	1σ	Ratio	1σ	Ratio	1σ	Age	1σ	Age	1σ	Age	1σ	Age	1σ	
SWA10a-020b	177	1007	0.18	2.78	0.14	0.3046	0.0043	14.77	0.22	0.3516	0.0043	0.211	0.005	3494	10	2800	14	1942	20	3863	80	
SWA10a-021	1137	2195	0.52	7.75	0.46	0.1936	0.0033	4.55	0.08	0.1706	0.0022	0.100	0.003	2773	13	1741	14	1015	12	1921	52	
SWA10a-022c	746	1512	0.49	0.9	0.38	0.2178	0.0059	7.14	0.20	0.2374	0.0039	0.073	0.004	2965	23	2129	25	1373	20	1427	70	
SWA10a-025	341	1847	0.18	3.13	0.25	0.2281	0.0052	6.38	0.15	0.2027	0.0031	0.128	0.006	3039	18	2030	21	1190	17	2431	100	
SWA10a-026	155	438	0.35			0.2405	0.0029	18.76	0.24	0.5659	0.0066	0.156	0.003	3123	8	3030	12	2891	27	2922	44	y
SWA10a-030	219	502	0.44	1.9	0.16	0.2380	0.0029	11.10	0.15	0.3385	0.0040	0.121	0.002	3106	9	2532	12	1879	19	2316	36	y
SWA10a-032	1973	4241	0.47	6.35	0.42	0.1627	0.0030	1.03	0.02	0.0461	0.0006	0.026	0.001	2484	14	720	10	290	4	518	16	
SWA10a-042c	335	1857	0.18	5.15	0.22	0.1928	0.0030	2.68	0.04	0.1007	0.0012	0.089	0.002	2766	11	1322	12	619	7	1718	40	
SWA10a-043	990	3203	0.31			0.1988	0.0031	3.18	0.05	0.1160	0.0015	0.252	0.006	2817	11	1452	12	707	8	4536	101	
SWA10a-047	2024	2918	0.69	9.27	0.58	0.2234	0.0037	2.87	0.05	0.0930	0.0012	0.050	0.001	3005	12	1373	13	573	7	992	27	
SWA10a-049c	599	878	0.68	3.25	0.35	0.2905	0.0047	14.04	0.24	0.3507	0.0045	0.126	0.003	3420	11	2753	16	1938	21	2397	60	
SWA10a-050c	105	251	0.42	3.92	0.27	0.2475	0.0039	9.75	0.16	0.2858	0.0036	0.132	0.003	3169	11	2412	15	1620	18	2501	60	
SWA10a-051c	108	167	0.65			0.3258	0.0067	28.17	0.59	0.6276	0.0090	0.169	0.006	3597	15	3425	20	3140	35	3164	105	
SWA10a-051r	75	605	0.12	0.74	0.09	0.2787	0.0061	14.57	0.31	0.3792	0.0050	0.149	0.006	3355	16	2788	20	2073	23	2801	100	
SWA10a-052c	362	783	0.46	4.93	0.25	0.2261	0.0029	11.07	0.15	0.3553	0.0042	0.174	0.003	3024	9	2529	13	1960	20	3238	54	
SWA10a-053	598	2114	0.28			0.1686	0.0026	3.56	0.06	0.1533	0.0020	0.045	0.001	2544	12	1540	13	919	11	883	20	
SWA10a-054	1299	1759	0.74			0.1797	0.0030	6.47	0.11	0.2614	0.0033	0.035	0.001	2650	12	2042	15	1497	17	687	17	
SWA10a-059c	957	1719	0.56	2.86	0.37	0.2030	0.0044	6.09	0.13	0.2176	0.0032	0.082	0.003	2851	16	1988	19	1269	17	1594	51	
SWA10a-063c	632	1693	0.37	2.5	0.29	0.1904	0.0046	5.36	0.13	0.2042	0.0031	0.084	0.003	2746	20	1878	21	1198	16	1637	59	
SWA10a-064c	145	197	0.74	0.8	0.29	0.3386	0.0055	31.98	0.53	0.6848	0.0083	0.193	0.005	3656	12	3550	16	3363	32	3559	88	
SWA10a-065	624	1638	0.38	3.07	0.28	0.1974	0.0037	5.08	0.10	0.1865	0.0023	0.082	0.003	2805	15	1833	16	1103	13	1595	51	
SWA10a-071	2539	4884	0.52	4.21	0.26	0.1725	0.0024	1.35	0.02	0.0567	0.0007	0.025	0.001	2582	11	867	9	355	4	502	10	
SWA10a-072c	1262	2301	0.55	2.57	0.27	0.1921	0.0032	3.21	0.05	0.1211	0.0015	0.045	0.001	2760	13	1459	13	737	9	885	22	
SWA10a-075	1074	3173	0.34	2.57	0.19	0.1546	0.0025	2.84	0.05	0.1333	0.0016	0.058	0.001	2398	13	1367	12	807	9	1149	27	
SWA10a-109c	821	1436	0.57	2.34	0.27	0.1892	0.0029	6.56	0.11	0.2518	0.0031	0.090	0.002	2735	12	2055	14	1448	16	1745	42	

				Ratios (corrected)								Ages (corrected; Ma)									
	Disc.	Correction type	^{204}Pb	^{207}Pb/^{206}Pb		^{207}Pb/^{235}U		^{206}Pb/^{238}U		^{208}Pb/^{232}Th		^{207}Pb/^{206}Pb		^{207}Pb/^{235}U		^{206}Pb/^{238}U		^{208}Pb/^{232}Th		Inc.?	
	%		cps	Ratio	1σ	Ratio	1σ	Ratio	1σ	Ratio	1σ	Age	1σ	Age	1σ	Age	1σ	Age	1σ	Int	W/A
SWA10a-020b	51.06	Disc	455	0.2894	0.0022	13.64	0.23	0.3418	0.0043	0.0901	0.0021	3415	11	2725	16	1895	21	1743	38		
SWA10a-021	61.8	Disc	918	0.1397	0.0042	3.03	0.13	0.1573	0.0024	0.0444	0.0008	2223	49	1415	32	942	13	878	16		
SWA10a-022c	59.02	Disc	286	0.2125	0.0043	6.89	0.24	0.2353	0.0042	0.0638	0.0011	2925	31	2098	31	1362	22	1250	20		
SWA10a-025	65.37	Disc	346	0.2087	0.0034	5.65	0.17	0.1964	0.0032	0.0533	0.0012	2895	25	1924	25	1156	17	1050	24		
SWA10a-026	9.21	None	52	0.2405	0.0014	18.76	0.24	0.5659	0.0066	0.1556	0.0025	3123	8	3030	12	2891	27	2922	44	y	y
SWA10a-030	44.59	Disc	203	0.2264	0.0017	10.36	0.17	0.3320	0.0041	0.0895	0.0012	3027	11	2468	16	1848	20	1733	22	y	
SWA10a-032	87.5	Disc	839	0.1170	0.0039	0.70	0.03	0.0431	0.0007	0.0124	0.0002	1911	56	536	19	272	4	249	5		
SWA10a-042c	79.16	Disc	413	0.1579	0.0024	2.08	0.05	0.0956	0.0012	0.0267	0.0008	2433	24	1142	17	588	7	532	16		
SWA10a-043	78.84	None	1779	0.1988	0.0015	3.18	0.05	0.1160	0.0015	0.2516	0.0063	2817	11	1452	12	707	8	4536	101		
SWA10a-047	81.87	Disc	1028	0.1608	0.0052	1.87	0.08	0.0844	0.0014	0.0235	0.0005	2464	51	1071	30	522	8	470	9		
SWA10a-049c	49.61	Disc	515	0.2721	0.0033	12.73	0.30	0.3393	0.0049	0.0899	0.0013	3318	18	2660	22	1883	23	1740	25		
SWA10a-050c	53.78	Disc	194	0.2235	0.0028	8.46	0.19	0.2746	0.0037	0.0741	0.0012	3006	19	2282	21	1564	19	1445	23	y	
SWA10a-051c	16.09	None	63	0.3258	0.0033	28.17	0.59	0.6276	0.0090	0.1695	0.0061	3597	15	3425	20	3140	35	3164	105		
SWA10a-051r	44.39	Disc	116	0.2746	0.0032	14.25	0.31	0.3764	0.0049	0.0997	0.0014	3332	17	2766	21	2060	23	1921	26		
SWA10a-052c	37.34	Disc	401	0.1944	0.0024	9.05	0.20	0.3378	0.0044	0.0924	0.0016	2780	19	2343	20	1876	21	1786	29		
SWA10a-053	68.36	None	184	0.1686	0.0012	3.56	0.06	0.1533	0.0020	0.0447	0.0010	2544	12	1540	13	919	11	883	20		
SWA10a-054	48.65	None	287	0.1797	0.0014	6.47	0.11	0.2614	0.0033	0.0346	0.0009	2650	12	2042	15	1497	17	687	17		
SWA10a-059c	59.22	Disc	578	0.1842	0.0036	5.37	0.18	0.2113	0.0034	0.0581	0.0009	2691	32	1880	28	1236	18	1141	18		
SWA10a-063c	59.82	Disc	2655	0.1738	0.0033	4.77	0.15	0.1991	0.0031	0.0550	0.0009	2595	31	1780	27	1170	17	1083	17		
SWA10a-064c	10.45	Disc	104	0.3347	0.0031	31.35	0.62	0.6793	0.0089	0.1767	0.0023	3639	14	3530	19	3342	34	3288	39		
SWA10a-065	64.07	Disc	472	0.1773	0.0028	4.42	0.12	0.1808	0.0024	0.0499	0.0007	2628	26	1716	22	1071	13	984	14		
SWA10a-071	87.12	Disc	1042	0.1434	0.0024	1.07	0.03	0.0543	0.0007	0.0153	0.0002	2269	28	741	14	341	4	307	4		
SWA10a-072c	76.33	Disc	488	0.1751	0.0025	2.85	0.07	0.1180	0.0016	0.0326	0.0004	2607	24	1369	19	719	9	648	9		
SWA10a-075	67.81	Disc	691	0.1366	0.0019	2.45	0.06	0.1299	0.0017	0.0368	0.0005	2185	24	1257	17	787	9	730	10		
SWA10a-109c	50.34	Disc	338	0.1736	0.0024	5.89	0.14	0.2459	0.0033	0.0680	0.0009	2593	22	1959	21	1417	17	1329	17		

						Ratios (uncorrected)								Ages (uncorrected; Ma)								
	Th	U	Th/U	Common Pb		$^{207}Pb/^{206}Pb$		$^{207}Pb/^{235}U$		$^{206}Pb/^{238}U$		$^{208}Pb/^{232}Th$		$^{207}Pb/^{206}Pb$		$^{207}Pb/^{235}U$		$^{206}Pb/^{238}U$		$^{208}Pb/^{232}Th$		Inc.?
	ppm	ppm		%	1σ	Ratio	1σ	Ratio	1σ	Ratio	1σ	Ratio	1σ	Age	1σ	Age	1σ	Age	1σ	Age	1σ	
SWA10a-116	723	1529	0.47			0.2078	0.0044	20.88	0.45	0.7309	0.0109	0.157	0.006	2888	16	3133	21	3537	41	2941	99	
SWA10a-123	617	1617	0.38	7.39	0.36	0.1850	0.0030	5.16	0.09	0.2024	0.0026	0.138	0.004	2698	12	1846	14	1188	14	2607	63	
SWA10a-128	272	705	0.39	6.4	0.49	0.2658	0.0064	20.43	0.49	0.5589	0.0089	0.341	0.014	3281	19	3112	23	2862	37	5935	210	
SWA10a-130	4497	4908	0.92	1.67	0.36	0.1674	0.0026	1.14	0.02	0.0495	0.0006	0.016	0.000	2532	12	773	9	311	4	311	7	
SWA10a-133c	1983	1381	1.44	3.94	1.32	0.2269	0.0072	10.84	0.33	0.3472	0.0058	0.111	0.006	3030	26	2510	28	1921	28	2135	113	
SWA10a-135	528	676	0.78			0.2380	0.0044	21.19	0.40	0.6464	0.0083	0.158	0.005	3106	14	3147	18	3214	32	2973	91	y
SWA10a-142	978	3077	0.32	3.19	0.27	0.1636	0.0034	2.73	0.06	0.1212	0.0017	0.059	0.002	2494	17	1336	16	737	10	1165	41	
SWA10a-145	442	728	0.61			0.2335	0.0038	15.49	0.26	0.4817	0.0061	0.119	0.003	3076	12	2846	16	2535	27	2275	58	
SWA10a-155	395	710	0.56	2.13	0.27	0.2315	0.0038	11.72	0.20	0.3675	0.0047	0.128	0.004	3063	12	2582	16	2018	22	2428	63	
RSA09-001c	305	892	0.34	3.49	0.31	0.2239	0.0046	11.19	0.23	0.3625	0.0049	0.175	0.006	3009	16	2539	19	1994	23	3255	111	y
RSA09-006	289	610	0.47	4.35	0.79	0.2072	0.0076	9.18	0.33	0.3217	0.0063	0.148	0.011	2883	33	2356	33	1798	30	2788	191	
RSA09-008	255	2405	0.11	2.36	0.22	0.1466	0.0038	1.94	0.05	0.0961	0.0014	0.059	0.003	2307	23	1096	17	591	8	1161	54	
RSA09-015c	514	1484	0.35	9.53	0.8	0.1998	0.0052	4.49	0.12	0.1631	0.0025	0.113	0.006	2825	22	1729	22	974	14	2166	101	
RSA09-021	336	537	0.63	2.98	0.46	0.2358	0.0055	14.32	0.33	0.4405	0.0063	0.166	0.007	3092	19	2771	22	2353	28	3101	122	
RSA09-024	214	732	0.29	9.39	0.94	0.2311	0.0081	7.23	0.25	0.2269	0.0042	0.213	0.015	3059	31	2140	31	1318	22	3895	246	y
RSA09-026	133	2947	0.05	2.31	0.11	0.1622	0.0030	4.35	0.08	0.1947	0.0025	0.297	0.009	2479	15	1704	15	1147	13	5257	147	
RSA09-030c	16	27	0.60			0.1863	0.0022	5.56	0.07	0.2165	0.0026	0.053	0.001	2709	9	1910	11	1263	14	1047	16	
RSA09-033	572	1280	0.45	1.15	0.37	0.2177	0.0056	13.17	0.34	0.4385	0.0071	0.140	0.007	2964	21	2692	25	2344	32	2654	118	
RSA09-036c	4967	1362	3.65			0.2672	0.0048	6.48	0.12	0.1760	0.0023	0.029	0.001	3290	13	2043	16	1045	13	577	17	
RSA09-036r	356	3298	0.11			0.1095	0.0026	2.09	0.05	0.1381	0.0022	0.281	0.012	1791	22	1144	17	834	12	5000	195	
RSA09-037	120	203	0.59	2.97	0.32	0.2251	0.0036	12.08	0.20	0.3892	0.0050	0.143	0.004	3018	12	2610	16	2119	23	2697	64	y
RSA09-038c	1871	3116	0.60			0.1823	0.0057	4.56	0.14	0.1816	0.0031	0.045	0.003	2674	28	1743	26	1076	17	890	51	
RSA09-041	246	528	0.47			0.2454	0.0047	14.59	0.29	0.4319	0.0060	0.089	0.003	3156	14	2789	19	2314	27	1728	56	
RSA09-053r	2	16	0.15			0.1960	0.0054	8.58	0.24	0.3175	0.0048	8.622	0.456	2794	24	2294	25	1778	23	45761	959	
RSA09-063c	521	1694	0.31	8.95	0.92	0.2162	0.0075	4.91	0.17	0.1646	0.0029	0.138	0.009	2953	31	1804	29	982	16	2614	163	

				Ratios (corrected)								Ages (corrected; Ma)									
	Disc.	Correction type	^{204}Pb	^{207}Pb/^{206}Pb		^{207}Pb/^{235}U		^{206}Pb/^{238}U		^{208}Pb/^{232}Th		^{207}Pb/^{206}Pb		^{207}Pb/^{235}U		^{206}Pb/^{238}U		^{208}Pb/^{232}Th		Inc.?	
	%		cps	Ratio	1σ	Ratio	1σ	Ratio	1σ	Ratio	1σ	Age	1σ	Age	1σ	Age	1σ	Age	1σ	Int	W/A
SWA10a-116	-28.98	None	306	0.2078	0.0021	20.88	0.45	0.7309	0.0109	0.1566	0.0057	2888	16	3133	21	3537	41	2941	99		
SWA10a-123	52.32	Disc	525	0.1329	0.0034	3.44	0.12	0.1874	0.0027	0.0532	0.0012	2137	44	1513	29	1107	14	1047	23		
SWA10a-128	12.63	Disc	730	0.2261	0.0050	16.31	0.59	0.5231	0.0092	0.1410	0.0035	3025	34	2895	35	2712	39	2667	63		
SWA10a-130	89.28	Disc	704	0.1559	0.0029	1.05	0.03	0.0486	0.0007	0.0136	0.0002	2411	30	726	16	306	4	273	4		
SWA10a-133c	39.72	Disc	2657	0.2015	0.0102	9.27	0.67	0.3335	0.0080	0.0909	0.0018	2839	79	2365	66	1855	39	1758	34		
SWA10a-135	-4.3	None	65	0.2380	0.0022	21.19	0.40	0.6464	0.0083	0.1585	0.0052	3106	14	3147	18	3214	32	2973	91	y	y
SWA10a-142	71.78	Disc	984	0.1412	0.0028	2.28	0.07	0.1173	0.0018	0.0331	0.0006	2241	33	1207	22	715	10	658	11		
SWA10a-145	21.31	None	216	0.2335	0.0018	15.49	0.26	0.4817	0.0061	0.1191	0.0032	3076	12	2846	16	2535	27	2275	58	y	
SWA10a-155	38.45	Disc	254	0.2181	0.0027	10.82	0.25	0.3597	0.0049	0.0973	0.0013	2967	19	2507	21	1981	23	1877	24		
RSA09-001c	36.83	Disc	389	0.2018	0.0032	9.73	0.27	0.3498	0.0052	0.0953	0.0017	2841	25	2410	26	1934	25	1840	30		
RSA09-006	39.16	Disc	85	0.1784	0.0072	7.57	0.45	0.3077	0.0070	0.0848	0.0018	2638	66	2181	54	1729	34	1646	34		
RSA09-008	75.61	Disc	437	0.1300	0.0026	1.68	0.05	0.0938	0.0014	0.0267	0.0005	2097	35	1001	21	578	8	532	10		
RSA09-015c	62.41	Disc	1225	0.1327	0.0073	2.70	0.19	0.1475	0.0029	0.0419	0.0010	2134	95	1328	53	887	16	829	20		
RSA09-021	26.7	Disc	129	0.2174	0.0042	12.81	0.42	0.4274	0.0069	0.1157	0.0018	2962	31	2666	31	2294	31	2212	33	y	
RSA09-024	57.46	Disc	231	0.1684	0.0089	4.77	0.35	0.2056	0.0048	0.0570	0.0022	2542	86	1780	61	1205	26	1121	41		
RSA09-026	55.7	Disc	977	0.1463	0.0018	3.84	0.09	0.1902	0.0024	0.0535	0.0028	2303	20	1600	18	1122	13	1053	54		
RSA09-030c	58.58	None	90	0.1863	0.0011	5.56	0.07	0.2165	0.0026	0.0532	0.0009	2709	9	1910	11	1263	14	1047	16	y	
RSA09-033	24.03	Disc	567	0.2106	0.0041	12.59	0.43	0.4335	0.0075	0.1177	0.0019	2910	31	2649	32	2321	34	2248	34		
RSA09-036c	73.6	None	1165	0.2672	0.0023	6.48	0.12	0.1760	0.0023	0.0290	0.0009	3290	13	2043	16	1045	13	577	17		
RSA09-036r	56.88	None	175	0.1095	0.0014	2.09	0.05	0.1381	0.0022	0.2807	0.0123	1791	22	1144	17	834	12	5000	195		
RSA09-037	32.86	Disc	167	0.2063	0.0029	10.74	0.28	0.3776	0.0054	0.1027	0.0015	2877	22	2501	24	2065	25	1976	27		
RSA09-038c	64.67	None	821	0.1823	0.0032	4.56	0.14	0.1816	0.0031	0.0450	0.0027	2674	28	1743	26	1076	17	890	51		
RSA09-041	31.74	None	718	0.2454	0.0023	14.59	0.29	0.4319	0.0060	0.0892	0.0030	3156	14	2789	19	2314	27	1728	56		
RSA09-053r	41.48	None	4916	0.1960	0.0030	8.58	0.24	0.3175	0.0048	8.6217	0.4565	2794	24	2294	25	1778	23	45761	959		
RSA09-063c	66.87	Disc	266	0.1554	0.0091	3.21	0.25	0.1499	0.0033	0.0419	0.0013	2406	97	1460	60	900	19	829	25		

						Ratios (uncorrected)								Ages (uncorrected; Ma)								
	Th	U	Th/U	Common Pb		$^{207}Pb/^{206}Pb$		$^{207}Pb/^{235}U$		$^{206}Pb/^{238}U$		$^{208}Pb/^{232}Th$		$^{207}Pb/^{206}Pb$		$^{207}Pb/^{235}U$		$^{206}Pb/^{238}U$		$^{208}Pb/^{232}Th$		Inc.?
	ppm	ppm		%	1σ	Ratio	1σ	Ratio	1σ	Ratio	1σ	Ratio	1σ	Age	1σ	Age	1σ	Age	1σ	Age	1σ	
RSA09-067	9	6	1.39			0.2303	0.0096	18.01	0.75	0.5672	0.0105	0.830	0.076	3054	40	2990	40	2896	43	12218	843	
RSA09-069	145	2012	0.07	1.04	0.06	0.1285	0.0024	3.57	0.07	0.2014	0.0027	0.157	0.005	2077	16	1542	15	1183	14	2951	92	
RSA09-070	159	2105	0.08	3.68	0.2	0.1367	0.0029	3.15	0.07	0.1674	0.0024	0.214	0.008	2186	18	1446	17	998	13	3921	138	
RSA09-073	461	1132	0.41	2.85	0.51	0.2071	0.0062	6.01	0.18	0.2105	0.0033	0.083	0.005	2883	26	1977	26	1231	18	1609	86	
RSA09-079	273	412	0.66			0.2251	0.0049	13.02	0.28	0.4201	0.0057	0.121	0.005	3017	17	2681	20	2261	26	2307	88	y
RSA09-092c	172	229	0.75	5.59	0.49	0.2370	0.0062	8.70	0.22	0.2663	0.0040	0.173	0.009	3100	21	2307	23	1522	20	3227	154	
RSA09-092r	86	2204	0.04	2.07	0.13	0.1105	0.0023	2.12	0.04	0.1390	0.0018	0.126	0.005	1808	19	1154	14	839	10	2407	95	
RSA09-097c	132	1041	0.13	2.68	0.14	0.1970	0.0037	7.73	0.15	0.2844	0.0037	0.258	0.009	2801	14	2200	17	1614	19	4645	138	
RSA09-097r	257	1665	0.15	3.66	0.3	0.1270	0.0040	1.53	0.05	0.0876	0.0014	0.086	0.005	2056	30	944	19	542	8	1676	94	
RSA09-102	305	3425	0.09	1.99	0.13	0.1233	0.0024	1.78	0.04	0.1049	0.0014	0.065	0.002	2005	16	1039	13	643	8	1281	43	
RSA09-104c	58	72	0.81			0.2442	0.0043	21.32	0.38	0.6334	0.0081	0.174	0.005	3147	13	3153	17	3163	32	3246	95	
RSA09-105	228	2358	0.10	2.09	0.08	0.1684	0.0024	5.43	0.08	0.2339	0.0029	0.210	0.005	2542	11	1889	13	1355	15	3854	78	
RSA09-107c	91	2331	0.04	1.97	0.1	0.1432	0.0028	3.08	0.06	0.1558	0.0020	0.210	0.007	2266	16	1427	15	934	11	3858	122	
RSA09-112c	38	82	0.46	3.54	0.29	0.2582	0.0044	19.65	0.33	0.5520	0.0069	0.236	0.007	3236	12	3074	16	2833	29	4277	111	
RSA09-112r	97	997	0.10	3	0.13	0.1553	0.0026	4.53	0.08	0.2116	0.0026	0.212	0.006	2405	13	1737	14	1237	14	3889	99	
RSA09-113c	388	462	0.84			0.2354	0.0051	11.84	0.26	0.3660	0.0052	0.096	0.004	3089	17	2592	20	2010	25	1848	66	
RSA09-115c	272	2461	0.11	13.38	0.45	0.1978	0.0031	6.23	0.10	0.2287	0.0029	0.619	0.015	2808	12	2009	14	1328	15	9735	185	
RSA09-125c	437	1322	0.33	3.05	0.24	0.1591	0.0030	5.26	0.10	0.2406	0.0032	0.114	0.003	2446	15	1863	16	1390	17	2179	63	
RSA09-131	265	5000	0.05	4.62	0.18	0.1314	0.0024	1.07	0.02	0.0593	0.0008	0.185	0.006	2117	16	739	10	371	5	3432	97	
RSA09-138	561	4773	0.12	0.99	0.09	0.1081	0.0022	1.11	0.02	0.0746	0.0010	0.035	0.001	1768	19	757	11	464	6	691	23	
RSA09-139	435	2759	0.16	2.34	0.15	0.1279	0.0027	1.66	0.04	0.0946	0.0013	0.068	0.002	2069	19	994	14	582	8	1323	46	
RSA09-142c	1240	877	1.41			0.2423	0.0063	4.21	0.11	0.1264	0.0019	0.092	0.005	3135	22	1676	21	767	11	1783	86	
RSA09-142r	486	3558	0.14	2.45	0.19	0.1208	0.0028	1.95	0.05	0.1171	0.0017	0.078	0.003	1969	21	1097	16	714	10	1512	63	
RSA09-146	224	3073	0.07	1.5	0.09	0.1102	0.0023	1.89	0.04	0.1247	0.0017	0.090	0.003	1802	18	1079	14	758	10	1745	54	
SWA03-001c	1032	3101	0.33			0.3337	0.0043	9.27	0.12	0.2015	0.0022	0.655	0.017	3634	9	2365	12	1183	12	10182	205	

				Ratios (corrected)								Ages (corrected; Ma)								
	Disc.	Correction type	^{204}Pb	^{207}Pb/^{206}Pb		^{207}Pb/^{235}U		^{206}Pb/^{238}U		^{208}Pb/^{232}Th		^{207}Pb/^{206}Pb		^{207}Pb/^{235}U		^{206}Pb/^{238}U		^{208}Pb/^{232}Th		Inc.?	
	%		cps	Ratio	1σ	Ratio	1σ	Ratio	1σ	Ratio	1σ	Age	1σ	Age	1σ	Age	1σ	Age	1σ	Int	W/A
RSA09-067	6.42	None	4323	0.2303	0.0060	18.01	0.75	0.5672	0.0105	0.8303	0.0763	3054	40	2990	40	2896	43	12218	843		
RSA09-069	44.26	Disc	317	0.1210	0.0013	3.33	0.07	0.1993	0.0026	0.0571	0.0013	1971	19	1487	16	1172	14	1122	25		
RSA09-070	49.84	Disc	366	0.1099	0.0024	2.44	0.08	0.1613	0.0024	0.0466	0.0019	1797	37	1255	24	964	13	921	37		
RSA09-073	61.23	Disc	376	0.1886	0.0053	5.32	0.23	0.2045	0.0036	0.0561	0.0009	2730	44	1872	37	1199	19	1103	18		
RSA09-079	29.68	None	229	0.2251	0.0025	13.02	0.28	0.4201	0.0057	0.1209	0.0049	3017	17	2681	20	2261	26	2307	88	y	
RSA09-092c	54.57	Disc	205	0.2016	0.0052	6.99	0.28	0.2514	0.0042	0.0685	0.0017	2839	40	2110	35	1446	22	1340	32	y	
RSA09-092r	49.26	Disc	154	0.0952	0.0017	1.79	0.05	0.1361	0.0018	0.0400	0.0010	1532	32	1040	18	822	10	792	20		
RSA09-097c	45.5	Disc	137	0.1794	0.0022	6.85	0.15	0.2768	0.0036	0.0763	0.0024	2648	19	2092	20	1575	18	1486	45		
RSA09-097r	70.51	Disc	166	0.0999	0.0036	1.16	0.06	0.0844	0.0014	0.0247	0.0008	1623	64	784	27	522	8	492	15		
RSA09-102	67.66	Disc	313	0.1088	0.0017	1.54	0.04	0.1028	0.0014	0.0298	0.0005	1780	27	948	16	631	8	593	11		
RSA09-104c	-0.65	None	28	0.2442	0.0021	21.32	0.38	0.6334	0.0081	0.1742	0.0055	3147	13	3153	17	3163	32	3246	95		
RSA09-105	48.99	Disc	585	0.1540	0.0014	4.86	0.08	0.2290	0.0027	0.0641	0.0019	2391	15	1796	15	1329	14	1255	36		
RSA09-107c	60.05	Disc	212	0.1292	0.0017	2.72	0.06	0.1528	0.0019	0.0435	0.0020	2087	22	1334	16	916	11	860	38		
RSA09-112c	13.78	Disc	77	0.2370	0.0030	17.40	0.40	0.5324	0.0070	0.1429	0.0022	3100	20	2957	22	2752	30	2700	39	y	
RSA09-112r	48.27	Disc	194	0.1342	0.0017	3.80	0.08	0.2053	0.0025	0.0582	0.0019	2154	22	1593	18	1203	13	1143	36		
RSA09-113c	40.67	None	98	0.2354	0.0026	11.84	0.26	0.3660	0.0052	0.0958	0.0036	3089	17	2592	20	2010	25	1848	66		
RSA09-115c	29.93	Disc	1455	0.0990	0.0049	2.70	0.16	0.1981	0.0029	0.0579	0.0061	1605	91	1329	45	1165	16	1138	116		
RSA09-125c	42.48	Disc	218	0.1374	0.0025	4.42	0.13	0.2333	0.0032	0.0660	0.0010	2194	31	1716	24	1352	17	1291	19		
RSA09-131	79.4	Disc	755	0.0969	0.0021	0.76	0.02	0.0566	0.0008	0.0166	0.0018	1564	40	571	14	355	5	332	36		
RSA09-138	74.4	Disc	348	0.1005	0.0014	1.02	0.02	0.0738	0.0010	0.0215	0.0003	1633	25	715	12	459	6	431	6		
RSA09-139	71.44	Disc	717	0.1104	0.0020	1.41	0.04	0.0923	0.0013	0.0267	0.0006	1806	31	891	17	569	8	532	11		
RSA09-142c	79.86	None	535	0.2423	0.0034	4.21	0.11	0.1264	0.0019	0.0922	0.0047	3135	22	1676	21	767	11	1783	86		
RSA09-142r	61.44	Disc	327	0.1027	0.0022	1.62	0.05	0.1142	0.0016	0.0333	0.0007	1673	40	977	20	697	9	661	13		
RSA09-146	56.64	Disc	202	0.0991	0.0014	1.68	0.04	0.1228	0.0016	0.0359	0.0007	1608	26	1001	15	747	9	713	14		
SWA03-001c	73.4	None	6685	0.3337	0.0019	9.27	0.12	0.2015	0.0022	0.6549	0.0168	3634	9	2365	12	1183	12	10182	205		

						Ratios (uncorrected)								Ages (uncorrected; Ma)								
	Th	U	Th/U	Common Pb		$^{207}Pb/^{206}Pb$		$^{207}Pb/^{235}U$		$^{206}Pb/^{238}U$		$^{208}Pb/^{232}Th$		$^{207}Pb/^{206}Pb$		$^{207}Pb/^{235}U$		$^{206}Pb/^{238}U$		$^{208}Pb/^{232}Th$		Inc.?
	ppm	ppm		%	1σ	Ratio	1σ	Ratio	1σ	Ratio	1σ	Ratio	1σ	Age	1σ	Age	1σ	Age	1σ	Age	1σ	
SWA03-003c	406	673	0.60	1.74	0.57	0.2324	0.0059	14.62	0.35	0.4560	0.0057	0.153	0.010	3068	22	2791	23	2422	25	2884	179	
SWA03-004c	275	1933	0.14	8.59	0.51	0.2291	0.0045	8.30	0.16	0.2629	0.0035	0.455	0.022	3045	15	2264	18	1505	18	7580	303	
SWA03-006c	384	580	0.66	1.03	0.26	0.2386	0.0033	16.92	0.23	0.5144	0.0057	0.156	0.005	3111	10	2930	13	2675	24	2937	80	y
SWA03-007c	447	552	0.81	1.84	0.36	0.2416	0.0034	17.86	0.25	0.5364	0.0060	0.172	0.005	3131	10	2982	14	2768	25	3201	91	y
SWA03-007r	789	1010	0.78	8.74	0.6	0.2657	0.0039	18.86	0.27	0.5151	0.0058	0.269	0.009	3281	10	3035	14	2678	25	4811	136	
SWA03-009c	418	870	0.48	3.21	0.39	0.2397	0.0032	16.18	0.20	0.4895	0.0049	0.171	0.005	3118	9	2887	12	2569	21	3197	82	y
SWA03-009r	457	828	0.55	8.29	0.51	0.2004	0.0027	6.08	0.08	0.2201	0.0026	0.121	0.003	2829	10	1988	12	1283	14	2307	62	
SWA03-010	532	734	0.72	4.3	0.41	0.2325	0.0029	12.16	0.15	0.3796	0.0040	0.141	0.004	3069	8	2617	12	2074	19	2665	63	
SWA03-011	416	1045	0.40	12.19	0.91	0.2376	0.0049	9.09	0.19	0.2775	0.0039	0.232	0.012	3104	16	2347	19	1579	19	4213	191	
SWA03-012	827	875	0.95	3.32	0.55	0.2348	0.0033	13.77	0.19	0.4255	0.0047	0.141	0.004	3085	10	2734	13	2285	21	2669	77	
SWA03-014c	735	592	1.24			0.2535	0.0059	21.05	0.49	0.6025	0.0088	0.150	0.008	3206	18	3141	22	3040	36	2821	146	
SWA03-014r	756	1389	0.54	21.63	1.78	0.2328	0.0065	4.68	0.13	0.1459	0.0022	0.142	0.011	3072	23	1763	23	878	13	2677	186	
SWA03-015	711	966	0.74	4.6	0.39	0.2194	0.0027	9.59	0.12	0.3169	0.0034	0.121	0.003	2977	8	2396	11	1775	17	2314	51	
SWA03-017c	802	864	0.93	3.83	0.62	0.2443	0.0036	15.62	0.24	0.4639	0.0056	0.158	0.005	3148	11	2854	15	2457	24	2958	92	
SWA03-018	436	574	0.76	1.74	0.56	0.2400	0.0038	14.15	0.23	0.4278	0.0050	0.130	0.005	3120	12	2760	15	2296	23	2470	87	y
SWA03-019	389	616	0.63	4.72	0.56	0.2380	0.0042	14.09	0.25	0.4294	0.0057	0.176	0.007	3107	13	2756	17	2303	26	3277	122	y
SWA03-020	378	607	0.62			0.2374	0.0057	18.21	0.43	0.5567	0.0082	0.136	0.008	3103	19	3001	23	2853	34	2574	136	y
SWA03-021c	503	700	0.72	3.87	0.33	0.2331	0.0029	13.57	0.18	0.4224	0.0049	0.162	0.004	3073	9	2720	12	2271	22	3035	67	
SWA03-022r	685	1091	0.63			0.2355	0.0070	12.79	0.35	0.3940	0.0074	0.480	0.028	3090	21	2664	26	2142	34	7928	384	
SWA03-023	367	470	0.78	2.28	0.55	0.2436	0.0040	17.96	0.30	0.5348	0.0068	0.173	0.007	3144	12	2988	16	2762	29	3217	117	y
SWA03-024	608	648	0.94	5.11	0.75	0.2429	0.0040	15.11	0.25	0.4513	0.0053	0.167	0.007	3139	12	2822	16	2401	24	3125	114	y
SWA03-025c	148	637	0.23	6.72	0.51	0.2502	0.0052	13.27	0.27	0.3847	0.0053	0.325	0.016	3186	15	2699	20	2098	24	5680	245	
SWA03-026	644	1070	0.60	5.1	0.65	0.2265	0.0044	8.15	0.16	0.2612	0.0035	0.112	0.005	3027	15	2248	18	1496	18	2154	94	
SWA03-029	424	589	0.72	1.3	0.4	0.2368	0.0035	16.22	0.25	0.4968	0.0060	0.150	0.005	3099	10	2890	14	2600	26	2832	88	y
SWA03-030	368	634	0.58	28.47	1.27	0.4170	0.0051	33.93	0.43	0.5903	0.0065	0.421	0.010	3972	8	3608	12	2990	26	7105	141	

				Ratios (corrected)								Ages (corrected; Ma)									
	Disc.	Correction type	^{204}Pb	^{207}Pb/^{206}Pb		^{207}Pb/^{235}U		^{206}Pb/^{238}U		^{208}Pb/^{232}Th		^{207}Pb/^{206}Pb		^{207}Pb/^{235}U		^{206}Pb/^{238}U		^{208}Pb/^{232}Th		Inc.?	
	%		cps	Ratio	1σ	Ratio	1σ	Ratio	1σ	Ratio	1σ	Age	1σ	Age	1σ	Age	1σ	Age	1σ	Int	W/A
SWA03-003c	24.18	Disc	345	0.2218	0.0050	13.70	0.48	0.4481	0.0066	0.1210	0.0016	2993	36	2729	33	2387	29	2309	29	y	y
SWA03-004c	51.09	Disc	872	0.1719	0.0048	5.70	0.23	0.2403	0.0038	0.0665	0.0048	2577	45	1931	35	1388	20	1301	90		
SWA03-006c	16.48	Disc	133	0.2324	0.0022	16.31	0.31	0.5091	0.0063	0.1369	0.0016	3068	15	2895	18	2653	27	2594	29	y	y
SWA03-007c	13.14	Disc	304	0.2304	0.0028	16.73	0.37	0.5266	0.0068	0.1417	0.0018	3055	19	2919	21	2727	29	2679	31	y	y
SWA03-007r	17.71	Disc	1350	0.2110	0.0048	13.68	0.47	0.4701	0.0069	0.1276	0.0024	2913	36	2727	33	2484	30	2427	43		
SWA03-009c	19.37	Disc	1229	0.2199	0.0029	14.37	0.33	0.4738	0.0057	0.1281	0.0015	2980	21	2774	22	2500	25	2436	28	y	
SWA03-009r	51.99	Disc	1351	0.1429	0.0042	3.98	0.16	0.2019	0.0030	0.0569	0.0010	2263	50	1630	33	1185	16	1118	19		
SWA03-010	35.19	Disc	1547	0.2053	0.0031	10.28	0.25	0.3632	0.0044	0.0988	0.0012	2869	24	2460	23	1998	21	1905	22	y	
SWA03-011	45.86	Disc	2422	0.1544	0.0080	5.19	0.35	0.2437	0.0045	0.0681	0.0021	2396	87	1851	57	1406	23	1332	41		
SWA03-012	28.7	Disc	1617	0.2141	0.0039	12.14	0.35	0.4114	0.0054	0.1115	0.0014	2937	29	2615	27	2221	25	2136	25	y	
SWA03-014c	6.54	None	1438	0.2535	0.0030	21.05	0.49	0.6025	0.0088	0.1498	0.0083	3206	18	3141	22	3040	36	2821	146		
SWA03-014r	14.18	Disc	3086	0.0660	0.0184	1.04	0.32	0.1144	0.0032	0.0349	0.0034	806	555	724	158	698	19	694	66		
SWA03-015	42.9	Disc	805	0.1897	0.0030	7.91	0.20	0.3024	0.0037	0.0829	0.0010	2739	25	2221	23	1703	18	1609	19		
SWA03-017c	24.27	Disc	1838	0.2207	0.0044	13.57	0.43	0.4461	0.0065	0.1206	0.0016	2986	31	2720	30	2378	29	2301	30	y	y
SWA03-018	30.46	Disc	1577	0.2294	0.0039	13.30	0.38	0.4204	0.0057	0.1132	0.0014	3048	27	2701	27	2262	26	2167	26		
SWA03-019	27.76	Disc	1678	0.2084	0.0044	11.75	0.39	0.4091	0.0062	0.1112	0.0017	2893	33	2585	31	2211	28	2130	31	y	
SWA03-020	9.99	None	1018	0.2374	0.0029	18.21	0.43	0.5567	0.0082	0.1358	0.0076	3103	19	3001	23	2853	34	2574	136	y	
SWA03-021c	28.41	Disc	1431	0.2088	0.0026	11.69	0.26	0.4060	0.0051	0.1103	0.0014	2896	19	2580	20	2197	23	2115	26	y	
SWA03-022r	35.94	None	143	0.2355	0.0032	12.79	0.35	0.3940	0.0074	0.4803	0.0282	3090	21	2664	26	2142	34	7928	384		
SWA03-023	13.62	Disc	1576	0.2297	0.0041	16.55	0.51	0.5226	0.0081	0.1407	0.0021	3050	27	2909	30	2710	34	2661	36	y	y
SWA03-024	25.03	Disc	1709	0.2110	0.0056	12.46	0.50	0.4283	0.0069	0.1162	0.0018	2913	41	2640	38	2298	31	2222	32	y	
SWA03-025c	36.56	Disc	1499	0.2080	0.0049	10.29	0.38	0.3588	0.0058	0.0975	0.0033	2890	36	2461	34	1977	27	1881	60	y	
SWA03-026	53.91	Disc	1839	0.1937	0.0053	6.62	0.27	0.2479	0.0041	0.0678	0.0011	2774	43	2062	36	1427	21	1326	22		
SWA03-029	18.76	Disc	1301	0.2289	0.0031	15.47	0.39	0.4903	0.0068	0.1321	0.0017	3044	21	2845	24	2572	29	2507	31	y	y
SWA03-030	33.97	Disc	8012	0.2503	0.0123	14.57	1.04	0.4222	0.0104	0.1128	0.0048	3187	75	2788	68	2271	47	2160	87		

						Ratios (uncorrected)								Ages (uncorrected; Ma)								
	Th	U	Th/U	Common Pb		$^{207}Pb/^{206}Pb$		$^{207}Pb/^{235}U$		$^{206}Pb/^{238}U$		$^{208}Pb/^{232}Th$		$^{207}Pb/^{206}Pb$		$^{207}Pb/^{235}U$		$^{206}Pb/^{238}U$		$^{208}Pb/^{232}Th$		Inc.?
	ppm	ppm		%	1σ	Ratio	1σ	Ratio	1σ	Ratio	1σ	Ratio	1σ	Age	1σ	Age	1σ	Age	1σ	Age	1σ	
SWA03-031c	178	465	0.38	1.75	0.15	0.2472	0.0027	21.26	0.24	0.6237	0.0068	0.224	0.004	3167	8	3150	11	3124	27	4085	65	
SWA03-031r	293	758	0.39	5.06	0.24	0.2379	0.0026	13.41	0.15	0.4088	0.0044	0.217	0.004	3106	8	2709	11	2209	20	3969	66	y
SWA03-032c	315	485	0.65	5.37	0.33	0.2370	0.0026	19.01	0.22	0.5820	0.0064	0.250	0.005	3100	8	3043	11	2957	26	4508	76	
SWA03-032r	625	773	0.81			0.2411	0.0030	18.31	0.22	0.5508	0.0058	0.153	0.004	3127	8	3006	12	2829	24	2872	68	y
SWA03-034c	315	524	0.60	0.85	0.26	0.1831	0.0023	5.51	0.07	0.2182	0.0026	0.066	0.002	2681	9	1902	12	1272	14	1291	31	
SWA03-035r	233	540	0.43			0.2525	0.0040	8.46	0.13	0.2431	0.0029	0.765	0.027	3201	11	2282	14	1403	15	11480	309	
SWA03-036	1374	1511	0.91	10.19	0.87	0.2368	0.0036	7.53	0.12	0.2305	0.0029	0.111	0.004	3099	11	2176	14	1337	15	2130	71	
SWA03-038c	406	519	0.78	3.63	0.71	0.2384	0.0045	16.25	0.31	0.4942	0.0067	0.176	0.008	3109	14	2892	18	2589	29	3275	139	y
SWA03-039c	459	772	0.59	5.59	0.8	0.2387	0.0049	15.54	0.32	0.4722	0.0066	0.204	0.011	3111	16	2849	20	2493	29	3747	179	y
SWA03-040	548	713	0.77	1.14	0.52	0.2440	0.0045	13.73	0.25	0.4082	0.0052	0.121	0.005	3146	14	2731	18	2207	24	2317	97	y
SWA03-041	531	521	1.02			0.2398	0.0036	15.72	0.24	0.4757	0.0056	0.130	0.005	3118	10	2860	14	2509	24	2469	84	y
SWA03-042	579	598	0.97			0.2411	0.0062	17.99	0.45	0.5412	0.0080	0.133	0.009	3127	21	2989	24	2788	33	2525	159	y
SWA03-043c	604	632	0.96			0.2310	0.0051	14.98	0.32	0.4703	0.0061	0.108	0.006	3059	18	2814	20	2485	27	2078	118	
SWA03-044	513	858	0.60	5.07	0.61	0.2394	0.0042	10.72	0.19	0.3247	0.0041	0.141	0.006	3116	13	2499	16	1812	20	2671	110	y
SWA03-045c	455	601	0.76			0.2240	0.0046	13.63	0.28	0.4413	0.0059	0.112	0.006	3010	16	2724	19	2357	26	2154	111	
SWA03-046c	566	673	0.84	2.05	0.84	0.2344	0.0056	14.25	0.33	0.4408	0.0059	0.139	0.009	3082	19	2766	22	2354	26	2632	162	y
SWA03-047c	310	413	0.75	5.57	1.17	0.2573	0.0071	21.22	0.58	0.5985	0.0091	0.237	0.017	3230	23	3149	26	3024	37	4295	286	
SWA03-048c	217	537	0.40			0.2451	0.0063	20.47	0.52	0.6061	0.0088	0.164	0.011	3153	21	3114	24	3054	35	3075	199	y
SWA03-048r	367	573	0.64	2.91	0.78	0.2385	0.0059	12.82	0.31	0.3897	0.0055	0.137	0.009	3110	20	2666	23	2122	25	2596	166	y
SWA03-049c	132	560	0.24			0.2430	0.0077	16.84	0.52	0.5028	0.0081	0.159	0.013	3140	28	2925	30	2626	35	2985	231	y
SWA03-050c	127	385	0.33	3.26	0.3	0.2424	0.0043	12.20	0.22	0.3653	0.0050	0.170	0.007	3136	13	2620	17	2007	24	3181	117	y
SWA03-050r	623	1329	0.47	13.4	0.74	0.1787	0.0028	3.66	0.06	0.1488	0.0020	0.113	0.004	2641	12	1564	13	894	11	2161	72	
SWA03-052	530	730	0.73	2.49	0.29	0.2408	0.0028	12.17	0.15	0.3665	0.0042	0.123	0.003	3125	8	2617	12	2013	20	2337	48	y
SWA03-053c	266	397	0.67	1.1	0.45	0.2367	0.0044	18.96	0.36	0.5811	0.0081	0.174	0.008	3098	14	3040	18	2953	33	3250	135	y
SWA03-053r	1465	2227	0.66	17.98	1	0.2490	0.0040	5.15	0.08	0.1501	0.0018	0.121	0.004	3178	11	1845	14	902	10	2301	81	

				Ratios (corrected)								Ages (corrected; Ma)									
	Disc.	Correction type	^{204}Pb	^{207}Pb/^{206}Pb		^{207}Pb/^{235}U		^{206}Pb/^{238}U		^{208}Pb/^{232}Th		^{207}Pb/^{206}Pb		^{207}Pb/^{235}U		^{206}Pb/^{238}U		^{208}Pb/^{232}Th		Inc.?	
	%		cps	Ratio	1σ	Ratio	1σ	Ratio	1σ	Ratio	1σ	Age	1σ	Age	1σ	Age	1σ	Age	1σ	Int	W/A
SWA03-031c	0.68	Disc	1103	0.2367	0.0015	19.99	0.30	0.6127	0.0071	0.1645	0.0021	3098	9	3091	14	3081	28	3078	36	y	
SWA03-031r	30.93	Disc	1232	0.2060	0.0021	11.02	0.21	0.3881	0.0047	0.1056	0.0019	2874	16	2525	18	2114	22	2028	35	y	
SWA03-032c	0.96	Disc	1294	0.2030	0.0026	15.42	0.35	0.5508	0.0071	0.1500	0.0022	2850	20	2841	22	2828	29	2825	39		
SWA03-032r	11.79	None	876	0.2411	0.0013	18.31	0.22	0.5508	0.0058	0.1527	0.0039	3127	8	3006	12	2829	24	2872	68	y	
SWA03-034c	57.05	Disc	1152	0.1775	0.0021	5.29	0.11	0.2163	0.0027	0.0597	0.0007	2629	19	1868	18	1262	14	1171	14		
SWA03-035r	62.2	None	918	0.2525	0.0018	8.46	0.13	0.2431	0.0029	0.7647	0.0270	3201	11	2282	14	1403	15	11480	309		
SWA03-036	57.28	Disc	2301	0.1689	0.0070	4.82	0.27	0.2070	0.0037	0.0574	0.0010	2547	68	1788	47	1213	19	1128	20		
SWA03-038c	17.95	Disc	1509	0.2159	0.0053	14.18	0.54	0.4763	0.0078	0.1290	0.0020	2951	38	2762	36	2511	34	2452	36		
SWA03-039c	19.93	Disc	1356	0.2033	0.0063	12.50	0.56	0.4458	0.0077	0.1214	0.0021	2853	49	2642	42	2376	34	2316	38		
SWA03-040	34.67	Disc	1772	0.2371	0.0040	13.19	0.38	0.4036	0.0058	0.1083	0.0015	3101	26	2694	27	2185	27	2079	27		
SWA03-041	23.54	None	1473	0.2398	0.0016	15.72	0.24	0.4757	0.0056	0.1299	0.0047	3118	10	2860	14	2509	24	2469	84		
SWA03-042	13.36	None	1569	0.2411	0.0033	17.99	0.45	0.5412	0.0080	0.1331	0.0089	3127	21	2989	24	2788	33	2525	159	y	
SWA03-043c	22.56	None	1061	0.2310	0.0026	14.98	0.32	0.4703	0.0061	0.1083	0.0065	3059	18	2814	20	2485	27	2078	118	y	y
SWA03-044	45.43	Disc	1777	0.2076	0.0048	8.82	0.31	0.3082	0.0046	0.0838	0.0013	2887	36	2320	32	1732	23	1626	25		
SWA03-045c	25.84	None	1107	0.2240	0.0023	13.63	0.28	0.4413	0.0059	0.1124	0.0061	3010	16	2724	19	2357	26	2154	111	y	y
SWA03-046c	26.95	Disc	1143	0.2218	0.0063	13.21	0.57	0.4318	0.0074	0.1166	0.0018	2994	44	2694	41	2314	33	2230	32	y	y
SWA03-047c	4.76	Disc	2019	0.2231	0.0090	17.38	1.03	0.5651	0.0121	0.1526	0.0030	3003	63	2956	57	2888	50	2870	52		
SWA03-048c	3.95	None	1204	0.2451	0.0034	20.47	0.52	0.6061	0.0088	0.1643	0.0115	3153	21	3114	24	3054	35	3075	199	y	
SWA03-048r	35.75	Disc	1525	0.2206	0.0061	11.51	0.49	0.3784	0.0066	0.1023	0.0016	2985	43	2565	40	2069	31	1968	30	y	y
SWA03-049c	19.92	None	1371	0.2430	0.0044	16.84	0.52	0.5028	0.0081	0.1591	0.0132	3140	28	2925	30	2626	35	2985	231		
SWA03-050c	40.3	Disc	1083	0.2222	0.0030	10.83	0.27	0.3533	0.0053	0.0954	0.0017	2997	21	2508	23	1950	25	1842	31		
SWA03-050r	32.03	Disc	1729	0.0769	0.0071	1.37	0.14	0.1289	0.0023	0.0387	0.0009	1119	183	875	62	782	13	768	17		
SWA03-052	40.21	Disc	1294	0.2256	0.0022	11.12	0.22	0.3574	0.0047	0.0964	0.0013	3021	15	2533	18	1970	22	1860	23		
SWA03-053c	5.1	Disc	1270	0.2301	0.0036	18.23	0.51	0.5747	0.0090	0.1547	0.0023	3052	24	3002	27	2927	37	2907	40	y	y
SWA03-053r	65.36	Disc	3957	0.1203	0.0097	2.04	0.20	0.1231	0.0024	0.0353	0.0010	1960	143	1130	66	749	14	701	20		

						Ratios (uncorrected)								Ages (uncorrected; Ma)								
	Th	U	Th/U	Common Pb		$^{207}Pb/^{206}Pb$		$^{207}Pb/^{235}U$		$^{206}Pb/^{238}U$		$^{208}Pb/^{232}Th$		$^{207}Pb/^{206}Pb$		$^{207}Pb/^{235}U$		$^{206}Pb/^{238}U$		$^{208}Pb/^{232}Th$		Inc.?
	ppm	ppm		%	1σ	Ratio	1σ	Ratio	1σ	Ratio	1σ	Ratio	1σ	Age	1σ	Age	1σ	Age	1σ	Age	1σ	
SWA03-054c	54	109	0.50	3.36	0.28	0.2704	0.0036	20.01	0.28	0.5367	0.0064	0.214	0.006	3308	9	3092	13	2769	27	3919	94	
SWA03-056c	503	656	0.77	4.79	0.63	0.2411	0.0038	17.15	0.28	0.5163	0.0067	0.190	0.007	3127	11	2944	16	2684	28	3513	117	y
SWA03-057c	688	1014	0.68	0.85	0.37	0.2243	0.0033	9.74	0.15	0.3151	0.0040	0.092	0.003	3012	11	2411	14	1766	19	1788	58	
SWA03-058c	675	809	0.84			0.2321	0.0037	13.53	0.21	0.4229	0.0050	0.119	0.004	3066	11	2717	15	2274	23	2267	78	
SWA03-060c	319	784	0.41	6.66	0.54	0.2349	0.0040	12.84	0.23	0.3967	0.0053	0.236	0.010	3086	12	2668	17	2154	25	4290	166	
RSA06-001c	105	183	0.57	2.62	0.27	0.2456	0.0036	14.95	0.23	0.4416	0.0055	0.159	0.004	3157	10	2812	14	2358	24	2990	63	
RSA06-002	659	1473	0.45	1.31	0.24	0.2029	0.0036	9.30	0.17	0.3324	0.0043	0.111	0.003	2849	14	2368	17	1850	21	2123	62	
RSA06-003	496	2073	0.24	2.91	0.14	0.1585	0.0019	2.95	0.04	0.1352	0.0016	0.073	0.001	2440	9	1396	10	818	9	1420	24	
RSA06-006c	1649	2442	0.68	4.03	0.41	0.1618	0.0027	2.75	0.05	0.1231	0.0016	0.049	0.001	2474	13	1341	13	749	9	976	27	
RSA06-015c	577	1038	0.56	1.61	0.49	0.2090	0.0059	8.93	0.25	0.3100	0.0050	0.103	0.005	2898	23	2331	25	1741	25	1975	98	
RSA06-018	365	1906	0.19	1.12	0.23	0.1866	0.0063	5.61	0.18	0.2182	0.0038	0.087	0.005	2712	30	1918	28	1273	20	1687	99	
RSA06-019c	35	60	0.59			0.2394	0.0039	19.48	0.33	0.5901	0.0076	0.166	0.004	3116	12	3066	16	2990	31	3101	77	
RSA06-021c	1601	1785	0.90	2.1	0.47	0.1803	0.0034	5.00	0.10	0.2014	0.0027	0.065	0.002	2655	15	1820	16	1183	14	1272	40	
RSA06-023	3969	635	6.25			0.2302	0.0051	10.83	0.24	0.3413	0.0045	0.015	0.001	3054	18	2509	21	1893	22	303	12	y
RSA06-025c	246	444	0.55	1.8	0.49	0.2275	0.0065	13.95	0.39	0.4448	0.0067	0.150	0.008	3035	24	2746	27	2372	30	2816	149	y
RSA06-030	1863	1902	0.98			0.1903	0.0043	4.29	0.10	0.1635	0.0023	0.034	0.001	2745	19	1691	19	976	13	674	28	
RSA06-035	836	1164	0.72			0.2069	0.0038	7.54	0.14	0.2644	0.0036	0.076	0.003	2881	14	2178	17	1512	18	1481	47	
RSA06-038	463	794	0.58	1.56	0.37	0.2235	0.0049	13.84	0.31	0.4491	0.0064	0.146	0.006	3006	17	2739	21	2391	29	2752	105	y
RSA06-039c	1796	674	2.66			0.2255	0.0060	15.54	0.41	0.4999	0.0079	0.050	0.003	3021	22	2849	25	2613	34	984	50	y
RSA06-045c	1187	4967	0.24	4	0.28	0.1690	0.0035	1.07	0.02	0.0460	0.0006	0.029	0.001	2548	17	739	11	290	4	580	22	
RSA06-048	683	826	0.83			0.2359	0.0056	21.56	0.52	0.6630	0.0098	0.163	0.007	3093	19	3164	23	3279	38	3060	130	
RSA06-052c	879	1985	0.44	2.54	0.39	0.1730	0.0043	4.02	0.10	0.1684	0.0026	0.067	0.003	2587	21	1638	20	1003	14	1306	59	
RSA06-055c	471	841	0.56	5.46	0.98	0.2055	0.0086	8.41	0.34	0.2968	0.0059	0.140	0.011	2870	38	2276	37	1676	29	2654	199	
RSA06-063	1401	3890	0.36	4.98	0.73	0.1014	0.0042	0.99	0.04	0.0711	0.0014	0.042	0.003	1650	44	700	21	443	9	832	65	
RSA06-065	499	751	0.66	1.19	0.56	0.2185	0.0064	12.10	0.35	0.4014	0.0063	0.123	0.007	2970	25	2612	27	2176	29	2349	130	

				Ratios (corrected)								Ages (corrected; Ma)									
	Disc.	Correction type	^{204}Pb	^{207}Pb/^{206}Pb		^{207}Pb/^{235}U		^{206}Pb/^{238}U		^{208}Pb/^{232}Th		^{207}Pb/^{206}Pb		^{207}Pb/^{235}U		^{206}Pb/^{238}U		^{208}Pb/^{232}Th		Inc.?	
	%		cps	Ratio	1σ	Ratio	1σ	Ratio	1σ	Ratio	1σ	Age	1σ	Age	1σ	Age	1σ	Age	1σ	Int	W/A
SWA03-054c	18.97	Disc	1078	0.2507	0.0024	17.92	0.35	0.5186	0.0069	0.1385	0.0020	3189	15	2986	19	2693	29	2621	36		
SWA03-056c	13.97	Disc	1546	0.2110	0.0047	14.30	0.50	0.4916	0.0080	0.1334	0.0021	2913	34	2770	33	2577	34	2531	37		
SWA03-057c	46.69	Disc	1349	0.2190	0.0029	9.43	0.22	0.3124	0.0042	0.0845	0.0011	2973	20	2381	21	1753	20	1639	20		
SWA03-058c	30.58	None	1086	0.2321	0.0017	13.53	0.21	0.4229	0.0050	0.1187	0.0043	3066	11	2717	15	2274	23	2267	78		
SWA03-060c	30.68	Disc	1588	0.1919	0.0045	9.80	0.34	0.3702	0.0056	0.1014	0.0022	2759	37	2416	32	2030	26	1952	39		
RSA06-001c	28.92	Disc	134	0.2297	0.0025	13.62	0.30	0.4300	0.0059	0.1158	0.0016	3050	17	2724	21	2306	27	2214	29		
RSA06-002	39.16	Disc	538	0.1944	0.0026	8.79	0.21	0.3280	0.0045	0.0897	0.0012	2780	21	2317	22	1829	22	1736	22		
RSA06-003	67.78	Disc	430	0.1381	0.0014	2.50	0.05	0.1313	0.0017	0.0371	0.0006	2204	17	1272	14	795	9	737	12		
RSA06-006c	70.04	Disc	361	0.1334	0.0035	2.17	0.08	0.1182	0.0018	0.0335	0.0005	2143	45	1173	27	720	10	666	9		
RSA06-015c	44.31	Disc	124	0.1987	0.0049	8.36	0.33	0.3050	0.0056	0.0832	0.0014	2816	39	2271	36	1716	27	1616	26		
RSA06-018	57.48	Disc	90	0.1792	0.0041	5.33	0.20	0.2158	0.0038	0.0595	0.0010	2646	36	1874	32	1260	20	1168	19		
RSA06-019c	5.07	None	100	0.2394	0.0019	19.48	0.33	0.5901	0.0076	0.1658	0.0044	3116	12	3066	16	2990	31	3101	77	y	
RSA06-021c	58.77	Disc	1286	0.1662	0.0039	4.52	0.16	0.1972	0.0030	0.0547	0.0008	2520	37	1734	30	1160	16	1077	14		
RSA06-023	43.68	None	284	0.2302	0.0027	10.83	0.24	0.3413	0.0045	0.0151	0.0006	3054	18	2509	21	1893	22	303	12		
RSA06-025c	24.86	Disc	165	0.2164	0.0051	13.03	0.48	0.4368	0.0071	0.1182	0.0018	2954	36	2682	35	2336	32	2259	32	y	y
RSA06-030	69.21	None	301	0.1903	0.0023	4.29	0.10	0.1635	0.0023	0.0339	0.0014	2745	19	1691	19	976	13	674	28		
RSA06-035	53.08	None	383	0.2069	0.0019	7.54	0.14	0.2644	0.0036	0.0761	0.0025	2881	14	2178	17	1512	18	1481	47		
RSA06-038	23.32	Disc	91	0.2138	0.0037	13.03	0.39	0.4421	0.0067	0.1198	0.0017	2934	26	2682	28	2360	30	2287	31	y	y
RSA06-039c	16.37	None	584	0.2255	0.0032	15.54	0.41	0.4999	0.0079	0.0499	0.0026	3021	22	2849	25	2613	34	984	50	y	
RSA06-045c	89.39	Disc	687	0.1412	0.0030	0.86	0.03	0.0441	0.0006	0.0125	0.0003	2242	34	630	15	278	4	250	5		
RSA06-048	-7.69	None	181	0.2359	0.0029	21.56	0.52	0.6630	0.0098	0.1634	0.0075	3093	19	3164	23	3279	38	3060	130	y	
RSA06-052c	63.79	Disc	177	0.1557	0.0038	3.52	0.13	0.1641	0.0026	0.0459	0.0007	2410	39	1533	29	980	15	906	14		
RSA06-055c	42.1	Disc	214	0.1690	0.0093	6.54	0.49	0.2806	0.0067	0.0778	0.0017	2548	89	2051	67	1595	34	1514	32		
RSA06-063	41.52	Disc	411	0.0629	0.0068	0.59	0.07	0.0675	0.0015	0.0208	0.0004	705	225	468	47	421	9	415	9		
RSA06-065	30.6	Disc	87	0.2111	0.0054	11.54	0.46	0.3966	0.0068	0.1076	0.0017	2914	40	2568	37	2153	31	2066	30	y	y

						Ratios (uncorrected)								Ages (uncorrected; Ma)								
	Th	U	Th/U	Common Pb		$^{207}Pb/^{206}Pb$		$^{207}Pb/^{235}U$		$^{206}Pb/^{238}U$		$^{208}Pb/^{232}Th$		$^{207}Pb/^{206}Pb$		$^{207}Pb/^{235}U$		$^{206}Pb/^{238}U$		$^{208}Pb/^{232}Th$		Inc.?
	ppm	ppm		%	1σ	Ratio	1σ	Ratio	1σ	Ratio	1σ	Ratio	1σ	Age	1σ	Age	1σ	Age	1σ	Age	1σ	
RSA06-071	403	4364	0.09	5.48	0.18	0.1217	0.0017	1.82	0.03	0.1083	0.0014	0.169	0.004	1981	11	1052	10	663	8	3155	61	
RSA06-073	358	494	0.73			0.2261	0.0047	14.91	0.30	0.4785	0.0062	0.136	0.005	3025	16	2810	19	2521	27	2578	89	y
RSA06-077c	234	1811	0.13	1.72	0.11	0.1596	0.0028	3.17	0.06	0.1442	0.0020	0.081	0.002	2452	14	1451	14	868	11	1573	44	
RSA06-080c	1211	1888	0.64	2.44	0.32	0.2201	0.0037	4.58	0.08	0.1509	0.0020	0.052	0.001	2981	13	1745	15	906	11	1032	28	
RSA06-083c	592	1362	0.43			0.2425	0.0087	8.98	0.31	0.2686	0.0048	0.073	0.005	3136	31	2336	32	1534	25	1428	93	
RSA06-087	966	1082	0.89			0.5666	0.0076	82.47	1.20	1.0558	0.0131	1.824	0.037	4425	9	4493	15	4646	41	20986	266	
RSA06-088c	133	467	0.28	3.45	0.23	0.2500	0.0046	9.69	0.18	0.2813	0.0039	0.147	0.004	3185	14	2406	17	1598	19	2764	79	
RSA06-092c	919	1925	0.48	0.65	0.31	0.1864	0.0048	4.66	0.12	0.1814	0.0029	0.055	0.003	2710	22	1760	22	1074	16	1080	48	
RSA06-093	510	689	0.74			0.2297	0.0101	12.25	0.52	0.3869	0.0084	0.079	0.006	3050	39	2624	40	2108	39	1538	115	y
RSA06-095	607	2947	0.21	0.51	0.13	0.1306	0.0032	1.67	0.04	0.0930	0.0014	0.031	0.001	2106	22	999	16	573	8	624	25	
RSA06-097c	499	672	0.74			0.2162	0.0050	13.87	0.33	0.4654	0.0072	0.119	0.005	2953	19	2741	22	2463	32	2272	92	
RSA06-100	334	542	0.62	1.86	0.46	0.2263	0.0057	12.17	0.30	0.3901	0.0056	0.130	0.006	3026	21	2618	23	2123	26	2462	112	y
RSA06-108	3414	1248	2.74			0.1844	0.0054	5.42	0.16	0.2134	0.0034	0.023	0.001	2693	26	1888	25	1247	18	451	24	
RSA06-112c	184	166	1.11			0.2375	0.0049	19.89	0.40	0.6076	0.0082	0.161	0.006	3103	16	3086	20	3060	33	3022	102	
RSA06-118c	1624	5687	0.29	6.48	0.27	0.1522	0.0021	1.97	0.03	0.0938	0.0012	0.072	0.002	2371	11	1105	10	578	7	1406	30	
RSA06-121	4817	585	8.24			0.2452	0.0092	16.27	0.60	0.4818	0.0095	0.038	0.003	3154	33	2893	36	2535	41	758	55	
RSA06-122c	1113	1831	0.61	3.56	0.28	0.1702	0.0023	2.68	0.04	0.1143	0.0014	0.046	0.001	2560	10	1323	10	698	8	902	18	
RSA06-125c	730	1613	0.45			0.1468	0.0068	2.52	0.11	0.1247	0.0029	0.035	0.003	2308	45	1279	33	758	17	689	62	
RSA06-130	1200	1371	0.88	6.26	0.8	0.2105	0.0047	5.91	0.13	0.2037	0.0029	0.085	0.004	2909	18	1963	20	1195	16	1646	68	
RSA06-139	835	1159	0.72			0.1586	0.0101	3.09	0.19	0.1410	0.0040	0.030	0.004	2441	63	1429	47	851	23	596	80	
RSA06-140	776	3018	0.26	1.09	0.14	0.1434	0.0024	1.85	0.03	0.0937	0.0013	0.035	0.001	2268	14	1064	12	577	7	690	20	
RSA06-142	385	1982	0.19	3.79	0.24	0.1435	0.0028	3.80	0.08	0.1924	0.0027	0.134	0.005	2270	16	1594	16	1134	15	2534	84	
RSA06-147c	557	2543	0.22	4.49	0.26	0.1593	0.0029	1.58	0.03	0.0721	0.0010	0.051	0.002	2448	14	964	12	449	6	1010	31	
SWA13a-001	98	132	0.74	0.77	0.21	0.2381	0.0029	16.88	0.22	0.5146	0.0061	0.149	0.002	3107	9	2928	13	2676	26	2805	43	y
SWA13a-002	1750	2135	0.82	2.02	0.26	0.2724	0.0033	3.56	0.05	0.0949	0.0011	0.030	0.001	3320	9	1542	10	585	7	594	10	

				Ratios (corrected)								Ages (corrected; Ma)									
	Disc.	Correction	^{204}Pb	^{207}Pb/^{206}Pb		^{207}Pb/^{235}U		^{206}Pb/^{238}U		^{208}Pb/^{232}Th		^{207}Pb/^{206}Pb		^{207}Pb/^{235}U		^{206}Pb/^{238}U		^{208}Pb/^{232}Th		Inc.?	
	%	type	cps	Ratio	1σ	Ratio	1σ	Ratio	1σ	Ratio	1σ	Age	1σ	Age	1σ	Age	1σ	Age	1σ	Int	W/A
RSA06-071	50.12	Disc	1509	0.0803	0.0019	1.13	0.04	0.1024	0.0013	0.0306	0.0016	1204	46	769	17	628	8	609	30		
RSA06-073	20.11	None	38	0.2261	0.0023	14.91	0.30	0.4785	0.0062	0.1360	0.0050	3025	16	2810	19	2521	27	2578	89	y	
RSA06-077c	67.3	Disc	347	0.1478	0.0016	2.89	0.06	0.1417	0.0021	0.0398	0.0007	2321	19	1379	17	854	12	788	14		
RSA06-080c	73.67	Disc	427	0.2046	0.0029	4.15	0.11	0.1472	0.0023	0.0401	0.0006	2863	23	1665	22	885	13	794	12		
RSA06-083c	57.16	None	222	0.2425	0.0048	8.98	0.31	0.2686	0.0048	0.0732	0.0050	3136	31	2336	32	1534	25	1428	93		
RSA06-087	-7	None	44892	0.5666	0.0036	82.47	1.20	1.0558	0.0131	1.8243	0.0372	4425	9	4493	15	4646	41	20986	266		
RSA06-088c	55.02	Disc	315	0.2290	0.0029	8.58	0.21	0.2716	0.0041	0.0731	0.0014	3045	20	2294	22	1549	21	1427	27		
RSA06-092c	64.92	Disc	371	0.1821	0.0035	4.52	0.15	0.1802	0.0032	0.0496	0.0008	2672	31	1735	28	1068	17	978	16		
RSA06-093	36.06	None	42	0.2297	0.0057	12.25	0.52	0.3869	0.0084	0.0790	0.0061	3050	39	2624	40	2108	39	1538	115	y	y
RSA06-095	75.36	Disc	166	0.1269	0.0021	1.62	0.05	0.0925	0.0015	0.0264	0.0004	2056	28	978	18	570	9	526	8		
RSA06-097c	19.91	None	107	0.2162	0.0026	13.87	0.33	0.4654	0.0072	0.1190	0.0051	2953	19	2741	22	2463	32	2272	92	y	y
RSA06-100	33.81	Disc	154	0.2148	0.0045	11.34	0.40	0.3828	0.0064	0.1037	0.0016	2942	34	2551	33	2089	30	1994	30	y	y
RSA06-108	58.87	None	323	0.1844	0.0030	5.42	0.16	0.2134	0.0034	0.0225	0.0012	2693	26	1888	25	1247	18	451	24		
RSA06-112c	1.74	None	27	0.2375	0.0024	19.89	0.40	0.6076	0.0082	0.1613	0.0059	3103	16	3086	20	3060	33	3022	102	y	
RSA06-118c	71.17	Disc	2611	0.1049	0.0026	1.27	0.04	0.0877	0.0012	0.0255	0.0006	1712	45	832	20	542	7	509	12		
RSA06-121	23.74	None	1193	0.2452	0.0052	16.27	0.60	0.4818	0.0095	0.0382	0.0028	3154	33	2893	36	2535	41	758	55		
RSA06-122c	74.22	Disc	123	0.1456	0.0023	2.21	0.06	0.1102	0.0015	0.0310	0.0004	2295	26	1185	18	674	9	617	8		
RSA06-125c	71.03	None	26	0.1468	0.0039	2.52	0.11	0.1247	0.0029	0.0347	0.0032	2308	45	1279	33	758	17	689	62		
RSA06-130	60.55	Disc	1439	0.1687	0.0064	4.44	0.24	0.1910	0.0036	0.0529	0.0009	2545	63	1720	45	1127	19	1043	18		
RSA06-139	69.34	None	104	0.1586	0.0060	3.09	0.19	0.1410	0.0040	0.0300	0.0041	2441	63	1429	47	851	23	596	80		
RSA06-140	76.89	Disc	285	0.1357	0.0015	1.73	0.04	0.0926	0.0013	0.0262	0.0004	2173	19	1021	14	571	8	523	7		
RSA06-142	45.95	Disc	303	0.1162	0.0024	2.97	0.10	0.1851	0.0028	0.0532	0.0012	1898	37	1399	25	1095	15	1048	22		
RSA06-147c	81.74	Disc	499	0.1275	0.0025	1.21	0.04	0.0689	0.0010	0.0196	0.0005	2063	34	805	17	429	6	393	9		
SWA13a-001	16.47	Disc	68	0.2333	0.0018	16.43	0.29	0.5106	0.0064	0.1373	0.0017	3075	12	2902	17	2659	27	2600	30		
SWA13a-002	85.82	Disc	1108	0.2607	0.0022	3.34	0.06	0.0930	0.0012	0.0248	0.0003	3251	13	1491	14	573	7	494	6		

						Ratios (uncorrected)								Ages (uncorrected; Ma)								
	Th	U	Th/U	Common Pb		$^{207}Pb/^{206}Pb$		$^{207}Pb/^{235}U$		$^{206}Pb/^{238}U$		$^{208}Pb/^{232}Th$		$^{207}Pb/^{206}Pb$		$^{207}Pb/^{235}U$		$^{206}Pb/^{238}U$		$^{208}Pb/^{232}Th$		Inc.?
	ppm	ppm		%	1σ	Ratio	1σ	Ratio	1σ	Ratio	1σ	Ratio	1σ	Age	1σ	Age	1σ	Age	1σ	Age	1σ	
SWA13a-003	225	317	0.71	0.6	0.26	0.2386	0.0036	14.81	0.23	0.4506	0.0056	0.129	0.003	3111	11	2803	15	2398	25	2445	56	y
SWA13a-004	208	304	0.68			0.2379	0.0046	18.25	0.36	0.5570	0.0077	0.146	0.005	3106	15	3003	19	2854	32	2748	86	y
SWA13a-005c	139	147	0.95			0.2391	0.0030	19.72	0.27	0.5986	0.0071	0.160	0.003	3114	9	3078	13	3024	29	2993	51	y
SWA13a-006	369	663	0.56	5.32	0.58	0.2591	0.0062	9.36	0.22	0.2620	0.0036	0.121	0.006	3241	19	2374	22	1500	19	2313	102	
SWA13a-008c	122	158	0.77			0.2401	0.0044	20.53	0.38	0.6202	0.0080	0.167	0.005	3121	14	3117	18	3111	32	3115	93	y
SWA13a-009	182	427	0.43			0.2381	0.0034	19.81	0.30	0.6035	0.0074	0.158	0.004	3108	10	3082	15	3044	30	2967	64	y
SWA13a-010	138	243	0.57			0.2421	0.0036	21.31	0.33	0.6384	0.0076	0.171	0.004	3134	11	3153	15	3183	30	3195	72	y
SWA13a-011	275	722	0.38	1.16	0.19	0.2375	0.0041	17.21	0.30	0.5257	0.0067	0.175	0.005	3103	13	2947	17	2723	28	3254	89	y
SWA13a-012c	186	243	0.77	1.59	0.32	0.2405	0.0036	17.74	0.28	0.5352	0.0068	0.166	0.004	3123	11	2976	15	2763	29	3101	69	y
SWA13a-014	446	342	1.30			0.2555	0.0031	11.03	0.15	0.3130	0.0037	0.056	0.001	3219	9	2525	12	1755	18	1095	18	
SWA13a-015c	44	73	0.61			0.2398	0.0031	21.37	0.30	0.6467	0.0079	0.165	0.003	3118	9	3156	14	3215	31	3091	54	y
SWA13a-016	306	612	0.50	1.19	0.22	0.2427	0.0039	18.49	0.31	0.5528	0.0072	0.175	0.005	3138	12	3016	16	2837	30	3265	80	y
SWA13a-017	126	207	0.61			0.2432	0.0043	20.18	0.36	0.6020	0.0077	0.160	0.005	3141	13	3100	17	3038	31	3004	83	y
SWA13a-018	411	453	0.91	2.93	0.5	0.2663	0.0047	16.07	0.29	0.4379	0.0057	0.144	0.004	3284	13	2881	17	2341	26	2725	78	
SWA13a-019	146	176	0.83			0.2444	0.0043	20.71	0.38	0.6147	0.0080	0.169	0.005	3149	13	3125	18	3089	32	3151	89	y
SWA13a-020	130	248	0.52	2.04	0.26	0.2409	0.0040	13.98	0.24	0.4209	0.0055	0.147	0.004	3126	12	2748	16	2265	25	2767	72	y
SWA13a-021c	165	210	0.78			0.2379	0.0054	15.55	0.35	0.4743	0.0068	0.125	0.005	3106	17	2850	21	2502	30	2386	91	y
SWA13a-024c	268	361	0.74			0.2500	0.0054	14.92	0.31	0.4331	0.0057	0.100	0.004	3185	16	2810	20	2319	25	1923	71	
SWA13a-025	124	199	0.62			0.2470	0.0036	18.62	0.28	0.5471	0.0064	0.133	0.003	3165	10	3022	14	2813	27	2527	55	
SWA13a-028	185	239	0.78			0.2392	0.0039	21.40	0.37	0.6488	0.0087	0.163	0.004	3114	12	3157	17	3223	34	3052	75	y
SWA13a-029	194	285	0.68			0.2386	0.0036	20.40	0.32	0.6200	0.0077	0.165	0.004	3110	11	3110	15	3110	31	3082	69	y
SWA13a-032	247	442	0.56	6.2	0.8	0.2383	0.0078	9.48	0.30	0.2890	0.0054	0.143	0.009	3109	26	2386	29	1636	27	2709	151	y
SWA13a-034	110	236	0.47	1.2	0.18	0.2464	0.0037	18.82	0.29	0.5538	0.0069	0.178	0.004	3162	11	3033	15	2841	29	3304	72	
SWA13a-035c	469	298	1.57			0.2403	0.0045	12.07	0.22	0.3643	0.0046	0.068	0.002	3122	14	2610	17	2003	22	1324	42	y
SWA13a-036	177	530	0.33	1.21	0.22	0.2549	0.0055	14.84	0.32	0.4221	0.0055	0.145	0.006	3216	17	2805	20	2270	25	2733	102	

				Ratios (corrected)								Ages (corrected; Ma)									
	Disc.	Correction	^{204}Pb	^{207}Pb/^{206}Pb		^{207}Pb/^{235}U		^{206}Pb/^{238}U		^{208}Pb/^{232}Th		^{207}Pb/^{206}Pb		^{207}Pb/^{235}U		^{206}Pb/^{238}U		^{208}Pb/^{232}Th		Inc.?	
	%	type	cps	Ratio	1σ	Ratio	1σ	Ratio	1σ	Ratio	1σ	Age	1σ	Age	1σ	Age	1σ	Age	1σ	Int	W/A
SWA13a-003	27.03	Disc	110	0.2348	0.0024	14.50	0.30	0.4479	0.0060	0.1203	0.0015	3085	15	2783	20	2386	26	2297	28	y	y
SWA13a-004	10.13	None	139	0.2379	0.0022	18.25	0.36	0.5570	0.0077	0.1457	0.0049	3106	15	3003	19	2854	32	2748	86	y	y
SWA13a-005c	3.64	None	62	0.2391	0.0014	19.72	0.27	0.5986	0.0071	0.1596	0.0029	3114	9	3078	13	3024	29	2993	51	y	y
SWA13a-006	58.63	Disc	532	0.2267	0.0055	7.75	0.29	0.2481	0.0040	0.0669	0.0012	3029	37	2203	34	1429	21	1308	23		
SWA13a-008c	0.41	None	66	0.2401	0.0021	20.53	0.38	0.6202	0.0080	0.1667	0.0054	3121	14	3117	18	3111	32	3115	93	y	y
SWA13a-009	2.59	None	58	0.2381	0.0016	19.81	0.30	0.6035	0.0074	0.1581	0.0037	3108	10	3082	15	3044	30	2967	64	y	y
SWA13a-010	-1.95	None	23	0.2421	0.0017	21.31	0.33	0.6384	0.0076	0.1713	0.0042	3134	11	3153	15	3183	30	3195	72	y	y
SWA13a-011	14.28	Disc	211	0.2304	0.0023	16.51	0.33	0.5196	0.0065	0.1399	0.0018	3055	15	2907	19	2698	28	2646	31		
SWA13a-012c	13.21	Disc	115	0.2308	0.0026	16.76	0.37	0.5267	0.0071	0.1417	0.0019	3057	17	2921	21	2728	30	2679	33		
SWA13a-014	51.69	None	306	0.2555	0.0015	11.03	0.15	0.3130	0.0037	0.0557	0.0009	3219	9	2525	12	1755	18	1095	18		
SWA13a-015c	-3.92	None	62	0.2398	0.0015	21.37	0.30	0.6467	0.0079	0.1652	0.0031	3118	9	3156	14	3215	31	3091	54	y	y
SWA13a-016	11.19	Disc	393	0.2355	0.0023	17.74	0.35	0.5462	0.0071	0.1467	0.0019	3090	15	2975	19	2809	30	2767	33	y	y
SWA13a-017	4.14	None	28	0.2432	0.0020	20.18	0.36	0.6020	0.0077	0.1602	0.0048	3141	13	3100	17	3038	31	3004	83	y	y
SWA13a-018	33.31	Disc	742	0.2490	0.0039	14.59	0.41	0.4250	0.0063	0.1136	0.0016	3179	24	2789	26	2283	28	2174	30		
SWA13a-019	2.42	None	93	0.2444	0.0021	20.71	0.38	0.6147	0.0080	0.1687	0.0052	3149	13	3125	18	3089	32	3151	89	y	y
SWA13a-020	31.6	Disc	57	0.2285	0.0026	12.99	0.29	0.4124	0.0056	0.1111	0.0015	3041	18	2679	21	2226	25	2129	27		
SWA13a-021c	23.39	None	64	0.2379	0.0027	15.55	0.35	0.4743	0.0068	0.1253	0.0051	3106	17	2850	21	2502	30	2386	91	y	y
SWA13a-024c	32.22	None	216	0.2500	0.0027	14.92	0.31	0.4331	0.0057	0.0998	0.0039	3185	16	2810	20	2319	25	1923	71		
SWA13a-025	13.73	None	89	0.2470	0.0016	18.62	0.28	0.5471	0.0064	0.1332	0.0031	3165	10	3022	14	2813	27	2527	55		
SWA13a-028	-4.49	None	29	0.2392	0.0019	21.40	0.37	0.6488	0.0087	0.1630	0.0043	3114	12	3157	17	3223	34	3052	75	y	y
SWA13a-029	-0.01	None	45	0.2386	0.0017	20.40	0.32	0.6200	0.0077	0.1647	0.0040	3110	11	3110	15	3110	31	3082	69	y	y
SWA13a-032	50.46	Disc	118	0.1984	0.0075	7.42	0.42	0.2710	0.0059	0.0740	0.0017	2813	59	2163	50	1546	30	1443	31		
SWA13a-034	11.94	Disc	121	0.2393	0.0021	18.05	0.34	0.5471	0.0069	0.1467	0.0018	3115	13	2992	18	2813	29	2767	33	y	y
SWA13a-035c	41.52	None	204	0.2403	0.0022	12.07	0.22	0.3643	0.0046	0.0677	0.0022	3122	14	2610	17	2003	22	1324	42	y	y
SWA13a-036	34.38	Disc	456	0.2478	0.0033	14.25	0.34	0.4170	0.0055	0.1115	0.0015	3171	20	2766	23	2247	25	2136	26		

						Ratios (uncorrected)								Ages (uncorrected; Ma)								
	Th	U	Th/U	Common Pb		$^{207}Pb/^{206}Pb$		$^{207}Pb/^{235}U$		$^{206}Pb/^{238}U$		$^{208}Pb/^{232}Th$		$^{207}Pb/^{206}Pb$		$^{207}Pb/^{235}U$		$^{206}Pb/^{238}U$		$^{208}Pb/^{232}Th$		Inc.?
	ppm	ppm		%	1σ	Ratio	1σ	Ratio	1σ	Ratio	1σ	Ratio	1σ	Age	1σ	Age	1σ	Age	1σ	Age	1σ	
SWA13a-037	172	384	0.45	3.64	0.3	0.2403	0.0044	11.19	0.21	0.3377	0.0044	0.148	0.005	3122	13	2539	17	1876	21	2782	79	y
SWA13a-039	181	206	0.88			0.2477	0.0056	17.52	0.39	0.5128	0.0072	0.134	0.005	3170	17	2964	21	2669	31	2550	93	
SWA13a-040	834	1575	0.53	8.75	0.41	0.2496	0.0034	4.51	0.07	0.1310	0.0016	0.080	0.002	3182	10	1732	12	793	9	1549	31	
SWA13a-041	121	147	0.82			0.2388	0.0038	18.60	0.30	0.5649	0.0069	0.156	0.004	3112	12	3021	15	2887	28	2928	75	y
SWA13a-042	88	167	0.53			0.2401	0.0042	20.38	0.36	0.6157	0.0077	0.181	0.006	3121	13	3110	17	3093	31	3360	97	
SWA13a-043	254	274	0.93			0.2404	0.0045	20.98	0.40	0.6328	0.0084	0.168	0.006	3123	15	3138	19	3161	33	3142	99	y
SWA13a-044	187	368	0.51			0.2416	0.0076	17.01	0.53	0.5103	0.0086	0.147	0.009	3130	28	2936	30	2658	37	2781	156	y
SWA13a-045	136	144	0.94			0.2386	0.0047	19.32	0.39	0.5873	0.0079	0.153	0.005	3110	15	3058	19	2978	32	2882	96	y
SWA13a-046c	498	918	0.54	0.91	0.35	0.2203	0.0049	9.61	0.22	0.3163	0.0043	0.097	0.004	2983	19	2398	21	1772	21	1863	75	
SWA13a-047	375	1283	0.29	2.34	0.32	0.2035	0.0055	4.57	0.12	0.1629	0.0025	0.072	0.004	2854	24	1744	22	973	14	1407	70	
SWA11-001c	153	343	0.45	1.09	0.33	0.2405	0.0043	18.77	0.32	0.5664	0.0062	0.178	0.008	3123	13	3030	16	2893	26	3305	134	y
SWA11-003	234	306	0.76	0.93	0.44	0.2423	0.0037	20.12	0.30	0.6026	0.0068	0.175	0.006	3135	11	3097	14	3040	27	3254	108	y
SWA11-004	256	515	0.50			0.2398	0.0036	19.61	0.29	0.5930	0.0066	0.161	0.006	3119	11	3072	14	3002	27	3019	97	y
SWA11-006	163	585	0.28			0.2415	0.0039	20.90	0.34	0.6276	0.0074	0.179	0.007	3130	12	3134	16	3140	29	3329	123	
SWA11-007	76	149	0.51			0.2402	0.0043	21.16	0.36	0.6390	0.0073	0.177	0.008	3121	13	3146	17	3185	29	3288	131	
SWA11-008	326	667	0.49	1.21	0.27	0.2429	0.0036	19.60	0.28	0.5856	0.0062	0.184	0.006	3139	10	3072	14	2971	25	3417	106	y
SWA11-010	422	591	0.71	4.62	0.48	0.2442	0.0035	15.23	0.22	0.4524	0.0053	0.175	0.005	3148	10	2830	14	2406	24	3263	94	y
SWA11-013	240	307	0.78			0.2412	0.0034	19.43	0.28	0.5844	0.0067	0.153	0.005	3128	10	3064	14	2967	27	2881	83	y
SWA11-014	219	623	0.35	1.51	0.33	0.2469	0.0051	19.41	0.40	0.5705	0.0077	0.200	0.011	3165	16	3063	20	2910	31	3677	177	y
SWA11-015	209	441	0.47	6.49	0.58	0.2643	0.0049	6.16	0.11	0.1691	0.0020	0.089	0.004	3273	14	1999	16	1007	11	1720	72	
SWA11-016	90	226	0.40			0.2425	0.0033	21.07	0.28	0.6304	0.0068	0.174	0.005	3136	9	3142	13	3151	27	3240	86	
SWA11-017	60	164	0.36			0.2419	0.0042	21.26	0.37	0.6377	0.0080	0.169	0.007	3132	13	3150	17	3180	31	3157	121	y
SWA11-020	302	398	0.76	4.24	0.81	0.2579	0.0055	20.39	0.44	0.5735	0.0078	0.211	0.011	3234	17	3110	21	2922	32	3877	190	
SWA11-023c	304	460	0.66	2.77	0.55	0.2398	0.0045	14.68	0.26	0.4441	0.0050	0.154	0.007	3119	14	2795	17	2369	22	2889	122	y
SWA11-024	352	860	0.41			0.2375	0.0048	18.40	0.37	0.5621	0.0073	0.142	0.007	3103	16	3011	19	2875	30	2676	125	y

				Ratios (corrected)								Ages (corrected; Ma)									
	Disc.	Correction type	^{204}Pb	^{207}Pb/^{206}Pb		^{207}Pb/^{235}U		^{206}Pb/^{238}U		^{208}Pb/^{232}Th		^{207}Pb/^{206}Pb		^{207}Pb/^{235}U		^{206}Pb/^{238}U		^{208}Pb/^{232}Th		Inc.?	
	%		cps	Ratio	1σ	Ratio	1σ	Ratio	1σ	Ratio	1σ	Age	1σ	Age	1σ	Age	1σ	Age	1σ	Int	W/A
SWA13a-037	44.27	Disc	161	0.2178	0.0032	9.77	0.25	0.3254	0.0045	0.0880	0.0014	2964	22	2413	24	1816	22	1705	25		
SWA13a-039	19.24	None	105	0.2477	0.0028	17.52	0.39	0.5128	0.0072	0.1345	0.0052	3170	17	2964	21	2669	31	2550	93		
SWA13a-040	77.74	Disc	1140	0.1933	0.0037	3.19	0.10	0.1195	0.0017	0.0327	0.0007	2771	31	1454	24	728	10	650	15		
SWA13a-041	8.97	None	34	0.2388	0.0018	18.60	0.30	0.5649	0.0069	0.1559	0.0043	3112	12	3021	15	2887	28	2928	75	y	y
SWA13a-042	1.14	None	36	0.2401	0.0020	20.38	0.36	0.6157	0.0077	0.1809	0.0057	3121	13	3110	17	3093	31	3360	97		
SWA13a-043	-1.56	None	47	0.2404	0.0022	20.98	0.40	0.6328	0.0084	0.1682	0.0057	3123	15	3138	19	3161	33	3142	99	y	y
SWA13a-044	18.28	None	230	0.2416	0.0042	17.01	0.53	0.5103	0.0086	0.1475	0.0088	3130	28	2936	30	2658	37	2781	156	y	y
SWA13a-045	5.3	None	33	0.2386	0.0024	19.32	0.39	0.5873	0.0079	0.1533	0.0055	3110	15	3058	19	2978	32	2882	96	y	y
SWA13a-046c	45.77	Disc	362	0.2146	0.0036	9.27	0.27	0.3135	0.0047	0.0849	0.0012	2941	26	2366	27	1758	23	1648	22		
SWA13a-047	69.81	Disc	345	0.1884	0.0039	4.13	0.14	0.1591	0.0027	0.0436	0.0008	2728	34	1660	28	952	15	863	15		
SWA11-001c	8.46	Disc	129	0.2338	0.0029	18.06	0.39	0.5602	0.0065	0.1506	0.0017	3078	20	2993	21	2867	27	2835	30	y	y
SWA11-003	3.23	Disc	33	0.2367	0.0032	19.48	0.46	0.5970	0.0076	0.1603	0.0019	3098	21	3066	23	3018	31	3005	33	y	y
SWA11-004	4.71	None	2	0.2398	0.0016	19.61	0.29	0.5930	0.0066	0.1611	0.0056	3119	11	3072	14	3002	27	3019	97	y	y
SWA11-006	-0.39	None	82	0.2415	0.0018	20.90	0.34	0.6276	0.0074	0.1790	0.0072	3130	12	3134	16	3140	29	3329	123		
SWA11-007	-2.54	None	38	0.2402	0.0021	21.16	0.36	0.6390	0.0073	0.1767	0.0076	3121	13	3146	17	3185	29	3288	131		
SWA11-008	5.95	Disc	224	0.2356	0.0024	18.79	0.35	0.5785	0.0066	0.1554	0.0017	3090	16	3031	18	2943	27	2919	30	y	y
SWA11-010	25.56	Disc	291	0.2155	0.0036	12.82	0.35	0.4315	0.0060	0.1169	0.0017	2948	27	2667	26	2313	27	2234	30		
SWA11-013	6.45	None	67	0.2412	0.0016	19.43	0.28	0.5844	0.0067	0.1532	0.0047	3128	10	3064	14	2967	27	2881	83	y	y
SWA11-014	9.2	Disc	273	0.2378	0.0034	18.42	0.47	0.5619	0.0080	0.1508	0.0021	3105	22	3012	25	2874	33	2839	37	y	y
SWA11-015	73.47	Disc	227	0.2246	0.0047	4.90	0.16	0.1581	0.0023	0.0427	0.0008	3014	33	1802	28	946	13	844	15		
SWA11-016	-0.58	None	41	0.2425	0.0014	21.07	0.28	0.6304	0.0068	0.1739	0.0050	3136	9	3142	13	3151	27	3240	86		
SWA11-017	-1.9	None	60	0.2419	0.0020	21.26	0.37	0.6377	0.0080	0.1691	0.0070	3132	13	3150	17	3180	31	3157	121	y	y
SWA11-020	9.88	Disc	350	0.2323	0.0061	17.59	0.71	0.5492	0.0094	0.1477	0.0024	3068	41	2967	39	2822	39	2784	42		
SWA11-023c	27.17	Disc	60	0.2228	0.0042	13.27	0.40	0.4319	0.0057	0.1166	0.0015	3001	30	2699	28	2314	26	2229	26		
SWA11-024	9.12	None	72	0.2375	0.0024	18.40	0.37	0.5621	0.0073	0.1416	0.0070	3103	16	3011	19	2875	30	2676	125	y	y

						Ratios (uncorrected)								Ages (uncorrected; Ma)								
	Th	U	Th/U	Common Pb		$^{207}Pb/^{206}Pb$		$^{207}Pb/^{235}U$		$^{206}Pb/^{238}U$		$^{208}Pb/^{232}Th$		$^{207}Pb/^{206}Pb$		$^{207}Pb/^{235}U$		$^{206}Pb/^{238}U$		$^{208}Pb/^{232}Th$		Inc.?
	ppm	ppm		%	1σ	Ratio	1σ	Ratio	1σ	Ratio	1σ	Ratio	1σ	Age	1σ	Age	1σ	Age	1σ	Age	1σ	
SWA11-025	614	716	0.86			0.2455	0.0036	18.01	0.27	0.5323	0.0063	0.146	0.005	3156	11	2990	14	2751	27	2762	85	y
SWA11-026	167	496	0.34	0.53	0.19	0.2521	0.0040	16.69	0.26	0.4800	0.0052	0.143	0.005	3198	11	2917	15	2527	23	2695	96	
SWA11-028c	166	403	0.41	1.58	0.24	0.2412	0.0036	17.88	0.26	0.5379	0.0057	0.183	0.006	3128	10	2983	14	2774	24	3404	105	y
SWA11-029	256	285	0.90			0.2446	0.0040	17.40	0.28	0.5162	0.0063	0.080	0.003	3150	11	2957	16	2683	27	1557	58	y
SWA11-030	228	309	0.74	2.83	0.51	0.2455	0.0039	17.34	0.28	0.5125	0.0062	0.173	0.007	3156	11	2954	16	2667	27	3231	113	y
SWA11-031	241	402	0.60			0.2414	0.0040	20.32	0.34	0.6105	0.0074	0.178	0.007	3129	12	3106	16	3072	30	3304	124	y
SWA11-032c	116	321	0.36	3.08	0.3	0.2516	0.0039	15.48	0.24	0.4465	0.0053	0.192	0.007	3195	11	2845	15	2379	24	3554	118	
SWA11-033	87	170	0.51	1.55	0.32	0.2411	0.0038	17.62	0.28	0.5303	0.0063	0.173	0.006	3127	11	2969	15	2743	27	3217	110	y
SWA11-037	150	341	0.44			0.2442	0.0046	20.23	0.37	0.6008	0.0076	0.169	0.008	3147	14	3102	18	3033	30	3148	138	y
SWA11-038	183	491	0.37	0.8	0.2	0.2452	0.0036	19.71	0.29	0.5830	0.0064	0.180	0.006	3154	10	3077	14	2961	26	3344	102	y
SWA11-040	214	378	0.57	2.16	0.32	0.2402	0.0034	14.04	0.20	0.4241	0.0048	0.144	0.004	3121	10	2753	13	2279	22	2715	78	y
SWA11-041	441	468	0.94			0.2461	0.0037	18.88	0.29	0.5563	0.0066	0.128	0.004	3160	11	3035	15	2851	28	2435	79	
SWA11-045	171	389	0.44	1	0.26	0.2439	0.0038	17.78	0.27	0.5288	0.0058	0.164	0.006	3146	11	2978	14	2736	24	3073	103	y
SWA11-046	115	201	0.57	0.61	0.29	0.2418	0.0036	18.64	0.28	0.5590	0.0065	0.161	0.005	3132	10	3023	14	2863	27	3014	91	y
SWA11-048	296	409	0.72	2.22	0.38	0.2487	0.0034	14.56	0.19	0.4246	0.0046	0.137	0.004	3176	9	2787	13	2281	21	2601	70	
SWA11-051	101	168	0.60	0.84	0.29	0.2445	0.0034	20.21	0.28	0.5998	0.0065	0.176	0.005	3149	10	3102	13	3029	26	3278	91	y
SWA11-052	111	170	0.65			0.2423	0.0050	20.47	0.42	0.6129	0.0083	0.165	0.008	3135	16	3114	20	3082	33	3094	146	y
SWA11-055	89	147	0.61			0.2427	0.0038	20.94	0.32	0.6262	0.0072	0.167	0.006	3137	11	3136	15	3134	29	3120	100	y
SWA11-057	171	629	0.27			0.2395	0.0058	20.38	0.49	0.6175	0.0089	0.156	0.009	3116	20	3110	23	3100	35	2937	164	y
SWA11-058c	118	201	0.59	0.74	0.31	0.2425	0.0037	19.43	0.29	0.5813	0.0065	0.169	0.006	3136	11	3063	14	2954	26	3161	99	y
SWA11-061	432	489	0.88	1.22	0.44	0.2401	0.0033	18.63	0.26	0.5629	0.0064	0.165	0.005	3121	10	3023	13	2879	26	3085	84	y
SWA11-062	443	675	0.66	1.09	0.39	0.2454	0.0038	18.99	0.28	0.5614	0.0060	0.167	0.006	3155	11	3041	14	2873	25	3128	107	y
SWA11-063	298	372	0.80			0.2437	0.0035	18.91	0.26	0.5630	0.0060	0.151	0.005	3144	10	3037	13	2879	25	2845	84	y
SWA11-065	102	215	0.47	2.69	0.28	0.2424	0.0032	15.50	0.21	0.4638	0.0051	0.174	0.005	3136	9	2846	13	2456	23	3238	84	y
SWA11-066	80	154	0.52			0.2406	0.0038	20.74	0.33	0.6254	0.0075	0.170	0.006	3124	11	3127	15	3131	30	3179	108	y

				Ratios (corrected)								Ages (corrected; Ma)									
	Disc.	Correction type	^{204}Pb	^{207}Pb/^{206}Pb		^{207}Pb/^{235}U		^{206}Pb/^{238}U		^{208}Pb/^{232}Th		^{207}Pb/^{206}Pb		^{207}Pb/^{235}U		^{206}Pb/^{238}U		^{208}Pb/^{232}Th		Inc.?	
	%		cps	Ratio	1σ	Ratio	1σ	Ratio	1σ	Ratio	1σ	Age	1σ	Age	1σ	Age	1σ	Age	1σ	Int	W/A
SWA11-025	15.76	None	86	0.2455	0.0017	18.01	0.27	0.5323	0.0063	0.1465	0.0048	3156	11	2990	14	2751	27	2762	85	y	
SWA11-026	25.09	Disc	218	0.2491	0.0023	16.40	0.29	0.4775	0.0054	0.1276	0.0014	3179	14	2900	17	2516	24	2427	25		
SWA11-028c	12.98	Disc	85	0.2316	0.0023	16.91	0.32	0.5294	0.0060	0.1424	0.0016	3063	15	2930	18	2739	25	2691	29		
SWA11-029	18.1	None	57	0.2446	0.0018	17.40	0.28	0.5162	0.0063	0.0801	0.0031	3150	11	2957	16	2683	27	1557	58	y	
SWA11-030	17.35	Disc	158	0.2283	0.0038	15.67	0.44	0.4980	0.0071	0.1341	0.0018	3040	26	2857	27	2605	31	2544	33		
SWA11-031	2.3	None	22	0.2414	0.0019	20.32	0.34	0.6105	0.0074	0.1776	0.0072	3129	12	3106	16	3072	30	3304	124	y	y
SWA11-032c	29.14	Disc	106	0.2330	0.0027	13.90	0.30	0.4327	0.0055	0.1163	0.0017	3073	18	2743	20	2318	25	2224	31	y	
SWA11-033	14.19	Disc	33	0.2317	0.0028	16.68	0.37	0.5221	0.0068	0.1404	0.0018	3064	18	2917	21	2708	29	2656	31	y	
SWA11-037	4.55	None	39	0.2442	0.0022	20.23	0.37	0.6008	0.0076	0.1685	0.0080	3147	14	3102	18	3033	30	3148	138	y	y
SWA11-038	7.21	Disc	86	0.2405	0.0021	19.18	0.34	0.5784	0.0067	0.1551	0.0018	3123	13	3051	17	2942	27	2913	31	y	y
SWA11-040	30.89	Disc	103	0.2271	0.0026	12.99	0.28	0.4149	0.0052	0.1118	0.0014	3031	18	2679	20	2237	24	2142	25		
SWA11-041	12.08	None	135	0.2461	0.0017	18.88	0.29	0.5563	0.0066	0.1280	0.0044	3160	11	3035	15	2851	28	2435	79	y	
SWA11-045	15.42	Disc	92	0.2379	0.0024	17.17	0.33	0.5235	0.0061	0.1405	0.0016	3106	16	2945	19	2714	26	2657	28	y	y
SWA11-046	10.3	Disc	57	0.2382	0.0024	18.24	0.36	0.5556	0.0070	0.1491	0.0018	3108	16	3003	19	2849	29	2809	32	y	y
SWA11-048	32.45	Disc	144	0.2353	0.0028	13.47	0.29	0.4152	0.0052	0.1115	0.0014	3088	19	2713	21	2239	23	2137	25	y	y
SWA11-051	4.32	Disc	47	0.2394	0.0024	19.63	0.38	0.5947	0.0071	0.1595	0.0018	3116	16	3073	19	3009	29	2991	32	y	y
SWA11-052	2.15	None	6	0.2423	0.0025	20.47	0.42	0.6129	0.0083	0.1654	0.0084	3135	16	3114	20	3082	33	3094	146	y	y
SWA11-055	0.14	None	7	0.2427	0.0017	20.94	0.32	0.6262	0.0072	0.1669	0.0058	3137	11	3136	15	3134	29	3120	100	y	y
SWA11-057	0.69	None	8	0.2395	0.0030	20.38	0.49	0.6175	0.0089	0.1564	0.0094	3116	20	3110	23	3100	35	2937	164	y	y
SWA11-058c	6.82	Disc	49	0.2380	0.0026	18.93	0.39	0.5770	0.0071	0.1548	0.0018	3107	17	3038	20	2936	29	2909	32	y	y
SWA11-061	8.88	Disc	104	0.2327	0.0031	17.84	0.43	0.5560	0.0074	0.1495	0.0019	3071	21	2981	23	2850	31	2816	33	y	
SWA11-062	10.51	Disc	134	0.2388	0.0030	18.29	0.41	0.5553	0.0067	0.1490	0.0017	3112	20	3005	22	2847	28	2807	30	y	y
SWA11-063	10.47	None	76	0.2437	0.0015	18.91	0.26	0.5630	0.0060	0.1512	0.0048	3144	10	3037	13	2879	25	2845	84	y	
SWA11-065	24.6	Disc	91	0.2260	0.0023	14.06	0.27	0.4513	0.0055	0.1217	0.0016	3024	16	2754	18	2401	24	2321	28		
SWA11-066	-0.26	None	0	0.2406	0.0017	20.74	0.33	0.6254	0.0075	0.1703	0.0062	3124	11	3127	15	3131	30	3179	108	y	y

						Ratios (uncorrected)								Ages (uncorrected; Ma)								
	Th	U	Th/U	Common Pb		$^{207}Pb/^{206}Pb$		$^{207}Pb/^{235}U$		$^{206}Pb/^{238}U$		$^{208}Pb/^{232}Th$		$^{207}Pb/^{206}Pb$		$^{207}Pb/^{235}U$		$^{206}Pb/^{238}U$		$^{208}Pb/^{232}Th$		Inc.?
	ppm	ppm		%	1σ	Ratio	1σ	Ratio	1σ	Ratio	1σ	Ratio	1σ	Age	1σ	Age	1σ	Age	1σ	Age	1σ	
SWA11-068	129	552	0.23			0.2397	0.0035	19.72	0.29	0.5970	0.0068	0.160	0.005	3118	10	3078	14	3018	27	3002	94	y
SWA11-073	257	331	0.78	1.47	0.45	0.2426	0.0036	18.83	0.28	0.5630	0.0065	0.170	0.006	3137	11	3033	14	2879	27	3176	100	y
SWA11-074	173	405	0.43	2.08	0.44	0.2424	0.0049	17.99	0.35	0.5386	0.0063	0.194	0.011	3135	16	2989	19	2777	26	3580	180	y
SWA11-077	356	542	0.66	3.86	0.56	0.2459	0.0042	13.76	0.23	0.4063	0.0049	0.153	0.006	3158	13	2734	16	2198	22	2874	111	y
SWA11-079	263	298	0.88			0.2424	0.0046	20.72	0.37	0.6201	0.0070	0.179	0.009	3136	14	3126	17	3110	28	3328	151	
SWA11-081	237	309	0.76			0.2408	0.0039	19.55	0.32	0.5888	0.0072	0.167	0.006	3125	12	3069	16	2984	29	3128	108	y
SWA11-084	168	255	0.66			0.2414	0.0043	21.18	0.38	0.6367	0.0081	0.183	0.008	3129	13	3147	17	3176	32	3391	135	
SWA11-085	293	390	0.75	1.17	0.46	0.2400	0.0037	17.42	0.27	0.5264	0.0061	0.156	0.006	3120	11	2958	15	2726	26	2930	97	y
SWA11-086	308	578	0.53			0.2448	0.0051	18.84	0.38	0.5580	0.0069	0.146	0.008	3152	16	3034	19	2858	29	2751	134	y
SWA11-088	168	459	0.37	0.47	0.2	0.2424	0.0036	20.61	0.30	0.6168	0.0068	0.180	0.006	3135	10	3120	14	3097	27	3350	105	y
SWA09-001c	135	178	0.76			0.2412	0.0060	16.54	0.41	0.4978	0.0074	0.097	0.004	3128	20	2909	23	2604	32	1872	69	y
SWA09-002	146	369	0.40	3.41	0.38	0.2455	0.0058	14.47	0.33	0.4273	0.0058	0.189	0.008	3156	19	2781	22	2294	26	3501	137	y
SWA09-004	102	206	0.49			0.2410	0.0080	19.65	0.64	0.5916	0.0098	0.169	0.011	3127	29	3074	31	2996	40	3159	186	y
SWA09-005c	175	332	0.53			0.2434	0.0056	17.58	0.40	0.5246	0.0075	0.086	0.003	3142	18	2967	22	2719	32	1660	57	y
SWA09-010	172	116	1.47			0.2414	0.0049	8.34	0.17	0.2508	0.0033	0.056	0.002	3129	15	2269	18	1443	17	1107	37	y
SWA09-011c	130	446	0.29			0.2393	0.0048	18.61	0.38	0.5641	0.0076	0.137	0.004	3115	16	3022	20	2883	31	2597	76	y
SWA09-012	88	119	0.74			0.2408	0.0046	20.04	0.38	0.6036	0.0075	0.161	0.005	3125	14	3093	18	3044	30	3010	93	y
SWA09-016	61	86	0.71			0.2414	0.0049	19.61	0.39	0.5890	0.0075	0.161	0.006	3129	16	3072	19	2986	31	3014	102	y
SWA09-017c	261	116	2.25			0.2446	0.0037	18.94	0.29	0.5615	0.0067	0.056	0.001	3150	11	3039	15	2873	27	1093	25	y
SWA09-018	631	637	0.99			0.3015	0.0054	16.51	0.30	0.3972	0.0051	0.086	0.003	3478	13	2907	17	2156	23	1668	50	
SWA09-021c	122	244	0.50			0.2430	0.0039	19.52	0.32	0.5828	0.0071	0.159	0.004	3139	12	3068	16	2960	29	2983	74	y
SWA09-023c	131	282	0.47			0.2434	0.0041	19.69	0.33	0.5869	0.0072	0.153	0.004	3142	12	3076	16	2977	29	2874	77	y
SWA09-025	1245	1330	0.94			0.2330	0.0053	4.86	0.11	0.1515	0.0021	0.031	0.001	3072	18	1796	19	909	11	611	26	
SWA09-026c	169	867	0.20			0.2450	0.0043	18.14	0.32	0.5372	0.0066	0.137	0.004	3153	13	2997	17	2772	28	2596	75	y
SWA09-027c	423	375	1.13			0.2856	0.0080	14.78	0.41	0.3754	0.0057	0.095	0.005	3394	23	2801	26	2055	27	1827	93	

				Ratios (corrected)								Ages (corrected; Ma)									
	Disc.	Correction type	^{204}Pb	^{207}Pb/^{206}Pb		^{207}Pb/^{235}U		^{206}Pb/^{238}U		^{208}Pb/^{232}Th		^{207}Pb/^{206}Pb		^{207}Pb/^{235}U		^{206}Pb/^{238}U		^{208}Pb/^{232}Th		Inc.?	
	%		cps	Ratio	1σ	Ratio	1σ	Ratio	1σ	Ratio	1σ	Age	1σ	Age	1σ	Age	1σ	Age	1σ	Int	W/A
SWA11-068	4.05	None	36	0.2397	0.0016	19.72	0.29	0.5970	0.0068	0.1601	0.0054	3118	10	3078	14	3018	27	3002	94	y	y
SWA11-073	9.34	Disc	122	0.2337	0.0033	17.88	0.44	0.5548	0.0074	0.1491	0.0019	3078	22	2983	24	2845	31	2809	33	y	y
SWA11-074	12.84	Disc	70	0.2297	0.0038	16.70	0.46	0.5274	0.0069	0.1420	0.0019	3050	26	2918	26	2730	29	2683	33	y	
SWA11-077	33.97	Disc	100	0.2220	0.0043	11.96	0.37	0.3906	0.0056	0.1055	0.0015	2996	30	2601	29	2125	26	2027	28		
SWA11-079	1.03	None	67	0.2424	0.0022	20.72	0.37	0.6201	0.0070	0.1790	0.0088	3136	14	3126	17	3110	28	3328	151		
SWA11-081	5.63	None	48	0.2408	0.0018	19.55	0.32	0.5888	0.0072	0.1674	0.0063	3125	12	3069	16	2984	29	3128	108	y	y
SWA11-084	-1.89	None	50	0.2414	0.0021	21.18	0.38	0.6367	0.0081	0.1827	0.0079	3129	13	3147	17	3176	32	3391	135		
SWA11-085	14.79	Disc	69	0.2329	0.0035	16.71	0.44	0.5203	0.0072	0.1399	0.0018	3072	23	2918	25	2700	30	2646	32	y	y
SWA11-086	11.49	None	24	0.2448	0.0025	18.84	0.38	0.5580	0.0069	0.1458	0.0076	3152	16	3034	19	2858	29	2751	134	y	y
SWA11-088	1.26	Disc	41	0.2395	0.0021	20.28	0.36	0.6140	0.0072	0.1646	0.0019	3117	14	3105	17	3086	29	3081	33	y	y
SWA09-001c	20.35	None	220	0.2412	0.0031	16.54	0.41	0.4978	0.0074	0.0971	0.0038	3128	20	2909	23	2604	32	1872	69	y	y
SWA09-002	30.78	Disc	311	0.2248	0.0041	12.79	0.39	0.4128	0.0060	0.1114	0.0018	3015	28	2664	28	2228	27	2134	32		
SWA09-004	5.26	None	83	0.2410	0.0046	19.65	0.64	0.5916	0.0098	0.1692	0.0108	3127	29	3074	31	2996	40	3159	186	y	y
SWA09-005c	16.59	None	243	0.2434	0.0029	17.58	0.40	0.5246	0.0075	0.0856	0.0031	3142	18	2967	22	2719	32	1660	57	y	y
SWA09-010	59.87	None	112	0.2414	0.0024	8.34	0.17	0.2508	0.0033	0.0563	0.0019	3129	15	2269	18	1443	17	1107	37	y	y
SWA09-011c	9.26	None	190	0.2393	0.0025	18.61	0.38	0.5641	0.0076	0.1371	0.0043	3115	16	3022	20	2883	31	2597	76	y	y
SWA09-012	3.25	None	11	0.2408	0.0022	20.04	0.38	0.6036	0.0075	0.1606	0.0053	3125	14	3093	18	3044	30	3010	93	y	y
SWA09-016	5.75	None	24	0.2414	0.0025	19.61	0.39	0.5890	0.0075	0.1608	0.0059	3129	16	3072	19	2986	31	3014	102	y	y
SWA09-017c	10.91	None	95	0.2446	0.0017	18.94	0.29	0.5615	0.0067	0.0556	0.0013	3150	11	3039	15	2873	27	1093	25	y	y
SWA09-018	44.47	None	586	0.3015	0.0026	16.51	0.30	0.3972	0.0051	0.0860	0.0027	3478	13	2907	17	2156	23	1668	50		
SWA09-021c	7.13	None	35	0.2430	0.0019	19.52	0.32	0.5828	0.0071	0.1590	0.0043	3139	12	3068	16	2960	29	2983	74	y	y
SWA09-023c	6.58	None	90	0.2434	0.0019	19.69	0.33	0.5869	0.0072	0.1528	0.0044	3142	12	3076	16	2977	29	2874	77	y	y
SWA09-025	75.2	None	539	0.2330	0.0028	4.86	0.11	0.1515	0.0021	0.0307	0.0013	3072	18	1796	19	909	11	611	26		
SWA09-026c	14.85	None	96	0.2450	0.0021	18.14	0.32	0.5372	0.0066	0.1370	0.0042	3153	13	2997	17	2772	28	2596	75	y	y
SWA09-027c	45.83	None	602	0.2856	0.0044	14.78	0.41	0.3754	0.0057	0.0946	0.0050	3394	23	2801	26	2055	27	1827	93		

						Ratios (uncorrected)								Ages (uncorrected; Ma)								
	Th	U	Th/U	Common Pb		$^{207}Pb/^{206}Pb$		$^{207}Pb/^{235}U$		$^{206}Pb/^{238}U$		$^{208}Pb/^{232}Th$		$^{207}Pb/^{206}Pb$		$^{207}Pb/^{235}U$		$^{206}Pb/^{238}U$		$^{208}Pb/^{232}Th$		Inc.?
	ppm	ppm		%	1σ	Ratio	1σ	Ratio	1σ	Ratio	1σ	Ratio	1σ	Age	1σ	Age	1σ	Age	1σ	Age	1σ	
SWA09-029c	375	352	1.07	1.93	0.74	0.2480	0.0057	19.55	0.44	0.5717	0.0076	0.172	0.007	3172	18	3069	22	2915	31	3215	126	y
SWA09-034c	76	150	0.50			0.2423	0.0051	20.83	0.43	0.6237	0.0083	0.168	0.006	3135	16	3131	20	3125	33	3133	112	y
SWA09-042c	256	258	0.99			0.2408	0.0055	19.85	0.44	0.5981	0.0079	0.150	0.006	3125	18	3084	21	3022	32	2825	111	y
SWA09-043c	266	231	1.15			0.2457	0.0032	17.23	0.24	0.5087	0.0060	0.070	0.001	3157	9	2948	13	2651	25	1368	26	y
SWA09-044c	73	113	0.65	0.56	0.21	0.2365	0.0032	18.34	0.25	0.5627	0.0066	0.161	0.003	3096	9	3008	13	2878	27	3011	57	
SWA09-045	4817	5479	0.88	4.98	0.48	0.1353	0.0021	0.69	0.01	0.0371	0.0005	0.015	0.000	2167	12	534	7	235	3	296	8	
SWA09-046	474	1177	0.40			0.2266	0.0060	12.76	0.34	0.4082	0.0065	0.120	0.006	3028	21	2662	25	2207	30	2282	111	
SWA09-048	3161	4712	0.67	14.01	1.13	0.2129	0.0053	1.11	0.03	0.0377	0.0005	0.026	0.001	2928	20	756	13	238	3	520	25	
SWA09-050	439	342	1.29			0.2311	0.0077	8.49	0.28	0.2664	0.0048	0.044	0.003	3060	28	2285	30	1523	24	876	52	
SWA02a-004c	797	1672	0.48	5.47	0.29	0.2109	0.0025	4.14	0.05	0.1424	0.0016	0.073	0.002	2913	8	1662	10	858	9	1423	29	
SWA02a-005c	846	1902	0.44	6.47	0.31	0.2131	0.0026	7.90	0.10	0.2688	0.0030	0.166	0.004	2929	8	2219	11	1535	15	3102	62	
SWA02a-006	337	868	0.39	2.07	0.23	0.1600	0.0023	3.66	0.06	0.1657	0.0020	0.067	0.002	2456	11	1562	12	988	11	1311	41	
SWA02a-007c	643	1427	0.45	7.03	0.37	0.2426	0.0032	5.98	0.08	0.1790	0.0019	0.114	0.003	3137	9	1974	11	1061	10	2187	55	
SWA02a-007r	809	2405	0.34	6.33	0.32	0.2048	0.0026	3.61	0.05	0.1278	0.0014	0.084	0.002	2865	9	1551	10	775	8	1627	38	
SWA02a-008	624	1064	0.59	5.58	0.39	0.2292	0.0032	9.19	0.13	0.2908	0.0034	0.153	0.005	3046	10	2357	13	1645	17	2884	83	
SWA02a-009	492	1318	0.37	11.28	0.79	0.2349	0.0048	5.52	0.11	0.1705	0.0020	0.170	0.009	3085	16	1904	17	1015	11	3170	150	
SWA02a-012c	222	535	0.42	3.27	0.26	0.3001	0.0042	17.02	0.24	0.4115	0.0047	0.179	0.005	3471	9	2936	14	2222	21	3328	94	
SWA02a-024c	223	441	0.51	1.62	0.26	0.2560	0.0040	18.27	0.27	0.5178	0.0057	0.179	0.006	3222	11	3004	14	2690	24	3322	110	
SWA02a-027c	943	1256	0.75	11.43	0.68	0.2469	0.0037	5.78	0.08	0.1697	0.0018	0.111	0.004	3165	10	1943	12	1010	10	2134	69	
SWA02a-030c	304	1074	0.28	0.73	0.14	0.2250	0.0034	14.81	0.24	0.4774	0.0061	0.158	0.006	3017	11	2803	15	2516	26	2970	98	
SWA02a-031c	704	2084	0.34	8.85	0.56	0.2104	0.0037	4.30	0.08	0.1484	0.0020	0.133	0.006	2909	13	1694	15	892	11	2524	101	
SWA02a-032	133	800	0.17	0.75	0.08	0.2392	0.0032	11.93	0.16	0.3617	0.0038	0.136	0.004	3115	9	2599	12	1990	18	2584	70	y
SWA02a-037c	656	2185	0.30	7.01	0.46	0.2045	0.0036	4.31	0.08	0.1528	0.0020	0.121	0.005	2863	13	1695	15	917	11	2315	92	
SWA02a-042c	330	1021	0.32	2	0.21	0.2366	0.0040	12.81	0.22	0.3929	0.0051	0.178	0.007	3097	13	2666	17	2136	24	3304	127	
SWA02a-043	251	2465	0.10	8.46	0.65	0.2379	0.0066	2.49	0.06	0.0759	0.0012	0.129	0.008	3106	21	1269	18	471	7	2444	147	

				Ratios (corrected)								Ages (corrected; Ma)									
	Disc.	Correction type	^{204}Pb	^{207}Pb/^{206}Pb		^{207}Pb/^{235}U		^{206}Pb/^{238}U		^{208}Pb/^{232}Th		^{207}Pb/^{206}Pb		^{207}Pb/^{235}U		^{206}Pb/^{238}U		^{208}Pb/^{232}Th		Inc.?	
	%		cps	Ratio	1σ	Ratio	1σ	Ratio	1σ	Ratio	1σ	Age	1σ	Age	1σ	Age	1σ	Age	1σ	Int	W/A
SWA09-029c	9.05	Disc	280	0.2364	0.0056	18.28	0.69	0.5607	0.0092	0.1505	0.0022	3096	35	3004	36	2869	38	2834	39	y	y
SWA09-034c	0.42	None	34	0.2423	0.0026	20.83	0.43	0.6237	0.0083	0.1677	0.0065	3135	16	3131	20	3125	33	3133	112	y	y
SWA09-042c	4.14	None	42	0.2408	0.0029	19.85	0.44	0.5981	0.0079	0.1500	0.0063	3125	18	3084	21	3022	32	2825	111	y	y
SWA09-043c	19.51	None	99	0.2457	0.0015	17.23	0.24	0.5087	0.0060	0.0701	0.0014	3157	9	2948	13	2651	25	1368	26	y	y
SWA09-044c	8.38	Disc	41	0.2330	0.0019	17.98	0.32	0.5595	0.0070	0.1504	0.0018	3073	12	2988	17	2865	29	2832	32		
SWA09-045	87.47	Disc	539	0.0986	0.0039	0.48	0.02	0.0352	0.0005	0.0103	0.0001	1598	70	397	17	223	3	207	3		
SWA09-046	31.9	None	261	0.2266	0.0032	12.76	0.34	0.4082	0.0065	0.1195	0.0061	3028	21	2662	25	2207	30	2282	111		
SWA09-048	90.08	Disc	1191	0.1114	0.0105	0.50	0.06	0.0324	0.0007	0.0094	0.0002	1822	164	410	38	206	4	188	4		
SWA09-050	56.13	None	118	0.2311	0.0042	8.49	0.28	0.2664	0.0048	0.0443	0.0027	3060	28	2285	30	1523	24	876	52		
SWA02a-004c	72.96	Disc	898	0.1747	0.0025	3.24	0.08	0.1346	0.0017	0.0372	0.0006	2603	23	1467	18	814	9	738	12		
SWA02a-005c	48.37	Disc	452	0.1700	0.0027	5.89	0.15	0.2514	0.0031	0.0696	0.0014	2557	25	1960	21	1446	16	1361	27		
SWA02a-006	62.07	Disc	881	0.1457	0.0020	3.26	0.08	0.1623	0.0021	0.0456	0.0006	2296	23	1472	18	969	11	902	12		
SWA02a-007c	69.5	Disc	701	0.1976	0.0032	4.53	0.12	0.1664	0.0021	0.0454	0.0010	2807	25	1737	21	992	11	898	20		
SWA02a-007r	74.46	Disc	818	0.1621	0.0028	2.68	0.07	0.1197	0.0015	0.0333	0.0007	2478	27	1322	19	729	8	662	14		
SWA02a-008	48.86	Disc	1453	0.1933	0.0033	7.32	0.20	0.2745	0.0036	0.0751	0.0014	2770	27	2151	24	1564	18	1464	25		
SWA02a-009	67.12	Disc	2035	0.1585	0.0070	3.31	0.19	0.1513	0.0024	0.0422	0.0016	2440	73	1482	45	908	13	835	31		
SWA02a-012c	42.11	Disc	352	0.2819	0.0025	15.47	0.28	0.3980	0.0049	0.1051	0.0017	3373	13	2845	17	2160	23	2021	30		
SWA02a-024c	19.54	Disc	199	0.2464	0.0024	17.31	0.33	0.5094	0.0060	0.1362	0.0016	3162	15	2952	18	2654	26	2582	29		
SWA02a-027c	69.26	Disc	813	0.1709	0.0058	3.54	0.16	0.1503	0.0022	0.0416	0.0010	2566	55	1537	36	903	12	824	19		
SWA02a-030c	19.5	Disc	133	0.2205	0.0019	14.41	0.25	0.4739	0.0060	0.1281	0.0016	2984	13	2777	17	2501	26	2436	29		
SWA02a-031c	69.11	Disc	1317	0.1496	0.0049	2.79	0.12	0.1353	0.0021	0.0379	0.0012	2341	55	1353	33	818	12	753	23		
SWA02a-032	41.5	Disc	159	0.2347	0.0015	11.61	0.16	0.3590	0.0037	0.0964	0.0011	3084	10	2574	13	1977	17	1861	20	y	
SWA02a-037c	68.84	Disc	1084	0.1569	0.0041	3.07	0.11	0.1421	0.0021	0.0397	0.0011	2422	43	1426	28	857	12	786	20		
SWA02a-042c	35.34	Disc	476	0.2243	0.0024	11.91	0.24	0.3851	0.0050	0.1039	0.0016	3012	17	2597	19	2100	23	1998	29		
SWA02a-043	86.51	Disc	235	0.1826	0.0061	1.75	0.08	0.0694	0.0012	0.0191	0.0013	2677	54	1027	30	433	7	382	26		

						Ratios (uncorrected)								Ages (uncorrected; Ma)								
	Th	U	Th/U	Common Pb		$^{207}Pb/^{206}Pb$		$^{207}Pb/^{235}U$		$^{206}Pb/^{238}U$		$^{208}Pb/^{232}Th$		$^{207}Pb/^{206}Pb$		$^{207}Pb/^{235}U$		$^{206}Pb/^{238}U$		$^{208}Pb/^{232}Th$		Inc.?
	ppm	ppm		%	1σ	Ratio	1σ	Ratio	1σ	Ratio	1σ	Ratio	1σ	Age	1σ	Age	1σ	Age	1σ	Age	1σ	
SWA02a-045c	621	2538	0.24	2.31	0.37	0.1980	0.0039	2.95	0.06	0.1080	0.0015	0.043	0.002	2810	15	1394	15	661	8	842	41	
SWA02a-046c	457	1167	0.39	26.77	1.96	0.3008	0.0089	2.46	0.06	0.0593	0.0010	0.099	0.006	3475	21	1260	19	371	6	1914	115	
SWA02a-047c	256	356	0.72			0.0599	0.0013	0.84	0.02	0.1022	0.0014	0.027	0.001	601	25	621	10	627	8	532	24	
SWA02a-048	653	1517	0.43	7.35	0.85	0.2263	0.0064	2.18	0.06	0.0698	0.0011	0.043	0.003	3026	22	1173	18	435	6	854	55	
SWA02a-052	848	1750	0.48			0.2367	0.0029	15.32	0.19	0.4697	0.0052	0.878	0.020	3098	9	2835	12	2482	23	12739	214	
SWA02a-054c	372	554	0.67			0.2414	0.0039	18.21	0.31	0.5474	0.0070	0.145	0.006	3129	12	3001	16	2814	29	2741	97	y
SWA02a-055	1043	4566	0.23	39.95	1.08	0.3736	0.0046	4.99	0.06	0.0969	0.0011	0.350	0.008	3806	8	1818	11	596	6	6068	124	
SWA02a-064c	681	556	1.22			0.2372	0.0040	18.84	0.33	0.5763	0.0074	0.156	0.006	3101	13	3034	17	2934	30	2934	106	y
RSA07-001	6535	4280	1.53	37.09	1.04	0.3481	0.0044	3.44	0.04	0.0717	0.0007	0.047	0.001	3699	8	1514	9	447	4	937	20	
RSA07-003	558	356	1.57			0.2475	0.0048	18.79	0.35	0.5508	0.0068	0.067	0.003	3169	14	3031	18	2829	28	1312	54	
RSA07-004	390	486	0.80	1.97	0.27	0.2425	0.0028	19.73	0.21	0.5902	0.0054	0.184	0.003	3136	7	3078	10	2990	22	3408	54	y
RSA07-014c	955	1543	0.62	20.69	0.88	0.2461	0.0036	5.74	0.08	0.1692	0.0016	0.148	0.004	3160	9	1938	11	1008	9	2796	73	
RSA07-014r	2575	1628	1.58			0.3036	0.0041	6.73	0.08	0.1607	0.0015	0.100	0.003	3489	8	2076	11	961	8	1922	46	
RSA07-021	133	426	0.31	1.71	0.24	0.2399	0.0042	16.38	0.28	0.4955	0.0058	0.183	0.007	3119	13	2899	16	2594	25	3402	119	y
RSA07-035	2271	667	3.41			0.3212	0.0060	15.60	0.28	0.3523	0.0041	0.078	0.003	3575	13	2853	17	1946	19	1522	61	
RSA07-046	2835	607	4.67			0.2641	0.0046	11.13	0.18	0.3057	0.0033	0.035	0.001	3271	12	2534	15	1720	16	695	26	
RSA07-050	9470	5304	1.79			0.3698	0.0087	2.85	0.06	0.0558	0.0007	0.041	0.002	3791	18	1368	17	350	4	820	45	
RSA07-051	384	482	0.80	4.58	0.94	0.2345	0.0053	13.80	0.30	0.4270	0.0056	0.158	0.009	3083	18	2736	21	2292	25	2965	153	
RSA07-057	33	36	0.93	15.22	0.78	0.2398	0.0037	11.58	0.16	0.3502	0.0037	0.198	0.005	3119	9	2571	13	1935	17	3659	82	
RSA07-069	503	353	1.42			0.2531	0.0041	17.51	0.26	0.5020	0.0053	0.089	0.003	3204	11	2963	15	2622	23	1721	55	
RSA07-079	533	1144	0.47	1.95	0.31	0.2222	0.0036	16.77	0.26	0.5478	0.0060	0.191	0.007	2996	12	2922	15	2816	25	3539	114	
RSA07-080c	583	131	4.46			0.2413	0.0052	16.54	0.34	0.4974	0.0065	0.022	0.001	3128	16	2909	20	2602	28	430	21	y
RSA07-080r	22323	4755	4.69			0.2717	0.0034	1.63	0.02	0.0434	0.0004	0.014	0.000	3316	7	981	7	274	2	286	6	
SWA05-001	632	538	1.17			0.2453	0.0030	11.48	0.14	0.3394	0.0037	0.067	0.002	3155	8	2563	12	1884	18	1302	29	y
SWA05-002c	124	119	1.04			0.2915	0.0039	27.96	0.38	0.6958	0.0080	0.167	0.004	3425	9	3418	13	3405	30	3119	78	

				Ratios (corrected)								Ages (corrected; Ma)									
	Disc.	Correction	^{204}Pb	^{207}Pb/^{206}Pb		^{207}Pb/^{235}U		^{206}Pb/^{238}U		^{208}Pb/^{232}Th		^{207}Pb/^{206}Pb		^{207}Pb/^{235}U		^{206}Pb/^{238}U		^{208}Pb/^{232}Th		Inc.?	
	%	type	cps	Ratio	1σ	Ratio	1σ	Ratio	1σ	Ratio	1σ	Age	1σ	Age	1σ	Age	1σ	Age	1σ	Int	W/A
SWA02a-045c	79.52	Disc	352	0.1829	0.0033	2.66	0.08	0.1055	0.0015	0.0290	0.0004	2679	29	1318	21	647	9	578	8		
SWA02a-046c	85.79	Disc	176	0.1053	0.0213	0.63	0.15	0.0434	0.0015	0.0126	0.0009	1719	401	496	91	274	9	253	19		
SWA02a-047c	-4.49	None	46	0.0599	0.0007	0.84	0.02	0.1022	0.0014	0.0267	0.0012	601	25	621	10	627	8	532	24		
SWA02a-048	87.17	Disc	256	0.1777	0.0072	1.58	0.09	0.0647	0.0012	0.0178	0.0004	2631	67	964	35	404	7	357	8		
SWA02a-052	23.91	None	4158	0.2367	0.0013	15.32	0.19	0.4697	0.0052	0.8781	0.0199	3098	9	2835	12	2482	23	12739	214		
SWA02a-054c	12.45	None	292	0.2414	0.0019	18.21	0.31	0.5474	0.0070	0.1453	0.0055	3129	12	3001	16	2814	29	2741	97	y	y
SWA02a-055	56.55	Disc	6175	0.0661	0.0163	0.53	0.14	0.0582	0.0014	0.0178	0.0037	810	510	432	94	365	8	356	74		
SWA02a-064c	6.78	None	203	0.2372	0.0019	18.84	0.33	0.5763	0.0074	0.1562	0.0061	3101	13	3034	17	2934	30	2934	106	y	y
RSA07-001	55.57	Disc	5937	0.0606	0.0150	0.38	0.10	0.0451	0.0010	0.0139	0.0005	624	470	325	74	285	6	279	9		
RSA07-003	13.26	None	1159	0.2475	0.0023	18.79	0.35	0.5508	0.0068	0.0671	0.0029	3169	14	3031	18	2829	28	1312	54	y	
RSA07-004	4.6	Disc	842	0.2305	0.0020	18.39	0.31	0.5785	0.0060	0.1557	0.0016	3056	13	3010	16	2943	24	2925	28		
RSA07-014c	47.69	Disc	2796	0.0922	0.0095	1.71	0.20	0.1342	0.0022	0.0395	0.0012	1472	189	1011	75	812	13	783	23		
RSA07-014r	77.62	None	4528	0.3036	0.0017	6.73	0.08	0.1607	0.0015	0.0997	0.0025	3489	8	2076	11	961	8	1922	46		
RSA07-021	19.44	Disc	878	0.2294	0.0026	15.41	0.32	0.4870	0.0059	0.1311	0.0017	3048	18	2841	20	2558	25	2490	29		
RSA07-035	52.48	None	3239	0.3212	0.0029	15.60	0.28	0.3523	0.0041	0.0782	0.0032	3575	13	2853	17	1946	19	1522	61		
RSA07-046	53.78	None	2232	0.2641	0.0022	11.13	0.18	0.3057	0.0033	0.0350	0.0013	3271	12	2534	15	1720	16	695	26	y	
RSA07-050	93.03	None	6813	0.3698	0.0045	2.85	0.06	0.0558	0.0007	0.0414	0.0023	3791	18	1368	17	350	4	820	45		
RSA07-051	27.38	Disc	1261	0.2056	0.0071	11.55	0.58	0.4074	0.0071	0.1108	0.0018	2871	54	2568	47	2203	33	2124	32		
RSA07-057	24.37	Disc	375	0.1328	0.0073	5.43	0.37	0.2969	0.0047	0.0842	0.0016	2135	93	1890	58	1676	23	1635	30		
RSA07-069	22.05	None	1162	0.2531	0.0019	17.51	0.26	0.5020	0.0053	0.0889	0.0030	3204	11	2963	15	2622	23	1721	55	y	
RSA07-079	5.64	Disc	1738	0.2099	0.0028	15.54	0.35	0.5371	0.0064	0.1458	0.0017	2905	20	2849	22	2771	27	2751	30		
RSA07-080c	20.41	None	769	0.2413	0.0026	16.54	0.34	0.4974	0.0065	0.0215	0.0011	3128	16	2909	20	2602	28	430	21		
RSA07-080r	93.54	None	3429	0.2717	0.0013	1.63	0.02	0.0434	0.0004	0.0142	0.0003	3316	7	981	7	274	2	286	6		
SWA05-001	46.25	None	341	0.2453	0.0013	11.48	0.14	0.3394	0.0037	0.0665	0.0015	3155	8	2563	12	1884	18	1302	29	y	y
SWA05-002c	0.78	None	159	0.2915	0.0017	27.96	0.38	0.6958	0.0080	0.1669	0.0045	3425	9	3418	13	3405	30	3119	78		

						Ratios (uncorrected)								Ages (uncorrected; Ma)								
	Th	U	Th/U	Common Pb		$^{207}Pb/^{206}Pb$		$^{207}Pb/^{235}U$		$^{206}Pb/^{238}U$		$^{208}Pb/^{232}Th$		$^{207}Pb/^{206}Pb$		$^{207}Pb/^{235}U$		$^{206}Pb/^{238}U$		$^{208}Pb/^{232}Th$		Inc.?
	ppm	ppm		%	1σ	Ratio	1σ	Ratio	1σ	Ratio	1σ	Ratio	1σ	Age	1σ	Age	1σ	Age	1σ	Age	1σ	
SWA05-002r	320	736	0.43	2.7	0.33	0.2340	0.0040	6.33	0.11	0.1961	0.0023	0.081	0.003	3080	12	2022	15	1155	12	1574	65	
SWA05-003	378	664	0.57			0.2350	0.0029	12.90	0.16	0.3981	0.0044	0.106	0.003	3087	9	2672	12	2160	20	2040	48	
SWA05-004	2254	5095	0.44			0.2713	0.0044	2.07	0.03	0.0554	0.0006	0.114	0.004	3314	11	1139	11	347	4	2175	81	
SWA05-006c	403	889	0.45			0.2428	0.0045	16.95	0.33	0.5065	0.0070	0.143	0.007	3139	14	2932	19	2642	30	2702	118	y
SWA05-007c	723	1160	0.62	1.39	0.35	0.2334	0.0036	11.35	0.18	0.3527	0.0043	0.111	0.004	3075	11	2552	15	1947	20	2132	71	
SWA05-007r	1217	6951	0.18			0.1238	0.0022	1.26	0.02	0.0740	0.0010	0.109	0.005	2011	15	829	10	460	6	2087	84	
SWA05-008c	853	853	1.00			0.2400	0.0037	9.79	0.14	0.2960	0.0031	0.066	0.002	3120	11	2416	13	1672	16	1290	45	
SWA05-008r	169	3872	0.04	7.19	0.41	0.1302	0.0025	1.16	0.02	0.0645	0.0007	0.254	0.012	2101	16	781	10	403	4	4567	200	
SWA05-009	164	246	0.67			0.2466	0.0034	18.77	0.26	0.5520	0.0061	0.137	0.004	3163	9	3030	13	2834	25	2603	71	y
SWA05-010c	152	243	0.63			0.2491	0.0039	19.90	0.32	0.5793	0.0070	0.150	0.005	3179	11	3086	15	2946	29	2831	94	y
SWA05-010r	30862	2864	10.78			0.2959	0.0056	4.40	0.08	0.1078	0.0014	0.018	0.001	3449	14	1712	16	660	8	360	17	
SWA05-011	139	341	0.41	1.77	0.29	0.2446	0.0042	12.79	0.22	0.3794	0.0045	0.137	0.006	3150	13	2665	16	2073	21	2600	101	y
SWA05-012c	122	228	0.53			0.2462	0.0034	19.19	0.26	0.5654	0.0063	0.119	0.003	3161	9	3052	13	2889	26	2266	61	y
SWA05-012r	526	1066	0.49			0.2217	0.0034	7.58	0.12	0.2481	0.0030	0.066	0.002	2993	11	2183	14	1428	16	1293	42	
SWA05-013	218	4425	0.05			0.0995	0.0022	0.88	0.02	0.0639	0.0009	0.188	0.010	1615	21	639	11	399	6	3480	169	
SWA05-016	154	291	0.53			0.2441	0.0035	21.08	0.31	0.6266	0.0073	0.187	0.006	3147	10	3142	14	3136	29	3463	94	
SWA05-017	117	254	0.46	1.83	0.31	0.2458	0.0038	14.63	0.22	0.4318	0.0047	0.147	0.005	3158	11	2792	14	2314	21	2765	90	y
SWA05-020	179	443	0.40			0.2409	0.0033	20.65	0.28	0.6219	0.0068	0.322	0.009	3126	9	3122	13	3118	27	5648	140	
SWA05-022c	113	211	0.53			0.2437	0.0035	20.97	0.30	0.6240	0.0071	0.184	0.006	3144	10	3137	14	3126	28	3418	97	
SWA05-022r	126	3018	0.04	8.05	0.3	0.1631	0.0022	3.39	0.05	0.1509	0.0017	0.636	0.018	2488	10	1503	11	906	10	9947	220	
SWA05-023r	298	4389	0.07	10.3	0.41	0.1928	0.0027	4.44	0.06	0.1669	0.0019	0.565	0.017	2766	10	1719	12	995	10	9050	222	
SWA05-025c	2152	1107	1.94			0.2588	0.0037	7.57	0.11	0.2122	0.0024	0.037	0.001	3239	10	2181	13	1240	13	728	22	
SWA05-025r	9508	9909	0.96			0.2919	0.0049	0.93	0.02	0.0230	0.0003	0.024	0.001	3427	12	665	8	147	2	489	19	

				Ratios (corrected)								Ages (corrected; Ma)									
	Disc.	Correction type	^{204}Pb	^{207}Pb/^{206}Pb		^{207}Pb/^{235}U		^{206}Pb/^{238}U		^{208}Pb/^{232}Th		^{207}Pb/^{206}Pb		^{207}Pb/^{235}U		^{206}Pb/^{238}U		^{208}Pb/^{232}Th		Inc.?	
	%		cps	Ratio	1σ	Ratio	1σ	Ratio	1σ	Ratio	1σ	Age	1σ	Age	1σ	Age	1σ	Age	1σ	Int	W/A
SWA05-002r	67.27	Disc	185	0.2173	0.0030	5.72	0.13	0.1908	0.0024	0.0516	0.0007	2961	21	1934	20	1126	13	1018	14		
SWA05-003	35.18	None	141	0.2350	0.0013	12.90	0.16	0.3981	0.0044	0.1062	0.0026	3087	9	2672	12	2160	20	2040	48		
SWA05-004	91.76	None	2354	0.2713	0.0020	2.07	0.03	0.0554	0.0006	0.1136	0.0045	3314	11	1139	11	347	4	2175	81		
SWA05-006c	19.27	None	128	0.2428	0.0023	16.95	0.33	0.5065	0.0070	0.1430	0.0067	3139	14	2932	19	2642	30	2702	118	y	y
SWA05-007c	41.7	Disc	123	0.2249	0.0029	10.78	0.25	0.3478	0.0045	0.0938	0.0012	3016	20	2505	21	1924	22	1813	22		
SWA05-007r	79.78	None	249	0.1238	0.0011	1.26	0.02	0.0740	0.0010	0.1088	0.0046	2011	15	829	10	460	6	2087	84		
SWA05-008c	52.45	None	220	0.2400	0.0016	9.79	0.14	0.2960	0.0031	0.0659	0.0024	3120	11	2416	13	1672	16	1290	45		
SWA05-008r	67.21	Disc	0	0.0755	0.0039	0.62	0.04	0.0599	0.0007	0.0180	0.0025	1081	101	492	23	375	4	361	49		
SWA05-009	12.85	None	83	0.2466	0.0015	18.77	0.26	0.5520	0.0061	0.1374	0.0040	3163	9	3030	13	2834	25	2603	71	y	y
SWA05-010c	9.14	None	90	0.2491	0.0018	19.90	0.32	0.5793	0.0070	0.1503	0.0054	3179	11	3086	15	2946	29	2831	94	y	y
SWA05-010r	84.76	None	3737	0.2959	0.0028	4.40	0.08	0.1078	0.0014	0.0180	0.0008	3449	14	1712	16	660	8	360	17		
SWA05-011	39.14	Disc	97	0.2339	0.0029	12.02	0.27	0.3726	0.0048	0.1002	0.0013	3079	19	2606	21	2042	22	1929	24		
SWA05-012c	10.66	None	27	0.2462	0.0015	19.19	0.26	0.5654	0.0063	0.1186	0.0034	3161	9	3052	13	2889	26	2266	61	y	y
SWA05-012r	58.02	None	194	0.2217	0.0016	7.58	0.12	0.2481	0.0030	0.0661	0.0022	2993	11	2183	14	1428	16	1293	42		
SWA05-013	77.56	None	252	0.0995	0.0012	0.88	0.02	0.0639	0.0009	0.1879	0.0099	1615	21	639	11	399	6	3480	169		
SWA05-016	0.44	None	0	0.2441	0.0016	21.08	0.31	0.6266	0.0073	0.1869	0.0055	3147	10	3142	14	3136	29	3463	94		
SWA05-017	30.92	Disc	106	0.2348	0.0028	13.72	0.29	0.4239	0.0051	0.1139	0.0014	3085	18	2731	20	2278	23	2180	25		
SWA05-020	0.34	None	305	0.2409	0.0015	20.65	0.28	0.6219	0.0068	0.3224	0.0092	3126	9	3122	13	3118	27	5648	140		
SWA05-022c	0.76	None	77	0.2437	0.0016	20.97	0.30	0.6240	0.0071	0.1842	0.0057	3144	10	3137	14	3126	28	3418	97		
SWA05-022r	54.03	Disc	1148	0.1042	0.0030	1.99	0.07	0.1387	0.0017	0.0403	0.0065	1700	51	1113	25	838	10	799	126		
SWA05-023r	57.38	Disc	1920	0.1190	0.0040	2.46	0.11	0.1497	0.0020	0.0430	0.0058	1941	58	1259	31	899	11	850	112		
SWA05-025c	67.5	None	543	0.2588	0.0017	7.57	0.11	0.2122	0.0024	0.0367	0.0011	3239	10	2181	13	1240	13	728	22		
SWA05-025r	96.72	None	2029	0.2919	0.0024	0.93	0.02	0.0230	0.0003	0.0245	0.0010	3427	12	665	8	147	2	489	19		

Appendix H – Zircon Hf-Isotope Analyses

The following information is presented for each analysis:

Measured ratios: Ratios of $^{176}Hf/^{177}Hf$, $^{178}Hf/^{177}Hf$, $^{180}Hf/^{177}Hf$, $^{176}Lu/^{177}Hf$, and $^{176}Yb/^{177}Hf$, and their associated uncertainties.

Total Hf: Total Hf signal intensity (V) and associated uncertainty.

Age: U-Pb age used in the calculation of initial $^{176}Hf/^{177}Hf$, εHf, and model age.

$^{176}Hf/^{177}Hf_i$: Initial ratio calculated at the specified age, and associated uncertainty.

εHf: Deviation (in parts per thousand) from the CHUR (CHondritic Uniform Reservoir) reference value at the specified age, and associated uncertainty.

T(DM)c: Crustal model age (in Ga) calculated from the intersection of an evolution line with Lu/Hf = 0.015 (average crust) with the DM (Depleted Mantle) line.

Samples are ordered from mafic to felsic.

	Measured ratios										Total Hf		Age		$^{176}Hf/^{177}Hf_i$		εHf		T(DM)c
	$^{176}Hf/^{177}Hf$	± 1σ	$^{178}Hf/^{177}Hf$	± 1σ	$^{180}Hf/^{177}Hf$	± 1σ	$^{176}Lu/^{177}Hf$	± 1σ	$^{176}Yb/^{177}Hf$	± 1σ	V	± 1σ	Ma	± 1σ	± 1σ		± 1σ		Ga
RSA03-001	0.280923	0.000013	1.467060	0.000027	1.886470	0.000120	0.000765	0.000059	0.028845	0.002500	3.53	0.04	3109	24	0.280877	0.000013	3.11	0.46	3.29
RSA03-007	0.280858	0.000024	1.467000	0.000045	1.886490	0.000180	0.000645	0.000035	0.022039	0.001300	3.64	0.05	3109	24	0.280819	0.000024	1.05	0.84	3.43
RSA03-011	0.280843	0.000015	1.467080	0.000044	1.886670	0.000180	0.000409	0.000020	0.013884	0.000960	3.51	0.11	3109	24	0.280819	0.000015	1.02	0.53	3.43
RSA03-012	0.280877	0.000009	1.467040	0.000032	1.886490	0.000084	0.000467	0.000019	0.016920	0.000820	3.62	0.05	3109	24	0.280849	0.000009	2.10	0.33	3.36
RSA03-013	0.280858	0.000019	1.466910	0.000027	1.886600	0.000071	0.000626	0.000069	0.025673	0.003200	3.51	0.04	3109	24	0.280821	0.000019	1.09	0.67	3.42
RSA03-014	0.280807	0.000016	1.466940	0.000021	1.886800	0.000070	0.000397	0.000040	0.013943	0.001600	3.42	0.07	3109	24	0.280783	0.000016	-0.24	0.56	3.51
RSA03-016	0.280817	0.000015	1.467020	0.000038	1.886640	0.000120	0.000306	0.000008	0.011655	0.000460	3.40	0.04	3109	24	0.280799	0.000015	0.31	0.53	3.47
RSA03-020	0.280925	0.000014	1.466960	0.000039	1.886700	0.000120	0.000829	0.000069	0.033160	0.003200	3.46	0.05	3109	24	0.280876	0.000014	3.04	0.49	3.30
RSA03-021	0.280817	0.000019	1.467060	0.000036	1.886920	0.000130	0.000388	0.000027	0.013365	0.001400	3.43	0.10	3109	24	0.280794	0.000019	0.14	0.67	3.49
RSA03-022	0.280806	0.000019	1.466960	0.000044	1.886910	0.000120	0.000403	0.000021	0.014554	0.001300	2.92	0.22	3109	24	0.280782	0.000019	-0.29	0.67	3.51
RSA03-023	0.280837	0.000021	1.466830	0.000034	1.886580	0.000120	0.000730	0.000073	0.029091	0.003100	3.25	0.04	3109	24	0.280793	0.000021	0.12	0.73	3.49
RSA03-024	0.280801	0.000018	1.466930	0.000046	1.886800	0.000087	0.000467	0.000030	0.019752	0.001500	3.71	0.03	3109	24	0.280773	0.000018	-0.60	0.63	3.53
RSA03-025	0.280839	0.000021	1.466890	0.000062	1.886610	0.000210	0.000490	0.000050	0.021383	0.002700	3.66	0.03	3109	24	0.280810	0.000021	0.70	0.73	3.45
RSA03-026	0.280882	0.000026	1.466990	0.000039	1.886500	0.000140	0.000493	0.000078	0.019390	0.003500	3.71	0.06	3109	24	0.280853	0.000026	2.23	0.91	3.35
RSA03-034	0.280814	0.000021	1.466920	0.000028	1.886840	0.000120	0.000258	0.000008	0.008841	0.000360	3.70	0.03	3109	24	0.280799	0.000021	0.30	0.73	3.47
RSA01-010c	0.280911	0.000017	1.467200	0.000035	1.886310	0.000092	0.000612	0.000045	0.020941	0.002000	2.80	0.08	3104.3	7.3	0.280875	0.000017	2.90	0.60	3.30
RSA01-011	0.280888	0.000024	1.467160	0.000036	1.886620	0.000150	0.000475	0.000047	0.017236	0.002000	2.72	0.14	3104.3	7.3	0.280860	0.000024	2.37	0.84	3.34
RSA01-013	0.280925	0.000016	1.467140	0.000028	1.886350	0.000095	0.000918	0.000033	0.031111	0.001700	2.24	0.05	3104.3	7.3	0.280870	0.000016	2.75	0.56	3.31
RSA01-018	0.280850	0.000009	1.467140	0.000018	1.886430	0.000078	0.000324	0.000010	0.009506	0.000300	3.56	0.06	3104.3	7.3	0.280831	0.000009	1.34	0.32	3.40
RSA01-022	0.280974	0.000014	1.467180	0.000028	1.886310	0.000073	0.000891	0.000065	0.029314	0.002200	2.49	0.06	3104.3	7.3	0.280921	0.000014	4.55	0.49	3.20
RSA01-027	0.280855	0.000017	1.467100	0.000024	1.886340	0.000110	0.000438	0.000020	0.012056	0.000620	2.63	0.05	3104.3	7.3	0.280829	0.000017	1.27	0.60	3.41
RSA01-033	0.280809	0.000014	1.467130	0.000032	1.886510	0.000061	0.000347	0.000011	0.008638	0.000380	2.75	0.03	3104.3	7.3	0.280788	0.000014	-0.17	0.49	3.50
RSA01-034	0.280826	0.000019	1.467210	0.000045	1.886940	0.000190	0.000438	0.000034	0.011502	0.000740	2.97	0.21	3104.3	7.3	0.280800	0.000019	0.24	0.67	3.47
RSA01-037	0.280791	0.000013	1.467040	0.000054	1.886640	0.000180	0.000749	0.000021	0.019694	0.000610	2.35	0.04	3104.3	7.3	0.280746	0.000013	-1.67	0.46	3.60
RSA01-043	0.280892	0.000017	1.467070	0.000036	1.886730	0.000110	0.000755	0.000049	0.026372	0.001900	2.66	0.05	3104.3	7.3	0.280847	0.000017	1.92	0.60	3.37
RSA01-046	0.280871	0.000018	1.467010	0.000025	1.886700	0.000130	0.000777	0.000017	0.027944	0.001200	2.55	0.05	3104.3	7.3	0.280825	0.000018	1.12	0.63	3.42
RSA01-049	0.280863	0.000017	1.467120	0.000026	1.886730	0.000095	0.000835	0.000035	0.027066	0.001300	2.45	0.06	3104.3	7.3	0.280813	0.000017	0.72	0.60	3.44
SWA18a-004	0.280921	0.000022	1.466860	0.000030	1.886610	0.000110	0.001289	0.000017	0.045792	0.000970	2.76	0.05	3117	21	0.280844	0.000022	2.10	0.77	3.37
SWA18a-007	0.280874	0.000022	1.466970	0.000084	1.886610	0.000340	0.001299	0.000016	0.034830	0.000760	2.79	0.05	3117	21	0.280796	0.000022	0.41	0.77	3.47
SWA18a-011c	0.280845	0.000025	1.467040	0.000056	1.886740	0.000120	0.000398	0.000005	0.010478	0.000150	1.63	0.04	3117	21	0.280821	0.000025	1.30	0.88	3.42

	Measured ratios										Total Hf		Age		$^{176}Hf/^{177}Hf_i$		εHf		T(DM)c
	$^{176}Hf/^{177}Hf$	± 1σ	$^{178}Hf/^{177}Hf$	± 1σ	$^{180}Hf/^{177}Hf$	± 1σ	$^{176}Lu/^{177}Hf$	± 1σ	$^{176}Yb/^{177}Hf$	± 1σ	V	± 1σ	Ma	± 1σ		± 1σ		± 1σ	Ga
SWA18a-012	0.280770	0.000011	1.467010	0.000028	1.886930	0.000071	0.000916	0.000034	0.028713	0.001300	3.30	0.06	3117	21	0.280715	0.000011	-2.48	0.39	3.66
SWA18a-016	0.280955	0.000017	1.467090	0.000045	1.886570	0.000140	0.001302	0.000029	0.045015	0.000880	2.69	0.04	3117	21	0.280877	0.000017	3.29	0.60	3.29
SWA18a-017c	0.280711	0.000014	1.467070	0.000019	1.886560	0.000059	0.002400	0.000070	0.079606	0.002200	2.50	0.03	3501	32	0.280549	0.000024	0.61	0.49	3.75
SWA18a-021	0.280963	0.000029	1.467030	0.000028	1.886850	0.000160	0.002062	0.000044	0.060685	0.001500	2.06	0.03	3117	21	0.280840	0.000029	1.95	1.02	3.38
SWA18a-029	0.280966	0.000032	1.467040	0.000066	1.886740	0.000200	0.001467	0.000065	0.041887	0.001800	2.30	0.05	3117	21	0.280878	0.000032	3.33	1.12	3.29
SWA18a-031	0.280966	0.000019	1.467100	0.000059	1.886660	0.000160	0.001508	0.000031	0.058148	0.001400	2.12	0.04	3117	21	0.280876	0.000019	3.24	0.67	3.29
SWA18a-033	0.280817	0.000011	1.467020	0.000018	1.886530	0.000087	0.000829	0.000050	0.026747	0.001900	2.83	0.09	3117	21	0.280767	0.000011	-0.62	0.39	3.54
SWA18a-036	0.280849	0.000012	1.466970	0.000033	1.886430	0.000096	0.000823	0.000046	0.024455	0.001500	1.98	0.07	3117	21	0.280800	0.000012	0.53	0.42	3.47
SWA18a-037	0.280841	0.000009	1.467040	0.000028	1.886550	0.000037	0.000778	0.000032	0.022235	0.000860	2.55	0.10	3117	21	0.280794	0.000009	0.34	0.32	3.48
SWA18a-039	0.280874	0.000009	1.467070	0.000026	1.886500	0.000065	0.001030	0.000046	0.035689	0.001900	3.25	0.04	3117	21	0.280812	0.000009	0.98	0.32	3.44
SWA18a-041	0.280890	0.000016	1.467020	0.000034	1.886600	0.000120	0.001033	0.000066	0.033431	0.001400	3.13	0.07	3117	21	0.280828	0.000016	1.54	0.56	3.40
RSA05-003	0.280831	0.000009	1.467270	0.000021	1.886620	0.000069	0.001853	0.000010	0.065759	0.000630	4.62	0.18	3100	17	0.280721	0.000009	-2.68	0.31	3.66
RSA05-005	0.280861	0.000017	1.467260	0.000030	1.886710	0.000110	0.002579	0.000035	0.083682	0.001100	2.19	0.11	3100	17	0.280708	0.000017	-3.15	0.60	3.69
RSA05-008	0.280836	0.000005	1.467280	0.000014	1.886800	0.000075	0.001934	0.000075	0.068700	0.001800	5.32	0.25	3100	17	0.280721	0.000005	-2.67	0.19	3.66
RSA05-011	0.280804	0.000016	1.467320	0.000029	1.886780	0.000078	0.001446	0.000025	0.040464	0.000550	2.78	0.05	3100	17	0.280718	0.000016	-2.78	0.56	3.66
RSA05-015	0.280797	0.000013	1.467350	0.000025	1.886850	0.000084	0.001538	0.000034	0.048571	0.000780	2.38	0.15	3100	17	0.280705	0.000013	-3.22	0.46	3.69
RSA05-016	0.280802	0.000014	1.467370	0.000037	1.886490	0.000090	0.003081	0.000100	0.129739	0.004300	4.91	0.12	3100	17	0.280619	0.000014	-6.32	0.49	3.89
RSA05-020	0.280876	0.000014	1.467270	0.000027	1.886510	0.000075	0.002117	0.000031	0.069173	0.001500	4.15	0.09	3100	17	0.280750	0.000014	-1.64	0.49	3.59
RSA05-022	0.280891	0.000012	1.467290	0.000027	1.886770	0.000063	0.001746	0.000047	0.068663	0.001500	4.52	0.21	3100	17	0.280787	0.000012	-0.32	0.42	3.51
RSA05-025	0.280890	0.000012	1.467320	0.000030	1.886840	0.000110	0.002234	0.000080	0.098931	0.003800	4.81	0.09	3100	17	0.280757	0.000012	-1.39	0.42	3.58
RSA05-026	0.280865	0.000014	1.467380	0.000034	1.886640	0.000083	0.002179	0.000150	0.085812	0.006100	3.38	0.08	3100	17	0.280735	0.000024	-2.16	0.49	3.62
RSA05-028	0.280848	0.000015	1.467320	0.000028	1.886530	0.000089	0.002926	0.000063	0.137496	0.003500	3.73	0.17	3100	17	0.280674	0.000015	-4.35	0.53	3.76
RSA05-030	0.280877	0.000015	1.467280	0.000031	1.886620	0.000087	0.002667	0.000120	0.091926	0.003600	2.72	0.15	3100	17	0.280718	0.000015	-2.77	0.53	3.66
RSA05-031	0.280899	0.000013	1.467330	0.000026	1.886470	0.000093	0.002950	0.000260	0.124176	0.012000	4.85	0.09	3100	17	0.280723	0.000013	-2.58	0.46	3.65
RSA05-036	0.280860	0.000015	1.467300	0.000036	1.886500	0.000099	0.002729	0.000099	0.122214	0.003400	4.74	0.16	3100	17	0.280698	0.000015	-3.50	0.53	3.71
RSA05-040	0.280821	0.000010	1.467280	0.000029	1.886550	0.000081	0.001562	0.000047	0.050088	0.001400	3.46	0.09	3100	17	0.280728	0.000010	-2.42	0.35	3.64
RSA05-043	0.280788	0.000018	1.467270	0.000046	1.886660	0.000120	0.002601	0.000088	0.098633	0.004200	3.02	0.31	3100	17	0.280633	0.000018	-5.80	0.63	3.86
RSA05-044	0.280889	0.000018	1.467320	0.000023	1.886740	0.000110	0.001668	0.000041	0.060821	0.000640	5.75	0.25	3100	17	0.280790	0.000018	-0.22	0.63	3.50
RSA05-049	0.280850	0.000015	1.467300	0.000026	1.886950	0.000100	0.002151	0.000048	0.078062	0.000510	4.91	0.25	3100	17	0.280722	0.000015	-2.63	0.53	3.66
RSA05-051	0.280806	0.000012	1.467180	0.000033	1.886550	0.000066	0.002998	0.000140	0.105378	0.005200	3.29	0.04	3100	17	0.280628	0.000012	-6.00	0.42	3.87

	Measured ratios										Total Hf		Age		$^{176}Hf/^{177}Hf_i$		εHf		T(DM)c
	$^{176}Hf/^{177}Hf$	± 1σ	$^{178}Hf/^{177}Hf$	± 1σ	$^{180}Hf/^{177}Hf$	± 1σ	$^{176}Lu/^{177}Hf$	± 1σ	$^{176}Yb/^{177}Hf$	± 1σ	V	± 1σ	Ma	± 1σ	± 1σ		± 1σ		Ga
RSA05-057	0.280843	0.000014	1.467280	0.000030	1.886870	0.000130	0.001680	0.000069	0.060364	0.001300	3.68	0.25	3100	17	0.280743	0.000014	-1.89	0.49	3.61
RSA05-061	0.280851	0.000010	1.467240	0.000025	1.886800	0.000070	0.001474	0.000056	0.056133	0.002100	3.50	0.25	3100	17	0.280763	0.000010	-1.16	0.35	3.56
RSA05-062	0.280876	0.000012	1.467190	0.000030	1.886470	0.000086	0.002628	0.000025	0.088290	0.000920	3.07	0.10	3100	17	0.280720	0.000012	-2.72	0.42	3.66
RSA05-067	0.280849	0.000011	1.467230	0.000021	1.886640	0.000072	0.000958	0.000027	0.036905	0.000980	3.61	0.13	3100	17	0.280792	0.000011	-0.14	0.39	3.50
RSA05-068	0.280929	0.000012	1.467230	0.000029	1.886760	0.000098	0.002114	0.000083	0.084219	0.000900	4.10	0.16	3100	17	0.280803	0.000012	0.26	0.42	3.47
RSA02-002	0.280936	0.000018	1.467040	0.000038	1.886880	0.000120	0.001499	0.000027	0.057396	0.001100	3.58	0.11	3111	26	0.280846	0.000018	2.06	0.63	3.36
RSA02-003	0.280882	0.000018	1.467020	0.000025	1.886490	0.000057	0.001616	0.000017	0.056202	0.001200	2.42	0.05	3111	26	0.280785	0.000018	-0.12	0.63	3.50
RSA02-005c	0.280873	0.000017	1.467030	0.000049	1.886910	0.000120	0.001612	0.000093	0.043943	0.002300	1.38	0.07	3111	26	0.280777	0.000017	-0.43	0.60	3.52
RSA02-006c	0.280754	0.000021	1.466890	0.000052	1.886790	0.000120	0.000354	0.000008	0.009653	0.000220	2.21	0.16	3111	26	0.280733	0.000021	-1.99	0.73	3.62
RSA02-006r	0.280904	0.000021	1.466920	0.000028	1.886720	0.000120	0.000847	0.000077	0.024744	0.002300	3.02	0.09	3111	26	0.280853	0.000021	2.30	0.73	3.35
RSA02-007c	0.280847	0.000011	1.466980	0.000029	1.886810	0.000060	0.001115	0.000004	0.039082	0.000240	3.04	0.06	3111	26	0.280780	0.000011	-0.30	0.39	3.51
RSA02-008c	0.280897	0.000013	1.466980	0.000025	1.886780	0.000057	0.000741	0.000034	0.018881	0.000790	4.37	0.04	3111	26	0.280853	0.000013	2.28	0.46	3.35
RSA02-010	0.280859	0.000011	1.467000	0.000025	1.886730	0.000070	0.001173	0.000033	0.038715	0.000250	3.09	0.04	3111	26	0.280789	0.000011	0.01	0.39	3.50
RSA02-012c	0.280806	0.000012	1.466890	0.000025	1.886650	0.000072	0.000310	0.000015	0.010373	0.000500	2.31	0.04	3111	26	0.280787	0.000012	-0.05	0.42	3.50
RSA02-014	0.281111	0.000023	1.466780	0.000025	1.886410	0.000053	0.002426	0.000091	0.081491	0.003500	3.23	0.05	3111	26	0.280966	0.000023	6.32	0.80	3.09
RSA02-019c	0.280903	0.000011	1.466940	0.000024	1.886630	0.000047	0.001342	0.000024	0.038506	0.001100	3.19	0.01	3111	26	0.280823	0.000011	1.21	0.39	3.42
RSA02-019r	0.280815	0.000011	1.466860	0.000024	1.886640	0.000066	0.000625	0.000032	0.018601	0.000590	3.23	0.21	3111	26	0.280778	0.000011	-0.39	0.39	3.52
RSA02-020	0.280895	0.000016	1.467030	0.000042	1.886620	0.000087	0.001506	0.000070	0.035441	0.001500	2.98	0.05	3111	26	0.280805	0.000016	0.58	0.56	3.46
RSA02-023	0.280728	0.000009	1.466960	0.000026	1.886730	0.000085	0.000072	0.000006	0.002216	0.000160	2.34	0.10	3111	26	0.280724	0.000009	-2.32	0.30	3.64
RSA02-027c	0.280741	0.000013	1.467040	0.000026	1.886690	0.000086	0.000037	0.000002	0.001432	0.000057	3.48	0.05	3111	26	0.280739	0.000013	-1.78	0.46	3.61
RSA02-029c	0.280893	0.000016	1.466990	0.000036	1.886200	0.000130	0.000843	0.000017	0.024222	0.000210	1.93	0.11	3111	26	0.280843	0.000016	1.92	0.56	3.37
RSA02-030	0.280967	0.000014	1.467020	0.000028	1.886450	0.000080	0.001277	0.000011	0.039072	0.000700	3.69	0.07	3111	26	0.280891	0.000014	3.63	0.49	3.26
RSA02-031	0.280705	0.000015	1.466920	0.000041	1.886710	0.000079	0.000311	0.000012	0.008844	0.000500	3.24	0.11	3111	26	0.280686	0.000015	-3.64	0.53	3.73
SWA07-005	0.280801	0.000010	1.467330	0.000030	1.887070	0.000057	0.001961	0.000055	0.051099	0.001600	1.97	0.09	3123	13	0.280683	0.000010	-3.47	0.35	3.73
SWA07-008	0.280636	0.000014	1.467270	0.000051	1.887220	0.000100	0.000666	0.000021	0.017607	0.000660	1.85	0.05	3123	13	0.280596	0.000014	-6.58	0.49	3.92
SWA07-011	0.280817	0.000022	1.467340	0.000071	1.887170	0.000110	0.001047	0.000011	0.030729	0.000570	1.34	0.05	3123	13	0.280754	0.000022	-0.95	0.77	3.57
SWA07-015	0.280843	0.000016	1.467300	0.000048	1.887090	0.000075	0.001511	0.000050	0.046644	0.001700	1.53	0.06	3123	13	0.280752	0.000016	-1.01	0.56	3.57
SWA07-018	0.280801	0.000018	1.467360	0.000065	1.887160	0.000110	0.001365	0.000080	0.038177	0.001900	1.38	0.06	3123	13	0.280719	0.000018	-2.20	0.63	3.64
SWA07-024	0.280875	0.000019	1.467590	0.000085	1.887180	0.000120	0.001081	0.000014	0.034270	0.001100	2.20	0.08	3123	13	0.280810	0.000019	1.04	0.67	3.44
SWA07-032	0.280775	0.000013	1.467250	0.000028	1.887250	0.000091	0.001131	0.000018	0.033135	0.000720	1.76	0.04	3123	13	0.280707	0.000013	-2.62	0.46	3.67

	Measured ratios										Total Hf		Age		$^{176}Hf/^{177}Hf_i$		εHf		T(DM)c
	$^{176}Hf/^{177}Hf$	± 1σ	$^{178}Hf/^{177}Hf$	± 1σ	$^{180}Hf/^{177}Hf$	± 1σ	$^{176}Lu/^{177}Hf$	± 1σ	$^{176}Yb/^{177}Hf$	± 1σ	V	± 1σ	Ma	± 1σ		± 1σ		± 1σ	Ga
SWA07-034	0.280772	0.000020	1.467390	0.000068	1.887270	0.000091	0.000957	0.000041	0.029863	0.002200	1.88	0.08	3123	13	0.280715	0.000020	-2.36	0.70	3.66
SWA07-048	0.280740	0.000015	1.467450	0.000059	1.887200	0.000056	0.001031	0.000023	0.030824	0.000470	1.63	0.06	3123	13	0.280678	0.000015	-3.66	0.53	3.74
SWA07-049	0.280767	0.000016	1.467310	0.000044	1.887060	0.000084	0.000717	0.000033	0.022395	0.001300	1.47	0.05	3123	13	0.280724	0.000016	-2.03	0.56	3.63
SWA07-054	0.280854	0.000022	1.467130	0.000130	1.886920	0.000190	0.000932	0.000021	0.031702	0.000940	1.89	0.08	3123	13	0.280798	0.000022	0.61	0.77	3.47
SWA07-055	0.280689	0.000029	1.467370	0.000071	1.887060	0.000100	0.001022	0.000054	0.025902	0.001500	1.12	0.04	3500	20	0.280620	0.000029	3.12	1.02	3.59
SWA07-059	0.280806	0.000014	1.467240	0.000044	1.886880	0.000095	0.001444	0.000023	0.043681	0.000660	1.45	0.06	3123	13	0.280719	0.000014	-2.19	0.49	3.64
SWA07-067	0.280858	0.000014	1.467320	0.000057	1.886940	0.000079	0.001216	0.000029	0.036931	0.001100	1.26	0.07	3123	13	0.280785	0.000014	0.15	0.49	3.50
SWA07-074	0.280745	0.000016	1.467300	0.000055	1.887020	0.000074	0.001699	0.000093	0.056685	0.003100	1.64	0.07	3490	24	0.280631	0.000016	3.26	0.56	3.58
SWA07-076	0.280853	0.000017	1.467280	0.000052	1.887030	0.000110	0.001013	0.000017	0.032006	0.000340	1.44	0.10	3123	13	0.280792	0.000017	0.40	0.60	3.48
SWA07-077	0.280603	0.000020	1.467460	0.000045	1.887150	0.000077	0.000658	0.000063	0.020144	0.001900	1.37	0.09	3536	18	0.280558	0.000020	1.76	0.70	3.71
SWA07-078	0.280949	0.000018	1.467210	0.000039	1.886950	0.000077	0.001645	0.000012	0.051660	0.000310	1.24	0.04	3123	13	0.280850	0.000018	2.47	0.63	3.35
SWA07-086	0.280927	0.000018	1.467310	0.000034	1.887280	0.000072	0.002082	0.000057	0.066313	0.001600	1.47	0.05	3123	13	0.280802	0.000018	0.76	0.63	3.46
SWA07-087	0.280810	0.000015	1.467350	0.000045	1.887040	0.000100	0.001413	0.000055	0.046103	0.001900	1.98	0.14	3514	32	0.280714	0.000015	6.81	0.53	3.37
SWA07-090	0.280631	0.000019	1.467530	0.000048	1.887090	0.000069	0.001188	0.000056	0.032312	0.001700	1.55	0.11	3417	18	0.280553	0.000019	-1.23	0.67	3.81
SWA07-097	0.280764	0.000015	1.467280	0.000041	1.887070	0.000088	0.000705	0.000025	0.022406	0.000950	1.77	0.07	3123	13	0.280722	0.000015	-2.11	0.53	3.64
RSA04-001r	0.280906	0.000020	1.466930	0.000049	1.886670	0.000260	0.001294	0.000033	0.036276	0.000830	2.47	0.15	3127	27	0.280828	0.000020	1.78	0.70	3.39
RSA04-002c	0.280964	0.000039	1.467060	0.000110	1.885940	0.000510	0.001501	0.000023	0.057701	0.000950	2.29	0.03	3127	27	0.280874	0.000039	3.40	1.37	3.29
RSA04-003r	0.280990	0.000058	1.466910	0.000100	1.886790	0.000460	0.001520	0.000029	0.038962	0.001500	1.66	0.10	3127	27	0.280899	0.000058	4.29	2.03	3.23
RSA04-006c	0.280952	0.000021	1.466980	0.000025	1.886610	0.000120	0.001652	0.000093	0.062117	0.003600	2.48	0.04	3127	27	0.280853	0.000021	2.66	0.73	3.34
RSA04-007c	0.280937	0.000024	1.467190	0.000041	1.886820	0.000240	0.001133	0.000078	0.037457	0.002100	3.15	0.12	3127	27	0.280869	0.000024	3.23	0.84	3.30
RSA04-009c	0.280875	0.000020	1.467020	0.000031	1.886620	0.000079	0.001252	0.000063	0.042900	0.002400	2.33	0.11	3127	27	0.280800	0.000020	0.77	0.70	3.46
RSA04-012	0.280910	0.000013	1.467120	0.000026	1.886780	0.000074	0.000829	0.000024	0.027006	0.000510	1.78	0.02	3127	27	0.280860	0.000013	2.92	0.46	3.32
RSA04-013c	0.280933	0.000022	1.467110	0.000034	1.886660	0.000100	0.001487	0.000100	0.047590	0.002600	2.49	0.09	3127	27	0.280844	0.000022	2.33	0.77	3.36
RSA04-015c	0.280869	0.000030	1.466890	0.000099	1.886570	0.000330	0.001757	0.000012	0.050508	0.000350	1.92	0.03	3127	27	0.280763	0.000030	-0.53	1.05	3.54
RSA08-006	0.280932	0.000014	1.467060	0.000034	1.886660	0.000077	0.000837	0.000029	0.027278	0.001200	3.29	0.05	3131	48	0.280882	0.000014	3.78	0.49	3.27
RSA08-016c	0.280985	0.000058	1.467080	0.000140	1.887030	0.000280	0.001863	0.000010	0.050987	0.000430	2.09	0.05	3131	48	0.280873	0.000058	3.47	2.03	3.29
RSA08-057	0.281060	0.000022	1.466910	0.000030	1.886770	0.000140	0.001718	0.000071	0.053798	0.001800	4.66	0.07	3131	48	0.280957	0.000022	6.45	0.77	3.10
SWA10a-001	0.280535	0.000005	1.467190	0.000018	1.886620	0.000027	0.001360	0.000048	0.064650	0.002300	7.19	0.17	3456	20	0.280444	0.000005	-4.18	0.17	4.03
SWA10a-003c	0.280813	0.000006	1.467170	0.000029	1.886730	0.000027	0.000954	0.000047	0.045609	0.002000	8.29	0.10	3123	15	0.280756	0.000006	-0.89	0.22	3.56
SWA10a-018	0.280450	0.000005	1.467240	0.000025	1.886750	0.000026	0.000952	0.000026	0.043655	0.001300	8.41	0.08	3469	26	0.280386	0.000005	-5.94	0.19	4.15

	Measured ratios										Total Hf		Age		$^{176}Hf/^{177}Hf_i$		εHf		T(DM)c
	$^{176}Hf/^{177}Hf$	± 1σ	$^{178}Hf/^{177}Hf$	± 1σ	$^{180}Hf/^{177}Hf$	± 1σ	$^{176}Lu/^{177}Hf$	± 1σ	$^{176}Yb/^{177}Hf$	± 1σ	V	± 1σ	Ma	± 1σ	± 1σ		± 1σ		Ga
SWA10a-019	0.280808	0.000009	1.467190	0.000023	1.886790	0.000027	0.001094	0.000016	0.048119	0.000750	6.63	0.09	3123	15	0.280742	0.000009	-1.37	0.31	3.59
SWA10a-020c	0.280503	0.000021	1.467120	0.000044	1.886420	0.000034	0.001810	0.000079	0.068807	0.003500	7.16	0.16	3502	20	0.280381	0.000021	-5.36	0.73	4.14
SWA10a-026	0.280856	0.000007	1.467240	0.000030	1.886560	0.000017	0.000992	0.000034	0.045074	0.001400	8.12	0.29	3123	15	0.280797	0.000007	0.56	0.24	3.47
SWA10a-030	0.280624	0.000018	1.467330	0.000055	1.886580	0.000087	0.001963	0.000022	0.062632	0.001100	2.76	0.17	3123	15	0.280506	0.000018	-9.78	0.63	4.13
SWA10a-049c	0.280515	0.000008	1.467420	0.000071	1.886570	0.000032	0.001261	0.000022	0.050164	0.000980	11.88	0.29	3420	22	0.280432	0.000008	-5.47	0.27	4.08
SWA10a-051c	0.280495	0.000006	1.467250	0.000032	1.886650	0.000024	0.001871	0.000038	0.089743	0.000480	7.37	0.13	3597	30	0.280365	0.000006	-3.68	0.20	4.10
SWA10a-051r	0.280554	0.000010	1.467240	0.000021	1.886590	0.000024	0.001893	0.000024	0.081651	0.002200	10.07	0.29	3355	32	0.280432	0.000010	-7.00	0.35	4.13
SWA10a-064c	0.280530	0.000009	1.467270	0.000037	1.886690	0.000026	0.002933	0.000120	0.136475	0.007100	7.24	0.18	3656	24	0.280323	0.000009	-3.79	0.32	4.15
SWA10a-128	0.280768	0.000016	1.467200	0.000077	1.886760	0.000044	0.001779	0.000068	0.066501	0.003400	11.50	0.13	3123	15	0.280661	0.000016	-4.26	0.56	3.78
SWA10a-135	0.280723	0.000012	1.467250	0.000048	1.886800	0.000050	0.002795	0.000020	0.092010	0.000790	6.30	0.04	3123	15	0.280555	0.000012	-8.03	0.42	4.02
SWA10a-145	0.280805	0.000019	1.467370	0.000077	1.886930	0.000049	0.001853	0.000057	0.078083	0.005500	9.32	0.23	3123	15	0.280694	0.000019	-3.10	0.67	3.70
SWA10a-155	0.280644	0.000024	1.467320	0.000100	1.886750	0.000088	0.002582	0.000110	0.089734	0.004600	4.56	0.18	3123	15	0.280489	0.000024	-10.39	0.84	4.16
RSA09-001c	0.280920	0.000010	1.467170	0.000032	1.886820	0.000022	0.003009	0.000072	0.163435	0.003800	9.59	0.19	3109	46	0.280740	0.000010	-1.77	0.35	3.61
RSA09-006	0.280921	0.000014	1.467130	0.000034	1.886730	0.000061	0.003468	0.000017	0.188033	0.001000	8.50	0.10	3109	46	0.280714	0.000014	-2.71	0.49	3.67
RSA09-021	0.280980	0.000014	1.467110	0.000049	1.886830	0.000053	0.002886	0.000130	0.142878	0.007200	8.01	0.12	3109	46	0.280808	0.000014	0.63	0.49	3.45
RSA09-024	0.280920	0.000012	1.467270	0.000026	1.886870	0.000023	0.003148	0.000120	0.152232	0.006200	9.48	0.38	3109	46	0.280732	0.000012	-2.07	0.42	3.63
RSA09-037	0.280915	0.000008	1.467270	0.000018	1.886910	0.000021	0.002566	0.000050	0.120996	0.003300	9.61	0.10	3109	46	0.280762	0.000008	-1.01	0.26	3.56
RSA09-041	0.280887	0.000019	1.467290	0.000120	1.886810	0.000049	0.001970	0.000056	0.067393	0.001100	11.10	0.18	3109	46	0.280769	0.000019	-0.74	0.67	3.54
RSA09-079	0.280886	0.000008	1.467250	0.000039	1.886880	0.000023	0.002609	0.000043	0.114536	0.002400	11.25	0.34	3109	46	0.280730	0.000008	-2.13	0.29	3.63
RSA09-092c	0.280996	0.000014	1.467160	0.000025	1.886780	0.000032	0.003929	0.000120	0.190367	0.005500	8.88	0.26	3109	46	0.280761	0.000014	-1.02	0.49	3.56
SWA03-003c	0.280841	0.000010	1.467220	0.000019	1.886880	0.000066	0.001638	0.000120	0.054443	0.002800	5.31	0.39	3152	20	0.280742	0.000010	-0.71	0.35	3.57
SWA03-006c	0.280884	0.000011	1.467230	0.000022	1.886590	0.000058	0.001976	0.000025	0.061414	0.000690	3.98	0.25	3152	20	0.280764	0.000011	0.09	0.39	3.52
SWA03-007c	0.280906	0.000009	1.467210	0.000021	1.886640	0.000057	0.001702	0.000037	0.060223	0.001300	3.83	0.14	3152	20	0.280803	0.000009	1.46	0.30	3.43
SWA03-009c	0.280884	0.000019	1.467180	0.000033	1.886550	0.000071	0.002413	0.000033	0.070780	0.001100	1.89	0.06	3152	20	0.280738	0.000019	-0.85	0.67	3.58
SWA03-010	0.280867	0.000013	1.467220	0.000036	1.886830	0.000100	0.002150	0.000042	0.062984	0.001300	2.21	0.04	3152	20	0.280737	0.000013	-0.89	0.46	3.58
SWA03-012	0.280896	0.000012	1.467210	0.000040	1.886570	0.000076	0.002652	0.000044	0.078646	0.001500	2.36	0.01	3152	20	0.280735	0.000012	-0.94	0.42	3.59
SWA03-017c	0.280975	0.000019	1.467160	0.000035	1.886410	0.000130	0.002883	0.000099	0.090963	0.003700	2.07	0.07	3152	20	0.280800	0.000019	1.37	0.67	3.44
SWA03-018	0.280848	0.000036	1.467120	0.000054	1.886330	0.000150	0.002291	0.000060	0.071149	0.002100	0.96	0.02	3152	20	0.280709	0.000036	-1.87	1.26	3.65
SWA03-019	0.280885	0.000011	1.467140	0.000029	1.886800	0.000064	0.002322	0.000059	0.066869	0.001500	3.01	0.06	3152	20	0.280744	0.000011	-0.62	0.39	3.57
SWA03-020	0.280906	0.000015	1.467200	0.000035	1.886610	0.000080	0.002579	0.000032	0.074525	0.000990	1.97	0.03	3152	20	0.280750	0.000015	-0.43	0.53	3.55

	Measured ratios										Total Hf		Age		$^{176}Hf/^{177}Hf_i$		εHf		T(DM)c
	$^{176}Hf/^{177}Hf$	± 1σ	$^{178}Hf/^{177}Hf$	± 1σ	$^{180}Hf/^{177}Hf$	± 1σ	$^{176}Lu/^{177}Hf$	± 1σ	$^{176}Yb/^{177}Hf$	± 1σ	V	± 1σ	Ma	± 1σ		± 1σ		± 1σ	Ga
SWA03-021c	0.280846	0.000012	1.467130	0.000017	1.886510	0.000057	0.002234	0.000063	0.067565	0.001700	3.27	0.05	3152	20	0.280711	0.000012	-1.82	0.42	3.64
SWA03-023	0.280838	0.000013	1.467170	0.000031	1.886800	0.000082	0.002045	0.000069	0.070781	0.001300	2.51	0.23	3152	20	0.280714	0.000013	-1.70	0.46	3.64
SWA03-024	0.280860	0.000013	1.467110	0.000019	1.886610	0.000064	0.002780	0.000120	0.099183	0.005500	3.05	0.05	3152	20	0.280692	0.000013	-2.50	0.46	3.69
SWA03-025c	0.280839	0.000007	1.467120	0.000014	1.886680	0.000045	0.001284	0.000057	0.049991	0.002500	5.11	0.22	3152	20	0.280761	0.000007	-0.02	0.25	3.53
SWA03-029	0.280913	0.000012	1.467240	0.000034	1.886710	0.000087	0.002396	0.000041	0.069671	0.001200	1.79	0.02	3152	20	0.280768	0.000012	0.22	0.42	3.51
SWA03-031c	0.280831	0.000010	1.467090	0.000018	1.886860	0.000048	0.001110	0.000048	0.043768	0.001700	2.79	0.13	3152	20	0.280764	0.000010	0.07	0.34	3.52
SWA03-031r	0.280874	0.000011	1.467160	0.000024	1.886850	0.000064	0.001692	0.000044	0.067484	0.002000	3.92	0.21	3152	20	0.280772	0.000011	0.35	0.39	3.50
SWA03-032c	0.280905	0.000013	1.467170	0.000029	1.887020	0.000089	0.001680	0.000032	0.069100	0.002700	2.50	0.12	3152	20	0.280803	0.000013	1.48	0.46	3.43
SWA03-032r	0.280877	0.000006	1.467130	0.000020	1.886740	0.000046	0.001710	0.000012	0.062071	0.001000	4.40	0.14	3152	20	0.280773	0.000006	0.41	0.22	3.50
SWA03-038c	0.280988	0.000019	1.467090	0.000038	1.886680	0.000110	0.002731	0.000035	0.081403	0.000820	2.20	0.03	3152	20	0.280823	0.000019	2.16	0.67	3.39
SWA03-039c	0.280899	0.000018	1.467270	0.000040	1.886860	0.000089	0.001913	0.000047	0.059468	0.001000	2.09	0.07	3152	20	0.280783	0.000018	0.76	0.63	3.48
SWA03-040	0.280875	0.000012	1.467370	0.000027	1.886840	0.000094	0.002309	0.000046	0.067648	0.001400	1.96	0.04	3152	20	0.280735	0.000012	-0.95	0.42	3.59
SWA03-041	0.280895	0.000011	1.467290	0.000031	1.887080	0.000098	0.001738	0.000051	0.064319	0.000850	3.29	0.16	3152	20	0.280790	0.000011	1.00	0.39	3.46
SWA03-043c	0.280882	0.000010	1.467370	0.000028	1.886890	0.000075	0.002508	0.000130	0.076335	0.003700	2.18	0.05	3152	20	0.280730	0.000010	-1.13	0.35	3.60
SWA03-044	0.280913	0.000024	1.467380	0.000047	1.887070	0.000170	0.001936	0.000025	0.071771	0.001100	1.80	0.07	3152	20	0.280796	0.000024	1.21	0.84	3.45
SWA03-045c	0.280958	0.000019	1.467190	0.000049	1.886570	0.000081	0.002837	0.000015	0.081894	0.000370	1.29	0.07	3152	20	0.280786	0.000019	0.87	0.67	3.47
SWA03-046c	0.280910	0.000013	1.467290	0.000031	1.886920	0.000085	0.002168	0.000066	0.094519	0.004100	3.48	0.10	3152	20	0.280779	0.000013	0.60	0.46	3.49
SWA03-048c	0.280811	0.000013	1.467290	0.000030	1.886830	0.000049	0.001182	0.000087	0.052161	0.004300	3.11	0.12	3152	20	0.280739	0.000013	-0.80	0.46	3.58
SWA03-048r	0.280847	0.000010	1.467270	0.000016	1.886800	0.000060	0.001285	0.000038	0.040710	0.001400	4.04	0.12	3152	20	0.280769	0.000010	0.26	0.33	3.51
SWA03-049c	0.280904	0.000014	1.467160	0.000025	1.886800	0.000092	0.002696	0.000048	0.083885	0.001100	1.84	0.04	3152	20	0.280741	0.000014	-0.75	0.49	3.57
SWA03-050c	0.280791	0.000013	1.467230	0.000023	1.886610	0.000079	0.001893	0.000054	0.055290	0.001700	2.51	0.08	3152	20	0.280676	0.000013	-3.04	0.46	3.72
SWA03-052	0.280903	0.000015	1.467290	0.000037	1.886740	0.000091	0.002148	0.000022	0.065050	0.000520	2.10	0.05	3152	20	0.280773	0.000015	0.40	0.53	3.50
SWA03-053c	0.280929	0.000018	1.467330	0.000040	1.886770	0.000130	0.001766	0.000084	0.056000	0.002500	2.11	0.18	3152	20	0.280822	0.000018	2.15	0.63	3.39
SWA03-056c	0.280886	0.000015	1.467260	0.000028	1.886800	0.000080	0.002219	0.000016	0.069137	0.001100	2.08	0.04	3152	20	0.280752	0.000015	-0.36	0.53	3.55
SWA03-058c	0.280949	0.000020	1.467290	0.000023	1.886900	0.000120	0.002344	0.000087	0.071394	0.002300	2.66	0.11	3152	20	0.280807	0.000020	1.61	0.70	3.42
SWA03-060c	0.280796	0.000017	1.467300	0.000035	1.886670	0.000110	0.002834	0.000042	0.079960	0.001300	1.20	0.09	3152	20	0.280624	0.000017	-4.89	0.60	3.84
RSA06-001c	0.280945	0.000010	1.467170	0.000030	1.886640	0.000039	0.002357	0.000079	0.072708	0.002900	11.43	0.17	3105	29	0.280804	0.000010	0.42	0.34	3.46
RSA06-019c	0.280789	0.000009	1.467200	0.000022	1.886830	0.000039	0.000735	0.000032	0.032210	0.001500	7.71	0.05	3105	29	0.280745	0.000009	-1.69	0.31	3.60
RSA06-025c	0.280884	0.000007	1.467250	0.000039	1.886790	0.000022	0.001849	0.000064	0.069858	0.002500	8.86	0.34	3105	29	0.280774	0.000007	-0.67	0.25	3.53
RSA06-038	0.280962	0.000011	1.467280	0.000037	1.886790	0.000047	0.002505	0.000046	0.087786	0.001900	7.82	0.23	3105	29	0.280813	0.000011	0.71	0.39	3.45

	Measured ratios										Total Hf		Age		$^{176}Hf/^{177}Hf_i$		εHf		T(DM)c
	$^{176}Hf/^{177}Hf$	± 1σ	$^{178}Hf/^{177}Hf$	± 1σ	$^{180}Hf/^{177}Hf$	± 1σ	$^{176}Lu/^{177}Hf$	± 1σ	$^{176}Yb/^{177}Hf$	± 1σ	V	± 1σ	Ma	± 1σ	± 1σ		± 1σ		Ga
RSA06-048	0.280905	0.000011	1.467340	0.000038	1.886660	0.000033	0.002177	0.000100	0.097889	0.003800	7.77	0.18	3105	29	0.280775	0.000011	-0.62	0.39	3.53
RSA06-055c	0.280922	0.000012	1.467190	0.000057	1.886760	0.000058	0.001690	0.000021	0.082125	0.002000	9.90	0.37	3105	29	0.280821	0.000012	1.02	0.42	3.43
RSA06-065	0.280918	0.000009	1.467190	0.000058	1.886770	0.000033	0.001867	0.000045	0.082152	0.002600	8.33	0.19	3105	29	0.280807	0.000009	0.50	0.33	3.46
RSA06-073	0.280863	0.000006	1.467290	0.000031	1.886750	0.000026	0.001253	0.000037	0.056532	0.001300	9.26	0.09	3105	29	0.280788	0.000006	-0.16	0.20	3.50
RSA06-088c	0.280824	0.000012	1.467330	0.000022	1.886850	0.000033	0.001367	0.000140	0.059558	0.006000	7.57	0.27	3105	29	0.280743	0.000012	-1.79	0.42	3.60
RSA06-100	0.280850	0.000012	1.467260	0.000042	1.886970	0.000034	0.002842	0.000045	0.089548	0.001600	5.87	0.11	3105	29	0.280681	0.000012	-3.99	0.42	3.75
RSA06-112c	0.280832	0.000006	1.467310	0.000024	1.886930	0.000027	0.000891	0.000013	0.038587	0.000490	6.03	0.15	3105	29	0.280779	0.000006	-0.49	0.22	3.52
RSA06-121	0.280928	0.000011	1.467260	0.000035	1.886920	0.000037	0.001966	0.000063	0.089085	0.004300	9.59	0.31	3105	29	0.280811	0.000011	0.64	0.39	3.45
SWA13a-001	0.280820	0.000005	1.467330	0.000016	1.886960	0.000030	0.001160	0.000037	0.043772	0.001600	6.68	0.15	3117.7	8.8	0.280751	0.000005	-1.20	0.16	3.58
SWA13a-003	0.280823	0.000009	1.467330	0.000037	1.887140	0.000048	0.001090	0.000045	0.041591	0.001600	8.45	0.15	3117.7	8.8	0.280758	0.000009	-0.95	0.32	3.56
SWA13a-004	0.280889	0.000011	1.467330	0.000028	1.887020	0.000031	0.002301	0.000150	0.090191	0.007500	10.35	0.18	3117.7	8.8	0.280751	0.000011	-1.18	0.39	3.58
SWA13a-005c	0.280898	0.000008	1.467330	0.000016	1.886980	0.000026	0.001511	0.000048	0.057227	0.001700	7.62	0.14	3117.7	8.8	0.280808	0.000008	0.83	0.29	3.45
SWA13a-008c	0.280881	0.000012	1.467360	0.000066	1.887220	0.000045	0.001135	0.000025	0.039740	0.001100	8.54	0.02	3117.7	8.8	0.280813	0.000012	1.02	0.42	3.44
SWA13a-009	0.280927	0.000008	1.467270	0.000018	1.887260	0.000027	0.001248	0.000020	0.041265	0.000190	10.78	0.27	3117.7	8.8	0.280852	0.000008	2.42	0.27	3.35
SWA13a-010	0.280997	0.000008	1.467160	0.000016	1.887240	0.000025	0.001762	0.000019	0.063255	0.000770	9.51	0.17	3117.7	8.8	0.280892	0.000008	3.82	0.27	3.26
SWA13a-011	0.281100	0.000013	1.466960	0.000047	1.887250	0.000085	0.002620	0.000009	0.074692	0.000240	5.08	0.28	3117.7	8.8	0.280943	0.000013	5.65	0.46	3.14
SWA13a-012c	0.280868	0.000012	1.467290	0.000026	1.886840	0.000048	0.001481	0.000044	0.063703	0.003100	8.13	0.07	3117.7	8.8	0.280779	0.000012	-0.18	0.42	3.51
SWA13a-015c	0.280805	0.000009	1.467330	0.000015	1.886900	0.000039	0.000877	0.000053	0.034708	0.002000	7.21	0.11	3117.7	8.8	0.280753	0.000009	-1.13	0.32	3.57
SWA13a-016	0.280819	0.000009	1.467890	0.000022	1.887270	0.000038	0.000805	0.000120	0.035654	0.006300	10.76	0.39	3117.7	8.8	0.280771	0.000009	-0.48	0.30	3.53
SWA13a-020	0.280911	0.000007	1.467270	0.000029	1.886690	0.000032	0.001145	0.000011	0.043217	0.001900	7.16	0.10	3117.7	8.8	0.280842	0.000007	2.07	0.23	3.37
SWA13a-021c	0.280895	0.000017	1.467210	0.000052	1.886530	0.000066	0.002002	0.000041	0.059372	0.001000	4.37	0.11	3117.7	8.8	0.280775	0.000017	-0.33	0.60	3.52
SWA13a-025	0.280885	0.000008	1.467280	0.000083	1.886680	0.000060	0.002076	0.000160	0.072594	0.005800	7.36	0.13	3117.7	8.8	0.280761	0.000008	-0.84	0.29	3.55
SWA13a-028	0.280959	0.000012	1.467220	0.000044	1.886680	0.000041	0.001480	0.000008	0.068796	0.000870	7.49	0.10	3117.7	8.8	0.280870	0.000012	3.06	0.42	3.30
SWA13a-029	0.280971	0.000007	1.467270	0.000031	1.886700	0.000043	0.001522	0.000019	0.065910	0.001700	6.93	0.05	3117.7	8.8	0.280880	0.000007	3.40	0.24	3.28
SWA13a-032	0.280937	0.000022	1.467360	0.000047	1.886640	0.000060	0.002313	0.000080	0.072710	0.002500	6.15	0.27	3117.7	8.8	0.280799	0.000022	0.51	0.77	3.47
SWA13a-034	0.280940	0.000007	1.467250	0.000031	1.886680	0.000038	0.001218	0.000044	0.044376	0.001300	9.82	0.17	3117.7	8.8	0.280867	0.000007	2.95	0.25	3.31
SWA13a-035c	0.280939	0.000017	1.467280	0.000062	1.886730	0.000037	0.002533	0.000150	0.083210	0.005400	7.59	0.50	3117.7	8.8	0.280787	0.000017	0.11	0.60	3.49
SWA13a-037	0.280943	0.000012	1.467220	0.000028	1.886800	0.000034	0.001050	0.000064	0.045586	0.003300	9.19	0.15	3117.7	8.8	0.280880	0.000012	3.41	0.42	3.28
SWA13a-039	0.281050	0.000007	1.467150	0.000028	1.886640	0.000033	0.001966	0.000051	0.072253	0.001800	7.17	0.08	3117.7	8.8	0.280932	0.000007	5.27	0.23	3.16
SWA13a-041	0.280821	0.000021	1.467260	0.000071	1.886720	0.000071	0.002001	0.000065	0.057943	0.001600	2.59	0.30	3117.7	8.8	0.280701	0.000021	-2.96	0.73	3.69

	Measured ratios										Total Hf		Age		$^{176}Hf/^{177}Hf_i$		εHf		T(DM)c
	$^{176}Hf/^{177}Hf$	± 1σ	$^{178}Hf/^{177}Hf$	± 1σ	$^{180}Hf/^{177}Hf$	± 1σ	$^{176}Lu/^{177}Hf$	± 1σ	$^{176}Yb/^{177}Hf$	± 1σ	V	± 1σ	Ma	± 1σ		± 1σ		± 1σ	Ga
SWA13a-043	0.280955	0.000013	1.467150	0.000025	1.886750	0.000030	0.001871	0.000130	0.083462	0.005900	7.01	0.10	3117.7	8.8	0.280843	0.000013	2.09	0.46	3.37
SWA13a-044	0.280867	0.000010	1.467140	0.000014	1.886750	0.000021	0.002115	0.000220	0.112493	0.012000	10.43	0.08	3117.7	8.8	0.280740	0.000010	-1.57	0.34	3.60
SWA13a-045	0.280887	0.000008	1.467200	0.000019	1.886730	0.000030	0.001267	0.000045	0.055170	0.001600	6.50	0.08	3117.7	8.8	0.280811	0.000008	0.95	0.27	3.44
SWA11-001c	0.280884	0.000012	1.467280	0.000043	1.887090	0.000053	0.001216	0.000050	0.040246	0.002000	1.80	0.06	3130	10	0.280811	0.000012	1.23	0.42	3.43
SWA11-003	0.280910	0.000015	1.467440	0.000028	1.886960	0.000074	0.000960	0.000012	0.033781	0.000690	1.36	0.05	3130	10	0.280852	0.000015	2.71	0.53	3.34
SWA11-004	0.280909	0.000016	1.467430	0.000040	1.886990	0.000076	0.001109	0.000032	0.038652	0.000630	1.43	0.06	3130	10	0.280842	0.000016	2.35	0.56	3.36
SWA11-008	0.280896	0.000016	1.467320	0.000058	1.886860	0.000100	0.001186	0.000004	0.037067	0.000200	1.89	0.03	3130	10	0.280825	0.000016	1.72	0.56	3.40
SWA11-013	0.280891	0.000010	1.467540	0.000052	1.886840	0.000076	0.001299	0.000037	0.038493	0.000670	1.65	0.14	3130	10	0.280813	0.000010	1.30	0.35	3.43
SWA11-014	0.280830	0.000016	1.467350	0.000048	1.886920	0.000066	0.000966	0.000010	0.027732	0.000560	1.63	0.06	3130	10	0.280772	0.000016	-0.16	0.56	3.52
SWA11-017	0.280810	0.000018	1.467200	0.000062	1.886870	0.000084	0.000782	0.000024	0.024481	0.000540	1.42	0.09	3130	10	0.280763	0.000018	-0.47	0.63	3.54
SWA11-023c	0.280879	0.000017	1.467240	0.000061	1.886950	0.000061	0.001347	0.000023	0.045480	0.001200	1.38	0.04	3130	10	0.280798	0.000017	0.77	0.60	3.46
SWA11-024	0.280883	0.000018	1.467340	0.000055	1.887030	0.000088	0.001386	0.000013	0.043429	0.000260	1.99	0.06	3130	10	0.280800	0.000018	0.83	0.63	3.46
SWA11-025	0.280947	0.000018	1.467250	0.000036	1.886990	0.000057	0.001807	0.000088	0.066098	0.002900	1.51	0.06	3130	10	0.280838	0.000018	2.21	0.63	3.37
SWA11-026	0.280870	0.000014	1.467300	0.000054	1.886960	0.000076	0.000802	0.000027	0.028046	0.000520	1.43	0.05	3130	10	0.280822	0.000014	1.62	0.49	3.41
SWA11-028c	0.280813	0.000019	1.467300	0.000052	1.887070	0.000087	0.000597	0.000026	0.021500	0.001100	1.38	0.03	3130	10	0.280777	0.000019	0.03	0.67	3.51
SWA11-029	0.280901	0.000016	1.467400	0.000049	1.886950	0.000089	0.001066	0.000025	0.037274	0.000720	1.21	0.04	3130	10	0.280837	0.000016	2.16	0.56	3.37
SWA11-030	0.280848	0.000020	1.467170	0.000097	1.887140	0.000130	0.001099	0.000042	0.041152	0.001500	1.24	0.04	3130	10	0.280782	0.000020	0.20	0.70	3.50
SWA11-031	0.280917	0.000017	1.467270	0.000049	1.886960	0.000075	0.001141	0.000012	0.038626	0.001300	1.13	0.05	3130	10	0.280848	0.000017	2.57	0.60	3.35
SWA11-032c	0.280853	0.000015	1.467270	0.000045	1.886940	0.000071	0.000822	0.000040	0.028467	0.001400	1.26	0.04	3130	10	0.280804	0.000015	0.97	0.53	3.45
SWA11-033	0.280843	0.000016	1.467220	0.000039	1.886830	0.000110	0.000915	0.000013	0.031284	0.000680	1.36	0.05	3130	10	0.280788	0.000016	0.42	0.56	3.48
SWA11-037	0.280867	0.000017	1.467230	0.000053	1.886940	0.000085	0.000713	0.000015	0.022737	0.000740	1.41	0.05	3130	10	0.280824	0.000017	1.70	0.60	3.40
SWA11-038	0.280824	0.000015	1.467290	0.000033	1.886940	0.000041	0.000575	0.000019	0.017538	0.000850	1.80	0.06	3130	10	0.280789	0.000015	0.47	0.53	3.48
SWA11-046	0.280861	0.000017	1.467100	0.000098	1.886870	0.000083	0.001277	0.000020	0.038061	0.000740	1.59	0.07	3130	10	0.280784	0.000017	0.28	0.60	3.49
SWA11-048	0.280849	0.000024	1.467440	0.000081	1.886910	0.000083	0.001130	0.000065	0.038381	0.001800	1.58	0.08	3130	10	0.280781	0.000024	0.17	0.84	3.50
SWA11-051	0.280876	0.000020	1.467220	0.000044	1.886850	0.000083	0.000688	0.000033	0.025345	0.001600	1.44	0.02	3130	10	0.280835	0.000020	2.08	0.70	3.38
SWA11-052	0.280899	0.000020	1.467300	0.000058	1.886970	0.000088	0.001143	0.000012	0.037150	0.000160	1.34	0.03	3130	10	0.280830	0.000020	1.92	0.70	3.39
SWA11-055	0.280765	0.000016	1.467260	0.000035	1.887200	0.000071	0.000550	0.000021	0.018160	0.000930	1.12	0.03	3130	10	0.280732	0.000016	-1.58	0.56	3.61
SWA11-058c	0.280834	0.000015	1.467230	0.000041	1.886920	0.000057	0.001005	0.000023	0.031967	0.000800	1.46	0.05	3130	10	0.280774	0.000015	-0.10	0.53	3.52
SWA11-061	0.280906	0.000018	1.467200	0.000057	1.887100	0.000092	0.001524	0.000043	0.048660	0.001500	1.22	0.04	3130	10	0.280814	0.000018	1.36	0.63	3.42
SWA11-062	0.280885	0.000014	1.467330	0.000055	1.887080	0.000078	0.001076	0.000056	0.035794	0.001900	1.65	0.06	3130	10	0.280820	0.000014	1.57	0.49	3.41

	Measured ratios										Total Hf		Age		$^{176}Hf/^{177}Hf_i$		εHf		T(DM)c
	$^{176}Hf/^{177}Hf$	± 1σ	$^{178}Hf/^{177}Hf$	± 1σ	$^{180}Hf/^{177}Hf$	± 1σ	$^{176}Lu/^{177}Hf$	± 1σ	$^{176}Yb/^{177}Hf$	± 1σ	V	± 1σ	Ma	± 1σ	± 1σ		± 1σ		Ga
SWA11-063	0.280897	0.000016	1.467300	0.000045	1.886980	0.000088	0.001287	0.000028	0.042282	0.001400	1.57	0.07	3130	10	0.280820	0.000016	1.54	0.56	3.41
SWA11-065	0.280802	0.000016	1.467290	0.000052	1.887050	0.000082	0.000843	0.000022	0.027196	0.000710	1.19	0.05	3130	10	0.280751	0.000016	-0.89	0.56	3.57
SWA11-066	0.280826	0.000018	1.467220	0.000052	1.887090	0.000084	0.000724	0.000010	0.023074	0.000460	1.30	0.06	3130	10	0.280782	0.000018	0.22	0.63	3.50
SWA11-068	0.280893	0.000014	1.467220	0.000045	1.886870	0.000068	0.001133	0.000023	0.035755	0.000450	2.10	0.06	3130	10	0.280825	0.000014	1.73	0.49	3.40
SWA11-073	0.280904	0.000016	1.467220	0.000043	1.887080	0.000084	0.001253	0.000076	0.040880	0.002500	1.39	0.02	3130	10	0.280829	0.000016	1.87	0.56	3.39
SWA11-074	0.280873	0.000016	1.467250	0.000033	1.886890	0.000075	0.001152	0.000059	0.038983	0.001500	1.58	0.06	3130	10	0.280804	0.000016	0.98	0.56	3.45
SWA11-081	0.280915	0.000016	1.467280	0.000040	1.887200	0.000072	0.000859	0.000049	0.028940	0.002200	1.31	0.02	3130	10	0.280863	0.000016	3.10	0.56	3.31
SWA11-085	0.280887	0.000020	1.467230	0.000039	1.887200	0.000072	0.001156	0.000005	0.038322	0.000610	1.35	0.03	3130	10	0.280818	0.000020	1.47	0.70	3.42
SWA11-086	0.280851	0.000014	1.467290	0.000055	1.887230	0.000110	0.001537	0.000052	0.057948	0.001700	1.50	0.04	3130	10	0.280759	0.000014	-0.63	0.49	3.55
SWA11-088	0.280872	0.000014	1.467360	0.000046	1.887140	0.000076	0.001108	0.000031	0.038456	0.001100	1.37	0.02	3130	10	0.280805	0.000014	1.04	0.49	3.44
SWA09-001c	0.280847	0.000006	1.467070	0.000028	1.886300	0.000042	0.001188	0.000027	0.041586	0.001200	7.57	0.17	3142	13	0.280775	0.000006	0.25	0.19	3.50
SWA09-002	0.280837	0.000023	1.467380	0.000110	1.886430	0.000059	0.003071	0.000027	0.107130	0.002100	5.56	0.55	3142	13	0.280652	0.000023	-4.16	0.80	3.78
SWA09-005c	0.280896	0.000012	1.467200	0.000056	1.886520	0.000042	0.001387	0.000016	0.055216	0.001200	11.12	0.16	3142	13	0.280812	0.000012	1.56	0.42	3.42
SWA09-010	0.280916	0.000007	1.467290	0.000046	1.886610	0.000026	0.001250	0.000052	0.040790	0.002300	7.26	0.18	3142	13	0.280841	0.000007	2.57	0.25	3.35
SWA09-011c	0.280842	0.000005	1.467240	0.000017	1.886490	0.000027	0.000255	0.000008	0.009543	0.000270	8.62	0.19	3142	13	0.280827	0.000005	2.07	0.18	3.39
SWA09-012	0.280914	0.000006	1.467130	0.000024	1.886420	0.000030	0.000807	0.000016	0.033142	0.000810	7.91	0.15	3142	13	0.280865	0.000006	3.45	0.22	3.30
SWA09-016	0.280954	0.000006	1.467140	0.000026	1.886580	0.000033	0.000728	0.000028	0.028424	0.000970	7.13	0.16	3142	13	0.280910	0.000006	5.04	0.21	3.20
SWA09-017c	0.280962	0.000008	1.466990	0.000025	1.886710	0.000033	0.000953	0.000035	0.039554	0.001700	8.52	0.16	3142	13	0.280904	0.000008	4.85	0.29	3.21
SWA09-018	0.281064	0.000023	1.466820	0.000030	1.886750	0.000031	0.002673	0.000029	0.120609	0.002400	10.10	0.24	3142	13	0.280903	0.000023	4.78	0.80	3.21
SWA09-021c	0.280974	0.000008	1.466940	0.000040	1.886940	0.000038	0.001217	0.000066	0.048744	0.002200	7.12	0.09	3142	13	0.280901	0.000008	4.71	0.27	3.22
SWA09-023c	0.280838	0.000007	1.467170	0.000023	1.886660	0.000023	0.001351	0.000023	0.065455	0.001600	7.89	0.11	3142	13	0.280756	0.000007	-0.42	0.25	3.55
SWA09-026c	0.280792	0.000005	1.467250	0.000022	1.886760	0.000021	0.000771	0.000041	0.037500	0.002700	11.14	0.28	3142	13	0.280745	0.000005	-0.82	0.19	3.57
SWA09-027c	0.280737	0.000029	1.467220	0.000130	1.886610	0.000052	0.002601	0.000054	0.100170	0.002300	4.99	0.20	3394	46	0.280567	0.000029	-1.27	1.02	3.79
SWA09-029c	0.280906	0.000014	1.467170	0.000050	1.886510	0.000031	0.002271	0.000036	0.118498	0.002600	8.34	0.07	3142	13	0.280769	0.000014	0.02	0.49	3.52
SWA09-034c	0.280858	0.000006	1.467160	0.000047	1.886500	0.000037	0.000941	0.000010	0.029487	0.000270	6.74	0.04	3142	13	0.280801	0.000006	1.17	0.21	3.44
SWA09-042c	0.280853	0.000006	1.467220	0.000023	1.886510	0.000029	0.000933	0.000014	0.043537	0.001000	8.64	0.12	3142	13	0.280797	0.000006	1.01	0.21	3.45
SWA09-043c	0.280817	0.000008	1.467240	0.000057	1.886550	0.000041	0.000547	0.000073	0.019686	0.002700	6.50	0.20	3142	13	0.280784	0.000008	0.56	0.27	3.48
SWA09-044c	0.280904	0.000009	1.467330	0.000039	1.886610	0.000036	0.001641	0.000014	0.051406	0.000290	6.45	0.07	3142	13	0.280805	0.000009	1.30	0.32	3.44
SWA02a-006	0.280939	0.000014	1.467210	0.000041	1.886860	0.000130	0.002528	0.000021	0.073443	0.000580	3.13	0.09	3119	30	0.280788	0.000014	0.15	0.49	3.49
SWA02a-012c	0.280689	0.000019	1.467230	0.000030	1.886940	0.000074	0.001497	0.000040	0.043529	0.001300	2.36	0.15	3471	18	0.280589	0.000019	1.32	0.67	3.69

	Measured ratios										Total Hf		Age		$^{176}Hf/^{177}Hf_i$		εHf		T(DM)c
	$^{176}Hf/^{177}Hf$	± 1σ	$^{178}Hf/^{177}Hf$	± 1σ	$^{180}Hf/^{177}Hf$	± 1σ	$^{176}Lu/^{177}Hf$	± 1σ	$^{176}Yb/^{177}Hf$	± 1σ	V	± 1σ	Ma	± 1σ		± 1σ		± 1σ	Ga
SWA02a-024c	0.280859	0.000014	1.467150	0.000027	1.886950	0.000081	0.001060	0.000130	0.045719	0.005500	1.82	0.04	3119	30	0.280795	0.000014	0.43	0.49	3.47
SWA02a-032	0.280791	0.000011	1.467190	0.000030	1.886860	0.000056	0.000978	0.000011	0.036059	0.000430	3.16	0.12	3119	30	0.280732	0.000011	-1.82	0.39	3.62
SWA02a-054c	0.280829	0.000009	1.467130	0.000023	1.886860	0.000052	0.001362	0.000045	0.046237	0.000850	2.83	0.16	3119	30	0.280747	0.000009	-1.28	0.32	3.58
SWA02a-064c	0.280897	0.000027	1.466990	0.000078	1.886770	0.000190	0.000898	0.000034	0.034233	0.001300	1.32	0.02	3119	30	0.280843	0.000027	2.13	0.94	3.37
RSA07-003	0.280799	0.000016	1.467180	0.000047	1.886470	0.000130	0.002203	0.000059	0.072501	0.002000	2.91	0.07	3167	34	0.280665	0.000016	-3.10	0.56	3.74
RSA07-004	0.280840	0.000011	1.467290	0.000022	1.886660	0.000046	0.002207	0.000150	0.067395	0.004400	4.12	0.19	3167	34	0.280706	0.000011	-1.65	0.39	3.64
RSA07-021	0.280840	0.000010	1.467200	0.000020	1.886220	0.000059	0.002513	0.000150	0.119761	0.007300	4.28	0.17	3167	34	0.280687	0.000010	-2.31	0.35	3.69
RSA07-046	0.280838	0.000015	1.467320	0.000025	1.886560	0.000099	0.002041	0.000065	0.078127	0.002300	4.94	0.32	3167	34	0.280714	0.000015	-1.36	0.53	3.63
RSA07-051	0.280891	0.000020	1.467190	0.000028	1.886210	0.000180	0.002441	0.000032	0.084459	0.000950	5.69	0.15	3167	34	0.280742	0.000020	-0.34	0.70	3.56
RSA07-080c	0.280803	0.000012	1.467330	0.000020	1.886510	0.000061	0.001353	0.000055	0.047193	0.000980	3.50	0.16	3167	34	0.280721	0.000012	-1.11	0.42	3.61
SWA05-001	0.280869	0.000010	1.467190	0.000023	1.886410	0.000097	0.001021	0.000038	0.033116	0.001400	3.45	0.05	3165	36	0.280807	0.000002	1.91	0.34	3.41
SWA05-002c	0.280891	0.000017	1.467090	0.000034	1.886380	0.000078	0.001436	0.000059	0.038625	0.001500	2.69	0.05	3165	36	0.280804	0.000004	1.80	0.60	3.42
SWA05-002r	0.280894	0.000016	1.467110	0.000034	1.886360	0.000100	0.001144	0.000034	0.035524	0.001200	2.51	0.14	3165	36	0.280824	0.000004	2.53	0.56	3.37
SWA05-006c	0.280897	0.000029	1.467050	0.000045	1.886320	0.000150	0.001653	0.000096	0.052959	0.003600	2.04	0.06	3165	36	0.280796	0.000007	1.54	1.02	3.44
SWA05-008c	0.280887	0.000013	1.467110	0.000022	1.886470	0.000058	0.001362	0.000033	0.040365	0.001000	3.12	0.06	3165	36	0.280804	0.000003	1.81	0.46	3.42
SWA05-009	0.280798	0.000021	1.467120	0.000042	1.886490	0.000093	0.000358	0.000003	0.010423	0.000095	2.92	0.05	3165	36	0.280776	0.000005	0.82	0.73	3.48
SWA05-010c	0.280848	0.000014	1.467140	0.000026	1.886570	0.000046	0.000752	0.000037	0.023680	0.001300	2.26	0.08	3165	36	0.280802	0.000004	1.74	0.49	3.43
SWA05-011	0.280866	0.000018	1.467120	0.000049	1.886410	0.000130	0.001066	0.000096	0.035984	0.003700	2.51	0.05	3165	36	0.280801	0.000005	1.71	0.63	3.43
SWA05-012c	0.280805	0.000010	1.467140	0.000025	1.886590	0.000065	0.000739	0.000033	0.021798	0.000590	2.05	0.05	3165	36	0.280760	0.000002	0.24	0.34	3.52
SWA05-017	0.280855	0.000023	1.467080	0.000047	1.886550	0.000140	0.001244	0.000047	0.043704	0.001800	2.61	0.03	3165	36	0.280779	0.000006	0.93	0.80	3.48